Synthesis of Chiral Saturated Heterocycles from Diazo Compounds for Pharmaceutical Screening Collections

A Thesis Submitted by

Alexander Joseph Boddy

In partial fulfilment of the requirements for the degree of

Doctor of Philosophy

Department of Chemistry

Imperial College London

Molecular Sciences Research Hub

White City Campus

London W12 0BZ

United Kingdom

2020

Declarations

Declaration of Originality

I, Alexander Joseph Boddy declare that this thesis and the work presented herein has been generated by me as a result of my own original research. Where I have consulted the published work of others this is clearly attributed. Where the thesis is based on work done by myself jointly with others, I have made clear exactly what was done by others and what I have contributed myself.

Copyright Declaration

The copyright of this thesis rests with the author. Unless otherwise indicated, its contents are licensed under a Creative Commons Attribution-NonCommercial 4.0 International Licence (CC BY-NC).

Under this licence, you may copy and redistribute the material in any medium or format. You may also create and distribute modified versions of the work. This is on the condition that: you credit the author and do not use it, or any derivative works, for a commercial purpose.

When reusing or sharing this work, ensure you make the licence terms clear to others by naming the licence and linking to the licence text. Where a work has been adapted, you should indicate that the work has been changed and describe those changes.

Please seek permission from the copyright holder for uses of this work that are not included in this licence or permitted under UK Copyright Law.

Acknowledgments

Firstly, I would like to thank Dr James Bull for providing me with the opportunity to undertake a PhD in his group. He has provided continual support and ideas throughout. His mentorship and supervision have taught me many valuable lessons and given me many opportunities, for which I will remain very grateful.

I would like to thank all members of the Bull group that I have worked with over the last 4 years. Special thanks to Dr Dominic Affron and Dr Rosemary Croft for their help at the start of my PhD. Daniele Antermite, Dr Maryne Dubois and Dr Sahra St. John-Campbell deserve a medal for putting up with me for four years. I reserve a special thank you to those friends at Imperial who have kept me grounded and remind me regularly that there is more to life: Edward Briggs, Stephanie Greed, Rainbow Lo, Megan Midson, Charlotte Zammit and Ahmed Carter.

I would like to thank Prof. Alan Spivey and Dr Christopher Cordier for their help throughout my time at Imperial. They have provided many ideas and encouragement which has benefited the project.

I would like to thank Imperial College and AstraZeneca for funding the project through an iCASE award. I would like to thank all the people I worked with at AZ (particularly Dr Steve Stokes and Dr Andrew Madin). I would especially like to thank Dr Emma Rivers for her support throughout my PhD and for making my time in Cambridge so enjoyable.

I am grateful to the mass spectrometry and NMR staff (Lisa Haigh, Peter Haycock and Corey Fulop) for their work, support and patience. I also thank Dr Andrew White for carrying out X-ray crystallography.

I thank Thomas Walton, Gracie Irvine, Edward Ringe, Mariana Garro and Harry McElligott for their friendship and support.

I am particularly thankful to have met Dr Camille Denis who I have had the pleasure of sharing my life with for the last 3 years. Thank you, Camille, for your constant love and support.

Finally, but most importantly, I would like to thank my family: Kevin, Sandra, Benjamin and Annabel. I am indebted to them for supporting me through University and my PhD. Without their love and guidance I would not have been able to make the most of these opportunities. Though I don’t express it in words, I am very grateful and hope I will make you proud.

Abstract

New synthetic methods that enable rapid access to new heterocyclic structures in biologically relevant chemical space provide important opportunities in drug discovery. In this thesis, novel saturated heterocycles were targeted as C(sp^3)-rich motifs to enrich existing pharmaceutical compound libraries.

Initially, the synthesis of 2,2-disubstituted saturated nitrogen heterocycles, as 2-aryl proline analogues, is described. These products are synthesised through an N–H insertion of diazo compounds followed by one-pot cyclisation using mild base. The use of the same method to access 4- to 7-membered scaffolds is shown. The flexibility of the methodology is demonstrated by application to drug and natural product functionalisation. The utility of the products is shown by various important derivatisation reactions.

Subsequently, the 4-membered azetidine products, synthesised by N–H insertion and cyclisation, are ring expanded to 6-membered 1,3-oxazinan-2-one products. Through exploration of the scope and mechanism of this 4- to 6-membered ring expansion a new methodology is developed for generating new leads for drug discovery.

Finally, the N–H insertion of diazo compounds is coupled with a new enantioselective cyclisation reaction to synthesise enantioenriched spiroazetidines. This cyclisation step makes use of a new asymmetric phase transfer catalyst to achieve high *er*. A range of spiroazetidines are synthesised and the mechanism of the asymmetric phase transfer catalysis is discussed.

A summary of specific conclusions and future work can be found at the end of each chapter. The final section provides experimental details.

Table of Contents

Abbreviations 10
Stereochemical Notation 11
1. Introduction 12
1.1 Approaches to Discovery of New Chemical Entities 12
1.1.1 The Hit Discovery Process 12
1.1.2 Pharmaceutical Screening Collections 12
1.1.3 Screening Methods in Drug Discovery 12
1.1.3.1 High Throughput Screening 12
1.1.3.2 Phenotypic Screening 13
1.1.3.3 Fragment Screening 13
1.1.3.4 DNA Encoded Libraries 13
1.1.3.5 In Silico Screening 14
1.1.3.6 Where do approved drugs come from? 14
1.1.4 Attrition in the Drug Discovery Pipeline 16
1.1.5 Physicochemical Properties of Drug Candidates 17
1.1.5.1 Lipophilicity 17
1.1.5.2 Aromatic Ring Count 18
1.1.5.3 Saturated Heterocycles 18
1.1.5.4 Molecular Topology 19
1.1.6 Lack of Diversity within Pharmaceutical Compound Collections 19
1.1.6.1 Lack of Synthetic Reaction Diversity 20
1.2 Synthetic Strategies to Overcome Attrition in Drug Discovery 20
1.2.1 Importance of Synthetic Chemistry for the Pharmaceutical Industry 20
1.2.2 Lead–Oriented Synthesis 21
1.2.3 Fragment–Oriented Synthesis 21
1.2.4 Diversity–Oriented Synthesis 23
1.2.4.1 Diversity–Oriented Synthesis and Lead–Oriented Synthesis 26
1.2.4.2 Diversity–Oriented Synthesis and Fragment–Oriented Synthesis 28
1.2.4.3 Assessment of the Diversity of Compound Libraries 31

1.2.5 Small Rings in Pharmaceuticals and Organic Synthesis 32
1.2.5.1 Fragment–Oriented Synthesis of Small Rings in the Bull Group 33
1.2.5.2 Fragment–Oriented Synthesis of Imidazolines, Pyrrolidines and Piperidines in the Bull Group 35
1.2.5.3 Novel Synthetic Methods as an Approach to New Fragments and Lead–Like Compounds (Summary) 37
1.3 Project Aims 39
2. Synthesis of Four- to Seven-Membered Saturated Nitrogen Heterocycles by N–H Insertion and Cyclisation 40
2.1 Saturated Nitrogen Heterocycles in Drug Discovery 40
2.2 General Strategies for the Synthesis of Saturated Nitrogen Heterocycles 40
2.3 2-Aryl Proline Analogues 42
2.3.1 Importance of 2-Aryl Proline Analogues 42
2.3.2 Synthetic Strategies to 2-Aryl Proline Analogues 43
2.3.3 Use of Diazo Compounds 44
2.4 Results and Discussion 46
2.4.1 Preliminary Work and Optimisation of N–H Insertion Reaction 46
2.4.2 Synthesis of Diester Azetidine, Pyrrolidine and Piperidine 47
2.4.3 Synthesis of 2-Aryl Proline Analogues 50
2.4.3.1 Synthesis of Protected Amine Starting Materials 50
2.4.3.2 Synthesis of Diazo Compounds 50
2.4.3.3 Scope of Azetidine Synthesis 52
2.4.3.4 Scope of Pyrrolidine Synthesis 54
2.4.3.5 Scope of Piperidine Synthesis 56
2.4.3.6 Synthesis of Larger Rings 58
2.4.3.7 Application of One-Pot Reaction to Late Stage Functionalisation 61
2.4.3.8 Functionalisation of Azetidine, Pyrrolidine, Piperidine and Azepane Scaffolds 66
2.4.3.9 Summary 71
2.4.4 Limitations of the N–H Insertion and Cyclisation Strategy 72

2.4.4.1 Scope of Diazo Compounds 72
2.4.4.2 Enantioselectivity 75
2.4.5 Conclusions and Future Work 78
3. Ring Expansion of Azetidines 79
3.1 Reactivity of Azetidines 79
3.1.1 Ring Strain of Azetidines 79
3.1.2 Ring Expansion and Ring Opening of Azetidines 80
3.2 1,3-Oxazinan-2-ones 81
3.2.1 1,3-Oxazinan-2-ones 81
3.2.2 1,3-Oxazinan-2-ones in Drug Discovery 81
3.2.3 Synthetic Approaches to 1,3-Oxazinan-2-ones 82
3.2.4 Synthesis of 1,3-Oxazinan-2-ones from Azetidines and Related Ring Expansions 83
3.3 Results and Discussion 84
3.3.1 Ring Expansion of Azetidine Carbamates: Initial Hit 84
3.3.2 Optimisation of Ring Expansion Reaction 85
3.3.3 Scope of 4- to 6-Membered Ring Expansion 87
3.3.4 Mechanism of the Ring Expansion 90
3.3.5 N–H Insertion/Cyclisation/Ring Expansion (NICE) Sequence 93
3.3.6 Functionalisation of 1,3-Oxazinan-2-one Scaffold 95
3.4 Conclusions and Future Work 97
4. Enantioselective Azetidine Spirocyclisation 99
4.1 Four-Membered Aza-Spirocycles in Synthesis and Drug Discovery 99
4.2 Spirocyclic Oxindoles in Synthesis and Drug Discovery 100
4.3 Asymmetric Phase Transfer Catalysis 103
4.3.1 Intermolecular Alkylation and Mechanism 103
4.3.2 Application of PTC to Spirocyclic Oxindoles and Intramolecular Alkylation 106
4.4 Results and Discussion 108
4.4.1 Optimisation of N–H and O–H Insertion of 3-Diazooxindoles 109
4.4.2 Scope of N–H Insertion and Racemic Spirooxindoles 111

4.4.2.1 Synthesis of Diazo Compounds 111
4.4.2.2 Synthesis of N–H Insertion Products 115
4.4.2.3 Synthesis of Racemic Spirooxindoles 118
4.4.3 Optimisation of Enantioselective Cyclisation 120
4.4.3.1 Synthesis of Catalysts 135
4.4.4 Reaction Scope of Enantioenriched Spirooxindoles 136
4.4.4.1 Testing Different Catalysts on Scale Up 136
4.4.4.2 Scope of Different Aromatic Rings 137
4.4.4.3 Scope of Different N-Substituents 138
4.4.4.4 One-Pot and Telescoped Reactions 139
4.4.4.5 Scope of Leaving Groups and Ring Size 140
4.4.5 Mechanism of Asymmetric Phase Transfer Catalysed Cyclisation 142
4.4.6 Conclusions and Future Work 150
5. Conclusions and Future Outlook 152
6. Experimental 154
6.1 General Experimental Considerations 154
6.2 Experimental Details and Characterisation Data 156
6.2.1 Synthesised Compounds in Chapter 2 156
6.2.1.1 Synthesis of Protected Amine Starting Materials 156
6.2.1.2 Synthesis of Diazo Compounds 163
6.2.1.3 Synthesis of 2,2-Diester Saturated Nitrogen Heterocycles 176
6.2.1.4 Synthesis of 2,2-Disubstituted Azetidines 178
6.2.1.5 Synthesis of 2,2-Disubstituted Pyrrolidines 187
6.2.1.6 Synthesis of 2,2-Disubstituted Piperidines 198
6.2.1.7 Synthesis of 2,2-Disubstituted Azepanes and Larger Rings 206
6.2.1.8 Late Stage Functionalisation 211
6.2.1.9 Functionalisation of Saturated Nitrogen Heterocycles 223
6.2.1.10 Compounds from Section 2.4.4 233
6.2.2 Synthesised Compounds from Chapter 3 240
6.2.2.1 Additional Diazo Compounds 240

6.2.2.2 Additional 2,2-Disubstituted Azetidines 241
6.2.2.3 Synthesis of 1,3-Oxazinan-2-ones 244
6.2.2.4 Synthesis of Oxazinanones by NICE Reaction 253
6.2.2.5 Functionalisation of 1,3-oxazinan-2-ones 258
6.2.2.6 HPLC Data for 1,3-Oxazinan-2-one Synthesis 263
6.2.3 Synthesised Compounds from Chapter 4 267
6.2.3.1 3-Diazooxindole Synthesis 267
6.2.3.2 Synthesis of Additional Protected Amine Starting Materials 286
6.2.3.3 N–H Insertion of 3-diazooxindoles 288
6.2.3.4 Racemic and Enantioselective Synthesis of Spirooxindoles 301
6.2.3.5 Synthesis of Phase Transfer Catalysts 322
6.2.3.6 Compounds from Conclusions and Future Work Section 4.4.6 346
6.2.3.7 HPLC Data for Spirooxindoles 349
7. Appendices 370
7.1 Literature Strategies for the Synthesis of Saturated Nitrogen Heterocycles 370
7.1.1 Azetidine Synthesis 370
7.1.2 Pyrrolidine Synthesis 372
7.1.3 Piperidine Synthesis 374
7.1.4 Azepane Synthesis 376
7.2 Representative NMR Spectra 378
7.3 X-Ray Crystal Structure Data 384
8. References 404

Abbreviations

ADMET	Absorption, distribution, metabolism, excretion and toxicity
API	Active pharmaceutical ingredient
aq	Aqueous
Ar	Aromatic ring
BIOS	Biology inspired oriented synthesis
Bn	Benzyl
Boc	*tert*-Butyloxycarbonyl
Bu	Butyl
Cbz	Carboxybenzyl
CNS	Central nervous system
CYP	Cytochrome P enzyme
DBU	1,8-diazabicyclo(5.4.0)undec-7-ene
DEL	DNA encoded library
DIBAL	Diisobutylaluminium hydride
DG	Directing group
DMA/DMF	*N*,*N*-dimethylacetamide/ dimethylformamide
DMAP	4-(dimethylamino)pyridine
DNA	Deoxyribonucleic acid
DOS	Diversity-oriented synthesis
Et	Ethyl
equiv	equivalents
FBDD	Fragment based drug discovery
FDA	Food and Drug Administration
Fsp^3	Fraction sp^3
GSK	GlaxoSmithKline
HBA	Hydrogen bond acceptors
HBD	Hydrogen bond donors
hERG	Human ether a-go-go-related gene
HTS	High-throughput screen/ing
IP	Intellectual property
cLog*P*/Log*P*	calculated water/octanol partition coefficient
LOS	Lead-oriented synthesis
LC/HRMS	Liquid chromatography/High resolution mass spectrometry
Me	Methyl
MIT	Massachusetts Institute of Technology
mp	Melting point
MPO	Multi-parameter optimisation
MW	Molecular weight
NICE	N–H Insertion/cyclisation/ring expansion
NME	New molecular entity
NMR	Nuclear magnetic resonance
Ns	Nosyl
*p*ABSA	*para*-Acetamidobenzenesulfonyl azide
PDC	Pyridinium dichromate
*p*TSA	*para*-Toluenesulfonic acid
PAINS	Pan-assay interference compounds
Pg	Protecting group
Ph	Phenyl
PK	Pharmacokinetics
ppm	Parts per million
PMP	*para*-methoxy phenyl

Abbreviations (continued)

PROTAC	Proteolysis targeting chimera	SPFE	Solid phase fluorous extraction
R&D	Research and development	TFA	Trifluoroacetic acid
Ro5	Rule of five	THF	Tetrahydrofuran
RSM	Recovered starting material	tPSA	Total Polar Surface Area
rt	room temperature	Ts	Tosyl
sat	saturated		

Stereochemical Notation

Throughout this thesis, representations of stereochemistry are consistent with the convention proposed by Maehr.[1] Solid and broken bold lines are used to indicate relative configuration and solid and broken wedges indicate absolute configuration. Where the former bold lines are used, the compound is racemic and the relative configuration is displayed. When solid and broken wedges are used, this is to indicate that the compound is enantioenriched or prepared as a single enantiomer, and the absolute configuration is shown.



racemic



enantioenriched

1. Introduction

1.1 Approaches to Discovery of New Chemical Entities

1.1.1 The Hit Discovery Process

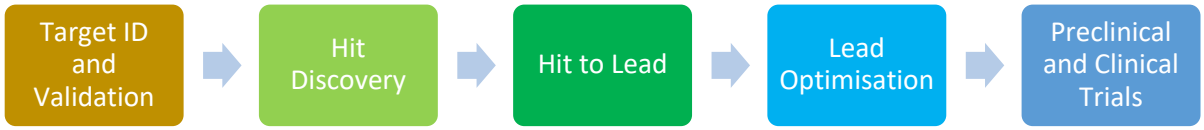


Figure 1: Schematic representation of the drug discovery pipeline.

The drug discovery process relies on the generation of a hit molecule against a selected, validated biological target, i.e. an enzyme or protein of interest. Generation of that hit compound typically results from screening of compounds in an assay to assess function which usually correlates to binding of the ligand with the target. This hit would then be tested with further assays in a hit validation process to assess selectivity, efficacy and initial safety testing i.e. in animal models to generate a lead candidate.[2] Upon selection of a lead candidate, this can be further optimised through analogue synthesis or derivatisation to investigate improvements in physicochemical properties, safety or efficacy. After lead optimisation the candidate may then enter clinical trials before potential approval as a drug for the disease criteria. This process may take 15–20 years, as well as up to $2.6 bn, from the start of the program to approval.[3] This high cost associated with the research and development of a drug, combined with the high rate of failure of pharmaceutical research programs, results in high market cost for new disease treatments.

1.1.2 Pharmaceutical Screening Collections

Pharmaceutical companies must maintain large numbers of compounds for screening purposes. These physical screening collections may number in the millions of compounds and require intensive effort and resource in order to procure, maintain and overhaul.[4] The screening collection used will have a large impact on the success of any hit screening programme (the properties and what constitutes a high quality compound collection will be discussed in Section 1.1.5).[5]

1.1.3 Screening Methods in Drug Discovery

1.1.3.1 High Throughput Screening

High-throughput screening (HTS), sometimes referred to as target based screening, has been the most common screening method utilised by the pharmaceutical industry (See Section 1.1.3.6 for discussion).[6] After advances in molecular biology in the 1980s, pharmaceutical

companies developed HTS to rapidly screen small-molecule libraries against biological targets. Prior to 2000 HTS was coupled with combinatorial chemistry in order to screen large numbers of compounds.[7] The success of HTS depends on the quality of the biology of the screen, i.e. target selection and validation; the size and diversity of the compound collection and the quality of the compounds (both chemical and physical).[8]

1.1.3.2 Phenotypic Screening

In contrast to HTS, phenotypic screening is target agnostic. Phenotypic screening was one of the only significant drug discovery methods available prior to the development of target-based HTS.[9] Phenotypic screening can directly assess a compounds ability to block or promote a phenotype relevant to disease. A hit's mechanism of action is then sought in order to be able to develop the hit in a similar manner to target based screening.[10] Although in recent decades HTS usurped phenotypic screening as the method of choice, phenotypic drug discovery has consistently been utilised for certain disease targets, i.e. in antibiotic drug discovery.[11]

1.1.3.3 Fragment Screening

Fragment based drug discovery (FBDD) has emerged in the last two decades as an alternative to HTS and phenotypic screening.[12] FBDD was enabled by the development of technology which allowed low molecular weight fragments with low affinities for targets to be detected using biophysical methods such as NMR spectroscopy or X-ray crystallography.[13] Being of low molecular weight, fewer fragments are necessary to cover a similar region of chemical space to a greater number of higher molecular weight compounds within a HTS. Yet, the low affinity of fragment hits means that they are particularly challenging to screen.[14] The desirable molecular properties of fragments in the context of organic synthesis will be discussed in Section 1.1.5.

1.1.3.4 DNA Encoded Libraries

Proposed by Brenner and Lerner in 1992, DNA encoded libraries (DELs) involve the generation of vast numbers of compounds tagged with a DNA barcode.[15] Enabled by developments in gene sequencing and the ability to amplify DNA sequences, DNA encoded libraries build compounds in a split-pool combinatorial approach and for each chemical step a unique DNA tag is added to a DNA strand attached to the compound by a linker.[16] The protein of interest is soaked with the DNA tagged compounds and then washed to reveal compounds that bind. The advantages of DNA encoded libraries include the ability to screen up to trillions of compounds in one experiment, obviating the necessity of an experiment per compound in HTS. Thus the cost is reduced compared to HTS where vast physical compound libraries must be maintained.[17] Challenges of this technology include hit validation, as there are a number of false positives generated with hits often resulting in no activity *in vitro* or *in vivo*, and the size

of the DNA tag can also lead to hindrance to target binding.[18] There are very specific requirements for organic synthesis to generate DELs, including compatibility with aqueous conditions and DNA.[19]

1.1.3.5 In Silico Screening

A potential route to expanding the number of compounds that can be screened is the use of computer aided drug design for screening of large virtual libraries of compounds *in silico*.[20] Coupled with protein structure, virtual chemical libraries can be screened in docking studies in order to generate a focussed library of compounds which can be screened in a physical assay.[21] This approach can help to focus synthesis efforts and reduce the number of compounds required to be physically synthesised.

1.1.3.6 Where do approved drugs come from?

At the start of the 21st century there was concern about the number of new drug approvals and the drug pipeline (Figure 2).[22] In recent years the number of drug approvals appears to be reaching levels not seen since before 2000. In this section we will discuss how these new drugs were discovered. In Section 1.1.4 the problem of attrition in the drug discovery pipeline which has contributed to the lower number of drug approvals between 2000 and 2016 will be discussed. In Section 1.1.5 the potential reasons why the number of approvals has recently increased will be discussed, with particular emphasis on the understanding of how to improve compound quality.

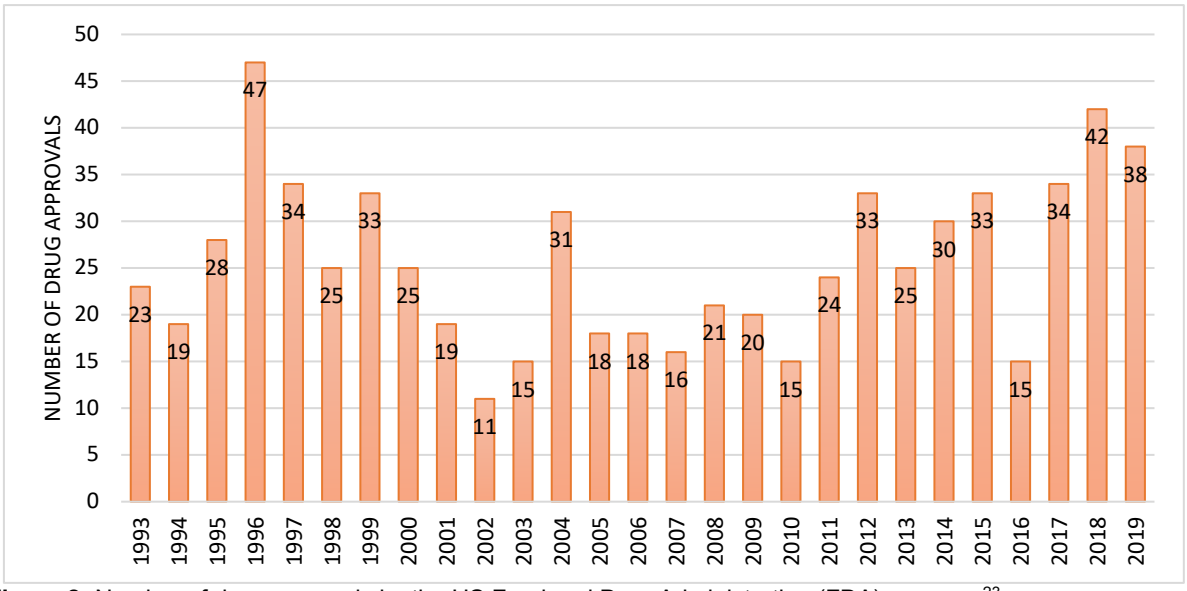


Figure 2: Number of drug approvals by the US Food and Drug Administration (FDA) per year.[23]

An analysis of all new medicine approvals by the FDA (between 1999 and 2008) by Swinney and Anthony at Roche showed that 100 medicines were discovered through target-based approaches (random HTS in a target based assay) and 58 medicines were discovered through

phenotypic screening (Figure 3A).[24] Swinney and Anthony emphasised that more first-in-class drugs were discovered by phenotypic screening than target based screening (28 vs. 17), with the remainder attributable to follower drugs (i.e. drugs with a known structure and mechanism of action). The authors argued that this made sense as target-based screening is easier once a disease target has already been validated. Eder and co-workers at Novartis re-evaluated this data in 2014 looking at the first-in-class drugs discovered between 1999 and 2013 (Figure 3B).[25] This analysis reclassified some of the medicines that Swinney and Anthony had classed as being discovered by phenotypic screening as being discovered by a target agnostic 'chemocentric' approach, i.e. from an identified natural product with bioactivity (aspirin). This placed a greater emphasis on the use of target based methods for the discovery of new drugs. In a more recent analysis of small molecule drug candidates (i.e. not-yet approved drugs) between 2016 and 2017, Brown and Boström showed that, after candidates developed from a prior disclosed compound, random HTS against a target generated the largest number of candidates (29%) (Figure 3C).[26]

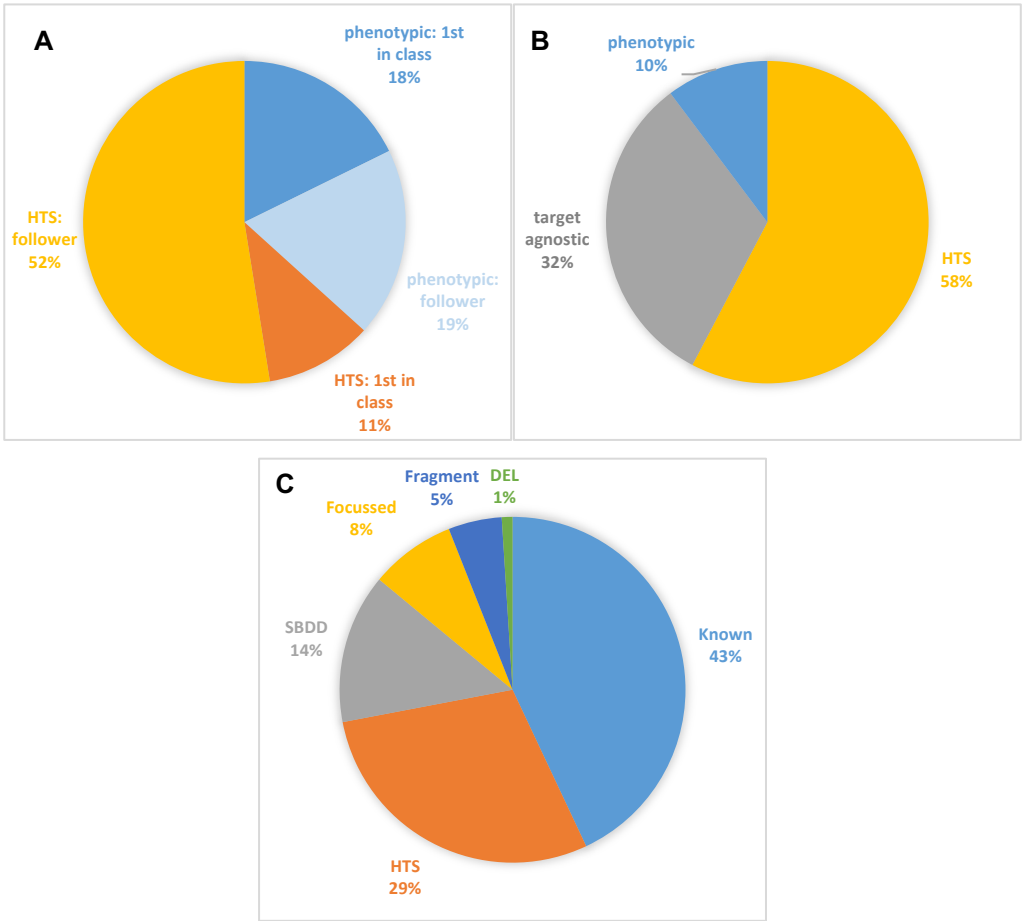


Figure 3: A: How new medicines were discovered between 1999 and 2008 according to ref 24. **B**: How new medicines were discovered between 1999 and 2013 according to ref 25. **C**: How new clinical candidates were discovered between 2016 and 2017.

These analyses clearly show that a significant proportion of new drug candidates have been discovered through a 'random' HTS. However, as demonstrated by Brown and Böstrom, the

diversity of different approaches has increased. This differentiation may have led to the increase in US FDA approvals in recent years. Though, it is telling that the proportion of candidate drugs discovered from known sources implies a lower success rate from other discovery routes for under-developed drug targets.

1.1.4 Attrition in the Drug Discovery Pipeline

As can be seen in Figure 2 the pharmaceutical industry has suffered from low rates of approval of new drugs over the last two decades and this is despite large leaps in technological development and resource investment.[27] The high attrition rate in the drug discovery pipeline remains a significant problem for pharmaceutical companies, particularly as new, difficult target modalities emerge and the existing standard of care must be improved upon in order to be approved by the FDA. The reliance on the "irrational" approach of HTS has been argued to be the underlying problem.[28] Others have defended the large impact that HTS has had (arguably the recent uptick in NME approvals may be due to the delayed success of HTS).[8] These authors argue that compound quality has a large impact on the outcome of a HTS and thus poor compound quality has led to the lower rates of NME approvals. An analysis of the attrition of 812 drug candidates from four major pharmaceutical companies between 2000–2010 showed the significant reduction in clinical candidates progressing through clinical trials (Figure 4A).[29] Reasons for termination of these candidates included clinical safety (11%), efficacy (9%), non-clinical toxicology (40%) and pharmacokinetics (PK) or bioavailability (5%) (Figure 4B). An earlier analysis by Kola and Landis of drug candidates between 1991–2000 showed similar trends and reasons for termination.[30] Failures in phase 3, though less numerous, pose a particular problem due to the extremely high sunk cost (Figure 4A).[31] The risk of termination of a project and the reason for that termination is related to the disease target. This kind of termination could be due to commercial reasons. However, poor choice of the correct disease target protein could lead to unwanted side-effects or poor efficacy *in vivo*. Therefore target selection and validation remains key for the development of a new drug, particularly in novel and more complex disease targets such as the CNS.[32]

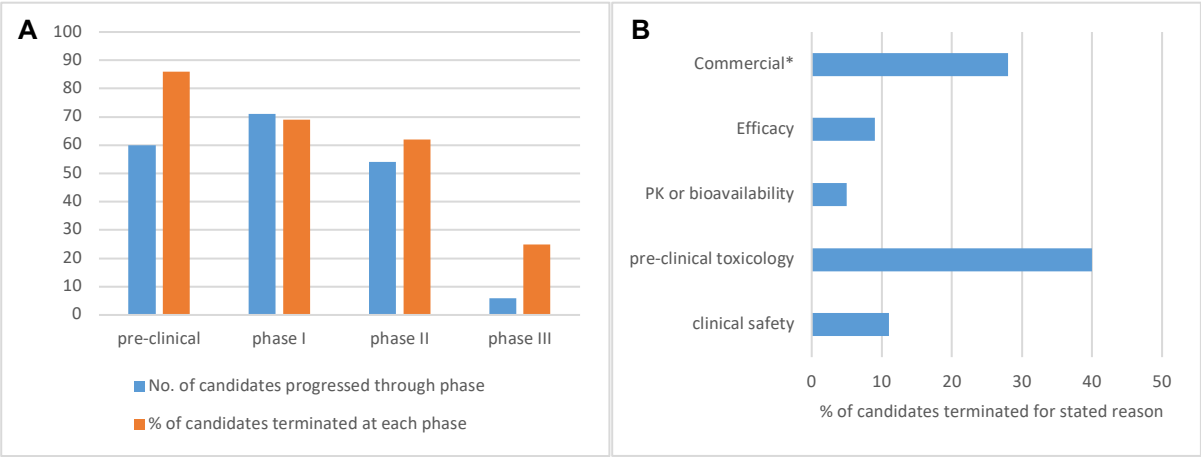


Figure 4: A: Analysis of candidate progression through drug discovery pipeline. **B**: Reasons for attrition between 2000 and 2010. * Commercial includes organisational rationalisation of company portfolio.

1.1.5 Physicochemical Properties of Drug Candidates

Whereas commercial reasons for termination of a drug candidate cannot be accounted for by a medicinal chemist, recent publications have linked the attrition rate attributed to efficacy, PK, toxicology and safety, to the physicochemical properties of drug candidates. Therefore, a medicinal chemist can influence the chances of a drug discovery programme's success through judicious choice of the drug candidate structure with the aim of limiting adverse Absorption, Distribution, Metabolism, Excretion and Toxicity (ADMET) outcomes.[33]

1.1.5.1 Lipophilicity

A significant realisation in the drug discovery community was the relationship between lipophilicity and drug failure related to toxicology issues.[34,35] In chasing potency against drug targets through increasing hydrophobic interactions, more drug candidates were observed to have ADMET issues such as poor solubility, higher promiscuity and the greater likelihood of drug-drug interactions (molecular obesity).[36] Some have attempted to relate simple descriptors such as log*P* and total polar surface area (tPSA) to the probability of a drug being toxic. The Lipinski 'Rule of 5' provided guidelines for the oral bioavailability of a drug.[37] Since this seminal work, workers at Pfizer related the safety of candidate molecules with tPSA and log*P*, where compounds with a log*P* > 3 and tPSA < 75 Å^2 were 2.5 times more likely to be toxic.[38] Also, Gleeson at GSK showed that candidates with a Mw < 400 and clogP < 4 had a greater chance of displaying beneficial ADMET properties.[39] These general rules should be viewed with some scepticism, indeed there have been many successful orally bioavailable drug candidates lying outside 'Lipinski space',[40] including recent large macrocycles and PROTAC degraders.[41] Yet the simplicity of these rules has been important and although newer, more complex analyses have been undertaken, they have yet to have the same impact as Lipinski's Ro5.[42] Indeed, these rules relating lipophilicity or tPSA are complicated by their dependence on intrinsic physicochemical properties of the compound, i.e. it has been observed that the probability of

toxicity outcomes depends also on whether the compound is neutral or basic.[43] A key challenge for medicinal chemists is to find the 'sweet spot' between providing potency while maintaining specificity and safety and understanding general rules regarding physicochemical properties can be important towards achieving this aim.[44]

1.1.5.2 Aromatic Ring Count

Related to this relationship between high lipophilicity and poor ADMET outcomes is the number of aromatic (benzenoid and heteroaromatic) rings in drugs.[45] In 2001, Hann calculated the average number of aromatic rings in orally available drugs as 1.6.[46] Ritchie and Macdonald at GSK showed that the overall number of aromatic rings in drugs decreased as candidates progressed through clinical trials indicating that a higher number of aromatic rings may be correlated with compound attrition.[47] Their analysis showed that increasing aromatic ring count led to increased lipophilicity and decreased solubility. The amount of plasma protein binding is linked with the potency and clearance of a drug.[48] Ritchie and Macdonald showed increasing aromatic ring count was correlated with higher plasma protein binding which would likely result in poorer potency and clearance. Inhibition of the human ether-a-go-go related gene (hERG) is related to detrimental cardiac-related side effects.[49] Inhibition of CYP450 enzymes, involved in the metabolism of drugs, can lead to drug-drug interactions *via* increased concentrations of a drug that would be metabolised by the CYP450 enzyme.[50] In their study, Ritchie and Macdonald showed that increasing aromatic ring count is proportional with higher inhibition of both hERG and CYP450 enzymes. It should be emphasised that aromatic rings do bring beneficial properties to drug compounds in specific and non-specific interactions provided by, for example, directional π–π stacking interactions or potency derived from lipophilicity.[51] Indeed, Ward and Beswick argue that there may be an area of 'safe' chemical space outside Lipinski Rof5 space (i.e. cLog*P* > 5) and a balanced approach to the use of aromatic rings in drugs should be taken.[52]

1.1.5.3 Saturated Heterocycles

Ritchie, Macdonald and co-workers at GSK extended this analysis of aromatic ring count related to drug developability to how these aromatic rings compare to saturated carbocycles and heterocycles.[53] This analysis showed that for many of the properties for which aromatic rings have a negative impact, saturated rings can provide a beneficial or, at least, neutral effect. The authors showed that replacing an aromatic ring with a saturated heterocycle can be beneficial for compound solubility, plasma protein binding and CYP enzyme inhibition.[54] A similar team from GSK showed that saturated heterocycles at least have similar developability compared to heteroaromatics.[55] Piperidines, for example, showed excellent solubility, plasma

protein binding and CYP450 inhibition properties. Saturated analogues of benzene rings can even provide similar stacking interactions with drug binding pockets.[56]

This realisation that saturated heterocycles could be beneficial motifs within drug discovery was made at a similar time to an emphasis on a higher fraction of sp^3-carbons (Fsp^3) in drug molecules. Lovering and co-workers showed that a higher Fsp^3 was related to improved ADMET properties.[57] Leeson and co-workers at AstraZeneca supported this hypothesis and argued that the Ar atom count – sp^3 atom count (Ar–sp^3) value should be negative for a drug candidate.[58] One of Lovering's key arguments is that increasing saturation also increases complexity and thus explores greater areas of chemical space without increasing molecular weight significantly.[57] Schreiber has corroborated this identification of structural complexity with greater protein binding.[59] However, Hann and co-workers have argued that a reduction in molecular complexity can have a positive influence on drug discovery.[46,60]

1.1.5.4 Molecular Topology

Increasing the Fsp^3 clearly impacts a compound's shape or topology as switching from an aromatic ring to a saturated analogue decreases the planarity of the compound.[61] In arguing for an 'escape from flatland' Lovering showed that increasing complexity (increased Fsp^3), and thus having inherently more 3D character, resulted in lower promiscuity and CYP enzyme inhibition.[62] Three-dimensional shape has also been highlighted as being of importance for binding certain proteins particularly for PPIs.[63] Therefore, increasing the number of 3D compounds in a screening collection could have a positive influence on the outcome of a drug discovery programme.[64] However, this correlation has also been associated with increasing the overall diversity of the collection to hit a greater number of targets rather than a fundamental beneficial advantage of 3D shape.[65]

1.1.6 Lack of Diversity within Pharmaceutical Compound Collections

Chemical space is an *n*-dimensional space populated by every conceivable molecule, where the coordinates are defined as the properties (Mw, lipophilicity, shape etc.) of each molecule.[66] Even a large screening collection (on the order of 10^6 compounds or more for a DEL) is orders of magnitude smaller than the vast number of possible drug-like molecules, which has been estimated to be ~10^{63} compounds.[67] While being too small (it is clearly unreasonable to suggest synthesising all possible drug-like molecules), pharmaceutical compound collections have been fundamentally criticised for lacking structural diversity.[68] Lipkus and co-workers' analysis of the CAS structural database in 2008, showed that nearly half of all small molecules were based on only 0.25% of known scaffolds or frameworks.[69] This top-heavy distribution of frameworks has continued in the last decade.[70] Taylor and co-workers analysed rings in drugs and showed that while 99% of drugs have four ring systems or less, drugs (as of 2014) only

contained 351 distinct ring systems of which 204 had only been used once.[71] They also showed that planar aromatic rings were prevalent, as 40% of these rings did not contain an sp^3–carbon. This is key in light of Lovering's argument for higher Fsp^3 and 3-dimensionality in drug candidates.[57,72] Structural and scaffold diversity has also been related to a greater chance of hitting more difficult drug targets and expanding the number of druggable targets.[65b,73]

Yet the question remains, why have pharmaceutical screening collections biased frameworks with flatter, aromatic rich compounds?

1.1.6.1 Lack of Synthetic Reaction Diversity

The answer is synthetic feasibility.[52] Analyses have shown that relatively few reactions dominate the total number of reactions that medicinal chemists carry out.[74] These analyses found that, other than deprotections and functional group interconversions, reactions such as amide bond formation and C–C bond formation, i.e. through Suzuki–Miyaura cross-coupling, are the most common. This is in general agreement with a similar analysis of reactions on process scale.[75] Reliance on these particular reactions has also led to a greater preponderance of certain substituents in drug candidates.[76] This has led to demand for the expansion of the medicinal chemist's toolkit for the synthesis of compounds with greater diversity.[77] Developing a drug requires large time and investment, and it is easy to see why utilising simple, efficient chemical processes to obtain drug candidates has been attractive.[22] However, this reliance on a few reactions has led to the aforementioned lack of diversity within screening collections and a consequent drop in pharmaceutical R&D productivity.[78]

1.2 Synthetic Strategies to Overcome Attrition in Drug Discovery

1.2.1 Importance of Synthetic Chemistry for the Pharmaceutical Industry

All drug discovery programmes require intensive synthetic effort to generate potential drug leads.[79] The importance of novel synthetic chemistry for driving innovation in the pharmaceutical industry should not be understated.[80] With more emphasis on new, difficult or less 'druggable' targets the requirement for the synthesis of more complex compounds enabled by new reaction discovery is likely to be necessary.[81] Despite the success and innovation of chemists within the pharmaceutical industry, new organic chemistry should be able to drive further innovation.[82] A cross-industry team has argued that organic synthesis can provide opportunities in drug discovery, for example by providing saturated heterocyclic rings in more flexible manners or pushing the boundaries of metal-catalysed cross-couplings, C–H activation chemistry or late-stage functionalisation.[83]

The synthesis of novel and diverse building blocks for construction of a drug compound is a strategy that has received attention to enrich screening collections.[84] Over the past two

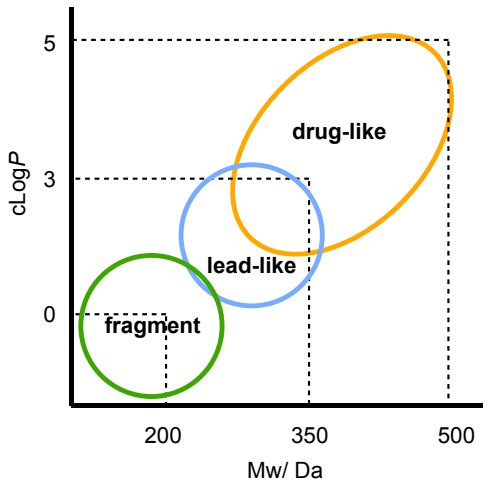
decades there have been a number of new strategies developed to guide synthetic effort towards the synthesis of screening compounds with desirable physicochemical properties.

1.2.2 Lead–Oriented Synthesis

A lead compound is the starting point for a lead-optimisation programme to deliver a drug candidate.[85] Due to the documented increase in molecular weight and lipophilicity through the drug discovery process, an emphasis has been placed on screening 'leads' of lower molecular weight and lipophilicity to increase the chance of success at a later stage of the pipeline.[86] In 2012 Churcher and co-workers proposed lead–oriented synthesis (LOS) as a strategy to provide lead-like molecules to increase the efficiency of the hit-to-lead and lead optimisation processes.[87] This team proposed that lead-like compounds should have low lipophilicity and molecular weight ($-1 < \text{cLog}P < 3$ and $200 < \text{Mw} < 350$ or $14 < \text{heavy atom count} < 26$). Another important aspect of lead-likeness is the exclusion of structural alerts or pan-assay interference compounds (PAINS) which can waste resource in lead-validation and HTS triage.[88] This approach for enrichment of screening collections has had significant uptake and success (the concept of lead–oriented synthesis is discussed further in Section 1.2.4.2).[89]

1.2.3 Fragment–Oriented Synthesis

In a similar vein to LOS, fragment–oriented synthesis aims to reduce the complexity of screening compounds in order to be able to cover a wider area of chemical space (*vide supra* Hann's argument in Section 1.1.5.3).[90] Fragments are smaller and have lower lipophilicity than lead-like compounds and can be grown or connected to build a typical drug-like molecule (Figure 6).[91] However, due to their size and hence lower affinity of hits, they require different screening approaches, i.e. more complex X–ray crystallography methods.[92] Astex, a pharmaceutical company specialising in fragment screening, have defined a 'rule-of-3' for fragments: Mw < 300 Da, no. of HBD < 3 and cLog$P$ < 3 (Figure 5).[93] More recently, workers at Astex revised these guidelines to a 'rule of 2': $140 < \text{Mw} < 230$ Da, $10 < \text{heavy atom count} < 16$, $0 < \text{cLog}P < 2$, no. of rotatable bonds between 0 and 3 and no. of chiral centres < 2.[94] This rule of 2 is only suitable for fragment screening using X-Ray crystallography due to the very low molecular weight of the fragments. As can be seen in Figure 3 FBDD has already started to have an impact on the discovery of new drug candidates.[95]



Lead-likeness	Astex Ro3	Astex Ro2
200 < Mw < 350	Mw < 300	140 < Mw <230
–1 < cLog *P*< 3	cLog*P* < 3	0 < cLog*P* < 2
14 < HAC < 26	no. of HBD < 3	10 < HAC < 16
		0 < no. of rot. bonds < 3
		no. of chiral centres < 2

Figure 5: Fragment, lead-like and drug-like chemical space and guidelines for the physicochemical properties of lead-like and fragment compounds. HAC = heavy atom count.[87,93,94]

Organic chemistry developments can also have a large impact on the synthesis of these low Mw fragments and influence the success of an FBDD programme.[94,96] In order to provide differentiated fragments some have emphasised the importance of the development of 3D compounds.[97] Of particular interest are 3D fragments which can be elaborated along defined vectors in a controlled manner to test biological hypotheses.[96,98] This elaboration would allow the growth or linking of fragments in a controlled direction in order to improve potency against a biological target. FBDD has become a standard approach within the pharmaceutical industry due to its success, in particular, with examples of inhibitors of less 'druggable' targets.[99]

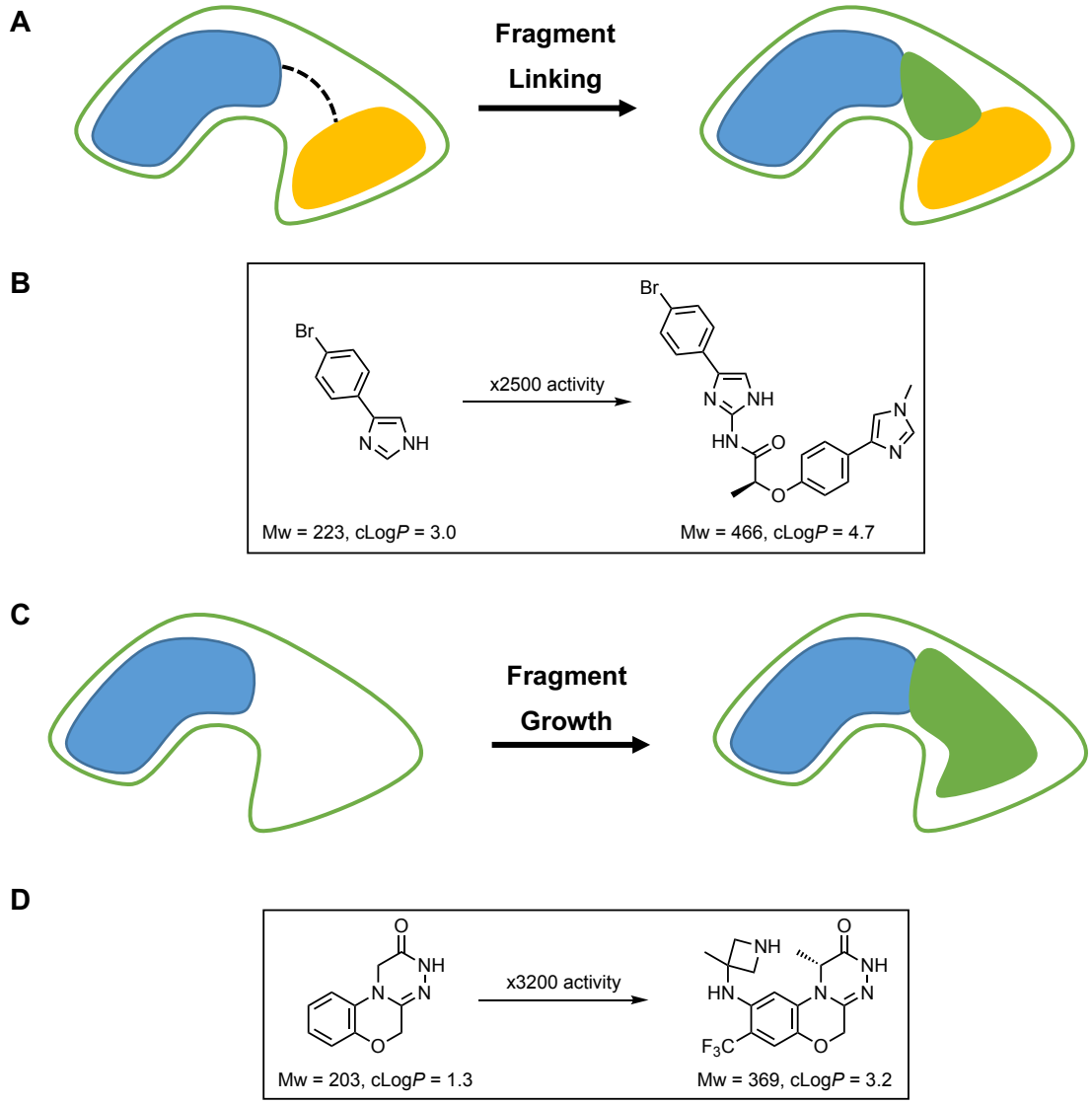


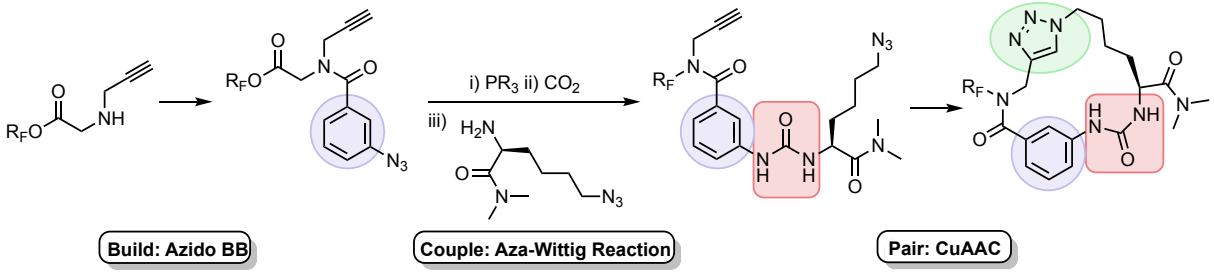
Figure 6: **A**: Schematic of fragment linking within a protein pocket.[100] **B**: Example of fragment linking from Blundell, Ascher, Abell and co-workers to produce a drug with high activity against *mycobacterium tuberculosis* Inosine-5'-monophosphate dehydrogenase to treat malaria.[101] **C**: Schematic of fragment growth within a protein pocket. **D**: Example of fragment growth by AbbVie to produce a drug lead with high activity against a protein kinase Cθ to treat a variety of diseases including arthritis.[102]

1.2.4 Diversity–Oriented Synthesis

Schreiber first proposed diversity–oriented synthesis (DOS) as an approach to promoting the increase in diversity of products synthesised to target biologically relevant pathways.[103] In contrast to target–oriented synthesis, where inspiration may come from a natural product to synthesise a target molecule to test a hypothesis. DOS aims to deliver maximum diversity through a minimal number of substrates, reaction conditions and chemical steps.[104] This diversity can be defined as appendage diversity, functional group diversity, stereochemical diversity or scaffold diversity. Clearly, for increasing the degree of diversity, scaffold/skeletal diversity will have the largest impact.[105] In being able to access high diversity in a short process

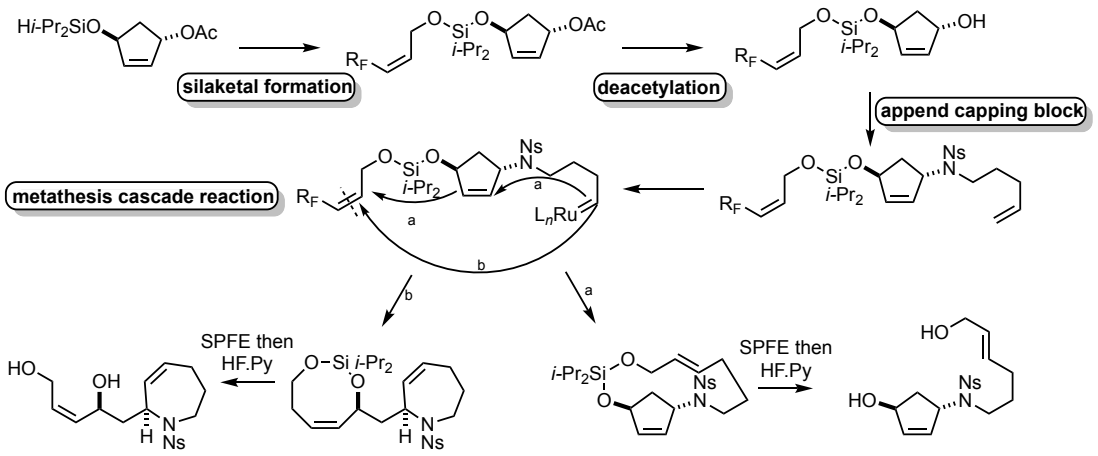
DOS can provide lead compounds for drug targets for which the biology or structure is not well understood.[106]

There are many approaches to the application of DOS.[107] A reagent-based approach uses similar starting materials combining these in a build/couple/pair approach by varying conditions to obtain a diverse range of products. An excellent example of this approach was demonstrated by Spring and co-workers where azide containing building blocks were coupled using the aza-Wittig reaction followed by a copper catalysed azide alkyne cycloaddition to build medicinally relevant macrocycles (Scheme 1).[108] Variation of the electrophilic coupling partner in the aza-Wittig step or variation of the cycloaddition chemistry in the pairing step allowed significant structural diversity.



Scheme 1: An example of a Build/Couple/Pair DOS by Spring and coworkers. R_F is a flourous tag.

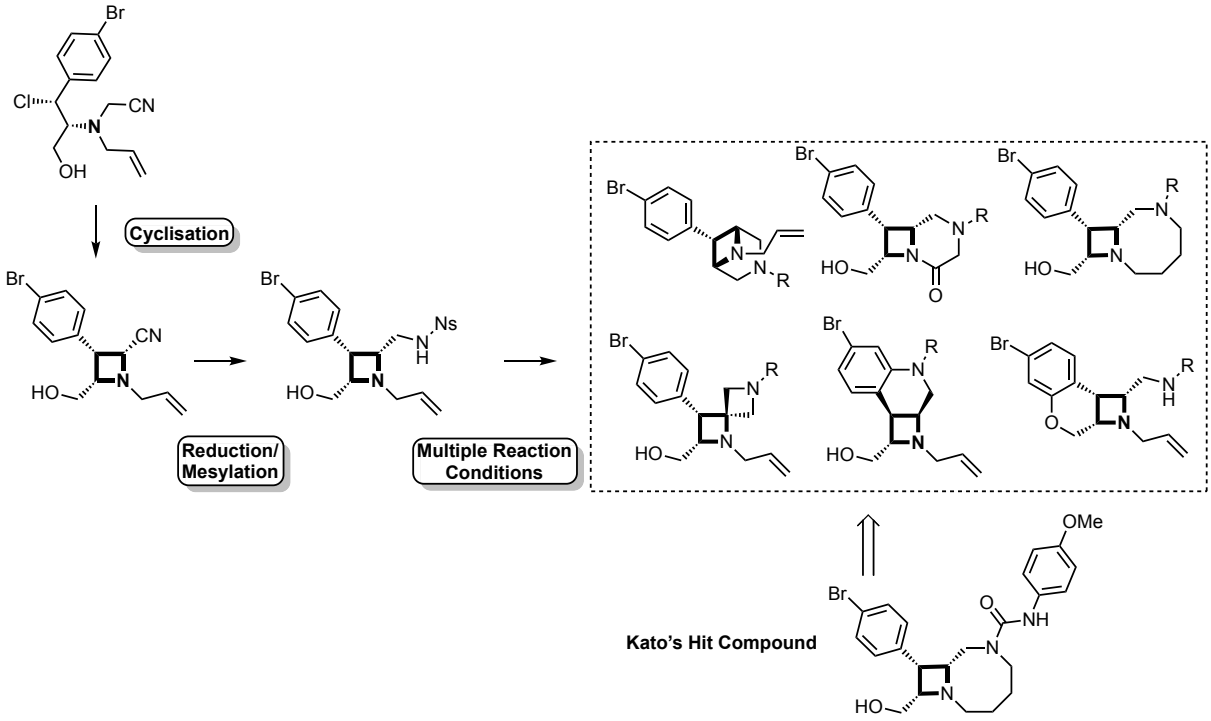
Another important example of a build/couple/pair strategy was developed by Nelson and co-workers where careful manipulation of reaction conditions allowed the generation of many scaffolds without significantly altering the substrates. (Scheme 2).[109] The key to this approach was the scope of ring-closing metathesis.[110] Where there is a difference between Spring's (Scheme 1) and Nelson's (Scheme 2) approaches lies in the variation of reaction conditions, where Nelson kept the same reagents and harnessed innate divergent substrate reactivity.



Scheme 2: Nelson's strategy to generate 80 distinct scaffolds through a Build/Couple/Pair Strategy. R_F is a fluorous tag. SPFE is solid phase flourous extraction.

Spring and Galloway have emphasised the importance of guiding DOS approaches towards biologically relevant chemical space.[111] Waldmann has articulated the term biology-oriented synthesis (BIOS) for DOS approaches biased towards natural product scaffolds, which Nelson's strategy conforms to.[112] There have been bodies of work which try to anchor the DOS approach in biologically relevant chemical space by biasing their synthesis around a 'privileged' structure (pDOS).[113] This is often, as Nelson's work, anchored in existing natural product or natural-product-like chemical space.[114] Others have utilised 'privileged' reaction modes in order to generate diversity in products.[115]

DOS has been a successful approach for generating biologically relevant compounds. Spring's example (Scheme 1) is one of many DOS approaches to biologically relevant macrocycles.[116,117] Nelson's DOS example (Scheme 2) is an excellent example of the synthesis of biologically relevant sp^3-rich saturated heterocycles.[118] Small ring heterocycles, in particular azetidines, have received much attention to target CNS diseases or malaria.[119] In order to design compounds for CNS applications the physicochemical properties must be specifically tuned to facilitate blood-brain barrier penetration.[120] Marcaurelle and co-workers at the Broad Institute of MIT and Harvard adapted ring-closing methodology developed by Couty[121] to generate a diverse library of azetidine scaffolds as a CNS-focussed library (Scheme 3).[119a] This library of compounds was included in a screen against malaria carried out by Kato and co-workers providing an azetidine-based hit compound.[119b,122]

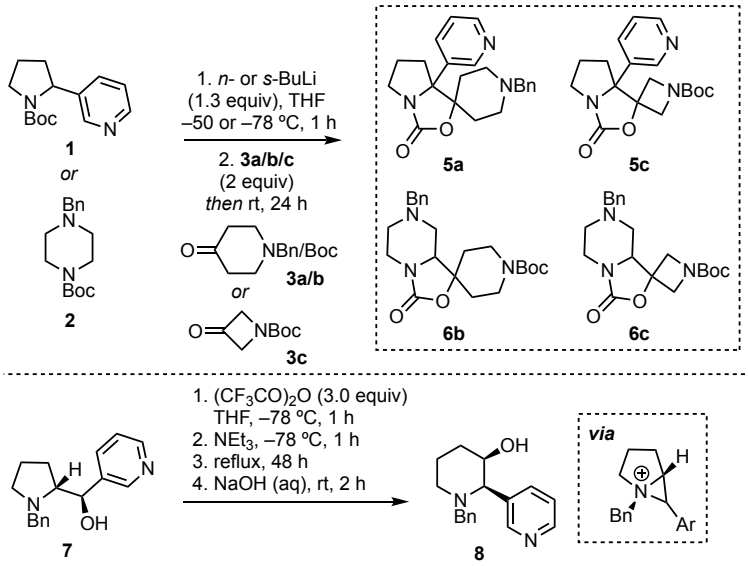


Scheme 3: B/C/P approach to a diverse azetidine-based compound library and derivation of an anti-malarial hit compound.

Marcaurelle's CNS focussed library (Scheme 3) was also described as lead-like. The principles of DOS in combination with the concepts of lead–oriented synthesis and fragment–oriented synthesis leads to diverse libraries of compounds with large potential for screening.

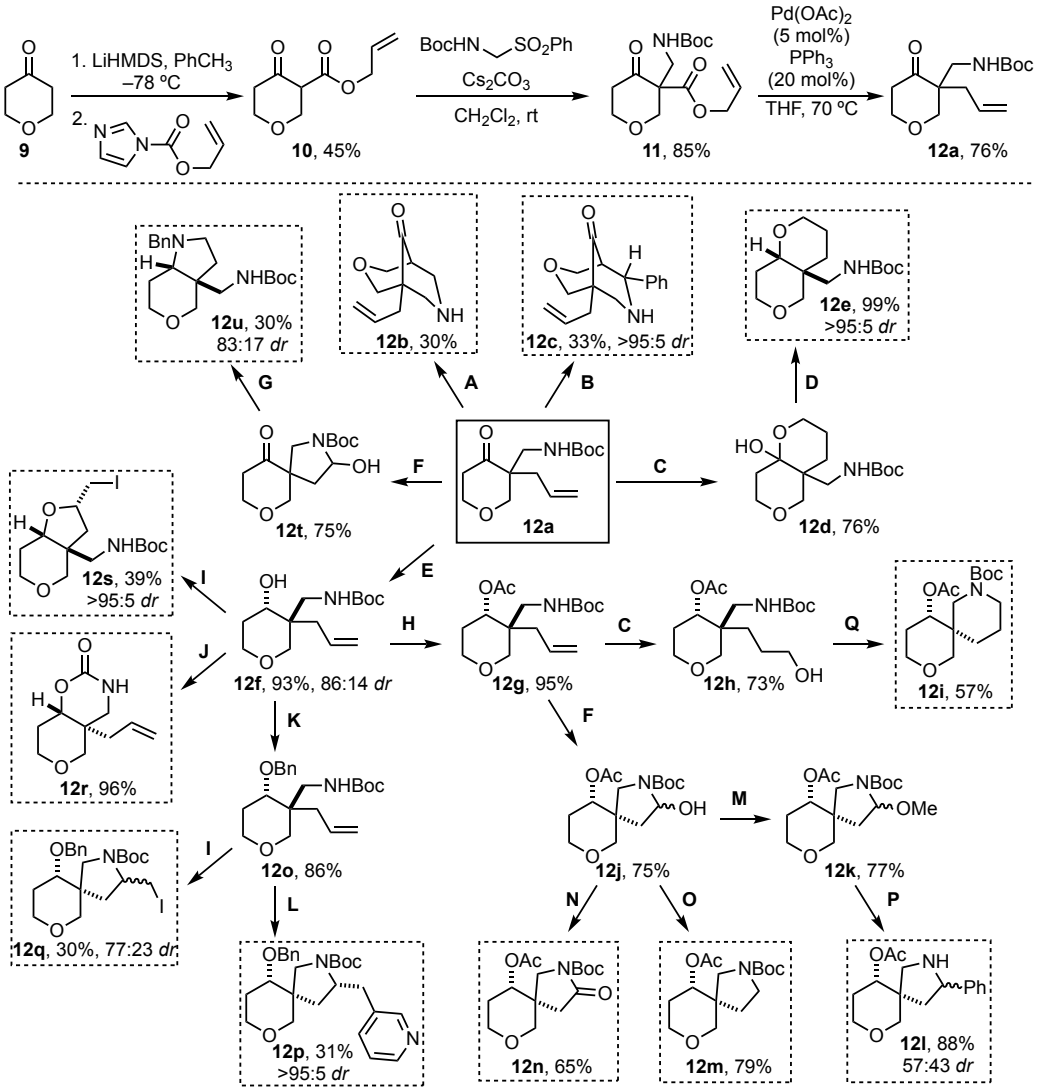
1.2.4.1 Diversity–Oriented Synthesis and Lead–Oriented Synthesis

Promoting diversity through DOS has been focussed using LOS on many occasions, with Rishton advocating this approach in 2008.[123] In particular, Nelson and Marsden have developed a number of LOS approaches towards diverse compound libraries.[124] In 2015 O'Brien and co-workers described a LOS approach to 3-D scaffolds containing piperazine, pyrrolidine and piperidine cores utilising α-lithiation chemistry.[125] Starting from *N*-Boc pyrrolidine **1** or piperazine **2**, fused scaffolds **5** and **6** could be synthesised by α-lithiation and trapping with the appropriate ketone **3a**, **b**, or **c**, followed by intramolecular cyclisation onto the carbamate group (Scheme 4). In the same report, O'Brien utilised a ring expansion[126] of pyrrolidine **7** via an intermediate aziridinium ion to deliver **8** (the use of ring expansion reactions as a complexity generating step will be revisited in Chapter 3).



Scheme 4: O'Brien's LOS by organolithium chemistry to 3-D scaffolds.[125]

Nelson has developed a modular synthesis of 30 lead-like scaffolds through use of a set of protection/deprotection, oxidation, reduction and cyclisation conditions (Scheme 5).[127] Nelson's approach makes use of a short and reliable synthetic route to multi-functional scaffolds such as THP **12a** with enolisable ketone, protected amine and alkene functional groups available. From this scaffold, bridged, fused and spirocyclic saturated heterocyclic scaffolds (**12b**–**u**) were generated from known reactions. Nelson then assessed these scaffolds using a CNS lead multiparameter optimisation (MPO) score after virtual elaboration.[128]

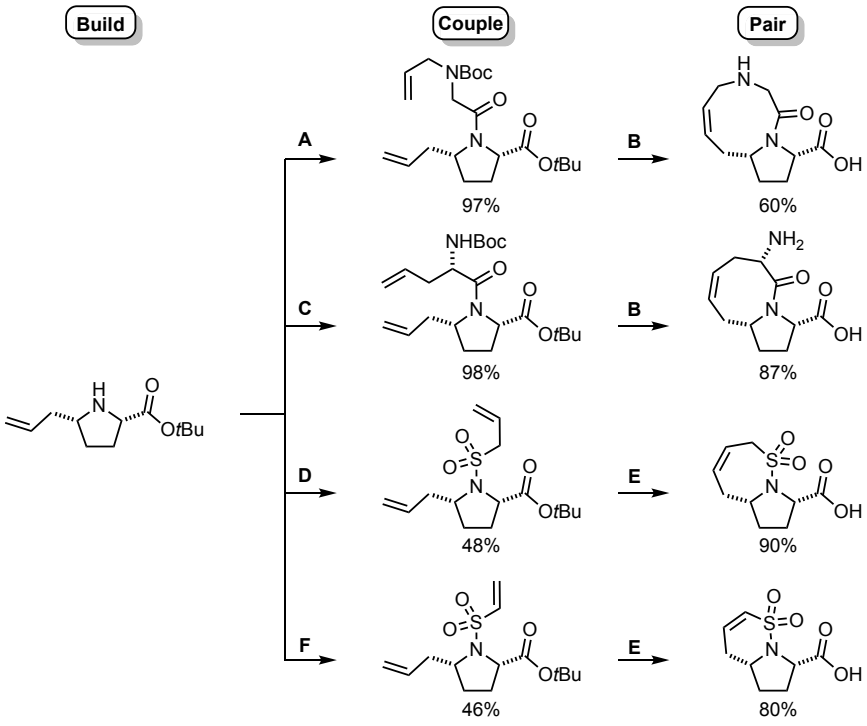


Scheme 5: Nelson's lead–oriented synthesis to scaffolds relevant for hit discovery in CNS chemical space. **A**: paraformaldehyde, TFA, MeOH, 65 ºC; **B**: PhCHO, TFA, MeOH, 65 ºC; **C**: disiamylborane, THF, 0 ºC then $NaBO_3$•$4H_2O$, THF:H_2O; **D**: Et_3SiH, TFA, CH_2Cl_2 then Boc_2O, Et_3N, CH_2Cl_2; **E**: *i*Bu_2AlH, CH_2Cl_2, –78 ºC; **F**: O_3, CH_2Cl_2, –78 ºC then Me_2S, CH_2Cl_2; **G**: $BnNH_2$, $NaBH(OAc)_3$,CH_2Cl_2; **H**: Ac_2O, pyridine; **I**: I_2, $NaHCO_3$, MeCN; **J**: *t*BuOK, THF, 0 ºC; **K**: NaH, BnBr, cat. Bu_4NI, THF, 0 ºC; **L**: 3-bromopyridine, 5 mol% $Pd(OAc)_2$, 10 mol% DPE-Phos, Cs_2CO_3, 1,4-dioxane, 105 ºC; **M**: cat. TsOH, MeOH; **N**: PDC, celite, CH_2Cl_2; **O**: $NaBH(OAc)_3$, AcOH; **P**: PhMgBr, CuBr•Me_2S, Et_2O•BF_3,Et_2O, 0 ºC; **Q**: MsCl, Et_3N, CH_2Cl_2 then TFA, CH_2Cl_2 then Et_3N, CH_2Cl_2 then Boc_2O, Et_3N, CH_2Cl_2. (No temperature indicates rt).

Nelson has recently established activity-directed synthesis which employs DOS principles to establish lead compounds in a structure-agnostic approach.[129] Through an array approach, reagents which can react in a promiscuous manner are subjected to reaction conditions and the crude reaction mixture screened directly in a biological assay. Once activity is established, the reaction can be repeated and products isolated to validate the product structure. This has been successful using carbenoid and Pd-mediated chemistry for identification of PPI inhibitors and anti-bacterials.[130]

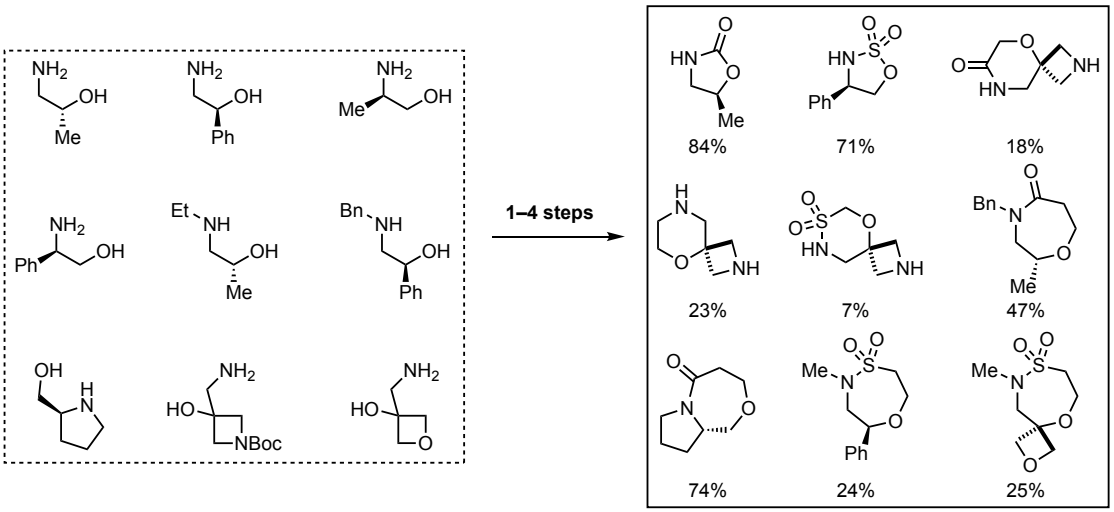
1.2.4.2 Diversity–Oriented Synthesis and Fragment–Oriented Synthesis

Related to the combination of LOS with DOS concepts, the utilisation of DOS principles for fragment–oriented synthesis has been demonstrated within the last decade.[131] The first report of the merging of these two concepts was by Young and co-workers at the Broad Institute of Harvard University.[132] Using a B/C/P approach, employing differentially *N*-substituted substituted pyrrolidines containing an allyl/ester group, and intramolecular cyclisations including ring closing metathesis or oxo-Michael reactions, bicyclic and spirocyclic fragments featuring stereochemical, functional group and scaffold diversity were synthesised. Scheme 6 shows a part of this strategy where a proline building block was synthesised in 5 steps (Build) followed by *N*-derivatisation (Couple) and olefin metathesis (Pair) to generate 5,6-, 5,7-, 5,8- and 5,9-fused fragments. In total, 35 fragment scaffolds were formed including all possible diastereomers by variation of the starting materials.



Scheme 6: A DOS strategy applied to fragment synthesis by Young and co-workers. **A**: *N*-Boc-*N*-allyl glycine, EDCI, Oxyma, NEt_3, CH_2Cl_2; **B**: Grubbs I, CH_2Cl_2, reflux then TFA; **C**: *(S)-N*-Boc-allyl glycine, EDCI, Oxyma, NEt_3, CH_2Cl_2; **D**: prop-2-ene-2-sulfonyl chloride, NEt_3, CH_2Cl_2, reflux; **E**: Grubbs II, CH_2Cl_2, reflux; **F**: 2-chlorosulfonyl chloride, NEt_3, CH_2Cl_2.

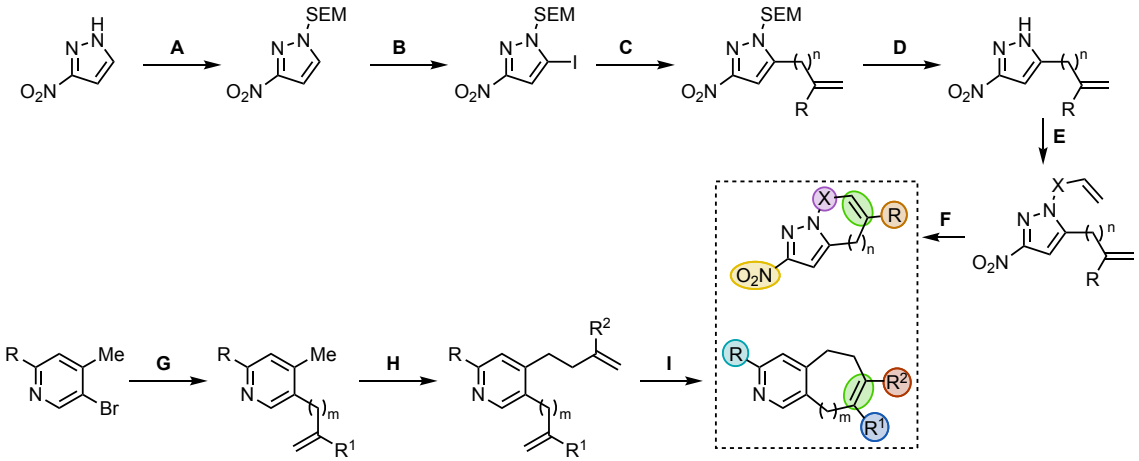
Schreiber, Phillips and co-workers at the Broad Institute and Bayer Pharma used a ‘pool’ of 9 chiral amino alcohol building blocks in short synthetic sequences to generate 45 chiral fragments of low molecular weight and high aqueous solubility (Scheme 7).[133] Notably the fragments were all saturated heterocycles including morpholines, lactams, sultams and sulfamidates.



Scheme 7: Use of 9 chiral amino alcohol building blocks to generate 45 chiral fragments in a DOS approach.[133]

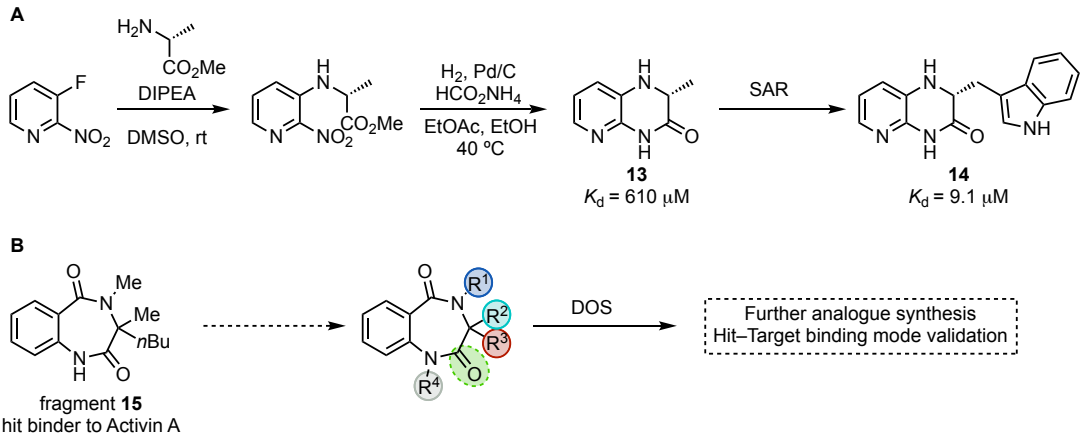
Nelson, Marsden and Spring have also developed fragment–oriented DOS approaches towards saturated heterocycles, emphasising their 3D shape and similarity to natural products.[134] Spirocycles are viewed as being particularly attractive screening compounds as their high 3-dimensionality and novelty results in opportunities in intellectual property (spirocycles will be discussed in greater detail in Chapter 4).[135] Related to Schreiber and Phillips' generation of spirocyclic fragments, Spring has utilised cycloaddition strategies to spirocyclic fragments.[136]

As discussed in Section 1.1.5.2 the number of aromatic rings in drugs is important. Although too many aromatic rings can lead to poor physicochemical properties, their inclusion is also important. Spring has developed a number of DOS strategies to fragments combining saturation and aromatic character.[137] In 2016, Spring described a DOS strategy focussed on pyrazole and pyridine scaffolds which could be elaborated in a diverse manner (Scheme 8).[138] The average physicochemical properties of the fragments compared favourably with commercial compound libraries.



Scheme 8: DOS of a partially saturated bicyclic fragment collection by Spring and co-workers with exploited points of diversification highlighted.[138] **A**: NaH, SEM-Cl, THF; **B**: LDA, I_2, THF; **C**: R'-BF_3K, Pd(dppf)Cl_2·CH_2Cl_2, K_2CO_3, THF:H_2O, 70 ºC or LDA, CuBr, allyl bromide, THF, –78 ºC to rt; **D**: TFA, CH_2Cl_2, rt; **E**: NaH, alkyl bromide, THF or DMF, 70 ºC; **F**: Grubbs II, CH_2Cl_2, 40 ºC or Hoveyda–Grubbs II, toluene, 110 ºC or CH_2Cl_2, rt; **G**: as **C** or allyltributyltin, $Pd(PPh_3)_4$, KF, toluene, 110 ºC or *i*-PrMgCl·LiCl, allyl bromide, THF, –15 ºC to rt; **H**: LDA, alkyl bromide, THF, –78 ºC, to rt; **I**: Grubbs II, CH_2Cl_2, 40 ºC.

Hung, Young and co-workers showed that a DOS strategy was suitable to targeting a specific target, in this case GSK3β.[139] A fragment screen using a library built as in Scheme 9[132] and through a two-step S_NAr/reduction protocol (Scheme 9A) gave a hit with moderate activity. Building from fragment **13** in a fragment-growing approach through a structure-activity relationship showed that **14** was a μM inhibitor of GSK3β (Scheme 9). Spring and a multi-institute team have recently demonstrated the potential of this type of fragment-focused DOS library in screening against three proteins.[140] The DOS library consisting of partially saturated fragments generated leads,[137,138] including **15**, which were further developed in a DOS approach for further screening (Scheme 9). This work showed how DOS can be used to generate hits but also can be used to elaborate leads in an efficient manner using defined exit vectors.



Scheme 9: **A**: Hung, Young and co-workers development of an inhibitor against GSK3β from a fragment derived from a DOS library. **B**: Spring's demonstration of the utility of fragment-focussed DOS libraries for hit-finding and analogue synthesis.

1.2.4.3 Assessment of the Diversity of Compound Libraries

The definition of diversity has been a controversial topic within the literature.[141] As discussed at the start of Section 1.2.4, DOS Compound libraries are often biased towards biologically relevant chemical space. However, how is this chemical space parameterised? There are a number of computational descriptors which are used to exemplify the diversity of compound libraries.[142] Chemical similarity is a complementary descriptor to diversity.[143] However, a compound that is similar (> 0.85 Tanimoto similarity)[144] to an active compound has only a 30% chance of being similarly active.[145] Though this may not be surprising considering that changing a compound's structure in a small way can have a significant effect on biological activity, the choice of molecular/similarity descriptor will dramatically bias the conclusion.[146]

Apart from molecular similarity, molecular shape is a particularly important descriptor due to the recent emphasis on increasing the complexity or Fsp^3 of screening compounds.[57,147] A principal moments of inertia (PMI) plot is a common computational technique employed to visualise the shape of a molecule (Figure 7).[148] The vertices of a PMI plot represent the extremes in terms of shape: rod-like, disc-like and spherical. Therefore, there has been a drive for compounds which populate chemical space away from the flat 'rod-disc' axis.[97] The 3D character of compounds can also be measured by the deviation of a compound's shape from an ideal plane of best fit.[149] A size-independent indication of molecular shape or 'globularity' is given by $C_{sp}{}^3/[C_{sp}{}^2 + C_{sp}{}^3]$.[59]

The size of a chemical library can also influence the conclusion on the diversity of that set.[150] It is important not to infer significance in conclusions drawn from a small data set.[151] Nelson and Marsden have developed a useful computational tool (lead-likeness and molecular analysis or LLAMA) to assess the lead-likeness of a screening library.[152] This tool allows virtual elaboration of building blocks or products to assess lead-likeness using a PMI plot for example.[153] This type of assessment was shown in recent work by Bull in collaboration with Eli Lilly. Bifunctional cyclopropanes were synthesised in a cobalt catalysed cyclopropanation of ethyl diazoacetate and vinyl sulfides.[154] Oxidation of the sulfide products, consequent sulfoxide–magnesium exchange and trapping with an electrophile or engagement in a Pd-catalysed Negishi cross-coupling allowed the synthesis of a wide variety of fragment and lead-like cyclopropanes. The Mw, ALog*P* relationship of these cyclopropanes was readily available through LLAMA, as well as a PMI plot showing the shape of the resultant compounds.

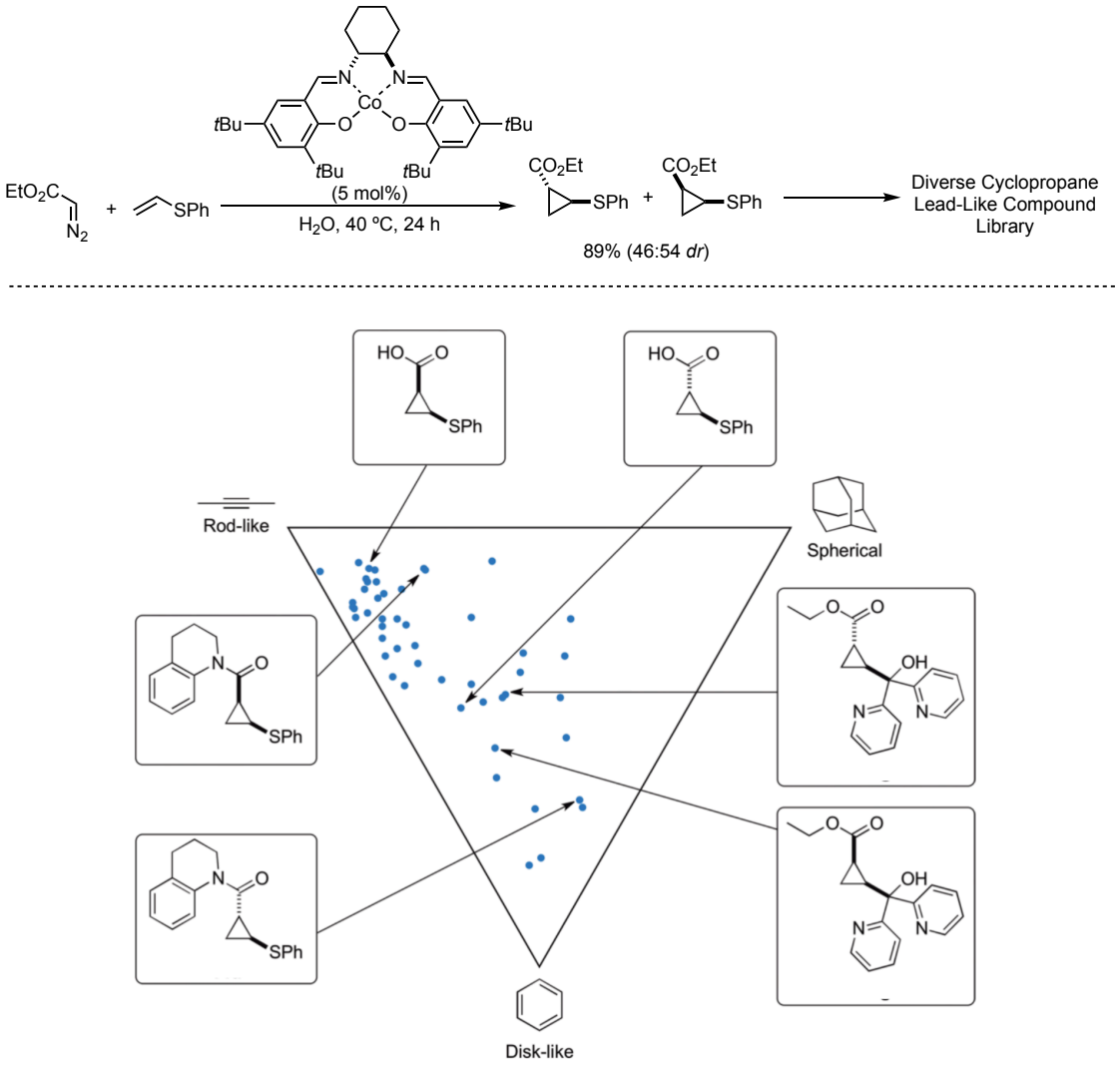


Figure 7: Co-Catalysed cyclopropanation to afford both *cis*- and *trans*-diastereomers of bifunctional cyclopropanes. PMI plot reproduced from reference 154 showing the diverse shape of some of the compounds formed in Bull's study.

1.2.5 Small Rings in Pharmaceuticals and Organic Synthesis

As discussed in Section 1.1.5.3, inclusion of a saturated heterocycle, in place of an aromatic ring, can be beneficial for the physicochemical properties, and hence developability, of a drug candidate. A subclass of saturated heterocycles that has received significant recent attention within medicinal chemistry are 4-membered rings, in particular oxetanes and azetidines. In 2006, Carreira showed that an oxetane ring was a suitable replacement group for methylene or *gem*-dimethyl motifs which could be at risk of metabolic attack.[155] Oxetanes have become an important motif within medicinal chemistry due to the beneficial properties, such as solubility, basicity, lipophilicity and metabolic stability, that they can impart (Figure 8).[156] Oxetanes can also be considered as bioisosteres[157] of carbonyl groups due to the similar size (1.2 Å for C=O vs. 2.1 Å for oxetane quaternary C–O distance) and lone pair arrangement.[158]



Figure 8: Strategic incorporation of an oxetane to reduce lipophilicity and clearance, while increasing solubility, developed by Merck.[159]

Azetidines can be used in a similar manner to oxetanes, often as a pendant group to modulate physicochemical properties or as a replacement group to provide hydrogen bond donor or acceptor abilities or modulate physicochemical properties. The exploration of azetidines in medicinal chemistry has been much more limited than their 2-azetidinone (β-lactam) analogues which feature widely in penicillin and cephalosporin antibiotics (Figure 9).[160] The reason for this lower uptake of azetidines may be due to the low number of synthetic methods to access them.[161] The properties and synthesis of aza-spirocycles as isosteres will be discussed in more detail in Section 4.1.

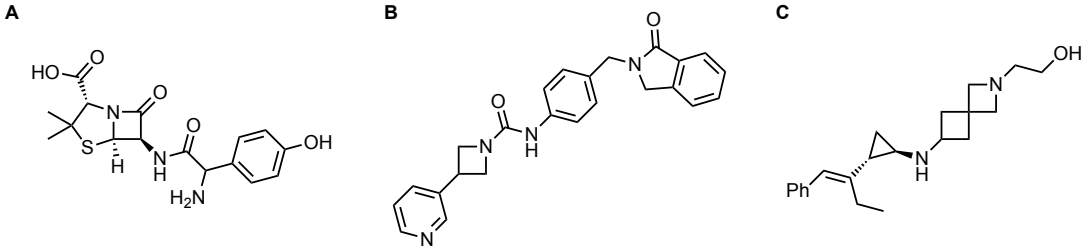
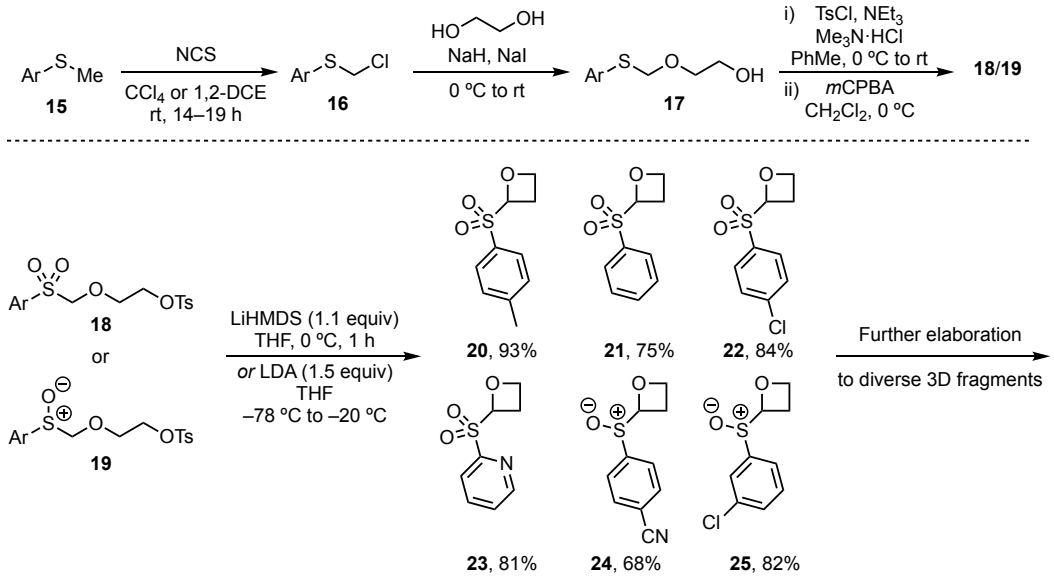


Figure 9: A: Beta-lactam containing antibiotic, amoxicillin. **B** and **C**: Recent examples of azetidine containing lead compounds developed by Novartis and Constellation Pharmaceuticals.[162]

1.2.5.1 Fragment–Oriented Synthesis of Small Rings in the Bull Group

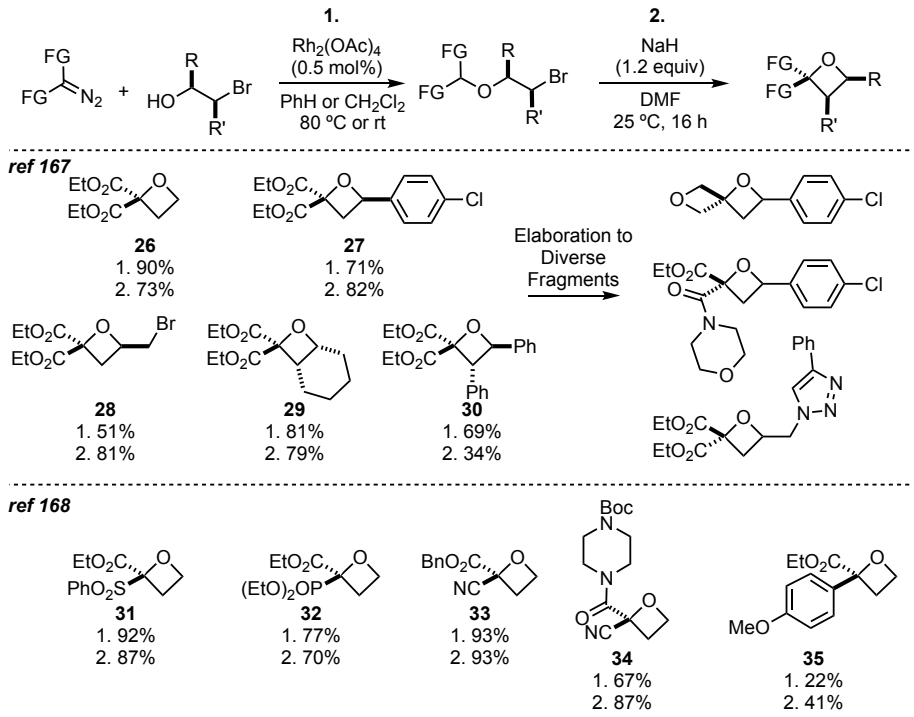
Towards new methods to access oxetane fragments, Bull and co-workers developed a route, underpinned by a C–C bond formation, to form 2-(aryl-sulfonyl)oxetanes as 3D fragments.[163] As an alternative to C–O bond formation, as in a Williamson etherification,[164] deprotonation of sulfonyl intermediate **18** led to cyclisation by C–C bond formation (Scheme 10). Sulfonyl oxetanes (i.e. **20**–**22**) were elaborated by α-lithiation, as well as directed *ortho*-metalation or transition-metal mediated cross couplings on the pendant aromatic. The sulfonyl oxetanes were found to be stable in acidic and basic media at 70 ºC (half-lifes for all tested >24 h), as well as showing good solubility and 3D shape.[165] Using sulfoxide intermediate **19** in a similar reaction process, the corresponding sulfinyl oxetanes (i.e. **23**–**25**) could be generated.[166]



Scheme 10: 2-(Aryl-sulfonyl/sulfinyl)oxetanes as 3D fragments developed by Bull and co-workers.[163,165,166]

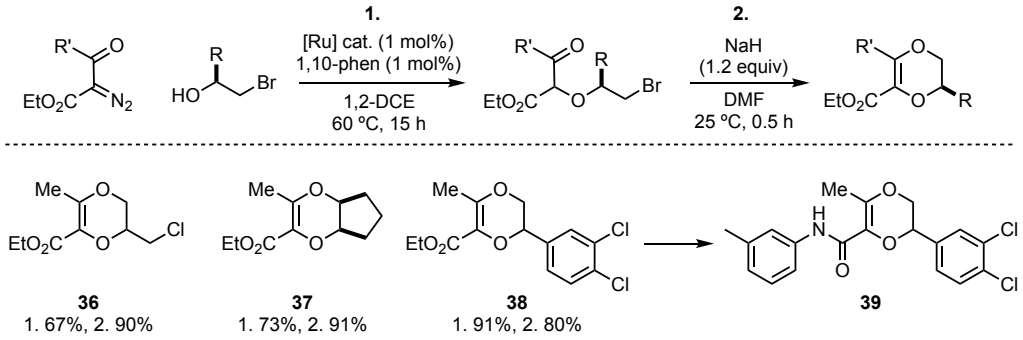
Bull and Davis developed an approach to 2,2-disubstituted oxetanes through a similar key C–C bond formation (Scheme 11).[167] Instead of using unstable α-chloro sulfide **16** (Scheme 10), diethyl diazomalonate was employed in a $Rh_2(OAc)_4$ catalysed O–H insertion reaction to form an intermediate which could be deprotonated to promote cyclisation. By doing so, this reduced the number of steps relative to Bull's prior work and allowed the synthesis of uncommon 2,2-disubstituted oxetanes. The highest yield for the O–H insertion reaction was observed when 2-bromoethanol was used. Subjection of the intermediate to strongly basic conditions (NaH in DMF) also gave the highest yield of oxetane **26**. High yields were obtained for O–H insertion of 2-substituted bromohydrins to form 2,2,4-trisubstituted oxetanes (i.e. **28**–**30**). This included retention of stereochemistry when an enantioenriched bromohydrin was employed. Highly substituted and fused oxetanes were formed in a 3-step bromohydrin formation, O–H insertion and cyclisation sequence. Additionally, manipulation of the ester groups as functional handles was demonstrated to synthesise diverse oxetane fragments.

Bull and co-workers further developed this 2-step O–H insertion and cyclisation strategy by diversifying the diazo reagent used.[168] This work expanded significantly the scope of 2,2-disubstituted oxetanes which could be accessed through this strategy. Scheme 11 shows the scope of functional groups additional to carboxylates, including amide, sulfonyl, cyano, phosphonate and aryl groups (oxetanes **31**–**35**). These functional groups present opportunities for divergent functionalisation of these 3D fragments, as well as, directly forming useful fragment compounds for screening in their own right.



Scheme 11: Bull's synthesis of diverse oxetane fragments through O–H insertion of a diazo compound and consequent base mediated C–C bond formation.

This strategy was shown to be adaptable to the synthesis of 6-membered oxygen-containing rings in further work by Bull and co-workers. Employing ketone containing diazo reagents in an O–H insertion reaction, catalysed by a Ru catalyst system, followed by cyclisation led to *O*-alkylation rather than *C*-alkylation (Scheme 12).[169] This 2-step process led to diverse 1,4-dioxenes (i.e. **36**–**38**) in high yields which could be further functionalised to afford lead-like compounds such as **39**.

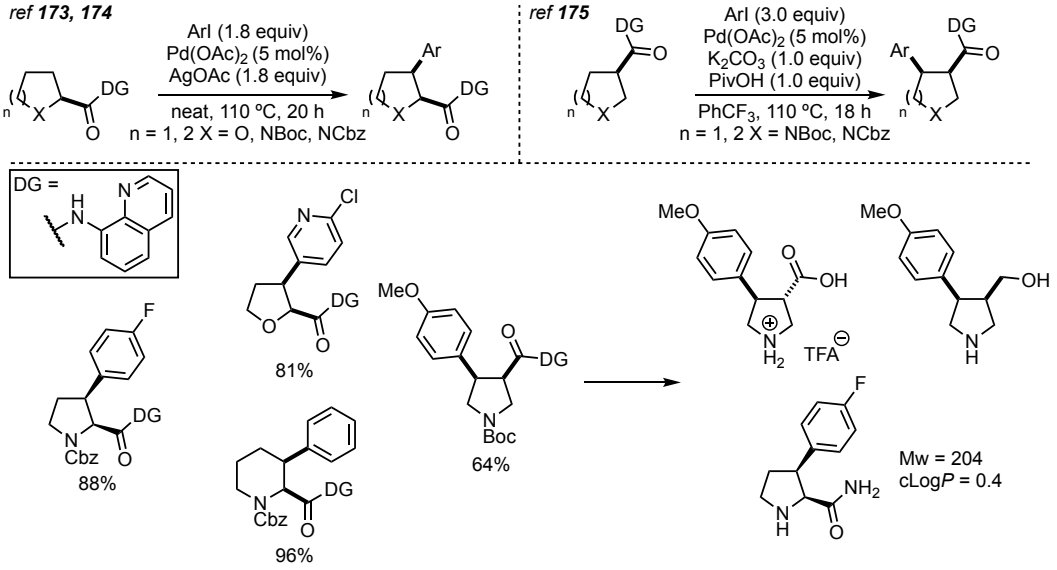


Scheme 12: Synthesis of diverse 1,4-dioxenes by Bull and co-workers. [Ru] cat. = $[CpRu(MeCN)_3]PF_6$.

1.2.5.2 Fragment–Oriented Synthesis of Pyrrolidines and Piperidines in the Bull Group

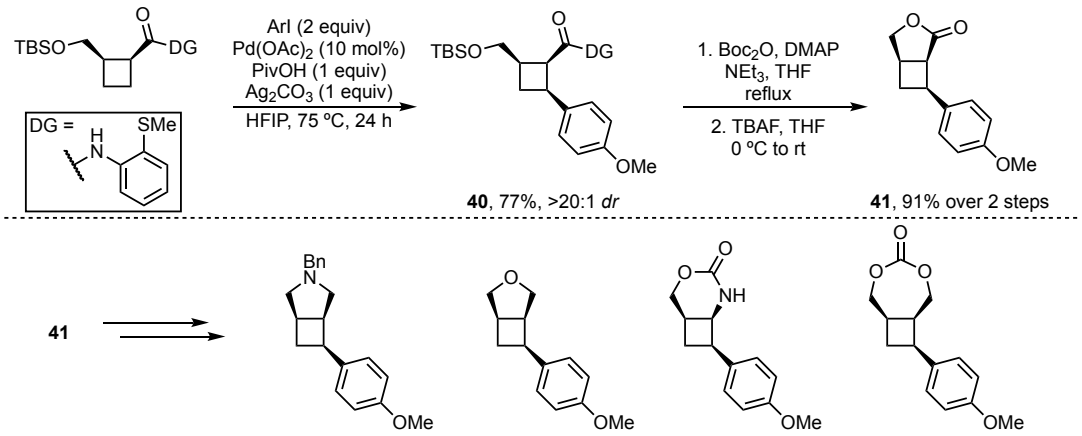
In light of the beneficial characteristics of saturated heterocycles *in combination with* aromatic rings (Sections 1.1.5.2 and 1.1.5.3), one potential avenue to form interesting lead-like compounds is arylation of saturated heterocycles. This is an approach which has been explored by the Bull group.

An attractive approach to arylation of saturated heterocycles is *via* C–H activation.[170] Initially developed by Daugulis,[171] Baran employed directed C–H activation of cyclobutanes in natural product synthesis.[172] Bull and co-workers developed a C(3)–H arylation of proline derivatives using Pd-catalysis (Scheme 13).[173] This was extended to other ring sizes and heterocycles to include piperidine, THF and THP rings.[174] In a further study, Bull and co-workers used a directing group at the C(3) position of pyrrolidines and piperidines to regio- and stereo-selectively arylate at the C(4) position, notably in the absence of silver salts.[175] Though the 8-aminoquinoline directing group was difficult to cleave in the initial reports, a significant advance in the synthesis of 3,4-disubstituted pyrrolidines and piperidines was the demonstration of numerous ways to do this, allowing access to a variety of fragments and building blocks.



Scheme 13: Fragment and building block synthesis through a C–H activation of saturated heterocycles. Conditions shown for C(3)–H activation are for NCbz pyrrolidine, for specific conditions for different ring sizes and heteroatoms see ref 174.

This directed C–H activation approach has been applied to a wide range of saturated ring types.[176] This includes C(3)-arylation of azetidines by Schreiber for the synthesis of an antimalarial agent.[177] Baran and co-workers utilised this C–H activation chemistry in combination with directing group removal and decarboxylative cross-coupling to build a variety of biologically relevant compounds.[178] Most recently, Spring utilised the directed C–H arylation of cyclobutanes[172,179] in combination with divergent functionalisation post-reaction to generate a library of sp^3-rich bicyclic fragments (Scheme 14).[180]



Scheme 14: C–H Arylation of cyclobutanes coupled with a divergent deprotection and functionalisation strategy to access fragment-like compounds.[180]

1.2.5.3 Novel Synthetic Methods as an Approach to New Fragments and Lead–Like Compounds (Summary)

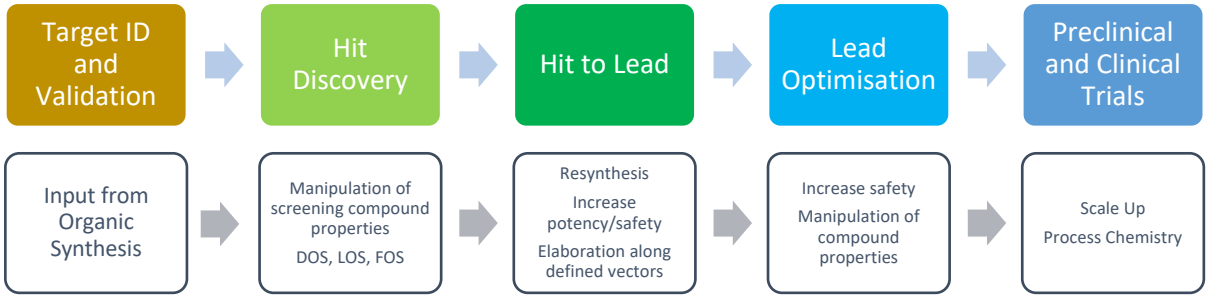


Figure 10: Drug discovery process as seen in Figure 1 and the importance of synthetic chemistry at each stage.

As discussed in Section 1.2.1 organic synthesis is incredibly important for the entire drug discovery process (Figure 10). In Sections 1.2.2 and 1.2.3 the concepts of lead–oriented synthesis and fragment–oriented synthesis were discussed relative to the requirement for guiding the molecular properties of new synthetic methods towards desirable areas of chemical space for screening compounds. These desirable properties were discussed in Section 1.1.5 and emphasised the need for new synthetic methodology to form 3D compounds with saturated heterocycles containing aromatic groups as being highly desirable. According to the principles of lead–oriented synthesis and fragment–oriented synthesis desirable compounds should have pre-installed functional handles which can be used for controlled elaboration to increase potency or modulate physicochemical properties in an efficient manner. In Section 1.2.4 the importance of diversity–oriented synthesis as a route to producing greater diversity within screening libraries was discussed. In particular when combined with the concepts of lead–oriented synthesis and fragment–oriented synthesis DOS has been shown to have significant success in producing valuable screening compounds in an efficient manner.

In Section 1.2.5.1 and 1.2.5.2 the Bull group's work on the development of new synthetic methodology for fragment and lead-like compound synthesis was discussed. These

approaches differ slightly from a typical DOS approach because novel synthetic methods were developed towards certain saturated heterocycles and this was exemplified to make a number of substrates, demonstrating their functionalisation to fragments and lead-like compounds.[181] Therefore, the synthetic strategy is key to this approach. Whereas many DOS approaches, i.e. Nelson's in Scheme 2, utilise known chemistry to build innovative scaffolds, the Bull group's approach has been to develop novel chemistry to build new scaffolds.

1.3 Project Aims

The research outlined in this thesis aimed to synthesise fragment and lead-like 3D saturated heterocycles for library synthesis to complement existing pharmaceutical screening collections. The primary aim was to further develop the modular strategy of oxetane synthesis developed previously within the Bull group. The project aimed to utilise the principles of DOS in combination with FOS and LOS by manipulating the starting materials to alter scaffold size as well as appendage and functional group diversity.

In order to explore a greater diversity of saturated heterocycles, saturated nitrogen heterocycles were targeted (Figure 11). With a particular emphasis placed on the combination of saturated nitrogen heterocycles with aromatic appendages as 2-aryl proline analogues. This work aimed to address some of the limitations of the Bull group's prior methodology: 1) avoidance of the use of NaH in DMF which has safety implications;[182] and 2) avoidance of the isolation of the cyclisation precursor. The development of this methodology is described in Chapter 2.

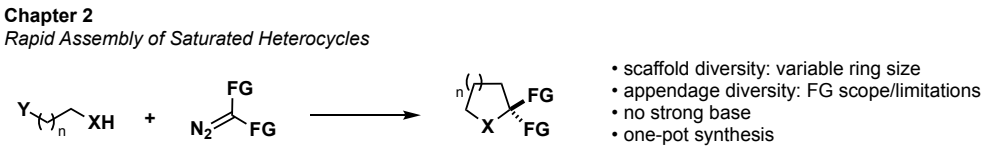


Figure 11: Planned modular synthesis of saturated heterocycles for screening collections.

The conversion of a scaffold into another unique scaffold in one step is desirable for generation of complexity and diversity. In Chapter 3 the discovery of a complexity generating ring expansion reaction is discussed (Figure 12). This reaction utilised the ring-strain of novel azetidine products (discussed in Chapter 2) in a 4- to 6-membered ring expansion to form further scaffolds of interest for medicinal chemistry.

Chapter 4 will address stereochemical diversity. Further development of the methodology developed in Chapter 2 will be discussed towards the achievement of high enantioselectivity using asymmetric phase transfer catalysis (Figure 12). This work also aimed to broaden the diversity of saturated heterocycles accessible for drug discovery by targeting enantioenriched spirocyclic azetidines.

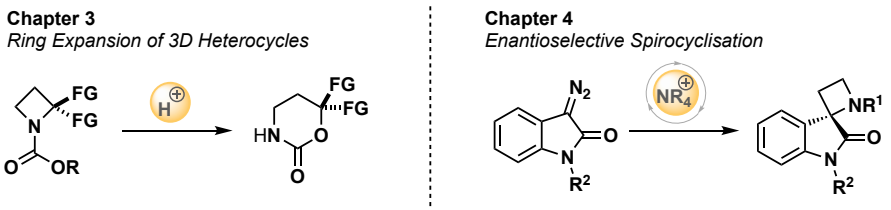


Figure 12: Complexity-generating ring expansion reaction and enantioselective spirocyclisation developed in this work.

2. Synthesis of Four- to Seven-Membered Saturated Nitrogen Heterocycles by N–H Insertion and Cyclisation

2.1 Saturated Nitrogen Heterocycles in Drug Discovery

As of 2014, 59% of small-molecule drugs contained a nitrogen heterocycle.[183] Saturated nitrogen heterocycles are among the most populous nitrogen heterocycles in US FDA approved drugs.[183] Piperidines and pyrrolidines being the first and fifth most frequent nitrogen heterocycles found in FDA approved drugs respectively.[183] Azetidines are starting to gain interest within medicinal chemistry, although they are still not as common as their 5- or 6-membered analogues.[184] Likewise, the seven-membered azepane ring is not common but does feature in a number of pharmaceuticals, in particular as a few specific substructures such as dibenzoazepines (Clomipramine, Figure 13).[185]

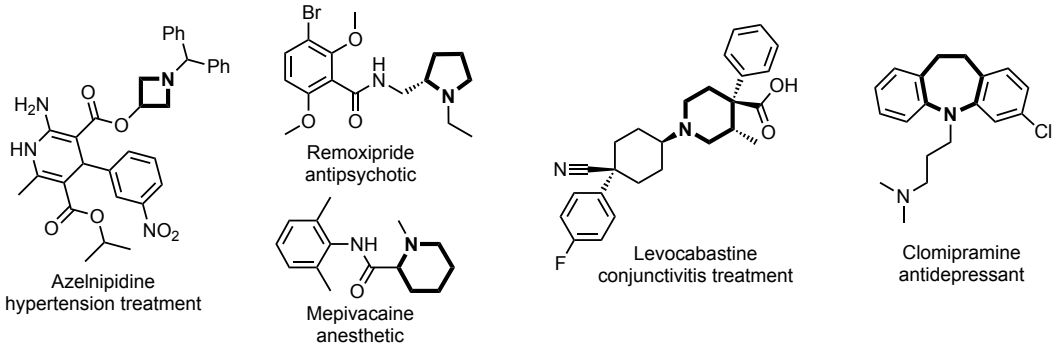


Figure 13: Selected examples of US FDA approved drugs containing 4–7-membered saturated nitrogen heterocycles and their treatment indications.

In Section 2.2 the general synthetic strategies used to access saturated nitrogen heterocycles will be covered. In Section 2.3 literature approaches to 2-aryl proline derivatives will be discussed because of the importance of this class of saturated nitrogen heterocycles for applications in drug discovery. This discussion of the state of the art will be followed by discussion of results for the development of a general strategy to 4- to 7-membered 2-aryl proline analogues.

2.2 General Strategies for the Synthesis of Saturated Nitrogen Heterocycles

There are many synthetic methods to access 4-, 5-, 6- and 7-membered saturated nitrogen heterocycles (See Appendix 7.1). Although some of these strategies can be flexible in terms of ring size, generally they are limited to a single ring size, i.e. there are few azetidine syntheses which can be readily changed to access higher homologues. General strategies that can easily afford multiple scaffolds are particularly desirable for DOS and hit discovery. In this section general strategies which can access multiple ring sizes by using modular reagents and similar reaction conditions will be presented.

In the past 12 years, Aggarwal has developed vinyl sulfonium salts or their precursor, (2-bromoethyl)sulfonium salts, as annulating agents with bis-nucleophiles to form 3- to 7-membered saturated nitrogen heterocycles (Scheme 15A).[186] This is simplest to envisage when a bis-nucleophile, such as a diamine, is used to react with a sulfonium salt as in Scheme 15A. For the synthesis of certain heterocycles, such as azetidines, the second nucleophilic displacement is promoted by an ester group, i.e. a masked nucleophile (Scheme 15B).[186b] As shown by these examples, there is significant variation in the approaches to the different heterocyclic ring sizes and this is the main drawback of these methods.

In 2013, Bode reported the use of reagents termed SnAP (tin-amino-protocol) reagents to effect an annulation of aldehydes by imine formation and radical ring closure (Scheme 15C).[187] Bode showed that this strategy was amenable to the synthesis of larger rings, including medium rings, albeit in lower yields.[188] The main drawback of this protocol is the use of a toxic tin reagent and Bode has developed two alternative protocols to avoid this. By using halogen amine radical protocol (HARP) reagents, amines with a pendant bromo-substituted pyridine, radical ring closure could occur to form tetrahydronapthyridines.[189] Using silicon (SLAP reagents) instead of tin, a photoredox catalysed cyclisation can be used, though this was less broad in scope than the SnAP reagents.[190] Since this work on photoredox-catalysed synthesis of saturated heterocycles, Romanov-Michailidis replaced the silicon in SLAP reagents with dihydropyridines and Bousquet and Bigot used carboxylic acids (CLAP reagents) in order to broaden scope.[191]

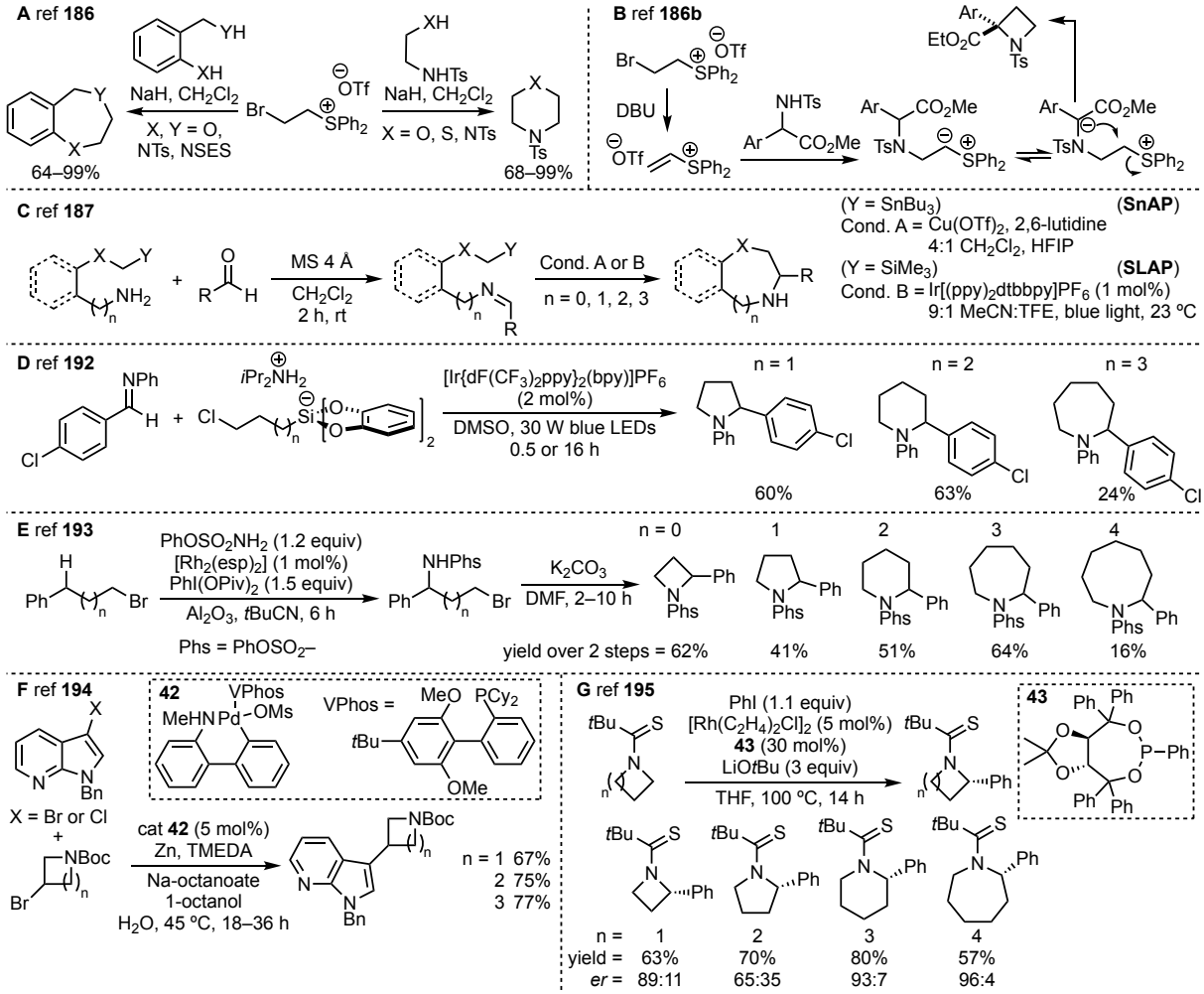
Molander recently reported a photocatalysed radical alkylation/cyclisation between ketimines and bis(catecholato)silicate radical precursors (Scheme 15D).[192] This reaction was suitable for the synthesis of α-aryl pyrrolidines, piperidines and azepanes, although the highest yield for azepane synthesis was 24%. 2,2-Disubstituted pyrrolidines were also demonstrated.

This year, Du Bois reported a C(sp^3)–H amination reaction, using $Rh_2(esp)_2$ as catalyst (see Section 2.3.3), to form a variety of bromide substituted aminoalkanes which could be cyclised, by C–N bond formation upon treatment with K_2CO_3, to a variety of ring sizes (3- to 8-membered rings, Scheme 15E).[193] The demonstrated scope focused on azetidine synthesis including a short total synthesis of a natural product. For higher homologues only monosubstituted examples were shown.

Apart from these general strategies that typically make use of a two-step coupling-cyclisation sequence, other significant strategies are functionalisation reactions which are generally applicable to different heterocycle ring sizes. For example, Buchwald demonstrated an aqueous Lipshutz–Negishi cross-coupling of alkyl bromides and aryl halides which is applicable to bromo-substituted azetidines, pyrrolidines and piperidines (Scheme 15F).[194]

Another example was demonstrated by Glorius who showed that using Rh^{I} catalysis enantioselective α-arylation of azetidines, pyrrolidines, piperidines and azepanes could be achieved (Scheme 15G).[195] The main limitation of these functionalisation methodologies is the requirement for *de novo* synthesis of the heterocycle for further functionalisation. For more complex substrates, *de novo* synthesis of each substrate heterocycle of different ring size may be very time-consuming.

Other distinct strategies include ring expansion of oxetanes or annulation of aza-oxyallyl cations.[196]



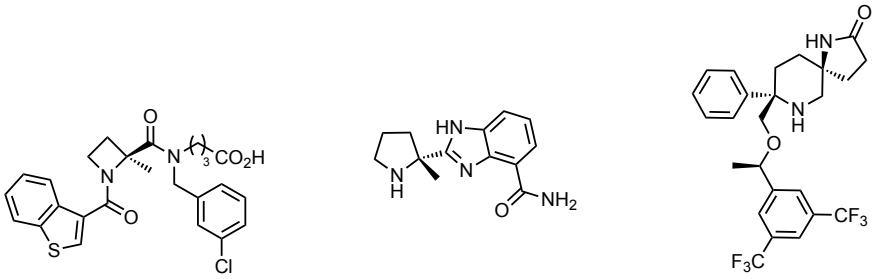
Scheme 15: Selected general strategies to saturated nitrogen heterocycles.

2.3 2-Aryl Proline Analogues

2.3.1 Importance of 2-Aryl Proline Analogues

2,2-Disubstituted saturated nitrogen heterocycles are widely represented in medicinal chemistry (Figure 14). In particular, those bearing an α-quaternary centre are attractive scaffolds and α-aryl proline analogues, as derivatives of the amino acid, can display wide bioactivities.[197] Strategies to access quaternary centres, particularly in a stereoselective

manner, are limited. Few of the strategies previously discussed are able to generate 2,2-disubstituted saturated nitrogen heterocycles of variable ring size.[198] Proline derivatives are used extensively in organocatalysis and quaternary derivatives could also see similar applications.[199]



GLPG0974
FFA2 receptor antagonist

veliparib
anti-cancer

rolapitant
NK_1 receptor antagonist

Figure 14: Examples of 2,2-disubstituted saturated nitrogen heterocycles in medicinal chemistry.

2.3.2 Synthetic Strategies to 2-Aryl Proline Analogues

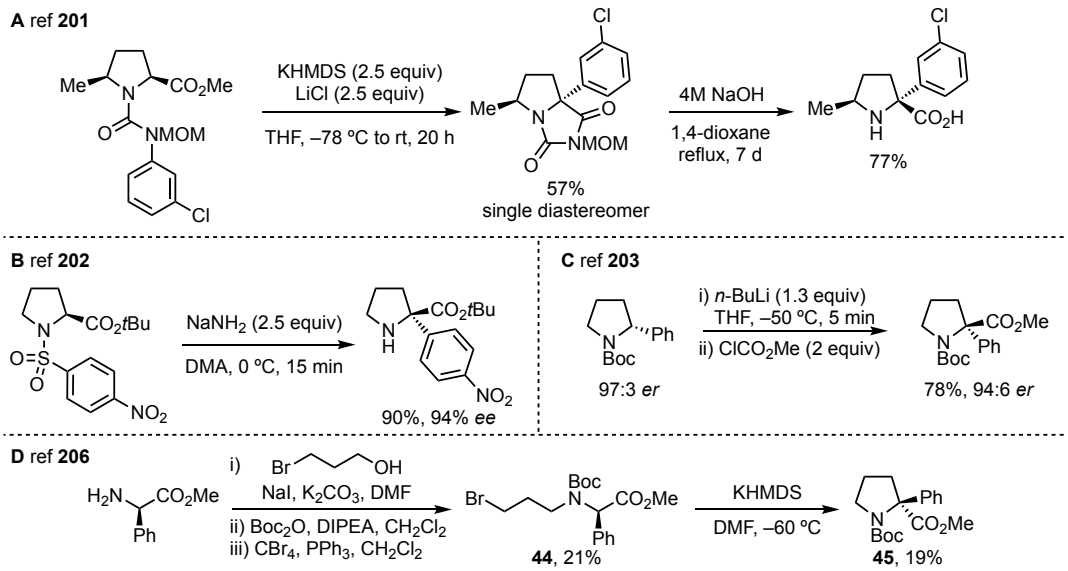
In the 1990s Harwood provided various routes to access morpholinone-fused pyrrolidines which could be reduced to the quaternary proline analogue.[200] Using a similar conceptual approach, Clayden could transform substituted prolines to the fused hydantoin through a cascade aryl migration and hydantoin formation reaction (Scheme 16A).[201] These hydantoins could then be cleaved to afford the 2-aryl proline analogue. The hydantoin formation, when substituted pyrrolidines were used, was diastereoselective. One limitation was the poor results obtained when electron rich aromatic rings were used, such as PMP, due to the requirement for nucleophilic attack at the *ipso*-carbon of the aromatic ring in the migration step.

Another route to enantioenriched α-aryl proline analogues is the base-mediated rearrangement of proline sulfonamides (Scheme 16B).[202] Best results were observed when using $NaNH_2$ as base in DMA at 0 ºC. Product was only observed when a NO_2- or NC-substituted aryl group was used due to a similar requirement, as in Clayden's work, for an electron sink to allow nucleophilic attack at the *ipso*-carbon of the aromatic ring.

One of the most general routes to α-aryl proline analogues is by α-lithiation of 2-aryl saturated nitrogen heterocycles. In 2012, Coldham and O'Brien reported the α-lithiation of *N*-Boc pyrrolidines and piperidines, using *n*-BuLi, to then trap with an electrophile and form 2,2-disubstituted pyrrolidines and piperidines.[203] If the reaction was carried out with enantioenriched α-aryl pyrrolidine[204] or piperidine at –50 ºC then the α-lithiated substrate was configurationally stable and upon trapping with an electrophile enantioenriched α-aryl proline analogues could be formed (Scheme 16C). Luisi has investigated the α-lithiation of azetidines.[491–493] Coldham has developed the α-lithiation of azepanes though this was more limited than with the piperidine due to the greater flexibility of the azepane ring.[205] This

approach is quite amenable for the synthesis of enantioenriched α-aryl proline analogues of ring size 5 and 6, though it necessitates the synthesis of the 2-aryl pyrrolidine or piperidine substrates in order to undergo lithiation.

Another route to α-aryl proline analogues is by cyclisation. Cossy formed pyrrolidine **45** in a low-yielding 4-step process from amino ester **44** in a controlled dialkylation sequence (Scheme 16D).[206] The *er* of the formed pyrrolidine was not stated, however, following deprotection/reprotection and reduction of the ester to an alcohol the *er* was 75:25, which was presumably due to erosion in the cyclisation step. Also see Aggarwal's approach to azetidines which was discussed in Section 2.2 (Scheme 15B).[186b]

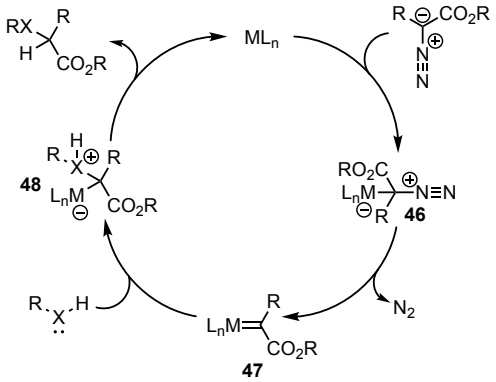


Scheme 16: Selected methods to access 2-aryl proline analogues.

2.3.3 Use of Diazo Compounds

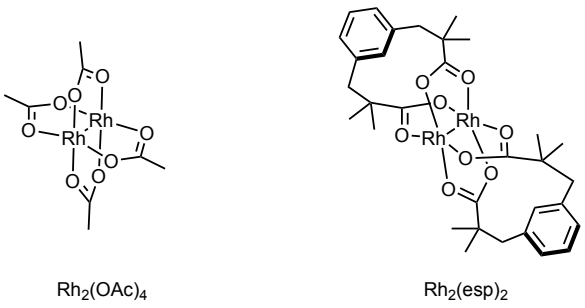
Diazo compounds have found extensive utility within modern organic synthesis.[207] $Rh_2(OAc)_4$ catalysed intramolecular N–H insertion has been extensively employed to access carbapenem antibiotics, including the synthesis of Thienamycin by MSD.[208] These X–H insertion reactions (X = O, NR, S) occur through the intermediacy of a metal carbene upon extrusion of nitrogen from the diazo compound.[209] As a late transition metal, Rh-carbene complexes are normally electrophilic (Fischer-type carbene), particularly as they are typically substituted with an electron-withdrawing group such as a carbonyl group.[209] For metal-catalysed X–H insertion reactions of diazo compounds the reaction is typically considered to be step-wise.[210] Though different transition metals may lead to different pathways and rate-determining steps, a typical mechanism involves the diazo compound acting as a nucleophile to attack an empty coordination site on the metal catalyst (Scheme 17). This consequently results in extrusion of nitrogen gas to afford a metal carbene complex **47**. In the case of Rh(II) catalysis the loss of N_2 is generally considered to be the rate determining step.[211] As mentioned, in the case of

Rh(II) catalysis the resultant metal carbene complex is electrophilic and the X–H nucleophile can attack to form an ylide, **48**. The [1,2]-proton shift to afford the product can have a surprisingly high activation barrier and the ylide intermediate has been trapped with an imine electrophile or can undergo competitive rearrangement.[212]



Scheme 17: General mechanism for metal catalysed X–H insertion reactions.

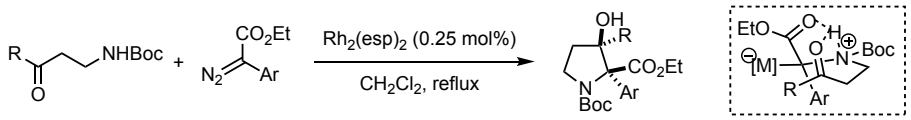
$Rh_2(OAc)_4$ is a common catalyst used to affect X–H insertion reactions. In 1973 Teyssié reported the use of $Rh_2(OAc)_4$ for O–H insertion reactions.[213] $Rh_2(OAc)_4$ exists as a dimer with a paddle-wheel type structure with two vacant coordination sites (Figure 15).[214] The reactivity of the Rh(II) can be altered by changing the ligand, for example Moody has shown that $Rh_2(NHCOCF_3)_4$ can be a superior catalyst for O–H insertion reactions.[215] Du Bois developed dimeric Rh(II) catalyst, $Rh_2(esp)_2$, as a catalyst for C–H amination.[216] The catalyst was designed to improve the stability of the Rh(II) dimer by addition of an appropriate linker, disfavouring ligand dissociation by a chelate effect. This extra stability allowed significant reduction in catalyst loadings due to the avoidance of ligand speciation or oxidation.[217]



$Rh_2(OAc)_4$ $Rh_2(esp)_2$

Figure 15: Structures of $Rh_2(OAc)_4$ and $Rh_2(esp)_2$.

Hu and Moody have independently developed N–H insertion and spontaneous aldol cyclisation methods to react donor-acceptor diazo compounds with β-amino ketones using $Rh_2(esp)_2$ as catalyst.[218] Moody showed *N*-Boc protected β-amino ketones as substrates rather than just *N*-aryl substrates (Scheme 18). The reactions were diastereoselective *via* a proposed stepwise mechanism where the ylide is intercepted and the nitrogen transfers the proton to the ketone, assisted by the ester group, resulting in the *cis*-product (with respect to the ester and alcohol).



Scheme 18: N–H insertion and aldol cyclisation to form polysubstituted pyrrolidines.

2.4 Results and Discussion

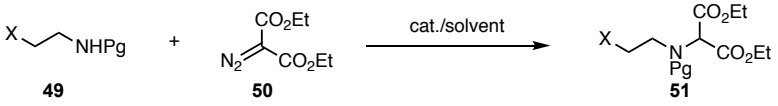
The methods outlined in Section 2.3 and Scheme 16 are limited in terms of the aromatic substituents that can be employed, in yield and the requirement for lengthy synthetic sequences, further substitution or lack of ability for facile modulation of ring size. Also, much of the research discussed in Sections 2.2 and 2.3 was published after the start of the research program detailed in this thesis. The aim of this research was to build on the strategy developed in the Bull group towards 2,2-disubstituted oxetane synthesis (Section 1.2.5.1, Scheme 11) in order to access a range of 2,2-disubstituted saturated nitrogen heterocycles. Of particular interest was the potential of this strategy to access 2-aryl proline derivatives of various ring sizes. This could potentially complement existing strategies by improving the scope of aromatic substituents while being able to produce 4–7-membered saturated nitrogen heterocycles using related simple building blocks in a short sequence.

Two key drawbacks of the previous methodology used to access oxetanes were the use of strong base in DMF for the cyclisation step and requirement for isolation of the intermediate. NaH in DMF has recently been highlighted as a safety concern and thus avoidance of this was a key aim.[182] Isolation of the intermediate was required due to the use of a strong base. Side-products remaining from the first step would likely require an excess of strong base to be used which would not be ideal. Therefore, key to removal of this requirement was identification of conditions amenable for mild base mediated cyclisation of the intermediate.

A concise account of this work can be found in *Angew. Chem. Int. Ed.*[219]

2.4.1 Preliminary Work and Optimisation of N–H Insertion Reaction

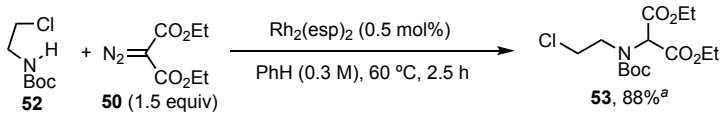
Before the start of this research Dr Dominic P. Affron carried out preliminary work in order to optimise the N–H insertion of diethyl diazomalonate **50** with different protected amines (Ts, Ns, Boc, Cbz, Scheme 19). Different catalysts in different solvents were investigated.



Scheme 19: N–H insertion of diethyl diazomalonate **50** with various protected amines.

Highest yields were observed with Ts when using $Rh_2(esp)_2$ in benzene. However, optimisation was continued with the Boc protecting group due to its foreseen greater ease of removal. Following iterative optimisation of the discrete variables, a design of experiments (DoE)

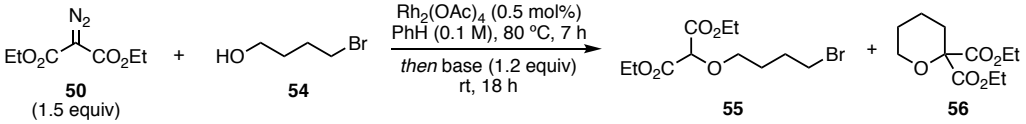
optimisation was carried out to optimise the continuous variables (diazo equiv, cat. loading, temperature, concentration and time). From this DoE optimisation various optimal conditions were generated. The equivalents of diazo compound were limited to 1.5 equiv and an 88% NMR yield of N–H insertion intermediate **53** was obtained using the optimised conditions as detailed below (Scheme 20).



Scheme 20: N–H insertion using Boc-protected amine **52** with Cl leaving group in benzene using optimised N–H insertion conditions. Work carried out by Dr Dominic P. Affron. [a] Yields calculated by ^{1}H NMR spectroscopy with respect to 1,3,5-trimethoxybenzene as an internal standard.

2.4.2 Synthesis of Diester Azetidine, Pyrrolidine and Piperidine

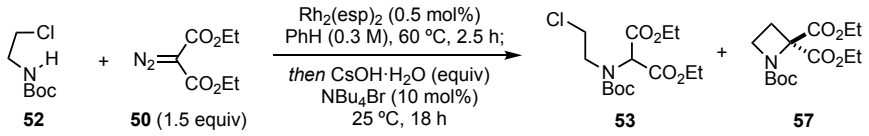
Preliminary work by Dr Dominic P. Affron had studied a one-pot process to synthesise tetrahydropyran (THP) **56**. Use of CsOH·H_2O gave the highest yield (Table 1) but only when combined with the use of a phase transfer catalyst, tetrabutylammonium bromide (TBAB).



entry	base	additive	yield of **55** (%)[a]	yield of **56** (%)[a]	total (%)[a]
1	CsOH·H_2O	none	75	0	75
2	CsOH·H_2O	TBAB (5 mol%)	0	80	80

Table 1: One-pot reaction to make THP **56** by Dr Dominic P. Affron. [a] Yields calculated by ^{1}H NMR spectroscopy with respect to 1,3,5-trimethoxybenzene as an internal standard.

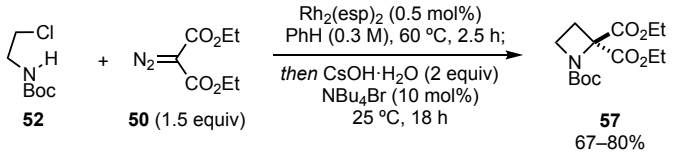
These conditions were combined with optimised conditions for the N–H insertion reaction of diazo **50** and Boc-protected amine **52** (Table 2). These results showed that use of 2 equiv of CsOH·H_2O was necessary for the consumption of the intermediate **53**.



entry	base equiv	yield of **53** (%)[a]	yield of **57** (%)[a]	total (%)[a]
1	1.25	15	53	78
2	1.50	5	61	77
3	1.75	3	66	80
4	2.00	1	68	79

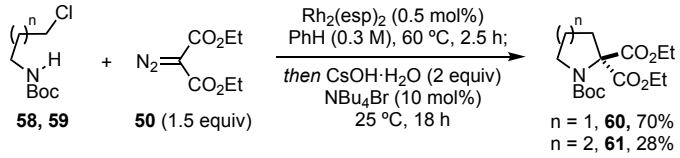
Table 2: One-pot reaction to make azetidine **57**. Reactions on 0.5 mmol scale. In each reaction ~10% of remaining **52** was observed. [a] Yields calculated by ^{1}H NMR spectroscopy with respect to 1,3,5-trimethoxybenzene as an internal standard.

Using these optimised conditions for the synthesis of diester azetidine **57** on 0.5 mmol scale gave isolated yields between 67% and 80% (Scheme 21). For the one-pot synthesis of this 4-membered ring this was considered acceptable and the synthesis of the 5- and 6-membered analogues was examined.



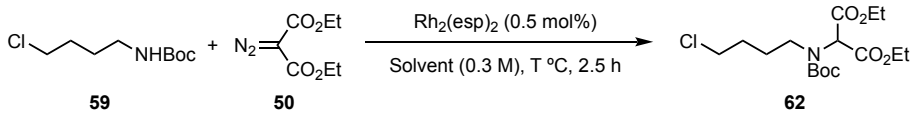
Scheme 21: One-pot reaction to make azetidine **57**. Reactions on 0.5 mmol scale.

The 5-membered pyrrolidine ring was synthesised in 70% yield under the optimised one-pot reaction conditions (Scheme 22). However, the piperidine ring was isolated in only 28% yield using these conditions.



Scheme 22: One-pot N–H insertion and cyclisation reaction to form pyrrolidine **60** and piperidine **61**. Reactions on 0.5 mmol scale.

The low yield for the synthesis of piperidine **61** was due to incomplete NH insertion reaction *and* cyclisation when n = 2. This may be explained by the greater distance of the electron-withdrawing chloride group from the reacting NH bond, thus resulting in a lower reactivity. Combined with the greater entropic barrier to cyclisation relative to the 4- and 5-membered ring syntheses led to a poorer result for the 6-membered ring. When the N–H insertion reaction was examined, full conversion of the protected amine **59** was observed upon increasing the equivalents of diazo compound **50** in CH_2Cl_2 at 40 ºC (Table 3).

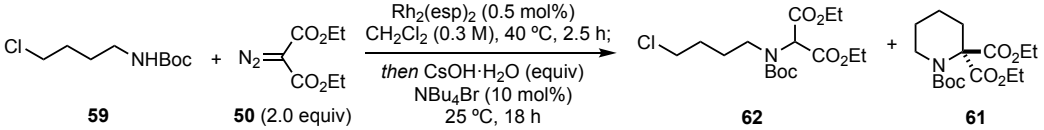


59 **50** **62**

entry	solvent	T (ºC)	**50** (equiv)	Conversion [a]
1	PhH	60	1.5	81
2	CH_2Cl_2	40	1.5	85
3	CH_2Cl_2	40	2.0	100

Table 3: N–H Insertion reaction using Boc-protected amine **59**. Reactions on 0.25 mmol scale. [a] Conversion determined by the ratio of **62**:**59** by ^{1}H NMR spectroscopy.

Increasing the amount of base used for the cyclisation afforded greater amounts of the cyclised product **61** (Table 4). Use of 4.0 equiv of $CsOH{\cdot}H_2O$ led to full conversion from the intermediate **62** (Table 4, Entry 3). Use of more equivalents of base led to a reduction in the recovered product (Entry 4).

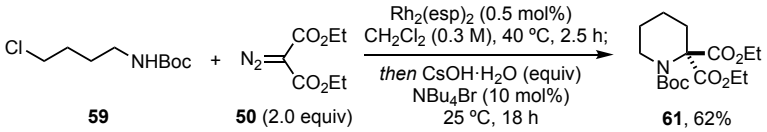


59 **50** (2.0 equiv) **62** **61**

entry	equiv of $CsOH{\cdot}H_2O$	Yield of **62** [a]	Yield of **61** [a]	Total
1	2.0	43	31	74
2	3.0	16	56	72
3	4.0	0	67	67
4	5.0	0	57	57

Table 4: One-pot reaction to synthesise piperidine **61** optimising the amount of base for the cyclisation. Entry 1 on 0.5 mmol scale, other reactions on 0.25 mmol scale. [a] Yields calculated by ^{1}H NMR spectroscopy with respect to 1,3,5-trimethoxybenzene as an internal standard.

Using these optimised conditions the six-membered piperidine ring was isolated in 62% yield (Scheme 23). The synthesis of these diester substituted saturated nitrogen heterocycles provided a set of conditions which could be taken forward for the synthesis of 2-aryl proline analogues.



59 **50** (2.0 equiv) **61**, 62%

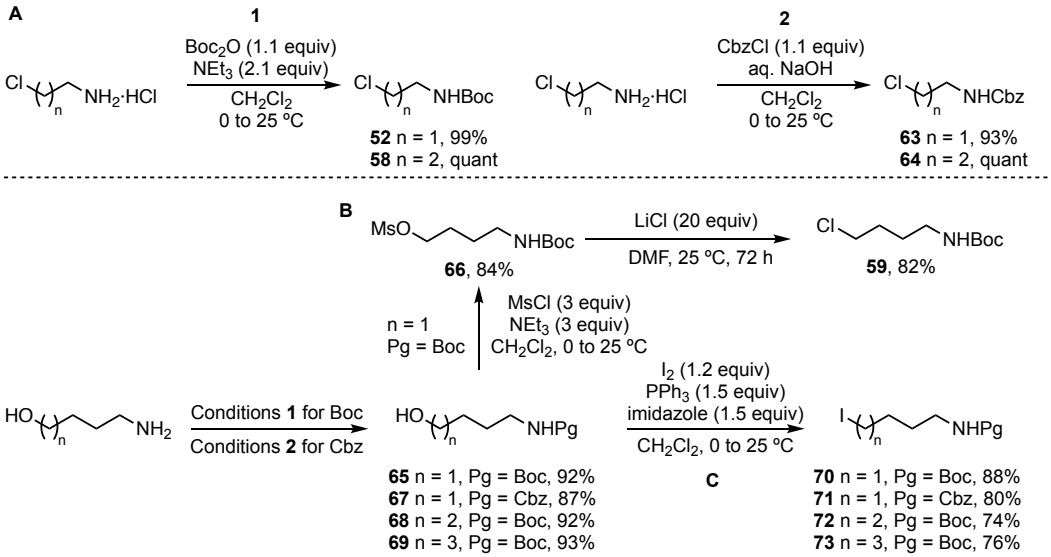
Scheme 23: Synthesis of piperidine **61** using modified conditions. Reaction on 0.25 mmol scale.

2.4.3 Synthesis of 2-Aryl Proline Analogues

As discussed in Section 2.3 the synthesis of 2-aryl proline analogues in a general manner whereby the nature of the aromatic substituent and ring size can be easily modulated would be a significant achievement. In Sections 2.4.1 and 2.4.2 the synthesis of diester substituted saturated nitrogen heterocycles showed how this could potentially be accomplished and showed that larger ring sizes may pose a challenge due to the entropic energy barrier to cyclisation.

2.4.3.1 Synthesis of Protected Amine Starting Materials

The protected amine starting materials that were used in this study can be considered as ambiphilic reagents which are attenuated nucleophiles with an electrophilic leaving group. This type of reagent has previously been used by Shi and co-workers at Bristol-Myers Squibb as an annulating agent.[220] The carbamate protected precursors to the azetidine and pyrrolidine rings can be synthesised by reaction of 2-chloroethylamine or 3-chloropropylamine with di-*tert*-butyl carbonate or benzyl chloroformate (Scheme 24A). For larger ring synthesis the corresponding chloride-substituted amines were not commercially available. In this case selective carbamate protection followed by mesylation and displacement with chloride using LiCl produced the appropriate amine with a Cl leaving group (Scheme 24B). For the synthesis of iodide substituted protected amines, the protected aminoalcohol was subjected to an Appel reaction (Scheme 24C).

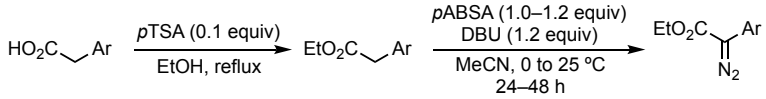


Scheme 24: Synthesis of protected amine starting materials.

2.4.3.2 Synthesis of Diazo Compounds

In order to explore the scope of 2-aryl proline analogue synthesis, a range of aryl-ester diazo compounds (aryldiazoacetates) were synthesised. The ester-aryl substrates with an activated

methylene group were typically prepared by esterification from the commercially available carboxylic acid (Figure 16). The majority of the ester-aryl diazo compounds were prepared using the Regitz diazo transfer,[221] according to a literature procedure using commercially available *p*-acetamidobenzenesulfonyl azide (*p*-ABSA).[222]



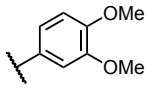
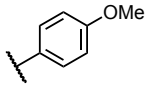
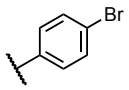
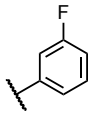
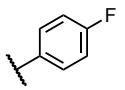
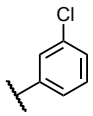
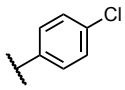
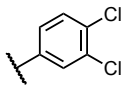
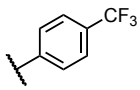
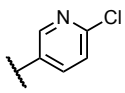
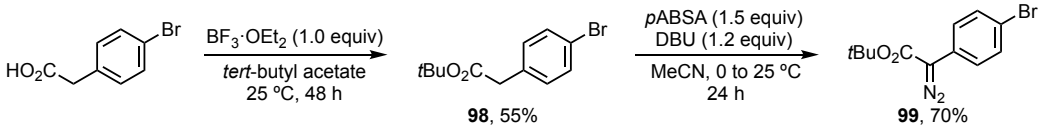
	Yield of Esterification (%)	Yield of Diazo Transfer (%)
	commercially available	**85**, 69%
	**74**, 84%	**86**, 36%
	**75**, 95%	**87**, 53%
	**76**, 97%	**88**, 87%
	**77**, 97%	**89**, 91%
	**78**, 44% [a]	**90**, 83% [a]
	**79**, 95%	**91**, 71%
	**80**, 94%	**92**, 95%
	**81**, 94%	**93**, 81%
	commercially available	**94**, 91%
	**82**, 95%	**95**, 91%
	**83**, 93%	**96**, 93%
	**84**, quant [b]	**97**, 72% [b]

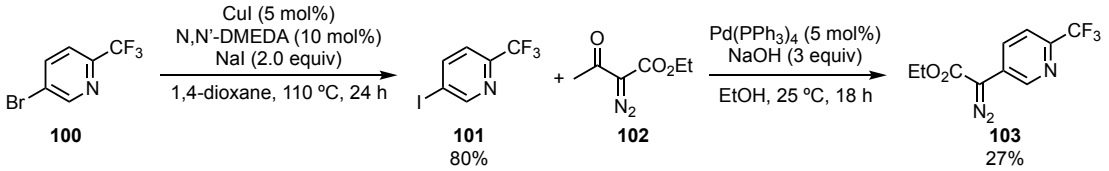
Figure 16: Synthesis of diazo compounds through esterification and Regitz diazo transfer. Esterification reactions on 10 to 30 mmol scale. Diazo transfer reactions on 5 to 28 mmol scale. [a] Reaction carried out by Sebastian Green. [b] Reaction carried out by Dr Dominic P. Affron.

tert-Butyl containing diazo compound **99** was synthesised from the corresponding carboxylic acid using $BF_3{\cdot}OEt_2$ as a Lewis acid in *tert*-butyl acetate as solvent in order to generate the *tert*-butyl carbocation which could be trapped in an S_N1 reaction with the carboxylic acid (Scheme 25).[398]



Scheme 25: Synthesis of *tert*-butyl ester containing diazo compound **99**. Esterification reaction on max. 5 mmol scale. Diazo transfer reaction on 5.0 mmol scale.

An alternative route to diazo compounds has been reported by Wang.[223] This methodology is able to cross-couple acyl diazo compound **102** and aryl iodides. This was studied and adapted slightly to achieve high yields (see discussion in Section 2.4.3.7). This method was used to synthesise diazo compound **103** where the corresponding aryl acetic acid is not commercially available (Scheme 26).



Scheme 26: Synthesis of heterocyclic diazo compound **103** from heteroaryl iodide. Reaction on 2.0 mmol scale.

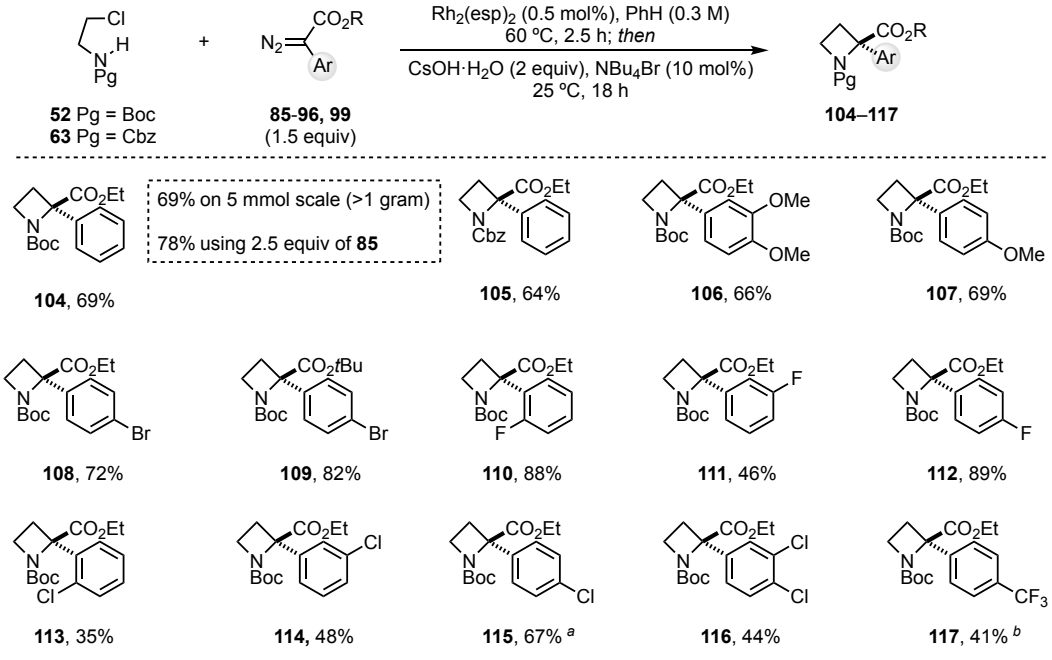
2.4.3.3 Scope of Azetidine Synthesis

A key aim when examining the scope of the reaction with respect to the aromatic substituent on the azetidine ring was i) the range of electronic properties that could be tolerated; ii) the ability to synthesise a wide library of azetidines with aromatic substituents that could be derivatised in a controlled manner in a structure activity relationship. This would enable a range of novel azetidines to be synthesised which could be used in a drug discovery programme.

Importantly, under the conditions as optimised for the synthesis of diester azetidine **57** (which gave between 67 and 80% yield) the 2-phenyl substituted azetidine **104** was afforded in 69% yield (Scheme 27). The reaction was scaled to 5 mmol scale to afford >1 g of the azetidine product with no loss in yield compared to 0.5 mmol scale. Additionally it was shown that increasing the equivalents of diazo compound **85** could increase the yield, though only by 9% from 69% to 78%. Use of protected amine **63** with a Cbz protecting group gave a similar yield to the Boc protecting group. Additionally different ester groups could be used i.e. bulky *tert*-butyl ester containing diazo compound **99** gave 82% yield of **109** compared to 72% yield for the ethyl ester analogue **108**.

Exploration of the different electronic properties of the aromatic ring showed that the reaction was tolerant of electron-rich and electron-poor aromatic rings (Scheme 27). For example

azetidine **107** with a *para*-OMe substituent on the aromatic ring gave the same yield as the unsubstituted example **104**. This was important as other methods to access 2-aryl proline analogues (discussed in Section 2.3) are typically limited to electron poor aromatic rings. The one-pot reaction was also tolerant of more electron poor aromatic substituents. More electron-deficient rhodium carbenes are more reactive and the rate of consumption of this reactive intermediate is likely effecting the yield in these cases. This can be clearly seen in the cases of azetidines **116** and **117** where the products were obtained in 44% and 41% yield respectively. Azetidine **117** required a slow addition of the diazo compound with an elevated equiv of diazo compound in order to obtain this yield (<10% yield under standard conditions, further discussion in Section 2.4.3.4). This trend in electronic properties is also observed with the cases of *para*-, *meta*- and *ortho*-Cl- or F-substituted aromatic rings. Moving these substituents from the *para*-position to the *meta*-position results in removal of any π-donation by these halogens and as such the resultant carbene is more electron-deficient. In comparison to the *meta*-F, the *ortho*-F substituted azetidine **110** is afforded in similar yield to the *para*-substituted analogue **112**. This is not mirrored in the case of *ortho*-Cl azetidine **113** as the yield decreases further. This could be explained by the steric hindrance caused by the Cl atom relative to the F atom or a similarly sized hydrogen atom. Additionally, *ortho*-substituted aryldiazo compounds have been reported to be twisted (a size-dependent effect) which would result in poor orbital overlap for π-electron donation and a much more similar yield to the *meta*-substituted analogue **114**.[224] In addition the greater steric hindrance may have resulted in a poorer yield for the cyclisation step (3% of uncyclised material was isolated in this reaction whereas this intermediate was not observed in other reactions).



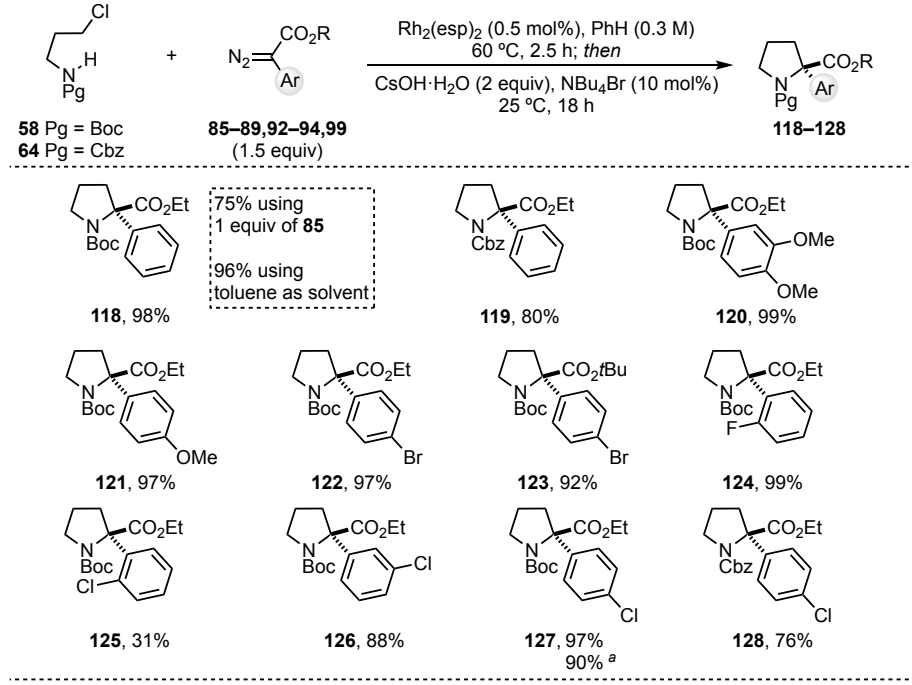
Scheme 27: Scope of azetidine synthesis varying the aromatic ring, protecting group and ester group. Reactions on 0.5 mmol scale. [a] Reaction on 2 mmol scale. [b] Slow addition of diazo compound using syringe pump over 1 h.

2.4.3.4 Scope of Pyrrolidine Synthesis

Having successfully demonstrated the scope of the one-pot N–H insertion and cyclisation reaction to synthesise a range of 2,2-disubstituted azetidines, the scope with respect to 5-membered ring synthesis was explored (Scheme 28).

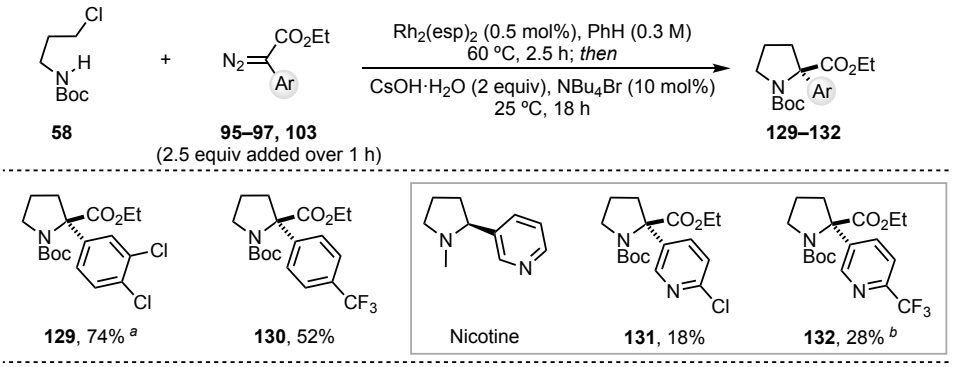
The key difference upon increasing the length of the carbon chain in the starting material to make pyrrolidines was the increase in yield relative to the 4-membered ring. Pyrrolidine **118**, a direct (protected) proline analogue, under the standard conditions was formed in 98% yield relative to 69% for azetidine **104**. This increase in yield could be attributed to the Cl group being removed further from the reacting NH bond (the effect of the chloride leaving group is clear in Section 2.4.3.5) or due to more facile ring closure to the 5-membered ring or a combination of these two factors. Decreasing the equivalents of diazo compound **85** to 1 equiv led to a reduced but still highly acceptable yield of 75%. It should be stressed that this is without slow addition of the diazo compound. Direct addition of the catalyst to a mixture of diazo **85** and starting material **58** leads to highly selective N–H insertion. It was also shown at this stage that the reaction gave a similar yield when benzene was replaced with, the less health hazardous alternative, toluene. A similar range of pyrrolidines could be synthesised as shown with azetidine synthesis, though this was almost uniformly in higher yield. Electron-rich and electron-poor aromatic rings were tolerated with *para*-OMe substituted diazo compound **87** and *para*-Cl substituted diazo compound **94** affording the same excellent yield of the pyrrolidine product.

Similar to the reaction to synthesise azetidine **113** with *o*-Cl substituted aryldiazoacetate **92**, pyrrolidine **125** gave a limited yield of 31%. In this reaction 45% of starting material **58** was recovered which is indicative of the initial N–H insertion step being problematic. This is likely due to the hindered nature of this diazo compound but also the resultant electron deficient carbene formed. Indeed, with other electron-poor aryldiazoacetates, such as **95**, under the standard N–H insertion conditions gave only 50% conversion with respect to protected amine **58**. This is likely due to the electron-deficient aromatic ring increasing the rate of carbene formation through promotion of nitrogen extrusion, which is typically considered to be the rate determining step.[211] Also, the resultant carbene will be highly reactive. This problem of conversion proved to be an issue for isolation of pyrrolidine **129**, due to co-elution with starting material **58**. Optimisation of this reaction by increasing the equiv of diazo **95** to 2.0 equiv and addition of this diazo over 1 h using a syringe pump led to improved conversion and gave an isolated yield of 74% (Scheme 29).



Scheme 28: Scope of azetidine synthesis varying the aromatic ring, protecting group and ester group. Reactions on 0.5 mmol scale. [a] Reaction on 3 mmol scale.

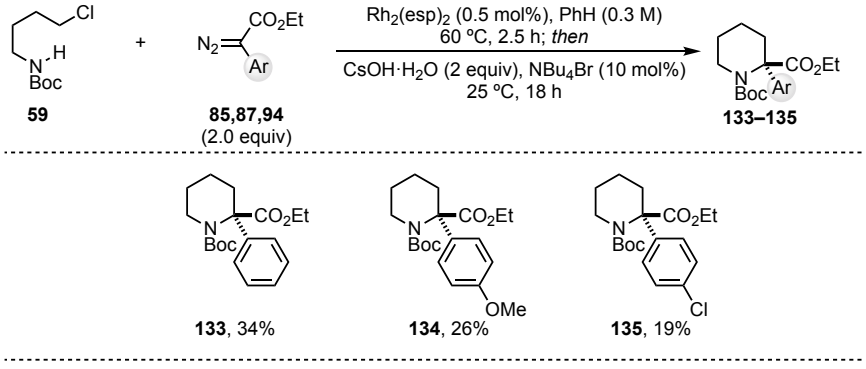
In a similar fashion, addition of 1.5 equiv of diazo **96** over 1 h only gave a 25% isolated yield of pyrrolidine **130**. Increasing the equivalents of diazo **96** added over 1 h to 2.5 equiv gave an isolated yield of 52% (Scheme 29). Nicotine is a well-known bioactive compound which is widely consumed as a stimulant through tobacco products. Nicotine analogues could provide interesting applications within the pharmaceutical and agrochemical industry.[225] Nicotine analogues could be produced in this one-pot reaction by using aryldiazo acetates with heteroaromatic substituents. In this case there was the potential for interaction between the lone pair of the nitrogen in the pyridine ring with Rh to form a Rh-ylide and thus inhibit the reaction. Therefore, to attenuate the nucleophilicity of the lone pair an electron-withdrawing substituent was used. Though the carbenes formed from these diazo compounds were likely to be very reactive, due to their electron-deficient nature, the desired pyrrolidines **131** and **132** could be isolated in 18% and 28% respectively.



Scheme 29: Synthesis of pyrrolidines with electron-poor aromatic and heteroaromatic substituted diazo compounds. Reactions on 0.5 mmol scale. [a] 2.0 equiv of diazo compound. [b] 0.15 mmol scale.

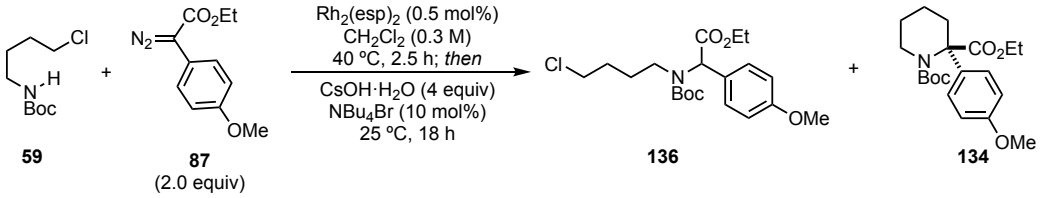
2.4.3.5 Scope of Piperidine Synthesis

Using the conditions optimised for azetidine and pyrrolidine synthesis for the synthesis of some different aryl substituted piperidines resulted in only poor yields (Scheme 30).



Scheme 30: Synthesis of piperidines **133**–**135** using conditions optimised for azetidine synthesis. Reactions on 0.5 mmol scale.

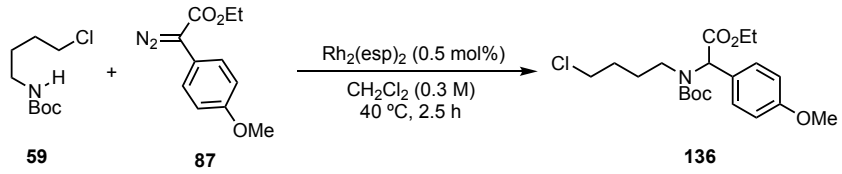
In Section 2.4.2, Scheme 25 diester substituted piperidine **61** was synthesised in 62% yield under modified N–H insertion and cyclisation conditions (relative to azetidine and pyrrolidine synthesis). From Scheme 30 it is clear that a similar set of conditions would be expected to be beneficial. However, when applying this set of conditions to ester-aryl diazo compound **87** a mixture of products was observed (Scheme 31). These products were determined to be protected amine starting material **59**, NH insertion intermediate **136** and cyclised product **134** in approximately equal proportions. This suggested that both N–H insertion and cyclisation were not complete under these conditions.



Yield of **59** [a] (%)	Yield of **136** [a] (%)	Yield of **134** [a] (%)	Total (%)
22	34	25	81

Scheme 31: Test of NH insertion reaction using diazo compound **87**. Reaction on 0.25 mmol scale. [a] Yields calculated by ^{1}H NMR spectroscopy with respect to 1,3,5-trimethoxybenzene as an internal standard.

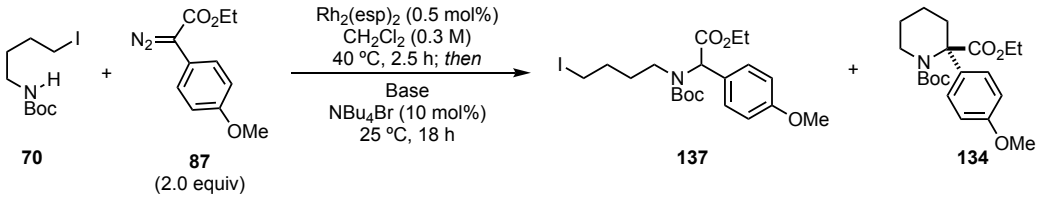
However, upon examination of the N–H insertion reaction without the consequent one-pot cyclisation, the yield for the N–H insertion was shown to be quantitative without any protected amine starting material **59** remaining (Table 5).



Entry	Equiv of **87**	Yield of **59** [a] (%)	Yield of **136** [a] (%)	Total (%)
1	2.0	0	quant	100
2	2.5	0	quant (99)	100

Table 5: Test of N–H insertion reaction using diazo compound **87**. Reactions on 0.25 mmol scale. Yield in parentheses indicates isolated yield.

This meant that protected starting material **59** was being regenerated in the second cyclisation step. It was hypothesised that this was occurring *via* deprotonation and consequent oxidative decomposition of the formed enolate due to the slow rate of 6-*exo*-tet cyclisation. Notably, increasing the amount of base for the cyclisation or increasing the temperature led to poorer product mass recovery (Table 6, Entries 1 and 2). Changing the leaving group to iodide was found to be critical in order to obtain high conversion to the desired piperidine product without formation of this side product (Table 6, Entry 3). Iodide, as a better leaving group than chloride, reduced the energy barrier to cyclisation leading to a higher rate of cyclisation. Using KOH (4 equiv) instead of CsOH gave a higher yield of the desired piperidine product (Table 6, Entry 4). Other bases such as NaOH, DBU or Cs_2CO_3 gave no product or <10% yield (not shown). Decreasing the equiv of KOH gave poorer conversion and increasing the equiv led to no improvement in yield (Table 6, Entries 4 and 5).

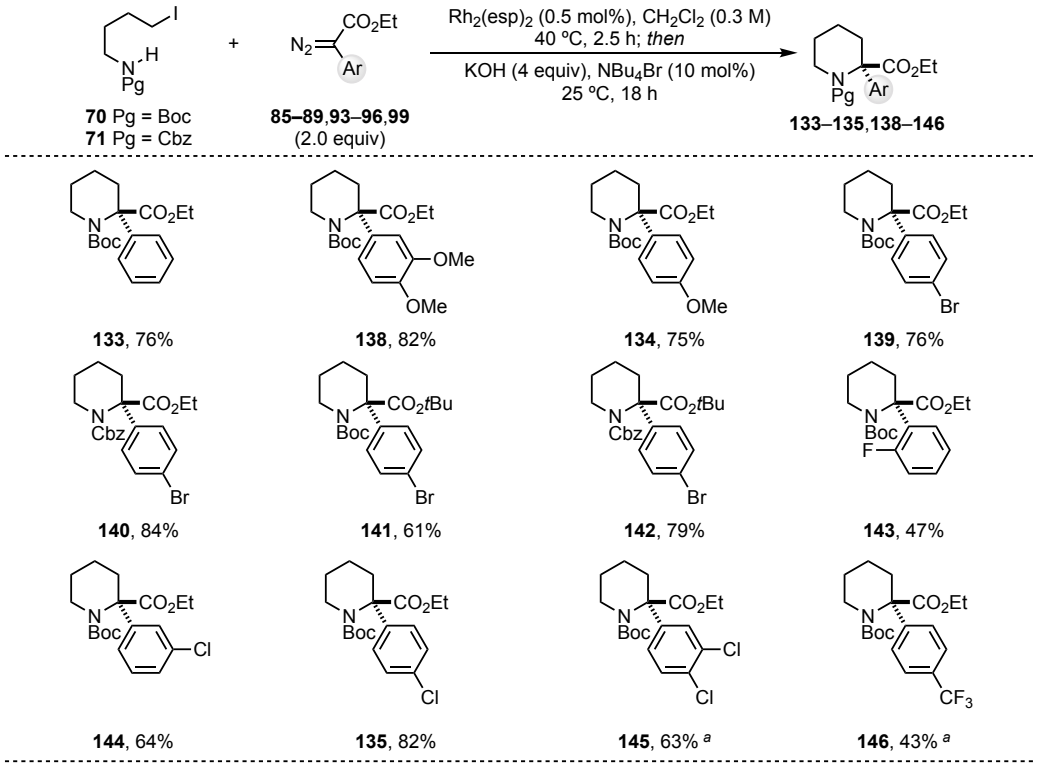


Entry	Base	Base equiv	Yield of **70** [a] (%)	Yield of **137** [a] (%)	Yield of **134** [a] (%)	Total (%)
1	CsOH	5.0	14	23	19	56
2[b]	CsOH	5.0	0	9	32	41
3	**KOH**	**4.0**	**0**	**0**	**94**	**94**
4	KOH	3.0	0	29	53	82
5	KOH	5.0	0	0	91	91

Table 6: Optimisation of conditions for one-pot N–H insertion and cyclisation to form piperidine **134**. Reactions on 0.25 mmol scale. [a] Yields calculated by ^{1}H NMR spectroscopy with respect to 1,3,5-trimethoxybenzene as an internal standard. [b] Cyclisation step carried out at 40 °C.

With the modified conditions a similar range of diazo compounds, as used in the synthesis of azetidines and pyrrolidines, could be employed for the synthesis of piperidines (Scheme 32). These 6-membered rings are analogues of pipecolic acid.[226] Though this type of product could feasibly be produced through α-lithiation,[203] their synthesis by cyclisation methods has previously been unexplored.

Overall 12 *N*-carbamate protected piperidines were synthesised with an average yield of 69% (43% to 84%). In terms of the scope with respect to the aromatic ring, similar trends were observed as with the smaller analogue synthesis. Lower yields were observed with the *ortho*-F substituted aryl piperidine **143**, as well as with more electron-poor diazo compounds **145** and **146**. However, with these more electron-poor aromatic substituents comparable yields to the azetidine and pyrrolidine were seen under the modified conditions. Piperidines **139–142** show how the protecting group and ester group can easily be modulated without significantly effecting the yield of the reaction, with the lowest yield for the bulky *N*-Boc protected *tert*-butyl ester piperidine **141**.

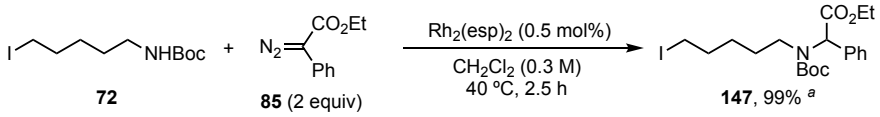


Scheme 32: Scope of azetidine synthesis varying the aromatic ring, protecting group and ester group. Reactions on 0.5 mmol scale. [a] 2.5 equiv of diazo added over 1 h.

2.4.3.6 Synthesis of Larger Rings

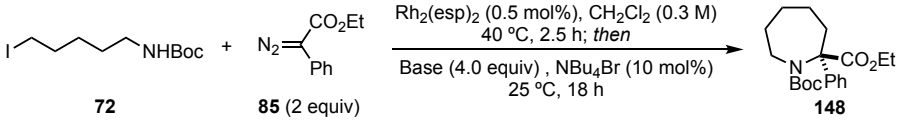
Due to the much lower relative rate of ring closure compared to 4–6-membered rings, 7-membered rings are often synthesised through rearrangement or ring expansion sequences.[227] As such the synthesis of 7-membered azepanes is limited (see Appendix 7.1.4) and most

commonly utilises ring expansion reactions to avoid the high entropic barrier to cyclisation. We were interested in investigating whether the developed N–H insertion and cyclisation strategy could be extended to azepane ring synthesis. A test of the N–H insertion reaction showed that the same yield as for 6-membered ring synthesis could be obtained (Scheme 33).



Scheme 33: N–H Insertion reaction for formation of intermediate **147** prior to azepane synthesis. Reaction on 0.25 mmol scale. [a] Yields calculated by ^{1}H NMR spectroscopy with respect to 1,3,5-trimethoxybenzene as an internal standard.

Having established that there would not be a problem in the N–H insertion step, the cyclisation step was tested in one-pot (Table 7). Using the conditions as applied to piperidine synthesis afforded only 26% of the desired azepane product (Table 7, Entry 1). However changing the base from KOH to CsOH (which had previously given the best results with the 4- and 5-membered ring synthesis) gave a high yield of the azepane (Table 7, Entry 2). Protected amine starting material **72** was being generated as a side-product in the cyclisation step but this was not further optimised.



Entry	Base	Yield of **72** [a] (%)	Yield of **148** [a] (%)	Total (%)
1	KOH	23	26	49
2	CsOH	32	67 (60)[b]	99

Table 7: One-pot reaction to access azepane **148**. Reactions on 0.25 mmol scale. [a] Yields calculated by ^{1}H NMR spectroscopy with respect to 1,3,5-trimethoxybenzene as an internal standard. [b] Yield in parenthesis is isolated yield on 0.5 mmol scale.

The ^{1}H NMR spectrum of azepane **148** was much more complex than spectra for similar compounds of smaller ring size (see Appendix 7.2 for representative examples, Figure 17). Seven-membered rings are more conformationally flexible than their five- or six-membered analogues and therefore can adopt more than one conformation at room temperature.[411] Obtaining ^{1}H NMR spectroscopy at 373 K and 233 K did not simplify the spectra significantly. Though at lower temperature significant broadening of certain peaks was observed. The compounds are also significantly rotameric due to the *N*-Boc group and high temperature NMR spectroscopy was not sufficient to resolve the rotamers. LCMS and HRMS confirmed the purity and identity of azepane **148**.

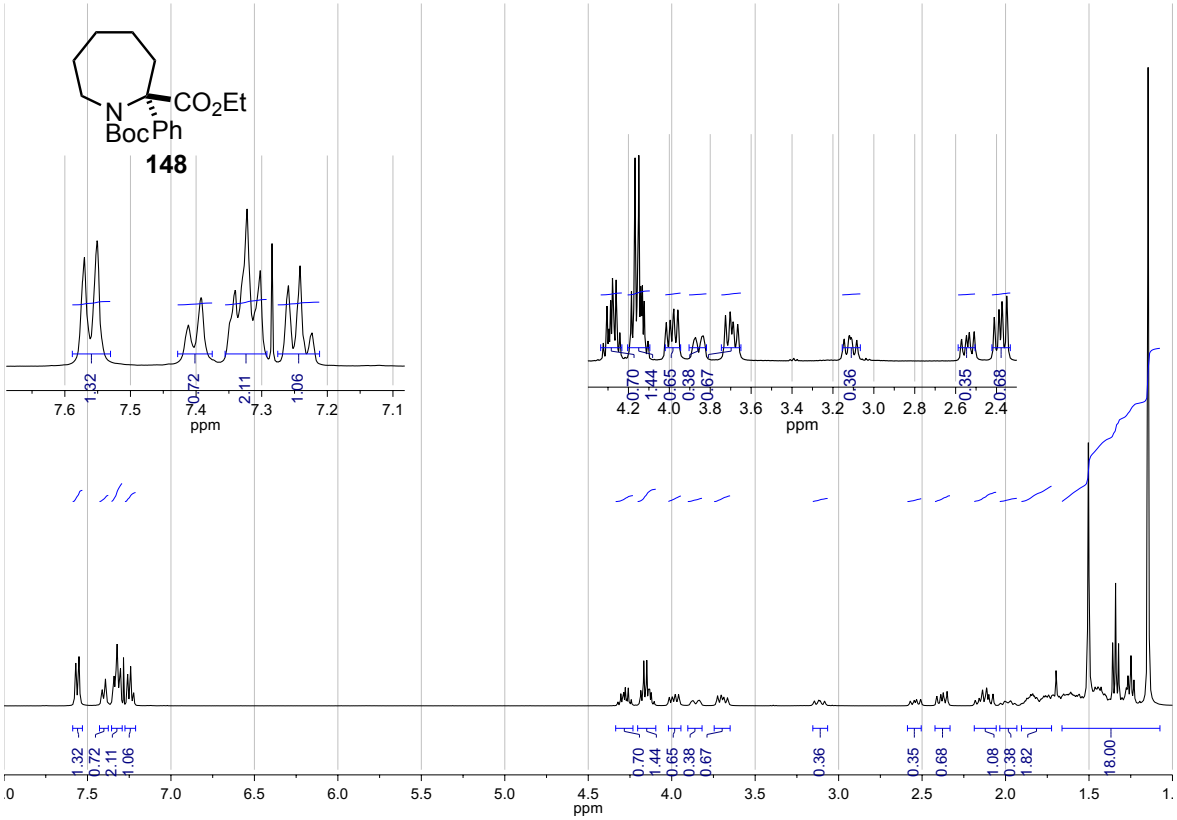
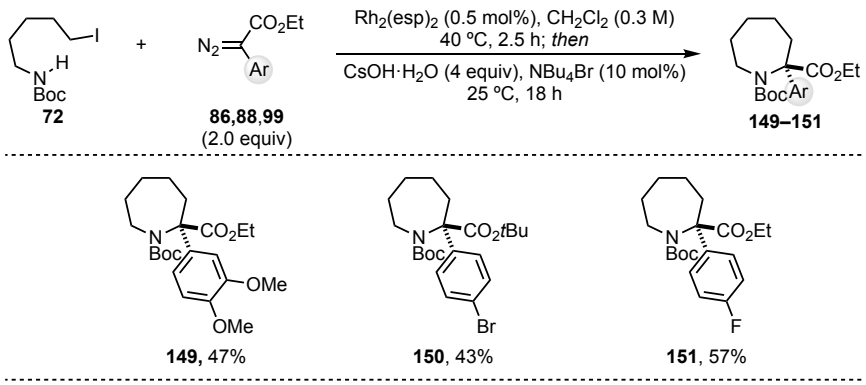


Figure 17: Room temperature ^{1}H NMR spectrum of azepane **148** displaying rotamers and restricted conformational flexibility which both affect the appearance of the spectrum.

Azepanes **149**, **150** and **151** were synthesised using the conditions described in Table 7 in 43 to 57% yield (Scheme 34). The yields for the synthesis of these azepanes was lower than for the 4-, 5- or 6-membered rings, however, this was most likely due to the lower rate of cyclisation and consequent side product formation *via* enolate decomposition.

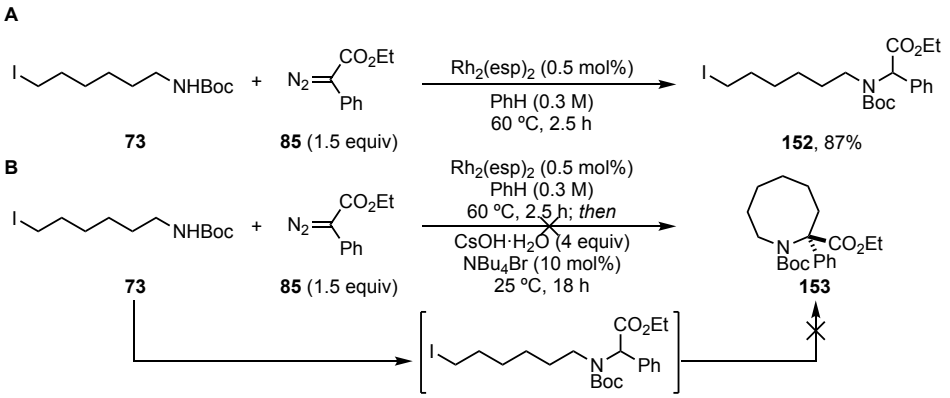


Scheme 34: Synthesis of azepanes in one-pot. Reactions on 0.5 mmol scale.

It was interesting to explore the limitations of the cyclisation to give 2,2-disubstituted saturated nitrogen heterocycles. Extending the carbon chain by adding a further methylene would, if successful, provide 8-membered azocane rings. 8-Membered rings are the first in the family of medium rings, which are more strained than 5-, 6- and 7-membered analogues due to

greater torsional (Pitzer) strain and transannular (Prelog) strain.[228] Both of these strain energies contribute to a higher enthalpic energy barrier to cyclisation, whereas the greater number of conformations that can be sampled by the longer carbon chain leads to a higher entropic energy barrier to cyclisation.

The N–H insertion reaction was tested successfully, affording an 87% isolated yield of intermediate **152** (Scheme 35A). However, no product was formed when the N–H insertion and cyclisation reaction was carried out in one-pot in order to form azocane **153** (Scheme 35B). No intermediate was observed at the end of the reaction so it is likely that this underwent degradation rather than 8-*exo*-tet cyclisation (note this was carried out in benzene rather than CH_2Cl_2). Considering the greater enthalpic and entropic barriers to desired cyclisation relative to 7-membered ring formation, this is perhaps not surprising. In order to construct 8-membered rings further substitution on the alkyl chain may be required, i.e. a benzo-fused system may reduce the entropic energy barrier to cyclisation through the Thorpe–Ingold effect.[188,229] Indeed, another strategy may be required altogether, i.e. use of ring-closing metathesis[230] or ring expansion.[231]



Scheme 35: Successful N–H insertion reaction to afford **153** and unsuccessful second cyclisation step when tested in one-pot. Reactions on 0.5 mmol scale.

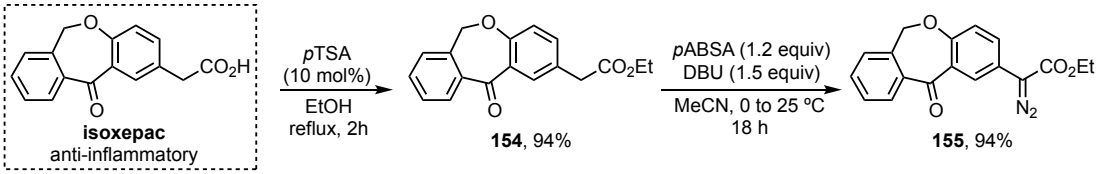
2.4.3.7 Application of One-Pot Reaction to Late Stage Functionalisation

Installation of medicinally relevant motifs at a late stage of a drug or natural product synthesis, termed late stage functionalisation, has recently received much attention from the medicinal chemistry and organic synthesis community.[232] Late stage functionalisation is a significant challenge for medicinal chemists due to the requirement to tolerate the functionality within complex drug molecules.[233]

We envisaged that we could exploit the arylacetic acid functionality[234] within drug compounds or append this to a drug compound in order to enable functionalisation with a saturated nitrogen heterocycle. This saturated nitrogen heterocycle would provide 3D shape to the drug

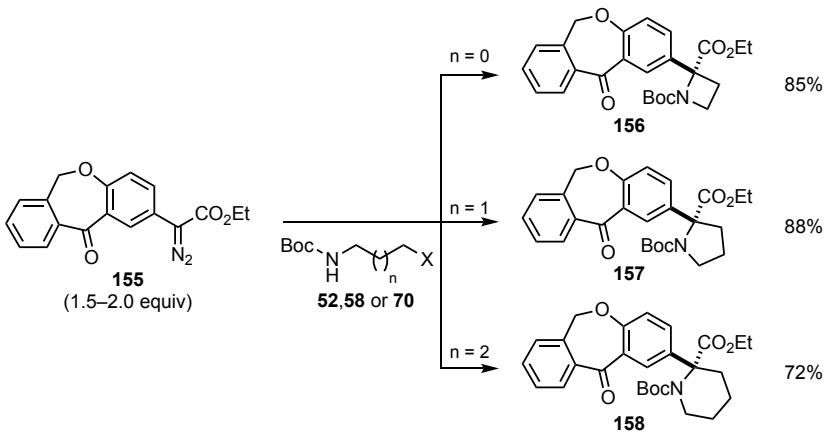
compound and provide further vectors for diversification through the protected nitrogen and ester.

Isoxepac is an arylacetic acid containing dibenzooxepine which has anti-inflammatory effects.[235] Esterification of isoxepac using an acid catalyst in ethanol under reflux afforded ester **154** which could be isolated with a basic workup (Scheme 36). Reaction of ester **154** with *p*ABSA in the presence of DBU gave diazo **155** in 94% yield in sufficient purity after workup as to not require column chromatography (Scheme 36).



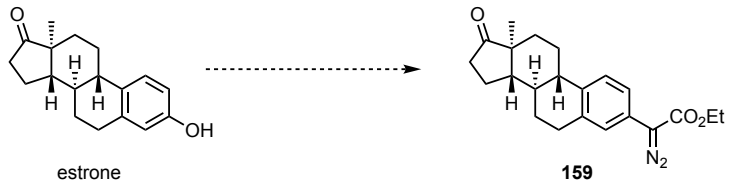
Scheme 36: Esterification and diazo transfer reactions to form diazo **155**. Esterification on 5.0 mmol scale. Diazo transfer on 3.4 mmol (1.0 g) scale.

The conditions developed for azetidine, pyrrolidine and piperidine synthesis (as discussed in Section 2.4.3.3–5) were applied using diazo **155** (Scheme 37). In the one-pot reaction the conditions were successful for the installation of the 4-, 5- and 6-membered rings to the drug compound. Azetidine **156** and pyrrolidine **157** were obtained in 85% and 88% yield respectively. Piperidine **158** was formed in a slightly lower yield of 72% using the modified conditions discussed in Section 2.4.3.5, i.e. using iodide as leaving group. This presented a proof of concept that an azetidine, pyrrolidine and piperidine could be installed at a late stage of a drug synthesis by exploiting an arylacetic acid functionality in above 64% yield over 4 steps with only one chromatographic purification.



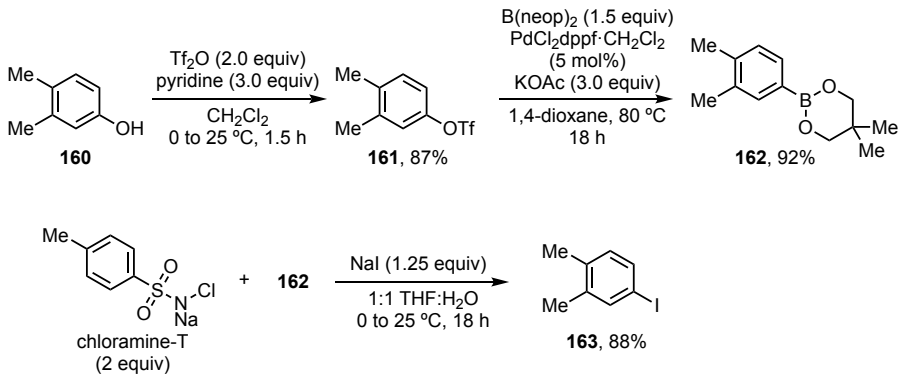
Scheme 37: Late stage installation of an azetidine, pyrrolidine and piperidine ring onto isoxepac scaffold. Reactions on 0.5 mmol scale. For n = 0 and 1, X = Cl, **155** (1.5 equiv), $Rh_2(esp)_2$ (0.5 mol%), PhH (0.3 M), 60 ºC, 2.5 h, then $CsOH{\cdot}H_2O$ (2 equiv), TBAB (10 mol%), 25 ºC, 18 h. For n = 2, X = I, **155** (2.0 equiv), $Rh_2(esp)_2$ (0.5 mol%), CH_2Cl_2 (0.3 M), 40 ºC, 2.5 h, then KOH (4 equiv), TBAB (10 mol%), 25 ºC, 18 h.

The late stage diversification of natural products is a complementary challenge to late stage functionalisation of drugs.[232a] We were interested in applying the developed methodology to functionalise estrone, a natural sex hormone (Scheme 38).[236]



Scheme 38: Proposed transformation of estrone phenol functionality to aryldiazo acetate.

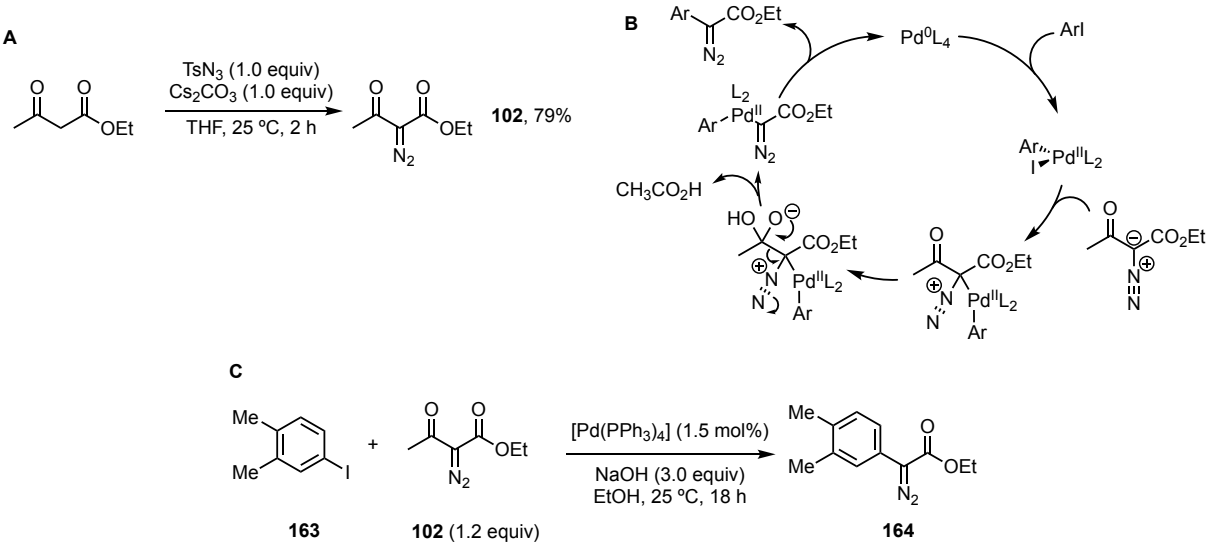
The aryl ester diazo functionality in **159** needed to be derived from the phenol. This was tested initially with a simpler phenol, 3,4-dimethyl phenol **160**, which has similar electronic properties (Scheme 39). Triflation to convert the phenol into a leaving group proceeded smoothly, followed by a Miyaura borylation reaction to furnish neopentyl boronate **162** in high yield. This was subjected to oxidative iodination to yield aryl iodide **163** in high yield.[237] The oxidative iodination may proceed through the formation of ICl upon reaction of NaI with chloramine-T which can then undergo reaction with the boronate to form an 'ate'-complex which can undergo reductive elimination to afford the aryl iodide *via* deboronation.



Scheme 39: Synthesis of aryl iodide **163** as a model system for estrone diversification. All reactions on > 2.0 mmol scale. neop = neopentyl glycol.

The successful reaction sequence to convert the phenol to iodide allowed the exploration of a reaction developed by Wang which could convert an aryl iodide to an aryldiazoacetate functionality by reaction with diazo **102** (previously discussed in Section 2.4.3.2).[223,238] Wang proposed that this reaction goes *via* oxidative addition of the aryl iodide to the Pd^0 catalyst followed by coordination of diazo **102** (Scheme 40B). Activation of the ketone by attack of hydroxide leads to loss of acetic acid and consequent reductive elimination generates the product. In a first attempt at employing the literature conditions[223] a 47%–51% yield was achieved comparable to a reported literature yield of 76% (this yield also proved to be variable/unreliable). As the yield for the estrone derivative would need to be maximised we decided to investigate which parameters were important to obtaining a high yield in this reaction (Scheme 40C). This showed that increasing the equiv of diazo **102** did not significantly

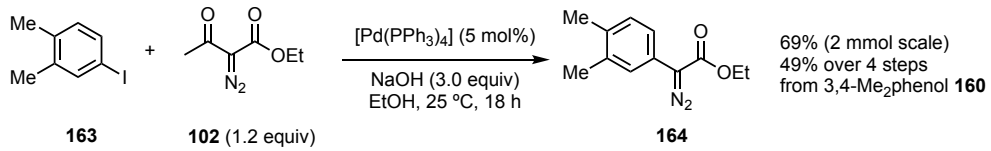
improve the yield of the cross-coupling (Entry 2). Increasing the loading of catalyst did give higher yield, with 5 mol% giving 80% yield (Entry 4). While more base decreased the yield, less base was not advantageous (Entry 5 and 6). The prior results suggested that catalyst deactivation, possibly due to the presence of moisture in the base could be responsible for the lower conversion. Indeed drying the base and using degassed solvent were both advantageous for the reaction (Entries 7 and 8).



Entry	Change	Yield of **163** [a] (%)	Yield of **164** [a] (%)	Total (%)
1	none	35	51	87
2	2 equiv **102**	43	56	99
3	3 mol% cat.	14	67	81
4	5 mol% cat.	9	80	89
5	6.0 equiv base	31	22	54
6	1.5 equiv NaOH [b]	39	60	99
7	dried NaOH [b,c]	10	72	82
8	degassed solvent [b,d]	11	75	86

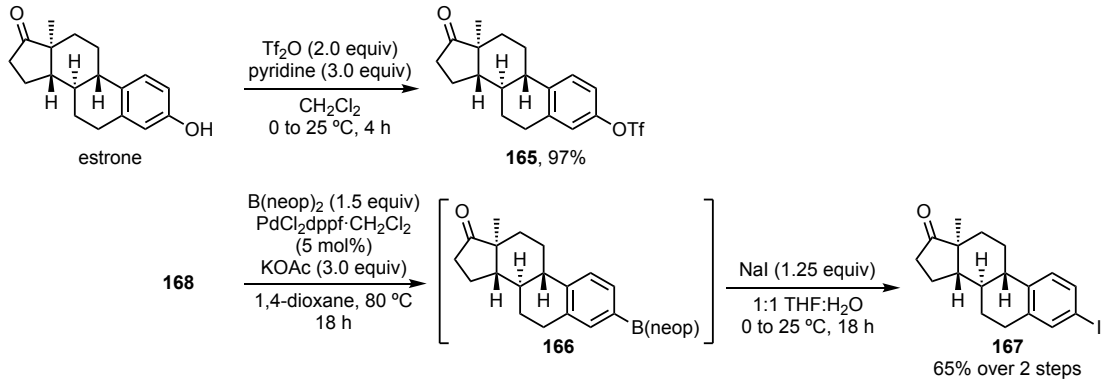
Scheme 40: **A**: Synthesis of diazo **164**. **B**: Mechanism of Wang's deacylative cross-coupling reaction. **C**: Optimisation of deacylative cross-coupling of **102** with aryl iodide **163**. [a] Yields calculated by ^{1}H NMR spectroscopy with respect to 1,3,5-trimethoxybenzene as an internal standard. [b] 3 mol% cat. [c] flame dried NaOH under Ar prior to addition of other reagents. [d] solvent degassed with Ar balloon for 10 min.

Scheme 40C represented a significant reoptimisation of the process of the cross-coupling reaction. This allowed more reliable yields to be achieved and allowed the large scale synthesis (300 mg, 2 mmol scale) of diazo **164** in 69% yield (Scheme 41).



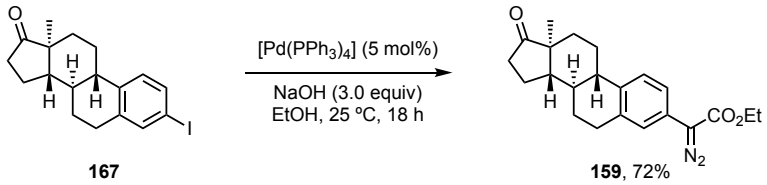
Scheme 41: Large scale synthesis of diazo **164**. Base flame-dried prior to addition of other reagents. EtOH degassed with Ar prior to use.

With optimisation of the 4 reaction steps from a phenol to an aryldiazoazecetate on the model system complete, this synthesis was carried out using estrone. Triflation proceeded in 97% isolated yield to afford **165** (Scheme 42). While the Miyaura borylation step was successful, column chromatography of boronate **166** proved difficult and a clean sample was only obtained on 0.5 mmol scale. A larger scale borylation afforded essentially quantitative conversion to the product, though this was only isolated in 80% purity (i.e. ~100% yield with an additional 20% impurity). This was used in the next step without further purification and the reaction successfully afforded aryl iodide **167** in 65% yield over 2 steps from triflate **165**.



Scheme 42: Synthesis of estrone derived aryl iodide **170** over 3 steps. Reactions on >3.9 mmol scale. neop = neopentyl glycol.

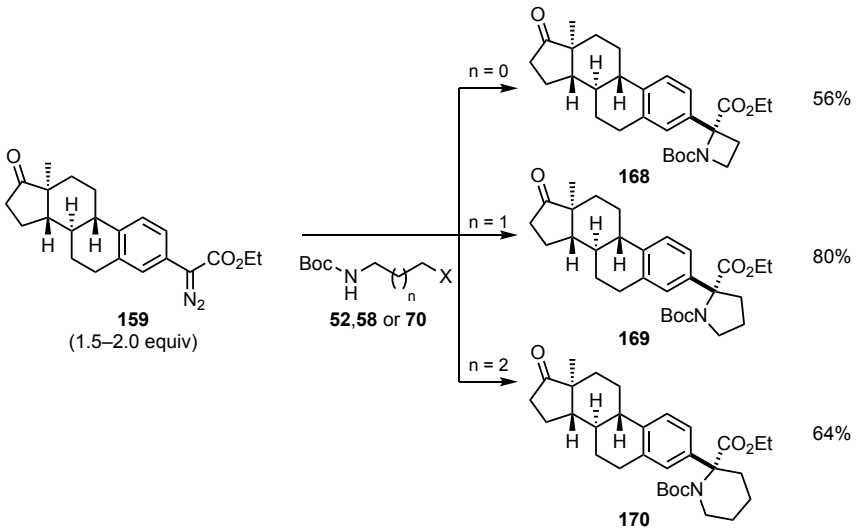
The deacylative cross-coupling conditions were applied to aryl iodide **170** which gave estrone diazo **162** in 72% yield (>0.5 g) (Scheme 43). This represented 45% over 4 steps from estrone.



Scheme 43*:* Synthesis of diazo **159** using previously discussed deacylative cross-coupling methodology. Reaction on 2.0 mmol scale.

Having executed a successful synthetic route to diazo **159** and with a significant quantity in hand, the late stage installation of the azetidine, pyrrolidine and piperidine rings was carried out. The azetidine was successfully installed in 56% yield which represents 25% in 6 steps from estrone (Scheme 44). The pyrrolidine was installed in a high 80% yield and the piperidine ring in 64% yield. Therefore each ring could be installed in over 25% yield in 6 steps from estrone allowing late stage diversification of estrone to 3 different products with high 3D shape,

due to the presence of the fully substituted carbon centre, and with further orthogonal vectors for functionalisation. It should be noted that it is assumed that these products were 1:1 mixtures of diastereomers due to the absence of stereocontrol in the cyclisation step and the remote centres of chirality in the steroid molecule.

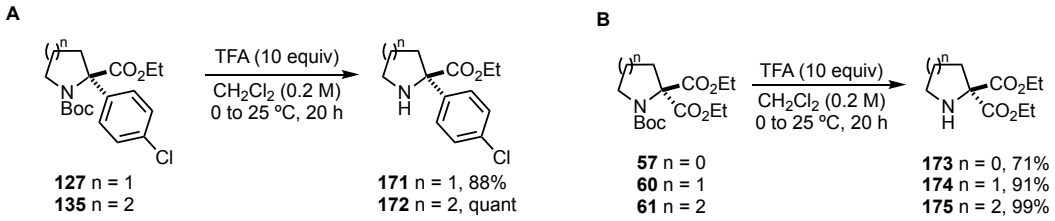


Scheme 44: Late stage installation of an azetidine, pyrrolidine and piperidine ring onto estrone scaffold. Reactions on 0.2 mmol scale. For n = 0 and 1, X = Cl, **162** (1.5 equiv), $Rh_2(esp)_2$ (0.5 mol%), PhH (0.3 M), 60 ºC, 2.5 h, then $CsOH·H_2O$ (2 equiv), TBAB (10 mol%), 25 ºC, 18 h. For n = 2, X = I, **162** (2.0 equiv), $Rh_2(esp)_2$ (0.5 mol%), CH_2Cl_2 (0.3 M), 40 ºC, 2.5 h, then KOH (4 equiv), TBAB (10 mol%), 25 ºC, 18 h.

2.4.3.8 Functionalisation of Azetidine, Pyrrolidine, Piperidine and Azepane Scaffolds

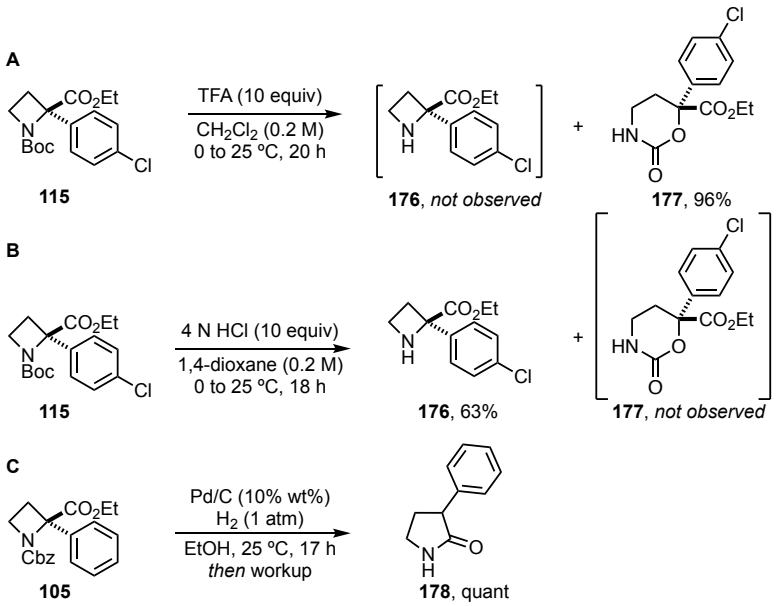
A key criteria by which this new synthetic methodology would be judged is its potential to have application within drug discovery. In order for the methodology described in this chapter to find application in hit discovery the demonstration of fast elaboration and diversification of the protected products was required. We envisaged that each product formed in the one-pot N–H insertion and cyclisation reaction process could be elaborated *via* 3 vectors: 1) *N*-Boc deprotection and derivatisation; 2) Ester hydrolysis and derivatisation; 3) Diversification of the aromatic ring i.e. by cross-coupling. This clearly opens many avenues for product derivatisation and we intended to demonstrate this with at least the 5-membered ring while trying to show that this was also applicable to other ring sizes. This section will detail the exploration of this functionalisation dealing with each vector in turn.

When considering *N*-Boc deprotection, treatment of pyrrolidine **127** or piperidine **135** with trifluoroacetic acid (TFA) in CH_2Cl_2 gave a high yield of amines **171** and **172** (Scheme 45A). The same conditions were successfully applied to *N*-Boc protected diester azetidine, pyrrolidine and piperidine **57**, **60** and **61** (Scheme 45B).



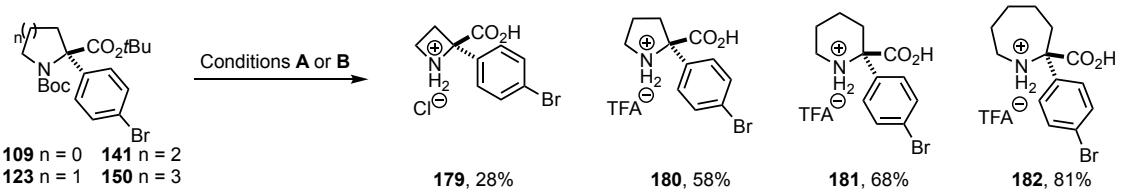
Scheme 45: *N*-Boc deprotection of **A**: pyrrolidine **127** and piperidine **135** and **B**: diester saturated nitrogen heterocycles **57**, **60** and **61**. Reactions on 0.1–0.2 mmol scale.

With the successful reaction of diester azetidine **57**, the same conditions were applied for the *N*-Boc deprotection of azetidine **115** (Scheme 46A). However, the expected azetidine product **176** was not observed. The product had the correct number of protons in the ^{1}H NMR spectrum to correspond to deprotected azetidine **176**. Though the signal assigned to the NH (at a chemical shift of 6.55 ppm) was significantly more deshielded than would be expected in a typical amine (though this was not definitive due to the variability of NH proton signals in ^{1}H NMR spectroscopy due to hydrogen bonding). The key evidence to dispute that product **176** was not the observed product was the ^{13}C NMR spectrum, where the quaternary carbon was more deshielded than expected (~83 ppm vs. 69 ppm) and the ^{13}C NMR spectrum showed the remaining presence of a carbon in a carbamate chemical environment at 153 ppm. The product was identified as 1,3-oxazinan-2-one **177** formed by a ring expansion of the azetidine (Scheme 46A). This ring expansion will be the focus of discussion in Chapter 3. By switching the acid from TFA to HCl in 1,4-dioxane instead of CH_2Cl_2, the ring expansion side product could be supressed and azetidine **176** was formed in 63% yield (Scheme 46B). An attempt was also made to deprotect the *N*-Cbz protected azetidine **105** using Pd/C under an atmosphere of H_2 (Scheme 46C). The crude reaction mixture indicated full conversion of the starting material and the formation of two products in a 5:1 mixture. After an SCX column to isolate the free azetidine, the majority product (not identified) converted to the minority product which was determined to be pyrrolidinone **178**. This was not further investigated due to the possibility to afford the desired free azetidine with judicious choice of acidic deprotection and the unclear mechanism by which this ring expansion was occurring.



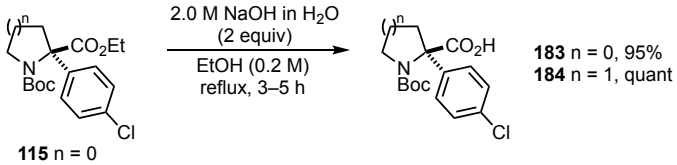
Scheme 46: **A**: Ring expansion of **115** upon treatment with TFA (0.2 mmol scale). **B**: Selective *N*-Boc deprotection of azetidine **115** using HCl in 1,4-dioxane (0.16 mmol scale). **C**: Ring expansion of azetidine **105** upon treatment with Pd/C under H_2 atmosphere and workup.

As discussed in Section 2.3 the synthesis of proline analogues of different ring size is an important synthetic challenge. We envisaged that we could access amino acids directly from the 2,2-disubstituted saturated nitrogen heterocycles if these were protected with an *N*-Boc group and a *tert*-butyl ester. Treatment of pyrrolidine **123**, piperidine **141** and azepane **150** with TFA in CH_2Cl_2 effectively deprotected the *N*-Boc protecting group and hydrolysed the *tert*-butyl ester in one-pot (Scheme 47). Azetidine **109** was subjected to a similar set of conditions, however, using HCl rather than TFA (TFA was tested and gave a complex mixture of products) allowed the azetidine amino acid **179** to be isolated as the HCl salt. The salts were purified by trituration with Et_2O and significant levels of side product were observed for the azetidine, presumably due to decomposition in the acidic media. This one-pot deprotection allowed the unnatural amino acids to be isolated as the TFA or HCl salts without chromatography.



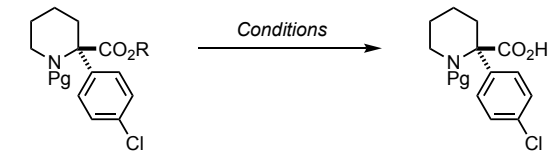
Scheme 47: Global one-pot deprotection of *N*-Boc protected *tert*-butyl ester substituted saturated nitrogen heterocycles. Conditions A: 1:1 4 N HCl in 1,4-dioxane: 1,4-dioxane, 40 ºC, 16 h. Conditions B: 1:1 TFA:CH_2Cl_2, 40 ºC, 16 h.

In order to allow selective diversification of the ester handle without *N*-Boc deprotection, hydrolysis under basic conditions (NaOH) was tested. High temperature was required in order to achieve full conversion in less than 24 h. Heating under reflux with 2.0 equiv of NaOH (2.0 M in H_2O) in EtOH gave full conversion and high yields for the synthesis of azetidine acid **183** and pyrrolidine acid **184** (Scheme 48).



Scheme 48: Ester hydrolysis of azetidine **115** and pyrrolidine **127**. Reactions on 0.2–1.0 mmol scale.

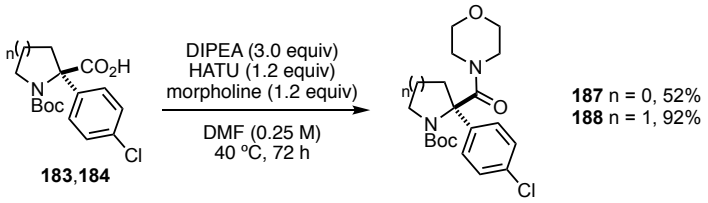
The analogous reaction for piperidine **135** proved more challenging than the smaller rings. Reaction with different bases at high temperature for multiple days led to poor conversion and in all cases recovery of the starting material **135**. This suggested much greater stability of the piperidine ester to basic hydrolysis. This is potentially due to the ring conformation and greater proximity of the ester group to the *N*-carbamate protecting group. This was somewhat validated by greater product formation when the *N*-protecting group was changed from Boc to Cbz (Table 8, Entry 4). Under basic conditions approximately 30% yield of the product was obtained with other side products. Due to the success of the ester hydrolysis in **141** to **181** (Scheme 47), we decided to apply an acidic hydrolysis to *N*-Cbz protected piperidine **142** which showed more promise (Table 8, Entry 5, piperidine **186** was observed by ^{1}H NMR spectroscopy, though this was not isolated in sufficient purity for characterisation). These samples were not analytically pure but showed that ester hydrolysis was much more tractable when using a less bulky *N*-protecting group and acidic or basic conditions could be applied.



Entry	Pg	R	Conditions	Time (h)	Result
1	Boc	Et	NaOH (2 M, 2 equiv) in EtOH (reflux)	72	No product **185**
2	Boc	Et	$LiOH·H_2O$ (5 equiv) in THF/H_2O, 80 ºC	120	<10% **185**
3	Boc	Et	30% KOH in H_2O, THF (5:1), 80 ºC	168	<10% **185**
4	Cbz	Et	NaOH (2 M, 4 equiv) in EtOH (reflux)	18	~30% **186**
5	Cbz	*t*Bu	TFA, CH_2Cl_2, 40 ºC	18	~30% **186**

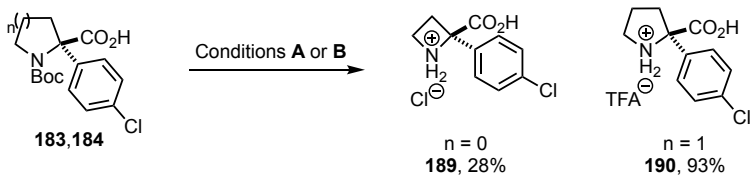
Table 8: Attempts to hydrolyse piperidines **135**, **140** and **142** using basic or acidic conditions.

With carboxylic acids **183** and **184** in hand it was possible to form amides using a peptide coupling reagent (Scheme 49). Treatment of **183** and **184** with HATU in the presence of DIPEA and morpholine allowed the formation of morpholine amides **187** and **188** in good yield. The lower yield for the azetidine product was due to the difficult isolation from the urea byproduct derived from HATU.



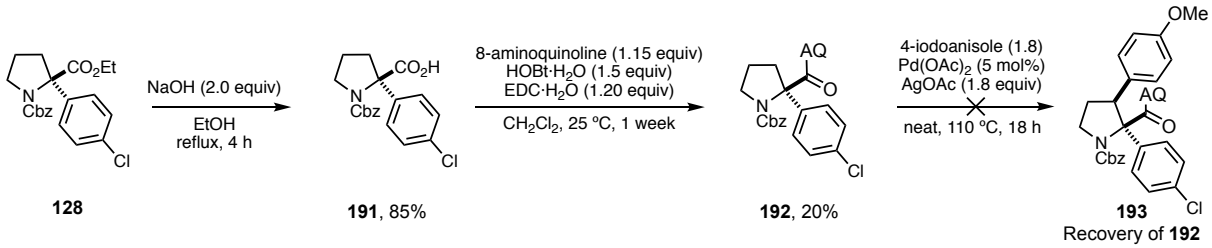
Scheme 49: Amide bond formation for derivatisation of ester handle. Reactions on 0.2 mmol scale.

From the same acids the Boc protecting group can be removed to provide an alternative route to the amino acids **189** and **190** (Scheme 50). This also demonstrates that, if desired, the ester handle can be derivatised and then the *N*-Boc group removed followed by *N*-derivatisation.



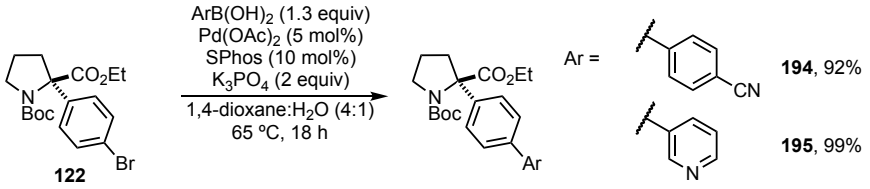
Scheme 50: Boc deprotection of carboxylic acids **183–184** to afford amino acids **189** and **190**. Conditions **A**: 4 N HCl in 1,4-dioxane, 1,4-dioxane, 25 ºC, 20 h. Conditions **B**: TFA, CH_2Cl_2, 25 ºC, 18 h.

The ester handle could be functionalised to install a directing group for C–H activation. Basic hydrolysis followed by amide bond formation and subsequent installation of the 8-aminoquinoline group formed **192** (Scheme 51). An attempt to promote a C–H arylation according to literature conditions previously discussed in Section 1.2.5.2,[173] was unsuccessful (Scheme 51). This result is likely due to the strict conformational requirements for the C–H arylation to occur. As a comparison, in the case of proline derivatives *N*-Boc protected examples gave poorer yields in the C–H arylation, likely due to the different conformation of the ring, compared to *N*-Cbz protected examples. In the case of pyrrolidine **192** it is possible that the aromatic ring may cause the amide group to be in an axial conformation resulting in a higher barrier for the transition state of the C–H activation step. Even if the amide group is equatorial the energy barrier may be too high due to the steric hindrance provided by the aromatic ring.



Scheme 51: Attempted C–H arylation of pyrrolidine **192** with an 8-aminoquinoline directing group. AQ = 8-amioquinoline.

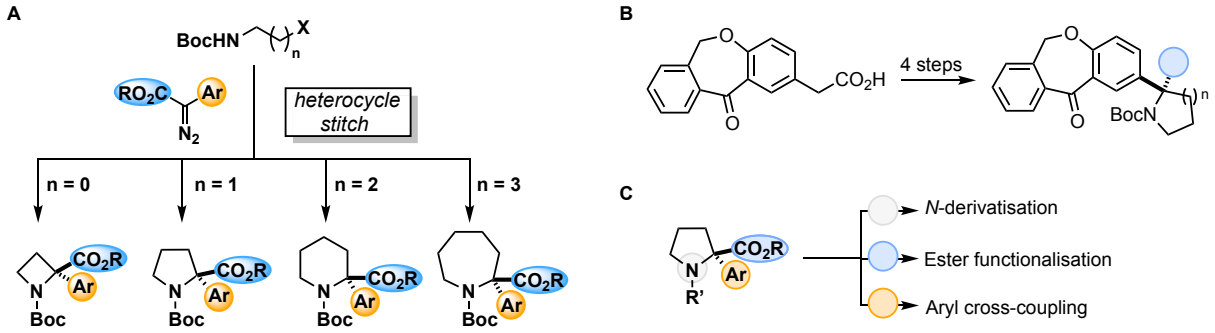
The third and final vector for derivatisation was the aromatic ring. This was demonstrated using pyrrolidine **122** with an aryl bromide substituent. Suzuki–Miyaura cross coupling[239] was successful with electron-withdrawing boronic acid coupling partners containing functionalisable or medicinally relevant motifs (Scheme 52). Using SPhos[240] as ligand with $Pd(OAc)_2$ as precatalyst gave high yields of the products.



Scheme 52: Suzuki–Miyaura cross-coupling using aryl bromide **122** with arylboronic acids. Reactions on 0.2 mmol scale.

2.4.3.9 Summary

In this section the synthesis of diverse saturated nitrogen heterocycles as α-aryl proline analogues has been demonstrated (Scheme 53). Four- to seven-membered rings have been synthesised in high yields using a Rh-catalysed N–H insertion reaction followed by a base mediated cyclisation in one-pot. The reaction was tolerant of a range of different aromatic substituents, including electron-rich and electron-poor aromatic rings, as well as different *N*-substituents and ester handles. The same conditions could be used to access each ring size with slightly modified conditions developed to achieve high yields of the piperidine and azepane system. The application of this methodology to late-stage functionalisation of a drug molecule and a natural product was shown in Section 2.4.3.7. This provided a rapid route to 3 topologically distinct analogues of two different bioactive compounds with greater 3D shape than the original bioactive molecule. Finally, functionalisation of the three orthogonal vectors: the *N* atom, the ester handle and the aromatic group, was demonstrated to provide a variety of lead-like compounds and building blocks including unnatural amino acids.



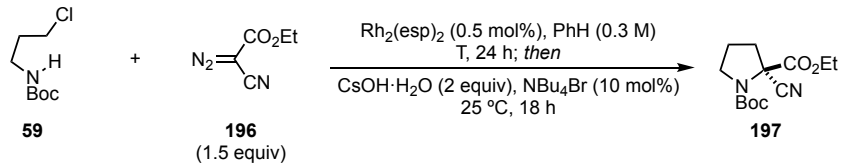
Scheme 53: **A**: Heterocycle stitch by N–H insertion and cyclisation to form 4–7-membered rings. **B**: Late stage heterocycle stitch to install saturated nitrogen heterocycles. **C**: Three routes to derivatisation of the saturated nitrogen heterocycles.

2.4.4 Limitations of the N–H Insertion and Cyclisation Strategy

2.4.4.1 Scope of Diazo Compounds

Section 2.4 has shown that four- to seven-membered rings could be generated in a short sequence from acceptor-acceptor (diester) and donor-acceptor (aryl-ester) diazo compounds in an N–H insertion/cyclisation process. However, a further way of increasing the diversity of products that could be generated using this methodology would be to broaden the types of diazo compounds utilised. This would provide further substituent diversity in the products in a rapid manner.

The stability of diazo compounds typically requires an electron-withdrawing group (acceptor).[241] This electron-withdrawing group is also required for the base-mediated cyclisation to reduce the pK_a of the generated cyclisation intermediate. A similar diazo compound to diethyl diazomalonate **50** (used in Section 2.4.1 and 2.4.2) is diazo **196**, with ester and cyano substituents. Under the conditions optimised for diazo **50** (which gave a 70% yield for the final cyclised pyrrolidine product **60**), a maximum yield of 18% for pyrrolidine **197** was achieved (Table 9, Entry 1 and 2). CH_2Cl_2 was used as solvent due to the high reactivity of diazo **196** and potential to undergo cyclopropanation with benzene.[242] Slow addition of the diazo compound did not change the yield (Entry 3). It is likely that increased equiv of diazo **196** would be required to improve the yield of **197** to synthetically useful levels. The presence of the –CN substituent clearly leads to higher reactivity of the diazo compound leading to greater dimerization of the generated metal-carbene.



Entry	T (ºC)	Yield (%)	
		59	**197**
1	30	64	16
2	60	61	18
3	60 [a]	58	17

Table 9: Synthesis of pyrrolidine **197** using diazo **196**. Reactions on 0.5 mmol scale. [a] Addition of diazo **196** over 1 h.

Further diversity in acceptor-acceptor diazo compounds was tested. Using ester-phosphonate diazo **198**, amide-phosphonate diazo **199**, ester-amide diazo **200** and ester-sulfonate diazo **201** all of which led to poor product yields using the standard N–H insertion and cyclisation conditions.

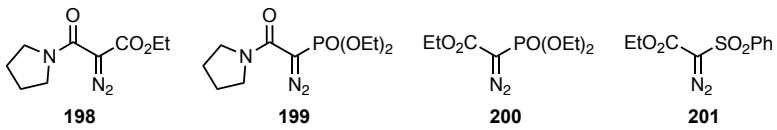
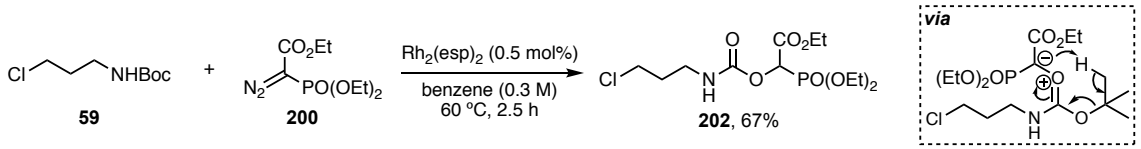


Figure 18: Diazo compounds that did not successfully undergo the desired reactivity under the N–H insertion conditions.

With diazo **198** a small amount (<5%) of N–H insertion product was observed. For diazos **198** and **199** there is a potential intramolecular C–H insertion pathway to form β-lactam products. Though significant amounts of this was not observed in the crude ^{1}H NMR spectrum. When phosphonate containing diazo **200** was subjected to the N–H insertion conditions, rearranged product **202** was isolated in 67% yield (Scheme 54). This carbamate product is presumed to form *via* carbonyl ylide formation with the metal-carbene. Consequent rearrangement through the *N*-Boc group would result in loss of the Boc group and formation of **202**. This type of reactivity was also observed with diazo **201**, though the rearranged product was not isolated with sufficient purity.

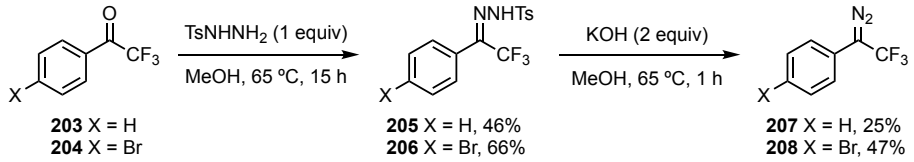


Scheme 54: Rearrangement of **200** upon reaction with **59** to form **202**. Reaction on 0.5 mmol scale.

This side reactivity shows how changing the substituent on the diazo compound can significantly affect the electronics and subsequent reactivity of the diazo compound. Also with respect to the broad range of diazo compounds employed by the Bull group for the synthesis of oxetanes,[168] clearly the range of diazo compounds compatible with the NH insertion

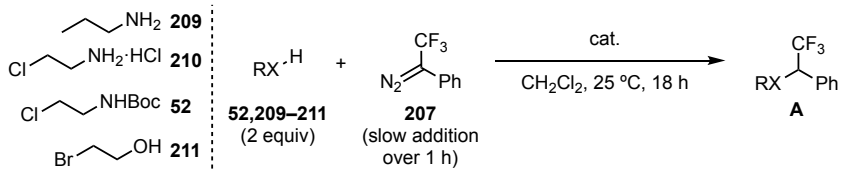
conditions are lower. This is likely due to the lower nucleophilicity of the NH bond in the carbamate protected amine, different catalyst employed and greater number of reaction pathways possible due to the presence of the carbamate protecting group.

Another type of donor-acceptor diazo compound that was tested was an aromatic-CF_3 substituted diazo, such as **207** and **208**.[243] These compounds could be prepared in two steps from the corresponding trifluoroacetophenone by tosylhydrazone formation followed by elimination of the tosyl group (Scheme 55).



Scheme 55: Synthesis of aryl–CF_3 substituted diazo compounds **207** and **208** from trifluoroacetophenones **203** and **204**.

Using conditions developed by Gouverneur for the X–H insertion of aryl–CF_3 diazo substituted diazo compounds,[244] propylamine gave a good yield for the N–H insertion product (Table 10, Entry 1). Additionally, the hydrochloride salt could be used with an additional base (Entry 2). However, Boc-protected amine **52** afforded no product under these conditions or when using $Rh_2(esp)_2$ as catalyst (Entry 3 and 4). Indeed, O–H insertion was moderately successful using 2-bromoethanol as substrate (Entry 5, O–H insertion was not previously shown by Gouverneur).

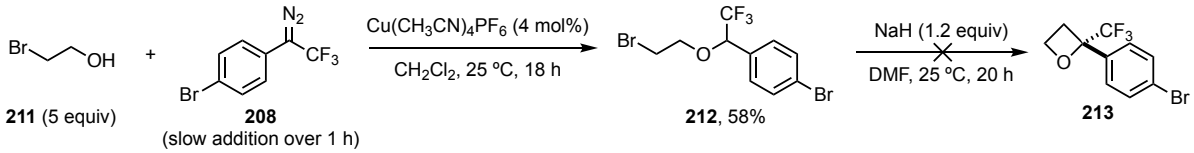


Entry	Nuc	cat.	Yield of **A** (%)[a]
1	**209**	$Cu(MeCN)_4PF_6$ [b]	49
2	**210** + NEt_3	$Cu(MeCN)_4PF_6$ [b]	72
3	**52**	$Cu(MeCN)_4PF_6$ [b]	0
4	**52**	$Rh_2(esp)_2$ (0.5 mol%)	0
5	**211**	$Cu(MeCN)_4PF_6$ [b]	28

Table 10: N–H and O–H insertion of CF_3 substituted diazo **207**. Reactions on 0.2 mmol scale. [a] Yields calculated by ^1H NMR spectroscopy with respect to 1,3,5-trimethoxybenzene as an internal standard. [b] 4 mol% loading.

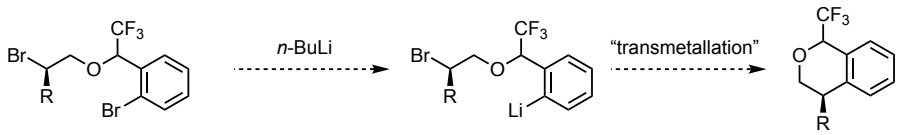
This reaction with 2-bromoethanol was scaled up using 5 equiv of alcohol **211** to afford cyclisation precursor **212** in 58% yield. This could be used to test the cyclisation to the oxetane as the N–H insertion to the Boc protected amine had not worked. Unfortunately, using strongly

basic conditions no oxetane product **213** was observed. Presumably due to the poor acidity of the proton which is required to be deprotonated.



Scheme 56: O–H insertion of diazo **208** followed by attempted cyclisation using NaH.

This work to expand the scope of diazo compounds in the synthesis of saturated nitrogen heterocycles showed the challenges faced when simple substitution of a group is desired. This work could be explored further, for example, for the synthesis of $–CF_3$ containing saturated oxygen or nitrogen heterocycles, the cyclisation step is likely to be the limiting step. Further work could examine stronger bases (*n*-BuLi or LiHMDS) to affect the deprotonation. Additionally, an alternative approach not requiring deprotonation could be examined, for example making use of Li-halogen exchange (Scheme 57).



Scheme 57: Proposed adaptation of OH/NH insertion and cyclisation methodology to access a diverse range of heterocycles.

2.4.4.2 Enantioselectivity

A key limitation of the methodology developed in Section 2.4 is the preparation of the products as racemates. As both the N–H insertion and cyclisation steps bear no stereochemical bias, i.e. no asymmetric information, both result in racemic mixtures of products. Proteins are asymmetric and thus can specifically bind to one enantiomer of a compound resulting in two enantiomers of a compound displaying widely different biological activity.[245] This can make the development of a chiral drug in enantiopure form important for reasons of high activity and safety (most notoriously exemplified by the drug Thalidomide).[246] However, many drugs that have chirality are marketed as racemates.[247] Indeed, the problem of chirality in early stage drug discovery is typically ignored in favour of more rapid achievement of hits, which if racemic would be reduced in activity by up to 50%.[248] Often, two enantiomers can be separated using chiral HPLC in order to test differential activity or safety. However, if one enantiomer has clear safety concerns (as in the case of thalidomide) or the activity of the compound needs to be boosted (a racemate will be limited to 50% potential activity by weight) then an asymmetric synthesis may be required.

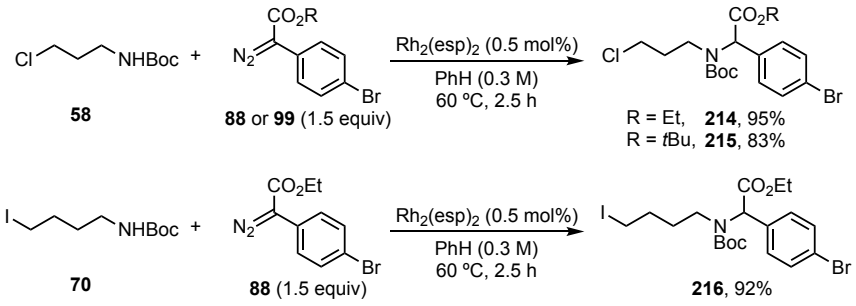
Asymmetric synthesis remains an exciting and challenging field within organic chemistry.[249] Asymmetric N–H insertion reactions using diazo compounds have been widely explored.[250]

Therefore, we could have explored an approach where the stereochemistry is controlled in the N–H insertion step. However, upon deprotonation of the intermediate this stereochemical information would likely be lost. There are a number of reports where the stereochemical information can be conserved in a deprotonation/cyclisation sequence, termed 'memory of chirality'.[251] Yet, these reactions typically require cryogenic temperatures and often specific substrate requirements leading to lack of generality in scope and utility on scale.

As the intermediate generated in the cyclisation step is planar, and if a 'memory of chirality' approach is ruled out, then one alternative is to add an external asymmetric component which can coordinate to the planar intermediate to induce enantioselectivity. One strategy could be asymmetric deprotonation. This involves deprotonation of a substrate with strong base, such as *n*-BuLi, in the presence of an asymmetric ligand, often a diamine such as sparteine.[252] This has been applied to the synthesis of pyrrolidines by cyclisation.[253] However, as this type of enantioinduction occurs during the deprotonation event, a prochiral substrate with two equivalent protons is required and so this cannot be applied to our system.

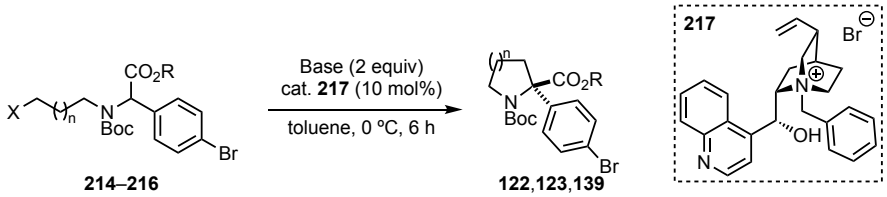
Another strategy would be to use a chiral cation which can coordinate to the already deprotonated substrate.[254] The field of asymmetric phase transfer catalysis involves the coordination of a chiral cation with a deprotonated substrate.[255] We had made use of phase transfer catalysis, using the racemic salt, tetrabutylammonium bromide, in order to increase the rate of cyclisation of the saturated nitrogen heterocycles by increasing the rate of deprotonation by transport of the base from the solid inorganic phase to the organic phase. Therefore, extension of our methodology by replacement of tetrabutylammonium bromide for an asymmetric phase transfer catalyst seemed a logical next step. Phase transfer catalysis does not require cryogenic temperatures and can be used on large scale with significant advantages for industrial application.[256]

We decided to explore the use of *cinchona* alkaloid derived quaternary ammonium salts as asymmetric phase transfer catalysts for the cyclisation step.[257] The N–H insertion intermediates (precursors to the 5- and 6-membered rings synthesised in Section 2.4.3.4 and 2.4.3.5) could be isolated in high yields (Scheme 58).



Scheme 58: N–H insertion of diazo **88** or **99** to form cyclisation precursors. Reactions on 0.5 to 2.0 mmol scale.

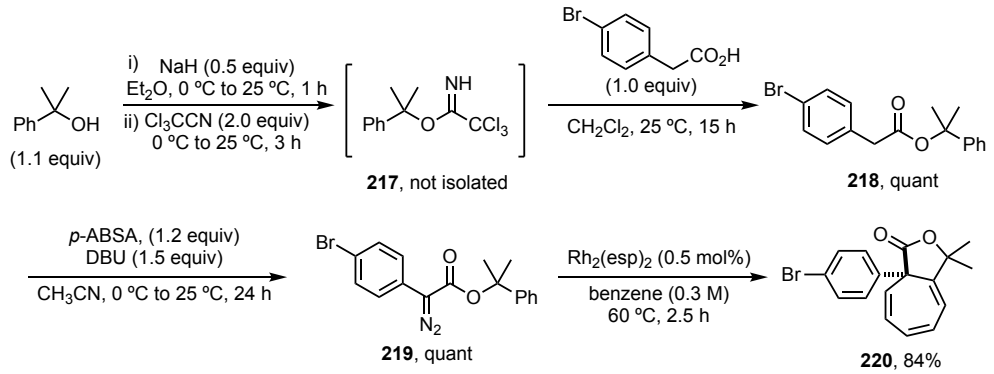
Use of *N*-benzyl cinchonidium bromide cat. **217** as asymmetric phase transfer catalyst did allow the formation of the 5- and 6-membered products (Table 11). However, stereoselectivities were uniformly poor.



Entry	R	X	n	Base	Yield of **122**, **123** or **139** (%)[a]	*er* [b]
1	Et	Cl	1	NaOH	27	55:45
2	*t*Bu	Cl	1	NaOH	50	50:50
3	Et	I	2	KOH	27	47:53

Table 11: Selected attempts to promote an enantioselective cyclisation using asymmetric phase transfer catalyst **217**. Reactions on 0.05 mmol scale. [a] Yields calculated by ^{1}H NMR spectroscopy with respect to 1,3,5-trimethoxybenzene as an internal standard. [b] *er* determined by HPLC analysis of crude reaction mixture on a chiral stationary phase.

One hypothesised route to improved enantioselectivity was altering the ester group to provide greater possibilities for aromatic interactions.[258] Diazo compound **219** was successfully synthesised on scale (Scheme 59). However, subjection of this diazo compound to the N–H insertion conditions (using **58**, not shown) formed product **220** instead of any desired N–H insertion product. This occurred by a Buchner reaction *via* a cyclopropane intermediate, which has been well-studied by Julia using acceptor-acceptor diazo compounds.[259]



Scheme 59: Synthesis of diazo compound **219** and Buchner reaction to form **220**. Reaction to **218** and **219** on 5.0 mmol scale. Buchner reaction to **220** on 0.5 mmol scale.

A common alternative to enantioselective synthesis is to use a chiral auxiliary in order to form diastereomers which can be separated. Cleavage of the chiral auxiliary will yield the enantioenriched compound.[260] Our attempts to utilise menthol esters[261] as chiral auxiliaries met with similar issues of reactivity as with cumyl ester containing diazo **219** in Scheme 59. Another route to enantioenriched compounds explored was the enzymatic resolution of

pyrrolidine **122**. However, this met with no success. This is perhaps not surprising considering that there are few reports of enzyme-mediated hydrolysis of bulky, tertiary esters.[262]

Whilst this avenue of further work is discussed further in Chapter 4, the enantioselective synthesis of the products synthesised in this chapter has not been successful. This may be due to the conformational flexibility of the precursor which could lead to 2 possible enolates and resultant complications in inducing enantioselectivity *via* one diastereomeric transition state. This led us to change the structure to a fixed conformation (see Chapter 4). For further discussion of phase transfer catalysis and a highly enantioselective application of asymmetric phase transfer catalysis in the synthesis of spirocyclic azetidines see Chapter 4.

2.4.5 Conclusions and Future Work

In Chapter 2 the development of a general strategy for the synthesis of 2,2-disubstituted saturated nitrogen heterocycles has been discussed. For a summary of the work developed see Section 2.4.3.9. High yields were achieved when using acceptor-acceptor diazo compounds and donor-acceptor diazo compounds to synthesise a variety of α-quaternary proline analogues. However, low yields were observed when using highly electron-withdrawing aromatic substituents, in particular, pyridine containing diazo compounds. This was despite using a higher loading of the diazo compound with a slow addition. Due to the importance of pyridine motifs within the pharmaceutical industry this is a significant drawback of the methodology. In Section 2.4.4.1 the scope of diazo compounds that gave poor yields or significant side reactions in the developed methodology was discussed. Further work could explore a wider range of diazo compounds by reoptimizing the reaction with different *N*-protecting groups or different catalysts. In order to improve the yield of pyridine containing diazo compounds, one potential avenue of further work (already under investigation in our laboratory) is the use of visible light instead of transition metal catalysis in order to decompose the diazo compound.[263] By removal of the metal this avoids any inhibition by ylide formation and as the metal-carbene is not formed different reactivity should be expected. This also has the advantage of removing the requirement for an expensive and non-abundant Rh catalyst. There is also the potential to adapt this methodology to flow synthesis.[264]

The further issue of the lack of stereocontrol has been discussed within Section 2.4.4.2. This issue will be discussed in more detail within Chapter 4.

3. Ring Expansion of Azetidines

The conversion of one scaffold into another useful scaffold in a step-efficient manner is a significant challenge within organic synthesis. The azetidine ring expansion discussed briefly in Section 2.4.3.8 (Scheme 46) represents a reaction belonging to this class of complexity-generating processes. We were interested in investigating this reaction further, particularly with respect to the scope of azetidines that could undergo this transformation and providing insight into the mechanism of this ring expansion reaction.

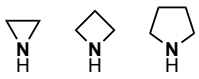
In this chapter the reactivity of azetidines and their use in ring expansion chemistry, particularly in contrast to aziridines will be discussed in Section 3.1. This will be followed by a discussion of the importance of 1,3-oxazinan-2-ones in drug discovery and literature methods to access this scaffold. In Section 3.3 the synthesis of 1,3-oxazinan-2-ones by a ring expansion of carbamate protected azetidines will be discussed.

A concise account of this work can be found in *Organic Letters*.[265]

3.1 Reactivity of Azetidines

3.1.1 Ring Strain of Azetidines

When considering the reactivity of azetidines it is useful to compare to the reactivity of the 3-membered and 5-membered analogues, aziridines and pyrrolidines. Ring strain in the azetidine ring has been calculated to be 105 kJ mol^{-1} which is comparable to the ring strain of an aziridine ring (calculated as 111 kJ mol^{-1} and experimentally determined as 113 kJ mol^{-1}).[266] The ring strain of the five-membered pyrrolidine ring is much lower at 24.8 kJ mol^{-1} (Figure 19).[267] This suggests that, in accordance with ring strain, the reactivity of an azetidine ring should be considered to be much closer to that of an aziridine than a pyrrolidine. For many ring opening or ring expansion reactions of aziridines or azetidines it is more appropriate to consider the reactivity of the aziridinium or azetidinium ion. Couty studied the rate of ring opening of aziridinium and azetidinium ions with DMAP and showed that azetidinium ions are much (1.7×10^4) less reactive than aziridinium ions.[268] When comparing the pK_as of the aziridine, azetidine and pyrrolidine, the azetidine is much closer to the pyrrolidine.[269,270] Basicity and nucleophilicity are proportional and are indicative of the availability of the nitrogen lone pair, so in some circumstances it is expected that azetidine reactivity will be closer to pyrrolidine reactivity than aziridine reactivity.[271] Hence, due to their high strain energy, azetidines can be viewed as highly reactive, yet their low rate of ring opening as an activated azetidinium ion means that in practice they are relatively stable. This makes azetidines highly interesting as relatively stable molecules that could be used in a variety of ring opening/expansion processes if the ring strain can be harnessed.



strain (kJ/mol)	**111**	**105**	**24.8**
pK_a	**8.0**	**11.3**	**11.3**

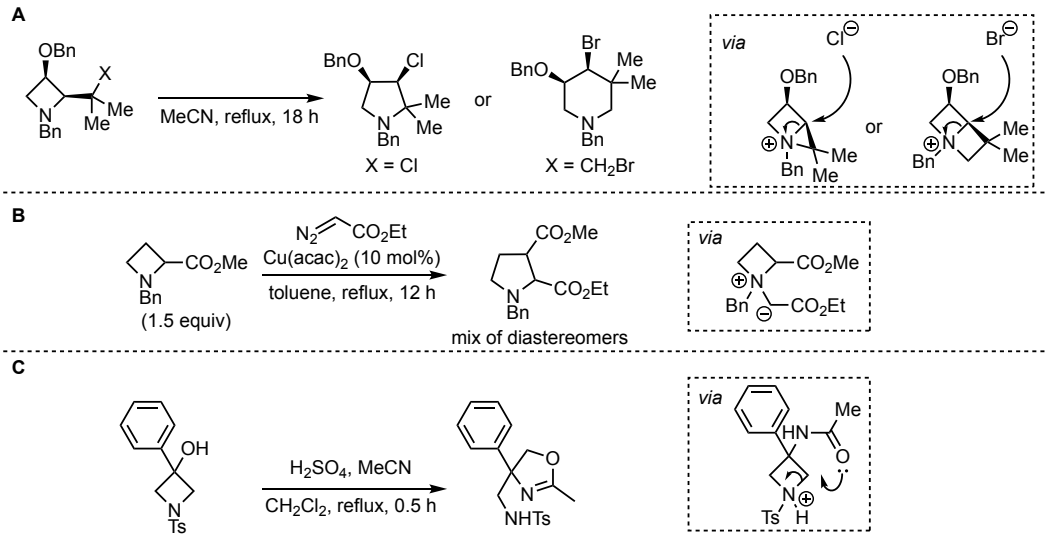
Figure 19: Comparison of the ring strain of aziridines, azetidines and pyrrolidines.

3.1.2 Ring Expansion and Ring Opening of Azetidines

The lower reactivity of azetidines relative to aziridines may be one reason why their reactivity is much less explored.[272] According to common terminology, azetidines bearing an *N*-alkyl, *N*-aryl or N–H are considered 'unactivated' and azetidines bearing an electron withdrawing substituent i.e. *N*-acyl, sulfonyl or carbamoyl are considered to be 'activated'.[273] This shows that the reactivity of an azetidine may be tuned by using a different *N*-substituent. Though the terms activated and unactivated implicitly suggest one is more reactive than another, this reflects the reactivity of the azetidine rather than the azetidinium ion, in fact an unactivated azetidine may be more reactive if the reactivity relies on Lewis basicity.

Many ring expansion methodologies using azetidines make use of a fused bicyclic azetidinium intermediate.[274] An early example of this was shown by De Kimpe where chloro- or bromo-substituted azetidines could be heated to yield pyrrolidines or piperidines (Scheme 60A).[275] These azetidinium intermediates are highly reactive towards nucleophilic attack (note these are 'unactivated' azetidines). Unactivated azetidines bearing an electron donating *N*-substituent can be treated with an electrophile to form an azetidinium ion which can then undergo ring expansion i.e. by 1,2-sigmatropic rearrangement (Scheme 60B, which actually proceeds via a diradical mechanism to form a mix of diastereomers).[276] Many other ring expansion reactions of azetidines proceed through a stepwise ring opening and ring closure sequence.[277]

There are also some examples of an azetidine substituent attacking the azetidine ring, in an intramolecular fashion, leading to ring opening. For example, Baxendale recently showed a cascade reaction of *N*-Ts protected 3-hydroxyazetidines with an acid mediated Ritter reaction followed by intramolecular ring opening of the azetidine (Scheme 60C).[278] Protonation of the azetidine to form the azetidinium ion was required for the cascade ring opening which produced oxazoline products.



Scheme 60: Selected examples of ring expansion and ring opening reactions of azetidines.

3.2 1,3-Oxazinan-2-ones

3.2.1 1,3-Oxazinan-2-ones

1,3-Oxazinan-2-ones are 6-membered cyclic carbamates (Figure 20). They are the 6-membered analogue of the more common 1,3-oxazolidin-2-one. 1,3-Oxazolidin-2-ones feature in a number of drug molecules including Linezolid, an antibiotic which is on the WHO essential medicines list.[279] Enantiopure oxazolidinones have found application in asymmetric synthesis, and are referred to as Evans auxiliaries, where they are used to control the stereochemical outcome of aldol reactions.[280] Vinyl benzoxazinanones have found application in palladium catalysis as π-allyl Pd-complex precursors which can extrude CO_2 to form an ambiphilic reagent for cycloaddition chemistry.[281]

3.2.2 1,3-Oxazinan-2-ones in Drug Discovery

1,3-Oxazinan-2-ones feature in a wide array of bioactive compounds including natural products and pharmaceuticals (Figure 20). They have been utilized as the core scaffold in anti-HIV,[282] antidiabetic,[283] anti-inflammatory[284] and anti-cancer compounds.[285] They have also found use as intermediates in organic synthesis, including in the synthesis of drug compounds and natural products.[286]

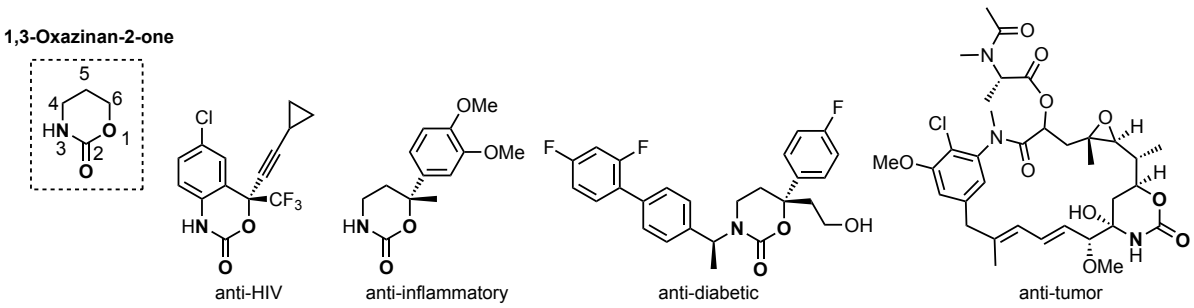


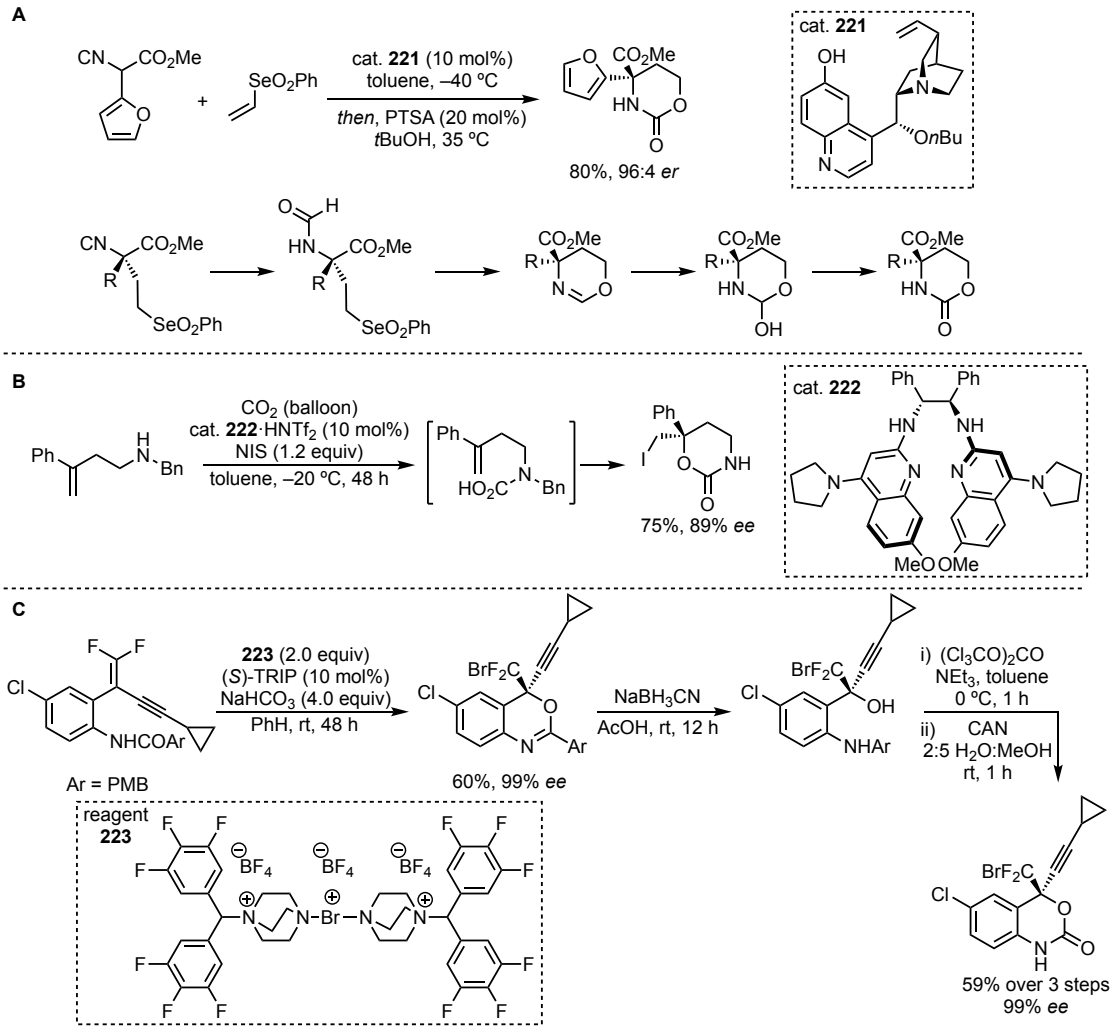
Figure 20: 1,3-Oxazinan-2-ones in drug discovery and natural products.

3.2.3 Synthetic Approaches to 1,3-Oxazinan-2-ones

Traditional approaches for the synthesis of 1,3-oxazinan-2-ones involve the reaction of an amino alcohol with a C_1 building block i.e. phosgene, triphosgene or carbonyldiimidazole (CDI).[287] There have been many other methods developed for the synthesis of a variety of differentially substituted 1,3-oxazinan-2-ones.[288] Most of these methods are limited to monosubstitution and disubstitution is more limited. An important exception to this is Zhu's use of phenyl vinyl selenones in a cascade reaction to generate 4,4-disubstituted 1,3-oxazinan-2-ones, including enantioenriched examples (Scheme 61A).[289]

An interesting approach to oxazinanones is the trapping of CO_2 with allylic or propargylic amines.[290] Recently, Johnston further developed this type of reaction for an enantioselective synthesis of 6,6-disubstituted 1,3-oxazinan-2-ones (Scheme 61B).[291] Using NIS with allyamines and a chiral acid catalyst **222** afforded high enantioselectivity of the oxazinanone products, though it was found that specific conditions including the water content and catalyst crystallinity were required for high conversion to be achieved.

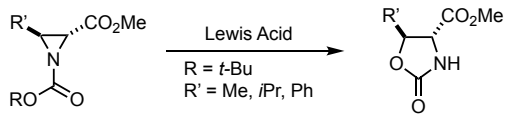
Very recently, Toste reported a chiral anion phase transfer catalysed bromocyclization to generate cyclised compounds with $–CF_2Br$ functional groups.[292] The developed reaction was used as a key step in the synthesis of an efavirenz analogue in high *ee* (Scheme 61C).



Scheme 61: Selected methods to access 1,3-oxazinan-2-ones.

3.2.4 Synthesis of 1,3-Oxazinan-2-ones from Azetidines and Related Ring Expansions

In 1997 and 1999, Tomasini reported the 3- to 5-membered ring expansion of *N*-acyl aziridines to afford 1,3-oxazolidin-2-ones.[293] The reaction was promoted by Brønsted acids or Lewis acids and was observed to be diastereoselective (Scheme 62). Related ring expansions of aziridines have been reported by Ha and Lee.[294] Gotor utilised a related cascade ring opening of aziridines to form the oxazolidinone core of Linezolid.[295]

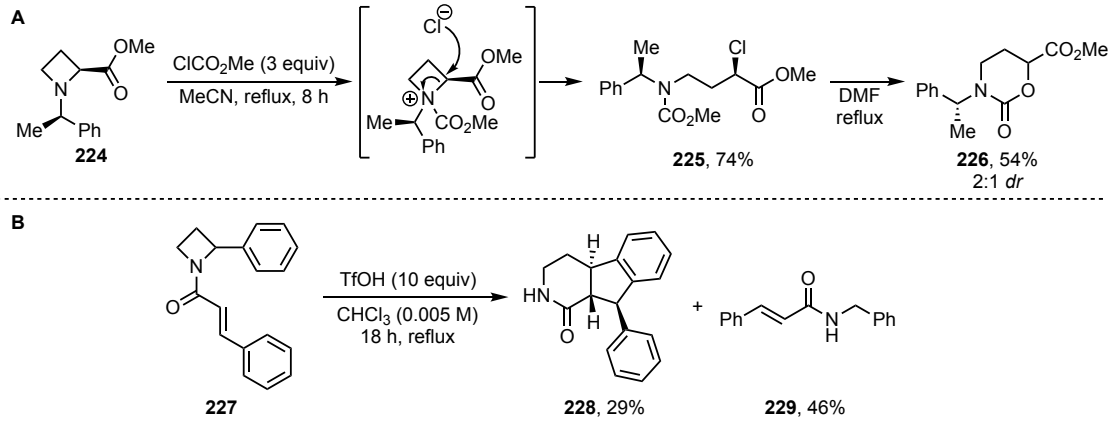


Scheme 62: Lewis acid catalysed ring expansion of *N*-acyl aziridines to 1,3-oxazolidin-2-ones by Tomasini.

Related ring expansions of azetidines to yield six-membered ring products are rarer. In 2007, Ha and Lee reacted azetidine **224** with methyl chloroformate which resulted in the ring opening to acyclic intermediate **225** (Scheme 63A). Heating **225** under reflux led to *O*-alkylation with resultant formation of oxazinanone **226**. This represents a related transformation to the ring

expansion reaction discussed in this chapter. Though only one example was shown and the reaction was carried out in a stepwise manner.

King and co-workers showed that TfOH could promote the ring expansion of azetidine **227** to give 6-membered ring **228** in low yield (Scheme 63B). Though no mechanism was proposed, this cascade reaction presumably results from a carbocation intermediate upon ring opening of the azetidine, followed by trapping with the alkene and consequent Friedel–Crafts alkylation. In addition, amide **229** was formed which was assumed to be due to acetylene elimination from the azetidine.



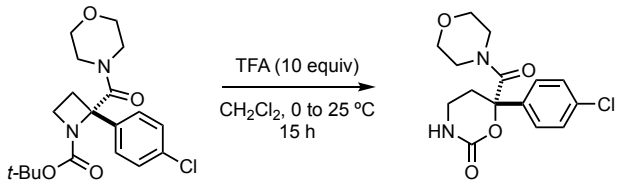
Scheme 63: Azetidine ring opening/closing to form a 1,3-oxazinan-2-one and ring expansion of an acyl-azetidine.

Though 3- to 5-membered ring expansions of aziridines have been well explored, except for the two above-mentioned examples, the related 4- to 6-membered ring expansion of azetidines has not been studied. As the azetidine ring displays similar ring strain to its 3-membered analogue, we were interested to see if we could harness this strain to synthesise 6-membered ring products.

3.3 Results and Discussion

3.3.1 Ring Expansion of Azetidine Carbamates: Initial Hit

Aside from the reaction previously discussed in Section 2.4.3.8, azetidine **187** was subjected to typical Boc-deprotection conditions, using TFA, which yielded oxazinanone **230** in 43% yield (Scheme 64). This was particularly interesting because this converted a functionalised azetidine into a new scaffold, which had no protecting groups or other groups not desirable for medicinal chemistry. With a Mw of 325 Da and Log*P*[296] of 0.91 and 7 non-carbon/hydrogen atoms, this product was immediately interesting as a compound of interest to be included in a pharmaceutical screening collection.



Scheme 64: Attempted Boc-deprotection of **187** and 1,3-oxazinan-2-one formed as the major product.

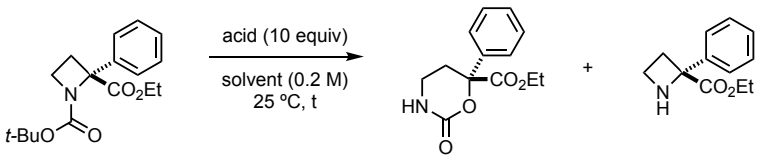
Given the interest in the synthesis of 1,3-oxazinan-2-ones and their use in drug discovery we were interested to explore this reaction further. The reaction is complementary to many of the methods discussed in Section 3.2.3 but is distinct due to the few number of reports which can form densely substituted carbon centres at the 6-position and as the oxazinanone is formed with no *N*-substituent. While the analogous ring expansion of aziridines is well explored (Section 3.2.4), the ring expansion of azetidines in one step has not been previously extensively investigated.

3.3.2 Optimisation of Ring Expansion Reaction

Although the reaction to form oxazinanone **177** in Section 2.4.3.8 gave very high yield (96% on small scale), we decided to test a range of acids and solvents to explore what would promote the reaction successfully. As one potential pathway by which this reaction was occurring was *via* positive charge build up at the benzylic site (the mechanism of the reaction is discussed in Section 3.3.4), a conscious decision was made not to bias the aromatic ring electronically and azetidine **104** was selected in order to optimise the reaction.

Carrying out the reaction on 0.2 mmol scale using TFA in CH_2Cl_2 gave a high yield of oxazinanone **231** with no Boc deprotection which would give azetidine **232** (Table 12, Entry 1). Changing the acid from TFA to HCl (4 M HCl in 1,4-dioxane) gave a mixture of products **231** and **232** in a 1:3 ratio (Entry 2). Carrying out the reaction in 1,4-dioxane gave an isolated yield of azetidine **232** 71% with no significant formation of the oxazinanone **231** (Entry 3). Using sulfonic acids (PTSA and CSA) gave mixtures of products without full conversion in 1 h (Entries 4 and 5). Acetic acid was not a strong enough acid to promote the reaction at this temperature or reaction time (Entry 6). TfOH, a much stronger acid than TFA or the other acids tested, gave 49% of the oxazinanone with a small amount of *N*-deprotected azetidine as a side product (Entry 7). Using $BF_3 \cdot OEt_2$ as a Lewis acid selectively formed the oxazinanone, though in lower yield than TFA (Entry 8). Using TFA as acid in different solvents showed that non-polar solvents were uniformly the best choice (Entries 9–12). Toluene and CH_2Cl_2 gave selective ring expansion in comparison to hexane which formed a mixture of oxazinanone:azetidine in a ratio of 3.5:1. Toluene was selected for further optimisation as it gave a similar yield to CH_2Cl_2 and is considered to be more sustainable and environmentally friendly.[297] Considering that the acid required for the transformation should be catalytic, it was interesting to try to reduce the

amount of TFA used. However, reducing the equivalents of TFA significantly slowed down the rate of reaction at 25 ºC (Entries 14 and 15). The reaction could presumably be carried out in TFA as solvent, yet TFA is not a desirable solvent.[297] We then sought to increase the rate of reaction by increasing the concentration of the toluene and in doing so reduce the amount of solvent waste upon scale up of the reaction. Performing the reaction with 5 equiv of TFA at 1.0 M concentration reduced the amount of TFA by half and the amount of toluene by 5 times, without a significant decrease in the yield of the reaction after 30 min (Entry 16). This resulted in an isolated yield of 76% for **231** in a more process friendly manner than the previous high yields obtained.



104 **231** **232**

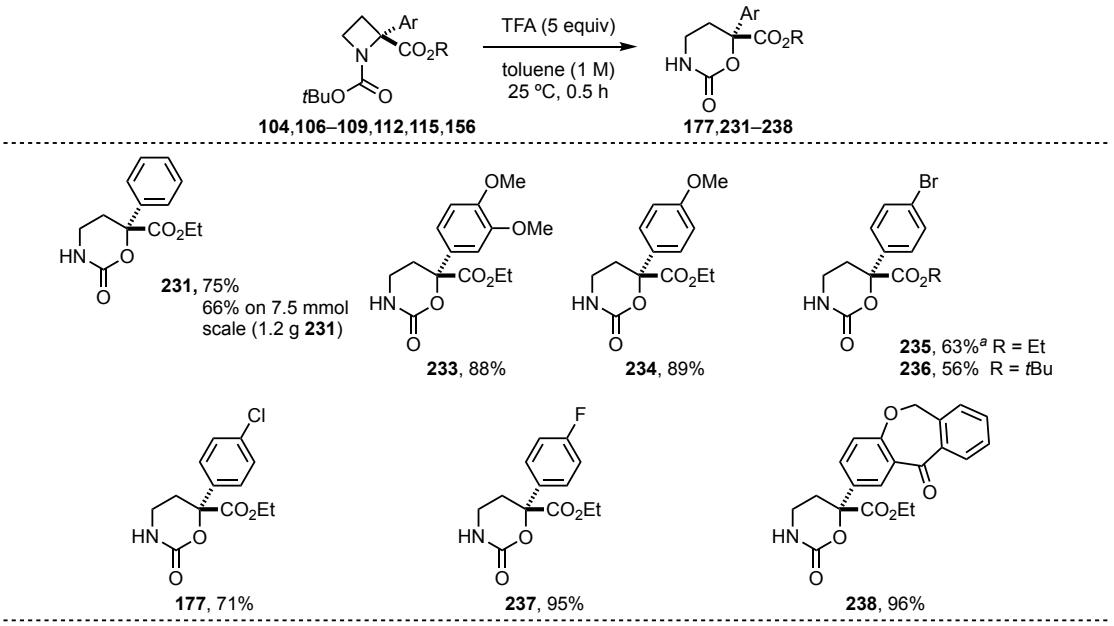
Entry	Acid	Solvent	t (h)	Yield (%) [a]			
				104	**231**	**232**	Total
1	TFA	CH_2Cl_2	1	0	89	0	89
2	4 M HCl [b]	CH_2Cl_2	1	0	22	65	87
3	4 M HCl [b]	1,4-dioxane	24	0	0	(71)	71
4	PTSA·H_2O	CH_2Cl_2	1	14	23	52	89
5	CSA	CH_2Cl_2	1	65	4	16	85
6	CH_3CO_2H	CH_2Cl_2	1	95	0	0	95
7	TfOH	CH_2Cl_2	1	0	49	7	56
8	BF_3·OEt_2 [c]	CH_2Cl_2	1	0	58	0	58
9	TFA	EtOAc	1	97	0	0	97
10	TFA	MeCN	1	0	6	3	9
11	TFA	hexane	1	0	77	22	99
12	TFA	toluene	1	0	93	0	93
13	TFA	toluene	0.16	0	94	0	94
14	TFA [c]	toluene	1.5	76	16	0	92
15	TFA [d]	toluene	0.5	40	53	0	93
16	TFA [d,e]	toluene	0.5	0	87 (76)	0	87

Table 12: Optimisation of ring expansion of azetidine **104** to 1,3-oxazinan-2-one **231**. Reactions on 0.2 mmol scale. [a] Yields calculated by ^{1}H NMR spectroscopy with respect to 1,3,5-trimethoxybenzene as an internal standard. Yields in parentheses are isolated. [b] Solution in 1,4-dioxane. [c] 2 equiv. [d] 5 equiv. [e] 1.0 M.

3.3.3 Scope of 4- to 6-Membered Ring Expansion

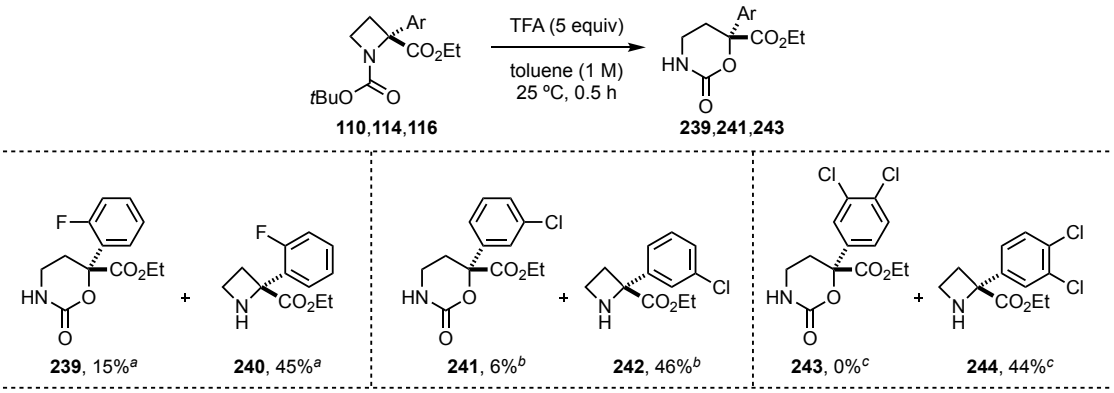
With optimal conditions in hand for the ring expansion of *N*-Boc protected azetidines to 1,3-oxazinan-2-ones the scope of aromatic and ester groups was studied. On 0.5 mmol scale 75% yield was obtained for oxazinanone **231** which is in agreement with the result from Table 12 on 0.2 mmol scale using the same conditions (Scheme 65). Scaling up this reaction to 7.5 mmol scale (15 × scale) gave only a small decrease in yield (66%) to afford 1.2 g of

oxazinanone **231**. High yields of the oxazinanone products were achieved when azetidines with electron-rich aromatic substituents were subjected to the ring expansion conditions. Aromatic substituents with *para*-Br, Cl or F were well tolerated with the yield correlated with the π-electron donating ability of the halogen (–F > –Cl > –Br).[298] The acid sensitive ester group –CO_2*t*Bu was well tolerated with no side-product formation observed due to ester hydrolysis. Isoxepac derived azetidine **156** was subjected to the reaction conditions to afford oxazinanone **238** in 96% yield.



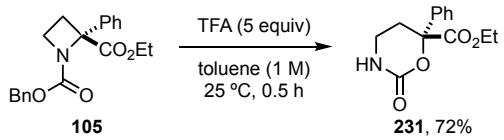
Scheme 65: Successful examples using optimised conditions for the ring expansion of *N*-Boc azetidines to 1,3-oxazinan-2-ones. Reactions on 0.5 mmol scale. [a] 10 equiv of TFA for 1 h.

Scheme 65 shows the successful substrates for the ring expansion reaction. All of these substrates are relatively electron-rich or have substituents which are able to donate π-electrons to the carbon where C–O bond formation occurs. When a –Cl or –F substituent was used in the *ortho*- or *meta*-position of the aromatic ring poor yields and conversion were observed. When *o*-F substituted substrate **110** was subjected to the reaction conditions a 1:3 product ratio (1,3-oxazinan-2-one **239**:deprotected azetidine **240**) was observed (Scheme 66). Inspection of the crude ^{1}H NMR spectrum showed that 24% of protected azetidine **110** was remaining after 0.5 h. While the *ortho*-fluoro substituent still has the same level of π-donation as *para*-fluoro, the σ-electron withdrawal is much greater due to the proximity to the reacting carbon. The trend for poorer conversion and yield upon increased σ-electron withdrawing ability and poorer π-electron donating ability was also observed with azetidines **114** and **116**.



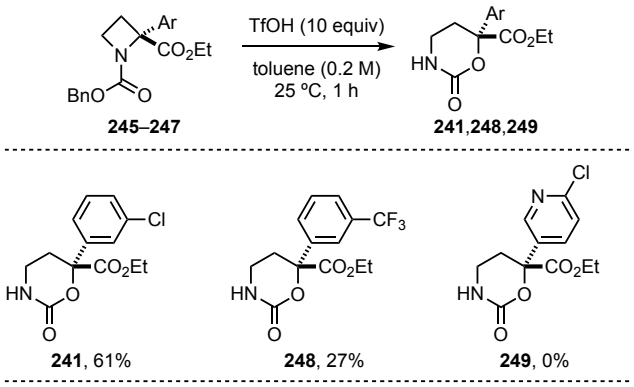
Scheme 66: Ring expansion of Boc protected azetidines with electron-poor aromatic substituents. [a] 76% conversion, **240** was not isolated, yields calculated by ^{1}H NMR spectroscopy with respect to 1,3,5-trimethoxybenzene as an internal standard. [b] 2 h reaction time, 79% conversion. [c] 52% conversion.

Clearly the poor yields achieved with more electron-poor aromatic rings, that had poor π-donating ability, was a challenge that needed to be overcome. A significant step in this direction came when using phenyl substituted Cbz-protected azetidine **105** which upon treatment with TFA under the standard conditions yielded oxazinanone **231** in essentially the same yield as when using a Boc-protected azetidine (Scheme 67).



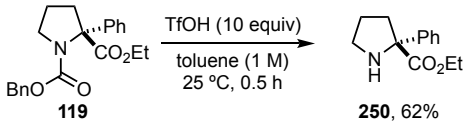
Scheme 67: Ring expansion of Cbz-protected azetidine **105** to 1,3-oxazinan-2-one **231**. Reaction on 0.1 mmol scale.

As the Cbz protecting group is much more resistant to acidic deprotection than the Boc protecting group, there was the possibility to use stronger acids in order to try to promote the ring expansion of Cbz-protected azetidines with electron poor aromatic substituents. It was hypothesised that a stronger acid would increase the rate and degree of protonation resulting in a greater possibility for the ring expansion reaction to occur. With Cbz-protected azetidine **245**, the reaction with TFA proceeded but the reaction progress was very slow. However, the reaction progressed smoothly with TfOH, which is a much stronger acid than TFA, affording oxazinanone **241** in 61% yield (Scheme 68). This represented a 10-fold increase compared to the reaction with Boc protected azetidine **114** when using TFA under the standard conditions. This was tested further with highly electron withdrawing aromatic rings including *meta*-CF_3 azetidine **246** and pyridyl substituted azetidine **247**. Oxazinanone **248** was isolated in 27% yield with full conversion observed by ^{1}H NMR spectroscopy from azetidine **246**. No product was observed when using azetidine **247** which may be due to protonation of the pyridine under the reaction conditions and inhibition of the reaction by the consequent increase of the electron-withdrawing character of the aromatic substituent. This demonstrated the limitation of this modified process to afford oxazinanones with electron-poor aromatic substituents.



Scheme 68: Scope of ring expansion of Cbz-protected azetidines with electron-withdrawing aromatic rings to 1,3-oxazinan-2-ones. Reactions on 0.1–0.2 mmol scale.

To establish whether the reaction required the ring strain of the azetidine to drive the reaction, Cbz-protected pyrrolidine **119** was subjected to the modified reaction conditions with TfOH (Scheme 69). These conditions were chosen as it was assumed that a strong acid may be required to promote the reaction with a lower ring strain and additionally the Cbz protecting group is more resistant to acidic deprotection (it was assumed that the acidic cleavage of the Boc group would be much faster than any 5- to 7-membered ring formation). No ring expansion was observed and only deprotected pyrrolidine **250** was isolated in the reaction. This suggests that, as expected, the ring strain of the azetidine is required to promote the ring expansion. The C=O stretch of the carbamate group in the IR spectrum also suggests that the azetidine lone pair is more available to protonation than in the pyrrolidine and piperidine (IR stretch for carbamate C=O in azetidine **110**, pyrrolidine **118** and piperidine **133** is 1706, 1690 and 1694 cm^{-1} respectively).

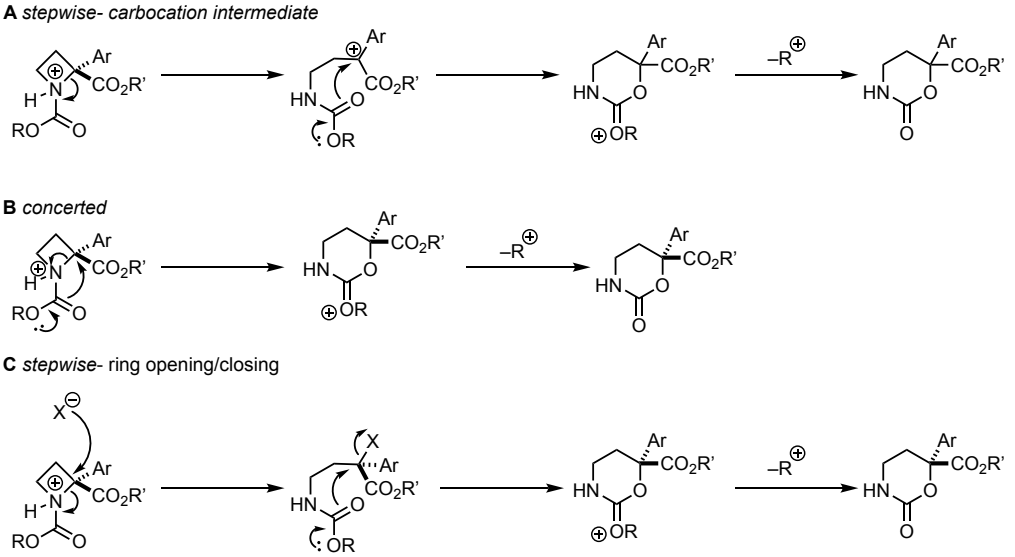


Scheme 69: Attempted 5- to 7-membered ring expansion with only Cbz-deprotection observed. Reaction on 0.05 mmol scale.

3.3.4 Mechanism of the Ring Expansion

There are multiple mechanisms that could be consistent with the observed ring expansion and the scope of the reaction. These mechanisms are detailed in Scheme 70. For all, the first step is assumed to be protonation on the nitrogen atom of the azetidine to form an azetidinium ion. There is clear evidence from the scope of the reaction that there is positive charge build up at the benzylic site due to the significant competing effects of π-electron donation/σ-electron withdrawal from substituents on the aromatic ring. The first proposed mechanism (A) occurs through a stepwise C–N bond cleavage to form a discrete carbocationic intermediate which is then trapped by C–O bond formation through the carbamate group. This is followed by loss of the R group (as R^+) from the carbamate group to afford the oxazinanone product. The second

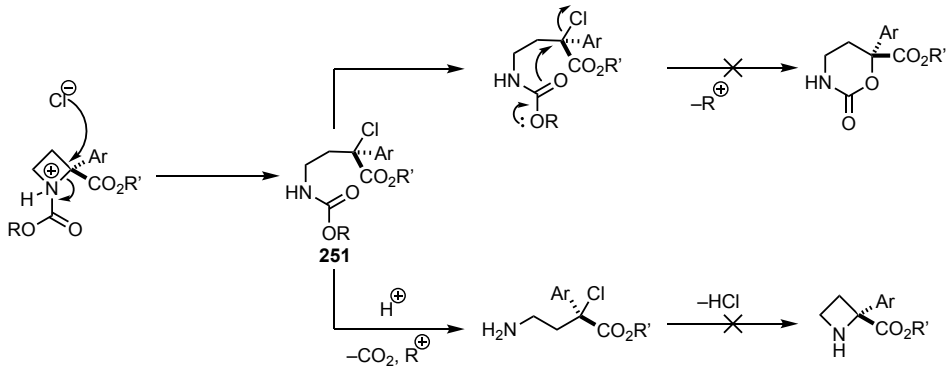
mechanism (B) occurs through a concerted C–O bond formation and C–N bond cleavage event. Upon protonation of the nitrogen atom, positive charge build up on the most substituted carbon atom results in C–N bond lengthening and weakening and *O*-alkylation *via* the carbamate group occurs at the same time as C–N bond cleavage. The third proposed mechanism (C) is more distinct from the A and B, here a nucleophile (likely the conjugate base of the acid) attacks the most substituted carbon atom where there is significant positive charge build up (similar to the reaction in Scheme 63A, Section 3.2.4). This is then followed by a ring closure through an oxygen of the carbamate group. A further option for each of these mechanisms would be that the ring expansion occurs through the formation of a carbamic acid and consequent trapping of this intermediate. However, subjection of Cbz-protected pyrrolidine **119** with TFA provided no reaction. This indicates that in the case of Cbz-protected azetidine **105** no carbamic acid would be formed and thus no reaction *via* this intermediate. Therefore, ring expansion with Cbz-protected azetidine **105** (Scheme 67) shows that it is likely that the intact carbamate reacts and the last step is loss of the R group.



Scheme 70: Possible reaction mechanisms for the ring expansion of azetidine carbamates to 1,3-oxazinan-2-ones.

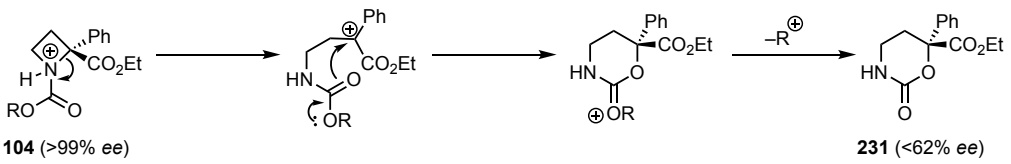
As a distinct mechanism from A and B, mechanism C can be discussed separately. One of the main reasons that this mechanism is not likely to be the dominant mechanism is the ring closure step. A *tert*-butyl or benzyl carbamate is not typically considered to be highly nucleophilic (we have already ruled out the carbamic acid as an intermediate) and thus any S_N2 displacement of X at the tertiary carbon centre would be exceedingly slow (if not impossible due to the nature of the tertiary carbon centre). Alternative S_N1 substitution from the tertiary carbon centre would essentially reduce mechanism C to mechanism A. The main difference remaining is whether the conjugate base of the acid aids ring opening of the azetidine. This is likely disputed by the differential reactivity of HCl, where significant Boc deprotection is observed. Attack of Cl^- in step 1 of mechanism A would lead to intermediate

251 (Scheme 71) similar to the reactivity observed by Ha and Lee (Section 3.2.4, Scheme 63A). It is difficult to see how this would proceed to form the unprotected azetidine as there would be no driving force for cyclisation (cyclisation would be reversible). Likewise, it is not expected that the trifluoroacetate anion would attack this tertiary carbon centre in order to aid ring opening.



Scheme 71: Pathway for azetidine deprotection or ring expansion *via* mechanism C, i.e. ring opening by conjugate base of HCl.

From this discussion, we can limit the choice of mechanism to A and B, i.e. either a stepwise or concerted mechanism. The main difference between the two mechanisms is whether a discrete carbocation intermediate is formed. As mechanism A proceeds through a planar carbocationic intermediate, enantioenriched starting material would be expected to undergo racemisation (assuming fast bond rotation). If the reaction proceeded through concerted mechanism B then the stereochemistry would be expected to be preserved in the oxazinanone product. In order to test this, a racemic mixture of azetidine **104** was separated using HPLC (see Section 6.2.2.6 for full details). Each enantiomer was subjected to the reaction conditions and the crude reaction mixture was subjected to HPLC analysis (Scheme 72). This showed that significant ablation of stereochemistry was observed during the reaction (>99% *ee* to <62% *ee*). Upon resubjecting enantioenriched product **231** to the reaction conditions, no change in the stereochemical ratio was observed. Additionally, the remaining starting material remained highly enantioenriched at the end of the reaction (>99% *ee*). This shows that the ablation in enantioenrichment is occurring during the reaction and indicates the formation of a carbocationic intermediate. Interestingly, the retention of some of the enantioenrichment (non-zero *ee*) suggested that the rate of ring closure by *O*-alkylation was fast enough to compete with rotation of the planar carbocationic intermediate.



104 (>99% *ee*) **231** (<62% *ee*)

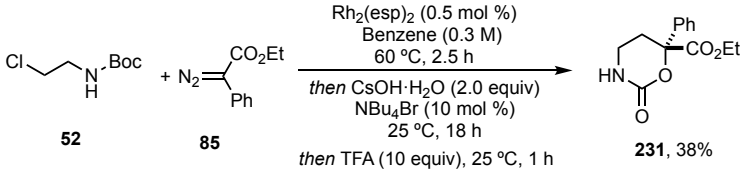
Scheme 72*:* Mechanistic rationale for the ring expansion reaction of azetidine carbamates to explain loss of enantioenrichment. It is assumed that the remaining enantioenrichment is due to retention of absolute configuration rather than inversion of configuration.

This evidence is sufficient to support stepwise mechanism A (Scheme 70), where a C–N bond cleavage forms a benzylic carbocation which is subsequently trapped by the carbamate group to form the 6-membered ring. Although mechanism B cannot be ruled out as a competitive pathway, our results show significant evidence of mechanism A.

3.3.5 N–H Insertion/Cyclisation/Ring Expansion (NICE) Sequence

Having established the scope of the reaction and investigated the mechanism of the transformation, we were interested in overcoming another potential limitation of the methodology: the requirement to synthesise the azetidine precursor. The azetidine starting materials could be accessed through the N–H insertion and cyclisation strategy previously described in Chapter 2. Some of these products can be difficult to isolate by column chromatography and if they are not desired for other diverse transformations then we wondered if their isolation could be avoided. Therefore, we aimed to access the 1,3-oxazinan-2-one desired products in 3 steps either in a one-pot or telescoped process (without isolation of the azetidine intermediate).

This was carried out initially using diazo **85** and Boc-protected amine **52** on 0.5 mmol scale (Scheme 73). The N–H insertion and cyclisation conditions (discussed in Chapter 2) were used to form azetidine **104** (isolated yield was 69% in Section 2.4.3.3). Directly to this reaction mixture TFA was added and the reaction mixture stirred for a further 1 h at 25 ºC. Oxazinanone **231** was then isolated in 38% yield. This represents only a small decrease in yield relative to the highest theoretical yield of 52% (i.e. if the isolated yields of the azetidine and one-step ring expansion reaction were combined).

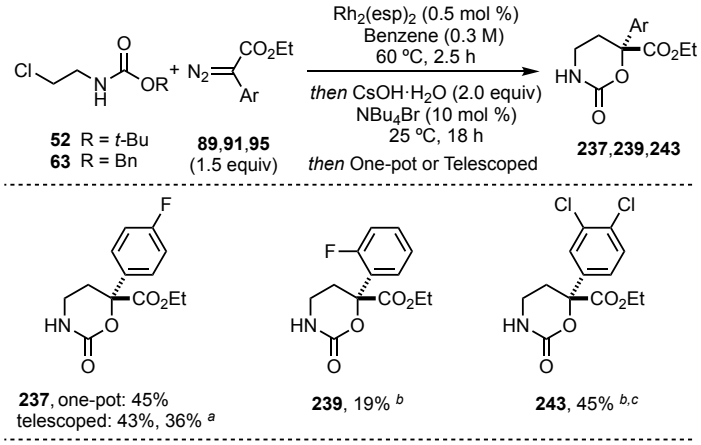


Scheme 73: One-pot NICE reaction to afford oxazinanone **231** over 3 steps. Reaction 0.5 mmol scale.

The one-pot reaction was then demonstrated to form oxazinanone **237** due to the presence of the *para*-F aromatic within a known treatment for diabetes (Section 3.2.2, Figure 20). Oxazinanone **237** was formed in 45% yield in 3 steps using the same one-pot methodology (Scheme 74). The purification of the oxazinanone was more difficult when using the one-pot methodology due to the presence of a number of side products due to the 3 different reaction steps. To overcome this a telescoped process was developed. Following the N–H insertion and cyclisation steps the crude reaction mixture was filtered through silica with CH_2Cl_2 followed by concentration to remove the solvent and then the ring expansion was carried out using the conditions developed in Section 3.3.2. This telescoped process simplified the purification of

oxazinanone **237** and gave a similar isolated yield to the one-pot process. This telescoped process was also more amenable for scale-up of the reaction. On 3 mmol scale oxazinanone **237** was formed in 36% yield to give 290 mg of oxazinanone from the acyclic precursors in 3 reaction steps and only one chromatographic purification.

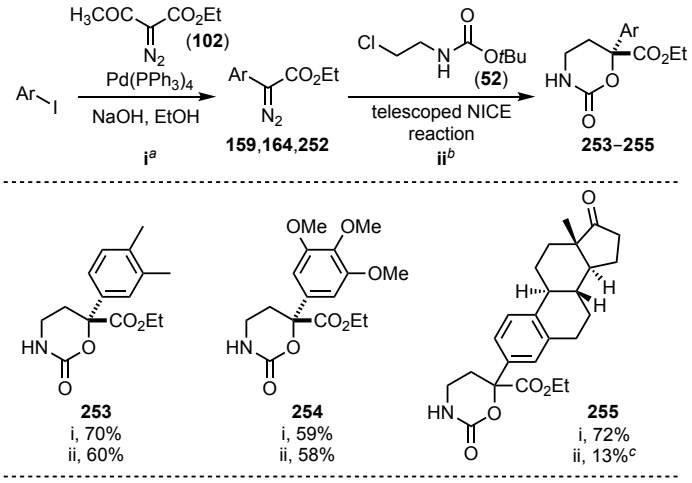
The ring expansion from linear precursors was then shown using the conditions adapted for aromatic groups with poor π-electron donating and significant σ-electron withdrawing substituents. Using TFA with Boc-protected azetidine **110** gave poor yield in the ring expansion reaction due to the high destabilisation of the carbocation intermediate and much greater competitive deprotection was observed. Carrying out the reaction with Cbz-protected amine **63** and diazo **89**, followed by addition of TfOH in one-pot to the formed Cbz-protected azetidine, gave oxazinanone **239** in 19% yield. This was a higher yield over 3 steps than previously observed using the standard ring expansion conditions over 1 step. Using the same conditions to synthesise **243** gave 45% yield over 3 steps. Using the previous conditions from Boc-protected azetidine **116** had given no product.



Scheme 74: One-pot and telescoped reactions to afford oxazinanones. Reactions on 0.5 mmol scale. One-pot: **52** (1.0 equiv), addition of TFA (10 equiv), 25 ºC, 1 h. Telescoped: **52** (1.0 equiv), filtration through silica with CH_2Cl_2, concentrate, addition of TFA (5 equiv), toluene, 25 ºC, 0.5 h. [a] 3 mmol scale. [b] One-pot using **63** (1.0 equiv), TfOH (10 equiv), 0.5–1.5 h. [c] 2.5 equiv of **95** used.

We then sought to demonstrate that a wider range of diazo compounds could be employed in the telescoped N–H insertion/cyclisation/ring expansion (NICE) sequence. By using the Pd-catalysed coupling of aryl iodides to prepare diazo compounds developed by Wang (previously discussed in Section 2.4.3.7) this reduced the synthesis of the diazo compound to the availability of the aryl iodide. Using this Pd-catalysed reaction three different diazo compounds were prepared and subjected to the telescoped NICE reaction (Scheme 75). The yields of the diazo synthesis were uniformly high. For diazo compounds **253** and **254** the telescoped NICE reactions gave very good 60% and 58% yields respectively (42% and 34% in 4 steps from the aryl iodide with 2 chromatographic purifications). Diazo **159** (previously synthesised in Section 2.4.3.7) was used in the telescoped reaction to form oxazinanone **255** in 13% yield. This

product is assumed to be a 1:1 mixture of diastereomers. Although the yield of the estrone containing oxazinanone **255** was disappointing, this represents 9% yield over 4 steps from a complex aryl iodide.

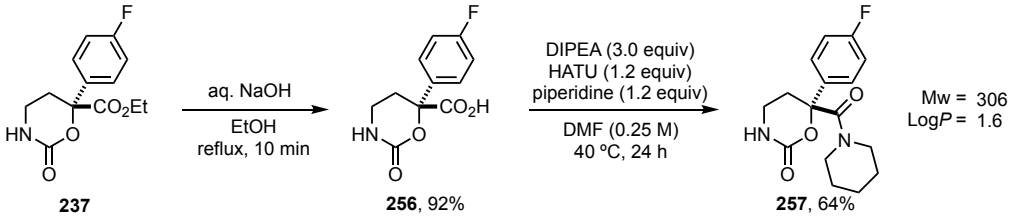


Scheme 75: Telescoped NICE reaction coupled with synthesis of diazo compound from aryl iodides to access oxazinanones in 4 steps. [a] Reactions on 2 mmol scale. [b] 0.5 mmol scale. [c] 0.2 mmol scale.

3.3.6 Functionalisation of 1,3-Oxazinan-2-one Scaffold

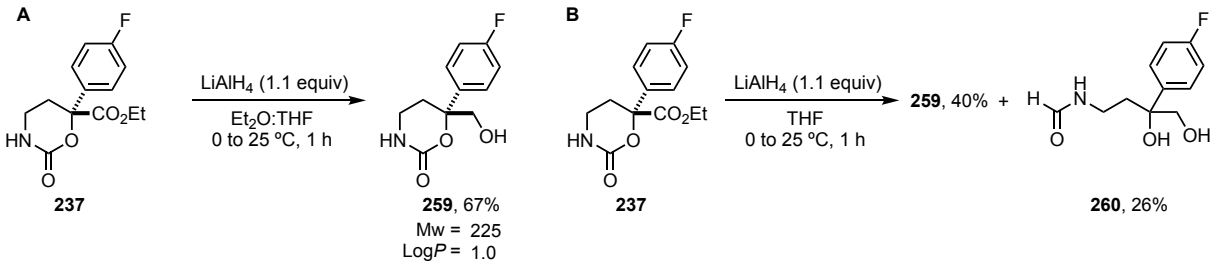
As discussed within Section 2.4.3.8, the ease of diversification of a compound determines their desirability as a lead in drug discovery. We envisaged that the 6,6-disubstituted 1,3-oxazinan-2-ones produced in the ring expansion detailed in this chapter could be readily elaborated by the ester handle and the carbamate nitrogen.

Firstly, the ester hydrolysis of oxazinanone **237** was shown to be very rapid when heating under reflux (Scheme 76). This is in comparison to the more hindered piperidine ring which was difficult to hydrolyse under similar conditions in Section 2.4.3.8. Arguably, this oxazinanone carboxylic acid **256**, readily formed in one step, is a useful screening compound in its own right. Although carboxylic acids can be used as screening compounds and within drug compounds,[299] they can pose toxicity issues.[300] Amide bond formation using piperidine with HATU as coupling agent afforded amide **257** in good yield. This oxazinanone is highly 3-dimensional and is an interesting lead-like compound for screening.



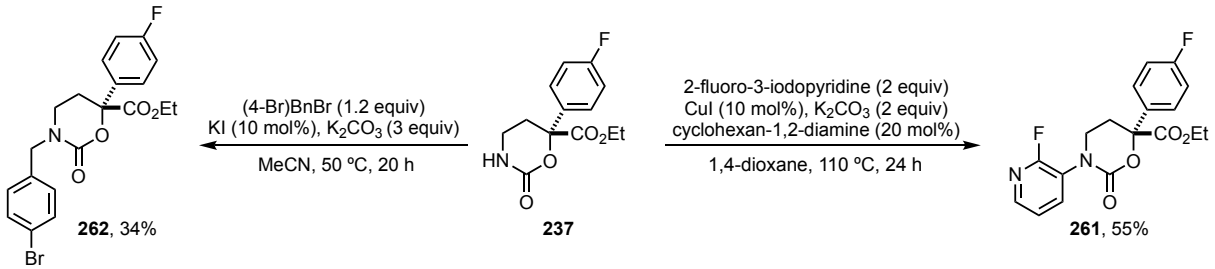
Scheme 76: Ester hydrolysis and amide bond formation using oxazinanone **237** to give lead-like compound **257**. Reactions on 0.2 mmol scale.

Reduction of the ester in the presence of the cyclic carbamate functionality was possible when using $LiAlH_4$ with a short reaction time to generate **259** as an interesting lead-like molecule with a low molecular weight and lipophilicity (Scheme 77A). The yield of this reaction was quite variable and in some cases the cyclic carbamate was reduced, with formamide **260** being isolated as a side product (Scheme 77B). Johnston reported that 1,3-oxazinan-2-ones could be reduced to the 1,3-amino alcohol at high temperature.[291] It is conceivable that heating formamide **260** with further equivalents of $LiAlH_4$ could form an acyclic amino alcohol.



Scheme 77: Reduction of the ester group in oxazinanone **237** and a common side product due to over-reduction of the cyclic carbamate.

Finally derivatisation of the 1,3-oxazinan-2-one scaffolds through the nitrogen atom was examined. Copper catalysed Ullmann coupling of an iodopyridine successfully afforded **261** in adequate yield (Scheme 78). Alkylation of the nitrogen proved more difficult than arylation. Using conditions such as NaH in DMF in order to deprotonate the carbamate NH and alkylate formed complex mixtures of products which were assumed to be due to competitive *O*-alkylation. Successful reaction conditions were found which heated the oxazinanone with 4-bromobenzyl bromide in the presence of KI and K_2CO_3 in order to promote the reaction through a Finkelstein reaction without deprotonation of the nitrogen atom (Scheme 78). These conditions resulted in a relatively low yield of oxazinanone **262** which could foreseeably be further functionalised through the aryl bromide.

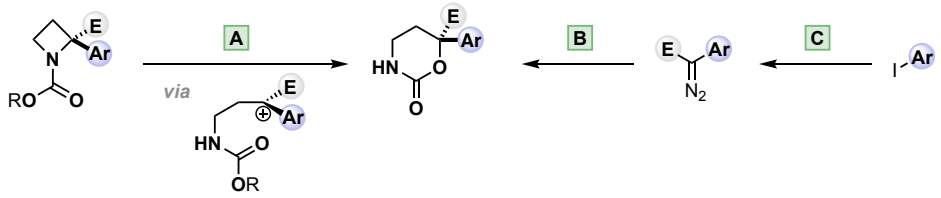


Scheme 78: *N*-alkylation and arylation demonstrated from oxazinanone **237**. Reactions on 0.1 mmol scale.

This section has shown how the 6,6-disubstituted 1,3-oxazinan-2-ones made by the ring expansion of azetidine carbamates can be readily diversified *via* the ester functional group and the carbamate nitrogen to access lead-like compounds.

3.4 Conclusions and Future Work

In this chapter the development of a new ring expansion of 2,2-disubstituted azetidine carbamates to form 6,6-disubstituted 1,3-oxazinan-2-ones has been discussed (Scheme 79A). Optimisation of the reaction gave process friendly conditions for the ring expansion of Boc-protected azetidines using TFA. High yields (up to 96% yield) were achieved for azetidines with aromatic rings with substituents that could stabilise benzylic carbocation formation. For azetidines with aromatic groups with carbocation destabilising substituents alternative conditions were developed with Cbz-protected azetidines using TfOH. Further to this, the products could be generated in a 3 or 4 step sequence from simple acyclic precursors in good yields and 1 or 2 chromatographic purifications (Scheme 79B and C). The 1,3-oxazinanone scaffolds could be functionalised in a divergent manner using the preinstalled vectors. This clearly demonstrated their potential utility to generate compounds for screening. Finally, in Section 3.3.4, the mechanism of the reaction was discussed and evidence suggested that the reaction proceeds through a benzylic carbocation.



Scheme 79: Synthesis of 1,3-oxazinan-2-ones by **A**: Ring expansion of 2,2-disubstituted azetidine carbamates; **B**: N–H insertion, cyclisation and ring expansion (NICE); **C**: From aryl iodides followed by NICE sequence.

There are a number of ways that the research discussed in this chapter could be further developed. Though the ester group is a useful functional group within the product oxazinanones, it is also electron-withdrawing and will contribute to the destabilisation of the benzylic carbocation. Therefore one potential way to improve the reactivity of azetidines with electron-withdrawing aromatic substituents would be to replace the ester group with a more neutral or electron-rich group. As an example, the reduction of the ester group (shown in Section 3.3.6) could be carried out prior to ring expansion, the $–CH_2OH$ group would be more electron-donating and thus stabilise the carbocation more (Figure 21). Additionally the reaction could be tested with 2-aryl azetidines synthesised by an alternative method to further explore the scope and generate monosubstituted oxazinanones.

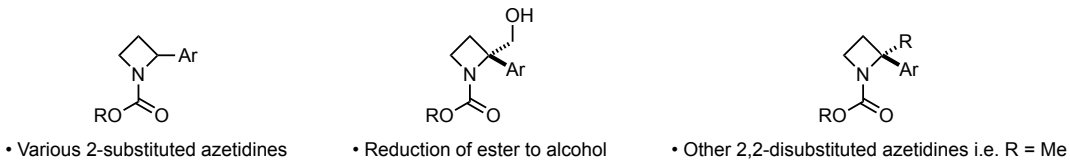
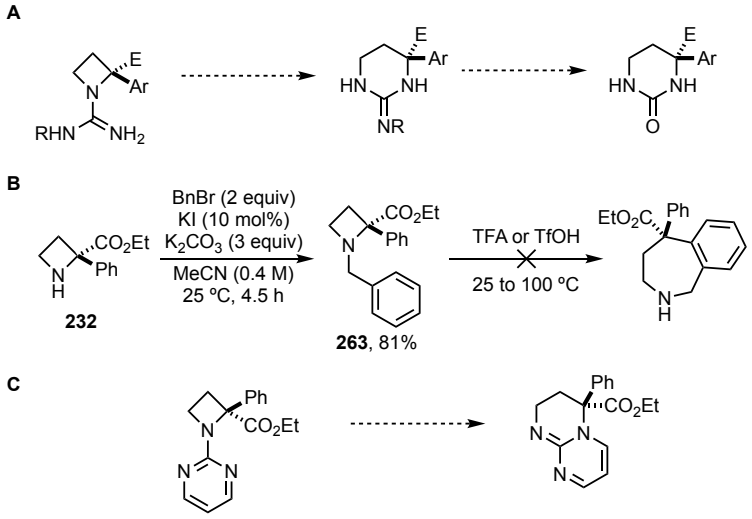


Figure 21: Further azetidines that could be tested within the developed methodology to access a wider variety of 1,3-oxazinan-2-ones.

A further interesting avenue of further work would be replacement of the carbamate group with another group which can be trapped by the formed carbocation. For example, a simple exchange of the carbamate group with a urea could form cyclic urea products (tetrahydropyrimidines). However, due to the chemoselectivity issue that this could present (*N*-alkylation vs. *O*-alkylation) this type of product could be accessed through the use of a guanidine group which would could cleave to form the cyclic urea (Scheme 80A). Using an *N*-aryl or -benzyl group could result in trapping of the carbocation through a Friedel–Crafts alkylation process. This was attempted with *N*-benzyl azetidine **263** however no reaction occurred, which is likely due to the altered reactivity of the azetidine (Scheme 80B).[301] The reasons for the failed ring opening is likely that the azetidine is now unactivated making ring opening more difficult. Additionally, the aromatic may need to be more electron rich in order to affect the Friedel–Crafts reaction. An alternative would be to use an *N*-heterocycle which could react through the nitrogen atom to form more complex rearranged products (Scheme 80C).



Scheme 80: Replacement of the carbamate functional group with **A**: different derivatives i.e. ureas or guanidines; **B**: alkyl or aromatic groups which could conceivably undergo Friedel–Crafts alkylation; **C**: *N*-heterocycles which could undergo rearrangement to complex products.

Synthesis of enantioenriched oxazinanones from enantioenriched azetidines would be difficult due to the established mechanism. Future work could attempt to promote an enantioselective ring closure through coordination of a chiral anion with the planar carbocationic intermediate. This could be through use of a strong chiral acid depending on the chiral conjugate base coordinating with the carbocation.

4. Enantioselective Azetidine Spirocyclisation

The importance of chirality in drug discovery was introduced in Section 2.4.4.2. So far, the methods developed in this Thesis (Chapters 2 and 3) produced racemic mixtures of compounds for screening. Arguably a racemic compound can be considered superior to an enantioenriched compound for screening as both compounds need to be screened for activity, so screening only racemic compounds reduces the number of screening experiments by 50%. However, if a hit is found with a racemic compound, the enantiomers must be tested for safety and efficacy purposes. Therefore, the provision of an enantioselective synthesis is desirable and enantioselective syntheses that can be scaled up in a cost-effective manner are highly sought after.

In this chapter the development of a phase transfer catalysed enantioselective cyclisation to spirocyclic azetidines will be discussed. Section 4.1 will discuss the use of aza-spirocycles in drug discovery and Section 4.2 will focus on spirocyclic oxindoles in synthesis and drug discovery. Section 4.3 introduces asymmetric phase transfer catalysis and its application to the synthesis of spirocycles. Section 4.4 presents the results of research to develop an asymmetric phase transfer catalysed cyclisation to spiroazetidine and spiropyrrolidine oxindoles.

4.1 Four-Membered Aza-Spirocycles in Synthesis and Drug Discovery

Spirocycles have recently gained significant attention within medicinal chemistry.[302] Possible advantages of spirocyclic structures over analogous monocyclic structures include greater complexity in three dimensions, greater aqueous solubility, lower lipophilicity and greater metabolic stability.[303] Spirocycles are inherently 3-dimensional due to the fully substituted carbon centre and typically dense functionalisation which places them within sp^3-rich chemical space.[304] One of the significant advantages of spirocycles in drug discovery is their relative novelty and as such underpopulated IP space, allowing pharmaceutical companies to explore these scaffolds without the danger of infringing on IP.[305] Four-membered spirocycles have received particular attention because of the combined advantages of spirocycles and small ring heterocycles in terms of physicochemical properties and occupation of novel IP space.[306]

In 2008, Carreira proposed 2,6-diazaspiro[3.3]heptane as a structural replacement for piperazine in drug discovery (Figure 22).[307] In a follow up study, Carreira synthesised a number of different aza-spirocycles and compared their lipophilicity, solubility, clearance and pK_a with their monocyclic analogues.[308] In general the results showed that the spirocycles displayed lower lipophilicity, higher pK_a, greater metabolic stability and higher solubility.[309] These studies

have led to the development of many more four-membered containing aza-spirocycles as structural replacements or conformational restriction.[310]

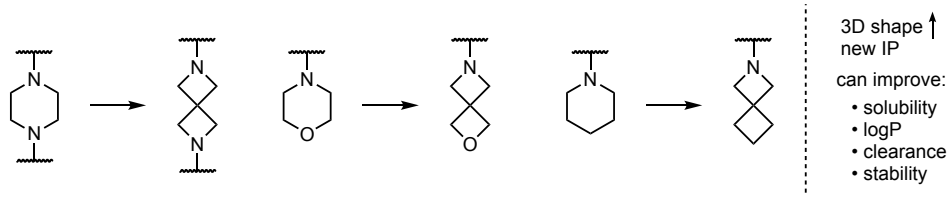


Figure 22: Spirocyclic replacements of saturated heterocycles commonly featured in pharmaceuticals and the potential benefits that these can have.

The developments in the synthesis and study of these spirocyclic replacements have led to numerous reports of their use in medicinal chemistry (Figure 23).[311]

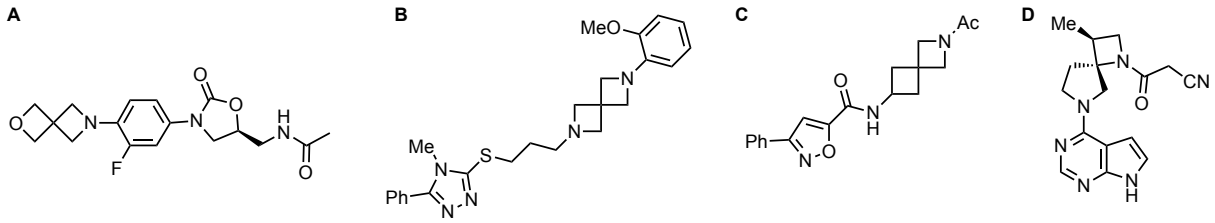


Figure 23: Examples of four-membered aza-spirocycles in medicinal chemistry. **A**: Linezolid analogue.[311a] **B**: Example of a diazaspiro alkane core in a study to develop Dopamine D_3 receptor antagonists.[311b] **C**: Fetal hemoglobin inducer for management of β-thalassemia and sickle cell disease by Asubio Pharma Co. [311d] **D**: Janus Kinase inhibitor (Delgocitinib) developed by Japan Tobacco Inc.[311e]

4.2 Spirocyclic Oxindoles in Synthesis and Drug Discovery

Spirocyclic oxindoles (also referred to as spirooxindoles and spiroindolones) are widespread within modern organic synthesis, drug discovery and natural product chemistry.[312] Spirooxindoles display a wide range of bioactivities (Figure 24), including use as anti-cancer and anti-viral agents.[313] The range of bioactive spirooxindoles includes 3- to 7- and even 8-membered spirocycles. A significant representative example of the use of a spiropyrrolidine oxindole in medicinal chemistry is MI-888 (Figure 24), which has had significant success and development as a p53-MDM2 inhibitor.[314] The success of this anti-cancer ligand, synthesised in a 1,3-dipolar cycloaddition, has inspired the development of further derivatives,[315] including proteolysis targeting chimeras (PROTACs)[316] and a molecular glue.[317]

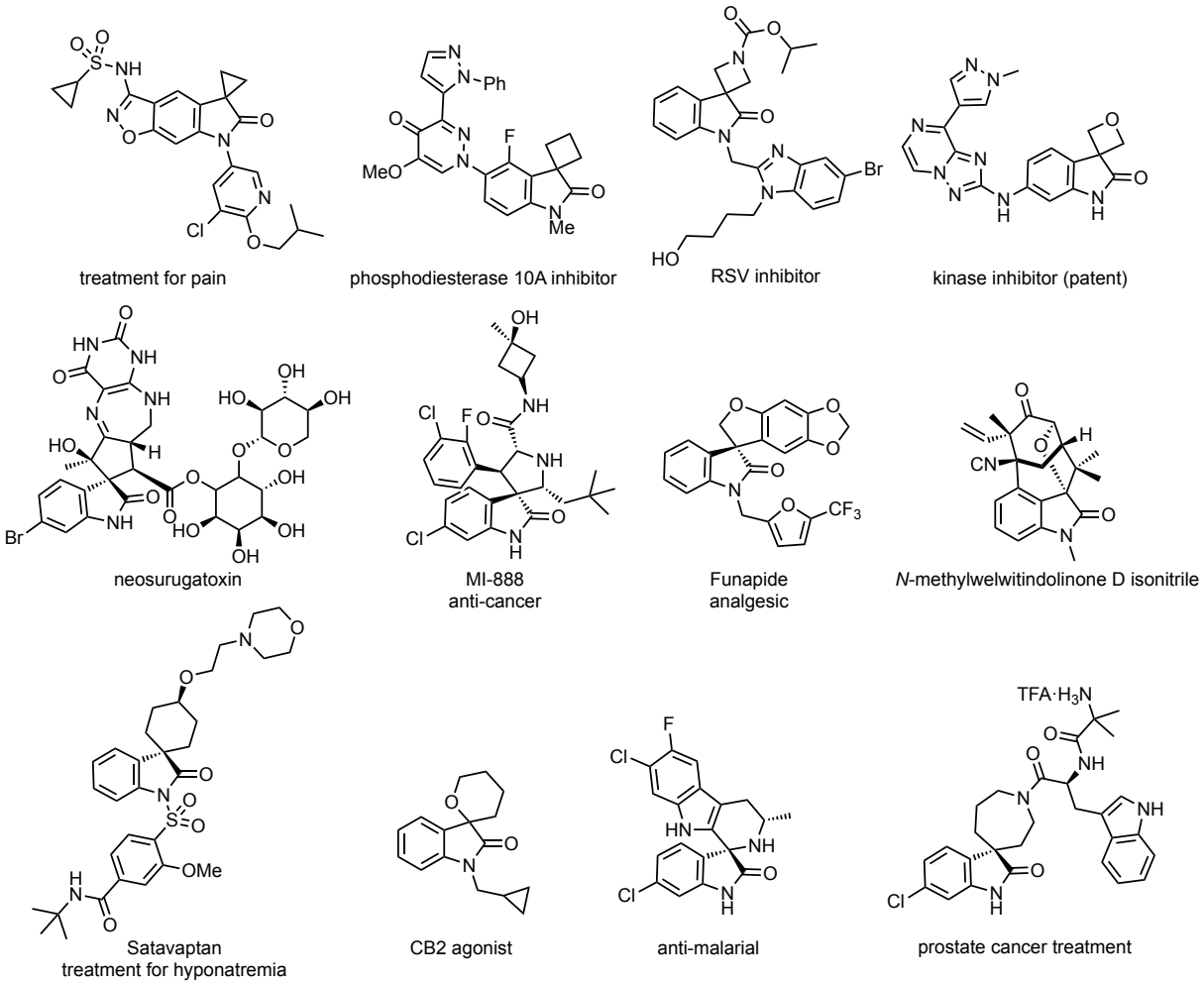
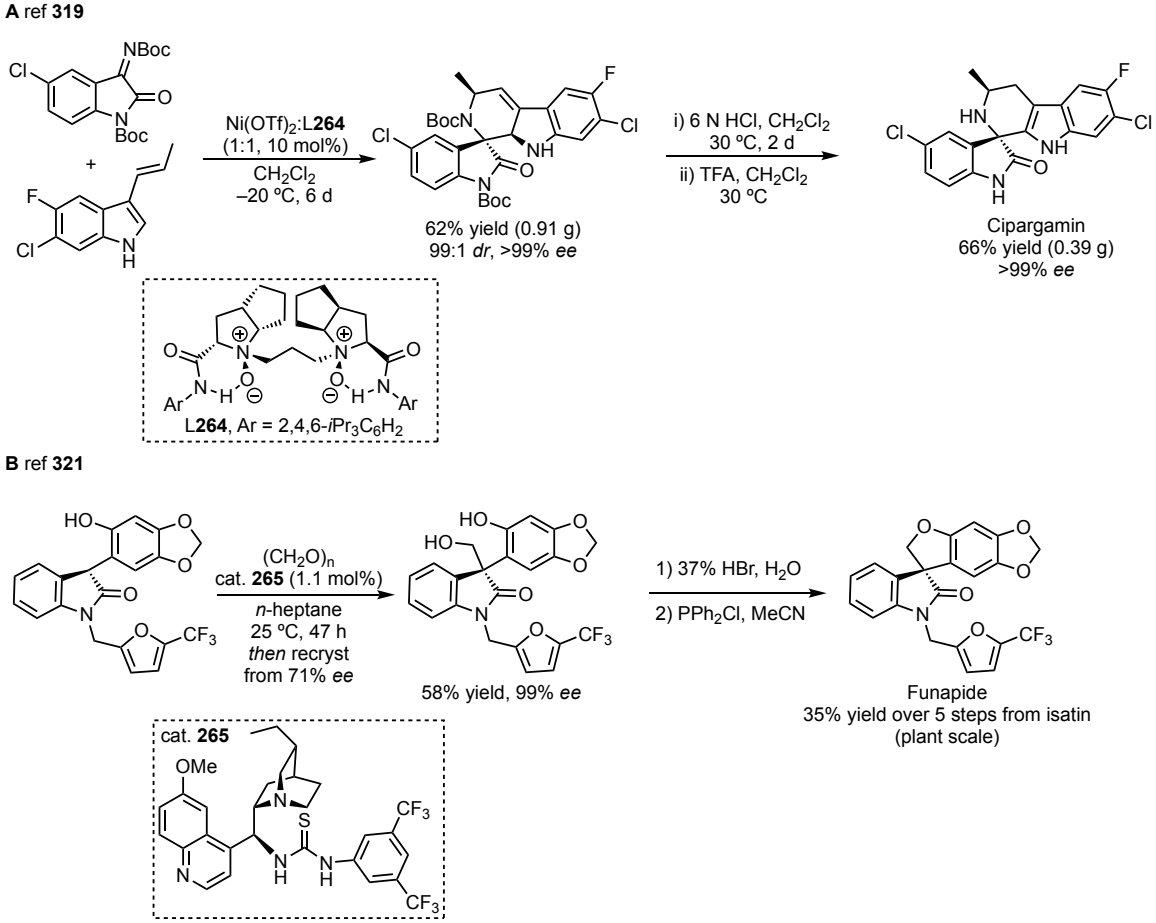


Figure 24: Selected examples of bioactive spirooxindoles with different saturated heterocyclic cores.

Another significant development in the use of spirooxindoles in medicinal chemistry is the development of cipargamin (NITD609/ KAE609) as an anti-malarial agent.[318] This has inspired the development of asymmetric syntheses (Scheme 81A).[319] A further example of the use of spirooxindoles in medicinal chemistry is Funapide (XEN402/TV-45070) licensed by Teva for the treatment of pain.[320] The success of this medicine has driven the development of enantioselective processes (Scheme 81B).[321] These examples clearly illustrate the medicinal importance of spirooxindoles and the necessity for the development of enantioselective methods (both within academia and industry) for their synthesis upon identification of the clinical candidate.



Scheme 81: Selected enantioselective methods developed for the synthesis of medicinal spirooxindoles.

Although Figure 24 includes a spiroazetidine (developed by WuXi AppTec and Buchang Pharmaceutical as an Respiratory Syncytial Virus (RSV) inhibitor),[322] the number of four-membered ring containing spirooxindoles is significantly lower than other ring sizes. An analysis of the literature publications in 2019 which include spirocyclic oxindoles shows that out of 482 publications only 9 included four-membered examples (Figure 25). This is despite a recent emphasis on the importance of four-membered ring containing spirocycles.[306] Therefore, despite the biological importance of spirooxindoles and the significant recent application of spirocyclic four-membered rings in drug discovery (Section 4.1), there has been relatively little research on spiroazetidinyl or spirooxetanyl oxindoles. Indeed, there are no stereoselective approaches to the unsymmetrical 3,2'-spiroazetidine motif in the literature, with most stereoselective methods limited to substituted β-lactams or their derivatives.[323]

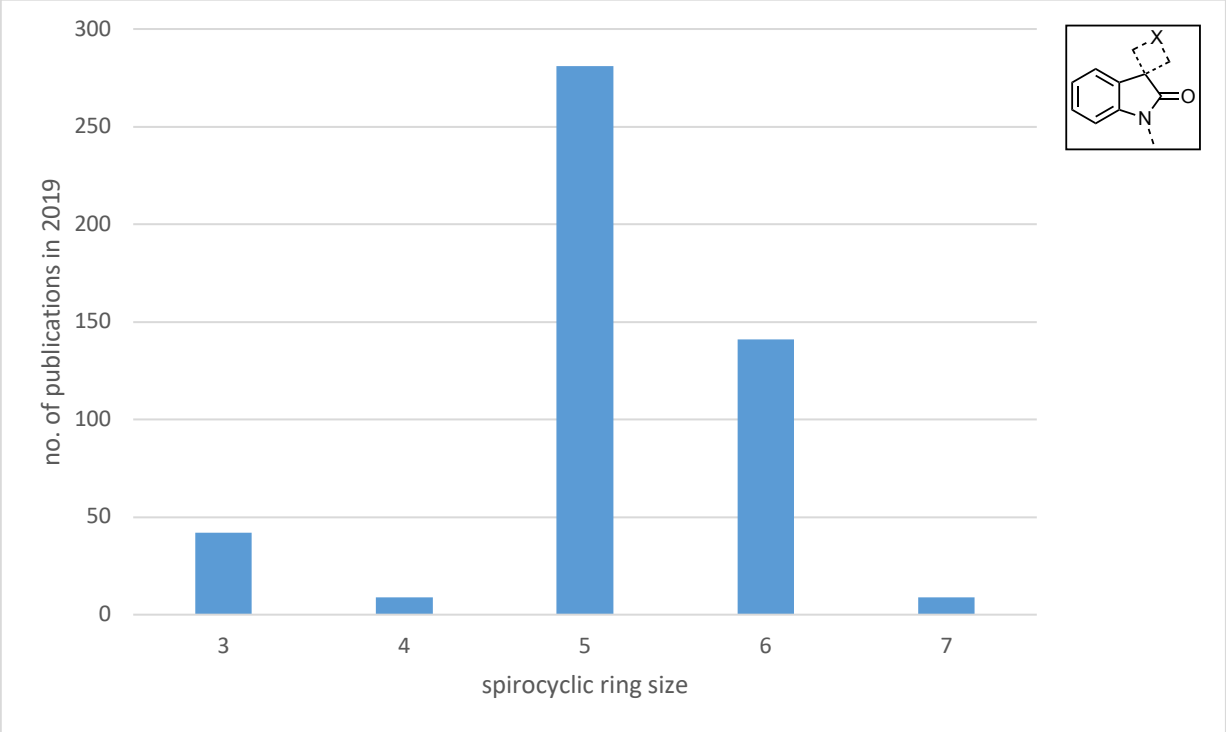
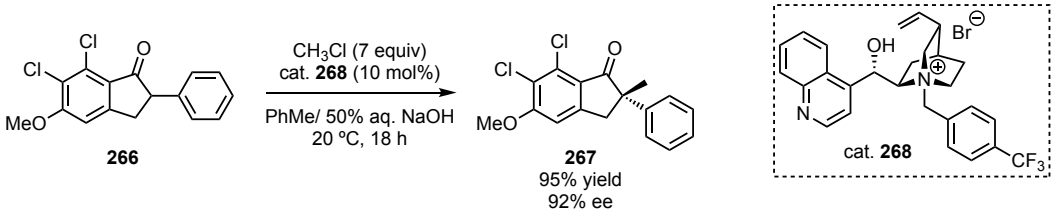


Figure 25: Comparison of the number of publications in 2019 for each ring size of spirocyclic oxindoles. Analysis carried out using SciFinder®.[324]

4.3 Asymmetric Phase Transfer Catalysis

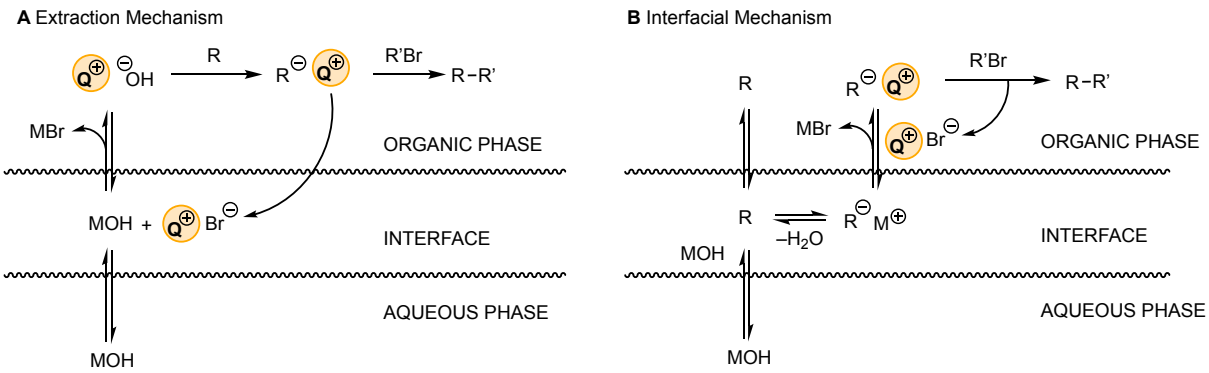
4.3.1 Intermolecular Alkylation and Mechanism

In 1971 Starks defined phase transfer catalysis as the rate enhancement of a reaction between two substrates which are partitioned in immiscible phases.[325] The prototypical phase transfer catalytic system involves an inorganic anion and an organic substrate, with a cation (typically a quaternary ammonium salt but phosphonium salts are also used) which can be soluble in both organic and inorganic media. Recently phase transfer catalysis using chiral anions with Brønsted acids, or even through hydrogen bonding catalysis with inorganic anions, has also been developed.[326] The emergence of the field of asymmetric phase transfer catalysis can be traced to 1984, when Dolling and co-workers at Merck used phase transfer catalyst (PTC) **268** derived from cinchonine for the intermolecular methylation of cyclic indanone **266** with high enantioselectivity (Scheme 82).[327] Since this work by Merck numerous asymmetric phase transfer catalysts have been developed.[328] Intermolecular alkylation is the reaction type that has dominated this research,[329] for example alkylation of glycine imines.[330] Intramolecular alkylation/cyclisation remains rarer than intermolecular examples.[331] This is likely due to the greater difficulty in controlling the rate of the racemic background reaction.



Scheme 82: Asymmetric phase transfer catalysed alkylation of indanone **266** developed by Merck.

There are two general mechanistic proposals for phase transfer catalysed reactions that involve aqueous bases.[332] These mechanisms differ in the location of the deprotonation event, either in the organic phase or at the interface of the two phases. For a typical phase transfer catalysed alkylation of an enolate, the extraction mechanism involves transport of the hydroxide anion to the interface to form a catalyst hydroxide complex ($Q^+ \cdot OH^-$) (Scheme 83A). This complex is then directly involved in the deprotonation event in the organic phase, forming a catalyst–substrate complex ($Q^+ \cdot R^-$), which upon alkylation can induce enantioselectivity due to the asymmetric environment created by the catalyst upon binding to the substrate. In the alternative interfacial mechanism, substrate deprotonation occurs at the interface, thus deprotonation to form the metal enolate is independent of the catalyst (Scheme 83B). The catalyst can then coordinate to the enolate. It is unclear whether this association occurs at the interface or within the organic medium. Regardless of the site of association, the catalyst–substrate complex can then undergo enantioselective alkylation.



Scheme 83: Extraction and interfacial mechanisms of phase transfer catalysis.

Significant evidence for the interfacial mechanism to be the dominant mechanism for enolate alkylations was provided by Merck.[333] This evidence can be summarised as: 1) In 50% NaOH in H_2O indanone **266** was deprotonated at the interface to form a separate phase (i.e. without the requirement of the catalyst); 2) Significant dependence of the rate of reaction on stirring rate; 3) Complex order in catalyst and electrophile (<1). The partitioning of the catalyst in each phase will clearly have an effect on the mechanism of the reaction.[334] The workers at Merck found that the quaternary ammonium catalyst was highly insoluble in benzene and that it forms dimers ($Q^+–OH\cdots{}^-O–Q^+Br^-$), upon deprotonation of one catalyst, which are more soluble in

benzene. This will create a lag time before the active catalyst is in the organic phase and can associate with the enolate at the interface.

The exact mechanism by which asymmetric phase transfer catalysts induce enantioselectivity remains obscure despite systematic attempts to study this by Denmark.[335] PTCs, in particular those that are *cinchona* alkaloid derived, have received little attention from computational chemists, most likely due to their large size and flexibility.[336] Building a model of enantioselectivity has historically relied on structure activity (enantioselectivity) relationships upon altering the catalyst structure.[335] Therefore, the exact model of asymmetric induction will be different depending on the exact reaction and substrate. A number of models have been proposed for intramolecular alkylations catalysed by PTCs. Generally, these reactions give highest yield and enantioselectivity in non-polar solvents which indicates a tight-ion pair (contact ion-pair, i.e. no solvent separates the cation and anion) between the catalyst and substrate in the transition state. Dolling and co-workers at Merck proposed that the reaction in Scheme 82 proceeds through an ion pair where the OH group of the ammonium salt coordinates to the enolate and the aromatic rings of the indanone π-stack with the aromatic rings of the catalyst (Figure 26A).[327,333] This model relies on the more electron rich phenyl ring interacting with the *N*-benzylic substituent of the catalyst to orient the substrate. The methyl chloride approaches from the opposite face to the catalyst, which acts as a steric shield to block one face of the substrate. This model has recently been disputed.[337] Through a theoretical approach, Pliego modelled the reaction developed by Merck and showed that the transition state lowest in energy is the one that places the chloride closest to the ammonium cation (Figure 26B). Therefore, the methyl chloride electrophile is between the catalyst and substrate and the cation interacts with the chloride anion as the C–Cl bond is broken. Pliego stated that there is no evidence of π-π stacking in the transition state and that the orientation is determined simply by the proximity of the chloride to the ammonium cation. It was argued that this explains the trend for poorer enantioselectivity when the Cl leaving group was replaced by Br and I in Merck's work. The model proposed by Dolling cannot account for this as the bromide and iodide would not impair the interaction between the catalyst and substrate. Whereas in the Pliego model a larger leaving group would clearly impair the catalyst-substrate interaction. While this variable could also be explained by a greater rate of racemic background reaction, this is assumed to be less significant for intermolecular alkylations vs. intramolecular alkylation.

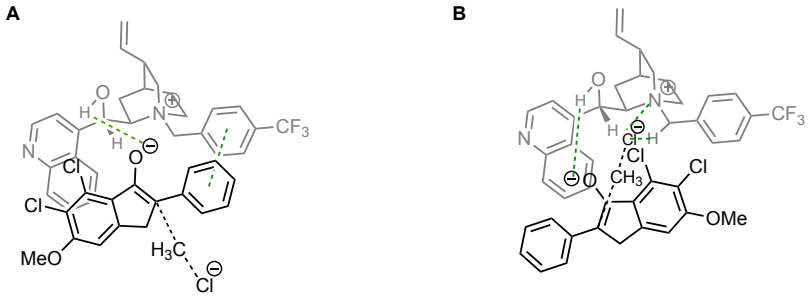
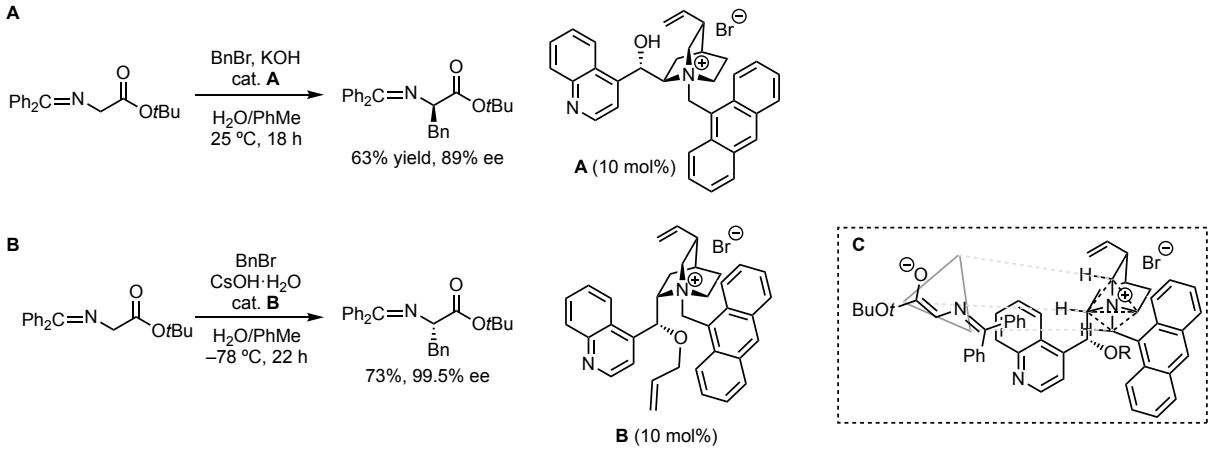


Figure 26: Models for the asymmetric induction of intermolecular alkylation (Scheme 82). **A**: Model proposed by Dolling. **B**: Model proposed by Pliego.

For the alkylation of glycine imines which has been intensively studied for different asymmetric phase transfer catalysts (see ref 330), both models suggest selective binding of the catalyst to one face of the *Z*-enolate.[338] The models differ in the importance placed on steric interactions which are primarily caused by the structural differences between the catalysts developed by Corey[328c] and Lygo (Scheme 84).[328b] Corey proposed the now commonly accepted tetrahedron model which relies on the catalyst ammonium cation presenting the positive charge on one face of a tetrahedron, with the other 3 faces being screened by steric repulsion (Scheme 84C). This tetrahedron model can be combined with the observation by Reetz that the positive charge of the ammonium cation is significantly delocalised onto the α-carbon atoms.[339] Therefore it is the ammonium α-C–H bonds which project the positive charge according to this tetrahedron model.



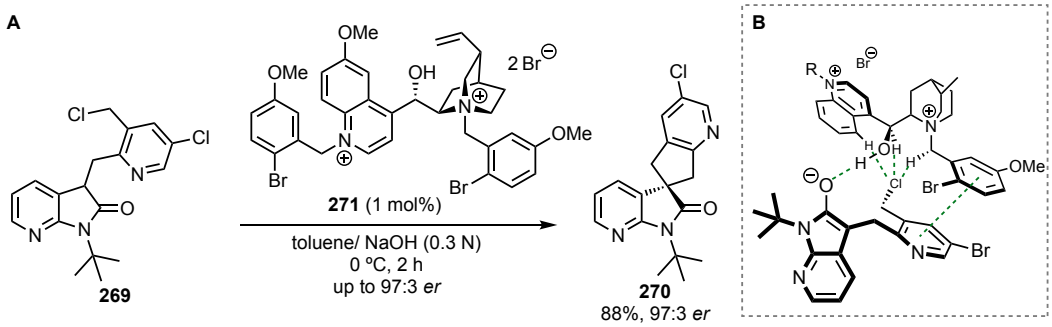
Scheme 84: Intermolecular alkylation catalysed by phase transfer catalysts **A** and **B** developed by Lygo (A) and Corey (B). Tetrahedron model for rationalising the stereochemical outcome (C).

4.3.2 Application of PTC to Spirocyclic Oxindoles and Intramolecular Alkylation

Asymmetric phase transfer catalysis has found significant application using oxindole or isatin-derived starting materials.[340] This is likely due to the low flexibility and potential for interactions through the carbonyl and aromatic group of the oxindole scaffold (*cf.* Section 4.3.1 and indanone **266**). Within the context of spirocyclic oxindole synthesis there are a number of examples of intramolecular reactions, though these tend to be limited to bespoke substitution

patterns in order to obtain high enantioselectivity.[341] For example, the initial process scale synthesis of Funapide (Scheme 81B) employed asymmetric phase transfer catalysis, though this was not progressed due to the requirement for protecting groups.[321]

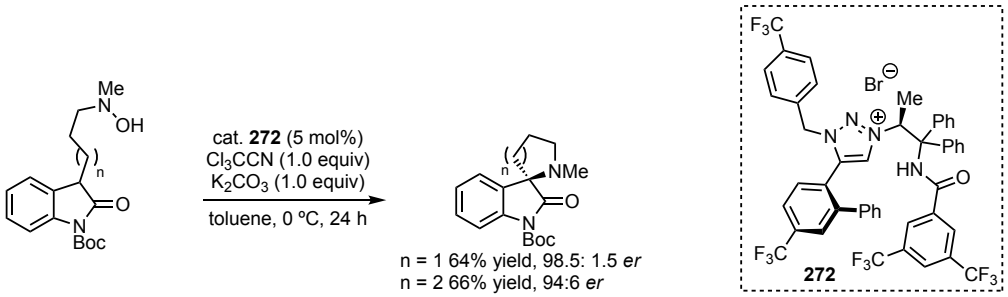
One notable example of intramolecular cyclisation applied to the synthesis of spirooxindoles using asymmetric phase transfer catalysis has recently been disclosed by Merck.[342] In order to access the core scaffold of candidate Calcitonin Gene-Related Peptide (CGRP) inhibitors for the treatment of migraine, an asymmetric phase transfer catalysed spirocyclisation to form spirocyclopentane oxindole **270** was developed (Scheme 85A). A *bis*-quaternised *cinchona* alkaloid was used to achieve up to 97:3 *er* of the product at 0 ºC for 2 h. The reaction mechanism was studied in collaboration with Houk (Scheme 85B).[343] Three key electrostatic interactions were proposed: 1) Hydrogen bonding between the hydroxyl group of the catalyst and the oxindole enolate; 2) A stabilising electrostatic interaction between the ammonium α-C–H bonds and the Cl leaving group (as in the Pliego model); 3) A π-π interaction between the fused pyridine of the substrate and the quinicludine *N*-benzyl substituent. This work also provided further evidence that the Pliego model of catalyst–substrate interaction through electrostatic interactions of the C–H bonds with the Cl leaving group was the lowest energy transition state. The reason for the privileged nature of the *bis*-quaternised catalysts over the more typical *mono*-quaternised catalysts was not explained, though Houk invoked a quinoline C–H···Cl interaction in the transition state (Scheme 85B). One factor also not discussed was how the additional quaternisation affects the partitioning of the catalyst between the aqueous and organic phases. The higher activity of this catalyst could feasibly be due to greater partitioning into the organic phase due to greater resemblance to the more soluble dimeric complexes of the ammonium catalysts.



Scheme 85: **A**: Asymmetric phase transfer catalysed intramolecular cyclisation developed by Merck. **B**: Model of asymmetric induction as studied by Houk.

Another example of enantioselective intramolecular cyclisation catalysed by a phase transfer catalyst has been developed by Ooi (Scheme 86).[344] Ooi used PTC **272** to induce enantioselectivity for the cyclisation of *O*-imino hydroxylamines. In this reaction, the nitrogen atom becomes electrophilic when the hydroxylamine reacts with trichloroacetonitrile to form

the *O*-imino hydroxylamine. High enantioselectivity was achieved for the intramolecular amination to form 5- and 6-membered rings. No model was proposed for how the triazolium catalyst **272** interacts with the substrate in this system. Developed by Ooi in 2011 these catalysts are highly modular with a key site being the hydrogen bond of the amide in close proximity to the triazolium cation.[345] However, a model for the asymmetric induction of these catalysts has not been proposed or validated and research will depend on structure-activity relationships.



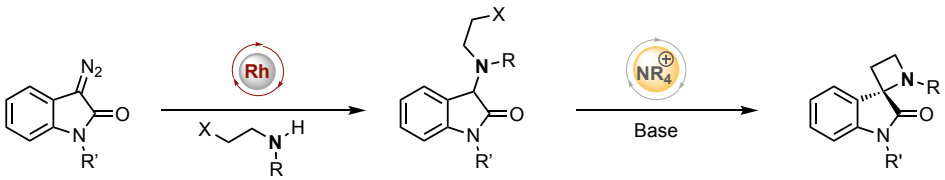
Scheme 86: Asymmetric phase transfer catalysed intramolecular cyclisation developed by Ooi.

The intramolecular cyclisations developed by Merck and Ooi represent significant advances in the field of asymmetric phase transfer catalysis and spirocyclic oxindole synthesis. The key disadvantages of these approaches are their limited scope. In terms of the system developed by Merck (Scheme 85), it is highly optimised to achieve high enantioselectivity. For example, removal of the pyridine nitrogen of the fused aromatic ring or the use of a methyl group instead of *tert*-butyl as oxindole *N*-substituent led to large decreases in enantioselectivity. This is likely due to the highly optimised nature of the catalyst which leads to low generality. Though this was not the aim of the paper, which aimed to synthesise a specific target compound. The only examples of enantioselective intramolecular cyclisation demonstrated by Ooi are the two shown in Scheme 86. This does not necessarily reflect the potential scope of the reaction but further examples would be needed to establish how the catalyst interacts with the substrate. This is coupled with the complexity of the catalyst, both in terms of structure and synthesis, and little development has been made in terms of how this catalyst could be optimised for other similar systems based on structure-activity knowledge.

4.4 Results and Discussion

This section will discuss research towards the development of an asymmetric phase transfer catalysed cyclisation reaction which was initially discussed in Section 2.4.4.2. It was interesting to see if the N–H insertion and cyclisation methodology developed in Chapter 2 could be developed to generate enantioenriched products (Scheme 87). Due to the importance of spirocyclic oxindoles in drug discovery and the greater rigidity over the non-spirocylic systems investigated in Section 2.4.4.2, 3-diazooxindoles were chosen as substrates for the N–H insertion reaction. In Section 4.1 the importance of four-membered ring containing spirocycles

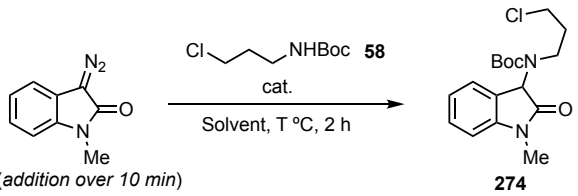
for drug discovery was discussed and in Section 4.2 it was shown that the number of methods to spiroazetidine oxindoles is extremely limited (Figure 25). Therefore, we were interested in the development of an asymmetric phase transfer catalyst to synthesise spiro-3,2'-azetidine oxindoles enantioselectively and demonstrate a general asymmetric phase transfer catalysed intramolecular cyclisation (see Section 4.3.2 for discussion of literature precedent).



Scheme 87: General reaction scheme summarising the target for Section 4.4.

4.4.1 Optimisation of N–H and O–H Insertion of 3-Diazooxindoles

Using the N–H insertion conditions employed in our previous work (Chapter 2), low yields were obtained for the N–H or O–H insertion of 3-diazooxindoles (<30% yield, not shown). Initial optimisation started with the O–H insertion of 3-bromoethanol with diazo **273**. The initial optimisation showed that a slow addition of the diazo compound was important for the reaction. Therefore, we started optimising the N–H insertion reaction using a slow addition of 3-diazooxindole **273** in CH_2Cl_2 over 10 min to a solution of amine **58** and $Rh_2(esp)_2$ in CH_2Cl_2 at 40 ºC (Table 13, Entry 1). Increasing the equiv of **58** was beneficial for the reaction but above 2 equiv no significant benefit in yield was observed (Entries 2–5). Changing the concentration showed that 0.1 M was optimal (Entry 6). Lower catalyst loading and switching solvent to toluene (less hazardous than CH_2Cl_2) gave the same yield (Entry 10 and 11). Lowering the reaction temperature to 25 ºC gave an improvement in the yield of the reaction (Entry 12), whereas higher temperatures gave lower yields (Entry 13 and 14). Testing different Rh catalysts all gave poorer results than $Rh_2(esp)_2$ (Entries 15–17).

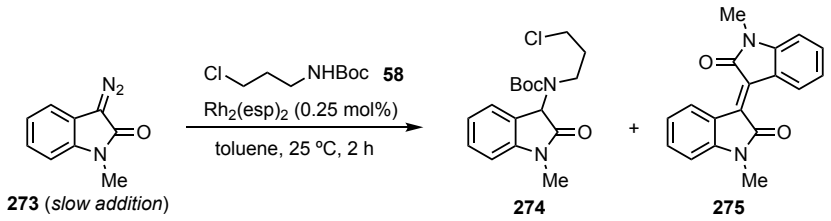


273 (*addition over 10 min*) **274**

Entry	Equiv of **58**	Conc (M)	Solvent	T (ºC)	Cat. (mol%)	Yield **274** (%) [a]
1	1	0.15	CH_2Cl_2	40	$Rh_2(esp)_2$ (0.5)	54
2	1.5	0.15	CH_2Cl_2	40	$Rh_2(esp)_2$ (0.5)	63
3	2	0.15	CH_2Cl_2	40	$Rh_2(esp)_2$ (0.5)	71
4	3	0.15	CH_2Cl_2	40	$Rh_2(esp)_2$ (0.5)	72
5	5	0.15	CH_2Cl_2	40	$Rh_2(esp)_2$ (0.5)	75
6	2	0.1	CH_2Cl_2	40	$Rh_2(esp)_2$ (0.5)	72
7	2	0.2	CH_2Cl_2	40	$Rh_2(esp)_2$ (0.5)	69
8	2	0.3	CH_2Cl_2	40	$Rh_2(esp)_2$ (0.5)	66
9	2	0.5	CH_2Cl_2	40	$Rh_2(esp)_2$ (0.5)	58
10	2	0.1	CH_2Cl_2	40	$Rh_2(esp)_2$ (0.25)	75
11	2	0.1	$PhCH_3$	40	$Rh_2(esp)_2$ (0.25)	75
12	**2**	**0.1**	**$PhCH_3$**	**25**	**$Rh_2(esp)_2$ (0.25)**	**85**
13	2	0.1	$PhCH_3$	60	$Rh_2(esp)_2$ (0.25)	76
14	2	0.1	$PhCH_3$	80	$Rh_2(esp)_2$ (0.25)	65
15	2	0.1	$PhCH_3$	25	$Rh_2(oct)_4$ (0.25)	55
16	2	0.1	$PhCH_3$	25	$Rh_2(OAc)_4$ (0.25)	21
17	2	0.1	$PhCH_3$	25	$Rh_2(TFA)_4$ (0.25)	19

Table 13: Selected optimisation of the N–H insertion reaction of 3-diazooxindole **273**. Reactions on 0.25 mmol scale. [a] Yields calculated by ^{1}H NMR spectroscopy with respect to 1,3,5-trimethoxybenzene as an internal standard.

The rate of the slow addition of the diazo compound was analysed and this showed that longer addition times did not improve the reaction yield (Table 14). When no slow addition was used more of dimer **275** was observed (Entry 1).



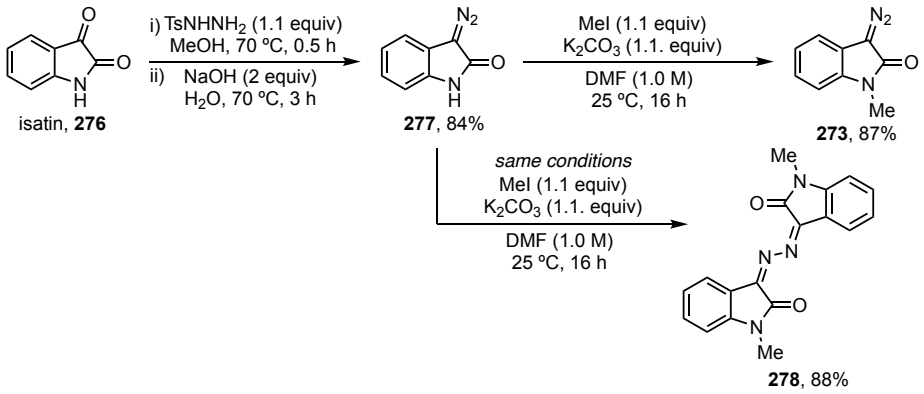
Entry	Addition time (min)	Yield (%) [a]	
		274	**275**
1	0	56	13
2	2	63	6
3	**10**	**89**	**0**
4	30	78	0
5	60	78	0

Table 14: Selected optimisation of N–H insertion reaction of 3-diazooxindole **273** varying addition time of diazo **273**. Reactions on 0.25 mmol scale. [a] Yields calculated by ^{1}H NMR spectroscopy with respect to 1,3,5-trimethoxybenzene as an internal standard.

4.4.2 Scope of N–H Insertion and Racemic Spirooxindoles

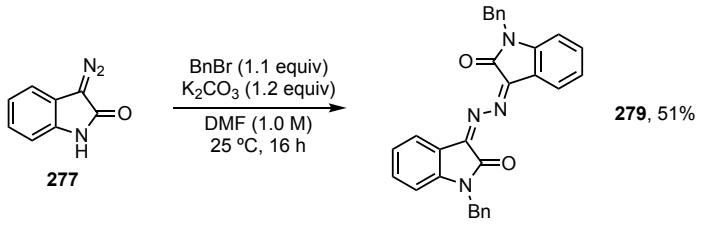
4.4.2.1 Synthesis of Diazo Compounds

The optimisation of the N–H insertion reaction discussed in Section 4.4.1 was carried out using diazo **273**. This was synthesised from isatin in a 3 step procedure (Scheme 88). First isatin was reacted with *N*-tosylhydrazide to form the *N*-tosylhydrazone, which was treated with NaOH in H_2O at 70 ºC to give unprotected diazo **277**. Methylation of diazo **277** in DMF afforded diazo **273** in good yield on large scale. However on some occasions, under the same conditions, a side reaction to form azine **278** was also observed. It remains unclear if the azine formation occurs after the methylation step.[346]



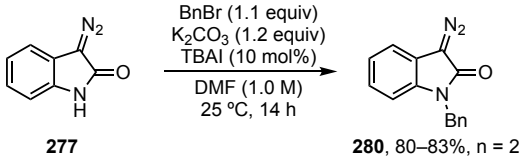
Scheme 88: Synthesis of diazo compounds **277** and **273** and observed side product **278** under the same reaction conditions as **273**. **277** formation on 40 mmol scale. Methylation reaction to **273** on 59 mmol scale and to **278** on 80 mmol scale.

Despite the potential side product formation, this approach to the *N*-protected diazo compounds was attractive due to the ability to react **277** with different electrophiles (as shown in Scheme 94). The alternative approach would be to react isatin with an electrophile and then form the diazo functionality. Yet this would result in a greater number of reactions overall. The reaction to form diazo **277** was carried out in a telescoped process, only requiring filtration of the *N*-tosylhydrazone intermediate. The unprotected diazo compounds could also typically be used in the protection step without column chromatography. While *N*-methyl diazo **273** could be formed using these conditions, benzylation proved more difficult and a similar azine side product was observed more often than with methylation (Scheme 89).



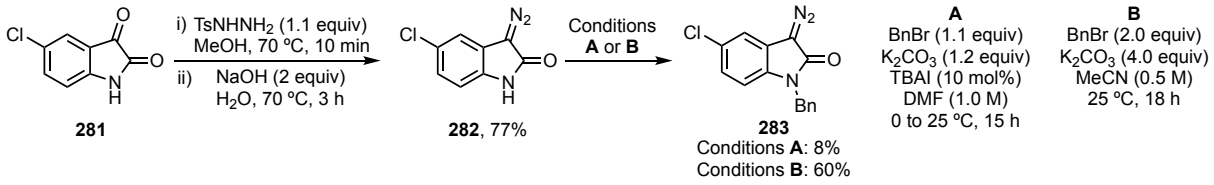
Scheme 89: *N*-Benzylation reaction to form azine **279**. Reaction on 10 mmol scale.

Two factors were hypothesised to promote azine formation: 1) acid catalysis through poor solubility of the base in DMF and 2) concentration in solvent and insolubility of product leading to a precipitation and consequent driving force for azine formation. Addition of a phase transfer catalyst to improve transport of the base into the organic solvent was found to be beneficial and reliable results for the benzylation of **277** were achieved when using tetrabutylammonium iodide (TBAI, Scheme 90).



Scheme 90: Beneficial effect of adding phase transfer catalyst, TBAI, to the benzylation of diazo **277**. Repeat reactions on 10 mmol scale.

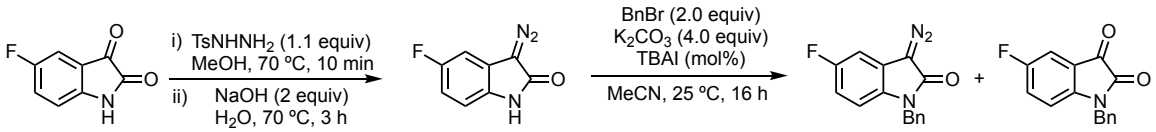
However, when differently substituted diazo compounds were used under these modified conditions significant side product formation was observed. For example, 5-chloroisatin **281** could be used to form diazo **282**, but under the benzylation conditions in DMF gave poor yields of the desired product. Application of different reaction conditions,[347] notably changing the reaction solvent from DMF to MeCN gave much improved results, even without added TBAI (Scheme 91).



281 **282**, 77% **283**
Conditions **A**: 8%
Conditions **B**: 60%

Scheme 91: Testing different conditions for substituted diazo compounds in the benzylation reaction. Reaction to form **282** on 10 mmol scale. Reactions on 2 or 4 mmol scale.

However, when these conditions were applied to other substituted diazo compounds including 5-fluoroisatin **284**, no product was obtained in the benzylation step (Table 15). The main side product was ketone **287**, with degradation of the diazo functional group to the ketone.[348] Addition of TBAI suppressed formation of side product **287** and gave a high yield of the desired product **286**.

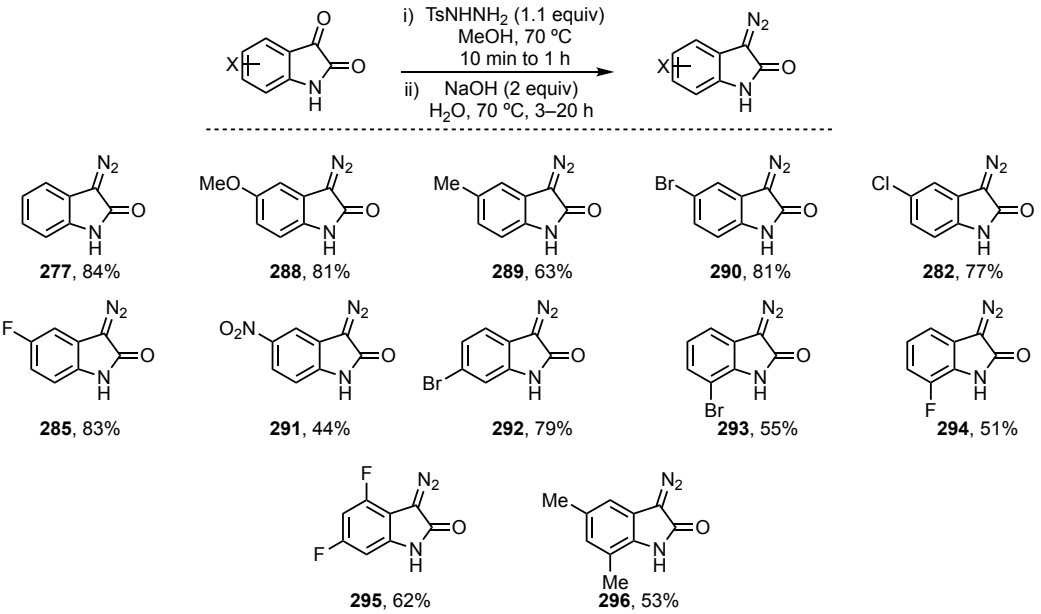


284 **285**, 62% [a] **286** **287**

Entry	TBAI loading	Yield (%)	
		286	**287**
1	0	-	54 [b]
2	20	(72)	-

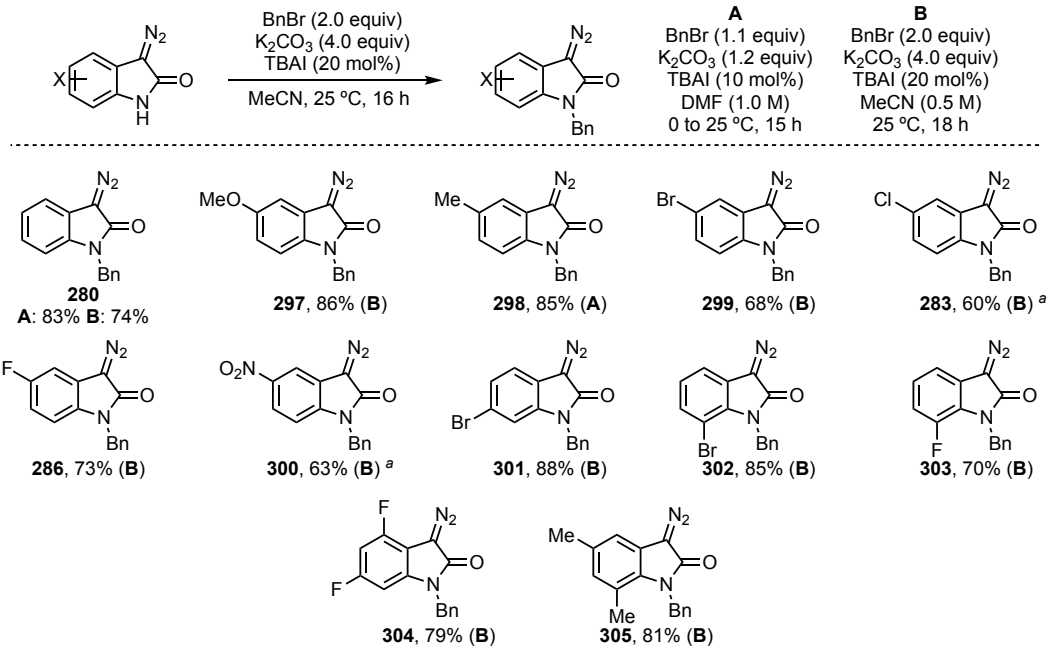
Table 15: Benzylation of diazo compound **286** and effect of adding TBAI. Isolated yields in parentheses. Reactions on 0.2 mmol scale. Yields in parentheses are isolated. [a] Reaction on 5.0 mmol scale. [b] Yields calculated by ^{1}H NMR spectroscopy with respect to 1,3,5-trimethoxybenzene as an internal standard.

With reliable conditions in hand, the diazo compounds required for this study were synthesised (Scheme 92). Generally high yields were achieved for the initial ketone to diazo transformation and the *N*-protection step.



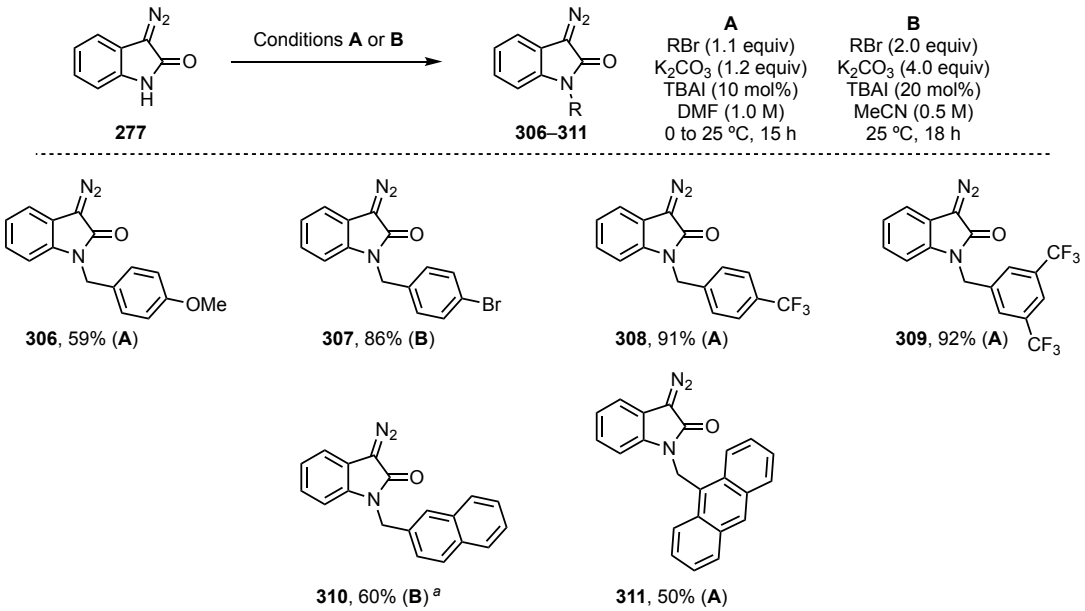
Scheme 92: Scope of diazo compound synthesis through *N*-tosylhydrazone formation and elimination of Ts group. Reactions on 3 to 40 mmol scale.

The exploration of conditions discussed within this section allowed the synthesis of a diverse array of 3-diazooxindoles all in good yields (60 to 86%, Scheme 93).



Scheme 93: Synthesis of *N*-benzyl diazo compounds with diverse substitution of the oxindole aromatic ring. Reactions on 2 to 10 mmol scale. [a] Reaction without TBAI added.

The synthesis of a variety of different alkyl substituted diazo compounds was also successful (Scheme 94).

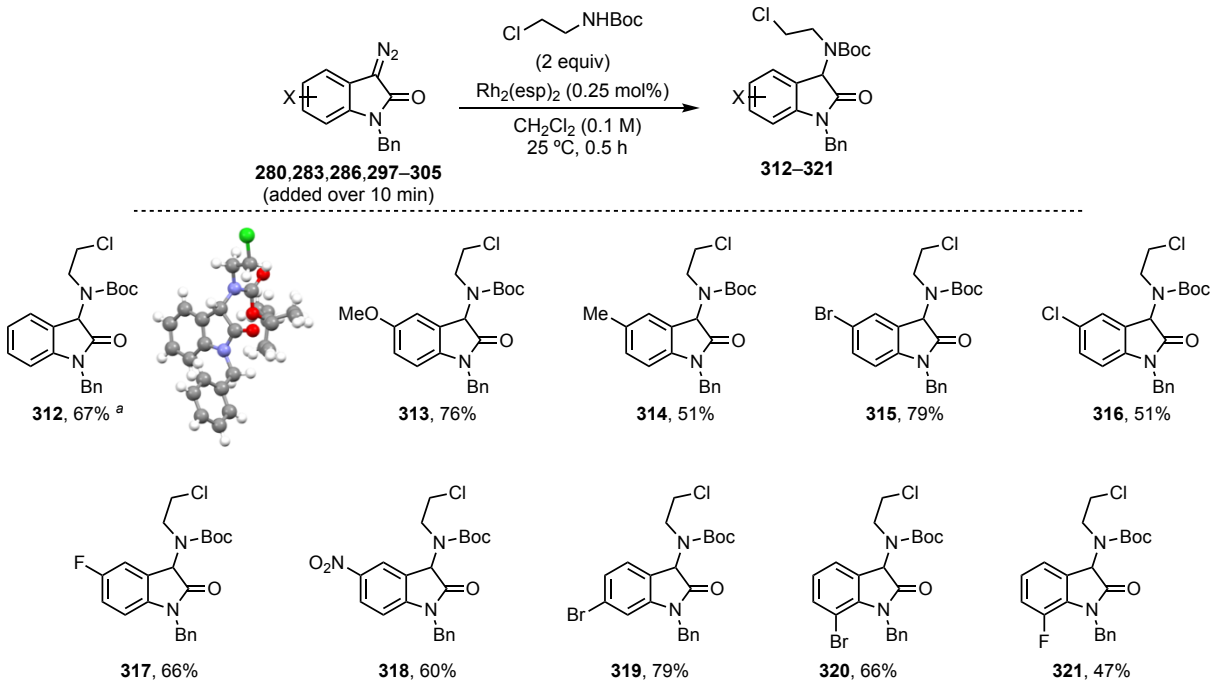


Scheme 94: Alkylation of 3-diazooxindole **277** to form a variety of diazo compounds for further synthesis. Reactions on 3 to 5 mmol scale.

4.4.2.2 Synthesis of N–H Insertion Products

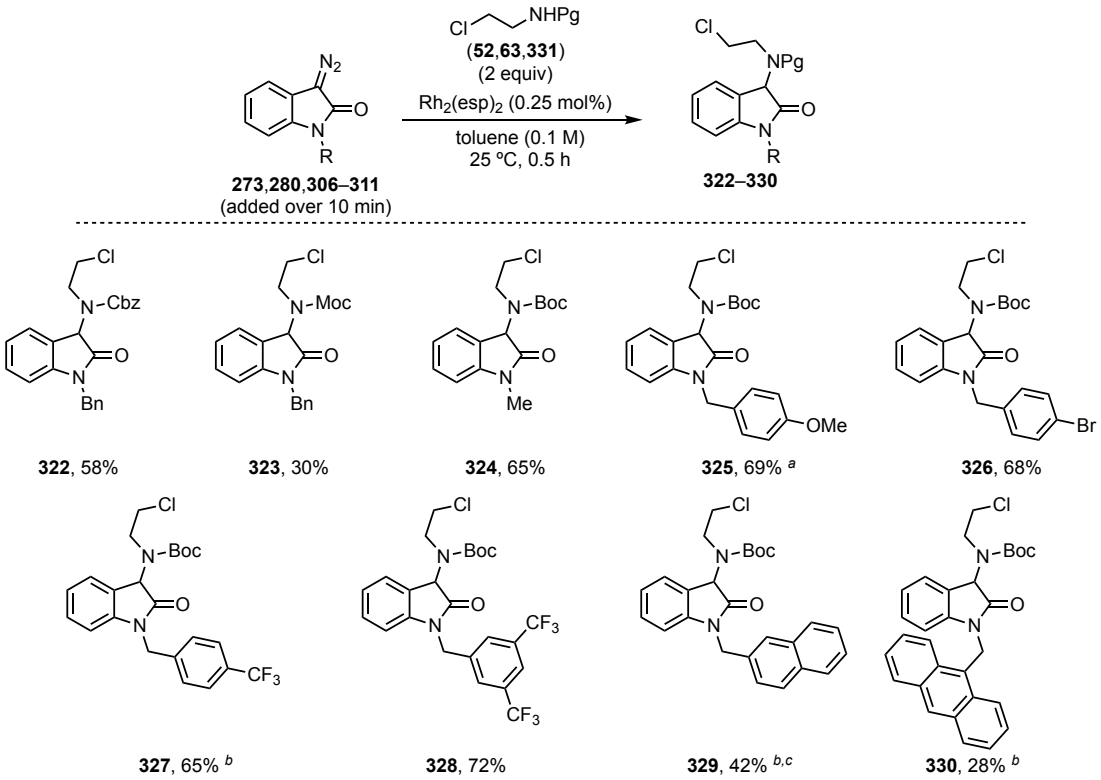
With optimised conditions for the N–H insertion reaction of 3-diazooxindoles (Section 4.4.1) a broad range of 3-diazooxindoles were tested. Notably, yields were reduced when carrying out the reaction on larger scale than the optimisation. This is likely due to a greater surface area impacting the rate of reaction during the slow addition combined with a different rate of stirring in a larger vessel. Despite this, a broad range of N–H insertion products were formed with yields typically not dependent on the electronics of the aromatic ring.

The main focus of this chapter is the synthesis of enantioenriched azetidines (For discussion see Section 4.4.3 and 4.4.4). As part of this investigation the N–H insertion reaction was carried out using a range of 3-diazooxindoles with a range of electronic properties (Scheme 95). Due to solubility reasons the optimised solvent (toluene) was not used for substituted diazo compounds and CH_2Cl_2 was used instead. Good yields (47% to 79%) were achieved for all of the diazo compounds on at least 1.0 mmol scale. This included both electron-rich and electron-poor oxindoles. Oxindole **312** which is later used as the model compound for the optimisation of the enantioselective cyclisation in Section 4.4.3 was successfully synthesised on 2 mmol scale in 67% yield. Synthesis on larger scale was mainly limited by the requirement for the slow addition of the diazo compound.



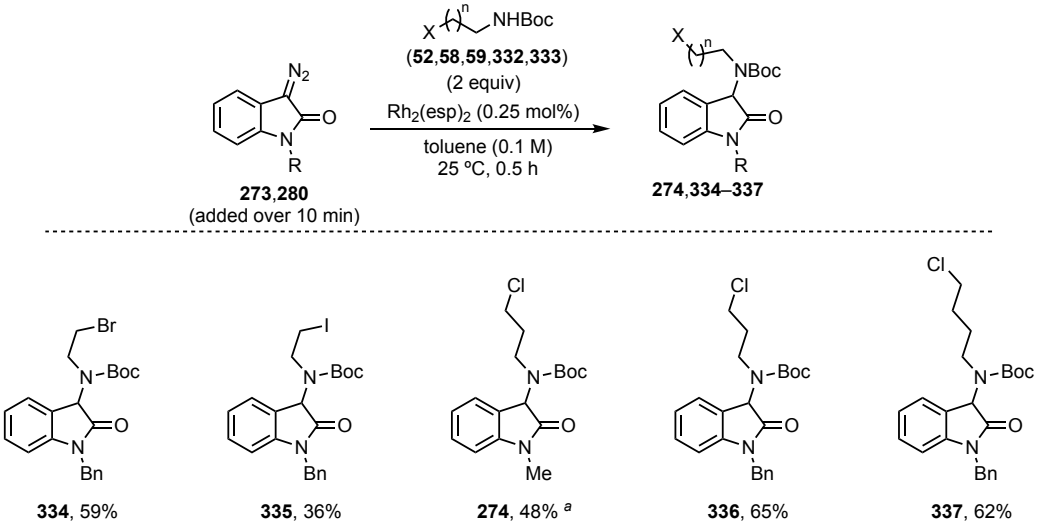
Scheme 95: Scope of N–H insertion reaction with different 3-diazooxindoles. Reactions on 1 mmol scale. [a] Reaction on 2 mmol scale in toluene. X-Ray crystal structure obtained for compound **312** and visualised using Mercury 2020.1[349] (see Appendix 7.3 for full details).

The scope with respect to the *N*-substituent of the oxindole and the protected amine starting material was also reasonably broad (Scheme 96). The Boc group could be replaced with Cbz or methoxycarbonyl (Moc) to give **321** and **322** in reasonable yield. Using *N*-methyl 3-diazooxindole **273** gave the same yield as with *N*-benzyl. The benzyl group could also be substituted and the yield of the reaction was not affected, although more bulky systems such as napthyl or anthracenyl gave lower yields.



Scheme 96: Scope of N–H insertion reaction with different 3-diazooxindoles varying *N*-substituents on the oxindole and protected amines. Reactions on 1 mmol scale. [a] Reaction on 0.75 mmol scale. [b] Reaction on 0.5 mmol scale. [c] Reaction in CH_2Cl_2.

The leaving group could be changed to afford **330** and **331** without significant reduction in yield for the N–H insertion reaction (Scheme 97). The carbon chain could also be extended to synthesise the precursors to the 5- and 6-membered rings without a significant reduction in yield compared to the azetidine precursor.

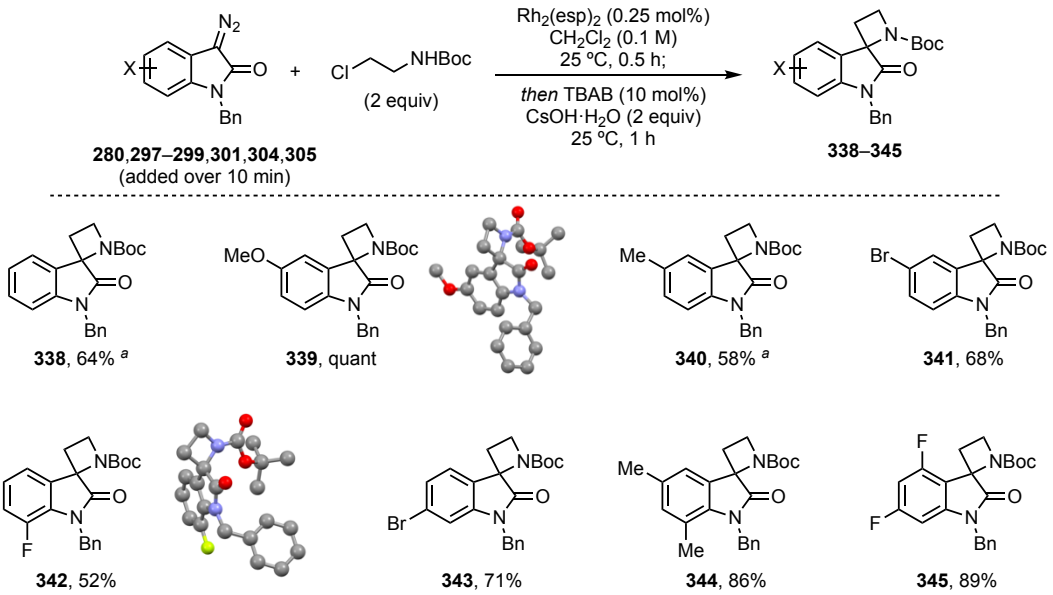


Scheme 97: Scope of N–H insertion reaction with different Boc-protected amines. Reactions on 1.0 mmol scale. [a] Reaction under non-optimised conditions, 0.25 mmol scale, 1.5 equiv **273**, 40 ºC in CH_2Cl_2, 1 h reaction time.

4.4.2.3 Synthesis of Racemic Spirooxindoles

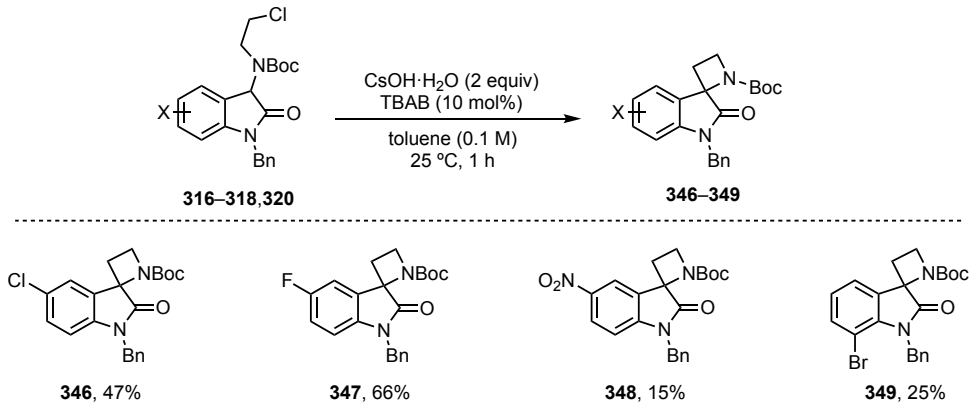
A prerequisite of an investigation into the synthesis of enantioenriched products is the synthesis of the racemic analogues. This is because of the requirement to compare the racemic and enantioenriched compounds using a chiral stationary phase, i.e. using HPLC or GC. Additionally, for the purposes of drug discovery, it is important to show that the racemate can be readily prepared, as this may be preferable due to cost and time efficiency.

There were two potential routes to the racemic spirooxindole products, either one-pot N–H insertion and cyclisation from 3-diazooxindoles or by cyclisation from the isolated N–H insertion intermediate. In most cases the one-pot reaction was carried out due to the greater time-efficiency. Upon application of the cyclisation conditions used in Chapter 2 in the one-pot reaction, a similar yield for the cyclised product was achieved as for the N–H insertion product (Scheme 98). Generally, the yields are very similar, although, some of the yields are actually higher than the N–H insertion reaction due to the smaller reaction scale (i.e. for **339**). For **339** and **342** the product structures were confirmed by X–ray crystallography.



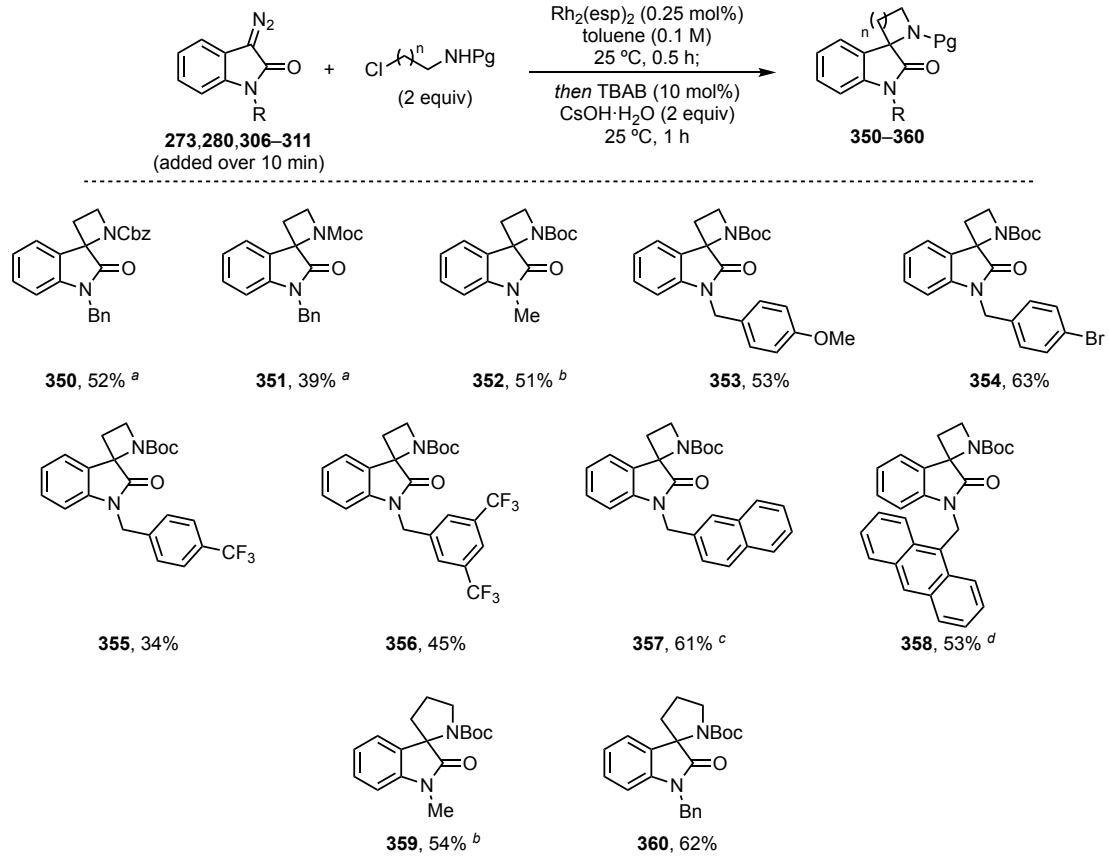
Scheme 98: Synthesis of racemic spiroazetidines with different substituents on the oxindole aromatic ring. Reactions on 0.25 mmol scale. [a] Reaction in toluene. X-Ray crystal structures were obtained for compounds **339** and **342** and visualised using Mercury[350] (for full details see Appendix 7.3).

In certain cases, the isolated product from the N–H insertion reaction was subjected to the cyclisation conditions to afford the spiroazetidine (Scheme 99). A few examples were synthesised in this way, which can be more practical than the one-pot reaction due to the simple reaction conditions and often simpler purification. The lowest yields were obtained for oxindoles **348** and **349**, which may have benefited from being run for a longer time (seen in Section 4.4.4.2).



Scheme 99: Synthesis of spiroazetidines from the isolated N–H insertion product. Reactions on 0.1 mmol scale.

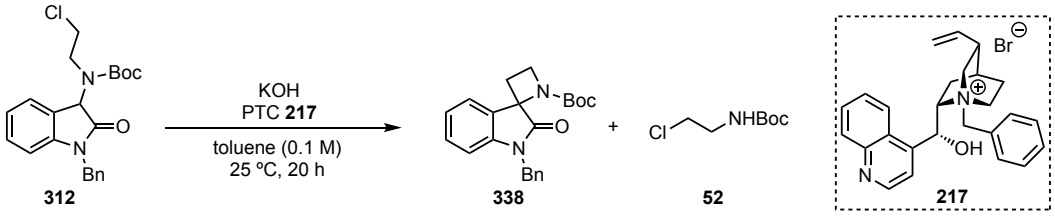
The one-pot N–H insertion and cyclisation was successful with the same substrates as in Scheme 96, with different *N*-substituents and ring sizes (Scheme 100). Yields were similar or slightly lower than the yields for the N–H insertion reactions shown in Scheme 96. Notably, the yield of anthracenyl protected spiroazetidine oxindole **358** was much higher due to a solvent switch from toluene to CH_2Cl_2, likely because of the increased solubility of the diazo compound. Pyrrolidines **359** and **360** were synthesised in the same yield as for the analogous azetidines. However, attempted cyclisation of 6-membered ring precursor **337** did not yield any piperidine product.



Scheme 100: Synthesis of racemic spiroazetidine and pyrrolidine oxindoles in one-pot. Standard conditions on 0.25 mmol scale. [a] Reaction on 0.5 mmol scale. [b] Reaction on 0.5 mmol scale in CH_2Cl_2. [c] Reaction on 0.1 mmol scale in CH_2Cl_2. [-d] CH_2Cl_2.

4.4.3 Optimisation of Enantioselective Cyclisation

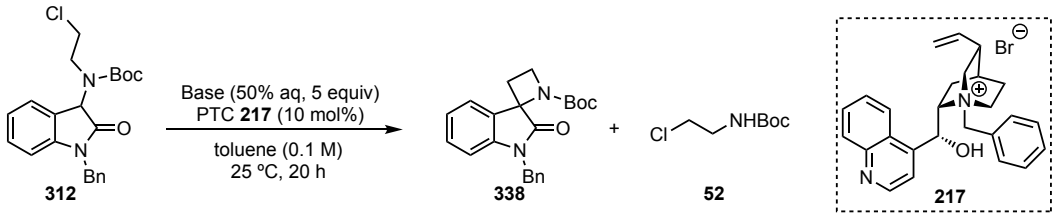
The optimisation of the enantioselective cyclisation started using intermediate **312** with commercially available PTC **217**, *N*-benzyl cinchonidium bromide. As discussed in Section 4.3 a key challenge for intramolecular alkylation reactions is the background or uncatalysed reaction which leads to the erosion of enantioselectivity. Initial results used 2 equiv of KOH, either solid or 50% aq., in toluene (Table 16). For each form of the base the reaction was run with and without PTC **217** (Table 16). Results showed low enantioselectivity, but the non-zero values were very promising in light of the results seen in Section 2.4.4.2. Higher yield and lower background reaction was observed for the reaction with 50% aq. KOH. An important realisation was the formation of **52** as a side product in the cyclisation reaction. This was presumed to be due to an oxidative decomposition of the enolate formed upon deprotonation, though the exact mechanism by which this occurs remains unclear.



Entry	Base	PTC loading (mol%)	Yield (%) [a]		**338** *er* [b]
			338	**52**	
1	s, 2 equiv	0	35	39	-
2	s, 2 equiv	10	41	29	42:58
3	50% aq, 2 equiv	0	15	17	-
4	50% aq, 2 equiv	10	77	23	43:57

Table 16: Test of asymmetric phase transfer catalysed cyclisation with and without PTC **217** with KOH as solid or aqueous base. Reactions on 0.05 mmol scale. [a] Yields calculated by ^{1}H NMR spectroscopy with respect to 1,3,5-trimethoxybenzene as an internal standard. [b] *er* determined by HPLC analysis of crude reaction mixture on a chiral stationary phase. HPLC reported according to elution time in column system stated in Experimental.

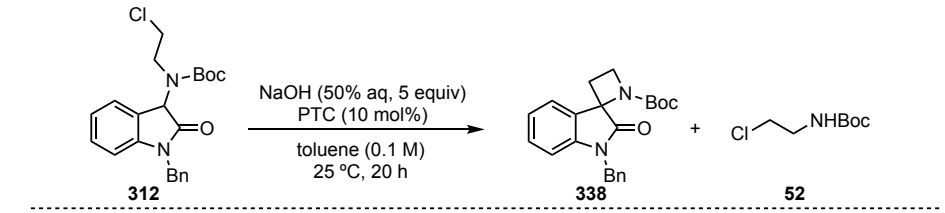
Following these results different inorganic bases as 50% aq. solutions were tested. Using 5 equiv of KOH gave a small increase in the yield of the spiroazetidine (Table 17, Entry 1). Screening different bases showed that hydroxide bases were clearly superior to carbonate bases in terms of yield (Entries 4 and 5). NaOH gave the highest yield and *er* (Table 17, Entry 2).

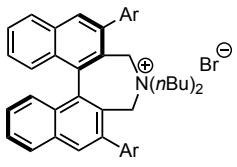


Entry	Base	Yield (%) [a]		**338** *er* [b]
		338	**52**	
1	KOH	23	14	42:58
2	NaOH	50	38	35:65
3	CsOH	22	16	40:60
4	Cs_2CO_3	2	4	40:60
5	K_2CO_3	4	9	40:60

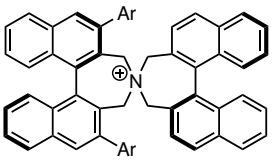
Table 17: Test of asymmetric phase transfer catalysed cyclisation with different bases. Reactions on 0.05 mmol scale. [a] Yields calculated by ^{1}H NMR spectroscopy with respect to 1,3,5-trimethoxybenzene as an internal standard. [b] *er* determined by HPLC analysis of crude reaction mixture on a chiral stationary phase. HPLC reported according to elution time in column system stated in Experimental.

Using the best conditions from Table 17, a screen of different classes of catalysts was carried out (Table 18). This screen included commercial catalysts including examples developed by Maruoka and Shibasaki (Table 18, Entries 1 to 3). Variations of the *cinchona* alkaloid included quininium catalyst **365,** as well as, the commercially available Corey catalyst **364** and an example of a *bis*-quaternised catalyst **366** (Entries 4 to 6). Of the Maruoka and Shibasaki catalysts, **362** gave a high enantioselectivity but poor yield. The Corey catalyst **364** gave poor yield and *er* while the *bis*-quaternised catalyst **366** gave no improvement over the *mono*-quaternised catalyst. Quininium catalyst **365** gave the same yield and *er* as the cinchonidium catalyst **217**, yet this result proved to be more reliable and so this was taken forward in further optimisation.

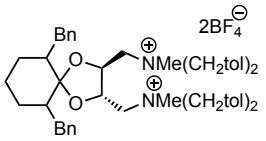




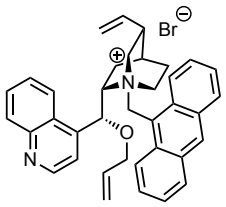
361
Ar = 3,4,5-$F_3C_6H_2$



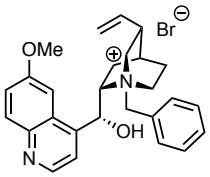
362
Ar = 3,4,5-$F_3C_6H_2$



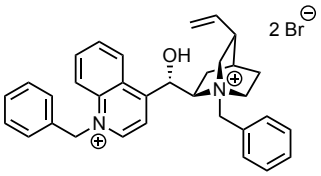
363



364



365



366

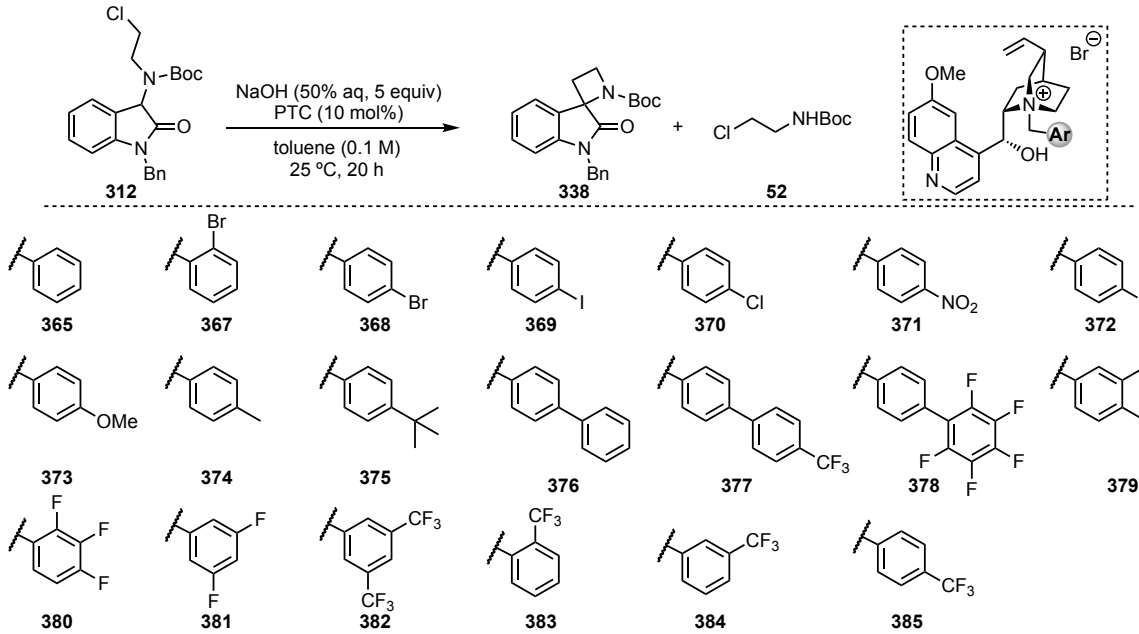
Entry	PTC	Yield (%) [a]		**338** *er* [b]
		338	**52**	
1	**361**	10	55	52:48
2	**362**	22	51	31:69
3	**363**	41	42	36:64
4	**364**	12	60	62:37
5	**365**	50	49	35:65
6	**366**	32	52	36:64

Table 18: Test of asymmetric phase transfer catalysed cyclisation with different catalyst classes. Reactions on 0.05 mmol scale. [a] Yields calculated by ^{1}H NMR spectroscopy with respect to 1,3,5-trimethoxybenzene as an internal standard. [b] *er* determined by HPLC analysis of crude reaction mixture on a chiral stationary phase. HPLC reported according to elution time in column system stated in Experimental.

At this point a number of catalysts derived from the alkylation of quinine were tested (Table 19). This study aimed to establish the required properties of the benzylic substituent for high yield and enantioselectivity. Most of the catalysts were prepared in a high throughput fashion without further purification of the salt after filtration. The unsubstituted *N*-benzyl quininium catalyst **365** gave 32% yield and 33:67 *er* (Table 19, Entry 1). *para*-Substituted benzyl groups with halide substituents (I, Br, Cl) gave improved enantioselectivity (Entries 3–5, 27:73 or 26:74 *er*). Other electron withdrawing substituents, for example, **371** or **372** gave poorer enantioselectivities (Entries 6 and 7). More electron donating substituents in the *para*-position of the aromatic ring also gave poorer enantioselectivities, for example **373** gave 41:59 *er* (Entries 8–11 and 14). Further electron withdrawing substituents in a biaryl system were tested and gave similar results to *para*-halogen containing aromatic rings (up to 25:75 *er*, Entries 12

and 13). Fluorinated aromatic rings are often used in asymmetric phase transfer catalysis. Poor results were seen except for *para*-CF_3 containing catalyst **385** which gave the highest enantioselectivity (21:79 *er*, Entry 20).

These results show a number of trends and provide important insight into the desired structure of the catalyst for this transformation. It was established that electron-withdrawing substituents in the *para*-position were privileged and gave higher enantioselectivities. For example, moving the *p*-CF_3 group to the *meta*- or *ortho*-positions led to poor yield and enantioselectivity (Entries 18 and 19). Even using a more electron-deficient aromatic (3,5-$(CF_3)_2C_6H_3$) gave poor enantioselectivity (Entry 17). Therefore it can be concluded that it is not just the electronic character that leads to the improvement in enantioselectivity, but also the position of the electron-withdrawing substituent. This could be due to different steric interactions in the transition state when the group is in the *ortho* or *meta* positions. Some of the tests in Table 19 were carried out with 20 mol% catalyst, generally this only had an effect on the yield of the reaction and provided more reliable results.

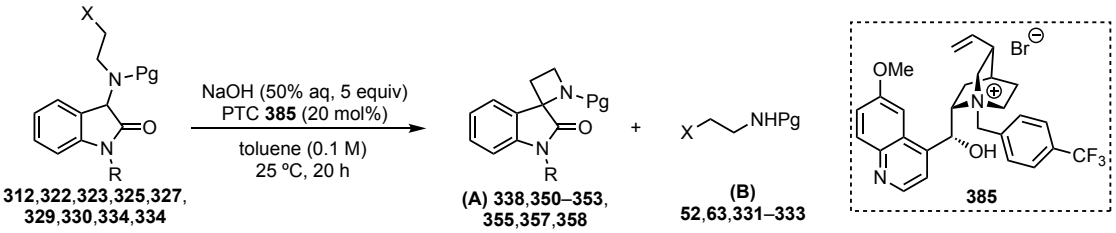


Entry	PTC	Yield (%) [a]		**338** *er* [b]
		338	**52**	
1	**365**	32	60	33:67
2	**367**	19	77	56:44
3	**368**	50	34	27:73
4	**369**	48	47	27:73
5	**370**	27	24	26:74
6	**371**	64	45	39:61
7	**372**	59	36	37:63
8	**373**	28	55	41:59
9	**374**	40	54	31:69
10	**375** [c]	48	45	32:68
11	**376** [c]	36	35	32:68
12	**377** [c]	74	26	25:75
13	**378** [c]	38	32	27:73
14	**379** [c]	23	52	34:66
15	**380**	15	75	49:51
16	**381**	14	46	48:52
17	**382**	19	45	56:44
18	**383** [c]	23	75	59:41
19	**384** [c]	9	15	42:58
20	**385**	48	49	21:79

Table 19: Test of asymmetric phase transfer catalysed cyclisation with different catalyst classes. Reactions on 0.05 mmol scale. [a] Yields calculated by ^{1}H NMR spectroscopy with respect to 1,3,5-trimethoxybenzene as an internal standard. [b] *er* determined by HPLC analysis of crude reaction mixture on a chiral stationary phase. [c] 20 mol% cat. used. HPLC reported according to elution time in column system stated in Experimental.

At this stage of the optimisation the substrate structure was modified to determine what effect changing the different *N*-protecting groups and the leaving group would have on the

enantioselectivity. Changing the leaving group from Cl to Br to I gave increased yield but poorer enantioselectivity (Table 20, Entries 1–3). Changing the amine protecting group from Boc to Cbz to Moc (CO_2Me) gave lower yields and enantioselectivities (Entries 4–5). Changing the protecting group on the oxindole part of the substrate did not lead to significant improvement in yield or *er* (Entries 6–10). These results showed that a larger, poorer nucleofuge would limit enantioselectivity. This observation is in accordance with the Pliego and Houk models for asymmetric phase transfer catalysis discussed in Section 4.3.2. Larger protecting groups gave poorer results which meant that the previously selected Boc group serendipitously had given the best result. In terms of the oxindole protecting group the benzyl group also seemed to be optimal in terms of yield and enantioselectivity. However, changing the electronics of this benzyl group did not significantly affect the yield or enantioselectivity. This screen resulted in the selection of substrate **312** with a Cl leaving group and Boc and Bn protecting groups for further optimisation.



312,**322**,**323**,**325**,**327**, **329**,**330**,**334**,**334**

(A) **338**,**350**–**353**, **355**,**357**,**358**

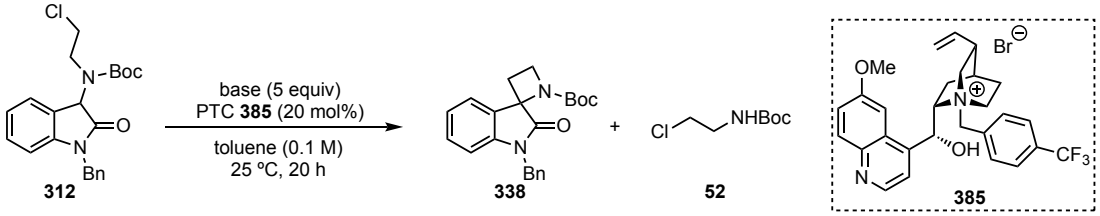
(B) **52**,**63**,**331**–**333**

385

Entry	X	Pg	R	Yield (%) [a]		**A** *er* [b]
				A	**B**	
1	Cl	Boc	Bn	60	39	23:77
2	Br	Boc	Bn	81	0	41:59
3	I	Boc	Bn	83	0	57:43
4	Cl	Cbz	Bn	33	31	62:38
5	Cl	Moc	Bn	45	51	57:43
6	Cl	Boc	Me	32	52	36:64
7	Cl	Boc	4-CF_3Bn	56	44	25:75
8	Cl	Boc	4-OMeBn	59	35	72:28
9	Cl	Boc	2-Menapthyl	39	72	21:79
10	Cl	Boc	9-Meanthryl	37	61	50:50

Table 20: Test of asymmetric phase transfer catalysed cyclisation changing leaving group and protecting groups. Reactions on 0.05 mmol scale. [a] Yields calculated by ^{1}H NMR spectroscopy with respect to 1,3,5-trimethoxybenzene as an internal standard. [b] *er* determined by HPLC analysis of crude reaction mixture on a chiral stationary phase. HPLC reported according to elution time in column system stated in Experimental.

Further extensive catalyst screens to try to improve the yield and enantioselectivity did not result in any benefits over PTC **385** under these conditions (not shown, further catalyst screen shown below in Table 26). Therefore different bases were re-examined (Table 21). Of the different hydroxide bases in aqueous solution NaOH still gave the highest enantioselectivity (Entries 1–4). However, changing the form of the hydroxide bases to solids gave very different results (Entries 5–8). Now KOH and CsOH gave higher yields and enantioselectivities (up to 8:92 *er* for CsOH, Entry 8). Notably, CsOH removed the issue of side product **52** forming by enolate decomposition. Using carbonate bases either did not afford the product or gave lower yield and enantioselectivity (Entry 9). Reducing the loading of base gave a lower *er* (Entry 10).

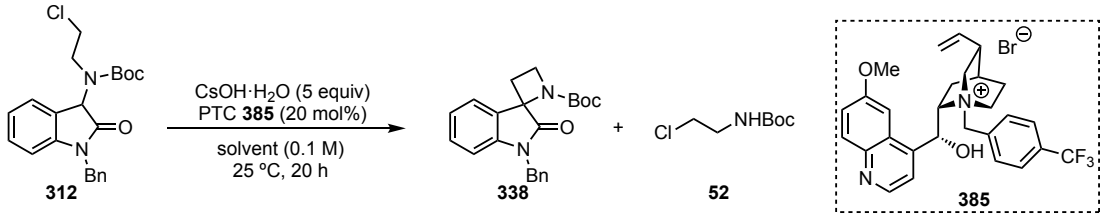


Entry	Base	Yield (%) [a]		**338** *er* [b]
		338	**52**	
1	LiOH (50% aq.)	70	30	32:68
2	NaOH (50% aq.)	60	34	25:75
3	KOH (50% aq.)	65	31	31:69
4	CsOH (50% aq.)	70	30	38:62
5	LiOH (s)	0	0	-
6	NaOH (s)	38	42	23:77
7	KOH (s)	63	24	14:86
8	$CsOH \cdot H_2O$ (s)	85	0	8:92
9	Cs_2CO_3 (s)	71	16	23:77
10	$CsOH \cdot H_2O$ (s, 2.5 equiv)	82	0	10:90

Table 21: Test of asymmetric phase transfer catalysed cyclisation changing base. Reactions on 0.05 mmol scale. [a] Yields calculated by ^1H NMR spectroscopy with respect to 1,3,5-trimethoxybenzene as an internal standard. [b] *er* determined by HPLC analysis of crude reaction mixture on a chiral stationary phase. HPLC reported according to elution time in column system stated in Experimental.

Clearly solid $CsOH \cdot H_2O$ was the superior base to use for the following optimisation. Different solvents were then examined (Table 22). Non-polar aromatic solvents gave superior results. Non-polar solvents being superior is in line with a tight ion-pair interaction. Mixed xylenes gave superior enantioselectivity and when the different xylene isomers were tested *meta*- and *ortho*-xylene gave higher enantioselectivity than *para*-xylene (Entries 3–6). More polar solvents,

relative to toluene and xylene, which are often used in asymmetric phase transfer catalysis, gave poorer yield and enantioselectivity (Entries 8 and 9).

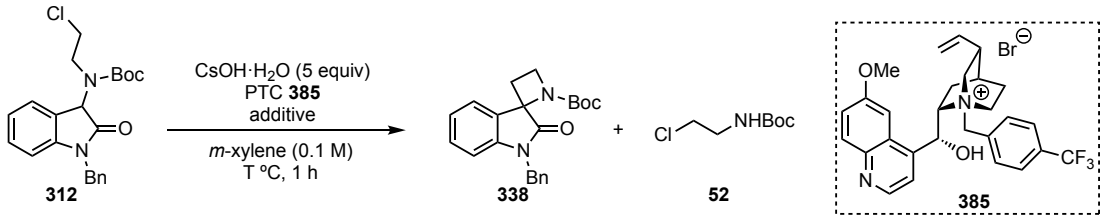


Entry	Solvent	Yield (%) [a]		**338** *er* [b]
		338	**52**	
1	toluene	85	0	8:92
2	benzene	65	0	12:88
3	xylenes	78	0	7:93
4	*p*-xylene	68	0	8:92
5	*m*-xylene	76	0	6:94
6	*o*-xylene	81	0	6:94
7	*m*-xylene [c]	81	0	6:94
8	CH_2Cl_2 [c]	49	13	33:67
9	Et_2O [c]	74	trace	37:63

Table 22: Test of asymmetric phase transfer catalysed cyclisation changing solvent. Reactions on 0.05 mmol scale. [a] Yields calculated by ^{1}H NMR spectroscopy with respect to 1,3,5-trimethoxybenzene as an internal standard. [b] *er* determined by HPLC analysis of crude reaction mixture on a chiral stationary phase. [c] 1 h reaction time. HPLC reported according to elution time in column system stated in Experimental.

At this point of the optimisation a range of variables were tested including temperature, catalyst loading, water content and effect of additives (Table 23). Previously, the reaction had been carried out at 25 ºC. Decreasing the temperature to 0 ºC led to significant inhibition of product formation and low *er* (Entry 1). Increasing the temperature above 20/25 ºC led to increased yield but reduction in *er* (Entries 4 and 5). Therefore the optimum temperature for this reaction remained between 20–25 ºC to maintain high yield and, most importantly, high *er*. Increasing and decreasing catalyst loading had a detrimental effect on yield and enantioselectivity and even though increasing the catalyst loading increased the yield, the *er* was not improved (Entries 6 and 7). Due to the presence of water in the solid CsOH base as the monohydroxide, it was important to determine the effect of water on the yield and enantioselectivity. Addition of 10 μL of water resulted in a drop in yield and *er*. Addition of more water led to much slower reaction rate and depressed product yields with poorer *er* and greater levels of side product **52** being observed (Entries 8–10). Drying the CsOH decreased the yield of the reaction but no

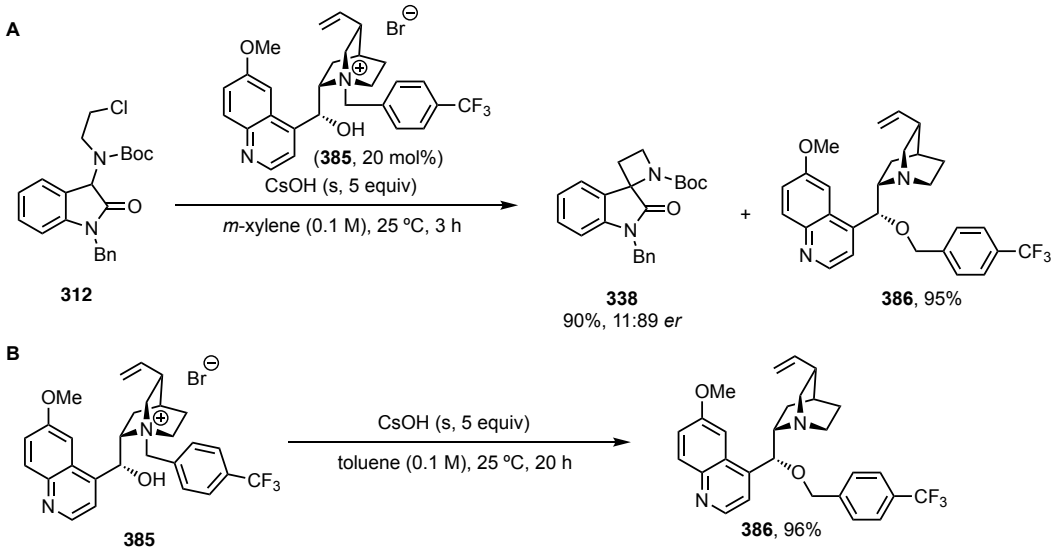
significant effect on the *er* (Entry 11). Grinding the dried base to increase the surface area resulted in higher yield (Entry 12). Addition of polar additives which, like H_2O, could similarly affect the dielectric constant led to poor yield and enantioselectivity in most cases (Entries 13–15). CsCl is likely to be the major inorganic byproduct of the reaction and addition of 1 equiv of this salt as a source of Cs^+ and Cl^- had very little effect on the reaction outcome (Entry 16).



Entry	PTC loading (mol%)	T (° C)	additive	Yield (%) [a]		**338** *er* [b]
				338	**52**	
1 [c]	20	0	-	19 (87) [d]	36	25:75
2	20	20	-	84	0	6:94
3	20	25	-	91	0	5:95
4	20	30	-	98	0	7:93
5	20	40	-	92	0	8:92
6	10	25	-	23	trace	10:90
7	40	25	-	89	0	6:94
8	20	25	H_2O (10 μL)	86	5	8:92
9	20	25	H_2O (50 μL)	22 (83) [d]	26	36:64
10	20	25	H_2O (100 μL)	13 (37) [d]	19	37:63
11	20	25	- [e]	49	trace	6:94
12	20	25	- [e,f]	75	0	5:95
13	20	25	HFIP (10 μL)	9 (66) [d]	10	39:61
14	20	25	urea (10 μL)	36	4	6:94
15	20	25	DMF (10 μL)	42	0	11:89
16	20	25	CsCl (1 equiv)	82	0	5:95

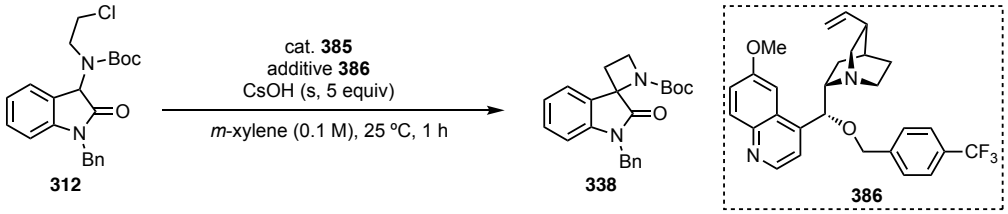
Table 23: Test of asymmetric phase transfer catalysed cyclisation with different temperatures, catalyst loading and additives. Reactions on 0.05 mmol scale. [a] Yields calculated by ^{1}H NMR spectroscopy with respect to 1,3,5-trimethoxybenzene as an internal standard. [b] *er* determined by HPLC analysis of crude reaction mixture on a chiral stationary phase. [c] In toluene. [d] Number in brackets indicates conversion of **312**. [e] dried CsOH. [f] CsOH ground with pestle and mortar. HPLC reported according to elution time in column system stated in Experimental.

Under the conditions optimised at this stage of the optimisation, the reaction was scaled up from 0.05 mmol scale to 0.20 mmol scale to test if the results could be reproduced. Scale up of the best reaction conditions at this point afforded spirocycle **338** in 90% yield with an *er* of 11:89 (Scheme 101A). Clearly this *er* is lower than seen in Table 21 and 22. One possible reason for this was the different rate of stirring upon scaling up the reaction which could affect the yield and enantioselectivity. The only significant byproduct of this reaction was isolated and determined to be **386**. This is derived from intramolecular *O*-alkylation of the catalyst. More typical catalyst degradation occurs *via* epoxide formation,[256,333] however, this was not observed in this reaction. This degradation pathway represents a novel pathway by which the catalyst can degrade. An independent reaction treating the catalyst with base (though at a much lower ratio than in the typical catalytic reaction) formed **386** in almost quantitative yield (Scheme 101B).



Scheme 101: **A**: Test of enantioselective cyclisation reaction at 0.2 mmol scale. **B**: Catalyst degradation under basic conditions. Reaction on 0.1 mmol scale. HPLC reported according to elution time in column system stated in Experimental.

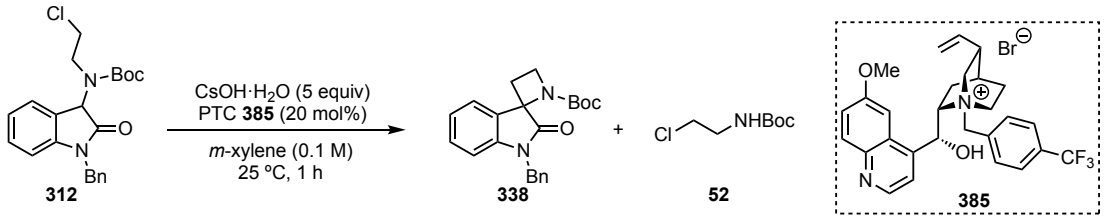
Adding this byproduct to the enantioselective cyclisation reaction had no effect and showed no catalytic activity (Table 24). Based on this evidence, this catalyst degradation pathway probably does not compete with catalytic activity and only slowly reduces the amount of active catalyst in the system.



Entry	PTC loading (mol%)	additive loading (mol%)	Yield (%) [a]		**338** *er* [b]
			338	**52**	
1 [c]	20	0	91	0	5:95
2	0	20	0	trace	-
3	20	20	87	0	5:95

Table 24: Effect of adding **386** to the reaction. Reactions on 0.05 mmol scale. [a] Yields calculated by ^{1}H NMR spectroscopy with respect to 1,3,5-trimethoxybenzene as an internal standard. [b] *er* determined by HPLC analysis of crude reaction mixture on a chiral stationary phase. HPLC reported according to elution time in column system stated in Experimental.

The result from Scheme 101A upon scaling up the reaction prompted an examination of the effect of stirring on the yield of the reaction. The results showed that, as expected for a phase transfer catalysed reaction, a low stirring rate caused diminished yield and enantioselectivity (Table 25, Entry 1). However, the results also showed that a higher stirring rate led to a sharp decrease in yield and enantioselectivity (>1000 rpm, Entry 6). While the lower stirring rate is in accordance with an interfacial phase transfer catalytic mechanism, where, reduction in stirring rate will lead to less catalyst-interface interaction resulting in poorer association of the catalyst. The result for higher stirring is less simple to explain. We have already shown that the surface area of the base is important to obtain a high yield. It is likely that a too vigourous stirring rate causes a physical disruption of the interface between the base and organic layer. It may also disrupt the partitioning of the catalyst into the organic layer which based on literature precedent will likely be dependent on the interaction of the catalyst with the solid base.

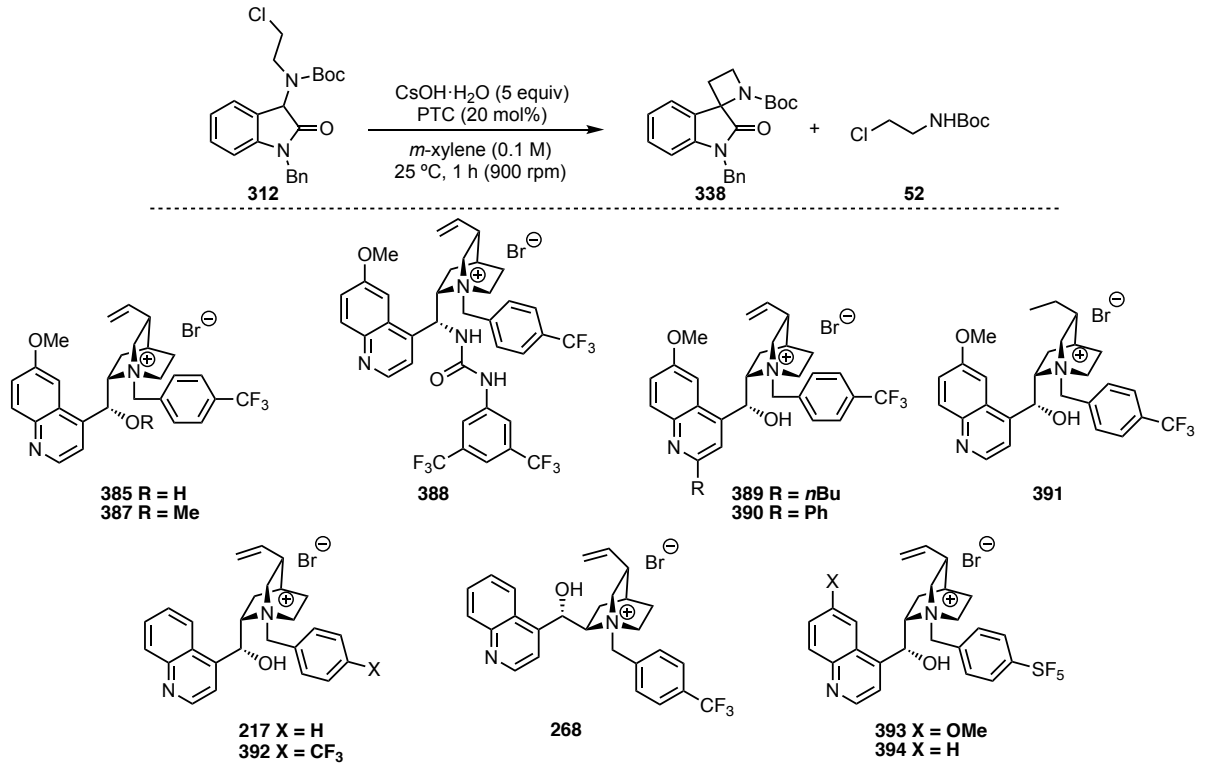


Entry	Stirring Rate (rpm)	Yield (%) [a]		**338** *er* [b]
		338	**52**	
1	500	27	7	15:85
2	700	89	0	7:93
3	800	98	0	6:94
4	900	87	0	5:95
5	900	92	0	5:95
6	1000	42	9	14:86
7	1100	23	5	15:85
8	1200	25	8	12:88
9	1500	24	27 [c]	30:70

Table 25: Effect of stirring rate on yield and enantioselectivity of enantioselective cyclisation. Reactions on 0.05 mmol scale. [a] Yields calculated by ^{1}H NMR spectroscopy with respect to 1,3,5-trimethoxybenzene as an internal standard. [b] *er* determined by HPLC analysis of crude reaction mixture on a chiral stationary phase. [c] 51% conversion from **312** (100% conversion in all other entries). HPLC reported according to elution time in column system stated in Experimental.

With a maximum *er* of 5:95 obtained in the enantioselective cyclisation thus far, a range of catalysts were tested to try to further improve the enantioselectivity while maintaining a high yield. Protection of the hydroxyl group of the catalyst by methylation gave lower yield and enantioselectivity (Table 26, Entry 2). This indicated that the hydroxyl group is important for substrate binding *via* hydrogen bonding. Urea catalyst **388** was tested, previously reported by Dixon, to try to improve hydrogen bonding.[350] However, cat. **388** gave poor results (Entry 3). Substitution of the quinoline group with either a Ph or *n*-Bu group resulted in relatively high yields but lower *er* than the control reaction (Entry 4 and 5). Sometimes using the hydrogenated starting material (i.e. alkane instead of alkene on quinicludine) can improve enantioselectivity presumably due to a slight change in catalyst conformation or solubility. However, using cat. **391** derived from hydroquinine gave lower *er* (Entry 6). A breakthrough came when commercial cat. **217** was retested under these conditions which gave 78% yield and 10:90 *er* (Entry 7). This was highly unexpected based on previous results using *N*-benzyl substituted catalysts. Testing cinchonidine derived cat. **392** gave very high yield and 4:96 *er* (Entry 8). Testing the pseudo-enantiomeric catalyst derived from cinchonine gave lower yield and slightly lower

enantioselectivity but importantly the opposite absolute configuration (Entry 9). We were then interested in trying to improve the enantioselectivity further by using a more electron-withdrawing group in the *para*-position. The SF_5 group is an under explored motif which has recently started to gain more attention within drug and agrochemical discovery, partly due to improved synthetic methods to access it.[351] The SF_5 group can be considered as a "super-CF_3" group. The σ_p Hammett value of SF_5 is 0.68, relative to 0.54 for CF_3 (σ_I: 0.55 vs. 0.39) and is much more similar in electronic character to bis-3,5-CF_3 than 4-CF_3.[352] Another interesting property that lends itself to phase transfer catalysis is the greater lipophilicity of the SF_5 group relative to the CF_3 group. We synthesised and tested the catalysts derived from quinine and cinchonidine. Cat. **393** showed no benefit when compared to analogous cat. **385** from quinine. However, cat. **394** derived from cinchonidine gave a similar high yield and a small but significant increase in enantioselectivity to 3:97 *er*.

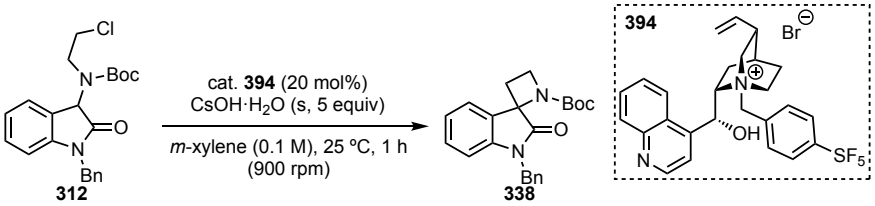


Entry	PTC	Yield (%) [a]		**338** *er* [b]
		338	**52**	
1	**385**	92	0	5:95
2	**387**	54	20	29:71
3	**388**	trace	10	-
4	**389**	87	0	13:87
5	**390**	71	8	8:92
6	**391**	85	0	10:90
7	**217**	78	0	10:90
8	**392**	97	0	4:96
9	**268**	89	0	93:7
10	**393**	78	0	10:90
11	**394**	92	0	3:97

Table 26: Final catalyst screen for the enantioselective cyclisation. Reactions on 0.05 mmol scale. [a] Yields calculated by ^{1}H NMR spectroscopy with respect to 1,3,5-trimethoxybenzene as an internal standard. [b] *er* determined by HPLC analysis of crude reaction mixture on a chiral stationary phase. HPLC reported according to elution time in column system stated in Experimental.

Throughout the optimisation process detailed in this section each variable was examined. However, it is useful to reexamine the variables after reaching the optimized conditions. Glorius

recently proposed a method of doing this whilst also providing a quick and simple way to assess the sensitivity of the reaction conditions to small alterations to selected variables.[353] This is the first time that this full assessment has been done for a reaction using an asymmetric phase transfer catalyst/chiral cation and the first fully reported assessment for an enantioselective reaction.[354] We chose the following 10 experiments (excluding control reaction) to assess the reaction sensitivity when changes were made to the standard conditions (Table 27).



Entry	Variable	Description	Yield of **338** [a]	Yield (±%)	*ee* [b]	*ee* (±%)
1	control	no deviation	94	-	94	-
2	low conc	0.09 M	98	4	94	0
3	high conc	0.11 M	90	–4	94	0
4	high H_2O	+ 5 µL H_2O	80	–14	94	0
5	low H_2O	flame-dried vial	98	4	94	0
6	low O_2	under Ar	100	6	90	–4
7	high T	35 °C	87	–7	91	–3
8	low T	15 °C	29	–65	68	–26
9	high stir	1150 rpm	33	–61	68	–26
10	low stir	650 rpm	27	–67	66	–28
11	big scale	1.0 mmol scale	72 (60)	–22	88	–6

Table 27: Sensitivity screen using optimised standard conditions. Reactions on 0.05 mmol scale unless otherwise stated. Reactions under air unless otherwise stated. [a] Yields calculated by ^{1}H NMR spectroscopy with respect to 1,3,5-trimethoxybenzene as an internal standard. [b] *er* determined by HPLC analysis of crude reaction mixture on a chiral stationary phase.

Figure 27 shows a radar plot of the data in Table 27. This demonstrates the change in yield and *ee* relative to the control reaction (Table 27, Entry 1). Qualitatively concentration, water and oxygen content have minimal impact on the yield and enantioselectivity of the reaction. As previously noted in Table 23, addition of water is negative. In this case, addition of 5 µL of water reduced the yield (–14%) but had no effect on the enantioselectivity of the reaction. Low oxygen content, by running the reaction under argon, increased the yield marginally, however, resulted in a lower enantioselectivity. As already seen and discussed in this section, the

reaction is much more sensitive to changes in temperature and stirring rate. Higher temperature led to reduced yield and enantioselectivity, though this was marginal relative to the control reaction. The differences in the yield and *er* were much more dramatic when the temperature was reduced by just 10 ºC. As observed in Table 25 changing the stirring rate, even just 250 rpm higher or lower, had a significant effect on the yield and the enantioselectivity. The yield and enantioselectivity differences shown in Figure 27 appear proportional. Importantly, when the reaction was scaled up (401 mg of **312**) the yield and *er* did decrease but not such that the yield and *er* were not synthetically useful. This large scale result was not optimised for stirring rate or vessel size and this is something to take into consideration for processing scaled up reactions.

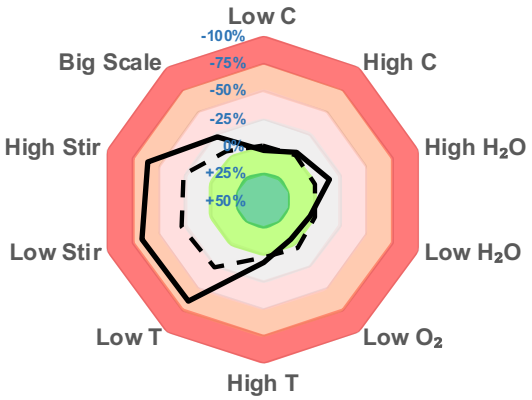
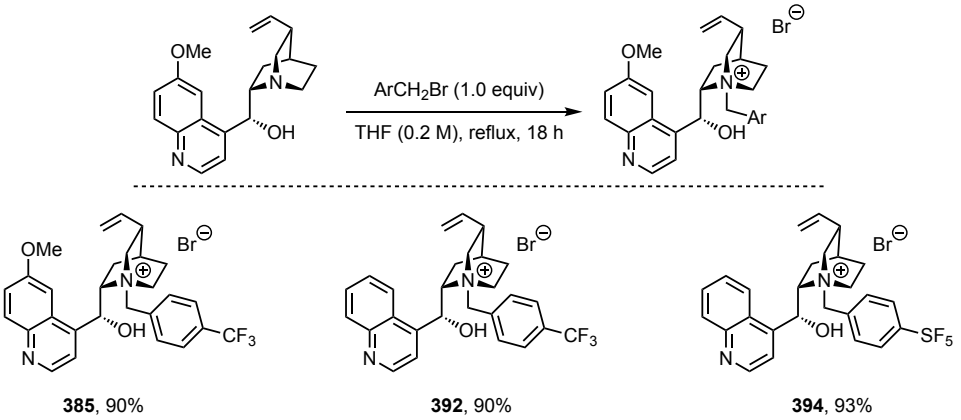


Figure 27: Radar plot to display the sensitivity of the reaction, raw data in Table 27. Bold line = yield. Dashed line = *ee*.

4.4.3.1 Synthesis of Catalysts

For full details of the synthesis of the catalysts used in the optimisation in this section see the experimental (Section 6.2.3.5). *Cinchona* alkaloids are natural and inexpensive compounds from the chiral pool. The quinicludine nitrogen can be alkylated to form a quaternary ammonium salt under neutral conditions. For example, PTCs **385**, **392** and **394** were synthesised through an alkylation using the appropriate substituted benzyl bromide (Scheme 102). Upon cooling to rt the solid was triturated with diethyl ether and used without further purification. The relevant benzyl bromides were commercially available.

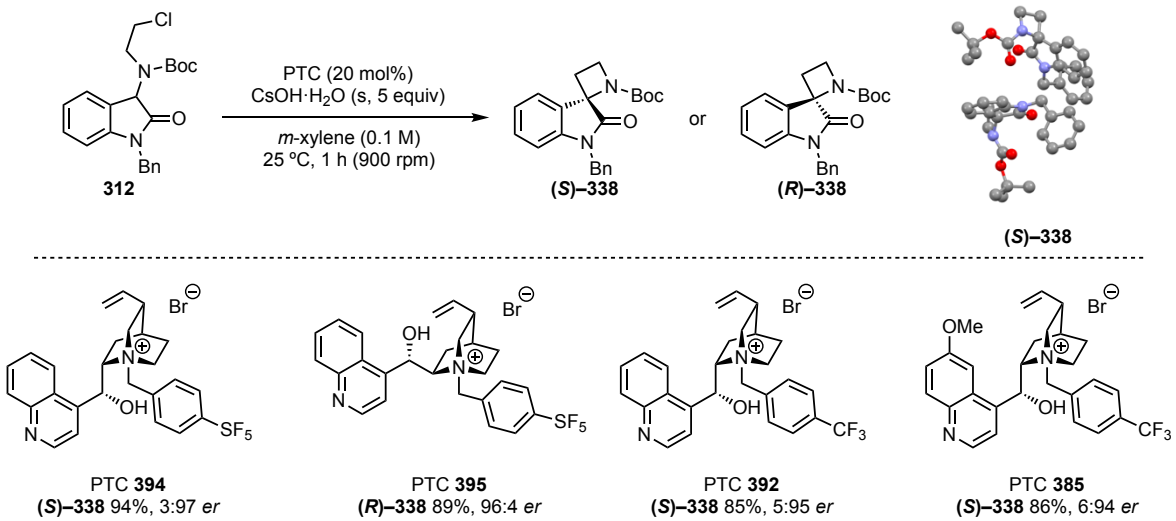


Scheme 102: Alkylation of cinchonidine with different substituted benzyl bromides. Reactions on 0.5 to 2.5 mmol scale.

4.4.4 Reaction Scope of Enantioenriched Spirooxindoles

4.4.4.1 Testing Different Catalysts on Scale Up

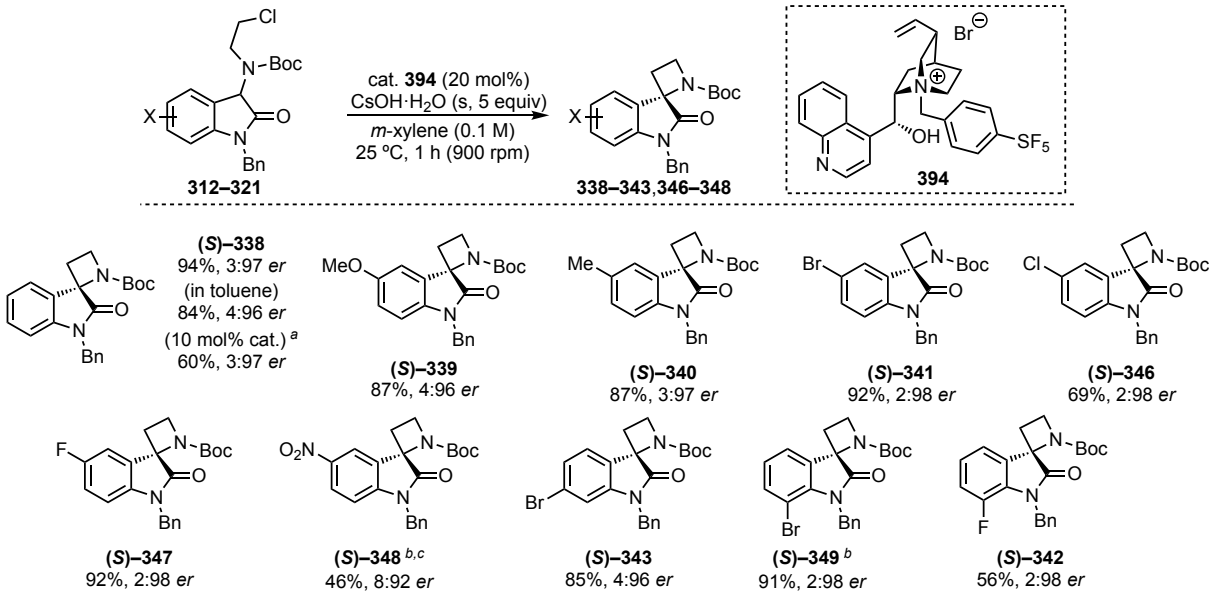
In Section 4.4.3 the optimisation of the asymmetric phase transfer catalysed cyclisation to form spiroazetidine oxindoles was described. The optimisation and sensitivity screen showed that stirring rate and therefore scale up of the reaction could lead to lower yield and enantioselectivity. However, scale up from 0.05 mmol scale to 0.20 mmol scale was successful without modification of the conditions when using cat. **394**. On this scale spiroazetidine **(*S*)–338** was afforded in 94% yield and 3:97 *er* (Scheme 103). When pseudoenantiomeric cat. **395** was employed the yield and enantioselectivity were slightly reduced. This showed that spiroazetidine **(*R*)–338** with the opposite absolute configuration could be afforded simply by changing the catalyst. Use of 4-CF_3 benzyl substituted catalysts **392** and **385** gave approximately 10% lower yield and 4 to 6% lower *ee*. This was a clear demonstration that cat. **394** was a superior catalyst. However, the required 4-SF_5-benzyl bromide starting material for catalyst synthesis is relatively expensive and may require synthesis. Therefore, it was important to show that the cheaper and more readily available 4-CF_3-benzyl bromide would afford the desired product in high yield and enantioselectivity.



Scheme 103: Enantioselective cyclisation of **312** with different catalysts. Reactions on 0.2 mmol scale. Isolated yields. *er* determined by HPLC analysis of product on a chiral stationary phase. HPLC reported according to elution time in column system stated in Experimental. X-Ray crystal structure shown for **338**, visualised using Mercury[350] (for full details see Appendix 7.3).

4.4.4.2 Scope of Different Aromatic Rings

Use of toluene instead of *m*-xylene reduced the yield by 10% and *ee* by 2% (Scheme 104). Using a lower catalyst loading (10 mol% vs. 20 mol%) gave a reduced yield but the same enantioselectivity. We then sought to demonstrate the scope with respect to the oxindole aromatic ring. When the oxindole aromatic was substituted with an electron-donating substituent high yields were obtained with a small reduction in enantioselectivity observed with OMe-substituted azetidine **339**. Very high enantioselectivities were observed when the aromatic ring was substituted with halogens (F, Cl, Br). Yields were variable with more electron poor aromatic rings giving lower yields (Cl, NO_2). A longer reaction time and higher catalyst loading was required to promote the cyclisation using NO_2-substituted starting material **318**, most likely due to the insolubility of this starting material which led to longer reaction times. Comparing 5-F substituted azetidine **347** with 7-F substituted azetidine **342**, only the yields were different and most importantly the enantioselectivities were not affected. Comparison of 5-Br substituted oxindole **341** with 6-Br and 7-Br oxindoles **343** and **349** shows that the yield is unaffected and the enantioselectivity was only slightly reduced for 6-Br substituted oxindole **343**.



Scheme 104: Scope of enantioselective cyclisation with respect to oxindole aromatic ring. Reactions on 0.2 mmol scale. Isolated yields. *er* determined by HPLC analysis of product on a chiral stationary phase. HPLC reported according to elution time in column system stated in Experimental. [a] 0.1 mmol scale. [b] 18 h reaction time. [c] 0.1 mmol scale, 40 mol% cat.

The absolute configuration of azetidines **343** and **349** was unambiguously determined through X-ray crystallography (Figure 28). The configuration was determined to be *S* according to the Cahn–Ingold–Prelog priority rules.[355] Azetidines synthesised using the same catalyst **394** have been assigned in analogy to the configuration of **343** and **349**.

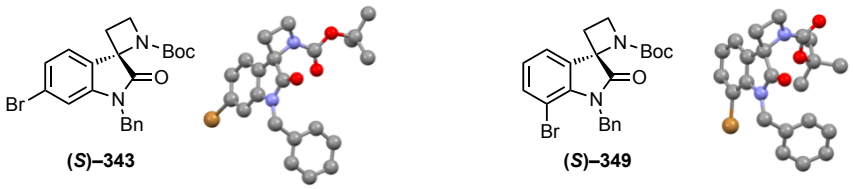
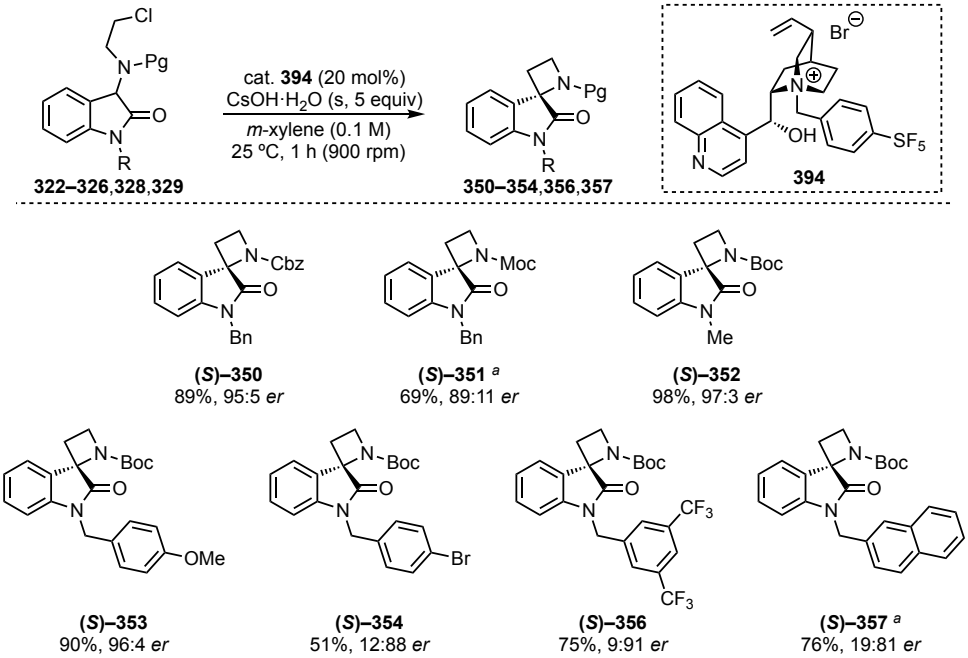


Figure 28: X-Ray crystal structures of azetidines **343** and **349** to unambiguously confirm the absolute configuration. Visualised using Mercury.[350] (For full details see Appendix 7.3).

4.4.4.3 Scope of Different N-Substituents

Having shown that the reaction was highly enantioselective with a range of electronically distinct fused aromatic rings, the two *N*-protecting groups were altered (Scheme 105). Changing the Boc protecting group on the amine portion of the starting material to Cbz and Moc resulted in lower yields and enantioselectivities. The similarly sized Cbz group gave only a marginally reduced yield and enantioselectivity and Moc, being much smaller, gave a significantly reduced, though arguably still impressive, yield and enantioselectivity of 69% and 89:11 *er*. When examining the oxindole *N*-substituent, it was surprising to see that when a methyl substituent was used the same enantioselectivity was observed when compared to a benzyl substituent. This suggests that the benzyl group is not required for high enantioselectivity to be obtained. The benzyl group could be substituted, for example, PMB protected azetidine **353** was afforded in high yield and 96:4 *er*. However, other substitution

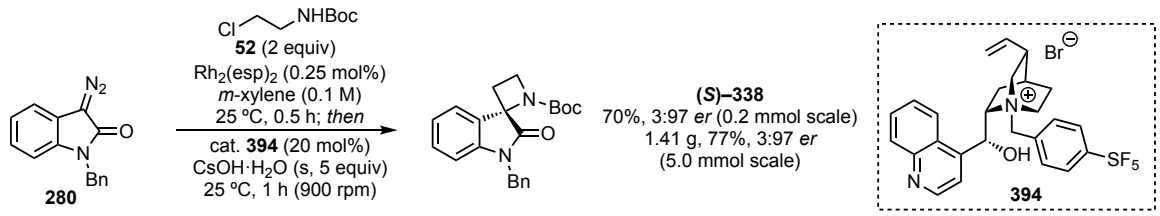
resulted in lower yield and enantioselectivity, which is likely due to the increased size and resultant increased steric demand in the catalyst active site.



Scheme 105: Scope of enantioselective cyclisation with respect to *N*-substituents. Reactions on 0.2 mmol scale. Isolated yields. *er* determined by HPLC analysis of product on a chiral stationary phase. HPLC reported according to elution time in column system stated in Experimental. [a] Reaction on 0.1 mmol scale.

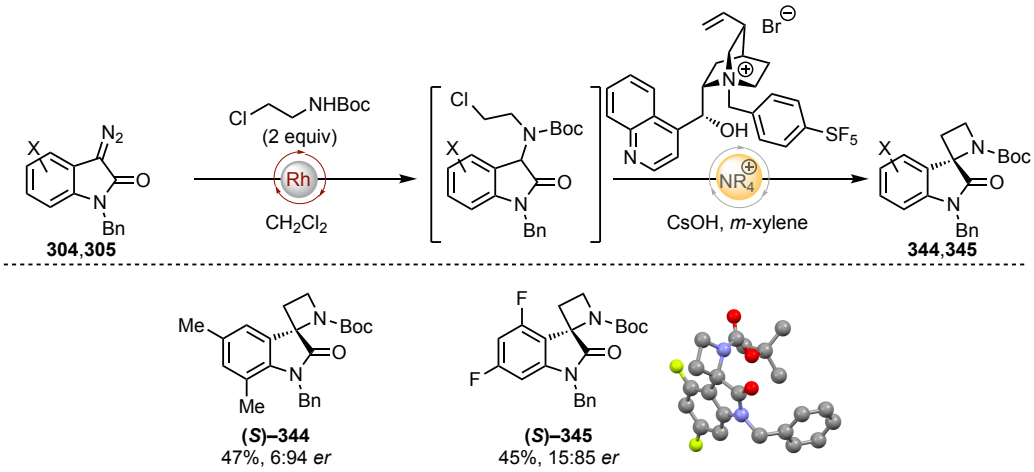
4.4.4.4 One-Pot and Telescoped Reactions

Section 4.4.4.2 and 4.4.4.3 established a broad scope of potential spirooxindoles that can be synthesised in highly enantioenriched manner through the developed asymmetric phase transfer catalytic system. As in Chapters 2 and 3, we were interested to remove the isolation of the intermediate and carry out an N–H insertion and enantioselective cyclisation in one-pot. The reaction was carried out successfully, simply by switching the solvent for the N–H insertion reaction from toluene to *m*-xylene to maintain a high enantioselectivity in the subsequent cyclisation step (Scheme 106). This one-pot reaction afforded spiroazetidine **338** in 70% yield over the 2 steps from diazo **280** without any reduction in the enantioselectivity relative to the cyclisation from the isolated NH insertion intermediate. This was scaled up to 5.0 mmol scale using 1.25 g of diazo **280** to afford 1.41 g of spiroazetidine **338** without a reduction in enantioselectivity and an improved 77% yield.



Scheme 106: One-pot N–H insertion and enantioselective cyclisation to spiroazetidine **338**. Reactions on 0.2 mmol or 5.0 mmol scale. Isolated yields. *er* determined by HPLC analysis of product on a chiral stationary phase. HPLC reported according to elution time in column system stated in Experimental.

The main limitation of this one-pot reaction is the generality to a broader range of diazo compounds. As the substituted diazo compounds are not very soluble in aromatic solvents such as toluene and *m*-xylene this would result in poor results for the initial step. Therefore, a telescoped process was investigated with CH_2Cl_2 used for the first step. Removal of this solvent was followed by addition of PTC **394** and *m*-xylene. This is because, as shown in Table 22, CH_2Cl_2 results in significant reduction in yield and enantioselectivity in the cyclisation step. The telescoped reaction was successful with disubstituted diazo compounds **304** and **305** and afforded the enantioenriched spiroazetidine oxindoles in good yield and enantioselectivity (Scheme 107). It is possible that some remaining traces of CH_2Cl_2 could have had a negative effect on the second step. However, this provided a proof of principle that the spiroazetidine products could be afforded in a rapid manner, removing the requirement for isolation and characterisation of the intermediate.

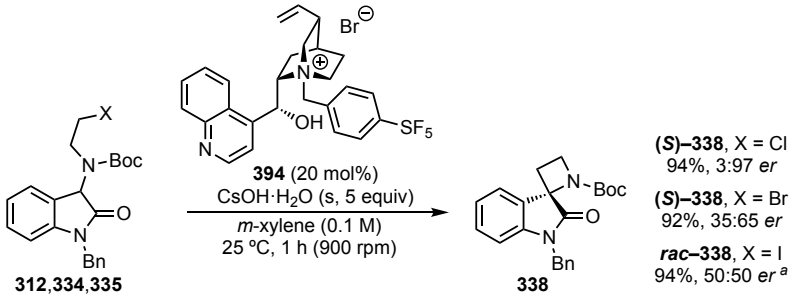


Scheme 107: Examples of spiroazetidine oxindoles synthesised in a telescoped process. Reactions on 0.2 mmol scale. Isolated yields. *er* determined by HPLC analysis of product on a chiral stationary phase. HPLC reported according to elution time in column system stated in Experimental. X-Ray crystal structure shown for **(*S*)–345**, visualised using Mercury[350] (for full details see Appendix 7.3).

4.4.4.5 Scope of Leaving Groups and Ring Size

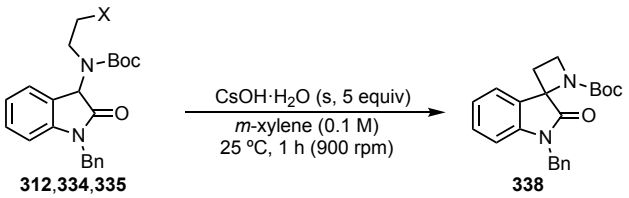
In the optimisation of the enantioselective cyclisation it had been clearly established that using Cl as leaving group gave superior enantioselectivity. However, we were interested to study this under the optimised conditions with cat. **394**. Using Br and I as leaving group gave the same yield under these conditions as when using Cl as leaving group (Scheme 108). However, using these better leaving groups led to much lower enantioselectivity. When using iodide as leaving group, racemic product was formed, even when using 40 mol% catalyst. There is clearly a correlation between larger leaving group and better nucleofuge with poorer enantioselectivity. It is expected that the chloride leaving group interacts with the ammonium cation upon C–Cl bond cleavage, as in the Pliego and Houk models of enantioselectivity (Section 4.3, for further discussion see Section 4.4.5). Therefore the observed reduction in enantioselectivity could be due to reduced substrate and catalyst interaction due to the leaving group size. However, the

reduction in enantioselectivity could also be due to a greater rate of racemic background reaction.



Scheme 108: Asymmetric phase transfer catalysed cyclisation when using different leaving groups. Reactions on 0.1 to 0.2 mmol scale. Isolated yields. *er* determined by HPLC analysis of product on a chiral stationary phase. HPLC reported according to elution time in column system stated in Experimental. [a] 40 mol% cat. **394**.

To test the background reaction, substrates **312**, **334** and **335** were subjected to the reaction conditions without adding PTC **394** (Table 28). No product was observed after 1 h with Cl as leaving group (Table 28, Entry 1). However, when Br and I were used as leaving group significant levels of background reaction were observed (Entries 2 and 3). This clearly indicates that the catalyst is not required for deprotonation of the substrate to form the enolate. This is evidence for an interfacial asymmetric phase transfer mechanism.

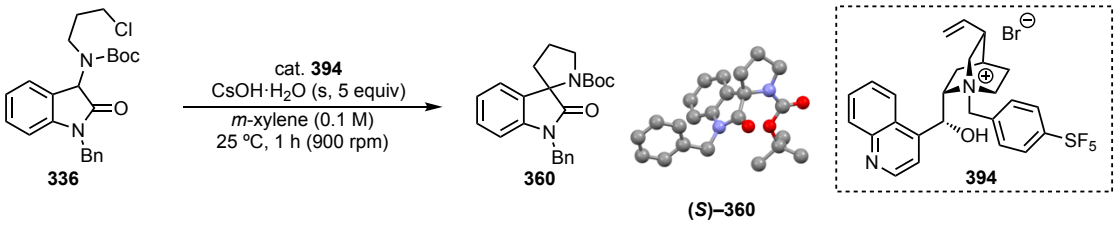


Entry	X	Yield of **338** (%) [a]
1 [b]	Cl	1
2	Br	67
3	I	100

Table 28: Non-catalysed cyclisation when using different leaving groups. Reactions on 0.05 mmol scale. [a] Yields calculated by ^{1}H NMR spectroscopy with respect to 1,3,5-trimethoxybenzene as an internal standard. [b] Reaction in toluene.

The catalysed and non-catalysed reaction to synthesise spiropyrrolidine oxindole **360** was then studied. Being able to modulate the ring size would increase the generality of the methodology. The non-catalysed reaction formed racemic pyrrolidine **360** in quantitative yield by ^{1}H NMR spectroscopy (Table 29). However, despite this racemic background reaction, the spiropyrrolidine was isolated in 96% yield and 17:83 *er* in the presence of cat. **394**. This enantioselectivity was higher than expected when the significant background reaction is taken into account. The faster rate of the background reaction compared to the four-membered ring (Table 28, Entry 1) is presumably because of the lower barrier for cyclisation due to the lower

strain energy of the five-membered ring. The enantioselectivity could also be affected by the additional methylene in the carbon chain which could result in poorer substrate-catalyst interaction.



Entry	cat. loading (mol%)	Yield of **360** (%) [a]	**360** *er* [b]
1 [c]	0	100	-
2	20	(96)	17:83

Table 29: Cyclisation of **336** to afford spiropyrrolidine **360** with and without phase transfer catalyst. Reactions on 0.20 mmol scale. [a] Yields calculated by ^{1}H NMR spectroscopy with respect to 1,3,5-trimethoxybenzene as an internal standard. [b] *er* determined by HPLC analysis of product on a chiral stationary phase. HPLC reported according to elution time in column system stated in Experimental. [c] Reaction on 0.05 mmol scale. X-Ray crystal structure obtained for **(*S*)–360** and visualised with Mercury (see Appendix 7.3 for full details).

As discussed in Section 4.3.2 the *cinchona* alkaloid derived phase transfer catalysts have been reported to be sparingly soluble in non-polar organic solvents. They have been proposed to form more soluble dimeric complexes upon deprotonation. Indeed, when stirred in toluene cat. **394** was observed to be insoluble. We hypothesised that prestirring the catalyst and base could lead to more catalyst entering the organic layer and improve reactivity. However, prestirring the base and catalyst prior to addition of the substrate did not improve reactivity.

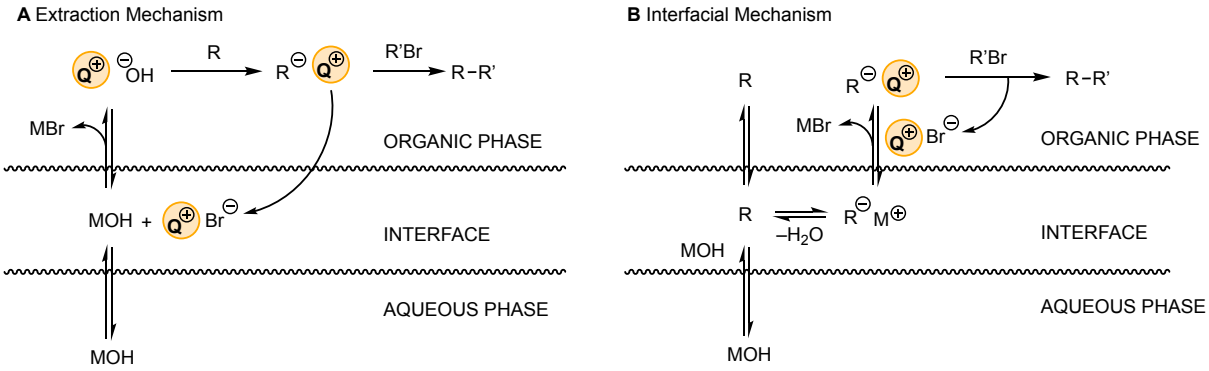
Towards six-membered ring synthesis, when substrate **337** was subjected to the reaction conditions to generate a spiropiperidine product, a poor yield of approximately 5% was obtained.

4.4.5 Mechanism of Asymmetric Phase Transfer Catalysed Cyclisation

In the previous two sections of this thesis the development and scope of a highly enantioselective phase transfer catalysed intramolecular cyclisation reaction was discussed. The observations from these sections can inform on two aspects of the mechanism of this reaction: 1) the phase transfer catalytic mechanism and 2) the mode of asymmetric induction.

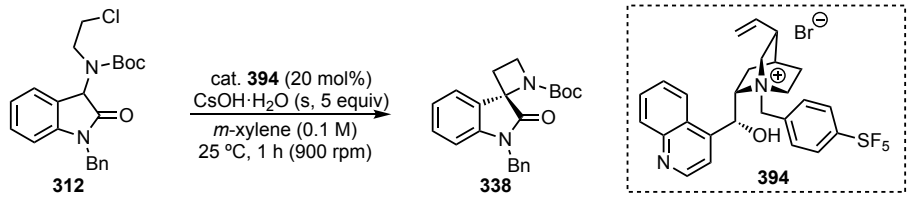
The two mechanisms of phase transfer catalysis, the extraction and interfacial mechanisms, were discussed in Section 4.3 (Scheme 83 is reproduced below). The first key piece of evidence to determine which phase transfer mechanism is operative, is the dependence of the reaction on stirring rate. In Tables 25 and 27 the reaction was shown to be sensitive to high and low stirring rates. The interfacial mechanism is typically dependant on stirring rate due to the requirement for deprotonation at the interface combined with catalyst-substrate

coordination. The extraction mechanism is not usually considered to be dependant on stirring rate as above a certain rate of stirring (300 rpm) catalyst-hydroxide transport is considered sufficient to allow deprotonation and then alkylation in the organic phase.[332] Another clear indication is the significant background reaction observed when better nucleofuges are used or when the energy barrier to cyclisation is lowered by changing from four- to five-membered ring formation. These background reactions (Table 28 and 29) show that the catalyst is not required for deprotonation to occur. This again implies that an interfacial mechanism is operative as in this mechanism the catalyst is not required for deprotonation. This is also why the interfacial mechanism is most applicable to enolate reactions where the pK_a of the enolisable proton lies between 16 and 23. The pK_a of the enolisable proton in oxindole is 18, which clearly lies within this boundary, so it is likely that the starting materials used in this study do also.[356] The acidity of the proton therefore allows deprotonation by hydroxide at the interface followed by coordination with the phase transfer catalyst. The extraction mechanism relies on the reduced hydration of the hydroxide ion, thus increasing the basicity, to allow for deprotonation in the presence of the phase transfer catalyst. Therefore, deprotonation would not be expected in the absence of the phase transfer catalyst.



Scheme 83: Extraction and interfacial mechanisms of phase transfer catalysis. Reproduced from Section 4.3.1.

Further evidence for an interfacial phase transfer catalytic mechanism was provided by monitoring the cyclisation of **312** to **338** (Figure 29). This showed that the starting material is rapidly deprotonated resulting in loss of any diagnostic ^{1}H NMR signals, however, this did not result in immediate product formation. Indeed, there is a lag before any product is formed and this steadily increases to give quantitative yield and 3:97 *er* after 1 h. This indicates that the starting material is deprotonated to form the metal enolate, which has a sufficiently long lifetime at the interface of the organic and aqueous layers. Then catalyst coordination can allow cyclisation to occur (further discussion on how this occurs below).



Entry	time (min)	Yield (%) [a]	
		312	**338**
1	0.5	92	0
2	1	83	0
3	1.5	47	0
4	2.5	29	0
5	5	10	0
6	10	2	5
7	30	0	60
8	60	0	100

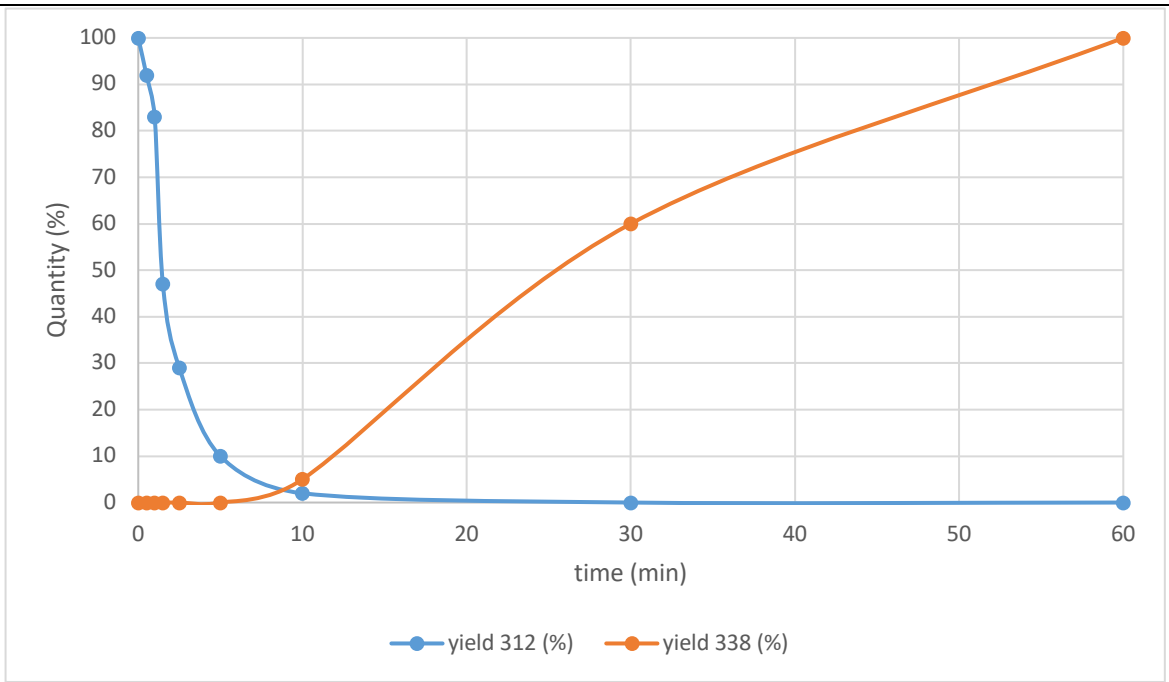
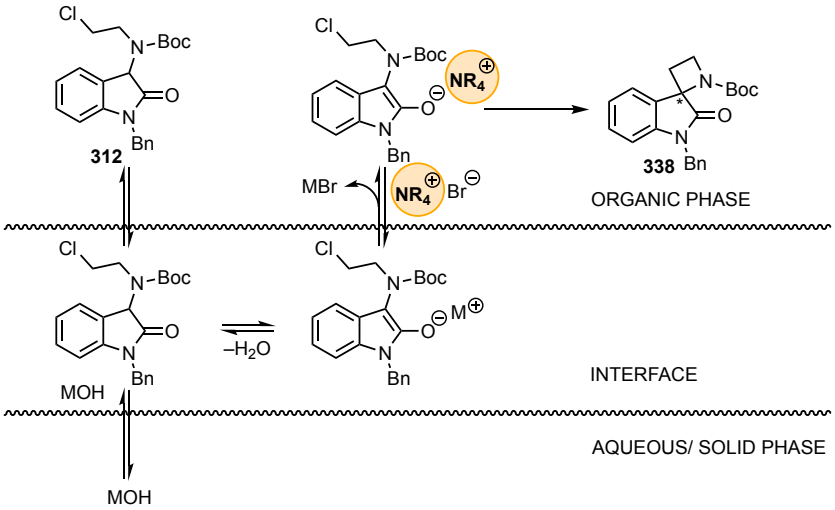


Figure 29: Sampling of reaction to form **338** catalysed by **394** over 1 h. Table and graph of results. [a] Yields calculated by ^{1}H NMR spectroscopy with respect to 1,3,5-trimethoxybenzene as an internal standard.

This data combined with the observations of deprotonation in the absence of the catalyst and dependence on stirring rate are consistent with an interfacial phase transfer catalytic mechanism rather than an extraction mechanism. An example mechanism is shown in Scheme 109. Here, the starting material **312** diffuses to the interface and can be deprotonated by the hydroxide, which in the case of the optimal conditions would be CsOH. The enolate then exists in equilibrium at the interface before coordination to the catalyst. In the final step the catalyst can promote the cyclisation reaction. Clearly, the chloride leaving group is vital for this

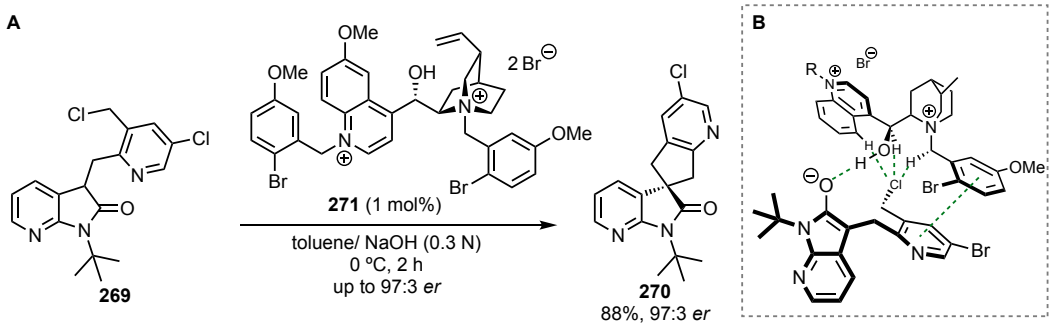
transformation to achieve high enantioselectivity. For the four membered ring formation, with Cl as leaving group, the energy barrier to cyclisation is too high in the absence of the catalyst. When the barrier to cyclisation is reduced, i.e. with Br or I as leaving group or in 5-membered ring formation, the enolate can spontaneously cyclise in the absence of the catalyst. In terms of different leaving groups, the nucleofuge will coordinate to the catalyst upon ring closure. The different counterions associated with the catalyst *can* have an effect on the lipophilicity of the catalyst and therefore the partitioning between the organic and aqueous phases, or in a solid inorganic/organic system the partitioning at the interface. Therefore, it is possible that additional iodide (generated upon cyclisation when using an iodide leaving group) makes the catalyst more lipophilic and thus reduces the amount of catalyst at the interface. However, in our optimisation changing the counterion of the catalyst from bromide to chloride had no effect on the result of the cyclisation.



Scheme 109: Generalised interfacial phase transfer catalytic mechanism for the spirocyclisation developed in this chapter.

Having determined that the operative phase transfer catalytic mechanism is most likely an interfacial mechanism the question remains as to how the catalyst interacts with the substrate in order to promote cyclisation and induce enantioselectivity. From the optimisation in Section 4.4.3, it was clear that high yield and enantioselectivity could only be achieved when non-polar aromatic solvents were employed. Even some solvents which normally can perform well in asymmetric phase transfer catalysis, i.e. CH_2Cl_2 and Et_2O, gave poor results in terms of enantioselectivity in this work. The preference for non-polar solvents indicates a tight-ion pair between the catalyst and substrate and indicates that the system can be treated similarly to literature precedent. Indeed, the literature precedent (discussed in Section 4.3.2) can be used to inform the asymmetric induction model for the reaction developed in this section. There are similarities between the intramolecular cyclisation reaction developed by Merck and further investigated by Houk (discussed in Section 4.3.2, Scheme 85 is reproduced below for clarity).

Therefore, the key interactions could be similar between the two reactions. However, one of the key interactions in the reaction developed by Merck was a π-interaction between the pyridine ring on the alkyl chain and the quinuclidine benzylic group. This is clearly absent in the reaction developed in Section 4.4. A further difference is the absence of the necessity for *bis*-quaternisation in the phase transfer catalyst in this work, which reduces the complexity of the system.



Scheme 85: **A**: Asymmetric phase transfer catalysed intramolecular cyclisation developed by Merck. **B**: Model of asymmetric induction as studied by Houk. Reproduced from Section 4.3.2.

One of the key interactions between the catalyst and the substrate is the interaction between the OH group of the catalyst and the enolate of the substrate. As described by Houk, this is a hydrogen bond which acts as one primary interaction between the catalyst and substrate. The stabilising effect of this interaction is suggested by the decrease in enantioselectivity of the azetidine formation when the OH group was replaced with OMe (Section 4.4.3, Table 26). Dependent on the charge distribution this hydrogen bond could lead to increased or reduced nucleophilicity of the enolate, but it clearly has a role to play in orienting the substrate prior to cyclisation.

Another key interaction emphasised by Pliego (Section 4.3.1) and Houk was the interaction between the ammonium cation (*via* the α-C–H bonds) and the leaving group of the substrate. This is supported in our work by the decreased enantioselectivity when Br and I are used. This would lead to reduced interaction with the catalyst due to the size of the nucleophile. Indeed, the catalyst can be considered to be activating the chloride electrophile to enable cyclisation as without the catalyst no cyclisation can occur. This activation occurs through stabilisation of the negative charge upon C–Cl bond cleavage, while also activating the C–Cl bond through greater polarisation by increasing electron density on Cl, leading to lengthening of the C–Cl bond.

A third key observation from Section 4.4.4.3 was the importance of a large protecting group on the alkylamine. A Boc protecting group gave superior enantioselectivity, with poorer enantioselectivity for CO_2Me as protecting group. This is due to the Boc group blocking one face of the substrate increasing the steric hindrance and promoting interaction between the

alkyl chloride of the substrate and the catalyst. Smaller leaving groups reduce this blocking effect and provide more flexibility for the amine to rotate.

Therefore, three key influences on the catalyst–substrate interaction are the OH···enolate hydrogen bond, the leaving group activation and the role of the large Boc group as a steric shield on one face of the enolate. These interactions cumulatively contribute significantly to providing an alternative cyclisation pathway with a reduced activation energy for one of the diastereomeric transition states. However, a further interaction is required to orientate the oxindole, i.e. the oxindole could rotate around the C–N bond resulting in the retention of the three aforementioned contributions but would result in the opposite absolute configuration. The remaining interactions are likely to be inter-aromatic in nature, i.e. between the aromatic groups of the catalyst and the oxindole.

When the scope of oxindole *N*-substituents was tested it was shown that the *N*-benzyl group gave no improvement in yield or *er* over the *N*-methyl group (both 3:97 *er*). This clearly shows that the *N*-benzyl aromatic group does not contribute to the catalyst–substrate interaction. Indeed, larger *N*-benzyl groups such as PMB or *para*-bromobenzyl led to decreased *er* and this could be attributed to greater steric hindrance and consequential poorer catalyst–substrate interaction. This is distinct from the work developed by Merck which required a bulky oxindole *N*-substituent to obtain high enantioselectivity. However, due to the presence of an *N*-Boc group in the reaction developed in Chapter 4 this fills this role in the asymmetric induction model.

It can be safely assumed that the inter-aromatic interaction stems from the fused oxindole aromatic ring and one of the two aromatic rings in the catalyst. Though there is little dependence on the electronics of this fused aromatic ring. The results from changing the electronics of the oxindole aromatic ring show that increasing the electron density on this aromatic ring reduces the enantioselectivity slightly, whereas, a more electron-deficient aromatic ring leads to slightly increased enantioselectivity.

Extensive catalyst optimisation was undertaken (Section 4.4.3) to achieve high yield and enantioselectivity in the azetidine products. One of the crucial aspects of this optimisation was finding the optimal quinoline and benzylic group. Altering the benzylic group to be electron-deficient gave the best results with CF_3 and SF_5 groups in the *para*-position being privileged. This group has a clear effect on the electron density at the benzylic CH_2, which has a role in stabilising the Cl leaving group in the transition state. Additionally, this aromatic ring could interact with the oxindole aromatic ring either by a π-π stacking interaction or through a C–H-π interaction. The oxindole aromatic ring should be considered as relatively electron-rich due to the conjugated enolate and nitrogen atom. The electronic trend of the fused aromatic ring could

be explained by Figure 30. The SF_5 group will polarise the aromatic ring resulting in a lower electron density at the *ipso*-carbon of the benzylic group, and this would have a positive electrostatic interaction when the oxindole aromatic ring is substituted with an electron-withdrawing substituent.

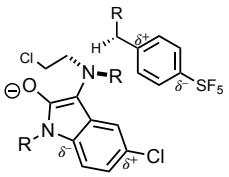


Figure 30: Polarity match of an oxindole with an electron-withdrawing substituent and the *para*-SF_5 benzyl group of the catalyst.

The quinoline group of the catalyst had a significant effect on the yield and enantioselectivity of the reaction. This group does not typically play an important role in models of enantioselective reactions in the literature,[357] including the intramolecular cyclisation developed by Merck and studied by Houk.[343] In the model developed by Houk, one of the quinoline C–H bonds (C6 of the quinoline) was implicated in a stabilising interaction with the leaving group. During the optimisation of the cyclisation (Section 4.4.3) changing the quinoline ring did have some significant effects on the yield and enantioselectivity. Most significantly removal of the OMe group of a quinine-derived catalyst by switching to a cinchonidine starting material, resulted in significant improvement in enantioselectivity. Additionally, substituting the quinoline ring at the 2-position with a phenyl or *n*-butyl group reduced enantioselectivity and yield. This could be due to disruption of an interaction with the fused oxindole or to increased steric bulk of the quinoline group leading to a poorer catalyst–substrate interaction i.e. by increasing the distance for hydrogen bond formation. The improvement in yield and enantioselectivity upon removal of the OMe group from the quinoline group could be due to an alteration in the electronics of the ring resulting in changes to any C–H interaction with the leaving group (as in Houk's model, Scheme 85B). The fused phenyl ring of the quinoline is more electron rich and due to the greater availability for π-interaction would likely interact with the oxindole aromatic as shown in Figure 31. However, if this was the prevailing model, the OMe group at this position would likely improve this π-interaction leading to higher enantioselectivity, and this is not observed. The OMe group would also result in greater steric hindrance and this could explain the poorer performance of quinine derived catalysts. Additionally, due to the conjugated enolate and nitrogen atom the oxindole aromatic would be expected to be relatively electron-rich, particularly in the absence of an electron-withdrawing substituent, and thus would be more likely to have poor electrostatic interactions with the quinoline group.

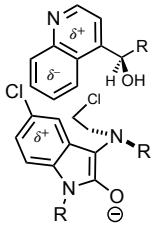


Figure 31: Polarity match between electron rich quinoline ring and electron-deficient oxindole aromatic.

As a result of the above discussion, two potential interactions can be proposed: 1) between the oxindole aromatic ring and the catalyst benzylic substituent and 2) between the oxindole aromatic ring and the catalyst quinoline group. Both of these models are shown in Figure 32. The final key piece of information to determine which model is dominant was the absolute configuration of the products. As shown in Figure 28, the products synthesised using cat. **394** were determined to be (*S*)-configured by X-ray crystallography. This indicates that model A from Figure 32 is the dominant transition state and that the dominant secondary interaction is between the benzylic aromatic ring and the fused oxindole aromatic. This also indicates that the quinoline group does not interact with the substrate in a direct π-interaction. The exact nature of the interaction between the benzylic group and the fused oxindole aromatic cannot be stated for certain, this could be a π-π interaction or C–H-π interaction. Direct implication of the SF_5 group in a π-interaction also cannot be ruled out.

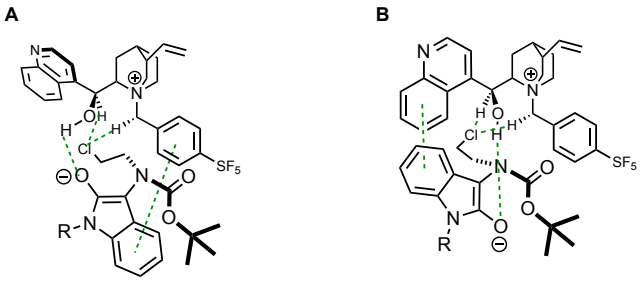


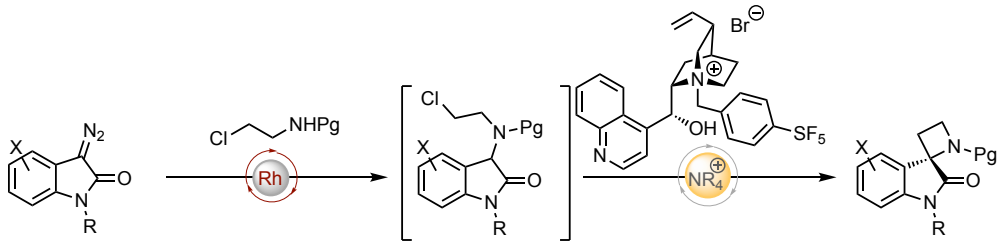
Figure 32: Potential models for asymmetric induction of the enantioselective cyclisation to spiroazetidine oxindoles.

In order to study the catalyst–substrate interactions extensively, computational studies would need to be carried out, including an application of how the transition state is distorted through the reaction coordinate.[358] However, this has not been carried out, mainly due to the high degrees of freedom of the catalyst and the resultant time and computational demand required.

We also know that the level of water in the system has a significant effect on the yield and enantioselectivity, with higher water levels leading to poorer yield and enantioselectivity. While difficult to know exactly why this may be, it could be due to greater levels of hydration leading to reduced availability of the catalyst and an alteration to the catalyst conformation. For example, water could disrupt hydrogen bonding between the catalyst and the substrate.

4.4.6 Conclusions and Future Work

In this chapter the development of a highly enantioselective synthesis of spiroazetidine oxindoles has been developed using phase transfer catalysis (Scheme 110). The scope of the reaction was broad with oxindoles substituted with electron-donating and withdrawing substituents affording azetidines with high yield and *er*. The *N*-substituents could be changed to provide a wide variety of spiroazetidine products. The ring size could also be altered to afford a spiropyrrolidine although the stereochemical induction was reduced by a more significant racemic background reaction. The developed methodology is general and not specific to a specific class of substrates, i.e. no bespoke substitution is required on the azetidine ring. This also represents the first stereoselective route to spiroazetidine oxindoles which are an under explored motif within drug discovery.



Scheme 110: Highly enantioselective synthesis of spiroazetidines by N–H insertion and asymmetric phase transfer catalysed cyclisation.

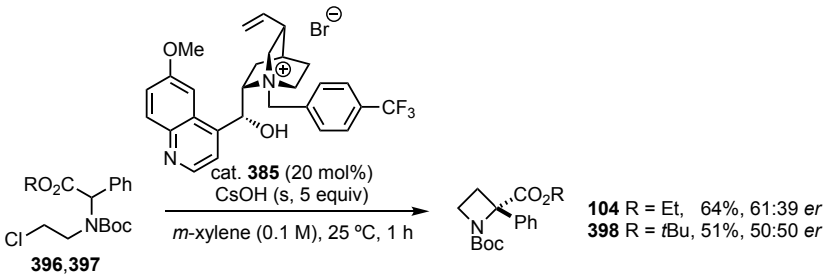
The observations made during the development of the reaction as well as in the scope of the reaction have led to significant insights into the mechanism of this transformation. An interfacial phase transfer mechanism has been proposed to be operative. The novel SF_5-containing phase transfer catalyst acts to activate the leaving group of the substrate to reduce the energy barrier for cyclisation to occur. Additional interactions between the catalyst and substrate further reduce the energy barrier to cyclisation for one of the diastereomeric transition states resulting in a highly enantioselective process. Confirmation of the absolute configuration of two of the azetidine products provided further insight into the model of asymmetric induction.

Further work should also aim to derivatise the enantioenriched products to demonstrate their utility for medicinal chemistry. This work would also show that, for example *N*-Boc deprotection can be carried out with retention of the high *er*. One of the benefits of the oxindole benzyl substituent is the potential to deprotect this while keeping the *N*-Boc group in place and *vice versa.* The derivatisation could also include demonstration of the ring expansion developed in Chapter 3. In particular, the development of a relationship between loss in stereochemistry and the Hammett parameter of oxindole substituents would be of interest. It would also be interesting to explore and optimise the cyclisation to 5-membered rings which was achieved in lower *er* than the azetidines in this work. Further work could also investigate the cyclisation to 6-membered or larger rings which were not successful under the current conditions.

One of the advantages of phase transfer catalysis is its potential application on large scale.[256] An example of a gram-scale synthesis was demonstrated without a reduction in enantioselectivity by understanding the key requirements of the reaction through a sensitivity screen. Also relevant to the potential applications of this methodology is the further exploration of the scope of products. For example, will the high enantioselectivity be maintained when a substituent is in the 4-position of the oxindole ring?

The spiroazetidine oxindoles synthesised in this chapter should be interesting for drug discovery. However, further work should attempt to apply the methodology and what has been learnt in this chapter to the products in Chapter 2. These non-spirocyclic structures are more challenging to synthesise enantioselectively due to the two diastereomeric enolates that can be formed (*E* or *Z*).

Indeed, during the development of the optimal conditions, conditions using cat. **385** were applied to precursor **396** (Scheme 111). Low enantioselectivity was observed, though this was notably non-zero, and this was compared to a background reaction which gave no product formation. Increasing the size of the ester group to influence the enolate geometry led to reduced yield, mainly due to lower conversion, and racemic product. Other ester groups such as benzyl proved to be too hydrolytically unstable. Even though this was a disappointing result, this could be optimised through catalyst design, i.e. applying SF_5 containing cat. **394** to this system could improve the enantioselectivity.



Scheme 111: Attempt to apply asymmetric phase transfer catalysed cyclisation conditions to the synthesis of non-spirocyclic azetidines.

5. Conclusions and Future Outlook

The aim of the research conducted in this thesis was to enable drug discovery efforts by developing synthetic methodology which could produce chemical matter within under explored chemical space in an efficient and robust manner. As such, novel saturated heterocycles were targeted as sp^3-rich motifs to enrich existing pharmaceutical compound libraries.

In Chapter 2 the development of methodology which could access 2,2-disubstituted saturated nitrogen heterocycles as 2-aryl proline analogues was discussed. This work fulfilled one of the key aims of this research project which was to provide a general methodology which could alter the skeletal diversity of the products through a simple change in the modular building blocks. This research could be used to generate a diverse library of saturated nitrogen heterocycles for screening purposes and to pursue structure-activity relationships upon target affinity identification.

In Chapter 3 the ring strain of the azetidine carbamates synthesised in Chapter 2 was harnessed in a complexity generating reaction. Again, this fulfilled the criteria of building diversity through a transformation from one skeleton to an under explored and valuable skeleton in one step. This work provided more compounds which would be desirable for medicinal chemistry as well as fundamental reaction understanding.

In Chapter 4 a cyclisation reaction to enantioenriched azetidines was developed. This cyclisation is a step forward in the research program as it overcomes one of the key limitations of the prior methodology, i.e. lack of stereocontrol. In the development of this enantioselective cyclisation, a new asymmetric phase transfer catalyst was developed which allowed up to 98:2 *er* to be achieved to the target products. Fundamental understanding of the reaction mechanism and the model of asymmetry has been achieved. This work should act as a stepping-stone to further developments in asymmetric catalysis using phase transfer catalysts, i.e. towards the development of an enantioselective variant of the research developed in Chapter 2.

The research in this thesis contributes to the fields of heterocycle synthesis, synthesis and ring expansion of small rings, diversity–oriented synthesis and asymmetric synthesis, most notably, asymmetric phase transfer catalysis. The work in each specific chapter has been summarised at the end of each chapter along with specific suggestions for future work. It is hoped that the research in this thesis can contribute to the further development of organic synthesis to enable discovery chemistry. There are many ways that the research in this thesis could be further developed. By reducing the complexity of the process, i.e. by employing visible light instead of metal catalysis for the decomposition of the diazo compound, a greater scope of diazo

compounds could conceivably be employed. Beyond the work developed in this thesis, the 2-step heterocycle construction that has now been developed within the Bull group should be suitable for application within an automated synthesiser.[359] This 'heterocycle-synthesis machine' could be coupled with further advances such as visible light mediated synthesis and flow chemistry to generate an efficient and advanced synthesis of heterocycles.[360] This could also allow the on-line change of modular components to be able to explore SAR in a rapid fashion.

6. Experimental

6.1 General Experimental Considerations

All non-aqueous reactions were carried out under an inert atmosphere (argon) with flame-dried glassware, using standard techniques. Anhydrous solvents were obtained by filtration through drying columns (CH_2Cl_2, toluene, THF, EtOH and DMF) or used as supplied (benzene, MeCN and *m*-xylene).

Flash chromatography was performed using 230–400 mesh silica, with the indicated solvent system according to standard techniques. Analytical thin-layer chromatography (TLC) was performed on precoated glass-backed silica gel plates. Visualization of the developed chromatogram was performed by UV absorbance (254 nm) and stained with aqueous potassium permanganate solution, a ninhydrin solution in ethanol or a phosphomolybdic acid solution in ethanol. Boc protected amine substrates and products were visualised using ninhydrin.

Infrared spectra (ν_{max}, FTIR ATR) were recorded in reciprocal centimetres (cm^{-1}). (br = broad, w = weak).

Nuclear magnetic resonance spectra were recorded on 400 or 500 MHz spectrometers. Chemical shifts for ^1H NMR spectra are recorded in parts per million from tetramethylsilane with the solvent resonance as the internal standard (chloroform: δ = 7.27 ppm, DMSO: δ = 2.50 ppm, CD_3OD: δ = 3.35 ppm, CF_3CO_2D: δ = 11.5 ppm). Data is reported as follows: chemical shift (multiplicity [s = singlet, d = doublet, t = triplet, q = quartet, p = pentet, m = multiplet and br = broad], coupling constant (in Hz), integration and assignment). ^{13}C NMR spectra were recorded with complete proton decoupling. Chemical shifts are reported in parts per million from tetramethylsilane with the solvent resonance as the internal standard ($^{13}CDCl_3$: δ = 77.0 ppm, $(^{13}CD_3)_2SO$: δ = 39.5 ppm, $^{13}CD_3OD$: δ = 49.0 ppm, $^{13}CF_3{}^{13}CO_2D$: δ = 164.2 ppm). Assignments of ^1H and ^{13}C spectra were based upon the analysis of δ and *J* values, as well as DEPT, COSY and HSQC experiments where appropriate. ^{19}F NMR spectra were recorded with or without complete proton decoupling. Decoupling is indicated as ($^{19}F\{^1H\}$) and where relevant this is stated in each assignment and spectrum. ^{19}F NMR spectra are indirectly referenced to $CFCl_3$, automatically *via* direct measurement of the absolute frequency of the deuterium lock signal by the spectrometer hardware.

For clarity NMR spectra are displayed as follows unless this would obscure signals: ^1H NMR spectra are displayed between 10 ppm and –0.5 ppm; ^{13}C NMR spectra are displayed between 210 ppm and 0 ppm; ^{19}F NMR spectra are displayed for the full sweep width as acquired.

All *tert*-butyloxycarbonyl (Boc) or carboxybenzyl (Cbz) containing compounds appeared as a mixture of rotamers in the NMR spectra at rt. For the majority of compounds, high temperature NMR experiments did not coalesce the signals or led to decomposition.

The high resolution mass spectrometry (HRMS) analyses were performed using electrospray ion source (ESI), pneumatically assisted electrospray (pNSI) or atomospheric pressure chemical ionisation (APCI). ESI was performed using a Waters LCT Premier equipped with an ESI source operated in positive or negative ion mode. The software used was MassLynx 4.1, this software does not account for the electron and all the calibrations/references are calculated accordingly, i.e. $[M+H]^+$ is detected and the mass is calibrated to output [M+H]. pNSI was performed using an Orbitrap XL in positive or negative ion mode. Samples are loop injected into or infused in a stream of H_2O/CH_3OH (1:1 at 50 μL/min) using an appropriate solvent for dissolution of the sample. Nebulization was pneumatically assisted by a flow of N_2 through a sheath around the capillary. APCI was carried out using a Thermo Fisher Q-Exactive in positive or negative ion mode.

Melting points were determined in open glass capillaries and are uncorrected.

Observed optical rotation (α') was measured at the indicated temperature (T ºC) and were converted to the corresponding specific rotations $[\alpha]_D^T$ in deg cm^2 g^{-1}, concentration (*c*) in g per 100 mL.

HPLC analyses were carried out using an Agilent 1260 Infinity Series system, employing Daicel Chiracel columns.

Reagents

Where the synthesis of a reagent is not stated, the reagent was commercially available.

Commercial reagents were used as supplied, or purified by standard techniques where necessary.

Catalyst purity: Bis[rhodium(α,α,α′,α′-tetramethyl-1,3-benzenedipropionic acid)] 96% (Aldrich 622623).

Notes:

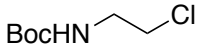
- Although we have not experienced any problems in the handling of azides or diazo reagents, extreme care should be taken when manipulating them due to their potentially explosive nature.[241]
- Melting points were not recorded for diazo compounds.
- For the diazo compounds synthesized, the resonance for the fully substituted C=N=N carbon in the ^{13}C NMR spectrum may not be seen due to quadrupole coupling to ^{14}N. Unless the ^{13}C resonance was observed it is not reported.

6.2 Experimental Details and Characterisation Data

6.2.1 Synthesised Compounds in Chapter 2

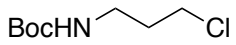
6.2.1.1 Synthesis of Protected Amine Starting Materials

tert-Butyl (2-chloroethyl)carbamate (52)



Triethylamine (4.70 mL, 33.7 mmol) was added dropwise to a stirred mixture of 2-chloroethylamine hydrochloride (3.00 g, 25.9 mmol) in CH_2Cl_2 (50 mL), and was subsequently cooled to 0 ºC. Di-*tert*-butyl dicarbonate (6.22 g, 28.5 mmol) was added portionwise carefully, then the solution was allowed to warm to 25 ºC for 18 h. H_2O (100 mL) and $CHCl_3$ (150 mL) were added, the organic and aqueous layers were separated, and the aqueous layer was extracted with further $CHCl_3$ (2 × 150 mL). The combined organic layers were then dried over Na_2SO_4, and the resulting solution was concentrated under reduced pressure. Purification by flash chromatography (15% EtOAc/pentane) afforded *tert*-butyl (2-chloroethyl)carbamate **52** (4.60 g, 99%) as a white solid. R_f 0.79 (20% EtOAc/pentane); mp = 27–28 ºC; ν_{max} (film)/cm^{-1} 3343 (NH), 2979, 1686 (C=O), 1511, 1366, 1247, 1162, 657; ^{1}H NMR (400 MHz, $CDCl_3$) δ 5.05 (br s, 1 H, NH), 3.63–3.53 (t, J = 5.7 Hz, 2 H, CH_2Cl), 3.49–3.40 (q, J = 5.7 Hz, 2 H, NCH_2), 1.43 (s, 9 H, $C(CH_3)_3$); ^{13}C NMR (101 MHz, $CDCl_3$) δ 155.6 (C=O), 79.7 ($C(CH_3)_3$), 44.2 (CH_2Cl), 42.4 (NCH_2), 28.3 ($C(CH_3)_3$). The observed characterisation data (IR, ^{1}H and ^{13}C NMR) was consistent with that previously reported in the literature.[361]

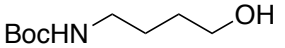
tert-Butyl (3-chloropropyl)carbamate (58)



Triethylamine (8.78 mL, 63.0 mmol) was added dropwise to a stirred mixture of 3-chloropropylamine hydrochloride (3.90 g, 30.0 mmol) in CH_2Cl_2 (60 mL) and stirred at 0 °C for 30 min. Di-*tert*-butyl dicarbonate (7.20 g, 33 mmol) was added to the stirred solution at 0 °C. After 5 min, the temperature was raised to 25 °C and stirred for 21 h. H_2O (100 mL) and $CHCl_3$ (100 mL) were added, the organic and aqueous layers were separated, and the aqueous layer was extracted with further $CHCl_3$ (2 × 100 mL). The combined organic layers were then dried over Na_2SO_4, and the resulting solution was concentrated under reduced pressure. Purification by flash chromatography (20 % EtOAc/pentane) afforded *tert*-butyl (3-chloroproyl)carbamate **58** (5.90 g, quant) as a white solid. R_f 0.42 (20% EtOAc/pentane); mp = 29–30 ºC (lit. = 32 ºC)[362]; ν_{max} (film)/cm^{-1} 3337 (br, NH), 2978, 1685 (C=O), 1518, 1366, 1251, 1164, 1119, 1074; ^{1}H NMR (400 MHz, $CDCl_3$) δ 4.68 (s, 1 H, NH), 3.59 (t, J = 6.4 Hz, 2 H, CH_2Cl), 3.28 (q, J = 6.4 Hz, 2 H, NCH_2), 1.97 (t, J = 6.4 Hz, 2 H, NCH_2CH_2), 1.44 (s, 9H, $C(CH_3)_3$); ^{13}C NMR (101 MHz, $CDCl_3$) δ 155.9 (C=O), 79.4 ($C(CH_3)_3$),

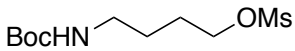
42.4 (CH_2Cl), 37.9 (NCH_2), 32.6 (NCH_2CH_2), 28.4 ($C(CH_3)_3$). The observed characterisation data (^1H and ^{13}C NMR) was consistent with that previously reported in the literature.[363]

tert-Butyl (4-hydroxybutyl)carbamate (65)



Triethylamine (8.80 mL, 63.0 mmol) was added dropwise to a stirred mixture of 4-aminobutanol (2.67 g, 30.0 mmol) in CH_2Cl_2 (60.0 mL) and stirred at 0 °C for 15 min. Di-*tert*-butyl dicarbonate (7.20 g, 33.0 mmol) was added to the stirred solution at 0 °C. After 5 min, the temperature was raised to 25 °C and stirred for 18 h. H_2O (150 mL) and $CHCl_3$ (150 mL) were added, the organic and aqueous layers were separated, and the aqueous layer was extracted with further $CHCl_3$ (2 × 150 mL). The combined organic layers were then dried over Na_2SO_4, and the resulting solution was concentrated under reduced pressure. Purification by flash chromatography (60% EtOAc/hexane) afforded *tert*-butyl (4-hydroxybutyl)carbamate **65** (5.20 g, 92%) as a white solid with a low melting point. R_f 0.13 (50% EtOAc/hexane); ν_{max} (film)/cm^{-1} 3337 (br, OH and NH), 2934, 1684 (C=O), 1521, 1365, 1276, 1250, 1166, 1058, 1039; ^1H NMR (400 MHz, $CDCl_3$) δ 4.75 (s br, 1 H, NH), 3.66–3.60 (m, 2 H, CH_2OH), 3.16–3.08 (m, 2 H, NCH_2), 2.44 (br s, 1 H, OH), 1.59–1.52 (m, 4 H, $NCH_2(CH_2)_2$), 1.42 (s, 9 H, $C(CH_3)_3$); ^{13}C NMR (101 MHz, $CDCl_3$) δ 156.1 (C=O), 79.1 ($C(CH_3)_3$), 62.2 (CH_2O), 40.2 (NCH_2), 29.6 (CH_2CH_2OH), 28.4 ($C(CH_3)_3$), 26.5 (NCH_2CH_2). The observed characterisation data (^1H and ^{13}C NMR) was consistent with that previously reported in the literature.[364]

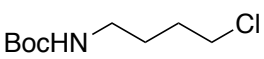
4-((_tert_-Butoxycarbonyl)amino)butyl methanesulfonate (66)



Methanesulfonyl chloride (6.00 mL, 78.0 mmol) was added to a stirred solution of *tert*-butyl (4-hydroxybutyl)carbamate **65** (4.92 g, 26.0 mmol) and triethylamine (10.90 mL, 78.0 mmol) in CH_2Cl_2 (130 mL) at 0 ºC. The reaction mixture was stirred for 1 h at 0 ºC and then for 3 h at 25 ºC. H_2O (100 mL) was added and the aqueous reaction mixture was extracted with CH_2Cl_2 (3 × 100 mL). The combined organic layers were dried over Na_2SO_4, filtered and concentrated under reduced pressure. Purification by flash chromatography (40% EtOAc/pentane) afforded 4-((*tert*-butoxycarbonyl)amino)butyl methanesulfonate **66** (5.82 g, 84%) as a white solid. R_f 0.20 (40% EtOAc/pentane); mp = 34–37 ºC; ν_{max} (film)/cm^{-1} 3400 (br, NH), 2977, 2939, 1690 (C=O), 1517, 1348, 1251, 1166, 931; ^1H NMR (400 MHz, $CDCl_3$) δ 4.63 (s br, 1 H, NH), 4.24 (t, J = 6.4 Hz, 2 H, CH_2OMs), 3.20–3.10 (m, 2 H, NCH_2), 3.00 (s, 3 H, SO_2CH_3), 1.82–1.74 (m, 2 H, CH_2CH_2OMs), 1.64–1.56 (m, 2 H, CH_2CH_2N), 1.43 (s, 9 H, $C(CH_3)_3$); ^{13}C NMR (101 MHz, $CDCl_3$) δ 156.0 (C=O), 79.2 ($C(CH_3)_3$), 69.6 (CH_2OMs), 39.7 (NCH_2), 37.3 (SO_2CH_3), 28.3 ($C(CH_3)_3$), 26.3 (CH_2CH_2OMs),

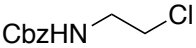
26.2 (CH_2CH_2N). The observed characterisation data (^1H and ^{13}C NMR) was consistent with that previously reported in the literature.[364]

tert-Butyl (4-chlorobutyl)carbamate (59)



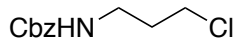
LiCl (17.5 g, 413 mmol) was added to 4-((*tert*-butoxycarbonyl)amino)butyl methanesulfonate **66** (5.52 g, 20.7 mmol) in DMF (210 mL). The reaction mixture was stirred at 25 ºC for 72 h, then water (100 mL) was added. The aqueous reaction mixture was extracted with EtOAc (4 × 100 mL), washed with brine (100 mL), then dried over Na_2SO_4, filtered and concentrated under reduced pressure. Purification by flash chromatography (30% Et_2O/pentane) afforded *tert*-butyl (4-chlorobutyl)carbamate **59** (3.53 g, 82%) as a white solid. R_f 0.25 (30% Et_2O/pentane); mp = 34–36 ºC; ν_{max} (film)/cm^{-1} 3333 (NH), 2978, 2940, 1682 (C=O), 1459, 1438, 1363, 1339, 1255, 1245, 1131, 1009, 968, 862, 808, 771, 674; ^1H NMR (400 MHz, $CDCl_3$) δ 4.54 (s br, 1 H, NH), 3.56 (t, J = 6.6 Hz, 2 H, CH_2Cl), 3.17 (q, J = 6.6 Hz, 2 H, NCH_2), 1.86–1.77 (m, 2 H, CH_2CH_2Cl), 1.69–1.60 (m, 2 H, NCH_2CH_2), 1.45 (s, 9 H, $C(CH_3)_3$); ^{13}C NMR (101 MHz, $CDCl_3$) δ 155.9 (C=O), 79.2 ($C(CH_3)_3$), 44.6 (CH_2Cl), 39.8 (NCH_2), 29.7 (CH_2CH_2Cl), 28.4 ($C(CH_3)_3$), 27.5 (NCH_2CH_2); HRMS (ESI$^+$) *m/z* Calculated for $C_9H_{18}NO_2{}^{35}ClNa$ [M+Na] 230.0918; Found 230.0920. The observed characterisation data (^1H NMR) was consistent with that previously reported in the literature.[365]

Benzyl (2-chloroethyl)carbamate (63)[366]



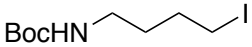
Benzyl chloroformate (3.14 mL, 22.0 mmol) was added dropwise over 5 min to a stirred solution of 2-chloroethylamine hydrochloride (2.32 g, 20.0 mmol) in aq. NaOH (10% in H_2O, 8.0 mL) at 0 °C. Further aq. NaOH (10%, 8.0 mL) was added and the temperature raised to 25 °C. After 24 h, the reaction mixture was diluted with CH_2Cl_2 (40 mL) and the aqueous and organic layers were separated. The aqueous layer was extracted further with CH_2Cl_2 (2 × 40 mL). The combined organic layers were dried over Na_2SO_4, filtered and concentrated under reduced pressure. Purification by flash chromatography (20% EtOAc/pentane) afforded benzyl (2-chloroethyl)carbamate **63** (3.97 g, 93%) as a colourless oil. R_f 0.33 (20% EtOAc/pentane); ν_{max} (film)/cm^{-1} 3327 (br, NH), 3034, 2960, 1695 (C=O), 1517, 1242, 1140, 1063, 996, 737, 696; ^1H NMR (400 MHz, $CDCl_3$) δ 7.43–7.30 (m, 5 H, 5 × HC_{Ph}), 5.25–5.10 (m, 3 H, NH and OCH_2Ph), 3.69–3.49 (m, 4 H, $N(CH_2)_2$); ^{13}C NMR (101 MHz, $CDCl_3$) δ 156.2 (C=O), 136.2 (C_{Ph} quat), 128.5 (2 × C_{Ph}), 128.2 (C_{Ph}), 128.1 (2 × C_{Ph}), 67.0 (OCH_2), 44.1 (CH_2Cl), 42.8 (NCH_2). The observed characterisation data (^1H and ^{13}C NMR) was consistent with that previously reported in the literature.[367]

Benzyl (3-chloropropyl)carbamate (64)[366]



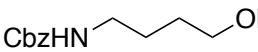
Benzyl chloroformate (3.14 mL, 22.0 mmol) was added dropwise over 5 min to a stirred solution of 3-chloropropylamine hydrochloride (2.60 g, 20.0 mmol) in aq. NaOH (10% in H_2O, 8.0 mL) at 0 °C. Further aq. NaOH (10%, 8.0 mL) was added and the temperature raised to 25 °C. After 24 h, the reaction mixture was diluted with CH_2Cl_2 (40 mL) and the aqueous and organic layers were separated. The aqueous layer was extracted further with CH_2Cl_2 (2 × 40 mL). The combined organic layers were dried over Na_2SO_4, filtered and concentrated under reduced pressure. Purification by flash chromatography (20% EtOAc/pentane), which afforded benzyl (3-chloropropyl)carbamate **64** (4.60 g, quant) as a colourless oil. R_f 0.28 (20% EtOAc/pentane); ν_{max} (film)/cm^{-1} 3325 (br, NH), 3063, 2972, 1689 (C=O), 1538, 1259, 1147, 744, 693; ^{1}H NMR (400 MHz, $CDCl_3$) δ 7.43–7.30 (m, 5 H, 5 × HC_{Ph}), 5.11 (s br, 2 H, OCH_2Ph), 4.89 (s br, 1 H, NH), 3.60 (t, J = 6.4 Hz, 2 H, CH_2Cl), 3.38 (q, J = 6.4 Hz, 2 H, NCH_2), 2.03 (q, J = 6.4 Hz, 2 H, NCH_2CH_2); ^{13}C NMR (101 MHz, $CDCl_3$) δ 156.4 (C=O), 136.4 (C_{Ph} quat), 128.5 (2 × C_{Ph}), 128.2 (2 × C_{Ph}), 128.1 (C_{Ph}), 66.7 (OCH_2), 42.2 (CH_2Cl), 38.3 (NCH_2), 32.3 (NCH_2CH_2). The observed characterisation data (^{1}H and ^{13}C NMR) was consistent with that previously reported in the literature.[366]

***tert*-Butyl (4-iodobutyl)carbamate (70)**[368]



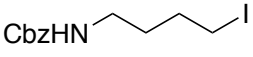
I_2 (1.22 g, 4.8 mmol) was added to a solution of PPh_3 (1.57 g, 6.0 mmol) and imidazole (408 mg, 6.0 mmol) in CH_2Cl_2 (8.0 mL) at 0 ºC. *tert*-Butyl (4-hydroxybutyl)carbamate **65** (757 mg, 4.0 mmol) was added to the mixture at 0 ºC and the mixture was stirred for 4 h at 25 ºC. Sat. aq. Na_2SO_3 (15 mL) was added and the resulting mixture stirred for 30 min. CH_2Cl_2 (30 mL) and the layers separated. The organic layer was washed with sat. aq. Na_2SO_3 (30 mL) and sat. brine (30 mL), then dried over Na_2SO_4. The solvent was removed under reduced pressure. Purification by flash chromatography (10% to 20% EtOAc/pentane) afforded *tert*-butyl (4-iodobutyl)carbamate **70** (1.05 g, 88%) as a yellow solid with a low melting point. R_f 0.43 (20% EtOAc/pentane); ν_{max} (film)/cm^{-1} 3350 (br s, NH), 2977, 1687 (C=O), 1518, 1365, 1251, 1171; ^{1}H NMR (400 MHz, $CDCl_3$) δ 4.54 (br s, 1 H, NH), 3.24–3.12 (m, 4 H, NCH_2 and CH_2I), 1.90–1.82 (m, 2 H, NCH_2CH_2), 1.64–1.56 (m, 2 H, CH_2CH_2I), 1.45 (s, 9 H, $C(CH_3)_3$); ^{13}C NMR (101 MHz, $CDCl_3$) δ 155.9 (C=O), 79.2 ($C(CH_3)_3$), 39.4 (NCH_2), 31.0 (NCH_2CH_2), 30.6 (CH_2CH_2I), 28.4 ($C(CH_3)_3$), 6.2 (CH_2I). The observed characterisation data (^{1}H and ^{13}C NMR) was consistent with that previously reported in the literature.[368]

Benzyl (4-hydroxybutyl)carbamate (67)



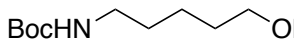
Benzyl chloroformate (0.31 mL, 2.2 mmol) was added dropwise over 5 min to a stirred solution of 4-aminobutanol (0.18 mL, 2.0 mmol) in aq. NaOH (10% in H_2O, 1.6 mL) at 0 °C. The reaction mixture was stirred at 25 ºC for 24 h, then CH_2Cl_2 (25 mL) was added. H_2O (25 mL) was added and the layers were separated. The aqueous layer was extracted with CH_2Cl_2 (2 × 25 mL). The combined organic layers were dried over Na_2SO_4, filtered and concentrated under reduced pressure. Purification by flash chromatography (60% EtOAc/hexane) afforded benzyl (4-hydroxybutyl)carbamate **67** (387 mg, 87%) as a white solid. R_f 0.13 (60% EtOAc/hexane); mp = 81–82 ºC [lit = 80–81 ºC][369]; ν_{max} (film)/cm^{-1} 3373 (br s, NH), 3327 (br s, OH), 2949, 2865, 1685 (C=O), 1532, 1463, 1454, 1337, 1268, 1235, 1138, 1104, 1056, 1010, 728, 696; ^{1}H NMR (400 MHz, $CDCl_3$) δ 7.39–7.29 (m, 5 H, 5 × HC_{Ph}), 5.18–5.07 (m, 2 H, OCH_2Ph), 4.96 (br s, 1 H, NH), 3.70–3.62 (m, 2 H, OCH_2), 3.28–3.14 (m, 2 H, NCH_2), 1.65–1.53 (m, 4 H, $NCH_2(CH_2)_2$); ^{13}C NMR (101 MHz, $CDCl_3$) δ 156.5 (C=O), 136.6 (C_{Ph} quat), 128.5 (2 × C_{Ph}), 128.1 (3 × C_{Ph}), 66.6 (OCH_2Ph), 62.3 (OCH_2), 40.8 (NCH_2), 29.6 (OCH_2CH_2), 26.5 (NCH_2CH_2). The observed characterisation data (^{1}H and ^{13}C NMR) was consistent with that previously reported in the literature.[370]

Benzyl (4-iodobutyl)carbamate (71)[368]



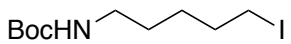
I_2 (426 mg, 1.7 mmol) was added to a solution of PPh_3 (550 mg, 2.1 mmol) and imidazole (143 mg, 2.1 mmol) in CH_2Cl_2 (2.8 mL) at 0 ºC. Benzyl (4-hydroxybutyl)carbamate **67** (311 mg, 1.4 mmol) was added to the mixture at 0 ºC and the mixture was stirred for 14 h at 25 ºC. Sat. aq. Na_2SO_3 (15 mL) was added then CH_2Cl_2 (30 mL) and the layers were separated. The organic layer was washed with sat. aq. Na_2SO_3 (30 mL) and sat. brine (30 mL), then dried over Na_2SO_4. The solvent was removed under reduced pressure. Purification by flash chromatography (20% Et_2O/pentane) afforded benzyl (4-iodobutyl)carbamate **71** (371 mg, 80%) as a pale yellow solid. R_f 0.13 (20% Et_2O/pentane); mp = 38–39 ºC (lit = 35–37 ºC)[371]; ν_{max} (film)/cm^{-1} 3335 (br s, NH), 2935, 1694 (C=O), 1524, 1247, 1175, 1131, 1015, 737, 697; ^{1}H NMR (400 MHz, $CDCl_3$) δ 7.40–7.30 (m, 5 H, 5 × HC_{Ph}), 5.17–5.08 (m, 2 H, OCH_2Ph), 4.75 (br s, 1 H, NH), 3.28–3.17 (m, 4 H, NCH_2 and CH_2I), 1.91–1.82 (m, 2 H, NCH_2CH_2), 1.68–1.59 (m, 2 H, CH_2CH_2I); ^{13}C NMR (101 MHz, $CDCl_3$) δ 156.4 (C=O), 136.5 (C_{Ph} quat), 128.5 (2 × C_{Ph}), 128.1 (3 × C_{Ph}), 66.7 (OCH_2Ph), 39.9 (NCH_2), 30.9 (NCH_2CH_2), 30.5 ($N(CH_2)_2CH_2$), 6.0 (CH_2I); HRMS (ESI$^+$) *m/z* Calculated for $C_{12}H_{17}NO_2{}^{127}I$ [M+H] 334.0304; Found 334.0308.

***tert*-Butyl (5-hydroxypentyl)carbamate (68)[372]**



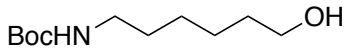
Triethylamine (1.53 mL, 11.0 mmol) was added dropwise to a stirred mixture of 5-aminopentanol (1.03 g, 10.0 mmol) in CH_2Cl_2 (20.0 mL) and stirred at 0 ºC. Di-*tert*-butyl dicarbonate (2.40 g, 11.0 mmol) was added to the stirred solution at 0 °C. After 5 min, the temperature was raised to 25 °C and stirred for 4 h. H_2O (50 mL) and $CHCl_3$ (50 mL) were added, the organic and aqueous layers were separated, and the aqueous layer was extracted with further $CHCl_3$ (3 × 50 mL). The combined organic layers were then dried over Na_2SO_4, filtered and the resulting solution was concentrated under reduced pressure. Purification by flash chromatography (80% EtOAc/hexane) afforded *tert*-butyl (5-hydroxypentyl)carbamate **68** (1.86 g, 92%) as a colourless oil. R_f 0.33 (70% EtOAc/hexane); ν_{max} (film)/cm^{-1} 3332 (br s, OH and NH), 2930, 2862, 1682 (C=O), 1522, 1364, 1247, 1164, 1011, 866, 780; ^{1}H NMR (400 MHz, $CDCl_3$) δ 4.64 (br s, 1 H, NH), 3.62 (t, J = 6.5 Hz, 2 H, CH_2OH), 3.11 (q, J = 6.5 Hz, 2 H, NCH_2), 2.03 (s, 1 H, OH), 1.61–1.33 (m, 15 H, $C(CH_3)_3$ and $NCH_2(CH_2)_3$); ^{13}C NMR (101 MHz, $CDCl_3$) δ 156.1 (C=O), 79.1 ($C(CH_3)_3$), 62.5 (CH_2OH), 40.4 (NCH_2), 32.2 (CH_2CH_2OH), 29.8 (NCH_2CH_2), 28.4 ($C(CH_3)_3$), 22.9 ($N(CH_2)_2CH_2$). The observed characterisation data (^{1}H and ^{13}C NMR) was consistent with that previously reported in the literature.[373]

***tert*-Butyl (5-iodopentyl)carbamate (72)[372]**



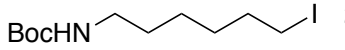
tert-Butyl (5-hydroxypentyl)carbamate **68** (1.86 g, 9.1 mmol) was added to a solution of I_2 (2.77 g, 10.9 mmol), PPh_3 (3.58 g, 13.7 mmol) and imidazole (933 mg, 13.7 mmol) in CH_2Cl_2 (18.2 mL) at 0 ºC and the mixture was stirred for 16 h at 25 ºC. Sat. aq. $Na_2S_2O_3$ (50 mL) and CH_2Cl_2 (50 mL) were added and the layers separated. The aqueous layer was extracted with further CH_2Cl_2 (50 mL). The combined organic layers were washed with sat. aq. $Na_2S_2O_3$ (50 mL) and sat. brine (50 mL), then dried over Na_2SO_4. The solvent was removed under reduced pressure. Purification by flash chromatography (20% to 30% Et_2O/pentane) afforded *tert*-butyl (5-iodopentyl)carbamate **72** (2.11 g, 74%) as a white solid with a low melting point. R_f 0.38 (30% Et_2O/pentane); ν_{max} (film)/cm^{-1} 3345 (br s, NH), 2929, 2859, 1685 (C=O), 1508, 1363, 1246, 1163, 1040, 978, 865, 779; ^{1}H NMR (400 MHz, $CDCl_3$) δ 4.45 (m, 1 H, NH), 3.18 (t, 2 H, J = 6.9 Hz, 2 H, CH_2I), 3.11 (q, J = 6.4 Hz, 2 H, NCH_2), 1.83 (p, J = 7.1 Hz, 2 H, ICH_2CH_2), 1.54–1.37 (m, 13 H, $C(CH_3)_3$ and $NCH_2(CH_2)_2$); ^{13}C NMR (101 MHz, $CDCl_3$) δ 155.9 (C=O), 79.1 ($C(CH_3)_3$), 40.3 (NCH_2), 33.0 (CH_2CH_2I), 29.0 (NCH_2CH_2), 28.4 ($C(CH_3)_3$), 27.6 ($N(CH_2)_2CH_2$), 6.7 (CH_2I). The observed characterisation data (^{1}H and ^{13}C NMR) was consistent with that previously reported in the literature.[374]

***tert*-Butyl (6-hydroxyhexyl)carbamate (69)**



Triethylamine (2.09 mL, 15.0 mmol) was added dropwise to a stirred mixture of 6-aminopentanol (1.29 g, 11.0 mmol) in CH_2Cl_2 (50.0 mL) and stirred at 0 ºC. Di-*tert*-butyl dicarbonate (2.18 g, 10.0 mmol) was added to the stirred solution at 0 °C. After 5 min, the temperature was raised to 25 °C and stirred for 18 h. CH_2Cl_2 (50 mL) was added and the reaction mixture was washed with sat. aq. NH_4Cl (50 mL), then sat. aq. $NaHCO_3$ (50 mL) and sat. aq. NaCl (50 mL). The combined organic layers were then dried over Na_2SO_4, filtered and the resulting solution was concentrated under reduced pressure to afford *tert*-butyl (6-hydroxyhexyl)carbamate **69** (2.01 g, 93%) as a colourless oil which was used without further purification. R_f 0.08 (60% Et_2O/hexane); ν_{max} (film)/cm^{-1} 3343 (br s, NH), 2976, 2931, 2859, 1685 (C=O), 1522, 1365, 1273, 1165, 731; ^{1}H NMR (400 MHz, $CDCl_3$) δ 4.57 (s, 1 H, NH), 3.63 (t, J = 5.9 Hz, 2 H, CH_2OH), 3.11 (q, J = 6.5 Hz, 2 H, NCH_2), 1.61–1.29 (m, 17 H, $NCH_2(CH_2)_4$ and $C(CH_3)_3$); ^{13}C NMR (101 MHz, $CDCl_3$) δ 156.0 (C=O), 78.9 ($C(CH_3)_3$), 62.2 (CH_2OH), 40.2 (NCH_2), 32.4 (CH_2CH_2OH), 29.8 (NCH_2CH_2), 28.3 ($C(CH_3)_3$), 26.3 ($N(CH_2)_3CH_2$), 25.2 ($N(CH_2)_2CH_2$). The observed characterisation data (IR, ^{1}H and ^{13}C NMR) was consistent with that previously reported in the literature.[375]

***tert*-Butyl (6-iodohexyl)carbamate (73)**



tert-Butyl (6-hydroxyhexy)carbamate **69** (1.74 g, 8.0 mmol) was added to a solution of I_2 (2.44 g, 9.6 mmol), PPh_3 (3.15 g, 9.6 mmol) and imidazole (824 mg, 12.0 mmol) in CH_2Cl_2 (18 mL) at 0 ºC and the mixture was stirred for 16 h at 25 ºC. Sat. aq. $Na_2S_2O_3$ (50 mL) and CH_2Cl_2 (50 mL) were added and the layers separated. The aqueous layer was extracted with further CH_2Cl_2 (50 mL). The combined organic layers were washed with sat. aq. $Na_2S_2O_3$ (50 mL) and sat. brine (50 mL), then dried over Na_2SO_4. The solvent was removed under reduced pressure. Purification by flash chromatography (25% Et_2O/hexane) afforded *tert*-butyl (6-iodohexyl)carbamate **73** (1.98 g, 76%) as a colourless oil which froze to afford a white solid. R_f 0.45 (50% Et_2O/hexane); mp = 22 ºC [lit mp = 24–25 ºC][376]; ν_{max} (film)/cm^{-1} 3358 (br s, NH), 2974, 2929, 2856, 1686 (C=O), 1508, 1364, 1247, 1164; ^{1}H NMR (400 MHz, $CDCl_3$) δ 4.72–4.45 (m, 1 H, NH), 3.12 (t, J = 7.0 Hz, 2 H, CH_2I), 3.04 (q, J = 6.5 Hz, 2 H, NCH_2), 1.76 (p, J = 7.0 Hz, CH_2CH_2I), 1.47–1.21 (m, 15 H, $NCH_2(CH_2)_3$ and $C(CH_3)_3$); ^{13}C NMR (101 MHz, $CDCl_3$) δ 155.8 (C=O), 78.7 ($C(CH_3)_3$), 40.2 (NCH_2), 33.2 (CH_2CH_2I), 29.9 ($CH_2(CH_2)I$), 29.7 (NCH_2CH_2), 28.3 ($C(CH_3)_3$), 25.5 ($N(CH_2)_2CH_2$), 6.9 (CH_2I). The observed characterisation data (IR, ^{1}H and ^{13}C NMR) was consistent with that previously reported in the literature.[376]

6.2.1.2 Synthesis of Diazo Compounds

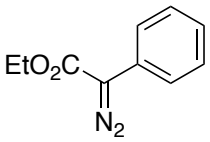
Diazo compound **50** was synthesised according to a procedure by Ellis[377] and samples were consistent with our previously reported data.[167,168]

p-Acetamidobenzenesulfonyl azide (*p*-ABSA) was purchased from TCI chemicals (product number: A1786) or synthesised according to a procedure by Hoye.[378]

Tosyl azide (TsN_3) was synthesised using a procedure by Zhao[379] and samples were consistent with our previously reported data.[168]

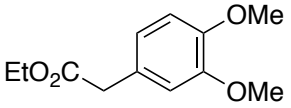
Esters and diazo compounds (**84** and **97**) were synthesised as previously reported by our group.[168] Diazo compounds were synthesised using a procedure adapted from Davies and co-workers.[380]

Ethyl 2-diazo-2-phenylacetate (85)



DBU (4.49 mL, 30 mmol) was added to a stirred solution of *p*-ABSA (7.2 g, 36 mmol) and ethyl 2-phenylacetate (4.11 g, 25 mmol) in CH_3CN (41.7 mL). The reaction mixture was stirred at 25 °C for 70 h. Saturated aq. NH_4Cl (150 mL) was added. The aqueous reaction mixture was extracted with Et_2O (3 × 150 mL). The combined organic layers were dried over Na_2SO_4 and concentrated under reduced pressure. The mixture was then taken up in 50% Et_2O/pentane, filtered and concentrated under reduced pressure. Flash column chromatography (3% Et_2O/pentane) afforded ethyl 2-diazo-2-phenylacetate **85** as a red-orange oil (3.26 g, 69%). R_f = 0.31 (3% Et_2O/pentane); IR (film)/ cm^{-1} 2983, 2079 (C=N=N out-of-phase), 1698 (C=O), 1598, 1575, 1499, 1479, 1465, 1450, 1394, 1370 (C=N=N in-phase), 1337, 1286, 1242, 1149, 1095, 1078, 1048, 1028, 986, 904, 859, 835, 752, 689, 666; ^{1}H NMR (400 MHz, $CDCl_3$) δ 7.52–7.48 (m, 2H), 7.42–7.37 (m, 2H, 2 × Ar-CH), 7.22–7.17 (m, 1H, Ar-CH), 4.35 (q, *J* = 7.1 Hz, 2H, C*H*$_2$CH$_3$), 1.36 (t, *J* = 7.1 Hz, 3H, CH$_2$C*H*$_3$); ^{13}C NMR (100 MHz, $CDCl_3$) δ 165.2 (CO_2), 128.9 (2 × Ar-C), 125.7 (Ar-C), 125.6 (Ar-C), 124.0 (2 × Ar-C), 61.0 (CH_2-O), 14.5 (*C*H$_3$CH$_2$). The observed characterisation data (IR, ^{1}H and ^{13}C NMR) was consistent with that previously reported in the literature.[381]

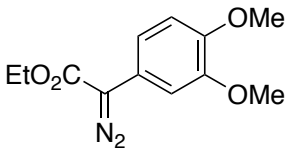
Ethyl 2-(3,4-dimethoxyphenyl)acetate (74)



A solution of 3,4-dimethoxyphenyl acetic acid (2.94 g, 15.0 mmol) and *p*-toluenesulfonic acid monohydrate (285 mg, 1.5 mmol) in ethanol (37.5 mL) was heated under reflux for 2 h. The solvent was then removed under reduced pressure. Saturated aq. $NaHCO_3$ (75 mL) was added and the product was extracted with EtOAc (2 × 75 mL). The organic extracts were combined, dried over Na_2SO_4, filtered and concentrated under reduced pressure to yield ethyl 2-(3,4-

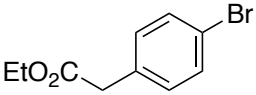
dimethoxyphenyl)acetate **74** (2.82 g, 84%) as a pale yellow oil which was used without further purification. R_f 0.12 (10% EtOAc/pentane); ν_{max} (film)/cm^{-1} 2937, 1729 (C=O), 1514, 1464, 1261, 1235, 1140, 1026, 763; ^{1}H NMR (400 MHz, $CDCl_3$) δ 6.85–6.80 (m, 3 H, 3 × HC_{Ar}), 4.15 (q, J = 7.2 Hz, 2 H, OCH_2CH$_3$), 3.88 (s, 3 H, OCH_3), 3.86 (s, 3 H, OCH_3), 3.55 (s, 2 H, CH_2), 1.25 (t, J = 7.2 Hz, 3 H, OCH_2CH_3); ^{13}C NMR (101 MHz, $CDCl_3$) δ 171.8 (C=O), 148.8 (OC_{Ar} quat), 148.0 (OC_{Ar} quat), 126.5 (C_{Ar} quat), 121.3 (C_{Ar}), 112.3 (C_{Ar}), 111.1 (C_{Ar}), 60.7 (OCH_2CH$_3$), 55.8 (d, 2 × OCH_3), 40.9 (CH_2), 14.1 (OCH_2CH_3). The observed characterisation data (IR, ^{1}H and ^{13}C NMR) was consistent with that previously reported in the literature.[382,383,384]

Ethyl 2-diazo-2-(3,4-dimethoxyphenyl)acetate (86)



DBU (1.97 mL, 13.2 mmol) was added dropwise over 2 min to a stirred solution of *p*-ABSA (3.17 g, 13.2 mmol) and ethyl 2-(3,4-dimethoxyphenyl)acetate **74** (2.47 g, 11.0 mmol) in CH_3CN (18.3 mL) at 0 °C. The reaction mixture was stirred at 25 °C for 48 h. Saturated aq. NH_4Cl (75 mL) was added. The aqueous reaction mixture was extracted with Et_2O (3 × 75 mL). 50% Et_2O/pentane (100 mL) was added and the mixture was filtered, washing with 50% Et_2O/pentane (100 mL), then concentrated under reduced pressure. The combined organic layers were dried over Na_2SO_4, filtered and concentrated under reduced pressure. Purification by flash chromatography (15% EtOAc/pentane) afforded ethyl 2-diazo-2-(3,4-dimethoxyphenyl)acetate **86** (0.98 g, 36%) as a red solid. R_f 0.27 (15% EtOAc/pentane); ν_{max} (film)/cm^{-1} 3001, 2966, 2078 (C=N=N out-of-phase), 1675 (C=O), 1582, 1516, 1456, 1374 (C=N=N in phase), 1326, 1265, 1248, 1057, 1040, 1026, 889, 864, 797, 766, 739; ^{1}H NMR (400 MHz, $CDCl_3$) δ 7.21 (d, J = 1.9 Hz, 1 H, HC_{Ar}), 6.92–6.85 (m, 2 H, 2 × HC_{Ar}), 4.33 (q, J = 7.2 Hz, 2 H, OCH_2CH$_3$), 3.91 (s, 3 H, OCH_3), 3.89 (s, 3 H, OCH_3), 1.35 (t, J = 7.2 Hz, 3 H, OCH_2CH_3); ^{13}C NMR (101 MHz, $CDCl_3$) δ 165.7 (C=O), 149.4 (OC_{Ar} quat), 147.3 (OC_{Ar} quat), 117.5 (C_{Ar} quat), 116.4 (C_{Ar}), 111.6 (C_{Ar}), 108.3 (C_{Ar}), 60.9 (OCH_2CH$_3$), 56.0 (OCH_3), 55.9 (OCH_3), 14.5 (OCH_2CH_3). The observed characterisation data (IR, ^{1}H and ^{13}C NMR) was consistent with that previously reported in the literature.[372,387]

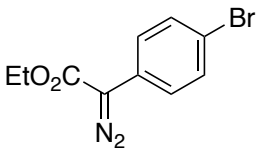
Ethyl 2-(4-bromophenyl)acetate (76)



A solution of 4-bromophenyl acetic acid (6.45 g, 30.0 mmol) and *p*-toluenesulfonic acid monohydrate (571 mg, 3.00 mmol) in ethanol (75 mL) was heated under reflux for 3 h. The solvent was then removed under reduced pressure, saturated aq. $NaHCO_3$ (150 mL) was added and the product was extracted with EtOAc (2 × 150 mL). The organic extracts were combined, dried over Na_2SO_4, filtered and concentrated under reduced pressure to yield ethyl 2-(4-bromophenyl)acetate **76**

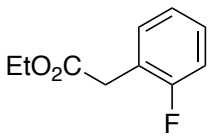
(7.08 g, 97%) as a white solid which was used without further purification. R_f 0.27 (5% Et_2O/pentane); mp = 31–32 ºC (lit. = 31 ºC)[385]; ν_{max} (film)/cm^{-1} 2982, 1731 (C=O), 1488, 1249, 1217, 1154, 1071, 1029, 1012, 801; ^{1}H NMR (400 MHz, $CDCl_3$) δ 7.45 (d, J = 8.5, 2 H, 2 × HC_{Ar}), 7.17 (d, J = 8.5 Hz, 2 H, 2 × HC_{Ar}), 4.16 (q, J = 7.1 Hz, 2 H, OCH_2CH_3), 3.57 (s, 2H, CH_2), 1.26 (t, J = 7.1 Hz, 3H, OCH_2CH_3); ^{13}C NMR (101 MHz, $CDCl_3$) δ 171.0 (C=O), 133.0 (C_{Ar} quat), 131.6 (2 × C_{Ar}), 131.0 (2 × C_{Ar}), 121.1 (BrC_{Ar} quat), 61.0 (OCH_2CH_3), 40.7 (CH_2), 14.1 (OCH_2CH_3). The observed characterisation data (IR, ^{1}H and ^{13}C NMR) was consistent with that previously reported in the literature.[386]

Ethyl 2-(4-bromophenyl)-2-diazoacetate (88)



DBU (4.49 mL, 30.0 mmol) was added dropwise over 2 min to a stirred solution of *p*-ABSA (6.00 g, 25.0 mmol) and ethyl 2-(4-bromophenyl)acetate **76** (6.08 g, 25.0 mmol) in CH_3CN (41.7 mL) at 0 °C. The reaction mixture was stirred at 25 °C for 24 h. Saturated aq. NH_4Cl (150 mL) was added and the aqueous reaction mixture was extracted with Et_2O (3 × 150 mL). The combined organic layers were dried over Na_2SO_4, filtered and concentrated under reduced pressure. 50% Et_2O/pentane (100 mL) was added and the mixture was filtered, washing with 50% Et_2O/pentane (100 mL), then concentrated under reduced pressure. Purification by flash chromatography (3% EtOAc/pentane) afforded ethyl 2-(4-bromophenyl)-2-diazoacetate **88** (5.84 g, 87%) as an orange solid. R_f 0.34 (3% EtOAc/pentane); ν_{max} (film)/cm^{-1} 2912, 2091 (C=N=N out-of-phase), 1692 (C=O), 1487, 1388 (C=N=N in phase), 1337, 1370, 1237, 1168, 1076, 991, 826, 814, 738; ^{1}H NMR (400 MHz, $CDCl_3$) δ 7.50 (d, J = 8.8 Hz, 2 H, 2 × HC_{Ar}), 7.38 (d, J = 8.8 Hz, 2 H, 2 × HC_{Ar}), 4.34 (q, J = 7.1 Hz, 2 H, OCH_2CH_3), 1.35 (t, J = 7.1 Hz, 3 H, OCH_2CH_3); ^{13}C NMR (101 MHz, $CDCl_3$) δ 164.8 (C=O), 132.0 (2 × C_{Ar}), 125.3 (2 × C_{Ar}), 124.9 (C_{Ar} quat), 119.2 (BrC_{Ar} quat), 61.2 (OCH_2CH_3), 14.5 (OCH_2CH_3). The observed characterisation data (IR, ^{1}H and ^{13}C NMR) was consistent with that previously reported in the literature.[387]

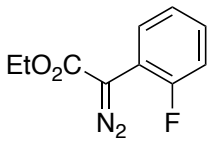
Ethyl 2-(2-fluorophenyl)acetate (77)



A solution of 2-fluorophenyl acetic acid (3.08 g, 20 mmol) and *p*-toluenesulfonic acid monohydrate (380 mg, 2.0 mmol) in ethanol (50 mL) was heated under reflux for 2 h. The solvent was then removed under reduced pressure, saturated aq. $NaHCO_3$ (100 mL) was added and the product was extracted with EtOAc (2 × 100 mL). The organic extracts were combined, dried over Na_2SO_4, filtered and concentrated under reduced pressure to yield ethyl 2-(2-fluorophenyl)acetate **77** (3.53 g, 97%) as a pale yellow oil which was used without further purification. R_f 0.19 (4% EtOAc/pentane);

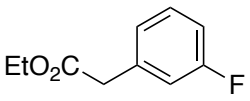
ν_{max} (film)/cm^{-1} 2984, 1734 (C=O), 1494, 1233, 1202, 1157, 1028, 755; ^{1}H NMR (400 MHz, $CDCl_3$) δ 7.30–7.24 (m, 2 H, 2 × HC_{Ar}), 7.14–7.04 (m, 2 H, 2 × HC_{Ar}), 4.18 (q, J = 7.2 Hz, 2 H, OCH_2CH_3), 3.68 (s, 2 H, CH_2), 1.27 (t, J = 7.2 Hz, 3 H, OCH_2CH_3); ^{13}C NMR (101 MHz, $CDCl_3$) δ 170.6 (C=O), 161.1 (d, J_{C-F} = 246.5 Hz, FC_{Ar} quat), 131.4 (d, J_{C-F} = 4.2 Hz, C_{Ar}), 128.9 (d, J_{C-F} = 8.3 Hz, C_{Ar}) 124.0 (d, J_{C-F} = 3.5 Hz, C_{Ar}), 121.5 (d, J_{C-F} = 15.8 Hz, C_{Ar}), 115.3 (d, J_{C-F} = 21.8 Hz, C_{Ar}), 61.0 (OCH_2CH_3), 34.5 (d, J_{C-F} = 3.0 Hz, CH_2C_{Ar}), 14.10 (OCH_2CH_3); ^{19}F{^{1}H} NMR (377 MHz, $CDCl_3$) δ –117.3. The observed characterisation data (^{1}H and ^{19}F NMR) was consistent with that previously reported in the literature.[388,389]

Ethyl 2-diazo-2-(2-fluorophenyl)acetate (89)



DBU (2.24 mL, 15.0 mmol) was added dropwise over 2 min to a stirred solution of *p*-ABSA (3.60 g, 15.0 mmol) and ethyl 2-(2-fluorophenyl)acetate **77** (2.73 g, 12.5 mmol) in CH_3CN (21.0 mL) at 0 °C. The reaction mixture was stirred at 25 °C for 24 h. Saturated aq. NH_4Cl (75 mL) was added. The aqueous reaction mixture was extracted with Et_2O (3 × 75 mL). The combined organic layers were dried over Na_2SO_4, filtered and concentrated under reduced pressure. 50% Et_2O/pentane (100 mL) was added and the mixture was filtered, washing with 50% Et_2O/pentane (100 mL), then concentrated under reduced pressure. Purification by flash chromatography (3% Et_2O/pentane) afforded ethyl 2-diazo-2-(2-fluorophenyl)acetate **89** (2.37 g, 91%) as an orange oil. R_f 0.27 (3% Et_2O/pentane); ν_{max} (film)/cm^{-1} 2984, 2092 (C=N=N out-of-phase), 1698 (C=O), 1496, 1369 (C=N=N in phase), 1345, 1284, 1240, 1170, 1147, 1088, 1029, 752, 654; ^{1}H NMR (400 MHz, $CDCl_3$) δ 7.71 (td, J = 7.7, 1.9 Hz, 1 H, HC_{Ar}), 7.28–7.16 (m, 2 H, 2 × HC_{Ar}), 7.12–7.06 (m, 1 H, HC_{Ar}), 4.34 (q, J = 7.2 Hz, 2 H, OCH_2CH_3), 1.35 (t, J = 7.2 Hz, 3 H, OCH_2CH_3); ^{13}C NMR (101 MHz, $CDCl_3$) δ 165.2 (C=O), 158.4 (d, J_{C-F} = 247.1 Hz, FC_{Ar} quat), 129.4 (C_{Ar}), 128.4 (d, J_{C-F} = 8.3 Hz, C_{Ar}), 124.6 (d, J_{C-F} = 3.5 Hz, C_{Ar}), 115.6 (d, J_{C-F} = 21.6 Hz, C_{Ar}), 113.9 (d, J_{C-F} = 11.8 Hz, C_{Ar} quat), 61.2 (OCH_2CH_3), 14.5 (OCH_2CH_3); ^{19}F{^{1}H} NMR (377 MHz, $CDCl_3$) δ –114.1. The observed characterisation data (IR, ^{1}H, ^{13}C and ^{19}F NMR) was consistent with that previously reported in the literature.[390]

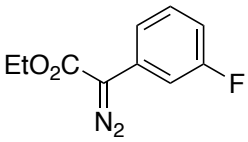
Ethyl 2-(3-fluorophenyl)acetate (78)



A solution of 3-fluorophenyl acetic acid (3.08 g, 20 mmol) and *p*-toluenesulfonic acid monohydrate (380 mg, 2.0 mmol) in ethanol (50 mL) was heated under reflux for 3 h. The solvent was then removed under reduced pressure, saturated aq. $NaHCO_3$ (30 mL) was added and the product was extracted with Et_2O (3 × 20 mL). The organic extracts were combined, dried over Na_2SO_4, filtered and concentrated under reduced pressure to yield ethyl 2-(3-fluorophenyl)acetate **78** (1.62 g, 44%)

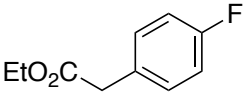
as a pale yellow oil which was used without further purification. R_f 0.29 (3% Et_2O/pentane); ν_{max} (film)/cm^{-1} 2983, 1732 (C=O), 1617, 1591, 1489, 1450, 1255, 1141, 1030, 962, 874, 776, 757, 721, 682; ^{1}H NMR (400 MHz, $CDCl_3$) δ 7.33–7.26 (m, 1 H, HC_{Ar}), 7.09–6.94 (m, 3 H, 3 × HC_{Ar}), 4.17 (q, J = 7.1 Hz, 2 H, OCH_2CH_3), 3.62 (s, 2 H, CH_2), 1.27 (t, J = 7.1 Hz, 3 H, OCH_2CH_3); ^{13}C NMR (101 MHz, $CDCl_3$) δ 171.0 (C=O), 162.8 (d, J_{C-F} = 246.1 Hz, FC_{Ar} quat), 136.4 (d, J_{C-F} = 7.9 Hz, C_{Ar} quat), 129.9 (d, J_{C-F} = 8.2 Hz, C_{Ar}), 124.9 (d, J_{C-F} = 2.4 Hz, C_{Ar}), 116.2 (d, J_{C-F} = 21.6 Hz, C_{Ar}), 114.0 (d, J_{C-F} = 21.0 Hz, C_{Ar}), 61.0 (OCH_2CH_3), 41.0 (CH_2), 14.1 (OCH_2CH_3); ^{19}F{^{1}H} NMR (377 MHz, $CDCl_3$) δ –113.2. The observed characterisation data (^{1}H and ^{19}F NMR) was consistent with that previously reported in the literature.[388,391]

Ethyl 2-diazo-2-(3-fluorophenyl)acetate (90)



DBU (0.90 mL, 6.0 mmol) was added dropwise over 1 min to a stirred solution of *p*-ABSA (1.44 g, 6.0 mmol) and ethyl 2-(3-fluorophenyl)acetate **78** (0.91 g, 5.0 mmol) in CH_3CN (8.3 mL) at 0 °C. The reaction mixture was stirred at 25 °C for 24 h. Saturated aq. NH_4Cl (30 mL) was added. The aqueous reaction mixture was extracted with Et_2O (3 × 30 mL). The combined organic layers were dried over Na_2SO_4, filtered and concentrated under reduced pressure. The mixture was taken up in 50% Et_2O/hexane (50 mL), filtered washing with 50% Et_2O/hexane (50 mL) and concentrated under reduced pressure. Purification by flash chromatography (3% Et_2O/pentane) afforded ethyl 2-diazo-2-(3-fluorophenyl)acetate **90** (0.86 g, 83%) as an orange liquid. R_f 0.30 (5% Et_2O/pentane); ν_{max} (film)/cm^{-1} 2983, 2080 (C=N=N out-of-phase), 1697 (C=O), 1580, 1490, 1444, 1369 (C=N=N in-phase), 1241, 1133, 1047, 884, 773, 679; ^{1}H NMR (400 MHz, $CDCl_3$) δ 7.38–7.30 (m, 2 H, 2 × HC_{Ar}), 7.17 (dq, J = 7.9, 0.9 Hz, 1 H, HC_{Ar}), 6.87 (tdd, J = 8.3, 2.5, 0.9 Hz, 1 H, HC_{Ar}), 4.35 (q, J = 7.1 Hz, 2 H, OCH_2CH_3), 1.36 (t, J = 7.1 Hz, 3 H, OCH_2CH_3); ^{13}C NMR (101 MHz, $CDCl_3$) δ 164.6 (C=O), 163.2 (d, J_{C-F} = 245.1 Hz, FC_{Ar} quat), 130.3 (d, J_{C-F} = 8.8 Hz, C_{Ar}), 128.3 (d, J_{C-F} = 9.3 Hz, C_{Ar} quat), 118.9 d, J_{C-F} = 2.6 Hz, C_{Ar}), 112.4 (J_{C-F} = 21.2 Hz, C_{Ar}), 111.1 (d, J_{C-F} = 25.5 Hz, C_{Ar}), 63.5 (CN_2 quat), 61.2 (OCH_2CH_3), 14.4 (OCH_2CH_3); ^{19}F{^{1}H} NMR (377 MHz, $CDCl_3$) δ –111.8. The observed characterisation data (IR, ^{1}H and ^{13}C NMR) was consistent with that previously reported in the literature.[392]

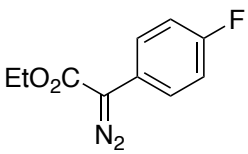
Ethyl 2-(4-fluorophenyl)acetate (79)



A solution of 4-fluorophenyl acetic acid (3.08 g, 20 mmol) and *p*-toluenesulfonic acid monohydrate (380 mg, 2.0 mmol) in ethanol (50 mL) was heated under reflux for 2 h. The solvent was then removed under reduced pressure, saturated aq. $NaHCO_3$ (100 mL) was added and the product was extracted

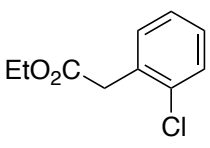
with Et_2O (2 × 100 mL). The organic extracts were combined, dried over Na_2SO_4, filtered and concentrated under reduced pressure to yield ethyl 2-(2-fluorophenyl)acetate **79** (3.41 g, 95%) as a pale yellow oil which was used without further purification. R_f 0.07 (2% Et_2O/pentane); ν_{max} (film)/cm^{-1} 2983, 1732 (C=O ester), 1509, 1369, 1300, 1254, 1221, 1153, 1095, 1030, 825, 798; ^{1}H NMR (400 MHz, $CDCl_3$) δ 7.30–7.24 (m, 2 H, 2 × HC_{Ar}), 7.04 (t, J = 8.8 Hz, 2 H, 2 × HC_{Ar}), 4.18 (q, J = 7.1 Hz, 2 H, OCH_2CH_3), 3.61 (s, 2 H, CH_2), 1.28 (t, J = 7.1 Hz, 3 H, OCH_2CH_3); ^{13}C NMR (101 MHz, $CDCl_3$) δ 171.4 (C=O), 162.0 (d, J_{C-F} = 245.7 Hz, FC_{Ar} quat), 130.8 (d, J_{C-F} = 8.0 Hz, 2 × C_{Ar}), 129.8 (d, J_{C-F} = 3.3 Hz, C_{Ar} quat), 115.4 (d, J_{C-F} = 21.7 Hz, 2 × C_{Ar}), 60.9 (OCH_2CH_3), 40.5 (CH_2), 14.1 (OCH_2CH_3); ^{19}F[^{1}H] NMR (377 MHz, $CDCl_3$) δ –115.9 (m). The observed characterisation data (IR, ^{1}H, ^{13}C and ^{19}F NMR) was consistent with that previously reported in the literature.[386]

Ethyl 2-diazo-2-(4-fluorophenyl)acetate (91)



DBU (1.79 mL, 12.0 mmol) was added dropwise over 1 min to a stirred solution of *p*-ABSA (2.88 g, 12.0 mmol) and ethyl 2-(4-fluorophenyl)acetate **79** (1.82 g, 10.0 mmol) in CH_3CN (16.6 mL) at 0 °C. The reaction mixture was stirred at 25 °C for 23 h. Saturated aq. NH_4Cl (75 mL) was added. The aqueous reaction mixture was extracted with Et_2O (3 × 75 mL). The combined organic layers were dried over Na_2SO_4, filtered and concentrated under reduced pressure. The mixture was taken up in 50% Et_2O/hexane (50 mL), filtered washing with 50% Et_2O/hexane (50 mL) and concentrated under reduced pressure. Purification by flash chromatography (1% to 3% Et_2O/hexane) afforded ethyl 2-diazo-2-(4-fluorophenyl)acetate **91** (1.48 g, 71%) as an orange solid. R_f 0.18 (3% Et_2O/hexane); ν_{max} (film)/cm^{-1} 2985, 2082 (C=N=N out-of-phase), 1698 (C=O), 1510, 1371 (C=N=N in-phase), 1341, 1244, 1234, 1163, 1155, 1045, 832, 740; ^{1}H NMR (400 MHz, $CDCl_3$) δ 7.45 (dd, J = 9.0, 5.1 Hz, 2 × HC_{Ar}), 7.10 (t, J = 8.8 Hz, 2 × HC_{Ar}), 4.34 (q, J = 7.1 Hz, 2 H, OCH_2CH_3), 1.35 (t, J = 7.1 Hz, 3 H, OCH_2CH_3); ^{13}C NMR (101 MHz, $CDCl_3$) δ 165.2 (C=O ester), 160.9 (d, J_{C-F} = 246.1 Hz, FC_{Ar} quat), 125.8 (d, J_{C-F} = 7.9 Hz, 2 × C_{Ar}), 121.3 (d, J_{C-F} = 3.1 Hz, C_{Ar} quat), 115.9 (d, J_{C-F} = 21.9 Hz, 2 × C_{Ar}), 62.5 (CN_2 quat), 61.0 (OCH_2CH_3), 14.4 (OCH_2CH_3); ^{19}F{^{1}H} NMR (377 MHz, $CDCl_3$) δ –116.4. The observed characterisation data (^{1}H and ^{13}C NMR) was consistent with that previously reported in the literature.[372]

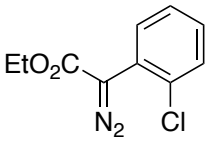
Ethyl 2-(2-chlorophenyl)acetate (80)



A solution of 2-chlorophenyl acetic acid (3.74 g, 20.0 mmol) and *p*-toluenesulfonic acid monohydrate (380 mg, 2.0 mmol) in ethanol (50 mL) was heated under reflux for 2 h. The solvent was then removed under

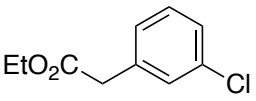
reduced pressure, saturated aq. $NaHCO_3$ (100 mL) was added and the product was extracted with EtOAc (2 × 100 mL). The organic extracts were combined, dried over Na_2SO_4, filtered and concentrated under reduced pressure to yield ethyl 2-(2-chlorophenyl)acetate **80** (3.74 g, 94%) as a colourless oil. R_f 0.46 (20% EtOAc/pentane); ν_{max} (film)/cm^{-1} 2983, 1733 (C=O), 1475, 1445, 1368, 1279, 1248, 1217, 1157, 1054, 1029, 743; ^{1}H NMR (400 MHz, $CDCl_3$) δ 7.42–7.37 (m, 1 H, HC_{Ar}), 7.32–7.20 (m, 3 H, HC_{Ar}), 4.19 (q, J = 7.2 Hz, 2 H, OCH_2CH_3), 3.78 (s, 2 H, CH_2), 1.27 (t, J = 7.2 Hz, 3 H, OCH_2CH_3); ^{13}C NMR (101 MHz, $CDCl_3$) δ 170.6 (C=O), 134.5 (ClC_{Ar} quat), 132.5 (C_{Ar} quat), 131.4 (C_{Ar}), 129.4 (C_{Ar}), 128.6 (C_{Ar}), 126.8 (C_{Ar}), 61.0 (OCH_2CH_3), 39.2 (CH_2), 14.1 (OCH_2CH_3); The observed characterisation data (IR, ^{1}H and ^{13}C NMR) was consistent with that previously reported in the literature.[393]

Ethyl 2-(2-chlorophenyl)-2-diazoacetate (92)



DBU (3.10 mL, 20.0 mmol) was added dropwise over 2 min to a stirred solution of *p*-ABSA (4.90 g, 20.0 mmol) and ethyl 2-(2-chlorophenyl)acetate **80** (3.38 g, 17.0 mmol) in CH_3CN (28.0 mL) at 0 °C. The reaction mixture was stirred at 25 °C for 24 h. Saturated aq. NH_4Cl (50 mL) was added and the aqueous reaction mixture was extracted with EtOAc (3 × 50 mL). 50% Et_2O/pentane (100 mL) was added and the mixture was filtered, washing with 50% Et_2O/pentane (100 mL), then concentrated under reduced pressure. The combined organic layers were dried over Na_2SO_4, filtered and concentrated under reduced pressure. Purification by flash chromatography (5% Et_2O/pentane) afforded ethyl 2-(2-chlorophenyl)-2-diazoacetate **92** (3.64 g, 95%) as an orange oil. R_f 0.18 (5% Et_2O/pentane); ν_{max} (film)/cm^{-1} 2982, 2090, 1698 (C=O), 1480, 1369, 1283, 1274, 1238, 1170, 1153, 1072, 1031, 752; ^{1}H NMR (400 MHz, $CDCl_3$) δ 7.56 (dd, J = 7.8, 1.8 Hz, 1 H, HC_{Ar}), 7.43 (dd, J = 7.8, 1.5 Hz, 1 H, HC_{Ar}), 7.36–7.26 (m, 2 H, 2 × HC_{Ar}) 4.32 (q, J = 7.1 Hz, 2 H, OCH_2CH_3), 1.34 (t, J = 7.1 Hz, 3 H, OCH_2CH_3); ^{13}C NMR (101 MHz, $CDCl_3$) δ 165.5 (C=O), 133.7 (C_{Ar} quat), 132.2 (C_{Ar}), 130.0 (C_{Ar}), 129.5 (C_{Ar}), 127.1 (C_{Ar}), 124.0 (C_{Ar} quat), 61.3 (OCH_2CH_3), 14.5 (OCH_2CH_3). The observed characterisation data (IR, ^{1}H and ^{13}C NMR) was consistent with that previously reported in the literature.[394]

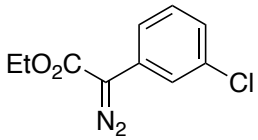
Ethyl 2-(3-chlorophenyl)acetate (81)



A solution of 3-chlorophenyl acetic acid (3.41 g, 20.0 mmol) and *p*-toluenesulfonic acid monohydrate (380 mg, 2.0 mmol) in ethanol (50 mL) was heated under reflux for 2 h. The solvent was then removed *in vacuo*. Saturated aq. $NaHCO_3$ (100 mL) was added and the product was extracted with EtOAc (2 × 100 mL). The organic extracts were combined, dried over Na_2SO_4 and concentrated under reduced pressure to yield ethyl 2-(3-chlorophenyl)acetate **81** (3.72 g, 94%)

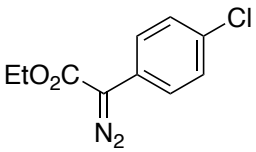
as a colourless oil which was used without further purification. R_f 0.19 (4% Et_2O/pentane); □$_{max}$ (film)/cm^{-1} 2982, 1732 (C=O), 1477, 1433, 1368, 1249, 1220, 1155, 1079, 1029, 682; ^{1}H NMR (400 MHz, $CDCl_3$) δ 7.31–7.29 (m, 1 H, HC_{Ar}), 7.28–7.24 (m, 2 H, 2 × HC_{Ar}), 7.21–7.15 (m, 1 H, HC_{Ar}), 4.17 (q, *J* = 7.2 Hz, 2 H, OCH_2CH_3), 3.59 (s, 2 H, CH_2), 1.27 (t, *J* = 7.2 Hz, 3 H, OCH_2CH_3); ^{13}C NMR (101 MHz, $CDCl_3$) δ ^{13}C NMR (101 MHz, Chloroform-*d*) δ 170.9 (C=O), 135.9 (C_{Ar}), 134.2 (C_{Ar} quat.), 129.7 (C_{Ar}), 129.4 (C_{Ar}), 127.4 (C_{Ar}), 127.2 (C_{Ar}), 61.0 (OCH_2CH_3), 40.9 (CH_2), 14.1 (OCH_2CH_3). The observed characterisation data (IR, ^{1}H and ^{13}C NMR) was consistent with that previously reported in the literature.[168]

Ethyl 2-(3-chlorophenyl)-2-diazoacetate (93)



DBU (2.24 mL, 15.0 mmol) was added dropwise over 2 min to a stirring solution of *p*-ABSA (3.60 g, 15.0 mmol) and ethyl 2-(3-chlorophenyl)acetate **81** (2.48 g, 12.5 mmol) in CH_3CN (21.0 mL) at 0 °C. The reaction mixture was stirred at 25 °C for 24 h. Saturated aq. NH_4Cl (75 mL) was added. The aqueous reaction mixture was extracted with Et_2O (3 × 75 mL). The combined organic layers were dried over Na_2SO_4 and concentrated under reduced pressure. Flash column chromatography (3% Et_2O/pentane) afforded ethyl 2-diazo-2-(3-chlorophenyl)acetate **93** (2.21 g, 81%) as an orange oil. R_f 0.42 (5% Et_2O/pentane); ν_{max} (film)/cm^{-1} 2992, 2091 (C=N=N out-of-phase), 1694 (C=O), 1592, 1558, 1391, 1372 (C=N=N in phase), 1240, 1167, 1049, 885, 776, 737, 681; ^{1}H NMR (400 MHz, $CDCl_3$) δ 7.56 (t, *J* = 1.7 Hz, 1 H, HC_{Ar}), 7.38–7.26 (m, 2 H, 2 × HC_{Ar}), 7.15 (dt, *J* = 7.5, 1.7 Hz, 1 H, HC_{Ar}), 4.35 (q, *J* = 7.2 Hz, 2 H, OCH_2CH_3), 1.36 (t, *J* = 7.2 Hz, 3 H, OCH_2CH_3); ^{13}C NMR (101 MHz, $CDCl_3$) δ 164.6 (C=O), 135.0 (C_{Ar} quat.), 130.0 (C_{Ar}), 127.9 (C_{Ar}), 125.6 (C_{Ar}), 123.6 (C_{Ar}), 121.5 (C_{Ar}), 61.2 (OCH_2CH_3), 14.4 (OCH_2CH_3). The observed characterisation data (IR, ^{1}H and ^{13}C NMR) was consistent with that previously reported in the literature.[168]

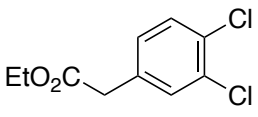
Ethyl 2-(4-chlorophenyl)-2-diazoacetate (94)



DBU (5.4 mL, 25.0 mmol) was added dropwise over 2 min to a stirred solution of *p*-ABSA (6.0 g, 25.0 mmol) and ethyl 2-(4-chlorophenyl)acetate (4.13 g, 20.8 mmol) in CH_3CN (34.7 mL). The reaction mixture was stirred at 25 °C for 24 h. Saturated aq. NH_4Cl (150 mL) was added. The aqueous reaction mixture was extracted with Et_2O (3 × 150 mL). The combined organic layers were dried over Na_2SO_4, filtered and concentrated under reduced pressure. Flash column chromatography (3% EtOAc/hexane) afforded ethyl 2-(4-chlorophenyl)-2-diazoacetate **94** (4.26 g, 91%) as an orange solid. R_f 0.15 (3 % EtOAc/hexane); ν_{max} (film)/cm^{-1} 2985, 2931, 2910, 2095 (C=N=N out-of-phase), 1901, 1691

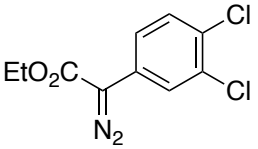
(C=O), 1651, 1592, 1562, 1493, 1481, 1456, 1443, 1394, 1372 (C=N=N out-of-phase), 1338, 1305, 1275, 1235, 1163, 1097, 1047, 1006, 993, 961, 822, 811, 733, 718, 700; ^{1}H NMR (400 MHz, $CDCl_3$) δ 7.43 (d, J = 8.9 Hz, 2 H, 2 × HC_{Ar}), 7.36 (d, J = 8.9 Hz, 2 H, 2 × HC_{Ar}), 4.34 (q, J = 7.1 Hz, 2 H, OCH_2CH_3), 1.35 (t, J = 7.1 Hz, 3 H, OCH_2CH_3); ^{13}C NMR (101 MHz, $CDCl_3$) δ 164.8 (C=O), 131.3 (ClC_{Ar} quat), 129.0 (2 × C_{Ar}), 125.0 (2 × C_{Ar}), 124.2 (C_{Ar} quat), 63.0 (CN_2 quat), 61.1 (OCH_2CH_3), 14.4 (OCH_2CH_3). The observed characterisation data (IR, ^{1}H and ^{13}C NMR) was consistent with that previously reported in the literature.[395]

Ethyl 2-(3,4-dichlorophenyl)acetate (82)



A solution of 3,4-dichlorophenyl acetic acid (3.08 g, 15.0 mmol) and *p*-toluenesulfonic acid monohydrate (285 mg, 1.50 mmol) in ethanol (37.5 mL) was heated under reflux for 2 h. The solvent was then removed under reduced pressure, saturated aq. $NaHCO_3$ (75 mL) was added and the product was extracted with EtOAc (2 × 75 mL). The organic extracts were combined, dried over Na_2SO_4, filtered and concentrated under reduced pressure to yield ethyl 2-(3,4-dichlorophenyl)acetate **82** (3.31 g, 95%) as a colourless oil which was used without further purification. R_f 0.20 (3% Et_2O/pentane); ν_{max} (film)/cm^{-1} 2983, 1732 (C=O), 1472, 1220, 1155, 1131, 1030, 822; ^{1}H NMR (400 MHz, $CDCl_3$) δ 7.41–7.37 (m, 2 H, 2 × HC_{Ar}), 7.13 (dd, J = 8.2, 2.1 Hz, 1 H, HC_{Ar}), 4.17 (q, J = 7.2 Hz, 2 H, OCH_2CH_3), 3.57 (s, 2 H, CH_2), 1.27 (t, J = 7.2 Hz, 3 H, OCH_2CH_3); ^{13}C NMR (101 MHz, $CDCl_3$) δ 170.6 (C=O), 134.1 (2 × ClC_{Ar} quat), 132.4 (C_{Ar} quat), 131.2 (C_{Ar}), 130.4 (C_{Ar}), 128.7 (C_{Ar}), 61.2 (OCH_2CH_3), 40.3 (CH_2), 14.1 (OCH_2CH_3). The observed characterisation data (IR, ^{1}H and ^{13}C NMR) was consistent with that previously reported in the literature.[393,396]

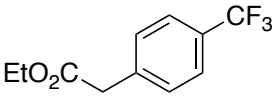
Ethyl 2-diazo-2-(3,4-dichlorophenyl)acetate (95)



DBU (2.33 mL, 15.6 mmol) was added dropwise over 2 min to a stirred solution of *p*-ABSA (3.75 g, 15.6 mmol) and ethyl 2-(3,4-dichlorophenyl)acetate **82** (3.03 g, 13.0 mmol) in CH_3CN (21.7 mL) at 0 °C. The reaction mixture was stirred at 25 °C for 24 h. Saturated aq. NH_4Cl (75 mL) was added and the aqueous reaction mixture was extracted with EtOAc (3 × 75 mL). The combined organic layers were dried over Na_2SO_4, filtered and concentrated under reduced pressure. 50% Et_2O/pentane (100 mL) was added and the mixture was filtered, washing with 50% Et_2O/pentane (100 mL), then concentrated under reduced pressure. Purification by flash chromatography (3% EtOAc/pentane) afforded ethyl 2-diazo-2-(3,4-dichlorophenyl)acetate **95** (3.08 g, 91%) as an orange solid. R_f 0.31 (3% EtOAc/pentane); ν_{max} (film)/cm^{-1} 3100, 2985, 2099 (C=N=N out-of-phase), 1685 (C=O), 1482, 1373 (C=N=N in

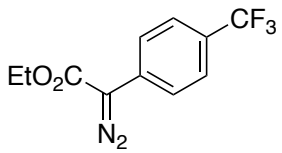
phase), 1346, 1239, 1170, 1022, 892, 808, 739; ^{1}H NMR (400 MHz, $CDCl_3$) δ 7.66 (d, J = 2.3 Hz, 1 H, HC_{Ar}), 7.44 (d, J = 8.6 Hz, 1 H, HC_{Ar}), 7.30 (dd, J = 8.6, 2.3 Hz, 1 H, HC_{Ar}), 4.35 (q, J = 7.2 Hz, 2 H, OCH_2CH_3), 1.35 (t, J = 7.2 Hz, 3 H, OCH_2CH_3); ^{13}C NMR (101 MHz, $CDCl_3$) δ 164.4 (C=O), 133.2 (ClC_{Ar} quat), 130.6 (C_{Ar}), 129.3 (ClC_{Ar} quat), 126.2 (C_{Ar} quat), 125.3 (C_{Ar}), 122.6 (C_{Ar}), 61.3 (OCH_2CH_3), 14.4 (OCH_2CH_3). The observed characterisation data (IR, ^{1}H and ^{13}C NMR) was consistent with that previously reported in the literature.[372,387]

Ethyl 2-(4-(trifluoromethyl)phenyl)acetate (83)



A solution of 4-(trifluoromethyl)phenyl acetic acid (2.04 g, 10.0 mmol) and *p*-toluenesulfonic acid monohydrate (190 mg, 1.0 mmol) in ethanol (25 mL) was heated under reflux for 2 h. The solvent was then removed *in vacuo*. Saturated aq. $NaHCO_3$ (50 mL) was added and the product was extracted with EtOAc (2 × 50 mL). The organic extracts were combined, dried over Na_2SO_4 and concentrated under reduced pressure to yield ethyl 2-(4-(trifluoromethyl)phenyl)acetate **83** (2.16 g, 93%) as a white solid which was used without further purification. R_f 0.21 (4% Et_2O/pentane); mp = 37–38 ºC [lit. = 37 ºC][397]; ν_{max} (film)/cm^{-1} 2992, 1719 (C=O), 1323, 1128, 1111, 1020, 886; ^{1}H NMR (400 MHz, $CDCl_3$) δ 7.60 (d, J = 8.1 Hz, 2 H, 2 × HC_{Ar}), 7.42 (d, J = 8.1 Hz, 2 H, 2 × HC_{Ar}), 4.18 (q, J = 7.2 Hz, 2 H, OCH_2CH_3), 3.68 (s, 2 H, CH_2), 1.27 (t, J = 7.2 Hz, 3 H, OCH_2CH_3); ^{13}C NMR (101 MHz, $CDCl_3$) δ 170.7 (C=O), 138.1 (C_{Ar} quat.), 129.6 (2 × C_{Ar}), 129.5 (q, $J_{C\text{-}F}$ = 33 Hz, $C_{Ar}(CF_3)$ quat.), 125.4 (q, $J_{C\text{-}F}$ = 4 Hz, 2 × C_{Ar}), 124.1 (q, $J_{C\text{-}F}$ = 273 Hz, CF_3), 61.1 (OCH_2CH_3), 41.1 (CH_2), 14.1 (OCH_2CH_3); ^{19}F{^{1}H} NMR (377 MHz, $CDCl_3$) δ –62.6 . The spectroscopic data for this compound is consistent with the available data in the literature (IR, ^{1}H and ^{13}C NMR).[168]

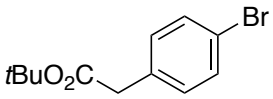
Ethyl 2-diazo-2-(4-(trifluoromethyl)phenyl)acetate (96)



DBU (1.39 mL, 9.3 mmol) was added dropwise over 2 min to a stirring solution of *p*-ABSA (2.23 g, 9.3 mmol) and ethyl 2-(4-(trifluoromethyl)phenyl)acetate **83** (1.80 g, 7.75 mmol) in CH_3CN (12.9 mL) at 0 °C. The reaction mixture was stirred at 25 °C for 24 h. Saturated aq. NH_4Cl (75 mL) was added. The aqueous reaction mixture was extracted with Et_2O (3 × 75 mL). The combined organic layers were dried over Na_2SO_4 and concentrated under reduced pressure. Flash column chromatography (3% Et_2O/pentane) afforded ethyl 2-diazo-2-(4-(trifluoromethyl)phenyl)acetate **96** (1.86 g, 93%) as an orange solid. R_f 0.46 (4% Et_2O/pentane); ν_{max} (film)/cm^{-1} 2989, 2093 (C=N=N out-of-phase), 1692 (C=O), 1618, 1373 (C=N=N in phase), 1320, 1241, 1154, 1111, 1095, 1069, 1010, 855, 820, 743; ^{1}H NMR (400 MHz, $CDCl_3$) δ 7.63 (s, 4 H, 4 × HC_{Ar}), 4.37 (q, J = 7.2 Hz, 2 H, OCH_2CH_3), 1.37 (t, J = 7.2 Hz,

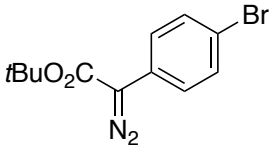
3 H, OCH_2CH_3); ^{13}C NMR (101 MHz, $CDCl_3$) δ 164.4 (C=O), 130.2 (C_{Ar} quat.), 127.5 (q, $J_{C\text{-}F}$ = 33 Hz, C_{Ar}), 125.8 (q, $J_{C\text{-}F}$ = 4 Hz, 2 × C_{Ar}), 124.1 (q, $J_{C\text{-}F}$ = 272 Hz, C_{Ar}), 123.4 (2 × C_{Ar}); $^{19}F\{^1H\}$ NMR (377 MHz, $CDCl_3$) δ –62.5. The observed characterisation data (IR, ^1H and ^{13}C NMR) was consistent with that previously reported in the literature.[168]

tert-Butyl 2-(4-bromophenyl)acetate (98)[398]



$BF_3{\cdot}OEt_2$ (0.62 mL, 5.0 mmol) was added dropwise over 1 min to a stirring solution of 4-bromophenylacetic acid (1.08 g, 5.0 mmol) in *tert*-butyl acetate (17 mL) at 25 ºC. The reaction mixture was stirred for 48 h, then H_2O (100 mL) was added. The aqueous reaction mixture was extracted with Et_2O (2 × 100 mL). The organic layers were washed with sat. aq. $NaHCO_3$ (100 mL), dried over Na_2SO_4, filtered and concentrated under reduced pressure. Purification by flash chromatography (2% Et_2O/pentane) afforded *tert*-butyl 2-(4-bromophenyl)acetate **98** (750 mg, 55%) as a colourless oil. R_f 0.22 (2% Et_2O/pentane); ν_{max} (film)/cm^{-1} 2978, 1730 (C=O), 1488, 1368, 1337, 1298, 1256, 1227, 1141, 1072, 1013, 956, 873, 835, 804, 774, 752, 738; ^1H NMR (400 MHz, $CDCl_3$) δ 7.45 (d, J = 8.4 Hz, 2 H, 2 × HC_{Ar}), 7.15 (d, J = 8.4 Hz, 2 H, 2 × HC_{Ar}), 3.48 (s, 2 H, CH_2), 1.44 (s, 9 H, $C(CH_3)_3$); ^{13}C NMR (101 MHz, $CDCl_3$) δ 170.3 (C=O), 133.6 (C_{Ar} quat), 131.5 (2 × C_{Ar}), 130.9 (2 × C_{Ar}), 120.8 (BrC_{Ar} quat), 81.1 ($C(CH_3)_3$), 42.0 (CH_2), 28.0 ($C(CH_3)_3$). The observed characterisation data (IR, ^1H and ^{13}C NMR) was consistent with that previously reported in the literature.[399,400]

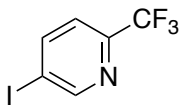
tert-Butyl 2-(4-bromophenyl)-2-diazoacetate (99)[401]



DBU (1.12 mL, 6.0 mmol) was added dropwise over 1 min to a stirred solution of *p*-ABSA (1.44 g, 7.5 mmol) and *tert*-butyl 2-(4-bromophenyl)acetate **98** (1.34 g, 5.0 mmol) in CH_3CN (16.7 mL) at 0 °C. The reaction mixture was stirred at 25 °C for 24 h. Saturated aq. NH_4Cl (50 mL) was added and the aqueous reaction mixture was extracted with Et_2O (3 × 50 mL). The organic layers were dried over Na_2SO_4, filtered and concentrated under reduced pressure. 50% Et_2O/pentane (50 mL) was added and the mixture was filtered, washing with 50% Et_2O/pentane (50 mL), then concentrated under reduced pressure. Purification by flash chromatography (2% Et_2O/pentane) afforded *tert*-butyl 2-(4-bromophenyl)-2-diazoacetate **99** (1.05 g, 70%) as an orange solid. R_f 0.29 (2% Et_2O/pentane); ν_{max} (film)/cm^{-1} 3004, 2930, 2976, 2086 (C=N=N out-of-phase), 1691 (C=O), 1490, 1456, 1392 (C=N=N in phase), 1369, 1345, 1279, 1246, 1190, 1147, 1077, 1012, 1002, 851, 828, 809, 741; ^1H NMR (400 MHz, $CDCl_3$) δ 7.47 (d, J = 8.9 Hz, 2 H, 2 × HC_{Ar}), 7.35 (d, J = 8.9 Hz, 2 H, 2 × HC_{Ar}), 1.55 (s, 9 H, $C(CH_3)_3$); ^{13}C NMR (101 MHz, $CDCl_3$) δ 164.1 (C=O ester), 131.9 (2 × C_{Ar}), 125.4 (C_{Ar}

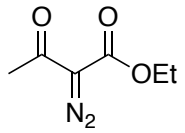
quat), 125.3 (2 × C_{Ar}), 119.0 (BrC_{Ar} quat), 82.3 ($C(CH_3)_3$), 63.5 (CN_2 quat), 28.4 ($C(CH_3)_3$). The observed characterisation data (IR, ^1H and ^{13}C NMR) was consistent with that previously reported in the literature.[402]

5-Iodo-2-(trifluoromethyl)pyridine (101)[403]



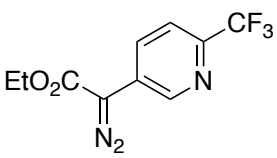
A solution of 5-bromo-2-(trifluoromethyl)pyridine (904 mg, 4.0 mmol), CuI (38.1 mg, 0.2 mmol), NaI (1.19 g, 8.0 mmol), N,N'-DMEDA (42 μL, 0.4 mmol) in 1,4-dioxane (8.0 mL) was stirred at 110 ºC for 24 h. The reaction mixture was cooled to rt and filtered through Celite washing with pentane. Concentration under reduced pressure afforded 5-iodo-2-(trifluoromethyl)pyridine **101** (892 mg, 82% containing ~2% 1,4-dioxane) as a white solid which was used without further purification. R_f 0.76 (20% Et_2O/pentane); mp = 81–83 ºC; ν_{max} (film)/cm^{-1} 3049, 1557, 1333, 1239, 1183, 1130, 1090, 1068, 1003, 859, 783, 699; ^1H NMR (400 MHz, $CDCl_3$) δ 8.96 (s, 1 H, HC_{Ar}), 8.26–8.20 (m, 1 H, HC_{Ar}), 7.48 (d, J = 8.2 Hz, 1 H, HC_{Ar}); ^{13}C NMR (101 MHz, $CDCl_3$) δ 156.2 (C_{Ar}), 147.1 (q, J_{C-F} = 34.8 Hz, CF_3C_{Ar} quat), 145.8 (C_{Ar}), 121.9 (q, J_{C-F} = 2.6 Hz, C_{Ar}), 121.4 (q, J_{C-F} = 273.6 Hz, CF_3), 96.9 (IC_{Ar} quat); $^{19}F\{^1H\}$ NMR (377 MHz, $CDCl_3$) δ –68.1. The observed characterisation data (^1H NMR) was consistent with that previously reported in the literature.[404]

Ethyl 2-diazo-3-oxobutanoate (102)[405]



Cs_2CO_3 (6.52 g, 20 mmol) was added portionwise to a stirred solution of ethyl 3-oxobutanoate (2.54 mL, 20 mmol) and TsN_3 (3.94 g, 20 mmol) in THF (200 mL) at 25 ºC. The reaction mixture was stirred at 25 ºC for 3 h, then the mixture was filtered through Celite, washing with Et_2O (200 mL) and concentrated under reduced pressure. Purification by flash chromatography (15% Et_2O/pentane) afforded ethyl 2-diazo-3-oxobutanoate **102** (2.88 g, 92%) as a yellow oil. R_f 0.22 (15% Et_2O/pentane); ν_{max} (film)/cm^{-1} 2986, 2134 (C=N=N out-of-phase), 1713 (C=O ketone), 1655 (C=O ester), 1364 (C=N=N in-phase), 1309, 1247, 1150, 1069, 1022, 964, 713; ^1H NMR (400 MHz, $CDCl_3$) δ 4.31 (q, J = 7.1 Hz, 2 H, OCH_2CH_3), 2.48 (s, 3 H, $COCH_3$), 1.34 (t, J = 7.1 Hz, 3 H, OCH_2CH_3); ^{13}C NMR (101 MHz, $CDCl_3$) δ 190.2 (C=O ketone), 161.4 (C=O ester), 61.4 (OCH_2CH_3), 28.2 ($COCH_3$), 14.3 (OCH_2CH_3). The observed characterisation data (IR, ^1H and ^{13}C NMR) was consistent with that previously reported in the literature.[406]

Ethyl 2-diazo-2-(6-(trifluoromethyl)pyridin-3-yl)acetate (103)



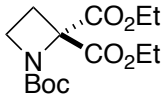
Adapted from a procedure by Wang.[223]

Ethyl 2-diazo-3-oxobutanoate **102** (0.33 mL, 2.4 mmol) was added to a solution of 5-iodo-2-(trifluoromethyl)pyridine **101** (546 mg, 2.0 mmol), $Pd(PPh_3)_4$ (116 mg, 0.1 mmol), dry NaOH* (240 mg, 6.0 mmol) in degassed EtOH (8.0 mL) and stirred at 25 ºC for 18 h. The reaction mixture was filtered through silica, washing with EtOAc (50 mL) and concentrated under reduced pressure. Purification by flash chromatography (10% Et_2O/pentane) afforded ethyl 2-diazo-2-(6-(trifluoromethyl)pyridin-3-yl)acetate **103** (140 mg, 27%) as a yellow solid. R_f 0.36 (10% Et_2O/pentane); ν_{max} (film)/cm^{-1} 2992, 2093 (C=N=N out-of-phase), 1680 (C=O), 1371 (C=N=N in-phase), 1341, 1257, 1237, 1172, 1133, 1087, 1017, 850, 741; ^1H NMR (400 MHz, $CDCl_3$) δ 8.78 (d, J = 2.2 Hz, 1 H, HC_{Ar}), 8.09 (dd, J = 8.4, 2.2 Hz, 1 H, HC_{Ar}), 7.67 (d, J = 8.4 Hz, 1 H, HC_{Ar}), 4.38 (q, J = 7.1 Hz, 2 H, OCH_2CH_3), 1.37 (t, J = 7.1 Hz, 3 H, OCH_2CH_3); ^{13}C NMR (101 MHz, $CDCl_3$) δ 163.8 (C=O), 144.8 (q, J_{C-F} = 35.2 Hz, F_3CC_{Ar} quat), 144.2 (C_{Ar}), 131.4 (C_{Ar}), 126.6 (C_{Ar} quat), 121.5 (q, J_{C-F} = 273.0 Hz, CF_3), 120.3 (q, J_{C-F} = 2.6 Hz, C_{Ar}), 61.7 (OCH_2CH_3), 14.4 (OCH_2CH_3); $^{19}F\{^1H\}$ NMR (377 MHz, $CDCl_3$) δ –67.7; HRMS (ASAP+) *m/z* Calculated for $C_{10}H_9N_3O_2F_3^+$ $[M+H]^+$ 260.0647; Found 260.0653.

*The NaOH was weighed and then dried over a flame in the vial.

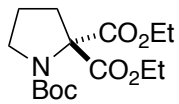
6.2.1.3 Synthesis of 2,2-Diester Saturated Nitrogen Heterocycles

1-(*tert*-Butyl) 2,2-diethyl azetidine-1,2,2-tricarboxylate (57)



$Rh_2(esp)_2$ (1.9 mg, 2.5 μmol) was added to a solution of *tert*-butyl (2-chloroethyl)carbamate **52** (90 mg, 0.50 mmol) and diethyl 2-diazomalonate **50** (140 mg, 0.75 mmol) in benzene (1.67 mL). The reaction vessel was sealed, purged with Ar and heated at 60 ºC for 2.5 h, then allowed to cool to rt. Tetrabutylammonium bromide (16 mg, 50 μmol) was added, followed by $CsOH·H_2O$ (168 mg, 1.00 mmol), and the reaction was stirred at 25 ºC for 18 h. The crude reaction mixture was then filtered through Celite, washing with EtOAc (10 mL), and concentrated under reduced pressure. Purification by flash chromatography (5% to 20% EtOAc/pentane) afforded 1-(*tert*-butyl) 2,2-diethyl azetidine-1,2,2-tricarboxylate **57** (121 mg, 80%) as a colourless oil. R_f 0.44 (20% EtOAc/pentane); ν_{max} (film)/cm^{-1} 2980, 1736 (C=O ester), 1708 (C=O carbamate), 1365, 1256, 1144, 1102, 1023; ^{1}H NMR (400 MHz, $CDCl_3$) δ 4.33–4.25 (m, 4 H, 2 × OCH_2CH$_3$), 3.95–3.90 (m, 2 H, NCH_2), 2.60 (t, *J* = 7.5 Hz, 2 H, NCH$_2$CH_2), 1.44 (s, 9 H, C(CH_3)$_3$), 1.32 (t, *J* = 7.1 Hz, 6 H, 2 × OCH$_2$CH_3); ^{1}H NMR (400 MHz, DMSO-d_6, 373 K) δ 4.23 (q, *J* = 7.1 Hz, 4 H, 2 × OCH_2CH$_3$), 3.80 (t, *J* = 7.6 Hz, 2 H, NCH_2), 2.55 (t, *J* = 7.5 Hz, 2H, NCH$_2$CH_2), 1.38 (s, 9 H, (C(CH_3)$_3$), 1.25 (t, *J* = 7.1 Hz, 6 H, 2 × OCH$_2$CH_3); ^{13}C NMR (101 MHz, $CDCl_3$) δ 168.5 (2 × C=O ester), 154.9 (C=O carbamate), 80.4 (*C*(CH$_3$)$_3$), 71.6 (NC quat), 61.9 (2 × O*C*H$_2$CH$_3$), 46.9 and 45.5 (NCH_2), 28.1 (C(*C*H$_3$)$_3$), 25.3 (NCH$_2$*C*H$_2$), 14.0 (2 × OCH$_2$*C*H$_3$); ^{13}C NMR (101 MHz, DMSO-d_6, 373 K) δ 167.2 (2 × C=O ester), 153.5 (C=O carbamate), 79.0 (*C*(CH$_3$)$_3$), 70.8 (NC quat), 60.8 (2 × O*C*H$_2$CH$_3$), 45.2 (NCH_2), 27.4 (C(*C*H$_3$)$_3$), 24.5 (NCH$_2$*C*H$_2$), 13.2 (2 × OCH$_2$*C*H$_3$); HRMS (ESI$^+$) *m/z* Calculated for $C_{14}H_{24}NO_6$ [M+H] 302.1604; Found 302.1590.

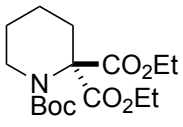
1-(*tert*-Butyl) 2,2-diethyl pyrrolidine-1,2,2-tricarboxylate (60)



$Rh_2(esp)_2$ (1.9 mg, 2.5 μmol) was added to a solution of *tert*-butyl (3-chloropropyl)carbamate **58** (97 mg, 0.50 mmol) and diethyl 2-diazomalonate **50** (140 mg, 0.75 mmol) in benzene (1.67 mL). The reaction vessel was sealed, purged with Ar and heated at 60 ºC for 2.5 h, then allowed to cool to rt. Tetrabutylammonium bromide (16 mg, 50 μmol) was added, followed by $CsOH·H_2O$ (168 mg, 1.00 mmol), and the reaction was stirred at 25 ºC for 18 h. The crude reaction mixture was then filtered through Celite, washing with EtOAc (10 mL), and concentrated under reduced pressure. Purification by flash chromatography (5% to 10% EtOAc/pentane) afforded 1-(*tert*-butyl) 2,2-diethyl pyrrolidine-1,2,2-tricarboxylate **60** (110 mg, 70%) as a colourless oil. R_f 0.26 (5% EtOAc/pentane); ν_{max} (film)/cm^{-1} 2980, 1747 (C=O ester), 1699 (C=O carbamate), 1385, 1365, 1256, 1159, 1111, 1028; ^{1}H NMR (400 MHz, $CDCl_3$) δ 4.31–4.21 (m, 4 H, 2 × OCH_2CH$_3$),

3.62–3.51 (m, 2 H, NCH_2), 2.52–2.44 (m, 2 H, $N(CH_2)_2CH_2$), 1.91–1.82 (m, 2 H, NCH_2CH_2), 1.47 and 1.41 (2 × s br, 9 H, $C(CH_3)_3$), 1.34–1.26 (m, 6 H, 2 × OCH_2CH_3); ^{13}C NMR (101 MHz, $CDCl_3$) δ 169.2 (2 × C=O ester), 153.5 (C=O carbamate), 80.6 and 80.0 ($C(CH_3)_3$), 71.8 (NC quat), 61.8 (2 × OCH_2CH_3), 47.4 (NCH_2), 38.3 and 36.7 (NCH_2CH_2), 28.3 and 28.1 ($C(CH_3)_3$), 23.7 and 22.9 ($N(CH_2)_2CH_2$), 14.08 (2 × OCH_2CH_3). The observed characterisation data (IR, ^{1}H and ^{13}C NMR) was consistent with that previously reported in the literature.[407]

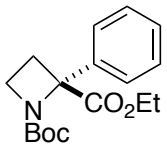
1-(*tert*-Butyl) 2,2-diethyl piperidine-1,2,2-tricarboxylate (61)



$Rh_2(esp)_2$ (1.0 mg, 1.25 μmol) was added to a solution of *tert*-butyl (4-chlorobutyl)carbamate **59** (52 mg, 0.25 mmol) and diethyl 2-diazomalonate **50** (93 mg, 0.50 mmol) in CH_2Cl_2 (1.67 mL). The reaction vessel was sealed, purged with Ar and heated at 40 ºC for 2.5 h, then allowed to cool to rt. Tetrabutylammonium bromide (8.0 mg, 25 μmol) was added, followed by $CsOH·H_2O$ (168 mg, 1.00 mmol), and the reaction was stirred at 25 ºC for 18 h. The crude reaction mixture was then filtered through Celite, washing with EtOAc (10 mL), and concentrated under reduced pressure. Purification by flash chromatography (2% Et_2O/CH_2Cl_2) afforded 1-(*tert*-butyl) 2,2-diethyl piperidine-1,2,2-tricarboxylate **61** (51 mg, 62%) as a colourless oil. R_f 0.28 (3% Et_2O/CH_2Cl_2); ν_{max} (film)/cm^{-1} 2980, 2941, 1736 (C=O ester), 1702 (C=O carbamate), 1363, 1344, 1272, 1237, 1155, 1137, 1114, 1065, 1028, 724; ^{1}H NMR (400 MHz, $CDCl_3$) δ 4.32–4.12 (m, 4 H, 2 × OCH_2CH_3), 3.38–3.29 (m, 2 H, NCH_2), 2.20–2.12 (t, J = 5.8 Hz, 2 H, $N(CH_2)_3CH_2$), 1.67–1.53 (s br, 2 H, NCH_2CH_2), 1.50–1.33 (m, 11 H, $C(CH_3)_3$ and $N(CH_2)_2CH_2$), 1.31–1.22 (t, J = 6.7 Hz, 6 H, 2 × OCH_2CH_3); ^{13}C NMR (101 MHz, $CDCl_3$) δ 168.8 (C=O ester), 156.3 and 156.1 (C=O carbamate), 81.5 and 80.5 ($C(CH_3)_3$), 69.7 and 69.1 (NC quat), 61.5 (OCH_2CH_3), 43.5 and 42.9 (NCH_2), 33.1 and 32.5 ($N(CH_2)_3CH_2$), 28.1 ($C(CH_3)_3$), 23.9 and 23.7 (NCH_2CH_2), 20.6 and 20.4 ($N(CH_2)_2CH_2$), 14.0 (OCH_2CH_3); HRMS (ESI$^+$) *m/z* Calculated for $C_{16}H_{28}NO_6$ [M+H] 330.1917; Found 330.1908.

6.2.1.4 Synthesis of 2,2-Disubstituted Azetidines

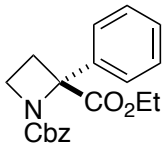
(±)–1-(*tert*-Butyl) 2-ethyl 2-phenylazetidine-1,2-dicarboxylate (104)



$Rh_2(esp)_2$ (1.9 mg, 2.5 μmol) was added to a solution of *tert*-butyl (2-chloroethyl)carbamate **52** (90 mg, 0.50 mmol) and ethyl 2-diazo-2-phenylacetate **85** (143 mg, 0.75 mmol) in benzene (1.67 mL). The reaction vessel was sealed, purged with Ar and heated at 60 ºC for 6 h, then allowed to cool to rt. Tetrabutylammonium bromide (16 mg, 50 μmol) was added, followed by $CsOH·H_2O$ (168 mg, 1.00 mmol), and the reaction was stirred at 25 ºC for 18 h. The crude reaction mixture was then filtered through Celite, washing with EtOAc (10 mL), and concentrated under reduced pressure. Purification by flash chromatography (5 to 10% EtOAc/pentane) afforded 1-(*tert*-butyl) 2-ethyl 2-phenylazetidine-1,2-dicarboxylate **104** (106 mg, 69%) as a colourless oil. R_f 0.18 (10% EtOAc/pentane); ν_{max} (film)/cm^{-1} 2977, 1736 (C=O ester), 1701 (C=O carbamate), 1362, 1230, 1151, 1087, 1022, 766, 696; ^{1}H NMR (400 MHz, $CDCl_3$) δ 7.50–7.27 (m, 5 H, 5 × HC_{Ph}), 4.34–4.12 (m, 3 H, OC*H*$_2$CH$_3$ and NCH*H*), 3.94–3.84 (m, 1 H, NC*H*H), 2.81–2.66 (m, 1 H, NCH_2CH*H*), 2.60–2.45 (m, 1 H, NCH_2C*H*H), 1.55–1.21 (m, 12 H, C(C*H*$_3$)$_3$ and OCH_2C*H*$_3$); ^{13}C NMR (101 MHz, $CDCl_3$) δ 171.5 (C=O ester), 155.9 (C=O carbamate), 140.4 (C_{Ph} quat), 127.7 (2 × C_{Ph}), 127.3 (2 × C_{Ph}), 126.4 (C_{Ph}), 80.3 and 80.0 (*C*(CH$_3$)$_3$), 73.4 and 73.2 (NC quat), 61.7 (O*C*H$_2$CH$_3$), 46.9 and 45.3 (NCH_2), 30.5 and 29.6 (NCH_2*C*H$_2$), 28.3 (C(*C*H$_3$)$_3$), 14.1 (OCH_2*C*H$_3$); HRMS (ESI$^+$) *m/z* Calculated for $C_{17}H_{24}NO_4$ [M+H] 306.1705; Found 306.1701.

Reaction on 5 mmol scale afforded 1.06 g, 69%. 2.5 h NH insertion step, purification by flash chromatography (10% to 15% EtOAc/pentane).

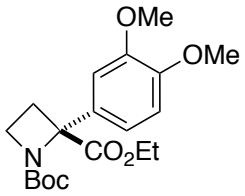
(±)–1-Benzyl 2-ethyl 2-phenylazetidine-1,2-dicarboxylate (105)



$Rh_2(esp)_2$ (1.9 mg, 2.5 μmol) was added to a solution of benzyl (2-chloroethyl)carbamate **63** (107 mg, 0.50 mmol) and ethyl 2-diazo-2-phenylacetate **85** (143 mg, 0.75 mmol) in benzene (1.67 mL). The reaction vessel was sealed, purged with Ar and heated at 60 ºC for 2.5 h, then allowed to cool to rt. Tetrabutylammonium bromide (16 mg, 50 μmol) was added, followed by $CsOH·H_2O$ (168 mg, 1.00 mmol), and the reaction was stirred at 25 ºC for 18 h. The crude reaction mixture was then filtered through Celite, washing with EtOAc (10 mL), and concentrated under reduced pressure. Purification by flash chromatography (15% EtOAc/pentane) afforded 1-benzyl 2-ethyl 2-phenylazetidine-1,2-dicarboxylate **105** (108 mg, 64%) as a colourless oil. R_f 0.19 (15% EtOAc/pentane); ν_{max} (film)/cm^{-1} 2977, 1706 (C=O), 1395, 1340, 1153, 1124, 1088, 695; ^{1}H NMR (400 MHz, $CDCl_3$) δ 7.61–7.10 (m, 10 H, 10 × HC_{Ph}), 5.29–5.09 (m, 2 H, CH_2Ph), 4.31–3.92 (m, 4 H, OC*H*$_2$CH$_3$ and NCH_2), 2.85–2.50 (m, 2 H, NCH_2C*H*$_2$), 1.26–1.08 (m, 3 H,

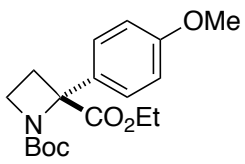
OCH_2CH_3); ^{13}C NMR (101 MHz, $CDCl_3$) δ 171.3 and 171.2 (C=O ester), 156.7 (C=O carbamate), 140.2 and 139.8 (C_{Ph} quat), 136.7 and 136.2 (C_{Ph} quat), 128.5 and 128.4 (2 × C_{Ph}), 128.0 (s br, 4 × C_{Ph}), 127.6 (2 × C_{Ph}), 126.5 and 126.4 (2 × C_{Ph}), 73.7 (NC quat), 66.9 (CH_2Ph), 61.9 (OCH_2CH_3), 46.8 and 45.7 (NCH_2), 31.0 and 30.0 (NCH_2CH_2), 14.0 (OCH_2CH_3); HRMS (ESI^+) *m/z* Calculated for $C_{20}H_{22}NO_4$ [M+H] 340.1549; Found 340.1535.

(±)–1-(*tert*-Butyl) 2-ethyl 2-(3,4-dimethoxyphenyl)azetidine-1,2-dicarboxylate (106)



$Rh_2(esp)_2$ (1.9 mg, 2.5 μmol) was added to a solution of *tert*-butyl (2-chloroethyl)carbamate **52** (90 mg, 0.50 mmol) and ethyl 2-diazo-2-(3,4-dimethoxyphenyl)acetate **86** (188 mg, 0.75 mmol) in benzene (1.67 mL). The reaction vessel was sealed, purged with Ar and heated at 60 ºC for 2.5 h, then allowed to cool to rt. Tetrabutylammonium bromide (16 mg, 50 μmol) was added, followed by $CsOH·H_2O$ (168 mg, 1.00 mmol), and the reaction was stirred at 25 ºC for 18 h. The crude reaction mixture was then filtered through Celite, washing with EtOAc (10 mL), and concentrated under reduced pressure. Purification by flash chromatography (25% EtOAc/pentane) afforded 1-(*tert*-butyl) 2-ethyl 2-(3,4-dimethoxyphenyl)azetidine-1,2-dicarboxylate **106** (121 mg, 66%) as a pale yellow oil. R_f 0.25 (25% EtOAc/pentane); ν_{max} (film)/cm^{-1} 2976, 1737 (C=O ester), 1700 (C=O carbamate), 1517, 1363, 1252, 1142, 1124, 1087, 1026, 763.4; ^1H NMR (400 MHz, $CDCl_3$) δ 7.15 (s br, 0.4 H, HC_{Ar}), 7.02–6.92 (m, 1.6 H, 2 × HC_{Ar}), 6.85 (d, J = 8.5 Hz, 1 H, HC_{Ar}), 4.35–4.09 (m, 3 H, NCH*H* and OCH_2CH_3), 3.92–3.82 (m, 7 H, NC*H*H and 2 × OCH_3), 2.81–2.42 (m, 2H, NCH_2CH_2), 1.54–1.23 (m, 12H, $C(CH_3)_3$ and OCH_2CH_3); ^{13}C NMR (101 MHz, $CDCl_3$) δ 171.6 (C=O ester), 156.0 (C=O carbamate), 148.2 (OC_{Ar} quat), 148.1 (OC_{Ar} quat), 133.0 (C_{Ar} quat), 118.8 (C_{Ar}), 110.4 (C_{Ar}), 110.0 (C_{Ar}), 80.3 and 79.9 ($C(CH_3)_3$), 73.2 and 73.0 (NC quat), 61.6 (OCH_2CH_3), 55.81 (OCH_3), 55.76 (OCH_3), 46.7 and 45.3 (NCH_2), 30.6 and 29.4 (NCH_2CH_2), 28.3 ($C(CH_3)_3$), 14.1 (OCH_2CH_3); HRMS (ESI^+) *m/z* Calculated for $C_{19}H_{28}NO_6$ [M+H] 366.1917; Found 366.1927.

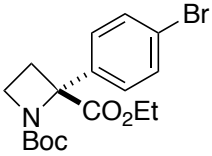
(±)–1-(*tert*-Butyl) 2-ethyl 2-(4-methoxyphenyl)azetidine-1,2-dicarboxylate (107)



$Rh_2(esp)_2$ (1.9 mg, 2.5 μmol) was added to a solution of *tert*-butyl (2-chloroethyl)carbamate **52** (90 mg, 0.50 mmol) and ethyl 2-diazo-2-(4-methoxyphenyl)acetate **87** (165 mg, 0.75 mmol) in benzene (1.67 mL). The reaction vessel was sealed, purged with Ar and heated at 60 ºC for 2.5 h, then allowed to cool to rt. Tetrabutylammonium bromide (16 mg, 50 μmol) was added, followed by $CsOH·H_2O$ (168 mg, 1.00 mmol), and the reaction was stirred at 25 ºC for 18 h. The crude reaction mixture was then filtered through Celite, washing with EtOAc (10 mL), and concentrated under reduced pressure. Purification by flash chromatography (20%

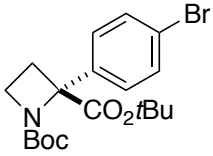
EtOAc/pentane) afforded 1-(*tert*-butyl) 2-ethyl 2-(4-methoxyphenyl)azetidine-1,2-dicarboxylate **107** (115 mg, 69%) as a colourless oil. R_f 0.30 (20% EtOAc/pentane); ν_{max} (film)/cm^{-1} 2977, 1736 (C=O ester), 1701 (C=O carbamate), 1514, 1363, 1247, 1151, 1085, 1026, 832, 752; ^{1}H NMR (400 MHz, $CDCl_3$) δ 7.47–7.28 (m, 2 H, HC_{Ar}), 7.06–6.70 (m, 2 H, HC_{Ar}), 4.33–4.19 (m, 2 H, OCH_2CH_3), 4.17–4.10 (m, 1 H, NC*H*H), 3.90–3.83 (m, 1 H, NCH*H*), 3.83 (s, 3 H, OCH_3), 2.76–2.59 (m, 1 H, NCH_2CHH), 2.59–2.42 (m, 1 H, NCH_2CHH), 1.52–1.25 (m, 12 H, $C(CH_3)_3$ and OCH_2CH_3); ^{13}C NMR (101 MHz, $CDCl_3$) δ 171.7 (C=O ester), 158.7 (OC_{Ar} quat), 155.9 (C=O carbamate), 133.0 and 132.5 (C_{Ar} quat), 127.7 (2 $\times$ C_{Ar}), 113.1 (2 $\times$ C_{Ar}), 80.2 and 79.9 ($C(CH_3)_3$), 73.1 and 72.9 (NC quat), 61.6 (OCH_2CH_3), 55.2 (OCH_3), 46.8 and 45.2 (NCH_2), 30.5 and 29.5 (NCH_2CH_2), 28.3 and 27.9 ($C(CH_3)_3$), 14.1 and 14.0 (OCH_2CH_3); HRMS (ESI$^+$) *m/z* Calculated for $C_{18}H_{26}NO_5$ [M+H] 336.1811; Found 336.1809.

(±)–1-(*tert*-Butyl) 2-ethyl 2-(4-bromophenyl)azetidine-1,2-dicarboxylate (108)



$Rh_2(esp)_2$ (1.9 mg, 2.5 μmol) was added to a solution of *tert*-butyl (2-chloroethyl)carbamate **52** (90 mg, 0.50 mmol) and ethyl 2-(4-bromophenyl)-2-diazoacetate **88** (202 mg, 0.75 mmol) in benzene (1.67 mL). The reaction vessel was sealed, purged with Ar and heated at 60 ºC for 2.5 h, then allowed to cool to rt. Tetrabutylammonium bromide (16 mg, 50 μmol) was added, followed by $CsOH{\cdot}H_2O$ (168 mg, 1.00 mmol), and the reaction was stirred at 25 ºC for 18 h. The crude reaction mixture was then filtered through Celite, washing with EtOAc (10 mL), and concentrated under reduced pressure. Purification by flash chromatography (10% EtOAc/pentane) afforded 1-(*tert*-butyl) 2-ethyl 2-(4-bromophenyl)azetidine-1,2-dicarboxylate **108** (138 mg, 72%) as a pale yellow oil. R_f 0.35 (15% EtOAc/pentane); ν_{max} (film)/cm^{-1} 2976, 1737 (C=O ester), 1701 (C=O carbamate), 1362, 1233, 1151, 1084, 1009, 976, 780; ^{1}H NMR (400 MHz, $CDCl_3$) δ 7.49 (br d, *J* = 8.1 Hz, 2 H, 2 $\times$ HC_{Ar}), 7.39–7.27 (m, 2 H, 2 $\times$ HC_{Ar}), 4.29–4.14 (m, 3 H, OCH_2CH_3 and NCH*H*), 3.89–3.83 (m, 1 H, NC*H*H), 2.80–2.63 (m, 1 H, NCH_2CHH), 2.56–2.37 (m, 1 H, NCH_2CHH), 1.58–1.21 (m, 12 H, $C(CH_3)_3$ and OCH_2CH_3); ^{13}C NMR (400 MHz, $CDCl_3$) δ 171.1 (C=O ester), 155.8 (C=O carbamate), 139.5 (C_{Ar} quat), 130.8 (2 $\times$ C_{Ar}), 128.2 (2 $\times$ C_{Ar}), 121.4 (BrC_{Ar} quat), 80.7 ($C(CH_3)_3$), 73.0 (NC quat), 61.9 (OCH_2CH_3), 46.9 and 45.4 (NCH_2), 30.5 and 29.5 (NCH_2CH_2), 28.3 ($C(CH_3)_3$), 14.1 (OCH_2CH_3); HRMS (ESI$^+$) *m/z* Calculated for $C_{17}H_{23}NO_4{}^{79}Br$ [M+H] 384.0810; Found 384.0820.

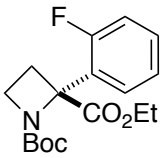
(±)–Di-*tert*-butyl 2-(4-bromophenyl)azetidine-1,2-dicarboxylate (109)



$Rh_2(esp)_2$ (1.9 mg, 2.5 μmol) was added to a solution of *tert*-butyl (2-chloroethyl)carbamate **52** (90 mg, 0.50 mmol) and *tert*-butyl 2-(4-bromophenyl)-2-diazoacetate **99** (223 mg, 0.75 mmol) in benzene

(1.67 mL). The reaction vessel was sealed, purged with Ar and heated at 60 ºC for 2.5 h, then allowed to cool to rt. Tetrabutylammonium bromide (16 mg, 50 μmol) was added, followed by $CsOH{\cdot}H_2O$ (168 mg, 1.00 mmol), and the reaction was stirred at 25 ºC for 18 h. The crude reaction mixture was then filtered through Celite, washing with EtOAc (10 mL), and concentrated under reduced pressure. Purification by flash chromatography (5% EtOAc/pentane) afforded di-*tert*-butyl 2-(4-bromophenyl)azetidine-1,2-dicarboxylate **109** (169 mg, 82%) as a pale yellow oil. R_f 0.16 (5% EtOAc/pentane); ν_{max} (film)/cm^{-1} 2976, 2932, 1732 (C=O ester), 1701 (C=O carbamate), 1490, 1477, 1364, 1289, 1245, 1147, 1087, 1010, 977, 911, 845, 831, 806, 782, 730; ^{1}H NMR (400 MHz, $CDCl_3$) δ 7.50–7.41 (m, 2 H, 2 × HC_{Ar}), 7.34–7.28 (d, J = 8.5 Hz, 2 H, 2 × HC_{Ar}), 4.15–4.08 (m, 1 H, NC*H*H), 3.88–3.78 (m, 1 H, NCH*H*), 2.68–2.58 (m, 1 H, NCH_2CHH), 2.50–2.35 (m, 1 H, NCH_2CHH), 1.59–1.35 (m, 18 H, 2 × $C(CH_3)_3$); ^{13}C NMR (101 MHz, $CDCl_3$) δ 170.1 and 169.7 (C=O ester), 156.3 and 155.8 (C=O carbamate), 140.3 and 139.7 (C_{Ar} quat), 130.7 and 130.6 (2 × C_{Ar}), 128.4 (2 × C_{Ar}), 121.3 (BrC_{Ar} quat), 82.3 and 82.2 ($C(CH_3)_3$ ester), 80.6 and 80.1 ($C(CH_3)_3$ carbamate), 73.4 and 73.1 (NC quat), 46.9 and 45.2 (NCH_2), 30.6 and 29.3 (NCH_2CH_2), 28.3 ($C(CH_3)_3$ carbamate), 27.8 ($C(CH_3)_3$ ester); HRMS (ESI$^+$) *m/z* Calculated for $C_{19}H_{27}NO_4{}^{79}Br$ [M+H] 412.1123; Found 412.1107.

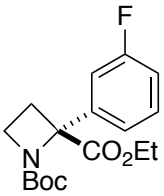
(±)–1-(*tert*-Butyl) 2-ethyl 2-(2-fluorophenyl)azetidine-1,2-dicarboxylate (110)



$Rh_2(esp)_2$ (1.9 mg, 2.5 μmol) was added to a solution of *tert*-butyl (2-chloroethyl)carbamate **52** (90 mg, 0.50 mmol) and ethyl 2-diazo-2-(2-fluorophenyl)acetate **89** (156 mg, 0.75 mmol) in benzene (1.67 mL). The reaction vessel was sealed, purged with Ar and heated at 60 ºC for 5 h, then allowed to cool to rt. Tetrabutylammonium bromide (16 mg, 50 μmol) was added, followed by $CsOH{\cdot}H_2O$ (168 mg, 1.00 mmol), and the reaction was stirred at 25 ºC for 18 h. The crude reaction mixture was then filtered through Celite, washing with EtOAc (10 mL), and concentrated under reduced pressure. Purification by flash chromatography (CH_2Cl_2 to 1% EtOAc/CH_2Cl_2) afforded 1-(*tert*-butyl) 2-ethyl 2-(2-fluorophenyl)azetidine-1,2-dicarboxylate **110** (142 mg, 88%) as a brown oil. R_f 0.15 (CH_2Cl_2); ν_{max} (film)/cm^{-1} 2978, 1734 (C=O ester), 1704 (C=O carbamate), 1357, 1263, 1213, 1192, 1150, 1104, 1083, 1025, 753; ^{1}H NMR (400 MHz, $CDCl_3$) δ 7.54–7.41 (m, 1 H, HC_{Ar}), 7.35–7.25 (m, 1 H, HC_{Ar}), 7.15 (t, J = 7.5 Hz, 1 H, HC_{Ar}), 7.04 (t, J = 8.9 Hz, 1 H, HC_{Ar}), 4.33–4.15 (m, 3 H, OCH_2CH_3 and NC*H*H), 3.92–3.85 (m, 1 H, NCH*H*), 2.96–2.82 (m, 1 H, NCH_2CHH), 2.50–2.39 (m, 1 H, NCH_2CHH), 1.56–1.21 (m, 12 H, OCH_2CH_3 and $C(CH_3)_3$); ^{13}C NMR (101 MHz, $CDCl_3$) δ 170.5 and 170.2 (C=O ester), 159.9 (d, J_{C-F} = 246.2 Hz, FC_{Ar} quat), 156.9 and 156.0 (C=O carbamate), 129.2 (s br, C_{Ar}), 128.5 (s br, C_{Ar} quat), 127.8 and 127.3 (C_{Ar}), 123.6 and 123.3 (C_{Ar}), 115.2 (d, J_{C-F} = 21.0 Hz,

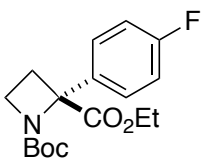
C_{Ar}), 80.7 and 80.4 ($C(CH_3)_3$), 71.5 (NC quat), 61.7 (OCH_2CH_3), 48.0 and 46.5 (NCH_2), 29.5 and 29.2 (NCH_2CH_2), 28.2 ($C(CH_3)_3$), 14.0 (OCH_2CH_3); $^{19}F\{^1H\}$ NMR (377 MHz, $CDCl_3$) δ –113.7 and –114.8; HRMS (ESI^+) *m/z* Calculated for $C_{17}H_{23}NO_4F$ [M+H] 324.1611; Found 324.1613.

(±)–1-(*tert*-Butyl) 2-ethyl 2-(3-fluorophenyl)azetidine-1,2-dicarboxylate (111)



$Rh_2(esp)_2$ (1.9 mg, 2.5 μmol) was added to a solution of *tert*-butyl (2-chloroethyl)carbamate **52** (90 mg, 0.50 mmol) and ethyl 2-diazo-2-(3-fluorophenyl)acetate **90** (156 mg, 0.75 mmol) in benzene (1.67 mL). The reaction vessel was sealed, purged with Ar and heated at 60 ºC for 2.5 h, then allowed to cool to rt. Tetrabutylammonium bromide (16 mg, 50 μmol) was added, followed by $CsOH{\cdot}H_2O$ (168 mg, 1.00 mmol), and the reaction was stirred at 25 ºC for 18 h. The crude reaction mixture was then filtered through Celite, washing with EtOAc (10 mL), and concentrated under reduced pressure. Purification by flash chromatography (15% EtOAc/ hexane) afforded 1-(*tert*-butyl) 2-ethyl 2-(3-fluorophenyl)azetidine-1,2-dicarboxylate **111** (75 mg, 46%) as a yellow solid. R_f 0.24 (15% EtOAc/hexane); mp = 41–43 ºC; ν_{max} (film)/cm^{-1} 2977, 2899, 1738 (C=O ester), 1701 (C=O carbamate), 1363, 1240, 1151, 1123, 1089, 779, 691; ^1H NMR (400 MHz, $CDCl_3$) δ 7.36–7.28 (m, 1 H, HC_{Ar}), 7.26–7.14 (m, 2 H, 2 × HC_{Ar}), 7.03–6.94 (m, 1 H, HC_{Ar}), 4.35–4.14 (m, 3 H, OCH_2CH_3 and NC*H*H), 3.87 (ddd, *J* = 9.1, 7.9, 4.6 Hz, 1 H, NCH*H*), 2.79–2.65 (m, 1 H, NCH_2CHH), 2.55–2.42 (m, 1 H, NCH_2CHH), 1.58–1.23 (m, 12 H, $C(CH_3)_3$ and OCH_2CH_3); ^{13}C NMR (101 MHz, $CDCl_3$) δ 171.0 (C=O ester), 162.4 (d, J_{C-F} = 243.9 Hz, FC_{Ar} quat), 156.4 and 155.8 (C=O carbamate), 143.3 and 143.0 (C_{Ar} quat), 129.2 (d, J_{C-F} = 8.1 Hz, C_{Ar}), 122.2 (br s, C_{Ar}), 114.2 (d, J_{C-F} = 21.0 Hz, C_{Ar}), 113.8 (d, J_{C-F} = 22.3 Hz, C_{Ar}), 80.7 and 80.3 ($C(CH_3)_3$), 73.0 (NC quat), 61.9 (OCH_2CH_3), 46.9 and 45.4 (NCH_2), 30.4 and 29.6 (NCH_2CH_2), 28.3 ($C(CH_3)_3$), 14.1 (OCH_2CH_3); $^{19}F\{^1H\}$ NMR (377 MHz, $CDCl_3$) δ –113.6 (br s); HRMS (ESI^+) *m/z* Calculated for $C_{17}H_{23}NO_4F$ [M+H] 324.1611; Found 324.1607.

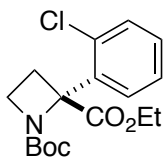
(±)–1-(*tert*-Butyl) 2-ethyl 2-(4-fluorophenyl)azetidine-1,2-dicarboxylate (112)



$Rh_2(esp)_2$ (1.9 mg, 2.5 μmol) was added to a solution of *tert*-butyl (2-chloroethyl)carbamate **52** (90 mg, 0.50 mmol) and ethyl 2-diazo-2-(4-fluorophenyl)acetate **91** (156 mg, 0.75 mmol) in benzene (1.67 mL). The reaction vessel was sealed, purged with Ar and heated at 60 ºC for 2.5 h, then allowed to cool to rt. Tetrabutylammonium bromide (16 mg, 50 μmol) was added, followed by $CsOH{\cdot}H_2O$ (168 mg, 1.00 mmol), and the reaction was stirred at 25 ºC for 18 h. The crude reaction mixture was then filtered through Celite, washing with EtOAc (10 mL), and concentrated under reduced pressure. Purification by flash chromatography (20%

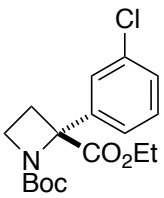
EtOAc/hexane) afforded 1-(*tert*-butyl) 2-ethyl 2-(4-fluorophenyl)azetidine-1,2-dicarboxylate **112** (144 mg, 89%) as a pale yellow oil. R_f 0.20 (20% EtOAc/hexane); ν_{max} (film)/cm^{-1} 2977, 2899, 1737 (C=O ester), 1701 (C=O carbamate), 1511, 1363, 1296, 1227, 1151, 1084, 1015, 977, 859, 836, 816, 780; ^{1}H NMR (400 MHz, $CDCl_3$) δ 7.50–7.34 (m, 2 H, 2 × HC_{Ar}), 7.04 (t, *J* = 8.5 Hz, 2 H, 2 × HC_{Ar}), 4.36–4.12 (m, 3 H, OC*H*$_2$CH$_3$ and NC*H*H), 3.91–3.83 (m, 1 H, NCH*H*), 2.79–2.62 (m, 1 H, NCH$_2$C*H*H), 2.58–2.40 (m, 1 H, NCH$_2$CH*H*), 1.62–1.21 (m, 12 H, OCH$_2$C*H*$_3$ and C(CH$_3$)$_3$); ^{13}C NMR (101 MHz, $CDCl_3$) δ 171.4 (C=O ester), 162.0 (d, J_{C-F} = 246.1 Hz, FC_{Ar} quat), 155.8 (C=O carbamate), 136.7 and 136.2 (C_{Ar} quat), 128.2 (2 × C_{Ar}), 114.6 (d, J_{C-F} = 22.6 Hz, 2 × C_{Ar}), 80.5 and 80.2 (*C*(CH$_3$)$_3$), 72.9 (br s, NC quat), 61.8 (O*C*H$_2$CH$_3$), 46.9 and 45.4 (NCH$_2$), 30.6 and 29.6 (NCH$_2$*C*H$_2$), 28.3 (C(*C*H$_3$)$_3$), 14.1 (OCH$_2$*C*H$_3$); ^{19}F{^{1}H} NMR (377 MHz, $CDCl_3$) δ –115.4 and –115.5; HRMS (ESI$^+$) *m/z* Calculated for $C_{17}H_{23}NO_4F$ [M+H] 324.1611; Found 324.1625.

(±)–1-(*tert*-Butyl) 2-ethyl 2-(2-chlorophenyl)azetidine-1,2-dicarboxylate (113)



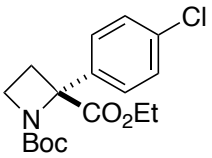
$Rh_2(esp)_2$ (1.9 mg, 2.50 μmol) was added to a solution of *tert*-butyl (2-chloroethyl)carbamate **52** (90 mg, 0.50 mmol) and ethyl 2-(2-chlorophenyl)-2-diazoacetate **92** (169 mg, 0.75 mmol) in benzene (1.67 mL). The reaction vessel was sealed, purged with Ar and heated at 60 ºC for 2.5 h, then allowed to cool to rt. Tetrabutylammonium bromide (16 mg, 50 μmol) was added, followed by CsOH·H$_2$O (168 mg, 1.00 mmol), and the reaction was stirred at 25 ºC for 18 h. The crude reaction mixture was then filtered through Celite, washing with EtOAc (10 mL), and concentrated under reduced pressure. Purification by flash chromatography (CH_2Cl_2) afforded 1-(*tert*-butyl) 2-ethyl 2-(2-chlorophenyl)azetidine-1,2-dicarboxylate **113** (60 mg, 35%) as a white solid. R_f 0.27 (CH_2Cl_2); mp = 63–64 ºC; ν_{max} (film)/cm^{-1} 2986, 1729 (C=O ester), 1702 (C=O carbamate), 1368, 1285, 1248, 1191, 1164, 1146, 1131, 1097, 1031, 1004, 765; ^{1}H NMR (400 MHz, $CDCl_3$) δ 7.51 (dd, *J* = 7.6, 1.9 Hz, 1 H, HC_{Ar}), 7.38–7.21 (m, 3 H, 3 × HC_{Ar}), 4.32–4.12 (m, 3 H, OC*H*$_2$CH$_3$ and NC*H*H), 3.87–3.78 (m, 1 H, NCH*H*), 3.15–3.04 (m, 1 H, NCH$_2$C*H*H), 2.44–2.34 (m, 1 H, NCH$_2$CH*H*), 1.55–1.36 (m, 9 H, C(CH$_3$)$_3$), 1.30–1.21 (m, 3 H, OCH$_2$C*H*$_3$); ^{13}C NMR (101 MHz, $CDCl_3$) δ 169.9 (C=O ester), 155.9 (C=O carbamate), 138.6 (C_{Ar}), 132.1 (ClC_{Ar} quat), 129.6 (C_{Ar}), 128.7 (C_{Ar}), 127.7 (C_{Ar}), 126.4 and 126.1 (C_{Ar} quat), 80.7 (*C*(CH$_3$)$_3$), 73.9 (NC quat), 61.7 (O*C*H$_2$CH$_3$), 47.6 and 46.1 (NCH$_2$), 29.8 (NCH$_2$*C*H$_2$), 28.2 (C(*C*H$_3$)$_3$), 13.9 (OCH$_2$*C*H$_3$); HRMS (ESI$^+$) *m/z* Calculated for $C_{17}H_{23}NO_4{}^{35}Cl$ [M+H] 340.1316; Found 340.1318.

(±)–1-(*tert*-Butyl) 2-ethyl 2-(3-chlorophenyl)azetidine-1,2-dicarboxylate (114)



$Rh_2(esp)_2$ (1.9 mg, 2.5 μmol) was added to a solution of *tert*-butyl (2-chloroethyl)carbamate **52** (90 mg, 0.50 mmol) and ethyl 2-diazo-2-(3-chlorophenyl)acetate **93** (168 mg, 0.75 mmol) in benzene (1.67 mL). The reaction vessel was sealed, purged with Ar and heated at 60 ºC for 5 h, then allowed to cool to rt. Tetrabutylammonium bromide (16 mg, 50 μmol) was added, followed by $CsOH·H_2O$ (168 mg, 1.00 mmol), and the reaction was stirred at 25 ºC for 18 h. The crude reaction mixture was then filtered through Celite, washing with EtOAc (10 mL), and concentrated under reduced pressure. Purification by flash chromatography (15% EtOAc/pentane) afforded 1-(*tert*-butyl) 2-ethyl 2-(3-chlorophenyl)azetidine-1,2-dicarboxylate **114** (81 mg, 48%) as a yellow oil. R_f 0.32 (15% EtOAc/pentane); ν_{max} (film)/cm^{-1} 2977, 1738 (C=O ester), 1702 (C=O carbamate), 1359, 1230, 1152, 1086, 781; ^{1}H NMR (400 MHz, $CDCl_3$) δ 7.49–7.23 (m, 4 H, 4 × HC_{Ar}), 4.34–4.12 (m, 3 H, O*C*$H_2$$CH_3$ and NC*H*H), 3.91–3.83 (m, 1 H, NCH*H*), 2.81–2.65 (m, 1 H, NCH_2C*H*H), 2.56–2.41 (m, 1 H, NCH_2CH*H*), 1.56–1.23 (m, 12H, OCH_2C*H*$_3$ and $C(CH_3)_3$); ^{13}C NMR (101 MHz, $CDCl_3$) δ 171.0 (C=O ester), 155.7 (C=O carbamate), 142.4 (C_{Ar} quat), 133.7 (ClC_{Ar} quat), 129.0 (C_{Ar}), 127.5 (C_{Ar}), 126.9 (br s, C_{Ar}), 124.7 (C_{Ar}), 80.8 (*C*$(CH_3)_3$), 72.9 (NC quat), 61.9 (O*C*$H_2$$CH_3$), 46.9 and 45.4 ($NCH_2$), 30.3 and 29.6 ($NCH_2$*C*$H_2$), 28.3 (C(*C*$H_3$)$_3$), 14.1 ($OCH_2$*C*$H_3$); HRMS (ESI$^+$) *m/z* Calculated for $C_{17}H_{23}NO_4{}^{35}Cl$ [M+H] 340.1316; Found 340.1324.

(±)–1-(*tert*-Butyl) 2-ethyl 2-(4-chlorophenyl)azetidine-1,2-dicarboxylate (115)



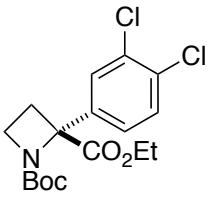
$Rh_2(esp)_2$ (1.9 mg, 2.5 μmol) was added to a solution of *tert*-butyl (2-chloroethyl)carbamate **52** (90 mg, 0.50 mmol) and ethyl 2-(4-chlorophenyl)-2-diazoacetate **94** (169 mg, 0.75 mmol) in benzene (1.67 mL). The reaction vessel was sealed, purged with Ar and heated at 60 ºC for 5 h, then allowed to cool to rt. Tetrabutylammonium bromide (16 mg, 50 μmol) was added, followed by $CsOH·H_2O$ (168 mg, 1.00 mmol), and the reaction was stirred at 25 ºC for 18 h. Saturated aq. NH_4Cl (10mL) was added to the reaction mixture and the aqueous reaction mixture was extracted with CH_2Cl_2 (3 × 10 mL). The combined organic layers were dried over Na_2SO_4, filtered and concentrated under reduced pressure. Purification by flash chromatography (15% EtOAc/hexane) afforded 1-(*tert*-butyl) 2-ethyl 2-(4-chlorophenyl)azetidine-1,2-dicarboxylate **115** (108 mg, 64%) as a colourless oil. R_f 0.22 (15% EtOAc/pentane); ν_{max} (film)/cm^{-1} 2977, 1737 (C=O ester), 1701 (C=O carbamate), 1362, 1233, 1089, 1013, 976, 858, 833, 780; ^{1}H NMR (400 MHz, $CDCl_3$) δ 7.46–7.30 (m, 4 H, 4 × HC_{Ar}), 4.34–4.12 (m, 3 H, O*C*$H_2$$CH_3$ and NCH*H*), 3.89–3.82 (m, 1 H, NC*H*H), 2.78–2.63 (m, 1 H, NCH_2CH*H*), 2.50–2.37 (m, 1 H, NCH_2C*H*H), 1.53–1.23 (m, 12 H, $C(CH_3)_3$ and OCH_2C*H*$_3$);

^{13}C NMR (101 MHz, $CDCl_3$) δ 171.1 (C=O ester), 155.8 (C=O carbamate), 138.9 (C_{Ar} quat), 133.1 (ClC_{Ar} quat), 128.1 and 127.9 (4 × C_{Ar}), 80.6 and 80.3 ($C(CH_3)_3$), 72.9 (NC quat), 61.9 (OCH_2CH_3), 46.9 and 45.4 (NCH_2), 30.5 and 29.5 (NCH_2CH_2), 28.2 ($C(CH_3)_3$), 14.1 (OCH_2CH_3); HRMS (ESI^+) *m/z* Calculated for $C_{17}H_{23}NO_4{}^{35}Cl$ [M+H] 340.1316; Found 340.1328.

Reaction on 2 mmol scale afforded **115**, 481 mg, 67% (Filtration through Celite followed by purification using 10% to 15% EtOAc/pentane).

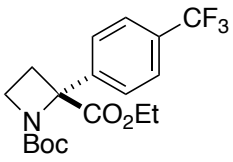
Reaction on 3 mmol scale afforded **115**, 488 mg, 48% (Filtration through Celite followed by purification using 10% EtOAc/pentane).

(±)–1-(*tert*-Butyl) 2-ethyl 2-(3,4-dichlorophenyl)azetidine-1,2-dicarboxylate (116)



$Rh_2(esp)_2$ (1.9 mg, 2.5 μmol) was added to a solution of *tert*-butyl (2-chloroethyl)carbamate **52** (90 mg, 0.50 mmol) and ethyl 2-diazo-2-(3,4-dichlorophenyl)acetate **95** (194 mg, 0.75 mmol) in benzene (1.67 mL). The reaction vessel was sealed, purged with Ar and heated at 60 ºC for 2.5 h, then allowed to cool to rt. Tetrabutylammonium bromide (16 mg, 50 μmol) was added, followed by $CsOH{\cdot}H_2O$ (168 mg, 1.00 mmol), and the reaction was stirred at 25 ºC for 18 h. The crude reaction mixture was then filtered through Celite, washing with EtOAc (10 mL), and concentrated under reduced pressure. Purification by flash chromatography (20% EtOAc/pentane) afforded 1-(*tert*-butyl) 2-ethyl 2-(3,4-dichlorophenyl)azetidine-1,2-dicarboxylate **116** (83 mg, 44%) as a yellow oil. R_f 0.25 (20% EtOAc/pentane); ν_{max} (film)/cm^{-1} 2977, 1738 (C=O ester), 1702 (C=O carbamate), 1363, 1230, 1152, 1136, 1088, 1029, 774; ^{1}H NMR (400 MHz, $CDCl_3$) δ 7.56 (s br, 1 H, HC_{Ar}), 7.46–7.38 (m, 1 H, HC_{Ar}), 7.35–7.21 (m, 1 H, HC_{Ar}), 4.35–4.12 (m, 3H, OCH_2CH_3 and NC*H*H), 3.89–3.82 (m, 1 H, NCH*H*), 2.77–2.63 (m, 1 H, NCH_2CHH), 2.51–2.39 (m, 1 H, NCH_2CHH), 1.55–1.24 (m, 12 H, OCH_2CH_3 and $C(CH_3)_3$); ^{13}C NMR (101 MHz, $CDCl_3$) δ 170.7 (C=O ester), 156.4 and 155.6 (C=O carbamate), 140.6 (C_{Ar} quat), 131.9 (ClC_{Ar} quat), 131.4 (ClC_{Ar} quat), 129.7 (C_{Ar}), 128.8 (C_{Ar}), 126.3 and 126.0 (C_{Ar}), 81.0 and 80.6 (NC quat), 72.5 ($C(CH_3)_3$), 62.1 (OCH_2CH_3), 46.9 and 45.5 (NCH_2), 30.3 and 29.5 (NCH_2CH_2), 28.3 ($C(CH_3)_3$), 14.1 (OCH_2CH_3); HRMS (ESI^+) *m/z* Calculated for $C_{17}H_{22}NO_4{}^{35}Cl_2$ [M+H] 374.9026; Found 374.9020.

(±)–1-(*tert*-Butyl) 2-ethyl 2-(4-(trifluoromethyl)phenyl)azetidine-1,2-dicarboxylate (117)

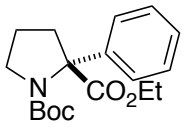


Ethyl 2-diazo-2-(4-(trifluoromethyl)phenyl)acetate **96** (323 mg, 1.25 mmol) in benzene (1.0 mL) was added slowly *via* syringe pump over 1 h to a solution of *tert*-butyl (2-chloroethyl)carbamate **52** (90 mg, 0.50 mmol) and $Rh_2(esp)_2$ (1.9 mg, 2.5 μmol) in benzene (0.67 mL) at

60 ºC. The reaction mixture was stirred at 60 °C for a further 2.5 h, then allowed to cool to rt. Tetrabutylammonium bromide (16 mg, 50 μmol) was added, followed by $CsOH{\cdot}H_2O$ (168 mg, 1.00 mmol), and the reaction was stirred at 25 ºC for 18 h. The crude reaction mixture was then filtered through Celite, washing with EtOAc (10 mL), and concentrated under reduced pressure. Purification by flash chromatography (15% EtOAc/pentane) afforded 1-(*tert*-butyl) 2-ethyl 2-(4-(trifluoromethyl)phenyl)azetidine-1,2-dicarboxylate **117** (76 mg, 41%) as a pale yellow oil. R_f 0.30 (15% EtOAc/pentane); ν_{max} (film)/cm^{-1} 2979, 1739 (C=O ester), 1702 (C=O carbamate), 1365, 1324, 1157, 1120, 1086, 1069, 1017, 843; ^{1}H NMR (400 MHz, $CDCl_3$) δ 7.70–7.50 (m, 4 H, 4 × HC_{Ar}), 4.36–4.16 (m, 3 H, OCH_2CH_3 and $NCHH$), 3.92–3.84 (m, 1 H, $NCHH$), 2.85–2.68 (m, 1 H, NCH_2CHH), 2.57–2.38 (m, 1 H, NCH_2CHH), 1.57–1.24 (m, 12 H, $C(CH_3)_3$ and OCH_2CH_3); ^{13}C NMR (101 MHz, $CDCl_3$) δ 170.9 (C=O ester), 156.6 and 155.9 (C=O carbamate), 144.8 and 144.4 (C_{Ar} quat), 129.5 (q, $J_{C–F}$ = 33.1 Hz, CF_3C_{Ar} quat), 127.0 and 126.9 (2 × C_{Ar}), 124.7 (2 × C_{Ar}), 124.2 (q, $J_{C–F}$ = 272.7 Hz, CF_3), 80.8 and 80.5 ($C(CH_3)_3$), 73.1 and 72.9 (NC quat), 62.0 (OCH_2CH_3), 47.0 and 45.5 (NCH_2), 30.5 and 29.6 (NCH_2CH_2), 28.3 ($C(CH_3)_3$), 14.1 (OCH_2CH_3); ^{19}F{^{1}H} NMR (377 MHz, $CDCl_3$) δ –62.5; HRMS (ESI^+) *m/z* Calculated for $C_{18}H_{23}NO_4F_3$ [M+H] 374.1579; Found 374.1579.

6.2.1.5 Synthesis of 2,2-Disubstituted Pyrrolidines

(±)–1-(*tert*-Butyl) 2-ethyl 2-phenylpyrrolidine-1,2-dicarboxylate (118)



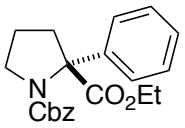
$Rh_2(esp)_2$ (1.9 mg, 2.5 μmol) was added to a solution of *tert*-butyl (3-chloropropyl)carbamate **58** (97 mg, 0.50 mmol) and ethyl 2-diazo-2-phenylacetate **85** (143 mg, 0.75 mmol) in benzene (1.67 mL). The reaction vessel was sealed, purged with Ar and heated at 60 ºC for 2.5 h, then allowed to cool to rt. Tetrabutylammonium bromide (16 mg, 50 μmol) was added, followed by $CsOH{\cdot}H_2O$ (168 mg, 1.00 mmol), and the reaction was stirred at 25 ºC for 18 h. The crude reaction mixture was then filtered through Celite, washing with EtOAc (10 mL), and concentrated under reduced pressure. Purification by flash chromatography (12.5% EtOAc/pentane) afforded 1-(*tert*-butyl) 2-ethyl 2-phenylpyrrolidine-1,2-dicarboxylate **118** (156 mg, 98%) as a white solid. R_f 0.30 (15% EtOAc/pentane); mp = 64–66 °C; ν_{max} (film)/cm^{-1} 2978, 1736 (C=O ester), 1690 (C=O carbamate), 1384, 1366, 1235, 1158, 1138, 1096, 751, 702; ^{1}H NMR (400 MHz; $CDCl_3$) δ 7.41–7.21 (m, 5 H, 5 × HC_{Ph}), 4.34–4.10 (m, 2 H, OCH_2CH_3), 3.78–3.57 (m, 2 H, NCH_2), 2.67–2.53 (m, 1 H, $N(CH_2)_2CHH$), 2.30–2.20 (m, 1 H, $N(CH_2)_2CHH$), 1.96–1.86 (m, 1 H, NCH_2CHH), 1.76–1.63 (m, 1H, NCH_2CHH), 1.50 (s, 3 H, $C(CH_3)_3$), 1.35–1.22 (m, 9 H, $C(CH_3)_3$ and OCH_2CH_3); ^{13}C NMR (101 MHz; $CDCl_3$) δ 172.7 (C=O ester), 153.9 (C=O carbamate), 140.6 (C_{Ph} quat), 127.5 and 127.3 (2 × C_{Ph}), 127.2 and 127.0 (2 × C_{Ph}), 126.8 (br s, C_{Ph}), 80.2 and 79.8 ($C(CH_3)_3$), 71.5 (NC quat), 61.4 (OCH_2CH_3), 47.9 (NCH_2), 43.6 and 41.9 ($N(CH_2)_2CH_2$), 28.4 and 28.0 ($C(CH_3)_3$), 23.5 and 22.6 (NCH_2CH_2), 14.2 (OCH_2CH_3). The observed characterisation data (IR, ^{1}H and ^{13}C NMR) was consistent with that previously reported in the literature.[408]

Reaction using toluene instead of benzene afforded **118** (153 mg, 96%). Purification by flash chromatography (1% to 2% Et_2O/CH_2Cl_2).

Reaction using 1:1 equiv of **58** to **85** afforded **118** (120 mg, 75%). Purification by flash chromatography (1% to 2% Et_2O/CH_2Cl_2)

Reaction using 1.5 equiv of **58** afforded **118** (128 mg, 80%). Purification by flash chromatography (CH_2Cl_2 to 1% to 3% Et_2O/CH_2Cl_2). Due to a similar R_f of the product and **58**, purification with excess **58** was more difficult.

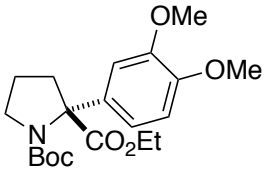
(±)–1-Benzyl 2-ethyl 2-phenylpyrrolidine-1,2-dicarboxylate (119)



$Rh_2(esp)_2$ (1.9 mg, 2.5 μmol) was added to a solution of benzyl (3-chloropropyl)carbamate **64** (114 mg, 0.50 mmol) and ethyl 2-diazo-2-phenylacetate **85** (143 mg, 0.75 mmol) in benzene (1.67 mL). The reaction

vessel was sealed, purged with Ar and heated at 60 ºC for 2.5 h, then allowed to cool to rt. Tetrabutylammonium bromide (16 mg, 50 μmol) was added, followed by $CsOH·H_2O$ (168 mg, 1.00 mmol), and the reaction was stirred at 25 ºC for 18 h. The crude reaction mixture was then filtered through Celite, washing with EtOAc (10 mL), and concentrated under reduced pressure. Purification by flash chromatography (1% EtOAc/CH_2Cl_2) afforded 1-benzyl 2-ethyl 2-phenylazetidine-1,2-dicarboxylate **119** (141 mg, 80%) as a colourless oil. R_f 0.14 (CH_2Cl_2); ν_{max} (film)/cm^{-1} 2981, 1741 (C=O ester), 1701 (C=O carbamate), 1404, 1351, 1243, 1221, 1163, 1130, 1096, 1025, 1008, 768, 695; ^{1}H NMR (400 MHz, $CDCl_3$) δ 7.47–7.17 (m, 9 H, 9 × HC_{Ph}), 7.08–7.01 (m, 1 H, HC_{Ph}), 5.27–5.12 (m, 1 H, *H*HCPh), 5.11–4.94 (m, 1 H, H*H*CPh), 4.28–4.14 (m, 1 H, OC*H*HCH_3), 4.06–3.69 (m, 3 H, OCH*H*CH_3 and NCH_2), 2.68–2.56 (m, 1 H, $N(CH_2)_2C$*H*H), 2.37–2.27 (m, 1 H, $N(CH_2)_2CH$*H*), 2.00–1.88 (m, 1 H, NCH_2C*H*H), 1.79–1.65 (m, 1 H, NCH_2CH*H*), 1.20 and 1.08 (2 × t, *J* = 7.1 Hz, 3 H, OCH_2C*H*$_3$); ^{13}C NMR (101 MHz, $CDCl_3$) δ 172.2 and 172.1 (C=O ester), 154.6 and 154.5 (C=O carbamate), 140.0 and 139.3 (C_{Ph} quat), 136.9 and 136.1 (C_{Ph} quat), 128.4, 128.1, 127.9, 127.91, 127.87, 127.7, 127.6, 127.5, 127.1 and 127.0 (10 × C_{Ph}), 72.1 and 71.6 (NC quat), 66.9 and 66.8 (CH_2Ph), 61.6 and 61.4 (OCH_2CH_3), 48.6 and 47.8 (NCH_2), 43.8 and 41.9 ($N(CH_2)_2CH_2$), 23.3 and 22.5 (NCH_2CH_2), 14.0 and 13.9 (OCH_2CH_3). The observed characterisation data (^{1}H NMR) was consistent with that previously reported in the literature.[409]

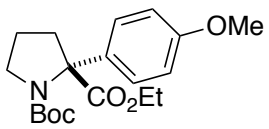
(±)–1-(*tert*-Butyl) 2-ethyl 2-(3,4-dimethoxyphenyl)pyrrolidine-1,2-dicarboxylate (120)



$Rh_2(esp)_2$ (1.9 mg, 2.5 μmol) was added to a solution of *tert*-butyl (3-chloropropyl)carbamate **58** (97 mg, 0.50 mmol) and ethyl 2-diazo-2-(3,4-dimethoxyphenyl)acetate **86** (188 mg, 0.75 mmol) in benzene (1.67 mL). The reaction vessel was sealed, purged with Ar and heated at 60 ºC for 2.5 h, then allowed to cool to rt. Tetrabutylammonium bromide (16 mg, 50 μmol) was added, followed by $CsOH·H_2O$ (168 mg, 1.00 mmol), and the reaction was stirred at 25 ºC for 18 h. The crude reaction mixture was then filtered through Celite, washing with EtOAc (10 mL), and concentrated under reduced pressure. Purification by flash chromatography (30% EtOAc/pentane) afforded 1-(*tert*-butyl) 2-ethyl 2-(3,4-dimethoxyphenyl)pyrrolidine-1,2-dicarboxylate **120** (189 mg, quant) as a yellow oil. R_f 0.21 (30% EtOAc/ pentane); ν_{max} (film)/cm^{-1} 2977, 1741 (C=O ester), 1693 (C=O carbamate), 1517, 1385, 1365, 1238, 1144, 1134, 1026, 764; ^{1}H NMR (400 MHz, $CDCl_3$) δ 6.98 (d, *J* = 2.2 Hz, 1 H, HC_{Ar}), 6.93–6.86 (m, 1 H, HC_{Ar}), 6.82 (d, *J* = 8.5 Hz, 1 H, HC_{Ar}), 4.34–4.10 (m, 2 H, OCH_2CH_3), 3.92–3.82 (m, 6 H, 2 × OCH_3), 3.75–3.59 (m, 2 H, NCH_2), 2.63–2.48 (m, 1 H, $N(CH_2)_2C$*H*H), 2.30–2.20 (m, 1 H, $N(CH_2)_2CH$*H*), 1.96–1.85 (m, 1 H, NCH_2C*H*H), 1.77–1.64 (m, 1 H, NCH_2CH*H*), 1.50 (s, 3 H, $C(CH_3)_3$), 1.35–1.24 (m, 9 H, OCH_2C*H*$_3$ and $C(CH_3)_3$); ^{13}C NMR (101 MHz, $CDCl_3$) δ 172.8 and

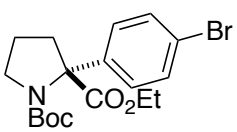
172.7 (C=O ester), 154.0 and 153.9 (C=O carbamate), 148.0 and 147.8 (OC_{Ar} quat), 147.9 and 147.7 (OC_{Ar} quat), 133.2 and 132.3 (C_{Ar} quat), 119.3 (C_{Ar}), 111.3 and 110.8 (C_{Ar}), 110.2 and 109.8 (C_{Ar}), 80.1 and 79.7 ($C(CH_3)_3$), 71.1 (NC quat), 61.3 (OCH_2CH_3), 55.8 ($2 \times OCH_3$), 47.8 (NCH_2), 43.6 and 41.7 ($N(CH_2)_2CH_2$), 28.3 and 28.0 ($C(CH_3)_3$), 23.4 and 22.5 (NCH_2CH_2), 14.1 (OCH_2CH_3); HRMS (ESI^+) *m/z* Calculated for $C_{20}H_{30}NO_6$ [M+H] 380.2073; Found 380.2084.

(±)–1-(*tert*-Butyl) 2-ethyl 2-(4-methoxyphenyl)pyrrolidine-1,2-dicarboxylate (121)



$Rh_2(esp)_2$ (1.9 mg, 2.5 μmol) was added to a solution of *tert*-butyl (3-chloropropyl)carbamate **58** (97 mg, 0.50 mmol) and ethyl 2-diazo-2-(4-methoxyphenyl)acetate **87** (165 mg, 0.75 mmol) in benzene (1.67 mL). The reaction vessel was sealed, purged with Ar and heated at 60 ºC for 2.5 h, then allowed to cool to rt. Tetrabutylammonium bromide (16 mg, 50 μmol) was added, followed by $CsOH{\cdot}H_2O$ (168 mg, 1.00 mmol), and the reaction was stirred at 25 ºC for 18 h. The crude reaction mixture was then filtered through Celite, washing with EtOAc (10 mL), and concentrated under reduced pressure. Purification by flash chromatography (20% EtOAc/pentane) afforded 1-(*tert*-butyl) 2-ethyl 2-(4-methoxyphenyl)pyrrolidine-1,2-dicarboxylate **121** (170 mg, 97%) as a colourless oil. R_f 0.28 (20% EtOAc/pentane); ν_{max} (film)/cm^{-1} 2978, 1743 (C=O ester), 1696 (C=O carbamate), 1513, 1388, 1248, 1161, 1031; ^1H NMR (400 MHz, $CDCl_3$) δ 7.37–7.24 (m, 2 H, $2 \times HC_{Ar}$), 6.92–6.83 (m, 2 H, $2 \times HC_{Ar}$), 4.34–4.21 (m, 1 H, $OCHHCH_3$), 4.21–4.10 (m, 1 H, $OCHHCH_3$), 3.84–3.78 (m, 3 H, OCH_3), 3.74–3.60 (m, 2 H, NCH_2), 2.63–2.49 (m, 1 H, $N(CH_2)_2CHH$), 2.28–2.20 (m, 1 H, $N(CH_2)_2CHH$), 1.95–1.85 (m, 1 H, NCH_2CHH), 1.74–1.62 (m, 1 H, NCH_2CHH), 1.50 (s, 3 H, $C(CH_3)_3$), 1.35–1.23 (m, 9 H, $C(CH_3)_3$ and OCH_2CH_3); ^{13}C NMR (101 MHz, $CDCl_3$) δ 172.9 and 172.8 (C=O ester), 158.4 and 158.3 (OC_{Ar} quat), 154.0 and 153.9 (C=O carbamate), 132.6 and 131.9 (C_{Ar} quat), 128.3 and 128.2 ($2 \times C_{Ar}$), 112.9 and 112.6 ($2 \times C_{Ar}$), 80.1 and 79.7 ($C(CH_3)_3$ quat), 71.1 and 71.0 (NC quat), 61.3 (OCH_2CH_3), 55.2 (OCH_3), 47.9 and 47.8 (NCH_2), 43.5 and 41.8 ($N(CH_2)_2CH_2$), 28.4 and 28.0 ($C(CH_3)_3$), 23.4 and 22.5 (NCH_2CH_2), 14.1 (OCH_2CH_3); HRMS (ESI^+) *m/z* Calculated for $C_{19}H_{28}NO_5$ [M+H] 350.1967; Found 350.1984.

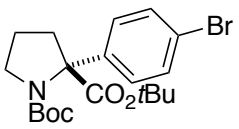
(±)–1-(*tert*-Butyl) 2-ethyl 2-(4-bromophenyl)pyrrolidine-1,2-dicarboxylate (122)



$Rh_2(esp)_2$ (1.9 mg, 2.5 μmol) was added to a solution of *tert*-butyl (3-chloropropyl)carbamate **58** (97 mg, 0.50 mmol) and ethyl 2-(4-bromophenyl)-2-diazoacetate **88** (169 mg, 0.75 mmol) in benzene (1.67 mL). The reaction vessel was sealed, purged with Ar and heated at 60 ºC for 5 h, then allowed to cool to rt. Tetrabutylammonium bromide (16 mg, 50 μmol) was

added, followed by $CsOH{\cdot}H_2O$ (168 mg, 1.00 mmol), and the reaction was stirred at 25 ºC for 18 h. The crude reaction mixture was then filtered through Celite, washing with EtOAc (10 mL), and concentrated under reduced pressure. Purification by flash chromatography (10% EtOAc/pentane) afforded 1-(*tert*-butyl) 2-ethyl 2-(4-bromophenyl)pyrrolidine-1,2-dicarboxylate **122** (193 mg, 97%) as a white solid. R_f 0.23 (10% EtOAc/pentane); mp = 59–62 ºC; ν_{max} (film)/cm^{-1} 2979, 1741 (C=O ester), 1695 (C=O carbamate), 1383, 1365, 1243, 1156, 1139, 1095, 1009, 822, 732; ^{1}H NMR (400 MHz; $CDCl_3$) δ 7.48–7.41 (m, 2 H, 2 × HC_{Ar}), 7.30–7.20 (m, 2 H, 2 × HC_{Ar}), 4.32–4.22 (m, 1 H, OC*H*HCH_3), 4.20–4.10 (m, 1 H, OC$HHCH_3$), 3.76–3.58 (m, 2 H, NCH_2), 2.64–2.51 (m, 1 H, $N(CH_2)_2CHH$), 2.24–2.16 (m, 1 H, $N(CH_2)_2CHH$), 1.97–1.87 (m, 1 H, NCH_2CHH), 1.73–1.60 (m, 1 H, NCH_2CHH), 1.49 (s, 3 H, $C(CH_3)_3$), 1.34–1.23 (m, 9 H, $C(CH_3)_3$ and OCH_2CH_3); ^{13}C NMR (101 MHz; $CDCl_3$) δ 172.3 and 172.2 (C=O ester), 154.1 and 153.7 (C=O carbamate), 139.8 and 139.0 (C_{Ar} quat), 130.6 (C_{Ar}), 130.4 (C_{Ar}), 129.1 (C_{Ar}), 128.9 (C_{Ar}), 121.0 and 120.9 (BrC_{Ar} quat), 80.5 and 80.1 ($C(CH_3)_3$), 71.2 and 71.1 (NC quat), 61.6 (OCH_2CH_3), 47.9 (NCH_2), 43.5 and 41.8 ($N(CH_2)_2CH_2$), 28.4 and 28.0 ($C(CH_3)_3$), 23.5 and 22.6 (NCH_2CH_2), 14.1 (OCH_2CH_3); HRMS (ESI^+) *m/z* Calculated for $C_{18}H_{25}NO_4{}^{79}Br$ [M+H] 398.0967; Found 398.0970.

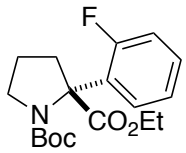
(±)–Di-*tert*-butyl 2-(4-bromophenyl)pyrrolidine-1,2-dicarboxylate (123)



$Rh_2(esp)_2$ (1.9 mg, 2.5 μmol) was added to a solution of *tert*-butyl (3-chloropropyl)carbamate **58** (97 mg, 0.50 mmol) and *tert*-butyl 2-(4-bromophenyl)-2-diazoacetate **99** (223 mg, 0.75 mmol) in benzene (1.67 mL). The reaction vessel was sealed, purged with Ar and heated at 60 ºC for 2.5 h, then allowed to cool to rt. Tetrabutylammonium bromide (16 mg, 50 μmol) was added, followed by $CsOH{\cdot}H_2O$ (168 mg, 1.00 mmol), and the reaction was stirred at 25 ºC for 18 h. The crude reaction mixture was then filtered through Celite, washing with EtOAc (10 mL), and concentrated under reduced pressure. Purification by flash chromatography (5% to 10% EtOAc/pentane) afforded di-*tert*-butyl 2-(4-bromophenyl)pyrrolidine-1,2-dicarboxylate **123** (196 mg, 92%) as a pale yellow oil. R_f 0.19 (5% EtOAc/pentane); ν_{max} (film)/cm^{-1} 2976, 2932, 1737 (C=O ester), 1697 (C=O carbamate), 1488, 1386, 1366, 1252, 1148, 1096, 1010, 773; ^{1}H NMR (400 MHz, $CDCl_3$) δ 7.46–7.41 (m, 2 H, 2 × HC_{Ar}), 7.32 and 7.24 (2 × d, *J* = 8.8 Hz, 2 H, 2 × HC_{Ar}), 3.76–3.68 (m, 1 H, NC*H*H), 3.63–3.57 (m, 1 H, NCH*H*), 2.60–2.48 (m, 1 H, $N(CH_2)_2CHH$), 2.22–2.13 (m, 1 H, $N(CH_2)_2CHH$), 1.96–1.85 (m, 1 H, NCH_2CHH), 1.77–1.58 (m, 1 H, NCH_2CHH), 1.52 and 1.46 (2 × s, 9 H, $C(CH_3)_3$ ester), 1.50 and 1.25 (2 × s, 9 H, $C(CH_3)_3$ carbamate); ^{13}C NMR (101 MHz, $CDCl_3$) δ 171.1 (C=O ester), 154.0 and 153.9 (C=O carbamate), 140.4 and 139.2 (C_{Ar} quat), 130.4 and 130.3 (2 × C_{Ar}), 129.2 and 128.9 (2 × C_{Ar}), 120.9 and 120.7 (BrC_{Ar} quat), 81.7 and 81.4 ($C(CH_3)_3$ ester), 80.5 and 79.8 ($C(CH_3)_3$

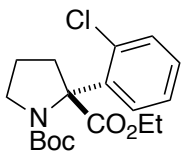
carbamate), 71.6 and 71.3 (NC quat), 48.14 and 48.06 (NCH_2), 44.1 and 42.0 ($N(CH_2)CH_2$), 28.5 and 28.0 ($C(CH_3)_3$ carbamate), 28.1 and 27.8 ($C(CH_3)_3$ ester), 23.6 and 22.6 (NCH_2CH_2); HRMS (ESI^+) *m/z* Calculated for $C_{20}H_{29}NO_4{}^{79}Br$ [M+H] 426.1280; Found 426.1289.

(±)-1-(*tert*-Butyl) 2-ethyl 2-(2-fluorophenyl)pyrrolidine-1,2-dicarboxylate (124)



$Rh_2(esp)_2$ (1.9 mg, 2.5 μmol) was added to a solution of *tert*-butyl (3-chloropropyl)carbamate **58** (97 mg, 0.50 mmol) and ethyl 2-(2-fluorophenyl)-2-diazoacetate **89** (156 mg, 0.75 mmol) in benzene (1.67 mL). The reaction vessel was sealed, purged with Ar and heated at 60 ºC for 5 h, then allowed to cool to rt. Tetrabutylammonium bromide (16 mg, 50 μmol) was added, followed by $CsOH·H_2O$ (168 mg, 1.00 mmol), and the reaction was stirred at 25 ºC for 18 h. The crude reaction mixture was then filtered through Celite, washing with EtOAc (10 mL), and concentrated under reduced pressure. Purification by flash chromatography (10% EtOAc/pentane) afforded 1-(*tert*-butyl) 2-ethyl 2-(2-fluorophenyl)pyrrolidine-1,2-dicarboxylate **124** (172 mg, quant) as a white solid. R_f 0.23 (10% EtOAc/pentane); mp = 85–88 ºC; ν_{max} (film)/cm^{-1} 2989, 1750 (C=O ester), 1688 (C=O carbamate), 1456, 1445, 1389, 1366, 1234, 1151, 1096, 1087, 1026, 770, 757; ^1H NMR (400 MHz, $CDCl_3$) δ 7.33–7.23 (m, 1 H, HC_{Ar}), 7.16–7.01 (m, 3 H, 3 × HC_{Ar}), 4.36–4.09 (m, 2 H, OCH_2CH_3), 3.82–3.52 (m, 2 H, NCH_2), 2.79–2.62 (m, 1 H, $N(CH_2)_2CHH$), 2.51–2.41 (m, 1 H, $N(CH_2)_2CHH$), 2.03–1.93 (m, 1 H, NCH_2CHH), 1.70–1.56 (m, 1 H, NCH_2CHH), 1.50 (s, 3 H, $C(CH_3)_3$), 1.36–1.21 (m, 9 H, $C(CH_3)_3$ and OCH_2CH_3); ^{13}C NMR (101 MHz, $CDCl_3$) δ 171.1 and 171.0 (C=O ester), 160.4 and 160.3 (2 × d, J_{C-F} = 247.3 Hz, FC_{Ar} quat), 154.1 and 153.8 (C=O carbamate), 129.2 (d, J_{C-F} = 8.5 Hz, C_{Ar}), 127.9 and 127.7 (2 × s br, C_{Ar} and C_{Ar} quat), 123.4 and 122.8 (C_{Ar}), 116.0 and 115.8 (2 × d, J_{C-F} = 23.1 Hz, C_{Ar}), 80.7 and 80.1 ($C(CH_3)_3$), 70.2 and 70.1 (NC quat), 61.5 (OCH_2CH_3), 47.9 and 47.8 (NCH_2), 40.6 and 39.2 ($N(CH_2)_2CH_2$), 28.4 and 28.0 ($C(CH_3)_3$), 23.7 and 22.9 (NCH_2CH_2), 14.0 (OCH_2CH_3); $^{19}F\{^1H\}$ NMR (377 MHz, $CDCl_3$) δ –107.5 and –107.9; HRMS (ESI^+) *m/z* Calculated for $C_{18}H_{25}NO_4F$ [M+H] 338.1768; Found 338.1762.

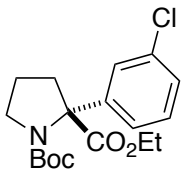
(±)–1-(*tert*-Butyl) 2-ethyl 2-(2-chlorophenyl)pyrrolidine-1,2-dicarboxylate (125)



$Rh_2(esp)_2$ (1.9 mg, 2.5 μmol) was added to a solution of *tert*-butyl (3-chloropropyl)carbamate **58** (97 mg, 0.50 mmol) and ethyl 2-(2-chlorophenyl)-2-diazoacetate **92** (169 mg, 0.75 mmol) in benzene (1.67 mL). The reaction vessel was sealed, purged with Ar and heated at 60 ºC for 2.5 h, then allowed to cool to rt. Tetrabutylammonium bromide (16 mg, 50 μmol) was added, followed by $CsOH·H_2O$ (168 mg, 1.00 mmol), and the reaction was stirred at 25 ºC for 18 h. The crude reaction mixture was then filtered through Celite, washing with EtOAc (10 mL), and

concentrated under reduced pressure. Purification by flash chromatography (1% EtOAc/CH_2Cl_2) afforded a mixture. Purification of the mixture by flash chromatography (15% EtOAc/pentane) afforded 1-(*tert*-butyl) 2-ethyl 2-(2-chlorophenyl)pyrrolidine-1,2-dicarboxylate **125** (54 mg, 31%) as a white solid. R_f 0.30 (15% EtOAc/pentane); mp = 69–70 ºC; ν_{max} (film)/cm^{-1} 2985, 2881, 1727 (C=O ester), 1692 (C=O carbamate), 1384, 1365, 1274, 1245, 1177, 1161, 1143, 1120, 1102, 1040, 774; ^{1}H NMR (400 MHz, $CDCl_3$) δ 7.43–7.36 (m, 1 H, HC_{Ar}), 7.26–7.16 (m, 3 H, 3 × HC_{Ar}), 4.34–4.10 (m, 2 H, OCH_2CH_3), 3.84–3.52 (m, 2 H, NCH_2), 2.92–2.77 (m, 1 H, $N(CH_2)_2CHH$), 2.72–2.64 (m, 1 H, $N(CH_2)_2CHH$), 2.00–1.90 (m, 1 H, NCH_2CHH), 1.68–1.17 (m, 13 H, NCH_2CHH, $C(CH_3)_3$ and OCH_2CH_3); ^{13}C NMR (101 MHz, $CDCl_3$) δ 171.0 and 170.7 (C=O ester), 153.8 (C=O carbamate), 137.6 and 137.2 (ClC_{Ar} quat), 133.2 (C_{Ar}), 131.2 (C_{Ar}), 128.5 (C_{Ar}), 128.2 and 128.0 (C_{Ar}), 126.4 and 125.8 (C_{Ar} quat), 80.6 and 80.1 ($C(CH_3)_3$), 72.2 (NC quat), 61.6 (OCH_2CH_3), 48.1 (NCH_2), 40.2 and 39.0 ($N(CH_2)_2CH_2$), 28.3 and 28.0 ($C(CH_3)_3$), 23.5 and 22.9 (NCH_2CH_2), 13.9 (OCH_2CH_3); HRMS (ESI^+) *m/z* Calculated for $C_{18}H_{25}NO_4{}^{35}Cl$ [M+H] 354.1472; Found 354.1482.

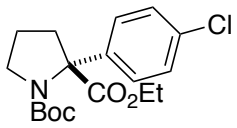
(±)–1-(*tert*-Butyl) 2-ethyl 2-(3-chlorophenyl)pyrrolidine-1,2-dicarboxylate (126)



$Rh_2(esp)_2$ (1.9 mg, 2.5 μmol) was added to a solution of *tert*-butyl (3-chloropropyl)carbamate **58** (97 mg, 0.50 mmol) and ethyl 2-(3-chlorophenyl)-2-diazoacetate **93** (168 mg, 0.75 mmol) in benzene (1.67 mL). The reaction vessel was sealed, purged with Ar and heated at 60 ºC for 5 h, then allowed to cool to rt. Tetrabutylammonium bromide (16 mg, 50 μmol) was added, followed by $CsOH·H_2O$ (168 mg, 1.00 mmol), and the reaction was stirred at 25 ºC for 18 h. The crude reaction mixture was then filtered through Celite, washing with EtOAc (10 mL), and concentrated under reduced pressure. Purification by flash chromatography (20% EtOAc/hexane) afforded 1-(*tert*-butyl) 2-ethyl 2-(3-chlorophenyl)pyrrolidine-1,2-dicarboxylate **126** (155 mg, 88%) as a yellow solid. R_f 0.23 (20% EtOAc/hexane); mp = 66–71 ºC; ν_{max} (film)/cm^{-1} 2978, 1742 (C=O ester), 1695 (C=O carbamate), 1382, 1365, 1244, 1158, 1139, 1104, 1095, 774, 709, 690; ^{1}H NMR (400 MHz, $CDCl_3$) δ 7.40 (s br, 0.6 H, HC_{Ar}), 7.30 (s br, 0.3 H, HC_{Ar}), 7.33–7.22 (m, 3 H, 3 × HC_{Ar}), 4.33–4.12 (m, 2 H, OCH_2CH_3), 3.78–3.58 (m, 2 H, NCH_2), 2.66–2.52 (m, 1 H, $N(CH_2)_2CHH$), 2.29–2.20 (m, 1 H, $N(CH_2)_2CHH$), 1.99–1.88 (m, 1 H, NCH_2CHH), 1.77–1.64 (m, 1 H, NCH_2CHH), 1.50 (s, 3 H, $C(CH_3)_3$), 1.35–1.23 (m, 9 H, $C(CH_3)_3$ and OCH_2CH_3); ^{13}C NMR (101 MHz, $CDCl_3$) δ 172.2 and 172.1 (C=O ester), 154.0 and 153.7 (C=O carbamate), 142.8 and 142.0 (C_{Ar} quat), 133.5 and 133.3 (ClC_{Ar} quat), 128.7 and 128.6 (C_{Ar}), 127.5 and 127.4 (C_{Ar}), 127.1 and 127.0 (C_{Ar}), 125.6 and 125.4 (C_{Ar}), 80.5 and 80.1 ($C(CH_3)_3$), 71.3 and 71.1 (NC quat), 61.6 (OCH_2CH_3), 47.9 (NCH_2), 43.5 and 41.8

($N(CH_2)_2CH_2$), 28.3 and 28.0 ($C(CH_3)_3$), 23.4 and 22.6 (NCH_2CH_2), 14.1 (OCH_2CH_3); HRMS (ESI^+) *m/z* Calculated for $C_{18}H_{25}NO_4{}^{35}Cl$ [M+H] 354.1472; Found 354.1472.

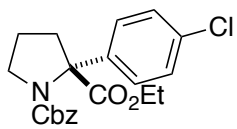
(±)–1-(*tert*-Butyl) 2-ethyl 2-(4-chlorophenyl)pyrrolidine-1,2-dicarboxylate (127)



$Rh_2(esp)_2$ (1.9 mg, 2.5 μmol) was added to a solution of *tert*-butyl (3-chloropropyl)carbamate **58** (97 mg, 0.50 mmol), ethyl 2-(4-chlorophenyl)-2-diazoacetate **94** (169 mg, 0.75 mmol) and benzene (1.67 mL). The reaction vessel was sealed, purged with Ar and heated at 60 ºC for 5 h, then allowed to cool to rt. Tetrabutylammonium bromide (16 mg, 50 μmol) was added, followed by $CsOH·H_2O$ (168 mg, 1.00 mmol), and the reaction was stirred at 25 ºC for 18 h. The crude reaction mixture was then filtered through Celite, washing with EtOAc (10 mL), and concentrated under reduced pressure. Purification by flash chromatography (12.5% EtOAc/pentane) afforded 1-(*tert*-butyl) 2-ethyl 2-(4-chlorophenyl)pyrrolidine-1,2-dicarboxylate **127** (171 mg, 97%) as a pale yellow solid. R_f 0.20 (12.5% EtOAc/pentane); mp = 50–53 ºC; ν_{max} (film)/cm^{-1} 2979, 1741 (C=O ester), 1695 (C=O carbamate), 1492, 1383, 1365, 1244, 1156, 1139, 1097, 1013, 772; ^1H NMR (400 MHz, $CDCl_3$) δ 7.36–7.27 (m, 4 H, 4 × HC_{Ar}), 4.32–4.23 (m, 1 H, $OCHHCH_3$), 4.21–4.11 (m, 1 H, $OCHHCH_3$), 3.75–3.59 (m, 2 H, NCH_2), 2.64–2.52 (m, 1 H, $N(CH_2)_2CHH$), 2.24–2.18 (m, 1 H, $N(CH_2)_2CHH$), 1.98–1.87 (m, 1 H, NCH_2CHH), 1.73–1.61 (m, 1 H, NCH_2CHH), 1.49 (s, 3 H, $C(CH_3)_3$), 1.34–1.23 (m, 9 H, $C(CH_3)_3$ and OCH_2CH_3); ^{13}C NMR (101 MHz, $CDCl_3$) δ 172.4 (C=O ester), 153.7 (C=O carbamate), 139.2 (C_{Ar} quat), 132.7 (ClC_{Ar} quat), 128.7 and 128.6 (2 × C_{Ar}), 127.6 and 127.5 (2 × C_{Ar}), 80.5 and 80.1 ($C(CH_3)_3$), 71.0 (NC quat), 61.6 (OCH_2CH_3), 47.9 (NCH_2), 43.6 and 41.8 ($N(CH_2)_2CH_2$), 28.4 and 28.0 ($C(CH_3)_3$), 23.5 and 22.6 (NCH_2CH_2), 14.1 (OCH_2CH_3); HRMS (ESI^+) *m/z* Calculated for $C_{18}H_{25}NO_4{}^{35}Cl$ [M+H] 354.1472; Found 354.1489.

Reaction performed on 3 mmol scale afforded **127** (0.95 g, 90%). 2.5 h NH insertion, purification by flash chromatography (10% to 15% EtOAc/pentane).

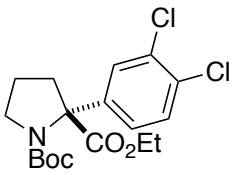
(±)-1-Benzyl 2-ethyl 2-(4-chlorophenyl)pyrrolidine-1,2-dicarboxylate (128)



$Rh_2(esp)_2$ (11.4 mg, 15.0 μmol) was added to a solution of benzyl (3-chloropropyl)carbamate **58** (683 mg, 3.0 mmol), ethyl 2-(4-chlorophenyl)-2-diazoacetate **94** (1.01 g, 4.5 mmol) in benzene (10.0 mL). The reaction vessel was sealed, purged with Ar and heated at 60 ºC for 2.5 h, then allowed to cool to rt. Tetrabutylammonium bromide (97 mg, 0.30 mmol) was added, followed by $CsOH·H_2O$ (1.01 g, 6.0 mmol), and the reaction was stirred at 25 ºC for 18 h. The crude reaction mixture was then filtered through Celite, washing with EtOAc (50 mL), and concentrated under reduced

pressure. Purification by flash chromatography (15% to 20% EtOAc/pentane) afforded 1-benzyl 2-ethyl 2-(4-chlorophenyl)pyrrolidine-1,2-dicarboxylate **128** (890 mg, 76%) as a pale yellow oil. R_f 0.32 (20% EtOAc/pentane); ν_{max} (film)/cm^{-1} 2983, 1739 (C=O ester), 1695 (C=O carbamate), 1405, 1353, 1245, 1135, 1098, 1012, 728, 696; ^{1}H NMR (400 MHz, $CDCl_3$) δ 7.43–7.21 (m, 8 H, 4 × HC_{Ph} and 4 × HC_{Ar}), 7.08–7.03 (m, 1 H, HC_{Ph}), 5.23–5.13 (m, 1 H, OC*H*HPh), 5.06–4.96 (m, 1 H, OCH*H*Ph), 4.26–4.14 (m, 1 H, OC*H*HCH$_3$), 4.94–3.95 (m, 0.5 H, OCH*H*CH$_3$), 3.91–3.68 (m, 2.5 H, OCH*H*CH$_3$ and NCH$_2$), 2.65–2.54 (m, 1 H, N(CH$_2$)$_2$C*H*H), 2.30–2.21 (m, 1 H, N(CH$_2$)$_2$CH*H*), 2.01–1.89 (m, 1 H, NCH$_2$C*H*H), 1.78–1.64 (m, 1 H, NCH$_2$CH*H*), 1.19 and 1.09 (2 × t, *J* = 7.1 Hz, 3 H, OCH$_2$C*H*$_3$); ^{13}C NMR (101 MHz, $CDCl_3$) δ 171.9 and 171.8 (C=O ester), 154.5 and 154.4 (C=O carbamate), 138.6 and 137.9 (C_{Ar} quat), 136.7 and 135.9 (C_{Ar} quat), 132.9 (ClC_{Ar} quat), 128.6, 128.5, 128.4, 128.1, 128.0, 127.9, 127.8, 127.7, 127.6 (9 × C_{Ar}), 71.7 and 71.1 (NC quat), 67.0 (OCH$_2$Ph), 61.7 and 61.6 (O*C*H$_2$CH$_3$), 48.5 and 47.8 (NCH$_2$), 43.7 and 41.9 (N(CH$_2$)$_2$*C*H$_2$), 23.3 and 22.5 (NCH$_2$*C*H$_2$), 13.9 (OCH$_2$*C*H$_3$); HRMS (ESI$^+$) *m/z* Calculated for $C_{21}H_{23}NO_4{}^{35}Cl$ [M+H] 388.1316; Found 388.1320.

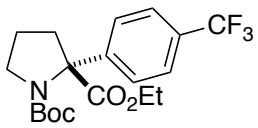
(±)–1-(*tert*-Butyl) 2-ethyl 2-(3,4-dichlorophenyl)pyrrolidine-1,2-dicarboxylate (129)



Ethyl 2-diazo-2-(3,4-dichlorophenyl)acetate **95** (259 mg, 1.0 mmol) in benzene (1.0 mL) was added slowly *via* syringe pump over 1 h to a stirred solution of *tert*-butyl (3-chloropropyl)carbamate **58** (97 mg, 0.50 mmol) and $Rh_2(esp)_2$ (1.9 mg, 2.5 μmol) in benzene (0.67 mL) at 60 °C. The reaction mixture was stirred at 60 °C for a further 2.5 h, then allowed to cool to rt. Tetrabutylammonium bromide (16 mg, 50 μmol) was added, followed by $CsOH{\cdot}H_2O$ (168 mg, 1.00 mmol), and the reaction was stirred at 25 ºC for 18 h. The crude reaction mixture was then filtered through Celite, washing with EtOAc (10 mL), and concentrated under reduced pressure. Purification by flash chromatography (15% EtOAc/pentane) afforded 1-(*tert*-butyl) 2-ethyl 2-(3,4-dichlorophenyl)pyrrolidine-1,2-dicarboxylate **129** (142 mg, 74%) as a yellow oil. R_f 0.30 (15% EtOAc/pentane); ν_{max} (film)/cm^{-1} 2978, 1741 (C=O ester), 1695 (C=O carbamate), 1380, 1365, 1244, 1155, 1135, 1098, 772; ^{1}H NMR (400 MHz, $CDCl_3$) δ 7.50 and 7.45 (2 × d, *J* = 2.3 Hz, 1 H, HC_{Ar}), 7.42–7.37 (m, 1 H, HC_{Ar}), 7.28–7.20 (m, 1 H, HC_{Ar}), 4.33–4.22 (m, 1 H, OC*H*HCH$_3$), 4.21–4.11 (m, 1 H, OCH*H*CH$_3$), 3.76– 3.61 (m, 2 H, NCH$_2$), 2.65–2.51 (m, 1 H, N(CH$_2$)$_2$C*H*H), 2.25–2.16 (m, 1 H, N(CH$_2$)$_2$CH*H*), 2.00–1.89 (m, 1 H, NCH$_2$C*H*H), 1.75–1.61 (m, 1 H, NCH$_2$CH*H*), 1.50 (s, 3 H, C(CH$_3$)$_3$), 1.35–1.23 (m, 9 H, OCH$_2$C*H*$_3$ and C(CH$_3$)$_3$); ^{13}C NMR (101 MHz, $CDCl_3$) δ 172.0 and 171.9 (C=O ester), 154.1 and 153.5 (C=O carbamate), 141.1 and 140.4 (C_{Ar} quat), 131.6 and 131.5 (ClC_{Ar} quat), 131.0 and 130.9 (ClC_{Ar} quat), 129.4, 129.3 and 129.2 (2 × C_{Ar}), 126.9 and 126.8 (C_{Ar}), 80.7 and 80.3 (*C*(CH$_3$)$_3$), 70.9 and 70.7 (NC quat), 61.7 (O*C*H$_2$CH$_3$), 47.9 (NCH$_2$), 43.4 and 41.8 (N(CH$_2$)$_2$*C*H$_2$), 28.3 and 28.0 (C(*C*H$_3$)$_3$),

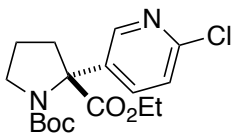
23.5 and 22.6 (NCH_2CH_2), 14.1 (OCH_2CH_3); HRMS (ESI^+) *m/z* Calculated for $C_{18}H_{24}NO_4{}^{35}Cl_2$ [M+H] 388.1082; Found 388.1080.

(±)–1-(*tert*-Butyl) 2-ethyl 2-(4-(trifluoromethyl)phenyl)pyrrolidine-1,2-dicarboxylate (130)



Ethyl 2-diazo-2-(4-(trifluoromethyl)phenyl)acetate **96** (323 mg, 1.25 mmol) in benzene (1.0 mL) was added slowly *via* syringe pump over 1 h to a solution of *tert*-butyl (3-chloropropyl)carbamate **58** (97 mg, 0.50 mmol) and $Rh_2(esp)_2$ (1.9 mg, 2.5 μmol) in benzene (0.67 mL) at 60 ºC. The reaction mixture was stirred at 60 °C for a further 2.5 h, then allowed to cool to rt. Tetrabutylammonium bromide (16 mg, 50 μmol) was added, followed by $CsOH{\cdot}H_2O$ (168 mg, 1.00 mmol), and the reaction was stirred at 25 ºC for 18 h. The crude reaction mixture was then filtered through Celite, washing with EtOAc (10 mL), and concentrated under reduced pressure. Purification by flash chromatography (CH_2Cl_2) afforded 1-(*tert*-butyl) 2-ethyl 2-(4-(trifluoromethyl)phenyl)pyrrolidine-1,2-dicarboxylate **130** (101 mg, 52%) as a pale yellow oil. R_f 0.27 (CH_2Cl_2); ν_{max} (film)/cm^{-1} 2981, 1744 (C=O ester), 1698 (C=O carbamate), 1387, 1367, 1327, 1248, 1162, 1125, 1098, 1071, 1017; ^1H NMR (400 MHz, $CDCl_3$) δ 7.60–7.46 (m, 4 H, 4 × HC_{Ar}), 4.32–4.11 (m, 2 H, OCH_2CH_3), 3.79–3.60 (m, 2 H, NCH_2), 2.68–2.54 (m, 1 H, $N(CH_2)_2CHH$), 2.27–2.18 (m, 1 H, $N(CH_2)_2CHH$), 1.98–1.88 (m, 1 H, NCH_2CHH), 1.72–1.60 (m, 1 H, NCH_2CHH), 1.49 (s, 3 H, $C(CH_3)_3$), 1.34–1.21 (m, 9 H, OCH_2CH_3 and $C(CH_3)_3$); ^{13}C NMR (101 MHz, $CDCl_3$) δ 172.1 and 172.0 (C=O ester), 154.1 and 153.6 (C=O carbamate), 144.8 and 144.0 (C_{Ar} quat), 129.1 (q, J_{C-F} = 32.4 Hz, CF_3C_{Ar} quat), 127.6 and 127.5 (2 × C_{Ar}), 124.2 and 124.1 (2 × q, J_{C-F} = 271.8 Hz, CF_3), 124.4 and 124.2 (2 × q, J_{C-F} = 3.5 Hz, 2 × C_{Ar}), 80.6 and 80.2 ($C(CH_3)_3$), 71.4 and 71.2 (NC quat), 61.6 (OCH_2CH_3), 47.9 (NCH_2), 43.6 and 41.8 ($N(CH_2)_2CH_2$), 28.3 and 27.9 ($C(CH_3)_3$), 23.4 and 22.5 (NCH_2CH_2), 14.0 (OCH_2CH_3); $^{19}F\{^1H\}$ NMR (377 MHz, $CDCl_3$) δ –62.45 and –62.54; HRMS (ESI^+) *m/z* Calculated for $C_{19}H_{25}NO_4F_3$ [M+H] 388.1736; Found 388.1742.

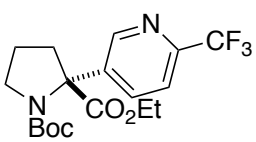
(±)-1-(*tert*-Butyl) 2-ethyl 2-(6-chloropyridin-3-yl)pyrrolidine-1,2-dicarboxylate (131)



Ethyl 2-(6-chloropyridin-3-yl)-2-diazoacetate **97** (282 mg, 1.25 mmol) in benzene (1.0 mL) was added slowly *via* syringe pump over 1 h to a solution of *tert*-butyl (3-chloropropyl)carbamate **58** (97 mg, 0.50 mmol) and $Rh_2(esp)_2$ (1.9 mg, 2.5 μmol) in benzene (0.67 mL) at 60 ºC. The reaction mixture was stirred at 60 °C for a further 2.5 h, then allowed to cool to rt. Tetrabutylammonium bromide (16 mg, 50 μmol) was added, followed by $CsOH{\cdot}H_2O$ (168 mg, 1.00 mmol), and the reaction was stirred at 25 ºC for 18 h. The crude reaction mixture was then filtered through Celite, washing with EtOAc (10 mL), and concentrated under reduced pressure. Purification by flash

chromatography (20% EtOAc/pentane) afforded 1-(*tert*-butyl) 2-ethyl 2-(6-chloropyridin-3-yl)pyrrolidine-1,2-dicarboxylate **131** (32 mg, 18%) as a yellow oil. R_f 0.17 (20% EtOAc/pentane); ν_{max} (film)/cm^{-1} 2980, 1740 (C=O ester), 1697 (C=O carbamate), 1456, 1386, 1366, 1289, 1160, 1137, 1109, 1019; ^{1}H NMR (400 MHz, $CDCl_3$) δ 8.40–8.33 (m, 1 H, HC_{Ar}), 7.74–7.68 (m, 1 H, HC_{Ar}), 7.31–7.25 (m, 1 H, HC_{Ar}), 4.33–4.10 (m, 2 H, OCH_2CH_3), 3.76–3.60 (m, 2 H, NCH_2), 2.65–2.52 (m, 1 H, $N(CH_2)CHH$), 2.22–2.13 (m, 1 H, $N(CH_2)CHH$), 2.02–1.92 (m, 1 H, NCH_2CHH), 1.75–1.61 (m, 1 H, NCH_2CHH), 1.47 (s, 3 H, $C(CH_3)_3$), 1.34–1.22 (m, 9 H, OCH_2CH_3 and $C(CH_3)_3$); ^{13}C NMR (101 MHz, $CDCl_3$) δ 171.9 and 171.8 (C=O ester), 154.1 and 153.4 (C=O carbamate), 150.0 (ClC_{Ar} quat), 148.6 (C_{Ar}), 138.3 and 138.0 (C_{Ar}), 135.3 and 134.6 (C_{Ar} quat), 123.0 and 122.8 (C_{Ar}), 81.0 and 80.5 ($C(CH_3)_3$), 69.7 and 69.5 (NC quat), 61.9 and 61.9 (OCH_2CH_3), 47.9 (NCH_2), 43.3 and 41.6 ($N(CH_2)_2CH_2$), 28.3 and 28.0 ($C(CH_3)_3$), 23.5 and 22.6 (NCH_2CH_2), 14.0 (OCH_2CH_3); HRMS (ESI$^+$) *m/z* Calculated for $C_{17}H_{24}N_2O_4{}^{35}Cl$ [M+H] 355.1425; Found 355.1434.

(±)–1-(*tert*-Butyl) 2-ethyl 2-(6-(trifluoromethyl)pyridin-3-yl)pyrrolidine-1,2-dicarboxylate (132)

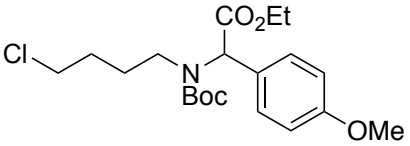


Ethyl 2-diazo-2-(6-(trifluoromethyl)pyridin-3-yl)acetate **103** (97 mg, 0.38 mmol) in benzene (0.30 mL) was added slowly *via* syringe pump over 1 h to a solution of *tert*-butyl (3-chloropropyl)carbamate **58** (29.1 mg, 0.15 mmol) and $Rh_2(esp)_2$ (0.6 mg, 0.75 μmol) in benzene (0.20 mL) at 60 ºC. The reaction mixture was stirred at 60 °C for a further 2.5 h, then allowed to cool to rt. Tetrabutylammonium bromide (16 mg, 50 μmol) was added, followed by $CsOH{\cdot}H_2O$ (168 mg, 1.00 mmol), and the reaction was stirred at 25 ºC for 18 h. The crude reaction mixture was then filtered through Celite, washing with EtOAc (10 mL), and concentrated under reduced pressure. Purification by flash chromatography (20% EtOAc/hexane) afforded 1-(*tert*-butyl) 2-ethyl 2-(6-(trifluoromethyl)pyridin-3-yl)pyrrolidine-1,2-dicarboxylate **132** (16 mg, 28%) as a yellow oil. R_f 0.15 (20% EtOAc/hexane); ν_{max} (film)/cm^{-1} 2982, 1741 (C=O ester), 1697 (C=O carbamate), 1386, 1368, 1339, 1250, 1140, 1103, 1086, 1023; ^{1}H NMR (400 MHz, $CDCl_3$) δ 8.79 and 8.73 (2 × d, J = 2.1 Hz, 1 H, HC_{Ar}), 7.95–7.89 (m, 1 H, HC_{Ar}), 7.68–7.63 (m, 1 H, HC_{Ar}), 4.36–4.26 (m, 1 H, $OCHHCH_3$), 4.24–4.14 (m, 1 H, $OCHHCH_3$), 3.82–3.62 (m, 2 H, NCH_2), 2.72–2.59 (m, 1 H, $N(CH_2)CHH$), 2.29–2.19 (m, 1 H, $N(CH_2)_2CHH$), 2.07–1.95 (m, 1 H, NCH_2CHH), 1.77–1.58 (m, 1 H, NCH_2CHH), 1.50 (s, 4 H, $C(CH_3)_3$), 1.37–1.23 (m, 8 H, $C(CH_3)_3$ and OCH_2CH_3); ^{13}C NMR (101 MHz, $CDCl_3$) δ 171.7 and 171.6 (C=O ester), 154.3 and 153.4 (C=O carbamate), 149.14 and 149.09 (C_{Ar}), 146.60 and 146.55 (2 × q, J_{C-F} = 34.8 Hz, F_3CC_{Ar} quat), 139.7 and 139.0 (C_{Ar} quat), 136.6 and 136.2 (C_{Ar}), 121.60 and 121.57 (2 × q, J_{C-F} = 273.8 Hz, CF_3), 119.3 and 119.1 (2 × q, J_{C-F} = 2.0 Hz, C_{Ar}), 81.2 and 80.7 ($C(CH_3)_3$), 70.1 and 69.9 (NC quat), 62.11

and 62.06 (O*C*H_2CH_3), 48.0 (NCH_2), 43.4 and 41.7 ($N(CH_2)_2CH_2$), 28.3 and 28.0 ($C(CH_3)_3$), 23.6 and 22.7 (NCH_2CH_2), 14.1 (OCH_2CH_3); $^{19}F\{^1H\}$ NMR (377 MHz, $CDCl_3$) δ –67.8 and –67.9; HRMS (ESI^+) *m/z* Calculated for $C_{18}H_{24}N_2O_4F_3$ [M+H] 389.1688; Found 389.1685.

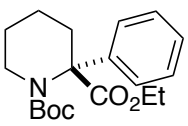
6.2.1.6 Synthesis of 2,2-Disubstituted Piperidines

(±)–Ethyl 2-((*tert*-butoxycarbonyl)(4-chlorobutyl)amino)-2-(4-methoxyphenyl)acetate (136)



$Rh_2(esp)_2$ (1.0 mg, 1.25 μmol) was added to a solution of *tert*-butyl (4-chlorobutyl)carbamate **59** (52 mg, 0.25 mmol) and ethyl 2-diazo-2-(4-methoxyphenyl)acetate **87** (110 mg, 0.50 mmol) in CH_2Cl_2 (0.83 mL). The reaction vessel was sealed, purged with Ar and heated at 40 ºC for 2.5 h, then allowed to cool to rt. The crude reaction mixture was then filtered through Celite, washing with EtOAc (10 mL), and concentrated under reduced pressure. Purification by flash chromatography (10% EtOAc/pentane) afforded ethyl 2-((*tert*-butoxycarbonyl)(4-chlorobutyl)amino)-2-(4-methoxyphenyl)acetate **136** (99 mg, 99%) as a pale yellow oil. R_f 0.30 (10% EtOAc/pentane); ν_{max} (film)/cm^{-1} 2977, 1742 (C=O ester), 1698 (C=O carbamate), 1514, 1366, 1304, 1250, 1176, 1149, 1031; ^{1}H NMR (400 MHz, $CDCl_3$) δ 7.21 (d, *J* = 8.6 Hz, 2 H, 2 × HC_{Ar}), 6.90 (d, *J* = 8.6 Hz, 2 H, 2 × HC_{Ar}), 5.75 and 5.45 (2 × br s, 1 H, CH), 4.24 (q, *J* = 7.1 Hz, 2 H, OCH_2CH_3), 3.83 (s, 3 H, OCH_3), 3.40–3.34 (m, 2 H, $ClCH_2$), 3.25–3.17 (m, 1 H, NC*H*H), 3.08–2.93 (m, 1 H, NCH*H*), 1.60–1.42 (m, 14 H, $C(CH_3)_3$ and $NCH_2(CH_2)_2$), 1.34–1.08 (m, 3 H, OCH_2CH_3); ^{13}C NMR (101 MHz, $CDCl_3$) δ 171.4 (C=O ester), 159.6 (OC_{Ar} quat), 155.9 (C=O carbamate), 130.5 (2 × C_{Ar}), 126.9 (C_{Ar} quat), 114.0 (2 × C_{Ar}), 80.4 ($C(CH_3)_3$), 61.9 (NCH), 61.2 (OCH_2CH_3), 55.3 (OCH_3), 44.6 ($ClCH_2$), 44.3 (NCH_2), 29.9 ($N(CH_2)CH_2$), 28.3 ($C(CH_3)_3$), 26.6 (NCH_2CH_2), 14.1 (OCH_2CH_3); HRMS (ESI$^+$) *m/z* Calculated for $C_{20}H_{31}NO_5Cl$ [M+H] 400.1891; Found 400.1900.

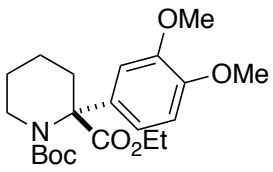
(±)-1-(*tert*-Butyl) 2-ethyl 2-phenylpiperidine-1,2-dicarboxylate (133)



$Rh_2(esp)_2$ (1.9 mg, 2.5 μmol) was added to a solution of *tert*-butyl (4-iodobutyl)carbamate **70** (150 mg, 0.50 mmol) and ethyl 2-diazo-2-phenylacetate **85** (190 mg, 1.0 mmol) in CH_2Cl_2 (1.67 mL). The reaction vessel was sealed, purged with Ar and heated at 40 ºC for 2.5 h, then allowed to cool to rt. Tetrabutylammonium bromide (16 mg, 50 μmol) was added, followed by KOH (112 mg, 2.0 mmol), and the reaction was stirred at 25 ºC for 18 h. The crude reaction mixture was then filtered through Celite, washing with EtOAc (10 mL), and concentrated under reduced pressure. Purification by flash chromatography (1% Et_2O/CH_2Cl_2) afforded 1-(*tert*-butyl) 2-ethyl 2-phenylpiperidine-1,2-dicarboxylate **133** (126 mg, 76%) as a colourless oil. R_f 0.30 (1% Et_2O/CH_2Cl_2); ν_{max} (film)/cm^{-1} 2977, 1739 (C=O ester), 1694 (C=O carbamate), 1365, 1156, 1052, 1030, 727, 698; ^{1}H NMR (400 MHz, $CDCl_3$) δ 7.38–7.27 (m, 4 H, 4 × HC_{Ph}), 7.25–7.20 (m, 1 H, HC_{Ph}), 4.23–4.08 (m, 2 H, OCH_2CH_3), 3.88–3.78 (m, 1 H, NC*H*H), 3.47–3.15 (br s,

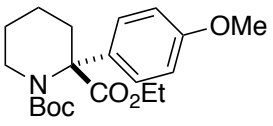
1 H, NCH*H*), 2.36–2.21 (m, 2 H, N(CH_2)$_3$CH_2), 1.77–1.12 (m, 16 H, NCH_2(CH_2)$_2$, C(CH_3)$_3$ and OCH_2CH_3); ^{13}C NMR (101 MHz, $CDCl_3$) δ 172.4 (C=O ester), 156.1 (C=O carbamate), 139.2 (br s, C_{Ph} quat), 127.6 (2 × C_{Ph}), 127.3 (2 × C_{Ph}), 126.6 (C_{Ph}), 80.3 (*C*(CH_3)$_3$), 67.3 (NC quat), 60.9 (O*C*H_2CH$_3$), 42.3 (NCH_2), 35.0 (br s, N(CH_2)$_3$*C*H_2), 27.9 (C(*C*H_3)$_3$), 23.5 (NCH_2*C*H_2), 18.8 (N(CH_2)$_2$*C*H_2), 14.0 (OCH_2*C*H_3). The observed characterisation data (IR, ^{1}H and ^{13}C NMR) was consistent with that previously reported in the literature.[408,410]

(±)–1-(*tert*-Butyl) 2-ethyl 2-(3,4-dimethoxyphenyl)piperidine-1,2-dicarboxylate (138)



$Rh_2(esp)_2$ (1.9 mg, 2.5 μmol) was added to a solution of *tert*-butyl (4-iodobutyl)carbamate **70** (150 mg, 0.50 mmol) and ethyl 2-diazo-2-(3,4-dimethoxyphenyl)acetate **86** (250 mg, 1.0 mmol) in CH_2Cl_2 (1.67 mL). The reaction vessel was sealed, purged with Ar and heated at 40 ºC for 2.5 h, then allowed to cool to rt. Tetrabutylammonium bromide (16 mg, 50 μmol) was added, followed by KOH (112 mg, 2.0 mmol), and the reaction was stirred at 25 ºC for 18 h. The crude reaction mixture was then filtered through cotton wool and then Celite, washing with EtOAc (20 mL), and concentrated under reduced pressure. Purification by flash chromatography (30% EtOAc/pentane) afforded 1-(*tert*-butyl) 2-ethyl 2-(3,4-dimethoxyphenyl)piperidine-1,2-dicarboxylate **138** (162 mg, 82%) as a pale yellow oil. R_f 0.06 (20% EtOAc/pentane); ν_{max} (film)/cm^{-1} 2936, 1736 (C=O ester), 1693 (C=O carbamate), 1515, 1365, 1254, 1145, 1027, 727; ^{1}H NMR (400 MHz, $CDCl_3$) δ 6.89 (d, *J* = 2.0 Hz, 1 H, HC_{Ar}), 6.83–6.75 (m, 2 H, 2 × HC_{Ar}), 4.16–4.03 (m, 2 H, OC*H*$_2$CH$_3$), 3.81 (br s, 7 H, NC*H*H and 2 × OCH_3), 3.28–3.09 (s br, 1 H, NCH*H*), 2.34–2.13 (m, 2 H, N(CH_2)$_3$CH_2), 1.64–1.11 (m, 16 H, NCH_2CH_2CH_2, C(CH_3)$_3$ and OCH_2CH_3); ^{13}C NMR (101 MHz, $CDCl_3$) δ 172.5 (C=O ester), 156.0 (C=O carbamate), 148.1 (OC_{Ar} quat), 147.7 (OC_{Ar} quat), 131.2 (br s, C_{Ar} quat), 119.8 (C_{Ar}), 111.2 (C_{Ar}), 110.2 (C_{Ar}), 80.2 (*C*(CH_3)$_3$), 66.8 (NC quat), 60.7 (O*C*H_2CH$_3$), 55.7 (OCH_3), 55.6 (OCH_3), 42.3 (NCH_2), 34.2 (N(CH_2)$_3$*C*H_2), 27.9 (C(*C*H_3)$_3$), 23.5 (NCH_2*C*H_2), 18.6 (N(CH_2)$_2$*C*H_2), 13.8 (OCH_2*C*H_3); HRMS (ESI$^+$) *m/z* Calculated for $C_{21}H_{32}NO_6$ [M+H] 394.2230; Found 394.2246.

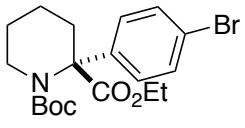
(±)–1-(*tert*-Butyl) 2-ethyl 2-(4-methoxyphenyl)piperidine-1,2-dicarboxylate (134)



$Rh_2(esp)_2$ (1.0 mg, 1.25 μmol) was added to a solution of *tert*-butyl (4-iodobutyl)carbamate **70** (75 mg, 0.25 mmol) and ethyl 2-diazo-2-(4-methoxyphenyl)acetate **87** (110 mg, 0.5 mmol) in CH_2Cl_2 (0.83 mL). The reaction vessel was sealed, purged with Ar and heated at 40 ºC for 2.5 h, then allowed to cool to rt. Tetrabutylammonium bromide (8.0 mg, 25 μmol) was added, followed by KOH (56.1 mg, 1.0 mmol), and the reaction was stirred at 25 ºC for 18 h. The crude reaction mixture was then filtered through Celite, washing with EtOAc (10 mL), and concentrated under reduced

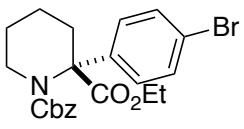
pressure. Purification by flash chromatography (10% to 15% EtOAc/pentane) afforded 1-(*tert*-butyl) 2-ethyl 2-(4-methoxyphenyl)piperidine-1,2-dicarboxylate **134** (68 mg, 75%) as a pale yellow oil. R_f 0.30 (15% EtOAc/pentane); ν_{max} (film)/cm^{-1} 2936, 1736 (C=O ester), 1693 (C=O carbamate), 1511, 1364, 1250, 1155, 1031, 832, 729; ^{1}H NMR (400 MHz, $CDCl_3$) δ 7.27 (d, J = 8.9 Hz, 2 × HC_{Ar}), 6.88 (d, J = 8.9 Hz, 2 × HC_{Ar}), 4.23–4.09 (m, 2 H, OCH_2CH_3), 3.91–3.84 (m, 1 H, NC*H*H), 3.82 (s, 3 H, OCH_3), 3.32–3.15 (s br, 1 H, NCH*H*), 2.36–2.19 (m, 2 H, $N(CH_2)_3CH_2$), 1.67–1.52 (m, 4 H, $NCH_2CH_2CH_2$), 1.44–1.33 (s br, 9 H, $C(CH_3)_3$), 1.24 (t, J = 7.1 Hz, 3 H, OCH_2CH_3); ^{13}C NMR (101 MHz, $CDCl_3$) δ 172.9 (C=O ester), 158.3 (OC_{Ar} quat), 156.2 (C=O carbamate), 130.7 (br s, C_{Ar} quat), 128.8 (2 × C_{Ar}), 113.1 (2 × C_{Ar} quat), 80.4 ($C(CH_3)_3$), 66.9 (NC quat), 60.9 (OCH_2CH_3), 55.2 (OCH_3), 42.4 (NCH_2), 34.4 (br s, $N(CH_2)_3CH_2$), 28.1 ($C(CH_3)_3$), 23.7 (NCH_2CH_2), 18.7 ($N(CH_2)_2CH_2$), 14.0 (OCH_2CH_3); HRMS (ESI$^+$) *m/z* Calculated for $C_{20}H_{30}NO_5$ [M+H] 364.2124; Found 364.2137.

(±)–1-(*tert*-Butyl) 2-ethyl 2-(4-bromophenyl)piperidine-1,2-dicarboxylate (139)



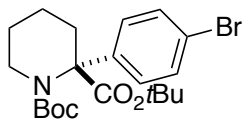
$Rh_2(esp)_2$ (1.9 mg, 2.5 μmol) was added to a solution of *tert*-butyl (4-iodobutyl)carbamate **70** (150 mg, 0.50 mmol) and ethyl 2-diazo-2-(4-bromophenyl)acetate **88** (269 mg, 1.0 mmol) in CH_2Cl_2 (1.67 mL). The reaction vessel was sealed, purged with Ar and heated at 40 ºC for 2.5 h, then allowed to cool to rt. Tetrabutylammonium bromide (16 mg, 50 μmol) was added, followed by KOH (112 mg, 2.0 mmol), and the reaction was stirred at 25 ºC for 18 h. The crude reaction mixture was then filtered through Celite, washing with EtOAc (20 mL), and concentrated under reduced pressure. Purification by flash chromatography (CH_2Cl_2 to 1% Et_2O/CH_2Cl_2) afforded 1-(*tert*-butyl) 2-ethyl 2-(4-bromophenyl)piperidine-1,2-dicarboxylate **139** (156 mg, 76%) as a pale yellow oil. R_f 0.19 (CH_2Cl_2); ν_{max} (film)/cm^{-1} 2977, 1737 (C=O ester), 1693 (C=O carbamate), 1488, 1456, 1365, 1272, 1238, 1198, 1155, 1095, 1052, 1032, 1008, 910; ^{1}H NMR (400 MHz, $CDCl_3$) δ 7.42 (d, J = 8.4 Hz, 2 H, 2 × HC_{Ar}), 7.22 (d, J = 8.4 Hz, 2 H, 2 × HC_{Ar}), 4.24–4.07 (m, 2 H, OCH_2CH_3), 3.86–3.71 (m, 1 H, NC*H*H), 3.51–3.01 (m, 1 H, NCH*H*), 2.31–2.04 (m, 2 H, $N(CH_2)_3CH_2$), 1.73–1.00 (m, 16 H, $NCH_2(CH_2)_2$), OCH_2CH_3 and $C(CH_3)_3$); ^{13}C NMR (101 MHz, $CDCl_3$) δ 172.1 (C=O ester), 155.8 (C=O carbamate), 138.4 (C_{Ar} quat), 130.7 (2 × C_{Ar}), 129.2 (2 × C_{Ar}), 120.7 (BrC_{Ar} quat), 80.6 ($C(CH_3)_3$), 67.0 (NC quat), 61.1 (OCH_2CH_3), 42.1 (NCH_2), 34.9 ($N(CH_2)_3CH_2$), 27.9 ($C(CH_3)_3$), 23.2 (NCH_2CH_2), 18.4 ($N(CH_2)_2CH_2$), 13.9 (OCH_2CH_3); HRMS (FTMS + pNSI) *m/z* Calculated for $C_{19}H_{27}NO_4{}^{79}Br^+$ $[M+H]^+$ 412.1118; Found 412.1116.

(±)–1-Benzyl 2-ethyl 2-(4-bromophenyl)piperidine-1,2-dicarboxylate (140)



$Rh_2(esp)_2$ (1.9 mg, 2.5 μmol) was added to a solution of benzyl (4-iodobutyl)carbamate **71** (167 mg, 0.50 mmol) and ethyl 2-diazo-2-(4-bromophenyl)acetate **88** (269 mg, 1.0 mmol) in CH_2Cl_2 (1.67 mL). The reaction vessel was sealed, purged with Ar and heated at 40 ºC for 2.5 h, then allowed to cool to rt. Tetrabutylammonium bromide (16 mg, 50 μmol) was added, followed by KOH (112 mg, 2.0 mmol), and the reaction was stirred at 25 ºC for 18 h. The crude reaction mixture was then filtered through Celite, washing with EtOAc (20 mL), and concentrated under reduced pressure. Purification by flash chromatography (25% EtOAc/hexane) afforded 1-benzyl 2-ethyl 2-(4-bromophenyl)piperidine-1,2-dicarboxylate **140** (188 mg, 84%) as a colourless oil. R_f 0.14 (20% EtOAc/hexane); ν_{max} (film)/cm^{-1} 2946, 2869, 1736 (C=O ester), 1698 (C=O carbamate), 1392, 1347, 1260, 1235, 1195, 1164, 1095, 1051, 1029, 1007, 732, 696; ^{1}H NMR (400 MHz, $CDCl_3$) δ 7.43 (d, J = 8.4 Hz, 2 H, 2 × HC_{Ar}), 7.32 (br s, 5 H, 5 × HC_{Ph}), 7.20 (d, J = 8.8 Hz, 2 H, 2 × HC_{Ar}), 5.10 (br s, 2 H, OCH_2Ph), 4.16–3.85 (m, 3 H, OCH_2CH_3 and NC*H*H), 3.35 (br s, 1 H, NCH*H*), 2.36–2.16 (m, 2 H, $N(CH_2)_3CH_2$), 1.75–1.51 (m, 3 H, NCH_2CH_2CHH), 1.34–1.21 (m, 1 H, $N(CH_2)_2$CH*H*), 1.15 (t, J = 7.1 Hz, 3 H, OCH_2CH_3); ^{13}C NMR (101 MHz, $CDCl_3$) δ 171.7 (C=O ester), 156.8 (C=O carbamate), 138.3 (br s, C_{Ar} quat), 136.1 (C_{Ph} quat), 131.0 (2 × C_{Ar}), 129.1 (2 × C_{Ar}), 128.3 (2 × C_{Ph}), 128.1 (2 × C_{Ph}), 128.0 (C_{Ph}), 121.0 (BrC_{Ar} quat), 67.6 (NC quat), 67.4 (OCH_2Ph), 61.4 (OCH_2CH_3), 42.7 (NCH_2), 35.0 (br s, $N(CH_2)_3CH_2$), 23.4 (NCH_2CH_2), 18.6 ($N(CH_2)_2CH_2$), 13.9 (OCH_2CH_3); HRMS (FTMS + pNSI) *m/z* Calculated for $C_{22}H_{25}NO_4{}^{79}Br^+$ $[M+H]^+$ 446.0961; Found 446.0960.

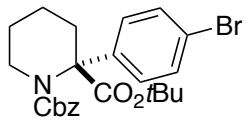
(±)–Di-*tert*-butyl 2-(4-bromophenyl)piperidine-1,2-dicarboxylate (141)



$Rh_2(esp)_2$ (1.9 mg, 2.5 μmol) was added to a solution of *tert*-butyl (4-iodobutyl)carbamate **70** (150 mg, 0.50 mmol) and *tert*-butyl 2-(4-bromophenyl)-2-diazoacetate **99** (297 mg, 1.0 mmol) in CH_2Cl_2 (1.67 mL). The reaction vessel was sealed, purged with Ar and heated at 40 ºC for 2.5 h, then allowed to cool to rt. Tetrabutylammonium bromide (16 mg, 50 μmol) was added, followed by KOH (112 mg, 2.0 mmol), and the reaction was stirred at 25 ºC for 18 h. The crude reaction mixture was then filtered through Celite, washing with EtOAc (20 mL), and concentrated under reduced pressure. Purification by flash chromatography (2.5% to 5% EtOAc/pentane) afforded di-*tert*-butyl 2-(4-bromophenyl)piperidine-1,2-dicarboxylate **141** (134 mg, 61%) as a pale yellow oil. R_f 0.31 (5% EtOAc/pentane); ν_{max} (film)/cm^{-1} 2976, 2935, 1731 (C=O ester), 1693 (C=O carbamate), 1488, 1456, 1391, 1365, 1272, 1251, 1150, 1095, 1076, 1051, 1010, 728; ^{1}H NMR (400 MHz, $CDCl_3$) δ 7.41 (d, J = 8.7 Hz, 2 H, 2 × HC_{Ar}), 7.33–7.23 (m, 2 H, 2 × HC_{Ar}), 3.97–3.02 (m, 2 H, NCH_2), 2.31–1.90 (m, 2 H, $N(CH_2)_3CH_2$), 1.78–0.94 (m, 22 H, $NCH_2(CH_2)_2$

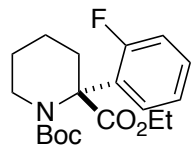
and 2 × $C(CH_3)_3$); ^{13}C NMR (101 MHz, $CDCl_3$) δ 170.8 (C=O ester), 155.9 (C=O carbamate), 138.9 (br s, C_{Ar} quat), 130.6 (2 × C_{Ar}), 129.0 (2 × C_{Ar}), 120.4 (BrC_{Ar} quat), 81.1 (*C*$(CH_3)_3$ ester), 80.2 (*C*$(CH_3)_3$ carbamate), 67.5 (NC quat), 42.3 (NCH_2), 34.2 ($N(CH_2)_3CH_2$), 28.1 ($C(CH_3)_3$ carbamate), 27.8 ($C(CH_3)_3$ ester), 23.3 (NCH_2CH_2), 18.6 ($N(CH_2)_3CH_2$); HRMS (ESI^+) *m/z* Calculated for $C_{21}H_{31}NO_4{}^{79}Br$ [M+H] 440.1436; Found 440.1429.

(±)–1-Benzyl 2-(tert-butyl) 2-(4-bromophenyl)piperidine-1,2-dicarboxylate (142)



$Rh_2(esp)_2$ (1.9 mg, 2.5 μmol) was added to a solution of benzyl (4-iodobutyl)carbamate **71** (167 mg, 0.50 mmol) and *tert*-butyl 2-(4-bromophenyl)-2-diazoacetate **99** (297 mg, 1.0 mmol) in CH_2Cl_2 (1.67 mL). The reaction vessel was sealed, purged with Ar and heated at 40 ºC for 2.5 h, then allowed to cool to rt. Tetrabutylammonium bromide (16 mg, 50 μmol) was added, followed by KOH (112 mg, 2.0 mmol), and the reaction was stirred at 25 ºC for 18 h. The crude reaction mixture was then filtered through Celite, washing with EtOAc (20 mL), and concentrated under reduced pressure. Purification by flash chromatography (10% EtOAc/hexane) afforded 1-benzyl 2-(tert-butyl) 2-(4-bromophenyl)piperidine-1,2-dicarboxylate **142** (187 mg, 79%) as a colourless oil. R_f 0.31 (15% EtOAc/hexane); ν_{max} (film)/cm^{-1} 2940, 1732 (C=O ester), 1701 (C=O carbamate), 1488, 1456, 1392, 1367, 1352, 1254, 1205, 1152, 1095, 1076, 1051, 1008, 961, 818, 794, 772, 734, 696; ^1H NMR (400 MHz, $CDCl_3$) δ 7.52–6.90 (m, 9 H, 9 × HC_{Ar}), 5.19–4.88 (m, 2 H, OCH_2Ph), 3.88–3.30 (m, 2 H, NCH_2), 2.35–2.25 (m, 1 H, $N(CH_2)_3CHH$), 2.14 (br s, 1 H, $N(CH_2)_3CHH$), 1.77–1.48 (m, 3 H, NCH_2CH_2CHH), 1.42–1.27 (m, 10 H, $N(CH_2)_2CHH$ and $OC(CH_3)_3$); ^{13}C NMR (101 MHz, $CDCl_3$) δ 170.4 (C=O ester), 156.8 (C=O carbamate), 139.6 (br s, C_{Ar} quat), 136.1 (C_{Ph} quat), 130.8 (2 × C_{Ar}), 128.8 (2 × C_{Ar}), 128.2 (2 × C_{Ph}), 128.0 (2 × C_{Ph}), 127.9 (C_{Ph}), 120.7 (BrC_{Ar} quat), 81.6 (*C*$(CH_3)_3$), 68.1 (NC quat), 67.2 (OCH_2Ph), 42.7 (NCH_2), 35.5 (br s, $N(CH_2)_3CH_2$), 27.7 ($C(CH_3)_3$), 23.3 (NCH_2CH_2), 18.7 ($N(CH_2)_3CH_2$); HRMS (FTMS + pNSI) *m/z* Calculated for $C_{24}H_{29}NO_4{}^{79}Br^+$ $[M+H]^+$ 474.1274; Found 474.1271.

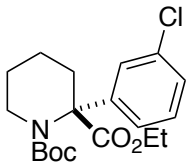
(±)–1-(*tert*-Butyl) 2-ethyl 2-(2-fluorophenyl)piperidine-1,2-dicarboxylate (143)



$Rh_2(esp)_2$ (1.9 mg, 2.5 μmol) was added to a solution of *tert*-butyl (4-iodobutyl)carbamate **70** (150 mg, 0.50 mmol) and ethyl 2-diazo-2-(2-fluorophenyl)acetate **89** (208 mg, 1.0 mmol) in CH_2Cl_2 (1.67 mL). The reaction vessel was sealed, purged with Ar and heated at 40 ºC for 2.5 h, then allowed to cool to rt. Tetrabutylammonium bromide (16 mg, 50 μmol) was added, followed by KOH (112 mg, 2.0 mmol), and the reaction was stirred at 25 ºC for 18 h. The crude reaction mixture was then filtered through Celite, washing with EtOAc (20 mL), and concentrated under reduced pressure. Purification by flash chromatography afforded 1-(*tert*-butyl) 2-ethyl 2-(2-

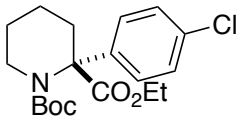
fluorophenyl)piperidine-1,2-dicarboxylate **143** (83 mg, 47%) as a colourless oil which froze at –20 ºC to give a white solid. R_f 0.23 (10% EtOAc/pentane); mp = 64–67 ºC; ν_{max} (film)/cm^{-1} 2978, 2936, 1736, 1694, 1486, 1447, 1383, 1364, 1272, 1248, 1234, 1218, 1154, 1132, 1095, 1055, 1032, 755; ^{1}H NMR (400 MHz, $CDCl_3$) δ 7.31–7.24 (m, 1 H, HC_{Ar}), 7.12–7.00 (m, 3 H, 3 $\times$ HC_{Ar}), 4.30–4.14 (m, 2 H, OCH_2CH_3), 3.83 (br s, 1 H, NC*H*H), 3.40 (br s, 1 H, NCH*H*), 2.61 (br s, 1 H, $N(CH_2)_3CHH$), 2.32–2.22 (m, 1 H, $N(CH_2)_3CHH$), 1.77–1.55 (m, 4 H, $NCH_2(CH_2)_2$), 1.53–1.12 (m, 12 H, OCH_2CH_3 and $C(CH_3)_3$); ^{13}C NMR (101 MHz, $CDCl_3$) δ 171 (C=O ester), 160.9 (d, J_{C-F} = 247.9 Hz, FC_{Ar} quat), 159.7 (C=O carbamate), 129.1 (d, J_{C-F} = 9.0 Hz, C_{Ar}), 128.8 (C_{Ar}), 126.4 (br s, C_{Ar} quat), 123.3 (C_{Ar}), 116.6 (d, J_{C-F} = 25.1 Hz, C_{Ar}), 80.6 ($C(CH_3)_3$), 67.2 (NC quat), 61.3 (OCH_2CH_3), 41.8 (NCH_2), 33.2 ($N(CH_2)_3CH_2$), 28.0 ($C(CH_3)_3$), 23.0 (NCH_2CH_2), 18.6 ($N(CH_2)_2CH_2$), 14.0 (OCH_2CH_3); ^{19}F{^{1}H} NMR (377 MHz, $CDCl_3$) δ –107.0; HRMS (FTMS + pNSI) *m/z* Calculated for $C_{19}H_{27}NO_4F^+$ $[M+H]^+$ 352.1919; Found 352.1921.

(±)–1-(*tert*-Butyl) 2-ethyl 2-(3-chlorophenyl)piperidine-1,2-dicarboxylate (144)



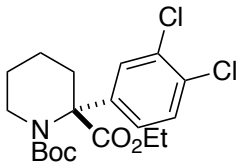
$Rh_2(esp)_2$ (1.9 mg, 2.5 μmol) was added to a solution of *tert*-butyl (4-iodobutyl)carbamate **70** (150 mg, 0.50 mmol) and ethyl 2-diazo-2-(3-chlorophenyl)acetate **93** (225 mg, 1.0 mmol) in CH_2Cl_2 (1.67 mL). The reaction vessel was sealed, purged with Ar and heated at 40 ºC for 2.5 h, then allowed to cool to rt. Tetrabutylammonium bromide (16 mg, 50 μmol) was added, followed by KOH (112 mg, 2.0 mmol), and the reaction was stirred at 25 ºC for 18 h. The crude reaction mixture was then filtered through Celite, washing with EtOAc (20 mL), and concentrated under reduced pressure. Purification by flash chromatography (1% to 2% Et_2O/CH_2Cl_2) afforded 1-(*tert*-butyl) 2-ethyl 2-(3-chlorophenyl)piperidine-1,2-dicarboxylate **144** (118 mg, 64%) as a yellow solid. R_f 0.16 (CH_2Cl_2); mp = 62–65 ºC; ν_{max} (film)/cm^{-1} 2978, 2936, 1735 (C=O ester), 1694 (C=O carbamate), 1487, 1447, 1383, 1364, 1272, 1248, 1234, 1218, 1154, 1132, 1095, 1055, 1032, 755; ^{1}H NMR (400 MHz, $CDCl_3$) δ 7.36 (br s, 1 H, HC_{Ar}), 7.31–7.21 (m, 3 H, 3 $\times$ HC_{Ar}), 4.28–4.13 (m, 2 H, OCH_2CH_3), 3.80 (br s, 1 H, NC*H*H), 3.15–3.12 (m, 1 H, NCH*H*), 2.34–2.10 (m, 2 H, $N(CH_2)_3CH_2$), 1.75–1.12 (m, 16 H, $NCH_2(CH_2)_2$, OCH_2CH_3 and $C(CH_3)_3$); ^{13}C NMR (101 MHz, $CDCl_3$) δ 172.1 (C=O ester), 155.9 (C=O carbamate), 142.1 (C_{Ar} quat), 133.7 (ClC_{Ar} quat), 128.9 (C_{Ar}), 127.6 (C_{Ar}), 126.9 (C_{Ar}), 125.6 (C_{Ar}), 80.7 ($C(CH_3)_3$), 67.2 (NC quat), 61.2 (OCH_2CH_3), 42.2 (NCH_2), 35.7 (br s, $N(CH_2)_3CH_2$), 28.0 ($C(CH_3)_3$), 23.3 (NCH_2CH_2), 18.5 ($N(CH_2)_2CH_2$), 14.0 (OCH_2CH_3); HRMS (FTMS + pNSI) *m/z* Calculated for $C_{19}H_{27}NO_4{}^{35}Cl^+$ $[M+H]^+$ 368.1623; Found 368.1626.

(±)–1-(*tert*-Butyl) 2-ethyl 2-(4-chlorophenyl)piperidine-1,2-dicarboxylate (135)



$Rh_2(esp)_2$ (1.9 mg, 2.5 μmol) was added to a solution of *tert*-butyl (4-iodobutyl)carbamate **70** (150 mg, 0.50 mmol) and ethyl 2-diazo-2-(4-chlorophenyl)acetate **94** (225 mg, 1.0 mmol) in CH_2Cl_2 (1.67 mL). The reaction vessel was sealed, purged with Ar and heated at 40 ºC for 2.5 h, then allowed to cool to rt. Tetrabutylammonium bromide (16 mg, 50 μmol) was added, followed by KOH (112 mg, 2.0 mmol), and the reaction was stirred at 25 ºC for 18 h. The crude reaction mixture was then filtered through cotton wool and then Celite, washing with EtOAc (20 mL), and concentrated under reduced pressure. Purification by flash chromatography (CH_2Cl_2) afforded 1-(*tert*-butyl) 2-ethyl 2-(4-chlorophenyl)piperidine-1,2-dicarboxylate **135** (150 mg, 82%) as a pale yellow oil. R_f 0.25 (CH_2Cl_2); ν_{max} (film)/cm^{-1} 2977, 2869, 1738 (C=O ester), 1694 (C=O carbamate), 1365, 1238, 1198, 1156, 1097, 1052, 1031, 1013; ^{1}H NMR (400 MHz, $CDCl_3$) δ 7.30 (s, 4 H, 4 × HC_{Ar}), 4.24–4.09 (m, 2 H, OCH_2CH$_3$), 3.86–3.76 (m, 1 H, NC*H*H), 3.32 (s br, 1 H, NCH*H*), 2.32–2.11 (m, 2 H, N$(CH_2)_3$CH_2), 1.73–1.51 (m, 4 H, $NCH_2(CH_2)_2$), 1.45–1.15 (m, 12 H, OCH_2CH_3 and $C(CH_3)_3$); ^{13}C NMR (101 MHz, $CDCl_3$) δ 172.2 (C=O ester), 155.8 (C=O carbamate), 138.0 (br s, C_{Ar} quat), 132.5 (ClC_{Ar} quat), 128.8 (2 × C_{Ar}), 127.7 (2 × C_{Ar}), 80.6 ($C(CH_3)_3$), 66.9 (NC quat), 61.1 (OCH_2CH_3), 42.1 (NCH_2), 35.2 (br s, N$(CH_2)_3CH_2$), 27.9 ($C(CH_3)_3$), 23.2 (NCH_2CH_2), 18.4 ($N(CH_2)_2CH_2$), 14.0 (OCH_2CH_3); HRMS (ESI$^+$) *m/z* Calculated for $C_{19}H_{27}NO_4{}^{35}Cl$ [M+H] 368.1629; Found 368.1631.

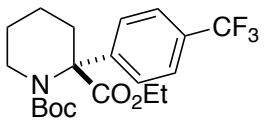
(±)-1-(*tert*-Butyl) 2-ethyl 2-(3,4-dichlorophenyl)piperidine-1,2-dicarboxylate (145)



Ethyl 2-diazo-2-(3,4-dichlorophenyl)acetate **95** (324 mg, 1.25 mmol) in CH_2Cl_2 (1.0 mL) was added slowly *via* syringe pump over 1 h to a solution of *tert*-butyl (4-iodobutyl)carbamate **70** (150 mg, 0.50 mmol) and $Rh_2(esp)_2$ (1.9 mg, 2.5 μmol) in CH_2Cl_2 (0.67 mL) at 40 ºC. Tetrabutylammonium bromide (16 mg, 50 μmol) was added, followed by KOH (112 mg, 2.0 mmol), and the reaction was stirred at 25 ºC for 18 h. The crude reaction mixture was then filtered through Celite, washing with EtOAc (20 mL), and concentrated under reduced pressure. Purification by flash chromatography (CH_2Cl_2) afforded 1-(*tert*-butyl) 2-ethyl 2-(3,4-dichlorophenyl)piperidine-1,2-dicarboxylate **145** (127 mg, 63%) as a pale yellow solid. R_f 0.23 (CH_2Cl_2); mp = 84–85 ºC; ν_{max} (film)/cm^{-1} 2973, 2899, 2870, 1730 (C=O ester), 1685 (C=O carbamate), 1471, 1391, 1374, 1363, 1281, 1241, 1200, 1160, 1096, 1056, 1034, 1025, 868, 777, 723; ^{1}H NMR (400 MHz, $CDCl_3$) δ 7.46 (br s, 1 H, HC_{Ar}), 7.41 (d, *J* = 8.6 Hz, 1 H, HC_{Ar}), 7.23 (br d, *J* = 8.6 Hz, 1 H, HC_{Ar}), 4.28–4.12 (m, 2 H, OCH_2CH$_3$), 3.89–3.71 (br s, 1 H, NC*H*H), 3.53–3.13 (m, 1 H, NCH*H*), 2.33–2.04 (m, 2 H, N$(CH_2)_3$CH_2), 1.80–1.10 (m, 16 H, $NCH_2(CH_2)_2$ and OCH_2CH_3 and $C(CH_3)_3$); ^{13}C NMR (101 MHz, $CDCl_3$) δ 172.0 (C=O ester), 155.8 (C=O

carbamate), 140.1 (br s, C_{Ar} quat), 131.8 (ClC_{Ar} quat), 130.8 (ClC_{Ar} quat), 129.6 (2 × C_{Ar}), 126.9 (C_{Ar}), 80.9 ($C(CH_3)_3$), 66.8 (NC quat), 61.4 (OCH_2CH_3), 42.0 (NCH_2), 35.5 ($N(CH_2)_3CH_2$), 28.0 ($C(CH_3)_3$), 23.1 (NCH_2CH_2), 18.3 ($N(CH_2)_2CH_2$), 14.0 (OCH_2CH_3); HRMS (FTMS + pNSI) *m/z* Calculated for $C_{19}H_{26}NO_4{}^{35}Cl_2{}^+$ $[M+H]^+$ 402.1233; Found 402.1232.

(±)–1-(*tert*-Butyl) 2-ethyl 2-(4-(trifluoromethyl)phenyl)piperidine-1,2-dicarboxylate (146)



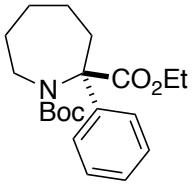
Ethyl 2-diazo-2-(4-(trifluoromethyl)phenyl)acetate **96** (323 mg, 1.25 mmol) in CH_2Cl_2 (1.0 mL) was added slowly *via* syringe pump over 1 h to a solution of *tert*-butyl (4-iodobutyl)carbamate **70** (150 mg, 0.50 mmol) and $Rh_2(esp)_2$ (1.9 mg, 2.5 μmol) in CH_2Cl_2 (0.67 mL) at 40 ºC. The reaction mixture was stirred at 40 °C for a further 2.5 h, then allowed to cool to rt. Tetrabutylammonium bromide (16 mg, 50 μmol) was added, followed by KOH (112 mg, 2.0 mmol), and the reaction was stirred at 25 ºC for 18 h. The crude reaction mixture was then filtered through Celite, washing with EtOAc (20 mL), and concentrated under reduced pressure. Purification by flash chromatography (CH_2Cl_2 to 1% Et_2O/CH_2Cl_2) afforded 1-(*tert*-butyl) 2-ethyl 2-(4-(trifluoromethyl)phenyl)piperidine-1,2-dicarboxylate **146** (86 mg, 43%) as a pale yellow oil. R_f 0.20 (CH_2Cl_2); ν_{max} (film)/cm^{-1} 2977, 2871, 1734 (C=O ester), 1695 (C=O carbamate), 1366, 1326, 1272, 1234, 1201, 1157, 1117, 1096, 1069, 1053, 1030, 1016, 730; ^1H NMR (400 MHz, $CDCl_3$) δ 7.58 (d, *J* = 8.4 Hz, 2 H, 2 × HC_{Ar}), 7.50 (d, *J* = 8.4 Hz, 2 H, 2 × HC_{Ar}), 4.28–4.13 (m, 2 H, OCH_2CH_3), 3.79 (br s, 1 H, NC*H*H), 3.39 (br s, 1 H, NCH*H*), 2.38–2.06 (m, 2 H, $N(CH_2)_3CH_2$), 1.83–1.03 (m, 16 H, $NCH_2(CH_2)_2$, OCH_2CH_3 and $C(CH_3)_3$); ^{13}C NMR (101 MHz, $CDCl_3$) δ 172.1 (C=O ester), 156.0 (C=O carbamate), 144.3 (br s, C_{Ar} quat), 129.0 (q, J_{C-F} = 32.4 Hz, CF_3C_{Ar} quat), 127.7 (br s, 2 × C_{Ar}), 124.6 (br s, 2 × C_{Ar}), 124.1 (q, J_{C-F} = 272.5 Hz, CF_3), 80.8 ($C(CH_3)_3$), 67.4 (NC quat), 61.4 (OCH_2CH_3), 42.2 (NCH_2), 35.6 ($N(CH_2)_3CH_2$), 28.0 ($C(CH_3)_3$), 23.6 (NCH_2CH_2), 18.5 ($N(CH_2)_2CH_2$), 14.0 (OCH_2CH_3); $^{19}F\{^1H\}$ NMR (377 MHz, $CDCl_3$) δ –62.5; HRMS (FTMS + pNSI) *m/z* Calculated for $C_{20}H_{27}NO_4F_3{}^+$ $[M+H]^+$ 402.1887; Found 402.1881.

6.2.1.7 Synthesis of 2,2-Disubstituted Azepanes and Larger Rings

As discussed by Moody and co-workers,[411] azepanes can sample multiple conformations of similar energy which complicates the room temperature NMR spectra. The NMR spectra for the synthesised azepanes (**148–151**) was further complicated by rotamers caused by the Boc group.

Variable temperature NMR spectroscopy (at 100 ºC) simplified the NMR spectra, however, the compounds were still observed to be rotameric.

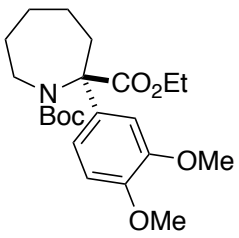
(±)–1-(*tert*-Butyl) 2-ethyl 2-phenylazepane-1,2-dicarboxylate (148)



$Rh_2(esp)_2$ (1.9 mg, 2.5 μmol) was added to a solution of *tert*-butyl (5-iodopentyl)carbamate **72** (157 mg, 0.50 mmol) and ethyl 2-diazo-2-phenylacetate **86** (190 mg, 1.0 mmol) in CH_2Cl_2 (1.67 mL). The reaction vessel was sealed, purged with Ar and heated at 40 ºC for 2.5 h, then allowed to cool to rt. Tetrabutylammonium bromide (16 mg, 50 μmol) was added, followed by $CsOH·H_2O$ (336 mg, 2.0 mmol), and the reaction was stirred at 25 ºC for 18 h. The crude reaction mixture was then filtered through Celite, washing with EtOAc (10 mL), and concentrated under reduced pressure. Purification by flash chromatography (5 to 10% EtOAc/hexane) then (75% CH_2Cl_2/$CHCl_3$ to CH_2Cl_2) afforded 1-(*tert*-butyl) 2-ethyl 2-phenylazepane-1,2-dicarboxylate **148** (104 mg, 60%) as a colourless oil. R_f 0.14 (CH_2Cl_2); ν_{max} (film)/cm^{-1} 2927, 1737 (C=O ester), 1691 (C=O carbamate), 1385, 1284, 1231, 1151, 1026, 697; ^{1}H NMR (400 MHz, $CDCl_3$) δ 7.57–7.52 (m, 1.2 H, HC_{Ph}), 7.42–7.37 (m, 0.7 H, HC_{Ph}), 7.34–7.28 (m, 2 H, 2 × HC_{Ph}), 7.26–7.20 (m, 1 H, HC_{Ph}), 4.32–4.22 (m, 0.7 H, OCH_2CH_3), 4.19–4.03 (m, 1.3 H, OCH_2CH_3), 3.97 (dd, *J* = 14.7, 7.6 Hz, 0.6 H, NC*H*H), 3.88–3.80 (m, 0.3 H, NC*H*H), 3.68 (dd, *J* = 14.7, 8.9 Hz, 0.6 H, NCH*H*), 3.11 (dd, *J* = 13.9, 10.5 Hz, 0.3 Hz, NCH*H*), 2.53 (dd, *J* = 15.3, 9.5 Hz, 0.3 H, $N(CH_2)_4CHH$), 2.37 (dd, *J* = 15.3, 9.4 Hz, 0.6 Hz, $N(CH_2)_4CHH$), 2.18–2.05 (m, 1 H, $N(CH_2)_4CHH$), 2.03–1.91 (m, 0.3 H, NCH_2CHH), 1.91–1.08 (m, 18 H, $NCH_2(CH_2)_3$, OCH_2CH_3 and $C(CH_3)_3$); ^{1}H NMR (500 MHz, DMSO-d_6, 373 K) δ 7.44 (br d, *J* = 7.8 Hz, 2 H, 2 × HC_{Ph}), 7.33–7.29 (m, 2 H, 2 × HC_{Ph}), 7.24–7.20 (m, 1 H, HC_{Ph}), 4.20–4.04 (m, 2 H, OCH_2CH_3), 3.90–3.82 (m, 1 H, NC*H*H), 3.37 (br s, 1 H, NCH*H*), 2.41–2.33 (m, 1 H, $N(CH_2)_4CHH$), 2.10 (ddd, *J* = 15.3, 9.8, 1.4 Hz, 1 H, $N(CH_2)_4CHH$), 1.79–1.68 (m, 2 H, NCH_2CH_2), 1.67–1.52 (m, 2 H, $N(CH_2)_3CH_2$), 1.50–1.14 (m, 14 H, $N(CH_2)_2CH_2$, OCH_2CH_3 and $C(CH_3)_3$); ^{1}H NMR (500 MHz, $CDCl_3$, 233 K) δ 7.57–7.47 (m, 1 H, HC_{Ph}), 7.36–7.30 (m, 3 H, 3 × HC_{Ph}), 7.28–7.23 (m, 1 H, HC_{Ph}), 4.30–4.21 (m, 0.6 H, OCH_2CH_3), 4.19–4.06 (m, 1.3 H, OCH_2CH_3), 4.04–3.35 (m, 1.4 H, NCH_2), 3.02 (br s, 0.3 H, NCH*H*), 2.53 (dd, *J* = 15.1, 9.7 Hz, 0.3 H, $N(CH_2)_4CHH$), 2.37 (dd, *J* = 15.2, 9.4 Hz, 0.6 H, $N(CH_2)_4CHH$), 2.12–1.94 (m, 1.4 H, $N(CH_2)_4CHH$ and NCH_2CHH), 1.89–1.00 (m, 18 H, $NCH_2(CH_2)_3$, OCH_2CH_3 and $C(CH_3)_3$); ^{13}C

NMR (101 MHz, $CDCl_3$) δ 173.4 and 172.6 (C=O ester), 156.0 and 155.7 (C=O carbamate), 142.7 and 140.3 (C_{Ph} quat), 127.7 and 127.5 (2 × C_{Ph}), 127.4 and 126.9 (2 × C_{Ph}), 126.8 and 126.4 (C_{Ph}), 80.6 and 80.0 ($C(CH_3)_3$), 71.0 and 70.1 (NC quat), 61.0 and 60.9 (OCH_2CH_3), 45.4 and 45.2 (NCH_2), 41.6 and 39.3 ($N(CH_2)_4CH_2$), 29.7 and 29.1 (NCH_2CH_2), 29.2 and 28.6 ($N(CH_2)_2CH_2$), 28.4 and 27.8 ($C(CH_3)_3$), 24.4 and 23.6 ($N(CH_2)_3CH_2$), 14.1 and 14.0 (OCH_2CH_3); ^{13}C NMR (126 MHz, DMSO-d_6, 373 K) δ 171.5 (C=O ester), 154.5 (C=O carbamate), 143.6 (C_{Ph} quat), 126.7 (2 × C_{Ph}), 126.4 (2 × C_{Ph}), 125.8 (C_{Ph}), 78.9 ($C(CH_3)_3$), 69.8 (NC quat), 59.9 (OCH_2CH_3), 44.4 (NCH_2), 28.5 (NCH_2CH_2), 27.6 ($N(CH_2)_3CH_2$), 27.3 ($C(CH_3)_3$), 23.2 ($N(CH_2)_2CH_2$), 13.2 (OCH_2CH_3) (Missing peak due to $N(CH_2)_4CH_2$ confirmed by HSQC to be beneath DMSO-d_6 residual solvent signal); ^{13}C NMR (126 MHz, $CDCl_3$, 233 K) δ 173.6 and 172.7 (C=O ester), 155.9 and 155.6 (C=O carbamate), 142.0 and 139.6 (C_{Ph} quat), 127.7 and 127.3 (2 × C_{Ph}), 126.8, 126.7 and 126.4 (3 × C_{Ph}), 80.6 and 80.0 ($C(CH_3)_3$), 70.5 and 69.5 (NC quat), 61.14 and 61.1 (OCH_2CH_3), 45.1 and 45.0 (NCH_2), 41.1 and 39.0 (2 × br s, $N(CH_2)_4CH_2$), 29.4 and 28.8 (NCH_2CH_2), 29.0 and 28.6 ($N(CH_2)_3CH_2$), 28.1 and 27.6 ($C(CH_3)_3$), 24.2 and 23.2 ($N(CH_2)_2CH_2$), 14.1 and 14.0 (OCH_2CH_3); HRMS (FTMS + pNSI) *m/z* Calculated for $C_{20}H_{30}NO_4^+$ $[M+H]^+$ 348.2172; Found 348.2169.

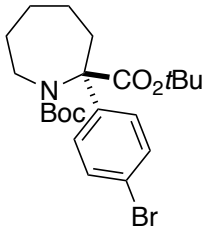
(±)–1-(*tert*-Butyl) 2-ethyl 2-(3,4-dimethoxyphenyl)azepane-1,2-dicarboxylate (149)



$Rh_2(esp)_2$ (1.9 mg, 2.5 μmol) was added to a solution of *tert*-butyl (5-iodopentyl)carbamate **72** (157 mg, 0.50 mmol) and ethyl 2-diazo-2-(3,4-dimethoxyphenyl)acete **86** (250 mg, 1.0 mmol) in CH_2Cl_2 (1.67 mL). The reaction vessel was sealed, purged with Ar and heated at 40 ºC for 2.5 h, then allowed to cool to rt. Tetrabutylammonium bromide (16 mg, 50 μmol) was added, followed by $CsOH·H_2O$ (336 mg, 2.0 mmol), and the reaction was stirred at 25 ºC for 18 h. The crude reaction mixture was then filtered through Celite, washing with EtOAc (10 mL), and concentrated under reduced pressure. Purification by flash chromatography (0 to 25% to 100% EtOAc/pentane) afforded **1**-(*tert*-butyl) 2-ethyl 2-(3,4-dimethoxyphenyl)azepane-1,2-dicarboxylate **149** (95 mg, 47%) as a colourless oil which slowly solidified to a white solid. R_f 0.25 (25% EtOAc/pentane); mp = 77–79 ºC; ν_{max} (film)/cm^{-1} 2974, 2929, 1737 (C=O ester), 1692 (C=O carbamate), 1513, 1461, 1387, 1230, 1141, 1019, 767; ^{1}H NMR (400 MHz, $CDCl_3$) δ 7.22 (d, *J* = 2.2 Hz, 0.5 H, HC_{Ar}), 7.03 (dd, *J* = 8.5, 2.2 Hz, 1 H, HC_{Ar}), 6.90 (dd, *J* = 8.5, 2.0 Hz, 0.4 H, HC_{Ar}), 6.83–6.78 (m, 1 H, HC_{Ar}), 4.29–4.19 (m, 0.6 H, OCH_2CH_3), 4.18–4.06 (m, 1.3 H, OCH_2CH_3), 3.98–3.74 (m, 7 H, NC*H*H and 2 × OCH_3), 3.66 (dd, *J* = 14.7, 8.9 Hz, 0.6 H, NCH*H*), 3.17–3.07 (m, 0.4 H, NCH*H*), 2.47 (dd, *J* = 15.2, 9.5 Hz, 0.4 H, $N(CH_2)_4CHH$), 2.33 (dd, *J* = 15.0, 9.1 Hz, 0.6 Hz, $N(CH_2)_4CHH$), 2.21–2.03 (m, 1 H, $N(CH_2)_4CHH$), 1.99–1.36 (m, 10 H, $NCH_2(CH_2)_3$ and $C(CH_3)_3$), 1.34–1.13 (m, 8 H, OCH_2CH_3 and $C(CH_3)_3$); ^{1}H NMR

(500 MHz, DMSO-d_6, 373 K) δ 7.07 (br s, 1 H, HC_{Ar}), 6.96 (dd, J = 8.6, 2.0 Hz, 1 H, HC_{Ar}), 6.90 (d, J = 8.6 Hz, 1 H, HC_{Ar}), 4.20–4.03 (m, 2 H, OCH_2CH_3), 3.88–3.72 (m, 7 H, NC*H*H and 2 × OCH_3), 3.33 (br s, 1 H, NCH*H*), 2.36 (dd, J = 15.1, 9.1 Hz, 1 H, $N(CH_2)_4CHH$), 2.11 (ddd, J = 15.2, 9.6, 1.2 Hz, 1 H, $N(CH_2)_4CHH$), 1.82–1.67 (m, 2 H, NCH_2CH_2), 1.66–1.18 (m, 16 H, $N(CH_2)_2CH_2CH_2$, $C(CH_3)_3$ and OCH_2CH_3); ^{13}C NMR (101 MHz, $CDCl_3$) δ 173.7 and 172.8 (C=O ester), 156.0 and 155.7 (C=O carbamate), 148.2 and 147.7 (OC_{Ar} quat), 147.9 and 147.4 (OC_{Ar} quat), 135.3 and 132.7 (C_{Ar} quat), 119.6 and 119.1 (C_{Ar}), 111.8 and 110.9 (C_{Ar}), 110.4 and 109.9 (C_{Ar}), 80.6 and 79.9 ($C(CH_3)_3$), 70.6 and 69.7 (NC quat), 61.0 and 60.9 (OCH_2CH_3), 55.80 and 55.75 (2 × OCH_3), 45.3 and 45.0 (NCH_2), 41.5 and 38.9 ($N(CH_2)_4CH_2$), 29.6 and 28.9 (NCH_2CH_2), 29.0 and 28.4 ($N(CH_2)_3CH_2$), 28.3 and 27.9 ($C(CH_3)_3$), 24.3 and 23.5 ($N(CH_2)_2CH_2$), 14.1 and 14.0 (OCH_2CH_3); ^{13}C NMR (126 MHz, DMSO-d_6, 373 K) δ 171.5 (C=O ester), 154.6 (C=O carbamate), 147.73 (OC_{Ar} quat), 147.65 (OC_{Ar} quat), 119.3 (C_{Ar}), 112.8 (C_{Ar}), 111.5 (C_{Ar}), 78.6 ($C(CH_3)_3$), 69.4 (NC quat), 59.8 (OCH_2CH_3), 55.6 (OCH_3), 55.5 (OCH_3), 44.3 (NCH_2), 28.4 (NCH_2CH_2), 27.4 ($N(CH_3)_2CH_2$), 27.3 ($C(CH_3)_3$), 23.1 ($N(CH_2)_3CH_2$), 13.2 (OCH_2CH_3) (Peak due to C_{Ar} quat in region 136–132 ppm not observed, peak due to $N(CH_2)_4CH_2$ confirmed to be underneath DMSO-d_6 residual solvent signal by HSQC); HRMS (FTMS + pNSI) *m/z* Calculated for $C_{22}H_{34}NO_6^+$ $[M+H]^+$ 408.2381; Found 408.2379.

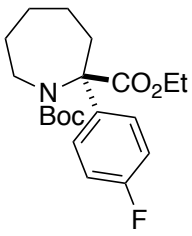
(±)–Di-*tert*-butyl 2-(4-bromophenyl)azepane-1,2-dicarboxylate (150)



$Rh_2(esp)_2$ (1.9 mg, 2.5 μmol) was added to a solution of *tert*-butyl (5-iodopentyl)carbamate **72** (157 mg, 0.50 mmol) and *tert*-butyl 2-(4-bromophenyl)-2-diazoacetate **99** (297 mg, 1.0 mmol) in CH_2Cl_2 (1.67 mL). The reaction vessel was sealed, purged with Ar and heated at 40 ºC for 2.5 h, then allowed to cool to rt. Tetrabutylammonium bromide (16 mg, 50 μmol) was added, followed by $CsOH·H_2O$ (336 mg, 2.0 mmol), and the reaction was stirred at 25 ºC for 18 h. The crude reaction mixture was then filtered through Celite, washing with EtOAc (10 mL), and concentrated under reduced pressure. Purification by flash chromatography (70% to 90% CH_2Cl_2/hexane) afforded di-*tert*-butyl 2-(4-bromophenyl)azepane-1,2-dicarboxylate **150** (97 mg, 43%) as a pale yellow waxy solid. R_f 0.31 (70% CH_2Cl_2/hexane); ν_{max} (film)/cm^{-1} 2974, 2923, 1733 (C=O ester), 1692 (C=O carbamate), 1387, 1241, 1144, 1006, 943, 816; ^{1}H NMR (400 MHz, $CDCl_3$) δ 7.50 and 7.27 (2 × d, J = 8.7 Hz, 2 H, 2 × HC_{Ar}), 7.44–7.40 (m, 2 H, 2 × HC_{Ar}), 3.99 (dd, J = 14.8, 8.5 Hz, 0.5 H, NC*H*H), 3.84–3.67 (m, 1 H, NC*H*H and NCH*H*), 3.26–3.17 (m, 0.5 H, NCH*H*), 2.43 (dd, J = 15.1, 9.5 Hz, 0.5 H, $N(CH_2)_4CHH$), 2.26 (dd, J = 15.1, 9.5 Hz, 0.5 H, $N(CH_2)_4CHH$), 2.10–1.22 (m, 21 H, $NCH_2(CH_2)_3$, $C(CH_3)_3$ ester and $C(CH_3)_3$ carbamate), 1.12 (s, 4 H, $C(CH_3)_3$ carbamate); ^{1}H NMR (500 MHz, DMSO-d_6, 373 K) δ 7.47 (d, J = 8.9 Hz, 2 H, 2 × HC_{Ar}), 7.44–

7.35 (m, 2 H, 2 × HC_{Ar}), 3.78 (ddd, *J* = 15.0, 7.5, 2.0 Hz, 1 H, NC*H*H), 3.47 (br s, 1 H, NCH*H*), 2.37–2.27 (m, 1 H, $N(CH_2)_4CHH$), 2.09–2.01 (m, 1 H, $N(CH_2)_4CHH$), 1.81–1.10 (m, 24 H, $NCH_2(CH_2)_3$, 2 × $C(CH_3)_3$); ^{13}C NMR (101 MHz, $CDCl_3$) δ 172.0 and 171.1 (C=O ester), 155.8 and 155.7 (C=O carbamate), 142.5 and 140.0 (C_{Ar} quat), 130.6 and 130.3 (2 × C_{Ar}), 129.3 and 129.0 (2 × C_{Ar}), 120.7 and 120.1 (BrC_{Ar} quat), 81.4 and 81.0 ($C(CH_3)_3$ ester), 80.9 and 80.0 ($C(CH_3)_3$ carbamate), 70.9 and 70.4 (NC quat), 45.6 and 45.5 (NCH_2), 41.6 and 39.9 ($N(CH_2)_3CH_2$), 29.9 and 29.4 (NCH_2CH_2), 29.1 and 28.9 ($N(CH_2)_2CH_2$), 28.4, 28.0, 27.9 and 27.8 (2 × $C(CH_3)_3$), 24.3 and 23.8 ($N(CH_2)_2CH_2$); ^{13}C NMR (126 MHz, DMSO-d_6, 373 K) δ 171.5 (C=O ester), 154.5 (C=O carbamate), 129.5 (2 × C_{Ar}), 128.8 (2 × C_{Ar}), 118.9 (BrC_{Ar} quat), 80.0 (2 × $C(CH_3)_3$), 70.0 (NC quat), 44.6 (NCH_2), 28.6 (NCH_2CH_2), 27.6 ($N(CH_2)_2CH_2$), 27.1 (2 × $C(CH_3)_3$), 23.2 ($N(CH_3)_2CH_2$), (Peak due to C_{Ar} quat in region 144–138 ppm not observed, peak due to $N(CH_2)_4CH_2$ confirmed to be underneath DMSO-d_6 residual solvent signal by HSQC); HRMS (FTMS + pNSI) *m/z* Calculated for $C_{22}H_{33}NO_4{}^{79}Br^+$ $[M+H]^+$ 454.1587; Found 454.1586.

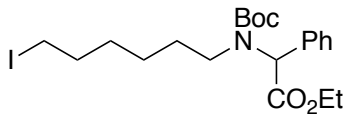
(±)–1-(*tert*-Butyl) 2-ethyl 2-(4-fluorophenyl)azepane-1,2-dicarboxylate (151)



$Rh_2(esp)_2$ (1.9 mg, 2.5 μmol) was added to a solution of *tert*-butyl (5-iodopentyl)carbamate **72** (157 mg, 0.50 mmol) and ethyl 2-diazo-2-(4-fluorophenyl)acetate **91** (208 mg, 1.0 mmol) in CH_2Cl_2 (1.67 mL). The reaction vessel was sealed, purged with Ar and heated at 40 ºC for 2.5 h, then allowed to cool to rt. Tetrabutylammonium bromide (16 mg, 50 μmol) was added, followed by $CsOH·H_2O$ (336 mg, 2.0 mmol), and the reaction was stirred at 25 ºC for 18 h. The crude reaction mixture was then filtered through Celite, washing with EtOAc (10 mL), and concentrated under reduced pressure. Purification by flash chromatography (10% EtOAc/hexane) afforded 1-(*tert*-butyl) 2-ethyl 2-(4-fluorophenyl)azepane-1,2-dicarboxylate **151** (105 mg, 57%) as a white solid. R_f 0.25 (10% EtOAc/hexane); mp = 85–86 ºC; ν_{max} (film)/cm^{-1} 2971, 2926, 1722 (C=O ester), 1685 (C=O carbamate), 1510, 1398, 1290, 1215, 1189, 1152, 1036, 988, 943, 828, 757, 723; ^{1}H NMR (400 MHz, $CDCl_3$) δ 7.55–7.49 (m, 1.2 H, 2 × HC_{Ar}), 7.38–7.33 (m, 0.7 H, 2 × HC_{Ar}), 7.03–6.96 (m, 2 H, 2 × HC_{Ar}), 4.31–4.22 (m, 0.6 H, OCH_2CH_3), 4.20–4.07 (m, 1.4 H, OCH_2CH_3), 3.92 (dd, *J* = 14.7, 7.7 Hz, 0.6 H, NC*H*H), 3.87–3.78 (m, 0.4 H, NC*H*H), 3.71 (dd, *J* = 14.7, 8.8 Hz, 0.6 H, NCH*H*), 3.14 (dd, *J* = 14.4, 10.5 Hz, 0.4 H, NCH*H*), 2.48 (dd, *J* = 14.9, 9.3 Hz, 0.4 H, $N(CH_2)_4CHH$), 2.33 (dd, *J* = 15.0, 9.3 Hz, 0.6 Hz, $N(CH_2)_4CHH$), 2.12–2.00 (m, 1 H, $N(CH_2)_4CHH$), 2.00–1.35 (m, 10 H, $NCH_2(CH_2)_3$ and $C(CH_3)_3$), 1.35–1.10 (m, 9 H, OCH_2CH_3 and $C(CH_3)_3$); ^{1}H NMR (500 MHz, DMSO-d_6, 373 K) δ 7.51–7.42 (m, 2 H, 2 × HC_{Ar}), 7.13–7.06 (m, 2 H, 2 × HC_{Ar}), 4.20–4.04 (m, 2 H , OCH_2CH_3), 3.89–3.80 (m, 1 H, NC*H*H), 3.39 (br s, 1 H, NCH*H*), 2.36 (dd, *J* = 15.2, 9.1 Hz, 1 H, $N(CH_2)_4CHH$), 2.08 (ddd, *J* = 15.4, 9.9, 1.2 Hz, 1 H, $N(CH_2)_4CHH$), 1.80–1.51 (m, 4 H,

NCH_2CH_2 and $N(CH_2)_3CH_2$), 1.49–1.10 (m, 14 H, $N(CH_2)_2CH_2$, OCH_2CH_3 and $C(CH_3)_3$); ^{13}C NMR (101 MHz, $CDCl_3$) δ 173.4 and 172.6 (C=O ester), 161.7 and 161.4 (2 × d, J_{C-F} = 246.7 Hz, FC_{Ar} quat), 156.0 and 155.6 (C=O carbamate), 138.5 and 136.2 (C_{Ar} quat), 128.9 and 128.8 (2 × d, J_{C-F} = 7.7 Hz, 2 × C_{Ar}), 114.3 and 114.1 (2 × d, J_{C-F} = 21.1 Hz, 2 × C_{Ar}), 80.8 and 80.2 ($C(CH_3)_3$), 70.6 and 69.7 (NC quat), 61.2 and 61.1 (OCH_2CH_3), 45.4 and 45.3 (NCH_2), 41.6 and 39.7 ($N(CH_2)_4CH_2$), 29.7 and 29.2 (NCH_2CH_2), 29.2 and 28.7 ($N(CH_2)_3CH_2$), 28.3 and 27.8 ($C(CH_3)_3$), 24.4 and 23.7 ($N(CH_2)_2CH_2$), 14.1 and 14.0 (OCH_2CH_3); ^{13}C NMR (126 MHz, DMSO-d_6, 373 K) δ 171.4 (C=O ester), 160.4 (d, J_{C-F} = 243.6 Hz, FC_{Ar} quat), 154.5 (C=O carbamate), 128.4 (d, J_{C-F} = 7.7 Hz, 2 × C_{Ar}), 113.3 (d, J_{C-F} = 21.4 Hz, 2 × C_{Ar}), 79.1 ($C(CH_3)_3$), 69.5 (NC quat), 60.0 (OCH_2CH_3), 44.4 (NCH_2), 28.5 (NCH_2CH_2), 27.6 ($N(CH_2)_3CH_2$), 27.3 ($C(CH_3)_3$), 23.2 ($N(CH_2)_2CH_2$), 13.2 (OCH_2CH_3) (Peak due to C_{Ar} quat in region 138–136 ppm not observed, peak due to $N(CH_2)_4CH_2$ confirmed to be underneath DMSO-d_6 residual solvent signal by HSQC); ^{19}F NMR (377 MHz, $CDCl_3$) δ –116.8 (m) and –117.2 (m); $^{19}F\{^1H\}$ NMR (377 MHz, DMSO-d_6, 373 K) δ –117.2; HRMS (FTMS + pNSI) *m/z* Calculated for $C_{20}H_{29}NO_4F^+$ $[M+H]^+$ 366.2075; Found 366.2079.

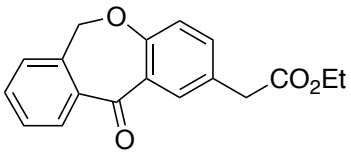
(±)–Ethyl 2-((*tert*-butoxycarbonyl)(6-iodohexyl)amino)-2-phenylacetate (152)



$Rh_2(esp)_2$ (1.9 mg, 2.5 μmol) was added to a solution of *tert*-butyl (6-iodohexyl)carbamate **73** (164 mg, 0.5 mmol) and ethyl 2-diazo-2-phenylacetate **85** (190 mg, 1.0 mmol) in benzene (1.67 mL). The reaction vessel was sealed, purged with Ar and heated at 60 ºC for 2.5 h, then allowed to cool to rt. The reaction mixture was cooled and the solvent was removed under reduced pressure. Purification by flash chromatography (70% CH_2Cl_2/hexane to CH_2Cl_2) afforded ethyl 2-((*tert*-butoxycarbonyl)(6-iodohexyl)amino)-2-phenylacetate **152** (206 mg, 87%) as a pale orange oil. R_f 0.33 (80% CH_2Cl_2/hexane); ν_{max} (film)/cm^{-1} 2976, 2932, 1743 (C=O ester), 1687 (C=O carbamate), 1454, 1392, 1366, 1299, 1253, 1208, 1177, 1146, 1026, 703; ^1H NMR (400 MHz, $CDCl_3$) δ 7.41–7.35 (m, 3 H, 3 × HC_{Ph}), 7.31–7.26 (m, 2 H, 2 × HC_{Ph}), 5.81 and 5.49 (2 × br s, 1 H, NCH), 4.25 (q, *J* = 7.1 Hz, OCH_2CH_3), 3.26–3.16 (m, 1 H, NC*H*H), 3.09 (t, 2 H, *J* = 7.0 Hz, CH_2I), 2.97 (br s, 1 H, NCH*H*), 1.71–1.62 (m, 2 H, NCH_2CH_2), 1.53–0.90 (m, 18 H, $C(CH_3)_3$, OCH_2CH_3 and $N(CH_2)_2(CH_2)_3$); ^{13}C NMR (101 MHz, $CDCl_3$) δ 171.1 (C=O ester), 156.1 (C=O carbamate), 135.3 (C_{Ph} quat), 129.2 (2 × C_{Ph}), 128.5 (2 × C_{Ph}), 128.3 (C_{Ph}), 80.3 ($C(CH_3)_3$), 62.5 (NCH), 61.2 (OCH_2CH_3), 45.4 (NCH_2), 33.2 (CH_2CH_2I), 29.9 (NCH_2CH_2), 28.8 ($N(CH_2)_2CH_2$), 28.4 ($C(CH_3)_3$), 25.6 ($N(CH_2)_3CH_2$), 14.1 (OCH_2CH_3), 6.9 (CH_2I); HRMS (ESI^+) *m/z* Calculated for $C_{21}H_{33}NO_4{}^{127}I$ [M+H] 490.1454; Found 490.1462.

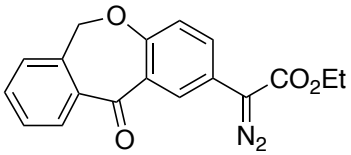
6.2.1.8 Late Stage Functionalisation

Ethyl 2-(11-oxo-6,11-dihydrodibenzo[*b*,*e*]oxepin-2-yl)acetate (154)



2-(11-Oxo-6,11-dihydrodibenzo[*b*,*e*]oxepin-2-yl)acetic acid (1.34 g, 5.0 mmol) and *para*-toluenesulfonic acid monohydrate (95 mg, 0.50 mmol) in EtOH (12.5 mL) were heated under reflux for 2 h. The reaction mixture was cooled to room temperature and the solvent was removed under reduced pressure. Sat. aq. $NaHCO_3$ (50 mL) was added and the aqueous reaction mixture was extracted with EtOAc (3 × 50 mL). Concentration under reduced pressure afforded ethyl 2-(11-oxo-6,11-dihydrodibenzo[*b*,*e*]oxepin-2-yl)acetate **154** (1.39 g, 94%) as a white solid which was used without further purification. R_f 0.11 (20% Et_2O/pentane); mp = 91–92 ºC (lit = 89–90 ºC)[412]; ν_{max} (film)/cm^{-1} 3061, 2982, 2926, 1732 (C=O ester), 1654 (C=O ketone), 1600, 1567, 1491, 1406, 1202, 1230, 1243, 1222, 1177, 1141, 1120, 1105, 1036, 1009, 823, 769, 695; ^{1}H NMR (400 MHz, $CDCl_3$) δ 8.12 (d, *J* = 2.2 Hz, 1 H, HC_{Ar}), 7.92–7.87 (m, 1 H, HC_{Ar}), 7.56 (td, *J* = 7.4, 1.1 Hz, 1 H, HC_{Ar}), 7.51–7.41 (m, 2 H, 2 × HC_{Ar}), 7.37 (d, *J* = 7.4 Hz, 1 H, HC_{Ar}), 7.04 (d, *J* = 8.4 Hz, 1 H, HC_{Ar}), 5.19 (s, 2 H, OCH_2Ar), 4.17 (q, *J* = 7.1 Hz, 2 H, OCH_2CH_3), 3.64 (s, 2 H, CH_2CO_2Et), 1.27 (t, *J* = 7.1 Hz, 3 H, OCH_2CH_3); ^{13}C NMR (101 MHz, $CDCl_3$) δ 190.8 (C=O ketone), 171.4 (C=O ester), 160.4 (OC_{Ar} quat), 140.4 (C_{Ar} quat), 136.3 (C_{Ar}), 135.5 (C_{Ar} quat), 132.7 (C_{Ar}), 132.4 (C_{Ar}), 129.4 (C_{Ar}), 129.2 (C_{Ar}), 127.9 (C_{Ar} quat), 127.8 (C_{Ar}), 125.1 (C_{Ar} quat), 121.0 (C_{Ar}), 73.6 (OCH_2Ar), 61.0 (OCH_2CH_3), 40.2 (CH_2CO_2Et), 14.2 (OCH_2CH_3). The observed characterisation data (^{1}H and ^{13}C NMR) was consistent with that previously reported in the literature.[413]

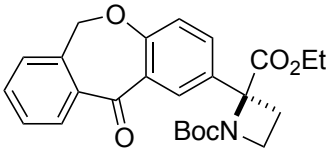
Ethyl 2-diazo-2-(11-oxo-6,11-dihydrodibenzo[*b*,*e*]oxepin-2-yl)acetate (155)



DBU (0.76 mL, 5.1 mmol) was added dropwise over 1 min to a stirred solution of *p*-ABSA (980 mg, 4.1 mmol) and ethyl 2-(11-oxo-6,11-dihydrodibenzo[*b*,*e*]oxepin-2-yl)acetate **154** (1.0 g, 3.4 mmol) in CH_3CN (5.67 mL) at 0 °C. The reaction mixture was stirred at 25 °C for 18 h. Saturated aq. NH_4Cl (50 mL) was added and the aqueous reaction mixture was extracted with Et_2O (3 × 50 mL). The organic layers were dried over Na_2SO_4, filtered and concentrated under reduced pressure. 50% Et_2O/pentane (50 mL) was added and the mixture was filtered, washing with 50% Et_2O/pentane (50 mL), then concentrated under reduced pressure to afford ethyl 2-diazo-2-(11-oxo-6,11-dihydrodibenzo[*b*,*e*]oxepin-2-yl)acetate **155** (1.03 g, 94%) as an orange solid which was used without further purification. R_f 0.11 (20% Et_2O/pentane); ν_{max} (film)/cm^{-1} 2982, 2936, 2085 (C=N=N in-phase), 1693 (C=O ester), 1652 (C=O ketone), 1599, 1490, 1474, 1408, 1371 (C=N=N out-of-phase), 1300, 1288, 1236, 1216, 1156, 1051, 1000, 841, 739; ^{1}H NMR (400 MHz, $CDCl_3$) δ 8.14 (d, *J* = 2.6 Hz, 1

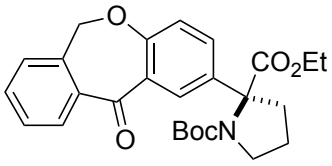
H, HC_{Ar}), 7.91 (d, *J* = 7.5 Hz, 1 H, HC_{Ar}), 7.82 (dd, *J* = 8.7, 2.4 Hz, 1 H, HC_{Ar}), 7.58 (td, *J* = 7.4, 0.8 Hz, 1 H, HC_{Ar}), 7.52–7.47 (m, 1 H, HC_{Ar}), 7.39 (d, *J* = 7.4 Hz, 1 H, HC_{Ar}), 7.12 (d, *J* = 8.7 Hz, 1 H, HC_{Ar}), 5.21 (s, 2 H, OCH_2Ar), 4.35 (q, *J* = 7.1 Hz, 2 H, OCH_2CH_3), 1.36 (t, *J* = 7.1 Hz, 3 H, OCH_2CH_3); ^{13}C NMR (101 MHz, $CDCl_3$) δ 190.4 (C=O ketone), 165.3 (C=O ester), 159.4 (OC_{Ar} quat), 140.2 (C_{Ar} quat), 135.4 (C_{Ar} quat), 132.8 (C_{Ar}), 131.9 (C_{Ar}), 129.5 (C_{Ar}), 129.3 (C_{Ar}), 127.8 (C_{Ar}), 126.7 (C_{Ar}), 125.4 (C_{Ar} quat), 121.7 (C_{Ar}), 119.6 (C_{Ar} quat), 73.6 (OCH_2Ar), 62.5 ($C=N_2$ quat), 61.1 (OCH_2CH_3), 14.5 (OCH_2CH_3); HRMS (ASAP+) *m/z* Calculated for $C_{18}H_{15}O_4^+$ $[M-N_2+H]^+$ 295.0970; Found 295.0972.

(±)–1-(*tert*-Butyl) 2-ethyl 2-(11-oxo-6,11-dihydrodibenzo[*b*,*e*]oxepin-2-yl)azetidine-1,2-dicarboxylate (156)



$Rh_2(esp)_2$ (1.9 mg, 2.5 μmol) was added to a solution of *tert*-butyl (2-chloroethyl)carbamate **52** (90 mg, 0.5 mmol) and ethyl 2-diazo-2-(11-oxo-6,11-dihydrodibenzo[*b*,*e*]oxepin-2-yl)acetate **155** (242 mg, 0.75 mmol) in benzene (1.67 mL). The reaction vessel was sealed, purged with Ar and heated at 60 ºC for 2.5 h, then allowed to cool to rt. Tetrabutylammonium bromide (16 mg, 50 μmol) was added, followed by $CsOH·H_2O$ (168 mg, 1.0 mmol), and the reaction was stirred at 25 ºC for 18 h. The crude reaction mixture was then filtered through Celite, washing with EtOAc (10 mL), and concentrated under reduced pressure. Purification by flash chromatography (20% EtOAc/pentane) afforded 1-(*tert*-butyl) 2-ethyl 2-(11-oxo-6,11-dihydrodibenzo[*b*,*e*]oxepin-2-yl)azetidine-1,2-dicarboxylate **156** (186 mg, 85%) as a white solid. R_f 0.28 (20% EtOAc/pentane); mp = 49–50 ºC; ν_{max} (film)/cm^{-1} 2977, 1737 (C=O ester), 1702 (C=O carbamate), 1648 (C=O ketone), 1488, 1365, 1301, 1206, 1153, 1144, 1130, 1090, 1016, 761, 730; ^1H NMR (400 MHz, $CDCl_3$) δ 8.38–8.21 (m, 1 H, HC_{Ar}), 7.89 (dd, *J* = 7.5, 0.8 Hz, 1 H, HC_{Ar}), 7.79–7.45 (m, 3 H, 3 × HC_{Ar}), 7.37 (d, *J* = 7.3 Hz, 1 H, HC_{Ar}), 7.05 (d, *J* = 8.7 Hz, 1 H, HC_{Ar}), 5.22 (s, 2 H, OCH_2Ar), 4.36–4.14 (m, 3 H, OCH_2CH_3 and NC*H*H), 3.92–3.85 (m, 1 H, NCH*H*), 2.80–2.47 (m, 2 H, NCH_2CH_2), 1.56–1.41 (m, 9 H, $C(CH_3)_3$), 1.38–1.24 (m, 3 H, OCH_2CH_3); ^{13}C NMR (101 MHz, $CDCl_3$) δ 190.8 (C=O ketone), 171.4 (C=O ester), 160.5 (OC_{Ar} quat), 155.8 (C=O carbamate), 140.6 (C_{Ar} quat), 135.4 (C_{Ar} quat), 134.5 and 134.3 (C_{Ar} quat), 133.7 (C_{Ar}), 132.7 (C_{Ar}), 130.1 (C_{Ar}), 129.4 (C_{Ar}), 129.2 (C_{Ar}), 127.8 (C_{Ar}), 124.5 (C_{Ar} quat), 120.4 and 120.2 (C_{Ar}), 80.8 and 80.2 ($C(CH_3)_3$), 73.6 (OCH_2Ar), 72.8 (NC quat), 61.9 (OCH_2CH_3), 46.9 and 45.4 (NCH_2), 30.1 and 29.3 (NCH_2CH_2), 28.3 ($C(CH_3)_3$), 14.2 (OCH_2CH_3); HRMS (FTMS + pNSI) *m/z* Calculated for $C_{25}H_{28}NO_6^+$ $[M+H]^+$ 438.1911; Found 438.1912.

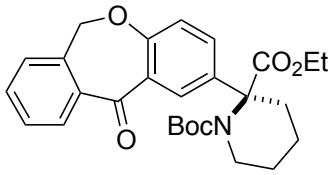
(±)–1-(*tert*-Butyl) 2-ethyl 2-(11-oxo-6,11-dihydrodibenzo[*b*,*e*]oxepin-2-yl)pyrrolidine-1,2-dicarboxylate (157)



$Rh_2(esp)_2$ (1.9 mg, 2.5 μmol) was added to a solution of *tert*-butyl (3-chloropropyl)carbamate **58** (97 mg, 0.5 mmol) and ethyl 2-diazo-2-(11-oxo-6,11-dihydrodibenzo[*b*,*e*]oxepin-2-yl)acetate **155** (242 mg, 0.75 mmol) in benzene (1.67 mL). The reaction vessel was sealed, purged with Ar and heated at 60 ºC for 2.5 h, then allowed to cool to rt. Tetrabutylammonium bromide (16 mg, 50 μmol) was added, followed by $CsOH·H_2O$ (168 mg, 1.0 mmol), and the reaction was stirred at 25 ºC for 18 h. The crude reaction mixture was then filtered through Celite, washing with EtOAc (10 mL), and concentrated under reduced pressure. Purification by flash chromatography (20% EtOAc/pentane) afforded 1-(*tert*-butyl) 2-ethyl 2-(11-oxo-6,11-dihydrodibenzo[*b*,*e*]oxepin-2-yl)pyrrolidine-1,2-dicarboxylate **157** (200 mg, 88%) as a white solid. R_f 0.21 (20% EtOAc/pentane); mp = 51–54 ºC; ν_{max} (film)/cm^{-1} 2978, 2874, 1738 (C=O ester), 1691 (C=O carbamate), 1647 (C=O ketone), 1486, 1387, 1366, 1297, 1286, 1244, 1160, 1146, 1121, 1104, 1016, 913, 761, 727; ^{1}H NMR (400 MHz, $CDCl_3$) δ 8.25 and 8.18 (2 × d, *J* = 2.5 Hz, 0.6 H, HC_{Ar}), 7.88 (dd, *J* = 7.6, 1.2 Hz, 1 H, HC_{Ar}), 7.60–7.42 (m, 3 H, 3 × HC_{Ar}), 7.36 (t, *J* = 7.0 Hz, 1 H, HC_{Ar}), 7.02 (dd, *J* = 8.7, 3.1 Hz, 1 H, HC_{Ar}), 5.22–5.16 (m, 2 H, OCH_2Ar), 4.36–4.10 (m, 2 H, OCH_2CH_3), 3.78–3.62 (m, 2 H, NCH_2), 2.67–2.52 (m, 1 H, $N(CH_2)_2CHH$), 2.35–2.23 (m, 1 H, $N(CH_2)_2CHH$), 1.99–1.88 (m, 1 H, NCH_2CHH), 1.78–1.63 (m, 1 H, NCH_2CHH), 1.53 (s, 3 H, $C(CH_3)_3$), 1.35–1.24 (m, 9 H, $C(CH_3)_3$ and OCH_2CH_3); ^{1}H NMR (400 MHz, DMSO-d_6, 373 K) δ 8.15–8.11 (m, 1 H, HC_{Ar}), 7.83–7.78 (m, 1 H, HC_{Ar}), 7.68–7.62 (m, 1 H, HC_{Ar}), 7.61–7.50 (m, 3 H, 3 × HC_{Ar}), 7.09–7.04 (m, 1 H, HC_{Ar}), 5.30–5.27 (m, 2 H, OCH_2Ar), 4.23–4.13 (m, 2 H, OCH_2CH_3), 3.67–3.57 (m, 2 H, NCH_2), 2.60–2.53 (m, 1 H, $N(CH_2)_2CHH$), 2.29–2.21 (m, 1 H, $N(CH_2)_2CHH$), 1.99–1.87 (m, 1 H, NCH_2CHH), 1.74–1.61 (m, 1 H, NCH_2CHH), 1.58–1.12 (m, 12 H, $C(CH_3)_3$ and OCH_2CH_3); ^{13}C NMR (101 MHz, $CDCl_3$) δ 190.5 and 190.3 (C=O ketone), 172.4 and 172.2 (C=O ester), 160.2 and 159.8 (OC_{Ar} quat), 153.8 and 153.5 (C=O carbamate), 140.3 and 140.2 (C_{Ar} quat), 135.4 and 135.1 (C_{Ar} quat), 134.9 and 134.1 (C_{Ar}), 134.0 and 133.3 (C_{Ar} quat), 132.3 and 132.2 (C_{Ar}), 130.4 and 129.7 (C_{Ar}), 129.2 and 129.1 (C_{Ar}), 128.9 and 128.8 (C_{Ar}), 127.40 and 127.35 (C_{Ar}), 123.9 (C_{Ar} quat), 119.7 and 119.2 (C_{Ar}), 80.1 and 79.8 ($C(CH_3)_3$), 73.3 and 73.2 (OCH_2Ar), 70.73 and 70.67 (NC quat), 61.2 (OCH_2CH_3), 47.7 and 47.6 (NCH_2), 43.0 and 41.1 ($N(CH_2)_2CH_2$), 28.1 and 27.7 ($C(CH_3)_3$), 23.1 and 22.3 (NCH_2CH_2), 13.8 (OCH_2CH_3); ^{13}C NMR (101 MHz, DMSO-d_6, 373 K) δ 189.4 (C=O ketone), 171.2 (C=O ester), 159.1 (OC_{Ar} quat), 152.7 (C=O carbamate), 139.5 (C_{Ar} quat), 135.4 (C_{Ar} quat), 134.2 (C_{Ar}), 134.0 (C_{Ar} quat), 132.2 (C_{Ar}), 129.2 (C_{Ar}), 128.5 (C_{Ar}), 128.2 (C_{Ar}), 127.6 (C_{Ar}), 123.5 (C_{Ar} quat), 118.9 (C_{Ar}), 78.8 ($C(CH_3)_3$), 72.5 (OCH_2Ar), 70.2 (NC quat), 60.4 (OCH_2CH_3), 47.4 (NCH_2), 41.6 ($N(CH_2)_2CH_2$),

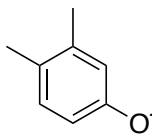
27.4 (C(CH_3)$_3$), 22.0 (NCH$_2$$CH_2$), 13.3 (OCH$_2$$CH_3$); HRMS (FTMS + pNSI) *m/z* Calculated for $C_{26}H_{30}NO_6^+$ $[M+H]^+$ 425.2068; Found 452.2070.

(±)–1-(*tert*-Butyl) 2-ethyl 2-(11-oxo-6,11-dihydrodibenzo[*b*,*e*]oxepin-2-yl)piperidine-1,2-dicarboxylate (158)



$Rh_2(esp)_2$ (1.9 mg, 2.5 μmol) was added to a solution of *tert*-butyl (4-iodobutyl)carbamate **60** (150 mg, 0.5 mmol) and ethyl 2-diazo-2-(11-oxo-6,11-dihydrodibenzo[*b*,*e*]oxepin-2-yl)acetate **155** (366 mg, 1.0 mmol) in CH_2Cl_2 (1.67 mL). The reaction vessel was sealed, purged with Ar and heated at 60 ºC for 2.5 h, then allowed to cool to rt. Tetrabutylammonium bromide (16 mg, 50 μmol) was added, followed by KOH (112 mg, 2.0 mmol), and the reaction was stirred at 25 ºC for 18 h. The crude reaction mixture was then filtered through Celite, washing with EtOAc (10 mL), and concentrated under reduced pressure. Purification by flash chromatography (10% EtOAc/pentane) afforded 1-(*tert*-butyl) 2-ethyl 2-(11-oxo-6,11-dihydrodibenzo[*b*,*e*]oxepin-2-yl)piperidine-1,2-dicarboxylate **158** (169 mg, 72%) as a white solid. R_f 0.40 (20% EtOAc/pentane); mp = 51–55 ºC; ν_{max} (film)/cm^{-1} 2977, 1734 (C=O ester), 1690 (C=O carbamate), 1648 (C=O ketone), 1486, 1366, 1299, 1279, 1243, 1199, 1157, 913, 729; ^{1}H NMR (400 MHz, $CDCl_3$) δ 8.14 (br s, 1 H, HC_{Ar}), 7.88 (dd, *J* = 7.6, 1.2 Hz, 1 H, HC_{Ar}), 7.58–7.52 (m, 2 H, 2 × HC_{Ar}), 7.47 (td, *J* = 7.6, 1.2 Hz, 1 H, HC_{Ar}), 7.37 (dd, *J* = 7.5, 0.8 Hz, 1 H, HC_{Ar}), 7.05 (d, *J* = 8.7 Hz, 1 H, HC_{Ar}), 5.20 (s, 2 H, OCH$_2$Ar), 4.20 (q, *J* = 7.1 Hz, 2 H, OC*H*$_2$CH$_3$), 3.97–3.86 (m, 1 H, NC*H*H), 3.30 (br s, 1 H, NCH*H*), 2.43–2.23 (m, 2 H, N(CH$_2$)$_3$C*H*$_2$), 1.75–1.15 (m, 16 H, NCH$_2$(C*H*$_2$)$_2$, C(CH$_3$)$_3$ and OCH$_2$C*H*$_3$); ^{13}C NMR (101 MHz, $CDCl_3$) δ 190.7 (C=O ketone), 172.7 (C=O ester), 160.3 (OC_{Ar} quat), 156.1 (C=O carbamate), 140.6 (C_{Ar} quat), 135.5 (C_{Ar}), 135.3 (C_{Ar} quat), 132.6 (C_{Ar}), 130.8 (C_{Ar}), 129.5 (C_{Ar}), 129.2 (C_{Ar}), 127.7 (C_{Ar}), 124.4 (C_{Ar} quat), 120.2 (C_{Ar}), 80.8 (*C*(CH$_3$)$_3$), 73.6 (OCH$_2$Ar), 66.9 (NC quat), 61.2 (O*C*H$_2$CH$_3$), 42.4 (NCH$_2$), 34.8 (br s, N(CH$_2$)$_3$*C*H$_2$), 28.2 (C(*C*H$_3$)$_3$), 23.6 (NCH$_2$*C*H$_2$), 18.6 (N(CH$_2$)$_2$*C*H$_2$), 14.1 (OCH$_2$*C*H$_3$) (The peak due to the C_{Ar} quat adjacent to the piperidine was not observed due to rotameric effects); HRMS (FTMS + pNSI) *m/z* Calculated for $C_{27}H_{32}NO_6^+$ $[M+H]^+$ 466.2224; Found 466.2221.

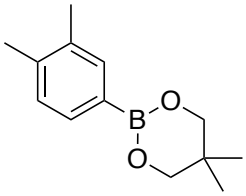
3,4-Dimethylphenyl trifluoromethanesulfonate (161)



Trifluoromethanesulfonic anhydride (1.68 mL, 10 mmol) was added dropwise over 2 min to a stirring solution of 3,4-dimethylphenol (611 mg, 5.0 mmol), pyridine (1.16 mL, 15.0 mmol) in CH_2Cl_2 (10 mL) at 0 ºC. The reaction mixture was heated to 25 ºC and stirred for a further 1 h then H_2O (50 mL) was added. The aqueous reaction mixture was extracted with CH_2Cl_2 (3 × 50 mL). The solvent was removed under

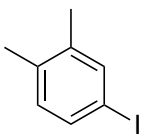
reduced pressure to afford 3,4-dimethylphenyl trifluoromethanesulfonate **161** (1.10 g, 87%) as a yellow oil which was used without further purification. R_f 0.75 (5% Et_2O/pentane); ν_{max} (film)/cm^{-1} 2927, 1496, 1422, 1208, 1141, 939, 852; ^1H NMR (400 MHz, $CDCl_3$) δ 7.19 (d, J = 8.3 Hz, 1 H, HC_{Ar}), 7.05 (d, J = 2.6 Hz, 1 H, HC_{Ar}), 7.01 (dd, J = 8.3, 2.6 Hz, 1 H, HC_{Ar}), 2.30 (s, 3 H, $ArCH_3$), 2.28 (s, 3 H, $ArCH_3$); ^{13}C NMR (101 MHz, $CDCl_3$) δ 147.6 (OC_{Ar} quat), 139.1 (C_{Ar} quat), 137.1 (C_{Ar} quat), 130.9 (C_{Ar}), 122.0 (C_{Ar}), 118.8 (q, J_{C-F} = 321.6 Hz, SO_2CF_3), 118.3 (C_{Ar}), 19.9 ($ArCH_3$), 19.2 ($ArCH_3$); $^{19}F\{^1H\}$ NMR (377 MHz, $CDCl_3$) δ –73.0. The observed characterisation data (IR, ^1H and ^{13}C NMR) was consistent with that previously reported in the literature.[414]

2-(3,4-Dimethylphenyl)-5,5-dimethyl-1,3,2-dioxaborinane (162)



A mixture of 3,4-dimethylphenyl trifluoromethanesulfonate **161** (835 mg, 3.3 mmol), bis(neopentyl glycolato)diboron (1.11 g, 4.9 mmol), $Pd(dppf)Cl_2{\cdot}CH_2Cl_2$ (133 mg, 0.16 mmol) and KOAc (968 mg, 9.8 mmol) in 1,4-dioxane (16 mL) was stirred at 80 ºC for 18 h. The reaction mixture was cooled to rt and filtered through celite, washing with EtOAc and concentrated under reduced pressure. Purification by flash chromatography (15% Et_2O/pentane) afforded 2-(3,4-dimethylphenyl)-5,5-dimethyl-1,3,2-dioxaborinane **162** (655 mg, 92%) as a white solid. R_f 0.40 (20% Et_2O/pentane); mp = 79–82 ºC; ν_{max} (film)/cm^{-1} 2960, 2872, 1613, 1478, 1418, 1339, 1310, 1285, 1225, 1180, 1120, 1003, 723, 701, 660; ^1H NMR (400 MHz, $CDCl_3$) δ 7.60 (s, 1 H, HC_{Ar}), 7.56 (d, J = 7.5 Hz, 1 H, HC_{Ar}), 7.16 (d, J = 7.5 Hz, 1 H, HC_{Ar}), 3.79 (s, 4 H, 2 × OCH_2), 2.30 (s, 6 H, 2 × $ArCH_3$), 1.04 (s, 6 H, $C(CH_3)_2$); ^{13}C NMR (101 MHz, $CDCl_3$) δ 139.4 (C_{Ar} quat), 135.6 (C_{Ar} quat), 135.1 (C_{Ar}), 131.5 (C_{Ar}), 129.0 (C_{Ar}), 72.3 (2 × OCH_2), 31.9 (OCH_2C quat), 21.9 ($C(CH_3)_2$), 19.9 ($ArCH_3$), 19.6 ($ArCH_3$) (The BC_{Ar} quat peak was not observed); ^{11}B NMR (128 MHz, $CDCl_3$) δ 27.0; HRMS (FTMS + pAPCI) *m/z* Calculated for $C_{13}H_{18}O_2{}^{10}B^+$ $[M–H]^+$ 216.1431; Found 216.1433.

4-Iodo-1,2-dimethylbenzene (163)

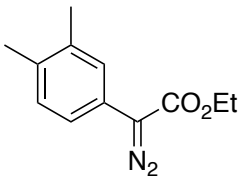


Adapted from a procedure by Burke.[415]

A solution of NaI (372 mg, 2.5 mmol) in H_2O (5 mL) was added to a solution of 2-(3,4-dimethylphenyl)-5,5-dimethyl-1,3,2-dioxaborinane **162** (436 mg, 2.0 mmol) in 1:1 THF/H_2O (0.8 mL) at 0 ºC. Chloroamine-T·$3H_2O$ (1.13 g, 4.0 mmol) in 1:1 THF/H_2O (8 mL) was added dropwise at 0 ºC. The reaction mixture was stirred at 25 ºC for 18 h. Sat. aq. $Na_2S_2O_3$ (50 mL) was added and the aqueous mixture was extracted with Et_2O (3 × 50 mL). The combined organic layers were dried over Na_2SO_4, filtered and concentrated under reduced

pressure. Purification by flash chromatography (pentane) afforded 4-iodo-1,2-dimethylbenzene **163** (464 mg, 88%) as a yellow oil. R_f 0.71 (pentane); ν_{max} (film)/cm^{-1} 2940, 2918, 1588, 1483, 1447, 1181, 848, 803; ^{1}H NMR (400 MHz, $CDCl_3$) δ 7.49 (s, 1 H, HC_{Ar}), 7.42 (dd, J = 7.9, 1.5 Hz, 1 H, HC_{Ar}), 6.88 (d, J = 7.9 Hz, 1 H, HC_{Ar}), 2.22 and 2.21 (2 × s, 6 H, 2 × $ArCH_3$); ^{13}C NMR (101 MHz, $CDCl_3$) δ 139.1 (C_{Ar} quat), 138.2 (C_{Ar}), 136.1 (C_{Ar} quat), 134.7 (C_{Ar}), 131.4 (C_{Ar}), 90.6 (IC_{Ar} quat), 19.4 ($ArCH_3$), 19.3 ($ArCH_3$). The observed characterisation data (^{1}H and ^{13}C NMR) was consistent with that previously reported in the literature.[416]

Ethyl 2-diazo-2-(3,4-dimethylphenyl)acetate (164)

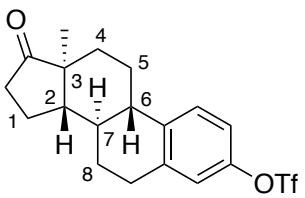


Adapted from a procedure by Wang.[223]

Ethyl 2-diazo-3-oxobutanoate **102** (0.33 mL, 2.4 mmol) was added to a solution of 4-iodo-1,2-dimethylbenzene **163** (464 mg, 2.0 mmol), $Pd(PPh_3)_4$ (116 mg, 0.1 mmol) and dry NaOH* (240 mg, 6.0 mmol) in degassed EtOH (8.0 mL) and stirred at 25 ºC for 18 h. The reaction mixture was filtered through silica, washing with EtOAc (50 mL) and concentrated under reduced pressure. Purification by flash chromatography (2% Et_2O/pentane) afforded ethyl 2-diazo-2-(3,4-dimethylphenyl)acetate **164** (300 mg, 69%) as an orange solid. R_f 0.21 (2% Et_2O/pentane); ν_{max} (film)/cm^{-1} 2972, 2920, 2079 (C=N=N out-of-phase), 1695 (C=O), 1505, 1372 (C=N=N in-phase), 1345, 1245, 1172, 1111, 892, 805, 706; ^{1}H NMR (400 MHz, $CDCl_3$) δ 7.27–7.24 (m, 1 H, HC_{Ar}), 7.22 (dd, J = 8.0, 1.9 Hz, 1 H, HC_{Ar}), 7.16 (d, J = 8.0 Hz, 1 H, HC_{Ar}), 4.33 (q, J = 7.1 Hz, 2 H, OCH_2CH_3), 2.28 and 2.26 (2 × s, 6 H, 2 × $ArCH_3$), 1.35 (t, J = 7.1 Hz, 3 H, OCH_2CH_3); ^{13}C NMR (101 MHz, $CDCl_3$) δ 165.6 (C=O), 137.3 (C_{Ar} quat), 134.4 (C_{Ar} quat), 130.2 (C_{Ar}), 125.3 (C_{Ar}), 122.5 (C_{Ar} quat), 121.7 (C_{Ar}), 60.9 (OCH_2CH_3), 19.9 ($ArCH_3$), 19.3 ($ArCH_3$), 14.5 (OCH_2CH_3). The observed characterisation data (^{1}H and ^{13}C NMR) was consistent with that previously reported in the literature.[223]

*The NaOH was weighed and then dried over a flame in the vial.

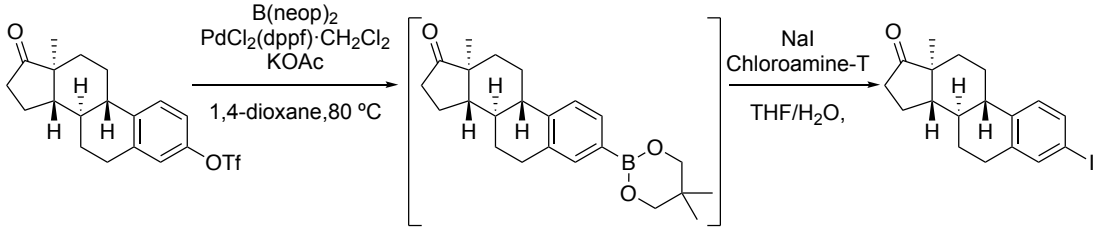
(8*R*,9*S*,13*S*,14*S*)-13-Methyl-17-oxo-7,8,9,11,12,13,14,15,16,17-decahydro-6*H*-cyclopenta[*a*]phenanthren-3-yl trifluoromethanesulfonate (165)



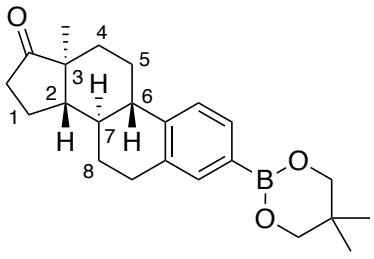
Trifluoromethanesulfonic anhydride (1.86 mL, 15 mmol) was added dropwise over 2 min to a stirring solution of estrone (1.35 g, 5.0 mmol) and pyridine (1.21 mL, 10.0 mmol) in CH_2Cl_2 (10 mL) at 0 ºC. The reaction mixture was heated to 25 ºC and stirred for a further 4 h then H_2O (50 mL) was added. The aqueous reaction mixture was extracted with CH_2Cl_2 (3 × 50 mL). The combined organic layers were dried over Na_2SO_4, filtered and

concentrated under reduced pressure. Purification by flash chromatography (20% to 30% Et_2O/pentane) afforded (8*R*,9*S*,13*S*,14*S*)-13-methyl-17-oxo-7,8,9,11,12,13,14,15,16,17-decahydro-6*H*-cyclopenta[*a*]phenanthren-3-yl trifluoromethanesulfonate **165** (1.94 g, 97%) as a white solid (addition of pentane aided solid formation). R_f 0.25 (20% Et_2O/pentane); mp = 82–83 ºC (lit = 87–88 ºC)[417]; ν_{max} (film)/cm^{-1} 2933, 2865, 1737 (C=O), 1490, 1417, 1249, 1204, 1138, 918, 898, 882, 837; ^{1}H NMR (400 MHz, $CDCl_3$) δ 7.35 (d, *J* = 8.7 Hz, 1 H, HC_{Ar}), 7.04 (dd, *J* = 8.7, 2.7 Hz, 1 H, HC_{Ar}), 7.00 (d, *J* = 2.7 Hz, 1 H, HC_{Ar}), 2.98–2.92 (m, 2 H, $ArCH_2$), 2.52 (dd, *J* = 19.1, 9.0 Hz, 1 H, ArCH), 2.45–2.38 (m, 1 H, C*H*HCO), 2.36–2.26 (m, 1 H, CH*H*CO), 2.22–1.95 (m, 4 H, 4 × CH*H*), 1.71–1.41 (m, 6 H, 4 × CH*H* and 2 × CH), 0.93 (s, 3 H, CH_3); ^{13}C NMR (101 MHz, $CDCl_3$) δ 220.3 (C=O), 147.6 (OC_{Ar} quat), 140.3 (C_{Ar} quat), 139.3 (C_{Ar} quat), 127.2 (C_{Ar}), 121.2 (C_{Ar}), 118.7 (q, *J* = 320.4 Hz, CF_3), 118.3 (C_{Ar}), 50.4 (C_2), 47.8 (C_3 quat), 44.1 (C_6), 37.7 (C_7), 35.8 (CH_2CO), 31.5 (C_4), 29.4 (CH_2Ar), 26.1 (C_8), 25.7 (C_5), 21.5 (C_1), 13.8 (CH_3); ^{19}F{^{1}H} (377 MHz, $CDCl_3$) δ –73.0. The observed characterisation data (^{1}H and ^{13}C NMR) was consistent with that previously reported in the literature.[418]

(8*R*,9*S*,13*S*,14*S*)-3-Iodo-13-methyl-6,7,8,9,11,12,13,14,15,16-decahydro-17*H*-cyclopenta[*a*]phenanthren-17-one (167)



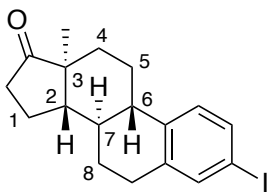
Adapted from a procedure by Burke.[415]



A solution of triflate **165** (1.96 g, 4.9 mmol), bis(neopentyl glycolato)diboron (1.65 g, 7.5 mmol), $Pd(dppf)Cl_2.CH_2Cl_2$ (200 mg, 0.25 mmol), KOAc (1.45 g, 15.0 mmol) in 1,4-dioxane (25 mL) was stirred at 80 ºC for 18 h. The reaction mixture was cooled to rt and filtered through Celite, washing with EtOAc (100 mL), then concentrated under reduced pressure. Purification by flash chromatography (50% EtOAc/hexane) afforded (8*R*,9*S*,13*S*,14*S*)-3-(5,5-dimethyl-1,3,2-dioxaborinan-2-yl)-13-methyl-6,7,8,9,11,12,13,14,15,16-decahydro-17*H*-cyclopenta[*a*]phenanthren-17-one **166** (2.09 g) as an impure off-white solid.

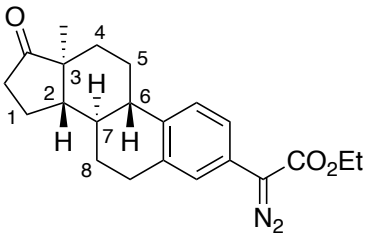
A reaction with 0.5 mmol scale of triflate (purification by flash chromatography (30% Et_2O/pentane) afforded pure (8*R*,9*S*,13*S*,14*S*)-3-(5,5-dimethyl-1,3,2-dioxaborinan-2-yl)-13-methyl-6,7,8,9,11,12,13,14,15,16-decahydro-17*H*-cyclopenta[*a*]phenanthren-17-one **166**

(101 mg, 55%) as a white solid. R_f 0.44 (50% EtOAc/hexane); mp = 229–231 ºC; ν_{max} (film)/cm^{-1} 2937, 1732 (C=O), 1477, 1422, 1310, 1273, 1249, 1178, 1127, 1007, 716, 708, 667; ^{1}H NMR (400 MHz, $CDCl_3$) δ 7.59 (d, J = 7.8 Hz, 1 H, HC_{Ar}), 7.56 (s, 1 H, HC_{Ar}), 7.31 (d, J = 7.8 Hz, 1 H, HC_{Ar}), 3.77 (s, 4 H, 2 × OCH_2), 2.97–2.91 (m, 2 H, $ArCH_2$), 2.56–2.43 (m, 2 H, C*H*HCO and CHAr), 2.38–2.30 (m, 1 H, CH*H*CO), 2.21–1.94 (m, 4 H, 4 × CH*H*), 1.71–1.39 (m, 6 H, 4 × CH*H* and 2 × CH), 1.03 (s, 6 H, $OCH_2C(CH_3)_2$), 0.92 (s, 3 H, CH_3); ^{13}C NMR (101 MHz, $CDCl_3$) δ 220.9 (C=O), 142.4 (C_{Ar} quat), 135.5 (C_{Ar} quat), 134.7 (C_{Ar}), 131.3 (C_{Ar}), 124.6 (C_{Ar}), 72.3 (2 × OCH_2), 50.6 (C_2), 48.0 (C_3 quat), 44.7 (C_6), 38.1 (C_7), 35.8 (CH_2CO), 31.9 (OCH_2C quat), 31.6 (C_4), 29.2 (CH_2Ar), 26.5 (C_8), 25.6 (C_5), 21.9 ($C(CH_3)_2$), 21.6 (C_1), 13.8 (CH_3) (The quaternary carbon adjacent to boron was not observed); ^{11}B NMR (128 MHz, $CDCl_3$) δ 27.0; HRMS (FTMS + pAPCI) *m/z* Calculated for $C_{23}H_{32}O_3{}^{10}B^+$ $[M+H]^+$ 366.2475; Found 366.2480.



A solution of NaI (871 mg, 5.85 mmol) in H_2O (12 mL) was added to a solution of impure **166** (1.43 g, 3.9 mmol) in 1:1 THF/H_2O (2.0 mL) at 0 ºC. Chloroamine-T·3H_2O (2.74 g, 9.75 mmol) in 1:1 THF/H_2O (20 mL) was added dropwise at 0 ºC. The reaction mixture was stirred at 25 ºC for 36 h. Sat. aq. $Na_2S_2O_3$ (100 mL) was added and the aqueous mixture was extracted with EtOAc (4 × 100 mL). The combined organic layers were dried over Na_2SO_4, filtered and concentrated under reduced pressure. Purification by flash chromatography (30% EtOAc/hexane) afforded (8*R*,9*S*,13*S*,14*S*)-3-iodo-13-methyl-6,7,8,9,11,12,13,14,15,16-decahydro-17*H*-cyclopenta[*a*]phenanthren-17-one **167** (829 mg, 65% over two steps). R_f 0.28 (20% EtOAc/hexane); mp = 225–228 ºC; ν_{max} (film)/cm^{-1} 2930, 2869, 1737 (C=O), 1478, 1453, 1009, 807; ^{1}H NMR (400 MHz, $CDCl_3$) δ 7.49–7.44 (m, 2 H, 2 × HC_{Ar}), 7.03 (d, J = 8.1 Hz, 1 H, HC_{Ar}), 2.91–2.85 (m, 2 H, $ArCH_2$), 2.52 (dd, J = 19.0, 8.8 Hz, 1 H, ArCH), 2.43–2.34 (m, 1 H, C*H*HCO), 2.30–1.93 (m, 5 H, CH*H*CO and 4 × C*H*H), 1.69–1.37 (m, 6 H, 4 × CH*H* and 2 × CH), 0.91 (s, 3 H, CH_3); ^{13}C NMR (101 MHz, $CDCl_3$) δ 220.5 (C=O), 139.5 (C_{Ar} quat), 139.1 (C_{Ar} quat), 137.7 (C_{Ar}), 134.7 (C_{Ar}), 127.4 (C_{Ar}), 91.1 (IC_{Ar} quat), 50.4 (C_2), 47.9 (C_3 quat), 44.1 (C_6), 37.8 (C_7), 35.8 (CH_2CO), 31.5 (C_4), 28.9 (CH_2Ar), 26.2 (C_8), 25.5 (C_5), 21.5 (C_1), 13.8 (CH_3). The observed characterisation data (^{1}H and ^{13}C NMR) was consistent with that previously reported in the literature.[419]

Ethyl 2-diazo-2-((8*R*,9*S*,13*S*,14*S*)-13-methyl-17-oxo-7,8,9,11,12,13,14,15,16,17-decahydro-6*H*-cyclopenta[*a*]phenanthren-3-yl)acetate (159)



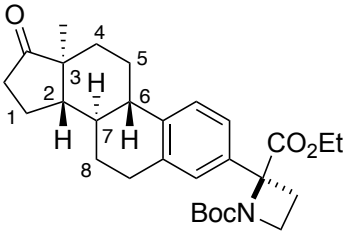
Adapted from a procedure by Wang.[223]

Ethyl 2-diazo-3-oxobutanoate **102** (0.33 mL, 2.4 mmol) was added to a solution of aryl iodide **167** (761 mg, 2.0 mmol), $Pd(PPh_3)_4$ (116 mg, 0.1 mmol), dry NaOH* (240 mg, 6.0 mmol) in degassed EtOH (8.0 mL) and stirred at 25 ºC for 18 h. The reaction mixture was filtered through silica, washing with EtOAc (50 mL) and concentrated under reduced pressure. Purification by flash chromatography (10% to 20% EtOAc/pentane) afforded ethyl 2-diazo-2-((8*R*,9*S*,13*S*,14*S*)-13-methyl-17-oxo-7,8,9,11,12,13,14,15,16,17-decahydro-6*H*-cyclopenta[*a*]phenanthren-3-yl)acetate **159** (527 mg, 72%) as an orange solid. R_f 0.21 (10% EtOAc/pentane); ν_{max} (film)/cm^{-1} 2937, 2856, 2093 (C=N=N out-of-phase), 1736 (C=O ketone), 1690 (C=O ester), 1502, 1453, 1371 (C=N=N in-phase), 1331, 1239, 1181, 1157, 1049, 813; ^{1}H NMR (400 MHz, $CDCl_3$) δ 7.32 (d, J = 8.9 Hz, 1 H, HC_{Ar}), 7.26–7.22 (m, 2 H, 2 × HC_{Ar}), 4.33 (q, J = 7.1 Hz, 2 H, OCH_2CH_3), 2.96–2.90 (m, 2 H, $ArCH_2$), 2.52 (dd, J = 19.1, 8.9 Hz, 1 H, ArCH), 2.46–2.39 (m, 1 H, C*H*HCO), 2.35–2.26 (m, 1 H, CH*H*CO), 2.21–1.93 (m, 4 H, 4 × C*H*H), 1.70–1.40 (m, 6 H, 4 × CH*H* and 2 × CH), 1.35 (t, J = 7.1 Hz, 3 H, OCH_2CH_3), 0.92 (s, 3 H, CH_3); ^{13}C NMR (101 MHz, $CDCl_3$) δ 220.7 (C=O ketone), 165.4 (C=O ester), 137.6 (C_{Ar} quat), 137.2 (C_{Ar} quat), 130.0 (C_{Ar}), 124.6 (C_{Ar}), 122.7 (C_{Ar} quat), 121.6 (C_{Ar}), 62.7 ($C=N_2$ quat), 60.9 (OCH_2CH_3), 50.4 (C_2), 48.0 (C_3 quat), 44.2 (C_6), 38.1 (C_7), 35.8 (CH_2CO), 31.5 (C_4), 29.5 (CH_2Ar), 26.4 (C_8), 25.7 (C_5), 21.6 (C_1), 14.5 (OCH_2CH_3), 13.8 (CH_3). The observed characterisation data (^{1}H and ^{13}C NMR) was consistent with that previously reported in the literature.[223]

*The NaOH was weighed and then dried over a flame in the vial.

(±)–1-(*tert*-Butyl) 2-ethyl 2-((8*R*,9*S*,13*S*,14*S*)-13-methyl-17-oxo-7,8,9,11,12,13,14,15,16,17-decahydro-6*H*-cyclopenta[*a*]phenanthren-3-yl)azetidine-1,2-dicarboxylate (168)

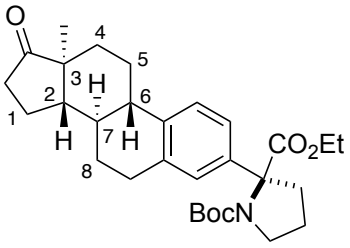
Note: Steroid derivatives are assumed to be a 1:1 mixture of diastereoisomers.



$Rh_2(esp)_2$ (0.8 mg, 1.0 μmol) was added to a solution of *tert*-butyl (2-chloroethyl)carbamate **52** (36 mg, 0.20 mmol) and ethyl 2-diazo-2-((8*R*,9*S*,13*S*,14*S*)-13-methyl-17-oxo-7,8,9,11,12,13,14,15,16,17-decahydro-6*H*-cyclopenta[*a*]phenanthren-3-yl)acetate **159** (110 mg, 0.30 mmol) in benzene (0.67 mL). The reaction vessel was sealed, purged with Ar and heated at 60 ºC for

2.5 h, then allowed to cool to rt. Tetrabutylammonium bromide (6.4 mg, 20 μmol) was added, followed by $CsOH{\cdot}H_2O$ (67 mg, 0.40 mmol), and the reaction was stirred at 25 ºC for 18 h. The crude reaction mixture was then filtered through Celite, washing with EtOAc (10 mL), and concentrated under reduced pressure. Purification by flash chromatography (20% EtOAc/pentane) afforded 1-(*tert*-butyl) 2-ethyl 2-((8*R*,9*S*,13*S*,14*S*)-13-methyl-17-oxo-7,8,9,11,12,13,14,15,16,17-decahydro-6*H*-cyclopenta[*a*]phenanthren-3-yl)azetidine-1,2-dicarboxylate **168** (54 mg, 56%) as a white solid. R_f 0.16 (20% EtOAc/pentane); ν_{max} (film)/cm^{-1} 2929, 1736 (C=O ketone/ester), 1702 (C=O carbamate), 1363, 1236, 1153, 1088, 1008, 775; mp = 60–65 ºC; ^{1}H NMR (400 MHz, $CDCl_3$) δ 7.33–7.13 (m, 3 H, 3 × HC_{Ar}), 4.35–4.10 (m, 3 H, OCH_2CH_3 and NC*H*H), 3.87 (td, *J* = 13.0, 8.5, 4.9 Hz, 1 H, NCH*H*), 3.02–2.86 (m, 2 H, $ArCH_2$), 2.80–2.63 (m, 1 H, NCH_2CHH), 2.59–2.39 (m, 3 H, ArCH, C*H*HCO and NCH_2CHH), 2.37–2.26 (m, 1 H, CH*H*CO), 2.22–1.93 (m, 4 H, C_1HH, C_4HH, C_5HH and C_8HH), 1.71–1.21 (m, 18 H, C_1HH, C_4HH, C_5HH, C_8HH, C_2H, C_7H, $C(CH_3)_3$ and OCH_2CH_3), 0.92 (s, 3 H, CH_3); ^{13}C NMR (101 MHz, $CDCl_3$) δ 220.8 (C=O ketone), 171.6 (C=O ester), 156.0 (C=O carbamate), 138.8 (C_{Ar} quat), 137.9 (C_{Ar} quat), 135.8 (C_{Ar} quat), 127.0 (C_{Ar}), 124.8 (C_{Ar}), 123.9 (C_{Ar}), 80.4 ($C(CH_3)_3$), 73.2 (NC quat), 61.7 (OCH_2CH_3), 50.5 (C_2), 48.0 (C_3 quat), 46.9 and 45.4 (NCH_2), 44.37 and 44.34 (C_6), 38.1 (C_7), 35.9 (CH_2CO), 31.6 (C_4), 30.3 and 29.6 (NCH_2CH_2), 29.5 (CH_2Ar), 28.4 ($C(CH_3)_3$), 26.5 (C_8), 25.64 and 25.60 (C_5), 21.6 (C_1), 14.2 (OCH_2CH_3), 13.8 (CH_3); HRMS (FTMS + p NSI) *m/z* Calculated for $C_{29}H_{40}NO_5^+$ $[M+H]^+$ 482.2901; Found 482.2895.

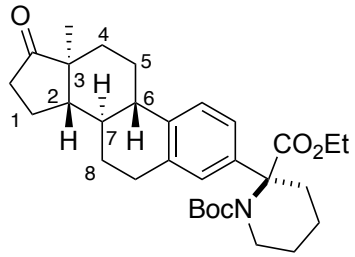
(±)–1-(*tert*-Butyl) 2-ethyl 2-((8*R*,9*S*,13*S*,14*S*)-13-methyl-17-oxo-7,8,9,11,12,13,14,15,16,17-decahydro-6*H*-cyclopenta[*a*]phenanthren-3-yl)pyrrolidine-1,2-dicarboxylate (169)



$Rh_2(esp)_2$ (0.8 mg, 1.0 μmol) was added to a solution of *tert*-butyl (3-chloropropyl)carbamate **58** (39 mg, 0.20 mmol) and ethyl 2-diazo-2-((8*R*,9*S*,13*S*,14*S*)-13-methyl-17-oxo-7,8,9,11,12,13,14,15,16,17-decahydro-6*H*-cyclopenta[*a*]phenanthren-3-yl)acetate **159** (110 mg, 0.30 mmol) in benzene (0.67 mL). The reaction vessel was sealed, purged with Ar and heated at 60 ºC for 2.5 h, then allowed to cool to rt. Tetrabutylammonium bromide (6.4 mg, 20 μmol) was added, followed by $CsOH{\cdot}H_2O$ (67 mg, 0.40 mmol), and the reaction was stirred at 25 ºC for 18 h. The crude reaction mixture was then filtered through Celite, washing with EtOAc (10 mL), and concentrated under reduced pressure. Purification by flash chromatography (20% EtOAc/pentane) afforded 1-(*tert*-butyl) 2-ethyl 2-((8*R*,9*S*,13*S*,14*S*)-13-methyl-17-oxo-7,8,9,11,12,13,14,15,16,17-decahydro-6*H*-cyclopenta[*a*]phenanthren-3-yl)pyrrolidine-1,2-

dicarboxyl-ate **169** (79 mg, 80%) as a white solid. R_f 0.25 (20% EtOAc/pentane); mp = 62–66 ºC; ν_{max} (film)/cm^{-1} 2977, 2930, 1738 (C=O ketone/ester), 1696 (C=O carbamate), 1389, 1366, 1245, 1155, 1137, 730; ^{1}H NMR (400 MHz, $CDCl_3$) δ 7.26–7.21 (m, 1 H, HC_{Ar}), 7.16–7.09 (m, 1 H, HC_{Ar}), 7.08–7.03 (m, 1 H, HC_{Ar}), 4.33–4.09 (m, 2 H, OCH_2CH_3), 3.70–3.58 (m, 2 H, NCH_2), 3.00–2.82 (m, 2 H, $ArCH_2$), 2.64–2.38 (m, 3 H, ArCH, C*H*HCO and $N(CH_2)_2CHH$), 2.37–2.22 (m, 2 H, CH*H*CO and $N(CH_2)CHH$), 2.21–1.84 (m, 5 H, C_1HH, C_4HH, C_5HH, C_8HH and NCH_2CHH), 1.78–1.40 (m, 10 H, C_1HH, C_4HH, C_5HH, C_8HH, C_2H, C_7H, NCH_2CHH and $C(CH_3)_3$), 1.35–1.23 (m, 9 H, OCH_2CH_3 and $C(CH_3)_3$), 0.94–0.89 (m, 3 H, CH_3); ^{13}C NMR (101 MHz, $CDCl_3$) δ 220.9 and 220.8 (C=O ketone), 172.8 (C=O ester), 154.0 (C=O carbamate), 138.3 and 138.2 (C_{Ar} quat), 137.9 and 137.1 (C_{Ar} quat), 135.3 and 135.1 (C_{Ar} quat), 127.8, 127.7 and 127.6 (C_{Ar}), 124.8, 124.6, 124.5 and 124.3 (2 × C_{Ar}), 80.1 and 79.7 ($C(CH_3)_3$), 71.3 (NC quat), 61.3 (OCH_2CH_3), 50.6 (C_2), 48.0 (C_3 quat), 47.9 (NCH_2), 44.3 (C_6), 43.4 and 41.7 ($N(CH_2)_2CH_2$), 38.2 (C_7), 35.9 (CH_2CO), 31.6 (C_4), 29.8 and 29.6 (CH_2Ar), 28.4 and 28.1 ($C(CH_3)_3$), 26.6 (C_8), 25.7 and 25.6 (C_5), 23.5 and 22.6 (NCH_2CH_2), 21.6 (C_1), 14.2 (OCH_2CH_3), 13.9 (CH_3); HRMS (FTMS + pNSI) *m/z* Calculated for $C_{30}H_{42}NO_5^+$ $[M+H]^+$ 496.3057; Found 496.3050.

(±)–1-(*tert*-Butyl) 2-ethyl 2-((8*R*,9*S*,13*S*,14*S*)-13-methyl-17-oxo-7,8,9,11,12,13,14,15,16,17-decahydro-6*H*-cyclopenta[*a*]phenanthren-3-yl)piperidine-1,2-dicarboxylate (170)



$Rh_2(esp)_2$ (0.8 mg, 1.0 μmol) was added to a solution of *tert*-butyl (4-iodobutyl)carbamate **70** (60 mg, 0.20 mmol) and ethyl 2-diazo-2-((8*R*,9*S*,13*S*,14*S*)-13-methyl-17-oxo-7,8,9,11,12,13,14,15,16,17-decahydro-6*H*-cyclopenta[*a*]phenanthren-3-yl)acetate **159** (147 mg, 0.40 mmol) in CH_2Cl_2 (0.67 mL). The reaction vessel was sealed, purged with Ar and heated at 60 ºC for 2.5 h, then allowed to cool to rt. Tetrabutylammonium bromide (6.4 mg, 20 μmol) was added, followed by KOH (45 mg, 0.80 mmol), and the reaction was stirred at 25 ºC for 18 h. The crude reaction mixture was then filtered through Celite, washing with EtOAc (10 mL), and concentrated under reduced pressure. Purification by flash chromatography (20% EtOAc/hexane) afforded 1-(*tert*-butyl) 2-ethyl 2-((8*R*,9*S*,13*S*,14*S*)-13-methyl-17-oxo-7,8,9,11,12,13,14,15,16,17-decahydro-6*H*-cyclopenta[*a*]phenanthren-3-yl)piperidine-1,2-dicarboxylate **170** (65 mg, 64%) as a white solid. R_f 0.18 (20% EtOAc/hexane); mp = 64–70 ºC; ν_{max} (film)/cm^{-1} 2930, 2865, 1736 (C=O ester/ketone), 1693 (C=O carbamate), 1454, 1364, 1253, 1155, 1051, 892, 775; ^{1}H NMR (400 MHz, $CDCl_3$) δ 7.26–7.22 (m, 1 H, HC_{Ar}), 7.10 (m, 1 H, HC_{Ar}), 7.00 (m, 1 H, HC_{Ar}), 4.26–4.10 (m, 2 H, OCH_2CH_3),

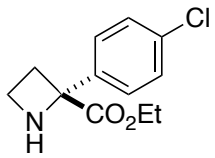
3.93–3.83 (m, 1 H, NC*H*H), 3.30–3.14 (br s, 1 H, NCH*H*), 2.99–2.82 (m, 2 H, $ArCH_2$), 2.51 (dd, *J* = 19.1, 8.9 Hz, 1 H, ArCH), 2.46–2.39 (m, 1 H, C*H*HCO), 2.38–1.92 (m, 7 H, CH*H*CO, $N(CH_2)_3CH_2$, C_1HH, C_4HH, C_5HH, C_8HH), 1.71–1.19 (m, 22 H, $NCH_2CH_2CH_2$, C_1HH, C_4HH, C_5HH, C_8HH, C_2H, C_7H, $C(CH_3)_3$ and OCH_2CH_3), 0.92 (s, 3 H, CH_3); ^{13}C NMR (101 MHz, $CDCl_3$) δ 220.8 (C=O ketone), 172.8 (C=O ester), 156.3 (C=O carbamate), 138.2 (C_{Ar} quat), 135.62 and 135.56 (C_{Ar} quat), 128.1 and 128.0 (C_{Ar}), 125.2 and 125.1 (C_{Ar}), 124.8 (C_{Ar}), 80.4 ($C(CH_3)_3$), 67.1 (NC quat), 60.9 (OCH_2CH_3), 50.5 (C_2), 48.0 (C_3 quat), 44.2 (C_6), 42.6 (NCH_2), 38.1 (C_7), 35.8 (CH_2CO), 34.6 (br s, $N(CH_2)_3CH_2$), 31.6 (C_4), 29.7 and 29.6 (CH_2Ar), 28.1 ($C(CH_3)_3$), 26.6 (C_8), 25.6 and 25.5 (C_5), 23.8 (NCH_2CH_2), 21.6 (C_1), 19.0 ($N(CH_2)_2CH_2$), 14.1 (OCH_2CH_3), 13.8 (CH_3) (The peak due to C_{Ar} quat adjacent to the piperidine was not observed due to rotameric effects); HRMS (FTMS + pNSI) *m/z* Calculated for $C_{31}H_{44}NO_5^+$ $[M+H]^+$ 510.3208; Found 510.3214.

6.2.1.9 Functionalisation of Saturated Nitrogen Heterocycles

General Procedure for Strong Cation Exchange (SCX) Column

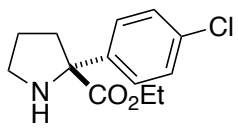
SCX cartridges (purchased from ThermoScientific) were selected with an appropriate capacity of stationary phase (5% w/v of crude product). The column was washed with three column volumes of methanol. The sample was then loaded onto the column in a minimum amount of solvent (1:1 MeOH/CH_2Cl_2). The column was washed through with three column volumes of MeOH and then with three column volumes of 5% NH_3 (28% aqueous solution)/MeOH to yield the free amine which was concentrated under reduced pressure.

(±)–Ethyl 2-(4-chlorophenyl)azetidine-2-carboxylate (176)



4 N HCl in 1,4-dioxane (0.25 mL) was added to a solution of 1-(*tert*-butyl) 2-ethyl 2-(4-chlorophenyl)azetidine-1,2-dicarboxylate **115** (54 mg, 0.16 mmol) in 1,4-dioxane (0.50 mL) at 0 ºC. The reaction mixture was stirred at 0 ºC for 15 min and then at 25 ºC for a further 18 h. The reaction mixture was concentrated under reduced pressure, then sat. aq. $NaHCO_3$ (20 mL) was added and the aqueous mixture was extracted with EtOAc (6 × 10 mL). The combined organic layers were combined, dried over Na_2SO_4 and concentrated under reduced pressure. Purification by flash chromatography afforded ethyl 2-(4-chlorophenyl)azetidine-2-carboxylate **176** (24 mg, 63%) as a brown oil. R_f 0.44 (0.02:1.98:98% NH_3:MeOH:CH_2Cl_2); ν_{max} (film)/cm^{-1} 3329 (w, NH), 2978, 1725 (C=O ester), 1490, 1246, 1105, 1091, 1014; ^{1}H NMR (400 MHz, $CDCl_3$) δ 7.35 (d, J = 8.8 Hz, 2 H, 2 × HC_{Ar}), 7.30 (d, J = 8.8 Hz, 2 H, 2 × HC_{Ar}), 4.27–4.17 (m, 2 H, OCH_2CH$_3$), 3.73–3.66 (m, 1 H, NC*H*H), 3.32 (ddd, J = 8.6, 7.4, 3.7 Hz, 1 H, NCH*H*), 2.92–2.85 (m, 1 H, NCH_2C*H*H), 2.76 (dt, J = 11.2, 8.6 Hz, 1 H, NCH_2NCH*H*), 1.23 (t, J = 7.1 Hz, 3 H, OCH_2CH_3); ^{13}C NMR (101 MHz, $CDCl_3$) δ 175.4 (C=O ester), 141.8 (C_{Ar} quat), 133.0 (ClC_{Ar} quat), 128.3 (2 × C_{Ar}), 126.7 (2 × C_{Ar}), 69.0 (NC quat), 61.8 (OCH_2CH$_3$), 41.8 (NCH_2), 32.7 (NCH_2CH_2), 14.0 (OCH_2CH_3); HRMS (ESI$^+$) *m/z* Calculated for $C_{12}H_{15}NO_2{}^{35}Cl$ [M+H] 240.0791; Found 240.0794.

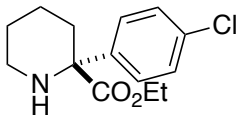
(±)–Ethyl 2-(4-chlorophenyl)pyrrolidine-2-carboxylate (171)



Trifluoroacetic acid (0.15 mL) was added to a stirred solution of 1-(*tert*-butyl) 2-ethyl 2-(4-chlorophenyl)pyrrolidine-1,2-dicarboxylate **127** (71 mg, 0.2 mmol) in CH_2Cl_2 (1.0 mL) at 0 ºC and stirred for 2 min. The reaction mixture was stirred at 25 ºC for a further 18 h. The solvent was removed under reduced pressure and purification by SCX column afforded ethyl 2-(4-chlorophenyl)pyrrolidine-2-carboxylate **172** (44 mg, 88%) as a yellow oil. R_f 0.71 (10% MeOH/CH_2Cl_2); ν_{max} (film)/cm^{-1} 3352 (NH), 2979, 1722 (C=O), 1489, 1243, 1181, 1091, 1014, 831, 787; ^{1}H NMR (400 MHz,

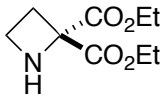
$CDCl_3$) δ 7.50 (d, *J* = 8.8 Hz, 2 H, 2 × HC_{Ar}), 7.29 (d, *J* = 8.8 Hz, 2 H, 2 × HC_{Ar}), 4.18–4.10 (m, 2 H, OCH_2CH_3), 3.12–3.06 (m, 2 H, NCH_2), 2.72 (ddd, *J* = 12.7, 8.0, 4.9 Hz, 1 H, $N(CH_2)_2CHH$), 2.04 (dt, *J* = 12.6, 8.3 Hz, 1 H, $N(CH_2)_2CHH$), 1.92–1.74 (m, 2 H, NCH_2CH_2), 1.21 (t, *J* = 7.1 Hz, 3 H, OCH_2CH_3); ^{13}C NMR (101 MHz, $CDCl_3$) δ 175.1 (C=O), 141.3 (C_{Ar} quat), 133.0 (ClC_{Ar} quat), 128.2 (2 × C_{Ar}), 127.7 (2 × C_{Ar}), 71.8 (NC quat), 61.7 (OCH_2CH_3), 45.8 (NCH_2), 36.9 ($N(CH_2)_2CH_2$), 24.7 (NCH_2CH_2), 14.0 (OCH_2CH_3); HRMS (ESI$^+$) *m/z* Calculated for $C_{13}H_{17}NO_2{}^{35}Cl$ [M+H] 254.0948; Found 254.0951.

(±)–Ethyl 2-(4-chlorophenyl)piperidine-2-carboxylate (172)



Trifluoroacetic acid (0.10 mL) was added to a stirred solution of 1-(*tert*-butyl) 2-ethyl 2-(4-chlorophenyl)piperidine-1,2-dicarboxylate **135** (37 mg, 0.10 mmol) in CH_2Cl_2 (0.5 mL) at 0 ºC. The reaction mixture was then stirred at 25 ºC for 15 h. Sat. aq. $NaHCO_3$ was added and the aqueous reaction mixture was extracted with EtOAc (6 × 10 mL). The organic layers were dried over Na_2SO_4, filtrered and the solvent was removed under reduced pressure to afford ethyl 2-(4-chlorophenyl)piperidine-2-carboxylate **172** (27 mg, quant) as a pale yellow oil. R_f 0.67 (5% MeOH/CH_2Cl_2); ν_{max} (film)/cm^{-1} 3341 (w br, NH), 2936, 1727 (C=O) 1492, 1217, 1123, 1094, 1014, 826, 752; ^{1}H NMR (400 MHz, $CDCl_3$) δ 7.44 (d, *J* = 8.8 Hz, 2 H, 2 × HC_{Ar}), 7.30 (d, *J* = 8.8 Hz, 2 H, 2 × HC_{Ar}), 4.25–4.17 (m, 2 H, OCH_2CH_3), 3.06–2.99 (m, 1 H, $NCHH$), 2.80–2.72 (m, 1 H, $NCHH$), 2.44–2.37 (m, 1 H, $N(CH_2)_3CHH$), 2.04–1.45 (m, 5 H, $N(CH_2)_3CHH$ and $NCH_2(CH_2)_2$), 1.25 (t, *J* = 7.1 Hz, 3 H, OCH_2CH_3); ^{13}C NMR (101 MHz, $CDCl_3$) δ 174.2 (C=O ester), 141.9 (C_{Ar} quat), 133.2 (ClC_{Ar} quat), 128.5 (2 × C_{Ar}), 126.7 (2 × C_{Ar}), 65.4 (NC quat), 61.2 (OCH_2CH_3), 43.7 (NCH_2), 35.2 ($N(CH_2)_3CH_2$), 24.9 (NCH_2CH_2), 22.4 ($N(CH_2)_2CH_2$), 14.2 (OCH_2CH_3); HRMS (FTMS + pNSI) *m/z* Calculated for $C_{14}H_{19}NO_2{}^{35}Cl^+$ [M+H]$^+$ 268.1099; Found 268.1101.

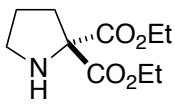
Diethyl azetidine-2,2-dicarboxylate (173)



Trifluoroacetic acid (0.10 mL) was added to a stirred solution of 1-(*tert*-butyl) 2,2-diethyl azetidine-1,2,2-tricarboxylate **57** (41 mg, 0.14 mmol) in CH_2Cl_2 (1 mL) at 0 ºC and stirred for 2 min. The reaction mixture was stirred at 25 ºC for a further 20 h. The solvent was removed under reduced pressure and purification by SCX column afforded diethyl azetidine-2,2-dicarboxylate **173** (20 mg, 71%) as a colourless oil. R_f 0.63 (95:5:1 CH_2Cl_2/MeOH/NEt_3); ν_{max} (film)/cm^{-1} 3337 (w, NH), 2982, 1733 (C=O), 1276, 1250, 1110, 1016; ^{1}H NMR (400 MHz, $CDCl_3$) δ 4.26 (q, *J* = 6.9 Hz, 4 H, 2 × OCH_2CH_3), 3.47 (t, *J* = 6.9 Hz, 2 H, NCH_2), 2.84–2.20 (m, 3 H, NCH_2CH_2 and NH), 1.28 (t, *J* = 6.9 Hz, 6 H, 2 × OCH_2CH_3); ^{13}C NMR (101 MHz, $CDCl_3$) δ 170.9 (2 × C=O), 68.8 (NC quat), 61.9 (2 ×

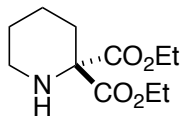
O*C*H$_2$CH$_3$), 42.1 (NCH$_2$), 27.7 (NCH$_2$*C*H$_2$), 14.0 (2 × OCH$_2$*C*H$_3$); HRMS (ESI$^+$) *m/z* Calculated for $C_9H_{16}NO_4$ [M+H] 202.1079; Found 202.1082.

Diethyl pyrrolidine-2,2-dicarboxylate (174)



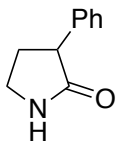
Trifluoroacetic acid (0.10 mL) was added to a stirred solution of 1-(*tert*-Butyl) 2,2-diethyl pyrrolidine-1,2,2-tricarboxylate **60** (59 mg, 0.19 mmol) in CH_2Cl_2 (1 mL) at 0 °C and stirred for 5 min. The reaction mixture was then stirred at 25 °C for 20 h. The solvent was removed under reduced pressure and saturated aqueous $NaHCO_3$ (10 mL) was added. The aqueous mixture was extracted with EtOAc (10 × 10 mL). The combined organic layers were dried over Na_2SO_4 and concentrated under reduced pressure to afford diethyl pyrrolidine-2,2-dicarboxylate **174** (39 mg, 97%) as a colourless oil. R_f 0.31 (5% MeOH/CH_2Cl_2); ν_{max} (film)/cm^{-1} 3360 (w, NH), 2981, 1729 (C=O), 1256, 1181, 1094, 1024, 860; ^{1}H NMR (400 MHz, $CDCl_3$) δ 4.27–4.18 (m, 4 H, 2 × OC*H*$_2$CH$_3$), 3.05 (t, *J* = 6.7 Hz, 2 H, NCH$_2$) 2.32 (t, *J* = 7.3 Hz, 2 H, N(CH$_2$)$_2$C*H*$_2$), 1.88–1.79 (m, 2 H, NCH$_2$C*H*$_2$), 1.27 (t, *J* = 7.1 Hz, 6 H, 2 × OCH$_2$C*H*$_3$); ^{13}C NMR (101 MHz, $CDCl_3$) δ 171.8 (2 × C=O), 72.0 (NC quat), 61.7 (2 × O*C*H$_2$CH$_3$), 47.2 (NCH$_2$), 33.0 (N(CH$_2$)$_2$*C*H$_2$), 25.5 (NCH$_2$*C*H$_2$), 14.0 (2 × OCH$_2$*C*H$_3$). The observed characterisation data (IR, ^{1}H and ^{13}C NMR) was consistent with that previously reported in the literature.[420]

Diethyl piperidine-2,2-dicarboxylate (175)



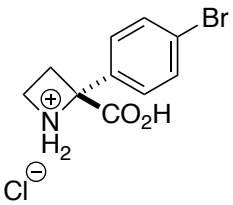
Trifluoroacetic acid (0.10 mL) was added to a stirred solution of 1-(*tert*-butyl) 2,2-diethyl piperidine-1,2,2-tricarboxylate **60** (48 mg, 0.15 mmol) in CH_2Cl_2 (0.5 mL) at 0 ºC. The reaction mixture was then stirred at 25 ºC for 15 h. Sat. aq. $NaHCO_3$ was added and the aqueous reaction mixture was extracted with EtOAc (6 × 10 mL). The organic layers were dried over Na_2SO_4, filtrered and the solvent was removed under reduced pressure to afford diethyl piperidine-2,2-dicarboxylate **175** (34 mg, quant) as a colourless oil. R_f 0.42 (5% MeOH/CH_2Cl_2); ν_{max} (film)/cm^{-1} 3368 (w br, NH), 2938, 2861, 1735 (C=O), 1293, 1228, 1209, 1127, 1172, 1102, 1075, 1022; ^{1}H NMR (400 MHz, $CDCl_3$) δ 4.21 (q, *J* = 7.1 Hz, 4 H, 2 × OC*H*$_2$CH$_3$), 2.83 (t, *J* = 5.6 Hz, 2 H, NCH$_2$), 2.52 (br s, 1 H, NH), 2.08–2.03 (m, 2 H, N(CH$_2$)$_3$C*H*$_2$), 1.62–1.48 (m, 4 H, NCH$_2$(C*H*$_2$)$_2$), 1.26 (t, *J* = 7.1 Hz, 6 H, 2 × OCH$_2$C*H*$_3$); ^{13}C NMR (101 MHz, $CDCl_3$) δ 170.5 (2 × C=O), 67.3 (NC quat), 61.6 (2 × O*C*H$_2$CH$_3$), 43.0 (NCH$_2$), 30.0 (N(CH$_2$)$_3$*C*H$_2$), 24.7 (NCH$_2$*C*H$_2$), 21.3 (N(CH$_2$)$_2$*C*H$_2$), 14.1 (2 × OCH$_2$*C*H$_3$). The observed characterisation data (IR, ^{1}H and ^{13}C NMR) was consistent with that previously reported in the literature.[420]

(±)–3-Phenylpyrrolidin-2-one (178)



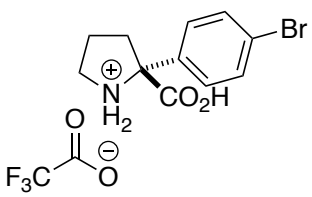
A solution of 1-(*tert*-butyl) 2-ethyl 2-(4-chlorophenyl)azetidine-1,2-dicarboxylate **105** (34 mg, 0.1 mmol) and palladium on carbon (3.4 mg, 10% w/w) in ethanol (1.0 mL) was stirred under an atmosphere of hydrogen at 25 ºC for 19 h. The reaction mixture was filtered through celite, washed with EtOAc and concentrated under reduced pressure. Purification by SCX column and washing with MeOH afforded 3-phenylpyrrolidin-2-one **178** (17 mg, quant) as a white solid. R_f 0.51 (0.05:4.95:95 NH_3:MeOH:CH_2Cl_2); mp = 83–84 ºC (lit = 82 ºC)[421]; ν_{max} (film)/cm^{-1} 3196 (br s, NH), 3088, 1687 (C=O), 1496, 1376, 1280, 753, 700; ^{1}H NMR (400 MHz, $CDCl_3$) δ 7.40–7.25 (m, 5 H, 5 × HC_{Ph}), 6.54 (br s, 1 H, NH), 3.64 (t, J = 9.0 Hz, 1 H, CH_2CHPh), 3.53–3.41 (m, 2 H, NCH_2), 2.68–2.57 (m, 1 H, NCH_2CHH), 2.33–2.21 (m, 1 H, NCH_2CHH); ^{13}C NMR (101 MHz, $CDCl_3$) δ 178.7 (C=O), 139.3 (C_{Ph} quat), 128.8 (2 × C_{Ph}), 128.0 (2 × C_{Ph}), 127.1 (C_{Ph}), 47.5 (CH_2CHPh), 40.5 (NCH_2), 30.8 (NCH_2CH_2); HRMS (ESI$^+$) *m/z* Calculated for $C_{10}H_{12}NO$ [M+H] 162.0919; Found 162.0924.

(±)–2-(4-Bromophenyl)-2-carboxyazetidin-1-ium chloride (179)



4 N HCl in 1,4-dioxane (0.25 mL) was added to a solution of di-*tert*-butyl 2-(4-bromophenyl)azetidine-1,2-dicarboxylate **109** (41 mg, 0.1 mmol) in 1,4-dioxane (0.25 mL). The solution was stirred at 40 ºC for 16 h. The reaction mixture was filtered, washing with Et_2O, then pentane and the solid was dried under reduced pressure to afford 2-(4-bromophenyl)-2-carboxyazetidin-1-ium chloride **179** (8 mg, 28%) as a white solid. mp = 136–139 ºC; ν_{max} (film)/cm^{-1} 3485–2395 (br m, OH and NH), 1716 (C=O), 1562, 1492, 1326, 1281, 1264, 1076, 1010, 816, 732; ^{1}H NMR (400 MHz, CD_3OD) δ 7.71 (d, J = 8.8 Hz, 2 H, 2 × HC_{Ar}), 7.39 (d, J = 8.8 Hz, 2 H, 2 × HC_{Ar}), 4.18 (dt, J = 10.3, 9.1 Hz, 1 H, NC*H*H), 3.93 (td, J = 10.0, 5.4 Hz, 1 H, NCH*H*), 3.37 (ddd, J = 12.6, 9.6, 8.8 Hz, 1 H, NCH_2CHH), 3.07 (ddd, J = 12.6, 9.3, 5.4 Hz, 1 H, NCH_2CHH); ^{13}C NMR (101 MHz, CD_3OD) δ 171.5 (C=O), 135.3 (C_{Ar} quat), 133.6 (2 × C_{Ar}), 128.5 (2 × C_{Ar}), 125.1 (BrC_{Ar} quat), 73.2 (NC quat), 42.9 (NCH_2), 29.8 (NCH_2CH_2); HRMS (FTMS + pNSI) *m/z* Calculated for $C_{10}H_{11}NO_2{}^{79}Br^+$ [M–Cl$^–$] 255.9968; Found 255.9970.

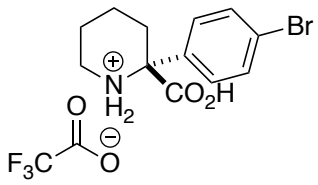
(±)-2-(4-Bromophenyl)-2-carboxypyrrolidin-1-ium 2,2,2-trifluoroacetate (180)



Trifluoroacetic acid (0.5 mL) was added to a solution of di-*tert*-butyl 2-(4-bromophenyl)pyrrolidine-1,2-dicarboxylate **123** (43 mg, 0.10 mmol) in CH_2Cl_2 (0.5 mL) at 25 ºC. The solution was then stirred at 40 ºC for 16 h. The reaction mixture was concentrated under reduced pressure and Et_2O/pentane added to precipitate a white solid. The solid was

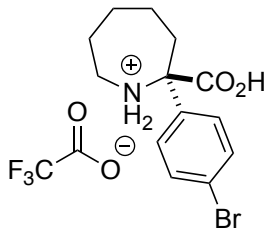
filtered, washing with Et_2O, then pentane. Concentration under reduced pressure afforded 2-(4-bromophenyl)-2-carboxypyrrolidin-1-ium 2,2,2-triforoacetate **180** (22 mg, 58%) as a white solid. mp > 250 ºC; ν_{max} (film)/cm^{-1} 3289–2215 (br, OH), 3054 (br s, NH), 2965, 2726, 1628 (s br, C=O), 1592 1490, 1450, 1436, 1399, 1348, 1328, 1312, 1187, 1139, 1074, 1045, 1008, 975, 888, 768, 713, 658; ^{1}H NMR (400 MHz, DMSO-*d*$_6$, 373 K) δ 7.55 (d, *J* = 8.5 Hz, 2 H, 2 × HC_{Ar}), 7.42 (d, *J* = 8.5 Hz, 2 H, 2 × HC_{Ar}), 3.38–3.29 (m, 1 H, NC*H*H), 3.17 (dt, *J* = 11.0, 8.0 Hz, 1 H, NCH*H*), 2.84–2.73 (m, 1 H, $N(CH_2)C$*H*H), 2.15–2.05 (m, 1 H, $N(CH_2)CH$*H*), 2.02–1.79 (m, 2 H, NCH_2C*H*$_2$); ^{13}C NMR (101 MHz, DMSO-*d*$_6$) δ 170.1 (C=O), 135.0 (C_{Ar} quat), 131.8 (2 × C_{Ar}), 128.7 (2 × C_{Ar}), 122.5 (BrC_{Ar} quat), 73.7 (NC quat), 44.3 (NCH_2), 32.9 ($N(CH_2)_2$*C*H_2), 21.7 (NCH_2*C*H_2); ^{19}F{^{1}H} NMR (377 MHz, DMSO-*d*$_6$) δ –68.7; ^{19}F{^{1}H} NMR (377 MHz, DMSO-*d*$_6$, 373 K) δ –73.4; HRMS (ESI$^+$) *m/z* Calculated for $C_{11}H_{13}NO_2{}^{79}Br$ [M–$CF_3CO_2^-$] 270.0130; Found 270.0133.

(±)–2-(4-Bromophenyl)-2-carboxypiperidin-1-ium 2,2,2-trifluoroacetate (181)



Trifluoroacetic acid (0.5 mL) was added to a solution of di-*tert*-butyl 2-(4-bromophenyl)piperidine-1,2-dicarboxylate **141** (44 mg, 0.10 mmol) in CH_2Cl_2 (0.5 mL) at 25 ºC. The solution was then stirred at 40 ºC for 16 h. The reaction mixture was concentrated under reduced pressure and Et_2O/pentane added to precipitate a white solid. Concentration under reduced pressure afforded 2-(4-bromophenyl)-2-carboxypiperidin-1-ium 2,2,2-trifluoroacetate **181** (27 mg, 68%) as a white solid. mp > 250 ºC; degradation observed at T > 250 ºC; ν_{max} (film)/cm^{-1} 3233–2163 (br, OH), 3037 (br, NH), 2944, 2866, 1690 (C=O) 1615, 1585, 1455, 1438, 1429, 1369, 1276, 1211, 1178, 1153, 1133, 1096, 1075, 1035, 1009, 815, 755, 718; ^{1}H NMR (400 MHz, DMSO-*d*$_6$) δ 7.74 (d, *J* = 8.6 Hz, 2 H, 2 × HC_{Ar}), 7.53 (d, *J* = 8.7 Hz, 2 H, 2 × HC_{Ar}), 3.21–3.04 (m, 2 H, NCH_2), 2.62–2.40 (m, 1 H, $N(CH_2)_3C$*H*H), 2.20–2.09 (m, 1 H, $N(CH_2)_3CH$*H*), 1.80–1.70 (m, 2 H, NCH_2C*H*$_2$), 1.64–1.43 (m, 2 H, $N(CH_2)_2C$*H*$_2$); ^{13}C NMR (101 MHz, DMSO-*d*$_6$) δ 170.0 (C=O), 134.8 (C_{Ar} quat), 132.1 (2 × C_{Ar}), 128.2 (2 × C_{Ar}), 122.9 (BrC_{Ar} quat), 65.2 (NC quat), 42.3 (NCH_2), 29.6 ($N(CH_2)_3CH_2$), 21.0 (NCH_2*C*H_2), 19.5 ($N(CH_2)_3$*C*H_2); ^{19}F{^{1}H} NMR (377 MHz, DMSO-*d*$_6$) δ –73.6; HRMS (ESI$^+$) *m/z* Calculated for $C_{12}H_{15}NO_2{}^{79}Br$ [M–$CF_3CO_2^-$] 284.0286; Found 284.0283.

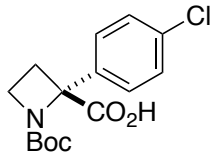
(±)–2-(4-Bromophenyl)-2-carboxyazepan-1-ium 2,2,2-trifluoroacetate (182)



Trifluoroacetic acid (0.20 mL) was added to a solution of di-*tert*-butyl 2-(4-bromophenyl)azepane-1,2-dicarboxylate **150** (24 mg, 0.05 mmol) in CH_2Cl_2 (0.20 mL) at 25 ºC. The solution was then stirred at 40 ºC for 16 h, then further CH_2Cl_2 (0.20 mL) was added. The reaction mixture was stirred at 40 ºC for a further 3 h, then concentrated under reduced pressure. Et_2O/pentane was added to precipitate a white solid. Concentration under reduced pressure afforded 2-(4-bromophenyl)-2-carboxyazepan-1-ium 2,2,2-trifluoroacetate **182** (17 mg, 81%) as a white solid. mp > 200 ºC; ν_{max} (film)/cm^{-1} 3064, 2930, 2870, 2631, 1610 (s br, C=O), 1454, 1491, 1372, 1118, 1077, 816, 768; ^{1}H NMR (400 MHz, CF_3CO_2D) δ 7.61 (d, *J* = 8.8 Hz, 2 H, 2 × HC_{Ar}), 7.30 (d, *J* = 8.8 Hz, 2 H, 2 × HC_{Ar}), 3.58–3.47 (m, 2 H, NCH_2), 2.97–2.88 (m, 1 H, $N(CH_2)_4CHH$), 2.72–2.62 (m, 1 H, $N(CH_2)_4CHH$), 2.06–1.75 (m, 6 H, $NCH_2(CH_2)_3$); ^{13}C NMR (101 MHz, CF_3CO_2D) δ 176.6 (C=O), 135.6 (2 × C_{Ar}), 133.8 (C_{Ar} quat), 129.2 (2 × C_{Ar}), 128.2 (BrC_{Ar} quat), 74.2 (NC quat), 48.4 (NCH_2), 33.4 ($N(CH_2)_4CH_2$), 29.0 (NCH_2CH_2), 28.1 ($N(CH_2)_2CH_2$), 24.5 ($N(CH_2)_3CH_2$); ^{19}F{^{1}H} NMR (377 MHz, DMSO-d_6) –68.7; HRMS (ESI$^+$) *m/z* Calculated for $C_{13}H_{17}NO_2{}^{79}Br$ [M–$CF_3CO_2^-$] 298.0443; Found 298.0453.

Note on TFA salts: All TFA salts were found to be sparingly soluble in DMSO, NMR at high temperatures was often required to obtain characterisation. It was found that characterisation data could be obtained in CF_3CO_2D which solvates the cation.

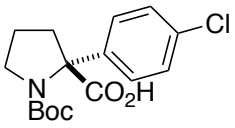
(±)–1-(*tert*-Butoxycarbonyl)-2-(4-chlorophenyl)azetidine-2-carboxylic acid (183)



NaOH (0.2 ml, 2.0 M in H_2O) was added to a solution of 1-(*tert*-butyl) 2-ethyl 2-(4-chlorophenyl)azetidine-1,2-dicarboxylate **115** (68 mg, 0.2 mmol) in EtOH (10.0 mL). The reaction mixture was stirred under reflux for 3 h then allowed to cool to rt. The solvent was removed under reduced pressure, H_2O (10 mL) was added and HCl (1 mL, 1.0 M in H_2O) was added to acidify the aqueous mixture. The aqueous mixture was extracted with EtOAc (4 × 10 mL) and the organic layers were dried over Na_2SO_4. Concentration under reduced pressure afforded 1-(*tert*-butoxycarbonyl)-2-(4-chlorophenyl)azetidine-2-carboxylic acid **183** (59 mg, 95%) as a white solid. R_f 0.14 (EtOAc); mp = 80–81 ºC; ν_{max} (film)/cm^{-1} 3712–2460 (br s, OH), 2977, 1707 (br s, 2 × C=O), 1493, 1394, 1368, 1155, 1094, 822, 733; ^{1}H NMR (400 MHz, $CDCl_3$) δ 7.38 (d, *J* = 8.5 Hz, 2 H, 2 × HC_{Ar}), 7.31 (d, *J* = 8.5 Hz, 2 H, 2 × HC_{Ar}), 4.04–3.91 (m, 2 H, NCH_2), 3.23–3.13 (m, 1 H, NCH_2CHH), 2.29–2.21 (m, 1 H, NCH_2CHH), 1.52 (s, 9 H, $C(CH_3)_3$); ^{13}C NMR (101 MHz, $CDCl_3$) δ 172.1 (C=O carboxylic acid), 157.6 (C=O carbamate), 136.8 (C_{Ar} quat), 134.5 (ClC_{Ar} quat), 129.2 (2 × C_{Ar}), 125.9 (2 × C_{Ar}), 83.5 ($C(CH_3)_3$), 74.5 (NC quat), 45.4

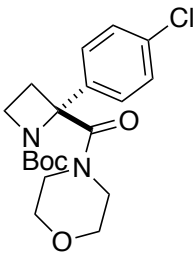
(NCH_2), 30.4 (NCH_2CH_2), 28.3 ($C(CH_3)_3$); HRMS (ESI^-) *m/z* Calculated for $C_{15}H_{17}NO_4{}^{35}Cl$ [M–H] 310.0846; Found 310.0851.

(±)–1-(*tert*-Butoxycarbonyl)-2-(4-chlorophenyl)pyrrolidine-2-carboxylic acid (184)



NaOH (1.0 ml, 2.0 M in H_2O) was added to a solution of 1-(*tert*-butyl) 2-ethyl 2-(4-chlorophenyl)pyrrolidine-1,2-dicarboxylate **127** (354 mg, 1.0 mmol) in EtOH (5.0 mL). The reaction mixture was stirred under reflux for 5 h then allowed to cool to rt. The solvent was removed under reduced pressure, H_2O (10 mL) was added and HCl (5 mL, 1.0 M in H_2O) was added to acidify the aqueous mixture. The aqueous mixture was extracted with EtOAc (4 × 10 mL) and the organic layers were dried over Na_2SO_4. Concentration of the dried organic layers under reduced pressure afforded 1-(*tert*-butoxycarbonyl)-2-(4-chlorophenyl)pyrrolidine-2-carboxylic acid **184** (326 mg, quant) as a white solid. R_f 0.44 (EtOAc); mp = 171–173 ºC; ν_{max} (film)/cm^{-1} 3200–2500 (br, OH), 2979, 1693 (br, 2 × C=O), 1395, 1369, 1158, 808, 731; ^1H NMR (400 MHz, $CDCl_3$) δ 7.33 (d, *J* = 8.7 Hz, 2 H, 2 × HC_{Ar}), 7.10 (d, *J* = 8.7 Hz, 2 H, 2 × HC_{Ar}), 3.75–3.61 (m, 2 H, NCH_2), 3.13–3.06 (m, 1 H, $N(CH_2)_2CHH$), 1.96–1.76 (m, 3 H, $N(CH_2)_2CHH$ and NCH_2CH_2), 1.49 (s, 9 H, $C(CH_3)_3$); ^{13}C NMR (101 MHz, $CDCl_3$) δ 171.7 (C=O carboxylic acid), 157.8 (C=O carbamate), 138.4 (C_{Ar} quat), 133.7 (ClC_{Ar} quat), 128.9 (2 × C_{Ar}), 125.9 (2 × C_{Ar}), 83.4 ($C(CH_3)_3$), 74.3 (NC quat), 50.0 (NCH_2), 41.6 ($N(CH_2)_2CH_2$), 28.3 ($C(CH_3)_3$), 23.3 (NCH_2CH_2); HRMS (ESI^+) *m/z* Calculated for $C_{16}H_{21}NO_4{}^{35}Cl$ [M+H] 326.1159; Found 326.1162.

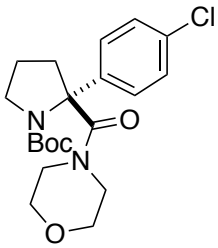
(±)–*tert*-Butyl 2-(4-chlorophenyl)-2-(morpholine-4-carbonyl)azetidine-1-carboxylate (187)



DIPEA (0.11 mL, 0.6 mmol) was added to a stirred solution of HATU (91 mg, 0.24 mmol), 1-(*tert*-butoxycarbonyl)-2-(4-chlorophenyl)azetidine-2-carboxylic acid **183** (62 mg, 0.2 mmol) in DMF (0.8 mL) and morpholine (21 μL, 0.24 mmol) at 40 ºC. The reaction mixture was stirred for 66 h. H_2O (10 mL) was added and the aqueous reaction mixture was extracted with EtOAc (4 × 10 mL). The combined organic layers were washed with brine (40 mL), dried over Na_2SO_4, filtered and concentrated under reduced pressure. Purification by flash chromatography (80% EtOAc/hexane to EtOAc) afforded *tert*-butyl 2-(4-chlorophenyl)-2-(morpholine-4-carbonyl)azetidine-1-carboxylate **187** (39 mg, 52%) as a white solid. R_f 0.13 (80% EtOAc/hexane); mp = 57–59 ºC; ν_{max} (film)/cm^{-1} 2975, 1687 (C=O carbamate), 1655 (C=O amide), 1389, 1364, 1238, 1152, 1114, 1094, 981, 825, 772; ^1H NMR (500 MHz, DMSO-d_6, 373 K) δ 7.49 (d, *J* = 8.9 Hz, 2 H, 2 × HC_{Ar}), 7.45 (d, *J* = 8.9 Hz, 2 H, 2 × HC_{Ar}), 3.83–3.78 (m, 1 H, NC*H*H), 3.77–3.71 (m, 1 H, NCH*H*), 3.52–3.37 (m, 4 H, 2 × NCH_2CH_2O), 3.32–3.08

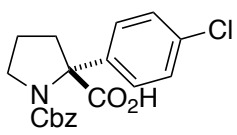
(m, 4 H, 2 × NCH_2CH_2O), 3.01–2.94 (m, 1 H, NCH_2CHH), 2.55–2.48 (m, 1 H, NCH_2CHH), 1.20 (s, 9 H, $C(CH_3)_3$), peaks due to NCH_2CH_2 are obscured by DMSO-d_6 solvent and H_2O signals but were confirmed by HSQC; ^{13}C NMR (126 MHz, DMSO-d_6, 373 K) δ 168.1 (C=O amide), 153.8 (C=O carbamate), 137.2 (C_{Ar} quat), 132.3 (ClC_{Ar} quat), 128.5 (2 × C_{Ar}), 127.5 (2 × C_{Ar}), 77.7 ($C(CH_3)_3$), 73.0 (NC quat), 64.9 (2 × OCH_2), 43.6 (br s, 3 × NCH_2), 27.44 ($C(CH_3)_3$), 27.35 (NCH_2CH_2); HRMS (ESI^+) *m/z* Calculated for $C_{19}H_{26}N_2O_4{}^{35}Cl$ [M+H] 381.1581; Found 381.1577.

(±)–*tert*-Butyl 2-(4-chlorophenyl)-2-(morpholine-4-carbonyl)pyrrolidine-1-carboxylate (188)



DIPEA (0.11 mL, 0.6 mmol) was added to a stirred solution of HATU (91 mg, 0.24 mmol), 1-(*tert*-butoxycarbonyl)-2-(4-chlorophenyl)pyrrolidine-2-carboxylic acid **184** (65 mg, 0.2 mmol) in DMF (0.8 mL) and morpholine (21 μL, 0.24 mmol) over 10 min at 40 ºC. The reaction mixture was stirred for a further 72 h. H_2O (10 mL) was added and the aqueous reaction mixture was extracted with EtOAc (6 × 10 mL). The combined organic layers were washed with brine (40 mL), dried over Na_2SO_4, filtered and concentrated under reduced pressure. Purification by flash chromatography (60% EtOAc/pentane) afforded *tert*-butyl 2-(4-chlorophenyl)-2-(morpholine-4-carbonyl)pyrrolidine-1-carboxylate **188** (73 mg, 92%) as a white solid. R_f 0.33 (60% EtOAc/pentane); mp = 142–145 ºC; ν_{max} (film)/cm^{-1} 2977, 2860, 1692 (C=O carbamate), 1649 (C=O amide), 1385, 1366, 1236, 1143, 1119, 1099, 732; ^1H NMR (400 MHz, DMSO-d_6, 373 K) δ 7.35–7.28 (m, 4 H, 4 × HC_{Ar}), 3.61–3.32 (m, 10 H, 2 × OCH_2 and 3 × NCH_2), 2.53–2.39 (m, 2 H, $N(CH_2)_2CH_2$), 1.94–1.84 (m, 1 H, NCH_2CHH), 1.78–1.65 (m, 1 H, NCH_2CHH), 1.29 (s, 9 H, $C(CH_3)_3$); ^{13}C NMR (101 MHz, DMSO-d_6, 373 K) δ 168.3 (C=O amide), 152.8 (C=O carbamate), 140.4 (C_{Ar} quat), 130.9 (ClC_{Ar} quat), 129.2 (2 × C_{Ar}), 126.4 (2 × C_{Ar}), 78.6 ($C(CH_3)_3$), 71.2 (NC quat), 65.2 (2 × OCH_2), 46.9 (NCH_2), 44.9 (2 × NCH_2), 27.5 ($C(CH_3)_3$), 21.7 (NCH_2CH_2) (Peak due to $N(CH_2)_2CH_2$ confirmed to be underneath DMSO-d_6 solvent peak by HSQC); HRMS (ESI^+) *m/z* Calculated for $C_{20}H_{28}N_2O_4{}^{35}Cl$ [M+H] 395.1738; Found 395.1732.

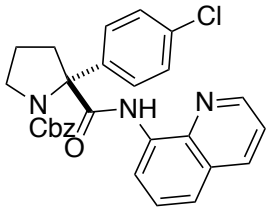
(±)–1-((Benzyloxy)carbonyl)-2-(4-chlorophenyl)pyrrolidine-2-carboxylic acid (191)



NaOH (2.0 ml, 2.0 M in H_2O) was added to a solution of 1-benzyl 2-ethyl 2-(4-chlorophenyl)pyrrolidine-1,2-dicarboxylate **128** (776 mg, 2.0 mmol) in EtOH (10.0 mL). The reaction mixture was stirred under reflux for 3.5 h then allowed to cool to rt. The solvent was removed under reduced pressure, H_2O (50 mL) was added and HCl (10 mL, 1.0 M in H_2O) was added to acidify the aqueous mixture. The aqueous

mixture was extracted with EtOAc (4 × 10 mL) and the organic layers were dried over Na_2SO_4. Concentration of the dried organic layers under reduced pressure afforded 1-((benzyloxy)carbonyl)-2-(4-chlorophenyl)pyrrolidine-2-carboxylic acid **191** (591 mg, 85%) as a white solid. R_f 0.31 (10% MeOH/CH_2Cl_2); ν_{max} (film)/cm^{-1} 3484 (br s, OH), 2957, 2687 (br s, 2 × C=O), 1492, 1412, 1356, 1339, 1223.7, 1180, 1099, 1013, 731, 697; ^{1}H NMR (400 MHz, $CDCl_3$) δ 7.98 (br s, 1 H, CO_2H), 7.41–7.30 (m, 5 H, 5 × HC_{Ar}), 7.22–7.09 (m, 4 H, 4 × HC_{Ar}), 5.17–4.98 (m, 2 H, OCH_2Ph), 3.76–3.62 (m, 2 H, NCH_2), 2.87–2.78 (m, 1 H, $N(CH_2)_2CHH$), 2.02–1.82 (m, 2 H, $N(CH_2)_2CH$*H* and NCH_2CHH), 1.77–1.65 (m, 1 H, NCH_2CH*H*); ^{13}C NMR (101 MHz, $CDCl_3$) δ 174.3 (C=O carboxylic acid), 156.4 (C=O carbamate), 138.6 (C_{Ar} quat), 136.0 (C_{Ar} quat), 133.0 (ClC_{Ar} quat), 128.5 (2 × C_{Ar}), 128.2 (C_{Ar}), 128.1 (2 × C_{Ar}), 127.9 (2 × C_{Ar}), 127.5 (2 × C_{Ar}), 73.7 (NC quat), 67.9 (OCH_2Ph), 48.8 (NCH_2), 41.8 ($N(CH_2)_2CH_2$), 23.3 (NCH_2CH_2); HRMS (ESI$^+$) *m/z* Calculated for $C_{19}H_{19}NO_4Cl$ [M+H] 360.1003; Found 360.0991.

(±)–Benzyl 2-(4-chlorophenyl)-2-(quinolin-8-ylcarbamoyl)pyrrolidine-1-carboxylate (192)



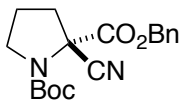
HOBt hydrate (230 mg, 1.5 mmol) was added to a solution of benzyl 2-(4-chlorophenyl)-2-(quinolin-8-ylcarbamoyl)pyrrolidine-1-carboxylate **191** (360 mg, 1.0 mmol), 8-aminoquinoline (166 mg, 1.15 mmol) and EDC·HCl (230 mg, 1.2 mmol), in CH_2Cl_2 (2.0 mL) and the resulting solution was stirred at 25 ºC for 7 days. The solvent was removed under reduced pressure, a solution of sat. aq. $NaHCO_3$ (20 mL) was added and the aqueous layer was extracted with EtOAc (3 × 50 mL). The combined organic extracts were dried with Na_2SO_4, filtered and the solvent was removed under reduced pressure. Purification by flash chromatography (10% Et_2O/CH_2Cl_2) afforded benzyl 2-(4-chlorophenyl)-2-(quinolin-8-ylcarbamoyl)pyrrolidine-1-carboxylate **192** (105 mg, 22%) as a pale yellow solid. R_f 0.65 (10% Et_2O/CH_2Cl_2); mp = 51–56 ºC; ν_{max} (film)/cm^{-1} 3320 (NH), 2952, 1693 (br s, 2 × C=O), 1524, 1486, 1399, 1327, 1132, 1013, 824, 791, 755, 733, 696; ^{1}H NMR (400 MHz, 373K, DMSO-d_6) δ 10.53 (br s, 1 H, NH), 8.68 (dd, *J* = 4.2, 1.7 Hz, 1 H, HC_{Ar}), 8.65 (dd, *J* = 7.6, 1.4 Hz, 1 H, HC_{Ar}), 8.34 (dd, *J* = 8.3, 1.7 Hz, 1 H, HC_{Ar}), 7.65 (dd, *J* = 8.3 Hz, 1.4 Hz, 1 H, HC_{Ar}), 7.60–7.53 (m, 2 H, 2 × HC_{Ar}), 7.46–7.42 (m, 2 H, 2 × HC_{Ar}), 7.41–7.36 (m, 2 H, 2 × HC_{Ar}), 7.10 (br s, 5 H, 5 × HC_{Ph}), 5.12–5.00 (m, 2 H, OCH_2Ph), 3.90–3.78 (m, 2 H, NCH_2), 2.99–2.89 (m, 2 H, $N(CH_2)_2CHH$), 2.36–2.28 (m, 1 H, $N(CH_2)_2CH$*H*), 2.05–1.95 (m, 1 H, NCH_2CHH), 1.87–1.77 (m, 1 H, NCH_2CH*H*); ^{13}C NMR (101 MHz, 373K, DMSO-d_6) δ 169.0 (C=O amide), 153.5 (C=O carbamate), 151.3 (C_{Ar} quat), 148.1 (C_{Ar}), 139.0 (C_{Ar} quat), 137.8 (C_{Ar} quat), 135.8 (C_{Ar}), 133.7 (ClC_{Ar} quat), 131.6 (C_{Ar} quat),

128.1 (2 × C_{Ar}), 127.42 (2 × C_{Ar}), 127.36 (C_{Ar}), 127.2 (C_{Ar} quat), 126.9 (2 × C_{Ar}), 126.8 (2 × C_{Ar}), 126.3 (C_{Ar}), 121.4 (2 × C_{Ar}), 115.4 (C_{Ar}), 73.4 (NC quat), 66.1 (OCH_2Ph), 48.3 (NCH_2), 42.0 ($N(CH_2)_2CH_2$), 22.1 (NCH_2CH_2); HRMS (ESI^+) *m/z* Calculated for $C_{28}H_{25}N_3O_3Cl^+$ $[M+H]^+$ 486.1579; Found 486.1587.

6.2.1.10 Compounds from Section 2.4.4

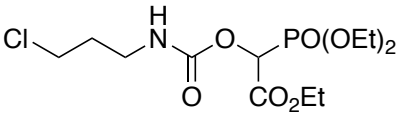
Diazo compounds **196** and **198–201** were synthesised as previously reported by Bull and coworkers[168] using procedures reported by Lee and Yuk.[405]

(±)–2-Benzyl 1-(*tert*-butyl) 2-cyanopyrrolidine-1,2-dicarboxylate (197)



$Rh_2(esp)_2$ (1.9 mg, 2.5 μmol) was added to a solution of *tert*-butyl (3-chloropropyl)carbamate **58** (97 mg, 0.50 mmol) and benzyl 2-cyano-2-diazoacetate **196** (151 mg, 0.75 mmol) in CH_2Cl_2 (1.67 mL). The reaction vessel was sealed, purged with Ar and heated at 60 ºC for 24 h, then allowed to cool to rt. Tetrabutylammonium bromide (16 mg, 50 μmol) was added, followed by $CsOH{\cdot}H_2O$ (168 mg, 1.00 mmol), and the reaction was stirred at 25 ºC for 18 h. The crude reaction mixture was then filtered through Celite, washing with EtOAc (10 mL), and concentrated under reduced pressure. Purification by flash chromatography (20% EtOAc/pentane) afforded 2-Benzyl 1-(*tert*-butyl) 2-cyanopyrrolidine-1,2-dicarboxylate **197** (29 mg, 18%) as a yellow oil. R_f 0.23 (20% EtOAc/pentane); ν_{max} (film)/cm^{-1} 2978, 1753 (C=O ester), 1701 (C=O carbamate), 1379, 1376, 1260, 1144, 1123, 739, 697; ^{1}H NMR (400 MHz, $CDCl_3$) δ 7.42–7.33 (m, 5 H, 5 × HC_{Ph}), 5.38–5.19 (m, 2 H, CH_2Ph), 3.72–3.50 (m, 2 H, NCH_2), 2.71–2.57 (m, 1 H, $N(CH_2)_2CHH$), 2.42–2.26 (m, 1 H, $N(CH_2)_2CHH$), 2.19–2.00 (m, 2 H, NCH_2CH_2), 1.47 (s, 3 H, $C(CH_3)_3$), 1.38 (s, 6 H, $C(CH_3)_3$); ^{13}C NMR (101 MHz, $CDCl_3$) δ 167.3 (C=O ester), 152.0 (C=O carbamate), 134.3 (C_{Ar} quat), 128.8 (2 × C_{Ar}), 128.6 (C_{Ar}), 128.5 (C_{Ar}), 128.1 (C_{Ar}), 117.5 (C≡N), 82.5 ($C(CH_3)_3$), 68.6 (CH_2Ph), 62.1 (NC quat), 47.3 and 47.2 (NCH_2), 39.5 and 38.3 ($N(CH_2)_2CH_2$), 28.2 and 28.0 ($C(CH_3)_3$), 24.3 and 23.4 (NCH_2CH_2); HRMS (ESI$^+$) *m/z* Calculated for $C_{18}H_{23}N_2O_4$ [M+H] 331.1658; Found 331.1670.

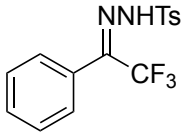
(±)–Ethyl 2-(((3-chloropropyl)carbamoyl)oxy)-2-(diethoxyphosphoryl)acetate (202)



$Rh_2(esp)_2$ (1.9 mg, 2.5 μmol) was added to a solution of *tert*-butyl (3-chloropropyl)carbamate **58** (97 mg, 0.50 mmol), ethyl 2-diazo-2-(diethoxyphosphoryl)acetate **200** (188 mg, 0.75 mmol) in benzene (1.67 mL). The reaction vessel was sealed, purged with Ar and heated at 60 ºC for 2.5 h. The reaction mixture was then allowed to cool to rt. The crude reaction mixture was then filtered through Celite, washing with EtOAc (10 mL), and concentrated under reduced pressure. Purification by flash chromatography (70% EtOAc/pentane) afforded ethyl 2-(((3-chloropropyl)carbamoyl)oxy)-2-(diethoxyphosphoryl)acetate **202** (120 mg, 67%) as a white solid. R_f 0.23 (70% EtOAc/pentane); mp = 52–53 ºC; ν_{max} (film)/cm^{-1} 3260 (br, NH), 2991, 1755 (C=O ester), 1734 (C=O carbamate), 1546, 1245 (P=O), 1212, 1141, 1060, 1007, 967, 931; ^{1}H NMR (400 MHz, $CDCl_3$) δ 5.57 (t, $J_{P\text{-}H}$ = 6.0 Hz, 1 H, NH), 5.40 (d, $J_{P\text{-}H}$ = 17.4 Hz, 1 H,

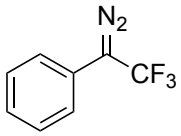
CHPO(OEt)$_2$), 4.34–4.16 (m, 6 H, OC*H*$_2$CH$_3$ and PO(OC*H*$_2$CH$_3$)$_2$), 3.58 (t, *J* = 6.4 Hz, 2 H, CH$_2$Cl), 3.36 (q, *J* = 6.4 Hz, 2 H, NCH$_2$), 2.04–1.93 (m, 2 H, NCH$_2$C*H*$_2$), 1.38–1.27 (m, 9 H, OCH$_2$C*H*$_3$ and PO(OCH$_2$C*H*$_3$)$_2$); ^{13}C NMR (101 MHz, CDCl$_3$) δ 165.7 (C=O ester), 154.7 (d, J_{C-P} = 12.2 Hz, C=O carbamate), 69.0 (d, J_{C-P} = 160.6 Hz, OCH), 63.9 (d, J_{C-P} = 6.6 Hz, PO(O*C*H$_2$CH$_3$)$_2$), 62.2 (O*C*H$_2$CH$_3$), 42.0 (CH$_2$Cl), 38.6 (NCH$_2$), 32.1 (NCH$_2$*C*H$_2$), 16.3 (d, J_{C-P} = 5.9 Hz, PO(OCH$_2$*C*H$_3$)$_2$), 14.0 (OCH$_2$*C*H$_3$); ^{31}P NMR (162 MHz, CDCl$_3$) δ 13.5; HRMS (ESI$^+$) *m/z* Calculated for C$_{12}$H$_{24}$NO$_7$^{35}ClP [M+H] 360.0979; Found 360.0973.

4-Methyl-*N*'-(2,2,2-trifluoro-1-phenylethylidene)benzenesulfonohydrazide (205)



Tosylhydrazide (3.72 g, 20 mmol) was added to trifluoroacetophenone (2.81 mL, 20 mmol) in MeOH (13 mL) and the mixture was heated to 65 ºC. After 15 h the reaction mixture was cooled to 0 ºC and pentane was added to aid precipitate formation. The precipitate was filtered and dried under reduced pressure to afford 4-methyl-*N*'-(2,2,2-trifluoro-1-phenylethylidene)benzenesulfonohydrazide **205** (3.14 g, 46%) as a white crystalline solid. ν_{max} (film)/cm^{-1} 3191, 1361, 1334, 1174, 1129, 1066, 988, 772, 682; ^{1}H NMR (400 MHz, CDCl$_3$) δ 7.99 (s, 1 H, NH), 7.82 (d, *J* = 8.3 Hz, 2 H, 2 × HC$_{Ar}$), 7.58–7.50 (m, 3 H, 3 × HC$_{Ph}$), 7.36 (d, *J* = 8.2 Hz, 2 H, 2 × HC$_{Ar}$), 7.27–7.22 (m, 2 H, 2 × HC$_{Ph}$), 2.47 (s, 3 H, CH$_3$); ^{13}C NMR (101 MHz, CDCl$_3$) δ 144.9 (C$_{Ph}$ quat), 141.6 (q, J_{C-F} = 35.9 Hz, C=N quat), 134.5 (C$_{Ar}$ quat), 131.5 (C$_{Ph}$), 130.0 (2 × C$_{Ar}$), 129.8 (2 × C$_{Ar}$), 128.1 (2 × C$_{Ar}$), 128.0 (2 × C$_{Ar}$), 125.2 (CH$_3$*C*$_{Ar}$ quat), 119.9 (q, J_{C-F} = 275.0 Hz, CF$_3$), 21.7 (CH$_3$); ^{19}F{^{1}H} NMR (377 MHz, CDCl$_3$) δ –63.3. The observed characterisation data (^{1}H, ^{13}C and ^{19}F NMR) was consistent with that previously reported in the literature.[422]

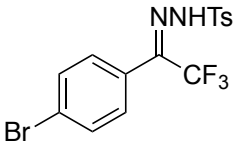
(1-Diazo-2,2,2-trifluoroethyl)benzene (207)



KOH (988 mg, 17.6 mmol) was added to a solution of 4-methyl-*N*'-(2,2,2-trifluoro-1-phenylethylidene)benzenesulfonohydrazide **205** (3.0 g, 8.8 mmol) in MeOH (22 mL). The reaction mixture was heated to 65 ºC for 1 h and then cooled to rt. H$_2$O (100 mL) was added and the aqueous mixture was extracted with pentane (3 × 100 mL). The combined organic layers were washed with sat. NaHCO$_3$ (50 mL), then sat. brine (50 mL) and dried over Na$_2$SO$_4$, filtered and concentrated under reduced pressure. Purification by flash chromatography (pentane), followed by distillation to remove residual pentane by gentle heating (T < 50 ºC) afforded (1-diazo-2,2,2-trifluoroethyl)benzene **207** (413 mg, 25%) as a volatile orange oil . R_f 0.68 (pentane); ν_{max} (film)/cm^{-1} 2080 (C=N=N out-of-phase), 1502, 1342 (C=N=N in-phase), 1297, 1141, 1096, 954, 746, 686; ^{1}H NMR (400 MHz, CDCl$_3$) δ 7.45–7.39 (m, 2 H, 2 × HC$_{Ph}$), 7.25–7.20 (m, 1 H, HC$_{Ph}$), 7.15–7.10 (m, 2 H, 2 × HC$_{Ph}$); ^{1}H NMR (400 MHz, C$_6$D$_6$) δ 6.99–6.93 (m, 2 H, 2 × HC$_{Ph}$), 6.85–6.80 (m, 1 H,

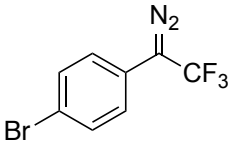
HC_{Ph}), 6.77–6.73 (m, 2 H, 2 × HC_{Ph}); ^{13}C NMR (101 MHz, $CDCl_3$) δ 129.4 (2 × C_{Ph}), 125.9 (C_{Ph}), 125.6 (q, $J_{C–F}$ = 268.7 Hz, CF_3), 123.5 (C_{Ph} quat), 122.2 (2 × C_{Ph}); ^{13}C NMR (101 MHz, C_6D_6) δ 130.1 (2 × C_{Ph}), 126.8 (q, $J_{C–F}$ = 269.8 Hz, CF_3), 126.5 (C_{Ph}), 124.1 (C_{Ph} quat), 123.0 (2 × C_{Ph}); $^{19}F\{^1H\}$ NMR (377 MHz, $CDCl_3$) δ –57.4; $^{19}F\{^1H\}$ NMR (377 MHz, C_6D_6) δ –57.6. The observed characterisation data (^1H NMR in $CDCl_3$, ^{13}C and ^{19}F NMR in C_6D_6) was consistent with that previously reported in the literature.[422,423]

_N_'-(1-(4-Bromophenyl)-2,2,2-trifluoroethylidene)-4-methylbenzenesulfonohydrazide (206)



Tosylhydrazide (1.86 g, 10.0 mmol) was added to 4'bromo-trifluoroacetophenone (2.53 g, 10.0 mmol) in toluene (5 mL) and the mixture was heated to 100 ºC. After 15 h the reaction mixture was cooled to 0 ºC and pentane was added. The precipitate was stirred for 30 min at 0 ºC, then filtered and dried under reduced pressure to afford _N_'-(1-(4-bromophenyl)-2,2,2-trifluoroethylidene)-4-methylbenzenesulfonohydrazide **206** (2.79 g, 66%) as a white crystalline solid. ν_{max} (film)/cm^{-1} 3176, 1357, 1170, 1133, 1070, 999, 876, 813; ^1H NMR (400 MHz, $CDCl_3$) δ 8.02 (s, 1 H, NH), 7.80 (d, J = 8.3 Hz, 2 H, 2 × HC_{Ar}), 7.67 (d, J = 8.5 Hz, 2 H, 2 × HC_{Ar}), 7.37 (d, J = 8.3 Hz, 2 H, 2 × HC_{Ar}), 7.14 (d, J = 8.5 Hz, 2 H, 2 × HC_{Ar}), 2.47 (s, 3 H, $ArCH_3$); ^{13}C NMR (101 MHz, $CDCl_3$) δ 145.1 (C_{Ar} quat), 140.2 (q, $J_{C–F}$ = 35.7 Hz, C=N quat), 134.3 (C_{Ar} quat), 133.3 (2 × C_{Ar}), 129.9 (2 × C_{Ar}), 129.8 (2 × C_{Ar}), 128.0 (2 × C_{Ar}), 126.4 (CH_3C_{Ar} quat), 123.9 (BrC_{Ar} quat), 119.7 (q, $J_{C–F}$ = 274.8 Hz, CF_3), 21.7 (CH_3); $^{19}F\{^1H\}$ NMR (377 MHz, $CDCl_3$) δ –68.2. The observed characterisation data (^1H NMR, ^{13}C NMR and ^{19}F NMR) was consistent with that previously reported in the literature.[422]

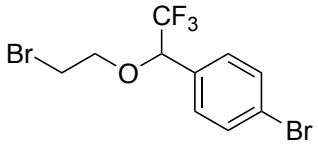
1-Bromo-4-(1-diazo-2,2,2-trifluoroethyl)benzene (208)



KOH (662 mg, 11.8 mmol) was added to a solution of _N_'-(1-(4-bromophenyl)-2,2,2-trifluoroethylidene)-4-methylbenzenesulfonohydrazide **206** (2.50 g, 5.9 mmol) in MeOH (14.8 mL). The reaction mixture was heated to 70 ºC for 1 h and then cooled to rt. H_2O (100 mL) was added and the aqueous mixture was extracted with CH_2Cl_2 (3 × 100 mL). The combined organic layers were washed with sat. brine (50 mL), dried over Na_2SO_4, filtered and concentrated under reduced pressure. Purification by flash chromatography (pentane) afforded 1-bromo-4-(1-diazo-2,2,2-trifluoroethyl)benzene **208** (738 mg, 47%) as an orange oil. R_f 0.75 (pentane); ν_{max} (film)/cm^{-1} 2080 (C=N=N out-of-phase), 1491, 1327 (C=N=N in-phase), 1301, 1264, 1170, 1144, 1100, 954, 813; ^1H NMR (400 MHz, $CDCl_3$) δ 7.52 (d, J = 8.9 Hz, 2 × HC_{Ar}), 6.99–6.94 (m, 2 H, 2 × HC_{Ar}); ^{13}C NMR (101 MHz, $CDCl_3$) δ), 132.6 and 132.5 (2 × C_{Ar}),

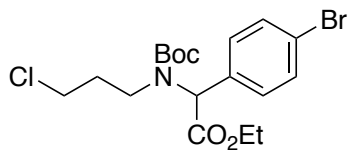
131.4 (C_{Ar} quat), 125.3 (q, J = 269.1 Hz, CF_3), 123.6 (2 × C_{Ar}), 122.7 (C=N_2), 119.5 (BrC_{Ar} quat); $^{19}F\{^1H\}$ NMR (377 MHz, $CDCl_3$) δ –57.5. The observed characterisation data (^1H, ^{13}C and ^{19}F NMR) was consistent with that previously reported in the literature.[422]

(±)–1-Bromo-4-(1-(2-bromoethoxy)-2,2,2-trifluoroethyl)benzene (212)



1-Bromo-4-(1-diazo-2,2,2-trifluoroethyl)benzene **208** (265 mg, 1.0 mmol) in CH_2Cl_2 (8.0 mL) was slowly added over 1 h *via* syringe pump to a stirred solution of 2-bromoethanol **211** (0.35 mL) and $Cu(MeCN)_4PF_6$ (15 mg, 40.0 μmol) in CH_2Cl_2 (5.0 mL) at 25 ºC. The reaction mixture was stirred for 18 h and then concentrated under reduced pressure. Purification by flash chromatography (1% to 3% Et_2O/pentane) afforded 1-bromo-4-(1-(2-bromoethoxy)-2,2,2-trifluoroethyl)benzene **212** (211 mg, 58%) as a colourless oil. R_f 0.13 (pentane); ν_{max} (film)/cm^{-1} 2967, 2889, 1592, 1491, 1264, 1170, 1126, 1074, 1010, 809, 727, 671; ^1H NMR (400 MHz, $CDCl_3$) δ 7.57 (d, J = 8.5 Hz, 2 H, 2 × HC_{Ar}), 7.35 (d, J = 8.5 Hz, 2 H, 2 × HC_{Ar}), 4.66 (q, J = 6.3 Hz, 1 H, $CHCF_3$), 3.86 (m, 2 H, OCH_2), 3.51–3.46 (m, 2 H, $BrCH_2$); ^{13}C NMR (101 MHz, $CDCl_3$) δ 131.9 (2 × C_{Ar}), 131.3 (C_{Ar} quat), 129.8 (2 × C_{Ar}), 124.0 (BrC_{Ar} quat), 123.3 (q, J = 282.6 Hz, CF_3), 79.6 (q, J = 31.6 Hz, $CHCF_3$), 70.6 (OCH_2), 29.2 ($BrCH_2$); $^{19}F\{^1H\}$ NMR (377 MHz, $CDCl_3$) δ –76.72 and –76.73; HRMS (EI^+) *m/z* Calculated for $C_{10}H_9OF_3{}^{79}Br_2$ $[M]^+$ 359.8972; Found 359.8979.

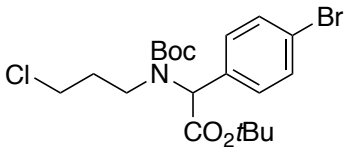
(±)–Ethyl 2-(4-bromophenyl)-2-((*tert*-butoxycarbonyl)(3-chloropropyl)amino)acetate (214)



$Rh_2(esp)_2$ (1.9 mg, 2.5 μmol) was added to a solution of *tert*-butyl (3-chloropropyl)carbamate **58** (97 mg, 0.50 mmol), ethyl 2-(4-bromophenyl)-2-diazoacetate **88** (202 mg, 0.75 mmol) in benzene (1.67 mL). The reaction vessel was sealed, purged with Ar and heated at 60 ºC for 2.5 h. The reaction mixture was then allowed to cool to rt. The crude reaction mixture was then filtered through Celite, washing with EtOAc (10 mL), and concentrated under reduced pressure. Purification by flash chromatography (90% CH_2Cl_2/hexane) afforded ethyl 2-(4-bromophenyl)-2-((*tert*-butoxycarbonyl)(3-chloropropyl)amino)acetate **214** (207 mg, 95%) as a white solid. R_f 0.22 (90% CH_2Cl_2/hexane); mp = 56–58 ºC; ν_{max} (film)/cm^{-1} 2978, 1744 (C=O ester), 1689 (C=O carbamate), 1394, 1367, 1151, 1011, 1026, 773; ^1H NMR (400 MHz, $CDCl_3$) δ 7.54–7.39 (m, 2 H, 2 × HC_{Ar}), 7.21–7.06 (m, 2 H, 2 × HC_{Ar}), 5.78–5.23 (m, 1 H, $HC(CO_2Et)$(Ar)), 4.29–4.12 (m, 2 H, OCH_2CH_3), 3.47–3.29 (m, 3 H, CH_2Cl and NC*H*H), 3.23–3.13 (m, 1 H, NCH*H*), 1.99–1.14 (m, 14 H, NCH_2CH_2, $C(CH_3)_3$, OCH_2CH_3); ^{13}C NMR (101 MHz, $CDCl_3$) δ 170.3 (C=O ester), 155.7 (C=O carbamate), 134.1 (C_{Ar} quat), 131.8 (2 × C_{Ar}), 130.7 (2 × C_{Ar}),

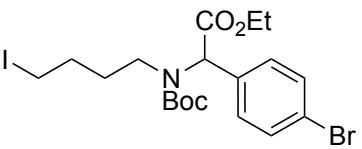
122.6 (BrC_{Ar} quat), 81.0 ($C(CH_3)_3$), 62.3 (NCH), 61.5 (OCH_2CH_3), 43.7 (CH_2Cl), 42.5 (NCH_2), 32.0 (NCH_2CH_2), 28.1 ($C(CH_3)_3$), 14.1 (OCH_2CH_3); HRMS (ESI^+) *m/z* Calculated for $C_{18}H_{26}NO_4ClBr$ [M+H] 434.0734; Found 434.0746.

(±)–*tert*-Butyl 2-(4-bromophenyl)-2-((*tert*-butoxycarbonyl)(3-chloropropyl)amino)acetate (215)



$Rh_2(esp)_2$ (1.9 mg, 2.5 μmol) was added to a solution of *tert*-butyl (3-chloropropyl)carbamate **58** (97 mg, 0.5 mmol), *tert*-butyl 2-(4-bromophenyl)-2-diazoacetate **99** (223 mg, 0.75 mmol) in benzene (1.67 mL). The reaction vessel was sealed, purged with Ar and heated at 60 ºC for 2.5 h. The reaction mixture was then allowed to cool to rt. The crude reaction mixture was concentrated under reduced pressure. Purification by flash chromatography (2.5% to 5% EtOAc/pentane) afforded *tert*-butyl 2-(4-bromophenyl)-2-((*tert*-butoxycarbonyl)(3-chloropropyl)amino)acetate **215** (191 mg, 83%) as a white solid. R_f 0.09 (2.5% EtOAc/pentane); mp = 82–83 ºC; ν_{max} (film)/cm^{-1} 2977, 1738 (C=O ester), 1690 (C=O carbamate), 1477, 1456, 1489, 1393, 1367, 1285, 1255, 1225, 1144, 1073, 1012, 908, 730; ^1H NMR (400 MHz, $CDCl_3$) δ 7.50 (d, *J* = 8.4 Hz, 2 H, 2 × HC_{Ar}), 7.18 (d, *J* = 8.4 Hz, 2 H, 2 × HC_{Ar}), 5.43 (br s, 1 H, NCH), 3.44–3.28 (m, 3 H, NCH_2 and $CHHCl$), 3.21–3.08 (m, 1 H, $CHHCl$), 1.94–1.83 (m, 1 H, NCH_2CHH), 1.74–1.40 (m, 19 H, NCH_2CHH and 2 × $C(CH_3)_3$); ^{13}C NMR (101 MHz, $CDCl_3$) δ 169.4 (C=O ester), 155.6 (C=O carbamate), 134.6 (br s, C_{Ar} quat), 131.7 (2 × C_{Ar}), 130.8 (2 × C_{Ar}), 122.4 (BrC_{Ar} quat), 82.1 ($C(CH_3)_3$ ester), 80.8 ($C(CH_3)$ carbamate), 63.0 (br s, NCH), 43.6 (NCH_2), 42.6 (CH_2Cl), 32.0 (NCH_2CH_2), 28.3 ($C(CH_3)_3$ ester), 28.0 ($C(CH_3)_3$ carbamate); HRMS (ESI^+) *m/z* Calculated for $C_{20}H_{30}NO_4{}^{35}Cl^{79}Br$ [M+H] 462.1047; Found 462.1056.

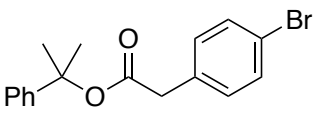
(±)–Ethyl 2-(4-bromophenyl)-2-((*tert*-butoxycarbonyl)(4-iodobutyl)amino)acetate (216)



$Rh_2(esp)_2$ (1.0 mg, 1.25 μmol) was added to a solution of *tert*-butyl (4-iodobutyl)carbamate **70** (299 mg, 1.0 mmol) and ethyl 2-diazo-2-(4-bromophenyl)acetate **88** (538 mg, 2.0 mmol) in CH_2Cl_2 (3.34 mL). The reaction vessel was sealed, purged with Ar and heated at 40 ºC for 2.5 h, then allowed to cool to rt. The crude reaction mixture was then concentrated under reduced pressure. Purification by flash chromatography (60% CH_2Cl_2/pentane) afforded ethyl 2-(4-bromophenyl)-2-((*tert*-butoxycarbonyl)(4-iodobutyl)amino)acetate **216** (496 mg, 92%) as a brown oil. R_f 0.20 (60% Et_2O/pentane); ν_{max} (film)/cm^{-1} 2976, 1743 (C=O ester), 1688 (C=O carbamate), 1489, 1454, 1393, 1366, 1291, 1251, 1146, 1072, 1027, 1011, 816, 769, 734; ^1H

NMR (400 MHz, $CDCl_3$) δ 7.50 (d, *J* = 8.4 Hz, 2 H, 2 × HC_{Ar}), 7.17 (d, *J* = 8.4 Hz, 2 H, 2 × HC_{Ar}), 5.73–5.22 (m, 1 H, NCH), 4.23 (q, *J* = 7.1 Hz, 2 H, OCH_2CH_3), 3.34–2.91 (m, 4 H, NCH_2 and CH_2I), 1.73–1.10 (m, 16 H, $NCH_2CH_2CH_2$ and OCH_2CH_3 and $C(CH_3)_3$); ^{13}C NMR (101 MHz, $CDCl_3$) δ 170.3 (C=O ester), 155.8 (C=O carbamate), 134.1 (C_{Ar} quat), 131.7 (2 × C_{Ar}), 130.7 (2 × C_{Ar} quat), 122.5 (BrC_{Ar} quat), 80.7 ($C(CH_3)_3$), 62.1 (NCH), 61.4 (OCH_2CH_3), 44.7 (NCH_2), 30.7 (NCH_2CH_2), 30.0 ($N(CH_2)_2CH_2$), 28.3 ($C(CH_3)_3$), 14.1 (OCH_2CH_3), 6.2 (CH_2I); HRMS (FTMS + pAPCI) *m/z* Calculated for $C_{14}H_{20}NO_2{}^{79}Br^{127}I^+$ $[M–(CO_2C(CH_3)_3)+H]^+$ 439.9717; Found 439.9698.

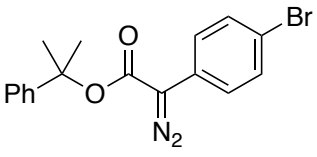
2-Phenylpropan-2-yl 2-(4-bromophenyl)acetate[424] (218)



2-phenyl-2-propanol (1.54 g, 11.0 mmol) in Et_2O (5.5 mL) was added to a solution of NaH (100.0 mg, 2.5 mmol) in Et_2O (10.0 mL) at 0 ºC). The reaction mixture was stirred at 25 ºC for 1 h. The reaction mixture was cooled to 0 ºC and trichloroacetonitrile (1.0 mL, 10.0 mmol) was added. The reaction mixture was stirred at 25 ºC for 3 h and then concentrated under reduced pressure. Pentane (50 mL) and MeOH (2 mL) were added and the mixture was stirred at 25 ºC for 10 min. The mixture was filtered through Celite, washing with pentane (20 mL). Concentration under reduced pressure afforded the crude imidate **217**.

4-Bromophenylacetic acid (1.08 g, 5.0 mmol) was added to the crude imidate in CH_2Cl_2 (5.0 mL) and the reaction mixture was stirred at 25 ºC for 15 h. The mixture was filtered through celite washing with CH_2Cl_2 (50 ml) and concentrated under reduced pressure. Purification by flash chromatography (5% to 10% Et_2O/pentane) afforded 2-phenylpropan-2-yl 2-(4-bromophenyl)acetate **218** (1.67 g, quant) as a pale yellow oil. R_f 0.25 (10% Et_2O/pentane); ν_{max} (film)/cm^{-1} 2981, 1733 (C=O), 1488, 1448, 1383, 1366, 1337, 1255, 1220, 1188, 1129, 1101, 1072, 1012, 961, 803, 764, 699; ^1H NMR (400 MHz, $CDCl_3$) δ 7.45 (d, *J* = 8.4 Hz, 2 H, 2 × HC_{Ar}), 7.33–7.20 (m, 5 H, 5 × HC_{Ph}), 7.15 (d, *J* = 8.4 Hz, 2 H, 2 × HC_{Ar}), 3.55 (s, 2 H, CH_2), 1.75 (s, 6 H, 2 × CH_3); ^{13}C NMR (101 MHz, $CDCl_3$) δ 169.4 (C=O), 145.4 (C_{Ph} quat), 133.2 (C_{Ar} quat), 131.5 (2 × C_{Ar}), 131.0 (2 × C_{Ar}), 128.2 (2 × C_{Ph}), 127.0 (C_{Ph}), 124.1 (2 × C_{Ph}), 121.0 (BrC_{Ar} quat), 82.3 ($CPh(CH_3)_2$), 41.9 (CH_2), 28.5 ($CPh(CH_3)_2$); HRMS (ES^-) *m/z* Calculated for $C_{17}H_{16}O_2{}^{79}Br$ [M–H] 331.0334; Found 331.0341.

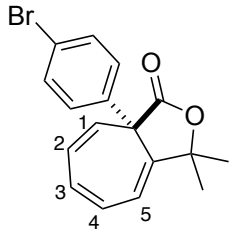
2-Phenylpropan-2-yl 2-(4-bromophenyl)-2-diazoacetate (219)



DBU (1.12 mL, 7.5 mmol) was added to a stirred solution of *p*-ABSA (1.44 g, 6.0 mmol) and 2-phenylpropan-2-yl 2-(4-bromophenyl)acetate **218** (1.67 g, 5.0 mmol) in CH_3CN (17 mL).

The reaction mixture was stirred at 25 °C for 24 h. Saturated aq. NH_4Cl (100 mL) was added. The aqueous reaction mixture was extracted with Et_2O (3 × 100 mL). The combined organic layers were dried over Na_2SO_4 and concentrated under reduced pressure. The mixture was then taken up in 50% Et_2O/pentane, filtered and concentrated under reduced pressure to afford 2-phenylpropan-2-yl 2-(4-bromoenyl)-2-diazoacetate **219** (1.8 g, quant) as an orange oil which was used without further purification. R_f 0.52 (5% Et_2O/pentane); ν_{max} (film)/cm^{-1} 2981, 2935, 2078 (C=N=N out-of-phase), 1698 (C=O), 1489, 1448, 1405, 1383, 1366 (C=N=N in-phase), 1310, 1276, 1189, 1168, 1131, 1016, 996, 730, 696; ^{1}H NMR (400 MHz, $CDCl_3$) δ 7.46 (d, J = 8.9 Hz, 2 H, 2 × HC_{Ar}), 7.43–7.31 (m, 6 H, 2 × HC_{Ar} and 4 × HC_{Ph}), 7.30–7.26 (m, 1 H, HC_{Ph}), 1.88 (s, 6 H, 2 × $OC(CH_3)_2Ph$); ^{13}C NMR (101 MHz, $CDCl_3$) δ 163.4 (C=O), 145.4 (C_{Ph} quat), 131.9 (2 × C_{Ar}), 128.4 (2 × C_{Ar}), 127.2 (C_{Ph}), 125.3 (2 × C_{Ph}), 125.0 (C_{Ar} quat), 124.2 (2 × C_{Ph}) 119.1 (BrC_{Ar} quat), 83.3 ($OC(CH_3)_2Ph$), 63.6 (CN_2 quat), 28.9 ($OC(CH_3)_2Ph$); HRMS (ESI$^+$) *m/z* Calculated for $C_{17}H_{15}N_2O_2{}^{79}BrNa$ [M+Na] 381.0215; Found 381.0222.

(±)–8a-(4-Bromophenyl)-3,3-dimethyl-3,8a-dihydro-1*H*-cyclohepta[*c*]furan-1-one (220)



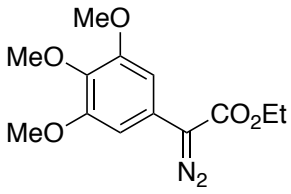
$Rh_2(esp)_2$ (1.9 mg, 2.5 μmol) was added to a solution of *tert*-butyl (3-chloropropyl)carbamate **58** (97 mg, 0.50 mmol) and 2-phenylpropan-2-yl 2-(4-bromophenyl)acetate **220** (269 mg, 0.75 mmol) in benzene (1.67 mL). The reaction vessel was sealed, purged with Ar and heated at 60 ºC for 2.5 h, then allowed to cool to rt. The crude reaction mixture was then filtered through Celite, washing with EtOAc (10 mL), and concentrated under reduced pressure. Purification by flash chromatography (5% Et_2O/pentane) afforded 8a-(4-Bromophenyl)-3,3-dimethyl-3,8a-dihydro-1*H*-cyclohepta[*c*]furan-1-one **220** (208 mg, 84%) as a white solid. R_f 0.23 (5% Et_2O/pentane); ν_{max} (film)/cm^{-1} 2982, 1754 (C=O ester), 1485, 1281, 1249, 1216, 1077, 1033, 1009, 928, 815, 702; ^{1}H NMR (400 MHz, $CDCl_3$) δ 7.32 (d, J = 8.7 Hz, 2 H, 2 × HC_{Ar}), 7.17 (d, J = 8.7 Hz, 2 H, 2 × HC_{Ar}), 6.51–6.41 (m, 2 H, H_3 and H_4), 6.37–6.25 (m, 2 H, H_2 and H_5), 5.78 (d, J = 9.2 Hz, 1 H, H_1), 1.79 (s, 3 H, CH_3), 1.57 (s, 3 H, CH_3); ^{13}C NMR (101 MHz, $CDCl_3$) δ 176.4 (C=O ester), 137.4 (C_5C quat), 135.5 (C_{Ar} quat), 130.8 (2 × C_{Ar}), 129.7 (C_2), 128.9 (2 × C_{Ar}), 128.8 (C_3 and BrC_{Ar} quat), 127.0 (C_5), 121.6 (C_1), 119.0 (C_4), 85.3 ($OC(CH_3)_2$ quat), 53.7 (C(O)*C*Ar quat), 31.3 (CH_3), 28.5 (CH_3); HRMS (ESI$^+$) *m/z* Calculated for $C_{17}H_{16}O_2Br$ [M+H] 331.0334; Found 331.0344.

6.2.2 Synthesised Compounds from Chapter 3

6.2.2.1 Additional Diazo Compounds

Ethyl 2-diazo-2-(3-(trifluoromethyl)phenyl)acetate **S1** was synthesised by Sebastian Green in analogous fashion to other ester-aryl diazo compounds (see Section 6.2.1.2).

Ethyl 2-diazo-2-(3,4,5-trimethoxyphenyl)acetate (252)

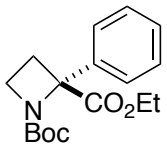


Adapted from a procedure by Wang.[223]

Ethyl 2-diazo-3-oxobutanoate **102** (0.33 mL, 2.4 mmol) was added to a solution of 5-iodo-1,2,3-trimethoxybenzene (588 mg, 2.0 mmol), $Pd(PPh_3)_4$ (116 mg, 0.1 mmol) and dry NaOH* (240 mg, 6.0 mmol) in degassed EtOH (8.0 mL) and stirred at 25 ºC for 18 h. The reaction mixture was filtered through silica, washing with EtOAc (50 mL) and concentrated under reduced pressure. Purification by flash chromatography (25% Et_2O/pentane) afforded ethyl 2-diazo-2-(3,4,5-trimethoxyphenyl)acetate **252** (340 mg, 59%) as an orange solid. R_f 0.24 (20% Et_2O/pentane); ν_{max} (film)/cm^{-1} 2976, 2943, 2078 (C=N=N out-of-phase), 1694 (C=O), 1578, 1509, 1446, 1393, 1378 (C=N=N in-phase), 1280, 1263, 1253, 1176, 1150, 1119, 1081, 1032, 897, 811, 731; ^{1}H NMR (400 MHz, $CDCl_3$) δ 6.74 (s, 2 H, 2 × HC_{Ar}), 4.33 (q, J = 7.1 Hz, 2 H, OCH_2CH_3), 3.87 (s, 6 H, 2 × OCH_3), 3.84 (s, 3 H, OCH_3), 1.35 (t, J = 7.1 Hz, 3 H, OCH_2CH_3); ^{13}C NMR (101 MHz, $CDCl_3$) δ 165.3 (C=O), 153.6 (2 × OC_{Ar} quat), 136.1 (OC_{Ar} quat), 120.8 (C_{Ar} quat), 101.5 (2 × C_{Ar}), 63.3 (C=N_2 quat), 61.0 (OCH_2CH_3), 60.9 (OCH_3), 56.1 (2 × OCH_3), 14.5 (OCH_2CH_3); HRMS (ESI^+) *m/z* Calculated for $C_{13}H_{17}N_2O_5$ [M+H] 281.1137; Found 281.1141. Note: Diazo **252** was observed to decompose at room temperature.

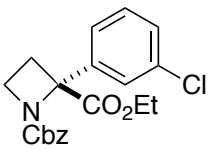
6.2.2.2 Additional 2,2-Disubstituted Azetidines

Large scale synthesis of (±)–1-(*tert*-butyl) 2-ethyl 2-phenylazetidine-1,2-dicarboxylate (104)



$Rh_2(esp)_2$ (56.9 mg, 75 μmol) was added to a solution of *tert*-butyl (2-chloroethyl)carbamate **52** (2.69 g, 15.0 mmol) and ethyl 2-diazo-2-phenylacetate **85** (4.28 g, 22.5 mmol) in toluene (50.0 mL). The reaction vessel was sealed, purged with Ar and heated at 60 ºC for 2.5 h, then allowed to cool to rt. Tetrabutylammonium bromide (483 mg, 1.5 mmol) was added, followed by $CsOH·H_2O$ (5.04 g, 30.0 mmol), and the reaction was stirred at 25 ºC for 18 h. The crude reaction mixture was then filtered through Celite, washing with EtOAc (200 mL), and concentrated under reduced pressure. Purification by flash chromatography (15 to 20% EtOAc/hexane) afforded 1-(*tert*-butyl) 2-ethyl 2-phenylazetidine-1,2-dicarboxylate **104** (1.97 g, 43%) as a pale yellow oil. R_f 0.18 (10% EtOAc/pentane); ν_{max} (film)/cm^{-1} 2977, 1736 (C=O ester), 1701 (C=O carbamate), 1362, 1230, 1151, 1087, 1022, 766, 696; ^{1}H NMR (400 MHz, $CDCl_3$) 7.50–7.27 (m, 5 H, 5 × HC_{Ph}), 4.34–4.12 (m, 3 H, OCH_2CH_3 and NCH), 3.94–3.84 (m, 1 H, NCH), 2.81–2.66 (m, 1 H, NCH_2CH), 2.60–2.45 (m, 1 H, NCH_2CH), 1.55–1.21 (m, 12 H, $C(CH_3)_3$ and OCH_2CH_3); ^{13}C NMR (101 MHz, $CDCl_3$) δ 171.5 (C=O ester), 155.9 (C=O carbamate), 140.4 (C_{Ph} quat), 127.7 (2 × C_{Ph}), 127.3 (2 × C_{Ph}), 126.4 (C_{Ph}), 80.3 and 80.0 ($C(CH_3)_3$), 73.4 and 73.2 (NC quat), 61.7 (OCH_2CH_3), 46.9 and 45.3 (NCH_2), 30.5 and 29.6 (NCH_2CH_2), 28.3 ($C(CH_3)_3$), 14.1 (OCH_2CH_3). The observed characterisation data was consistent with that previously reported above.[219]

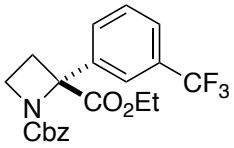
(±)–1-Benzyl 2-ethyl 2-(3-chlorophenyl)azetidine-1,2-dicarboxylate (245)



$Rh_2(esp)_2$ (3.8 mg, 5.0 μmol) was added to a solution of benzyl (2-chloroethyl)carbamate **63** (214 mg, 1.0 mmol) and ethyl 2-diazo-2-(3-chlorophenyl)acetate **245** (337 mg, 1.5 mmol) in benzene (3.33 mL). The reaction vessel was sealed, purged with Ar and heated at 60 ºC for 2.5 h, then allowed to cool to rt. Tetrabutylammonium bromide (32 mg, 0.1 mmol) was added, followed by $CsOH·H_2O$ (336 mg, 2.00 mmol), and the reaction was stirred at 25 ºC for 18 h. The crude reaction mixture was then filtered through Celite, washing with EtOAc (50 mL), and concentrated under reduced pressure. Purification by flash chromatography (20% EtOAc/hexane) afforded 1-benzyl 2-ethyl 2-(3-chlorophenyl)azetidine-1,2-dicarboxylate **245** (212 mg, 57%) as a pale yellow oil. R_f 0.25 (20% EtOAc/hexane); ν_{max} (film)/cm^{-1} 2972, 1706 (br s, C=O ester and carbamate), 1446, 1478, 1395, 1339, 1230, 1154, 1124, 777, 764, 739, 696, 689; ^{1}H NMR (400 MHz, $CDCl_3$) δ 7.51–7.22 (m, 9 H, 5 × HC_{Ph} and 4 × HC_{Ar}), 5.30–5.07 (m, 2 H, OCH_2Ph),

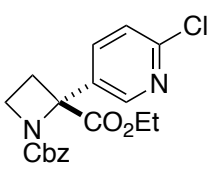
4.32–3.90 (m, 4 H, OC*H*$_2$CH$_3$ and NCH$_2$), 2.76 (br s, 1 H, NCH$_2$C*H*H), 2.63–2.46 (m, 1 H, NCH$_2$CH*H*), 1.26–1.09 (m, 3 H, OCH$_2$C*H*$_3$); ^{13}C NMR (101 MHz, $CDCl_3$) δ 170.6 (C=O ester), 156.7 and 156.5 (C=O carbamate), 142.3 and 141.8 (C_{Ar} quat), 136.5 and 135.9 (C_{Ph} quat), 133.9 (ClC_{Ar} quat), 129.2 (C_{Ar}), 128.4 (2 $\times$ C_{Ph}), 128.1 (2 $\times$ C_{Ph} and 1 $\times$ C_{Ar}), 127.7 (C_{Ar}), 126.8 (C_{Ph}), 124.8 (br s, C_{Ar}), 73.1 (NC quat), 67.0 (OCH$_2$Ph), 62.0 (O*C*H$_2$CH$_3$), 46.8 and 45.7 (NCH$_2$), 30.9 and 30.0 (NCH$_2$*C*H$_2$), 13.9 (OCH$_2$*C*H$_3$); HRMS (ESI$^+$) *m/z* Calculated for $C_{20}H_{21}NO_4{}^{35}Cl$ [M+H] 374.1159; Found 374.1164.

(±)–1-Benzyl 2-ethyl 2-(3-(trifluoromethyl)phenyl)azetidine-1,2-dicarboxylate (246)



Ethyl 2-diazo-2-(3-(trifluoromethyl)phenyl)acetate **S1** (484 mg, 1.88 mmol) in benzene (1.5 mL) was added slowly *via* syringe pump over 1 h to a solution of benzyl (2-chloroethyl)carbamate **63** (160 mg, 0.75 mmol) and $Rh_2(esp)_2$ (2.8 mg, 3.75 μmol) in benzene (1.0 mL) at 60 ºC. The reaction mixture was stirred at 60 °C for a further 2.5 h, then allowed to cool to rt. Tetrabutylammonium bromide (24 mg, 75.0 μmol) was added, followed by $CsOH{\cdot}H_2O$ (252 mg, 1.50 mmol), and the reaction was stirred at 25 ºC for 18 h. The crude reaction mixture was then filtered through Celite, washing with EtOAc (50 mL), and concentrated under reduced pressure. Purification by flash chromatography (20% EtOAc/pentane) afforded 1-benzyl 2-ethyl 2-(3-(trifluoromethyl)phenyl)azetidine-1,2-dicarboxylate **246** (227 mg, 74%) as a pale yellow oil. R_f 0.11 (15% EtOAc/pentane); ν_{max} (film)/cm^{-1} 2978, 1707 (s br, 2 $\times$ C=O), 1394, 1331, 1226, 1156, 1118, 697; ^{1}H NMR (400 MHz, $CDCl_3$) δ 7.76–7.19 (m, 9 H, 5 $\times$ HC_{Ph} and 4 $\times$ HC_{Ar}), 5.29–5.06 (m, 2 H, OCH$_2$Ph), 4.33–3.91 (m, 4 H, OC*H*$_2$CH$_3$ and NC*H*$_2$), 2.86–2.75 (m, 1 H, NCH$_2$C*H*H), 2.65–2.47 (m,1 H, NCH$_2$CH*H*), 1.23–1.09 (m, 3 H, OCH$_2$C*H*$_3$); ^{13}C NMR (101 MHz, $CDCl_3$) δ 170.6 (C=O ester), 156.7 (br s, C=O carbamate), 141.3 and 141.0 (C_{Ar} quat), 136.3 and 135.8 (C_{Ph} quat), 130.4 and 130.0 (2 $\times$ C_{Ar}), 128.41, 128.35 and 128.1 (3 $\times$ br s, 5 $\times$ C_{Ph} and C_{Ar}), 124.39 and 124.36 (m, C_{Ar}), 124.1 (q, J_{C-F} = 271.7 Hz, CF_3), 123.4 (C_{Ar}), 73.2 (NC quat), 67.1 (OCH$_2$Ph), 62.1 (O*C*H$_2$CH$_3$), 46.8 and 45.8 (NCH$_2$), 30.9 and 30.0 (NCH$_2$*C*H$_2$), 13.9 (OCH$_2$*C*H$_3$); ^{19}F{^{1}H} NMR (377 MHz, $CDCl_3$) δ –62.46 and –62.50; HRMS (FTMS + pNSI) *m/z* Calculated for $C_{21}H_{21}NO_4F_3^+$ $[M+H]^+$ 408.1417; Found 408.1413.

(±)–1-Benzyl 2-ethyl 2-(6-chloropyridin-3-yl)azetidine-1,2-dicarboxylate (247)

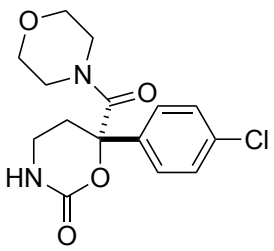


Ethyl 2-(6-chloropyridin-3-yl)-2-diazoacetate **97** (1.13 g, 5.0 mmol) in benzene (2.17 mL) was added slowly *via* syringe pump over 1 h to a solution of benzyl (2-chloroethyl)carbamate **63** (427 mg, 2.0 mmol) and $Rh_2(esp)_2$ (7.6 mg, 10 μmol) in benzene (4.5 mL) at 60 ºC. The reaction mixture was stirred at 60 °C for a further 2.5 h, then allowed to cool to rt. Tetrabutylammonium bromide

(65 mg, 0.2 mmol) was added, followed by $CsOH{\cdot}H_2O$ (672 mg, 4.0 mmol), and the reaction was stirred at 25 ºC for 18 h. The crude reaction mixture was then filtered through Celite, washing with EtOAc (100 mL), and concentrated under reduced pressure. Purification by flash chromatography (30% to 40% EtOAc/pentane) afforded 1-benzyl 2-ethyl 2-(6-chloropyridin-3-yl)azetidine-1,2-dicarboxylate **247** (133 mg, 18%) as a brown oil. R_f 0.13 (30% EtOAc/pentane); ν_{max} (film)/cm^{-1} 2978, 2900, 1707 (br s, 2 × C=O), 1588, 1457, 1394, 1338, 1238, 1156, 1103, 1014, 738, 697; ^{1}H NMR (400 MHz, $CDCl_3$) δ 8.43 (br s, 1 H, HC_{Ar}), 7.84 and 7.67 (2 × d, J = 7.5 Hz, 1 H, HC_{Ar}), 7.49–7.12 (m, 6 H, HC_{Ar} and 5 × HC_{Ph}), 5.25–5.06 (m, 2 H, OCH_2Ph), 4.32–3.85 (m, 4 H, OCH_2CH_3 and NCH_2), 2.80–2.68 (m, 1 H, NCH_2CHH), 2.62–2.43 (m, 1 H, NCH_2CHH), 1.20–1.06 (m, 3 H, OCH_2CH_3); ^{13}C NMR (101 MHz, $CDCl_3$) δ 170.1 (C=O ester), 156.8 and 156.3 (C=O carbamate), 150.4 (ClC_{Ar} quat), 148.0 (C_{Ar}), 137.5 and 137.1 (C_{Ph} quat), 136.1 and 135.5 (C_{Ar} quat), 135.0 and 134.5 (C_{Ar}), 128.4 (2 × C_{Ph}), 128.1 (2 × C_{Ph}), 127.8 (C_{Ph}), 123.3 (C_{Ar}), 71.3 and 71.2 (NC quat), 67.2 and 67.1 (OCH_2Ph), 62.3 (OCH_2CH_3), 47.0 and 46.0 (NCH_2), 30.5 and 29.5 (NCH_2CH_2), 13.8 (OCH_2CH_3); HRMS (ESI^+) *m/z* Calculated for $C_{19}H_{20}N_2O_4{}^{35}Cl$ [M+H] 375.1112; Found 375.1096.

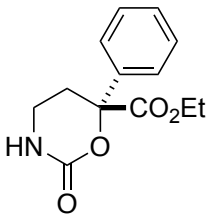
6.2.2.3 Synthesis of 1,3-Oxazinan-2-ones

(±)–6-(4-Chlorophenyl)-6-(morpholine-4-carbonyl)-1,3-oxazinan-2-one (230)



Trifluoroacetic acid (0.10 mL) was added to a stirred solution of of *tert*-butyl 2-(4-chlorophenyl)-2-(morpholine-4-carbonyl)azetidine-1-carboxylate **187** (28 mg, 0.075 mmol) in CH_2Cl_2 (0.40 mL) at 0 ºC. The reaction mixture was then stirred at 25 ºC for 15 h. The solvent was removed under reduced pressure, saturated aq. $NaHCO_3$ (10 mL) and saturated brine (25 mL) was added and the aqueous mixture was extracted with $CHCl_3$:2-propanol (3:1, 6 × 10 mL). The solvent was removed under reduced pressure. Purification by flash chromatography NH_3/MeOH/CH_2Cl_2 (0.05:4.95:95%) afforded 6-(4-chlorophenyl)-6-(morpholine-4-carbonyl)-1,3-oxazinan-2-one **230** (10 mg, 43%) as a yellow solid. R_f 0.18 (0.05:4.95:95 NH_3:MeOH:CH_2Cl_2); mp = 188–190 ºC; ν_{max} (film)/cm^{-1} 3283 (br s, NH), 2924, 2858, 1721 (C=O carbamate), 1642 (C=O amide), 1490, 1436, 1319, 1115, 1085, 1006, 730; ^{1}H NMR (400 MHz, $CDCl_3$) δ 7.43–7.34 (m, 4 H, 2 × HC_{Ar}), 5.77 (br s, 1 H, NH), 3.74–3.56 (m, 6 H, 2 × OC*H*H, HNC*H*HCH$_2$, NC*H*HCH$_2$O and NC*H*$_2$CH$_2$O), 3.54–3.46 (m, 1 H, OCH*H*), 3.33–3.25 (m, 1 H, NCH*H*CH$_2$O), 3.24–3.17 (m, 1 H, HNCH*H*CH$_2$), 3.16–3.09 (m, 1 H, OCH*H*), 2.77 (dt, 1 H, *J* = 14.0, 4.5 Hz, HNCH$_2$C*H*H), 2.02–1.92 (m, 1 H, HNCH$_2$CH*H*); ^{13}C NMR (101 MHz, $CDCl_3$) δ 166.9 (C=O amide), 152.4 (C=O carbamate), 137.7 (C_{Ar} quat), 134.6 (C_{Ar} quat), 129.3 (2 × C_{Ar}), 125.3 (2 × C_{Ar}), 84.9 (OC quat), 66.7 (O*C*H$_2$), 66.4 (O*C*H$_2$), 47.1 (N*C*H$_2$CH$_2$O), 43.8 (NCH$_2$*C*H$_2$O), 37.7 (HNCH$_2$), 32.7 (HNCH$_2$*C*H$_2$); HRMS (ESI$^+$) *m/z* Calculated for $C_{15}H_{18}N_2O_4{}^{35}Cl$ [M+H] 325.0955; Found 325.0958.

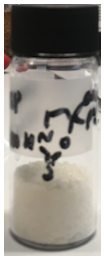
(±)–Ethyl 2-oxo-6-phenyl-1,3-oxazinane-6-carboxylate (231)



Trifluoroacetic acid (0.19 mL, 2.5 mmol) was added to a stirred solution of 1-(*tert*-butyl) 2-ethyl 2-phenylazetidine-1,2-dicarboxylate **104** (153 mg, 0.5 mmol) in toluene (0.5 mL) at 25 ºC and stirred for 30 min. The reaction mixture was concentrated and purified by flash chromatography (2% to 3% MeOH/CH_2Cl_2) to afford ethyl 2-oxo-6-phenyl-1,3-oxazinane-6-carboxylate **231** (93 mg, 75%) as an off-white solid. R_f 0.25 (EtOAc); mp = 141–145 ºC; ν_{max} (film)/cm^{-1} 3266 (br, NH), 2983, 1710 (s br, 2 × C=O), 1489, 1449, 1408, 1312, 1271, 1203, 1139, 1096, 1074, 1015, 760, 734, 698; ^{1}H NMR (400 MHz, $CDCl_3$) δ 7.61–7.56 (m, 2 H, 2 × HC_{Ph}), 7.43–7.33 (m, 3 H, 3 × HC_{Ph}), 6.59 (br s, 1 H, NH), 4.27–4.18 (m, 2 H, OC*H*$_2$CH$_3$), 3.41–3.26 (m, 2 H, NCH$_2$), 2.75 (dt, *J* = 13.8, 4.9 Hz, 1 H, NCH$_2$C*H*H), 2.33 (ddd, *J* = 13.8, 9.2, 5.9 Hz, 1 H, NCH$_2$CH*H*), 1.23 (t, *J* = 7.1 Hz, 3 H, OCH$_2$C*H*$_3$); ^{13}C NMR (101 MHz, $CDCl_3$) δ 169.9 (C=O ester), 153.1 (C=O carbamate), 137.4 (C_{Ph} quat), 128.72 (C_{Ph}), 128.66 (2 × C_{Ph}), 124.9 (2 ×

C_{Ph}), 83.2 (OC quat), 62.4 (O*C*H_2CH_3), 37.1 (NCH_2), 29.2 (NCH_2CH_2), 13.9 (OCH_2CH_3); HRMS (ESI^+) *m/z* Calculated for $C_{13}H_{16}NO_4$ [M+H] 250.1079; Found 250.1079.

Gram Scale Synthesis of **231**

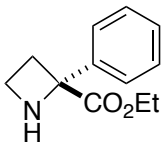


Trifluoroacetic acid (2.87 mL, 37.5 mmol) was added to a stirred solution of 1-(*tert*-butyl) 2-ethyl 2-phenylazetidine-1,2-dicarboxylate **104** (2.29 g, 7.5 mmol) in toluene (7.5 mL) at 25 ºC and stirred for 30 min. The reaction mixture was concentrated and purified by flash chromatography (EtOAc) to afford ethyl 2-oxo-6-phenyl-1,3-oxazinane-6-carboxylate **231** (1.23 g, 66%) as an off-white solid. The observed characterisation data was identical to that reported previously for **231** above.

From 1-benzyl 2-ethyl 2-phenylazetidine-1,2-dicarboxylate **105**:

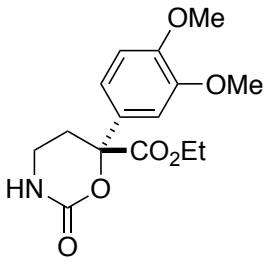
Trifluoroacetic acid (38 μL, 0.5 mmol) was added to a stirred solution of 1-(*tert*-butyl) 2-ethyl 2-phenylazetidine-1,2-dicarboxylate **105** (34 mg, 0.1 mmol) in toluene (0.1 mL) at 25 ºC and stirred for 30 min. The reaction mixture was concentrated and purified by flash chromatography (2% MeOH/CH_2Cl_2) to afford ethyl 2-oxo-6-phenyl-1,3-oxazinane-6-carboxylate **231** (18 mg, 72%) as an off-white solid. The observed characterisation data was identical to that reported previously for **231** above.

(±)–Ethyl 2-phenylazetidine-2-carboxylate (232)



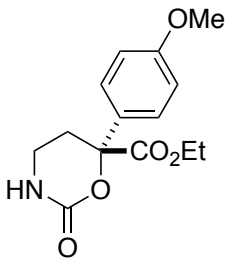
4 N HCl in 1,4-dioxane (3.8 mL) was added dropwise to a stirred solution of 1-(*tert*-butyl) 2-ethyl 2-phenylazetidine-1,2-dicarboxylate **104** (458 mg, 1.5 mmol) in 1,4-dioxane (6.0 mL) at 0 ºC. The reaction mixture was stirred at 25 ºC for 24 h then diluted with 1 M HCl (40 mL). The aqueous reaction mixture was extracted with EtOAc (2 × 40 mL). The aqueous layer was basified with sat. aq. $NaHCO_3$ (50 mL) and extracted with EtOAc (5 × 25 mL). The combined organic layers were dried over Na_2SO_4 and filtered. Concentration under reduced pressure afforded ethyl 2-phenylazetidine-2-carboxylate **232** (220 mg, 71%) as a yellow oil. R_f 0.36 (EtOAc); ν_{max} (film)/cm^{-1} 3325 (NH), 2974, 2874, 1722 (C=O), 1241, 1103, 1014, 775, 731, 697; ^1H NMR (400 MHz, $CDCl_3$) δ 7.42–7.38 (m, 2 H, 2 × HC_{Ph}), 7.37–7.32 (m, 2 H, 2 × HC_{Ph}), 7.29–7.23 (m, 1 H, HC_{Ph}), 4.28–4.11 (m, 2 H, O*C*H_2CH_3), 3.69 (td, *J* = 8.5, 7.4 Hz, 1 H, NC*H*H), 3.34 (ddd, *J* = 8.5, 7.3, 3.9 Hz, 1 H, NCH*H*), 2.94–2.77 (m, 2 H, NCH_2CH_2), 1.23 (d, *J* = 7.1 Hz, 3 H, OCH_2CH_3); ^{13}C NMR (101 MHz, $CDCl_3$) δ 175.7 (C=O), 143.1 (C_{Ph} quat), 128.1 (2 × C_{Ph}), 127.1 (C_{Ph}), 125.1 (2 × C_{Ph}), 69.4 (NC quat), 61.6 (O*C*H_2CH_3), 41.8 (NCH_2), 32.4 (NCH_2CH_2), 14.0 (OCH_2CH_3); HRMS (FTMS + pNSI) *m/z* Calculated for $C_{12}H_{16}NO_2^+$ $[M+H]^+$ 206.1176; Found 206.1176.

(±)–Ethyl 6-(3,4-dimethoxyphenyl)-2-oxo-1,3-oxazinane-6-carboxylate (233)



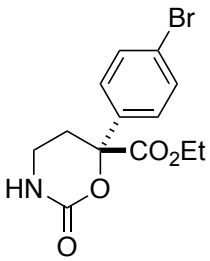
Trifluoroacetic acid (38 μL, 0.50 mmol) was added to a stirred solution of 1-(*tert*-butyl) 2-ethyl 2-(3,4-dimethoxyphenyl)azetidine-1,2-dicarboxylate **106** (36.5 mg, 0.10 mmol) in toluene (0.10 mL) at 25 ºC and stirred for 30 min. The reaction mixture was concentrated and purified by flash chromatography (3% MeOH/CH_2Cl_2) to afford ethyl 6-(4-methoxyphenyl)-2-oxo-1,3-oxazinane-6-carboxylate **233** (27 mg, 88%) as a white solid. R_f 0.05 (2% MeOH/CH_2Cl_2); mp = 108–111 ºC; ν_{max} (film)/cm^{-1} 3282 (br s, NH), 2939, 1710 (br s, C=O ester/carbamate), 1516, 1460, 1413, 1262, 1202, 1166, 1144, 1090, 1020, 808, 760, 692; ^{1}H NMR (400 MHz, $CDCl_3$) δ 7.13–7.06 (m, 2 H, 2 × HC_{Ar}), 6.87 (d, *J* = 8.4 Hz, 1 H, HC_{Ar}), 6.33 (s, 1 H, NH), 4.23 (q, *J* = 7.1 Hz, 2 H, OCH_2CH_3), 3.90 and 3.89 (2 × s, 6 H, 2 × OCH_3), 3.38–3.32 (m, 2 H, NCH_2), 2.75 (dt, *J* = 13.8, 4.3 Hz, 1 H, NCH_2CHH), 2.37–2.26 (m, 1 H, NCH_2CHH), 1.24 (q, *J* = 7.1 Hz, 3 H, OCH_2CH_3); ^{13}C NMR (101 MHz, $CDCl_3$) δ 170.0 (C=O ester), 153.3 (C=O carbamate), 149.3 (OC_{Ar} quat), 149.0 (OC_{Ar} quat), 129.8 (C_{Ar} quat), 117.4 (C_{Ar}), 110.9 (C_{Ar}), 108.2 (C_{Ar}), 83.1 (OC quat), 62.5 (OCH_2CH_3), 56.0 (OCH_3), 55.9 (OCH_3), 37.2 (NCH_2), 29.0 (NCH_2CH_2), 14.0 (OCH_2CH_3); HRMS (ESI$^+$) *m/z* Calculated for $C_{15}H_{20}NO_6$ [M+H] 310.1291; Found 310.1295.

(±)–Ethyl 6-(4-methoxyphenyl)-2-oxo-1,3-oxazinane-6-carboxylate (234)



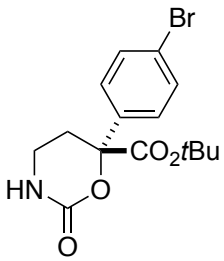
Trifluoroacetic acid (38 μL, 0.50 mmol) was added to a stirred solution of 1-(*tert*-butyl) 2-ethyl 2-(4-methoxyphenyl)azetidine-1,2-dicarboxylate **107** (34 mg, 0.10 mmol) in toluene (0.10 mL) at 25 ºC and stirred for 30 min. The reaction mixture was concentrated and purified by flash chromatography (3% MeOH/CH_2Cl_2) to afford ethyl 6-(4-methoxyphenyl)-2-oxo-1,3-oxazinane-6-carboxylate **234** (25 mg, 89%) as a white solid. R_f 0.21 (3% MeOH/CH_2Cl_2); mp = 175–176 ºC; ν_{max} (film)/cm^{-1} 3241 (br s, NH), 3138, 2942, 1741 (C=O ester), 1702 (C=O carbamate), 1511, 1492, 1462, 1445, 1411, 1326, 1308, 1302, 1254, 1199, 1182, 1145, 1122, 1090, 1031, 1005, 822, 799, 763, 695; ^{1}H NMR (400 MHz, $CDCl_3$) δ 7.50 (d, *J* = 8.9 Hz, 2 H, 2 × HC_{Ar}), 6.91 (d, *J* = 8.9 Hz, 2 H, 2 × HC_{Ar}), 6.36 (br s, 1 H, NH), 4.22 (q, *J* = 7.1 Hz, 2 H, OCH_2CH_3), 3.81 (s, 3 H, OCH_3), 3.39–3.26 (m, 2 H, NCH_2), 2.72 (dt, *J* = 13.8, 4.8 Hz, 1 H, NCH_2CHH), 2.32 (ddd, *J* = 13.8, 8.3, 2.6 Hz, 1 H, NCH_2CHH), 1.23 (t, *J* = 7.1 Hz, 3 H, OCH_2CH_3); ^{13}C NMR (101 MHz, $CDCl_3$) δ 171.1 (C=O ester), 159.8 (OC_{Ar} quat), 153.1 (C=O carbamate), 129.5 (C_{Ar} quat), 126.4 (2 × C_{Ar}), 114.0 (2 × C_{Ar}), 83.0 (OC quat), 62.4 (OCH_2CH_3), 55.3 (OCH_3), 37.1 (NCH_2), 29.0 (NCH_2CH_2), 14.0 (OCH_2CH_3); HRMS (ESI$^+$) *m/z* Calculated for $C_{14}H_{18}NO_5$ [M+H] 280.1185; Found 280.1187.

(±)–Ethyl 6-(4-bromophenyl)-2-oxo-1,3-oxazinane-6-carboxylate (235)



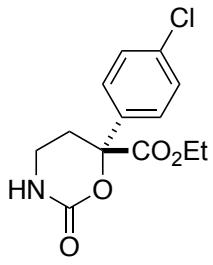
Trifluoroacetic acid (38 μL, 0.50 mmol) was added to a stirred solution of 1-(*tert*-butyl) 2-ethyl 2-(4-bromophenyl)azetidine-1,2-dicarboxylate **108** (38 mg, 0.10 mmol) in toluene (0.10 mL) at 25 ºC and stirred for 30 min. After 30 min further trifluoroacetic acid (38 μL, 0.50 mmol) was added and the mixture was stirred for a further 30 min. The reaction mixture was concentrated and purified by flash chromatography (80% EtOAc/pentane to EtOAc) to afford ethyl 6-(4-bromophenyl)-2-oxo-1,3-oxazinane-6-carboxylate **235** (21 mg, 63%) as a white solid. R_f 0.23 (3% MeOH/CH_2Cl_2); mp = 122–125 ºC; ν_{max} (film)/cm^{-1} 3241 (br s, NH), 3138, 2980, 2941, 1741 (C=O ester), 1705 (C=O carbamate), 1485, 1462, 1410, 1338, 1324, 1277, 1255, 1199, 1185, 1145, 1122, 1090, 1024, 1007, 967, 820, 779, 723, 700, 685; ^{1}H NMR (400 MHz, $CDCl_3$) δ 7.55 (d, *J* = 8.8 Hz, 2 H, 2 × HC_{Ar}), 7.48 (d, *J* = 8.8 Hz, 2 H, 2 × HC_{Ar}), 5.53 (br s, 1 H, NH), 4.28–4.20 (m, 2 H, OC*H*$_2$CH$_3$), 3.43–3.28 (m, 2 H, NCH_2), 2.75 (dt, *J* = 13.9, 4.8 Hz, 1 H, NCH_2CHH), 2.33–2.22 (ddd, *J* = 14.0, 9.4, 6.4 Hz, 1 H, NCH_2CHH), 1.25 (t, *J* = 7.1 Hz, 3 H, OCH_2CH_3); ^{13}C NMR (101 MHz, $CDCl_3$) δ 169.5 (C=O ester), 152.7 (C=O carbamate), 136.5 (C_{Ar} quat), 131.9 (2 × C_{Ar}), 126.8 (2 × C_{Ar}), 123.1 (BrC_{Ar} quat), 82.9 (OC quat), 62.7 (OCH_2CH_3), 37.1 (NCH_2), 29.2 (NCH_2CH_2), 13.9 (OCH_2CH_3); HRMS (ESI$^+$) *m/z* Calculated for $C_{13}H_{15}NO_4{}^{79}Br$ [M+H] 328.0184; Found 328.0184.

(±)–*tert*-Butyl 6-(4-bromophenyl)-2-oxo-1,3-oxazinane-6-carboxylate (236)



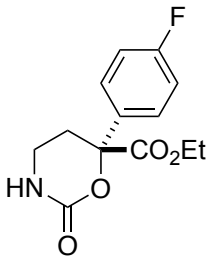
Trifluoroacetic acid (38 μL, 0.5 mmol) was added to a stirred solution of di-*tert*-butyl 2-(4-bromophenyl)azetidine-1,2-dicarboxylate **109** (41 mg, 0.10 mmol) in toluene (0.10 mL) at 25 ºC and stirred for 30 min. The reaction mixture was concentrated and purified by flash chromatography (2% MeOH/CH_2Cl_2) to afford *tert*-butyl 6-(4-bromophenyl)-2-oxo-1,3-oxazinane-6-carboxylate **236** (20 mg, 56%) as a white solid. R_f 0.20 (3% MeOH/CH_2Cl_2); mp = 185–188 ºC; ν_{max} (film)/cm^{-1} 3263 (br s, NH), 2979, 1724 (br s, C=O ester/carbamate), 1489, 1397, 1370, 1321, 1160, 1096, 840; ^{1}H NMR (400 MHz, $CDCl_3$) δ 7.53 (d, *J* = 8.8 Hz, 2 H, 2 × HC_{Ar}), 7.47 (d, *J* = 8.8 Hz, 2 H, 2 × HC_{Ar}), 5.94 (br s, 1 H, NH), 3.43–3.30 (m, 2 H, NCH_2), 2.71 (dt, *J* = 13.8, 4.6 Hz, 1 H, NCH_2CHH), 2.22 (ddd, *J* = 13.8, 9.7, 6.3 Hz, 1 H, NCH_2CHH), 1.43 (s, 9 H, $C(CH_3)_3$); ^{13}C NMR (101 MHz, $CDCl_3$) δ 168.4 (C=O ester), 152.7 (C=O carbamate), 136.9 (C_{Ar} quat), 131.7 (2 × C_{Ar}), 126.8 (2 × C_{Ar}), 122.9 (BrC_{Ar} quat), 83.8 ($C(CH_3)_3$), 83.0 (OC quat), 37.3 (NCH_2), 29.2 (NCH_2CH_2), 27.7 ($C(CH_3)_3$); HRMS (ESI$^+$) *m/z* Calculated for $C_{15}H_{19}NO_4{}^{79}Br$ [M+H] 356.0497; Found 356.0503.

(±)–Ethyl 6-(4-chlorophenyl)-2-oxo-1,3-oxazinane-6-carboxylate (177)



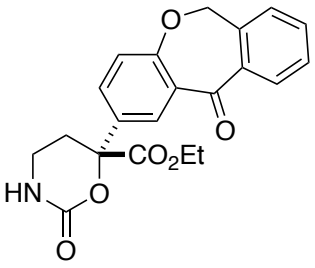
Trifluoroacetic acid (77 μL, 1.0 mmol) was added to a stirred solution of 1-(*tert*-butyl) 2-ethyl 2-(4-chlorophenyl)azetidine-1,2-dicarboxylate **115** (68 mg, 0.20 mmol) in toluene (0.20 mL) at 25 ºC and stirred for 30 min. The reaction mixture was concentrated and purified by flash chromatography (2% MeOH/CH_2Cl_2) to afford ethyl 6-(4-chlorophenyl)-2-oxo-1,3-oxazinane-6-carboxylate **177** (40 mg, 71%) as a white solid. R_f 0.23 (3% MeOH/CH_2Cl_2); mp = 116–118 ºC; ν_{max} (film)/cm^{-1} 3242 (br s, NH), 3137, 2981, 2941, 1485, 1462, 1411, 1338, 1324, 1301, 1277, 1255, 1199, 1185, 1145, 1122, 1089, 1024, 1007, 861, 779, 763, 723, 685, 701; ^{1}H NMR (400 MHz, $CDCl_3$) δ 7.54 (d, *J* = 8.7 Hz, 2 H, 2 × HC_{Ar}), 7.38 (d, *J* =, 8.7 Hz, 2 H, 2 × HC_{Ar}), 6.55 (br s, 1 H, NH), 4.23 (q, *J* = 7.1 Hz, 2 H, OC*H*$_2$CH$_3$), 3.40–3.28 (m, 2 H, NCH_2), 2.74 (dt, *J* = 13.8, 4.7 Hz, 1 H, NCH_2CHH), 2.27 (ddd, *J* = 14.0, 9.3, 5.9 Hz, 1 H, NCH_2CHH), 1.23 (t, *J* = 7.1 Hz, 3 H, OCH_2CH_3); ^{13}C NMR (101 MHz, $CDCl_3$) δ 169.6 (C=O ester), 152.8 (C=O carbamate), 136.0 (C_{Ar} quat), 134.9 (ClC_{Ar} quat), 128.9 (2 × C_{Ar}), 126.5 (2 × C_{Ar}), 82.8 (OC quat), 62.7 (O*C*H$_2$CH$_3$), 37.1 (NCH_2), 29.2 (NCH_2CH_2), 13.9 (OCH_2CH_3); HRMS (ESI$^+$) *m/z* Calculated for $C_{13}H_{15}NO_4{}^{35}Cl$ [M+H] 284.0690; Found 284.0689.

(±)–Ethyl 6-(4-fluorophenyl)-2-oxo-1,3-oxazinane-6-carboxylate (237)



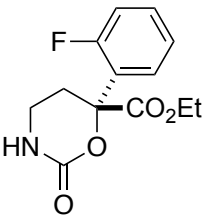
Trifluoroacetic acid (77 μL, 1.0 mmol) was added to a stirred solution of 1-(*tert*-butyl) 2-ethyl 2-(4-fluorophenyl)azetidine-1,2-dicarboxylate **112** (65 mg, 0.20 mmol) in toluene (0.20 mL) at 25 ºC and stirred for 30 min. The reaction mixture was concentrated and purified by flash chromatography (3% MeOH/CH_2Cl_2) to afford ethyl 6-(4-fluorophenyl)-2-oxo-1,3-oxazinane-6-carboxylate **237** (37 mg, 95%) as a white solid. R_f 0.28 (3% MeOH/CH_2Cl_2); mp = 115–118 ºC; ν_{max} (film)/cm^{-1} 3236 (br s, NH), 3136, 1732 (C=O ester), 1705 (C=O carbamate), 1511, 1493, 1415, 1332, 1222, 1207, 1142, 1121, 1012, 813, 744, 709; ^{1}H NMR (400 MHz, $CDCl_3$) δ 7.61–7.55 (m, 2 H, 2 × HC_{Ar}), 7.12–7.05 (m, 2 H, 2 × HC_{Ar}), 6.46 (br s, 1 H, NH), 4.23 (q, *J* = 7.1 Hz, 2 H, OC*H*$_2$CH$_3$), 3.41–3.28 (m, 2 H, NCH_2), 2.75 (dt, *J* = 13.8, 4.6 Hz, 1 H, NCH_2CHH), 2.29 (ddd, *J* = 13.8, 9.2, 6.2 Hz, 1 H, NCH_2CHH), 1.23 (t, *J* = 7.1 Hz, 3 H, OCH_2CH_3); ^{13}C NMR (101 MHz, $CDCl_3$) δ 169.7 (C=O ester), 162.8 (d, J_{C-F} = 247.8 Hz, FC_{Ar} quat), 153.0 (C=O carbamate), 133.3 (d, J_{C-F} = 2.9 Hz, C_{Ar} quat), 127.0 (d, J_{C-F} = 8.3 Hz, 2 × C_{Ar}), 115.7 (d, J_{C-F} = 21.9 Hz, 2 × C_{Ar}), 82.9 (OC quat), 62.6 (O*C*H$_2$CH$_3$), 37.1 (NCH_2), 29.2 (NCH_2CH_2), 13.9 (OCH_2CH_3); ^{19}F{^{1}H} NMR (377 MHz, $CDCl_3$) δ –113.0; HRMS (ESI$^+$) *m/z* Calculated for $C_{13}H_{15}NO_4F$ [M+H] 268.0985; Found 268.0993.

(±)–Ethyl 2-oxo-6-(11-oxo-6,11-dihydrodibenzo[*b*,*e*]oxepin-2-yl)-1,3-oxazinane-6-carboxylate (238)



Trifluoroacetic acid (38 μL, 0.50 mmol) was added to a stirred solution of 1-(*tert*-butyl) 2-ethyl 2-(11-oxo-6,11-dihydrodibenzo[*b*,*e*]oxepin-2-yl)azetidine-1,2-dicarboxylate **156** (44 mg, 0.10 mmol) in toluene (0.10 mL) at 25 ºC and stirred for 30 min. The reaction mixture was concentrated and purified by flash chromatography (70% EtOAc/pentane) to afford ethyl 2-oxo-6-(11-oxo-6,11-dihydrodibenzo[b,e]oxepin-2-yl)-1,3-oxazinane-6-carboxylate **238** (37 mg, 96%) as a white solid. R_f 0.20 (70% EtOAc/pentane); mp = 78–80 ºC; ν_{max} (film)/cm^{-1} 3280 (br s, NH), 2982, 1715 (br s, C=O ester and carbamate), 1648 (C=O ketone), 1484, 1297, 1271, 1200, 1092, 1010, 760, 727; ^{1}H NMR (400 MHz, $CDCl_3$) δ 8.38 (d, *J* = 2.5 Hz, 1 H, HC_{Ar}), 7.88 (dd, *J* = 7.7, 1.2 Hz, 1 H, HC_{Ar}), 7.78 (dd, *J* = 8.7, 2.6 Hz, 1 H, HC_{Ar}), 7.58 (td, *J* = 7.5, 1.4 Hz, 1 H, HC_{Ar}), 7.49 (td, *J* = 7.6, 1.2 Hz, 1 H, HC_{Ar}), 7.38 (dd, *J* = 7.6, 0.9 Hz, 1 H, HC_{Ar}), 7.10 (d, *J* = 8.7 Hz, 1 H, HC_{Ar}), 6.30 (br s, 1 H, NH), 5.21 (s, 2 H, OCH_2Ar), 4.25 (q, *J* = 7.1 Hz, 2 H, OCH_2CH_3), 3.42–3.36 (m, 2 H, NCH_2), 2.84 (dt, *J* = 13.8, 4.6 Hz, 1 H, NCH_2CHH), 2.39 (dt, *J* = 13.8, 7.9 Hz, 1 H, NCH_2CHH), 1.26 (t, *J* = 7.1 Hz, 3 H, OCH_2CH_3); ^{13}C NMR (101 MHz, $CDCl_3$) δ 190.5 (C=O ketone), 170.0 (C=O ester), 161.4 (OC_{Ar} quat), 152.8 (C=O carbamate), 140.3 (C_{Ar} quat), 135.2 (C_{Ar} quat), 132.9 (C_{Ar}), 132.4 (C_{Ar}), 131.3 (C_{Ar} quat), 129.44 (C_{Ar}), 129.37 (C_{Ar}), 128.7 (C_{Ar}), 127.9 (C_{Ar}), 125.0 (C_{Ar} quat), 121.5 (C_{Ar}), 82.8 (OC quat), 73.5 (OCH_2Ar), 62.6 (OCH_2CH_3), 37.2 (NCH_2), 28.7 (NCH_2CH_2), 14.0 (OCH_2CH_3); HRMS (FTMS + pNSI) *m/z* Calculated for $C_{21}H_{20}NO_6^+$ $[M+H]^+$ 382.1285; Found 382.1288.

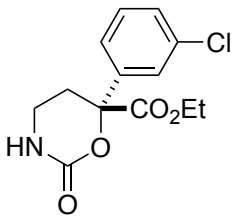
(±)–Ethyl 6-(2-fluorophenyl)-2-oxo-1,3-oxazinane-6-carboxylate (239)



Trifluoroacetic acid (77 μL, 1.0 mmol) was added to a stirred solution of 1-(*tert*-butyl) 2-ethyl 2-(4-fluorophenyl)azetidine-1,2-dicarboxylate **110** (65 mg, 0.20 mmol) in toluene (0.20 mL) at 25 ºC and stirred for 30 min. The reaction mixture was concentrated and purified by flash chromatography (2% MeOH/CH_2Cl_2) to afford ethyl 6-(2-fluorophenyl)-2-oxo-1,3-oxazinane-6-carboxylate **239** (4 mg, 15%) as a white solid. R_f 0.22 (70% EtOAc/pentane); mp = 170–172 ºC; ν_{max} (film)/cm^{-1} 3242 (br s, NH), 3125, 2948, 1748 (C=O ester), 1699 (C=O carbamate), 1491, 1408, 1320, 1276, 1249, 1202, 1147, 1120, 1102, 1079, 1017, 758, 689; ^{1}H NMR (400 MHz, $CDCl_3$) δ 7.61–7.55 (m, 1 H, HC_{Ar}), 7.41–7.33 (m, 1 H, HC_{Ar}), 7.21 (td, *J* = 7.6, 0.8 Hz, 1 H, HC_{Ar}), 7.08 (m, 1 H, HC_{Ar}), 6.43 (br s, 1 H, NH), 4.31–4.18 (m, 2 H, OCH_2CH_3), 3.46–3.37 (m, 1 H, $NCHH$), 3.24–3.14 (m, 1 H, $NCHH$), 2.82–2.72 (dt, *J* = 13.9, 5.8 Hz, 1 H, NCH_2CHH), 2.50 (ddd, *J* = 13.6, 7.7, 5.2 Hz, 1 H, NCH_2CHH), 1.23 (t, *J* = 7.1 Hz, 3 H,

OCH_2CH_3); ^{13}C NMR (101 MHz, $CDCl_3$) δ 168.5 (C=O ester), 159.3 (d, J_{C-F} = 248.6 Hz, FC_{Ar} quat), 152.6 (C=O carbamate), 130.7 (d, J_{C-F} = 8.6 Hz, C_{Ar}), 127.6 (d, J_{C-F} = 2.8 Hz, C_{Ar}), 125.4 (d, J_{C-F} = 11.9 Hz, C_{Ar} quat), 124.4 (d, J_{C-F} = 3.0 Hz, C_{Ar}), 116.3 (d, J_{C-F} = 22.5, C_{Ar}), 81.9 (OC quat), 62.5 (OCH_2CH_3), 36.9 (NCH_2), 27.4 (d, J_{C-F} = 4.7 Hz, NCH_2CH_2), 13.8 (OCH_2CH_3); ^{19}F NMR (377 MHz, $CDCl_3$) δ –112.9 (m); HRMS (ESI^+) *m/z* Calculated for $C_{13}H_{15}NO_4F$ [M+H] 268.0985; Found 268.0983.

(±)–Ethyl 6-(3-chlorophenyl)-2-oxo-1,3-oxazinane-6-carboxylate (241)



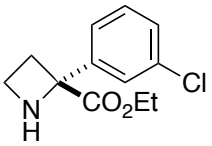
From 1-(tert-butyl) 2-ethyl 2-(3-chlorophenyl)azetidine-1,2-dicarboxylate **114**

Trifluoroacetic acid (38 μL, 0.50 mmol) was added to a stirred solution of 1-(*tert*-butyl) 2-ethyl 2-(3-chlorophenyl)azetidine-1,2-dicarboxylate **114** (34 mg, 0.10 mmol) in toluene (0.10 mL) at 25 ºC and stirred for 2 h. 1 M aq. HCl (20 mL) was added and the aqueous reaction mixture was extracted with EtOAc (3 × 20 mL). The combined organic layers were dried over Na_2SO_4, filtered and concentrated under reduced pressure. Purification by flash chromatography (2% $MeOH/CH_2Cl_2$) afforded ethyl 6-(3-chlorophenyl)-2-oxo-1,3-oxazinane-6-carboxylate **241** (2 mg, 6%).

From 1-benzyl 2-ethyl 2-(3-chlorophenyl)azetidine-1,2-dicarboxylate **245**:

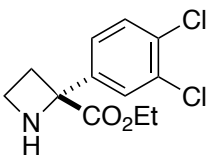
TfOH (88 μL, 1.0 mmol) was added to a stirred solution of 1-benzyl 2-ethyl 2-(3-chlorophenyl)azetidine-1,2-dicarboxylate **245** (37 mg, 0.10 mmol) in toluene (0.50 mL) at 25 ºC and stirred for 1 h. Sat. aq. $NaHCO_3$ (20 mL) was slowly added and the aqueous reaction mixture was extracted with EtOAc (5 × 20 mL). The combined organic layers were dried over Na_2SO_4, filtered and concentrated under reduced pressure. Purification by flash chromatography (80% EtOAc/pentane) afforded ethyl 6-(3-chlorophenyl)-2-oxo-1,3-oxazinane-6-carboxylate **241** (17 mg, 61%) as a white solid. R_f 0.33 (80% EtOAc/pentane); mp = 151–155 ºC; ν_{max} (film)/cm^{-1} 3248 (NH), 3139, 2919, 1728 (C=O ester), 1711 (C=O carbamate), 1492, 1477, 1404, 1327, 1274, 1250, 1226, 1120, 1106, 1078, 1027, 1013, 774, 714; ^1H NMR (400 MHz, $CDCl_3$) δ 7.64–7.61 (m, 1 H, HC_{Ar}), 7.52–7.47 (m, 1 H, HC_{Ar}), 7.37–7.34 (m, 2 H, 2 × HC_{Ar}), 5.75 (br s, 1 H, NH), 4.30–4.21 (m, 2 H, OCH_2CH_3), 3.43–3.29 (m, 2 H, NCH_2), 2.76 (dt, *J* = 13.9, 4.7 Hz, 1 H, NCH_2CHH), 2.29 (ddd, *J* = 13.9, 9.6, 6.0 Hz, 1 H, NCH_2CHH), 1.26 (t, *J* = 7.1 Hz, 3 H, OCH_2CH_3); ^{13}C NMR (101 MHz, $CDCl_3$) δ 169.4 (C=O ester), 152.6 (C=O carbamate), 139.4 (C_{Ar} quat), 134.8 (ClC_{Ar} quat), 130.0 (C_{Ar}), 129.0 (C_{Ar}), 125.4 (C_{Ar}), 123.2 (C_{Ar}), 82.7 (OC quat), 62.8 (OCH_2CH_3), 37.1 (NCH_2), 29.3 (NCH_2CH_2), 13.9 (OCH_2CH_3); HRMS (ESI^+) *m/z* Calculated for $C_{13}H_{15}NO_4{}^{35}Cl$ [M+H] 284.0690; Found 284.0703.

(±)–Ethyl 2-(3-chlorophenyl)azetidine-2-carboxylate (242)



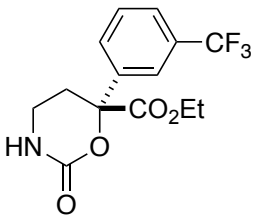
Trifluoroacetic acid (38 μL, 0.50 mmol) was added to a stirred solution of 1-(*tert*-butyl) 2-ethyl 2-(3-chlorophenyl)azetidine-1,2-dicarboxylate **114** (34 mg, 0.10 mmol) in toluene (0.10 mL) at 25 ºC and stirred for 2 h. 1 M aq. HCl (20 mL) was added and the aqueous reaction mixture was extracted with EtOAc (3 × 20 mL). The aqueous layer was basified with 1 M NaOH (50 mL) and extracted with EtOAc (6 × 20 mL). The combined organic layers from the second extraction were concentrated to afford ethyl 2-(3-chlorophenyl)azetidine-2-carboxylate **242** (11 mg, 46%) as a yellow oil. R_f 0.40 (0.05:4.95:95 NH_3:MeOH:CH_2Cl_2); ν_{max} (film)/cm^{-1} 3337 (w, NH), 2979, 1727 (C=O ester), 1596, 1573, 1475, 1247, 1108, 787, 710; ^{1}H NMR (400 MHz, $CDCl_3$) δ 7.44–7.41 (m, 1 H, HC_{Ar}), 7.30–7.21 (m, 3 H, 3 × HC_{Ar}), 4.28–4.14 (m, 2 H, O*C*H_2CH$_3$), 3.74–3.65 (m, 1 H, NC*H*H), 3.33 (ddd, *J* = 12.1, 8.5, 3.7 Hz, 1 H, NCH*H*), 2.89 (ddd, *J* = 11.2, 8.5, 3.7 Hz, 1 H, NCH_2C*H*H), 2.77 (dt, *J* = 11.2, 8.6 Hz, 1 H, NCH_2CH*H*), 1.25 (t, *J* = 7.1 Hz, 3 H, OCH_2C*H*$_3$); ^{13}C NMR (101 MHz, $CDCl_3$) δ 175.2 (C=O), 145.2 (C_{Ar} quat), 134.2 (ClC_{Ar} quat), 129.4 (C_{Ar}), 127.3 (C_{Ar}), 125.7 (C_{Ar}), 123.4 (C_{Ar}), 69.0 (NC quat), 61.9 (O*C*H_2CH$_3$), 41.9 (NCH_2), 32.6 (NCH_2*C*H_2), 14.0 (OCH_2*C*H_3); HRMS (ESI$^+$) *m/z* Calculated for $C_{12}H_{15}NO_2{}^{35}Cl$ [M+H] 240.0791; Found 240.0794.

(±)–Ethyl 2-(3,4-dichlorophenyl)azetidine-2-carboxylate (244)



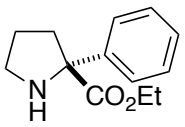
Trifluoroacetic acid (38 μL, 0.50 mmol) was added to a stirred solution of 1-(*tert*-butyl) 2-ethyl 2-(3,4-dichloromophenyl)azetidine-1,2-dicarboxylate **116** (37 mg, 0.10 mmol) in toluene (0.10 mL) at 25 ºC and stirred for 30 min. The reaction mixture was concentrated and purified by SCX column to afford ethyl 2-(3,4-dichlorophenyl)azetidine-2-carboxylate **244** (12 mg, 44%) as a yellow oil. R_f 0.50 (0.05:4.95:95% NH_3:MeOH:CH_2Cl_2); ν_{max} (film)/cm^{-1} 3324 (w, NH), 2979, 2875, 1727 (C=O ester), 1465, 1247, 1221, 1106, 1030; ^{1}H NMR (400 MHz, $CDCl_3$) δ 7.54 (d, *J* = 2.1 Hz, 1 H, HC_{Ar}), 7.40 (d, *J* = 8.4 Hz, 1 H, HC_{Ar}), 7.25 (dd, *J* = 8.4, 2.1 Hz, 1 H, HC_{Ar}), 4.29–4.15 (m, 2 H, O*C*H_2CH$_3$), 3.74–3.66 (m, 1 H, NC*H*H), 3.32 (ddd, *J* = 8.6, 7.4, 3.7 Hz, 1 H, NCH*H*), 2.88 (ddd, *J* = 11.2, 8.6, 3.7 Hz, 1 H, NCH_2C*H*H), 2.73 (dt, *J* = 11.2, 8.6 Hz, 1 H, NCH_2CH*H*), 1.25 (t, *J* = 7.1 Hz, 3 H, OCH_2C*H*$_3$); ^{13}C NMR (101 MHz, $CDCl_3$) δ 174.9 (C=O ester), 143.5 (C_{Ar} quat), 132.3 (ClC_{Ar} quat), 131.3 (ClC_{Ar} quat), 130.1 (C_{Ar}), 127.6 (C_{Ar}), 124.8 (C_{Ar}), 68.6 (NC quat), 62.1 (O*C*H_2CH$_3$), 41.8 (NCH_2), 32.8 (NCH_2*C*H_2), 14.1 (OCH_2*C*H_3); HRMS (ESI$^+$) *m/z* Calculated for $C_{12}H_{14}NO^{35}Cl_2$ [M+H] 274.0402; Found 274.0400.

(±)–Ethyl 2-oxo-6-(3-(trifluoromethyl)phenyl)-1,3-oxazinane-6-carboxylate (248)



TfOH (0.18 mL, 2.0 mmol) was added to a stirred solution of 1-benzyl 2-ethyl 2-(3-(trifluoromethyl)phenyl)azetidine-1,2-dicarboxylate **246** (82 mg, 0.20 mmol) in toluene (1.0 mL) at 25 ºC and stirred for 1 h. Sat. aq. $NaHCO_3$ (20 mL) was slowly added and the aqueous reaction mixture was extracted with EtOAc (5 × 20 mL). The combined organic layers were dried over Na_2SO_4, filtered and concentrated under reduced pressure. Purification by flash chromatography (EtOAc) afforded ethyl 2-oxo-6-(3-(trifluoromethyl)phenyl)-1,3-oxazinane-6-carboxylate **248** (17 mg, 27%) as a white solid. R_f 0.30 (EtOAc); mp = 115–117 ºC; ν_{max} (film)/cm^{-1} 3250 (NH), 3138, 1744 (C=O ester), 1715 (C=O carbamate), 1327, 1267, 1238, 1167, 1115, 1070; ^{1}H NMR (400 MHz, CD_3OD) δ 7.96–7.90 (m, 2 H, 2 × HC_{Ar}), 7.77–7.73 (m, 1 H, HC_{Ar}), 7.71–7.61 (m, 1 H, HC_{Ar}), 4.33–4.21 (m, 2 H, OCH_2CH_3), 3.40–3.29 (m, 2 H, NCH_2 obscured by residual CH_3OH), 2.95–2.88 (m, 1 H, NCH_2CHH), 2.37 (ddd, *J* = 14.0, 9.6, 6.7 Hz, 1 H, NCH_2CHH), 1.25 (t, *J* = 7.1 Hz, 3 H, OCH_2CH_3); ^{1}H NMR (400 MHz, $CDCl_3$) δ 7.90–7.88 (m, 1 H, HC_{Ar}), 7.85–7.82 (m, 1 H, HC_{Ar}), 7.67–7.64 (m, 1 H, HC_{Ar}), 7.58–7.53 (m, 1 H, HC_{Ar}), 5.23 (br s, 1 H, NH), 4.32–4.20 (m, 2 H, OCH_2CH_3), 3.47–3.34 (m, 2 H, NCH_2), 2.87–2.80 (m, 1 H, NCH_2CHH), 2.31 (ddd, *J* = 13.9, 10.0, 6.1 Hz, 1 H, NCH_2CHH), 1.26 (t, *J* = 7.1 Hz, 3 H, OCH_2CH_3); ^{13}C NMR (101 MHz, CD_3OD) δ 170.7 (C=O ester), 154.9 (C=O carbamate), 140.6 (C_{Ar} quat), 132.1 (q, J_{C-F} = 32.8 Hz, C_{Ar}), 130.8 (C_{Ar}), 130.2 (C_{Ar}), 126.7 (q, *J* = 4.0 Hz, C_{Ar}), 125.4 (q, J_{C-F} = 271.6 Hz, CF_3), 123.1 (q, J_{C-F} = 4.0 Hz, C_{Ar}), 84.3 (OC quat), 63.9 (OCH_2CH_3), 37.8 (NCH_2), 29.9 (NCH_2CH_2), 14.2 (OCH_2CH_3); ^{19}F{^{1}H} NMR (377 MHz, CD_3OD) δ –64.2; HRMS (FTMS + pNSI) *m/z* Calculated for $C_{14}H_{15}NO_4F_3^+$ $[M+H]^+$ 318.0948; Found 318.0950.

(±)–Ethyl 2-phenylpyrrolidine-2-carboxylate (250)

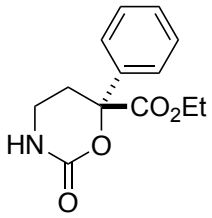


TfOH (44 μL, 0.5 mmol) was added to a stirred solution of 1-benzyl 2-ethyl 2-phenylazetidine-1,2-dicarboxylate **119** (18 mg, 0.05 mmol) in toluene (0.25 mL) at 25 ºC and stirred for 1 h. Sat. aq. $NaHCO_3$ (20 mL) was slowly added and the aqueous reaction mixture was extracted with EtOAc (5 × 20 mL). The combined organic layers were dried over Na_2SO_4, filtered and concentrated under reduced pressure. Purification by flash chromatography (30% EtOAc/pentane) afforded ethyl 2-phenylpyrrolidine-2-carboxylate **250** (8 mg, 62%) as a colourless oil. R_f 0.27 (40% EtOAc/pentane); ν_{max} (film)/cm^{-1} 3349 (NH), 2980, 2873, 1721 (C=O), 1447, 1242, 1180, 1096, 1025, 729, 698; ^{1}H NMR (400 MHz, $CDCl_3$) δ 7.56–7.51 (m, 2 H, 2 × HC_{Ph}), 7.35–7.29 (m, 2 H, 2 × HC_{Ph}), 7.28–7.23 (m, 1 H, HC_{Ph}), 4.20–4.09 (m, 2 H, OCH_2CH_3), 3.14–3.05 (m, 2 H, NCH_2), 2.76 (ddd, *J* = 12.7, 8.1, 4.8 Hz, 1 H, $N(CH_2)_2CHH$), 2.07 (dt, *J* = 12.6, 8.5 Hz, 1 H, $N(CH_2)_2CHH$), 1.94–1.75

(m, 2 H, NCH_2CH_2), 1.21 (t, *J* = 7.1 Hz, 3 H, OCH_2CH_3); ^{13}C NMR (101 MHz, $CDCl_3$) δ 175.6 (C=O), 142.9 (C_{Ph} quat), 128.1 (2 × C_{Ph}), 127.1 (C_{Ph}), 126.1 (2 × C_{Ph}), 72.3 (NC quat), 61.5 (OCH_2CH_3), 45.7 (NCH_2), 36.7 ($N(CH_2)_2CH_2$), 24.6 (NCH_2CH_2), 14.1 (OCH_2CH_3); HRMS (ESI^+) *m/z* Calculated for $C_{13}H_{18}NO_2$ [M+H] 220.1338; Found 220.1347.

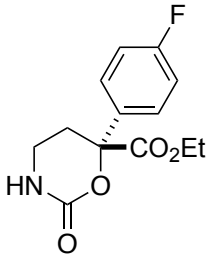
6.2.2.4 Synthesis of Oxazinanones by NICE Reaction

(±)–Ethyl 2-oxo-6-phenyl-1,3-oxazinane-6-carboxylate (231)



$Rh_2(esp)_2$ (1.9 mg, 2.5 μmol) was added to a solution of *tert*-butyl (2-chloroethyl)carbamate **52** (90 mg, 0.50 mmol) and ethyl 2-diazo-2-phenylacetate **85** (143 mg, 0.75 mmol) in benzene (1.67 mL). The reaction vessel was sealed, purged with Ar and heated at 60 ºC for 2.5 h, then allowed to cool to rt. Tetrabutylammonium bromide (16 mg, 50 μmol) was added, followed by $CsOH·H_2O$ (168 mg, 1.00 mmol), and the reaction was stirred at 25 ºC for 18 h. TFA (0.38 mL, 5.0 mmol) was added and the reaction mixture was stirred for 1 h. Sat. aq. $NaHCO_3$ (40 mL) was slowly added, then the aqueous reaction mixture was extracted with EtOAc (5 × 40 mL). The combined organic layers were dried over Na_2SO_4, filtered and concentrated under reduced pressure. Purification by flash chromatography (2% MeOH/CH_2Cl_2) afforded ethyl 2-oxo-6-phenyl-1,3-oxazinane-6-carboxylate **231** (48 mg, 38%) as a white solid. The observed characterisation data was identical to that reported previously for **231** above.

(±)–Ethyl 6-(4-fluorophenyl)-2-oxo-1,3-oxazinane-6-carboxylate (237)



One-pot procedure

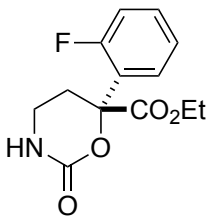
$Rh_2(esp)_2$ (1.9 mg, 2.5 μmol) was added to a solution of *tert*-butyl (2-chloroethyl)carbamate **52** (90 mg, 0.50 mmol) and ethyl 2-diazo-2-(4-fluorophenyl)acetate **91** (156 mg, 0.75 mmol) in benzene (1.67 mL). The reaction vessel was sealed, purged with Ar and heated at 60 ºC for 2.5 h, then allowed to cool to rt. Tetrabutylammonium bromide (16 mg, 50 μmol) was added, followed by $CsOH·H_2O$ (168 mg, 1.00 mmol), and the reaction was stirred at 25 ºC for 18 h. TFA (0.38 mL, 5.0 mmol) was added and the reaction mixture was stirred for 1 h. Sat. aq. $NaHCO_3$ (40 mL) was slowly added, then the aqueous reaction mixture was extracted with EtOAc (5 × 40 mL). The combined organic layers were dried over Na_2SO_4, filtered and concentrated under reduced pressure. Purification by flash chromatography (2% MeOH/ CH_2Cl_2) afforded ethyl 6-(4-fluorophenyl)-2-oxo-1,3-oxazinane-6-carboxylate **237** (60 mg, 45%) as a white solid. The observed characterisation data was identical to that reported previously for **237** above.

Telescoped procedure

$Rh_2(esp)_2$ (1.9 mg, 2.5 μmol) was added to a solution of *tert*-butyl (2-chloroethyl)carbamate **52** (90 mg, 0.50 mmol) and ethyl 2-diazo-2-(4-fluorophenyl)acetate **91** (156 mg, 0.75 mmol) in benzene (1.67 mL). The reaction vessel was sealed, purged with Ar and heated at 60 ºC for 2.5 h, then allowed to cool to rt. Tetrabutylammonium bromide (16 mg, 50 μmol) was added, followed by $CsOH·H_2O$ (168 mg, 1.00 mmol), and the reaction was stirred at 25 ºC for 18 h. The crude reaction mixture was then filtered through silica, eluting with CH_2Cl_2 (10 mL), and concentrated under reduced pressure. The crude reaction mixture was transferred to a dry reaction flask and concentrated under reduced pressure. TFA (0.19 mL, 2.5 mmol) was added to the crude reaction mixture in toluene (0.50 mL) and stirred at 25 ºC for 0.5 h. The crude reaction mixture was concentrated. Purification by flash chromatography (2% MeOH/CH_2Cl_2) afforded ethyl 6-(4-fluorophenyl)-2-oxo-1,3-oxazinane-6-carboxylate **237** (57 mg, 43%) as a white solid. The observed characterisation data was identical to that reported previously for **237** above.

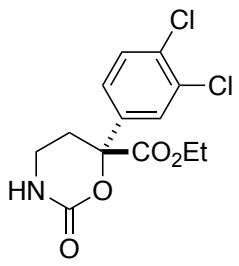
Telescoped procedure on 3.0 mmol scale afforded ethyl 6-(4-fluorophenyl)-2-oxo-1,3-oxazinane-6-carboxylate **237** (289 mg, 36%).

(±)–Ethyl 6-(2-fluorophenyl)-2-oxo-1,3-oxazinane-6-carboxylate (239)



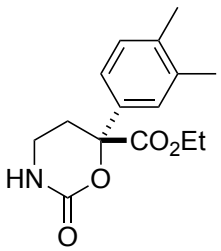
$Rh_2(esp)_2$ (1.9 mg, 2.5 μmol) was added to a solution of benzyl (2-chloroethyl)carbamate **63** (90 mg, 0.50 mmol) and ethyl 2-diazo-2-(2-fluorophenyl)acetate **89** (156 mg, 0.75 mmol) in benzene (1.67 mL). The reaction vessel was sealed, purged with Ar and heated at 60 ºC for 2.5 h, then allowed to cool to rt. Tetrabutylammonium bromide (16 mg, 50 μmol) was added, followed by $CsOH·H_2O$ (168 mg, 1.00 mmol), and the reaction was stirred at 25 ºC for 18 h. TfOH (0.44 mL, 5.0 mmol) was added and the reaction mixture was stirred for a further 1.5 h. Sat. aq. $NaHCO_3$ (40 mL) was slowly added and the aqueous reaction mixture was extracted with EtOAc (5 × 40 mL). The combined organic layers were dried over Na_2SO_4, filtered and concentrated under reduced pressure. Purification by flash chromatography (70% EtOAc/pentane) afforded ethyl 6-(2-fluorophenyl)-2-oxo-1,3-oxazinane-6-carboxylate **239** (26 mg, 19%) as a white solid. The observed characterisation data was identical to that reported previously for **239** above.

(±)–Ethyl 6-(3,4-dichlorophenyl)-2-oxo-1,3-oxazinane-6-carboxylate (243)



Ethyl 2-diazo-2-(3,4-dichlorophenyl)acetate **95** (324 mg, 1.25 mmol) in benzene (1.0 mL) was added slowly *via* syringe pump over 1 h to a solution of benzyl (2-chloroethyl)carbamate **63** (107 mg, 0.50 mmol) and $Rh_2(esp)_2$ (1.9 mg, 2.5 μmol) in benzene (0.67 mL) at 60 ºC. The reaction mixture was stirred at 60 °C for a further 2.5 h, then allowed to cool to rt. Tetrabutylammonium bromide (16 mg, 50 μmol) was added, followed by $CsOH·H_2O$ (168 mg, 1.50 mmol), and the reaction was stirred at 25 ºC for 18 h. TfOH (0.45 mL, 5.0 mmol) was added dropwise and the reaction mixture was stirred for 30 min. Sat. aq. $NaHCO_3$ (40 mL) was slowly added and the aqueous reaction mixture was extracted with EtOAc (5 × 40 mL). The combined organic layers were dried over Na_2SO_4, filtered and concentrated under reduced pressure. Purification by flash chromatography (EtOAc) afforded ethyl 6-(3,4-dichlorophenyl)-2-oxo-1,3-oxazinane-6-carboxylate **243** (78 mg, 45%) as a pale yellow solid. R_f 0.19 (EtOAc); mp = 86–90 ºC; ν_{max} (film)/cm^{-1} 3343 (NH), 2985, 1707 (br s, 2 × C=O), 1256, 1170, 1010, 1033; ^{1}H NMR (400 MHz, DMSO-d_6) δ 7.75–7.71 (m, 2 H, 2 × HC_{Ar}), 7.58 (br s, 1 H, NH), 7.51 (dd, J = 8.6, 2.3 Hz, 1 H, HC_{Ar}), 4.22–4.12 (m, 2 H, OCH_2CH_3), 3.18–3.05 (m, 2 H, NCH_2), 2.68 (dt, J = 13.8, 4.7 Hz, 1 H, NCH_2CHH), 2.32 (ddd, J = 14.0, 9.2, 6.2 Hz, 1 H, NCH_2CHH), 1.14 (t, J = 7.1 Hz, 3 H, OCH_2CH_3); ^{13}C NMR (101 MHz, DMSO-d_6) δ 169.1 (C=O ester), 150.7 (C=O carbamate), 138.9 (C_{Ar} quat), 131.6 (ClC_{Ar} quat), 131.5 (ClC_{Ar} quat), 131.0 (C_{Ar}), 127.3 (C_{Ar}), 125.7 (C_{Ar}), 81.7 (OC quat), 62.3 (OCH_2CH_3), 36.1 (NCH_2), 28.0 (NCH_2CH_2), 13.8 (OCH_2CH_3); HRMS (FTMS + pNSI) *m/z* Calculated for $C_{13}H_{14}NO_4{}^{35}Cl_2{}^+$ $[M+H]^+$ 318.0294; Found 318.0299.

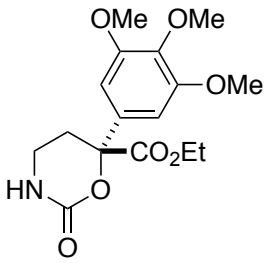
(±)–Ethyl 6-(3,4-dimethylphenyl)-2-oxo-1,3-oxazinane-6-carboxylate (253)



$Rh_2(esp)_2$ (1.9 mg, 2.5 μmol) was added to a solution of *tert*-butyl (2-chloroethyl)carbamate **52** (90 mg, 0.50 mmol) and ethyl 2-diazo-2-(3,4-dimethylphenyl)acetate **164** (164 mg, 0.75 mmol) in benzene (1.67 mL). The reaction vessel was sealed, purged with Ar and heated at 60 ºC for 2.5 h, then allowed to cool to rt. Tetrabutylammonium bromide (16 mg, 50 μmol) was added, followed by $CsOH·H_2O$ (168 mg, 1.00 mmol), and the reaction was stirred at 25 ºC for 18 h. The crude reaction mixture was then filtered through silica, eluting with CH_2Cl_2 (10 mL), and concentrated under reduced pressure. The crude reaction mixture was transferred to a dry reaction flask and concentrated. TFA (0.19 mL, 2.5 mmol) was added to the crude reaction mixture in toluene (0.50 mL) and stirred at 25 ºC for 0.5 h. The crude reaction mixture was concentrated. Purification by flash chromatography (80% EtOAc/hexane) afforded ethyl 6-(3,4-dimethylphenyl)-2-oxo-1,3-oxazinane-6-carboxylate **253** (83 mg, 60%) as

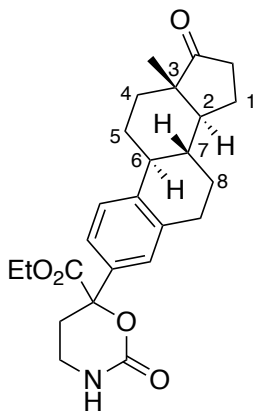
a white solid. R_f 0.31 (EtOAc); mp = 167–169 ºC; ν_{max} (film)/cm^{-1} 3236 (NH), 3140, 2916, 1745 (C=O ester), 1713 (C=O carbamate), 1489, 1411, 1327, 1256, 1193, 1121, 1095, 1015, 777; ^{1}H NMR (400 MHz, $CDCl_3$) δ 7.36 (d, J = 1.5 Hz, 1 H, HC_{Ar}), 7.30–7.26 (m, 1 H, HC_{Ar}), 7.15 (d, J = 8.0 Hz, 1 H, HC_{Ar}), 6.25 (br s, 1 H, NH), 4.28–4.16 (m, 2 H, OCH_2CH_3), 3.40–3.26 (m, 2 H, NCH_2), 2.72 (dt, J = 13.8, 5.0 Hz, 1 H, NCH_2CHH), 2.37–2.23 (m, 7 H, NCH_2CHH and 2 × $ArCH_3$), 1.24 (t, J = 7.1 Hz, 3 H, OCH_2CH_3); ^{13}C NMR (101 MHz, $CDCl_3$) δ 170.1 (C=O ester), 153.1 (C=O carbamate), 137.3 (CH_3C_{Ar} quat), 137.1 (CH_3C_{Ar} quat), 134.8 (C_{Ar} quat), 129.9 (C_{Ar}), 126.0 (C_{Ar}), 122.3 (C_{Ar}), 83.2 (OC quat), 62.4 (OCH_2CH_3), 37.2 (NCH_2), 29.1 (NCH_2CH_2), 19.9 ($ArCH_3$), 19.4 ($ArCH_3$), 14.0 (OCH_2CH_3); HRMS (ESI$^+$) *m/z* Calculated for $C_{15}H_{20}NO_4$ [M+H] 278.1392; Found 278.1404.

(±)–Ethyl 2-oxo-6-(3,4,5-trimethoxyphenyl)-1,3-oxazinane-6-carboxylate (254)



$Rh_2(esp)_2$ (1.9 mg, 2.5 μmol) was added to a solution of *tert*-butyl (2-chloroethyl)carbamate **52** (90 mg, 0.50 mmol) and ethyl 2-diazo-2-(3,4,5-trimethoxyphenyl)acetate **252** (215 mg, 0.75 mmol) in benzene (1.67 mL). The reaction vessel was sealed, purged with Ar and heated at 60 ºC for 2.5 h, then allowed to cool to rt. Tetrabutylammonium bromide (16 mg, 50 μmol) was added, followed by $CsOH{\cdot}H_2O$ (168 mg, 1.00 mmol), and the reaction was stirred at 25 ºC for 18 h. The crude reaction mixture was then filtered through silica, eluting with EtOAc (10 mL), and concentrated under reduced pressure. The crude reaction mixture was transferred to a dry reaction flask and concentrated. TFA (0.19 mL, 2.5 mmol) was added to the crude reaction mixture in toluene (0.50 mL) and stirred at 25 ºC for 0.5 h. The crude reaction mixture was concentrated. Purification by flash chromatography (EtOAc) afforded ethyl 2-oxo-6-(3,4,5-trimethoxyphenyl)-1,3-oxazinane-6-carboxylate **254** (98 mg, 58%) as a pale yellow solid. R_f 0.23 (EtOAc); mp = 159–163 ºC; ν_{max} (film)/cm^{-1} 3275 (br s, NH), 2940, 1718 (br s, C=O ester/ carbamate), 1591, 1491, 1456, 1416, 1329, 1246, 1125, 1097, 1007; ^{1}H NMR (400 MHz, $CDCl_3$) δ 6.79 (s, 2 H, 2 × HC_{Ar}), 6.23 (br s, 1 H, NH), 4.31–4.18 (m, 2 H, OCH_2CH_3), 3.87 (s, 6 H, 2 × OCH_3), 3.85 (s, 3 H, OCH_3), 3.41–3.29 (m, 2 H, NCH_2), 2.74 (dt, J = 13.9, 4.8 Hz, 1 H, NCH_2CHH), 2.29 (ddd, J = 13.9, 9.0, 6.5 Hz, 1 H, NCH_2CHH), 1.26 (t, 3 H, OCH_2CH_3); ^{13}C NMR (101 MHz, $CDCl_3$) δ 169.8 (C=O ester), 153.3 (2 × OC_{Ar} quat), 152.9 (C=O carbamate), 138.3 (OC_{Ar} quat), 132.9 (C_{Ar} quat), 102.2 (2 × C_{Ar}), 83.1 (OC quat), 62.6 (OCH_2CH_3), 60.8 (OCH_3), 56.3 (2 × OCH_3), 37.2 (NCH_2), 29.5 (NCH_2CH_2), 14.0 (OCH_2CH_3); HRMS (ESI$^+$) *m/z* Calculated for $C_{16}H_{22}NO_7$ [M+H] 340.1396; Found 340.1388.

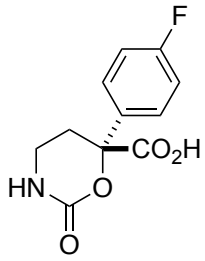
(±)–Ethyl 6-((8*R*,9*S*,13*S*,14*S*)-13-methyl-17-oxo-7,8,9,11,12,13,14,15,16,17-decahydro-6*H*-cyclopenta[*a*]phenanthren-3-yl)-2-oxo-1,3-oxazinane-6-carboxylate (mixture of diastereomers) (255)



$Rh_2(esp)_2$ (0.8 mg, 1.0 μmol) was added to a solution of *tert*-butyl (2-chloroethyl)carbamate **52** (36 mg, 0.20 mmol) and diazo **159** (110 mg, 0.30 mmol) in benzene (0.67 mL). The reaction vessel was sealed, purged with Ar and heated at 60 ºC for 2.5 h, then allowed to cool to rt. Tetrabutylammonium bromide (6.4 mg, 20 μmol) was added, followed by $CsOH·H_2O$ (67 mg, 0.40 mmol), and the reaction was stirred at 25 ºC for 18 h. The crude reaction mixture was then filtered through silica, eluting with EtOAc (10 mL), and concentrated under reduced pressure. The crude reaction mixture was transferred to a dry reaction flask and concentrated. TFA (0.08 mL, 1.0 mmol) was added to the crude reaction mixture in toluene (0.20 mL) and stirred at 25 ºC for 0.5 h. The crude reaction mixture was concentrated. Purification by flash chromatography (80% EtOAc/hexane) afforded ethyl 6-((8*R*,9*S*,13*S*,14*S*)-13-methyl-17-oxo-7,8,9,11,12,13,14,15,16,17-decahydro-6*H*-cyclopenta[*a*]phenanthren-3-yl)-2-oxo-1,3-oxazinane-6-carboxylate **255** (11 mg, 13%) as a white solid (the product is assumed to be a 1:1 mixture of diastereomers). R_f 0.13 (70% EtOAc/hexane); mp = 95–97 ºC; ν_{max} (film)/cm^{-1} 3268 (w br, NH), 2929, 1733 (2 × C=O), 1491, 1454, 1407, 1319, 1203, 1096, 730; ^1H NMR (400 MHz, $CDCl_3$) δ 7.37–7.29 (m, 3 H, 3 × HC_{Ar}), 5.96 (s, 1 H, NH), 4.29–4.16 (m, 2 H, OCH_2CH_3), 3.41–3.27 (m, 2 H, NCH_2), 2.97–2.90 (m, 2 H, $ArCH_2$), 2.78–2.69 (m, 1 H, NCH_2CHH), 2.52 (dd, *J* = 19.1, 9.0 Hz, 1 H, ArCH), 2.47–2.37 (m, 1 H, C*H*HCO), 2.36–2.26 (m, 1 H, CH*H*CO), 2.22–1.93 (m, 5 H, 4 × C*H*H and NCH_2CHH), 1.72–1.40 (m, 6 H, 4 × CH*H* and 2 × CH), 1.26 (td, *J* = 7.1, 1.6 Hz, 3 H, OCH_2CH_3), 0.91 (s, 3 H, CH_3); ^{13}C NMR (101 MHz, $CDCl_3$) δ 220.7 (C=O ketone), 170.0 (C=O ester), 152.9 (C=O carbamate), 140.4 (C_{Ar} quat), 137.0 (C_{Ar} quat), 134.8 (C_{Ar} quat), 125.7 (C_{Ar}), 125.53 and 125.47 (C_{Ar}), 122.26 and 122.23 (C_{Ar}), 83.2 (OC quat), 62.5 (OCH_2CH_3), 50.5 (C_2), 47.9 (C_3 quat), 44.3 (C_6), 37.9 (C_7), 37.3 (NCH_2), 35.8 (CH_2CO), 31.5 (C_4), 29.5, 29.4, 29.3 and 29.2 (CH_2Ar and NCH_2CH_2), 26.4 (C_8), 25.6 (C_5), 21.6 (C_1), 14.0 (OCH_2CH_3), 13.8 (CH_3); HRMS (ESI^+) *m/z* Calculated for $C_{25}H_{32}NO_5$ [M+H] 426.2280; Found 426.2282.

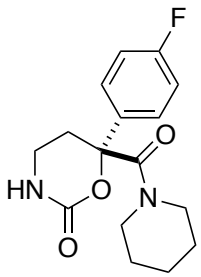
6.2.2.5 Functionalisation of 1,3-oxazinan-2-ones

(±)–6-(4-Fluorophenyl)-2-oxo-1,3-oxazinane-6-carboxylic acid (256)



NaOH (2 M aq, 0.2 mL) was added to a solution of ethyl 6-(4-fluorophenyl)-2-oxo-1,3-oxazinane-6-carboxylate **237** (53.5 mg, 0.2 mmol) in EtOH (1.0 mL). The reaction mixture was heated under reflux for 10 min, then cooled to rt. The solvent was removed under reduced pressure, then 1 M aq. HCl (10 mL) was added and the aqueous mixture was extracted with EtOAc (6 × 10 mL). The combined organic layers were dried over Na_2SO_4, filtered and concentrated under reduced pressure to afford 6-(4-fluorophenyl)-2-oxo-1,3-oxazinane-6-carboxylic acid **256** (41 mg, 92%) as a white solid. R_f 0.38 (EtOAc); mp = 152–153 ºC; ν_{max} (film)/cm^{-1} 3333 (OH), 2919, 2850, 1716 (C=O carbamate), 1661 (br s, C=O carboxylic acid), 1602, 1509, 1459, 1276, 1232, 1224, 1212, 1165, 1118, 1089, 840, 740, 702, 675; ^{1}H NMR (400 MHz, DMSO-d_6) δ 13.60 (br s, 1 H, CO_2H), 7.60–7.52 (m, 2 H, 2 × HC_{Ar}), 7.42 (br s, 1 H, NH), 7.31–7.23 (m, 2 H, 2 × HC_{Ar}), 3.19–3.07 (m, 2 H, NCH_2), 2.63 (dt, J = 13.7, 4.1 Hz, 1 H, NCH_2CHH), 2.29–2.18 (m, 1 H, NCH_2CHH); ^{13}C NMR (101 MHz, DMSO-d_6) δ 171.2 (C=O carboxylic acid), 160.9 (d, J_{C-F} = 245.1 Hz, FC_{Ar} quat), 151.3 (C=O carbamate), 134.8 (d, J_{C-F} = 2.5 Hz, C_{Ar} quat), 127.5 (d, J_{C-F} = 8.6 Hz, 2 × C_{Ar}), 115.3 (d, J_{C-F} = 21.5 Hz, 2 × C_{Ar}), 81.9 (OC quat), 36.4 (NCH_2), 28.1 (NCH_2CH_2); ^{19}F{^{1}H} NMR (377 MHz, $CDCl_3$) δ –113.8; HRMS (ESI$^-$) *m/z* Calculated for $C_{11}H_9NO_4F$ [M–H] 238.0516; Found 238.0523.

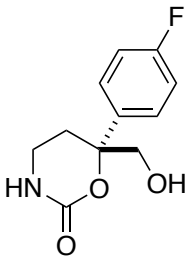
(±)–6-(4-Fluorophenyl)-6-(piperidine-1-carbonyl)-1,3-oxazinan-2-one (257)



DIPEA (0.1 mL) was added to a solution of HATU (80 mg, 0.21 mmol), piperidine (21 μL) and 6-(4-fluorophenyl)-2-oxo-1,3-oxazinane-6-carboxylic acid **256** (42 mg, 0.18 mmol) in DMF (0.72 mL). The reaction mixture was stirred at 40 ºC for 24 h then H_2O (20 mL) was added. EtOAc (20 mL) was added to the aqueous mixture and the layers were separated. Sat. brine (10 mL) was added to aid separation. The aqueous layer was extracted with EtOAc (5 × 20 mL). The combined organic layers were washed with brine (20 mL), dried over Na_2SO_4, filtered and concentrated under reduced pressure. Purification by flash chromatography (2% MeOH/CH_2Cl_2 followed by EtOAc) afforded 6-(4-fluorophenyl)-6-(piperidine-1-carbonyl)-1,3-oxazinan-2-one **257** (39 mg, 64%) as a white solid. R_f 0.28 (EtOAc); mp = 177–180 ºC; ν_{max} (film)/cm^{-1} 3279 (br s, NH), 2937, 2859, 1718 (C=O carbamate), 1634 (C=O amide), 1509, 1444, 1318, 1229, 1025, 1086, 731; ^{1}H NMR (400 MHz, $CDCl_3$) δ 7.46–7.40 (m, 2 H, 2 × HC_{Ar}), 7.13–7.06 (m, 2 H, 2 × HC_{Ar}), 5.69 (br s, 1 H, NH), 3.68–3.57 (m, 2 H, 2 × NC*H*H), 3.52–3.43 (m, 2 H, 2 × NCH*H*), 3.37–3.28 (m, 1 H, NHC*H*H),

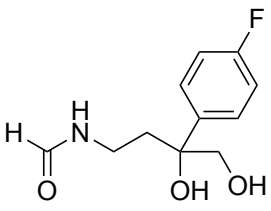
3.22–3.15 (m, 1 H, NHCH*H*), 2.78 (dt, *J* = 13.9, 4.4 Hz, 1 H, NHCH$_2$C*H*H), 1.95 (ddd, *J* = 14.0, 9.7, 6.0 Hz, 1 H, NHCH$_2$CH*H*), 1.60–1.44 (m, 4 H, 2 × NCH$_2$C*H*$_2$), 1.43–1.33 (m, 1 H, N(CH$_2$)$_2$C*H*H), 0.98–0.85 (m, 1 H, N(CH$_2$)CH*H*); ^{13}C NMR (101 MHz, $CDCl_3$) δ 166.6 (C=O amide), 162.4 (d, J_{C-F} = 247.7 Hz, FC$_{Ar}$ quat), 152.8 (C=O carbamate), 135.6 (d, J_{C-F} = 3.0 Hz, C$_{Ar}$ quat), 125.8 (d, J_{C-F} = 8.3 Hz, 2 × C$_{Ar}$), 115.9 (d, J_{C-F} = 21.8 Hz, 2 × C$_{Ar}$), 85.1 (OC quat), 47.3 (NCH$_2$), 44.7 (NCH$_2$), 37.8 (NHCH$_2$), 33.1 (NHCH$_2$*C*H$_2$), 25.7 (NCH$_2$*C*H$_2$), 25.6 (NCH$_2$*C*H$_2$), 24.3 (N(CH$_2$)$_2$*C*H$_2$); ^{19}F NMR (377 MHz, $CDCl_3$) δ –113.6 (m); HRMS (ESI$^+$) *m/z* Calculated for $C_{16}H_{20}NO_3F$ [M+H] 307.1458; Found 307.1466.

(±)–6-(4-Fluorophenyl)-6-(hydroxymethyl)-1,3-oxazinan-2-one (259)



$LiAlH_4$ (4.1 mg, 0.11 mmol) in 1.8:1 Et_2O:THF (2.8 mL) was added dropwise over 10 min to a solution of ethyl 6-(4-fluorophenyl)-2-oxo-1,3-oxazinane-6-carboxylate **237** (27 mg, 0.1 mmol) in Et_2O (0.2 mL) at 0 ºC. The reaction mixture was stirred for a further 50 min at 25 ºC then sat. aq. NH_4Cl (20 mL) was added and the mixture was filtered into a separating funnel. The aqueous reaction mixture was extracted with EtOAc (4 × 20 mL) and the combined organic layers were dried over Na_2SO_4, filtered and concentrated under reduced pressure. Purification by flash chromatography (5% MeOH/CH_2Cl_2) afforded 6-(4-fluorophenyl)-6-(hydroxymethyl)-1,3-oxazinan-2-one **257** (15 mg, 67%) as a white solid. R_f 0.10 (5% MeOH/CH_2Cl_2); mp = 185–187 ºC; ν_{max} (film)/cm^{-1} 3443 (br s, OH), 3242 (NH), 2917, 1720 (C=O), 1656, 1601, 1491, 1479, 1441, 1330, 1163, 1136, 1113, 1076, 1049, 982, 841, 768; ^{1}H NMR (400 MHz, CD_3OD) δ 7.50–7.45 (m, 2 H, 2 × HC$_{Ar}$), 7.22–7.15 (m, 2 H, 2 × HC$_{Ar}$), 3.73 (d, *J* = 12.2 Hz, 1 H, C*H*HOH), 3.68 (d, *J* = 12.2 Hz, 1 H, CH*H*OH), 3.33–3.27 (m, 1 H, NC*H*H), 2.98–2.90 (m, 1 H, NCH*H*), 2.45–2.39 (m, 2 H, NCH$_2$C*H*$_2$); ^{13}C NMR (101 MHz, CD_3OD) δ 163.9 (d, J_{C-F} = 245.2 Hz, FC$_{Ar}$), 156.7 (C=O), 137.2 (d, J_{C-F} = 3.1 Hz, C$_{Ar}$), 128.6 (d, J_{C-F} = 8.1 Hz, 2 × C$_{Ar}$), 116.5 (d, J_{C-F} = 21.8 Hz, 2 × C$_{Ar}$), 86.3 (OC quat), 70.1 (CH$_2$OH), 37.2 (NCH$_2$), 26.7 (NCH$_2$*C*H$_2$); ^{19}F NMR (377 MHz, CD_3OD) δ –116.8 (m); HRMS (ESI$^+$) *m/z* Calculated for $C_{11}H_{13}NO_3F$ [M+H] 226.0879; Found 226.0890.

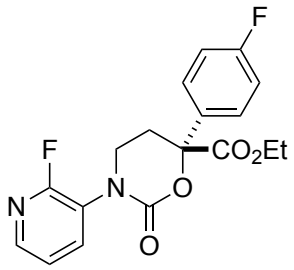
***N*-(3-(4-Fluorophenyl)-3,4-dihydroxybutyl)formamide (260)**



Ethyl 6-(4-fluorophenyl)-2-oxo-1,3-oxazinane-6-carboxylate **237** (27 mg, 0.1 mmol) in THF (0.75 mL) was added dropwise over 10 min to a solution of $LiAlH_4$ (4.1 mg, 0.11 mmol) in THF (0.25 mL) at 0 ºC. The reaction mixture was stirred for a further 1 h at 25 ºC then sat. aq. NH_4Cl (20 mL) was added and the mixture was filtered into a separating funnel. The aqueous reaction mixture was extracted with EtOAc (4 × 20 mL) and the combined

organic layers were dried over Na_2SO_4, filtered and concentrated under reduced pressure. Purification by flash chromatography (5% to 10% MeOH/CH_2Cl_2) afforded 6-(4-Fluorophenyl)-6-(hydroxymethyl)-1,3-oxazinan-2-one **259** (9 mg, 40%) then *N*-(3-(4-fluorophenyl)-3,4-dihydroxybutyl)formamide **260** (6 mg, 26%) as a white solid. R_f 0.30 (10% MeOH/CH_2Cl_2); mp = 102–104 ºC; ν_{max} (film)/cm^{-1} 3332 (br s, OH), 2926, 1655 (C=O), 1510, 1383, 1226, 839; ^{1}H NMR (400 MHz, CD_3OD) δ 7.97 (s, 1 H, CHO), 7.57–7.50 (m, 2 H, 2 × HC_{Ar}), 7.13–7.06 (m, 2 H, 2 × HC_{Ar}), 3.68–3.61 (m, 2 H, OCH_2Ar), 3.27–3.18 (m, 1 H, NCH_2CHH), 3.14–3.04 (m, 1 H, NCH_2CHH), 2.14–2.08 (m, 2 H, NCH_2); ^{13}C NMR (101 MHz, CD_3OD) δ 163.7 (C=O), 163.2 (d, J_{C-F} = 243.6 Hz, FC_{Ar} quat), 141.1 (d, J_{C-F} = 2.9 Hz, C_{Ar} quat), 128.7 (d, J_{C-F} = 8.0 Hz, 2 × C_{Ar}), 115.6 (d, J_{C-F} = 21.4 Hz, 2 × C_{Ar}), 76.9 (HOC quat), 71.3 ($HOCH_2$), 38.3 (NCH_2CH_2), 34.7 (NCH_2); ^{19}F{^{1}H} NMR (377 MHz, CD_3OD) δ –118.9; HRMS (ESI$^-$) *m/z* Calculated for $C_{11}H_{13}NO_3F$ [M–H] 226.0879; Found 226.0884.

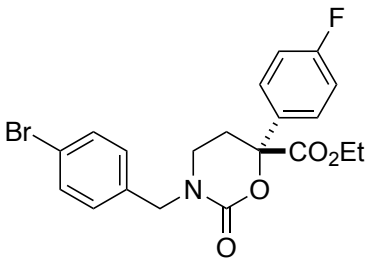
(±)–Ethyl 6-(4-fluorophenyl)-3-(2-fluoropyridin-3-yl)-2-oxo-1,3-oxazinane-6-carboxylate (261)



A solution of ethyl 6-(4-fluorophenyl)-2-oxo-1,3-oxazinane-6-carboxylate **237** (27 mg, 0.1 mmol), 2-fluoro-3-iodopyridine (44 mg, 0.2 mmol), CuI (1.9 mg, 10 μmol), K_2CO_3 (28 mg, 0.2 mmol) and cyclohexan-1,2-diamine (2.4 μL, 20 μmol) in 1,4-dioxane was stirred at 110 ºC for 24 h. The reaction mixture was allowed to cool to rt, then the mixture was filtered through celite washing with EtOAc (20 mL) and the crude product was concentrated under reduced pressure. Purification by flash chromatography (60% EtOAc/pentane) afforded ethyl 6-(4-fluorophenyl)-3-(2-fluoropyridin-3-yl)-2-oxo-1,3-oxazinane-6-carboxylate **261** (20 mg, 55%) as a white solid. R_f 0.13 (50% EtOAc/pentane); mp = 139–141 ºC; ν_{max} (film)/cm^{-1} 3064, 2907, 2967, 1703 (s br, 2 × C=O), 1603, 1577, 1450, 1323, 1252, 1223, 1159, 1092, 1006, 965, 917, 828; ^{1}H NMR (400 MHz, $CDCl_3$) δ 8.18 (m, 1 H, HC_{Ar}), 7.81–7.75 (m, 1 H, HC_{Ar}), 7.67–7.61 (m, 2 H, 2 × HC_{Ar}), 7.27–7.25 (m, 1 H, HC_{Ar}), 7.16–7.09 (m, 2 H, 2 × HC_{Ar}), 4.36–4.24 (m, 2 H, OCH_2CH_3), 3.74–3.66 (m, 1 H, NCHH), 3.61–3.54 (m, 1 H, NCHH), 2.97 (ddd, *J* = 13.9, 5.2, 4.1 Hz, 1 H, NCH_2HH), 2.55 (ddd, *J* = 13.9, 10.1, 5.9 Hz, 1 H, NCH_2CHH), 1.29 (t, *J* = 7.1 Hz, 3 H, OCH_2CH_3); ^{13}C NMR (101 MHz, $CDCl_3$) δ 169.6 (C=O ester), 163.0 (d, *J* = 249.0 Hz, FC_{Ar} quat), 158.6 (d, *J* = 241.6 Hz, $FC_{Ar}N$ quat), 150.7 (C=O carbamate), 139.9 (d, J_{C-F} = 2.9 Hz, C_{Ar} quat), 132.8 (d, J_{C-F} = 2.9 Hz, C_{Ar} quat), 127.0 (d, J_{C-F} = 8.4 Hz, 2 × C_{Ar}), 124.5 (d, J_{C-F} = 27.7 Hz, C_{Ar}), 122.2 (d, J_{C-F} = 4.2 Hz, C_{Ar}), 115.8 (d, J_{C-F} = 21.8 Hz, 2 × C_{Ar}), 83.5 (OC quat), 63.0 (OCH_2CH_3), 45.4 (NCH_2), 30.4 (NCH_2CH_2), 14.0 (OCH_2CH_3) (the peak due to NC_{Ar} quat was not observed);

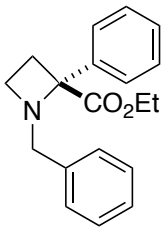
$^{19}F\{^{1}H\}$ NMR (377 MHz, $CDCl_3$) δ –74.9, –112.5; HRMS (ESI$^+$) *m/z* Calculated for $C_{18}H_{17}N_2O_4F_2$ [M+H] 363.1156; Found 363.1154.

(±)–Ethyl 3-(4-bromobenzyl)-6-(4-fluorophenyl)-2-oxo-1,3-oxazinane-6-carboxylate (262)



A solution of ethyl 6-(4-fluorophenyl)-2-oxo-1,3-oxazinane-6-carboxylate **237** (27 mg, 0.1 mmol), 4-bromobenzyl bromide (30 mg, 0.12 mmol), KI (1.7 mg, 10 μmol) and K_2CO_3 (42 mg, 0.3 mmol) in MeCN (0.25 mL) was stirred at 50 ºC for 20 h. The reaction was allowed to cool to rt and H_2O (25 mL) was added. The aqueous reaction mixture was extracted with EtOAc (3 × 25 mL) and the combined organic layers were dried over Na_2SO_4, filtered and concentrated under reduced pressure. Purification by flash chromatography (25% to 40% EtOAc/pentane) followed by purification by flash chromatography (2% Et_2O/CH_2Cl_2) afforded ethyl 3-(4-bromobenzyl)-6-(4-fluorophenyl)-2-oxo-1,3-oxazinane-6-carboxylate **262** (15 mg, 34%) as a white solid. R_f 0.18 (1% Et_2O/CH_2Cl_2); mp = 105–107 ºC; ν_{max} (film)/cm^{-1} 3049, 2974, 2929, 1737 (C=O ester), 1692 (C=O carbamate), 1513, 1439, 1267, 1170, 1010, 824, 753; ^{1}H NMR (400 MHz, $CDCl_3$) δ 7.60–7.54 (m, 2 H, 2 × HC_{Ar}), 7.44 (d, *J* = 8.4 Hz, 2 H, 2 × HC_{Ar}), 7.15–7.05 (m, 4 H, 4 × HC_{Ar}), 4.59 (d, *J* = 15.0 Hz, 1 H, NC*H*HAr), 4.44 (d, *J* = 15.0 Hz, 1 H, NCH*H*Ar), 4.23–4.11 (m, 2 H, OCH_2CH_3), 3.25–3.17 (m, 1 H, NC*H*H), 3.16–3.08 (m, 1 H, NCH*H*), 2.80–2.72 (m, 1 H, NCH_2CHH), 2.33 (ddd, *J* = 13.9, 9.7, 6.1 Hz, 1 H, NCH_2CHH), 1.19 (t, *J* = 7.1 Hz, 3 H, OCH_2CH_3); ^{13}C NMR (101 MHz, $CDCl_3$) δ 169.8 (C=O ester), 162.9 (d, $J_{C–F}$ = 248.3 Hz, FC_{Ar} quat), 152.1 (C=O carbamate), 135.2 (C_{Ar} quat), 133.1 (d, $J_{C–F}$ = 2.7 Hz, C_{Ar} quat), 131.8 (2 × C_{Ar}), 129.7 (2 × C_{Ar}), 127.0 (d, $J_{C–F}$ = 8.4 Hz, 2 × C_{Ar}), 121.8 (BrC_{Ar} quat), 115.6 (d, $J_{C–F}$ = 21.7 Hz, 2 × C_{Ar}), 82.5 (OC quat), 62.6 (OCH_2CH_3), 52.0 (NCH_2Ar), 41.8 (NCH_2), 30.0 (NCH_2CH_2), 13.9 (OCH_2CH_3); $^{19}F\{^{1}H\}$ NMR (377 MHz, $CDCl_3$) δ –112.8; HRMS (ESI$^+$) *m/z* Calculated for $C_{20}H_{20}NO_4F^{79}Br$ [M+H] 436.0560; Found 436.0554.

(±)–Ethyl 1-benzyl-2-phenylazetidine-2-carboxylate (263)



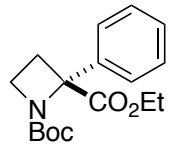
Benzyl bromide (0.10 mL, 0.8 mmol) was added to a stirred solution of ethyl 2-phenylazetidine-2-carboxylate **232** (82 mg, 0.4 mmol), KI (6.6 mg, 40 μmol) and K_2CO_3 (166 mg, 1.2 mmol) in MeCN (1.0 mL). The reaction mixture was stirred at 25 ºC for 4.5 h then H_2O (50 mL) was added. The aqueous reaction mixture was extracted with EtOAc (3 × 30 mL). The combined organic layers were dried over Na_2SO_4, filtered and concentrated under reduced pressure. Purification by flash chromatography (2% to 5% to 100% Et_2O/pentane) afforded ethyl 1-benzyl-2-phenylazetidine-2-carboxylate **263** (95 mg, 81%) as a colourless oil. R_f 0.15 (2% Et_2O/pentane); ν_{max} (film)/cm^{-1}

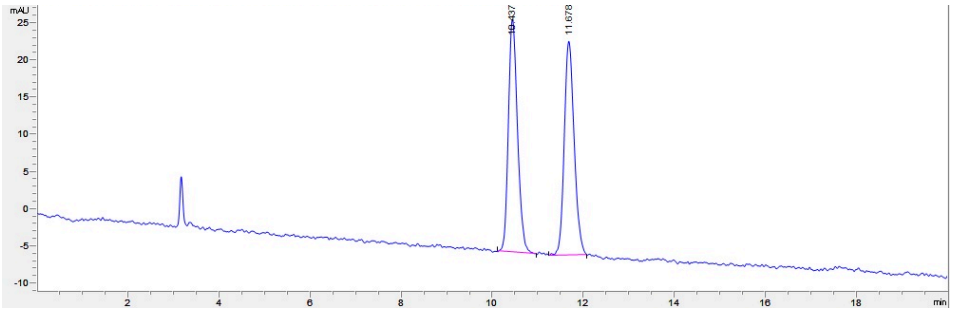
2967, 2832, 1722 (C=O), 1215, 1100, 1025, 738, 697; ^{1}H NMR (400 MHz, $CDCl_3$) δ 7.48–7.25 (m, 10 H, 10 × HC_{Ph}), 4.36–4.28 (m, 2 H, OCH_2CH_3), 3.98 (d, *J* = 13.0 Hz, 1 H, NC*H*HPh), 3.50 (d, *J* = 13.0 Hz, 1 H, NCH*H*Ph), 3.33–3.22 (m, 2 H, NCH_2), 2.98 (ddd, *J* = 11.3, 7.9, 3.6 Hz, 1 H, NCH_2CHH), 2.35 (dt, *J* = 10.7, 8.1 Hz, 1 H, NCH_2CHH), 1.31 (t, *J* = 7.1 Hz, 3 H, OCH_2CH_3); ^{13}C NMR (101 MHz, $CDCl_3$) δ 172.4 (C=O), 142.4 (C_{Ph} quat), 138.2 (C_{Ph} quat), 128.5 (2 × C_{Ph}), 128.32 (2 × C_{Ph}), 128.25 (2 × C_{Ph}), 127.2 (C_{Ph}), 127.0 (C_{Ph}), 125.3 (2 × C_{Ph}), 74.6 (NC quat), 60.9 (OCH_2CH_3), 57.4 (NCH_2Ph), 49.9 (NCH_2), 30.1 (NCH_2CH_2), 14.4 (OCH_2CH_3); HRMS (ESI^+) *m/z* Calculated for $C_{19}H_{22}NO_2$ [M+H] 296.1651; Found 296.1647.

6.2.2.6 HPLC Data for 1,3-Oxazinan-2-one Synthesis

(±)–1-(*tert*-Butyl) 2-ethyl 2-phenylazetidine-1,2-dicarboxylate 104

Conditions: Chiralpak IE 3-column, 95:5 *n*-hexane:*i*-PrOH, flow rate: 1 mL·min^{-1}, 35 ºC. UV detection wavelength: 210.4 nm.





#	Time	Area	Height	Width	Area%	Symmetry
1	10.437	441	31.5	0.2155	50.153	0.762
2	11.678	438.3	28.9	0.2311	49.847	0.837

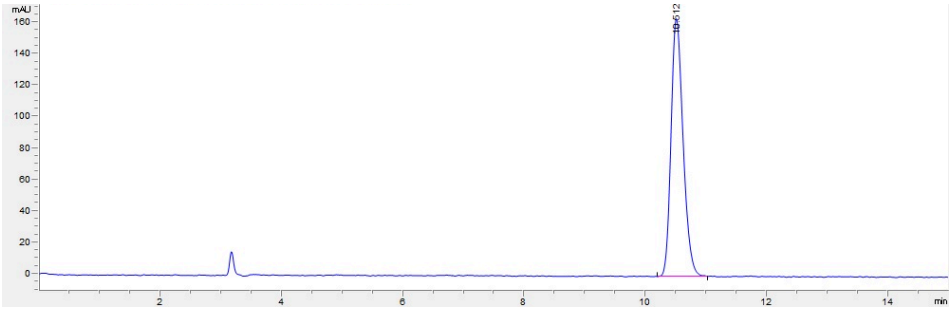
Separation of enantiomers of (±)-1-(*tert*-Butyl) 2-ethyl 2-phenylazetidine-1,2-dicarboxylate 104

A racemic mixture of 1-(*tert*-Butyl) 2-ethyl 2-phenylazetidine-1,2-dicarboxylate **104** was separated by chiral HPLC.

Conditions: Chiralpak IE 3-column, 95:5 *n*-hexane:*i*-PrOH, flow rate: 1 mL·min^{-1}, 35 ºC. UV detection wavelength: 210.4 nm.

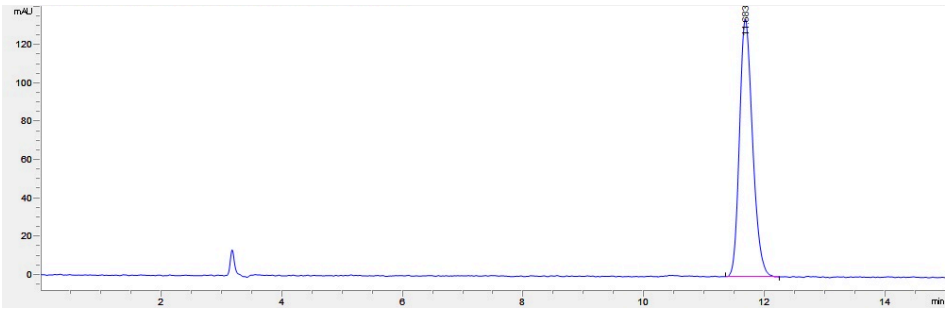
A 10 mg/mL solution of 1-(*tert*-Butyl) 2-ethyl 2-phenylazetidine-1,2-dicarboxylate **104** was injected and the HPLC outlet was collected in vials, changing every 15 s. This was repeated to afford 3 mg each of the two enantiomers with high enantiopurity.

Enantiomer at t = 10.5 min



#	Time	Area	Height	Width	Area%	Symmetry
1	10.512	2269.8	164.6	0.2109	100.000	0.751

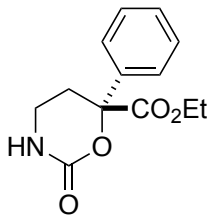
Enantiomer at t = 11.7 min

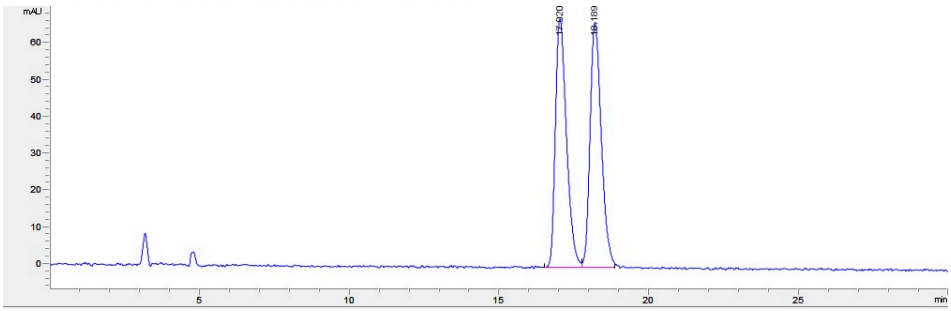


#	Time	Area	Height	Width	Area%	Symmetry
1	11.683	2026.8	134.3	0.2321	100.000	0.765

(±)–Ethyl 2-oxo-6-phenyl-1,3-oxazinane-6-carboxylate 231

Conditions: Chiralpak ID 3-column, 80:20 *n*-hexane:*i*-PrOH, flow rate: 1 mL·min^{-1}, 35 ºC. UV detection wavelength: 210.4 nm.

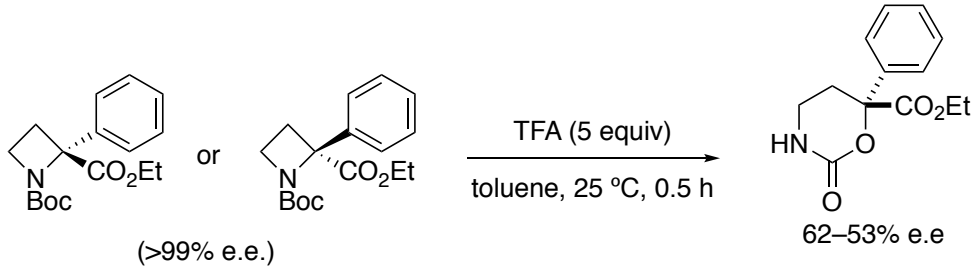




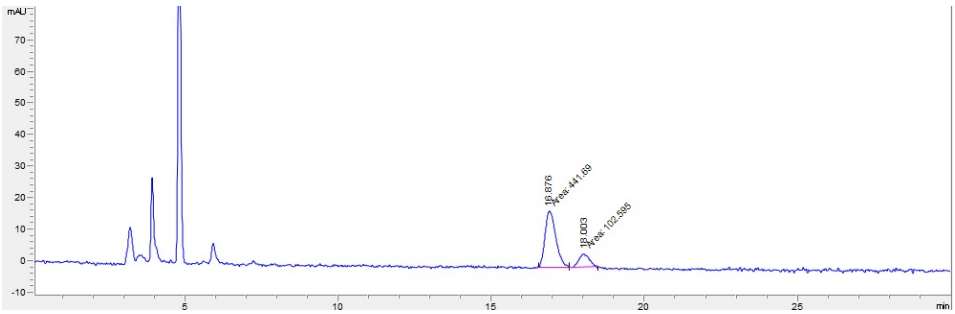
#	Time	Area	Height	Width	Area%	Symmetry
1	17.02	1740.1	67.4	0.3751	49.990	0.643
2	18.189	1740.9	66.6	0.3931	50.010	0.72

Subjection of enantiomer of 1-(*tert*-butyl) 2-ethyl 2-phenylazetidine-1,2-dicarboxylate 231 to reaction conditions

A stock solution of trifluoroacetic acid in toluene (10 μL, 0.38 mL TFA/ 1 mL toluene) was added to a solution of 1-(*tert*-butyl) 2-ethyl 2-phenylazetidine-1,2-dicarboxylate **104** (e.e. > 99%) (3 mg) at 25 ºC and stirred for 30 min. The reaction mixture was concentrated under reduced pressure and a sample taken for HPLC analysis.

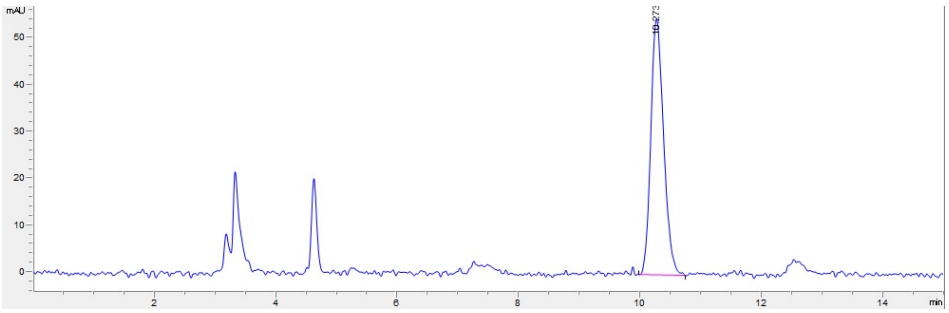


HPLC trace of ethyl 2-oxo-6-phenyl-1,3-oxazinane-6-carboxylate 231 formed



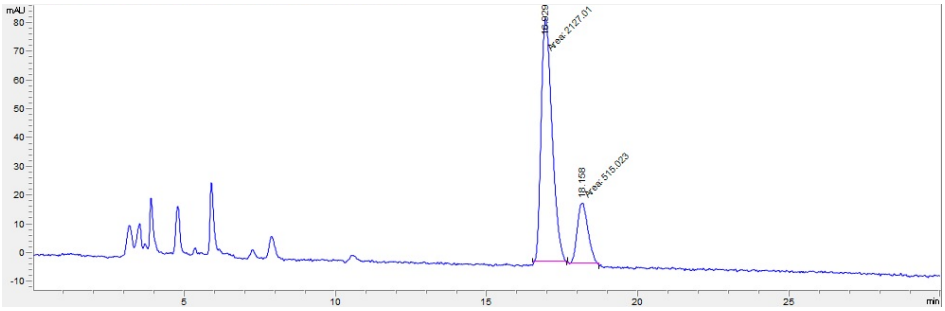
#	Time	Area	Height	Width	Area%	Symmetry
1	16.876	441.7	17.9	0.4119	81.151	0.66
2	18.003	102.6	4.3	0.3993	18.849	0.909

HPLC trace of remaining starting material 104



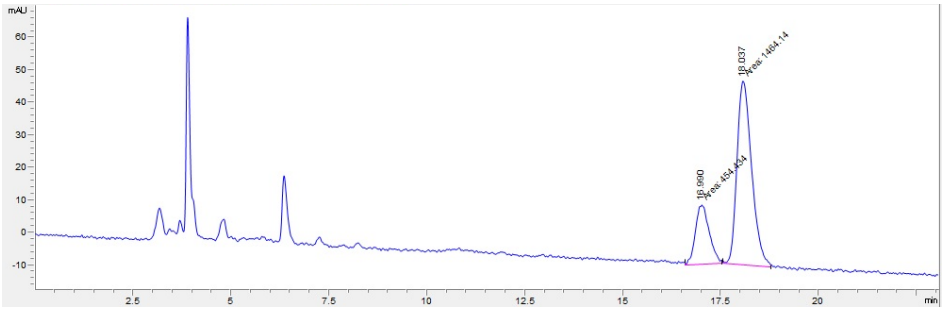
#	Time	Area	Height	Width	Area%	Symmetry
1	10.273	811	54.9	0.2084	100.000	0.762

HPLC trace of product 231 formed resubjected to reaction condtions



#	Time	Area	Height	Width	Area%	Symmetry
1	16.929	2127	84.7	0.4183	80.507	0.646
2	18.158	515	21.1	0.4076	19.493	0.982

HPLC trace when opposite enantiomer of 104 was subjected to reaction conditions

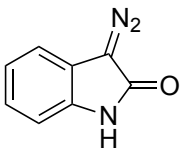


#	Time	Area	Height	Width	Area%	Symmetry
1	16.99	454.4	18.3	0.4133	23.686	0.855
2	18.037	1464.1	56.3	0.4335	76.314	0.667

6.2.3 Synthesised Compounds from Chapter 4

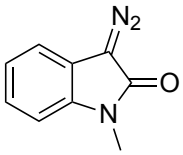
6.2.3.1 3-Diazooxindole Synthesis

3-Diazoindolin-2-one (277)



Tosylhydrazide (7.66 g, 44.0 mmol) in MeOH (40 mL) was heated to 70 ºC to solubilise the hydrazide. The mixture was cooled to rt and isatin (5.90 g, 40.0 mmol) was added. The reaction mixture was stirred at 70 ºC for 10 min, then cooled to rt. The solid was filtered, then transferred to a new reaction flask. H_2O (200 mL) was added, then NaOH (3.20 g, 80.0 mmol) was added and the reaction mixture was stirred at 70 ºC for 3 h. The aqueous reaction mixture was extracted with EtOAc (3 × 200 mL) and the combined organic layers were dried over Na_2SO_4, filtered and concentrated under reduced pressure. The crude reaction mixture was dry-loaded onto silica (CH_2Cl_2). Purification by flash chromatography (60% EtOAc/hexane to EtOAc) afforded 3-diazoindolin-2-one **277** (5.37 g, 84%) as an orange solid. R_f 0.30 (60% EtOAc/hexane); ν_{max} (film)/cm^{-1} 3019 (br s, NH), 2080 (C=N=N out-of-phase), 1674 (C=O), 1614, 1394 (C=N=N in-phase), 1208, 1096, 988, 742; ^{1}H NMR (400 MHz, $CDCl_3$) δ 9.52–9.37 (br d, 1 H, NH), 7.19 (d, J = 7.9 Hz, 1 H, HC_{Ar}), 7.15 (dd, J = 7.7, 1.3 Hz, 1 H, HC_{Ar}), 7.08 (dt, J = 7.6, 1.1 Hz, 1 H, HC_{Ar}), 7.05–7.01 (m, 1 H, HC_{Ar}); ^{13}C NMR (101 MHz, $CDCl_3$) δ 169.5 (C=O quat), 132.0 (NC_{Ar} quat), 125.5 (C_{Ar}), 122.1 (C_{Ar}), 118.3 (C_{Ar}), 117.2 (C_{Ar} quat), 110.8 (C_{Ar}), 61.5 ($C=N_2$). The observed characterisation data (^{1}H and ^{13}C NMR) was consistent with that previously reported in the literature.[425]

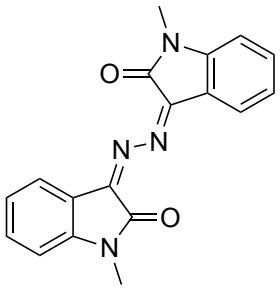
3-Diazo-1-methylindolin-2-one (273)



MeI (4.04 mL, 64.9 mmol) was added dropwise to a solution of 3-diazoindolin-2-one **277** (9.38 g, 59.0 mmol) and K_2CO_3 (8.97 g, 64.9 mmol) in DMF (65.0 mL) at 25 ºC. The reaction mixture was stirred for 24 h, then H_2O (250 mL) was added followed by EtOAc (250 mL). The layers were separated and the aqueous layer extracted with EtOAc (2 × 250 mL). The combined organic layers were dried over Na_2SO_4, filtered and concentrated under reduced pressure. Purification by flash chromatography (50% EtOAc/heptane) afforded 3-diazo-1-methylindolin-2-one **273** (8.86 g, 87%) as a red solid. R_f 0.30 (50% Et_2O/pentane); ν_{max} (film)/cm^{-1} 2087 (C=N=N out-of-phase), 1674 (C=O amide), 1607, 1398, 1368 (C=N=N in-phase), 1312, 1249, 1197, 1118, 1088, 1018, 734, 697; ^{1}H NMR (400 MHz, $CDCl_3$) δ 7.23–7.18 (m, 2 H, 2 × HC_{Ar}), 7.12–7.07 (m, 1 H, HC_{Ar}), 6.94–6.91 (m, 1 H, HC_{Ar}), 3.33 (s, 3 H, NCH_3); ^{13}C NMR (101 MHz, $CDCl_3$) δ 166.8 (C=O), 134.4 (NC_{Ar} quat), 125.4 (C_{Ar}), 122.0 (C_{Ar}), 118.2 (C_{Ar}), 116.6 (C_{Ar} quat), 108.6 (C_{Ar}), 26.8 (CH_3).

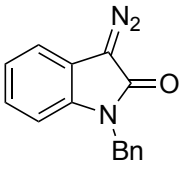
The observed characterisation data (^{1}H and ^{13}C NMR) was consistent with that previously reported in the literature.[426]

(3*Z*,3'*Z*)-3,3'-(Hydrazine-1,2-diylidene)bis(1-methylindolin-2-one) (278)



Tosylhydrazide (20.5 g, 110 mmol) in MeOH (100 mL) was heated to 60 ºC to solubilise the hydrazide. The mixture was cooled to rt and isatin (14.7 g, 100 mmol) was added. The reaction mixture was stirred at 60 ºC for 1 h, then cooled to rt. The solid was filtered, then transferred to a new reaction flask. H_2O (700 mL) was added, then NaOH (8.0 g, 200 mmol) was added and the reaction mixture was stirred at 70 ºC for 2.5 h. The aqueous reaction mixture was extracted with EtOAc (3 × 200 mL) and the combined organic layers were dried over Na_2SO_4, filtered and concentrated under reduced pressure. MeI (5.48 mL) was added dropwise to a solution of crude 3-diazoindolin-2-one **277** (12.5 g, 80.0 mmol) and K_2CO_3 (12.16 g, 88.0 mmol) in DMF (200 mL) at 25 ºC. The reaction mixture was stirred for 18 h and filtered and the filtered solid was dried to afford (3*Z*,3'*Z*)-3,3'-(hydrazine-1,2-diylidene)bis(1-methylindolin-2-one) (assumed to be Z,Z' stereoisomer) **278** (11.2 g, 88%) as an orange solid. R_f 0.09 (50% EtOAc/hexane); mp = decomposition observed at 205 ºC [lit = decomposition observed at 251 ºC][427]; ν_{max} (film)/cm^{-1} 1716 (C=O),1608,1467, 1374, 1334, 1104, 785, 733; ^{1}H NMR (400 MHz, $CDCl_3$) δ 7.77–7.74 (m, 2 H, 2 × HC_{Ar}), 7.42 (td, *J* = 7.8, 1.3 Hz, 2 H, 2 × HC_{Ar}), 7.05 (td, *J* = 7.7, 0.9 Hz, 2 H, 2 × HC_{Ar}), 6.86 (d, *J* = 7.9 Hz, 2 H, 2 × HC_{Ar}), 3.32 (s, 6 H, 2 × NCH_3); ^{13}C NMR (101 MHz, $CDCl_3$) δ 162.8 (2 × C=O), 145.9 (2 × NC_{Ar} quat), 144.5 (2 × C=N), 133.7 (2 × C_{Ar}), 129.1 (2 × C_{Ar}), 123.3 (2 × C_{Ar}), 115.5 (2 × C_{Ar} quat), 108.6 (2 × C_{Ar}), 26.0 (2 × NCH_3); HRMS (FTMS + pAPCI) *m/z* Calculated for $C_{18}H_{15}N_4O_2^+$ $[M+H]^+$ 319.1190; Found 319.1191.

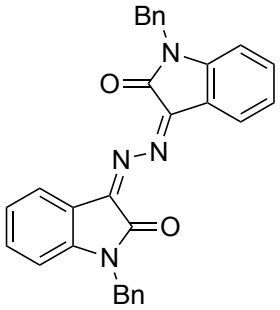
1-Benzyl-3-diazoindolin-2-one (280)



BnBr (1.30 mL, 11.0 mmol) was added to a stirred solution of 3-diazoindolin-2-one **277** (1.59 g, 10.0 mmol), K_2CO_3 (1.66 g, 12.0 mmol) and TBAI (370 mg, 1.0 mmol) in DMF (10.0 mL) at 25 ºC. The reaction mixture was stirred for 18 h, then H_2O (100 mL) was added and the aqueous reaction mixture was extracted with EtOAc (2 × 100 mL). The combined organic layers were washed with brine (2 × 100 mL), dried over Na_2SO_4, filtered and concentrated under reduced pressure to afford 1-benzyl-3-diazoindolin-2-one **280** (2.06 g, 83%) as an orange solid. R_f 0.50 (50% Et_2O/hexane); ν_{max} (film)/cm^{-1} 2117 (C=N=N out-of-phase), 1662 (C=O), 1610, 1342 (C=N=N in-phase), 1167, 734, 697; ^{1}H NMR (400 MHz, $CDCl_3$) δ 7.34–7.29 (m, 4 H, 4 × HC_{Ar}), 7.28–7.25 (m, 1 H, HC_{Ar}), 7.23–7.20 (m, 1 H, HC_{Ar}), 7.12–7.05 (m, 2 H, 2 × HC_{Ar}), 6.85–6.82 (m, 1 H, HC_{Ar}), 5.04 (s, 2 H,

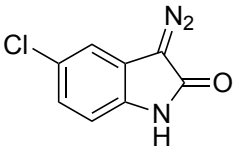
NCH_2Ph); ^{13}C NMR (101 MHz, $CDCl_3$) δ 166.8 (C=O), 136.0 (NC_{Ar} quat), 133.6 (C_{Ph} quat), 128.7 (2 × C_{Ph}), 127.6 (C_{Ph}), 127.2 (2 × C_{Ph}), 125.4 (C_{Ar}), 122.1 (C_{Ar}), 118.2 (C_{Ar}), 116.7 (C_{Ar} quat), 109.5 (C_{Ar}), 44.2 (NCH_2Ph). The observed characterisation data (^1H, ^{13}C NMR and IR) was consistent with that previously reported in the literature.[426]

(3*Z*,3'*Z*)-3,3'-(Hydrazine-1,2-diylidene)bis(1-benzylindolin-2-one) (279)



BnBr (1.31 mL, 11.0 mmol) was added dropwise to a stirred solution of 3-diazoindolin-2-one **277** (1.59 g, 10.0 mmol) and K_2CO_3 (1.66 g, 12.0 mmol) in DMF (10.0 mL) at 25 ºC. The reaction mixture was stirred for 16 h then the reaction mixture was filtered and the isolated solid was dried to afford (3*Z*,3'*Z*)-3,3'-(hydrazine-1,2-diylidene)bis(1-benzylindolin-2-one) (assumed to be Z,Z' stereoisomer) **279** (1.15 g, 50%) as a dark purple solid. R_f 0.38 (50% EtOAc/hexane); mp = >200 ºC [lit = 187–189 ºC][428]; ν_{max} (film)/cm^{-1} 1711 (C=O), 1603, 1465, 1346, 1178, 1100, 727; ^1H NMR (400 MHz, $CDCl_3$) δ 7.85 (d, *J* = 7.5 Hz, 2 H, 2 × HC_{Ar}), 7.40–7.28 (m, 12 H, 12 × HC_{Ar}), 7.04 (t, *J* = 7.6 Hz, 2 H, 2 × HC_{Ar}), 6.75 (d, *J* = 7.9 Hz, 2 H, 2 × HC_{Ar}), 5.02 (s, 4 H, 2 × NCH_2Ph); ^{13}C NMR (101 MHz, $CDCl_3$) δ 163.2 (2 × C=O), 145.4 (2 × NC_{Ar} quat), 145.3 (2 × C=N), 135.0 (2 × C_{Ph} quat), 134.0 (2 × C_{Ar}), 129.6 (2 × C_{Ar}), 128.9 (4 × C_{Ph}), 127.9 (2 × C_{Ph}), 127.3 (4 × C_{Ph}), 123.6 (2 × C_{Ar}), 116.0 (2 × C_{Ar} quat), 109.9 (2 × C_{Ar}), 44.0 (2 × NCH_2Ph). HRMS (FTMS + pAPCI) *m/z* Calculated for $C_{30}H_{23}N_4O_2^+$ $[M+H]^+$ 471.1816; Found 471.1814.

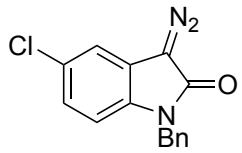
5-Chloro-3-diazoindolin-2-one (282)



Tosylhydrazide (1.92 g, 11.0 mmol) in MeOH (10 mL) was heated to 70 ºC to solubilise the hydrazide. The mixture was cooled to rt and 5-chloroisatin (1.82 g, 10.0 mmol) was added. The reaction mixture was stirred at 70 ºC for 10 min, then cooled to rt. The solid was filtered, then transferred to a new reaction flask. H_2O (50 mL) was added, then NaOH (0.8 g, 20.0 mmol) was added and the reaction mixture was stirred at 70 ºC for 19 h. The aqueous reaction mixture was extracted with EtOAc (3 × 200 mL) and the combined organic layers were dried over Na_2SO_4, filtered and concentrated under reduced pressure to afford 5-chloro-3-diazoindolin-2-one **282** (1.49 g, 77%) as an orange solid which was used without further purification. R_f 0.25 (50% EtOAc/hexane); ν_{max} (film)/cm^{-1} 3254 (br s, NH), 2091 (C=N=N out-of-phase), 1696 (C=O), 1648, 1472, 1241, 1394, 1282, 1189, 1070, 887, 861, 701; ^1H NMR (400 MHz, DMSO-d_6) δ 10.77 (s, 1 H, NH), 7.54 (d, *J* = 2.0 Hz, 1 H, HC_{Ar}), 7.09 (dd, *J* = 8.3, 2.0 Hz, 1 H, HC_{Ar}), 6.88 (d, *J* = 8.3 Hz, 1 H, HC_{Ar}); ^{13}C NMR (101 MHz, DMSO-d_6) δ 167.3 (C=O), 131.3 (NC_{Ar}

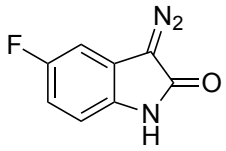
quat), 125.2 (C_{Ar} quat), 124.7 (C_{Ar}), 119.0 (C_{Ar} quat), 118.9 (C_{Ar}), 110.9 (C_{Ar}), 60.7 ($C{=}N_2$ quat); HRMS (FTMS + pAPCI) *m/z* Calculated for $C_8H_5N_3OCl^+$ $[M+H]^+$ 194.0116; Found 194.0110.

1-Benzyl-5-chloro-3-diazoindolin-2-one (283)



Benzyl bromide (0.48 mL, 4.0 mmol) was added to a solution of 5-chloro-3-diazoindolin-2-one **282** (390 mg, 2.0 mmol) and K_2CO_3 (550 mg, 4.0 mmol) in MeCN (4.0 mL) at 25 ºC. The reaction mixture was stirred for 18 h at 25 ºC. CH_2Cl_2 (50 mL) was added and the reaction mixture was extracted with H_2O (3 × 50 mL). The combined organic layers were dried over Na_2SO_4, filtered and concentrated under reduced pressure. Purification by flash chromatography (20% to 30% EtOAc/hexane) afforded 1-benzyl-5-chloro-3-diazoindolin-2-one **283** (338 mg, 60%) as an orange solid. R_f 0.31 (30% EtOAc/hexane); ν_{max} (film)/cm^{-1} 3034, 3064, 2095 (C=N=N out-of-phase), 1681 (C=O), 1610, 1476, 1446, 1387 (C=N=N in-phase), 1170, 1118; ^{1}H NMR (400 MHz, $CDCl_3$) δ 7.36–7.25 (m, 5 H, 5 × HC_{Ph}), 7.19 (d, J = 2.0 Hz, 1 H, HC_{Ar}), 7.05 (dd, J = 8.4, 2.0 Hz, 1 H, HC_{Ar}), 6.72 (d, J = 8.4 Hz, 1 H, HC_{Ar}), 5.01 (s, 2 H, NCH_2Ph); ^{13}C NMR (101 MHz, $CDCl_3$) δ 166.3 (C=O), 135.5 (C_{Ar} quat), 132.1 (C_{Ar} quat), 128.8 (2 × C_{Ph}), 127.8 (C_{Ph}), 127.6 (C_{Ar} quat), 127.2 (2 × C_{Ph}), 125.4 (C_{Ar}), 118.3 (C_{Ar} quat), 118.2 (C_{Ar}), 110.3 (C_{Ar}), 44.4 (NCH_2Ph); HRMS (FTMS + pAPCI) *m/z* Calculated for $C_{15}H_{11}N_3OCl^+$ $[M+H]^+$ 284.0585; Found 284.0580.

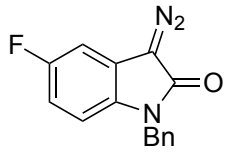
3-Diazo-5-fluoroindolin-2-one (285)



Tosylhydrazide (958 mg, 5.5 mmol) in MeOH (5.0 mL) was heated to 70 ºC to solubilise the hydrazide. The mixture was cooled to rt and 5-fluoroisatin (826 mg, 5.0 mmol) was added. The reaction mixture was stirred at 70 ºC for 10 min, then cooled to rt. The solid was filtered, then transferred to a new reaction flask. H_2O (50 mL) was added, then NaOH (0.4 g, 10.0 mmol) was added and the reaction mixture was stirred at 70 ºC for 3 h. The aqueous reaction mixture was extracted with EtOAc (3 × 100 mL) and the combined organic layers were dried over Na_2SO_4, filtered and concentrated under reduced pressure to afford 3-diazo-5-fluoroindolin-2-one **285** (735 mg, 83%) as an orange solid which was used without further purification. R_f 0.32 (40% EtOAc/hexane); ν_{max} (film)/cm^{-1} 3284, 2087 (C=N=N out-of-phase), 1685 (C=O), 1651, 1476, 1402, 1286, 1245, 1189, 906, 846, 805; ^{1}H NMR (400 MHz, DMSO-d_6) δ 10.68 (br s, 1 H, NH), 7.40 (dd, J = 9.0, 2.5 Hz, 1 H, HC_{Ar}), 6.94–6.84 (m, 2 H, 2 × HC_{Ar}); ^{13}C NMR (101 MHz, DMSO-d_6) δ 167.6 (C=O quat), 157.6 (d, J_{C-F} = 235.2 Hz, FC_{Ar} quat), 128.9 (C_{Ar}), 118.5 (d, J_{C-F} = 11.4 Hz, C_{Ar} quat), 111.6 (d, J_{C-F} = 24.1 Hz, C_{Ar}), 111.5 (d, J_{C-F} = 9.0 Hz, C_{Ar}), 106.6 (d, J_{C-F} = 27.8 Hz, C_{Ar} quat), 61.2 ($C{=}N_2$ quat); ^{19}F{^{1}H} NMR (377 MHz, DMSO-d_6) δ –122.0. The

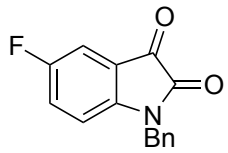
observed characterisation data (IR, ^{1}H and ^{13}C NMR) was consistent with that previously reported in the literature.[429]

1-Benzyl-3-diazo-5-fluoroindolin-2-one (286)



Benzyl bromide (0.32 mL, 2.7 mmol) was added to a solution of 3-diazo-5-fluoroindolin-2-one **285** (239 mg, 1.35 mmol), K_2CO_3 (746 mg, 5.4 mmol) and TBAI (100 mg, 0.27 mmol) in MeCN (2.7 mL) at 25 ºC. The reaction mixture was stirred for 14 h at 25 ºC. CH_2Cl_2 (50 mL) was added and the reaction mixture was extracted with sat. aq. $NaHCO_3$ (3 × 50 mL). The combined organic layers were dried over Na_2SO_4, filtered and concentrated under reduced pressure. Purification by flash chromatography (30% Et_2O/pentane) afforded 1-benzyl-3-diazo-5-fluoroindolin-2-one **286** (261 mg, 73%) as an orange solid. R_f 0.31 (30% Et_2O/pentane); ν_{max} (film)/cm^{-1} 3064, 2926, 2087 (C=N=N out-of-phase), 1674 (C=O), 1603, 1476, 1394 (C=N=N in-phase), 1357, 1297, 1159, 850, 783; ^{1}H NMR (400 MHz, $CDCl_3$) δ 7.36–7.25 (m, 5 H, 5 × HC_{Ph}), 6.96 (dd, J = 8.0, 2.4 Hz, 1 H, HC_{Ar}), 6.83–6.77 (m, 1 H, HC_{Ar}), 6.71 (dd, J = 8.6, 4.2 Hz, 1 H, HC_{Ar}), 5.02 (s, 2 H, NCH_2Ph); ^{13}C NMR (101 MHz, $CDCl_3$) δ 166.5 (C=O quat), 158.8 (d, $J_{C–F}$ = 239.8 Hz, FC_{Ar} quat), 135.7 (C_{Ar} quat), 129.6 (C_{Ar} quat), 128.8 (2 × C_{Ph}), 127.7 (C_{Ph}), 127.2 (2 × C_{Ph}), 117.9 (d, $J_{C–F}$ = 10.7 Hz, C_{Ar} quat), 112.1 (d, $J_{C–F}$ = 23.9 Hz, C_{Ar}), 110.0 (d, $J_{C–F}$ = 8.7 Hz, C_{Ar}), 105.8 (d, $J_{C–F}$ = 27.3 Hz, C_{Ar}), 61.5 (s, $C=N_2$ quat), 44.4 (NCH_2Ph); $^{19}F\{^{1}H\}$ NMR (377 MHz, $CDCl_3$) δ –120.4. The observed characterisation data (IR, ^{1}H, ^{13}C and ^{19}F NMR) was consistent with that previously reported in the literature.[430]

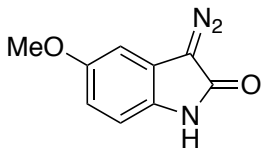
1-Benzyl-5-fluoroindoline-2,3-dione (287)[431]



Benzyl bromide (0.71 mL, 6.0 mmol) was added to a solution of 5-fluoroisatin (330 mg, 2.0 mmol) and K_2CO_3 (691 mg, 5.0 mmol) in DMF (10 mL) at 25 ºC. The reaction mixture was stirred for 62 h at 25 ºC. CH_2Cl_2 (50 mL) and H_2O (50 mL) were added and the layers were separated. The aqueous layer was extracted with CH_2Cl_2 (2 × 50 mL). The combined organic layers were washed with H_2O (3 × 50 mL), dried over Na_2SO_4, filtered and concentrated under reduced pressure. Purification by flash chromatography (30% EtOAc/hexane) afforded 1-benzyl-5-fluoroindoline-2,3-dione **287** (510 mg, quant) as a red solid. R_f 0.11 (20% EtOAc/hexane); mp = 131–133 ºC [lit. mp = 130–133 ºC][432]; ν_{max} (film)/cm^{-1} 3064, 1730 (2 × C=O ketone), 1621, 1480, 1331, 1264, 1170, 1133, 887, 824, 783, 697; ^{1}H NMR (400 MHz, $CDCl_3$) δ 7.40–7.30 (m, 6 H, 5 × HC_{Ph} and HC_{Ar}), 7.20 (td, J = 8.6, 2.7 Hz, 1 H, HC_{Ar}), 6.74 (dd, J = 8.6, 3.6 Hz, 1 H, HC_{Ar}), 4.94 (s, 2 H, NCH_2Ph); ^{13}C NMR (101 MHz, $CDCl_3$) δ 182.6 (C=O ketone), 159.2 (d, $J_{C–F}$ = 245.9 Hz, FC_{Ar} quat), 158.0 (C=O amide), 146.7 (NC_{Ar} quat), 134.1 (C_{Ph} quat), 129.0

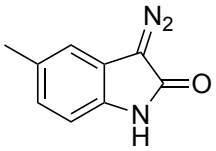
(2 × C_{Ph}), 128.2 (C_{Ph}), 127.3 (2 × C_{Ph}), 124.6 (d, J_{C-F} = 23.8 Hz, C_{Ar}), 118.2 (d, J_{C-F} = 6.9 Hz, C_{Ar} quat), 112.3 (d, J_{C-F} = 19.4 Hz, C_{Ar}), 112.2 (C_{Ar}), 44.1 (NCH_2); $^{19}F\{^1H\}$ NMR (377 MHz, $CDCl_3$) δ –117.9. The observed characterisation data (^1H, ^{13}C and ^{19}F NMR) was consistent with that previously reported in the literature.[433]

3-Diazo-5-methoxyindolin-2-one (288)



Tosylhydrazide (1.92 g, 11.0 mmol) in MeOH (10.0 mL) was heated to 70 ºC to solubilise the hydrazide. The mixture was cooled to rt and 5-methoxyisatin (1.77 g, 10.0 mmol) was added. The reaction mixture was stirred at 70 ºC for 25 min, then cooled to rt. The solid was filtered, then transferred to a new reaction flask. H_2O (100 mL) was added, then NaOH (0.8 g, 20.0 mmol) was added and the reaction mixture was stirred at 70 ºC for 3 h. The aqueous reaction mixture was extracted with EtOAc (3 × 100 mL) and the combined organic layers were dried over Na_2SO_4, filtered and concentrated under reduced pressure to afford 3-diazo-5-methoxyindolin-2-one **288** (1.54 g, 81%) as an orange solid which was used without further purification. R_f 0.20 (60% EtOAc/hexane); ν_{max} (film)/cm^{-1} 3094 (br s, NH), 3030, 2885, 2832, 2788, 2087 (C=N=N out-of-phase), 1666 (C=O), 1595, 1480, 1413, 1379 (C=N=N in-phase), 1308, 1264, 1197, 1148, 1010, 902, 787, 727; ^1H NMR (400 MHz, $CDCl_3$) δ 10.46 (br s, 1 H, NH), 7.11 (d, J = 2.5 Hz, 1 H, HC_{Ar}), 6.80 (d, J = 8.5 Hz, 1 H, HC_{Ar}), 6.66 (dd, J = 8.5, 2.5 Hz, 1 H, HC_{Ar}), 3.71 (s, 3 H, OCH_3); ^{13}C NMR (101 MHz, $CDCl_3$) δ 167.9 (C=O), 154.7 (OC_{Ar} quat), 126.3 (NC_{Ar} quat), 118.0 (C_{Ar} quat), 111.4 (C_{Ar}), 110.4 (C_{Ar}), 105.3 (C_{Ar}), 60.7 (CN_2 quat), 55.5 (OCH_3). The observed characterisation data (IR, ^1H and ^{13}C NMR) was consistent with that previously reported in the literature.[429]

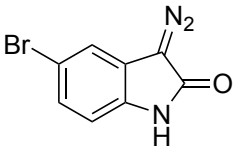
3-Diazo-5-methylindolin-2-one (289)



Tosylhydrazide (575 mg, 3.3 mmol) in MeOH (3.0 mL) was heated to 70 ºC to solubilise the hydrazide. The mixture was cooled to rt and 5-methylisatin (484 mg, 3.0 mmol) was added. The reaction mixture was stirred at 70 ºC for 30 min, then cooled to rt. The solid was filtered, then transferred to a new reaction flask. H_2O (30 mL) was added, then NaOH (240 mg, 6.0 mmol) was added and the reaction mixture was stirred at 70 ºC for 4 h. The aqueous reaction mixture was extracted with EtOAc (3 × 200 mL) and the combined organic layers were dried over Na_2SO_4, filtered and concentrated under reduced pressure. The crude reaction mixture was dry-loaded onto silica (CH_2Cl_2). Purification by flash chromatography (50% to 60% EtOAc/hexane) afforded 3-diazo-5-methylindolin-2-one **289** (325 mg, 63%) as an orange solid which was used without further purification. R_f 0.30 (50% EtOAc/hexane); ν_{max} (film)/cm^{-1} 3150, 3056, 3027, 2102 (C=N=N out-of-phase), 1677 (C=O), 1484, 1387 (C=N=N in-phase), 1208, 805, 671; ^1H NMR

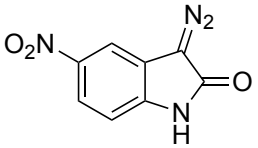
(400 MHz, $CDCl_3$) δ 9.16 (br s, 1 H, NH), 7.02–7.01 (m, 1 H, HC_{Ar}), 6.98–6.95 (m, 1 H, HC_{Ar}), 6.90 (d, *J* = 8.0 Hz, 1 H, HC_{Ar}), 2.37 (s, 3 H, CH_3); ^{13}C NMR (101 MHz, $CDCl_3$) δ 169.3 (C=O), 131.8 (C_{Ar} quat), 129.6 (C_{Ar} quat), 126.3 (C_{Ar}), 118.9 (C_{Ar}), 117.3 (C_{Ar} quat), 110.4 (C_{Ar}), 21.2 (CH_3); HRMS (FTMS + pAPCI) *m/z* Calculated for $C_9H_8N_3O^+$ $[M+H]^+$ 174.0662; Found 174.0662.

5-Bromo-3-diazoindolin-2-one (290)



Tosylhydrazide (1.69 g, 9.7 mmol) in MeOH (8.8 mL) was heated to 70 ºC to solubilise the hydrazide. The mixture was cooled to rt and 5-bromoisatin (2.00 g, 8.8 mmol) was added. The reaction mixture was stirred at 70 ºC for 10 min, then cooled to rt. The solid was filtered, then transferred to a new reaction flask. H_2O (88 mL) was added, then NaOH (664 mg, 16.6 mmol) was added and the reaction mixture was stirred at 70 ºC for 16 h. The aqueous reaction mixture was extracted with EtOAc (3 × 100 mL) and the combined organic layers were dried over Na_2SO_4, filtered and concentrated under reduced pressure to afford 5-bromo-3-diazoindolin-2-one **290** (1.69 g, 81%) as an orange solid which was used without further purification. R_f 0.18 (50% EtOAc/hexane); ν_{max} (film)/cm^{-1} 3265 (br s, NH), 3101, 2095 (C=N=N out-of-phase), 1700 (C=O), 1648, 1469, 1394 (C=N=N in-phase), 1282, 1245, 1193, 1059, 1014, 821; ^1H NMR (400 MHz, DMSO-d_6) δ 10.80 (s, 1 H, NH), 7.68 (d, *J* = 1.8 Hz, 1 H, HC_{Ar}), 7.23 (dd, *J* = 8.3, 1.9 Hz, 1 H, HC_{Ar}), 6.84 (d, *J* = 8.3 Hz, 1 H, HC_{Ar}); ^{13}C NMR (101 MHz, DMSO-d_6) δ 167.3 (C=O quat), 131.7 (NC_{Ar} quat), 127.5 (C_{Ar}), 121.7 (C_{Ar}), 119.5 (C_{Ar} quat), 112.8 (C_{Ar} quat), 111.5 (C_{Ar}), 60.5 ($C=N_2$ quat); HRMS (FTMS + p APCI) *m/z* Calculated for $C_8H_5N_3O^{79}Br^+$ $[M+H]^+$ 237.9611; Found 237.9601.

3-Diazo-5-nitroindolin-2-one (291)

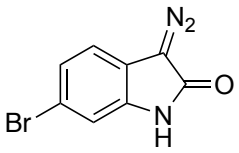


Tosylhydrazide (958 mg, 5.5 mmol) in MeOH (5.0 mL) was heated to 70 ºC to solubilise the hydrazide. The mixture was cooled to rt and 5-nitroisatin (961 mg, 5.0 mmol) was added. The reaction mixture was stirred at 70 ºC for 10 min, then cooled to rt. The solid was filtered, then transferred to a new reaction flask. H_2O (50 mL) was added, then NaOH (0.4 g, 10.0 mmol) was added and the reaction mixture was stirred at 70 ºC for 3 h. The aqueous reaction mixture was extracted with EtOAc (3 × 100 mL) and the combined organic layers were dried over Na_2SO_4, filtered and concentrated under reduced pressure. Purification by flash chromatography (50% EtOAc/hexane to 20% Et_2O/CH_2Cl_2 to 50% Et_2O/CH_2Cl_2)* to afford 3-diazo-5-nitroindolin-2-one **291** (450 mg, 44%) as a yellow solid. R_f 0.19 (50% EtOAc/hexane); ν_{max} (film)/cm^{-1} 3105 (br s, NH), 2837, 2132 (C=N=N out-of-phase), 1700 (C=O amide), 1614, 1513 (NO_2), 1461, 1379 (C=N=N in-phase), 1342 (NO_2), 1200, 1156, 1088, 883, 820, 768,

738, 675; ^{1}H NMR (400 MHz, $CDCl_3$) δ 11.4 (br s, 1 H, NH), 8.47 (d, J = 2.3 Hz, 1 H, HC_{Ar}), 8.03 (dd, J = 8.7, 2.3 Hz, 1 H, HC_{Ar}), 7.07 (d, J = 8.7 Hz, 1 H, HC_{Ar}); ^{13}C NMR (101 MHz, $CDCl_3$) δ 167.5 (C=O), 141.7 (NO_2C_{Ar} quat), 138.1 (NC_{Ar} quat), 121.5 (C_{Ar}), 118.3 (C_{Ar} quat), 114.9 (C_{Ar}), 109.6 (C_{Ar}), 61.7 (CN_2 quat); HRMS (FTMS – p APCI) *m/z* Calculated for $C_8H_3N_4O_3^-$ $[M–H]^-$ 203.0211; Found 203.0205.

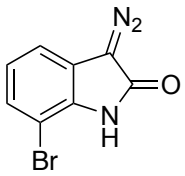
* The crude material was dry loaded with CH_2Cl_2 but did not elute with 50% EtOAc/hexane. The residual CH_2Cl_2 was difficult to remove and **291** was used in the next step with this residual solvent.

6-Bromo-3-diazoindolin-2-one (292)



Tosylhydrazide (1.92 g, 11.0 mmol) in MeOH (10 mL) was heated to 70 ºC to solubilise the hydrazide. The mixture was cooled to rt and 6-bromoisatin (2.26 g, 10.0 mmol) was added. The reaction mixture was stirred at 70 ºC for 10 min, then cooled to rt. The solid was filtered, then transferred to a new reaction flask. H_2O (100 mL) was added, then NaOH (800 mg, 20.0 mmol) was added and the reaction mixture was stirred at 70 ºC for 16 h. The aqueous reaction mixture was extracted with EtOAc (3 × 100 mL) and the combined organic layers were dried over Na_2SO_4, filtered and concentrated under reduced pressure to afford 6-bromo-3-diazoindolin-2-one **292** (1.87 g, 79%) as a red solid which was used without further purification. R_f 0.35 (50% EtOAc/hexane); ν_{max} (film)/cm^{-1} 3120, 2084 (C=N=N out-of-phase), 1681 (C=O), 1599, 1484, 1397 (C=N=N in-phase), 1327, 1208, 1170, 1107, 1055, 995, 910, 861, 801, 742; ^{1}H NMR (400 MHz, DMSO-d_6) δ 10.80 (br s, 1 H, NH), 7.37 (d, J = 8.2 Hz, 1 H, HC_{Ar}), 7.16 (dd, J = 8.2, 1.7 Hz, 1 H, HC_{Ar}), 7.03 (d, J = 1.7 Hz, 1 H, HC_{Ar}); ^{13}C NMR (101 MHz, DMSO-d_6) δ 167.4 (C=O), 133.9 (NC_{Ar} quat), 123.7 (C_{Ar}), 120.8 (C_{Ar}), 117.2 (C_{Ar} quat), 116.5 (C_{Ar} quat), 112.5 (C_{Ar}), 60.5 (CN_2 quat); HRMS (FTMS + pAPCI) *m/z* Calculated for $C_8H_5N_3O^{79}Br^+$ $[M+H]^+$ 237.9611; Found 237.9613.

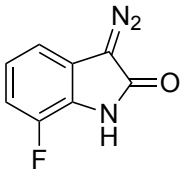
7-Bromo-3-diazoindolin-2-one (293)



Tosylhydrazide (766 mg, 4.4 mmol) in MeOH (4.0 mL) was heated to 70 ºC to solubilise the hydrazide. The mixture was cooled to rt and 7-bromoisatin (904 mg, 4.0 mmol) was added. The reaction mixture was stirred at 70 ºC for 1 h, then cooled to rt. The solid was filtered, then transferred to a new reaction flask. H_2O (40 mL) was added, then NaOH (320 mg, 8.0 mmol) was added and the reaction mixture was stirred at 70 ºC for 16 h. The aqueous reaction mixture was extracted with EtOAc (3 × 100 mL) and the combined organic layers were dried over Na_2SO_4, filtered and concentrated under reduced pressure to afford 7-bromo-3-diazoindolin-2-one **293** (526 mg,

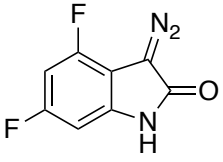
55%) as an orange solid which was used without further purification. R_f 0.48 (50% EtOAc/hexane); ν_{max} (film)/cm^{-1} 3109, 3027, 2982, 2773, 2717, 2076 (C=N=N out-of-phase), 1670 (C=O), 1607, 1439, 1379 (C=N=N in-phase), 1323, 1290, 1226, 1185, 1010, 954, 760, 697; ^{1}H NMR (400 MHz, DMSO-d_6) δ 10.99 (br s, 1 H, NH), 7.45 (d, J = 7.6 Hz, 1 H, HC_{Ar}), 7.28 (dd, J = 8.1, 0.8 Hz, 1 H, HC_{Ar}), 6.96 (t, J = 7.8 Hz, 1 H, HC_{Ar}); ^{13}C NMR (101 MHz, DMSO-d_6) δ 167.3 (C=O), 131.5 (NC_{Ar} quat), 127.5 (C_{Ar}), 122.7 (C_{Ar}), 118.8 (C_{Ar} quat), 118.2 (C_{Ar}), 102.3 (BrC_{Ar} quat), 61.4 (CN_2 quat); HRMS (FTMS + pAPCI) *m/z* Calculated for $C_8H_5N_3O^{79}Br^+$ $[M+H]^+$ 237.9611; Found 237.9608.

3-Diazo-7-fluoroindolin-2-one (294)



Tosylhydrazide (1.92 g, 11.0 mmol) in MeOH (10.0 mL) was heated to 70 ºC to solubilise the hydrazide. The mixture was cooled to rt and 7-fluoroisatin (1.65 g, 10.0 mmol) was added. The reaction mixture was stirred at 70 ºC for 10 min, then cooled to rt. The solid was filtered, then transferred to a new reaction flask. H_2O (100 mL) was added, then NaOH (0.8 g, 20.0 mmol) was added and the reaction mixture was stirred at 70 ºC for 5 h. The aqueous reaction mixture was extracted with EtOAc (3 × 100 mL) and the combined organic layers were dried over Na_2SO_4, filtered and concentrated under reduced pressure to afford 3-diazo-7-fluoroindolin-2-one **294** (912 mg, 51%) as an orange solid which was used without further purification. R_f 0.37 (50% EtOAc/hexane); ν_{max} (film)/cm^{-1} 3123 (br s, NH), 3034, 2993, 2102 (C=N=N out-of-phase), 1636 (C=O), 1599, 1390 (C=N=N in-phase), 1334, 1249, 1215, 1182, 885, 869, 768, 697; ^{1}H NMR (400 MHz, DMSO-d_6) δ 11.19 (br s, 1 H, NH), 7.31–7.26 (m, 1 H, HC_{Ar}), 7.04–6.96 (m, 2 H, 2 × HC_{Ar}); ^{13}C NMR (101 MHz, DMSO-d_6) δ 167.3 (C=O quat), 146.6 (d, J_{C-F} = 241.2 Hz, FC_{Ar} quat), 122.0 (d, J_{C-F} = 6.3 Hz, C_{Ar}), 120.1 (d, J_{C-F} = 6.1 Hz, C_{Ar} quat), 119.6 (d, J_{C-F} = 15.1 Hz, C_{Ar} quat), 115.3 (d, J_{C-F} = 2.9 Hz, C_{Ar}), 111.4 (d, J_{C-F} = 17.3 Hz, C_{Ar}), 61.1 ($C=N_2$ quat); ^{19}F{^{1}H} NMR (377 MHz, DMSO-d_6) δ –133.3; HRMS (FTMS + pAPCI) *m/z* Calculated for $C_8H_5N_3O^+$ $[M+H]^+$ 178.0411; Found 178.0414.

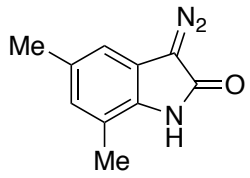
3-Diazo-4,6-difluoroindolin-2-one (295)



Tosylhydrazide (1.92 g, 11.0 mmol) in MeOH (10.0 mL) was heated to 70 ºC to solubilise the hydrazide. The mixture was cooled to rt and 4,6-difluoroisatin (1.83 g, 10.0 mmol) was added. The reaction mixture was stirred at 70 ºC for 10 min, then cooled to rt. The solid was filtered, then transferred to a new reaction flask. H_2O (100 mL) was added, then NaOH (0.8 g, 20.0 mmol) was added and the reaction mixture was stirred at 70 ºC for 1 h. The aqueous reaction mixture was extracted with EtOAc (3 × 100 mL) and the combined organic layers were dried over

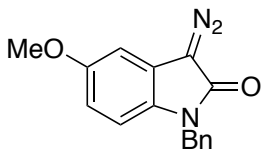
Na_2SO_4, filtered and concentrated under reduced pressure to afford 3-diazo-4,6-difluoroindolin-2-one **295** (1.21 g, 62%) as an orange solid which was used without further purification. R_f 0.40 (60% EtOAc/hexane); ν_{max} (film)/cm^{-1} 3079 (br s, NH), 2851, 2788, 2747, 2099 (C=N=N out-of-phase), 1674 (C=O), 1636, 1607, 1513, 1454, 1402, 1342 (C=N=N in-phase), 1252, 1167, 1118, 1066, 984, 783, 734; ^{1}H NMR (400 MHz, DMSO-d_6) δ 11.10 (br s, 1 H, NH), 6.97–6.89 (m, 1 H, HC_{Ar}), 6.71–6.67 (m, 1 H, HC_{Ar}); ^{13}C NMR (101 MHz, DMSO-d_6) δ 167.4 (C=O), 160.4 (dd, J_{C-F} = 241.9, 12.4 Hz, FC_{Ar} quat), 154.8 (dd, J_{C-F} = 244.2, 14.8 Hz, FC_{Ar} quat), 135.0 (dd, J_{C-F} = 14.3, 10.7 Hz, NC_{Ar} quat), 100.0 (d, J_{C-F} = 19.5 Hz, C_{Ar} quat), 96.7 (dd, J_{C-F} = 27.6, 23.7 Hz, C_{Ar}), 95.1 (d, J_{C-F} = 27.8 Hz, C_{Ar}), 58.4 (CN_2 quat); ^{19}F{^{1}H} NMR (377 MHz, DMSO-d_6) δ –113.2, –122.4; HRMS (ESI$^-$) *m/z* Calculated for $C_8H_2N_3OF_2$ [M–H] 194.0166; Found 194.0172.

3-Diazo-5,7-dimethylindolin-2-one (296)



Tosylhydrazide (1.92 g, 11.0 mmol) in MeOH (10.0 mL) was heated to 70 ºC to solubilise the hydrazide. The mixture was cooled to rt and 5,7-dimethylisatin (1.75 g, 10.0 mmol) was added. The reaction mixture was stirred at 70 ºC for 20 min, then cooled to rt. The solid was filtered, then transferred to a new reaction flask. H_2O (100 mL) was added, then NaOH (0.8 g, 20.0 mmol) was added and the reaction mixture was stirred at 70 ºC for 3 h. The aqueous reaction mixture was extracted with EtOAc (3 × 100 mL) and the combined organic layers were dried over Na_2SO_4, filtered and concentrated under reduced pressure to afford 3-diazo-5,7-dimethylindolin-2-one **296** (1.00 g, 53%) as a dark orange solid which was used without further purification. R_f 0.55 (50% EtOAc/pentane); ν_{max} (film)/cm^{-1} 3124 (NH), 3008, 2907, 2818, 2087 (C=N=N out-of-phase), 1670 (C=O), 1461, 1431, 1379 (C=N=N in-phase), 1327, 1200, 1096, 1036, 962, 895, 772, 705; ^{1}H NMR (400 MHz, DMSO-d_6) δ 10.59 (br s, 1 H, NH), 7.03 (s, 1 H, HC_{Ar}), 6.72 (s, 1 H, HC_{Ar}), 2.23 (s, 1 H, $ArCH_3$), 2.18 (s, 1 H, $ArCH_3$); ^{13}C NMR (101 MHz, DMSO-d_6) δ 168.3 (C=O), 130.2 (C_{Ar} quat), 129.0 (C_{Ar} quat), 127.3 (C_{Ar}), 119.1 (C_{Ar} quat), 117.1 (C_{Ar}), 116.6 (C_{Ar} quat), 60.1 (CN_2 quat), 20.7 ($ArCH_3$), 16.3 ($ArCH_3$); HRMS (ESI$^+$) *m/z* Calculated for $C_{12}H_{13}N_4O$ [M+CH_3CN+H] 229.1089; Found 229.1084.

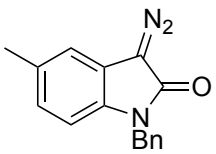
1-Benzyl-3-diazo-5-methoxyindolin-2-one (297)



Benzyl bromide (0.95 mL, 8.0 mmol) was added to a solution of 3-diazo-5-methoxyindolin-2-one **288** (757 mg, 4.0 mmol), K_2CO_3 (2.21 g, 16.0 mmol) and TBAI (300 mg, 0.8 mmol) in MeCN (8.0 mL) at 25 ºC. The reaction mixture was stirred for 19 h at 25 ºC. CH_2Cl_2 (100 mL) was added and the reaction mixture was extracted with sat. aq. $NaHCO_3$ (3 × 100 mL). The

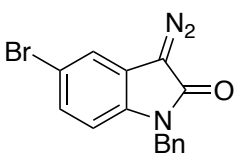
combined organic layers were dried over Na_2SO_4, filtered and concentrated under reduced pressure. Purification by flash chromatography (30% EtOAc/hexane; dry loaded with CH_2Cl_2) afforded 1-benzyl-3-diazo-5-methoxyindolin-2-one **297** (956 mg, 86%) as a pale brown solid. R_f 0.29 (30% EtOAc/hexane); ν_{max} (film)/cm^{-1} 3060, 3029, 3000, 2933, 2833, 2084 (C=N=N out-of-phase), 1670 (C=O), 1591, 1479, 1436, 1389 (C=N=N in-phase), 1353, 1329, 1295, 1284, 1238, 1220, 1197, 1165, 1034, 797, 772, 731; ^{1}H NMR (400 MHz, $CDCl_3$) δ 7.35–7.22 (m, 5 H, 5 × HC_{Ph}), 6.80 (d, J = 2.3 Hz, 1 H, HC_{Ar}), 6.70 (d, J = 8.6 Hz, 1 H, HC_{Ar}), 6.64 (dd, J = 8.6, 2.3 Hz, 1 H, HC_{Ar}), 5.00 (s, 2 H, NCH_2Ph), 3.79 (s, 3 H, OCH_3); ^{13}C NMR (101 MHz, $CDCl_3$) δ 166.6 (C=O), 155.6 (OC_{Ar} quat), 136.0 (C_{Ph} quat), 128.6 (2 × C_{Ph}), 127.52 (C_{Ph}), 127.48 (C_{Ar} quat), 127.2 (2 × C_{Ph}), 117.7 (C_{Ar} quat), 111.0 (C_{Ar}), 110.0 (C_{Ar}), 104.7 (C_{Ar}), 61.2 (CN_2 quat), 55.7 (OCH_3), 44.3 (NCH_2Ph); HRMS (ESI$^+$) *m/z* Calculated for $C_{16}H_{14}N_3O_2$ [M+H] 280.1086; Found 280.1091.

1-Benzyl-3-diazo-5-methylindolin-2-one (298)



Benzyl bromide (0.13 mL, 1.1 mmol) was added to a solution of 3-diazo-5-methylindolin-2-one **289** (173 mg, 1.0 mmol), TBAI (37 mg, 0.1 mmol) and K_2CO_3 (166 mg, 1.2 mmol) in DMF (10 mL) at 0 ºC. The reaction mixture was stirred for 19 h at 25 ºC. Sat. aq. NaCl (100 mL) was added and extracted with EtOAc (2 × 100 mL). The combined organic layers were washed with sat. aq. NaCl (3 × 100 mL), dried over Na_2SO_4, filtered and concentrated under reduced pressure. Purification by flash chromatography (25% Et_2O/pentane) afforded 1-benzyl-3-diazo-5-methylindolin-2-one **298** (223 mg, 85%) as an orange solid. R_f 0.40 (30% Et_2O/pentane); ν_{max} (film)/cm^{-1} 2091 (C=N=N out-of-phase), 1670 (C=O), 1487, 1387 (C=N=N in-phase), 1182, 1122, 801, 719; ^{1}H NMR (400 MHz, $CDCl_3$) δ 7.34–7.23 (m, 5 H, 5 × HC_{Ph}), 7.04–7.03 (m, 1 H, HC_{Ar}), 6.90 (ddd, J = 8.0, 1.6, 0.7 Hz, 1 H, HC_{Ar}), 6.71 (d, J = 8.0 Hz, 1 H, HC_{Ar}), 5.01 (s, 2 H, NCH_2Ph), 2.34 (s, 3 H, $ArCH_3$); ^{13}C NMR (101 MHz, $CDCl_3$) δ 167.0 (C=O), 136.1 (C_{Ar} quat), 131.8 (C_{Ar} quat), 131.5 (C_{Ar} quat),128.7 (2 × C_{Ph}), 127.6 (C_{Ph}), 127.2 (2 × C_{Ph}), 126.0 (C_{Ar}), 118.9 (C_{Ar}), 116.8 (C_{Ar}), 116.8 (C_{Ar} quat), 109.3 (C_{Ar}), 44.3 (NCH_2Ph), 21.1 ($ArCH_3$); HRMS (ESI$^+$) *m/z* Calculated for $C_{16}H_{14}N_3O$ [M+H] 264.1137; Found 264.1135.

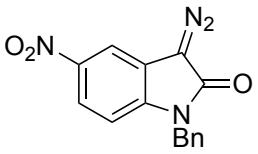
1-Benzyl-5-bromo-3-diazoindolin-2-one (299)



Benzyl bromide (1.19 mL, 10.0 mmol) was added to a solution of 5-bromo-3-diazoindolin-2-one **290** (1.19 g, 5.0 mmol) and K_2CO_3 (2.76 g, 20.0 mmol) in MeCN (10 mL) at 25 ºC. The reaction mixture was stirred for 14 h at 25 ºC. CH_2Cl_2 (100 mL) was added and the reaction mixture was extracted with sat. aq. $NaHCO_3$ (3 × 100 mL). The combined organic layers were dried

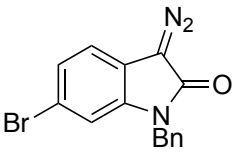
over Na_2SO_4, filtered and concentrated under reduced pressure. Purification by flash chromatography (10% to 20% EtOAc/hexane) afforded 1-benzyl-5-bromo-3-diazoindolin-2-one **299** (1.11 g, 68%) as an orange solid. R_f 0.27 (20% EtOAc/hexane); ν_{max} (film)/cm^{-1} 3030, 3064, 2091 (C=N=N out-of-phase), 1677, 1607, 1476, 1439, 1387 (C=N=N in-phase), 1353, 1170, 1118, 801, 701; ^{1}H NMR (400 MHz, $CDCl_3$) δ 7.35–7.25 (m, 6 H, 5 × HC_{Ph} and HC_{Ar}), 7.19 (dd, J = 8.4, 1.9 Hz, 1 H, HC_{Ar}), 6.67 (d, J = 8.4 Hz, 1 H, HC_{Ar}), 5.01 (s, 2 H, NCH_2Ph); ^{13}C NMR (101 MHz, $CDCl_3$) δ 166.1 (C=O), 135.5 (C_{Ph} quat), 132.5 (NC_{Ar} quat), 128.8 (2 × C_{Ph}), 128.2 (C_{Ar}), 127.8 (C_{Ph}), 127.2 (2 × C_{Ph}), 120.9 (C_{Ar}), 118.7 (C_{Ar} quat), 114.7 (C_{Ar} quat), 110.8 (C_{Ar}), 44.4 (NCH_2Ph); HRMS (FTMS + pAPCI) *m/z* Calculated for $C_{15}H_{11}N_3O^{79}Br^+$ $[M+H]^+$ 328.0080; Found 328.0076.

1-Benzyl-3-diazo-5-nitroindolin-2-one (300)



Benzyl bromide (0.48 mL, 4.0 mmol) was added to a solution of 3-diazo-5-nitroindolin-2-one **291** (408 mg, 2.0 mmol) and K_2CO_3 (553 mg, 4.0 mmol) in MeCN (4.0 mL) at 25 ºC. The reaction mixture was stirred for 14 h at 25 ºC. CH_2Cl_2 (50 mL) was added and the reaction mixture was extracted with H_2O (3 × 50 mL). The combined organic layers were dried over Na_2SO_4, filtered and concentrated under reduced pressure. Purification by flash chromatography (dry loaded with CH_2Cl_2, eluted with 40% to 60% Et_2O/pentane to CH_2Cl_2 then CH_2Cl_2 to 10% Et_2O/CH_2Cl_2) afforded 1-benzyl-3-diazo-5-nitroindolin-2-one **300** (372 mg, 63%) as a yellow solid. R_f 0.15 (30% Et_2O/pentane); ν_{max} (film)/cm^{-1} 3064, 2113 (C=N=N out-of-phase), 1685 (C=O), 1610, 1517, 1484, 1387 (C=N=N in-phase), 1338, 1170, 1092, 734; ^{1}H NMR (400 MHz, $CDCl_3$) δ 8.14 (d, J = 2.2 Hz, 1 H, HC_{Ar}), 8.05 (dd, J = 8.7, 2.2 Hz, 1 H, HC_{Ar}), 7.38–7.26 (m, 5 H, 5 × HC_{Ph}), 6.90 (d, J = 8.7 Hz, 1 H, HC_{Ar}), 5.09 (s, 2 H, NCH_2Ph); ^{13}C NMR (101 MHz, $CDCl_3$) δ 163.1 (C=O quat), 143.0 (O_2NC_{Ar} quat), 138.3 (NC_{Ar} quat), 134.9 (C_{Ph} quat), 129.0 (2 × C_{Ph}), 128.2 (C_{Ph}), 127.3 (2 × C_{Ph}), 122.0 (C_{Ar}), 118.0 (C_{Ar} quat), 113.6 (C_{Ar}), 108.9 (C_{Ar}), 44.7 (NCH_2Ph). The observed characterisation data (IR, ^{1}H and ^{13}C NMR) was consistent with that previously reported in the literature.[430]

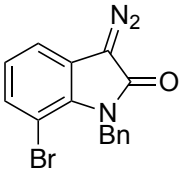
1-Benzyl-6-bromo-3-diazoindolin-2-one (301)



Benzyl bromide (1.19 mL, 10.0 mmol) was added to a solution of 6-bromo-3-diazoindolin-2-one **292** (1.19 g, 5.0 mmol) and K_2CO_3 (2.76 g, 20.0 mmol) in MeCN (10 mL) at 25 ºC. The reaction mixture was stirred for 14 h at 25 ºC. CH_2Cl_2 (100 mL) was added and the reaction mixture was extracted with sat. aq. $NaHCO_3$ (3 × 100 mL). The organic layers were dried over Na_2SO_4, filtered and concentrated under reduced pressure. Purification by flash chromatography (20%

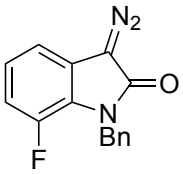
to 30% Et_2O/pentane) afforded 1-benzyl-6-bromo-3-diazoindolin-2-one **301** (1.45 g, 88%) as an orange solid. R_f 0.37 (30% Et_2O/pentane); ν_{max} (film)/cm^{-1} 3064, 3030, 2087 (C=N=N out-of-phase), 1677 (C=O), 1603, 1580, 1476, 1394 (C=N=N in-phase), 1349, 1256, 1170, 1115, 1062, 910, 861, 798, 731; ^{1}H NMR (400 MHz, $CDCl_3$) δ 7.37–7.26 (m, 5 H, 5 × HC_{Ph}), 7.18 (dd, J = 8.1, 1.7 Hz, 1 H, HC_{Ar}), 7.05 (d, J = 8.1 Hz, 1 H, HC_{Ar}), 6.97 (d, J = 1.7 Hz, 1 H, HC_{Ar}), 4.99 (s, 2 H, NCH_2Ph); ^{13}C NMR (101 MHz, $CDCl_3$) δ 166.4 (C=O quat), 135.4 (C_{Ph} quat), 134.6 (NC_{Ar} quat), 128.8 (2 × C_{Ph}), 127.8 (C_{Ph}), 127.2 (2 × C_{Ph}), 124.9 (C_{Ar}), 119.1 (C_{Ar}), 118.5 (C_{Ar} quat), 115.5 (C_{Ar} quat), 112.6 (C_{Ar}), 60.9 (CN_2 quat), 44.3 (NCH_2Ph); HRMS (ESI$^+$) *m/z* Calculated for $C_{15}H_{11}N_3O^{79}Br$ [M+H]$^+$ 328.0080; Found 328.0081.

1-Benzyl-7-bromo-3-diazoindolin-2-one (302)



Benzyl bromide (0.33 mL, 2.8 mmol) was added to a solution of 7-bromo-3-diazoindolin-2-one **293** (340 mg, 1.4 mmol) and K_2CO_3 (773 mg, 5.6 mmol) in MeCN (3.0 mL) at 25 ºC. The reaction mixture was stirred for 16 h at 25 ºC. CH_2Cl_2 (50 mL) was added and the reaction mixture was extracted with sat. aq. $NaHCO_3$ (3 × 50 mL). The organic layers were dried over Na_2SO_4, filtered and concentrated under reduced pressure. Purification by flash chromatography (20% to 30% Et_2O/pentane) afforded 1-benzyl-7-bromo-3-diazoindolin-2-one **302** (390 mg, 85%) as a dark orange solid. R_f 0.43 (30% Et_2O/pentane); ν_{max} (film)/cm^{-1} 3064, 3030, 2094 (C=N=N out-of-phase), 1685 (C=O), 1446, 1394 (C=N=N in-phase), 1334, 1156, 1126, 772, 719; ^{1}H NMR (400 MHz, $CDCl_3$) δ 7.34–7.14 (m, 7 H, 5 × HC_{Ph} and 2 × HC_{Ar}), 6.95 (t, J = 7.8 Hz, 1 H, HC_{Ar}), 5.53 (s, 2 H, NCH_2Ph); ^{13}C NMR (101 MHz, $CDCl_3$) δ 167.0 (C=O), 137.6 (C_{Ph} quat), 130.94 (NC_{Ar} quat), 130.89 (C_{Ar}), 128.5 (2 × C_{Ph}), 127.1 (C_{Ph}), 126.3 (2 × C_{Ph}), 123.2 (C_{Ar}), 119.6 (C_{Ar} quat), 117.1 (C_{Ar}), 103.3 (BrC_{Ar} quat), 45.0 (NCH_2Ph). The observed characterisation data (^{1}H NMR) was consistent with that previously reported in the literature.[434]

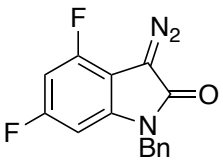
1-Benzyl-3-diazo-7-fluoroindolin-2-one (303)



Benzyl bromide (0.71 mL, 6.0 mmol) was added to a solution of 3-diazo-7-fluoroindolin-2-one **294** (531 mg, 3.0 mmol), K_2CO_3 (1.66 g, 12.0 mmol) and TBAI (222 mg, 0.6 mmol) in MeCN (6.0 mL) at 25 ºC. The reaction mixture was stirred for 19 h at 25 ºC. CH_2Cl_2 (100 mL) was added and the reaction mixture was extracted with sat. aq. $NaHCO_3$ (3 × 100 mL). The combined organic layers were dried over Na_2SO_4, filtered and concentrated under reduced pressure. Purification by flash chromatography (30% Et_2O/pentane) afforded 1-benzyl-3-diazo-7-fluoroindolin-2-one **303** (557 mg, 70%) as an orange solid. R_f 0.28 (30% Et_2O/pentane); ν_{max} (film)/cm^{-1} 3064, 3034, 2091 (C=N=N out-of-phase), 1685 (C=O), 1625, 1592, 1491, 1469, 1394 (C=N=N in-phase),

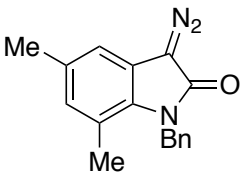
1334, 1241, 1156, 768, 716; ^{1}H NMR (400 MHz, $CDCl_3$) δ 7.39–7.24 (m, 5 H, 5 × HC_{Ph}), 7.03–6.96 (m, 2 H, 2 × HC_{Ar}), 6.90–6.84 (m, 1 H, HC_{Ar}), 5.17 (s, 2 H, NCH_2Ph); ^{13}C NMR (101 MHz, $CDCl_3$) δ 166.2 (C=O quat), 147.8 (d, J_{C-F} = 244.0 Hz, FC_{Ar} quat), 137.1 (C_{Ph} quat), 128.6 (2 × C_{Ph}), 127.6 (C_{Ph}), 127.5 (2 × C_{Ph}), 122.7 (d, J_{C-F} = 7.1 Hz, C_{Ar}), 120.5 (d, J_{C-F} = 11.4 Hz, NC_{Ar} quat), 119.5 (d, J_{C-F} = 5.5 Hz, C_{Ar} quat), 114.1 (d, J_{C-F} = 2.9 Hz, C_{Ar}), 112.8 (d, J_{C-F} = 19.6 Hz, C_{Ar}), 46.0 (d, J_{C-F} = 4.7 Hz, NCH_2Ph); ^{19}F{^{1}H} NMR (377 MHz, $CDCl_3$) δ –133.2. The observed characterisation data (IR, ^{1}H, ^{13}C and ^{19}F NMR) was consistent with that previously reported in the literature.[434]

1-Benzyl-3-diazo-4,6-difluoroindolin-2-one (304)



Benzyl bromide (0.95 mL, 8.0 mmol) was added to a solution of 3-diazo-4,6-difluoroindolin-2-one **295** (780 mg, 4.0 mmol), K_2CO_3 (2.21 g, 16.0 mmol) and TBAI (300 mg, 0.8 mmol) in MeCN (8.0 mL) at 25 ºC. The reaction mixture was stirred for 19 h at 25 ºC. CH_2Cl_2 (100 mL) was added and the reaction mixture was extracted with sat. aq. $NaHCO_3$ (3 × 100 mL). The combined organic layers were dried over Na_2SO_4, filtered and concentrated under reduced pressure. Purification by flash chromatography (10% EtOAc/hexane) afforded 1-benzyl-3-diazo-4,6-difluoroindolin-2-one **304** (907 mg, 79%) as an orange solid. R_f 0.20 (10% EtOAc/hexane); ν_{max} (film)/cm^{-1} 3086, 3066, 3031, 2925, 2093 (C=N=N out-of-phase), 1687 (C=O), 1643, 1599, 1498, 1461, 1437, 1402, 1388 (C=N=N in-phase), 1356, 1319, 1297, 1216, 1180, 1073, 1094, 1073, 1029, 955, 929, 824, 730, 696, 669; ^{1}H NMR (400 MHz, $CDCl_3$) δ 7.37–7.26 (m, 5 H, 5 × HC_{Ph}), 6.60–6.50 (m, 1 H, HC_{Ar}), 6.45–6.41 (m, 1 H, HC_{Ar}), 4.99 (s, 2 H, NCH_2Ph); ^{13}C NMR (101 MHz, $CDCl_3$) δ 166.7 (C=O), 162.2 (dd, J_{C-F} = 245.3, 12.0 Hz, FC_{Ar} quat), 155.2 (dd, J_{C-F} = 246.7, 14.2 Hz, FC_{Ar} quat), 135.5 (dd, J_{C-F} = 13.2, 10.4 Hz, NC_{Ar} quat), 135.1 (C_{Ph} quat), 128.9 (2 × C_{Ph}), 128.0 (C_{Ph}), 127.2 (2 × C_{Ph}), 99.4 (dd, J_{C-F} = 20.0, 3.0 Hz, C_{Ar} quat), 97.6 (dd, J_{C-F} = 27.5, 23.1 Hz, C_{Ar}), 94.7 (dd, J_{C-F} = 28.2, 3.5 Hz, C_{Ar}), 59.1 (CN_2 quat), 44.7 (NCH_2Ph); ^{19}F{^{1}H} NMR (377 MHz, $CDCl_3$) δ –111.96 (d, J_{F-F} = 4.5 Hz), –121.68 (d, J_{F-F} = 4.5 Hz); HRMS (ESI$^+$) *m/z* Calculated for $C_{15}H_{10}N_3OF_2$ [M+H] 286.0792; Found 286.0804.

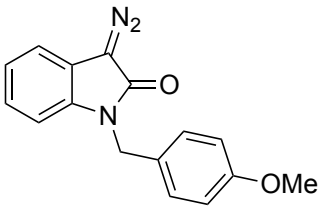
1-Benzyl-3-diazo-5,7-dimethylindolin-2-one (305)



Benzyl bromide (0.95 mL, 8.0 mmol) was added to a solution of 3-diazo-5,7-dimethylindolin-2-one **296** (749 mg, 4.0 mmol), K_2CO_3 (2.21 g, 16.0 mmol) and TBAI (300 mg, 0.8 mmol) in MeCN (8.0 mL) at 25 ºC. The reaction mixture was stirred for 19 h at 25 ºC. CH_2Cl_2 (100 mL) was added and the reaction mixture was extracted with sat. aq. $NaHCO_3$ (3 × 100 mL). The combined organic layers were dried over Na_2SO_4, filtered and concentrated under reduced

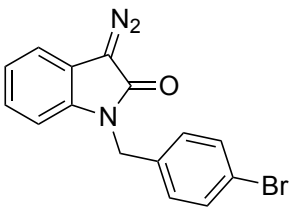
pressure. Purification by flash chromatography (10% to 15% EtOAc/hexane; dry loaded with CH_2Cl_2) afforded 1-benzyl-3-diazo-5,7-dimethylindolin-2-one **305** (899 mg, 81%) as an orange solid. R_f 0.13 (10% EtOAc/hexane); ν_{max} (film)/cm^{-1} 3062, 3029, 2919, 2864, 2085 (C=N=N out-of-phase), 1677 (C=O), 1592, 1470, 1446, 1418, 1392, 1380, 1347 (C=N=N in-phase), 1331, 1154, 11234, 842, 722, 697; ^{1}H NMR (400 MHz, $CDCl_3$) δ 7.33–7.28 (m, 2 H, 2 × HC_{Ph}), 7.26–7.21 (m, 1 H, HC_{Ph}), 7.14–7.11 (m, 2 H, 2 × HC_{Ph}), 6.91 (s, 1 H, HC_{Ar}), 6.68 (s, 1 H, HC_{Ar}), 5.29 (s, 2 H, NCH_2Ph), 2.32 (s, 3 H, $ArCH_3$), 2.27 (s, 3 H, $ArCH_3$); ^{13}C NMR (101 MHz, $CDCl_3$) δ 167.7 (C=O), 137.9 (C_{Ar} quat), 131.8 (C_{Ar} quat), 130.1 (C_{Ar}), 129.7 (C_{Ar} quat), 128.8 (2 × C_{Ph}), 127.1 (C_{Ph}), 125.6 (2 × C_{Ph}), 120.4 (C_{Ar} quat), 117.2 (C_{Ar} quat), 116.8 (C_{Ar}), 45.5 (NCH_2Ph), 28.8 ($ArCH_3$), 18.7 ($ArCH_3$). The observed characterisation data (IR, ^{1}H and ^{13}C NMR) was consistent with that previously reported in the literature.[430]

3-Diazo-1-(4-methoxybenzyl)indolin-2-one (306)



1-(Bromomethyl)-4-methoxybenzene (0.63 mL, 4.4 mmol) was added dropwise to a solution of 3-diazoindolin-2-one **277** (637 mg, 4.0 mmol), TBAI (148 mg, 0.4 mmol) and K_2CO_3 (663 mg, 4.8 mmol) in DMF (40 mL) at 0 ºC. The reaction mixture was stirred for 15 h at 25 ºC. Sat. aq. NaCl (50 mL) was added and extracted with EtOAc (3 × 50 mL). The combined organic layers were washed with sat. aq. NaCl (2 × 50 mL), dried over Na_2SO_4, filtered and concentrated under reduced pressure. Purification by flash chromatography (30% EtOAc/hexane) afforded 3-Diazo-1-(4-methoxybenzyl)indolin-2-one **306** (494 mg, 59%) as an orange solid. R_f 0.36 (30% EtOAc/hexane); ν_{max} (film)/cm^{-1} 3056, 2997, 2933, 2833, 2084 (C=N=N out-of-phase), 1674 (C=O), 1610, 1513, 1465, 1398, 1338, 1301, 1245, 1200, 1167, 1103, 1029, 842, 809, 738; ^{1}H NMR (400 MHz, $CDCl_3$) δ 7.26 (d, J = 8.7 Hz, 2 H, 2 × HC_{Ar}), 7.20–7.17 (m, 1 H, HC_{Ar}), 7.10 (td, J = 7.6, 1.4 Hz, 1 H, HC_{Ar}), 7.05 (td, J = 7.6, 1.2 Hz, 1 H, HC_{Ar}), 6.88 – 6.82 (m, 3 H, 3 × HC_{Ar}), 4.95 (s, 2 H, NCH_2Ar), 3.76 (s, 3 H, OCH_3); ^{13}C NMR (101 MHz, $CDCl_3$) δ 166.7 (C=O), 158.9 (OC_{Ar} quat), 133.5 (NC_{Ar} quat), 128.6 (2 × C_{Ar}), 128.0 (C_{Ar} quat), 125.3 (C_{Ar}), 122.0 (C_{Ar}), 118.1 (C_{Ar}), 116.6 (C_{Ar} quat), 114.0 (2 × C_{Ar}), 109.4 (C_{Ar}), 60.7 (CN_2 quat), 55.1 (OCH_3), 43.6 (NCH_2Ar). The observed characterisation data (IR, ^{1}H and ^{13}C NMR) was consistent with that previously reported in the literature.[435]

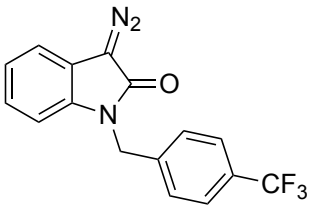
1-(4-Bromobenzyl)-3-diazoindolin-2-one (307)



1-Bromo-4-(bromomethyl)benzene (2.00 g, 8.0 mmol) was added dropwise to a solution of 3-diazoindolin-2-one **277** (636 mg, 4.0 mmol), TBAI (309 mg, 0.4 mmol) and K_2CO_3 (2.24 g, 16.0 mmol) in MeCN (8.0 mL) at 25 ºC. The reaction mixture was stirred for 19 h

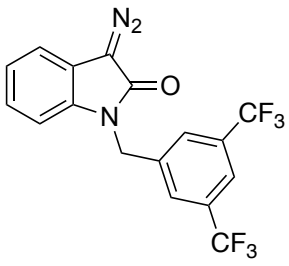
at 25 ºC. CH_2Cl_2 (50 mL) was added and the reaction mixture was extracted with sat. aq. $NaHCO_3$ (3 × 50 mL). The combined organic layers were dried over Na_2SO_4, filtered and concentrated under reduced pressure. Purification by flash chromatography (10% to 20% EtOAc/hexane) afforded 1-(4-Bromobenzyl)-3-diazoindolin-2-one **307** (1.13 g, 86%) as an orange solid. R_f 0.30 (20% EtOAc/hexane); ν_{max} (film)/cm^{-1} 3056, 2930, 2084 (C=N=N out-of-phase), 1674 (C=O), 1607, 1484, 1435, 1398, 1338 (C=N=N in-phase), 1204, 1163, 1103, 1070, 1010, 850; ^{1}H NMR (400 MHz, $CDCl_3$) δ 7.44 (d, J = 8.4 Hz, 2 H, 2 × HC_{Ar}), 7.23–7.16 (m, 3 H, 3 × HC_{Ar}), 7.15–7.05 (m, 2 H, 2 × HC_{Ar}), 6.81–6.78 (m, 1 H, HC_{Ar}), 4.97 (s, 2 H, NCH_2Ar); ^{13}C NMR (101 MHz, $CDCl_3$) δ 166.7 (C=O), 135.0 (C_{Ar} quat), 133.3 (C_{Ar} quat), 131.8 (2 × C_{Ar}), 129.0 (2 × C_{Ar}), 125.4 (C_{Ar}), 122.3 (C_{Ar}), 121.6 (C_{Ar} quat), 118.3 (C_{Ar}), 116.7 (C_{Ar} quat), 109.3 (C_{Ar}), 60.8 (CN_2 quat), 43.6 (NCH_2Ar). The observed characterisation data (IR, ^{1}H and ^{13}C NMR) was consistent with that previously reported in the literature.[436]

3-Diazo-1-(4-(trifluoromethyl)benzyl)indolin-2-one (308)



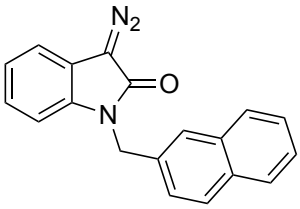
1-(Bromomethyl)-4-(trifluoromethyl)benzene (1.31 g, 5.5 mmol) was added to a solution of 3-diazoindolin-2-one **277** (796 mg, 5.0 mmol), TBAI (185 mg, 0.5 mmol) and K_2CO_3 (829 mg, 6.0 mmol) in DMF (50 mL) at 0 ºC. The reaction mixture was stirred for 15 h at 25 ºC. Sat. aq. NaCl (100 mL) was added and extracted with EtOAc (3 × 100 mL). The combined organic layers were washed with sat. aq. NaCl (2 × 100 mL), dried over Na_2SO_4, filtered and concentrated under reduced pressure. Purification by flash chromatography (20% EtOAc/hexane) afforded 3-diazo-1-(4-(trifluoromethyl)benzyl)indolin-2-one **308** (1.45 g, 91%) as an orange solid. R_f 0.38 (30% EtOAc/hexane); ν_{max} (film)/cm^{-1} 2095 (C=N=N out-of-phase), 1670 (C=O), 1607, 1469, 1402, 1066, 1156, 1103, 1066, 947, 854, 746, 686; ^{1}H NMR (400 MHz, $CDCl_3$) δ 7.59 (d, J = 8.1 Hz, 2 H, 2 × HC_{Ar}), 7.42 (d, J = 8.1 Hz, 2 H, 2 × HC_{Ar}), 7.26–7.23 (m, 1 H, HC_{Ar}), 7.15–7.07 (m, 2 H, 2 × HC_{Ar}), 6.81–6.77 (m, 1 H, HC_{Ar}), 5.09 (s, 2 H, NCH_2Ar); ^{13}C NMR (101 MHz, $CDCl_3$) δ 166.8 (C=O), 140.0 (C_{Ar} quat), 133.3 (C_{Ar} quat), 130.0 (q, $J_{C–F}$ = 33 Hz, $C_{Ar}CF_3$ quat), 127.5 (2 × C_{Ar}), 125.8 (q, $J_{C–F}$ = 4 Hz, 2 × C_{Ar}), 125.5 (C_{Ar}), 124.0 (q, $J_{C–F}$ = 273 Hz, CF_3), 122.5 (C_{Ar}), 118.4 (C_{Ar}), 116.8 (C_{Ar} quat), 109.3 (C_{Ar}), 43.8 (NCH_2Ar); ^{19}F{^{1}H} NMR (377 MHz, $CDCl_3$) δ –62.6; HRMS (ESI$^+$) *m/z* Calculated for $C_{16}H_{11}N_3OF_3$ [M+H] 318.0854; Found 318.0854.

1-(3,5-Bis(trifluoromethyl)benzyl)-3-diazoindolin-2-one (309)



1-(Bromomethyl)-3,5-bis(trifluoromethyl)benzene (0.81 mL, 4.4 mmol) was added to a solution of 3-diazoindolin-2-one **277** (637 mg, 4.0 mmol), TBAI (148 mg, 0.4 mmol) and K_2CO_3 (663mg, 4.8 mmol) in DMF (40 mL) at 0 ºC. The reaction mixture was stirred for 15 h at 25 ºC. Sat. aq. NaCl (100 mL) was added and extracted with EtOAc (3 × 100 mL). The combined organic layers were washed with sat. aq. NaCl (3 × 100 mL), dried over Na_2SO_4, filtered and concentrated under reduced pressure. Purification by flash chromatography (30% EtOAc/hexane) afforded 1-(3,5-bis(trifluoromethyl)benzyl)-3-diazoindolin-2-one **309** (1.42 g, 92%) as an orange solid. R_f 0.32 (40% EtOAc/hexane); ν_{max} (film)/cm^{-1} 2084 (C=N=N out-of-phase), 1696 (C=O), 1379 (C=N=N in-phase), 1342, 1275, 1163, 1126, 1044, 1010, 962, 846, 734, 705; ^{1}H NMR (400 MHz, $CDCl_3$) δ 7.81 (s, 1 H, HC_{Ar}), 7.75 (s, 2 H, 2 × HC_{Ar}), 7.28–7.25 (m, 1 H, HC_{Ar}), 7.18–7.11 (m, 2 H, 2 × HC_{Ar}), 6.80–6.77 (m, 1 H, HC_{Ar}), 5.13 (s, 2 H, NCH_2Ar); ^{13}C NMR (101 MHz, $CDCl_3$) δ 166.7 (C=O), 138.8 (C_{Ar} quat), 132.9 (C_{Ar} quat), 132.2 (q, J_{C-F} = 33.4 Hz, 2 × CF_3C_{Ar} quat), 127.4 (q, J_{C-F} = 3.6 Hz, 2 × C_{Ar}), 125.6 (C_{Ar}), 123.2 (q, J_{C-F} = 272.9 Hz, 2 × CF_3 quat), 122.7 (C_{Ar}), 121.9 (m, C_{Ar}), 118.6 (C_{Ar}), 116.8 (C_{Ar} quat), 108.9 (C_{Ar}), 61.1 (CN_2 quat), 43.5 (NCH_2Ar); ^{19}F{^{1}H} NMR (377 MHz, $CDCl_3$) δ –62.8; HRMS (FTMS + p APCI) *m/z* Calculated for $C_{17}H_{10}N_3OF_6$ $[M+H]^+$ 386.0723; Found 386.0718.

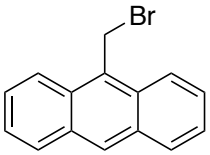
3-Diazo-1-(naphthalen-2-ylmethyl)indolin-2-one (310)



2-Bromonapthalene (243 mg, 1.1 mmol) in DMF (2 mL) was added to a solution of 3-diazoindolin-2-one **277** (478 mg, 3.0 mmol), K_2CO_3 (829 mg, 6.0 mmol) in MeCN (6.0 mL) at 25 ºC. The reaction mixture was stirred for 16 h then CH_2Cl_2 (50 mL) was added and the organic layer was extracted with H_2O (3 × 50 mL). The combined organic layers were dried over Na_2SO_4, filtered and concentrated under reduced pressure. Purification by flash chromatography (30% to 40% Et_2O/pentane) afforded 3-diazo-1-(naphthalen-2-ylmethyl)indolin-2-one **310** (593 mg, 66%) as an orange-red solid. R_f 0.13 (30% Et_2O/hexane); ν_{max} (film)/cm^{-1} 3054, 2085 (C=N=N out-of-phase), 1672 (C=O), 1608, 1467, 1375 (C=N=N in-phase), 1337, 1166, 1102, 740; ^{1}H NMR (400 MHz, $CDCl_3$) δ 7.84–7.75 (m, 4 H, 4 × HC_{Ar}), 7.51–7.43 (m, 3 H, 3 × HC_{Ar}), 7.24–7.19 (m, 1 H, HC_{Ar}), 7.10–7.03 (m, 2 H, 2 × HC_{Ar}), 6.90–6.85 (m, 1 H, HC_{Ar}), 5.20 (s, 2 H, NCH_2Ar); ^{13}C NMR (101 MHz, $CDCl_3$) δ 166.9 (C=O), 133.6 (NC_{Ar} quat), 133.5 (C_{Ar} quat), 133.2 (C_{Ar} quat), 132.8 (C_{Ar} quat), 128.7 (C_{Ar}), 127.72 (C_{Ar}), 127.66 (C_{Ar}), 126.3 (C_{Ar}), 126.1 (C_{Ar}), 126.0 (C_{Ar}), 125.4 (C_{Ar}), 125.2 (C_{Ar}), 122.2 (C_{Ar}), 118.2

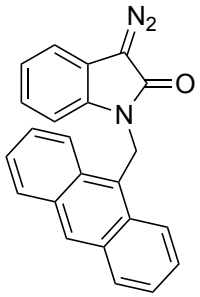
(C_{Ar}), 116.7 (C_{Ar} quat), 109.6 (C_{Ar}), 44.5 (NCH_2Ar); HRMS (ESI^+) *m/z* Calculated for $C_{19}H_{14}N_3O$ [M+H] 300.1137; Found 300.1132.

9-(Bromomethyl)anthracene (S2)[437]



PBr_3 (1.12 mL, 12.0 mmol) was added to a stirred solution of 9-hydroxymethylanthracene (2.08 g, 10.0 mmol) in toluene (50 mL) at 0 ºC. The reaction mixture was stirred at 0 ºC for 1 h, then the temperature was raised to 25 ºC and stirred for 2 h. The reaction mixture was washed with H_2O (50 mL), sat. brine (50 mL), dried over Na_2SO_4, filtered and concentrated under reduced pressure until a yellow solid started to precipitate. Cold hexane (10 mL) was added and mixture was filtered, washing with cold hexane (100 mL). Removal of the solvent under reduced pressure afforded 9-(bromomethyl)anthracene **S2** (1.98 g, 73%) as a yellow solid. R_f 0.27 (30% EtOAc/hexane); mp = 143–145 ºC (lit. = 140–142 ºC)[438]; ν_{max} (film)/cm^{-1} 3029, 3051, 1195, 882, 837, 786, 691, 727; ^1H NMR (400 MHz, $CDCl_3$) δ 8.52 (s, 1 H, HC_{Ar}), 8.32 (d, *J* = 8.9 Hz, 2 H, 2 × HC_{Ar}), 8.06 (d, *J* = 8.5 Hz, 2 H, 2 × HC_{Ar}), 7.69–7.64 (m, 2 H, 2 × HC_{Ar}), 7.56–7.50 (m, 2 H, 2 × HC_{Ar}), 5.57 (s, 2 H, CH_2Br); ^{13}C NMR (101 MHz, $CDCl_3$) δ 131.6 (2 × C_{Ar} quat), 129.7 (2 × C_{Ar} quat), 129.3 (2 × C_{Ar}), 129.2 (C_{Ar}), 127.9 (C_{Ar} quat), 126.8 (2 × C_{Ar}), 125.4 (2 × C_{Ar}), 123.5 (2 × C_{Ar}), 26.9 (CH_2Br). The observed characterisation data (^1H and ^{13}C NMR) was consistent with that previously reported in the literature.[437]

1-(Anthracen-9-ylmethyl)-3-diazoindolin-2-one (311)

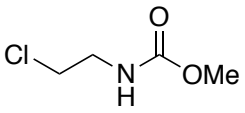


3-Diazoindolin-2-one **277** (478 mg, 3.0 mmol) in DMF (5.0 mL) was added to a solution of 9-(bromomethyl)anthracene **S2** (895 mg, 3.3 mmol), K_2CO_3 (1.2 equiv) and TBAI (111 mg, 0.3 mmol) in DMF (10.0 mmol) at 25 ºC. The reaction mixture was stirred for 22 h then brine (100 mL) was added followed by EtOAc (100 mL) and the layers were separated. The aqueous layer was extracted with EtOAc (2 × 100 mL). The combined organic layers were washed with brine (100 mL), dried over Na_2SO_4, filtered and concentrated under reduced pressure. Purification by flash chromatography (10% to 20% EtOAc/hexane) afforded 1-(anthracen-9-ylmethyl)-3-diazoindolin-2-one **311** (529 mg, 50%) as a pale orange solid. R_f 0.30 (20% EtOAc/hexane); ν_{max} (film)/cm^{-1} 3053, 2084 (C=N=N out-of-phase), 1665 (C=O), 1590, 1479, 1467, 1398, 1381 (C=N=N in-phase), 1347, 1332, 1156, 906, 889, 784, 721; ^1H NMR (400 MHz, $CDCl_3$) δ 8.54–8.47 (m, 3 H, 3 × HC_{Ar}), 8.06–8.02 (m, 2 H, 2 × HC_{Ar}), 7.65–7.60 (m, 2 H, 2 × HC_{Ar}), 7.54–7.49 (m, 2 H, 2 × HC_{Ar}), 7.06–7.03 (m, 1 H, HC_{Ar}), 6.84 (td, *J* = 7.6, 0.9 Hz, 1 H, HC_{Ar}), 6.65 (td, *J* = 8.0, 1.1 Hz, 1 H, HC_{Ar}), 6.34 (d, *J* = 8.0 Hz, 1 H, HC_{Ar}), 6.01 (s, 2 H, NCH_2Ar); ^{13}C NMR (101 MHz, $CDCl_3$) δ 166.8 (C=O), 133.9 (NC_{Ar} quat), 131.3 (2

× C_{Ar} quat), 130.8 (2 × C_{Ar} quat), 129.5 (2 × C_{Ar}), 129.0 (C_{Ar}), 126.9 (2 × C_{Ar}), 126.0 (C_{Ar} quat), 125.2 (C_{Ar}), 125.0 (2 × C_{Ar}), 123.7 (2 × C_{Ar}), 121.7 (C_{Ar}), 117.9 (C_{Ar}), 116.6 (C_{Ar} quat), 110.6 (C_{Ar}), 60.9 (CN_2 quat), 38.1 (NCH_2Ph); HRMS (ESI^+) *m/z* Calculated for $C_{23}H_{16}N_3O$ [M+H] 350.1293; Found 350.1305.

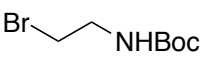
6.2.3.2 Synthesis of Additional Protected Amine Starting Materials

Methyl (2-chloroethyl)carbamate (331)



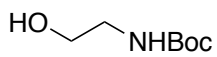
Methyl chloroformate (0.77 mL, 10.0 mmol) was added dropwise to a solution of 2-chloroethylamine hydrochloride (1.28 g, 11.0 mmol) and triethylamine (3.1 mL, 22.0 mmol) in CH_2Cl_2 (50 mL) at 0 ºC. The reaction mixture was stirred for 17 h at 25 ºC, then sat. aq. NH_4Cl (50 mL) was added and the aqueous reaction mixture was extracted with CH_2Cl_2 (3 × 50 mL). The combined organic layers were dried over Na_2SO_4, filtered and concentrated under reduced pressure. Purification by flash chromatography (30% Et_2O/pentane) afforded methyl (2-chloroethyl)carbamate **331** (881 mg, 64%) as a colourless oil. R_f 0.14 (20% Et_2O/pentane); ν_{max} (film)/cm^{-1} 3332 (br s, NH), 2958, 1696 (C=O carbamate), 1523, 1437, 1247, 1194, 1067, 1010, 779; ^{1}H NMR (400 MHz, $CDCl_3$) δ 5.23 and 5.08 (2 × br s, 1 H, NH), 3.75–3.65 (br s, 3 H, OCH_3), 3.60 (br t, J = 5.6 Hz, 2 H, CH_2Cl), 3.51 (br q, J = 5.6 Hz, 2 H, NCH_2); ^{1}H NMR (400 MHz, DMSO-d_6) δ 7.40 and 7.05 (2 × br s, 1 H, NH), 3.58 (t, J = 6.3 Hz, 2 H, CH_2Cl), 3.53 (s, 3 H, OCH_3), 3.29 (q, J = 6.1 Hz, 2 H, NCH_2); ^{13}C NMR (101 MHz, $CDCl_3$) δ 156.9 (C=O), 52.3 (OCH_3), 44.0 (NCH_2), 42.8 (CH_2Cl); ^{13}C NMR (101 MHz, DMSO-d_6) δ 156.7 (C=O), 51.4 (OCH_3), 43.4 (NCH_2), 42.3 (CH_2Cl). The observed characterisation data (IR and ^{1}H NMR in DMSO-d_6) was consistent with that previously reported in the literature.[439]

***tert*-Butyl (2-bromoethyl)carbamate (332)**



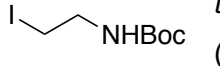
Triethylamine (2.09 mL, 15.0 mmol) was added dropwise to a stirred mixture of 2-bromoethylamine hydrobromide (2.25 g, 11.0 mmol) in CH_2Cl_2 (80 mL), and was subsequently cooled to 0 ºC. Di-*tert*-butyl dicarbonate (2.18 g, 10.0 mmol) was added portionwise, then the solution was warmed to 25 ºC for 18 g. Sat. aq. NH_4Cl (100 mL) and CH_2Cl_2 (100 mL) were added and the layers were separated. The organic layer was washed. with sat. aq. NH_4Cl (100 mL) then sat. aq. $NaHCO_3$ (2 × 100 mL) and sat. aq. brine (2 × 100 mL), dried over Na_2SO_4, filtered and concentrated under reduced pressure. Purification by flash chromatography (0 to 20% EtOAc/hexane) afforded *tert*-butyl (2-bromoethyl)carbamate **332** (1.43 g, 64%) as a white solid with a low melting point. R_f 0.16 (10% EtOAc/hexane); ν_{max} (film)/cm^{-1} 3347 (br s, NH), 2976, 1687 (C=O), 1508, 1365, 1269, 1248, 1159; ^{1}H NMR (400 MHz, $CDCl_3$) δ 5.16 (br s, 1 H, NH), 3.50–3.35 (m, 4 H, NCH_2CH_2), 1.38 (s, 9 H, $C(CH_3)_3$); ^{13}C NMR (101 MHz, $CDCl_3$) δ 155.5 (C=O), 79.5 ($C(CH_3)_3$), 42.2 (NCH_2), 32.4 (CH_2Br), 28.2 ($C(CH_3)_3$). The observed characterisation data (IR, ^{1}H and ^{13}C NMR) was consistent with that previously reported in the literature.[440]

***tert*-Butyl (2-hydroxyethyl)carbamate (S3)**



Ethanolamine (3.02 mL, 50.0 mmol) was added to a solution of di-*tert*-butyl dicarbonate (12.0 g, 55.0 mmol) in CH_2Cl_2 (100 mL) at 0 ºC. The reaction mixture was stirred at 25 ºC for 16 h then CH_2Cl_2 (100 mL) and sat. aq. $NaHCO_3$ (100 mL) were added and the layers separated. The organic layer was washed with sat. aq. $NaHCO_3$ (2 × 100 mL), dried over Na_2SO_4 and concentrated under reduced pressure to afford *tert*-butyl (2-hydroxyethyl)carbamate **S3** (6.11 g, 76%) as a colourless oil which was used without further purification. R_f 0.16 (60% EtOAc/hexane); ν_{max} (film)/cm^{-1} 3355 (br s, NH), 2976, 2934, 1685 (C=O), 1509, 1457, 1366, 1274, 1249, 1165, 1118, 1064, 1000, 971, 865, 779; ^{1}H NMR (400 MHz, $CDCl_3$) δ 5.17 (br s, 1 H, NH), 3.69–3.62 (m, 2 H, OCH_2), 3.29–3.20 (m, 3 H, NCH_2 and OH), 1.42 (s, 9 H, $C(CH_3)_3$); ^{13}C NMR (101 MHz, $CDCl_3$) δ 156.8 (C=O), 79.6 ($C(CH_3)_3$), 62.3 (OCH_2), 43.0 (NCH_2), 28.3 ($C(CH_3)_3$). The observed characterisation data (^{1}H and ^{13}C NMR) was consistent with that previously reported in the literature.[441]

***tert*-Butyl (2-iodoethyl)carbamate (333)**



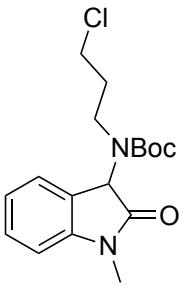
tert-Butyl (2-hydroxyethyl)carbamate **S3** (806 mg, 5.0 mmol) in CH_2Cl_2 (10 mL) was added dropwise to a stirred solution of PPh_3 (1.31 g, 5.0 mmol), I_2 (1.52 g, 6.0 mmol) and imidazole (343 mg, 5.0 mmol) in CH_2Cl_2 (40 mL) at 25 ºC. The reaction mixture was stirred at 25 ºC for 2.5 h then H_2O (50 mL) was added and the layers separated. The organic layer was washed with sat. aq. sodium thiosulfate (2 × 50 mL), sat. brine (50 mL), dried over Na_2SO_4 and concentrated under reduced pressure. Purification by flash chromatography (50% to 100% CH_2Cl_2/pentane) afforded *tert*-butyl (2-iodoethyl)carbamate **333** (880 mg, 65%) as a pale yellow solid. R_f 0.28 (50% CH_2Cl_2/pentane); mp = 42–44 ºC [lit mp = 42–43 ºC][442]; ν_{max} (film)/cm^{-1} 3350 (br s, NH), 2977, 1677 (C=O), 1513, 1362, 1297, 1270, 1192, 1158, 1135, 1045, 1025, 933, 919, 861, 784; ^{1}H NMR (400 MHz, $CDCl_3$) δ 4.94 (br s, 1 H, NH), 3.49 (q, J = 6.3 Hz, 2 H, NCH_2), 3.24 (t, J = 6.3 Hz, 2 H, ICH_2), 1.45 (s, 9 H, $C(CH_3)_3$); ^{13}C NMR (101 MHz, $CDCl_3$) δ 155.4 (C=O), 79.8 ($C(CH_3)_3$), 42.9 (NCH_2), 28.3 ($C(CH_3)_3$), 6.0 (ICH_2). The observed characterisation data (^{1}H and ^{13}C NMR) was consistent with that previously reported in the literature.[442]

6.2.3.3 N–H Insertion of 3-diazooxindoles

General Procedure **A**

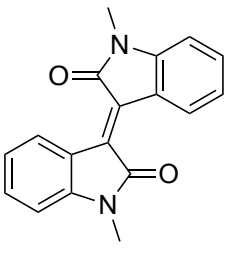
A solution of diazo (1.0 equiv) in CH_2Cl_2 or toluene (0.16 M) was slowly added over 10 min to a stirred solution of the appropriate protected amine (2.0 equiv) and $Rh_2(esp)_2$ (0.25 mol%) in CH_2Cl_2 or toluene (0.3 M) at 25 ºC. The remaining diazo solution was washed with CH_2Cl_2 or toluene (1 M) to ensure quantitative transfer. After 30 min the reaction mixture was concentrated under reduced pressure. Purification by flash chromatography afforded the NH insertion product.

(±)–*tert*-Butyl (3-chloropropyl)(1-methyl-2-oxoindolin-3-yl)carbamate (274)



A solution of diazo **273** (66 mg, 0.38 mmol) in CH_2Cl_2 (0.9 mL) was slowly added over 10 min to a stirred solution of protected amine **52** (48 mg, 0.25 mmol) and $Rh_2(esp)_2$ (0.9 mg, 1.25 μmol) in CH_2Cl_2 (0.67 mL) at 40 ºC. The remaining solution of diazo **273** was washed with CH_2Cl_2 (0.1 mL) to ensure quantitative transfer. After 2 h at 40 ºC the reaction mixture was concentrated under reduced pressure. Purification by flash chromatography (heptane to 30% EtOAc/heptane) afforded *tert*-butyl (3-chloropropyl)(1-methyl-2-oxoindolin-3-yl)carbamate **274** (41 mg, 48%) as a brown oil. R_f 0.20 (30% EtOAc/heptane); ν_{max} (film)/cm^{-1} 2984, 2954, 2928, 1720 (C=O amide), 1689 (C=O carbamate), 1609, 1495, 1471, 1457, 1417, 1362, 1375, 1353, 1336, 1282, 1154, 1121, 1084, 766; ^{1}H NMR (400 MHz, DMSO-d_6, 373 K) δ 7.31 (tt, J = 7.7, 1.1 Hz, 1 H, HC_{Ar}), 7.22–7.19 (m, 1 H, HC_{Ar}), 7.05 (td, J = 7.6, 0.9 Hz, 1 H, HC_{Ar}), 6.96 (d, J = 7.8 Hz, 1 H, HC_{Ar}), 5.01 (br s, 1 H, NCH), 3.76–3.66 (m, 2 H, CH_2Cl), 3.64–3.39 (m, 2 H, NCH_2), 3.13 (s, 3 H, NCH_3), 2.13–2.02 (m, 2 H, NCH_2CH_2), 1.29–1.07 (br s, 9 H, $C(CH_3)_3$); ^{13}C NMR (101 MHz, DMSO-d_6, 373 K) δ 173.2 (C=O amide), 153.4 (C=O carbamate), 143.1 (NC_{Ar} quat), 127.9 (C_{Ar}), 126.4 (C_{Ar} quat), 122.0 (C_{Ar}), 121.4 (C_{Ar}), 107.7 (C_{Ar}), 79.2 ($C(CH_3)_3$), 59.4 (NCH), 45.6 (NCH_2), 42.0 (CH_2Cl), 31.6 (NCH_2CH_2), 27.1 ($C(CH_3)_3$), 25.4 (NCH_3); HRMS (ESI$^+$) *m/z* Calculated for $C_{17}H_{23}N_2O_3{}^{35}Cl$ [M+Na] 361.1295; Found 361.1295.

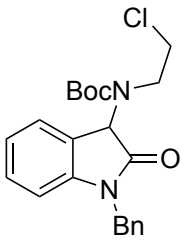
(*E*)-1,1'-Dimethyl-[3,3'-biindolinylidene]-2,2'-dione (275)



A solution of diazo **273** (66 mg, 0.38 mmol) in CH_2Cl_2 (0.5 mL) was slowly added over 10 min to a stirred solution of 3-bromopropan-1-ol (35 mg, 0.25 mmol) and $[Cu(MeCN)_4]PF_6$ (4.7 mg, 0.01 mmol) in CH_2Cl_2 (0.2 mL) at 40 ºC. The remaining solution of diazo **273** was washed with CH_2Cl_2 (0.1 mL) to ensure quantitative transfer. The reaction mixture was stirred for 18 h at 40 ºC and then concentrated under reduced pressure. Purification by flash

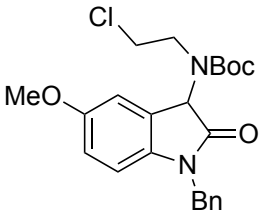
chromatography (50% CH_2Cl_2/heptane to CH_2Cl_2) afforded (*E*)-1,1'-dimethyl-[3,3'-biindolinylidene]-2,2'-dione **275** (34 mg, 62%) as a purple solid. R_f 0.22 (CH_2Cl_2); mp = 275 ºC [lit = 268 ºC][443]; ν_{max} (film)/cm^{-1} 1677 (C=O), 1603, 1469, 1370, 1334, 1076, 772; ^{1}H NMR (400 MHz, $CDCl_3$) δ 9.24–9.22 (m, 2 H, 2 × HC_{Ar}), 7.39 (td, *J* = 7.7, 1.2 Hz, 2 H, 2 × HC_{Ar}), 7.08 (td, *J* = 8.0, 1.2 Hz, 2 H, 2 × HC_{Ar}), 6.80 (dd, *J* = 7.8, 0.5 Hz, 2 H, 2 × HC_{Ar}), 3.30 (s, 6 H, 2 × NCH_3); ^{13}C NMR (101 MHz, $CDCl_3$) δ 168.0 (2 × C=O), 145.2 (2 × NC_{Ar} quat), 133.4 (2 × C_{Ar} quat), 132.4 (2 × C_{Ar}), 129.9 (2 × C_{Ar}), 122.4 (2 × C_{Ar}), 121.6 (*C*=*C*), 107.6 (2 × C_{Ar}), 26.1 (2 × NCH_3). The observed characterisation data (^{1}H and ^{13}C NMR) was consistent with that previously reported in the literature.[444]

(±)–*tert*-Butyl (1-benzyl-2-oxoindolin-3-yl)(2-chloroethyl)carbamate (312)



Following general procedure **A** on 1.0 mmol scale using diazo **280** and protected amine **52** in toluene. Purification by flash chromatography (25% Et_2O/pentane) afforded *tert*-butyl (1-benzyl-2-oxoindolin-3-yl)(2-chloroethyl)carbamate **312** (264 mg, 67%) as a pale brown solid. R_f 0.10 (25% Et_2O/hexane); mp = 112–114 ºC; ν_{max} (film)/cm^{-1} 2978, 1703 (2 × C=O), 1608, 1485, 1447, 1365, 1334, 1241, 1156, 738, 701; ^{1}H NMR (400 MHz, DMSO-*d*$_6$) δ 7.46–7.14 (m, 7 H, 7 HC_{Ar}), 7.07–6.93 (m, 2 H, 2 × HC_{Ar}), 5.26 (s, 1 H, NCH), 5.11–4.60 (m, 2 H, NCH_2Ph), 4.00–3.70 (m, 4 H, $N(CH_2)_2$), 1.38 and 0.87 (2 × s, 9 H, $C(CH_3)_3$); ^{13}C NMR (101 MHz, DMSO-*d*$_6$) δ 174.2 (C=O amide), 153.5 (C=O carbamate), 142.3 (NC_{Ar} quat), 136.5 (C_{Ar} quat), 128.5, 128.4, 128.1, 127.7, 127.5, 127.2 (6 × C_{Ar} and C_{Ar} quat), 122.6 (C_{Ar}), 122.1 (C_{Ar}), 108.8 (C_{Ar}), 79.9 ($C(CH_3)_3$), 60.2 (NCH), 50.7 (NCH_2), 42.9 (NCH_2Ph), 41.9 (CH_2Cl), 27.8 and 27.2 ($C(CH_3)_3$); HRMS (ESI$^+$) *m/z* Calculated for $C_{24}H_{28}N_3O_3Na^{35}Cl$ [M+CH_3CN+Na] 464.1717; Found 464.1716.

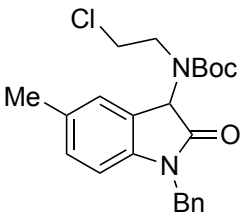
(±)–*tert*-Butyl (1-benzyl-5-methoxy-2-oxoindolin-3-yl)(2-chloroethyl)carbamate (313)



Following general procedure **A** on 1.0 mmol scale using diazo **297** and protected amine **52** in CH_2Cl_2. Purification by flash chromatography (20% to 25% to 30% EtOAc/pentane) afforded *tert*-butyl (1-benzyl-5-methoxy-2-oxoindolin-3-yl)(2-chloroethyl)carbamate **313** (328 mg, 76%) as a white solid. R_f 0.13 (20% EtOAc/pentane); ν_{max} (film)/cm^{-1} 2973, 2930, 1697 (2 × C=O), 1602, 1491, 1454, 1364, 1333, 1435, 1406, 1279, 1247, 1176, 1151, 1081, 1062, 1035, 855, 807, 762, 727; ^{1}H NMR (400 MHz, $CDCl_3$) δ 7.44–7.22 (m, 5 H, 5 × HC_{Ph}), 6.97 and 6.91 (2 × br s, 1 H, HC_{Ar}), 6.87–6.70 (m, 2 H, 2 × HC_{Ar}), 5.22 (s, 1 H, NCH), 5.04 (d, *J* = 15.5 Hz, 0.5 H, NC*H*HPh), 4.90 and 4.84 (2 × d, *J* = 15.6 Hz, 1 H, NCH*H*Ph), 4.60 (d, *J* = 15.5 Hz, 0.5 H, NC*H*HPh), 3.98–3.65 (m, 7 H, $N(CH_2)_2$ and OCH_3), 1.38 and 0.89 (2 ×

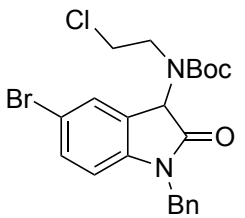
s, 9 H, $C(CH_3)_3$); ^{13}C NMR (101 MHz, $CDCl_3$) δ 173.8 (C=O amide), 155.4 (OC_{Ar} quat), 153.5 (C=O carbamate), 136.6 and 136.3 (C_{Ar} quat), 135.8 and 135.7 (C_{Ar} quat), 129.1 (C_{Ar} quat), 128.5 and 128.4 (2 × C_{Ph}), 127.7, 127.4 and 127.2 (3 × C_{Ph}), 112.4 (C_{Ar}), 110.6 and 110.0 (C_{Ar}), 109.2 (C_{Ar}), 80.3 and 79.9 ($C(CH_3)_3$), 60.5 (NCH), 55.6 and 55.4 (OCH_3), 50.7 (NCH_2), 43.0 and 42.8 (NCH_2Ph), 42.0 (CH_2Cl), 27.8 and 27.3 ($C(CH_3)_3$); HRMS (FTMS – pAPCI) *m/z* Calculated for $C_{23}H_{26}N_2O_4{}^{35}Cl^-$ $[M–H]^-$ 429.1587; Found 429.1574.

(±)–*tert*-Butyl (1-benzyl-5-methyl-2-oxoindolin-3-yl)(2-chloroethyl)carbamate (314)



Following general procedure **A** on 0.9 mmol scale using diazo **298** and protected amine **52** in CH_2Cl_2. Purification by flash chromatography (30% Et_2O/pentane) afforded *tert*-butyl (1-benzyl-5-methyl-2-oxoindolin-3-yl)(2-chloroethyl)carbamate **314** (196 mg, 51%) as a brown solid. R_f 0.19 (30% Et_2O/pentane); mp = 147–148 ºC; ν_{max} (film)/cm^{-1} 2973, 2924, 2869, 1702 (2 × C=O), 1495, 1415, 1365, 1334, 1244, 1154, 1132, 825, 741, 703; ^1H NMR (400 MHz, DMSO-d_6) δ 7.44–7.22 (m, 5 H, 5 × HC_{Ph}), 7.15–6.96 (m, 2 H, 2 × HC_{Ar}), 6.85–6.66 (m, 1 H, HC_{Ar}), 5.20 (s, 1 H, NCH), 5.04 and 4.91 (2 × d, *J* = 15.4 Hz, 1 H, NC*H*HPh), 4.83 and 4.60 (2 × d, *J* = 15.4 Hz, 1 H, NCH*H*Ph), 3.97–3.64 (m, 4 H, NCH_2CH_2), 2.27–2.22 (s, 3 H, $ArCH_3$), 1.39 and 0.88 (s, 9 H, $C(CH_3)_3$); ^{13}C NMR (101 MHz, DMSO-d_6) δ 174.0 (C=O amide), 153.5 (C=O carbamate), 139.9 (NC_{Ar} quat), 136.5 (C_{Ph} quat), 131.1 (C_{Ar} quat), 128.5, 128.1, 127.6, 127.4 and 127.2 (5 × C_{Ph}, C_{Ar} and C_{Ar} quat), 123.3 (C_{Ar}), 108.8 and 108.5 (C_{Ar}), 80.3 and 79.8 ($C(CH_3)_3$), 60.3 (NCH), 50.7 (NCH_2), 42.9 and 42.8 (NCH_2Ar), 41.8 (CH_2Cl), 27.8 and 27.2 ($C(CH_3)_3$), 20.6 ($ArCH_3$); HRMS (ESI^+) *m/z* Calculated for $C_{23}H_{28}N_2O_3{}^{35}Cl$ [M+H] 415.1788; Found 415.1800.

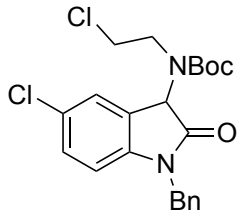
(±)–*tert*-Butyl (1-benzyl-5-bromo-2-oxoindolin-3-yl)(2-chloroethyl)carbamate (315)



Following general procedure **A** on 1.0 mmol scale using diazo **299** and protected amine **52** in CH_2Cl_2. Purification by flash chromatography (20% to 30% Et_2O/pentane) afforded *tert*-butyl (1-benzyl-5-bromo-2-oxoindolin-3-yl)(2-chloroethyl)carbamate **315** (377 mg, 79%) as a white solid. R_f 0.29 (30% Et_2O/pentane); mp = 57–59 ºC; ν_{max} (film)/cm^{-1} 2974, 2930, 1698 (br s, 2 × C=O), 1608, 1481, 1455, 1406, 1366, 1331, 1291, 1248, 1154, 1113, 1081, 807, 698; ^1H NMR (400 MHz, $CDCl_3$) δ 7.52–7.23 (m, 7 H, 7 × HC_{Ar}), 6.95 and 6.77 (2 × d, *J* = 8.2 Hz, 1 H, HC_{Ar}), 5.38–5.21 (m, 1 H, NCH), 5.05 and 4.94 (2 × d, *J* = 15.9 Hz, 1 H, NC*H*HPh), 4.86 and 4.66 (2 × d, *J* = 15.9 Hz, 1 H, NCH*H*Ph), 3.98–3.66 (m, 4 H, NCH_2CH_2), 1.37 and 0.90 (2 × br s, 9 H, $C(CH_3)_3$); ^{13}C NMR (101 MHz, $CDCl_3$) δ 173.8 and 173.3 (C=O amide), 153.3 (C=O carbamate), 141.7 and 141.5 (NC_{Ar} quat), 136.1 and 135.9 (C_{Ph} quat), 130.7 (C_{Ar}), 130.2 (C_{Ar}

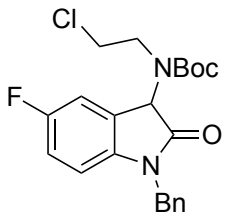
quat), 128.6 and 128.4 (2 × C_{Ph}), 127.7 and 127.5 (2 × C_{Ph}), 127.3 and 127.2 (C_{Ph}), 125.8 and 125.6 (C_{Ar}), 114.0 (BrC_{Ar} quat), 110.9 and 110.8 (C_{Ar}), 80.6 and 80.2 ($C(CH_3)_3$), 60.0 (NCH), 50.7 (NCH_2), 43.0 and 42.8 (NCH_2Ph), 42.4 and 42.0 (CH_2Cl), 27.8 and 27.2 ($C(CH_3)_3$); HRMS (FTMS – pAPCI) *m/z* Calculated for $C_{22}H_{23}N_2O_3{}^{35}Cl^{79}Br^-$ $[M-H]^-$ 477.0586; Found 477.0567.

(±)–*tert*-Butyl (1-benzyl-5-chloro-2-oxoindolin-3-yl)(2-chloroethyl)carbamate (316)



Following general procedure **A** on 1.0 mmol scale using diazo **283** and protected amine **52** in CH_2Cl_2. Purification by flash chromatography (CH_2Cl_2 to 2% Et_2O/CH_2Cl_2 to 4% Et_2O/CH_2Cl_2) afforded *tert*-butyl (1-benzyl-5-chloro-2-oxoindolin-3-yl)(2-chloroethyl)carbamate **316** (224 mg, 51%) as a pale yellow solid. R_f 0.52 (2% Et_2O/CH_2Cl_2); mp = 60–63 ºC; ν_{max} (film)/cm^{-1} 2971, 2926, 1689 (br s, 2 × C=O), 1610, 1480, 1428, 1364, 1327, 1245, 1152, 1078, 809, 738, 697; ^{1}H NMR (400 MHz, DMSO-d_6) δ 7.45–7.10 (m, 7 H, 7 × HC_{Ar}), 7.02–6.83 (m, 1 H, HC_{Ar}), 5.33 (br s, 1 H, NCH), 5.10–4.84 and 4.77–4.61 (m, 2 H, NCH_2Ph), 3.98–3.67 (m, 4 H, NCH_2CH_2), 1.37 and 0.90 (2 × s, 9 H, $C(CH_3)_3$); ^{13}C NMR (101 MHz, DMSO-d_6) δ 173.9 and 173.5 (C=O amide), 153.3 (C=O carbamate), 141.3 and 141.1 (NC_{Ar} quat), 136.2 and 135.9 (C_{Ph} quat), 129.9 (C_{Ar} quat), 128.6, 128.4, 127.9, 127.7, 127.6, 127.3, 127.2, 126.8, 126.4 (6 × C_{Ar} and C_{Ar} quat), 122.9 (C_{Ar}), 110.2 (C_{Ar}), 80.6 and 80.2 ($C(CH_3)_3$), 60.1 (NCH), 50.7 (NCH_2), 43.0 and 42.8 (NCH_2Ph), 42.4 and 42.0 (CH_2Cl), 27.8 and 27.2 ($C(CH_3)_3$); HRMS (ESI$^+$) *m/z* Calculated for $C_{22}H_{25}N_2O_3{}^{35}Cl_2$ [M+H] 435.1242; Found 435.1247.

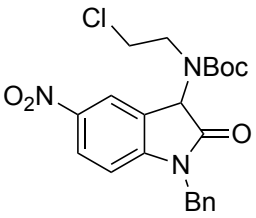
(±)–*tert*-Butyl (1-benzyl-5-fluoro-2-oxoindolin-3-yl)(2-chloroethyl)carbamate (317)



Following general procedure **A** on 1.0 mmol scale using diazo **286** and protected amine **52** in CH_2Cl_2. Purification by flash chromatography (30% Et_2O/pentane) afforded *tert*-butyl (1-benzyl-5-fluoro-2-oxoindolin-3-yl)(2-chloroethyl)carbamate **317** (275 mg, 66%) as a brown solid. R_f 0.26 (30% Et_2O/pentane); mp = 87–88 ºC; ν_{max} (film)/cm^{-1} 2974, 2930, 1700 (br s, 2 × C=O), 1487, 1454, 1409, 1364, 1334, 1290, 1249, 1156, 809, 772, 693; ^{1}H NMR (400 MHz, DMSO-d_6) δ 7.44–7.14 (m, 6 H, 6 × HC_{Ar}), 7.13–7.00 (m, 1 H, HC_{Ar}), 6.99–6.94 and 6.82–6.77 (2 × m, 1 H, HC_{Ar}), 5.31 (s, 1 H, NCH), 5.05 and 4.92 (2 × d, J =16.0, 15.5 Hz, 1 H, NC*H*HPh), 4.87 and 4.65 (2 × d, J = 16.0, 15.5 Hz, 1 H, NCH*H*Ph), 3.96–3.69 (m, 4 H, NCH_2CH_2), 1.37 and 0.90 (2 × s, 9 H, $C(CH_3)_3$); ^{13}C NMR (101 MHz, DMSO-d_6) δ 174.1 and 173.6 (C=O amide), 158.5 (d, J_{C-F} = 237.2 Hz, FC_{Ar} quat), 153.3 (C=O carbamate), 138.6 and 138.4 (C_{Ar} quat), 136.3 and 136.1 (C_{Ph} quat), 129.7 and 129.7 (C_{Ar} quat), 128.6 and 128.4 (2 × C_{Ph}), 127.8, 127.5, 127.3 and 127.2 (3 × C_{Ph}), 114.3 and 114.1 (C_{Ar}), 110.8 and 110.6 (C_{Ar}), 109.6 and 109.6 (C_{Ar}), 80.5 and 80.1 ($C(CH_3)_3$), 60.4 (NCH), 50.6 (NCH_2), 43.0 and 42.9 (NCH_2Ph), 42.3

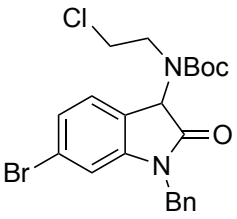
and 42.0 (CH_2Cl), 27.8 and 27.2 ($C(CH_3)_3$); $^{19}F\{^1H\}$ NMR (377 MHz, DMSO-d_6) δ –121.2; HRMS (ESI^+) *m/z* Calculated for $C_{22}H_{25}N_2O_3F^{35}Cl$ [M+H] 419.1538; Found 419.1533.

(±)–*tert*-Butyl (1-benzyl-5-nitro-2-oxoindolin-3-yl)(2-chloroethyl)carbamate (318)



Following general procedure **A** on 0.95 mmol scale using diazo **300** and protected amine **52** in CH_2Cl_2. Purification by flash chromatography (40% Et_2O/pentane) afforded *tert*-butyl (1-benzyl-5-nitro-2-oxoindolin-3-yl)(2-chloroethyl)carbamate **318** (254 mg, 60%) as a white solid. R_f 0.34 (50% Et_2O/pentane); mp = 67–69 ºC; ν_{max} (film)/cm^{-1} 2973, 2926, 1735 (C=O amide), 1698 (C=O carbamate), 1611, 1517, 1444, 1406, 1388, 1366, 1331, 1248, 1152, 1124, 1071, 884, 823, 750; ^1H NMR (400 MHz, DMSO-d_6) δ 8.28–8.15 (m, 2 H, 2 × HC_{Ar}), 7.47–7.23 and 7.07–7.03 (m, 6 H, HC_{Ar} and 5 × HC_{Ph}), 5.48 and 5.37 (2 × s, 1 H, NCH), 5.17–4.94 and 4.87–4.79 (m, 2 H, NCH_2Ph), 4.04–3.73 (m, 4 H, NCH_2CH_2), 1.36 and 0.87 (2 × s, 9 H, $C(CH_3)_3$); ^{13}C NMR (101 MHz, DMSO-d_6) δ 174.8 and 174.5 (C=O amide), 153.4 and 153.1 (C=O carbamate), 148.4 and 148.2 (NC_{Ar} quat), 142.6 (NO_2C_{Ar} quat), 135.6 and 135.5 (C_{Ph} quat), 128.9, 128.7, 128.5, 127.80, 127.75, 127.5, 127.2 (5 × C_{Ph} and C_{Ar} quat), 125.5 (C_{Ar}), 118.3 and 118.2 (C_{Ar}), 109.0 (C_{Ar}), 80.9 and 80.5 ($C(CH_3)_3$), 60.0 and 59.8 (NCH), 50.7 (NCH_2), 43.3 and 43.1 (NCH_2Ph), 42.6 and 42.2 (CH_2Cl), 27.8 and 27.2 ($C(CH_3)_3$); HRMS (ESI^+) *m/z* Calculated for $C_{22}H_{25}N_3O_5^{35}Cl$ [M+H] 446.1483; Found 446.1477.

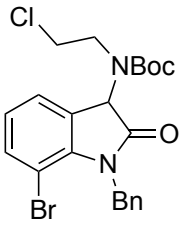
(±)–*tert*-Butyl (1-benzyl-6-bromo-2-oxoindolin-3-yl)(2-chloroethyl)carbamate (319)



Following general procedure **A** on 1.0 mmol scale using diazo **301** and protected amine **52** in CH_2Cl_2. Purification by flash chromatography (25% Et_2O/pentane) afforded *tert*-butyl (1-benzyl-6-bromo-2-oxoindolin-3-yl)(2-chloroethyl)carbamate **319** (377 mg, 79%) as a white solid. R_f 0.33 (30% Et_2O/pentane); mp = 57–60 ºC; ν_{max} (film)/cm^{-1} 2973, 2929, 1720 (C=O amide), 1701 (C=O carbamate), 1606, 1589, 1484, 1454, 1439, 1426, 1405, 1366, 1333, 1290, 1249, 1153, 1105, 927, 875, 800, 741, 724, 697, 670; ^1H NMR (400 MHz, DMSO-d_6) δ 7.48–7.03 (m, 8 H, 8 × HC_{Ar}), 5.26 (s, 1 H, NCH), 5.04 and 4.95 (2 × d, *J* = 15.6 and 16.0 Hz, 1 H, NC*H*HPh), 4.89 and 4.73 (2 × d, *J* = 16.0 and 15.6 Hz, 1 H, NCH*H*Ph), 3.99–3.65 (m, 4 H, NCH_2CH_2), 1.36 and 0.91 (2 × s, 9 H, $C(CH_3)_3$); ^{13}C NMR (101 MHz, DMSO-d_6) δ 174.2 and 173.8 (C=O amide), 153.3 (C=O carbamate), 144.1 and 143.9 (NC_{Ar} quat), 136.2 and 135.9 (C_{Ph} quat), 128.6 and 128.4 (2 × C_{Ph}), 127.7, 127.5, 127.3, 127.2 and 127.1 (3 × C_{Ph} and C_{Ar} quat), 124.7 and 124.4 (2 × C_{Ar}), 120.7 (BrC_{Ar} quat), 111.9 and 111.7 (C_{Ar}), 80.5 and 80.1 ($C(CH_3)_3$), 59.8 (NCH), 50.7 (NCH_2), 42.9 and 42.7 (NCH_2Ph), 42.3 and 42.0 (CH_2Cl), 27.8

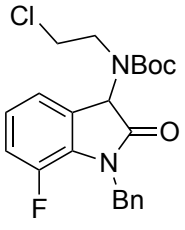
and 27.2 (C(CH_3)$_3$); HRMS (FTMS – pAPCI) *m/z* Calculated for $C_{22}H_{23}N_2O_3{}^{35}Cl^{79}Br^-$ $[M–H]^-$ 477.0586; Found 477.0604.

(±)–*tert*-Butyl (1-benzyl-7-bromo-2-oxoindolin-3-yl)(2-chloroethyl)carbamate (320)



Following general procedure **A** on 0.85 mmol scale using diazo **302** and protected amine **52** in CH_2Cl_2. Purification by flash chromatography (20% to 30% Et_2O/pentane) afforded *tert*-butyl (1-benzyl-7-bromo-2-oxoindolin-3-yl)(2-chloroethyl)carbamate **320** (269 mg, 66%) as a white solid. R_f 0.45 (30% Et_2O/pentane); mp = 128–130 ºC; ν_{max} (film)/cm^{-1} 2974, 2928, 1728 (C=O amide), 1694 (C=O carbamate), 1608, 1450, 1418, 1357, 1327, 1251, 1200, 1175, 1149, 1115, 1019, 1075, 963, 917, 850, 882, 768, 749, 729, 659; ^{1}H NMR (400 MHz, DMSO-d_6) δ 7.45–7.20 (m, 7 H, 7 × HC_{Ar}), 7.04–6.94 (m, 1 H, HC_{Ar}), 5.44 (s, 1 H, NCH), 5.31 (d, J = 16.7 Hz, NC*H*HPh), 5.26 (d, J = 16.7 Hz, NCH*H*Ph), 3.97–3.73 (m, 4 H, NCH_2CH_2), 1.37 and 1.00 (2 × s, 9 H, C(CH_3)$_3$); ^{13}C NMR (101 MHz, DMSO-d_6) δ 175.2 (C=O amide), 153.2 (C=O carbamate), 139.54 and 139.45 (NC_{Ar} quat), 137.7 and 137.6 (C_{Ph} quat), 133.7 (C_{Ar}), 131.4 (C_{Ar} quat), 128.4 and 128.2 (2 × C_{Ph}), 127.0 and 126.7 (C_{Ph}), 126.3 and 126.1 (2 × C_{Ph}), 124.1 (C_{Ar}), 122.2 (C_{Ar}), 101.4 (BrC_{Ar} quat), 80.7 and 80.4 (*C*(CH_3)$_3$), 59.6 (NCH), 50.7 (NCH_2), 44.0 (NCH_2Ph), 41.9 (CH_2Cl), 27.8 and 27.3 (C(*C*H_3)$_3$); HRMS (FTMS – pAPCI) *m/z* Calculated for $C_{22}H_{23}N_2O_3{}^{35}Cl^{79}Br^-$ $[M–H]^-$ 477.0586; Found 477.0589.

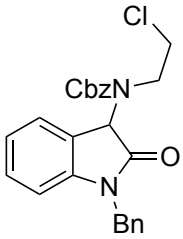
(±)–*tert*-Butyl (1-benzyl-7-fluoro-2-oxoindolin-3-yl)(2-chloroethyl)carbamate (321)



Following general procedure **A** on 1.0 mmol scale using diazo **303** and protected amine **52** in CH_2Cl_2. Purification by flash chromatography (30% Et_2O/pentane) afforded *tert*-butyl (1-benzyl-7-fluoro-2-oxoindolin-3-yl)(2-chloroethyl)carbamate **321** (197 mg, 47%) as a pale brown gum. R_f 0.30 (30% Et_2O/pentane); ν_{max} (film)/cm^{-1} 2974, 2933, 2868, 1726 (C=O amide), 1702 (C=O carbamate), 1631, 1474, 1455, 1366, 1338, 1292, 1182, 1152, 1126, 1082, 1068, 766, 721, 697; ^{1}H NMR (400 MHz, $CDCl_3$) δ 7.38–7.24 (m, 5 H, 5 × HC_{Ar}), 7.22–7.12 (m, 2 H, 2 × HC_{Ar}), 7.10–6.98 (m, 1 H, HC_{Ar}), 5.39 (s, 1 H, NCH), 5.13 and 5.02 (2 × d, J = 16.0, 15.7 Hz, 1 H, NC*H*HPh), 4.93 and 4.76 (2 × d, J = 16.0, 15.7 Hz, NCH*H*Ph), 3.98–3.71 (m, 4 H, NCH_2CH_2), 1.37 and 0.92 (2 × s, 9 H, C(CH_3)$_3$); ^{13}C NMR (101 MHz, $CDCl_3$) δ 174.1 and 173.7 (C=O amide), 153.3 (C=O carbamate), 146.7 (d, $J_{C–F}$ = 242 Hz, FC_{Ar} quat), 137.1 (C_{Ar} quat), 131.0 (C_{Ar} quat), 128.5, 128.3, 127.5 and 127.2 (4 × C_{Ar} and C_{Ar} quat), 126.6 (C_{Ar}), 123.34 and 123.28 (C_{Ar}), 119.1 (C_{Ar}), 116.2 (d, $J_{C–F}$ = 19.6 Hz, C_{Ar}), 80.6 and 80.2 (*C*(CH_3)$_3$), 60.2 (NCH), 50.7 (NCH_2), 44.8 and 44.7 (NCH_2Ph), 42.4 and 42.0 (CH_2Cl), 27.8 and 27.2 (C(*C*H_3)$_3$);

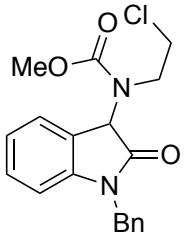
$^{19}F\{^{1}H\}$ NMR (377 MHz, DMSO-d_6) δ –135.5, –135.8 (br s); HRMS (ESI$^+$) *m/z* Calculated for $C_{22}H_{25}N_2O_3F^{35}Cl$ [M+H] 419.1538; Found 419.1532.

(±)–Benzyl (1-benzyl-2-oxoindolin-3-yl)(2-chloroethyl)carbamate (322)



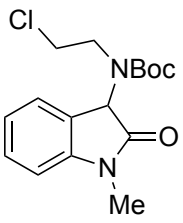
Following general procedure **A** on 1.0 mmol scale using diazo **280** and protected amine **63** in toluene. Purification by flash chromatography (CH_2Cl_2 to 2% EtOAc/CH_2Cl_2) afforded benzyl (1-benzyl-2-oxoindolin-3-yl)(2-chloroethyl)carbamate **322** (253 mg, 58%) as a brown gummy solid. R_f 0.33 (2% EtOAc/CH_2Cl_2); mp = 110–112 ºC; ν_{max} (film)/cm^{-1} 3026, 2922, 1701 (2 × C=O), 1655, 1439, 1420, 1284, 1156, 1178, 1005, 907, 746, 662; ^{1}H NMR (400 MHz, DMSO-d_6) δ 7.42–7.10 (m, 12 H, 12 × HC_{Ar}), 7.06–6.97 (m, 1 H, HC_{Ar}), 6.87–6.79 and 6.63–6.55 (m, 1 H, HC_{Ar}), 5.36 (br s, 1 H, NCH), 5.13 (s, 1 H, OC*H*HPh), 4.97–4.75 and 4.62–4.40 (m, 3 H, OCH*H*Ph and NCH_2Ph), 4.08–3.70 (m, 4 H, NCH_2CH_2); ^{13}C NMR (101 MHz, DMSO-d_6) δ 173.7 and 173.4 (C=O amide), 154.5 and 154.2 (C=O carbamate), 142.5 and 142.2 (NC_{Ar} quat), 136.3, 136.2 and 135.6 (2 × C_{Ph} quat), 128.5, 128.4, 128.1, 128.0 (4 × C_{Ph} and C_{Ar} quat), 127.6, 127.4, 127.3, 127.2, 126.9 (6 × C_{Ph} and C_{Ar}), 123.2 and 123.0 (C_{Ar}), 122.4 and 122.2 (C_{Ar}), 109.1 (C_{Ar}), 67.0 and 66.7 (OCH_2Ph), 60.4 and 60.1 (NCH), 51.5 and 50.5 (NCH_2), 42.9 (NCH_2Ph), 42.0 and 41.8 (CH_2Cl); HRMS (ESI$^+$) *m/z* Calculated for $C_{25}H_{23}N_2O_3Na^{35}Cl$ [M+Na] 457.1295; Found 457.1306.

(±)–Methyl (1-benzyl-2-oxoindolin-3-yl)(2-chloroethyl)carbamate (323)



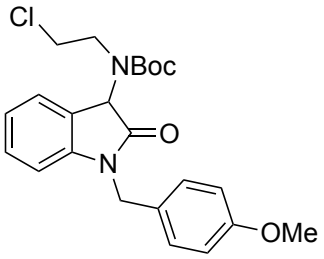
Following general procedure **A** on 1.0 mmol scale using diazo **280** and protected amine **331** in toluene. Purification by flash chromatography (CH_2Cl_2 to 2% Et_2O/CH_2Cl_2) afforded methyl (1-benzyl-2-oxoindolin-3-yl)(2-chloroethyl)carbamate **323** (106 mg, 30%) as a brown gummy solid. R_f 0.27 (90% CH_2Cl_2/pentane); ν_{max} (film)/cm^{-1} 3060, 2956, 1707 (br s, 2 × C=O), 1614, 1469, 1361, 1174, 753; ^{1}H NMR (400 MHz, $CDCl_3$) δ 7.37–7.19 (m, 7 H, 7 × HC_{Ar}), 7.09–7.02 (m, 1 H, HC_{Ar}), 6.81–6.62 (m, 1 H, HC_{Ar}), 5.09–4.74 (m, 3 H, NCH_2Ph and NCH), 3.86–3.44 (m, 7 H, NCH_2CH_2Cl and OCH_3); ^{13}C NMR (101 MHz, $CDCl_3$) δ 173.5 (C=O amide), 156.3 (C=O carbamate), 142.9 and 142.5 (NC_{Ar} quat), 135.4 (C_{Ph} quat), 129.4, 128.8 127.8, 127.7, 127.5, 127.2 (5 × C_{Ph}, C_{Ar} and $C_{Ar.}$ quat), 124.9 and 124.0 (C_{Ar}), 123.0 (C_{Ar}), 109.5 (C_{Ar}), 60.5 (NCH), 53.5 and 53.2 (OCH_3 and NCH_2), 44.0 (NCH_2Ph), 41.1 (CH_2Cl); HRMS (ESI$^+$) *m/z* Calculated for $C_{19}H_{20}N_2O_3^{35}Cl$ [M+H] 359.1162; Found 359.1154.

(±)–*tert*-Butyl (2-chloroethyl)(1-methyl-2-oxoindolin-3-yl)carbamate (324)



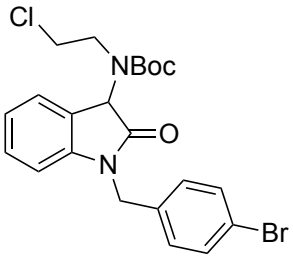
Following general procedure **A** on 1.0 mmol scale using diazo **273** and protected amine **52** in toluene. Purification by flash chromatography (50% Et_2O/pentane) afforded *tert*-butyl (2-chloroethyl)(1-methyl-2-oxoindolin-3-yl)carbamate **324** (210 mg, 65%) as a white solid. R_f 0.19 (50% Et_2O/pentane); mp = 123–124 ºC; ν_{max} (film)/cm^{-1} 2982, 1716 (C=O amide), 1697 (C=O carbamate), 1609, 1456, 1441, 1370, 1245, 1156, 1120, 1088, 759, 731; ^{1}H NMR (400 MHz, DMSO-d_6) δ 7.35–7.23 (m, 2 H, 2 × HC_{Ar}), 7.09–6.95 (m, 2 H, 2 × HC_{Ar}), 5.06 (br s, 1 H, NCH), 3.67–3.94 (m, 4 H, $N(CH_2)_2$), 3.11 (s, 3 H, NCH_3), 1.35 and 0.92 (2 × s, 9 H, $C(CH_3)_3$); ^{13}C NMR (101 MHz, DMSO-d_6) δ 174.0 (C=O amide), 153.5 (C=O carbamate), 143.3 (NC_{Ar} quat), 128.3 (C_{Ar}), 127.6 (C_{Ar} quat), 122.5 (C_{Ar}), 122.0 (C_{Ar}), 108.2 (C_{Ar}), 79.7 ($C(CH_3)_3$), 60.2 (NCH), 50.7 (NCH_2), 41.9 (CH_2Cl), 27.8 and 27.3 ($C(CH_3)_3$), 26.0 (NCH_3); HRMS (ESI$^+$) *m/z* Calculated for $C_{16}H_{22}N_2O_3{}^{35}Cl$ [M+H] 325.1319; Found 325.1324.

(±)–*tert*-Butyl (2-chloroethyl)(1-(4-methoxybenzyl)-2-oxoindolin-3-yl)carbamate (325)



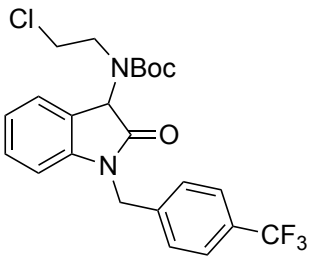
Following general procedure **A** on 1.0 mmol scale using diazo **306** and protected amine **52** in toluene. Purification by flash chromatography (30% to 40% Et_2O/pentane) afforded *tert*-butyl (2-chloroethyl)(1-(4-methoxybenzyl)-2-oxoindolin-3-yl)carbamate **325** (138 mg, 64%) as a pale yellow solid. R_f 0.11 (25% Et_2O/pentane); mp = 107–110 ºC; ν_{max} (film)/cm^{-1} 2971, 2933, 1718 (C=O amide), 1692 (C=O carbamate), 1610, 1439, 1364, 1338, 1245, 1156, 1126, 753, 727; ^{1}H NMR (400 MHz, DMSO-d_6) δ 7.40–7.15 (m, 4 H, 4 × HC_{Ar}), 7.06–6.95 (m, 2 H, 2 × HC_{Ar}), 6.92–6.82 (m, 2 H, 2 × HC_{Ar}), 5.21 (s, 1 H, NCH), 4.99 and 4.85 (2 × d, J = 15.1 Hz, 1 H, NC*H*HAr), 4.80 and 4.57 (2 × d, J = 15.1 Hz, 1 H, NCH*H*Ar), 3.99–3.66 (m, 7 H, NCH_2CH_2 and OCH_3), 1.39 and 0.86 (2 × s, 9 H, $C(CH_3)_3$); ^{13}C NMR (101 MHz, DMSO-d_6) δ 174.1 (C=O amide), 159.6 and 158.5 (OC_{Ar} quat), 153.5 (C=O carbamate), 142.4 and 142.3 (NC_{Ar} quat), 129.2, 128.6, 128.4, 128.1 and 127.7 (4 × C_{Ar} and C_{Ar} quat), 122.5 (C_{Ar} quat), 122.0 (C_{Ar}), 113.9 and 113.8 (2 × C_{Ar}), 109.1 and 108.8 (C_{Ar}), 80.4 and 79.8 ($C(CH_3)_3$), 60.2 (NCH), 55.0 (OCH_3), 50.7 (NCH_2), 42.4 and 42.3 (NCH_2Ar), 41.9 (CH_2Cl), 27.8 and 27.2 ($C(CH_3)_3$); HRMS (ESI$^+$) *m/z* Calculated for $C_{23}H_{27}N_2O_4Na^{35}Cl$ [M+Na] 453.1557; Found 453.1551.

(±)–*tert*-Butyl (1-(4-bromobenzyl)-2-oxoindolin-3-yl)(2-chloroethyl)carbamate (326)



Following general procedure **A** on 1.0 mmol scale using diazo **307** and protected amine **52** in toluene. Purification by flash chromatography (30% Et_2O/pentane) afforded *tert*-butyl (1-(4-bromobenzyl)-2-oxoindolin-3-yl)(2-chloroethyl)carbamate **326** (325 mg, 68%) as a white solid. R_f 0.18 (30% Et_2O/pentane); mp = 58–60 ºC; ν_{max} (film)/cm^{-1} 2975, 2932, 1720 (C=O amide), 1703 (C=O carbamate), 1613, 1487, 1467, 1407, 1365, 1293, 1249, 1156, 1012, 750, 731; ^{1}H NMR (400 MHz, DMSO-d_6) δ 7.55 and 7.49 (2 × d, J = 8.2 Hz, 2 H, 2 × HC_{Ar}), 7.42–7.16 (m, 4 H, 4 × HC_{Ar}), 7.08–6.94 and 6.85–6.80 (2 × m, 2 H, 2 × HC_{Ar}), 5.25 (s, 1 H, NCH), 5.04 and 4.92 (d, J = 15.9 Hz, 1 H, NC*H*H), 4.85 and 4.63 (d, J = 15.7 Hz, 1 H, NCH*H*), 4.00–3.69 (m, 4 H, NCH_2CH_2), 1.37 and 0.87 (2 × br s, 9 H, $C(CH_3)_3$); ^{13}C NMR (101 MHz, DMSO-d_6) δ 174.3 and 173.7 (C=O amide), 153.5 and 153.4 (C=O carbamate), 142.2 and 142.1 (NC_{Ar} quat), 136.0 and 135.8 (C_{Ar} quat), 131.4 and 131.3 (2 × C_{Ar}), 130.0 and 129.6 (2 × C_{Ar} and C_{Ar} quat), 128.3 and 128.2 (C_{Ar}), 127.7 and 127.6 (C_{Ar}), 122.7 and 122.2 (C_{Ar}), 120.6 (BrC_{Ar} quat), 108.9 and 108.7 (C_{Ar}), 80.4 and 79.9 ($C(CH_3)_3$), 60.2 (NCH), 50.7 (NCH_2), 42.3, 42.2 and 42.0 (NCH_2Ar and CH_2Cl), 27.8 and 27.2 ($C(CH_3)_3$); HRMS (FTMS – pAPCI) *m/z* Calculated for $C_{22}H_{23}N_2O_3{}^{35}Cl^{79}Br^-$ $[M–H]^-$ 477.0586; Found 477.0587.

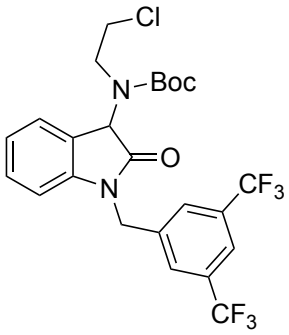
(±)–*tert*-Butyl (2-chloroethyl)(2-oxo-1-(4-(trifluoromethyl)benzyl)indolin-3-yl)carbamate (327)



Following general procedure **A** on 1.0 mmol scale using diazo **308** and protected amine **52** in toluene. Purification by flash chromatography (40% Et_2O/pentane) afforded *tert*-butyl (2-chloroethyl)(2-oxo-1-(4-(trifluoromethyl)benzyl)indolin-3-yl)carbamate **327** (151 mg, 65%) as an off-white solid. R_f 0.26 (40% Et_2O/pentane); mp = 52–55 ºC; ν_{max} (film)/cm^{-1} 2974, 2933, 1692 (2 × C=O), 1614, 1469, 1409, 1364, 1320, 1249, 1156, 1111, 1018, 910, 850, 749; ^{1}H NMR (400 MHz, DMSO-d_6) δ 7.75–7.65 (m, 4 H, 4 × HC_{Ar}), 7.32 (t, J = 8.3 Hz, 1 H, HC_{Ar}), 7.28–7.16 (m, 1 H, HC_{Ar}), 7.09–6.96 and 6.86–6.81 (m, 2 H, 2 × HC_{Ar}), 5.28 (s, 1 H, NCH), 5.16 and 5.06 (2 × d, J = 16.0 Hz, 1 H, NC*H*HPh), 4.98 and 4.79 (1 × d, J = 16.0 Hz, 1 H, NCH*H*Ph), 4.00–3.69 (m, 4 H, NCH_2CH_2), 1.37 and 0.87 (2 × s, 9 H, $C(CH_3)_3$); ^{13}C NMR (101 MHz, DMSO-d_6) δ 174.3 and 173.8 (C=O amide), 153.4 (C=O carbamate), 142.2 and 142.0 (C_{Ar} quat), 141.3 and 141.2 (C_{Ar} quat), 128.3 (2 × C_{Ar}), 128.2, 128.0, 128.0 and 127.7 (2 × C_{Ar} and C_{Ar} quat), 125.4 and 125.2 (2 × C_{Ar}), 122.8 and 122.7 (C_{Ar} quat), 122.3 (C_{Ar}), 108.9 and 108.7 (C_{Ar}), 80.4 and 80.0 ($C(CH_3)_3$), 60.2 (NCH), 50.8 (NCH_2), 42.5 and 42.4 (NCH_2Ar), 41.9 (CH_2Cl), 27.8 and

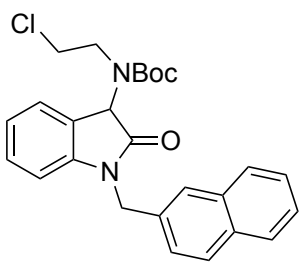
27.1 (C(CH_3)$_3$) (CF_3 quat was not observed or was obscured by other signals); $^{19}F\{^1H\}$ NMR (377 MHz, DMSO-d_6) δ –61.0 and –61.1; HRMS (ESI$^-$) *m/z* Calculated for $C_{23}H_{23}N_2O_3F_3{}^{35}Cl_3$ [M–H] 467.1349; Found 467.1356.

(±)–*tert*-Butyl (1-(3,5-bis(trifluoromethyl)benzyl)-2-oxoindolin-3-yl)(2-chloroethyl)carbamate (328)



Following general procedure **A** on 0.5 mmol scale using diazo **309** and protected amine **52** in toluene. Purification by flash chromatography (30% Et_2O/pentane) afforded *tert*-butyl (1-(3,5-bis(trifluoromethyl)benzyl)-2-oxoindolin-3-yl)(2-chloroethyl)carbamate **328** (160 mg, 60%) as a pale orange solid. R_f 0.17 (30% Et_2O/pentane); mp = 67–70 ºC; ν_{max} (film)/cm^{-1} 2986, 2933, 1729 (C=O amide), 1702 (C=O carbamate), 1465, 1414, 1341, 1277, 1157, 1126, 1010, 907, 882, 747, 737, 713; ^1H NMR (400 MHz, DMSO-d_6) δ 8.16 (s, 2 H, 2 × HC_{Ar}), 8.05 and 7.97 (2 × s, 1 H, HC_{Ar}), 7.37–7.32 (m, 1 H, HC_{Ar}), 7.28 and 7.18 (2 × t, *J* = 7.6 Hz, 1 H, HC_{Ar}), 7.15–6.98 and 6.86–6.77 (m, 2 H, 2 × HC_{Ar}), 5.36–5.10 (m, 2 H, NCH and NC*H*HAr), 5.01–4.90 (m, 1 H, NCH*H*Ar), 4.01–3.69 (m, 4 H, NCH_2CH_2), 1.34 and 0.82 (2 × s, 9 H, C(CH_3)$_3$); ^{13}C NMR (101 MHz, DMSO-d_6) δ 174.9 and 174.0 (C=O amide), 153.6 and 153.4 (C=O carbamate), 142.1 and 142.0 (C_{Ar} quat), 140.3 and 140.2 (C_{Ar} quat), 130.7 and 130.5 (2 × q, J_{C-F} = 33 Hz, 2 × $C_{Ar}CF_3$ quat), 129.0, 128.5, 128.4, 128.0 and 126.8 (3 × C_{Ar} and C_{Ar} quat), 123.4 (q, J_{C-F} = 273 Hz, 2 × CF_3 quat), 123.3 and 123.0 (C_{Ar}), 122.6 (C_{Ar}), 121.6 and 121.2 (C_{Ar}), 108.9 (C_{Ar}), 80.6 and 80.0 (*C*(CH_3)$_3$), 60.7 and 60.4 (NCH), 51.5 and 51.0 (NCH_2), 42.5, 42.2 and 42.0 (NCH_2Ar and CH_2Cl), 27.8 and 27.3 (C(*C*H_3)$_3$); $^{19}F\{^1H\}$ NMR (377 MHz, DMSO-d_6) δ –61.26 and –61.34; HRMS (FTMS – pAPCI) *m/z* Calculated for $C_{24}H_{22}N_2O_3F_6{}^{35}Cl^-$ $[M–H]^-$ 535.1229; Found 535.1228.

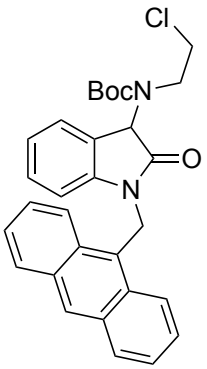
(±)–*tert*-Butyl (2-chloroethyl)(1-(naphthalen-2-ylmethyl)-2-oxoindolin-3-yl)carbamate (310)



Following general procedure **A** on 0.5 mmol scale using diazo **310** and protected amine **52** in CH_2Cl_2. Purification by flash chromatography (30% Et_2O/pentane) afforded *tert*-butyl (2-chloroethyl)(1-(naphthalen-2-ylmethyl)-2-oxoindolin-3-yl)carbamate **310** (95 mg, 42%) as a white solid. R_f 0.20 (50% Et_2O/hexane); mp = 74–76 ºC; ν_{max} (film)/cm^{-1} 3055, 2974, 2929, 1718 (C=O amide), 1701 (C=O carbamate), 1614, 1467, 1364, 1339, 1247, 1154, 747; ^1H NMR (400 MHz, $CDCl_3$) δ 7.97–7.83 (m, 4 H, 4 × HC_{Ar}), 7.58–7.44 (m, 3 H, 3 × HC_{Ar}), 7.35–7.28 (m, 1 H, HC_{Ar}),

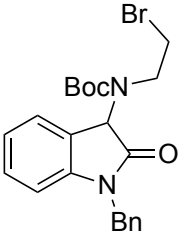
7.25–7.12 (m, 1 H, HC_{Ar}), 7.06–6.97 (m, 2 H, 2 × HC_{Ar}), 5.30 (s, 1 H, NCH), 5.25 (d, *J* = 15.5 Hz, 0.5 H, NC*H*HAr), 5.14 (d, *J* = 16.2 Hz, 0.5 H, NCH*H*Ar), 5.01 (d, *J* = 16.2 Hz, 0.5 H, NCH*H*Ar), 4.79 (d, *J* = 15.5 Hz, 0.5 H, NC*H*HAr), 4.01–3.73 (m, 4 H, $N(CH_2)_2$), 1.41 and 0.88 (2 × s, 9 H, $C(CH_3)_3$); ^{13}C NMR (101 MHz, $CDCl_3$) δ 174.4 (C=O amide), 153.5 (C=O carbamate), 142.3 (NC_{Ar} quat), 134.0 and 133.8 (C_{Ar} quat), 132.8 (C_{Ar} quat), 132.3 (C_{Ar} quat), 128.3 (C_{Ar}), 128.2 (C_{Ar} quat), 127.6 (2 × C_{Ar}), 126.4 (C_{Ar}), 126.1 (C_{Ar}), 126.0 (C_{Ar}), 125.9 (C_{Ar}), 125.6 (C_{Ar}), 122.7 (C_{Ar}), 122.2 (C_{Ar}), 108.8 (C_{Ar}), 79.9 ($C(CH_3)_3$), 60.3 (NCH), 50.8 (NCH_2), 43.2 (NCH_2Ar), 42.0 (CH_2Cl), 27.9 and 27.2 ($C(CH_3)_3$); HRMS (ESI^+) *m/z* Calculated for $C_{26}H_{28}N_2O_3{}^{35}Cl$ [M+H] 451.1788; Found 451.1795.

(±)–*tert*-Butyl (1-(anthracen-9-ylmethyl)-2-oxoindolin-3-yl)(2-chloroethyl)carbamate (330)



Following general procedure **A** on 0.5 mmol scale using diazo **311** and protected amine **52** in toluene. Purification by flash chromatography (CH_2Cl_2 to 10% Et_2O/CH_2Cl_2) afforded *tert*-butyl (1-(anthracen-9-ylmethyl)-2-oxoindolin-3-yl)(2-chloroethyl)carbamate **330** (70 mg, 28%) as a pale brown solid. R_f 0.25 (CH_2Cl_2); mp = 150–153 ºC; ν_{max} (film)/cm^{-1} 2974, 2910, 1719 (C=O amide), 1686 (C=O carbamate), 1611, 1484, 1462, 1368, 1351, 1296, 1271, 1251, 1157, 908, 752, 736; ^1H NMR (400 MHz, $CDCl_3$) δ 8.68 (s, 1 H, HC_{Ar}), 8.60–8.50 (m, 2 H, 2 × HC_{Ar}), 8.16 (d, *J* = 8.3 Hz, 2 H, 2 × HC_{Ar}), 7.71–7.53 (m, 4 H, 4 × HC_{Ar}), 7.24–7.15 (m, 1 H, HC_{Ar}), 6.91–6.78 (m, 2 H, 2 × HC_{Ar}), 6.41–6.22 (m, 1 H, HC_{Ar}), 6.08–5.88 and 5.74–5.63 (m, 2 H, NCH_2Ar), 5.20 (s, 1 H, NCH), 4.02–3.70 (m, 4 H, $N(CH_2)_2$), 1.41 and 0.87 (2 × s, 9 H, $C(CH_3)_3$); ^{13}C NMR (101 MHz, $CDCl_3$) δ 174.4 (C=O amide), 153.5 (C=O carbamate), 142.5 (NC_{Ar} quat), 130.9 (2 × C_{Ar}), 130.4 and 130.3 (C_{Ar}), 129.5 and 129.4 (3 × C_{Ar}), 128.6 (C_{Ar} quat), 128.0 and 127.9 (2 × C_{Ar} quat), 127.0 and 126.8 (2 × C_{Ar}), 126.5 (C_{Ar} quat), 125.3 (3 × C_{Ar}), 124.0 and 123.8 (C_{Ar}), 122.6 (C_{Ar} quat), 122.0 (C_{Ar} quat), 109.2 (C_{Ar}), 79.9 ($C(CH_3)_3$), 60.0 (NCH), 50.6 (NCH_2), 42.0 (CH_2Cl), 37.4 (CH_2Ar), 27.8 and 27.2 ($C(CH_3)_3$); HRMS (ESI^+) *m/z* Calculated for $C_{30}H_{30}N_2O_3{}^{35}Cl$ [M+H] 501.1945; Found 501.1944.

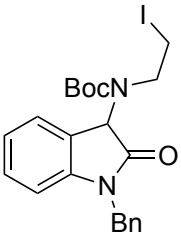
(±)–*tert*-Butyl (1-benzyl-2-oxoindolin-3-yl)(2-bromoethyl)carbamate (334)



Following general procedure **A** on 1.0 mmol scale using diazo **280** and protected amine **332** in toluene. Purification by flash chromatography (30% Et_2O/pentane) afforded *tert*-butyl (1-benzyl-2-oxoindolin-3-yl)(2-bromoethyl)carbamate **334** (263 mg, 59%) as a white solid. R_f 0.18 (30% Et_2O/pentane); mp = 113–115 ºC; ν_{max} (film)/cm^{-1} 2974, 1696 (br s, 2 × C=O),

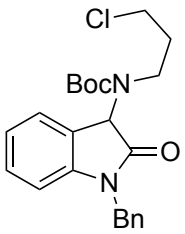
1613, 1467, 1454, 1364, 1149, 747; ^{1}H NMR (400 MHz, $CDCl_3$) δ 7.42–7.17 (m, 7 H, 7 × HC_{Ar}), 7.09–7.00 (m, 1 H, HC_{Ar}), 6.81–6.71 (m, 1 H, HC_{Ar}), 5.27–4.78 and 4.59–4.45 (m, 2 H, NCH_2Ph), 4.75–4.62 (m, 1 H, NCH), 4.11-3.93 (br s, 1 H, NC*H*H), 3.77–3.62 (m, 1 H, NCH*H*), 3.60–3.32 (m, 2 H, CH_2Br), 1.53 and 0.97 (2 × br s, 9 H, $C(CH_3)_3$); ^{13}C NMR (101 MHz, $CDCl_3$) δ 174.2 and 173.7 (C=O amide), 154.9 and 153.7 (C=O carbamate), 142.8 and 142.5 (NC_{Ar} quat), 135.7 and 135.4 (C_{Ph} quat), 129.3, 128.8, 128.6 (2 × C_{Ph} and C_{Ar}), 127.8, 127.7 and 127.2 (3 × C_{Ph}), 125.3 and 124.2 (C_{Ar} quat), 122.9 and 122.6 (2 × C_{Ar}), 106.5 and 108.8 (C_{Ar}), 81.5 and 81.2 ($C(CH_3)_3$), 61.8 and 59.1 (NCH), 52.5 (NCH_2), 44.1 and 44.0 (NCH_2Ph), 30.0 and 28.7 (CH_2Br), 28.2 and 27.6 ($C(CH_3)_3$); HRMS (ESI$^+$) *m/z* Calculated for $C_{24}H_{28}N_3O_3Na^{79}Br$ [M+CH_3CN+Na] 508.1212; Found 508.1207.

(±)–*tert*-Butyl (1-benzyl-2-oxoindolin-3-yl)(2-iodoethyl)carbamate (335)



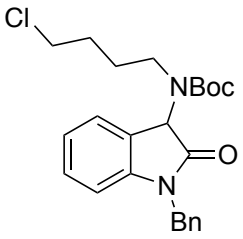
Following general procedure **A** on 0.88 mmol scale using diazo **280** and protected amine **333** in toluene. Purificaton by flash chromatography (CH_2Cl_2 to 1% to 3% Et_2O/CH_2Cl_2 then 30% Et_2O/pentane) afforded *tert*-butyl (1-benzyl-2-oxoindolin-3-yl)(2-iodoethyl)carbamate **335** (155 mg, 36%) as an off-white solid. R_f 0.45 (50% Et_2O/pentane); mp = 111–112 ºC; ν_{max} (film)/cm^{-1} 2974, 1696 (br s, 2 × C=O), 1613, 1487, 1467, 1453, 1407, 1364, 1281, 1148, 748, 697; ^{1}H NMR (400 MHz, $CDCl_3$) δ 7.43–7.19 (m, 7 H, 7 × HC_{Ar}), 7.10–7.01 (m, 1 H, HC_{Ar}), 6.81–6.72 (m, 1 H, HC_{Ar}), 5.74 (br s, 1 H, NCH rotamer), 5.29–4.97 (m, 1 H, NC*H*HPh), 4.90–4.75 and 4.70–4.42 (m, 1 H, NCH rotamer and NCH*H*Ph), 4.18–3.80 (2 × br s, 1 H, NC*H*H), 3.62–3.02 (m, 3 H, NCH*HCH*$_2$), 1.54 and 0.98 (2 × s, 9 H, $C(CH_3)_3$); ^{1}H NMR (400 MHz, DMSO-d_6) δ 7.46–7.15 (m, 7 H, 7 × HC_{Ar}), 7.07–6.92 and 6.86–6.81 (m, 2 H, 2 × HC_{Ar}), 5.26 (s, 1 H, NCH), 5.10–5.01, 4.98–4.83 and 4.68–4.60 (m, 2 H, NCH_2Ph), 3.94–3.78 (m, 1 H, NC*H*H), 3.49–3.29 (m, 3 H, NCH*HCH*$_2$), 1.39 and 0.87 (2 × br s, 9 H, $C(CH_3)_3$); ^{13}C NMR (101 MHz, $CDCl_3$) δ 174.0 and 173.7 (C=O amide), 153.6 (C=O carbamate), 142.8 and 142.6 (NC_{Ar} quat), 135.5 (C_{Ph} quat), 129.3, 128.9 (C_{Ar} and 2 × C_{Ph}), 127.8, 127.7 and 127.2 (3 × C_{Ph}), 125.3 and 124.2 (C_{Ar} quat), 123.0 and 122.6 (2 × C_{Ar}), 109.5 and 108.9 (C_{Ar}), 81.5 and 81.2 ($C(CH_3)_3$), 61.5 and 59.0 (NCH), 53.5 (NCH_2), 44.1 and 44.0 (NCH_2Ph), 28.3 and 27.6 ($C(CH_3)_3$), 1.6 (CH_2I); ^{13}C NMR (101 MHz, DMSO-d_6) δ 174.2 (C=O amide), 153.3 (C=O carbamate), 142.3 (NC_{Ar} quat), 136.5 and 136.3 (C_{Ph} quat), 128.6, 128.5, 128.1, 127.7, 127.4, 127.2 (5 × C_{Ph}, C_{Ar} and C_{Ar} quat), 122.7 (C_{Ar}), 122.2 and 122.1 (C_{Ar}), 108.8 (C_{Ar}), 80.4 and 79.9 ($C(CH_3)_3$), 59.9 (NCH), 51.7 and 51.6 (NCH_2), 42.9 and 42.8 (NCH_2Ph), 27.8 and 27.2 ($C(CH_3)_3$), 3.0 (CH_2I); HRMS (ESI$^+$) *m/z* Calculated for $C_{22}H_{26}N_2O_3{}^{127}I$ [M+H] 493.0988; Found 493.0992.

(±)–*tert*-Butyl (1-benzyl-2-oxoindolin-3-yl)(3-chloropropyl)carbamate (336)



Following general procedure **A** on 2.0 mmol scale using diazo **280** and protected amine **58** in toluene. Purification by flash chromatography (CH_2Cl_2 to 3% Et_2O/CH_2Cl_2) afforded *tert*-butyl (1-benzyl-2-oxoindolin-3-yl)(3-chloropropyl)carbamate **336** (270 mg, 65%) as a brown solid. R_f 0.40 (3% Et_2O/CH_2Cl_2); mp = 104–105 ºC; ν_{max} (film)/cm^{-1} 2980, 2947, 2931, 1718 (C=O amide), 1699 (C=O carbamate), 1612, 1417, 1362, 1347, 1250, 1149, 746, 700; ^{1}H NMR (400 MHz, DMSO-d_6, 373 K) δ 7.43–7.39 (m, 2 H, 2 × HC_{Ar}), 7.35–7.30 (m, 2 H, 2 × HC_{Ar}), 7.29–7.20 (m, 3 H, 3 × HC_{Ar}), 7.05–7.01 (m, 1 H, HC_{Ar}), 6.88 (d, J = 8.1 Hz, 1 H, HC_{Ar}), 5.21 (br s, 1 H, NCH), 5.00 (d, J = 15.8 Hz, 1 H, PhC*H*H), 4.76 (d, J = 15.8 Hz, 1 H, PhCH*H*), 3.75–3.40 (m, 4 H, NCH_2CH_2CH_2Cl), 2.16–2.02 (m, 2 H, NCH_2CH_2), 1.19 (br s, 9 H, C(CH_3)$_3$); ^{13}C NMR (101 MHz, DMSO-d_6, 373 K) δ 173.4 (C=O amide), 153.5 (C=O carbamate), 142.2 (NC_{Ar} quat), 135.8 (C_{Ph} quat), 127.9 (2 × C_{Ph} and C_{Ar}), 127.8 (C_{Ph}), 126.9 (2 × C_{Ph}), 126.7 (C_{Ar}), 122.3 (C_{Ar} quat), 121.6 (C_{Ar}), 108.4 (C_{Ar}), 79.4 (*C*(CH$_3$)$_3$), 59.5 (NCH), 45.6 (NCH_2), 42.8 (NCH_2Ph), 42.1 (CH_2Cl), 31.6 (NCH_2CH_2), 27.2 (C(*C*H$_3$)$_3$); HRMS (ESI$^+$) *m/z* Calculated for $C_{23}H_{28}N_2O_3{}^{35}Cl$ [M+H] 415.1791; Found 415.1788.

(±)–*tert*-Butyl (1-benzyl-2-oxoindolin-3-yl)(4-chlorobutyl)carbamate (337)



Following general procedure **A** on 1.0 mmol scale using diazo **280** and protected amine **59** in toluene. Purification by flash chromatography (30% Et_2O/pentane) afforded *tert*-butyl (1-benzyl-2-oxoindolin-3-yl)(4-chlorobutyl)carbamate **337** (266 mg, 62%) as a brown gum. R_f 0.26 (30% Et_2O/pentane); ν_{max} (film)/cm^{-1} 2974, 2930, 1722 (C=O amide), 1692 (C=O carbamate), 1614, 1487, 1416, 1364, 1297, 1152, 749, 697; ^{1}H NMR (400 MHz, DMSO-d_6) δ 7.45–7.16 (m, 7 H, 7 × HC_{Ar}), 7.06–6.91 (m, 2 H, 2 × HC_{Ar}), 5.15–5.05 and 4.95–4.83 (m, 2 H, NC*H*HPh and NCH), 4.60 (d, J = 15.5 Hz, 1 H, NCH*H*Ph), 3.79–3.48 (m, 4 H, NCH_2 and CH_2Cl), 1.92–1.73 (m, 4 H, $NCH_2(CH_2)_2$), 1.38 and 0.88 (2 × s, 9 H, C(CH$_3$)$_3$); ^{13}C NMR (101 MHz, DMSO-d_6) δ 174.4 (C=O amide), 153.6 (C=O carbamate), 142.4 (NC_{Ar} quat), 136.5 (C_{Ph} quat), 128.5, 128.1 and 128.0 (3 × C_{Ar}), 127.6, 127.4 and 127.3 (4 × C_{Ar}), 122.3 (C_{Ar} quat), 122.0 (C_{Ar}), 108.7 (C_{Ar}), 79.2 (*C*(CH$_3$)$_3$), 59.8 (NCH), 48.2 (NCH_2Ph), 45.2 and 45.1 (CH_2Cl), 42.9 (NCH_2), 29.2 ($N(CH_2)_2CH_2$), 27.9 and 27.3 (C(*C*H$_3$)$_3$), 26.2 (NCH_2CH_2); HRMS (ESI$^+$) *m/z* Calculated for $C_{24}H_{29}N_2O_3Na^{35}Cl$ [M+Na] 451.1764; Found 451.1763.

6.2.3.4 Racemic and Enantioselective Synthesis of Spirooxindoles

General Procedure **B** (One-Pot)

A solution of diazo (1.0 equiv) in CH_2Cl_2 or toluene (0.16 M) was slowly added over 10 min to a stirred solution of the appropriate protected amine (2.0 equiv) and $Rh_2(esp)_2$ (0.25 mol%) in CH_2Cl_2 or toluene (0.3 M) at 25 ºC. The remaining diazo solution was washed with CH_2Cl_2 or toluene (1 M) to ensure quantitative transfer. After 30 min, $CsOH{\cdot}H_2O$ (2 equiv) and tetrabutylammonium bromide (10 mol%) were added and the reaction mixture was stirred for the stated time (0.5–3 h) at 25 ºC. The reaction mixture was filtered through celite, washing with Et_2O (25 mL) and concentrated under reduced pressure followed by purification by flash chromatography.

General Procedure **C** (From cyclisation precursor)

From the stated cyclisation precursor in toluene or CH_2Cl_2 (0.1 M), $CsOH{\cdot}H_2O$ (2 equiv) and tetrabutylammonium bromide (10 mol%) were added and the reaction mixture was stirred for the stated time (0.5–3 h) at 25 ºC. The reaction mixture was filtered through celite, washing with Et_2O (25 mL) and concentrated under reduced pressure followed by purification by flash chromatography.

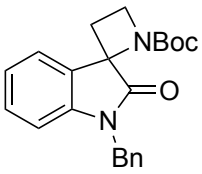
General Procedure **D** (Enantioselective)

$CsOH{\cdot}H_2O$ (5 equiv) was added and to the stated cyclisation precursor and stated catalyst (20 mol%) in *m*-xylene (0.1 M) and the reaction stirred (900 rpm) at 25 ºC for 1 h. The reaction mixture was filtered through celite, washing with Et_2O (25 mL) and concentrated under reduced pressure followed by purification by flash chromatography.

General Procedure **E** (Telescoped Enantioselective)

A solution of diazo (1.0 equiv) in CH_2Cl_2 (0.16 M) was slowly added over 10 min to a stirred solution of the appropriate protected amine (2.0 equiv) and $Rh_2(esp)_2$ (0.25 mol%) in CH_2Cl_2 (0.3 M) at 25 ºC. The remaining diazo solution was washed with CH_2Cl_2 (1 M) to ensure quantitative transfer. After 30 min, the solvent was removed under reduced pressure. Then cat. **394** (20 mol%) and *m*-xylene (0.1 M) were added. $CsOH{\cdot}H_2O$ (5 equiv) was added and the reaction mixture was stirred (900 rpm) at 25 ºC for 1 h. The reaction mixture was filtered through celite, washing with Et_2O (25 mL) and concentrated under reduced pressure followed by purification by flash chromatography.

(±)–*tert*-Butyl 1'-benzyl-2'-oxospiro[azetidine-2,3'-indoline]-1-carboxylate (338)



Following general procedure **B** on 0.5 mmol scale using diazo **280** and protected amine **52** in toluene. Purification by flash chromatography (40% Et_2O/pentane) afforded *tert*-butyl 1'-benzyl-2'-oxospiro[azetidine-2,3'-indoline]-1-carboxylate **338** (116 mg, 64%) as a brown solid. R_f 0.14 (40% Et_2O/pentane); mp = 41–43 ºC; ν_{max} (film)/cm^{-1} 2973, 1718 (C=O amide), 1701 (C=O carbamate), 1614, 1467, 1363, 1346, 1177, 1146, 1099, 966, 748, 695; ^{1}H NMR (400 MHz, $CDCl_3$) δ 7.49–7.44 (m, 1 H, HC_{Ar}), 7.39–7.13 (m, 6 H, 6 × HC_{Ar}), 7.11–7.02 (m, 1 H, HC_{Ar}), 6.74 and 6.62 (2 × d, *J* = 7.8 Hz, 1 H, HC_{Ar}), 5.06–4.69 (m, 2 H, NCH_2Ph), 4.37–4.24 (m, 1 H, NC*H*H), 4.15–4.00 (m, 1 H, NCH*H*), 2.76–2.68 and 2.64–2.56 (2 × m, 1 H, NCH_2CHH), 2.54–2.46 (m, 1 H, NCH_2CHH), 1.45 and 1.05 (2 × br s, 9 H, $C(CH_3)_3$); ^{1}H NMR (400 MHz, DMSO-*d*$_6$) δ 7.59–7.55 (m, 1 H, HC_{Ar}), 7.42–7.19 (m, 6 H, 6 × HC_{Ar}), 7.11–7.03 (m, 1 H, HC_{Ar}), 6.96 and 6.78 (2 × d, *J* = 7.8 Hz, 1 H, HC_{Ar}), 5.00–4.74 (m, 2 H, NCH_2Ph), 4.16–3.98 (m, 2 H, NCH_2), 2.58–2.44 (NCH_2CH_2), 1.36 and 0.94 (2 × s, 9 H, $C(CH_3)_3$); ^{13}C NMR (101 MHz, $CDCl_3$) δ 175.7 and 175.3 (C=O amide), 155.2 and 154.4 (C=O carbamate), 142.7 and 142.6 (NC_{Ar} quat), 135.6 and 135.5 (C_{Ph} quat), 129.5 and 129.5 (C_{Ar}), 129.1 (C_{Ar} quat), 128.7 and 128.6 (2 × C_{Ph}), 127.7 (2 × C_{Ph}), 127.4 and 127.1 (C_{Ph}), 123.6 and 123.4 (C_{Ar}), 122.9 (C_{Ar}), 109.3 and 108.7 (C_{Ar}), 80.4 and 80.0 ($C(CH_3)_3$), 68.6 and 68.3 (NC quat), 47.3 and 45.8 (NCH_2), 43.9 and 43.8 (NCH_2Ph), 28.3 and 27.8 ($C(CH_3)_3$), 27.54 and 27.51 (NCH_2CH_2); ^{13}C NMR (101 MHz, DMSO-*d*$_6$) δ 175.3 and 175.2 (C=O amide), 154.8 and 154.4 (C=O carbamate), 143.0 and 142.8 (NC_{Ar} quat), 136.7 and 136.5 (C_{Ar} quat), 130.0 (C_{Ar}), 129.12, 129.06, 129.0 (3 × C_{Ar}), 128.2, 128.0, 127.8, 127.6 (2 × C_{Ar} and C_{Ar} quat), 124.4 and 124.1 (C_{Ar}), 123.2 (C_{Ar}), 109.6 and 109.3 (C_{Ar}), 80.2 and 79.5 ($C(CH_3)_3$), 68.8 and 68.3 (NC quat), 47.5 and 46.1 (NCH_2), 43.4 and 43.2 (NCH_2Ph), 28.5 and 27.9 ($C(CH_3)_3$), 27.5 and 27.3 (NCH_2CH_2); HRMS (ESI$^+$) *m/z* Calculated for $C_{22}H_{24}N_2O_3Na$ [M+Na] 387.1685; Found 387.1676.

(–)–*tert*-Butyl 1'-benzyl-2'-oxospiro[azetidine-2,3'-indoline]-1-carboxylate ((*S*)–338)

Following general procedure **D** on 0.2 mmol scale using cyclisation precursor **312** and cat. **394** with purification by flash chromatography (40% Et_2O/pentane) afforded *tert*-butyl 1'-benzyl-5'-fluoro-2'-oxospiro[azetidine-2,3'-indoline]-1-carboxylate **(*S*)–338** (68 mg, 94%) as a pale yellow solid. The characterisation data observed was consistent with the above. The *er* of the product was 3:97 [Chiralpak ID column, 90:10 *n*-hexane:*i*-PrOH, flow rate: 1 mL min^{-1}, 35 ºC, UV detection wavelength: 254 nm, *rac* **338** retention times 18.03 and 27.55 min]; $[\alpha]_D^{22} = -55$ (*c* = 0.62, CH_2Cl_2).

(+)–*tert*-Butyl 1'-benzyl-2'-oxospiro[azetidine-2,3'-indoline]-1-carboxylate ((*R*)–338)

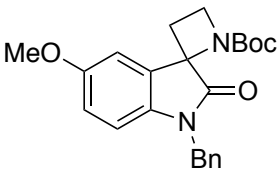
Following general procedure **D** on 0.2 mmol scale using cyclisation precursor **312** and cat. **395** with purification by flash chromatography (50% Et_2O/pentane) afforded *tert*-butyl 1'-benzyl-5'-fluoro-2'-oxospiro[azetidine-2,3'-indoline]-1-carboxylate **(*R*)–338** (65 mg, 89%) as a pale yellow solid. The characterisation data observed was consistent with the above. The *er* of the product was 96:4 [Chiralpak ID column, 90:10 *n*-hexane:*i*-PrOH, flow rate: 1 mL min^{-1}, 35 ºC, UV detection wavelength: 254 nm, *rac* **338** retention times 18.03 and 27.55 min]; $[\alpha]_D^{22} = +38^{\circ}$ (*c* = 1.83, Et_2O).

One-pot synthesis of (–)–*tert*-butyl 1'-benzyl-2'-oxospiro[azetidine-2,3'-indoline]-1-carboxylate (*S*)–338 on gram-scale



A solution of diazo **280** (1.25 g, 5.0 mmol) in toluene (30 mL) was slowly added over 10 min to a stirred solution of protected amine **52** (1.80 g, 10.0 mmol) and $Rh_2(esp)_2$ (9.5 mg, 12.5 μmol) in toluene (18 mL) at 25 ºC. The remaining diazo was quantitatively added using toluene (2.0 mL). After 30 min, cat. **394** (592 mg, 1.0 mmol) and $CsOH{\cdot}H_2O$ (4.20 g, 25 mmol) were added and the reaction mixture was stirred for 1 h at 25 ºC. The reaction mixture was filtered through celite, washing with Et_2O (200 mL) and concentrated under reduced pressure. Purification by flash chromatography (40% Et_2O/pentane) afforded *tert*-Butyl 1'-benzyl-2'-oxospiro[azetidine-2,3'-indoline]-1-carboxylate **(*S*)–338** (1.41 g, 77%) as a pale brown solid. The observed characterisation data was consistent with the above. The *er* of the product was 3:97 [Chiralpak ID column, 90:10 *n*-hexane:*i*-PrOH, flow rate: 1 mL min^{-1}, 35 ºC, UV detection wavelength: 254 nm, *rac* **338** retention times 18.03 and 27.55 min].

(±)–*tert*-Butyl 1'-benzyl-5'-methoxy-2'-oxospiro[azetidine-2,3'-indoline]-1-carboxylate (339)



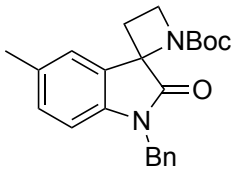
Following general procedure **B** on 0.25 mmol scale using diazo **297** and protected amine **52** in CH_2Cl_2. Purification by flash chromatography (40% EtOAc/hexane) afforded *tert*-butyl 1'-benzyl-5'-methoxy-2'-oxospiro[azetidine-2,3'-indoline]-1-carboxylate **339** (100 mg, quant) as an off-white solid. R_f 0.19 (30% EtOAc/hexane); mp = 166–167 ºC; ν_{max} (film)/cm^{-1} 2973, 2896, 1718 (C=O amide), 1702 (C=O carbamate), 1604, 1495, 1477, 1435, 1389, 1366, 1178, 1154, 1036; ^{1}H NMR (400 MHz, $CDCl_3$) δ 7.38–7.22 (m, 5 H, 5 × HC_{Ar}), 7.09 and 7.07 (2 × d, *J* = 2.5 Hz, 1 H, HC_{Ar}), 6.74 and 6.68 (2 × dd, *J* = 8.5, 2.5 Hz, 1 H, HC_{Ar}), 6.62 and 6.51 (2 × d, *J* = 8.5 Hz, 1 H, HC_{Ar}), 5.02 and 4.97 (2 × d, *J* = 15.5 Hz, 1 H, NC*H*HPh), 4.86 and 4.67 (2 × d, *J* = 15.5 Hz, 1 H, NCH*H*Ph), 4.37–4.24 (m, 1 H, NC*H*H), 4.15–3.98 (m, 1 H,

NCH*H*), 3.79 and 3.77 (2 × s, 3 H, OCH_3), 2.76–2.68 and 2.64–2.56 (2 × m, 1 H, NCH_2CHH), 2.53–2.44 (m, 1 H, NCH_2CHH), 1.45 and 1.08 (2 × s, 9 H, $C(CH_3)_3$); ^{13}C NMR (101 MHz, $CDCl_3$) δ 175.5 and 175.1 (C=O amide), 156.3 (OC_{Ar} quat), 155.3 and 154.5 (C=O carbamate), 136.1 and 136.0 (C_{Ar} quat), 135.7 and 135.6 (C_{Ar} quat), 130.4 and 129.8 (C_{Ar} quat), 128.73 and 128.69 (2 × C_{Ph}), 127.70 and 127.67 (2 × C_{Ph}), 127.4 and 127.2 (C_{Ph}), 114.1 and 114.0 (C_{Ar}), 111.0 and 110.5 (C_{Ar}), 109.8 and 109.3 (C_{Ar}), 80.5 and 80.1 ($C(CH_3)_3$), 69.0 and 68.8 (NC quat), 55.9 and 55.8 (OCH_3), 47.4 and 45.9 (NCH_2), 44.1 and 43.9 (NCH_2Ph), 28.4 and 27.9 ($C(CH_3)_3$), 27.7 (NCH_2CH_2); HRMS (FTMS – pAPCI) *m/z* Calculated for $C_{23}H_{25}N_2O_4^-$ [M–H]$^-$ 393.1820; Found 393.1813.

(–)–*tert*-Butyl 1'-benzyl-5'-methoxy-2'-oxospiro[azetidine-2,3'-indoline]-1-carboxylate ((*S*)–339)

Following general procedure **D** on 0.2 mmol scale using cyclisation precursor **313** and cat. **394** with purification by flash chromatography (30% EtOAc/pentane) afforded *tert*-Butyl 1'-benzyl-5'-methoxy-2'-oxospiro[azetidine-2,3'-indoline]-1-carboxylate **(*S*)–339** (69 mg, 87%) as a white solid. The characterisation data observed was consistent with the above. The *er* of the product was 4:96 [Chiralpak IA column, 80:20 *n*-hexane:*i*-PrOH, flow rate: 1 mL min^{-1}, 35 ºC, UV detection wavelength: 254 nm, *rac* **339** retention times 8.40 and 13.11 min]; $[\alpha]_D^{22} = -80$ (*c* = 0.45, Et_2O).

(±)–*tert*-Butyl 1'-benzyl-5'-methyl-2'-oxospiro[azetidine-2,3'-indoline]-1-carboxylate (340)



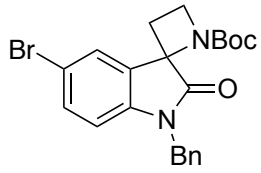
Following general procedure **B** on 0.25 mmol scale using diazo **298** and protected amine **52** in toluene. Purification by flash chromatography (40% Et_2O/pentane) afforded *tert*-butyl 1'-benzyl-5'-methyl-2'-oxospiro[azetidine-2,3'-indoline]-1-carboxylate **340** (55 mg, 58%) as a maroon solid. R_f 0.20 (40% Et_2O/pentane); mp = 65–66 ºC; ν_{max} (film)/cm^{-1} 3027, 2967, 2919, 2894, 1718 (C=O amide), 1701 (C=O carbamate), 1602, 1496, 1455, 1477, 1388, 1363, 1340, 1299, 1176, 1146, 969, 807, 775, 761, 731, 714, 697; ^1H NMR (400 MHz, DMSO-d_6) δ 7.42–7.19 (m, 6 H, 6 × HC_{Ar}), 7.07 and 7.02 (2 × ddd, *J* = 7.9, 1.6, 0.6 Hz, 1 H, HC_{Ar}), 6.83 and 6.65 (2 × d, *J* = 8.0 Hz, 1 H, HC_{Ar}), 4.95 (d, *J* = 15.6 Hz, 1 H, NC*H*HPh), 4.79 and 4.73 (2 × d, *J* = 15.9 Hz, 1 H, NCH*H*Ph), 4.15–3.97 (m, 2 H, NCH_2), 2.58–2.42 (m, 2 H, NCH_2CH_2), 2.28 and 2.26 (2 × s, 3 H, $ArCH_3$), 1.36 and 0.96 (2 × s, 9 H, $C(CH_3)_3$); ^{13}C NMR (101 MHz, DMSO-d_6) δ 174.8 and 174.6 (C=O amide), 154.3 and 154.0 (C=O carbamate), 140.1 and 140.0 (C_{Ar} quat), 136.3 and 136.0 (C_{Ar} quat), 131.8 (C_{Ar} quat), 129.6, 128.7, 128.5 and 128.4 (3 × C_{Ar} and C_{Ar} quat), 127.6 and 127.4 (2 × C_{Ar}), 127.2 and 127.1 (C_{Ar}), 124.5 and 124.3 (C_{Ar}), 108.9 and

108.6 (C_{Ar}), 79.7 and 79.0 ($C(CH_3)_3$), 68.4 and 67.9 (NC quat), 47.0 and 45.6 (NCH_2), 42.9 and 42.7 (NCH_2Ph), 28.0 and 27.5 ($C(CH_3)_3$), 27.0 and 26.8 (NCH_2CH_2), 20.1 ($ArCH_3$); HRMS (ESI^+) *m/z* Calculated for $C_{23}H_{26}N_2O_3Na$ [M+Na] 401.1841; Found 401.1848.

(–)–*tert*-Butyl 1'-benzyl-5'-methyl-2'-oxospiro[azetidine-2,3'-indoline]-1-carboxylate ((*S*)–340)

Following general procedure **D** on 0.2 mmol scale using cyclisation precursor **314** and cat. **394** with purification by flash chromatography (40% Et_2O/pentane) afforded *tert*-butyl 1'-benzyl-5'-methyl-2'-oxospiro[azetidine-2,3'-indoline]-1-carboxylate **(*S*)–340** (66 mg, 87%) as a pale yellow solid. The characterisation data observed was consistent with the above. The *er* of the product was 3:97 [Chiralpak ID column, 90:10 *n*-hexane:*i*-PrOH, flow rate: 1 mL min^{-1}, 35 ºC, UV detection wavelength: 254 nm, *rac* **340** retention times 15.79 and 24.07 min]; $[\alpha]_D^{22} = -25$ (*c* = 0.55, Et_2O).

(±)–*tert*-Butyl 1'-benzyl-5'-bromo-2'-oxospiro[azetidine-2,3'-indoline]-1-carboxylate (341)

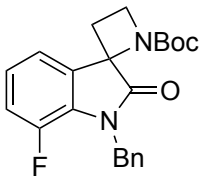


Following general procedure **B** on 0.25 mmol scale using diazo **299** and protected amine **52** in CH_2Cl_2. Purification by flash chromatography (30% to 40% Et_2O/pentane) afforded *tert*-butyl 1'-benzyl-5'-bromo-2'-oxospiro[azetidine-2,3'-indoline]-1-carboxylate **341** (76 mg, 68%) as a white solid. R_f 0.19 (30% Et_2O/pentane); mp = 64–65 ºC; ν_{max} (film)/cm^{-1} 2974, 2897, 1726 (C=O amide), 1702 (C=O carbamate), 1610, 1476, 1429, 1366, 1344, 1176, 1152, 734; ^1H NMR (400 MHz, $CDCl_3$) δ 7.59 and 7.58 (2 × d, *J* = 1.9 Hz, 1 H, HC_{Ar}), 7.40–7.16 (m, 6ii H, 6 × HC_{Ar}), 6.60 and 6.49 (2 × d, *J* = 8.3 Hz, 1 H, HC_{Ar}), 5.04 and 4.98 (2 × d, *J* = 15.7 Hz, 1 H, NC*H*HPh), 4.86 and 4.67 (2 × d, *J* = 15.7 Hz, NCH*H*Ph), 4.36–4.24 (m, 1 H, NC*H*H), 4.13–3.98 (m, 1 H, NCH*H*), 2.76–2.68 and 2.64–2.56 (m, 1 H, NCH_2CHH), 2.55–2.45 (NCH_2CHH), 1.45 and 1.09 (2 × br s, 9 H, $C(CH_3)_3$); ^{13}C NMR (101 MHz, $CDCl_3$) δ 175.3 and 174.8 (C=O amide), 155.2 and 154.3 (C=O carbamate), 141.8 and 141.7 (NC_{Ar} quat), 135.2 and 135.0 (C_{Ph} quat), 132.4 and 132.3 (C_{Ar}), 131.1 and 130.6 (C_{Ar} quat), 128.9 and 128.8 (2 × C_{Ph}), 127.9, 127.6, 127.13, 127.07 , 126.8 (3 × C_{Ph} and C_{Ar}), 115.7 and 115.5 (C_{Ar} quat), 110.9 and 110.3 (C_{Ar}), 80.8 and 80.4 ($C(CH_3)_3$), 68.4 and 68.1 (NC quat), 47.4 and 45.9 (NCH_2), 44.1 and 43.9 (NCH_2Ph), 28.3 and 27.9 ($C(CH_3)_3$), 27.6 and 27.5 (NCH_2CH_2); HRMS (FTMS + pAPCI) *m/z* Calculated for $C_{22}H_{23}N_2O_3{}^{79}Br^{\cdot+}$ $[M+H]^{\cdot+}$ 442.0887; Found 442.0902.

(–)–*tert*-Butyl 1'-benzyl-5'-bromo-2'-oxospiro[azetidine-2,3'-indoline]-1-carboxylate ((*S*)–341)

Following general procedure **D** on 0.2 mmol scale using cyclisation precursor **315** and cat. **394** with purification by flash chromatography (40% Et_2O/pentane) afforded *tert*-butyl 1'-benzyl-5'-bromo-2'-oxospiro[azetidine-2,3'-indoline]-1-carboxylate **(*S*)–341** (89 mg, 92%) as a white solid. The characterisation data observed was consistent with the above. The *er* of the product was 2:98 [Chiralpak IC column, 90:10 *n*-hexane:*i*-PrOH, flow rate: 1 mL min^{-1}, 35 ºC, UV detection wavelength: 254 nm, *rac* **341** retention times 14.60 and 18.19 min]; $[\alpha]_D^{22} = -79$ (*c* = 0.63, CH_2Cl_2).

(±)–*tert*-Butyl 1'-benzyl-7'-fluoro-2'-oxospiro[azetidine-2,3'-indoline]-1-carboxylate (342)



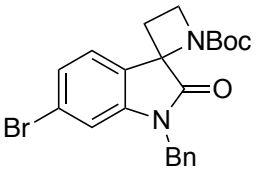
Following general procedure **B** using protected amine **52** (90 mg, 0.5 mmol) and diazo **303** (67 mg, 0.25 mmol) in CH_2Cl_2. Purification by flash chromatography (40% Et_2O/pentane then 2% Et_2O/CH_2Cl_2) afforded *tert*-butyl 1'-benzyl-7'-fluoro-2'-oxospiro[azetidine-2,3'-indoline]-1-carboxylate **342** (50 mg, 52%) as a white solid. R_f 0.16 (30% Et_2O/pentane); mp = 151–153 ºC; ν_{max} (film)/cm^{-1} 2974, 2933, 2896, 1727 (C=O carbamate), 1702 (C=O amide), 1633, 1487, 1472, 1365, 1345, 1245, 1170, 1153, 782, 727, 699; ^{1}H NMR (400 MHz, $CDCl_3$) δ 7.45–7.38 (m, 2 H, 2 × HC_{Ar}), 7.35–7.22 (m, 4 H, 4 × HC_{Ar}), 7.07–6.91 (m, 2 H, 2 × HC_{Ar}), 5.13–5.06 and 4.96–4.91 (2 × m, 2 H, NCH_2Ph), 4.36–4.24 (m, 1 H, NC*H*H), 4.12–3.98 (m, 1 H, NCH*H*), 2.75–2.68 and 2.63–2.55 (m, 1 H, NCH_2CHH), 2.52–2.43 (m, 1 H, NCH_2CHH), 1.45 and 1.04 (2 × s, 9 H, $(CH_3)_3$); ^{13}C NMR (101 MHz, $CDCl_3$) δ 175.6 and 175.1 (C=O amide), 155.2 and 154.2 (C=O carbamate), 148.4 and 146.0 (2 × d, J_{C-F} = 244.3 Hz, FC_{Ar} quat), 136.8 (C_{Ph} quat), 135.1 and 131.6 (2 × d, J_{C-F} = 2.7 Hz, C_{Ar} quat), 129.2 (d, J_{C-F} = 8.5 Hz, C_{Ar} quat), 128.6, 128.5, 128.1, 127.7 and 127.4 (5 × C_{Ph}), 123.7 and 123.6 (2 × d, J_{C-F} = 6.4 Hz, C_{Ar}), 119.6 and 119.4 (2 × d, J_{C-F} = 2.6 Hz, C_{Ar}), 117.8 and 117.7 (2 × d, J_{C-F} = 19.8 Hz, C_{Ar}), 80.8 and 80.3 ($C(CH_3)_3$), 68.6 and 68.4 (NC quat), 47.3 and 45.9 (NCH_2), 45.6 and 45.5 (NCH_2Ph), 28.3, 28.0, 27.9 and 27.8 ($C(CH_3)_3$ and NCH_2CH_2); ^{19}F{^{1}H} NMR (377 MHz, $CDCl_3$) δ –134.1, –134.2; HRMS (ESI^+) *m/z* Calculated for $C_{22}H_{27}N_3O_3F$ [M+NH_4] 400.2036; Found 400.2042.

(–)–*tert*-Butyl 1'-benzyl-7'-fluoro-2'-oxospiro[azetidine-2,3'-indoline]-1-carboxylate ((*S*)–342)

Following general procedure **D** on 0.2 mmol scale using cyclisation precursor **321** and cat. **394** with purification by flash chromatography (40% Et_2O/pentane) afforded *tert*-butyl 1'-benzyl-7'-fluoro-2'-oxospiro[azetidine-2,3'-indoline]-1-carboxylate **(*S*)–342** (41 mg, 56%) as a white solid. The characterisation data observed was consistent with the above. The *er* of the product

was 2:98 [Chiralpak ID column, 90:10 *n*-hexane:*i*-PrOH, flow rate: 1 mL min^{-1}, 35 ºC, UV detection wavelength: 254 nm, *rac* **342** retention times 12.32 and 18.44 min]; $[\alpha]_D^{22} = -32$ (*c* = 1.95, Et_2O).

(±)–*tert*-Butyl 1'-benzyl-6'-bromo-2'-oxospiro[azetidine-2,3'-indoline]-1-carboxylate (343)

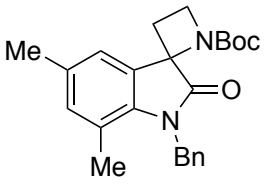


Following general procedure **B** on 0.25 mmol scale using diazo **301** and protected amine **52** in CH_2Cl_2. Purification by flash chromatography (40% Et_2O/pentane) afforded *tert*-butyl 1'-benzyl-6'-bromo-2'-oxospiro[azetidine-2,3'-indoline]-1-carboxylate **343** (79 mg, 71%) as a pale brown solid. R_f 0.17 (30% Et_2O/pentane); mp = 140–141 ºC; ν_{max} (film)/cm^{-1} 2974, 2931, 2896, 1727 (C=O amide), 1702 (C=O carbamate), 1608, 1487, 1428, 1389, 1366, 1338, 1178, 1154, 1114, 731; ^{1}H NMR (400 MHz, $CDCl_3$) δ 7.37–7.26 (m, 6 H, 6 × HC_{Ar}), 7.23 and 7.19 (2 × dd, *J* = 7.9, 1.6 Hz, 1 H, HC_{Ar}), 6.88 and 6.77 (2 × d, *J* = 1.6 Hz, 1 H, HC_{Ar}), 5.02, 4.96, 4.85 and 4.66 (4 × d, *J* = 15.9 or 15.5 Hz, 2 H, NCH_2Ph), 4.36–4.24 (m, 1 H, NC*H*H), 4.11–3.98 (m, 1 H, NCH*H*), 2.74–2.66 and 2.63–2.56 (m, 1 H, NCH_2CHH), 2.52–2.44 (m, 1 H, NCH_2CHH), 1.44 and 1.08 (2 × s, 9 H, $C(CH_3)_3$); ^{13}C NMR (101 MHz, $CDCl_3$) δ 175.7 and 175.2 (C=O amide), 154.3 (C=O carbamate), 144.1 and 144.0 (NC_{Ar} quat), 135.1 and 135.0 (C_{Ph} quat), 128.9 and 128.9 (2 × C_{Ph}), 128.1, 128.0, 128.0 and 127.1 (3 × C_{Ph} and C_{Ar} quat), 125.9 and 125.8 (C_{Ar}), 125.0 (C_{Ar}), 123.3 and 123.1 (BrC_{Ar} quat), 112.7 and 112.1 (C_{Ar}), 80.8 and 80.4 ($C(CH_3)_3$), 68.2 and 68.0 (NC quat), 47.4 and 45.9 (NCH_2), 44.1 and 44.0 (NCH_2Ph), 28.3 and 28.0 ($C(CH_3)_3$), 27.6 and 27.4 (NCH_2CH_2); HRMS (FTMS + pAPCI) *m/z* Calculated for $C_{22}H_{23}N_2O_3{}^{79}Br^{\cdot+}$ $[M]^{\cdot+}$ 442.0887; Found 442.0879.

(–)–*tert*-Butyl 1'-benzyl-6'-bromo-2'-oxospiro[azetidine-2,3'-indoline]-1-carboxylate ((*S*)–343)

Following general procedure **D** on 0.2 mmol scale using cyclisation precursor **319** and cat. **394** with purification by flash chromatography (40% Et_2O/pentane) afforded *tert*-butyl 1'-benzyl-6'-bromo-2'-oxospiro[azetidine-2,3'-indoline]-1-carboxylate **(*S*)–343** (76 mg, 85%) as a white solid. The characterisation data observed was consistent with the above. The *er* of the product was 4:96 [Chiralpak ID column, 90:10 *n*-hexane:*i*-PrOH, flow rate: 1 mL min^{-1}, 35 ºC, UV detection wavelength: 254 nm, *rac* **343** retention times 11.36 and 14.89 min]; $[\alpha]_D^{22} = -35$ (*c* = 0.8, Et_2O).

(±)–*tert*-Butyl 1'-benzyl-5',7'-dimethyl-2'-oxospiro[azetidine-2,3'-indoline]-1-carboxylate (344)

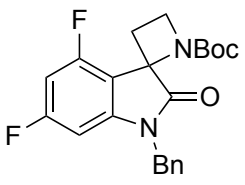


Following general procedure **B** using diazo **305** and protected amine **52** in CH_2Cl_2 on 0.25 mmol scale. Purification by flash chromatography (40% Et_2O/pentane) afforded *tert*-butyl 1'-benzyl-5',7'-dimethyl-2'-oxospiro[azetidine-2,3'-indoline]-1-carboxylate **344** (84 mg, 86%) as a white solid. R_f 0.28 (50% Et_2O/pentane); mp = 165–167 ºC; ν_{max} (film)/cm^{-1} 2895, 2973, 1718 (C=O amide), 1701 (C=O carbamate), 1604, 1480, 1454, 1389, 1365, 1347, 1252, 1169, 1153, 977, 859, 731; ^{1}H NMR (400 MHz, $CDCl_3$) δ 7.34–7.15 (m, 6 H, 6 × HC_{Ar}), 6.79 and 6.74 (2 × s, 1 H, HC_{Ar}), 5.28 and 5.27 (2 × d, J = 16.7 Hz, 1 H, NC*H*H), 5.08 and 4.98 (2 × d, J = 16.7 Hz, 1 H, NCH*H*), 4.36–4.21 (m, 1 H, NC*H*H), 4.16–4.09 and 4.07–3.98 (2 × m, 1 H, NCH*H*), 2.79–2.71 and 2.63–2.56 (2 × m, 1 H, NCH_2CHH), 2.54–2.43 (m, 1 H, NCH_2CHH), 1.45 and 1.16 (2 × s, 9 H, $C(CH_3)_3$); ^{13}C NMR (101 MHz, $CDCl_3$) δ 176.7 and 176.3 (C=O amide), 155.2 and 154.6 (C=O carbamate), 138.3 and 138.1 (C_{Ar} quat), 137.5 (C_{Ar} quat), 134.1 and 133.7 (C_{Ar}), 132.6 (C_{Ar} quat), 130.1 and 129.5 (C_{Ar} quat), 128.7 (2 × C_{Ph}), 127.2 and 126.9 (C_{Ph}), 125.9 (2 × C_{Ph}), 122.4 and 122.1 (C_{Ar}), 119.6 and 119.3 (C_{Ar} quat), 80.4 and 80.0 ($C(CH_3)_3$), 68.4 and 68.1 (NC quat), 47.3 and 45.9 (NCH_2), 45.1 (NCH_2Ph), 28.4, 28.1, 28.0 and 27.8 ($C(CH_3)_3$ and NCH_2CH_2), 20.72 and 20.67 ($ArCH_3$), 18.5 ($ArCH_3$); HRMS (FTMS + pAPCI) *m/z* Calculated for $C_{19}H_{21}N_2O^+$ $[M–(C_5H_9O_2)+2H]^+$ 293.1648; Found 293.1641.

(–)–*tert*-Butyl 1'-benzyl-5',7'-dimethyl-2'-oxospiro[azetidine-2,3'-indoline]-1-carboxylate ((*S*)–344)

Following general procedure **E** on 0.2 mmol scale using diazo **305**, protected amine **52** and cat. **394** with purification by flash chromatography (40% to 50% Et_2O/pentane) afforded *tert*-butyl 1'-benzyl-5',7'-dimethyl-2'-oxospiro[azetidine-2,3'-indoline]-1-carboxylate **(*S*)–344** (37 mg, 47%) as a white solid. The characterisation data observed was consistent with the above. The *er* of the product was 6:94 [Chiralpak IE column, 90:10 *n*-hexane:*i*-PrOH, flow rate: 1 mL min^{-1}, 35 ºC, UV detection wavelength: 254 nm, *rac* **344** retention times 26.88 and 33.08 min]; $[\alpha]_D^{22} = -40$ (c = 0.2, Et_2O).

(±)–*tert*-Butyl 1'-benzyl-4',6'-difluoro-2'-oxospiro[azetidine-2,3'-indoline]-1-carboxylate (345)



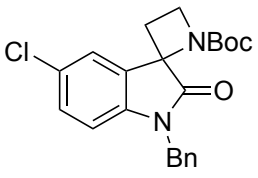
Following general procedure **B** using diazo **304** and protected amine **52** on in CH_2Cl_2 on 0.25 mmol scale. Purification by flash chromatography (30% Et_2O/pentane) afforded *tert*-butyl 1'-benzyl-4',6'-difluoro-2'-oxospiro[azetidine-2,3'-indoline]-1-carboxylate **345** (89 mg, 89%) as a

white solid. R_f 0.30 (30% Et_2O/pentane); mp = 152–154 ºC; ν_{max} (film)/cm^{-1} 2974, 2932, 2899, 1735 (C=O amide), 1701 (C=O carbamate), 1638, 1611, 1502, 1459, 1366, 1342, 1262, 1133, 1103, 967, 829, 700; ^{1}H NMR (400 MHz, $CDCl_3$) δ 7.37–7.25 (m, 5 H, 5 × HC_{Ph}), 6.54–6.42 (m, 1 H, HC_{Ar}), 6.35–6.31 and 6.23–6.19 (2 × m, 1 H, HC_{Ar}), 4.96 and 4.95 (2 × d, J = 15.5 Hz, 1 H, NC*H*H), 4.84 and 4.71 (2 × d, J = 15.5 Hz, NCH*H*Ph), 4.28–4.07 (m, 2 H, NC*H*$_2$), 2.78–2.60 (m, 2 H, NCH_2CH_2), 1.44 and 1.09 (2 × s, 9 H, $C(CH_3)_3$); ^{13}C NMR (101 MHz, $CDCl_3$) δ 175.2 and 174.9 (C=O amide), 165.5 and 163.0 (FC_{Ar} quat), 158.0 and 156.2 (FC_{Ar} quat), 154.8 and 153.9 (C=O carbamate), 145.6 (C_{Ar} quat), 134.8 and 134.7 (C_{Ph} quat), 129.0 and 128.9 (2 × C_{Ph}), 128.1 and 127.8 (C_{Ph}), 127.7 and 127.2 (2 × C_{Ph}), 98.4, 98.3, 98.1, 97.9 (C_{Ar}), 94.8 and 94.2 (2 × dd, $J_{C–F}$ = 27.3, 3.0 Hz, C_{Ar}), 80.7 and 80.2 ($C(CH_3)_3$), 66.9 and 66.6 (NC quat), 47.1 and. 45.5 (NCH_2), 44.5 and 44.4 (NCH_2Ph), 28.3 and 27.9 ($C(CH_3)_3$), 25.7 and 25.4 (NCH_2CH_2); ^{19}F{^{1}H} NMR (377 MHz, $CDCl_3$) δ –105.7 and –106.1 (2 × d, $J_{F–F}$ = 8.1 Hz), –116.5 and –117.4 (2 × d, $J_{F–F}$ = 8.1 Hz); HRMS (FTMS – pAPCI) *m/z* Calculated for $C_{22}H_{21}N_2O_3^-$ [M–H]$^-$ 399.1515; Found 399.1510.

(–)–*tert*-Butyl 1'-benzyl-4',6'-difluoro-2'-oxospiro[azetidine-2,3'-indoline]-1-carboxylate ((*S*)–345)

Following general procedure **E** on 0.2 mmol scale using diazo **305,** protected amine **52** and cat. **394** with purification by flash chromatography (30% Et_2O/pentane) afforded *tert*-butyl 1'-benzyl-4',6'-difluoro-2'-oxospiro[azetidine-2,3'-indoline]-1-carboxylate **(*S*)–345** (36 mg, 45%) as a white solid. The characterisation data observed was consistent with the above. The *er* of the product was 15:85 [Chiralpak ID column, 90:10 *n*-hexane:*i*-PrOH, flow rate: 1 mL min^{-1}, 35 ºC, UV detection wavelength: 254 nm, *rac* **345** retention times 9.92 and 11.34 min]; $[\alpha]_D^{22} = -28$ (*c* = 0.85, Et_2O).

(±)–*tert*-Butyl 1'-benzyl-5'-chloro-2'-oxospiro[azetidine-2,3'-indoline]-1-carboxylate (346)



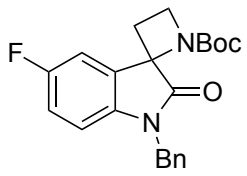
Following general procedure **C** on 0.1 mmol scale using cyclisation precursor **316**. Purification by flash chromatography (30% Et_2O/pentane) afforded *tert*-butyl 1'-benzyl-5'-chloro-2'-oxospiro[azetidine-2,3'-indoline]-1-carboxylate **346** (22 mg, 47%) as an off-white solid. R_f 0.20 (30% Et_2O/pentane); mp = 62–63 ºC; ν_{max} (film)/cm^{-1} 2974, 2930, 2896, 1700 (br s, 2 × C=O), 1614, 1484, 1364, 1297, 1260, 1148, 1077, 969, 813, 738, 701; ^{1}H NMR (400 MHz, DMSO-d_6) δ 7.74 and 7.72 (2 × d, J = 2.2 Hz, 1 H, HC_{Ar}), 7.40–7.22 (m, 6 H, 6 × HC_{Ar}), 6.99 and 6.80 (2 × d, J = 8.4 Hz, 1 H, HC_{Ar}), 5.04–4.76 (m, 2 H, NCH_2Ph), 4.14–3.96 (m, 2 H, NCH_2), 2.60–2.43 (m, 2 H, NCH_2CH_2), 1.37 and 0.96 (2 × s, 9 H, $C(CH_3)_3$); ^{13}C NMR

(101 MHz, DMSO-d_6) δ 174.6 and 174.4 (C=O amide), 154.3 and 153.6 (C=O carbamate), 141.4 and 141.2 (C_{Ar} quat), 135.9 and 135.6 (C_{Ph} quat), 130.6 and 130.4 (C_{Ar} quat), 129.3 (br s, C_{Ar}), 128.6 and 128.5 (2 × C_{Ar}), 127.7 and 127.6 (2 × C_{Ar}), 127.3, 127.1 and 126.9 (C_{Ar} quat and C_{Ar}), 124.3 and 124.1 (C_{Ar}), 110.6 and 110.4 (C_{Ar}), 79.9 and 79.2 ($C(CH_3)_3$), 68.1 and 67.6 (NC quat), 47.1 and 45.7 (NCH_2), 43.0 and 42.8 (NCH_2Ph), 27.9 and 27.4 ($C(CH_3)_3$), 26.7 and 26.6 (NCH_2CH_2); HRMS (ESI^+) *m/z* Calculated for $C_{22}H_{23}N_2O_3NaCl$ [M+Na] 421.1295; Found 421.1284.

(–)–*tert*-Butyl 1'-benzyl-5'-chloro-2'-oxospiro[azetidine-2,3'-indoline]-1-carboxylate ((*S*)–346)

Following general procedure **D** on 0.2 mmol scale using cyclisation precursor **316** and cat. **394** with purification by flash chromatography (40% Et_2O/pentane) afforded *tert*-butyl 1'-benzyl-5'-chloro-2'-oxospiro[azetidine-2,3'-indoline]-1-carboxylate **(*S*)–346** (55 mg, 69%) as a pale yellow solid. The characterisation data observed was consistent with the above. The *er* of the product was 2:98 [Chiralpak IE column, 90:10 *n*-hexane:*i*-PrOH, flow rate: 1 mL min^{-1}, 35 ºC, UV detection wavelength: 254 nm, *rac* **346** retention times 16.27 and 20.00 min]; $[\alpha]_D^{22} = -95$ (*c* = 0.65, Et_2O).

(±)–*tert*-Butyl 1'-benzyl-5'-fluoro-2'-oxospiro[azetidine-2,3'-indoline]-1-carboxylate (347)



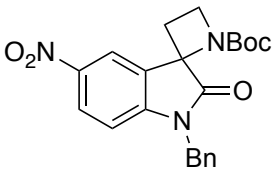
Following general procedure **C** on 0.1 mmol scale using cyclisation precursor **317**. Purification by flash chromatography (CH_2Cl_2 to 2% Et_2O/CH_2Cl_2 to 4% Et_2O/CH_2Cl_2) afforded *tert*-butyl 1'-benzyl-5'-fluoro-2'-oxospiro[azetidine-2,3'-indoline]-1-carboxylate **347** (18 mg, 66%) as a white solid. R_f 0.10 (CH_2Cl_2); mp = 142–145 ºC; ν_{max} (film)/cm^{-1} 2974, 2930, 1722 (2 × C=O), 1491, 1457, 1364, 1156; ^1H NMR (400 MHz, $CDCl_3$) δ 7.37–7.19 (m, 6 H, 6 × HC_{Ar}), 6.92 and 6.85 (2 × td, *J* = 8.8, 2.5 Hz, 1 H, HC_{Ar}), 6.64 and 6.53 (2 × dd, *J* = 8.6, 4.0 Hz, 1 H, HC_{Ar}), 5.04 and 4.98 (2 × d, *J* = 15.8 and 15.5 Hz, 1 H, NC*H*HPh), 4.87 and 4.68 (2 × d, *J* = 15.8 and 15.5 Hz, NCH*H*Ph), 4.38–4.26 (m, 1 H, NC*H*H), 4.12–3.99 (m, 1 H, NCH*H*), 2.76–2.57 (m, 1 H, NCH_2CHH), 2.54–2.45 (m, 1 H, NCH_2CHH), 1.45 and 1.09 (2 × s, 9 H, $C(CH_3)_3$); ^{13}C NMR (101 MHz, $CDCl_3$) δ 175.6 and 175.2 (C=O amide), 159.51 and 159.42 (2 × d, $J_{C–F}$ = 241.7 Hz, FC_{Ar} quat), 155.3 and 154.3 (C=O carbamate), 138.6 and 138.4 (C_{Ar} quat), 135.3 and 135.2 (C_{Ar} quat), 130.7 and 130.1 (2 × d, $J_{C–F}$ = 7.6 Hz, C_{Ar} quat), 128.8 (2 × C_{Ar}), 127.9, 127.6, 127.5 and 127.1 (3 × C_{Ar}), 115.8 and 115.7 (2 × d, $J_{C–F}$ = 23.4 Hz, C_{Ar}), 111.8 and 111.6 (2 × d, $J_{C–F}$ = 25.1 Hz, C_{Ar}), 110.0 and 109.4 (2 × d, $J_{C–F}$ = 8.0 Hz, C_{Ar}), 80.8 and 80.3 ($C(CH_3)_3$), 68.7 and 68.4 (NC quat), 47.4 and 45.9 (NCH_2), 44.1 and 44.0 (NCH_2Ph), 28.3 and 27.9 ($C(CH_3)_3$),

27.62 and 26.55 (NCH_2CH_2); ^{19}F NMR (377 MHz, $CDCl_3$) δ –119.9 and –120.2; HRMS (ESI^+) *m/z* Calculated for $C_{22}H_{27}N_3O_3F$ [M+NH_4] 400.2036; Found 400.2030.

(–)–*tert*-Butyl 1'-benzyl-5'-fluoro-2'-oxospiro[azetidine-2,3'-indoline]-1-carboxylate ((*S*)–347)

Following general procedure **D** on 0.2 mmol scale using cyclisation precursor **317** and cat. **394** with purification by flash chromatography (40% Et_2O/pentane) afforded *tert*-butyl 1'-benzyl-5'-fluoro-2'-oxospiro[azetidine-2,3'-indoline]-1-carboxylate **(*S*)–347** (71 mg, 92%) as a white solid. The characterisation data observed was consistent with the above. The *er* of the product was 2:98 [Chiralpak ID column, 90:10 *n*-hexane:*i*-PrOH, flow rate: 1 mL min^{-1}, 35 ºC, UV detection wavelength: 254 nm, *rac* **347** retention times 14.06 and 34.18 min]; $[\alpha]_D^{22} = -37$ (*c* = 0.38, Et_2O).

(±)–*tert*-Butyl 1'-benzyl-5'-nitro-2'-oxospiro[azetidine-2,3'-indoline]-1-carboxylate (348)



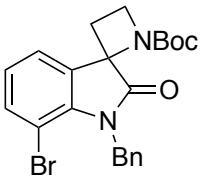
Following general procedure **C** using cyclisation intermediate **318** on 0.1 mmol scale. Purification by flash chromatography (CH_2Cl_2 to 1% to 2% Et_2O/CH_2Cl_2) afforded *tert*-butyl 1'-benzyl-5'-nitro-2'-oxospiro[azetidine-2,3'-indoline]-1-carboxylate **348** (6 mg, 15%) as a white solid. R_f 0.16 (CH_2Cl_2); mp = 75–77 ºC; ν_{max} (film)/cm^{-1} 2976, 1737 (C=O amide), 1702 (C=O carbamate), 1616, 1521, 1489, 1388, 1367, 1335 (N-O stretch), 1176, 1156; ^1H NMR (400 MHz, $CDCl_3$) δ 8.38 and 8.37 (2 × d, *J* = 2.2 Hz, 1 H, HC_{Ar}), 8.22 and 8.14 (2 × dd, *J* = 8.6, 2.2 Hz, HC_{Ar}), 7.39–7.28 (m, 5 H, 5 × HC_{Ph}), 6.84 and 6.70 (2 × d, *J* = 8.6 Hz, 1 H, HC_{Ar}), 5.12 (d, *J* = 15.5 Hz, 0.5 H, NC*H*HPh), 5.07 (d, *J* = 16.0 Hz, 0.5 H, NCH*H*Ph), 4.92 (d, *J* = 16.0 Hz, 0.5 H, NCH*H*Ph), 4.73 (d, *J* = 15.5 Hz, 0.5 H, NC*H*HPh), 4.41–4.31 (m, 1 H, NC*H*H), 4.18–4.05 (m, 1 H, NCH*H*), 2.78–2.55 (m, 2 H, NCH_2CH_2), 1.45 and 1.07 (2 × s, 9 H, $C(CH_3)_3$); ^{13}C NMR (101 MHz, $CDCl_3$) δ 176.1 (C=O amide), 155.2 (C=O carbamate), 148.3 (NC_{Ar} quat), 143.8 and 143.7 (NO_2CAr quat), 134.5 and 134.3 (C_{Ph} quat), 130.0 and 129.4 (C_{Ar} quat), 129.1 and 129.0 (2 × C_{Ph}), 128.3 and 128.0 (C_{Ph}), 127.7 and 127.2 (2 × C_{Ph}), 126.7 and 126.6 (C_{Ar}), 119.8 and 119.5 (C_{Ar}), 109.1 and 108.4 (C_{Ar}), 81.3 and 80.8 ($C(CH_3)_3$), 67.9 and 67.5 (NC quat), 47.4 and 46.0 (NCH_2), 44.4 and 44.3 (NCH_2Ph), 28.3 and 27.9 ($C(CH_3)_3$), 27.6 and 27.3 (NCH_2CH_2); HRMS (FTMS – pAPCI) *m/z* Calculated for $C_{22}H_{23}N_3O_5Cl^-$ [M+Cl]$^-$ 444.1332; Found 444.1331.

(–)–*tert*-Butyl 1'-benzyl-5'-nitro-2'-oxospiro[azetidine-2,3'-indoline]-1-carboxylate ((*S*)–348)

Following general procedure **D** on 0.1 mmol scale using cyclisation precursor **318** and cat. **394** (40 mol%) with 18 h reaction time and purification by flash chromatography (50%

Et_2O/pentane) afforded *tert*-Butyl 1'-benzyl-5'-nitro-2'-oxospiro[azetidine-2,3'-indoline]-1-carboxylate **(*S*)–348** (19 mg, 46%) as a white solid. The characterisation data observed was consistent with the above. The *er* of the product was 8:92 [Chiralpak IF column, 90:10 *n*-hexane:*i*-PrOH, flow rate: 1 mL min^{-1}, 35 ºC, UV detection wavelength: 254 nm, *rac* **348** retention times 14.65 and 16.43 min]; $[\alpha]_D^{22} = -90$ (*c* = 0.20, Et_2O).

(±)–*tert*-Butyl 1'-benzyl-7'-bromo-2'-oxospiro[azetidine-2,3'-indoline]-1-carboxylate (349)

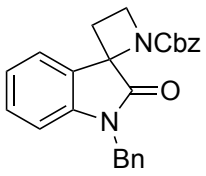


Following general procedure **C** on 0.1 mmol scale using cyclisation precursor **320** and in toluene. Purification by flash chromatography (40% Et_2O/pentane) afforded *tert*-butyl 1'-benzyl-7'-bromo-2'-oxospiro[azetidine-2,3'-indoline]-1-carboxylate **349** (11 mg, 25%) as a white solid. R_f 0.30 (40% Et_2O/pentane); mp = 67–68 ºC; ν_{max} (film)/cm^{-1} 2973, 2933, 1731 (C=O amide), 1703 (C=O carbamate), 1612, 1450, 1390, 1366, 1346, 1161, 1123, 731; ^1H NMR (400 MHz, $CDCl_3$) δ 7.47–7.38 (m, 2 H, 2 × HC_{Ar}), 7.35–7.21 (m, 5 H, 5 × HC_{Ph}), 7.01–6.92 (m, 1 H, HC_{Ar}), 5.50–5.30 (m, 2 H, NCH_2Ph), 4.37–4.24 (m, 1 H, NC*H*H), 4.13–3.99 (m, 1 H, NCH*H*), 2.76–2.69 and 2.64–2.56 (m, 1 H, NCH_2CHH), 2.55–2.44 (m, 1 H, NCH_2CHH), 1.44 and 1.15 (2 × s, 9 H, $C(CH_3)_3$); ^{13}C NMR (101 MHz, $CDCl_3$) δ 176.6 and 176.2 (C=O amide), 155.2 and 154.2 (C=O carbamate), 140.3 (NC_{Ar} quat), 137.3 and 137.2 (C_{Ph} quat), 135.5 and 135.4 (C_{Ar}), 132.5 and 132.0 (C_{Ar} quat), 128.49 and 128.5 (2 × C_{Ph}), 127.2 and 126.9 (C_{Ph}), 126.7 and 126.4 (2 × C_{Ph}), 124.32 and 124.27 (C_{Ar}), 122.9 and 122.7 (C_{Ar}), 102.7 and 102.3 (BrC_{Ar} quat), 80.8 and 80.5 ($C(CH_3)_3$), 68.0 and 67.8 (NC quat), 47.3 and 45.9 (NCH_2), 44.7 and 44.6 (NCH_2Ph), 28.3, 28.1, 28.0 and 27.8 ($C(CH_3)_3$ and NCH_2CH_2); HRMS (FTMS + pAPCI) *m/z* Calculated for $C_{22}H_{23}N_2O_3{}^{79}Br^{\cdot+}$ $[M]^{\cdot+}$ 442.0887; Found 442.0874.

(+)–*tert*-Butyl 1'-benzyl-7'-bromo-2'-oxospiro[azetidine-2,3'-indoline]-1-carboxylate ((*S*)–349)

Following general procedure **D** on 0.1 mmol scale using cyclisation precursor **320** and cat. **394** with purification by flash chromatography (40% Et_2O/pentane) afforded *tert*-butyl 1'-benzyl-7'-bromo-2'-oxospiro[azetidine-2,3'-indoline]-1-carboxylate **(*S*)–349** (40 mg, 91%) as a white solid. The characterisation data observed was consistent with the above. The *er* of the product was 2:98 [Chiralpak ID column, 90:10 *n*-hexane:*i*-PrOH, flow rate: 1 mL min^{-1}, 35 ºC, UV detection wavelength: 254 nm, *rac* **349** retention times 14.33 and 24.52 min]; $[\alpha]_D^{22} = +8$ (*c* = 0.5, Et_2O).

(±)–Benzyl 1'-benzyl-2'-oxospiro[azetidine-2,3'-indoline]-1-carboxylate (350)

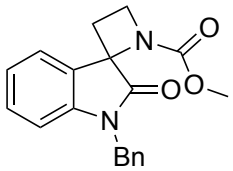


Following general procedure **B** on 0.5 mmol scale using diazo **280** and protected amine **63** in toluene. Purification by flash chromatography (50% to 70% Et_2O/hexane) afforded benzyl 1'-benzyl-2'-oxospiro[azetidine-2,3'-indoline]-1-carboxylate **350** (113 mg, 52%) as a pale brown solid. R_f 0.30 (50% EtOAc/hexane); mp = 45–48 ºC; ν_{max} (film)/cm^{-1} 3029, 2961, 2894, 1702 (br s, 2 × C=O), 1612, 1466, 1454, 1402, 1342, 1177, 1130, 1098, 747, 729, 693; ^{1}H NMR (400 MHz, DMSO-d_6) δ 7.67–7.60 (m, 1 H, HC_{Ar}), 7.42–7.21 (m, 7 H, 7 × HC_{Ar}), 7.19–7.05 (m, 4 H, 4 × HC_{Ar}), 6.86 and 6.78 (2 × d, J = 7.8 Hz, 1 H, HC_{Ar}), 6.75–6.71 (m, 1 H, HC_{Ar}), 5.08–4.92 (m, 2 H, OCH_2Ph), 4.85–4.70 (m, 2 H, NCH_2Ph), 4.24–4.08 (m, 2 H, NCH_2), 2.66–2.52 (m, 2 H, NCH_2CH_2); ^{13}C NMR (101 MHz, DMSO-d_6) δ 174.5 and 174.4 (C=O amide), 154.4 and 154.1 (C=O carbamate), 142.3 (C_{Ar} quat), 136.4, 136.2 and 135.9 (2 × C_{Ar} quat), 129.9 and 129.7 (C_{Ar} quat), 128.6, 128.47, 128.45, 128.3, 128.1, 128.0, 127.7, 127.4, 127.3, 127.03, 126.95 (10 × C_{Ar}), 126.2 (C_{Ar}), 124.1 and 124.0 (C_{Ar}), 123.0 and 122.8 (C_{Ar}), 109.3 (C_{Ar}), 68.3 and 67.9 (NC quat), 66.1 and 65.5 (OCH_2Ph), 47.0 and 45.9 (NCH_2Ph), 42.8 (NCH_2), 27.6 and 27.4 (NCH_2CH_2); HRMS (ESI$^+$) *m/z* Calculated for $C_{25}H_{23}N_2O_3$ [M+H] 399.1709; Found 399.1720.

(–)–Benzyl 1'-benzyl-2'-oxospiro[azetidine-2,3'-indoline]-1-carboxylate ((*S*)–350)

Following general procedure **D** on 0.2 mmol scale using cyclisation precursor **322** cat. **394** with purification by flash chromatography (30% to 40% EtOAc/hexane) afforded benzyl 1'-benzyl-2'-oxospiro[azetidine-2,3'-indoline]-1-carboxylate **(*S*)–350** (71 mg, 89%) as a white gummy solid. The characterisation data observed was consistent with the above. The *er* of the product was 95:5 [Chiralpak IA column, 80:20 *n*-hexane:*i*-PrOH, flow rate: 1 mL min^{-1}, 35 ºC, UV detection wavelength: 254 nm, *rac* **350** retention times 16.03 and 15.14 min]; $[\alpha]_D^{22} = -49$ (c = 0.84, Et_2O).

(±)–Methyl 1'-benzyl-2'-oxospiro[azetidine-2,3'-indoline]-1-carboxylate (351)



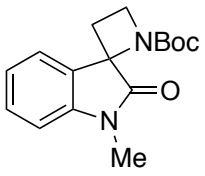
Following general procedure **B** on 0.5 mmol scale using diazo **280** and protected amine **331** in toluene. Purification by flash chromatography (20% to 30% EtOAc/pentane) afforded methyl 1'-benzyl-2'-oxospiro[azetidine-2,3'-indoline]-1-carboxylate **351** (63 mg, 39%) as a pink solid. R_f 0.29 (40% EtOAc/pentane); mp = 102–104 ºC; ν_{max} (film)/cm^{-1} 3030, 2960, 2896, 1700 (br s, 2 × C=O), 1614, 1450, 1349, 1182, 753, 697; ^{1}H NMR (400 MHz, $CDCl_3$) δ 7.51–7.47 (m, 1 H, HC_{Ar}), 7.39–7.15 (m, 6 H, 6 × HC_{Ar}), 7.12–7.04 (m, 1 H, HC_{Ar}), 6.70 and 6.62 (2 × d, J = 7.8 Hz, 1 H, HC_{Ar}), 5.19, 5.03, 4.88 and 4.64 (4 × d, J = 15.9 Hz, NCH_2Ph), 4.42–4.31 (m, 1 H, NC*H*H), 4.18–4.10 (m, 1 H, NCH*H*), 3.68 and 3.43 (2 × s, 3 H, OCH_3), 2.78–2.67 (m,

1 H, NCH_2CHH), 2.61–2.51 (m, 1 H, NCH_2CHH); ^{13}C NMR (101 MHz, $CDCl_3$) δ 175.3 and 175.0 (C=O amide), 155.9 and 155.7 (C=O carbamate), 142.7 and 142.4 (C_{Ar} quat), 135.5 and 135.3 (C_{Ar} quat), 129.8 (C_{Ar}), 128.8 and 128.7 (2 × C_{Ar}), 127.7, 127.4, 127.2 and 127.0 (4 × C_{Ar}), 123.6 (C_{Ar}), 123.1 and 123.1 (C_{Ar} quat), 109.5 and 109.2 (C_{Ar}), 68.7 and 68.3 (NC quat), 52.5 and 52.3 (OCH_3), 47.2 and 46.2 (NCH_2Ph), 43.9 and 43.7 (NCH_2), 28.3 and 27.9 (NCH_2CH_2); HRMS (ESI^+) *m/z* Calculated for $C_{19}H_{19}N_2O_3$ [M+H] 323.1396; Found 323.1383.

(–)–Methyl 1'-benzyl-2'-oxospiro[azetidine-2,3'-indoline]-1-carboxylate ((*S*)–351)

Following general procedure **D** on 0.1 mmol scale using cyclisation precursor **323** cat. **394** with purification by flash chromatography (40% EtOAc/hexane) afforded methyl 1'-benzyl-2'-oxospiro[azetidine-2,3'-indoline]-1-carboxylate **(*S*)–351** (22 mg, 69%) as a white solid. The characterisation data observed was consistent with the above. The *er* of the product was 89:11 [Chiralpak IA column, 80:20 *n*-hexane:*i*-PrOH, flow rate: 1 mL min^{-1}, 35 ºC, UV detection wavelength: 254 nm, *rac* **351** retention times 8.79 and 9.89 min]; $[\alpha]_D^{22} = -65$ (*c* = 1.05, CH_2Cl_2).

(±)–*tert*-Butyl 1'-methyl-2'-oxospiro[azetidine-2,3'-indoline]-1-carboxylate (352)

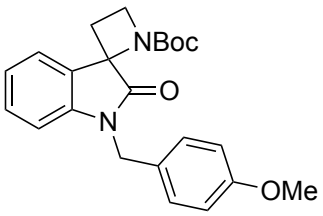


A solution of diazo **273** (87 mg, 0.5 mmol) in CH_2Cl_2 (2.5 mL) was slowly added over 10 min to a stirred solution of *tert*-butyl (2-chloroethyl)carbamate **52** (180 mg, 1.0 mmol) and $Rh_2(esp)_2$ (1.9 mg, 2.5 μmol) in CH_2Cl_2 (2.0 mL) at 25 ºC. The remaining diazo **273** was dissolved in CH_2Cl_2 (0.5 mL) to ensure quantitative transfer. After 30 min, $CsOH·H_2O$ (168 mg, 2.0 mmol) and tetrabutylammonium bromide (16 mg, 10 mol%) were added and the reaction mixture was stirred for 3 h at 25 ºC. The reaction mixture was filtered through celite, washing with EtOAc (25 mL) and concentrated under reduced pressure. Purification by flash chromatography (0 to 50% EtOAc/heptane) afforded *tert*-butyl 1'-methyl-2'-oxospiro[azetidine-2,3'-indoline]-1-carboxylate **352** (73 mg, 51%) as a colourless gum. R_f 0.30 (50% EtOAc/heptane); ν_{max} (film)/cm^{-1} 2892, 2974, 1700 (br s, 2 × C=O), 1614, 1495, 1364, 1249, 1126, 1014, 969, 749, 693; ^1H NMR (400 MHz, DMSO-d_6, 373 K) δ 7.53 (d, *J* = 7.3 Hz, 1 H, HC_{Ar}), 7.34 (td, *J* = 7.7, 1.1 Hz, 1 H, HC_{Ar}), 7.10 (t, *J* = 7.5 Hz, 1 H, HC_{Ar}), 6.96 (d, *J* = 7.8 Hz, 1 Hz, HC_{Ar}), 4.08–3.97 (m, 2 H, NCH_2), 3.13 (s, 3 H, NCH_3), 2.52–2.41 (m, NCH_2CH_2), 1.44–0.97 (br d, 9 H, $C(CH_3)_3$); ^{13}C NMR (101 MHz, DMSO-d_6, 373 K) δ 174.0 (C=O amide), 153.4 (C=O carbamate), 143.2 (NC_{Ar} quat), 129.0 (C_{Ar}), 128.3 (C_{Ar} quat), 122.8 (C_{Ar}), 121.9 (C_{Ar}), 107.6 (C_{Ar}), 78.4 ($C(CH_3)_3$), 45.1 (NCH_2), 27.2 ($C(CH_3)_3$), 26.1 (NCH_2CH_2), 25.3 (NCH_3); HRMS (ESI^+) *m/z* Calculated for $C_{18}H_{23}N_3O_3Na$ [M+CH_3CN+Na] 352.1637; Found 352.1625.

(–)–*tert*-Butyl 1'-methyl-2'-oxospiro[azetidine-2,3'-indoline]-1-carboxylate ((*S*)–352)

Following general procedure **D** on 0.2 mmol scale using cyclisation precursor **324** and cat. **394** with purification by flash chromatography (10% Et_2O/CH_2Cl_2) afforded *tert*-butyl 1'-methyl-2'-oxospiro[azetidine-2,3'-indoline]-1-carboxylate **(*S*)–352** (57 mg, 98%) as a colourless gum. The characterisation data observed was consistent with the above. The *er* of the product was 97:3 [Chiralpak IA column, 95:5 *n*-hexane:*i*-PrOH, flow rate: 1 mL min^{-1}, 35 ºC, UV detection wavelength: 254 nm, *rac* **352** retention times 11.51 and 12.95 min]; $[\alpha]_D^{22} = -50$ (*c* = 2.4, Et_2O).

(±)–*tert*-Butyl 1'-(4-methoxybenzyl)-2'-oxospiro[azetidine-2,3'-indoline]-1-carboxylate (353)



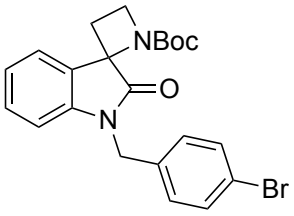
Following general procedure **B** using diazo **306** and protected amine **52** on 0.25 mmol scale in toluene. Purification by flash chromatography (50% Et_2O/pentane) afforded *tert*-butyl 1'-(4-methoxybenzyl)-2'-oxospiro[azetidine-2,3'-indoline]-1-carboxylate **353** (52 mg, 53%) as a pale yellow solid. R_f 0.22 (50% Et_2O/pentane); mp = 55–58 ºC; ν_{max} (film)/cm^{-1} 2971, 2896, 1700 (br s, 2 × C=O), 1614, 1465, 1349, 1245, 1148, 1029, 969, 835, 746; ^{1}H NMR (400 MHz, DMSO-d_6) δ 7.58–7.54 (m, 1H, HC_{Ar}), 7.37–7.20 (m, 3 H, HC_{Ar}), 7.08 and 7.06 (dt, *J* = 7.4, 0.7 Hz, 1 H, HC_{Ar}), 6.99 and 6.80 (d, *J* = 7.8 Hz, 1 H, HC_{Ar}), 6.89 and 6.86 (2 × d, *J* = 8.7 Hz, 2 H, 2 × HC_{Ar}), 4.89 (d, *J* = 15.3 Hz, 1 H, NC*H*HAr), 4.76 and 4.70 (2 × d, *J* = 15.3 Hz, 1 H, NCH*H*Ar), 4.16–3.98 (m, 2 H, NCH_2), 3.71 (s, 3 H, OCH_3), 2.57–2.43 (m, 2 H, NCH_2CH_2), 1.37 and 0.94 (2 × s, 9 H, $C(CH_3)_3$); ^{13}C NMR (101 MHz, DMSO-d_6) δ 174.7 and 174.6 (C=O amide), 158.6 and 158.5 (OC_{Ar} quat), 154.3 and 153.9 (C=O carbamate), 142.5 and 142.3 (C_{Ar} quat), 129.5, 129.4, 129.1, 128.7, 128.6, 128.4, 128.2 and 127.8 (3 × C_{Ar} and 2 × C_{Ar} quat), 123.8 and 123.6 (C_{Ar}), 122.6 (C_{Ar}), 113.9 and 113.8 (2 × C_{Ar}), 109.2 and 108.9 (C_{Ar}), 79.7 and 79.0 ($C(CH_3)_3$), 68.3 and 67.8 (NC quat), 55.03 and 54.99 (OCH_3), 47.0 and 46.0 (NCH_2), 42.3 and 42.1 (NCH_2Ar), 28.0 and 27.4 ($C(CH_3)_3$), 27.0 and 26.7 (NCH_2CH_2); HRMS (ESI^+) *m/z* Calculated for $C_{23}H_{26}N_2O_4Na$ [M+Na] 417.1790; Found 417.1790.

(–)–*tert*-Butyl 1'-(4-methoxybenzyl)-2'-oxospiro[azetidine-2,3'-indoline]-1-carboxylate ((*S*)–353)

Following general procedure **D** on 0.2 mmol scale using cyclisation precursor **325** and cat. **394** with purification by flash chromatography (50% Et_2O/pentane) afforded *tert*-butyl 1'-(4-methoxybenzyl)-2'-oxospiro[azetidine-2,3'-indoline]-1-carboxylate **(*S*)–353** (71 mg, 90%) as a white solid. The characterisation data observed was consistent with the above. The *er* of the product was 96:4 [Chiralpak IA column, 90:10 *n*-hexane:*i*-PrOH, flow rate: 1 mL min^{-1}, 35 ºC,

UV detection wavelength: 254 nm, *rac* **353** retention times 12.00 and 14.68 min]; $[\alpha]_D^{22} = -36$ (*c* = 1.85, Et_2O).

(±)–*tert*-Butyl 1'-(4-bromobenzyl)-2'-oxospiro[azetidine-2,3'-indoline]-1-carboxylate (354)

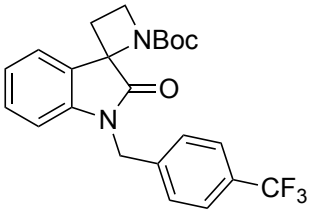


Following general procedure **B** on 0.25 mmol scale using diazo **307** and protected amine **52** in toluene. Purification by flash chromatography (40% Et_2O/pentane) afforded *tert*-butyl 1'-(4-bromobenzyl)-2'-oxospiro[azetidine-2,3'-indoline]-1-carboxylate **354** (70 mg, 63%) as a pale brown solid. R_f 0.24 (40% Et_2O/pentane); mp = 135–136 ºC; ν_{max} (film)/cm^{-1} 2974, 2931, 2894, 1723 (C=O amide), 1701 (C=O carbamate), 1616, 1488, 1467, 1364, 1178, 1152, 750; ^1H NMR (400 MHz, $CDCl_3$) δ 7.50–7.42 (m, 3 H, 3 × HC_{Ar}), 7.30–7.14 (m, 3 H, 3 × HC_{Ar}), 7.12–7.04 (m, 1 H, HC_{Ar}), 6.69 and 6.58 (2 × d, *J* = 7.8 Hz, 1 H, HC_{Ar}), 5.04 and 4.97 (2 × d, *J* = 15.9 Hz, 1 H, NC*H*HAr), 4.73 and 4.67 (2 × d, *J* = 15.9 Hz, 1 H, NCH*H*Ar), 4.36–4.23 (m, 1 H, NC*H*H), 4.15–4.08 and 4.06–4.00 (m, 1 H, NCH*H*), 2.75–2.67 and 2.63–2.56 (m, 1 H, NCH_2CHH), 2.55–2.46 (m, 1 H, NCH_2CHH), 1.44 and 1.05 (2 × br s, 9 H, $C(CH_3)_3$); ^{13}C NMR (101 MHz, $CDCl_3$) δ 175.8 and 175.3 (C=O amide), 154.4 (C=O carbamate), 142.5 and 142.3 (NC_{Ar} quat), 134.7 and 134.5 (C_{Ar} quat), 131.9 and 131.8 (2 × C_{Ar}), 129.64, 129.58, 129.4, 129.1, 129.0, 128.6 (3 × C_{Ar} and C_{Ar} quat), 123.9 and 123.6 (C_{Ar}), 123.1 (C_{Ar}), 121.7 and 121.4 (C_{Ar} quat), 109.1 and 108.6 (C_{Ar}), 80.6 and 80.1 ($C(CH_3)_3$), 68.6 and 68.4 (NC quat), 47.4 and 45.9 (NCH_2), 43.4 and 43.2 (NCH_2Ar), 28.3 and 27.9 ($C(CH_3)_3$), 27.6 and 27.5 (NCH_2CH_2); HRMS (FTMS + pAPCI) *m/z* Calculated for $C_{22}H_{23}N_2O_3{}^{79}Br^{+\cdot}$ $[M]^{+\cdot}$ 442.0887; Found 442.0873.

(–)-*tert*-Butyl 1'-(4-bromobenzyl)-2'-oxospiro[azetidine-2,3'-indoline]-1-carboxylate ((*S*)–354)

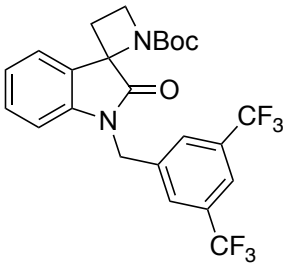
Following general procedure **D** on 0.2 mmol scale using cyclisation precursor **326** and cat. **394** with purification by flash chromatography (40% Et_2O/pentane) afforded *tert*-butyl 1'-(4-bromobenzyl)-2'-oxospiro[azetidine-2,3'-indoline]-1-carboxylate **(*S*)–354** (45 mg, 51%) as a pale brown solid. The characterisation data observed was consistent with the above. The *er* of the product was 12:88 [Chiralpak ID column, 90:10 *n*-hexane:*i*-PrOH, flow rate: 1 mL min^{-1}, 35 ºC, UV detection wavelength: 254 nm, *rac* **354** retention times 14.96 and 21.63 min]; $[\alpha]_D^{22} = -24$ (*c* = 0.25, CH_2Cl_2).

(±)–*tert*-Butyl 2'-oxo-1'-(4-(trifluoromethyl)benzyl)spiro[azetidine-2,3'-indoline]-1-carboxylate (355)



Following general procedure **B** on 0.25 mmol scale using diazo **308** and protected amine **52** in toluene. Purification by flash chromatography (40% Et_2O/pentane) afforded *tert*-butyl 2'-oxo-1'-(4-(trifluoromethyl)benzyl)spiro[azetidine-2,3'-indoline]-1-carboxylate **355** (37 mg, 34%) as a pale yellow solid. R_f 0.20 (40% Et_2O/pentane); mp = 52–55 ºC; ν_{max} (film)/cm^{-1} 2974, 1700 (br s, 2 × C=O), 1614, 1364, 1323, 1156, 1115, 1018, 749; ^{1}H NMR (400 MHz, DMSO-d_6) δ 7.75–7.56 (m, 5 H, 5 × HC_{Ar}), 7.29 and 7.24 (2 × td, J = 7.7, 1.2 Hz, 1 H, HC_{Ar}), 7.11 and 7.08 (2 × td, J = 7.7, 0.7 Hz, 1 H, HC_{Ar}), 7.01 and 6.81 (2 × d, J = 7.8 Hz, 1 H, HC_{Ar}), 5.14–5.01 (m, 1 H, NC*H*HAr), 4.92 and 4.90 (2 × d, J = 16.4 Hz, NCH*H*Ar), 4.16–3.98 (m, 2 H, NCH_2), 2.61–2.45 (m, 2 H, NCH_2CH_2), 1.36 and 0.91 (2 × s, 9 H, $C(CH_3)_3$); ^{13}C NMR (101 MHz, DMSO-d_6) δ 174.9 and 174.8 (C=O amide), 154.4 and 153.8 (C=O carbamate), 142.3 and 142.1 (C_{Ar} quat), 141.1 and 140.9 (C_{Ar} quat), 129.6 (C_{Ar}), 128.6 and 128.4 (C_{Ar} quat), 128.5 (2 × C_{Ar}), 127.8 (C_{Ar}), 125.5 and 125.3 (2 × q, $J_{C–F}$ = 4 Hz, 2 × C_{Ar}), 124.0 and 123.7 (C_{Ar} quat), 122.9 (C_{Ar}), 109.0 and 108.7 (C_{Ar}), 79.8 and 79.0 ($C(CH_3)_3$), 68.2 and 67.7 (NC quat), 47.1 and 45.6 (NCH_2), 42.5 and 42.3 (NCH_2Ar), 27.9 and 27.4 ($C(CH_3)_3$), 26.83 and 26.77 (NCH_2CH_2) (CF_3 quat was not observed); ^{19}F{^{1}H} NMR (377 MHz, DMSO-d_6) δ –56.2 and –56.3; HRMS (ESI$^+$) *m/z* Calculated for $C_{23}H_{23}N_2O_3F_3Na$ [M+Na] 455.1558; Found 455.1555.

(±)–*tert*-Butyl 1'-(3,5-bis(trifluoromethyl)benzyl)-2'-oxospiro[azetidine-2,3'-indoline]-1-carboxylate (356)



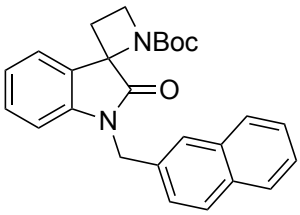
Following general procedure **B** on 0.25 mmol scale using diazo **309** and protected amine **52** in toluene. Purification by flash chromatography (40% Et_2O/pentane then 2% Et_2O/CH_2Cl_2) afforded *tert*-butyl 1'-(3,5-bis(trifluoromethyl)benzyl)-2'-oxospiro[azetidine-2,3'-indoline]-1-carboxylate **356** (56 mg, 45%) as a pale orange solid. R_f 0.14 (30% Et_2O/pentane); ν_{max} (film)/cm^{-1} 2974, 1692 (2 × C=O), 1618, 1366, 1282, 1174, 1126, 973, 906, 753, 708; ^{1}H NMR (400 MHz, DMSO-d_6) δ 8.19 and 8.16 (2 × s, 2 H, 2 × HC_{Ar}), 8.08 and 7.99 (2 × s, 1 H, HC_{Ar}), 7.62 and 7.59 (2 × dd, 1 H, J = 7.4, 0.8 Hz, 1 H, HC_{Ar}), 7.35 (td, J = 7.7, 1.3 Hz, 0.4 Hz, HC_{Ar}), 7.28–7.21 (m, 1 H, HC_{Ar}), 7.13 and 7.10 (2 × td, J = 7.6, 0.9 Hz, 1 H, HC_{Ar}), 6.86 (d, J = 7.8 Hz, 0.6 Hz, HC_{Ar}), 5.34, 5.08 and 4.91 (2 × d and s, 2 H, NCH_2Ar), 4.17–3.96 (m, 2 H, NCH_2), 2.59–2.44 (m, 2 H, NCH_2CH_2), 1.36 and 0.80 (2 × s, 9 H, $C(CH_3)_3$); ^{13}C NMR (101 MHz, DMSO-d_6) δ 175.0 (C=O amide), 154.7 and 153.6 (C=O carbamate), 142.2 and 142.0 (C_{Ar} quat), 140.0 and 139.8 (C_{Ar} quat),

130.5 and 130.4 (2 × q, J_{C-F} = 33 Hz, 2 × $C_{Ar}CF_3$ quat), 129.8, 129.2, 128.7, 128.4 and 128.2 (3 × C_{Ar}), 124.3 and 123.8 (C_{Ar}), 123.3 (q, J_{C-F} = 273 Hz, 2 × CF_3), 123.1 (2 × C_{Ar}), 121.1 (C_{Ar} quat), 108.8 and 108.7 (C_{Ar}), 80.0 and 78.8 ($C(CH_3)_3$), 68.2 and 67.7 (NC quat), 47.2 and 45.6 (NCH_2), 42.3 and 41.8 (NCH_2Ar), 27.8 and 27.1 ($C(CH_3)_3$), 26.9 and 26.4 (NCH_2CH_2); $^{19}F\{^1H\}$ NMR (377 MHz, DMSO-d_6) δ –61.2 and –61.3; HRMS (FTMS + pAPCI) *m/z* Calculated for $C_{24}H_{22}N_2O_3F_6^{\cdot+}$ $[M+H]^{\cdot+}$ 500.1529; Found 500.1517.

(–)–*tert*-Butyl 1'-(3,5-bis(trifluoromethyl)benzyl)-2'-oxospiro[azetidine-2,3'-indoline]-1-carboxylate ((*S*)–356)

Following general procedure **D** on 0.2 mmol scale using cyclisation precursor **328** cat. **394** with purification by flash chromatography (30% Et_2O/pentane) afforded *tert*-Butyl 1'-(3,5-bis(trifluoromethyl)benzyl)-2'-oxospiro[azetidine-2,3'-indoline]-1-carboxylate **(*S*)–356** (75 mg, 75%) as a white solid. The characterisation data observed was consistent with the above. The *er* of the product was 9:91 [Chiralpak IC column, 98.5:1.5 *n*-hexane:*i*-PrOH, flow rate: 1 mL min^{-1}, 35 ºC, UV detection wavelength: 254 nm, *rac* **356** retention times 14.12 and 23.59 min]; $[\alpha]_D^{22} = -75$ (*c* = 1.52, Et_2O).

(±)–*tert*-Butyl 1'-(naphthalen-2-ylmethyl)-2'-oxospiro[azetidine-2,3'-indoline]-1-carboxylate (357)



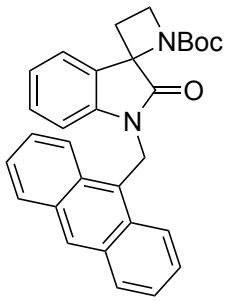
Following general procedure **B** on 0.1 mmol scale using diazo **310.** and protected amine **52** in CH_2Cl_2. Purification by flash chromatography (40% EtOAc/hexane) afforded *tert*-butyl 1'-(naphthalen-2-ylmethyl)-2'-oxospiro[azetidine-2,3'-indoline]-1-carboxylate **357** (25 mg, 61%) as a pale brown solid. R_f 0.17 (30% EtOAc/hexane); mp = 71–73 ºC; ν_{max} (film)/cm^{-1} 2975, 2892, 1722 (C=O amide), 1692 (C=O carbamate), 1612, 137, 1355, 1178, 1142, 745; ^1H NMR (400 MHz, $CDCl_3$) δ 7.98–7.77 (m, 4 H, 4 × HC_{Ar}), 7.61–7.45 (m, 4 H, 4 × HC_{Ar}), 7.26 and 7.20 (2 × t, *J* = 7.8 Hz, 1 H, HC_{Ar}), 7.11–7.00 (m, 1.6 H, 2 × HC_{Ar}), 6.82 (d, *J* = 7.8 Hz, 0.4 Hz, HC_{Ar}), 5.19 and 5.14 (2 × d, *J* = 16.0 Hz, 1 H, NC*H*HAr), 4.95 and 4.94 (2 × d, *J* = 16.0 Hz, 1 H, NCH*H*Ar), 4.19–3.99 (m, 2 H, NCH_2), 2.66–2.47 (m, 2 H, NCH_2CH_2), 1.40 and 0.92 (2 × s, 9 H, $C(CH_3)_3$); ^{13}C NMR (101 MHz, $CDCl_3$) δ 175.0 and 174.9 (C=O amide), 154.5 and 153.9 (C=O carbamate), 142.6 and 142.4 (NC_{Ar} quat), 133.8 and 133.4 (C_{Ar} quat), 132.9 (C_{Ar} quat), 132.3 and 132.2 (C_{Ar} quat), 129.6 (C_{Ar}), 128.7 and 128.5 (C_{Ar} quat), 128.3 and 128.1 (C_{Ar}), 127.59, 127.55 and 127.4 (2 × C_{Ar}), 126.4, 126.2, 126.0, 125.8, 125.5 and 125.4 (4 × C_{Ar}), 124.0 and 123.7 (C_{Ar}), 122.7 (C_{Ar}), 109.1 and 108.9 (C_{Ar}), 79.8 and 79.0 ($C(CH_3)_3$), 68.3 and 67.8 (NC quat), 47.1 and 45.7 (NCH_2), 43.2 and

42.8 (NCH_2Ar), 28.0 and 27.4 ($C(CH_3)_3$), 26.8 (NCH_2CH_2); HRMS (ESI^+) *m/z* Calculated for $C_{26}H_{26}N_2O_3Na$ [M+Na] 437.1841; Found 437.1827.

(–)–*tert*-Butyl 1'-(naphthalen-2-ylmethyl)-2'-oxospiro[azetidine-2,3'-indoline]-1-carboxylate ((*S*)–357)

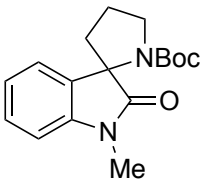
Following general procedure **D** on 0.1 mmol scale using cyclisation precursor **329** and cat. **394** with purification by flash chromatography (30% Et_2O/pentane) afforded *tert*-Butyl 1'-(3,5-bis(trifluoromethyl)benzyl)-2'-oxospiro[azetidine-2,3'-indoline]-1-carboxylate **(*S*)–357** (31 mg, 76%) as a white solid. The characterisation data observed was consistent with the above. The *er* of the product was 19:81 [Chiralpak ID column, 90:10 *n*-hexane:*i*-PrOH, flow rate: 1 mL min^{-1}, 35 ºC, UV detection wavelength: 254 nm, *rac* **357** retention times 20.34 and 28.31 min]; $[\alpha]_D^{22} = -49$ (*c* = 0.85, Et_2O).

(±)–*tert*-Butyl 1'-(anthracen-9-ylmethyl)-2'-oxospiro[azetidine-2,3'-indoline]-1-carboxylate (358)



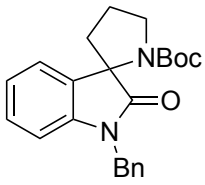
Following general procedure **B** on 0.25 mmol scale using diazo **311** and protected amine **52** in CH_2Cl_2. Purification by flash chromatography (50% to 60% Et_2O/hexane) afforded *tert*-butyl 1'-(anthracen-9-ylmethyl)-2'-oxospiro[azetidine-2,3'-indoline]-1-carboxylate **358** (61 mg, 53%) as a pale brown solid. R_f 0.26 (40% EtOAc/hexane); mp = 197–199 ºC; ν_{max} (film)/cm^{-1} 3053, 2974, 1719 (C=O amide), 1686 (C=O carbamate), 1611, 1484, 1462, 1367, 1351, 1337, 1157, 752, 727; ^1H NMR (400 MHz, $CDCl_3$) δ 8.69–8.66 (m, 1 H, HC_{Ar}), 8.59–8.53 (m, 2 H, 2 × HC_{Ar}), 8.17–8.12 (m, 2 H, 2 × HC_{Ar}), 7.69–7.53 (m, 4 H, 4 × HC_{Ar}), 7.47–7.42 (m, 1 H, HC_{Ar}), 6.93–6.77 (m, 2 H, 2 × HC_{Ar}), 6.29–6.25 (m, 0.6 H, HC_{Ar}), 6.15 (d, *J* = 7.8 Hz, 0.4 Hz, 0.4 Hz, HC_{Ar}), 6.00 and 5.99 (2 × d, *J* = 15.6 Hz, NC*H*H), 5.89 and 5.82 (2 × d, *J* = 15.6 Hz, NCH*H*), 4.25–3.98 (m, 2 H, NCH_2), 2.61–2.37 (m, 2 H, NCH_2CH_2), 1.41 and 0.80 (2 × d, 9 H, $C(CH_3)_3$); ^{13}C NMR (101 MHz, $CDCl_3$) δ 175.0 and 174.7 (C=O amide), 154.3 and 153.7 (C=O carbamate), 142.6 and 142.3 (NC_{Ar} quat), 130.9, 130.42 and 130.36 (C_{Ar} and C_{Ar} quat), 129.5, 129.4, 129.2, 129.1 (2 × C_{Ar} and C_{Ar} quat), 128.9 and 128.6 (2 × C_{Ar} quat), 126.9 and 126.8 (2 × C_{Ar}), 126.31 and 126.26 (2 × C_{Ar} quat), 125.3 (3 × C_{Ar}), 124.1, 123.9, 123.7 and 123.5 (3 × C_{Ar}), 122.5 (C_{Ar}), 109.4 and 109.2 (C_{Ar}), 79.8 and 78.9 ($C(CH_3)_3$), 68.2 and 67.8 (NC quat), 47.0 and 45.7 (NCH_2), 37.2 and 37.1 (NCH_2Ar), 28.0, 27.7, 27.3 and 27.1 (NCH_2CH_2 and $C(CH_3)_3$); HRMS (ESI^+) *m/z* Calculated for $C_{30}H_{29}N_2O_3$ [M+H] 465.2178; Found 465.2171.

(±)–*tert*-Butyl 1-methyl-2-oxospiro[indoline-3,2'-pyrrolidine]-1'-carboxylate (359)



A solution of diazo **273** (87 mg, 0.5 mmol) in CH_2Cl_2 (2.5 mL) was slowly added over 10 min to a stirred solution of *tert*-butyl (2-chloroethyl)carbamate **58** (180 mg, 1.0 mmol) and $Rh_2(esp)_2$ (1.9 mg, 2.5 μmol) in CH_2Cl_2 (2.0 mL) at 25 ºC. The remaining diazo **273** was dissolved in CH_2Cl_2 (0.5 mL) to ensure quantitative transfer. After 30 min, $CsOH{\cdot}H_2O$ (168 mg, 2 mmol) and tetrabutylammonium bromide (16 mg, 10 mol%) were added and the reaction mixture was stirred for 0.5 h at 25 ºC. The reaction mixture was filtered through celite, washing with EtOAc (25 mL) and concentrated under reduced pressure. Purification by flash chromatography (50% EtOAc/heptane) afforded *tert*-butyl 1-methyl-2-oxospiro[indoline-3,2'-pyrrolidine]-1'-carboxylate **359** (82 mg, 54%) as a pink solid. R_f 0.30 (50% EtOAc/heptane); mp = 87–89 ºC; ν_{max} (film)/cm^{-1} 2974, 2881, 1715 (C=O amide), 1689 (C=O carbamate), 1614, 1472, 1390, 1252, 1156, 1126, 753; ^{1}H NMR (500 MHz, DMSO-d_6, 373 K) δ 7.32–7.25 (m, 2 H, 2 × HC_{Ar}), 7.03 (t, J = 7.5 Hz, 1 H, HC_{Ar}), 6.95 (d, J = 7.7 Hz, 1 H, HC_{Ar}), 3.74–3.67 (m, 1 H, NC*H*H), 3.64–3.57 (m, 1 H, NCH*H*), 3.13 (s, 3 H, NCH_3), 2.25–2.18 (m, 1 H, $N(CH_2)_2CHH$), 2.17–2.07 (m, 2 H, NCH_2CH_2), 2.05–1.98 (m, 1 H, $N(CH)_2CHH$), 1.01 (br s, 9 H, $C(CH_3)_3$); ^{13}C NMR (101 MHz, DMSO-d_6, 373 K) δ 176.1 (C=O amide), 151.7 (C=O carbamate), 142.6 (NC_{Ar} quat), 132.0 (C_{Ar} quat), 127.8 (C_{Ar}), 121.6 (C_{Ar}), 121.1 (C_{Ar}), 107.5 (C_{Ar}), 78.3 ($C(CH_3)_3$), 65.9 (NC quat), 47.3 (NCH_2), 38.5 ($N(CH_2)_2CH_2$), 27.1 ($C(CH_3)_3$), 25.5 (NCH_3), 22.0 (NCH_2CH_2); HRMS (ESI$^+$) *m/z* Calculated for $C_{19}H_{25}N_3O_3Na$ [M+CH_3CN+Na] 366.1794; Found 366.1806.

(±)–*tert*-Butyl 1-benzyl-2-oxospiro[indoline-3,2'-pyrrolidine]-1'-carboxylate (360)



Following general procedure **B** on 0.25 mmol scale using diazo **280** and protected amine **58** in toluene. Purification by flash chromatography (50% Et_2O/hexane) afforded *tert*-butyl 1-benzyl-2-oxospiro[indoline-3,2'-pyrrolidine]-1'-carboxylate **360** (59 mg, 62%) as a brown solid. R_f 0.26 (50% Et_2O/hexane); mp = 145–146 ºC; ν_{max} (film)/cm^{-1} 2975, 2889, 1726 (C=O amide), 1689 (C=O carbamate), 1610, 1489, 1467, 1382, 1362, 1179, 1157, 1114, 762, 697; ^{1}H NMR (400 MHz, DMSO-d_6, 373 K) δ 7.41–7.36 (m, 2 H, 2 × HC_{Ar}), 7.35–7.30 (m, 2 H, 2 × HC_{Ar}), 7.29–7.24 (m, 2 H, 2 × HC_{Ar}), 7.23–7.17 (m, 1 H, HC_{Ar}), 7.01 (t, J = 7.4 Hz, 1 H, HC_{Ar}), 6.86 (br s, 1 H, HC_{Ar}), 5.02 (br s, 1 H, NC*H*HPh), 4.69 (br s, 1 H, NCH*H*Ph), 3.77–3.62 (m, 2 H, NCH_2), 2.32–2.02 (m, 4 H, $NCH_2(CH_2)_2$), 1.00 (br s, 9 H, $C(CH_3)_3$); ^{13}C NMR (101 MHz, DMSO-d_6, 373 K) δ 176.4 (C=O amide), 151.7 (C=O carbamate), 141.6 (NC_{Ar} quat), 135.9 (C_{Ar} quat), 127.9 (2 × C_{Ar}), 127.6 (C_{Ar}), 131.9 (C_{Ar} quat), 126.8 (2 × C_{Ar}), 126.7 (C_{Ar}), 121.8 (C_{Ar}), 121.3 (C_{Ar}), 108.2 (C_{Ar}), 78.6 ($C(CH_3)_3$), 66.0 (NC quat), 47.5 (NCH_2), 42.7 (NCH_2Ph), 27.1 ($C(CH_3)_3$), 22.0

($N(CH_2)_2CH_2$), peak due to NCH_2CH_2 obscured by DMSO residual solvent signal confirmed by HSQC; HRMS (ESI^+) *m/z* Calculated for $C_{23}H_{26}N_2O_3Na$ [M+Na] 401.1841; Found 481.1850.

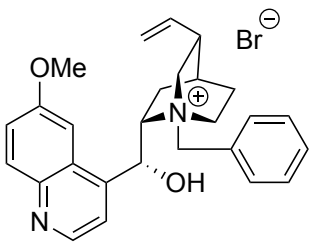
(–)–*tert*-Butyl 1-benzyl-2-oxospiro[indoline-3,2'-pyrrolidine]-1'-carboxylate ((*S*)–360)

Following general procedure **D** on 0.2 mmol scale using cyclisation precursor **336** and cat. **394** with purification by flash chromatography (40% Et_2O/pentane) afforded *tert*-butyl 1-benzyl-2-oxospiro[indoline-3,2'-pyrrolidine]-1'-carboxylate **(*S*)–360** (73 mg, 96%) as a pale orange solid solid. The characterisation data observed was consistent with the above. The *er* of the product was 17:83 [Chiralpak ID column, 80:20 *n*-hexane:*i*-PrOH, flow rate: 1 mL min^{-1}, 35 ºC, UV detection wavelength: 254 nm, *rac* **360** retention times 10.54 and 15.55 min]; $[\alpha]_D^{22} = -8$ (*c* = 1.85, Et_2O).

6.2.3.5 Synthesis of Phase Transfer Catalysts

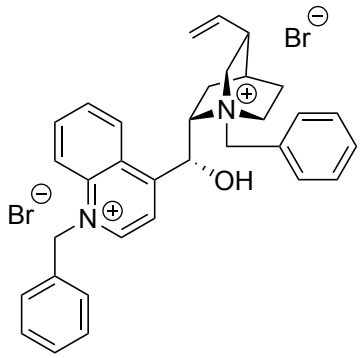
Catalysts **217** and **361–364** are commercially available. Catalysts **367**–**385** (Table 19, p. 125) were synthesised analogous to **365** below and used without further purification. Synthesis and characterisation of catalysts **365**, **371**, **377**, **378** and **385** are provided below as examples for catalysts used in Table 19.

(1*S*,2*S*,4*S*,5*R*)-1-Benzyl-2-((*R*)-hydroxy(6-methoxyquinolin-4-yl)methyl)-5-vinylquinuclidin-1-ium bromide (365)



A solution of quinine (162 mg, 0.5 mmol) and benzyl bromide (60 μL, 0.5 mmol) in THF (2.5 mL) was heated to 70 ºC for 18 h. The reaction was cooled to rt and Et_2O was added. The reaction was stirred for approx. 0.5 h then the precipitate was filtered, washing with Et_2O. The collected solid was dried to afford (1*S*,2*S*,4*S*,5*R*)-1-benzyl-2-((*R*)-hydroxy(6-methoxyquinolin-4-yl)methyl)-5-vinylquinuclidin-1-ium bromide **365** (226 mg, 91%) as a brown solid. $[\alpha]_D^{22} = -173$ (*c* = 0.3, MeOH) [lit = –205 (*c* = 0.51, MeOH)][445]; R_f 0.15 (10% MeOH/CH_2Cl_2); mp = 165–168 ºC [lit = 168–170 ºC][446]; ν_{max} (film)/cm^{-1} 3187 (br s, OH), 2945, 1618, 1510, 1457, 1361, 1323, 1226, 1029, 913, 828, 764, 708; ^{1}H NMR (400 MHz, $CDCl_3$) δ 8.63 (d, *J* = 4.6 Hz, 1 H, HC_{Ar}), 7.91 (d, *J* = 9.2 Hz, 1 H, HC_{Ar}), 7.76 (d, *J* = 7.1 Hz, 2 H, 2 × HC_{Ar}), 7.65 (d, *J* = 4.6 Hz, 1 H, HC_{Ar}), 7.41 – 7.20 (m, 5 H, 5 × HC_{Ar}), 6.63 (d, *J* = 4.1 Hz, 1 H, N^+CH), 6.42 (d, *J* = 6.1 Hz, 1 H, OH), 5.89 (d, *J* = 12.0 Hz, 1 H, N^+CHH), 5.58 (ddd, *J* = 17.3, 10.4, 6.9 Hz, 1 H, $CH{=}CH_2$), 5.07 (d, *J* = 17.1 Hz, 1 H, $CH{=}CHH$), 4.92 (d, *J* = 10.4 Hz, 1 H, $CH{=}CHH$), 4.87–4.72 (m, 2 H, N^+CHHAr and N^+CHH), 4.00–3.92 (m, 4 H, $CHOH$ and OCH_3), 3.74–3.66 (m, 1 H, N^+CHH), 3.44–3.37 (m, 1 H, N^+CHH), 3.09–3.00 (m, 1 H, N^+CHH), 2.55 (q, *J* = 7.0 Hz, 1 H, $CHCH{=}CH_2$), 2.33–2.17 (m, 2 H, $NCHCHH$ and NCH_2CHH), 1.98–1.93 (m, 1 H, $N(CH_2)_2CH$), 1.75–1.65 (m, 1 H, NCH_2CHH), 1.57–1.47 (m, 1 H, $NCHCHH$); ^{13}C NMR (101 MHz, $CDCl_3$) δ 158.0 (OC_{Ar} quat), 147.0 (C_{Ar}), 143.63 (C_{Ar} quat), 143.59 (C_{Ar} quat), 136.3 ($CH{=}CH_2$), 133.8 (2 × C_{Ar}), 131.3 (C_{Ar}), 130.4 (C_{Ar}), 129.1 (2 × C_{Ar}), 126.9 (C_{Ar} quat), 126.0 (C_{Ar} quat), 121.3 (C_{Ar}), 120.4 (C_{Ar}), 117.8 ($CH{=}CH_2$), 102.0 (C_{Ar}), 69.3 (CHOH), 63.9 (N^+CH), 63.4 (N^+CH_2Ar), 60.4 (N^+CH_2), 56.3 (OCH_3), 51.1 (N^+CH_2), 38.0 ($CHCH{=}CH_2$), 26.8 ($N(CH_2)_2CH$), 24.7 ($NCHCH_2$), 21.4 (NCH_2CH_2). The observed characterisation data (^{1}H and ^{13}C NMR) was consistent with that previously reported in the literature.[446]

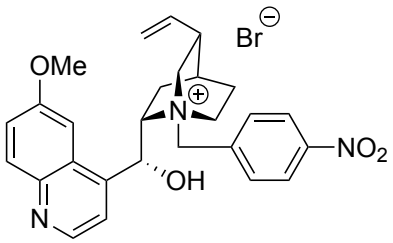
(1*S*,2*S*,4*S*,5*R*)-1-Benzyl-2-((*R*)-(1-benzylquinolin-1-ium-4-yl)(hydroxy)methyl)-5-vinylquinuclidin-1-ium bromide (366)[342]



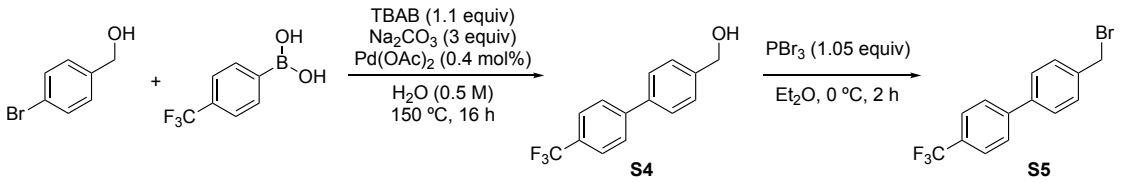
A slurry of cinchonidine (118 mg, 0.4 mmol) and benzyl bromide (0.12 mL, 1.0 mmol) in 2-propanol (0.1 mL) and DMF (0.72 mL) was degassed with Argon, heated to 70 ºC under Argon atmosphere and stirred for 7 h. The reaction mixture was cooled to rt and EtOAc (10 mL) was added over 10 min with vigorous stirring. The resulting slurry was stirred overnight, filtered and rinsed with EtOAc (2 × 10 mL) and hexane (2 × 10 mL). The solid was dried under vacuum to afford (1*S*,2*S*,4*S*,5*R*)-1-benzyl-2-((*R*)-(1-benzylquinolin-1-ium-4-yl)(hydroxy)methyl)-5-vinylquinuclidin-1-ium bromide **366** (223 mg, 87%) as an off-white solid. $[\alpha]_D^{22} = -47$ (*c* = 0.2, MeOH); R_f 0.05* (50% MeOH/CH_2Cl_2); mp = 200–201 ºC [lit = 228–230 ºC][447]; ν_{max} (film)/cm^{-1} 3101 (s br, OH), 2943, 1617, 1602, 1588, 1533, 1497, 1455, 1166, 1125, 1011, 939, 770, 754, 715; ^{1}H NMR (400 MHz, $CDCl_3$) δ 9.86 (d, *J* = 6.3 Hz, 1 H, HC_{Ar}), 8.81 (d, *J* = 8.6 Hz, 1 H, HC_{Ar}), 8.62 (d, *J* = 8.9 Hz, 1 H, HC_{Ar}), 8.52 (d, *J* = 6.2 Hz, 1 H, HC_{Ar}), 8.30–8.24 (m, 1 H, HC_{Ar}), 8.12 (m, 1 H, HC_{Ar}), 7.84–7.77 (m, 2 H, 2 × HC_{Ph}), 7.60–7.56 (m, 3 H, 3 × HC_{Ph}), 7.47–7.35 (m, 5 H, 5 × HC_{Ph}), 7.31 (d, *J* = 5.1 Hz, 1 H, OH), 6.85 (d, *J* = 4.3 Hz, 1 H, N^+CH), 6.48–6.37 (m, 2 H, $N_{Ar}{}^+CH_2$), 5.74–5.63 (m, 1 H, CH_2=C*H*), 5.30–5.14 (m, 3 H, N^+CH_2Ph and C*H*H=CH), 4.98–4.92 (m, 1 H, CH*H*=CH), 4.33 (t, *J* = 10.6 Hz, 1 H, N^+CHHCH), 4.09 (t, *J* = 9.1 Hz, 1 H, C*H*OH), 3.97–3.89 (m, 1 H, N^+CHHCH_2), 3.37–3.19 (m, 2 H, N^+CHHCH_2 and N^+CHHCH), 2.77–2.66 (m, 1 H, N^+CH_2CH), 2.13–1.97 (m, 3 H, CH bridgehead, N^+CH_2CHH and N^+CHCHH), 1.90–1.70 (br t, *J* = 10.5 Hz, N^+CH_2CHH), 1.49–1.39 (m, 1 H, N^+CHCHH); ^{13}C NMR (101 MHz, $CDCl_3$) δ 158.1 (C_{Ar} quat), 149.5 (C_{Ar}), 138.1 (CH_2=*C*H), 137.1 (C_{Ph} quat), 135.3 (C_{Ar}), 133.8 (2 × C_{Ph}), 133.7 (C_{Ar} quat), 130.6 (C_{Ar}), 130.1 (C_{Ph} quat), 129.1 (2 × C_{Ph}), 128.9 (2 × C_{Ph}), 128.8 (C_{Ph}), 127.8 (C_{Ph}), 127.5 (2 × C_{Ph}), 126.8 (C_{Ar}), 126.2 (C_{Ar} quat), 121.6 (C_{Ar}), 120.0 (C_{Ar}), 116.6 (*C*H_2=CH), 67.2 (CHOH), 64.7 (N^+CH), 62.5 (N^+CH_2Ph), 60.0 ($N_{Ar}{}^+CH_2Ph$), 59.4 ($N^+CH_2CH_2$), 50.6 (N^+CH_2CH), 36.8 (CH_2=CH*C*H), 26.0 (CH bridgehead), 24.2 (NCH_2CH_2), 21.1 ($NCHCH_2$). The observed characterisation data (^{1}H and ^{13}C NMR) was consistent with that previously reported in the literature.[342]

* The compound did not move significantly by TLC even when using very polar solvent systems and the spot streaked with a small amount remaining on the baseline of the TLC plate.

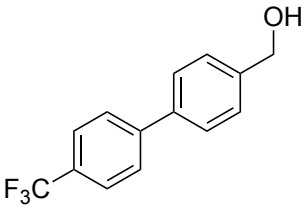
(1*S*,2*S*,4*S*,5*R*)-2-((*R*)-Hydroxy(6-methoxyquinolin-4-yl)methyl)-1-(4-nitrobenzyl)-5-vinylquinuclidin-1-ium bromide (371)



A solution of quinine (162 mg, 0.5 mmol) and 1-(bromomethyl)-4-nitrobenzene (108 mg, 0.5 mmol) in THF (2.5 mL) was heated to 70 ºC for 16 h. The reaction was cooled to rt and Et_2O was added. The reaction was stirred for approx. 0.5 h then the precipitate was filtered. The collected solid was dried to afford (1*S*,2*S*,4*S*,5*R*)-2-((*R*)-hydroxy(6-methoxyquinolin-4-yl)methyl)-1-(4-nitrobenzyl)-5-vinylquinuclidin-1-ium bromide **371** (93 mg, 75%) as an off-white solid. $[\alpha]_D^{21}$ = –156 (*c* = 0.5, CH_2Cl_2); R_f 0.23 (10% MeOH/CH_2Cl_2); mp = 233–235 ºC (decomposition observed); ν_{max} (film)/cm^{-1} 3176 (br s, OH), 2982, 1621, 1521, 1472, 1431, 1346, 1226, 1029, 921, 857, 824, 701; ^{1}H NMR (400 MHz, $CDCl_3$) δ 8.70 (d, *J* = 4.5 Hz, 1 H, HC_{Ar}), 8.11–8.05 (m, 4 H, 4 × HC_{Ar}), 7.94–7.91 (m, 1 H, HC_{Ar}), 7.73 (d, *J* = 4.5 Hz, 1 H, HC_{Ar}), 7.26–7.22 (m, 2 H, HC_{Ar}), 6.59 (d, *J* = 6.4 Hz, 1 H, N^+CH), 6.36 (d, *J* = 6.6 Hz, 1 H, OH), 6.13 (d, *J* = 12.0 Hz, 1 H, N^+CHHAr), 5.56 (ddd, *J* = 17.1, 10.5, 6.6 Hz, 1 H, CH_2=C*H*), 5.32 (d, *J* = 12.0 Hz, 1 H, N^+CHHAr), 5.20–5.13 (m, 1 H, C*H*H=CH), 4.95 (d, *J* = 10.2 Hz, 1 H, CH*H*=CH), 4.93–4.82 (m, 1 H, N^+CHH), 4.04 (t, *J* = 8.9 Hz, 1 H, C*H*OH), 3.95–4.85 (m, 4 H, OCH_3 and N^+CHH), 3.36 (dd, *J* = 11.1, 1.40 Hz, 1 H, N^+CHH), 3.04 (td, *J* = 11.5, 6.0 Hz, 1 H, N^+CHH), 2.62–2.54 (m, 1 H, CH_2=CHC*H*), 2.32–2.16 (m, 2 H, NCHC*H*H and NCH_2CHH), 2.05–2.00 (m, 1 H, $N(CH_2)_2CH$), 1.81–1.70 (m, 1 H, NCHCH*H*), 1.53–1.43 (m, 1 H, NCH_2CHH); ^{13}C NMR (101 MHz, $CDCl_3$) δ 158.1 (OC_{Ar} quat), 148.7 (C_{Ar} quat), 147.1 (C_{Ar}), 143.8 (C_{Ar} quat), 142.9 (C_{Ar} quat), 135.9 (*C*H=CH_2), 135.2 (2 × C_{Ar}), 134.2 (C_{Ar} quat), 131.7 (C_{Ar} quat), 125.9 (C_{Ar}), 123.7 (2 × C_{Ar}), 120.8 (C_{Ar}), 120.6 (C_{Ar}), 118.1 (CH=*C*H_2), 102.2 (C_{Ar}), 69.3 (CHOH), 64.4 (N^+CH), 61.2 (N^+CH_2Ar), 60.7 (N^+CH_2), 56.4 (OCH_3), 51.6 (N^+CH_2), 37.8 (*C*HCH=CH_2), 26.5 ($N(CH_2)_2CH$), 24.9 ($NCHCH_2$), 21.8 (NCH_2CH_2); HRMS (ESI^+) *m/z* Calculated for $C_{27}H_{30}N_3O_4^+$ [M–Br^-] 460.2231; Found 460.2221.

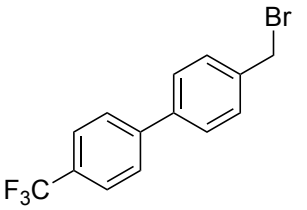


(4'-(Trifluoromethyl)-[1,1'-biphenyl]-4-yl)methanol (S4)[448]



4-Bromobenzyl alcohol (187 mg, 1.0 mmol), (4-(trifluoromethyl)phenyl)boronic acid (209 mg, 1.1 mmol), TBAB (322 mg, 1.0 mmol), Na_2CO_3 (318 mg, 3.0 mmol) and $Pd(OAc)_2$ (0.9 mg, 4.0 μmol) were added to a vial. The vial was evacuated and backfilled with N_2 (3 ×) then H_2O (2.0 mL) was added and the reaction was stirred at 150 ºC for 16 h. The vial was cooled to rt then EtOAc (20 mL) and H_2O (20 mL) was added and the layers were separated. The aqueous layer was extracted with EtOAc (3 × 20 mL). The combined organic layers were dried over Na_2SO_4, filtered and concentrated under reduced pressure. Purification by flash chromatography (20% EtOAc/hexane) afforded (4'-(trifluoromethyl)-[1,1'-biphenyl]-4-yl)methanol **S4** (209 mg, 83%) as a white solid. R_f 0.28 (20% EtOAc/hexane); mp = 148–150 ºC; ν_{max} (film)/cm^{-1} 3401 (br s, OH), 1399, 1335, 1170, 1128, 1076, 1016, 811; ^{1}H NMR (400 MHz, $CDCl_3$) δ 7.70 (s, 4 H, 4 × HC_{Ar}), 7.62 (d, J = 8.3 Hz, 2 H, 2 × HC_{Ar}), 7.49 (d, J = 8.3 Hz, 2 H, 2 × HC_{Ar}), 4.78 (s, 2 H, CH_2Br); ^{13}C NMR (101 MHz, $CDCl_3$) δ 144.3 (C_{Ar} quat), 140.9 (C_{Ar} quat), 139.1 (C_{Ar} quat), 129.4 (q, $J_{C–F}$ = 32 Hz, $C_{Ar}CF_3$ quat), 127.6 (2 × C_{Ar}), 127.4 (2 × C_{Ar}), 127.3 (2 × C_{Ar}), 125.7 (q, $J_{C–F}$ = 4 Hz, 2 × C_{Ar}), 124.3 (q, $J_{C–F}$ = 272 Hz, CF_3), 64.9 (CH_2OH); ^{19}F{^{1}H} NMR (377 MHz, $CDCl_3$) δ –62.4. The observed characterisation data (^{1}H and ^{13}C NMR) was consistent with that previously reported in the literature.[448]

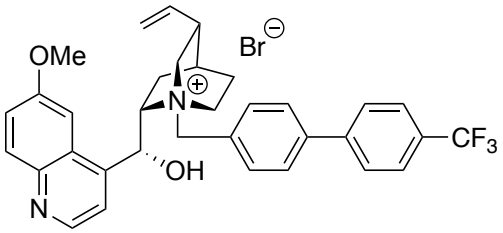
4-(Bromomethyl)-4'-(trifluoromethyl)-1,1'-biphenyl (S5)[449]



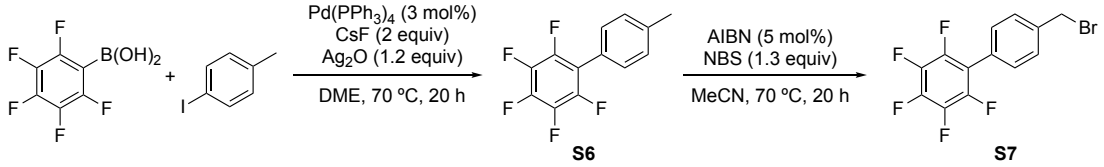
Phosphorus tribromide (59 μL, 0.63 mmol) was added dropwise to a solution of (4'-(trifluoromethyl)-[1,1'-biphenyl]-4-yl)methanol **S4** (151 mg, 0.6 mmol) in Et_2O (3.0 mL) at 0 ºC. The reaction mixture was stirred for 2 h at 0 ºC then H_2O (20 mL) was added. The aqueous reaction mixture was extracted with EtOAc (3 × 20 mL). The combined organic layers were washed with sat. aq. NaCl (30 mL), dried over Na_2SO_4, filtered and concentrated under reduced pressure. Purification by flash chromatography (10% EtOAc/hexane) afforded 4-(bromomethyl)-4'-(trifluoromethyl)-1,1'-biphenyl **S6** (91 mg, 48%) as a white solid. R_f 0.73 (40% EtOAc/hexane); mp = 77–79 ºC; ν_{max} (film)/cm^{-1} 1616, 1398, 1329, 1167, 1124, 1113, 1073, 832, 820; ^{1}H NMR (400 MHz, $CDCl_3$) δ 7.73–7.67 (m, 4 H, 4 × HC_{Ar}), 7.59 (d, J = 8.3 Hz, 2 H, 2 × HC_{Ar}), 7.51 (d, J = 8.3 Hz, 2 H, 2 × HC_{Ar}), 4.56 (s, 2 H,

CH_2Br); ^{13}C NMR (101 MHz, $CDCl_3$) δ 143.9 (C_{Ar} quat), 139.8 (C_{Ar} quat), 137.8 (C_{Ar} quat), 129.7 (2 × C_{Ar}), 129.6 (q, J_{C-F} = 33 Hz, $C_{Ar}CF_3$ quat), 127.7 (2 × C_{Ar}), 127.4 (2 × C_{Ar}), 125.8 (q, J_{C-F} = 4 Hz, 2 × C_{Ar}), 124.2 (q, J_{C-F} = 272 Hz, CF_3), 33.0 (CH_2Br); $^{19}F\{^1H\}$ NMR (377 MHz, $CDCl_3$) δ –62.5. The observed characterisation data (^1H NMR) was consistent with that previously reported in the literature.[450]

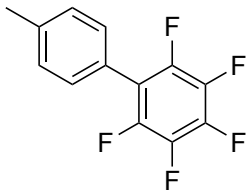
(1*S*,2*S*,4*S*,5*R*)-2-((*R*)-Hydroxy(6-methoxyquinolin-4-yl)methyl)-1-((4'-(trifluoromethyl)-[1,1'-biphenyl]-4-yl)methyl)-5-vinylquinuclidin-1-ium bromide (377)



A mixture of quinine (32 mg, 0.1 mmol) and 4-(bromomethyl)-4'-(trifluoromethyl)-1,1'-biphenyl **S5** (32 mg, 0.1 mmol) in THF (0.5 mL) was heated to 70 ºC for 36 h. The reaction was cooled and Et_2O (2.5 mL) was added. The reaction was stirred for approx. 0.5 h then the precipitate was filtered. Purification by flash chromatography (10% MeOH/CH_2Cl_2) afforded (1*S*,2*S*,4*S*,5*R*)-2-((*R*)-hydroxy(6-methoxyquinolin-4-yl)methyl)-1-((4'-(trifluoromethyl)-[1,1'-biphenyl]-4-yl)methyl)-5-vinylquinuclidin-1-ium **377** (30 mg, 47%) as a pale brown solid. $[\alpha]_D^{17}$ = –180 (*c* = 0.1, $CHCl_3$); R_f 0.51 (20% MeOH/CH_2Cl_2); mp = 188–191 ºC; ν_{max} (film)/cm^{-1} 3198 (br s, OH), 2948, 1618, 1510, 1327, 1241, 1167, 1126, 828, 731; ^1H NMR (400 MHz, $CDCl_3$) δ 8.71 (d, *J* = 4.5 Hz, 1 H, HC_{Ar}), 7.97 (d, *J* = 9.2 Hz, 1 H, HC_{Ar}), 7.87 (d, *J* = 8.2 Hz, 2 H, 2 × HC_{Ar}), 7.76 (d, *J* = 4.5 Hz, 1 H, HC_{Ar}), 7.68 (d, *J* = 8.2 Hz, 2 H, 2 × HC_{Ar}), 7.57 (d, *J* = 8.1 Hz, 2 H, 2 × HC_{Ar}), 7.52 (d, *J* = 8.3 Hz, 2 H, 2 × HC_{Ar}), 7.32 (d, *J* = 2.6 Hz, 1 H, HC_{Ar}), 7.27 (dd, *J* = 9.2, 2.6 Hz, 1 H, HC_{Ar}), 6.83 (d, *J* = 5.7 Hz, 1 H, OH), 6.70–6.65 (s, 1 H, N^+CH), 6.15 (d, *J* = 12.1 Hz, 1 H, N^+CHHAr), 5.60 (ddd, *J* = 17.2, 10.4, 6.9 Hz, 1 H, $CH_2=CH$), 5.15 (d, *J* = 17.1 Hz, 1 H, $CHH=CH$), 5.07–4.93 (m, 3 H, N^+CHHAr, $CHH=CH$ and N^+CHH), 3.94–3.88 (s, 4 H, OCH_3 and $CHOH$), 3.57–3.43 (m, 2 H, N^+CH_2), 3.16 (dt, *J* = 11.4, 6.0 Hz, 1 H, N^+CHH), 2.64–2.56 (m, 1 H, $CH_2=CHCH$), 2.36– 2.18 (m, 2 H, N^+CHCHH and N^+CH_2CHH), 2.06–2.00 (m, 1 H, $N^+(CH_2)_2CH$), 1.80–1.70 (m, 1 H, N^+CH_2CHH), 1.53–1.43 (m, 1 H, N^+CHCHH); ^{13}C NMR (101 MHz, $CDCl_3$) δ 158.0 (OC_{Ar} quat), 147.5 (C_{Ar}), 144.2 (C_{Ar} quat), 143.0 (C_{Ar} quat), 142.9 (C_{Ar} quat), 141.6 (C_{Ar} quat), 136.2 ($CH_2=CH$), 134.5 (2 × C_{Ar}), 132.0 (C_{Ar} quat), 130.1 (q, J_{C-F} = 33 Hz, $C_{Ar}CF_3$ quat), 127.8 (2 × C_{Ar}), 127.3 (2 × C_{Ar}), 126.8 (C_{Ar} quat), 126.0 (C_{Ar}), 125.9 (q, J_{C-F} = 4 Hz, 2 × C_{Ar}), 124.0 (q, J_{C-F} = 272 Hz, CF_3), 120.6 (C_{Ar}), 120.5 (C_{Ar}), 118.1 ($CH_2=CH$), 102.2 (C_{Ar}), 69.5 (CHOH), 64.5 (N^+CH), 63.0 (N^+CH_2Ar), 61.1 (N^+CH_2), 56.3 (OCH_3), 51.1 (N^+CH_2), 38.1 ($CH_2=CHCH$), 26.7 ($N^+(CH_2)_2CH$), 24.9 ($N^+CH_2CH_2$), 21.8 (N^+CHCH_2); $^{19}F\{^1H\}$ NMR (377 MHz, $CDCl_3$) δ –62.6; HRMS (FTMS + pAPCI) *m/z* Calculated for $C_{34}H_{34}N_2O_2F_3^+$ [M–Br^-] 559.2567; Found 559.2572

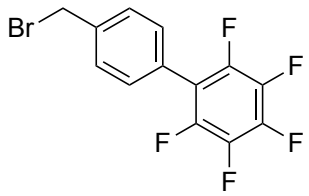


2,3,4,5,6-Pentafluoro-4'-methyl-1,1'-biphenyl (S6)[451]



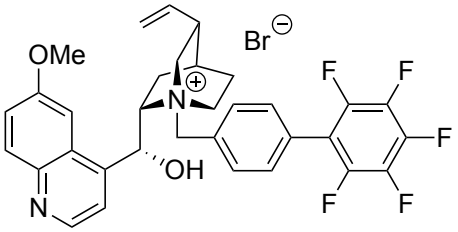
A mixture of 2,3,4,5,6-pentafluorobenzeneboronic acid (117 mg, 0.55 mmol), 4-iodotoluene (109 mg, 0.5 mmol), $Pd(PPh_3)_4$ (17 mg, 0.015 mmol), CsF (152 mg, 1.0 mmol), Ag_2O (139 mg, 0.6 mmol) in DME (1.5 mL) was degassed with Ar then heated at 70 ºC for 19 h. The reaction mixture was filtered through celite washing with EtOAc (20 mL) and concentrated under reduced pressure. Purification by flash chromatography (pentane) afforded 2,3,4,5,6-pentafluoro-4'-methyl-1,1'-biphenyl **S6** (118 mg, 91%) as a white solid. R_f 0.56 (hexane); mp = 120–121 ºC [lit = 119–120 ºC][452]; ν_{max} (film)/cm^{-1} 2926, 1484, 977, 772; ^{1}H NMR (400 MHz, $CDCl_3$) δ 7.32 (s, 4 H, 4 × HC_{Ar}), 2.43 (s, 3 H, $ArCH_3$); ^{13}C NMR (101 MHz, $CDCl_3$) δ 145.3 and 142.9 (2 × m, 2 × FC_{Ar}), 141.4 (m, FC_{Ar}), 139.4 (C_{Ar} quat), 139.0 and 136.5 (2 × m, 2 × FC_{Ar}), 130.0 (2 × C_{Ar}), 129.4 (2 × C_{Ar}), 123.3 (C_{Ar} quat), 115.9 (m, C_{Ar} quat), 21.3 ($ArCH_3$); ^{19}F{^{1}H} NMR (377 MHz, $CDCl_3$) δ –143.4 (dd, $J_{F–F}$ = 23.0, 8.1 Hz, 2 × FC_{Ar}), –156.1 (t, $J_{F–F}$ = 21.0 Hz, 2 × FC_{Ar}), –162.4 (td, $J_{F–F}$ = 22.5, 8.1 Hz, FC_{Ar}). The observed characterisation data (IR, ^{1}H and ^{13}C NMR) was consistent with that previously reported in the literature.[451]

4'-(Bromomethyl)-2,3,4,5,6-pentafluoro-1,1'-biphenyl (S7)



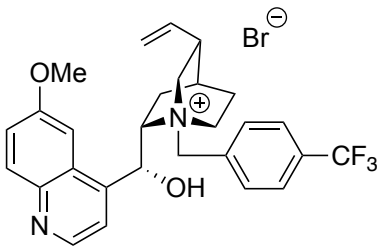
AIBN (0.8 mg, 5 μmol) was added to a solution of 2,3,4,5,6-pentafluoro-4'-methyl-1,1'-biphenyl **S6** (26 mg, 0.1 mmol) and NBS (23 mg, 0.13 mmol) in MeCN and heated to 70 ºC for 21 h. The reaction mixture was cooled to rt and filtered through celite, washing with pentane (20 mL) and concentrated under reduced pressure. Purification by flash chromatography (hexane) afforded 4'-(bromomethyl)-2,3,4,5,6-pentafluoro-1,1'-biphenyl **S7** (19 mg, 56%) as a white solid. R_f 0.42 (pentane); mp = 105–108 ºC; ν_{max} (film)/cm^{-1} 1491, 984; ^{1}H NMR (400 MHz, $CDCl_3$) δ 7.54 (d, J = 8.4 Hz, 2 H, 2 × HC_{Ar}), 7.44–7.40 (m, 2 H, 2 × HC_{Ar}), 4.55 (s, 2 H, CH_2Br); ^{13}C NMR (101 MHz, $CDCl_3$) δ 145.4 and 142.9 (2 × m, 2 × FC_{Ar}), 141.8 (m, FC_{Ar}), 139.1 and 136.6 (2 × m, 2 × FC_{Ar}), 138.9 (C_{Ar} quat), 130.6 (2 × C_{Ar}), 129.4 (2 × C_{Ar}), 126.4 (C_{Ar} quat), 115.2 (C_{Ar} quat), 32.5 (CH_2Br); ^{19}F{^{1}H} NMR (377 MHz, $CDCl_3$) δ –143.1 (dd, $J_{F–F}$ = 22.9, 8.0 Hz, 2 × FC_{Ar}), –155.0 (t, $J_{F–F}$ = 21.1 Hz, FC_{Ar}), –161.9 (td, $J_{F–F}$ = 21.1, 7.9 Hz, 2 × FC_{Ar}); HRMS (FTMS + pAPCI) *m/z* Calculated for $C_{13}H_7F_5{}^{79}Br^+$ $[M+H]^+$ 336.9646; Found 336.9641.

(1*S*,2*S*,4*S*,5*R*)-2-((*R*)-Hydroxy(6-methoxyquinolin-4-yl)methyl)-1-((2',3',4',5',6'-pentafluoro-[1,1'-biphenyl]-4-yl)methyl)-5-vinylquinuclidin-1-ium bromide (378)



A mixture of quinine (48 mg, 0.15 mmol) and 4'-(bromomethyl)-2,3,4,5,6-pentafluoro-1,1'-biphenyl **S7** (50 mg, 0.15 mmol) in THF (0.75 mL) was heated to 70 ºC for 22 h. The reaction was cooled and Et_2O (2.5 mL) was added. The reaction was stirred for approx. 0.5 h then the precipitate was filtered. The collected solid was dried to afford (1*S*,2*S*,4*S*,5*R*)-2-((*R*)-hydroxy(6-methoxyquinolin-4-yl)methyl)-1-((2',3',4',5',6'-pentafluoro-[1,1'-biphenyl]-4-yl)methyl)-5-vinylquinuclidin-1-ium bromide **378** (72 mg, 73%) as a pale brown solid. $[\alpha]_D^{17}$ = –96 (*c* = 0.25, CH_2Cl_2); R_f 0.09 (10% MeOH/CH_2Cl_2); mp = 180–185 ºC (decomposition observed); ν_{max} (film)/cm^{-1} 3213 (br s, OH), 2982, 2948, 1621, 1510, 992; ^{1}H NMR (400 MHz, $CDCl_3$) δ 8.68 (d, *J* = 4.5 Hz, 1 H, HC_{Ar}), 7.98–7.93 (m, 3 H, 3 × HC_{Ar}), 7.71 (d, *J* = 4.5 Hz, 1 H, HC_{Ar}), 7.39 (d, *J* = 8.1 Hz, 2 H, 2 × HC_{Ar}), 7.32 (d, *J* = 2.5 Hz, 1 H, HC_{Ar}), 7.27 (dd, *J* = 9.2, 2.5 Hz, 1 H, HC_{Ar}), 6.69 (d, *J* = 6.2 Hz, 1 H, N^+CH), 6.42 (d, *J* = 6.8 Hz, 1 H, OH), 6.20 (d, *J* = 12.0 Hz, 1 H, N^+CHHAr), 5.59 (ddd, *J* = 17.2, 10.4, 6.9 Hz, 1 H, $CH_2=CH$), 5.13 (d, *J* = 16.9 Hz, 1 H, CHH=CH), 5.00–4.90 (t, *J* = 12.0 Hz, 3 H, N^+CHHAr, N^+CHH and CHH=CH), 3.99–3.93 (m, 4 H, CHOH and OCH_3), 3.65 (ddd, *J* = 12.9, 5.8, 2.5 Hz, 1 H, N^+CHH), 3.48 (dd, *J* = 12.6, 10.7, 1 H, N^+CHH), 3.11 (td, *J* = 11.4, 6.4 Hz, 1 H, N^+CHH), 2.64–2.55 (m, 1 H, $CH_2=CHCH$), 2.37–2.23 (m, 2 H, N^+CHCHH and N^+CH_2CHH), 2.06–2.00 (m, 1 H, $N(CH_2)_2CH$), 1.82–1.72 (m, 1 H, NCH_2CHH), 1.58–1.48 (m, 1 H, NCHCHH); ^{13}C NMR (101 MHz, $CDCl_3$) δ 158.0 (OC_{Ar} quat), 147.2 (C_{Ar}), 145.2 and 142.8 (2 × m, 2 × FC_{Ar}), 144.1 (C_{Ar} quat), 143.0 (C_{Ar} quat), 139.1 (m, 2 × FC_{Ar}), 136.6 (m, FC_{Ar}), 136.1 ($CH_2=CH$), 134.3 (2 × C_{Ar}), 131.7 (C_{Ar}), 130.7 (2 × C_{Ar}), 128.6 (C_{Ar} quat), 128.3 (C_{Ar} quat), 125.9 (C_{Ar} quat), 121.1 (C_{Ar}), 120.5 (C_{Ar}), 117.9 ($CH_2=CH$), 114.5 (m, C_{Ar} quat), 101.8 (C_{Ar}), 69.5 (CHOH), 63.9 (N^+CH), 62.3 (N^+CH_2Ar), 60.4 (N^+CH_2), 56.3 (OCH_3), 51.2 (N^+CH_2), 37.9 ($CH_2=CHCH$), 26.8 ($N(CH_2)_2CH$), 24.8 (NCH_2CH_2), 21.5 ($NCHCH_2$); ^{19}F{^{1}H} NMR (377 MHz, $CDCl_3$) δ –143.1 (dd, $J_{F–F}$ = 22.8, 8.2 Hz, 2 × FC_{Ar}), –153.8 (t, $J_{F–F}$ = 20.9 Hz, FC_{Ar}), –161.3 (td, $J_{F–F}$ = 22.0, 7.9 Hz, 2 × FC_{Ar}); HRMS (FTMS + pAPCI) *m/z* Calculated for $C_{33}H_{30}N_2O_2F_5^+$ [M–Br^-] 581.2222; Found 581.2214.

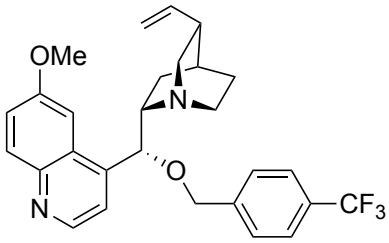
(1*S*,2*S*,4*S*,5*R*)-2-((*R*)-Hydroxy(6-methoxyquinolin-4-yl)methyl)-1-(4-(trifluoromethyl)benzyl)-5-vinylquinuclidin-1-ium bromide (385)



A solution of quinine (324 mg, 1.0 mmol) and 4-(trifluromethyl)benzyl bromide (239 mg, 1.0 mmol) in THF (5.0 mL) was heated to 70 ºC for 22 h. The reaction was cooled to rt and Et_2O was added. The reaction was stirred for approx. 0.5 h then the precipitate was filtered. The collected solid was dried to afford (1*S*,2*S*,4*S*,5*R*)-2-((*R*)-hydroxy(6-methoxyquinolin-4-yl)methyl)-1-(4-(trifluoromethyl)benzyl)-5-vinylquinuclidin-1-ium bromide **385** (505 mg, 90%) as a white solid. $[\alpha]_D^{17}$ = –180 (*c* = 0.1, MeOH) [lit = –153 (c = 0.18, MeOH)][453]; R_f 0.38 (5% MeOH/CH_2Cl_2); mp = >225 ºC [lit = 185–187 ºC][453]; ν_{max} (film)/cm^{-1} 3171 (OH), 1619, 1508, 1429, 1327, 1224, 1163, 1122, 1030, 1022, 856, 826; ^{1}H NMR (400 MHz, DMSO-d_6) δ 8.82 (d, *J* = 4.5 Hz, 1 H, HC_{Ar}), 8.03 (d, *J* = 9.2 Hz, 1 H, HC_{Ar}), 7.99–7.90 (m, 4 H, 4 × HC_{Ar}), 7.76 (d, *J* = 4.5 Hz, 1 H, HC_{Ar}), 7.51 (dd, *J* = 9.2, 2.6 Hz, 1 H, HC_{Ar}), 7.38 (d, *J* = 2.6 Hz, 1 H, HC_{Ar}), 6.72 (d, *J* = 3.7 Hz, 1 H, OH), 6.59–6.55 (m, 1 H, N^+CH), 5.74 (ddd, *J* = 17.3, 10.4, 6.9 Hz, 1 H, C*H*=CH_2), 5.49 (d, *J* = 12.4 Hz, 1 H, N^+C*H*HAr), 5.14–5.07 (m, 1 H, CH=C*H*H), 5.03–4.98 (m, 1 H, CH=CH*H*), 4.79 (d, *J* = 12.3 Hz, 1 H, N^+CH*H*Ar), 4.28–4.23 (m, 1 H, N^+C*H*H), 4.00 (s, 3 H, OCH_3), 3.89–3.81 (m, 1 H, C*H*OH), 3.70 (dd, *J* = 12.4, 5.7 Hz, 1 H, N^+C*H*H), 3.39–3.30 (m, 1 H, N^+CH*H*, confirmed by HSQC), 3.29–3.19 (m, 1 H, N^+CH*H*), 2.72–2.62 (m, 1 H, CH_2=CHC*H*), 2.29–2.20 (m, 1 H, NCH_2C*H*H), 2.19–2.08 (m, 1 H, NCHC*H*H), 2.03–1.97 (m, 1 H, N(CH_2)$_2$C*H*), 1.87–1.76 (m, 1H, NCHCH*H*), 1.50–1.40 (m, 1 H, NCH_2CH*H*); ^{1}H NMR (400 MHz, $CDCl_3$) δ 8.67 (d, *J* = 4.5 Hz, 1 H, HC_{Ar}), 7.98 (d, *J* = 8.1 Hz, 2 H, 2 × HC_{Ar}), 7.94 (d, *J* = 9.0 Hz, 1 H, HC_{Ar}), 7.70 (d, *J* = 4.5 Hz, 1 H, HC_{Ar}), 7.56 (d, *J* = 8.1 Hz, 2 H, 2 × HC_{Ar}), 7.29–7.23 (m, 2 H, 2 × HC_{Ar}), 6.62 (d, *J* = 6.6 Hz, 1 H, N^+CH), 6.38 (d, *J* = 6.7 Hz, 1 H, OH), 6.09 (d, *J* = 12.0 Hz, 1 H, N^+CH*H*Ar), 5.55 (ddd, *J* = 17.2, 10.4, 6.7 Hz, 1 H, C*H*=CH_2), 5.18–5.07 (m, 2 H, N^+CH*H*Ar and CH=C*H*H), 4.96–4.82 (m, 2 H CH=CH*H* and N^+C*H*H), 4.06–3.88 (m, 4 H, OCH_3 and C*H*OH), 3.81–3.71 (m, 1 H, N^+C*H*H), 3.40–3.30 (m, 1 H, N^+CH*H*), 3.03 (td, *J* = 11.5, 6.1 Hz, 1 H, N^+CH*H*), 2.54 (d, *J* = 7.3 Hz, 1 H, CH_2=CHC*H*), 2.32–2.16 (m, 2 H, NCH_2C*H*H and NCHC*H*H), 2.04–1.96 (m, 1 H, N(CH_2)$_2$C*H*), 1.77–1.67 (m, 1 H, NCHCH*H*), 1.54–1.44 (m, 1 H, NCH_2CH*H*); ^{13}C NMR (101 MHz, DMSO-d_6) δ 157.4 (OC_{Ar} quat), 147.4 (C_{Ar}), 143.8 (C_{Ar} quat), 143.7 (C_{Ar} quat), 138.0 (CH_2=*C*H), 134.5 (2 × C_{Ar}), 132.6 (C_{Ar} quat), 131.5 (C_{Ar}), 130.4 (q, J_{C-F} = 32 Hz, $C_{Ar}CF_3$ quat), 125.8 (2 × C_{Ar}), 125.3 (C_{Ar} quat), 124.0 (q, *J* = 272 Hz, CF_3), 121.4 (C_{Ar}), 120.3 (C_{Ar}) 116.6 (*C*H_2=CH), 102.1 (C_{Ar}), 68.6 (CHOH), 63.6 (N^+CH), 62.3 (N^+CH_2Ar), 59.2 (N^+CH_2), 56.0 (OCH_3), 50.8 (N^+CH_2), 37.0 (CH_2=CH*C*H), 25.9 (N(CH_2)$_2$*C*H), 24.2 (NCH*C*H_2), 20.3 (NCH_2*C*H_2); ^{13}C NMR (101 MHz, $CDCl_3$) δ 158.0

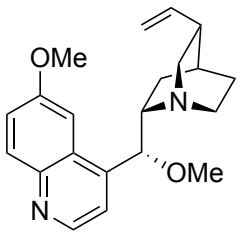
(OC_{Ar} quat), 147.3 (C_{Ar}), 144.1 (C_{Ar} quat), 142.8 (C_{Ar} quat), 135.9 (*C*H=CH_2), 134.4 (2 × C_{Ar}), 132.3 (q, J_{C-F} = 33 Hz, CF_3C_{Ar} quat), 131.7 (C_{Ar} quat), 131.2 (C_{Ar} quat), 125.9 (C_{Ar}), 125.7 (2 × C_{Ar}), 123.4 (q, J_{C-F} = 273 Hz, CF_3), 121.2 (C_{Ar}), 120.5 (C_{Ar}), 117.8 (CH=*C*H_2), 101.7 (C_{Ar}), 69.1 (CHOH), 63.9 (N^+CH), 61.6 (N^+CH_2Ar), 60.2 (N^+CH_2), 56.3 (OCH_3), 51.4 (N^+CH_2), 37.9 (*C*HCH=CH_2), 26.6 ($N(CH_2)_2$*C*H), 24.8 (NCH_2CH_2), 21.6 (NCH_2CH_2); ^{19}F NMR (377 MHz, DMSO-d_6) δ –61.3; ^{19}F{^{1}H} NMR (377 MHz, $CDCl_3$) δ –63.1. The observed characterisation data (^{1}H in DMSO-d_6) was consistent with that previously reported in the literature.[454]

(1*S*,2*S*,4*S*,5*R*)-2-((*R*)-(6-Methoxyquinolin-4-yl)((4-(trifluoromethyl)benzyl)oxy)methyl)-5-vinylquinuclidine (386)



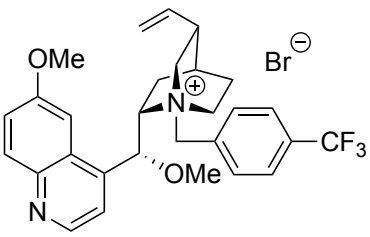
Cesium hydroxide monohydrate (84 mg, 0.5 mmol) was added to a solution of 1*S*,2*S*,4*S*,5*R*)-2-((*R*)-hydroxy(6-methoxyquinolin-4-yl)methyl)-1-(4-(trifluoromethyl)benzyl)-5-vinylquinuclidin-1-ium bromide **385** (56 mg, 0.1 mmol) in toluene (1.0 mL) and the mixture was stirred at 25 ºC for 17 h. The reaction mixture was filtered through celite, washing with Et_2O (25 mL) and concentrated under reduced pressure to afford (1*S*,2*S*,4*S*,5*R*)-2-((*R*)-(6-methoxyquinolin-4-yl)((4-(trifluoromethyl)benzyl)oxy)methyl)-5-vinylquinuclidine **386** (46 mg, 96%) as a colourless gummy solid. $[\alpha]_D^{17} = -29$ (*c* = 1.18, $CHCl_3$); R_f 0.50 (Et_2O); ν_{max} (film)/cm^{-1} 2934, 2795, 2762, 1620, 1508, 1324, 1238, 1161, 1121, 1105, 1066, 1019, 854; ^{1}H NMR (400 MHz, $CDCl_3$) δ 8.75 (d, *J* = 4.4 Hz, 1 H, HC_{Ar}), 8.06 (d, *J* = 9.2 Hz, 1 H, HC_{Ar}), 7.56 (d, *J* = 8.1 Hz, 2 H, 2 × HC_{Ar}), 7.46–7.39 (m, 3 H, 3 × HC_{Ar}), 7.27 (dd, *J* = 15.9, 3.5 Hz, 2 H, 2 × HC_{Ar}), 6.32–6.19 (m, 1 H, CH_2=C*H*), 5.14 (dd, *J* = 10.3, 1.9 Hz, 1 H, C*H*H=CH), 5.10–5.03 (m, 1 H, CH*H*=CH), 4.14 (d, *J* = 1.7 Hz, 1 H, C*H*OCH_2Ar), 3.97 (s, 3 H, OCH_3), 3.56 (d, *J* = 14.0 Hz, 1 H, OC*H*HAr), 3.48 (d, *J* = 14.0 Hz, 1 H, OCH*H*Ar), 3.04–2.97 (m, 1 H, NC*H*H), 2.86 (d, *J* = 10.7 Hz, 1 H, NCH), 2.75 (d, *J* = 10.0 Hz, 1 H, NC*H*H), 2.46 (dd, *J* = 8.7, 3.1 Hz, 1 H, CH_2=CHC*H*), 2.34–2.24 (m, 1 H, NCH*H*), 2.15 (td, *J* = 10.5, 3.7 Hz, 1 H, NCH*H*), 1.99–1.87 (m, 2 H, NCHC*H*H and NCH_2C*H*H), 1.78–1.64 (m, 3 H, N(CH_2)C*H*, NCHCH*H* and NCH_2CH*H*); ^{13}C NMR (101 MHz, $CDCl_3$) δ 157.9 (OC_{Ar} quat), 148.0 (C_{Ar}), 143.9 (C_{Ar} quat), 143.2 (C_{Ar} quat), 141.8 (C_{Ar} quat), 138.1 (CH_2=*C*H), 131.8 (C_{Ar}), 129.1 (q, J_{C-F} = 32 Hz, $C_{Ar}CF_3$ quat), 128.8 (2 × C_{Ar}), 127.4 (C_{Ar} quat), 124.3 (q, J_{C-F} = 273 Hz, CF_3 quat), 125.1 (q, J_{C-F} = 4 Hz, 2 × C_{Ar}), 121.6 (C_{Ar}), 116.8 (C_{Ar}), 116.5 (*C*H_2=CH), 101.0 (C_{Ar}), 62.6 (OCH_2Ar), 61.3 (NCH), 58.9 (NCH_2), 55.6 (OCH_3), 55.4 (*C*HOCH_2Ar), 53.7 (NCH_2), 43.4 (CH_2=CH*C*H), 36.9 ($N(CH_2)_2$*C*H), 28.7 (NCH*C*H_2 and NCH_2CH_2); ^{19}F{^{1}H} NMR (377 MHz, $CDCl_3$) δ –62.3; HRMS (ESI$^+$) *m/z* Calculated for $C_{28}H_{30}N_2O_2F_3$ [M+H] 483.2259; Found 483.2245.

(1*S*,2*S*,4*S*,5*R*)-2-((*R*)-Methoxy(6-methoxyquinolin-4-yl)methyl)-5-vinylquinuclidine (S8)



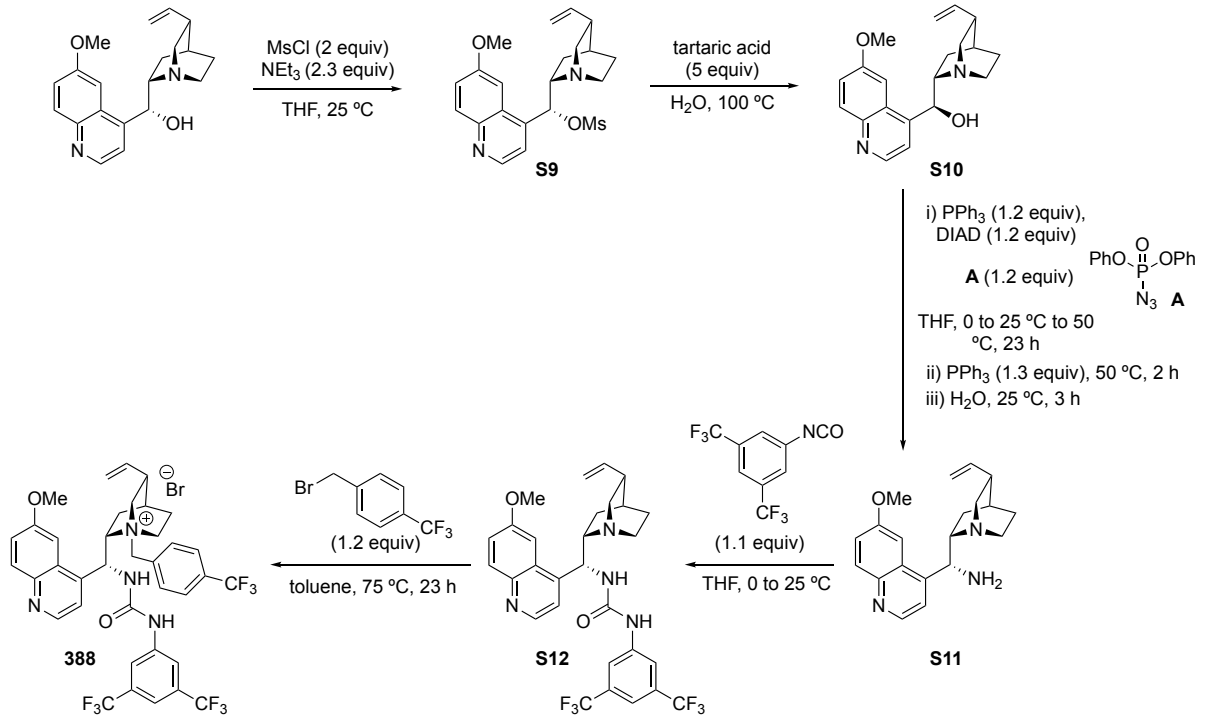
NaH (60% dispersion in mineral oil, 1.0 g, 25.0 mmol) was added portionwise to a solution of quinine (3.24 g, 10.0 mmol) in DMF (33 mL) at 0 ºC and stirred for 1 h at 0 ºC. MeI (0.62 mL, 10.0 mmol) was added dropwise at 0 ºC and the reaction mixture was stirred for 24 h at 25 ºC. Sat. aq. brine (50 mL) was added and the aqueous reaction mixture was extracted with EtOAc (3 × 50 mL). The combined organic layers were dried over Na_2SO_4, filtered and concentrated under reduced pressure. Purification by flash chromatography afforded (1*S*,2*S*,4*S*,5*R*)-2-((*R*)-methoxy(6-methoxyquinolin-4-yl)methyl)-5-vinylquinuclidine **S8** (1.63 g, 48%) as a yellow gum. $[\alpha]_D^{17}$ = –144 (*c* = 1.17, $CHCl_3$) [lit = –172 (*c* = 0.90, $CHCl_3$)][455]; R_f 0.18 (10% MeOH/CH_2Cl_2); ν_{max} (film)/cm^{-1} 2933, 2866, 1618, 1506, 1472, 1226, 1111, 1059, 1025, 913, 857, 716; ^{1}H NMR (400 MHz, $CDCl_3$) δ 8.77 (d, *J* = 4.5 Hz, 1 H, HC_{Ar}), 8.05 (d, *J* = 9.5 Hz, 1 H, HC_{Ar}), 7.45–7.35 (m, 3 H, 3 × HC_{Ar}), 5.70 (ddd, *J* = 17.5, 10.3, 7.6 Hz, 1 H, C*H*=CH_2), 5.14 (br s, 1 H, C*H*OCH_3), 5.01–4.86 (m, 2 H, CH=C*H*$_2$), 3.98 (s, 3 H, $ArOCH_3$), 3.51 (s, 1 H, NC*H*H), 3.34 (s, 3 H, OCH_3), 3.22–3.09 (m, 2 H, NC*H*H and NCH), 2.82–2.65 (m, 2 H, 2 × NCH*H*), 2.34 (s, 1 H, C*H*CH=CH_2), 1.85 (s, 3 H, NCHC*H*H, NCH_2CHH and $N(CH_2)_2CH$), 1.63–1.47 (m, 2 H, NCHCH*H* and NCH_2CHH); ^{13}C NMR (101 MHz, $CDCl_3$) δ 158.0 (OC_{Ar} quat), 147.3 (C_{Ar}), 144.5 (C_{Ar} quat), 143.9 (C_{Ar} quat), 141.1 (CH_2=*C*H), 131.7 (C_{Ar}), 127.3 (C_{Ar} quat), 121.8 (C_{Ar}), 118.5 (*C*H_2=CH), 114.7 (C_{Ar}), 101.1 (C_{Ar}), 82.0 (*C*HOCH_3), 59.8 (NCH), 57.0 (OCH_3), 56.6 (NCH_2), 56.0 ($ArOCH_3$), 43.2 (NCH_2), 39.5 (*C*HCH=CH_2), 27.7 ($N(CH_2)_2CH$), 27.1 ($NCHCH_2$), 21.4 (NCH_2CH_2). The observed characterisation data (IR, ^{1}H and ^{13}C NMR) was consistent with that previously reported in the literature.[456]

(1*S*,2*S*,4*S*,5*R*)-2-((*R*)-methoxy(6-methoxyquinolin-4-yl)methyl)-1-(4-(trifluoromethyl)benzyl)-5-vinylquinuclidin-1-ium bromide (387)

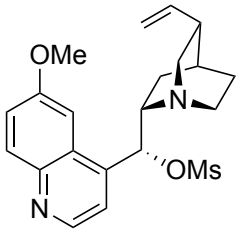


A solution of (1*S*,2*S*,4*S*,5*R*)-2-((*R*)-Methoxy(6-methoxyquinolin-4-yl)methyl)-5-vinylquinuclidine **S8** (338 mg, 1.0 mmol) and 4-(trifluromethyl)benzyl bromide (239 mg, 1.0 mmol) in THF (5.0 mL) was heated to 70 ºC for 18 h. The reaction was cooled to rt and Et_2O was added. The reaction was stirred for approx. 0.5 h then the precipitate was filtered. The collected solid was purified by flash chromatography (10% MeOH/CH_2Cl_2) afforded (1*S*,2*S*,4*S*,5*R*)-2-((*R*)-methoxy(6-methoxyquinolin-4-yl)methyl)-1-(4-(trifluoromethyl)benzyl)-5-vinylquinuclidin-1-ium bromide **387** (287 mg, 50%) as a pale yellow solid. $[\alpha]_D^{17}$ = –216 (*c* = 0.5, CH_3OH); R_f 0.11 (10% MeOH/CH_2Cl_2); ν_{max} (film)/cm^{-1} 2952, 1621, 1506, 1323, 1238, 1170, 1126, 1070, 1021, 910, 857, 723; ^{1}H NMR (400 MHz, CD_3OD) δ 8.85 (d, *J* = 4.5 Hz, 1 H, HC_{Ar}), 8.09 (d, *J* = 9.3 Hz,

1 H, HC_{Ar}), 8.02 (d, *J* = 8.1 Hz, 2 H, 2 × HC_{Ar}), 7.94 (d, *J* = 8.1 Hz, 2 H, 2 × HC_{Ar}), 7.83 (d, *J* = 4.5 Hz, 1 H, HC_{Ar}), 7.58 (dd, *J* = 9.3, 2.6 Hz, 1 H, HC_{Ar}), 7.49 (d, *J* = 2.4 Hz, 1 H, HC_{Ar}), 6.39 (s, 1 H, N^+CH), 5.77 (ddd, *J* = 17.3, 10.4, 7.0 Hz, 1 H, CH_2=C*H*), 5.53 (d, *J* = 12.3 Hz, 1 H, N^+C*H*HAr), 5.18 (dt, *J* = 17.2, 1.1 Hz, 1 H, C*H*H=CH), 5.08 (dt, *J* = 10.5, 1.1 Hz, 1 H, CH*H*=CH), 4.92 (d, *J* = 12.3 Hz, 1 H, N^+CH*H*Ar), 4.30–4.20 (m, 1 H, N^+C*H*H), 4.11 (s, 3 H, $ArOCH_3$), 4.02–3.95 (m, 1 H, C*H*OCH_3), 3.74–3.64 (m, 4 H, OCH_3 and N^+C*H*H), 3.58–3.42 (m, 2 H, 2 × N^+CH*H*), 2.80–2.71 (m, 1 H, CH_2=CHC*H*), 2.56–2.48 (m, 1 H, NCHC*H*H), 2.40–2.29 (m, 1 H, NCH_2C*H*H), 2.16–2.11 (m, 1 H, $N(CH_2)_2$C*H*), 2.02–1.91 (m, 1 H, NCH_2CH*H*), 1.73 – 1.63 (m, 1 H, NCHCH*H*); ^{13}C NMR (101 MHz, CD_3OD) δ 160.3 (OC_{Ar} quat), 148.2 (C_{Ar}), 145.3 (C_{Ar} quat), 141.5 (C_{Ar} quat), 138.4 (CH_2=*C*H), 135.8 (2 × C_{Ar}), 133.6 (q, $J_{C–F}$ = 33 Hz, *C*$_{Ar}CF_3$ quat), 132.9 (C_{Ar} quat), 132.0 (C_{Ar}), 128.3 (C_{Ar} quat), 127.2 (q, $J_{C–F}$ = 4 Hz, 2 × C_{Ar}), 125.3 (q, $J_{C–F}$ = 272 Hz, CF_3), 123.6 (C_{Ar}), 121.6 (C_{Ar}), 117.8 (*C*H_2=CH), 102.5 (C_{Ar}), 75.6 (N^+CH), 70.7 (*C*HOCH_3), 65.2 (N^+CH_2), 61.8 (N^+CH_2), 57.3 (OCH_3), 56.7 ($ArOCH_3$), 53.1 (N^+CH_2), 39.1 (CH_2=CH*C*H), 28.1 ($N(CH_2)_2$*C*H), 25.8 (NCH_2*C*H_2), 22.2 (NCH*C*H_2); ^{19}F{^{1}H} NMR (377 MHz, CD_3OD) δ –64.5; HRMS (FTMS + pAPCI) *m/z* Calculated for $C_{29}H_{32}N_2O_2F_3^+$ [M–Br^-] 497.2410; Found 497.2395.

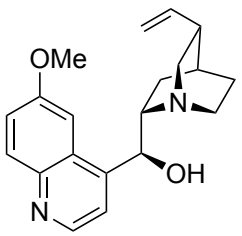


(*R*)-(6-Methoxyquinolin-4-yl)((1*S*,2*S*,4*S*,5*R*)-5-vinylquinuclidin-2-yl)methyl methanesulfonate (S9)[457]



Mesyl chloride (1.54 mL, 20.0 mL) was added dropwise to a solution of quinine (3.24 g, 10.0 mmol) and NEt_3 (3.20 mL, 23.0 mmol) in THF (40 mL) at 0 ºC. The reaction mixture was stirred for 24 h then sat. aq. $NaHCO_3$ (100 mL) was added. The aqueous reaction mixture was extracted with CH_2Cl_2 (3 × 50 mL). The combined organic layers were dried over Na_2SO_4, filtered and concentrated under reduced pressure. Purification by flash chromatography (10% MeOH/EtOAc) afforded (*R*)-(6-methoxyquinolin-4-yl)((1*S*,2*S*,4*S*,5*R*)-5-vinylquinuclidin-2-yl)methyl methanesulfonate **S9** (2.62 g, 65%) as a pale yellow solid. $[\alpha]_D^{17} = -66$ (*c* = 1, $CHCl_3$) [lit = –71.9 (*c* = 0.92, CH_2Cl_2)][458]; R_f 0.30 (10% MeOH/EtOAc); mp = 120–123 ºC [lit = 114–116.5 ºC][458]; ν_{max} (film)/cm^{-1} 2944, 2911, 2870, 1621, 1510, 1476, 1357, 1260, 1223, 1170, 1021, 984, 924, 869, 831, 678; ^{1}H NMR (400 MHz, $CDCl_3$) δ 8.79 (d, *J* = 4.3 Hz, 1 H, HC_{Ar}), 8.05 (d, *J* = 9.2 Hz, 1 H, HC_{Ar}), 7.50–7.34 (m, 3 H, 3 × HC_{Ar}), 6.18 (s, 1 H, HCOMs), 5.82 (ddd, *J* = 17.3, 9.8, 7.4 Hz, 1 H, CH_2=C*H*), 5.05–4.97 (m, 2 H, CH_2=CH), 3.96 (s, 3 H, OCH_3), 3.41 (br s, 1 H, NC*H*H), 3.17–3.06 (m, 1 H, NC*H*H), 3.03–2.92 (m, 1 H, NCH), 2.71–2.52 (m, 5 H, SO_2CH_3 and 2 × NCH*H*), 2.28 (br s, 1 H, CH_2=CHC*H*), 2.12–1.98 (s, 1 H, NCHC*H*H), 1.91 (br s, 1 H, N(CH_2)C*H*), 1.82–1.50 (m, 3 H, NCH_2CH_2 and NCHCH*H*); ^{13}C NMR (101 MHz, $CDCl_3$) δ 158.3 (OC_{Ar} quat), 147.4 (C_{Ar}), 144.9 (C_{Ar} quat), 141.4 (C_{Ar}), 132.1 (C_{Ar}), 126.4 (CH_2=CH), 122.2 (C_{Ar}), 119.3 (br s, C_{Ar} quat), 114.6 (CH_2=CH), 100.7 (br s, C_{Ar}), 59.7 (br s, NCH), 56.4 (NCH_2), 55.7 (OCH_3), 42.2 (br s, NCH_2), 39.4 (*C*HCH=CH_2), 39.1 (SO_2CH_3), 27.5 (N(CH_2)$_2$*C*H), 27.2 (NCH*C*H_2), 24.9 (NCH_2CH_2) (the signal due to CHOMs was not observed, the signal due to NC_{Ar} quat expected at ~143 ppm was not observed). The observed characterisation data (IR, ^{1}H and ^{13}C NMR) was consistent with that previously reported in the literature.[458]

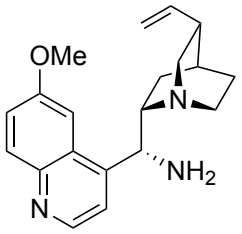
(*S*)-(6-Methoxyquinolin-4-yl)((1*S*,2*S*,4*S*,5*R*)-5-vinylquinuclidin-2-yl)methanol (S10)



Tartaric acid (3.75 g, 25.0 mmol) was added to a solution of (*R*)-(6-Methoxyquinolin-4-yl)((1*S*,2*S*,4*S*,5*R*)-5-vinylquinuclidin-2-yl)methyl methanesulfonate (2.01 g, 5.0 mmol) in H_2O (50 mL) and heated at 100 ºC for 19 h. The reaction mixture was cooled to rt, then solid $NaHCO_3$ was added until no significant effervescence was observed. The aqueous reaction mixture was extracted with CH_2Cl_2 (3 × 100 mL). The combined organic layers were washed with sat. aq. $NaHCO_3$ (100 mL), dried over Na_2SO_4, filtered and concentrated under reduced pressure to afford (*S*)-(6-methoxyquinolin-4-yl)((1*S*,2*S*,4*S*,5*R*)-5-vinylquinuclidin-2-yl)methanol **S10** (1.41 g, 87%) as a brown solid. $[\alpha]_D^{17} = +30$ (*c* = 1.35, $CHCl_3$) [lit = +43.3 (*c* =

1.0, EtOH)][459]; R_f 0.06 (20% MeOH/CH_2Cl_2); mp = 67–70 ºC [lit = 175 ºC][460]; ν_{max} (film)/cm^{-1} 3243 (br s, OH), 2930, 2863, 1618, 1506, 1472, 1357, 1320, 1238, 1081, 1025, 988, 913, 854, 716; ^{1}H NMR (400 MHz, $CDCl_3$) δ 8.75 (d, *J* = 4.5 Hz, 1 H, HC_{Ar}), 8.04 (d, *J* = 9.2 Hz, 1 H, HC_{Ar}), 7.66 (d, *J* = 2.8 Hz, 1 H, HC_{Ar}), 7.43–7.37 (m, 2 H, 2 × HC_{Ar}), 5.76 (ddd, *J* = 17.1, 10.3, 7.5 Hz, 1 H, CH_2=C*H*), 5.06–4.95 (m, 3 H, C*H*$_2$=CH and C*H*OH), 3.96 (s, 3 H, OCH_3), 3.33–3.08 (m, 3 H, 2 × NCH*H* and NCH), 2.86–2.77 (m, 2 H, 2 × NCH*H*), 2.39–2.30 (m, 1 H, CH_2=CHC*H*), 1.77–1.72 (m, 1 H, N(CH_2)$_2$C*H*), 1.66–1.60 (m, 2 H, NCHC*H*H and NCH_2C*H*H), 1.53–1.44 (m, 1 H, NCHCH*H*), 0.98 (ddt, *J* = 13.5, 7.8, 1.8 Hz, 1 H, NCH_2CH*H*); ^{13}C NMR (101 MHz, $CDCl_3$) δ 157.5 (OC_{Ar} quat), 147.6 (C_{Ar}), 144.9 (C_{Ar} quat), 144.3 (C_{Ar} quat), 141.4 (CH_2=*C*H), 131.7 (C_{Ar}), 128.2 (C_{Ar} quat), 121.3 (C_{Ar}), 120.1 (C_{Ar}), 114.7 (*C*H_2=CH), 102.6 (C_{Ar}), 71.4 (*C*HOH), 61.6 (NCH), 55.9 (NCH_2), 55.5 (OCH_3), 40.8 (NCH_2), 39.9 (CH_2=CHC*H*), 28.0 (N(CH_2)$_2$*C*H), 27.3 (NCH*C*H_2), 25.2 (NCH_2*C*H_2). The observed characterisation data (^{1}H and ^{13}C NMR) was consistent with that previously reported in the literature.[461]

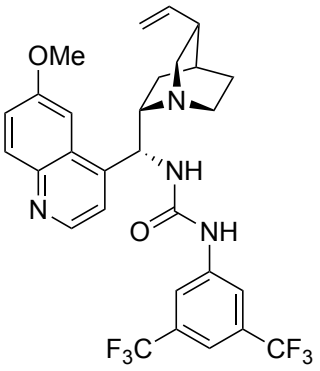
(*R*)-(6-Methoxyquinolin-4-yl)((1*S*,2*S*,4*S*,5*R*)-5-vinylquinuclidin-2-yl)methanamine (S11)



DIAD (1.02 mL, 5.16 mmol) was added to a stirred solution of *S*)-(6-methoxyquinolin-4-yl)((1*S*,2*S*,4*S*,5*R*)-5-vinylquinuclidin-2-yl)methanol **S10** (1.40 g, 4.3 mmol) and PPh_3 (1.35 g, 5.16 mmol) in THF (16 mL) at 0 ºC. A solution of diphenyl phosphoryl azide (1.11 mL, 5.16 mmol) in THF (8 mL) was added dropwise at 0 ºC. The temperature was raised to 25 ºC and stirred for 24 h then heated to 50 ºC for 2 h. PPh_3 (1.46 g, 5.6 mmol) was added at 50 ºC and the reaction mixture stirred at 50 ºC for 1 h. H_2O (1.0 mL) was added and the reaction mixture was stirred at 25 ºC for 3 h then concentrated under reduced pressure. The crude reaction mixture was dissolved in CH_2Cl_2 (20 mL) and 1 M HCl (20 mL) was added. The layers were separated and the aqueous layer was extracted with CH_2Cl_2 (3 × 20 mL). 1 M NaOH (40 mL) was added to the aqueous layer (pH > 7) and the aqueous layer was extracted with CH_2Cl_2 (2 × 20 mL) followed by EtOAc (2 × 20 mL). The organic layers were combined, filtered and concentrated under reduced pressure. Purification by flash chromatography (10% to 20% MeOH/CH_2Cl_2 to 1% NEt_3 + 20% MeOH/CH_2Cl_2) afforded (*R*)-(6-methoxyquinolin-4-yl)((1*S*,2*S*,4*S*,5*R*)-5-vinylquinuclidin-2-yl)methanamine **S11** (0.94 g, 68%) as a yellow solid. $[\alpha]_D^{17} = -33$ (*c* = 0.3, $CHCl_3$) [lit = –53.6 (*c* = 0.3, $CHCl_3$)][462]; R_f 0.06 (10% MeOH/CH_2Cl_2); mp = 53–56 ºC; ν_{max} (film)/cm^{-1} 3370 and 3280 (br s, NH), 2937, 2863, 1621, 1538, 1506, 1472, 1230, 1029, 910, 850, 731; ^{1}H NMR (400 MHz, $CDCl_3$) δ 8.74 (d, *J* = 4.6 Hz, 1 H, HC_{Ar}), 8.01 (d, *J* = 9.2 Hz, 1 H, HC_{Ar}), 7.50 (d, *J* = 2.4 Hz, 1 H, HC_{Ar}), 7.39–7.33 (m, 2 H, 2 × HC_{Ar}), 5.86 (ddd, *J* = 17.4, 10.4, 7.4 Hz, 1 H, CH_2=C*H*), 5.09–5.02 (m, 2 H, C*H*$_2$=CH), 4.98–4.83 (m, 1 H, C*H*NH_2), 4.00 (s, 3 H, OCH_3), 3.42–3.18 (m, 2 H, NC*H*H and NCH), 3.11 (dd, *J* = 13.6, 10.2

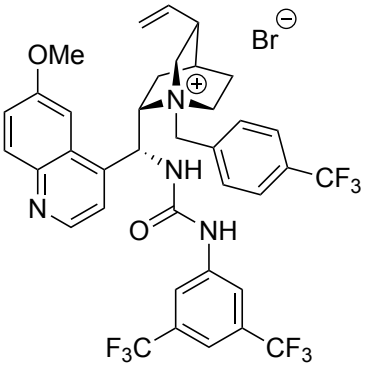
Hz, 1 H, NC*H*H), 2.81–2.60 (m, 2 H, 2 × NCH*H*), 2.40–2.31 (m, 1 H, CH_2=CHC*H*), 2.09–2.00 (m, 1 H, NCHC*H*H), 1.98–1.91 (m, 1 H, $N(CH_2)_2C$*H*), 1.80–1.71 (m, 1 H, NCH_2C*H*H), 1.65–1.55 (m, 2 H, NCH_2CH*H* and NCHCH*H*); ^{13}C NMR (101 MHz, $CDCl_3$) δ 158.0 (OC_{Ar} quat), 148.6 (br s, C_{Ar} quat), 147.7 (C_{Ar}), 144.8 (C_{Ar} quat), 141.0 (br s, CH_2=*C*H), 131.9 (C_{Ar}), 127.4 (C_{Ar} quat), 121.5 (C_{Ar}), 118.1 (C_{Ar}), 115.0 (*C*H_2=CH), 101.2 (C_{Ar}), 60.5 (NCH), 56.03 (NCH_2), 55.95 (OCH_3), 52.9 (br s, $CHNH_2$), 42.2 (NCH_2), 39.2 (CH_2=CH*C*H), 27.6 ($N(CH_2)_2$*C*H), 27.2 ($NCHCH_2$), 25.2 (br s, NCH_2CH_2). The observed characterisation data (^{1}H and ^{13}C NMR) was consistent with that previously reported in the literature.[463]

1-(3,5-Bis(trifluoromethyl)phenyl)-3-((*R*)-(6-methoxyquinolin-4-yl)((1*S*,2*S*,4*S*,5*R*)-5-vinylquinuclidin-2-yl)methyl)urea (S12)



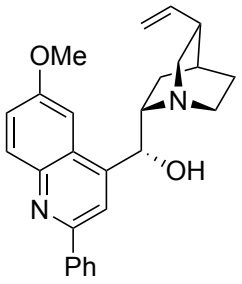
3-5-bis(trifluoromethyl)phenyl isocyanate (0.29 mL, 1.65 mmol) was added dropwise to a solution of (*R*)-(6-methoxyquinolin-4-yl)((1*S*,2*S*,4*S*,5*R*)-5-vinylquinuclidin-2-yl)methanamine **S11** (485 mg, 1.5 mmol) in THF (1.5 mL) at 0 ºC. The reaction mixture was stirred at 25 ºC for 15 h then concentrated under reduced pressure. Purification by flash chromatography (5 to 10% MeOH/CH_2Cl_2) afforded 1-(3,5-bis(trifluoromethyl)phenyl)-3-((*R*)-(6-methoxyquinolin-4-yl)((1*S*,2*S*,4*S*,5*R*)-5-vinylquinuclidin-2-yl)methyl)urea **S12** (705 mg, 81%). $[\alpha]_D^{15} = -26$ (*c* = 1.0, CH_2Cl_2); R_f 043 (10% MeOH/CH_2Cl_2); mp = 142–146 ºC; ν_{max} (film)/cm^{-1} 3302 (br s, NH), 3083, 2941, 1674 (C=O), 1621 (C=C), 1566 (C=C), 1510, 1472, 1387, 1275, 1230, 1126, 1029, 880, 850, 731; ^{1}H NMR (400 MHz, $CDCl_3$) δ 8.51 (s, 1 H, NH), 8.39 (d, *J* = 4.0 Hz, 1 H, HC_{Ar}), 7.89 (s, 2 H, 2 × HC_{Ar}), 7.57 (d, *J* = 8.3 Hz, 1 H, HC_{Ar}), 7.51–7.43 (m, 2 H, 2 × HC_{Ar}), 7.22 (d, *J* = 4.2 Hz, 1 H, HC_{Ar}), 7.16–7.11 (m, 1 H, HC_{Ar}), 5.99–5.75 (m, 3 H, NH, C*H*=CH_2 and C*H*NHCO), 5.14–5.11 (m, 1 H, CH=C*H*H), 5.09 (d, *J* = 1.0 Hz, 1 H, CH=CH*H*), 3.93 (s, 3 H, OCH_3), 3.46–3.32 (s, 1 H, NC*H*H), 3.15 (t, *J* = 10.9 Hz, 1 H, NCH), 3.02–2.72 (2 × br s, 2 H, NCH*H* and NC*H*H), 2.59 (br s, 1 H, NCH*H*), 2.36 (br s, 1 H, CH_2=CHC*H*), 2.08 (t, *J* = 10.9 Hz, 1 H, NCH_2C*H*H), 1.97–1.71 (m, 3 H, $N(CH_2)_2C$*H*, NCH_2CH*H* and NCHC*H*H), 1.63–1.51 (m, 1 H, NCHCH*H*); ^{13}C NMR (101 MHz, $CDCl_3$) δ 158.5 (OC_{Ar} quat), 155.0 (C=O), 146.5 (C_{Ar}), 145.8 (C_{Ar} quat), 143.6 (C_{Ar} quat), 141.2 (C_{Ar}), 140.9 (CH_2=*C*H), 132.1 (q, J_{C-F} = 33 Hz, 2 × $C_{Ar}CF_3$ quat), 129.8 (C_{Ar}), 128.2 (C_{Ar} quat), 123.1 (q, J_{C-F} = 274 Hz, 2 × CF_3), 122.7 (C_{Ar}), 118.8 (C_{Ar} quat), 117.7 (2 × C_{Ar}), 115.4 (*C*H_2=CH), 114.8 (C_{Ar}), 101.5 (C_{Ar}), 58.1 (NCH), 55.9 (NCH_2), 55.7 (OCH_3), 50.2 (*C*HNHCO), 41.5 (NCH_2), 39.2 (CH_2=CH*C*H), 27.3 ($N(CH_2)_2$*C*H), 27.1 (NCH_2CH_2), 25.1 ($NCHCH_2$); ^{19}F{^{1}H} NMR (377 MHz, $CDCl_3$) δ –63.1; HRMS (ESI$^+$) *m/z* Calculated for $C_{29}H_{29}N_4O_2F_6$ [M+H] 579.2195; Found 579.2203.

(1*S*,2*S*,4*S*,5*R*)-2-((*R*)-(3-(3,5-Bis(trifluoromethyl)phenyl)ureido)(6-methoxyquinolin-4-yl)methyl)-1-(4-(trifluoromethyl)benzyl)-5-vinylquinuclidin-1-ium bromide (388)



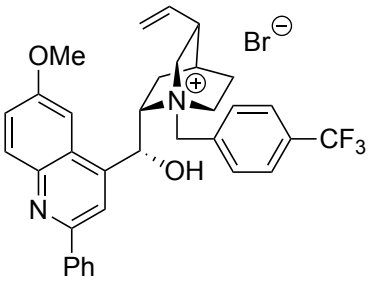
A mixture of 1-(3,5-bis(trifluoromethyl)phenyl)-3-((*R*)-(6-methoxyquinolin-4-yl)((1*S*,2*S*,4*S*,5*R*)-5-vinylquinuclidin-2-yl)methyl)urea **S12** (400 mg, 0.69 mmol) and 4-(trifluromethyl)benzyl bromide (198 mg, 0.83 mmol) in toluene (11.5 mL) was heated to 75 ºC for 23 h. The reaction was cooled and concentrated under reduced pressure. Purification by flash chromatography (5% to 10% to 20% MeOH/Et_2O) afforded (1*S*,2*S*,4*S*,5*R*)-2-((*R*)-(3-(3,5-bis(trifluoromethyl)phenyl)ureido)(6-methoxyquinolin-4-yl)methyl)-1-(4-(trifluoromethyl)benzyl)-5-vinylquinuclidin-1-ium bromide **388** (321 mg, 57%) as a yellow solid. $[\alpha]_D^{14}$ = +8 (*c* = 1.0, CH_2Cl_2); R_f 0.38 (15% MeOH/CH_2Cl_2); mp = 175–178 ºC ; ν_{max} (film)/cm^{-1} 3220 (NH), 3083, 3004, 1692 (C=O), 1621 (C=C), 1573 (C=C), 1510, 1472, 1431, 1387, 1323, 1275, 1223, 1170, 1126, 1070, 1021, 939, 910, 854; ^{1}H NMR (400 MHz, $CDCl_3$) δ 10.12 (s, 1 H, NH), 9.01 (d, *J* = 9.9 Hz, 1 H, NH), 8.68 (d, *J* = 4.6 Hz, 1 H, HC_{Ar}), 8.09 (s, 2 H, 2 × HC_{Ar}), 7.94 (d, *J* = 9.2 Hz, 1 H, HC_{Ar}), 7.73 (d, *J* = 4.7 Hz, 1 H, HC_{Ar}), 7.62 (s, 4 H, 4 × HC_{Ar}), 7.48 (s, 1 H, HC_{Ar}), 7.33 (d, *J* = 2.4 Hz, 1 H, HC_{Ar}), 7.30–7.25 (m, 1 H, HC_{Ar}), 6.83 (d, *J* = 10.1 Hz, 1 H, N^+CH), 5.58 (ddd, *J* = 17.1, 10.4, 6.7 Hz, 1 H, CH_2=C*H*), 5.43 (d, *J* = 12.5 Hz, 1 H, N^+CHHAr), 5.16–5.08 (m, 2 H, N^+CHHAr and C*H*H=CH), 5.02 (d, *J* = 10.3 Hz, 1 H, CH*H*=CH), 4.17–4.07 (m, 2 H, C*H*NHCO and N^+CHH), 3.91 (s, 3 H, OCH_3), 3.71–3.63 (m, 1 H, N^+CHH), 3.51 (t, *J* = 11.5 Hz, 1 H, N^+CHH), 3.29–3.19 (m, 1 H, N^+CHH), 2.80–2.60 (m, 2 H, CH_2=CHC*H* and N^+CH_2CHH), 2.55 (dd, *J* = 13.5, 7.6 Hz, 1 H, N^+CHCHH), 2.14–2.09 (m, 1 H, $N(CH_2)_2CH$), 1.91–1.72 (m, 2 H, NCHCH*H* and NCH_2CHH); ^{13}C NMR (101 MHz, $CDCl_3$) δ 158.6 (OC_{Ar} quat), 155.4 (C=O), 147.5 (C_{Ar}), 144.3 (C_{Ar} quat), 140.7 (C_{Ar}), 140.1 (CH_2=*C*H), 135.5 (C_{Ar}), 133.6 (2 × C_{Ar}), 133.3 (q, J_{C-F} = 33 Hz, $C_{Ar}CF_3$ quat), 132.5 (C_{Ar}), 132.0 (q, J_{C-F} = 33 Hz, 2 × $C_{Ar}CF_3$ quat), 130.0 (C_{Ar} quat), 127.3 (part of q (other peaks obscured), CF_3 quat), 126.5 (q, *J* = 4 Hz, 2 × C_{Ar}), 125.7 (C_{Ar} quat), 123.2 (q, J_{C-F} = 273 Hz, 2 × CF_3), 120.4 (C_{Ar} quat), 120.3 (C_{Ar}), 118.4 (C_{Ar} quat), 118.1 (2 × C_{Ar}), 115.7 (*C*H_2=CH), 101.8 (C_{Ar}), 68.2 (*C*HNHCO), 63.4 (N^+CH_2Ar), 61.9 (N^+CH_2), 55.8 (OCH_3), 51.4 (N^+CH), 47.6 (N^+CH_2), 37.8 (CH_2=CH*C*H), 26.4 ($N^+(CH_2)_2CH$), 24.5 ($N^+CH_2CH_2$), 23.6 (N^+CHCH_2); ^{19}F{^{1}H} NMR (377 MHz, $CDCl_3$) δ –62.9, –63.2; HRMS (ESI^+) *m/z* Calculated for $C_{37}H_{34}N_4O_2F_9$ [M–Br^-] 737.2538; Found 737.2543.

(*R*)-(6-Methoxy-2-phenylquinolin-4-yl)((1*S*,2*S*,4*S*,5*R*)-5-vinylquinuclidin-2-yl)methanol (S13)[464]



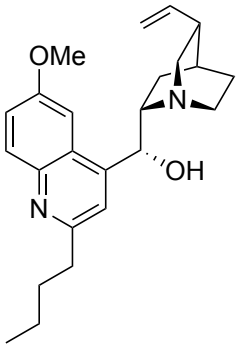
A solution of quinine (487 mg, 1.5 mmol) in MTBE (75 mL) was cooled to –10 ºC. PhLi (1.79 M in dibutyl ether, 2.56 mL, 4.58 mmol) was added over 5 min and was stirred for a further 25 min then slowly raised to 25 ºC then stirred for 4 h at 25 ºC. Acetic acid (1.0 mL) was added to the reaction at 0 ºC, then H_2O (2.5 mL) and EtOAc (2.5 mL) were added. I_2 (0.6 g) was added at 25 ºC, then sat. aq. $Na_2S_2O_3$ (10 mL) was added, followed by aq. NH_3 (28%, 5 mL) and the reaction mixture was stirred vigorously for 15 min. The layers were separated and the organic layer was washed with sat. aq. NaCl (10 mL). The combined aqueous layers were washed with CH_2Cl_2 (3 × 25 mL). The combined organic layers were dried over Na_2SO_4, filtered and concentrated under reduced pressure. Purification by flash chromatography (8:1:0.5:0.5 to 7:1:1.5:0.5 hexane:EtOAc:MeOH:NEt_3) afforded (*R*)-(6-methoxy-2-phenylquinolin-4-yl)((1*S*,2*S*,4*S*,5*R*)-5-vinylquinuclidin-2-yl)methanol **S13** (189 mg, 31%) as a pale yellow solid. $[\alpha]_D^{17} = -24$ (*c* = 0.25, $CHCl_3$) [lit = –43.9 (*c* = 1.0, EtOH)][465]; R_f 0.15 (7:1:1.5:0.5 hexane:EtOAc:MeOH:NEt_3); mp = 137–138 ºC [lit = 145–147 ºC][465]; ν_{max} (film)/cm^{-1} 3700–2300 (br s, OH), 2933, 2863, 1618 (C=C), 1498, 1450, 1349, 1226, 1029, 906, 831, 731, 693; ^{1}H NMR (400 MHz, $CDCl_3$) δ 8.01 (d, *J* = 9.2 Hz, 1 H, HC_{Ar}), 7.92–7.88 (m, 2 H, 2 × HC_{Ar}), 7.80 (s, 1 H, HC_{Ar}), 7.39–7.32 (m, 3 H, 3 × HC_{Ar}), 7.26 (dd, *J* = 9.2, 2.6 Hz, 1 H, HC_{Ar}), 7.07 (d, *J* = 2.6 Hz, 1 H, HC_{Ar}), 5.67 (ddd, *J* = 17.6, 10.3, 7.7 Hz, 1 H, CH_2=C*H*), 5.40 (d, *J* = 3.1 Hz, 1 H, C*H*OH), 4.95 – 4.82 (m, 2 H, CH_2=CH), 3.81 (s, 3 H, OCH_3), 3.49–3.38 (m, 1 H, NC*H*H), 3.06–2.97 (m, 2 H, NCH and NC*H*H), 2.62–2.51 (m, 2 H, 2 × NCH*H*), 2.26–2.18 (m, 1 H, CH_2=CHC*H*), 1.81–1.66 (m, 3 H, NCHC*H*H, NCH_2C*H*H and $N(CH_2)_2$C*H*), 1.48–1.36 (m, 2 H, NCHCH*H* and NCH_2CH*H*); ^{13}C NMR (101 MHz, $CDCl_3$) δ 157.4 (OC_{Ar} quat), 154.3 (C_{Ar} quat), 148.5 (C_{Ar} quat), 144.0 (C_{Ar} quat), 141.7 (C_{Ar}), 139.3 (CH_2=*C*H), 131.4 (C_{Ar} quat), 128.8 (C_{Ar}), 128.5 (2 × C_{Ar}), 127.1 (2 × C_{Ar}), 125.3 (C_{Ar} quat), 121.5 (C_{Ar}), 116.3 (*C*H_2=CH), 114.2 (C_{Ar}), 101.3 (C_{Ar}), 71.9 (*C*HOH), 59.8 (NCH), 56.9 (NCH_2), 55.5 (OCH_3), 43.1 (NCH_2), 39.8 (CH_2=CH*C*H), 27.8 ($N(CH_2)_2$*C*H), 27.4 (NCH_2*C*H_2), 21.1 (NCH*C*H_2). The observed characterisation data (^{1}H and ^{13}C NMR) was consistent with that previously reported in the literature.[466]

(1*S*,2*S*,4*S*,5*R*)-2-((*R*)-Hydroxy(6-methoxy-2-phenylquinolin-4-yl)methyl)-1-(4-(trifluoromethyl)benzyl)-5-vinylquinuclidin-1-ium bromide (390)



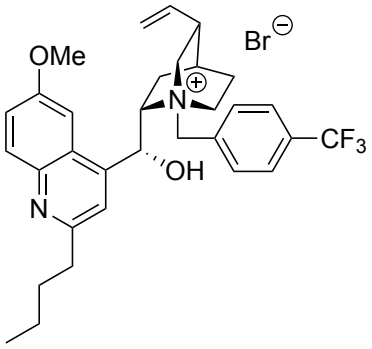
A mixture of (*R*)-(6-methoxy-2-phenylquinolin-4-yl)((1*S*,2*S*,4*S*,5*R*)-5-vinylquinuclidin-2-yl)methanol **S13** (80 mg, 0.16 mmol) and 4-(trifluromethyl)benzyl bromide (39 mg, 0.16 mmol) in toluene (1.0 mL) was heated to 75 ºC for 23 h. The reaction was cooled and concentrated under reduced pressure. Purification by flash chromatography (5% MeOH/CH_2Cl_2) afforded (1*S*,2*S*,4*S*,5*R*)-2-((*R*)-hydroxy(6-methoxy-2-phenylquinolin-4-yl)methyl)-1-(4-(trifluoromethyl)benzyl)-5-vinylquinuclidin-1-ium bromide **390** (66 mg, 65%) as a white solid. $[\alpha]_D^{17} = -120$ (*c* = 0.25, CH_3OH); R_f 0.42 (10% MeOH/CH_2Cl_2); ν_{max} (film)/cm^{-1} 3202 (br s, OH), 2982, 2948, 1621 (C=C), 1498, 1349, 1327, 1230, 1170, 1129, 1070, 1021, 831; ^{1}H NMR (400 MHz, $CDCl_3$) δ 8.22 (s, 1 H, HC_{Ar}), 8.13 (d, *J* = 7.4 Hz, 2 H, 2 × HC_{Ar}), 8.00–7.94 (m, 3 H, 3 × HC_{Ar}), 7.55 (d, *J* = 8.0 Hz, 2 H, 2 × HC_{Ar}), 7.46 (t, *J* = 7.5 Hz, 2 H, 2 × HC_{Ar}), 7.39 (t, *J* = 7.2 Hz, 1 H, HC_{Ar}), 7.27–7.25 (m, 1 H, HC_{Ar}), 7.22 (dd, *J* = 9.2, 2.4 Hz, 1 H, HC_{Ar}), 6.77–6.70 (m, 1 H,), 6.61 (s, 1 H, N^+CH), 6.02 (d, *J* = 12.0 Hz, 1 H, N^+CHHAr), 5.51 (ddd, *J* = 17.1, 10.5, 6.7 Hz, 1 H, CH_2=C*H*), 5.29 (d, *J* = 12.0 Hz, 1 H, N^+CHHAr), 5.10 (d, *J* = 17.1 Hz, 1 H, C*H*H=CH), 4.93–4.80 (m, 2 H, CH*H*=CH and N^+CHH), 4.03 (t, *J* = 8.7 Hz, 1 H, N^+CHH), 3.89 (s, 3 H, OCH_3), 3.82–3.74 (m, 1 H, C*H*OH), 3.29 (t, *J* = 11.7 Hz, 1 H, N^+CHH), 3.01 (td, *J* = 11.3, 5.7 Hz, 1 H, N^+CHH), 2.54–2.45 (m, 1 H, CH_2=CHC*H*), 2.30–2.14 (m, 2 H, N^+CHCHH and N^+CH_2CHH), 2.00–1.87 (s, 1 H, $N(CH_2)_2CH$), 1.68 (t, *J* = 11.3 Hz, 1 H, N^+CH_2CHH), 1.47–1.37 (m, 1 H, N^+CHCHH); ^{13}C NMR (101 MHz, $CDCl_3$) δ 157.8 (OC_{Ar} quat), 154.3 (C_{Ar} quat), 144.3 (C_{Ar} quat), 143.3 (C_{Ar} quat), 139.2 (CH_2=*C*H), 136.0 (C_{Ar} quat), 134.4 (2 × C_{Ar}), 132.4 (q, J_{C-F} = 4 Hz, $C_{Ar}CF_3$ quat), 132.1 (C_{Ar}), 131.1 (C_{Ar} quat), 129.0 (C_{Ar}), 128.7 (2 × C_{Ar}), 127.3 (2 × C_{Ar}), 125.9 (q, J_{C-F} = 3 Hz, 2 × C_{Ar}), 124.8 (C_{Ar} quat), 123.4 (q (obscured by other peaks), J_{C-F} = 273 Hz, CF_3), 120.7 (C_{Ar}), 118.2 (C_{Ar}), 118.0 (*C*H_2=*C*H), 102.1 (C_{Ar}), 69.3 (CHOH), 65.0 (N^+CH), 62.0 (N^+CH_2Ar), 60.7 (N^+CH_2), 56.2 (OCH_3), 51.3 (N^+CH_2), 37.9 (CH_2=CH*C*H), 26.6 ($N^+(CH_2)_2CH$), 24.9 ($N^+CH_2CH_2$), 21.9 (N^+CHCH); ^{19}F{^{1}H} NMR (377 MHz, $CDCl_3$) δ –63.0. HRMS (ESI^+) *m/z* Calculated for $C_{34}H_{34}N_2O_2F_3$ [M–Br^-] 559.2572; Found 559.2574.

(*R*)-(2-Butyl-6-methoxyquinolin-4-yl)((1*S*,2*S*,4*S*,5*R*)-5-vinylquinuclidin-2-yl)methanol (S14)[466]



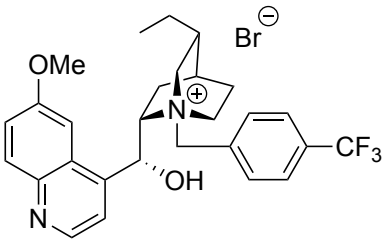
n-BuLi (1.54 M in hexanes, 3.90 mL, 6.0 mmol) was added to quinine (649 mg, 2.0 mmol) suspended in MTBE (10 mL) at –10 ºC. After 20 min at –10 ºC, the reaction mixture was stirred at 25 ºC for 1 h. AcOH (0.9 mL) was added, followed by H_2O (10 mL) and EtOAc (10 mL). I_2 (<0.5 g) was added to the stirred solution until a dark colour persisted. Then sat. aq. $Na_2S_2O_3$ (10 mL) was added followed by aq. NH_3 (~20%, 5 mL). The layers were separated and the organic layer was washed with CH_2Cl_2 (2 × 30 mL). The combined organic layers were dried over Na_2SO_4, filtered and concentrated under reduced pressure. Purification by flash chromatography (10:1:1 toluene:MeOH:NEt_3) afforded (*R*)-(2-butyl-6-methoxyquinolin-4-yl)((1*S*,2*S*,4*S*,5*R*)-5-vinylquinuclidin-2-yl)methanol **S14** (381 mg, 50%) as a white solid. $[\alpha]_D^{17}$ = –60 (*c* = 0.5, CH_2Cl_2); R_f 0.31 (10:1:1 toluene:MeOH:NEt_3); mp = 57–61 ºC; ν_{max} (film)/cm^{-1} 3400–2500 (br s, OH), 2922, 2855, 1618, 1561, 1502, 1450, 1349, 1259, 1230, 1163, 1096, 1029, 992, 939, 906, 828, 667; ^{1}H NMR (400 MHz, $CDCl_3$) δ 7.88 (d, *J* = 9.2 Hz, 1 H, HC_{Ar}), 7.39 (s, 1 H, HC_{Ar}), 7.24 (dd, *J* = 9.2, 2.7 Hz, 1 H, HC_{Ar}), 7.14 (d, *J* = 2.7 Hz, 1 H, HC_{Ar}), 5.70 (ddd, *J* = 17.9, 10.3, 7.8 Hz, 1 H, C*H*=CH_2), 5.49 (d, *J* = 3.3 Hz, 1 H, C*H*OH), 4.97–4.87 (m, 2 H, CH=CH_2), 3.86 (s, 3 H, OCH_3), 3.57–3.47 (m, 1 H, NC*H*H), 3.09–3.01 (m, 2 H, NCH and NC*H*H), 2.74 (dd, *J* = 8.9, 6.8 Hz, 2 H, $ArCH_2$), 2.69–2.59 (m, 2 H, 2 × NCH*H*), 2.28–2.20 (m, 1 H, C*H*CH=CH_2), 1.81–1.67 (m, 3 H, N$(CH_2)_2$C*H*, NCHC*H*H and NCH_2C*H*H), 1.66–1.56 (m, 2 H, $ArCH_2CH_2$), 1.52–1.38 (m, 2 H, NCHCH*H* and NCH_2CHH), 1.27 (h, *J* = 7.3 Hz, 2 H, Ar$(CH_2)_2CH_2$), 0.84 (t, *J* = 7.3 Hz, 3 H, Ar$(CH_2)_3CH_3$); ^{13}C NMR (101 MHz, $CDCl_3$) δ 160.0 (CH_2C_{Ar} quat), 157.0 (OC_{Ar} quat), 148.0 (C_{Ar} quat), 143.7 (C_{Ar} quat), 141.9 (*C*H=CH_2), 130.6 (C_{Ar}), 124.8 (C_{Ar} quat), 120.9 (C_{Ar}), 118.5 (C_{Ar}), 114.3 (CH=*C*H_2), 101.4 (C_{Ar}), 71.9 (*C*HOH), 59.9 (NCH), 57.1 (NCH_2), 55.6 (OCH_3), 43.3 (NCH_2), 40.0 (*C*HCH=CH_2), 38.7 ($ArCH_2$), 32.1 ($ArCH_2CH_2$), 27.9 (N$(CH_2)_2$*C*H), 27.6 (NCH*C*H_2), 22.6 (Ar$(CH_2)_2CH_2$), 21.3 (NCH_2CH_2), 13.9 (Ar$(CH_2)_3CH_2$). The observed characterisation data (^{1}H and ^{13}C NMR) was consistent with that previously reported in the literature.[466]

(1*S*,2*S*,4*S*,5*R*)-2-((*R*)-(2-Butyl-6-methoxyquinolin-4-yl)(hydroxy)methyl)-1-(4-(trifluoromethyl)benzyl)-5-vinylquinuclidin-1-ium bromide (389)



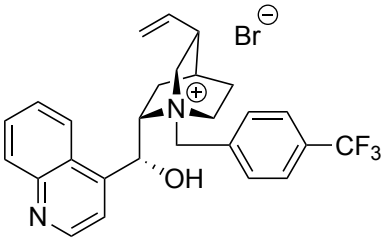
A solution of **S14** (95 mg, 0.25 mmol) and 4-(trifluromethyl)benzyl bromide (60 mg, 0.25 mmol) in THF (1.25 mL) was heated to 70 ºC for 23 h. The reaction was cooled to rt and Et_2O was added. The reaction was stirred for approx. 0.5 h then the precipitate was filtered. The collected solid was dried to afford (1*S*,2*S*,4*S*,5*R*)-2-((*R*)-(2-butyl-6-methoxyquinolin-4-yl)(hydroxy)methyl)-1-(4-(trifluoromethyl)benzyl)-5-vinylquinuclidin-1-ium bromide **389** (65 mg, 42%) as an off-white crystalline solid. $[\alpha]_D^{17} = -112$ (*c* = 0.25, $CHCl_3$); mp = 169–170 ºC; R_f 0.44 (10% MeOH/CH_2Cl_2); ν_{max} (film)/cm^{-1} 3213 (br s, OH), 2956, 1621, 1506, 1323, 1230, 1170, 1129, 1066, 1021, 857, 828, 731; ^{1}H NMR (400 MHz, $CDCl_3$) δ 8.02 (d, *J* = 8.0 Hz, 2 H, 2 × HC_{Ar}), 7.95 (d, *J* = 9.2 Hz, 1 H, HC_{Ar}), 7.69 (s, 1 H, HC_{Ar}), 7.61 (d, *J* = 8.0 Hz, 2 H, 2 × HC_{Ar}), 7.28–7.24 (m, 1 H, HC_{Ar}), 7.17 (d, *J* = 2.6 Hz, 1 H, HC_{Ar}), 6.65 (d, *J* = 6.6 Hz, 1 H, N^+CH), 6.38 (d, *J* = 6.8 Hz, 1 H, OH), 6.27 (d, *J* = 12.0 Hz, 1 H, N^+CHHAr), 5.55 (ddd, *J* = 17.2, 10.4, 6.9 Hz, 1 H, $CH=CH_2$), 5.12 (d, *J* = 17.6, 0.7 Hz, 1 H, CH=CHH), 5.02–4.92 (m, 3 H, N^+CHHAr, CH=CHH and N^+CHH), 3.93–3.84 (m, 4 H, OCH_3 and CHOH), 3.61–3.53 (m, 1 H, N^+CHH), 3.46–3.38 (m, 1 H, N^+CHH), 3.06 (td, *J* = 11.4, 6.2 Hz, 1 H, N^+CHH), 2.90 (dd, *J* = 8.8, 7.0 Hz, 2 H, $ArCH_2$), 2.62–2.53 (m, 1 H, $CHCH=CH_2$), 2.39–2.29 (m, 1 H, NCHCHH), 2.28–2.19 (m, 1 H, NCH_2CHH), 2.06–2.01 (m, 1 H, $N(CH_2)_2CH$), 1.81–1.71 (m, 3 H, $ArCH_2CH_2$ and NCHCHH), 1.51–1.37 (m, 3 H, $Ar(CH_2)_2CH_2$ and NCH_2CHH), 0.96 (t, *J* = 7.4 Hz, 3 H, $Ar(CH_2)_3CH_3$); ^{13}C NMR (101 MHz, $CDCl_3$) δ 160.3 (CH_2C_{Ar} quat), 157.4 (OC_{Ar} quat), 143.9 (C_{Ar} quat), 142.8 (C_{Ar} quat), 136.0 ($CH=CH_2$), 134.4 (C_{Ar}), 132.6 (q, J_{C-F} = 32.9 Hz, $C_{Ar}CF_3$ quat), 131.4 (C_{Ar}), 130.9 (C_{Ar} quat), 126.0 (q, J_{C-F} = 3.1 Hz, 2 × C_{Ar}), 124.1 (C_{Ar}), 123.4 (q, J_{C-F} = 272.6 Hz, CF_3 quat), 120.9 (C_{Ar}), 120.1 (C_{Ar}), 118.2 ($CH=CH_2$), 102.2 (C_{Ar}), 69.8 (CHOH), 64.0 (N^+CH), 62.3 (N^+CH_2Ar), 61.1 (N^+CH_2), 56.2 (OCH_3), 51.4 (N^+CH_2), 38.8 ($ArCH_2$), 38.0 ($CHCH=CH_2$), 32.2 ($ArCH_2CH_2$), 26.6 ($N(CH_2)_2CH$), 24.8 ($NCHCH_2$), 22.7 ($Ar(CH_2)_2CH_2$), 21.6 (NCH_2CH_2), 14.0 ($Ar(CH_2)_3CH_3$); $^{19}F\{^1H\}$ NMR (377 MHz, $CDCl_3$) δ –63.1; HRMS (ESI^+) *m/z* Calculated for $C_{32}H_{38}N_2O_2F_3$ [M–Br] 539.2885; Found 539.2881.

(1*S*,2*S*,4*S*,5*R*)-5-Ethyl-2-((*R*)-hydroxy(6-methoxyquinolin-4-yl)methyl)-1-(4-(trifluoromethyl)benzyl)quinuclidin-1-ium bromide (391)



A mixture of dihydroquinine (163 mg, 0.5 mmol) and 4-(trifluromethyl)benzyl bromide (120 mg, 0.50 mmol) in THF (2.5 mL) was heated to 70 ºC for 15.5 h. The reaction was cooled and Et_2O was added. The reaction was stirred for approx. 0.5 h then the precipitate was filtered. The collected solid was dried to afford (1*S*,2*S*,4*S*,5*R*)-5-ethyl-2-((*R*)-hydroxy(6-methoxyquinolin-4-yl)methyl)-1-(4-(trifluoromethyl)benzyl)quinuclidin-1-ium bromide **391** (224 mg, 79%) as a white solid. $[\alpha]_D^{17} = -108$ (*c* = 1.06, CH_2Cl_2); R_f 0.20 (10% MeOH/CH_2Cl_2); mp = 236–238 ºC (decomposition observed); ν_{max} (film)/cm^{-1} 3213 (OH), 2963, 1621, 1510, 1327, 1241, 1170, 1129, 1070, 1021, 857, 828; ^{1}H NMR (400 MHz, $CDCl_3$) δ 8.69 (d, *J* = 4.5 Hz, 1 H, HC_{Ar}), 8.01–7.94 (m, 3 H, 3 × HC_{Ar}), 7.69 (d, *J* = 4.5 Hz, 1 H, HC_{Ar}), 7.58 (d, *J* = 8.1 Hz, 2 H, HC_{Ar}), 7.29–7.25 (m, 2 H, 2 × HC_{Ar}), 6.62 (d, *J* = 6.6 Hz, 1 H, N^+CH), 6.35 (d, *J* = 6.7 Hz, 1 H, OH), 6.08 (d, *J* = 12.0 Hz, 1 H, N^+CHHAr), 4.91 (d, *J* = 12.0 Hz, 1 H, N^+CHHAr), 4.87–4.78 (m, 1 H, N^+CHH), 3.99–3.88 (m, 4 H, OCH_3 and C*H*OH), 3.51–3.44 (m, 1 H, N^+CHH), 3.32 (dd, *J* = 12.4, 10.7 Hz, 1 H, N^+CHH), 2.97 (td, *J* = 11.4, 6.4 Hz, 1 H, N^+CHH), 2.31–2.18 (m, 2 H, N^+CH_2CHH and N^+CHCHH), 1.99–1.91 (m, 1 H, $N^+(CH_2)_2CH$), 1.74–1.58 (m, 2 H, N^+CH_2CH and N^+CH_2CHH), 1.47–1.38 (m, 1 H, N^+CHCHH), 1.29–1.08 (m, 2 H, CH_3CH_2), 0.66 (t, *J* = 7.3 Hz, 3 H, CH_3CH_2); ^{13}C NMR (101 MHz, $CDCl_3$) δ 158.0 (OC_{Ar} quat), 147.4 (C_{Ar}), 144.1 (C_{Ar} quat), 142.9 (C_{Ar} quat), 134.4 (2 × C_{Ar}), 132.4 (q, J_{C-F} = 33 Hz, $C_{Ar}CF_3$ quat), 131.9 (C_{Ar} quat), 131.1 (C_{Ar} quat), 125.9 (3 × C_{Ar}), 123.5 (q, J_{C-F} = 273 Hz, CF_3), 120.8 (C_{Ar}), 120.6 (C_{Ar}), 102.1 (C_{Ar}), 69.5 (CHOH), 64.0 (N^+CH), 62.9 (N^+CH_2Ar), 62.1 (N^+CH_2), 56.3 (OCH_3), 51.4 (N^+CH_2), 36.0 (N^+CH_2CH), 26.0 (CH_3CH_2), 25.2 ($N^+CH_2CH_2$), 23.9 ($N^+(CH_2)_2CH$), 21.3 (N^+CHCH_2), 11.2 (CH_3CH_2); ^{19}F{^{1}H} NMR (377 MHz, $CDCl_3$) δ –63.0; HRMS (FTMS + pAPCI) *m/z* Calculated for $C_{28}H_{32}N_2O_2F_3^+$ [M–Br$^-$] 485.2410; Found 485.2391.

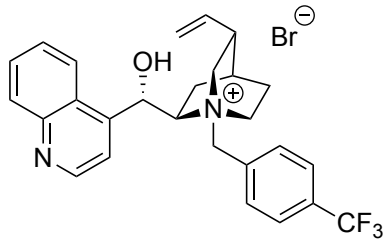
(1*S*,2*S*,4*S*,5*R*)-2-((*R*)-Hydroxy(quinolin-4-yl)methyl)-1-(4-(trifluoromethyl)benzyl)-5-vinylquinuclidin-1-ium bromide (392)



A solution of cinchonidine (147 mg, 0.5 mmol) and 4-(trifluromethyl)benzyl bromide (120 mg, 0.5 mmol) in THF (2.5 mL) was heated to 70 ºC for 23 h. The reaction was cooled to rt and Et_2O was added. The reaction was stirred for approx. 0.5 h then the precipitate was filtered. The collected solid was dried to afford (1*S*,2*S*,4*S*,5*R*)-2-((*R*)-hydroxy(quinolin-4-yl)methyl)-1-(4-(trifluoromethyl)benzyl)-5-vinylquinuclidin-1-ium bromide **392** (240 mg, 90%) as a white solid.

$[\alpha]_D^{17}$ = –130 (*c* = 0.2, MeOH) [lit = –159 (*c* = 0.1, MeOH)][467]; mp = 235–237 ºC (decomposition observed) [lit = 222–223][467]; R_f 0.30 (10% MeOH/CH_2Cl_2); ν_{max} (film)/cm^{-1} 3183 (br s, OH), 2982, 2952, 1323, 1167, 1118, 1066, 921, 857, 775, 731; ^{1}H NMR (400 MHz, $CDCl_3$) δ 8.80 (d, *J* = 4.5 Hz, HC_{Ar}), 8.16–8.11 (m, 1 H, HC_{Ar}), 7.88 (d, *J* = 7.8 Hz, 2 H, 2 × HC_{Ar}), 7.79 (d, *J* = 4.5 Hz, 1 H, HC_{Ar}), 7.58–7.53 (m, 1 H, HC_{Ar}), 7.42 (d, *J* = 7.8 Hz, 2 × HC_{Ar}), 7.07–7.00 (m, 2 H, 2 × HC_{Ar}), 6.55–6.47 (m, 2 H, N^+CH and OH), 6.29 (d, *J* = 11.9 Hz, N^+CHHAr), 5.59 (d, *J* = 11.9 Hz, N^+CHHAr), 5.43–5.28 (m, 2 H, CH=CH_2), 4.94–4.90 (m, 1 H, CH=CHH), 4.71–4.62 (m, 1 H, N^+CHH), 4.24–4.16 (m, 1 H, N^+CHH), 3.99–3.92 (m, 1 H, $CHOH$), 3.06–2.90 (m, 2 H, 2 × N^+CHH), 2.52–2.44 (m, 1 H, $CHCH{=}CH_2$), 2.13–2.03 (m, 1 H, $NCHCHH$), 1.96–1.91 (m, 1 H, $N(CH_2)_2CH$), 1.90–1.81 (m, 1 H, NCH_2CHH), 1.66–1.55 (m, 1 H, $NCHCHH$), 1.05–0.95 (m, 1 H, NCH_2CHH); ^{13}C NMR (101 MHz, $CDCl_3$) δ 149.2 (C_{Ar}), 146.8 (C_{Ar} quat), 144.1 (C_{Ar} quat), 135.6 ($CH{=}CH_2$), 134.4 (2 × C_{Ar}), 132.1 (q, $J_{C–F}$ = 32.7 Hz, CF_3C_{Ar} quat), 131.0 (C_{Ar} quat), 129.4 (C_{Ar}), 128.3 (C_{Ar}), 127.2 (C_{Ar}), 125.3 (q, $J_{C–F}$ = 3.4 Hz, 2 × C_{Ar}), 123.6 (q, $J_{C–F}$ = 272.4 Hz, CF_3 quat), 123.2 (C_{Ar} quat), 122.6 (C_{Ar}), 119.6 (C_{Ar}), 117.9 ($CH{=}CH_2$), 67.1 (CHOH), 65.2 (N^+CH), 60.8 (N^+CH_2Ar), 60.0 (N^+CH_2), 50.5 (N^+CH_2), 37.7 ($CHCH{=}CH_2$), 26.2 ($N(CH_2)_2CH$), 25.0 ($NCHCH_2$), 22.5 (NCH_2CH_2); ^{19}F{^{1}H} NMR (377 MHz, $CDCl_3$) δ –63.1; HRMS (ESI^+) *m/z* Calculated for $C_{27}H_{28}N_2OF_3$ [M–Br] 453.2154; Found 453.2157. Compound previously characterised in DMSO-*d*^{6}.[467]

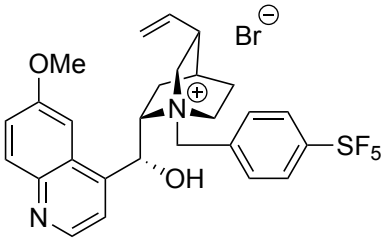
(1*S*,2*R*,4*S*,5*R*)-2-((*S*)-Hydroxy(quinolin-4-yl)methyl)-1-(4-(trifluoromethyl)benzyl)-5-vinylquinuclidin-1-ium bromide (268)



A solution of cinchonine (147 mg, 0.5 mmol) and 4-(trifluromethyl)benzyl bromide (120 mg, 0.5 mmol) in THF (2.5 mL) was heated to 70 ºC for 23 h. The reaction was cooled to rt and Et_2O was added. The reaction was stirred for approx. 0.5 h then the precipitate was filtered. The collected solid was dried to afford (1*S*,2*R*,4*S*,5*R*)-2-((*S*)-hydroxy(quinolin-4-yl)methyl)-1-(4-(trifluoromethyl)benzyl)-5-vinylquinuclidin-1-ium bromide **268** (227 mg, 85%) as a white solid. $[\alpha]_D^{21}$ = +150 (*c* = 0.16, MeOH) [lit = +135 (*c* = 0.50, MeOH)][468]; R_f 0.23 (10% MeOH/CH_2Cl_2); mp = 240–245 ºC (decomposition observed) [lit = 244–246 ºC (with decomp.)][468]; ν_{max} (film)/cm^{-1} 3183 (br s, OH), 2960, 2878, 1327, 1126, 865, 779; ^{1}H NMR (400 MHz, $CDCl_3$) δ 8.83 (d, *J* = 4.5 Hz, 1 H, HC_{Ar}), 8.25 (d, *J* = 8.1 Hz, 1 H, HC_{Ar}), 7.87–7.79 (m, 3 H, 3 × HC_{Ar}), 7.51 (dd, *J* = 8.3, 1.2 Hz, 1 H, HC_{Ar}), 7.39 (d, *J* = 8.1 Hz, 2 H, 2 × HC_{Ar}), 7.01–6.89 (m, 2 H, 2 × HC_{Ar}), 6.57 (d, *J* = 5.6 Hz, 1 H, N^+CH), 6.53–6.36 (m, 2 H, OH and N^+CHHAr), 5.82 (ddd, *J* = 17.4, 10.4, 7.2 Hz, 1 H, $CH{=}CH_2$), 5.43–5.31 (m, 1 H, N^+CHHAr), 5.26–5.15 (m, 2 H,

CH=C*H*$_2$), 4.53–4.44 (m, 1 H, N$^+$C*H*H), 4.24–4.05 (m, 2 H, N$^+$C*H*H and C*H*OH), 3.16 (t, *J* = 11.4 Hz, 1 H, N$^+$CH*H*), 2.69–2.59 (m, 1 H, N$^+$CH*H*), 2.29 (q, *J* = 8.8 Hz, 1 H, C*H*CH=CH$_2$), 2.14–2.05 (m, 1 H, NCHC*H*H), 1.89–1.66 (m, 3 H, N(CH$_2$)$_2$C*H*, NCH$_2$C*H*H and NCHCH*H*), 0.77–0.68 (m, 1 H, NCH$_2$CH*H*); ^{1}H NMR (400 MHz, DMSO-*d*$_6$) δ 8.99 (d, *J* = 4.5 Hz, 1 H, HC$_{Ar}$), 8.44–8.38 (m, 1 H, HC$_{Ar}$), 8.12–8.03 (m, 3 H, 3 × HC$_{Ar}$), 7.96 (d, *J* = 8.2 Hz, 2 H, 2 × HC$_{Ar}$), 7.88–7.81 (m, 2 H, 2 × HC$_{Ar}$), 7.78–7.72 (m, 1 H, HC$_{Ar}$), 6.84 (dd, *J* = 14.8, 4.2 Hz, 1 H, OH), 6.55–6.50 (m, 1 H, N$^+$CH), 6.00 (ddd, *J* = 17.3, 10.7, 7.0 Hz, 1 H, C*H*=CH$_2$), 5.31 (d, *J* = 12.3 Hz, 1 H, N$^+$C*H*HAr), 5.26–5.19 (m, 2 H, CH=C*H*$_2$), 5.12 (d, *J* = 12.3 Hz, 1 H, N$^+$CH*H*Ar), 4.31–4.23 (m, 1 H, N$^+$C*H*H), 4.13–4.03 (m, 1 H, N$^+$C*H*H), 3.97 (t, *J* = 9.2 Hz, 1 H, C*H*OH), 3.48 (t, *J* = 11.4 Hz, 1 H, N$^+$CH*H*), 3.05–2.91 (m, 1 H, N$^+$CH*H*), 2.65 (q, *J* = 8.4 Hz, 1 H, *C*HCH=CH$_2$), 2.34–2.22 (m, 1 H, NCHC*H*H), 1.89–1.85 (m, 1 H, N(CH$_2$)$_2$C*H*), 1.79–1.71 (m, 2 H, NCH$_2$C*H*H and NCHC*H*H), 1.10–1.00 (m, 1 H, NCHCH*H*); ^{13}C NMR (101 MHz, DMSO-*d*$_6$) δ 150.1 (C$_{Ar}$), 147.6 (C$_{Ar}$ quat), 144.9 (C$_{Ar}$ quat), 137.1 (*C*H=CH$_2$), 134.7 (2 × C$_{Ar}$), 132.6 (C$_{Ar}$ quat), 130.3 (q, *J*$_{C–F}$ = 31.9 Hz, CF$_3$*C*$_{Ar}$ quat), 129.7 (C$_{Ar}$), 129.4 (C$_{Ar}$), 127.2 (C$_{Ar}$), 125.7 (q, *J*$_{C–F}$ = 3.1 Hz, 2 × C$_{Ar}$), 124.3 (C$_{Ar}$), 124.01 (q, *J*$_{C–F}$ = 272.5 Hz, *C*F$_3$ quat), 123.98 (C$_{Ar}$ quat), 120.1 (C$_{Ar}$), 117.0 (CH=*C*H$_2$), 67.3 (*C*HOH), 64.6 (N$^+$CH), 61.2 (N$^+$*C*H$_2$Ar), 56.0 (N$^+$CH$_2$), 53.9 (N$^+$CH$_2$), 36.6 (*C*HCH=CH$_2$), 26.2 (N(CH$_2$)*C*H), 22.9 (NCH*C*H$_2$), 20.7 (NCH$_2$*C*H$_2$); ^{19}F{^{1}H} NMR (377 MHz, DMSO-*d*$_6$) δ –61.3. The observed characterisation data (IR, ^{1}H and ^{13}C NMR in DMSO-*d*$_6$) was consistent with that previously reported in the literature.[468]

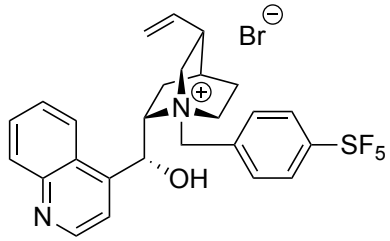
(1*S*,2*S*,4*S*,5*R*)-2-((*R*)-Hydroxy(6-methoxyquinolin-4-yl)methyl)-1-(4-(pentafluoro-λ^6-sulfaneyl)benzyl)-5-vinylquinuclidin-1-ium bromide (393)



A solution of quinine (65 mg, 0.20 mmol) and (4-(bromomethyl)phenyl)pentafluoro-λ^6-sulfane (59 mg, 0.20 mmol) in THF (1.0 mL) was heated to 70 ºC for 15 h. The reaction was cooled to rt and Et$_2$O was added. The reaction was stirred for approx. 0.5 h then the precipitate was filtered. The collected solid was dried to afford (1*S*,2*S*,4*S*,5*R*)-2-((*R*)-hydroxy(6-methoxyquinolin-4-yl)methyl)-1-(4-(pentafluoro-λ^6-sulfaneyl)benzyl)-5-vinylquinuclidin-1-ium bromide **393** (93 mg, 75%) as a white solid. $[\alpha]_D^{22} = -120$ (*c* = 0.25, CH$_2$Cl$_2$); *R*$_f$ (10% MeOH/CH$_2$Cl$_2$); mp = 190–192 ºC; ν$_{max}$ (film)/cm^{-1} 3216 (br s, OH), 2962, 1621, 1510, 1472, 1241, 846; ^{1}H NMR (400 MHz, CDCl$_3$) δ 8.69 (d, *J* = 4.5 Hz, HC$_{Ar}$), 8.02 (d, *J* = 8.4 Hz, 2 × HC$_{Ar}$), 7.93 (d, *J* = 9.0 Hz, 1 H, HC$_{Ar}$), 7.91–7.66 (m, 3 H, 3 × HC$_{Ar}$), 7.27–7.22 (m, 2 H, 2 × HC$_{Ar}$), 6.65–6.60 (m, 1 H, N$^+$CH), 6.31 (br d, *J* = 5.5 Hz, OH), 6.06 (d, *J* = 11.9 Hz, N$^+$C*H*HAr), 5.52 (ddd, *J* = 17.2, 10.5, 6.8 Hz, C*H*=CH$_2$), 5.14–5.03 (m, 2 H, CH=C*H*H and N$^+$CH*H*Ar), 4.87–4.77 (m, 2 H, CH=CH*H* and N$^+$C*H*H), 4.06–3.90 (m, 5 H, C*H*OH, OCH$_3$ and N$^+$C*H*H), 3.29 (dd, *J* = 11.1,

1.5 Hz, N^+CHH), 3.02–2.92 (m, 1 H, N^+CHH), 2.56–2.47 (m, 1 H, NCH_2CH), 2.33–2.13 (m, 2 H, NCH_2CHH and $NCHCHH$), 2.02–1.97 (m, 1 H, $N(CH_2)_2CH$), 1.78–1.69 (m, 1 H, $NCHCHH$), 1.55–1.45 (m, 1 H, NCH_2CHH); ^{13}C NMR (101 MHz, $CDCl_3$) δ 158.1 (OC_{Ar} quat), 155.1 (p, J_{C-F} = 18.0 Hz, SF_5C_{Ar} quat), 147.2 (C_{Ar}), 143.9 (C_{Ar} quat), 143.0 (C_{Ar} quat), 135.9 ($CH=CH_2$), 134.5 (2 × C_{Ar}), 131.7 (C_{Ar} quat), 131.1 (C_{Ar} quat), 126.6 (br s, 2 × C_{Ar}), 125.9 (C_{Ar}), 121.2 (C_{Ar}), 120.5 (C_{Ar}), 118.0 ($CH=CH_2$), 101.9 (C_{Ar}), 69.6 ($CHOH$), 63.9 (N^+CH), 61.4 (N^+CH_2Ar), 60.5 (N^+CH_2), 56.4 (OCH_3), 51.4 (N^+CH_2), 37.8 ($CHCH=CH_2$), 26.7 ($N(CH_2)_2CH$), 24.8 ($NCHCH_2$), 21.5 (NCH_2CH_2); $^{19}F\{^1H\}$ NMR (377 MHz, $CDCl_3$) δ 83.0 (q, J_{F-F} = 151 Hz, F_{ax}), 62.5 (d, J_{F-F} = 150 Hz, 4 × F_{eq}); HRMS (ESI^+) *m/z* Calculated for $C_{27}H_{30}N_2O_2SF_5$ [M–Br] 541.1948; Found 541.1941.

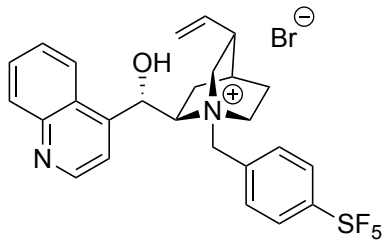
(1*S*,2*S*,4*S*,5*R*)-2-((*R*)-Hydroxy(quinolin-4-yl)methyl)-1-(4-(pentafluoro-λ^6-sulfaneyl)benzyl)-5-vinylquinuclidin-1-ium bromide (394)



A solution of cinchonidine (736 mg, 2.5 mmol) and (4-(bromomethyl)phenyl)pentafluoro-λ^6-sulfane (743 mg, 2.5 mmol) in THF (12.5 mL) was heated to 70 ºC for 14 h. The reaction was cooled to rt and Et_2O was added. The reaction was stirred for approx. 0.5 h then the precipitate was filtered. The collected solid was dried to afford (1*S*,2*S*,4*S*,5*R*)-2-((*R*)-hydroxy(quinolin-4-yl)methyl)-1-(4-(pentafluoro-λ^6-sulfaneyl)benzyl)-5-vinylquinuclidin-1-ium bromide **394** (1.38 g, 93%) as a white solid. $[\alpha]_D^{22} = -144$ (*c* = 0.5, CH_2Cl_2); R_f 0.30 (10% MeOH/CH_2Cl_2); mp = 220–223 ºC (decomposition observed); ν_{max} (film)/cm^{-1} 3183 (br s, OH), 2986, 1510, 921, 839, 731; ^1H NMR (400 MHz, $CDCl_3$) δ 8.81 (d, *J* = 4.5 Hz, 1 H, HC_{Ar}), 8.19–8.13 (m, 1 H, HC_{Ar}), 7.97 (d, *J* = 8.3 Hz, 2 H, 2 × HC_{Ar}), 7.79 (d, *J* = 4.5 Hz, 1 H, HC_{Ar}), 7.69–7.64 (m, 1 H, HC_{Ar}), 7.61 (d, *J* = 8.5 Hz, 2 H, 2 × HC_{Ar}), 7.18–7.12 (m, 2 H, 2 × HC_{Ar}), 6.55 (d, *J* = 5.9 Hz, 1 H, OH), 6.50–6.46 (m, 1 H, N^+CH), 6.18 (d, *J* = 12.0 Hz, 1 H, N^+CHHAr), 5.62 (d, *J* = 12.0 Hz, 1 H, N^+CHHAr), 5.45–5.35 (m, 1 H, $CH=CH_2$), 5.28 (dd, *J* = 17.3, 0.6 Hz, 1 H, $CH=CHH$), 4.93 (dd, *J* = 10.3, 1.3 Hz, 1 H, $CH=CHH$), 4.72–4.62 (m, 1 H, N^+CHH), 4.16 (br t, *J* = 9.2 Hz, 1 H, $CHOH$), 3.96–3.88 (m, 1 H, N^+CHH), 3.10–2.93 (m, 2 H, 2 × N^+CHH), 2.55–2.48 (m, 1 H, $CHCH=CH_2$), 2.15–2.06 (m, 1 H, $NCHCHH$), 1.98–1.92 (m, 1 H, $N(CH_2)_2CH$), 1.91–1.83 (m, 1 H, NCH_2CHH), 1.70–1.59 (m, 1 H, $NCHCHH$), 1.08–0.98 (m, 1 H, NCH_2CHH); ^{13}C NMR (101 MHz, $CDCl_3$) δ 155.0 (p, J_{C-F} = 17.7 Hz, SF_5C_{Ar} quat), 149.3 (C_{Ar}), 146.9 (C_{Ar} quat), 144.4 (C_{Ar} quat), 135.6 ($CH=CH_2$), 134.5 (2 × C_{Ar}), 131.1 (C_{Ar} quat), 129.6 (C_{Ar}), 128.7 (C_{Ar}), 127.4 (C_{Ar}), 126.3 (br s, 2 × C_{Ar}), 123.5 (C_{Ar} quat), 122.8 (C_{Ar}), 119.8 (C_{Ar}), 118.1 ($CH=CH_2$), 67.7 (CHOH), 65.1 (N^+CH), 60.8 (N^+CH_2Ar), 60.3 (N^+CH_2), 50.9 (N^+CH_2), 37.8 ($CHCH=CH_2$), 26.2 ($N(CH_2)_2CH$), 25.0 ($NCHCH_2$), 22.4 (NCH_2CH_2); $^{19}F\{^1H\}$ NMR (377 MHz, $CDCl_3$) δ 82.6 (p, J_{F-F} = 150 Hz, F_{ax}), 62.5 (d, J_{F-F}

= 150 Hz, 4 × F_{eq}); HRMS (ESI$^+$) *m/z* Calculated for $C_{26}H_{28}N_2OSF_5$ [M–Br] 511.1843; Found 511.1847.

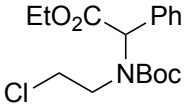
(1*S*,2*R*,4*S*,5*R*)-2-((*S*)-Hydroxy(quinolin-4-yl)methyl)-1-(4-(pentafluoro-λ^6-sulfaneyl)benzyl)-5-vinylquinuclidin-1-ium bromide (395)



A solution of cinchonine (736 mg, 2.5 mmol) and (4-(bromomethyl)phenyl)pentafluoro-λ^6-sulfane (743 mg, 2.5 mmol) in THF (12.5 mL) was heated to 70 ºC for 14 h. The reaction was cooled to rt and Et_2O was added. The reaction was stirred for approx. 0.5 h then the precipitate was filtered. The collected solid was dried to afford (1*S*,2*R*,4*S*,5*R*)-2-((*S*)-hydroxy(quinolin-4-yl)methyl)-1-(4-(pentafluoro-λ^6-sulfaneyl)benzyl)-5-vinylquinuclidin-1-ium bromide **395** (1.35 g, 91%) as a white solid. $[\alpha]_D^{17}$ = +104 (*c* = 0.75, CH_2Cl_2); R_f 0.55 (10% MeOH/CH_2Cl_2); mp = 224–227 ºC (decomposition observed); ν_{max} (film)/cm^{-1} 3179 (br s, OH), 2952, 1510, 921, 839, 731; ^{1}H NMR (400 MHz, $CDCl_3$) δ 8.84 (d, *J* = 4.6 Hz, 1 H, HC_{Ar}), 8.29 (d, *J* = 8.3 Hz, 1 H, HC_{Ar}), 7.93–7.86 (m, 3 H, 3 × HC_{Ar}), 7.64–7.58 (m, 3 H, 3 × HC_{Ar}), 7.11–7.06 (m, 1 H, HC_{Ar}), 7.03–6.98 (m, 1 H, HC_{Ar}), 6.66 (2 × d, *J* = 5.3 Hz, 1 H, OH), 6.48–6.33 (m, 2 H, N$^+$CH and N$^+$C*H*HAr), 5.82 (ddd, *J* = 17.4, 10.4, 7.2 Hz, 1 H, C*H*=CH_2), 5.38 and 5.32 (2 × d, 11.9 Hz, 1 H, N$^+$CH*H*Ar), 5.26 (d, *J* = 10.4 Hz, 1 H, CH=C*H*H), 5.20 (d, *J* = 17.1 Hz, CH=CH*H*), 4.53–4.44 (m, 1 H, N$^+$C*H*H), 4.22–4.03 (m, 2 H, N$^+$C*H*H and C*H*OH), 3.20 (t, *J* = 11.4 Hz, 1 H, N$^+$CH*H*), 2.65–2.55 (m, 1 H, N$^+$CH*H*), 2.34 (q, *J* = 8.9 Hz, 1 H, C*H*CH=CH_2), 2.13–2.04 (m, 1 H, NCHC*H*H), 1.83–1.67 (m, 3 H, NCH_2CH_2CH), 0.75–0.66 (m, 1 H, NCHCH*H*); ^{13}C NMR (101 MHz, $CDCl_3$) δ 155.0 (p, $J_{C–F}$ = 18.5 Hz, F_5SC_{Ar} quat), 149.3 (C_{Ar}), 146.8 (C_{Ar} quat), 144.0 (C_{Ar} quat), 134.7 (*C*H=CH_2), 134.3 (2 × C_{Ar}), 131.0 (C_{Ar} quat), 129.4 (C_{Ar}), 128.5 (C_{Ar}), 127.2 (C_{Ar}), 126.1 (2 × C_{Ar}), 123.3 (C_{Ar} quat), 123.1 (C_{Ar}), 119.6 (C_{Ar}), 118.4 (CH=*C*H_2), 67.2 (CHOH), 65.5 (N$^+$CH), 59.8 (N$^+$$CH_2$Ar), 56.5 (N$^+$$CH_2$), 54.1 (N$^+$$CH_2$), 37.8 (*C*HCH=$CH_2$), 26.9 (N($CH_2$)$_2$*C*H), 23.6 (NCH*C*$H_2$), 21.7 (NCH$_2$*C*$H_2$); ^{19}F{^{1}H} NMR (377 MHz, $CDCl_3$) δ 82.4 (p, $J_{F–F}$ = 150 Hz, F_{ax}), 62.5 (d, $J_{F–F}$ = 150 Hz, 4 × F_{eq}); HRMS (ESI$^+$) *m/z* Calculated for $C_{26}H_{28}N_2OSF_5$ [M–Br] 511.1843; Found 511.1846.

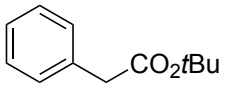
6.2.3.6 Compounds from Conclusions and Future Work Section 4.4.6

(±)–Ethyl 2-((*tert*-butoxycarbonyl)(2-chloroethyl)amino)-2-phenylacetate (396)



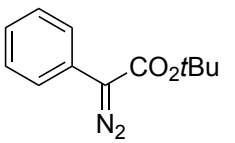
$Rh_2(esp)_2$ (3.8 mg, 5.0 μmol) was added to a solution of protected amine **52** (179 mg, 1.0 mmol) and ethyl 2-diazo-2-phenylacetate **85** (285 mg, 1.5 mmol) in benzene (3.33 mL). The reaction mixture was heated to 60 ºC and stirred for 2.5 h. The reaction mixture was cooled to rt and filtered through celite, washing with EtOAc (20 mL) and then concentrated under reduced pressure. Purification by flash chromatography (5% EtOAc/pentane) afforded ethyl 2-((*tert*-butoxycarbonyl)(2-chloroethyl)amino)-2-phenylacetate **396** (292 mg, 85%) as a pale yellow oil. R_f 0.25 (5% EtOAc/pentane); ν_{max} (film)/cm^{-1} 2977, 1741 (C=O ester), 1696 (C=O carbamate), 1456, 1392, 1366, 1252, 1206, 1148, 1099, 1025, 904, 773, 749, 701; ^{1}H NMR (400 MHz, $CDCl_3$) δ 7.43–7.36 (m, 3 H, 3 × HC_{Ph}), 7.30–7.25 (m, 2 H, 2 × HC_{Ph}), 5.92 and 5.61 (2 × br s, 1 H, NCH), 4.32–4.22 (m, 2 H, O*C*H_2CH$_3$), 3.52–3.26 (m, 3 H, NCH_2*C*H), 3.24–3.12 and 3.00–2.88 (2 × m, 1 H, NCH$_2$CH*H*), 1.51 (br s, 9 H, C(CH$_3$)$_3$), 1.32–1.24 (m, 3 H, OCH$_2$CH_3); ^{13}C NMR (101 MHz, $CDCl_3$) δ 170.9 (C=O ester), 155.6 (C=O carbamate), 134.8 (C_{Ph} quat), 129.0 (br s, 4 × C_{Ph}), 128.8 (C_{Ph}), 81.2 (*C*(CH$_3$)$_3$), 63.6 and 62.1 (NCH), 61.4 (O*C*H$_2$CH$_3$), 46.4 (CH$_2$Cl), 40.9 and 40.6 (NCH$_2$), 28.3 (C(*C*H$_3$)$_3$), 14.1 (OCH$_2$*C*H$_3$); HRMS (ESI$^+$) *m/z* Calculated for $C_{17}H_{25}NO_4{}^{35}Cl$ [M+H] 342.1472; Found 342.1481.

***tert*-Butyl 2-phenylacetate (S15)[469]**



DMAP (730 mg, 6.0 mmol) was added to a mixture of phenyl acetic acid (2.72 g, 20.0 mmol) and di-*tert*-butyl decarbonate (9.61 g, 44.0 mmol) in *t*-BuOH (50 mL) at 0 ºC. The reaction mixture was stirred at 30 ºC for 19 h. The reaction mixture was concentrated under reduced pressure. Purification by flash chromatography afforded *tert*-butyl 2-phenylacetate **S15** (2.38 g, 62%) as a colourless oil. R_f 0.26 (2% Et_2O/pentane); ν_{max} (film)/cm^{-1} 2978, 1730 (C=O), 1454, 1368, 1297, 1256, 1137, 742, 697; ^{1}H NMR (400 MHz, $CDCl_3$) δ 7.35–7.24 (m, 5 H, 5 × HC_{Ph}), 3.54 (s, 2 H, PhCH$_2$), 1.45 (s, 9 H, C(CH$_3$)$_3$); ^{13}C NMR (101 MHz, $CDCl_3$) δ 170.9 (C=O), 134.7 (C_{Ph} quat), 129.2 (2 × C_{Ph}), 128.4 (2 × C_{Ph}), 126.8 (C_{Ph}), 80.8 (*C*(CH$_3$)$_3$), 42.6 (PhCH$_2$), 28.0 (C(*C*H$_3$)$_3$). The observed characterisation data (IR, ^{1}H and ^{13}C NMR) was consistent with that previously reported in the literature.[470]

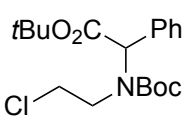
***tert*-Butyl 2-diazo-2-phenylacetate (S16)**



DBU (2.24 mL, 15.0 mmol) was added dropwise to a solution of *tert*-butyl 2-phenylacetate **S15** (1.92 g, 10.0 mmol) and *p*-ABSA (2.88 g, 12.0 mmol) in MeCN (33 mL) at 0 ºC. The reaction mixture was stirred for 64 h then sat. aq. NH_4Cl (50 mL) was added. The aqueous reaction mixture was extracted with Et_2O (3 ×

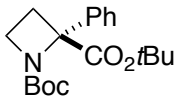
50 mL). The combined organic layers were concentrated under reduced pressure, then 50% Et_2O/pentane (100 mL) was added and the mixture was filtered then concentrated under reduced pressure. Purification by flash chromatography (2% Et_2O/pentane) afforded *tert*-butyl 2-diazo-2-phenylacetate **S16** (1.20 g, 55%) as an low melting point orange solid. R_f 0.47 (2% Et_2O/pentane); ν_{max} (film)/cm^{-1} 2978, 2080 (C=N=N out-of-phase), 1700 (C=O), 1498, 1349 (C=N=N in-phase), 1245, 1141, 1006, 757; ^{1}H NMR (400 MHz, $CDCl_3$) δ 7.50–7.47 (m, 2 H, 2 × HC_{Ph}), 7.41–7.35 (m, 2 H, 2 × HC_{Ph}), 7.20–7.15 (m, 1 H, HC_{Ph}), 1.57 (s, 9 H, $C(CH_3)_3$); ^{13}C NMR (101 MHz, $CDCl_3$) δ 164.5 (C=O), 128.8 (2 × C_{Ph}), 126.1 (C_{Ph} quat), 125.5 (C_{Ph}), 123.9 (2 × C_{Ph}), 82.0 ($C(CH_3)_3$), 28.4 ($C(CH_3)_3$). The observed characterisation data (IR, ^{1}H and ^{13}C NMR) was consistent with that previously reported in the literature.[471]

(±)–*tert*-Butyl 2-((*tert*-butoxycarbonyl)(2-chloroethyl)amino)-2-phenylacetate (397)



$Rh_2(esp)_2$ (3.8 mg, 5.0 μmol) was added to a solution of protected amine **52** (180 mg, 1.0 mmol) and *tert*-butyl 2-diazo-2-phenylacetate **S16** (327 mg, 1.5 mmol) in benzene (3.33 mL). The reaction mixture was heated to 60 ºC and stirred for 2.5 h. The reaction mixture was cooled to rt and filtered through celite, washing with EtOAc (20 mL) and then concentrated under reduced pressure. Purification by flash chromatography (5% to 10% EtOAc/pentane) afforded *tert*-butyl 2-((*tert*-butoxycarbonyl)(2-chloroethyl)amino)-2-phenylacetate **397** (272 mg, 74%) as a pale orange oil. R_f 0.19 (5% EtOAc/pentane); ν_{max} (film)/cm^{-1} 2978, 1737 (C=O ester), 1700 (C=O carbamate), 1454, 1394, 1293, 1252, 1144, 753, 701; ^{1}H NMR (400 MHz, $CDCl_3$) δ 7.44–7.35 (m, 3 H, 3 × HC_{Ph}), 7.31–7.25 (m, 2 H, 2 × HC_{Ph}), 5.77 and 5.33 (2 × br s, 1 H, NCH), 3.51–3.23 (m, 3 H, NCH_2CHH), 3.18–3.05 and 2.98–2.87 (m, 1 H, NCH_2CH*H*), 1.51 and 1.49 (2 × br s, 18 H, 2 × $C(CH_3)_3$); ^{13}C NMR (101 MHz, $CDCl_3$) δ 170.0 (C=O ester), 155.6 and 155.0 (C=O carbamate), 135.3 and 134.6 (C_{Ph} quat), 129.1 (2 × C_{Ph}), 128.9 (2 × C_{Ph}), 128.5 (br s, C_{Ph}), 82.1 ($C(CH_3)_3$ ester), 81.0 ($C(CH_3)_3$ carbamate), 63.9 and 62.2 (NCH), 46.5 and 46.4 (CH_2Cl), 40.9 and 40.7 (NCH_2), 28.3 ($C(CH_3)_3$ ester), 28.0 ($C(CH_3)_3$ carbamate); HRMS (ESI$^+$) *m/z* Calculated for $C_{19}H_{29}NO_4{}^{35}Cl$ [M+H] 370.1785; Found 370.1792.

(±)–Di-*tert*-butyl 2-phenylazetidine-1,2-dicarboxylate (398)



$CsOH·H_2O$ (34mg, 0.2 mmol) was added to a solution of *tert*-butyl 2-((*tert*-butoxycarbonyl)(2-chloroethyl)amino)-2-phenylacetate **397** (37 mg, 0.1 mmol) and tetrabutylammonium bromide (3.0 mg, 0.01 mmol) in toluene (0.3 mL). The reaction mixture was stirred for 20 h then filtered through celite, washing with Et_2O (20 mL) and concentrated under reduced pressure. Purification by flash chromatography (20% Et_2O/pentane) afforded di-*tert*-butyl 2-phenylazetidine-1,2-dicarboxylate **398** (15mg, 45%) as

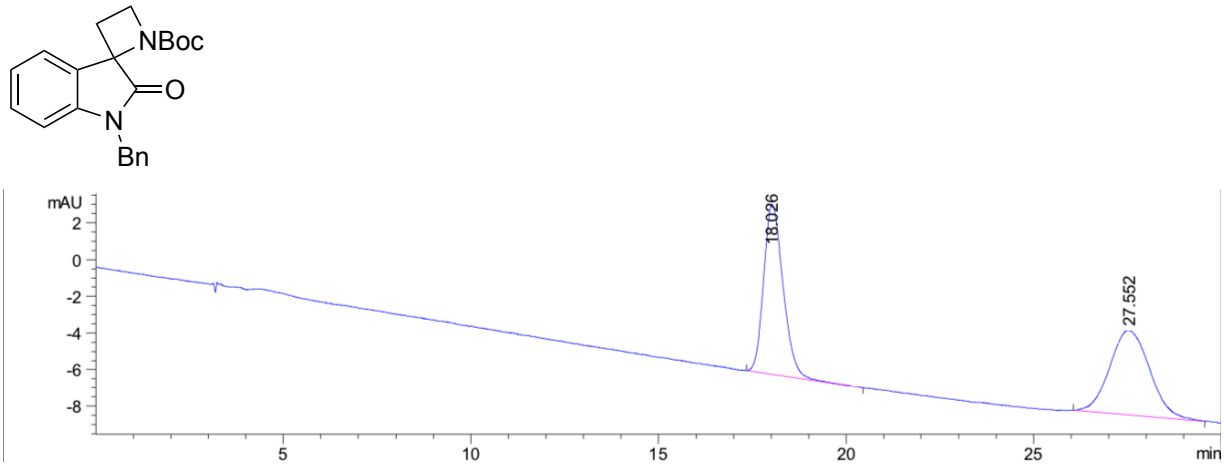
a colourless oil. R_f 0.26 (20% Et_2O/pentane); ν_{max} (film)/cm^{-1} 2975, 1735 (C=O ester), 1704 (C=O carbamate), 1365, 1249, 1152, 1088; ^1H NMR (400 MHz, $CDCl_3$) δ 7.46–7.41 (m, 2 H, 2 $\times$ HC_{Ph}), 7.38–7.32 (m, 2 H, 2 $\times$ HC_{Ph}), 7.31–7.24 (m, 1 H, HC_{Ph}), 4.13 (q, J = 7.8 Hz, 1 H, NC*H*H), 3.87 (ddd, J = 9.0, 8.0, 4.6 Hz, 1 H, NCH*H*), 2.71–2.62 (m, 1 H, NCH_2CHH), 2.55–2.44 (m, 1 H, NCH_2CHH), 1.52, 1.49 and 1.41 (3 $\times$ s, 18 H, 2 $\times$ $C(CH_3)_3$); ^{13}C NMR (101 MHz, $CDCl_3$) δ 170.3 (C=O ester), 156.0 (C=O carbamate), 140.6 and 136.5 (C_{Ar} quat), 127.7, 127.5, 127.1 and 126.5 (5 $\times$ C_{Ar}), 82.0 ($C(CH_3)_3$ ester), 80.3 and 79.8 ($C(CH_3)_3$ carbamate), 73.8 (NC quat), 47.0 and 45.2 (NCH_2), 30.7 and 29.5 (NCH_2CH_2), 28.4 and 27.9 (2 $\times$ $C(CH_3)_3$); HRMS (ESI^+) *m/z* Calculated for $C_{19}H_{28}NO_4$ [M+H] 334.2018; Found 334.2020.

6.2.3.7 HPLC Data for Spirooxindoles

***tert*-Butyl 1'-benzyl-2'-oxospiro[azetidine-2,3'-indoline]-1-carboxylate (338)**

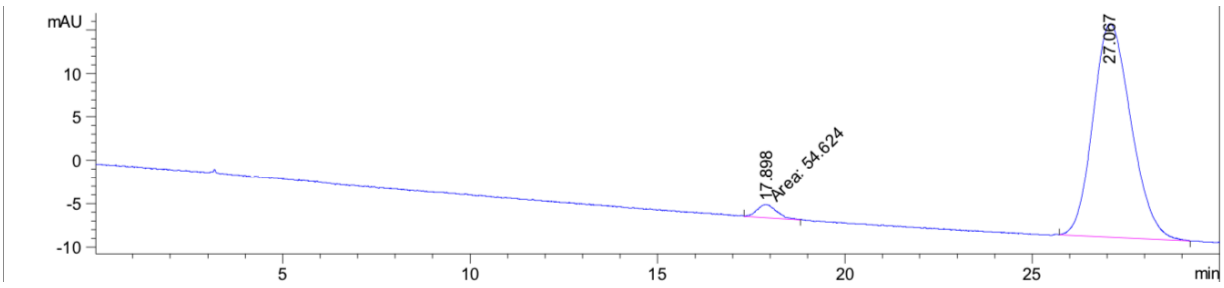
Conditions: Chiralpak ID column, 90:10 *n*-hexane:*i*-PrOH, flow rate: 1 mL min^{-1}, 35 ºC, UV detection wavelength: 254 nm

(±)–338



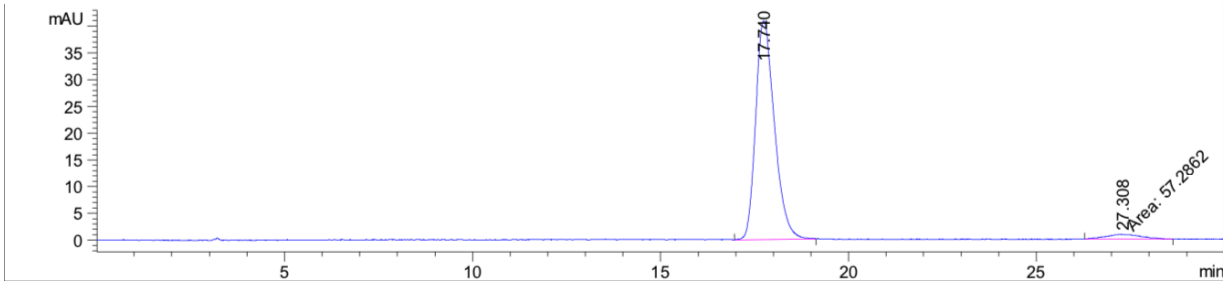
Peak #	Ret Time [min]	Type	Width [min]	Area [mAU*s]	Height [mAU]	Area %
1	18.026	BB	0.5456	333.15030	9.26355	49.3461
2	27.552	BB	0.8746	341.97998	4.63588	50.6539
Totals :				675.13028	13.89943	

(–)–(*S*)–338



Peak #	Ret Time [min]	Type	Width [min]	Area [mAU*s]	Height [mAU]	Area %
1	17.898	MM	0.6028	54.62404	1.51019	3.0559
2	27.067	BB	0.8755	1732.89771	24.55142	96.9441
Totals :				1787.52175	26.06161	

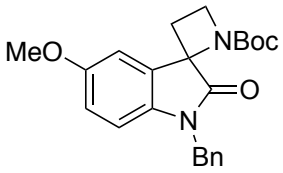
(+)–(*R*)–338



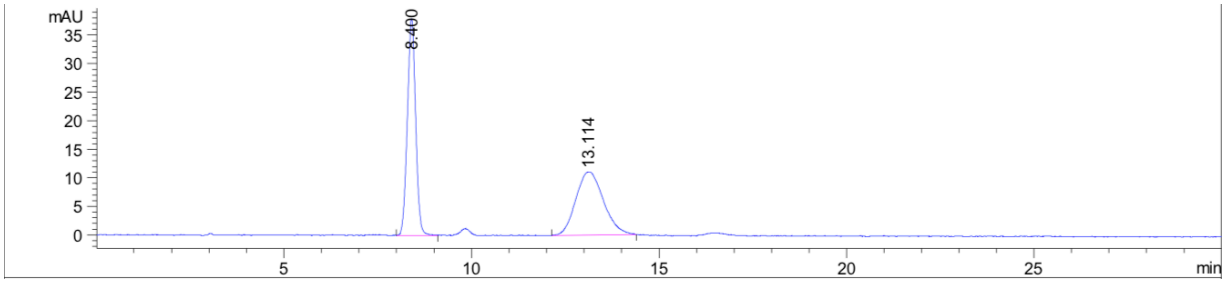
Peak #	Ret Time [min]	Type	Width [min]	Area [mAU*s]	Height [mAU]	Area %
1	17.740	BB	0.5269	1417.22314	40.83775	96.1149
2	27.308	PM	1.0938	57.28624	8.72885e-1	3.8851
Totals :				1474.50938	41.71063	

tert-Butyl 1'-benzyl-5'-methoxy-2'-oxospiro[azetidine-2,3'-indoline]-1-carboxylate (339)

Conditions: Chiralpak IA column, 80:20 *n*-hexane:*i*-PrOH, flow rate: 1 mL min^{-1}, 35 ºC, UV detection wavelength: 254 nm

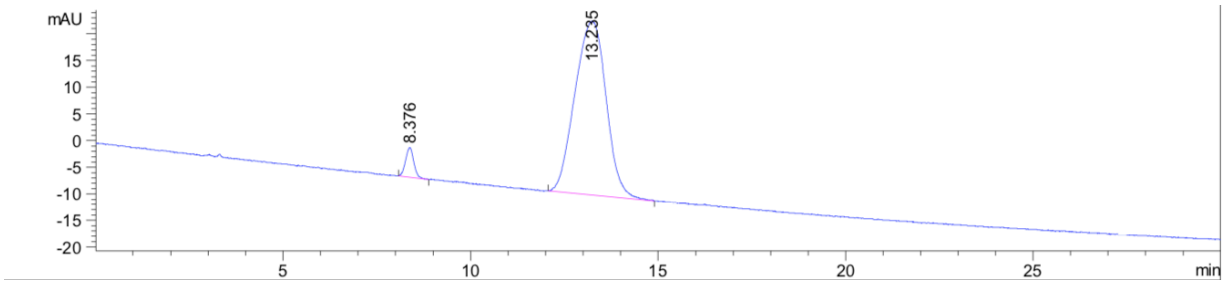


(±)–339



Peak #	Ret Time [min]	Type	Width [min]	Area [mAU*s]	Height [mAU]	Area %
1	8.400	BB	0.2396	583.41754	37.90751	50.8066
2	13.114	BB	0.6100	564.89215	11.05798	49.1934
Totals :				1148.30969	48.96549	

(–)–(*S*)–339

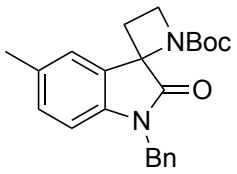


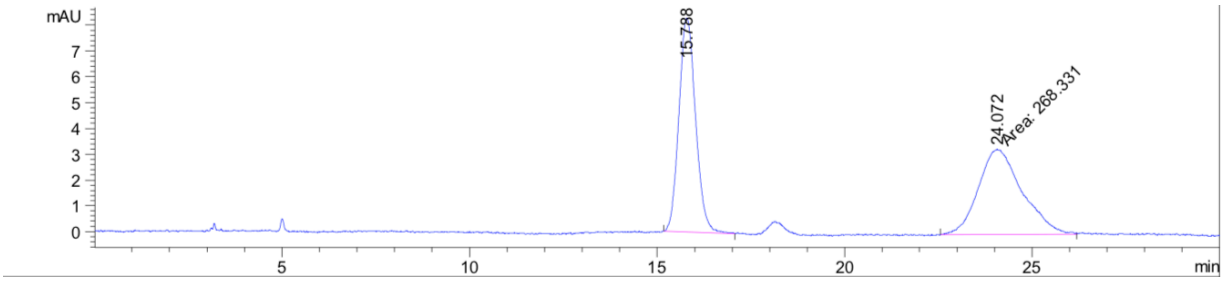
Peak #	Ret Time [min]	Type	Width [min]	Area [mAU*s]	Height [mAU]	Area %
1	8.376	BB	0.2253	84.58729	5.56446	4.3018
2	13.235	BB	0.6867	1881.75085	32.63501	95.6982
Totals :				1966.33814	38.19947	

***tert*-Butyl 1'-benzyl-5'-methyl-2'-oxospiro[azetidine-2,3'-indoline]-1-carboxylate (340)**

Conditions: Chiralpak ID column, 90:10 *n*-hexane:*i*-PrOH, flow rate: 1 mL min^{-1}, 35 ºC, UV detection wavelength: 254 nm

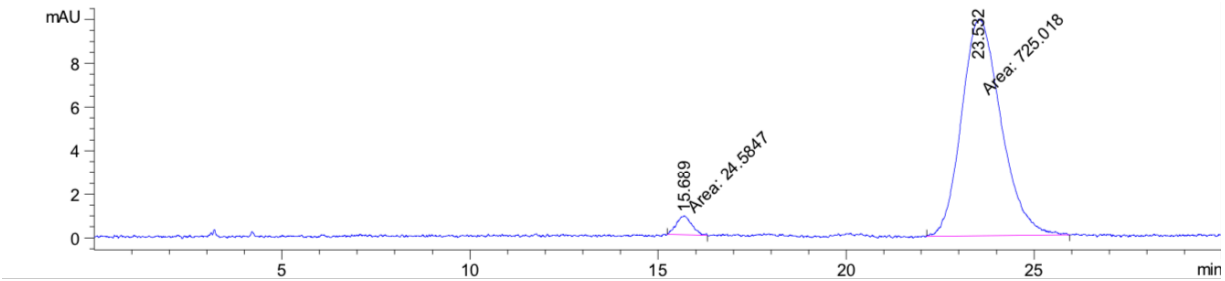
(±)–340





Peak #	Ret Time [min]	Type	Width [min]	Area [mAU*s]	Height [mAU]	Area %
1	15.788	BB	0.4610	256.26868	8.28246	48.8503
2	24.072	PM	1.3500	268.33084	3.31263	51.1497
Totals :				524.59952	11.59509	

(–)–(*S*)–340

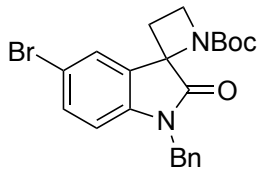


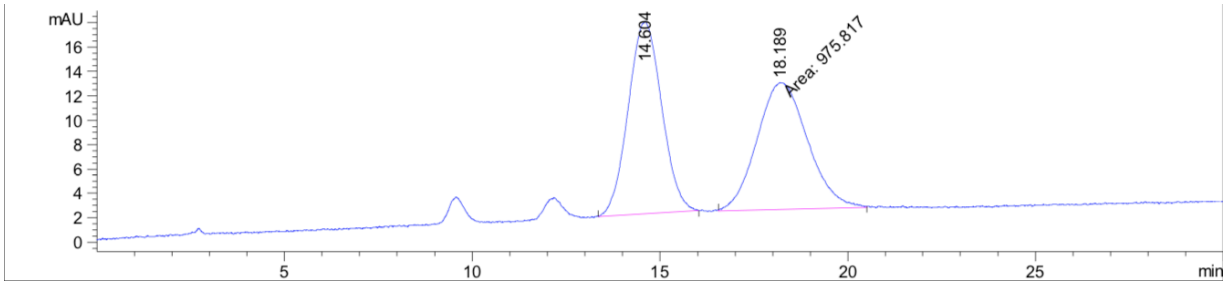
Peak #	Ret Time [min]	Type	Width [min]	Area [mAU*s]	Height [mAU]	Area %
1	15.689	PP	0.4787	24.58469	8.55947e-1	3.2797
2	23.532	MP	1.2158	725.01837	9.93894	96.7203
Totals :				749.60307	10.79488	

***tert*-Butyl 1'-benzyl-5'-bromo-2'-oxospiro[azetidine-2,3'-indoline]-1-carboxylate (341)**

Conditions: Chiralpak IC column, 90:10 *n*-hexane:*i*-PrOH, flow rate: 1 mL min^{-1}, 35 ºC, UV detection wavelength: 254 nm

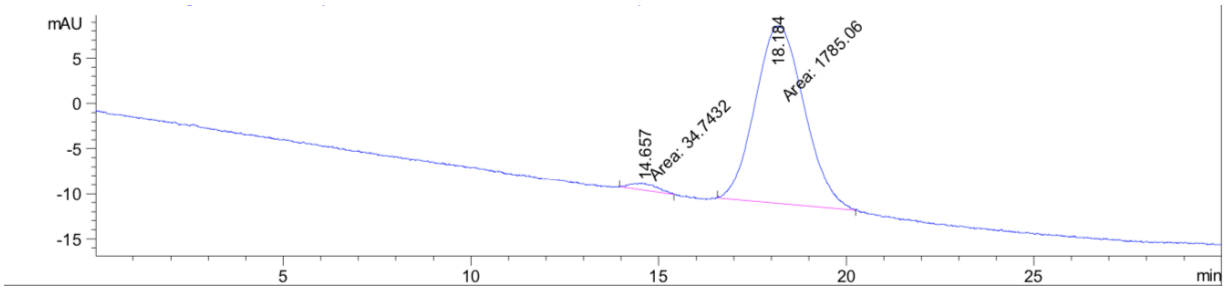
(±)–341





Peak #	Ret Time [min]	Type	Width [min]	Area [mAU*s]	Height [mAU]	Area %
1	14.604	BB	0.7431	978.13226	15.78033	50.0593
2	18.189	MM	1.5618	975.81659	10.41315	49.9407
Totals :				1953.94885	26.19347	

(–)–(*S*)–341

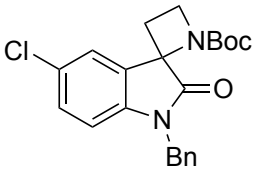


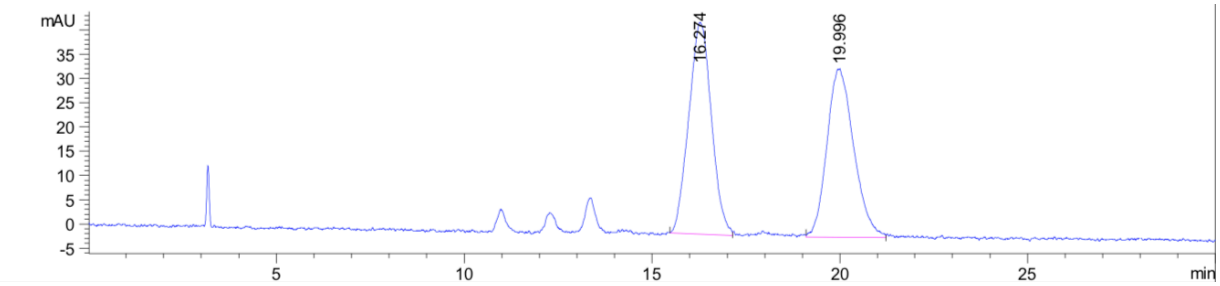
Peak #	Ret Time [min]	Type	Width [min]	Area [mAU*s]	Height [mAU]	Area %
1	14.657	PP	0.8110	34.74319	7.14008e-1	1.9092
2	18.184	MM	1.5118	1785.05896	19.67957	98.0908
Totals :				1819.80215	20.39358	

***tert*-Butyl 1'-benzyl-5'-chloro-2'-oxospiro[azetidine-2,3'-indoline]-1-carboxylate (346)**

Conditions: Chiralpak IE column, 90:10 *n*-hexane:*i*-PrOH, flow rate: 1 mL min^{-1}, 35 ºC, UV detection wavelength: 254 nm

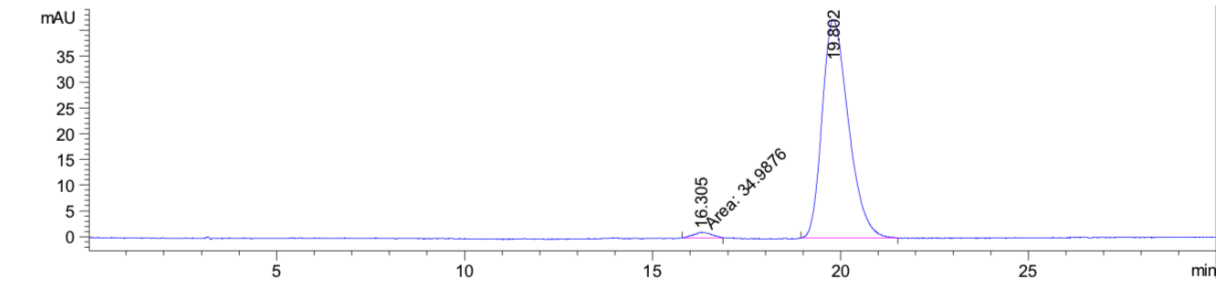
(±)–346





Peak #	Ret Time [min]	Type	Width [min]	Area [mAU*s]	Height [mAU]	Area %
1	16.274	BV	0.5034	1831.85645	43.67122	51.5426
2	19.996	VV	0.5968	1722.20837	34.71099	48.4574
Totals :				3554.06482	78.38221	

(–)–(*S*)–346

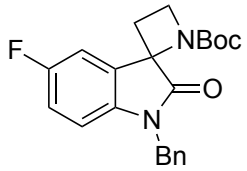


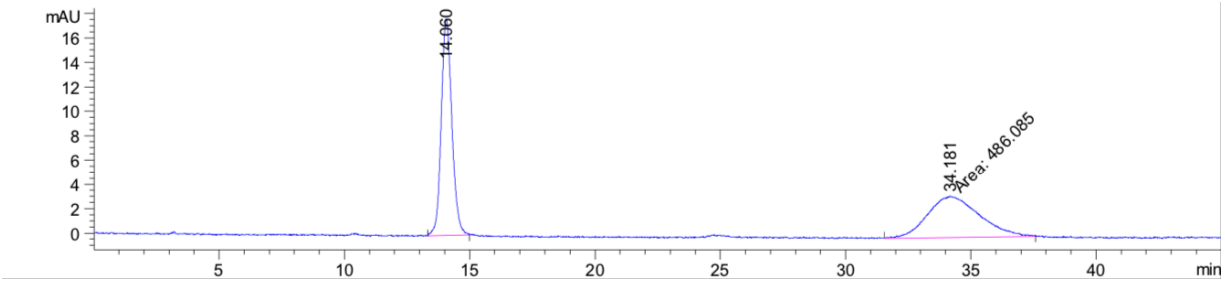
Peak #	Ret Time [min]	Type	Width [min]	Area [mAU*s]	Height [mAU]	Area %
1	16.305	MM	0.5448	34.98760	1.07041	1.6718
2	19.802	BB	0.7035	2057.87939	42.30371	98.3282
Totals :				2092.86699	43.37411	

tert-Butyl 1'-benzyl-5'-fluoro-2'-oxospiro[azetidine-2,3'-indoline]-1-carboxylate (347)

Conditions: Chiralpak ID column, 90:10 *n*-hexane:*i*-PrOH, flow rate: 1 mL min^{-1}, 35 ºC, UV detection wavelength: 254 nm

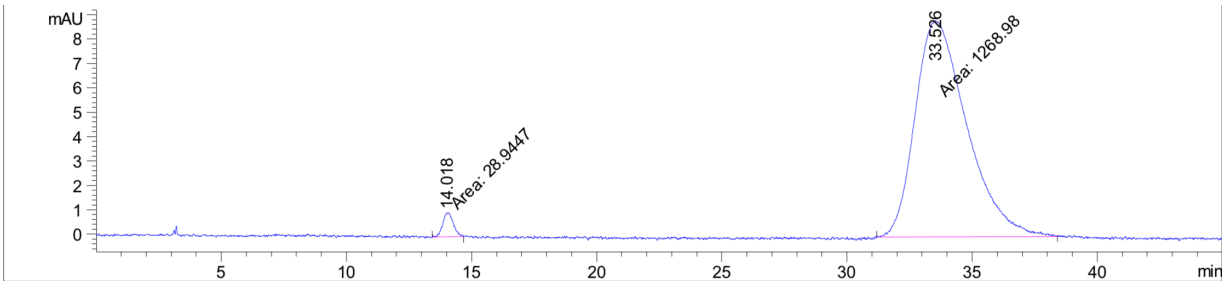
(±)–347





Peak #	Ret Time [min]	Type	Width [min]	Area [mAU*s]	Height [mAU]	Area %
1	14.060	BB	0.4468	520.76111	17.72309	51.7220
2	34.181	MM	2.3896	486.08478	3.39033	48.2780
Totals :				1006.84589	21.11343	

(–)–(*S*)–347

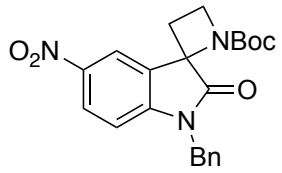


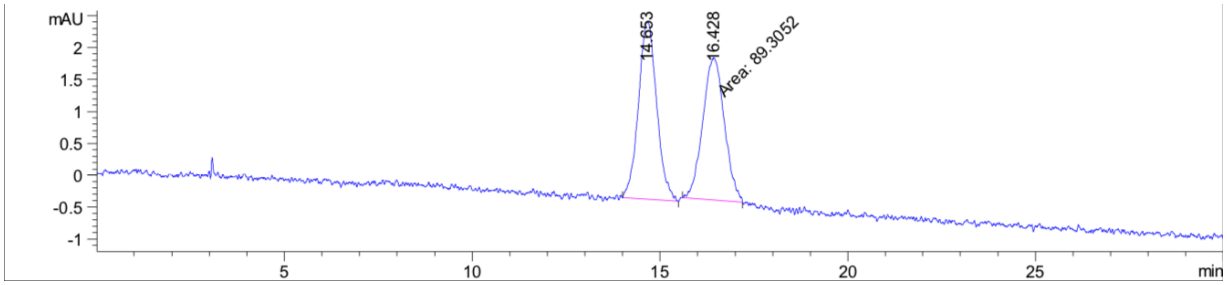
Peak #	Ret Time [min]	Type	Width [min]	Area [mAU*s]	Height [mAU]	Area %
1	14.018	MP	0.4917	28.94473	9.81207e-1	2.2301
2	33.526	PM	2.3872	1268.98315	8.85965	97.7699
Totals :				1297.92788	9.84086	

***tert*-Butyl 1'-benzyl-5'-nitro-2'-oxospiro[azetidine-2,3'-indoline]-1-carboxylate (348)**

Conditions: Chiralpak IF column, 90:10 *n*-hexane:*i*-PrOH, flow rate: 1 mL min^{-1}, 35 ºC, UV detection wavelength: 254 nm

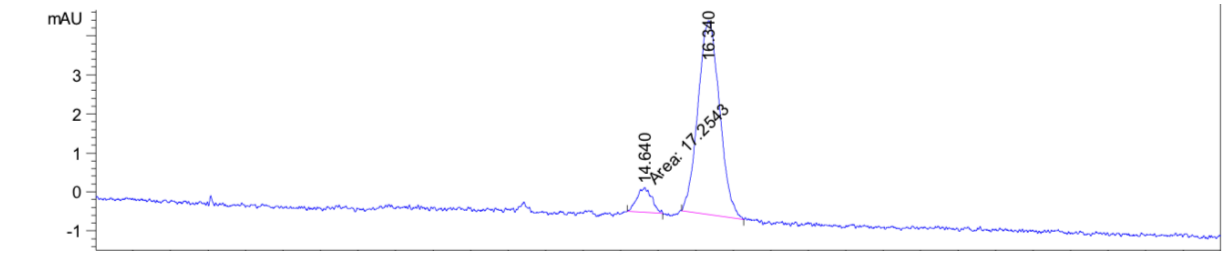
(±)–348





Peak #	Ret Time [min]	Type	Width [min]	Area [mAU*s]	Height [mAU]	Area %
1	14.653	BB	0.4144	94.33975	2.79078	51.3707
2	16.428	PP	0.6676	89.30518	2.22955	48.6293
Totals :				183.64493	5.02033	

(–)–(*S*)–348

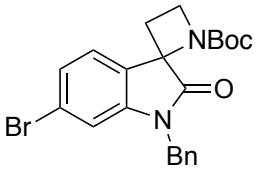


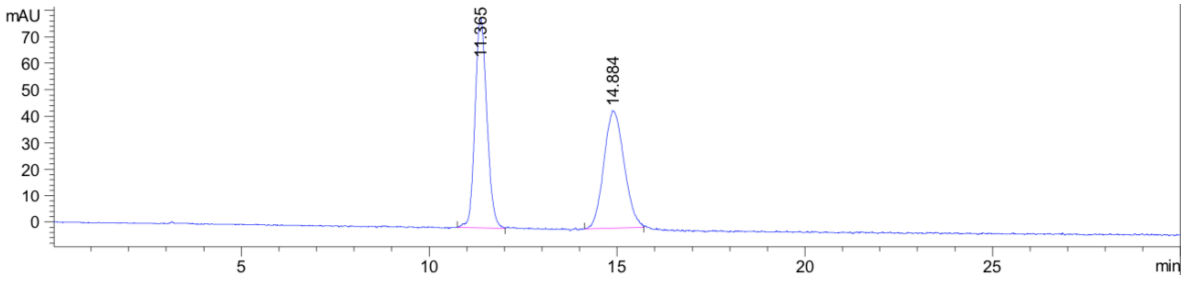
Peak #	Ret Time [min]	Type	Width [min]	Area [mAU*s]	Height [mAU]	Area %
1	14.640	PP	0.4519	17.25432	6.36379e-1	7.9902
2	16.340	BB	0.4907	198.68871	4.96717	92.0098
Totals :				215.94303	5.60355	

***tert*-butyl 1'-benzyl-6'-bromo-2'-oxospiro[azetidine-2,3'-indoline]-1-carboxylate (343)**

Conditions: Chiralpak IC column, 90:10 *n*-hexane:*i*-PrOH, flow rate: 1 mL min^{-1}, 35 ºC, UV detection wavelength: 254 nm

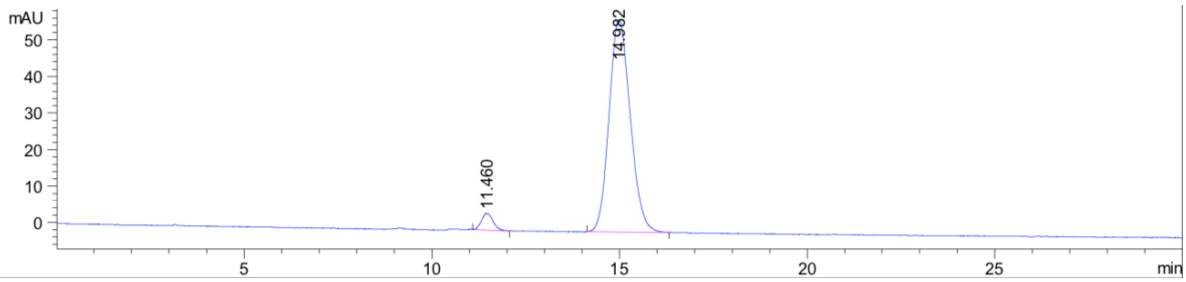
(±)–343





Peak #	Ret Time [min]	Type	Width [min]	Area [mAU*s]	Height [mAU]	Area %
1	11.365	BV	0.3298	1744.56006	79.56335	51.0347
2	14.884	BV	0.4514	1673.82007	44.64238	48.9653
Totals :				3418.38013	124.20573	

(–)–(*S*)–343

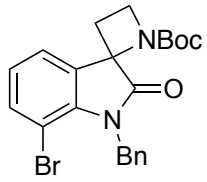


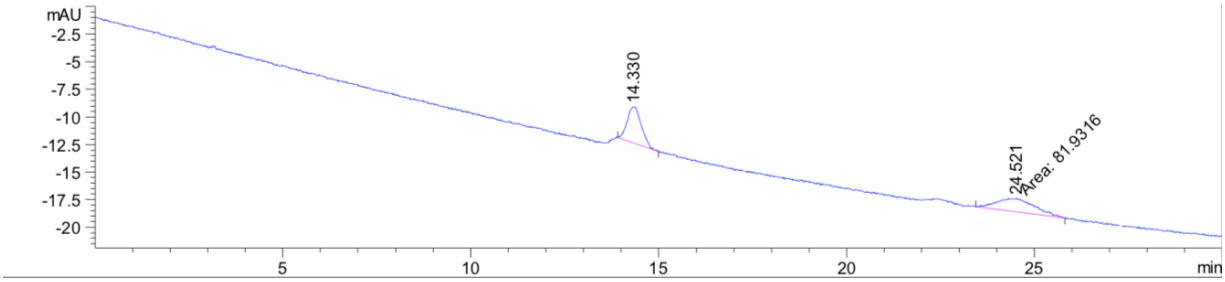
Peak #	Ret Time [min]	Type	Width [min]	Area [mAU*s]	Height [mAU]	Area %
1	11.460	BB	0.2978	96.84792	4.55978	4.0686
2	14.982	BB	0.6121	2283.53540	58.15580	95.9314
Totals :				2380.38332	62.71559	

tert-Butyl 1'-benzyl-7'-bromo-2'-oxospiro[azetidine-2,3'-indoline]-1-carboxylate (349)

Conditions: Chiralpak IC column, 90:10 *n*-hexane:*i*-PrOH, flow rate: 1 mL min^{-1}, 35 ºC, UV detection wavelength: 254 nm

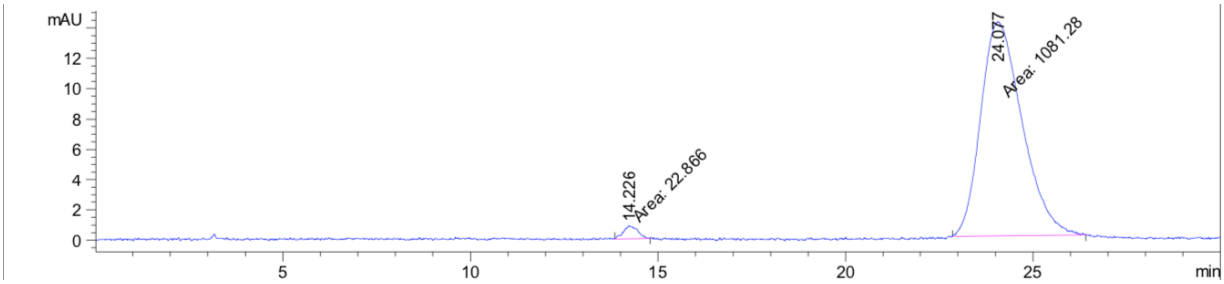
(±)–349





Peak #	Ret Time [min]	Type	Width [min]	Area [mAU*s]	Height [mAU]	Area %
1	14.330	BB	0.3275	84.98497	3.24541	50.9146
2	24.521	PP	1.1325	81.93165	1.20573	49.0854
Totals :				166.91662	4.45114	

(+)–(*S*)–349

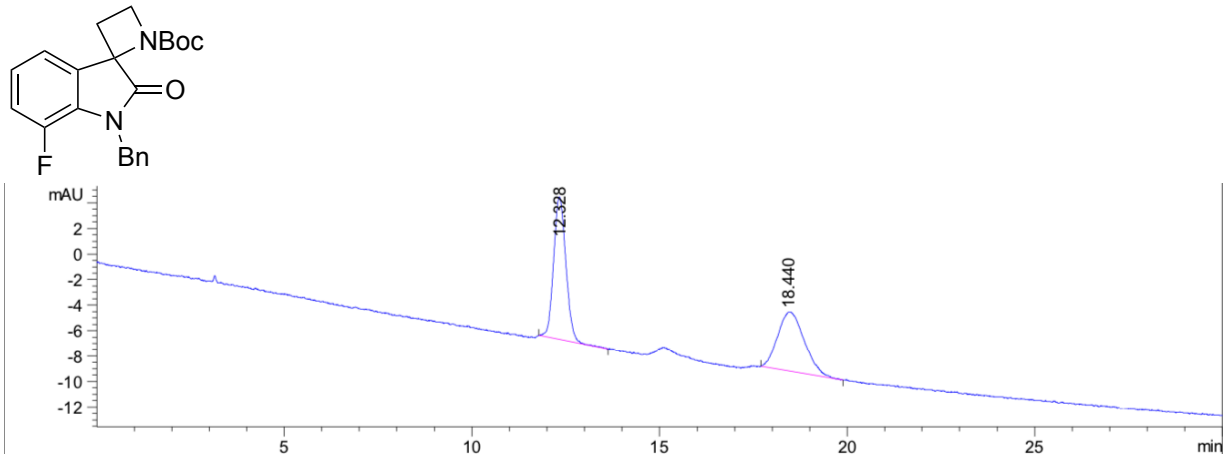


Peak #	Ret Time [min]	Type	Width [min]	Area [mAU*s]	Height [mAU]	Area %
1	14.226	MM	0.4404	22.86604	8.65271e-1	2.0709
2	24.077	PM	1.2770	1081.27954	14.11210	97.9291
Totals :				1104.14558	14.97737	

***tert*-Butyl 1'-benzyl-7'-fluoro-2'-oxospiro[azetidine-2,3'-indoline]-1-carboxylate (342)**

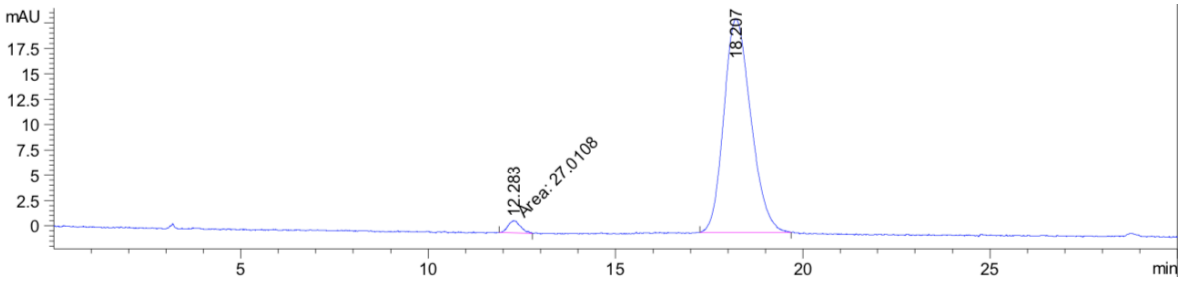
Conditions: Chiralpak ID column, 90:10 *n*-hexane:*i*-PrOH, flow rate: 1 mL min^{-1}, 35 ºC, UV detection wavelength: 254 nm

(±)–342



Peak #	Ret Time [min]	Type	Width [min]	Area [mAU*s]	Height [mAU]	Area %
1	12.328	BB	0.3419	254.60260	11.17275	52.4086
2	18.440	BB	0.6037	231.20050	4.63665	47.5914
Totals :				485.80310	15.80941	

(–)–(*S*)–342

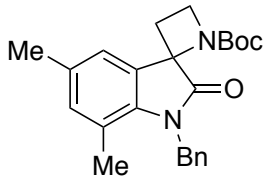


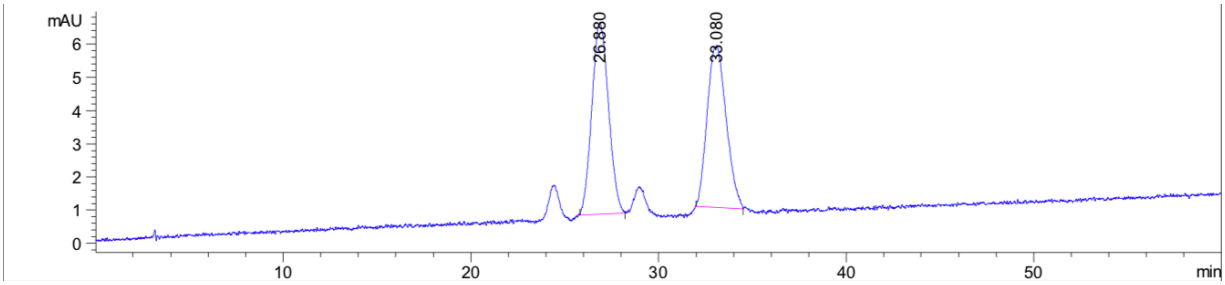
Peak #	Ret Time [min]	Type	Width [min]	Area [mAU*s]	Height [mAU]	Area %
1	12.283	MP	0.3790	27.01079	1.18786	2.4858
2	18.207	BB	0.7005	1059.60339	21.07650	97.5142
Totals :				1086.61419	22.26437	

***tert*-Butyl 1'-benzyl-5',7'-dimethyl-2'-oxospiro[azetidine-2,3'-indoline]-1-carboxylate (344)**

Conditions: Chiralpak IE column, 90:10 *n*-hexane:*i*-PrOH, flow rate: 1 mL min^{-1}, 35 ºC, UV detection wavelength: 254 nm

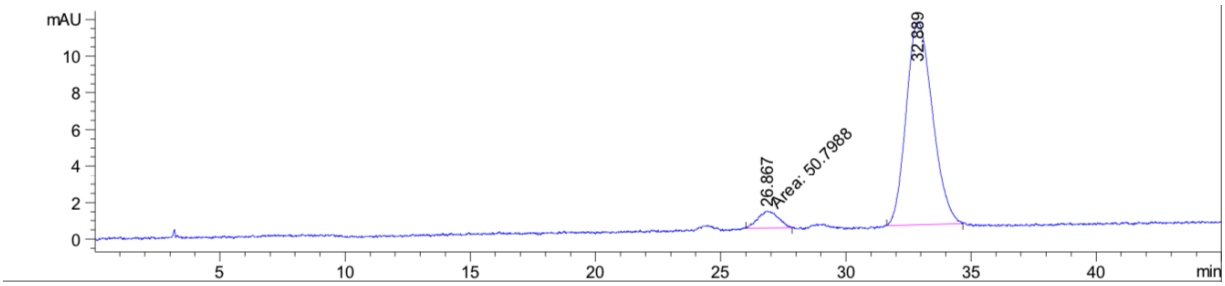
(±)–344





Peak #	Ret Time [min]	Type	Width [min]	Area [mAU*s]	Height [mAU]	Area %
1	26.880	BB	0.7374	357.44885	5.78069	51.0496
2	33.080	BB	0.8312	342.75040	4.88152	48.9504
Totals :				700.19925	10.66221	

(–)–(*S*)–344

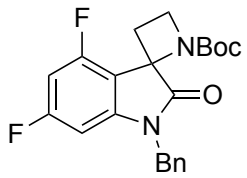


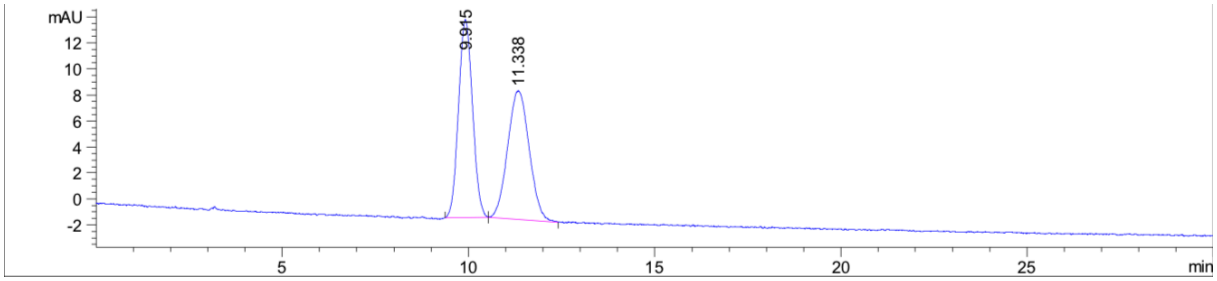
Peak #	Ret Time [min]	Type	Width [min]	Area [mAU*s]	Height [mAU]	Area %
1	26.867	PP	0.9263	50.79882	9.14001e-1	5.9034
2	32.889	BB	0.8649	809.70593	11.10130	94.0966
Totals :				860.50476	12.01530	

***tert*-Butyl 1'-benzyl-4',6'-difluoro-2'-oxospiro[azetidine-2,3'-indoline]-1-carboxylate (345)**

Conditions: Chiralpak ID column, 90:10 *n*-hexane:*i*-PrOH, flow rate: 1 mL min^{-1}, 35 ºC, UV detection wavelength: 254 nm

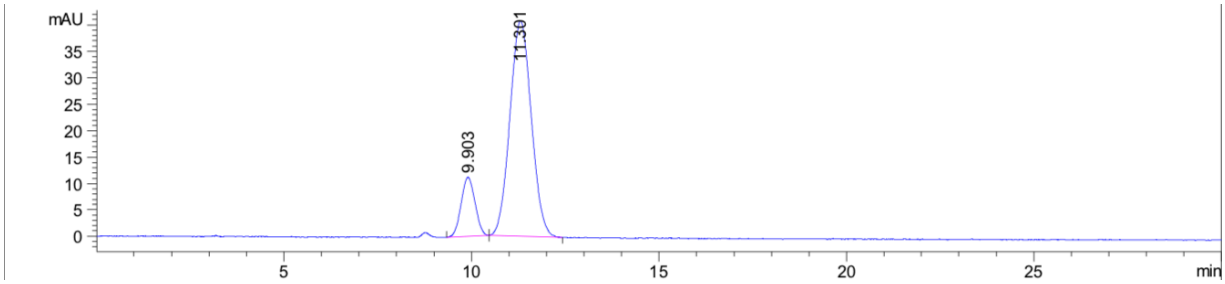
(±)–345





Peak #	Ret Time [min]	Type	Width [min]	Area [mAU*s]	Height [mAU]	Area %
1	9.915	BB	0.4001	397.16812	15.23955	50.0326
2	11.338	BB	0.4841	396.65027	9.88595	49.9674
Totals :				793.81839	25.12550	

(–)–(*S*)–345

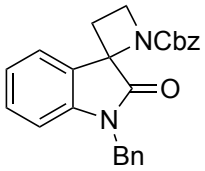


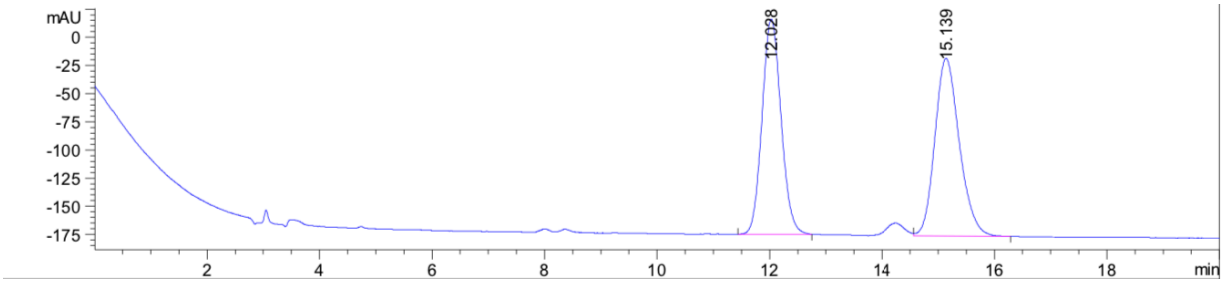
Peak #	Ret Time [min]	Type	Width [min]	Area [mAU*s]	Height [mAU]	Area %
1	9.903	BB	0.3777	289.13007	11.25432	15.1140
2	11.301	BB	0.5982	1623.87109	40.81146	84.8860
Totals :				1913.00116	52.06577	

Benzyl 1'-benzyl-2'-oxospiro[azetidine-2,3'-indoline]-1-carboxylate (350)

Conditions: Chiralpak IA column, 80:20 *n*-hexane:*i*-PrOH, flow rate: 1 mL min^{-1}, 35 ºC, UV det

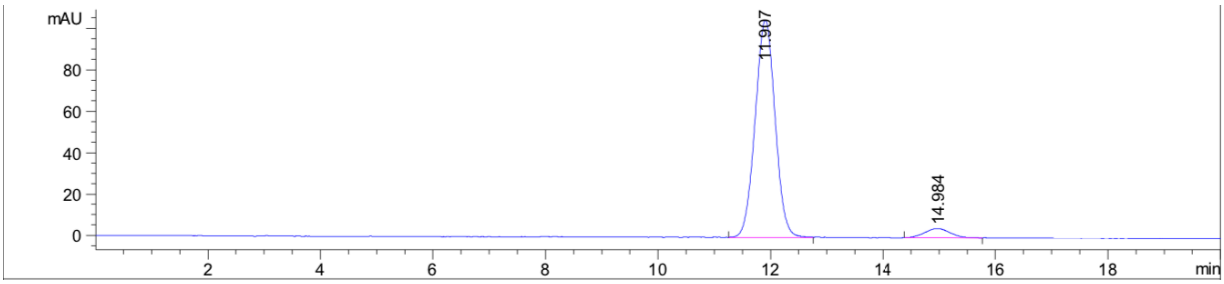
(±)–350





Peak #	Ret Time [min]	Type	Width [min]	Area [mAU*s]	Height [mAU]	Area %
1	12.028	BB	0.3675	4479.76172	191.11395	48.3737
2	15.139	VB	0.4574	4780.98584	157.85286	51.6263
Totals :				9260.74756	348.96681	

(–)–(*S*)–350

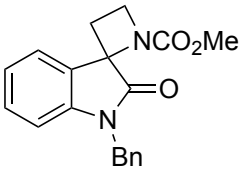


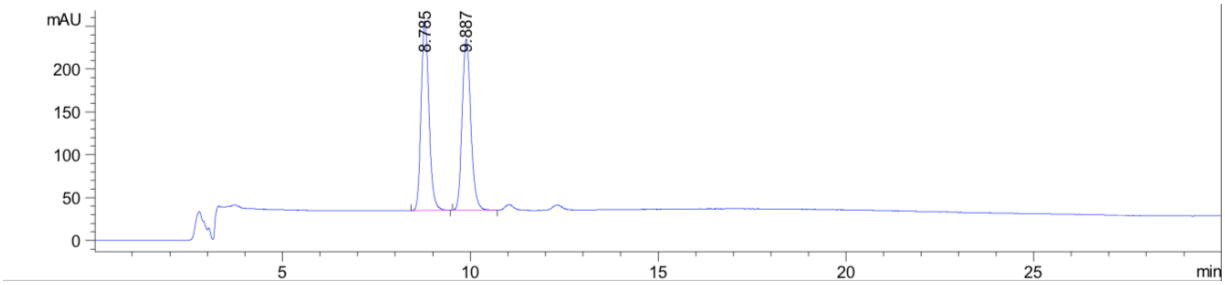
Peak #	Ret Time [min]	Type	Width [min]	Area [mAU*s]	Height [mAU]	Area %
1	11.907	BB	0.3812	2581.89502	104.88249	94.8984
2	14.984	BB	0.3936	138.79991	4.42879	5.1016
Totals :				2720.69493	109.31128	

Methyl 1'-benzyl-2'-oxospiro[azetidine-2,3'-indoline]-1-carboxylate (351)

Conditions: Chiralpak IA column, 80:20 *n*-hexane:*i*-PrOH, flow rate: 1 mL min^{-1}, 35 ºC, UV detection wavelength: 254 nm

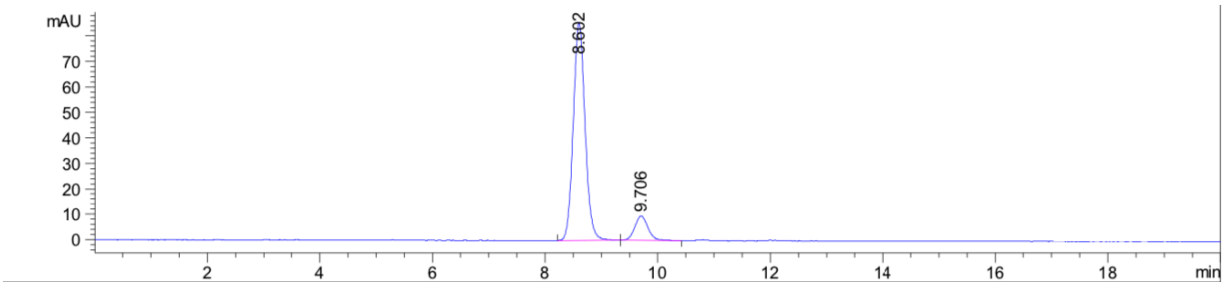
(±)–351





Peak #	Ret Time [min]	Type	Width [min]	Area [mAU*s]	Height [mAU]	Area %
1	8.785	BB	0.2223	3190.69800	221.16893	50.0000
2	9.887	BB	0.2462	3190.69702	199.92406	50.0000
Totals :				6381.39502	421.09299	

(–)–(*S*)–351

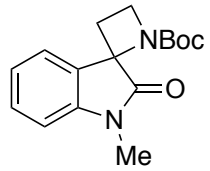


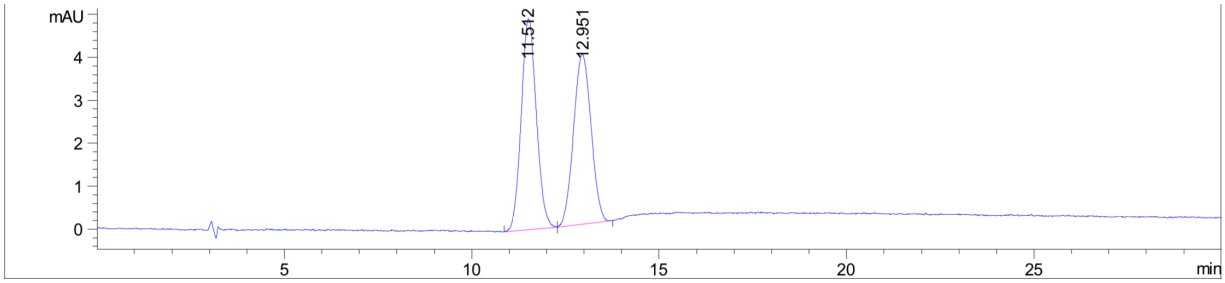
Peak #	Ret Time [min]	Type	Width [min]	Area [mAU*s]	Height [mAU]	Area %
1	8.602	BB	0.2240	1245.56458	85.49292	88.6550
2	9.706	BB	0.2507	159.39255	9.65243	11.3450
Totals :				1404.95712	95.14535	

tert-Butyl 1'-methyl-2'-oxospiro[azetidine-2,3'-indoline]-1-carboxylate (352)

Conditions: Chiralpak IA column, 95:5 *n*-hexane:*i*-PrOH, flow rate: 1 mL min^{-1}, 35 ºC, UV detection wavelength: 254 nm

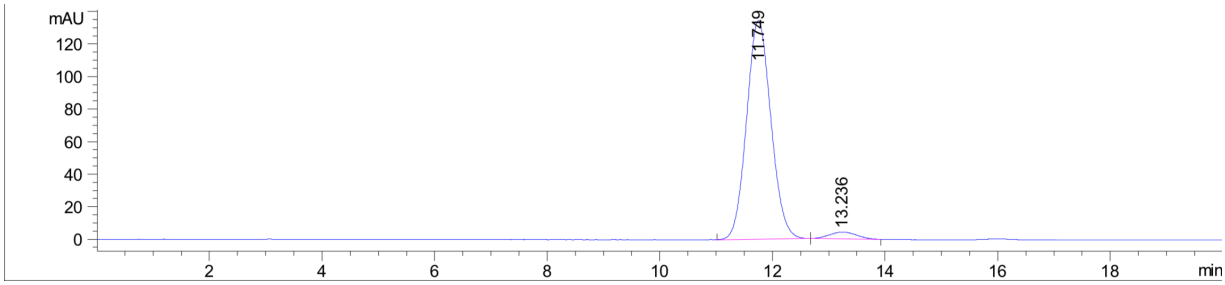
(±)–352





Peak #	Ret Time [min]	Type	Width [min]	Area [mAU*s]	Height [mAU]	Area %
1	11.512	BB	0.4287	138.43642	4.91338	51.7541
2	12.951	BB	0.4895	129.05222	3.96786	48.2459
Totals :				267.48863	8.88124	

(–)–(*S*)–352

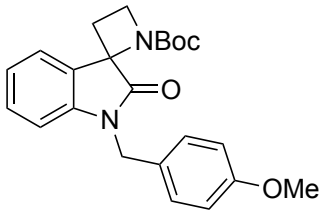


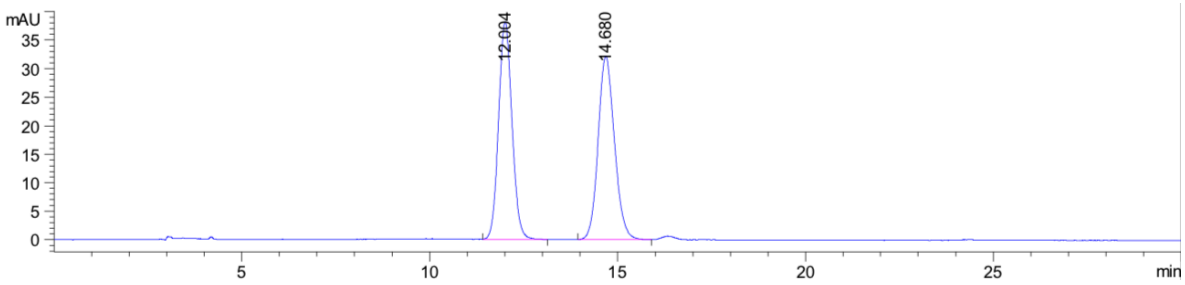
Peak #	Ret Time [min]	Type	Width [min]	Area [mAU*s]	Height [mAU]	Area %
1	11.749	BB	0.4663	4034.90308	134.37186	96.6522
2	13.236	BB	0.4017	139.76117	4.16239	3.3478
Totals :				4174.66425	138.53424	

***tert*-Butyl 1'-(4-methoxybenzyl)-2'-oxospiro[azetidine-2,3'-indoline]-1-carboxylate (353)**

Conditions: Chiralpak IA column, 90:10 *n*-hexane:*i*-PrOH, flow rate: 1 mL min^{-1}, 35 ºC, UV detection wavelength: 254 nm

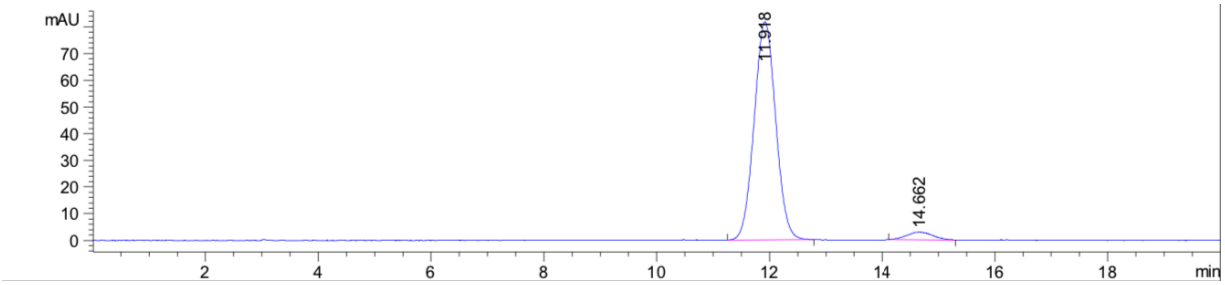
(±)–353





Peak #	Ret Time [min]	Type	Width [min]	Area [mAU*s]	Height [mAU]	Area %
1	12.004	BB	0.3849	944.28143	38.13831	49.3758
2	14.680	BB	0.4599	968.15479	32.09934	50.6242
Totals :				1912.43622	70.23765	

(–)–(*S*)–353

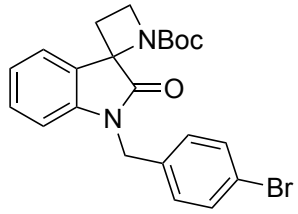


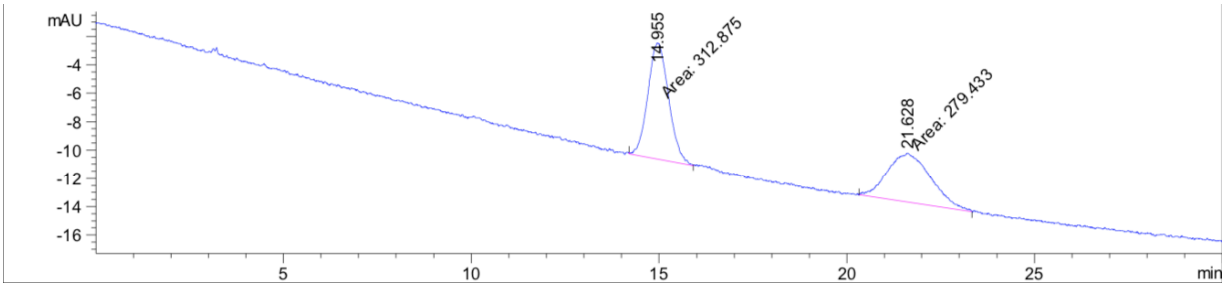
Peak #	Ret Time [min]	Type	Width [min]	Area [mAU*s]	Height [mAU]	Area %
1	11.918	BB	0.4158	2170.44214	81.73095	95.9089
2	14.662	BB	0.4039	92.58223	2.88870	4.0911
Totals :				2263.02437	84.61965	

***tert*-Butyl 1'-(4-bromobenzyl)-2'-oxospiro[azetidine-2,3'-indoline]-1-carboxylate (354)**

Conditions: Chiralpak ID column, 90:10 *n*-hexane:*i*-PrOH, flow rate: 1 mL min^{-1}, 35 ºC, UV detection wavelength: 254 nm

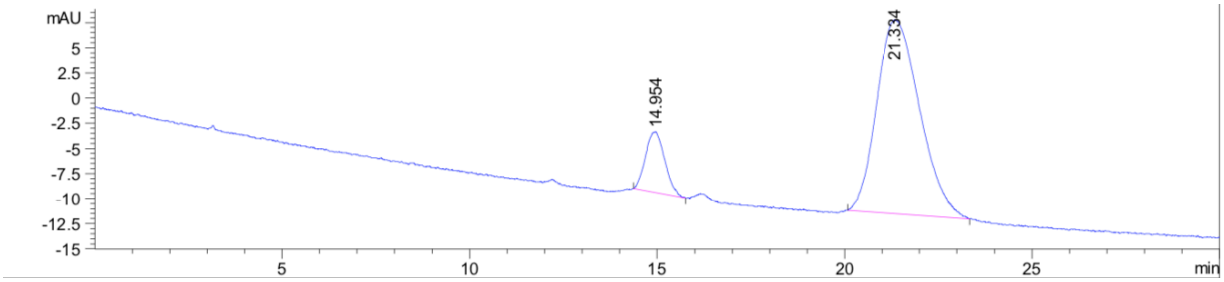
(±)–354





Peak #	Ret Time [min]	Type	Width [min]	Area [mAU*s]	Height [mAU]	Area %
1	14.955	MM	0.6401	312.87549	8.14698	52.8231
2	21.628	PP	1.3424	279.43311	3.46921	47.1769
Totals :				592.30859	11.61620	

(–)–(*S*)–354

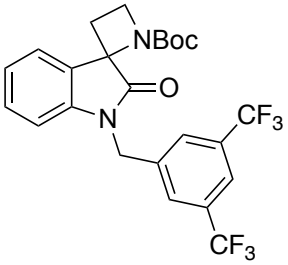


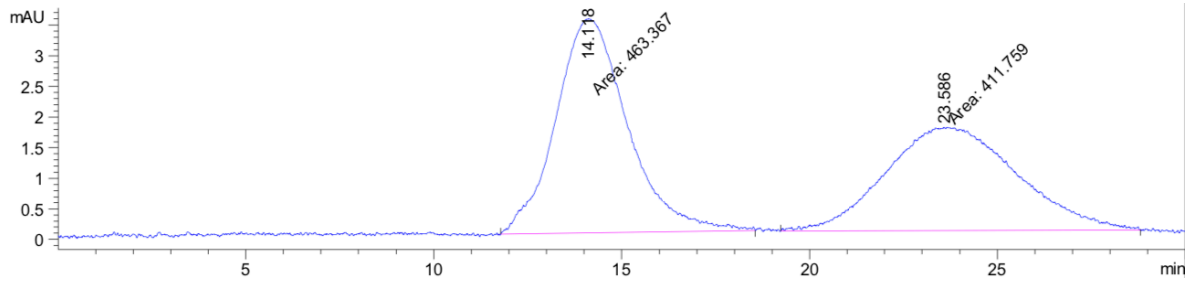
Peak #	Ret Time [min]	Type	Width [min]	Area [mAU*s]	Height [mAU]	Area %
1	14.954	BB	0.4303	215.12451	6.02916	12.2580
2	21.334	BB	0.9431	1539.85327	19.29395	87.7420
Totals :				1754.97778	25.32312	

***tert*-Butyl 1'-(3,5-bis(trifluoromethyl)benzyl)-2'-oxospiro[azetidine-2,3'-indoline]-1-carboxylate (356)**

Conditions: Chiralpak IC column, 98.5:1.5 *n*-hexane:*i*-PrOH, flow rate: 1 mL min^{-1}, 35 ºC, UV detection wavelength: 254 nm

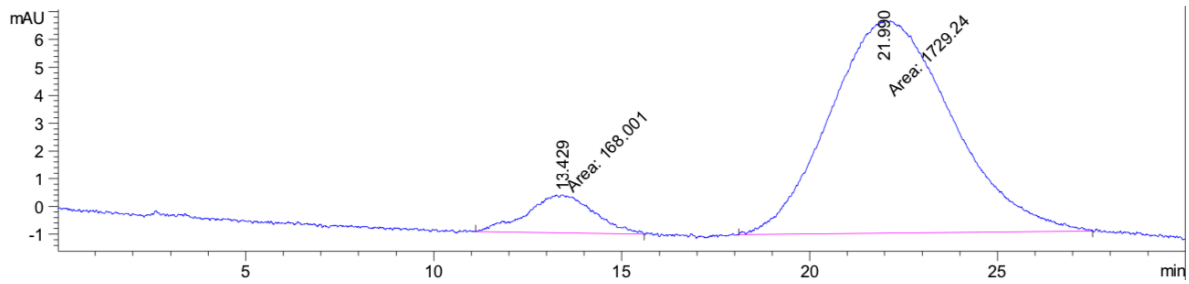
(±)–356





Peak #	Ret Time [min]	Type	Width [min]	Area [mAU*s]	Height [mAU]	Area %
1	14.118	PP	2.2116	463.36749	3.49198	52.9486
2	23.586	PM	4.0581	411.75876	1.69109	47.0514
Totals :				875.12625	5.18307	

(–)–(*S*)–356

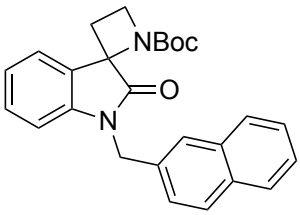


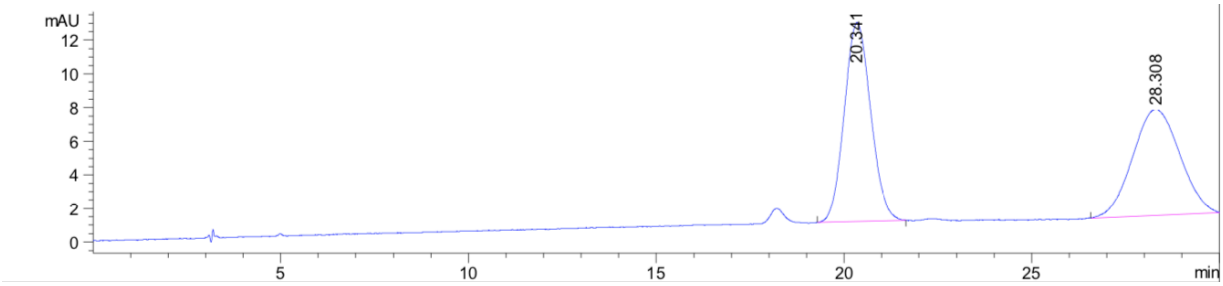
Peak #	Ret Time [min]	Type	Width [min]	Area [mAU*s]	Height [mAU]	Area %
1	13.429	MP	2.0608	168.00090	1.35869	8.8550
2	21.990	PP	3.7638	1729.23853	7.65734	91.1450
Totals :				1897.23943	9.01602	

***tert*-Butyl 1'-(naphthalen-2-ylmethyl)-2'-oxospiro[azetidine-2,3'-indoline]-1-carboxylate (357)**

Conditions: Chiralpak ID column, 90:10 *n*-hexane:*i*-PrOH, flow rate: 1 mL min^{-1}, 35 ºC, UV detection wavelength: 254 nm

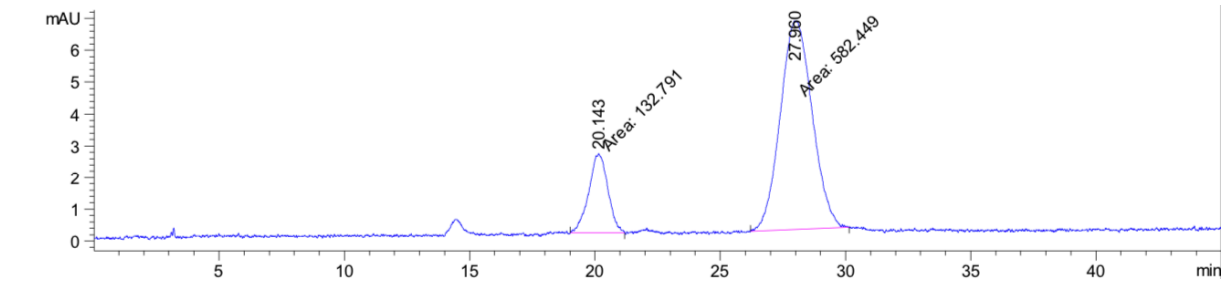
(±)–357





Peak #	Ret Time [min]	Type	Width [min]	Area [mAU*s]	Height [mAU]	Area %
1	20.341	BB	0.6875	545.33740	11.09324	51.2982
2	28.307	BBA	1.0254	517.73627	5.92523	48.7018
Totals :				1063.07367	17.01847	

(–)–(*S*)–357

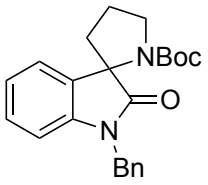


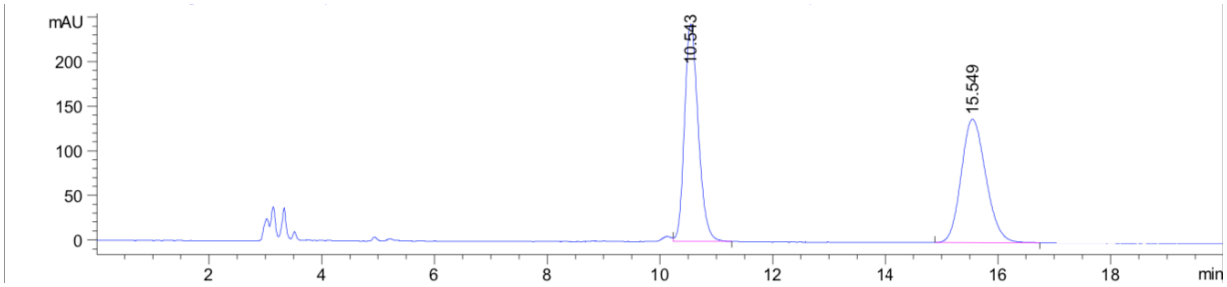
Peak #	Ret Time [min]	Type	Width [min]	Area [mAU*s]	Height [mAU]	Area %
1	20.143	PP	0.8829	132.79059	2.50682	18.5659
2	27.960	PP	1.4783	582.44928	6.56684	81.4341
Totals :				715.23987	9.07366	

tert-Butyl 1-benzyl-2-oxospiro[indoline-3,2'-pyrrolidine]-1'-carboxylate (360)

Conditions: Chiralpak ID column, 80:20 *n*-hexane:*i*-PrOH, flow rate: 1 mL min^{-1}, 35 ºC, UV detection wavelength: 254 nm

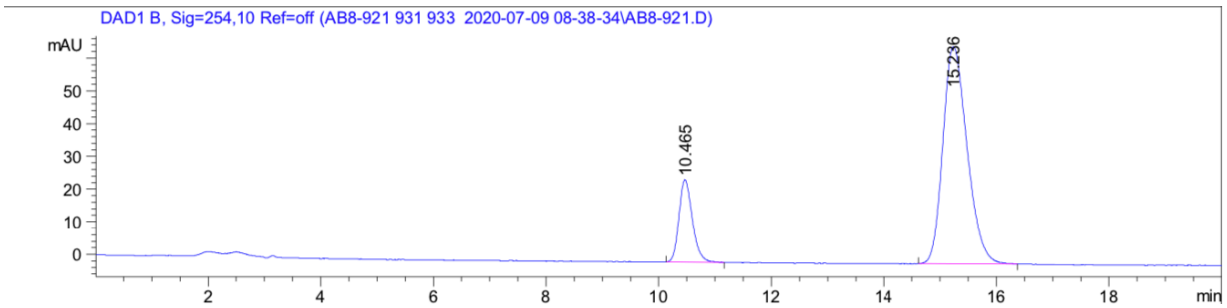
(±)–360





Peak #	Ret Time [min]	Type	Width [min]	Area [mAU*s]	Height [mAU]	Area %
1	10.543	VV	0.2634	4129.20264	244.09178	49.4999
2	15.549	BB	0.4605	4212.64063	138.63885	50.5001
Totals :				8341.84326	382.73064	

(–)–(*S*)–360



Peak #	Ret Time [min]	Type	Width [min]	Area [mAU*s]	Height [mAU]	Area %
1	10.465	BB	0.2553	416.95822	25.16654	17.3319
2	15.236	BB	0.4576	1988.76379	66.36789	82.6681
Totals :				2405.72202	91.53443	

7. Appendices

7.1 Literature Strategies for the Synthesis of Saturated Nitrogen Heterocycles

In this section exemplar synthetic strategies for the synthesis of 4- to 7-membered saturated nitrogen heterocycles are presented.

7.1.1 Azetidine Synthesis

Azetidines are interesting for medicinal chemistry but also due to their reactivity as their high ring strain, but relatively high stability, in certain protected forms, allows for interesting yet controlled reactivity (see Chapter 3). Traditional approaches to azetidines have extensively utilised cyclisation reactions, such as the reaction of a nucleophile with a bis-electrophile to form a 4-substituted azetidine. For example, Hillier treated 2-substituted-1,3-propanediols with triflic anhydride to form the bis-triflate which could be consequently attacked by an amine to form the 3-substituted azetidine.[472] Another approach to azetidines is *via* reduction of azetidin-2-ones which are more commonly accessed.[161,473]

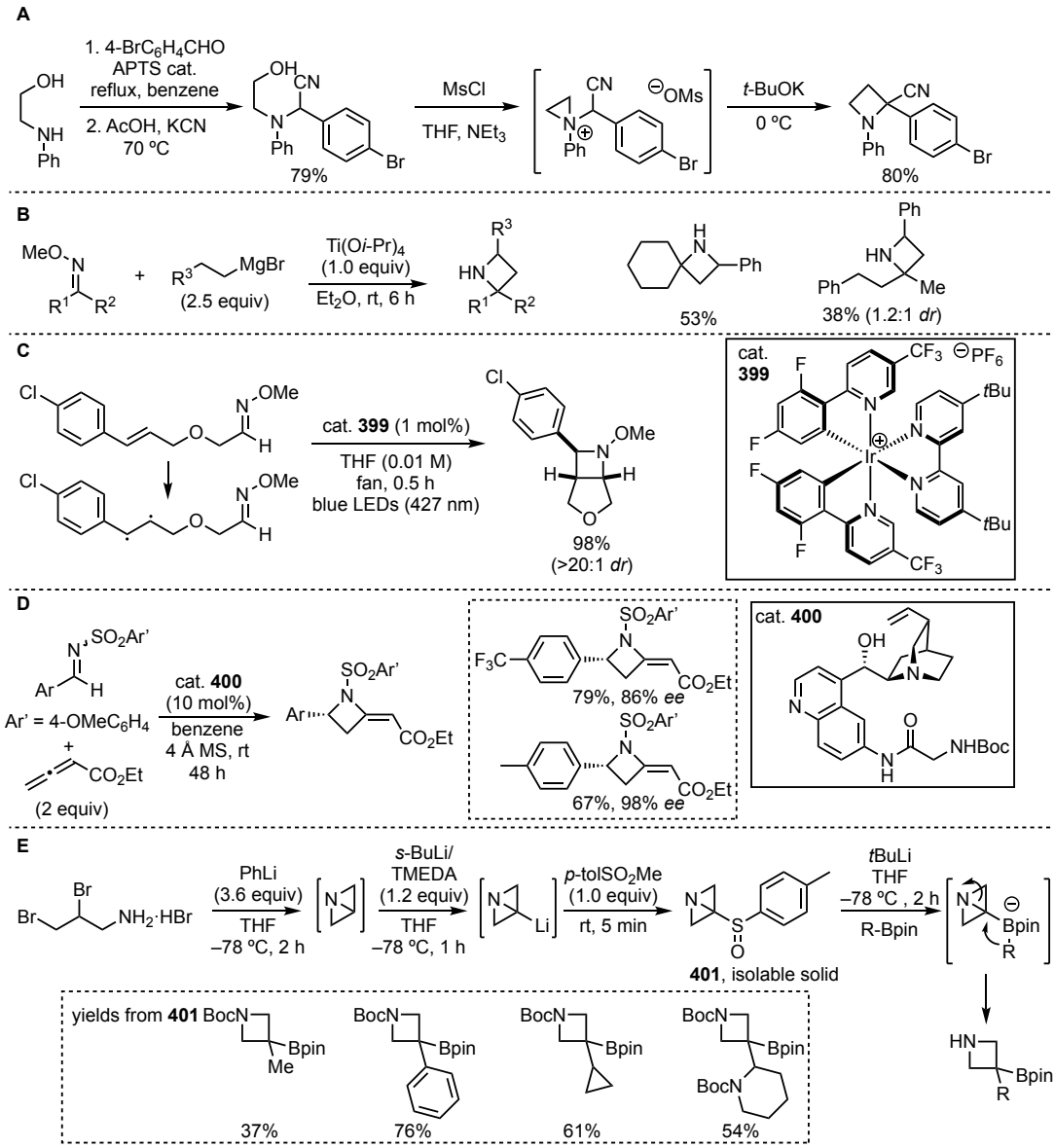
Couty has reported a reliable cyclisation methodology relying on an anionic ring closure, which was used by Marcaurelle and co-workers in a DOS strategy (see Scheme 102).[474] An example of this methodology is given in Scheme 102A.[475] Fossey described an iodocyclisation to 2,4-disubstituted azetidines in a diastereoselective reaction from homoallyl amines.[476,477] The iodomethyl substituted azetidines were found to be thermally unstable to ring expansion but could be trapped with a nucleophile i.e. an amine to form stable *cis*-azetidine products. Kürti showed that Grignard reagents reacted with oxime ethers in a Kulinkovich-type mechanism to afford unprotected azetidine products (Scheme 102B).[478]

The Paternò-Büchi reaction is the photochemically allowed cycloaddition of an alkene with a carbonyl to afford an oxetane product.[479] In this reaction the photoexcitation of the carbonyl group generates the singlet state radical which followed by intersystem crossing to the triplet state radical can react with the C=C double bond. In order to apply this reaction to imine cycloaddition, in an *aza*-Paternò-Büchi reaction, the key challenge is to overcome the lack of photoreactivity of imines.[480] This lower reactivity is due to alternative relaxation pathways, including through imine isomerisation upon excitation from the ground state.[481] Maruoka has used *N*-tosyl imines to undergo [2+2]-cycloaddition with alkenes, albeit with limited scope due to the narrow requirements for the imine precursor.[482] Sivagaru developed an enantioselective *aza*-Paternò-Buchi reaction using an enamide which could be excited to the triplet state using a xanthone sensitiser.[483] Schindler and co-workers have recently reported a visible light mediated intramolecular *aza*-Paternò-Buchi reaction between alkenes and oximes.[484] Similar

to the work by Sivagaru, Schindler's reaction relies on the selective activation of the alkene (over the imine) to a triplet excited state to then undergo [2+2]-cycloaddition (Scheme 102C).

Further advances have been made in [2+2]-cycloaddition using DABCO for a Baylis–Hillmann type reaction of allenes and imines[485] or *cinchona*-alkaloid derived catalysts for enantioselective synthesis of azetidines or β-lactams.[486,487] A notable example of this type of [2+2]-cycloaddition is the use of *cinchona* alkaloid derivative **400** as a nucleophilic catalyst to promote the enantioselective cyclisation of *N*-tosylimines and allenoates by Zhu (Scheme 102D).[488]

Another approach to diverse azetidines is through direct functionalisation of intact azetidines. This may be *via* C–H arylation[177], Friedel–Crafts reactions[489] or through development of novel cross-coupling methodologies.[490] Luisi has studied the lithiation of α-aryl azetidines and found that when using an electron withdrawing *N*-substituent (Boc) α-lithiation occurred, allowing α-functionalisation through electrophile trapping.[491] Use of an electron donating *N*-substituent (Me) led to preferred *ortho*-lithiation of the α-aryl substituent.[492] More recently, Luisi reported the α-lithiation of azetidine borane complexes.[493] 2,2-Disubstituted azetidines can also be made through a Sommelet–Hauser rearrangement of azetidinium ions upon treatment with base.[494] Aggarwal has reported the synthesis of sulfoxide **401** as a stable crystalline solid which can undergo sulfoxide-Li exchange forming lithiated azabicyclopropane (Scheme 102E).[495] Reaction with a boronate ester followed by 1,2-rearrangement, driven by release of ring strain, afforded 3,3-disubstituted azetidines, with a boron substituent for further diversification.



Scheme 102: Selected examples of modern azetidine synthesis. APTS = 1,3,6-pyrenetrisulfonic acid.

7.1.2 Pyrrolidine Synthesis

The range of available synthetic methodologies to access diverse pyrrolidines is much more explored than for azetidines. The diverse range of cyclisation methodologies is likely due to the greater ease of cyclisation vs. the four-membered analogue. Ring closure to afford a five-membered ring does not suffer from the same enthalpic cost of forming the strained four-membered ring and does not have a significant entropic cost as with larger ring sizes. Consequently, ring closure to afford the pyrrolidine ring will be selective, in cases where other ring sizes may also be formed.

[3+2]-Cycloaddition of an azomethine ylide (derived from an imine) and an alkene is now a mature method to access multi-substituted pyrrolidines.[496] This method has recently been employed on scale by Abbvie to a cystic fibrosis transmembrane receptor protein modulator

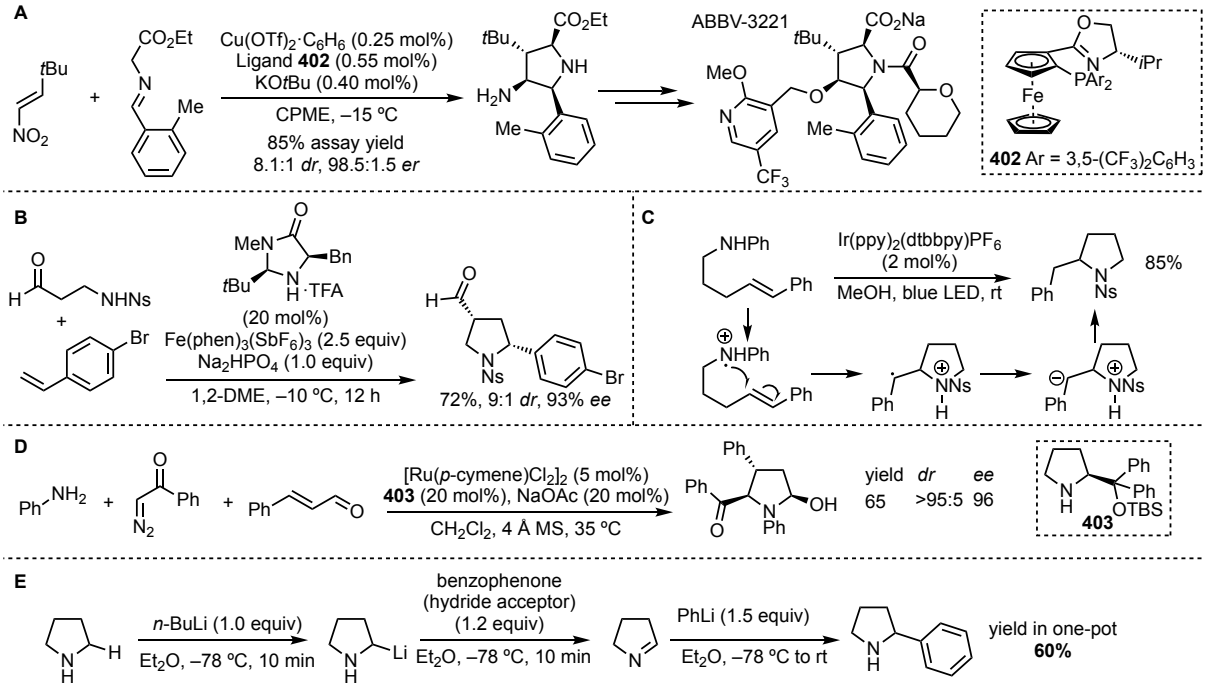
ABBV-3221 (Scheme 103A).[497] MacMillan showed that aldehydes β-amino aldehydes could be coupled with olefins using iminium catalysis in a SOMO-activated enantioselective [3+2]-cycloaddition (Scheme 103B). Related to [3+2]-cycloaddition are *aza*-Cope rearrangements as developed initially by Overman towards pyrrolidine synthesis.[498]

Another method for pyrrolidine synthesis which has been extensively explored is hydroamination, whereby an amine reacts directly with an alkene or alkyne.[499] Widenhoefer and Hartwig developed gold, platinum and rhodium catalysis to move away from rare-earth metal catalysts.[500,501] Ackermann then showed that Lewis or Brønsted acids could promote the reaction, and showed an enantioselective variant using a chiral phosphoric acid, albeit in low *ee*.[502] Since 2011, significant advances have been made in enantioselective hydroamination reactions to pyrrolidines.[503] Knowles has disclosed a photoredox catalysed hydroamination (Scheme 103C).[504] Related transformations involve nucleopalladation followed by intramolecular amination and either nucleophilic displacement or oxidation.[505]

A useful method to pyrrolidines is cycloisomerisation whereby dienes or enynes can be coupled together,[506] this includes recent electrochemical enyne cyclisation.[507] Other methods which proceed through ring closure include intramolecular reductive amination,[508] Ugi multicomponent reactions[509] or iodocyclisation.[510] Intramolecular C(sp^3)–H amination is a well-precedented method to access pyrrolidines.[511] Muñiz has developed an I_2-catalysed Hofmann–Löffler reaction using an equivalent of a hypervalent iodine oxidant using visible light or a photoredox catalyst.[512] Direct C(sp^3)–H amination has also been achieved using transition metal catalysis.[513] C–H insertion of nitrenes (from azides)[514,515] or carbenes (from diazo compounds, *N*-tosylhydrazones or triazoles) is also an established method.[516] Lacour synthesised 2,2-disubstituted pyrrolidines from 2-pyrrolidinones by reaction with diazo compounds, followed by a 1,2-acyl shift, in the presence of a copper catalyst.[517] Hu recently showed an enantioselective three-component coupling to form 2,3,5-trisubstituted pyrrolidines from diazo compounds, anilines and α,β-unsaturated aldehydes (Scheme 103D).[518]

Recently, significant advances have been made in the functionalisation of intact pyrrolidines.[519] In particular MacMillan has developed numerous photoredox approaches for the α-functionalisation of pyrrolidines by vinylation or arylation.[520,521] These advances in photoredox approaches has been concurrent with advances in metal-catalysed C–H activation[522] as well as electrochemical approaches.[523] Fu has developed enantioconvergent cross-couplings of alkyl-zinc reagents with electrophiles (lithiation of the 2-position is discussed in Section 2.2).[524] A significant advance in pyrrolidine functionalisation was made recently by Seidel where unprotected pyrrolidines could be arylated at the 2-position *via* an cyclic imine intermediate (Scheme 103E). Many of these functionalisation approaches are flexible in ring

size and can, for example, be applied to piperidine rings due to the similar proximity and reactivity of the α-C–H bond.



Scheme 103: Selected modern methods for pyrrolidine synthesis and functionalisation.

7.1.3 Piperidine Synthesis

Many of the synthetic methodologies designed for pyrrolidine synthesis can be extended for the synthesis of piperidines, in particular functionalisation methodologies. This is due to the low enthalpic cost upon six-membered ring formation and variable entropic cost. In some circumstances 6-membered rings may be formed by ring closure in a similar fashion to pyrrolidines.[525] However, there are circumstances where 6-membered ring formation is not favourable due to a high entropic barrier and there are even examples where 4-membered ring formation can occur preferentially.[526]

One route to piperidines that is relatively unexplored for pyrrolidine synthesis is hydrogenation.[527] Glorius and Charette have reported efficient asymmetric hydrogenation methods of pyridines.[528] Qu showed that pyridinium salts could be hydrogenated using an Ir catalytic system (Scheme 104A).[529] More recently Glorius generated fluorinated piperidines through asymmetric hydrogenation employing a Rh catalyst and HBpin (Scheme 104B).[530]

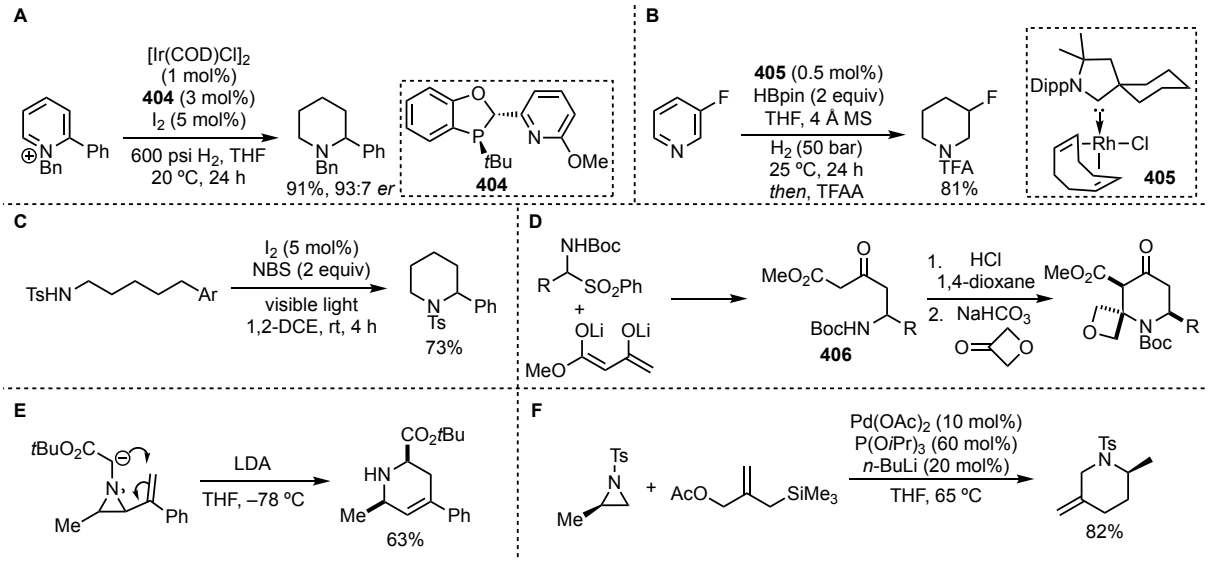
Muñiz has demonstrated that C(sp^3)–H amination using I_2 under visible light can be applied for ring closure to piperidines as well as pyrrolidines (ref 512).[531] By generation of the benzylic radical (weakest C–H bond) preferentially, the 1,5-HAT mechanism could be overridden (Scheme 104C). de Bruin was able to use a similar strategy to cause six-membered ring formation in a Co-catalysed carbene formation.[532] Building on prior work to synthesise 5-

membered rings,[516d] Sun showed that allenes (from combination of carbenes with alkynes) would undergo intramolecular cyclisation to piperidines.[533] Liu has shown that alkyl-Heck reactions can be utilised in a selective 6-*endo*-*trig* ring closure *via* a radical pathway.[534] Clarke has shown that 2-spiropiperidines can be generated in a modular fashion through synthesis of an intermediate **406** followed by ring closure (Scheme 104D).[535]

A classical approach to piperidines is nucleophilic displacement of a bis-electrophile.[536] A more sophisticated alternative is Ir-catalysed *in situ* oxidation of an appropriate diol to the aldehyde in order to react with an amine ultimately forming a piperidine product.[537] Hydroamination towards piperidine products can represent a challenge in favouring anti-Markovnikov 6-*endo*-trig cyclisation over Markovnikov 5-*exo*-trig cyclisation. Hartwig was able to form piperidines in a 6-*endo*-trig cyclisation selectively using a Rh catalyst.[538] Since Hartwig's publication, there have been many reports synthesising piperidines by reacting amines with alkenes in an intramolecular cyclisation.[539]

Cycloaddition or annulation reactions are another common route to multisubstituted piperidines. [3+3]-, [4+2]- and [5+1]-cycloadditions or annulations have all been reported.[540] Ring expansion on pyrrolidine-fused aziridinium ylides can form piperidines.[541] The ring expansion of aziridines has been exploited by Coldham in a 3,2-sigmatropic rearrangement (Scheme 104E).[542] Harrity developed a [3+3]-cycloaddition harnessing the ring strain of aziridines (Scheme 104F).[543]

As stated many of the functionalisation reactions applied to pyrrolidines can be applied the six-membered analogue. C–H Activation has been applied to functionalise at diverse positions in piperidines.[170] Of note, is the C4-arylation of piperidines using a directing group on the nitrogen atom by Sanford.[544] Another route to functionalise piperidines includes Suzuki–Miyaura cross-coupling of a vinyl boronate followed by hydrogenation.[545]



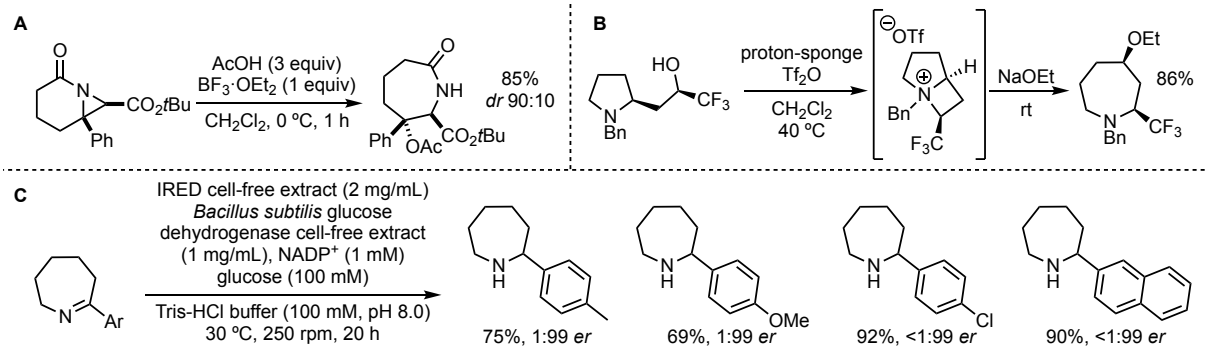
Scheme 104: Selected modern methods for piperidine synthesis.

7.1.4 Azepane Synthesis

As seven-membered analogues of the previously discussed saturated heterocycles, azepanes are much less common and there are fewer procedures for their synthesis. Due to the much lower relative rate of ring closure compared to 4–6-membered rings, 7-membered rings are often synthesised through rearrangement or ring expansion sequences.227

Ring expansion of bicyclic systems has recently been adopted to access these 7-membered rings.[546] Cossy has shown that azabicyclic systems such as **407** will ring open regioselectively *via* the aziridinium ion under acidic conditions to form 7-membered rings (Scheme 105A).[546a] Couty and Cossy have shown that ring expansion of pyrrolidines *via* bicyclic azetidinium ions can form azepanes (Scheme 105B).[547] Another common route to azepanes is by Schmidt rearrangement of six-membered cyclic ketones followed by reduction of the formed azepanone.[548] Moody has performed a similar 6- to 7-membered ring expansion using ethyl diazoacetate and $BF_3 \cdot OEt_2$.[411]

Cyclisation strategies include ring-closing metathesis[549], silyl-*aza*-Prins cyclisation[550] and reductive amination.[551] Another route to azepanes is reduction of the corresponding cyclic imine.[552] However, due to the entropic barrier to cyclisation the equilibrium for cyclised imine versus uncyclised amine lies towards the uncyclised starting material. One approach around this is distillation to drive the equilibrium to the cyclised imine *via* azeotropic removal of water.[552] Turner and Clayden showed that enzyme catalysed reduction of the imine *in situ* could be used to drive the equilibrium towards product (Scheme 105C).[553]

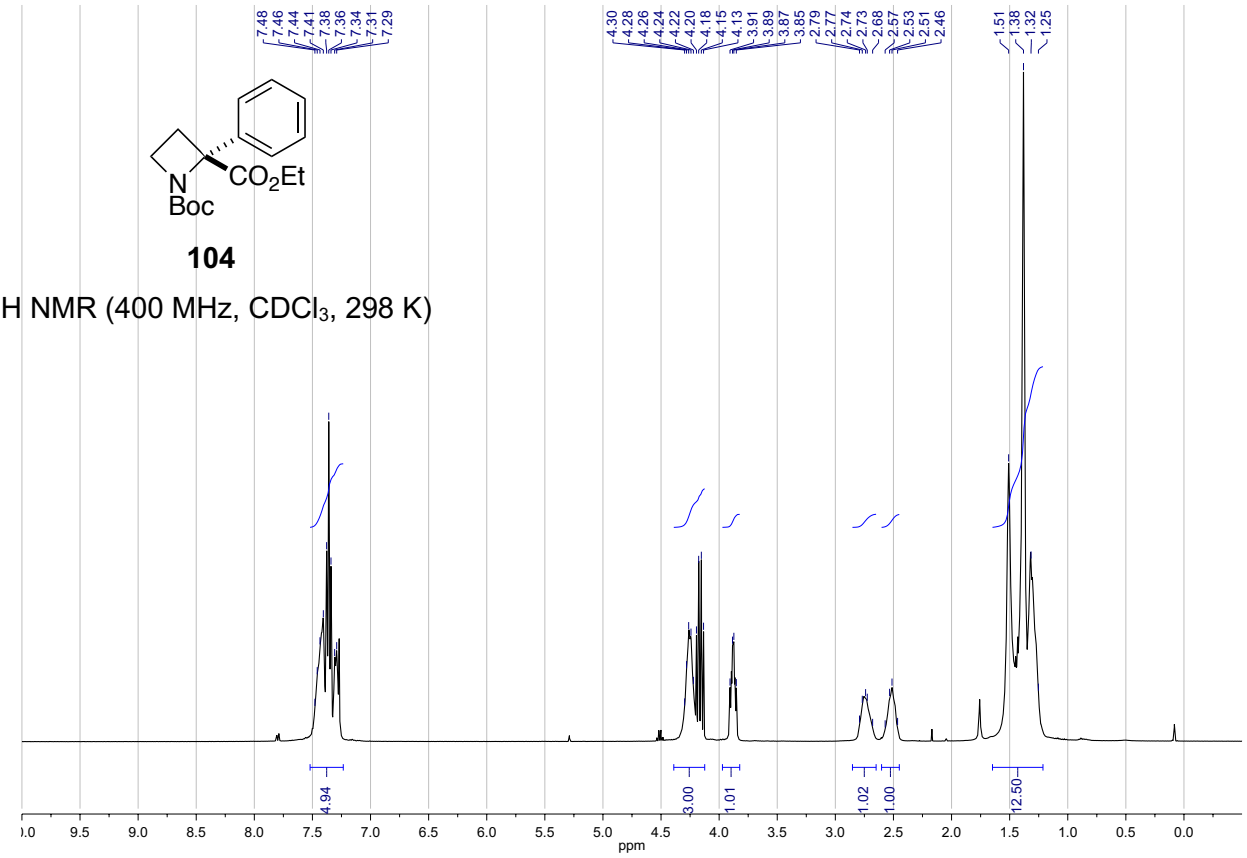


Scheme 105: Selected modern methods for azepane synthesis. Proton sponge = 1,8-bis(dimethylamino)naphthalene.

7.2 Representative NMR Spectra

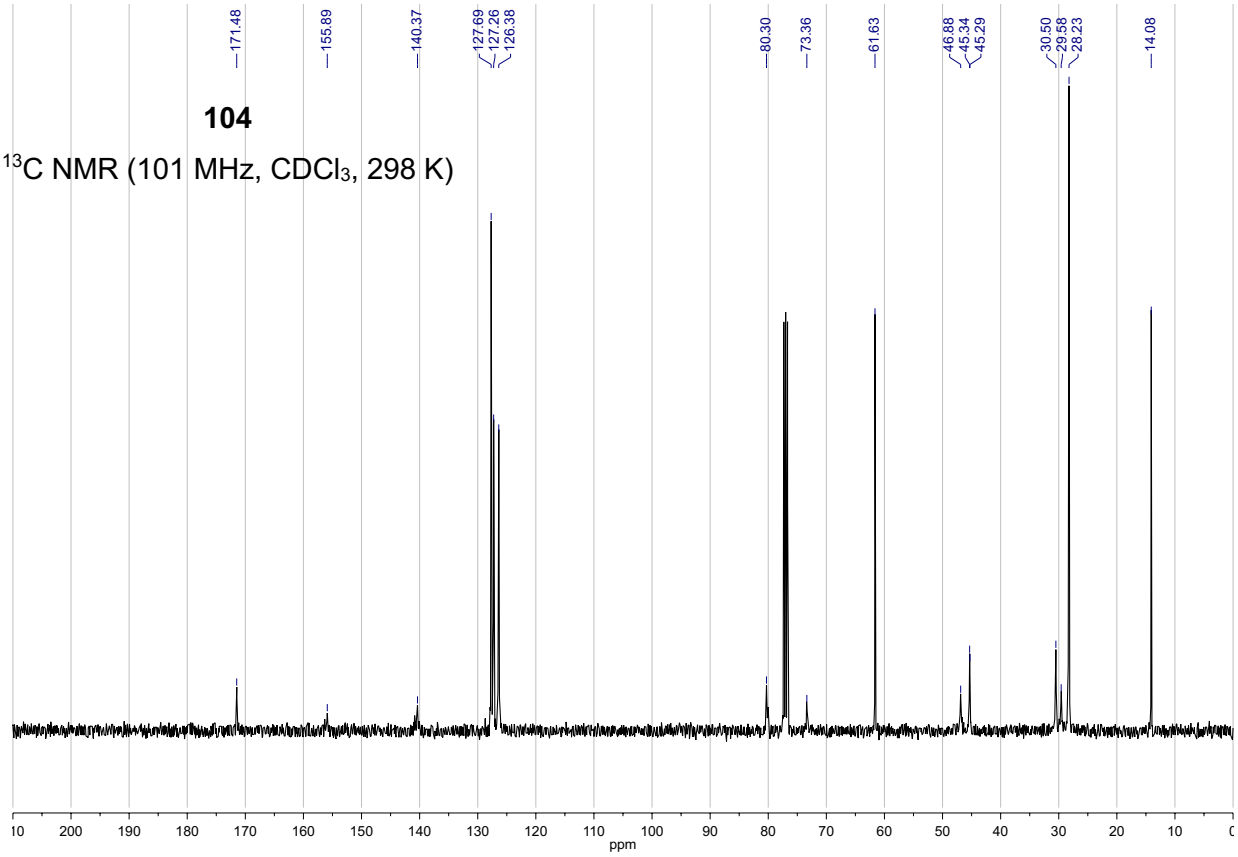
104

^{1}H NMR (400 MHz, $CDCl_3$, 298 K)



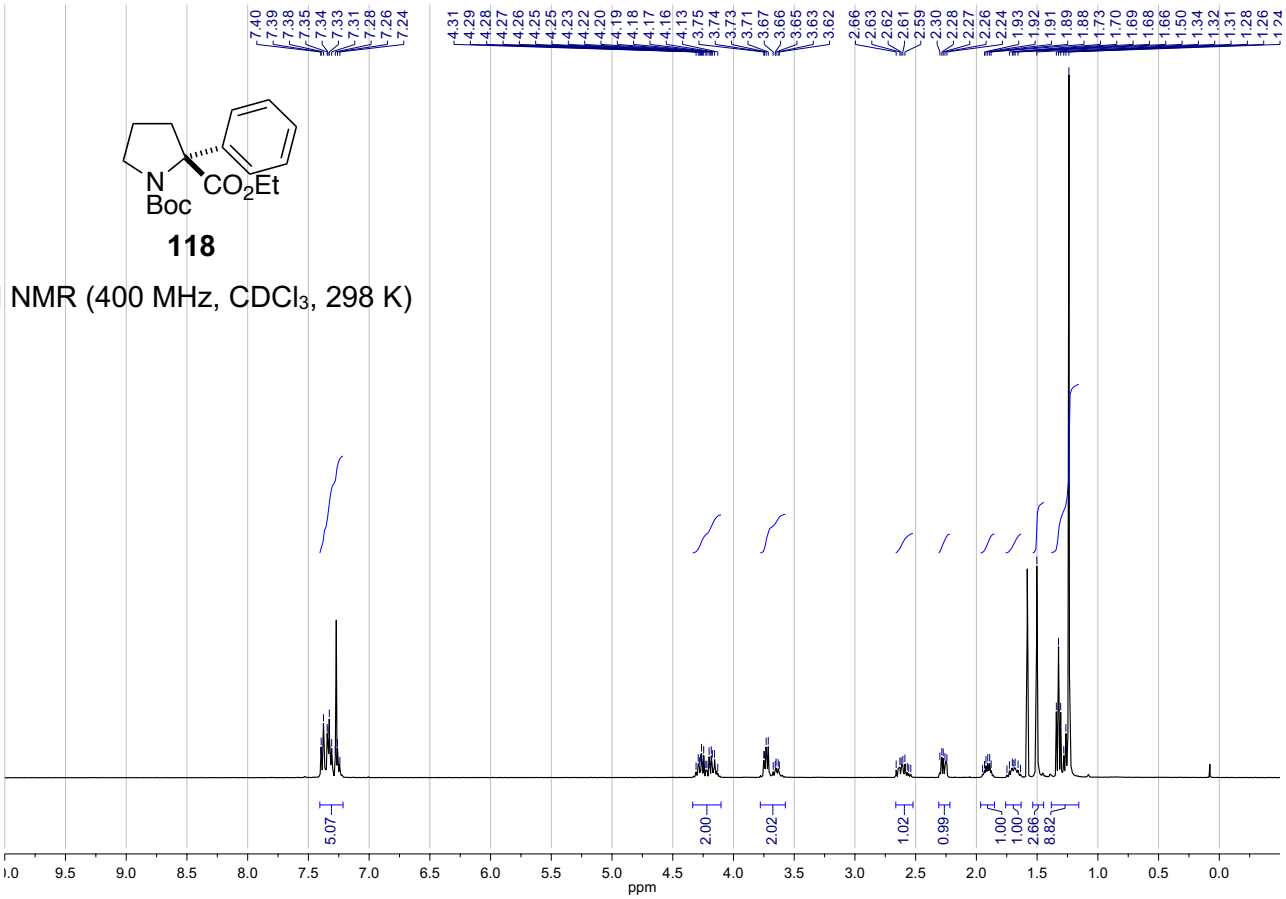
104

^{13}C NMR (101 MHz, $CDCl_3$, 298 K)



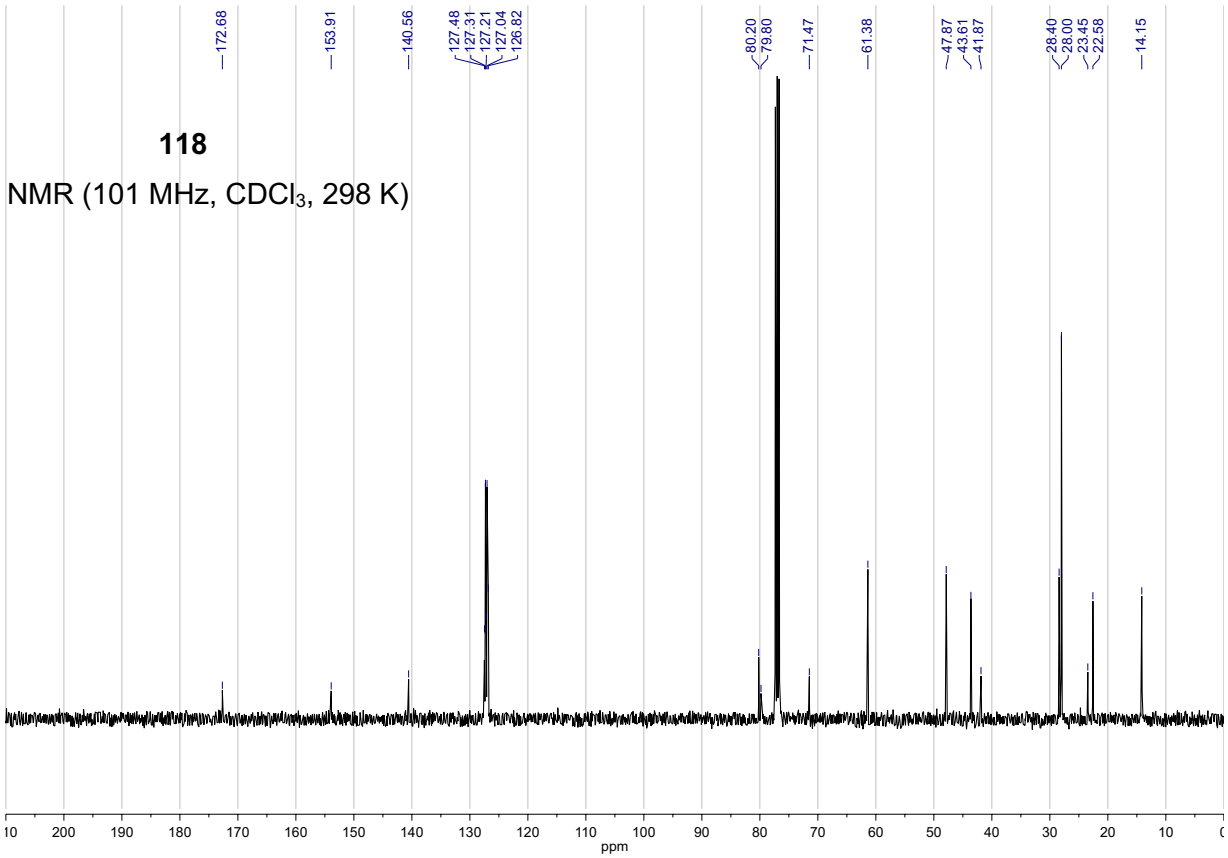
118

^{1}H NMR (400 MHz, $CDCl_3$, 298 K)



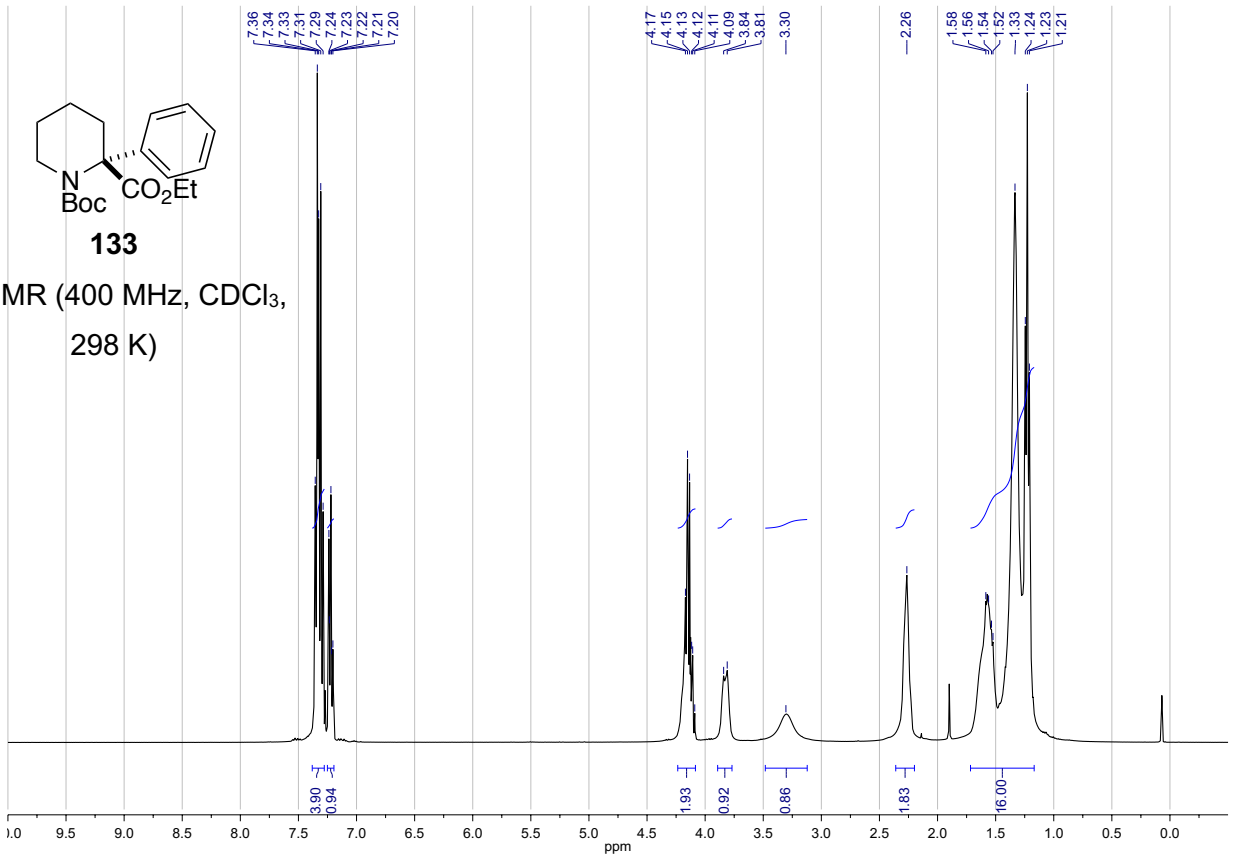
118

^{13}C NMR (101 MHz, $CDCl_3$, 298 K)



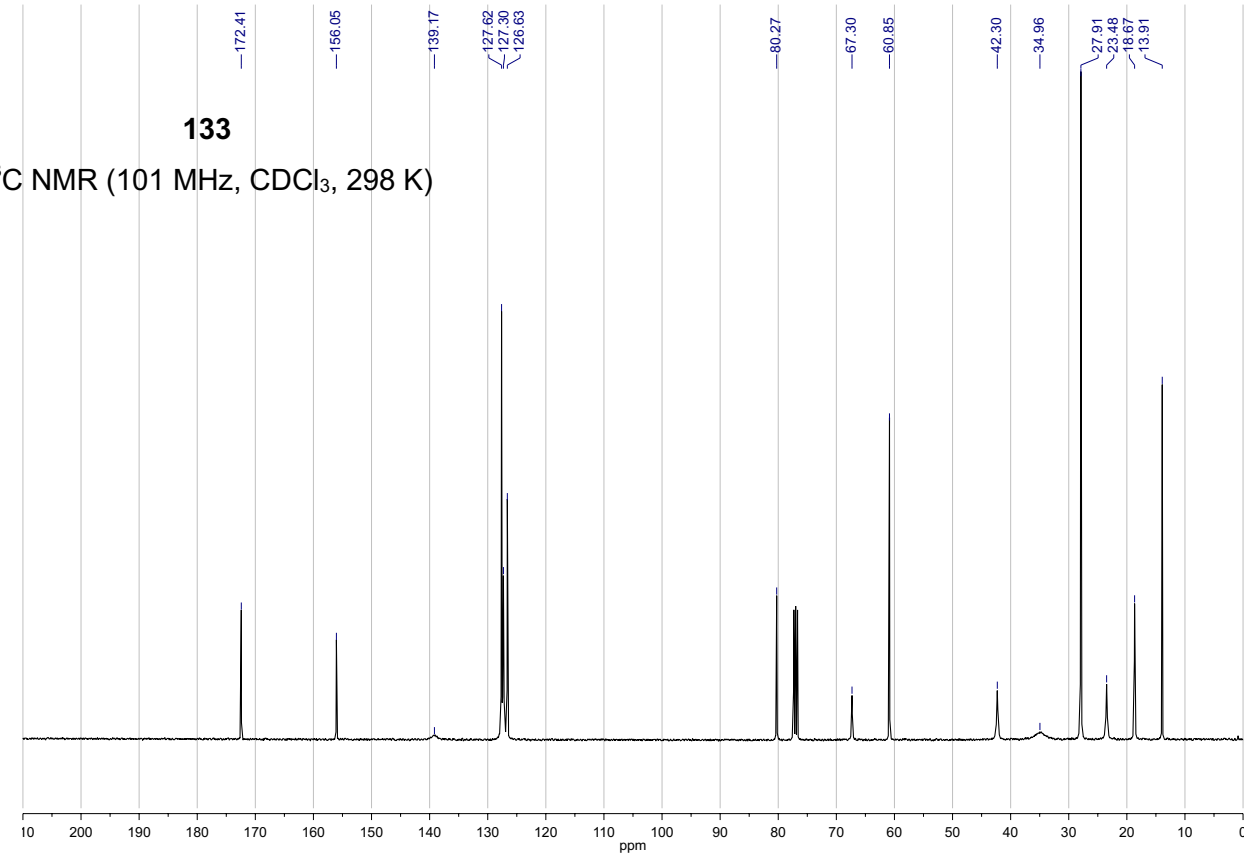
133

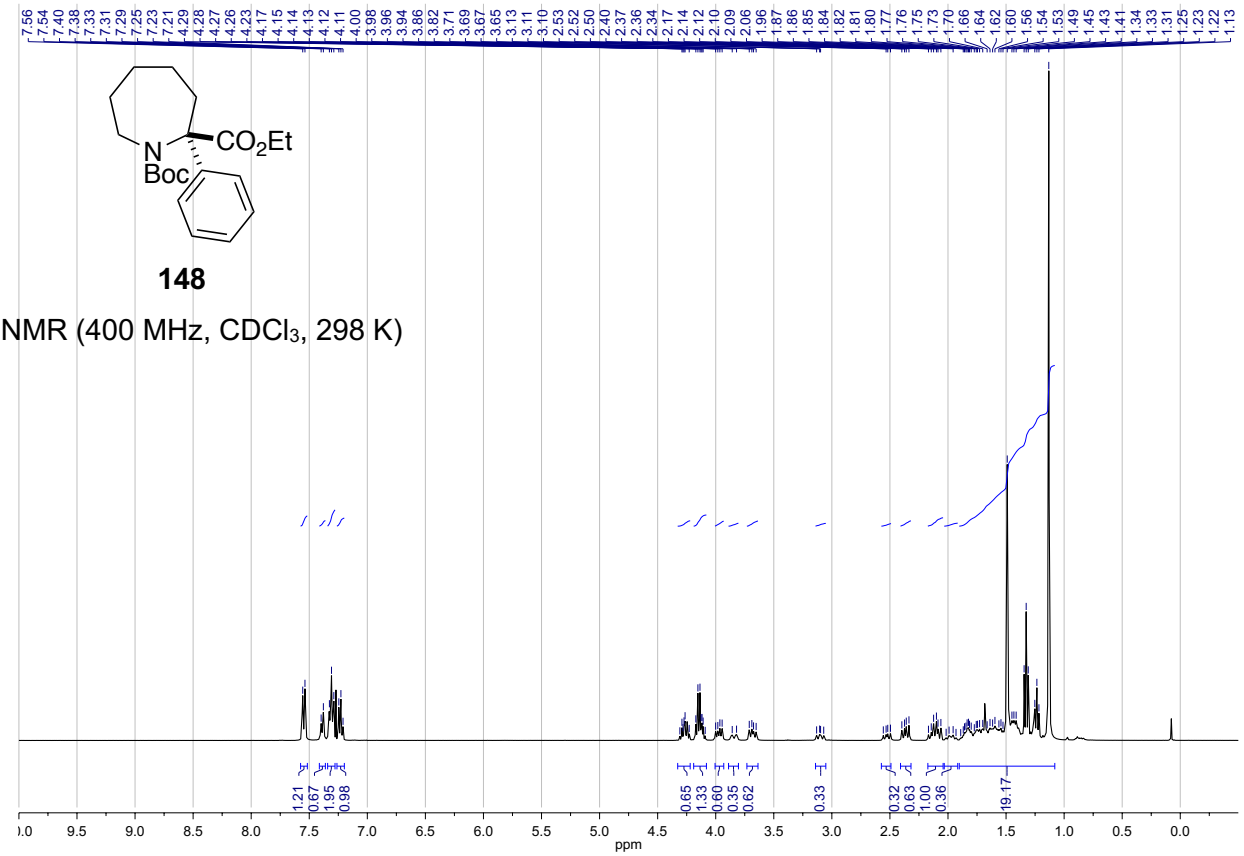
^{1}H NMR (400 MHz, $CDCl_3$, 298 K)



133

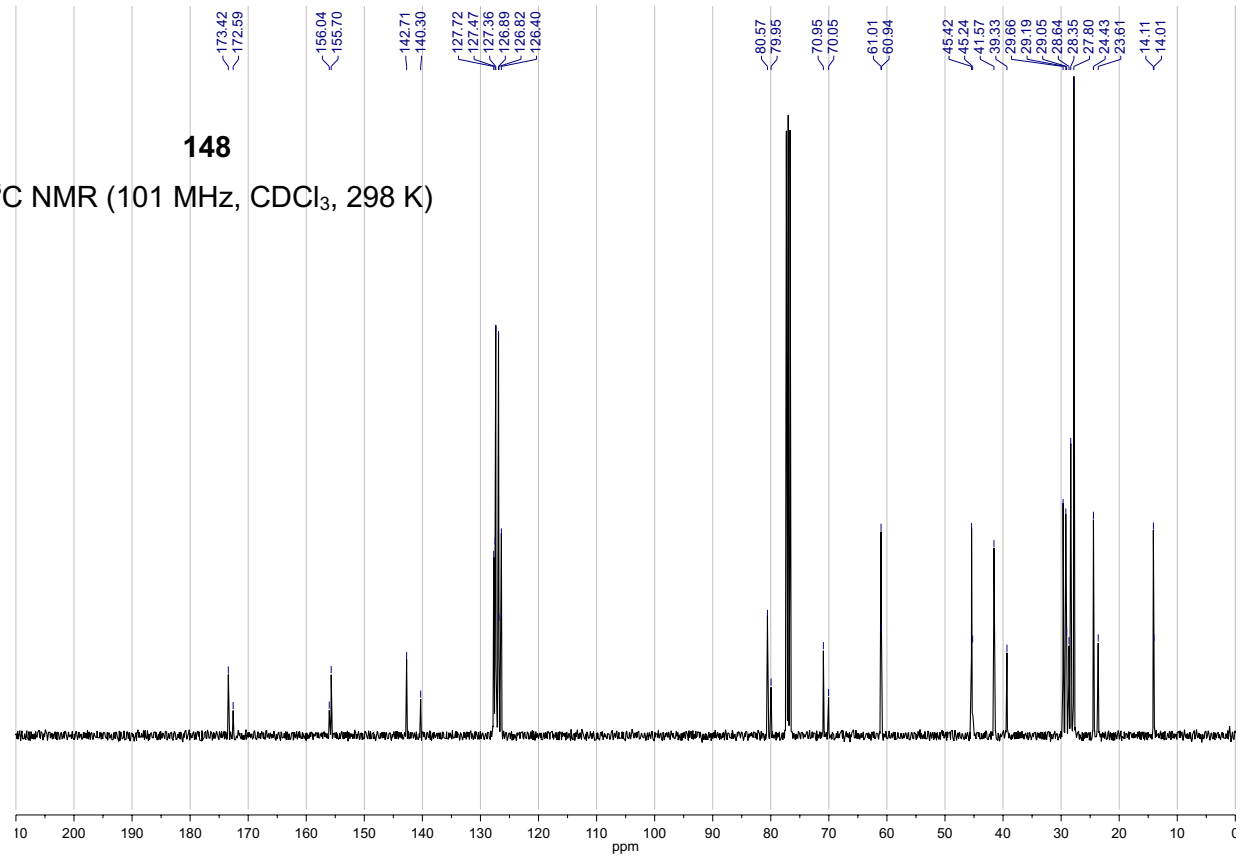
^{13}C NMR (101 MHz, $CDCl_3$, 298 K)





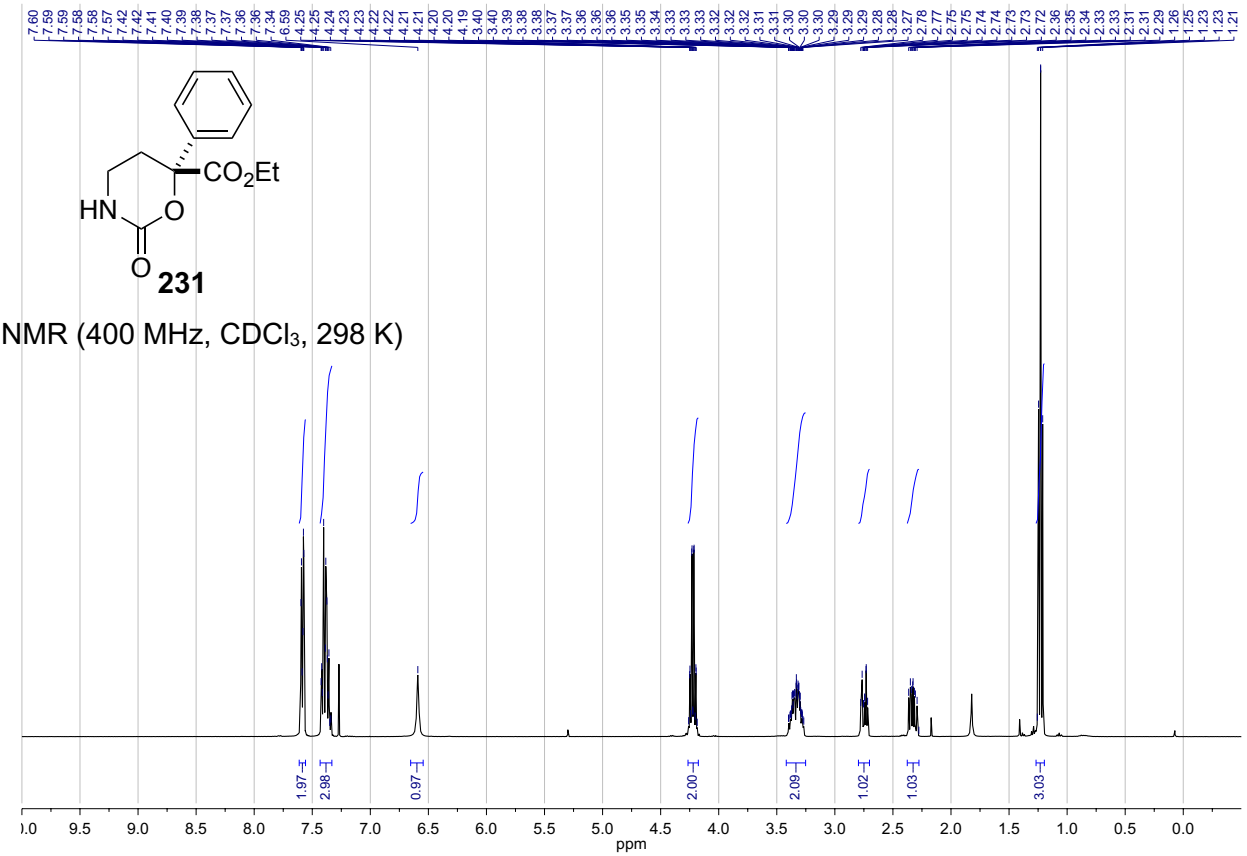
148

^{1}H NMR (400 MHz, $CDCl_3$, 298 K)

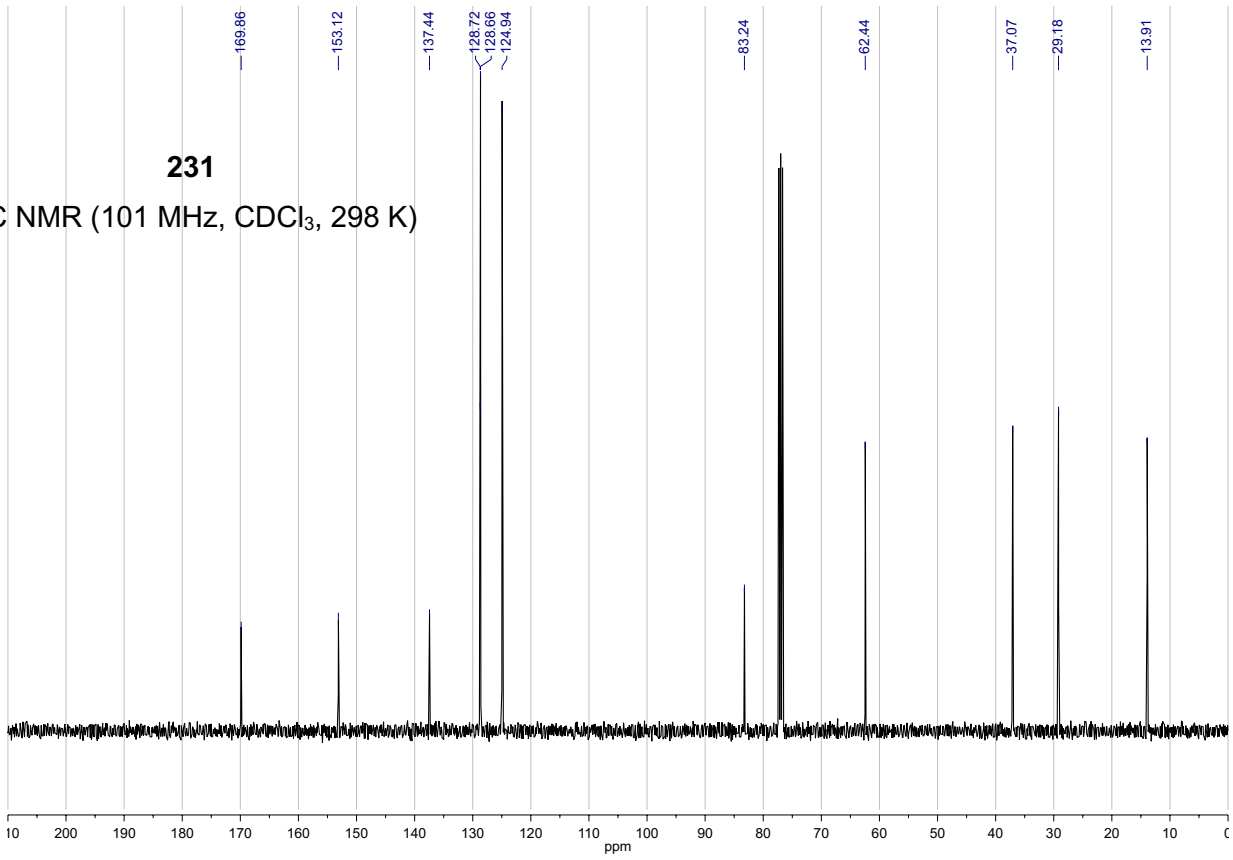


148

^{13}C NMR (101 MHz, $CDCl_3$, 298 K)

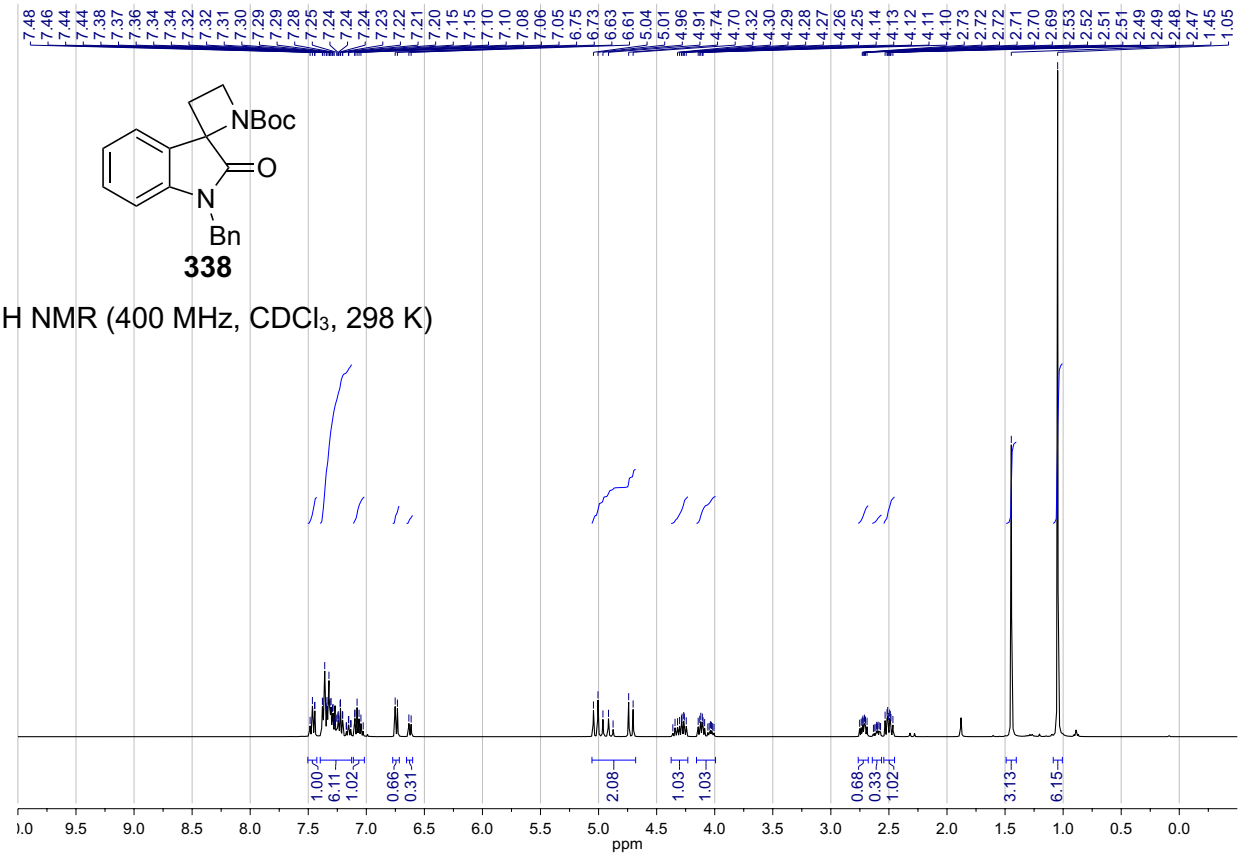


^{1}H NMR (400 MHz, $CDCl_3$, 298 K)



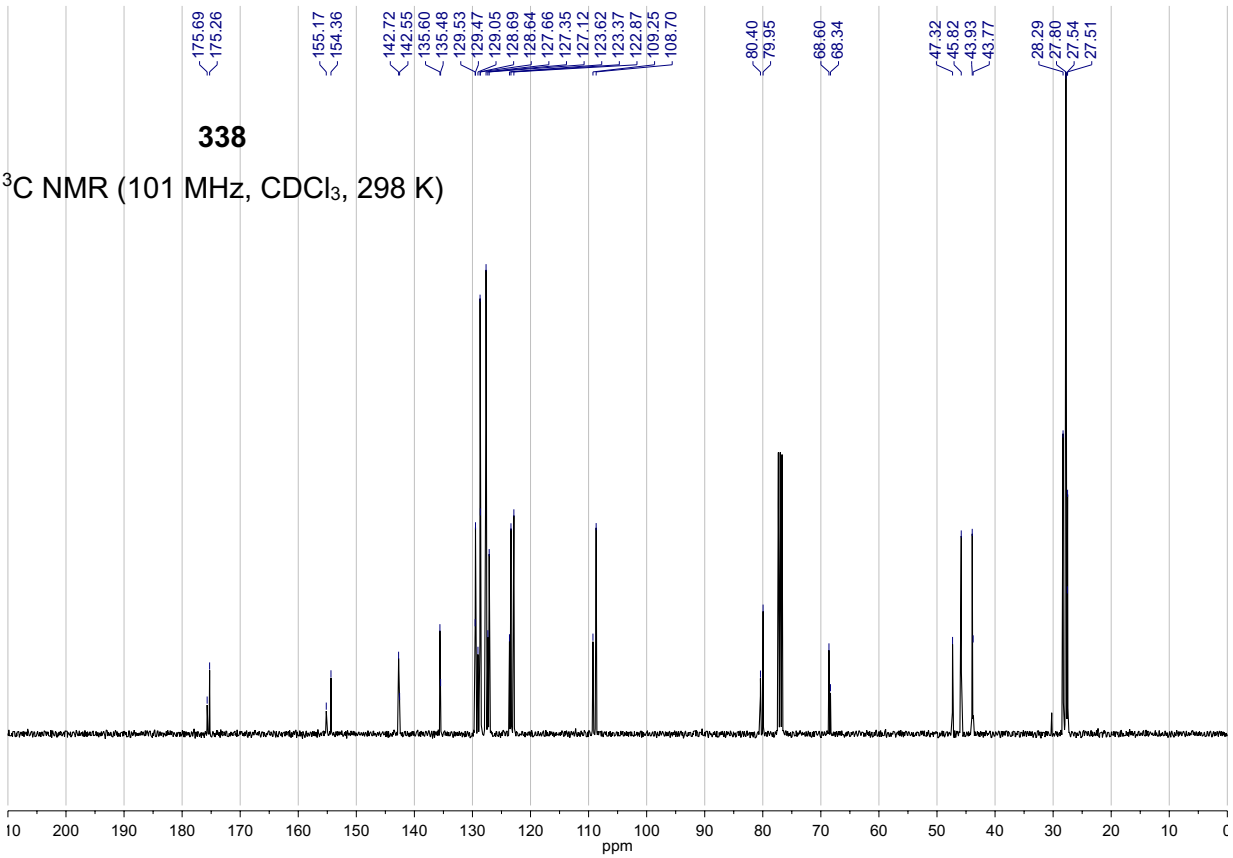
231

^{13}C NMR (101 MHz, $CDCl_3$, 298 K)



338

^{1}H NMR (400 MHz, $CDCl_3$, 298 K)

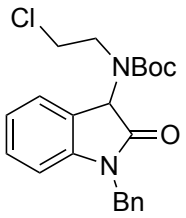


338

^{13}C NMR (101 MHz, $CDCl_3$, 298 K)

7.3 X-Ray Crystal Structure Data

(±)–*tert*-Butyl (1-benzyl-2-oxoindolin-3-yl)(2-chloroethyl)carbamate (312)



Identification code	JAB2001
Formula	C22 H25 Cl N2 O3
Formula weight	400.89
Temperature	173(2) K
Diffractometer, wavelength	Agilent Xcalibur 3 E, 0.71073 Å
Crystal system, space group	Monoclinic, $P2_1/c$
Unit cell dimensions	a = 9.4777(4) Å α = 90°
	b = 9.8446(4) Å β = 95.696(4)°
	c = 22.6335(9) Å γ = 90°
Volume, Z	2101.37(14) $Å^3$, 4
Density (calculated)	1.267 Mg/m^3
Absorption coefficient	0.206 mm^{-1}
F(000)	848
Crystal colour / morphology	Colourless blocks
Crystal size	0.519 x 0.374 x 0.288 mm^3
θ range for data collection	2.676 to 28.237°
Index ranges	-10<=h<=12, -8<=k<=12, -20<=l<=29
Reflns collected / unique	6956 / 4203 [R(int) = 0.0218]
Reflns observed [F>4σ(F)]	2959
Absorption correction	Analytical
Max. and min. transmission	0.962 and 0.941
Refinement method	Full-matrix least-squares on F^2
Data / restraints / parameters	4203 / 55 / 271
Goodness-of-fit on F^2	1.045
Final R indices [F>4σ(F)]	R1 = 0.0455, wR2 = 0.0939
R indices (all data)	R1 = 0.0745, wR2 = 0.1102
Largest diff. peak, hole	0.234, -0.383 $eÅ^{-3}$
Mean and maximum shift/error	0.000 and 0.000

Bond lengths [Å] and angles [°] for JAB2001.

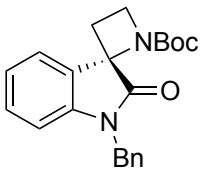
N(1)-C(2)	1.370(2)
N(1)-C(9)	1.411(2)

N(1)-C(10)	1.445(2)
C(2)-O(2)	1.215(2)
C(2)-C(3)	1.539(3)
C(3)-N(17)	1.454(2)
C(3)-C(4)	1.507(2)
C(4)-C(5)	1.375(3)
C(4)-C(9)	1.388(2)
C(5)-C(6)	1.390(3)
C(6)-C(7)	1.379(3)
C(7)-C(8)	1.393(3)
C(8)-C(9)	1.379(2)
C(10)-C(11)	1.508(2)
C(11)-C(16)	1.380(3)
C(11)-C(12)	1.386(3)
C(12)-C(13)	1.385(3)
C(13)-C(14)	1.374(3)
C(14)-C(15)	1.374(3)
C(15)-C(16)	1.389(3)
N(17)-C(18)	1.365(2)
N(17)-C(24)	1.458(2)
C(18)-O(18)	1.211(2)
C(18)-O(19)	1.345(2)
O(19)-C(20')	1.465(17)
O(19)-C(20)	1.469(3)
C(20)-C(22)	1.513(5)
C(20)-C(23)	1.515(4)
C(20)-C(21)	1.518(4)
C(20')-C(22')	1.510(14)
C(20')-C(21')	1.512(14)
C(20')-C(23')	1.516(14)
C(24)-C(25)	1.506(3)
C(25)-Cl(26)	1.791(2)

C(2)-N(1)-C(9)	111.24(15)
C(2)-N(1)-C(10)	123.41(15)
C(9)-N(1)-C(10)	124.86(15)
O(2)-C(2)-N(1)	125.88(18)
O(2)-C(2)-C(3)	126.76(17)
N(1)-C(2)-C(3)	107.35(15)
N(17)-C(3)-C(4)	118.23(15)
N(17)-C(3)-C(2)	114.23(15)
C(4)-C(3)-C(2)	102.64(14)
C(5)-C(4)-C(9)	119.59(17)
C(5)-C(4)-C(3)	131.92(17)
C(9)-C(4)-C(3)	108.42(15)
C(4)-C(5)-C(6)	119.00(18)
C(7)-C(6)-C(5)	120.75(18)
C(6)-C(7)-C(8)	120.99(18)
C(9)-C(8)-C(7)	117.21(17)
C(8)-C(9)-C(4)	122.45(17)
C(8)-C(9)-N(1)	127.76(16)
C(4)-C(9)-N(1)	109.78(15)
N(1)-C(10)-C(11)	114.74(15)
C(16)-C(11)-C(12)	118.55(18)
C(16)-C(11)-C(10)	122.93(17)
C(12)-C(11)-C(10)	118.52(17)
C(13)-C(12)-C(11)	120.8(2)
C(14)-C(13)-C(12)	120.0(2)
C(13)-C(14)-C(15)	120.0(2)
C(14)-C(15)-C(16)	119.9(2)
C(11)-C(16)-C(15)	120.8(2)
C(18)-N(17)-C(3)	122.50(15)
C(18)-N(17)-C(24)	117.56(15)

C(3)-N(17)-C(24)	119.71(15)
O(18)-C(18)-O(19)	126.66(18)
O(18)-C(18)-N(17)	123.68(18)
O(19)-C(18)-N(17)	109.66(16)
C(18)-O(19)-C(20')	124.9(9)
C(18)-O(19)-C(20)	120.48(19)
O(19)-C(20)-C(22)	108.3(3)
O(19)-C(20)-C(23)	111.6(3)
C(22)-C(20)-C(23)	113.2(3)
O(19)-C(20)-C(21)	101.4(3)
C(22)-C(20)-C(21)	110.0(3)
C(23)-C(20)-C(21)	111.6(3)
O(19)-C(20')-C(22')	106(2)
O(19)-C(20')-C(21')	107(2)
C(22')-C(20')-C(21')	112.3(13)
O(19)-C(20')-C(23')	108.5(17)
C(22')-C(20')-C(23')	112.0(12)
C(21')-C(20')-C(23')	110.8(12)
N(17)-C(24)-C(25)	111.31(16)
C(24)-C(25)-Cl(26)	109.23(14)

tert-Butyl (_S_)-1'-benzyl-2'-oxospiro[azetidine-2,3'-indoline]-1-carboxylate ((_S_)–338)



Identification code	JAB2020
Formula	C22 H24 N2 O3
Formula weight	364.43
Temperature	173(2) K
Diffractometer, wavelength	Agilent Xcalibur PX Ultra A, 1.54184 Å
Crystal system, space group	Orthorhombic, $P2_12_12_1$
Unit cell dimensions	a = 12.9504(3) Å α = 90°
	b = 15.1729(4) Å β = 90°
	c = 20.2983(5) Å γ = 90°
Volume, Z	3988.51(18) $Å^3$, 8
Density (calculated)	1.214 Mg/m^3
Absorption coefficient	0.652 mm^{-1}
F(000)	1552
Crystal colour / morphology	Colourless blocks
Crystal size	0.470 x 0.404 x 0.181 mm^3
θ range for data collection	3.637 to 73.370°
Index ranges	-14<=h<=15, -18<=k<=16, -24<=l<=16
Reflns collected / unique	12231 / 7615 [R(int) = 0.0590]
Reflns observed [F>4σ(F)]	5585
Absorption correction	Analytical

Max. and min. transmission	0.901 and 0.802
Refinement method	Full-matrix least-squares on F^2
Data / restraints / parameters	7615 / 0 / 494
Goodness-of-fit on F^2	1.030
Final R indices [F>4σ(F)]	R1 = 0.0533, wR2 = 0.1173
R indices (all data)	R1 = 0.0827, wR2 = 0.1445
Absolute structure parameter	0.1(2)
Largest diff. peak, hole	0.181, -0.202 eÅ^{-3}
Mean and maximum shift/error	0.000 and 0.000

Bond lengths [Å] and angles [°] for JAB2020.

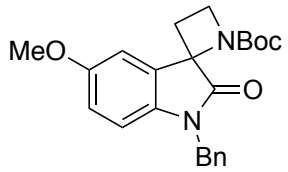
N(1A)-C(2A)	1.369(6)
N(1A)-C(9A)	1.414(5)
N(1A)-C(10A)	1.450(6)
C(2A)-O(2A)	1.221(6)
C(2A)-C(3A)	1.540(7)
C(3A)-N(17A)	1.457(6)
C(3A)-C(4A)	1.490(6)
C(3A)-C(19A)	1.558(6)
C(4A)-C(5A)	1.392(7)
C(4A)-C(9A)	1.397(6)
C(5A)-C(6A)	1.391(7)
C(6A)-C(7A)	1.380(7)
C(7A)-C(8A)	1.394(7)
C(8A)-C(9A)	1.386(6)
C(10A)-C(11A)	1.510(6)
C(11A)-C(16A)	1.383(6)
C(11A)-C(12A)	1.397(7)
C(12A)-C(13A)	1.405(8)
C(13A)-C(14A)	1.370(8)
C(14A)-C(15A)	1.382(7)
C(15A)-C(16A)	1.399(7)
N(17A)-C(20A)	1.360(6)
N(17A)-C(18A)	1.468(6)
C(18A)-C(19A)	1.549(7)
C(20A)-O(20A)	1.219(6)
C(20A)-O(21A)	1.346(6)
O(21A)-C(22A)	1.482(5)
C(22A)-C(25A)	1.513(7)
C(22A)-C(24A)	1.519(7)
C(22A)-C(23A)	1.521(7)
N(1B)-C(2B)	1.360(6)
N(1B)-C(9B)	1.413(6)
N(1B)-C(10B)	1.449(6)
C(2B)-O(2B)	1.228(6)
C(2B)-C(3B)	1.534(7)
C(3B)-N(17B)	1.472(6)
C(3B)-C(4B)	1.502(7)
C(3B)-C(19B)	1.562(6)
C(4B)-C(5B)	1.383(7)
C(4B)-C(9B)	1.399(6)
C(5B)-C(6B)	1.399(8)
C(6B)-C(7B)	1.388(8)
C(7B)-C(8B)	1.393(8)
C(8B)-C(9B)	1.378(7)
C(10B)-C(11B)	1.515(6)
C(11B)-C(12B)	1.386(6)

C(11B)-C(16B)	1.388(7)
C(12B)-C(13B)	1.390(7)
C(13B)-C(14B)	1.379(7)
C(14B)-C(15B)	1.383(7)
C(15B)-C(16B)	1.389(7)
N(17B)-C(20B)	1.368(6)
N(17B)-C(18B)	1.478(6)
C(18B)-C(19B)	1.552(7)
C(20B)-O(20B)	1.207(6)
C(20B)-O(21B)	1.348(6)
O(21B)-C(22B)	1.479(6)
C(22B)-C(24B)	1.500(8)
C(22B)-C(25B)	1.515(8)
C(22B)-C(23B)	1.520(7)

C(2A)-N(1A)-C(9A)	110.7(4)
C(2A)-N(1A)-C(10A)	123.5(4)
C(9A)-N(1A)-C(10A)	125.8(4)
O(2A)-C(2A)-N(1A)	125.1(5)
O(2A)-C(2A)-C(3A)	126.6(4)
N(1A)-C(2A)-C(3A)	108.3(4)
N(17A)-C(3A)-C(4A)	119.7(4)
N(17A)-C(3A)-C(2A)	112.9(4)
C(4A)-C(3A)-C(2A)	102.3(4)
N(17A)-C(3A)-C(19A)	87.9(3)
C(4A)-C(3A)-C(19A)	121.1(4)
C(2A)-C(3A)-C(19A)	113.3(4)
C(5A)-C(4A)-C(9A)	119.3(4)
C(5A)-C(4A)-C(3A)	131.3(4)
C(9A)-C(4A)-C(3A)	109.4(4)
C(6A)-C(5A)-C(4A)	118.7(4)
C(7A)-C(6A)-C(5A)	121.0(5)
C(6A)-C(7A)-C(8A)	121.5(5)
C(9A)-C(8A)-C(7A)	117.0(4)
C(8A)-C(9A)-C(4A)	122.5(4)
C(8A)-C(9A)-N(1A)	128.2(4)
C(4A)-C(9A)-N(1A)	109.3(4)
N(1A)-C(10A)-C(11A)	114.2(4)
C(16A)-C(11A)-C(12A)	119.3(4)
C(16A)-C(11A)-C(10A)	122.6(4)
C(12A)-C(11A)-C(10A)	118.1(4)
C(11A)-C(12A)-C(13A)	119.5(5)
C(14A)-C(13A)-C(12A)	120.6(5)
C(13A)-C(14A)-C(15A)	120.0(5)
C(14A)-C(15A)-C(16A)	119.9(5)
C(11A)-C(16A)-C(15A)	120.5(4)
C(20A)-N(17A)-C(3A)	123.4(4)
C(20A)-N(17A)-C(18A)	130.2(4)
C(3A)-N(17A)-C(18A)	94.6(4)
N(17A)-C(18A)-C(19A)	87.9(4)
C(18A)-C(19A)-C(3A)	87.5(4)
O(20A)-C(20A)-O(21A)	127.2(4)
O(20A)-C(20A)-N(17A)	122.4(4)
O(21A)-C(20A)-N(17A)	110.3(4)
C(20A)-O(21A)-C(22A)	119.8(4)
O(21A)-C(22A)-C(25A)	109.3(4)
O(21A)-C(22A)-C(24A)	110.5(4)
C(25A)-C(22A)-C(24A)	112.8(4)
O(21A)-C(22A)-C(23A)	102.5(4)
C(25A)-C(22A)-C(23A)	110.7(4)
C(24A)-C(22A)-C(23A)	110.6(5)
C(2B)-N(1B)-C(9B)	110.9(4)
C(2B)-N(1B)-C(10B)	124.2(4)

C(9B)-N(1B)-C(10B)	124.9(4)
O(2B)-C(2B)-N(1B)	125.6(5)
O(2B)-C(2B)-C(3B)	125.7(4)
N(1B)-C(2B)-C(3B)	108.6(4)
N(17B)-C(3B)-C(4B)	120.5(4)
N(17B)-C(3B)-C(2B)	112.2(4)
C(4B)-C(3B)-C(2B)	102.3(4)
N(17B)-C(3B)-C(19B)	88.1(3)
C(4B)-C(3B)-C(19B)	121.8(4)
C(2B)-C(3B)-C(19B)	112.1(4)
C(5B)-C(4B)-C(9B)	120.4(5)
C(5B)-C(4B)-C(3B)	130.8(4)
C(9B)-C(4B)-C(3B)	108.7(4)
C(4B)-C(5B)-C(6B)	118.0(5)
C(7B)-C(6B)-C(5B)	120.8(5)
C(6B)-C(7B)-C(8B)	121.6(5)
C(9B)-C(8B)-C(7B)	117.0(5)
C(8B)-C(9B)-C(4B)	122.2(5)
C(8B)-C(9B)-N(1B)	128.3(4)
C(4B)-C(9B)-N(1B)	109.4(4)
N(1B)-C(10B)-C(11B)	112.6(4)
C(12B)-C(11B)-C(16B)	119.0(4)
C(12B)-C(11B)-C(10B)	120.0(4)
C(16B)-C(11B)-C(10B)	121.0(4)
C(11B)-C(12B)-C(13B)	120.8(4)
C(14B)-C(13B)-C(12B)	119.5(4)
C(13B)-C(14B)-C(15B)	120.4(5)
C(14B)-C(15B)-C(16B)	119.7(4)
C(11B)-C(16B)-C(15B)	120.5(4)
C(20B)-N(17B)-C(3B)	121.0(4)
C(20B)-N(17B)-C(18B)	128.5(4)
C(3B)-N(17B)-C(18B)	93.4(3)
N(17B)-C(18B)-C(19B)	88.3(4)
C(18B)-C(19B)-C(3B)	87.2(4)
O(20B)-C(20B)-O(21B)	126.6(5)
O(20B)-C(20B)-N(17B)	123.3(4)
O(21B)-C(20B)-N(17B)	110.1(4)
C(20B)-O(21B)-C(22B)	120.3(4)
O(21B)-C(22B)-C(24B)	110.7(5)
O(21B)-C(22B)-C(25B)	109.6(4)
C(24B)-C(22B)-C(25B)	111.6(6)
O(21B)-C(22B)-C(23B)	102.7(4)
C(24B)-C(22B)-C(23B)	111.2(5)
C(25B)-C(22B)-C(23B)	110.6(5)

tert-Butyl 1'-benzyl-5'-methoxy-2'-oxospiro[azetidine-2,3'-indoline]-1-carboxylate ((±)–339)



Identification code	JAB2011
Formula	C23 H26 N2 O4
Formula weight	394.46
Temperature	173(2) K
Diffractometer, wavelength	Agilent Xcalibur 3 E, 0.71073 Å

Crystal system, space group	Monoclinic, $P2_1/c$
Unit cell dimensions	a = 13.9967(7) Å α = 90°
	b = 7.7675(3) Å β = 95.354(4)°
	c = 18.8888(7) Å γ = 90°
Volume, Z	2044.62(16) $Å^3$, 4
Density (calculated)	1.281 Mg/m^3
Absorption coefficient	0.088 mm^{-1}
F(000)	840
Crystal colour / morphology	Colourless hexagonal tablets
Crystal size	0.542 x 0.388 x 0.112 mm^3
θ range for data collection	2.724 to 28.282°
Index ranges	-12<=h<=18, -9<=k<=6, -24<=l<=17
Reflns collected / unique	7181 / 4112 [R(int) = 0.0360]
Reflns observed [F>4σ(F)]	3010
Absorption correction	Analytical
Max. and min. transmission	0.990 and 0.970
Refinement method	Full-matrix least-squares on F^2
Data / restraints / parameters	4112 / 0 / 267
Goodness-of-fit on F^2	1.031
Final R indices [F>4σ(F)]	R1 = 0.0502, wR2 = 0.1027
R indices (all data)	R1 = 0.0755, wR2 = 0.1174
Largest diff. peak, hole	0.245, -0.184 $eÅ^{-3}$
Mean and maximum shift/error	0.000 and 0.000

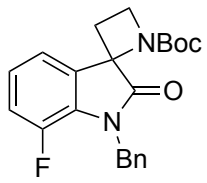
Bond lengths [Å] and angles [°] for JAB2011.

N(1)-C(2)	1.363(2)
N(1)-C(9)	1.415(2)
N(1)-C(10)	1.447(2)
C(2)-O(2)	1.215(2)
C(2)-C(3)	1.541(3)
C(3)-N(17)	1.468(2)
C(3)-C(4)	1.504(2)
C(3)-C(19)	1.556(2)
C(4)-C(5)	1.380(2)
C(4)-C(9)	1.387(2)
C(5)-C(6)	1.391(2)
C(6)-O(26)	1.375(2)
C(6)-C(7)	1.392(2)
C(7)-C(8)	1.388(2)
C(8)-C(9)	1.379(2)
C(10)-C(11)	1.512(2)
C(11)-C(16)	1.385(2)
C(11)-C(12)	1.386(2)
C(12)-C(13)	1.381(3)
C(13)-C(14)	1.381(3)
C(14)-C(15)	1.379(3)
C(15)-C(16)	1.381(3)
N(17)-C(20)	1.345(2)

N(17)-C(18)	1.452(2)
C(18)-C(19)	1.553(3)
C(20)-O(20)	1.206(2)
C(20)-O(21)	1.345(2)
O(21)-C(22)	1.477(2)
C(22)-C(25)	1.505(3)
C(22)-C(23)	1.506(2)
C(22)-C(24)	1.506(3)
O(26)-C(27)	1.415(2)

C(2)-N(1)-C(9)	111.17(15)
C(2)-N(1)-C(10)	124.48(16)
C(9)-N(1)-C(10)	124.35(15)
O(2)-C(2)-N(1)	126.22(18)
O(2)-C(2)-C(3)	126.20(17)
N(1)-C(2)-C(3)	107.58(16)
N(17)-C(3)-C(4)	117.32(15)
N(17)-C(3)-C(2)	113.41(14)
C(4)-C(3)-C(2)	102.90(14)
N(17)-C(3)-C(19)	86.94(13)
C(4)-C(3)-C(19)	119.07(14)
C(2)-C(3)-C(19)	117.59(16)
C(5)-C(4)-C(9)	121.37(16)
C(5)-C(4)-C(3)	130.27(16)
C(9)-C(4)-C(3)	108.35(15)
C(4)-C(5)-C(6)	117.58(16)
O(26)-C(6)-C(5)	124.42(15)
O(26)-C(6)-C(7)	114.56(15)
C(5)-C(6)-C(7)	121.01(16)
C(8)-C(7)-C(6)	120.89(17)
C(9)-C(8)-C(7)	117.82(16)
C(8)-C(9)-C(4)	121.31(16)
C(8)-C(9)-N(1)	128.69(16)
C(4)-C(9)-N(1)	110.00(15)
N(1)-C(10)-C(11)	113.65(14)
C(16)-C(11)-C(12)	118.38(17)
C(16)-C(11)-C(10)	119.80(16)
C(12)-C(11)-C(10)	121.81(16)
C(13)-C(12)-C(11)	120.62(19)
C(12)-C(13)-C(14)	120.56(19)
C(15)-C(14)-C(13)	119.18(19)
C(14)-C(15)-C(16)	120.25(19)
C(15)-C(16)-C(11)	120.99(18)
C(20)-N(17)-C(18)	132.29(15)
C(20)-N(17)-C(3)	128.73(14)
C(18)-N(17)-C(3)	96.14(13)
N(17)-C(18)-C(19)	87.59(13)
C(18)-C(19)-C(3)	88.67(13)
O(20)-C(20)-N(17)	124.76(16)
O(20)-C(20)-O(21)	127.02(16)
N(17)-C(20)-O(21)	108.16(15)
C(20)-O(21)-C(22)	122.63(14)
O(21)-C(22)-C(25)	109.79(15)
O(21)-C(22)-C(23)	101.87(15)
C(25)-C(22)-C(23)	110.38(16)
O(21)-C(22)-C(24)	109.22(14)
C(25)-C(22)-C(24)	112.84(19)
C(23)-C(22)-C(24)	112.17(18)
C(6)-O(26)-C(27)	117.39(14)

tert-Butyl 1'-benzyl-7'-fluoro-2'-oxospiro[azetidine-2,3'-indoline]-1-carboxylate ((±)–342)



Identification code	JAB2010
Formula	C22 H23 F N2 O3
Formula weight	382.42
Temperature	173(2) K
Diffractometer, wavelength	Agilent Xcalibur 3 E, 0.71073 Å
Crystal system, space group	Triclinic, P-1
Unit cell dimensions	a = 9.0794(11) Å α = 107.981(10)°
	b = 10.1910(11) Å β = 93.178(10)°
	c = 10.6587(13) Å γ = 95.593(9)°
Volume, Z	929.78(19) $Å^3$, 2
Density (calculated)	1.366 Mg/m^3
Absorption coefficient	0.098 mm^{-1}
F(000)	404
Crystal colour / morphology	Colourless blocks
Crystal size	0.522 x 0.230 x 0.168 mm^3
θ range for data collection	2.419 to 28.204°
Index ranges	-11<=h<=11, -13<=k<=9, -13<=l<=14
Reflns collected / unique	5368 / 3664 [R(int) = 0.0296]
Reflns observed [F>4σ(F)]	2675
Absorption correction	Analytical
Max. and min. transmission	0.987 and 0.966
Refinement method	Full-matrix least-squares on F^2
Data / restraints / parameters	3664 / 0 / 257
Goodness-of-fit on F^2	1.060
Final R indices [F>4σ(F)]	R1 = 0.0539, wR2 = 0.1188
R indices (all data)	R1 = 0.0783, wR2 = 0.1408
Largest diff. peak, hole	0.239, -0.233 $eÅ^{-3}$
Mean and maximum shift/error	0.000 and 0.000

Bond lengths [Å] and angles [°] for JAB2010.

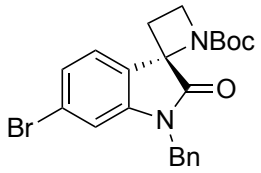
N(1)-C(2)	1.369(3)
N(1)-C(9)	1.416(2)
N(1)-C(10)	1.456(3)
C(2)-O(2)	1.219(2)
C(2)-C(3)	1.533(3)
C(3)-N(17)	1.469(3)

C(3)-C(4)	1.501(3)
C(3)-C(19)	1.559(3)
C(4)-C(5)	1.378(3)
C(4)-C(9)	1.395(3)
C(5)-C(6)	1.389(3)
C(6)-C(7)	1.383(3)
C(7)-C(8)	1.384(3)
C(8)-F(8)	1.358(2)
C(8)-C(9)	1.373(3)
C(10)-C(11)	1.506(3)
C(11)-C(12)	1.381(3)
C(11)-C(16)	1.390(3)
C(12)-C(13)	1.388(3)
C(13)-C(14)	1.383(3)
C(14)-C(15)	1.376(3)
C(15)-C(16)	1.384(3)
N(17)-C(20)	1.345(3)
N(17)-C(18)	1.455(3)
C(18)-C(19)	1.555(3)
C(20)-O(20)	1.213(2)
C(20)-O(21)	1.345(3)
O(21)-C(22)	1.482(2)
C(22)-C(23)	1.513(3)
C(22)-C(25)	1.521(3)
C(22)-C(24)	1.523(3)

C(2)-N(1)-C(9)	110.54(17)
C(2)-N(1)-C(10)	122.19(18)
C(9)-N(1)-C(10)	127.27(18)
O(2)-C(2)-N(1)	125.8(2)
O(2)-C(2)-C(3)	126.2(2)
N(1)-C(2)-C(3)	107.97(18)
N(17)-C(3)-C(4)	118.81(16)
N(17)-C(3)-C(2)	113.19(17)
C(4)-C(3)-C(2)	103.23(17)
N(17)-C(3)-C(19)	87.22(16)
C(4)-C(3)-C(19)	120.76(18)
C(2)-C(3)-C(19)	113.83(17)
C(5)-C(4)-C(9)	120.3(2)
C(5)-C(4)-C(3)	131.7(2)
C(9)-C(4)-C(3)	107.98(17)
C(4)-C(5)-C(6)	119.4(2)
C(7)-C(6)-C(5)	120.6(2)
C(6)-C(7)-C(8)	119.4(2)
F(8)-C(8)-C(9)	120.37(19)
F(8)-C(8)-C(7)	118.9(2)
C(9)-C(8)-C(7)	120.7(2)
C(8)-C(9)-C(4)	119.60(18)
C(8)-C(9)-N(1)	130.2(2)
C(4)-C(9)-N(1)	110.16(18)
N(1)-C(10)-C(11)	114.65(16)
C(12)-C(11)-C(16)	118.8(2)
C(12)-C(11)-C(10)	118.87(18)
C(16)-C(11)-C(10)	122.3(2)
C(11)-C(12)-C(13)	121.1(2)
C(14)-C(13)-C(12)	119.7(2)
C(15)-C(14)-C(13)	119.6(2)
C(14)-C(15)-C(16)	120.7(2)
C(15)-C(16)-C(11)	120.2(2)
C(20)-N(17)-C(18)	132.34(19)
C(20)-N(17)-C(3)	131.14(19)
C(18)-N(17)-C(3)	96.06(16)
N(17)-C(18)-C(19)	87.85(16)

C(18)-C(19)-C(3)	88.58(15)
O(20)-C(20)-N(17)	123.6(2)
O(20)-C(20)-O(21)	127.49(19)
N(17)-C(20)-O(21)	108.93(17)
C(20)-O(21)-C(22)	122.41(15)
O(21)-C(22)-C(23)	102.81(14)
O(21)-C(22)-C(25)	108.45(17)
C(23)-C(22)-C(25)	111.56(18)
O(21)-C(22)-C(24)	110.56(17)
C(23)-C(22)-C(24)	110.17(18)
C(25)-C(22)-C(24)	112.83(17)

tert-Butyl (_S_)-1'-benzyl-6'-bromo-2'-oxospiro[azetidine-2,3'-indoline]-1-carboxylate ((_S_)–343)



Identification code	JAB2019
Formula	C22 H23 Br N2 O3
Formula weight	443.33
Temperature	173(2) K
Diffractometer, wavelength	Agilent Xcalibur PX Ultra A, 1.54184 Å
Crystal system, space group	Orthorhombic, $P2_12_12_1$
Unit cell dimensions	a = 9.3712(3) Å α = 90°
	b = 13.2604(3) Å β = 90°
	c = 16.8619(5) Å γ = 90°
Volume, Z	2095.35(10) $Å^3$, 4
Density (calculated)	1.405 Mg/m^3
Absorption coefficient	2.873 mm^{-1}
F(000)	912
Crystal colour / morphology	Colourless blocks
Crystal size	0.453 x 0.344 x 0.213 mm^3
θ range for data collection	4.242 to 73.320°
Index ranges	-11<=h<=11, -13<=k<=16, -20<=l<=13
Reflns collected / unique	6304 / 3993 [R(int) = 0.0489]
Reflns observed [F>4σ(F)]	3433
Absorption correction	Analytical
Max. and min. transmission	0.641 and 0.445
Refinement method	Full-matrix least-squares on F^2
Data / restraints / parameters	3993 / 0 / 254
Goodness-of-fit on F^2	1.036
Final R indices [F>4σ(F)]	R1 = 0.0448, wR2 = 0.1054

R indices (all data)	R1 = 0.0562, wR2 = 0.1182
Absolute structure parameter	-0.04(2)
Largest diff. peak, hole	0.574, -0.567 eÅ^{-3}
Mean and maximum shift/error	0.000 and 0.001

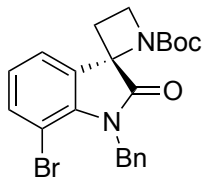
Bond lengths [Å] and angles [°] for JAB2019.

N(1)-C(2)	1.358(7)
N(1)-C(9)	1.407(7)
N(1)-C(10)	1.454(7)
C(2)-O(2)	1.214(7)
C(2)-C(3)	1.555(8)
C(3)-N(17)	1.472(7)
C(3)-C(4)	1.488(8)
C(3)-C(19)	1.563(8)
C(4)-C(5)	1.380(8)
C(4)-C(9)	1.402(7)
C(5)-C(6)	1.392(8)
C(6)-C(7)	1.378(8)
C(7)-C(8)	1.401(8)
C(7)-Br(7)	1.898(5)
C(8)-C(9)	1.376(7)
C(10)-C(11)	1.517(9)
C(11)-C(12)	1.383(9)
C(11)-C(16)	1.399(8)
C(12)-C(13)	1.389(10)
C(13)-C(14)	1.377(11)
C(14)-C(15)	1.388(12)
C(15)-C(16)	1.377(10)
N(17)-C(20)	1.349(7)
N(17)-C(18)	1.472(7)
C(18)-C(19)	1.549(8)
C(20)-O(20)	1.217(6)
C(20)-O(21)	1.347(6)
O(21)-C(22)	1.474(6)
C(22)-C(24)	1.514(8)
C(22)-C(23)	1.517(8)
C(22)-C(25)	1.532(9)

C(2)-N(1)-C(9)	111.4(4)
C(2)-N(1)-C(10)	124.0(5)
C(9)-N(1)-C(10)	124.6(5)
O(2)-C(2)-N(1)	127.5(6)
O(2)-C(2)-C(3)	124.5(5)
N(1)-C(2)-C(3)	107.9(4)
N(17)-C(3)-C(4)	119.5(5)
N(17)-C(3)-C(2)	113.7(4)
C(4)-C(3)-C(2)	102.2(4)
N(17)-C(3)-C(19)	87.3(4)
C(4)-C(3)-C(19)	121.4(5)
C(2)-C(3)-C(19)	113.3(5)
C(5)-C(4)-C(9)	120.4(5)
C(5)-C(4)-C(3)	130.4(5)
C(9)-C(4)-C(3)	109.1(4)
C(4)-C(5)-C(6)	118.8(5)
C(7)-C(6)-C(5)	119.2(5)
C(6)-C(7)-C(8)	123.8(5)
C(6)-C(7)-Br(7)	118.4(4)
C(8)-C(7)-Br(7)	117.7(4)
C(9)-C(8)-C(7)	115.4(5)
C(8)-C(9)-C(4)	122.4(5)
C(8)-C(9)-N(1)	128.2(5)

C(4)-C(9)-N(1)	109.4(5)
N(1)-C(10)-C(11)	114.3(5)
C(12)-C(11)-C(16)	118.7(6)
C(12)-C(11)-C(10)	119.7(6)
C(16)-C(11)-C(10)	121.4(6)
C(11)-C(12)-C(13)	120.6(6)
C(14)-C(13)-C(12)	120.9(7)
C(13)-C(14)-C(15)	118.3(7)
C(16)-C(15)-C(14)	121.6(7)
C(15)-C(16)-C(11)	119.8(6)
C(20)-N(17)-C(3)	123.8(4)
C(20)-N(17)-C(18)	132.5(4)
C(3)-N(17)-C(18)	95.0(4)
N(17)-C(18)-C(19)	87.8(4)
C(18)-C(19)-C(3)	88.4(4)
O(20)-C(20)-O(21)	126.5(5)
O(20)-C(20)-N(17)	123.1(5)
O(21)-C(20)-N(17)	110.4(4)
C(20)-O(21)-C(22)	120.3(4)
O(21)-C(22)-C(24)	109.9(5)
O(21)-C(22)-C(23)	103.5(5)
C(24)-C(22)-C(23)	110.1(5)
O(21)-C(22)-C(25)	110.0(4)
C(24)-C(22)-C(25)	112.7(5)
C(23)-C(22)-C(25)	110.3(5)

tert-Butyl (_S_)-1'-benzyl-7'-bromo-2'-oxospiro[azetidine-2,3'-indoline]-1-carboxylate ((_S_)–349)



Identification code	JAB2018
Formula	C22 H23 Br N2 O3
Formula weight	443.33
Temperature	173(2) K
Diffractometer, wavelength	Agilent Xcalibur PX Ultra A, 1.54184 Å
Crystal system, space group	Monoclinic, $P2_1$
Unit cell dimensions	a = 8.8565(3) Å α = 90°
	b = 11.1338(3) Å β = 90.987(3)°
	c = 10.0946(3) Å γ = 90°
Volume, Z	995.25(5) $Å^3$, 2
Density (calculated)	1.479 Mg/m^3
Absorption coefficient	3.025 mm^{-1}
F(000)	456
Crystal colour / morphology	Colourless blocks
Crystal size	0.431 x 0.322 x 0.258 mm^3
θ range for data collection	4.381 to 73.467°

Index ranges	-10<=h<=9, -13<=k<=13, -8<=l<=12
Reflns collected / unique	5879 / 3779 [R(int) = 0.0381]
Reflns observed [F>4σ(F)]	3453
Absorption correction	Analytical
Max. and min. transmission	0.564 and 0.429
Refinement method	Full-matrix least-squares on F^2
Data / restraints / parameters	3779 / 1 / 257
Goodness-of-fit on F^2	1.052
Final R indices [F>4σ(F)]	R1 = 0.0424, wR2 = 0.1043
R indices (all data)	R1 = 0.0488, wR2 = 0.1162
Absolute structure parameter	0.00(3)
Largest diff. peak, hole	0.261, -0.265 eÅ^{-3}
Mean and maximum shift/error	0.000 and 0.000

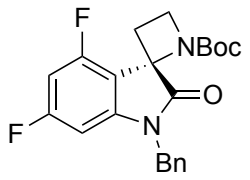
Bond lengths [Å] and angles [°] for JAB2018.

N(1)-C(2)	1.379(8)
N(1)-C(9)	1.414(8)
N(1)-C(10)	1.471(8)
C(2)-O(2)	1.206(8)
C(2)-C(3)	1.519(9)
C(3)-N(17)	1.474(8)
C(3)-C(4)	1.494(9)
C(3)-C(19)	1.571(8)
C(4)-C(5)	1.372(9)
C(4)-C(9)	1.399(8)
C(5)-C(6)	1.401(10)
C(6)-C(7)	1.379(11)
C(7)-C(8)	1.396(9)
C(8)-C(9)	1.398(9)
C(8)-Br(8)	1.884(6)
C(10)-C(11)	1.525(8)
C(11)-C(12)	1.382(9)
C(11)-C(16)	1.382(9)
C(12)-C(13)	1.394(10)
C(13)-C(14)	1.383(10)
C(14)-C(15)	1.388(9)
C(15)-C(16)	1.393(10)
N(17)-C(20)	1.342(8)
N(17)-C(18)	1.432(8)
C(18)-C(19)	1.535(10)
C(20)-O(20)	1.217(8)
C(20)-O(21)	1.341(7)
O(21)-C(22)	1.478(7)
C(22)-C(25)	1.516(8)
C(22)-C(24)	1.520(8)
C(22)-C(23)	1.523(8)

C(2)-N(1)-C(9)	110.6(5)
C(2)-N(1)-C(10)	119.7(5)
C(9)-N(1)-C(10)	129.6(5)
O(2)-C(2)-N(1)	125.7(6)
O(2)-C(2)-C(3)	126.3(6)
N(1)-C(2)-C(3)	108.0(5)
N(17)-C(3)-C(4)	116.4(5)
N(17)-C(3)-C(2)	114.2(6)

C(4)-C(3)-C(2)	103.4(4)
N(17)-C(3)-C(19)	86.1(4)
C(4)-C(3)-C(19)	120.9(7)
C(2)-C(3)-C(19)	116.1(5)
C(5)-C(4)-C(9)	122.4(6)
C(5)-C(4)-C(3)	129.0(6)
C(9)-C(4)-C(3)	108.5(5)
C(4)-C(5)-C(6)	119.0(6)
C(7)-C(6)-C(5)	119.1(6)
C(6)-C(7)-C(8)	122.2(6)
C(7)-C(8)-C(9)	118.6(6)
C(7)-C(8)-Br(8)	116.6(5)
C(9)-C(8)-Br(8)	124.6(5)
C(8)-C(9)-C(4)	118.6(5)
C(8)-C(9)-N(1)	131.9(5)
C(4)-C(9)-N(1)	109.5(5)
N(1)-C(10)-C(11)	113.8(5)
C(12)-C(11)-C(16)	119.4(6)
C(12)-C(11)-C(10)	120.4(6)
C(16)-C(11)-C(10)	120.2(6)
C(11)-C(12)-C(13)	120.0(7)
C(14)-C(13)-C(12)	121.0(6)
C(13)-C(14)-C(15)	118.6(6)
C(14)-C(15)-C(16)	120.5(6)
C(11)-C(16)-C(15)	120.5(6)
C(20)-N(17)-C(18)	133.6(6)
C(20)-N(17)-C(3)	129.8(5)
C(18)-N(17)-C(3)	96.3(5)
N(17)-C(18)-C(19)	88.9(5)
C(18)-C(19)-C(3)	88.4(5)
O(20)-C(20)-O(21)	127.7(6)
O(20)-C(20)-N(17)	122.8(6)
O(21)-C(20)-N(17)	109.5(5)
C(20)-O(21)-C(22)	121.0(5)
O(21)-C(22)-C(25)	109.5(5)
O(21)-C(22)-C(24)	110.2(5)
C(25)-C(22)-C(24)	112.3(5)
O(21)-C(22)-C(23)	102.3(4)
C(25)-C(22)-C(23)	111.5(5)
C(24)-C(22)-C(23)	110.7(5)

tert-Butyl (_S_)-1'-benzyl-4',6'-difluoro-2'-oxospiro[azetidine-2,3'-indoline]-1-carboxylate ((_S_)–345)



Identification code	JAB2009
Formula	C22 H22 F2 N2 O3
Formula weight	400.41
Temperature	173(2) K
Diffractometer, wavelength	Agilent Xcalibur PX Ultra A, 1.54184 Å
Crystal system, space group	Orthorhombic, $P2_12_12_1$
Unit cell dimensions	a = 9.3708(2) Å α = 90°

	b = 12.1170(3) Å β = 90°
	c = 18.0973(4) Å γ = 90°
Volume, Z	2054.87(9) $Å^3$, 4
Density (calculated)	1.294 Mg/m^3
Absorption coefficient	0.827 mm^{-1}
F(000)	840
Crystal colour / morphology	Colourless blocks
Crystal size	0.364 x 0.308 x 0.262 mm^3
θ range for data collection	4.391 to 73.659°
Index ranges	-11<=h<=11, -14<=k<=15, -22<=l<=22
Reflns collected / unique	34661 / 4118 [R(int) = 0.0631]
Reflns observed [F>4σ(F)]	3405
Absorption correction	Analytical
Max. and min. transmission	0.849 and 0.802
Refinement method	Full-matrix least-squares on F^2
Data / restraints / parameters	4118 / 0 / 266
Goodness-of-fit on F^2	1.052
Final R indices [F>4σ(F)]	R1 = 0.0582, wR2 = 0.1491
R indices (all data)	R1 = 0.0720, wR2 = 0.1643
Absolute structure parameter	-0.21(10)
Largest diff. peak, hole	0.427, -0.250 $eÅ^{-3}$
Mean and maximum shift/error	0.000 and 0.000

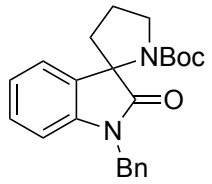
Bond lengths [Å] and angles [°] for JAB2009.

N(1)-C(2)	1.377(5)
N(1)-C(9)	1.385(5)
N(1)-C(10)	1.463(5)
C(2)-O(2)	1.220(5)
C(2)-C(3)	1.532(5)
C(3)-N(17)	1.463(5)
C(3)-C(4)	1.480(6)
C(3)-C(19)	1.563(6)
C(4)-C(5)	1.370(6)
C(4)-C(9)	1.402(5)
C(5)-F(5)	1.358(5)
C(5)-C(6)	1.370(7)
C(6)-C(7)	1.367(7)
C(7)-F(7)	1.355(5)
C(7)-C(8)	1.386(6)
C(8)-C(9)	1.387(5)
C(10)-C(11)	1.497(6)
C(11)-C(12)	1.337(7)
C(11)-C(16)	1.411(6)
C(12)-C(13)	1.416(9)
C(13)-C(14)	1.361(11)
C(14)-C(15)	1.369(10)
C(15)-C(16)	1.368(8)
N(17)-C(20)	1.345(6)
N(17)-C(18)	1.471(6)

C(18)-C(19)	1.542(7)
C(20)-O(20)	1.202(5)
C(20)-O(21)	1.340(5)
O(21)-C(22)	1.467(5)
C(22)-C(25)	1.506(9)
C(22)-C(23)	1.518(8)
C(22)-C(24)	1.523(9)

C(2)-N(1)-C(9)	110.8(3)
C(2)-N(1)-C(10)	123.0(3)
C(9)-N(1)-C(10)	126.2(3)
O(2)-C(2)-N(1)	125.7(4)
O(2)-C(2)-C(3)	126.0(4)
N(1)-C(2)-C(3)	108.3(3)
N(17)-C(3)-C(4)	119.1(3)
N(17)-C(3)-C(2)	114.5(3)
C(4)-C(3)-C(2)	102.0(3)
N(17)-C(3)-C(19)	87.7(3)
C(4)-C(3)-C(19)	118.7(4)
C(2)-C(3)-C(19)	115.5(4)
C(5)-C(4)-C(9)	118.4(4)
C(5)-C(4)-C(3)	132.1(4)
C(9)-C(4)-C(3)	109.5(3)
F(5)-C(5)-C(4)	118.8(4)
F(5)-C(5)-C(6)	118.9(4)
C(4)-C(5)-C(6)	122.3(4)
C(7)-C(6)-C(5)	116.7(4)
F(7)-C(7)-C(6)	117.6(4)
F(7)-C(7)-C(8)	116.9(4)
C(6)-C(7)-C(8)	125.5(4)
C(7)-C(8)-C(9)	115.0(4)
N(1)-C(9)-C(8)	128.5(4)
N(1)-C(9)-C(4)	109.5(3)
C(8)-C(9)-C(4)	122.0(4)
N(1)-C(10)-C(11)	113.5(3)
C(12)-C(11)-C(16)	120.8(5)
C(12)-C(11)-C(10)	122.7(4)
C(16)-C(11)-C(10)	116.5(4)
C(11)-C(12)-C(13)	119.3(6)
C(14)-C(13)-C(12)	119.0(6)
C(13)-C(14)-C(15)	121.8(6)
C(16)-C(15)-C(14)	119.1(6)
C(15)-C(16)-C(11)	119.6(6)
C(20)-N(17)-C(3)	128.6(3)
C(20)-N(17)-C(18)	129.7(4)
C(3)-N(17)-C(18)	95.0(3)
N(17)-C(18)-C(19)	88.2(3)
C(18)-C(19)-C(3)	88.3(3)
O(20)-C(20)-O(21)	127.4(4)
O(20)-C(20)-N(17)	123.0(4)
O(21)-C(20)-N(17)	109.5(3)
C(20)-O(21)-C(22)	122.0(3)
O(21)-C(22)-C(25)	111.1(5)
O(21)-C(22)-C(23)	102.4(4)
C(25)-C(22)-C(23)	112.2(6)
O(21)-C(22)-C(24)	107.4(5)
C(25)-C(22)-C(24)	112.1(6)
C(23)-C(22)-C(24)	111.1(6)

tert-Butyl 1-benzyl-2-oxospiro[indoline-3,2'-pyrrolidine]-1'-carboxylate ((_S_)–360)



Identification code	JAB2016
Formula	C23 H26 N2 O3
Formula weight	378.46
Temperature	173(2) K
Diffractometer, wavelength	Agilent Xcalibur PX Ultra A, 1.54184 Å
Crystal system, space group	Monoclinic, $P2_1$
Unit cell dimensions	a = 8.7487(9) Å α = 90°
	b = 13.4090(11) Å β = 110.630(10)°
	c = 9.3797(6) Å γ = 90°
Volume, Z	1029.78(16) $Å^3$, 2
Density (calculated)	1.221 Mg/m^3
Absorption coefficient	0.649 mm^{-1}
F(000)	404
Crystal colour / morphology	Colourless blocks
Crystal size	0.270 x 0.208 x 0.191 mm^3
θ range for data collection	5.038 to 73.219°
Index ranges	-10<=h<=8, -13<=k<=16, -7<=l<=11
Reflns collected / unique	3406 / 2654 [R(int) = 0.0601]
Reflns observed [F>4σ(F)]	1878
Absorption correction	Analytical
Max. and min. transmission	0.911 and 0.877
Refinement method	Full-matrix least-squares on F^2
Data / restraints / parameters	2654 / 1 / 257
Goodness-of-fit on F^2	1.049
Final R indices [F>4σ(F)]	R1 = 0.0506, wR2 = 0.1005
R indices (all data)	R1 = 0.0795, wR2 = 0.1208
Absolute structure parameter	0.1(5)
Largest diff. peak, hole	0.144, -0.194 $eÅ^{-3}$
Mean and maximum shift/error	0.000 and 0.000

Bond lengths [Å] and angles [°] for JAB2016.

N(1)-C(2)	1.363(6)
N(1)-C(9)	1.405(6)
N(1)-C(10)	1.458(6)
C(2)-O(2)	1.222(6)

C(2)-C(3)	1.551(7)
C(3)-N(17)	1.454(6)
C(3)-C(4)	1.511(7)
C(3)-C(20)	1.532(7)
C(4)-C(5)	1.375(8)
C(4)-C(9)	1.399(6)
C(5)-C(6)	1.398(8)
C(6)-C(7)	1.390(8)
C(7)-C(8)	1.388(8)
C(8)-C(9)	1.382(7)
C(10)-C(11)	1.502(7)
C(11)-C(12)	1.376(9)
C(11)-C(16)	1.393(7)
C(12)-C(13)	1.393(9)
C(13)-C(14)	1.389(10)
C(14)-C(15)	1.379(13)
C(15)-C(16)	1.380(10)
N(17)-C(21)	1.349(7)
N(17)-C(18)	1.470(6)
C(18)-C(19)	1.528(8)
C(19)-C(20)	1.539(7)
C(21)-O(21)	1.216(6)
C(21)-O(22)	1.356(6)
O(22)-C(23)	1.454(6)
C(23)-C(25)	1.505(8)
C(23)-C(26)	1.506(7)
C(23)-C(24)	1.530(6)

C(2)-N(1)-C(9)	111.3(4)
C(2)-N(1)-C(10)	123.9(4)
C(9)-N(1)-C(10)	124.8(4)
O(2)-C(2)-N(1)	124.8(5)
O(2)-C(2)-C(3)	126.9(4)
N(1)-C(2)-C(3)	108.2(4)
N(17)-C(3)-C(4)	115.4(4)
N(17)-C(3)-C(20)	102.3(4)
C(4)-C(3)-C(20)	115.4(5)
N(17)-C(3)-C(2)	114.2(4)
C(4)-C(3)-C(2)	101.6(4)
C(20)-C(3)-C(2)	108.2(4)
C(5)-C(4)-C(9)	119.3(5)
C(5)-C(4)-C(3)	131.9(4)
C(9)-C(4)-C(3)	108.8(4)
C(4)-C(5)-C(6)	119.7(5)
C(7)-C(6)-C(5)	119.4(6)
C(8)-C(7)-C(6)	122.1(5)
C(9)-C(8)-C(7)	117.0(5)
C(8)-C(9)-C(4)	122.4(5)
C(8)-C(9)-N(1)	127.8(4)
C(4)-C(9)-N(1)	109.8(4)
N(1)-C(10)-C(11)	112.3(5)
C(12)-C(11)-C(16)	119.5(6)
C(12)-C(11)-C(10)	121.2(5)
C(16)-C(11)-C(10)	119.3(6)
C(11)-C(12)-C(13)	121.1(6)
C(14)-C(13)-C(12)	119.0(8)
C(15)-C(14)-C(13)	119.6(7)
C(14)-C(15)-C(16)	121.2(7)
C(15)-C(16)-C(11)	119.4(8)
C(21)-N(17)-C(3)	125.9(4)
C(21)-N(17)-C(18)	120.3(4)
C(3)-N(17)-C(18)	113.7(4)
N(17)-C(18)-C(19)	103.2(4)

C(18)-C(19)-C(20)	103.4(5)
C(3)-C(20)-C(19)	103.8(4)
O(21)-C(21)-N(17)	124.6(5)
O(21)-C(21)-O(22)	126.1(5)
N(17)-C(21)-O(22)	109.3(4)
C(21)-O(22)-C(23)	121.8(4)
O(22)-C(23)-C(25)	109.7(5)
O(22)-C(23)-C(26)	110.8(5)
C(25)-C(23)-C(26)	112.8(5)
O(22)-C(23)-C(24)	102.1(4)
C(25)-C(23)-C(24)	111.2(5)
C(26)-C(23)-C(24)	109.7(4)

8. References

1 H. Maehr, *J. Chem. Educ.* **1985**, *62*, 114–120.

2 J. Holenz, P. Stoy, *Bioorg. Med. Chem. Lett.* **2019**, *29*, 517–524.

3 A. Smith, *Nature* **2002**, *418*, 453–459.

4 S. J. Lane, D. S. Eggleston, K. A. Brinded, J. C. Hollerton, N. L. Taylor, S. A. Readshaw, *Drug Discov. Today* **2006**, *11*, 267–272.

5 G. Harper, S. Pickett, D. Green, *Comb. Chem. High Throughput Screen.* **2004**, *7*, 63–70.

6 J. Inglese, D. S. Auld, *Wiley Encycl. Chem. Biol.*, John Wiley & Sons, Inc., Hoboken, NJ, USA, **2008**.

7 R. Liu, X. Li, K. S. Lam, *Curr. Opin. Chem. Biol.* **2017**, *38*, 117–126.

8 R. Macarron, M. N. Banks, D. Bojanic, D. J. Burns, D. A. Cirovic, T. Garyantes, D. V. S. Green, R. P. Hertzberg, W. P. Janzen, J. W. Paslay, et al., *Nat. Rev. Drug Discov.* **2011**, *10*, 188–195.

9 H. Al-Ali, *Med. Chem. Commun.* **2016**, *7*, 788–798.

10 J. Hughes, S. Rees, S. Kalindjian, K. Philpott, *Br. J. Pharmacol.* **2011**, *162*, 1239–1249.

11 W. E. Childers, K. M. Elokely, M. Abou-Gharbia, *ACS Med. Chem. Lett.* **2020**, doi: 10.1021/acsmedchemlett.0c00006.

12 D. A. Erlanson, R. S. McDowell, T. O'Brien, *J. Med. Chem.* **2004**, *47*, 3463–3482.

13 S. B. Shuker, P. J. Hajduk, R. P. Meadows, S. W. Fesik, *Science* **1996**, *274*, 1531–1534.

14 R. Carr, H. Jhoti, *Drug Discov. Today* **2002**, *7*, 522–527.

15 a) S. Brenner, R. A. Lerner, *Proc. Natl. Acad. Sci. U. S. A.* **1992**, *89*, 5381. b) R. Lerner, K. Janda, S. Brenner, J. Nielsen, ENCODED COMBINATORIAL CHEMICAL LIBRARIES, PCT Int. Appl. WO9320242, 1993.

16 a) M. A. Clark, R. A. Acharya, C. C. Arico-Muendel, S. L. Belyanskaya, D. R. Benjamin, N. R. Carlson, P. A. Centrella, C. H. Chiu, S. P. Creaser, J. W. Cuozzo, et al., *Nat. Chem. Biol.* **2009**, *5*, 647–654. b) L. Mannocci, M. Leimbacher, M. Wichert, J. Scheuermann, D. Neri, *Chem. Commun.* **2011**, *47*, 12747–12753. c) D. T. Flood, C. Kingston, J. C. Vantourout, P. E. Dawson, P. S. Baran, *Isr. J. Chem.* **2020**, 268–280.

17 R. A. Goodnow, C. E. Dumelin, A. D. Keefe, *Nat. Rev. Drug Discov.* **2017**, *16*, 131–147.

18 K. Götte, S. Chines, A. Brunschweiger, *Tetrahedron Lett.* **2020**, *61*, 151889.

19 M. Song, G. T. Hwang, *J. Med. Chem.* **2020**, *63*, 6578–6599.

20 A. Leach, *Drug Discov. Today* **2000**, *5*, 326–336.

21 W. P. Walters, *J. Med. Chem.* **2019**, *62*, 1116–1124.

22 J. W. Scannell, A. Blanckley, H. Boldon, B. Warrington, *Nat. Rev. Drug Discov.* **2012**, *11*, 191–200.

23 A. Mullard, *Nat. Rev. Drug Discov.* **2020**, *19*, 79–84.

24 D. C. Swinney, J. Anthony, *Nat. Rev. Drug Discov.* **2011**, *10*, 507–519.

25 J. Eder, R. Sedrani, C. Wiesmann, *Nat. Rev. Drug Discov.* **2014**, *13*, 577–587.

26 D. G. Brown, J. Boström, *J. Med. Chem.* **2018**, *61*, 9442–9468.

27 K. C. Nicolaou, *Angew. Chem. Int. Ed.*, **2014**, *53*, 9128–9140.

28 a) R. Lahana, *Drug Discov. Today* **2003**, *8*, 655–656. b) J.-P. Garnier, *Harv. Bus. Rev.* **2008**, *86*, 68–76.

29 M. J. Waring, J. Arrowsmith, A. R. Leach, P. D. Leeson, S. Mandrell, R. M. Owen, G. Pairaudeau, W. D. Pennie, S. D. Pickett, J. Wang, et al., *Nat. Rev. Drug Discov.* **2015**, *14*, 475–486.

30 I. Kola, J. Landis, *Nat. Rev. Drug Discov.* **2004**, *3*, 711–715.

31 a) D. A. Parasrampuria, L. Z. Benet, A. Sharma, *AAPS J.* **2018**, *20*, 46. b) S. Galson, C. P. Austin, E. Khandekar, L. D. Hudson, J. A. DiMasi, R. Califf, J. A. Wagner, *Nat. Rev. Drug Discov.* **2020**, doi: 10.1038/d41573-020-00167-0.

32 a) M. E. Bunnage, *Nat. Chem. Biol.* **2011**, *7*, 335–339. b) D. Cook, D. Brown, R. Alexander, R. March, P. Morgan, G. Satterthwaite, M. N. Pangalos, *Nat. Rev. Drug Discov.* **2014**, *13*, 419–431.
33 P. D. Leeson, B. Springthorpe, *Nat. Rev. Drug Discov.* **2007**, *6*, 881–890.
34 M. J. Waring, *Expert Opin. Drug Discov.* **2010**, *5*, 235–248.
35 J. A. Arnott, S. L. Planey, *Expert Opin. Drug Discov* **2012**, *7*, 863–875.
36 a) A. P. Hill, R. J. Young, *Drug Discov. Today* **2010**, *15*, 648–655. b) M. M. Hann, *MedChemComm* **2011**, *2*, 349–355.
37 C. A. Lipinski, F. Lombardo, B. W. Dominy, P. J. Feeney, *Adv. Drug Deliv. Rev.* **1997**, *23*, 3–25.
38 J. D. Hughes, J. Blagg, D. A. Price, S. Bailey, G. A. DeCrescenzo, R. V. Devraj, E. Ellsworth, Y. M. Fobian, M. E. Gibbs, R. W. Gilles, et al., *Bioorg. Med. Chem. Lett.* **2008**, *18*, 4872–4875.
39 M. P. Gleeson, *J. Med. Chem.* **2008**, *51*, 817–834.
40 a) D. A. Degoey, H. J. Chen, P. B. Cox, M. D. Wendt, *J. Med. Chem.* **2018**, *61*, 2636–2651. b) M. D. Shultz, *J. Med. Chem.* **2019**, *62*, 1701–1714.
41 M. Pettersson, C. M. Crews, *Drug Discov. Today Technol.* **2019**, *31*, 15–27.
42 a) D. A. DeGoey, H.-J. Chen, P. B. Cox, M. D. Wendt, *J. Med. Chem.* **2018**, *61*, 2636–2651. b) J. M. Sanders, D. C. Beshore, J. C. Culberson, J. I. Fells, J. E. Imbriglio, H. Gunaydin, A. M. Haidle, M. Labroli, B. E. Mattioni, N. Sciammetta, et al., *J. Med. Chem.* **2017**, *60*, 6771–6780. c) L. Z. Benet, C. M. Hosey, O. Ursu, T. I. Oprea, *Adv. Drug Deliv. Rev.* **2016**, *101*, 89–98.
43 T. Yukawa, R. Naven, *ACS Med. Chem. Lett.* **2020**, *11*, 203–209.
44 a) M. M. Hann, G. M. Keserü, *Nat. Rev. Drug Discov.* **2012**, *11*, 355–365. b) P. D. Leeson, R. J. Young, *ACS Med. Chem. Lett.* **2015**, *6*, 722–725.
45 R. J. Young, D. V. S. Green, C. N. Luscombe, A. P. Hill, *Drug Discov. Today* **2011**, *16*, 822–830.
46 M. M. Hann, A. R. Leach, G. Harper, *J. Chem. Inf. Comput. Sci.* **2001**, *41*, 856–864.
47 T. J. Ritchie, S. J. F. Macdonald, *Drug Discov. Today* **2009**, *14*, 1011–1020.
48 G. L. Trainor, *Expert Opin. Drug Discov.* **2007**, *2*, 51–64.
49 C. Jamieson, E. M. Moir, Z. Rankovic, G. Wishart, *J. Med. Chem.* **2006**, *49*, 5029–5046.
50 D. Lewis, *Drug Discov. Today* **2002**, *7*, 918–925.
51 E. A. Meyer, R. K. Castellano, F. Diederich, *Angew. Chem. Int. Ed.* **2003**, *42*, 1210–1250.
52 S. E. Ward, P. Beswick, *Expert Opin. Drug Discov.* **2014**, *9*, 995–1003.
53 T. J. Ritchie, S. J. F. MacDonald, R. J. Young, S. D. Pickett, *Drug Discov. Today* **2011**, *16*, 164–171.
54 T. J. Ritchie, S. J. F. Macdonald, *Eur. J. Med. Chem.* **2016**, *124*, 1057–1068.
55 T. J. Ritchie, S. J. F. Macdonald, S. Peace, S. D. Pickett, C. N. Luscombe, *MedChemComm* **2012**, *3*, 1062.
56 H. Gunaydin, M. D. Bartberger, *ACS Med. Chem. Lett.* **2016**, *7*, 341–344.
57 F. Lovering, J. Bikker, C. Humblet, *J. Med. Chem.* **2009**, *52*, 6752–6756.
58 P. D. Leeson, S. A. St-Gallay, M. C. Wenlock, *MedChemComm* **2011**, *2*, 91–105.
59 P. A. Clemons, N. E. Bodycombe, H. A. Carrinski, J. A. Wilson, A. F. Shamji, B. K. Wagner, A. N. Koehler, S. L. Schreiber, *Proc. Natl. Acad. Sci. U. S. A.* **2010**, *107*, 18787–18792.
60 A. R. Leach, M. M. Hann, *Curr. Opin. Chem. Biol.* **2011**, *15*, 489–496.
61 J. Meyers, M. Carter, N. Y. Mok, N. Brown, *Future Med. Chem.* **2016**, *8*, 1753–1767.
62 F. Lovering, *MedChemComm* **2013**, *4*, 515–519.
63 S. Kortagere, M. D. Krasowski, S. Ekins, *Trends Pharmacol. Sci.* **2009**, *30*, 138–147.
64 B. Cox, V. Zdorichenko, P. B. Cox, K. I. Booker-Milburn, R. Paumier, L. D. Elliott, M. Robertson-Ralph, G. Bloomfield, *ACS Med. Chem. Lett.* **2020**, *11*, 1185–1190.

65 a) A. R. Leach, V. J. Gillet, R. A. Lewis, R. Taylor, *J. Med. Chem.* **2010**, *53*, 539–558. b) K. E. Prosser, R. W. Stokes, S. M. Cohen, *ACS Med. Chem. Lett.* **2020**, *11*, 1292–1298.

66 U. Lessel, C. Lemmen, *ACS Med. Chem. Lett.* **2019**, *10*, 1504–1510.

67 a) R. S. Bohacek, C. McMartin, W. C. Guida, *Med. Res. Rev.* **1996**, *16*, 3–50. b) C. M. Dobson, *Nature* **2004**, *432*, 824–828. c) C. A. Lipinski, A. Hopkins, *Nature* **2004**, *432*, 855–861.

68 a) M. Krier, G. Bret, D. Rognan, *J. Chem. Inf. Model.* **2006**, *46*, 512–524. b) A. A. Shelat, R. K. Guy, *Nat. Chem. Biol.* **2007**, *3*, 442–446.

69 A. H. Lipkus, Q. Yuan, K. A. Lucas, S. A. Funk, W. F. Bartelt, R. J. Schenck, A. J. Trippe, *J. Org. Chem.* **2008**, *73*, 4443–4451.

70 A. H. Lipkus, S. P. Watkins, K. Gengras, M. J. McBride, T. J. Wills, *J. Org. Chem.* **2019**, *84*, 13948–13956.

71 R. D. Taylor, M. MacCoss, A. D. G. Lawson, *J. Med. Chem.* **2014**, *57*, 5845–5859.

72 M. Aldeghi, S. Malhotra, D. L. Selwood, A. W. E. Chan, *Chem. Biol. Drug Des.* **2014**, *83*, 450–461.

73 M. Garcia-Castro, S. Zimmermann, M. G. Sankar, K. Kumar, *Angew. Chem. Int. Ed.* **2016**, *55*, 7586–7605.

74 a) S. D. Roughley, A. M. Jordan, *J. Med. Chem.* **2011**, *54*, 3451–3479. b) D. G. Brown, J. Boström, *J. Med. Chem.* **2016**, *59*, 4443–4458. c) N. Schneider, D. M. Lowe, R. A. Sayle, M. A. Tarselli, G. A. Landrum, *J. Med. Chem.* **2016**, *59*, 4385–4402. d) J. Boström, D. G. Brown, *Drug Discov. Today* **2016**, *21*, 701–703.

75 a) R. W. Dugger, J. A. Ragan, D. H. B. Ripin, *Org. Process Res. Dev.* **2005**, *9*, 253–258. b) J. S. Carey, D. Laffan, C. Thomson, M. T. Williams, *Org. Biomol. Chem.* **2006**, *4*, 2337–2347. c) A. C. Flick, C. A. Leverett, H. X. Ding, E. McInturff, S. J. Fink, C. J. Helal, J. C. DeForest, P. D. Morse, S. Mahapatra, C. J. O'Donnell, *J. Med. Chem.* **2020**, doi: 10.1021/acs.jmedchem.0c00345.

76 D. G. Brown, M. M. Gagnon, J. Boström, *J. Med. Chem.* **2015**, *58*, 2390–2405.

77 J. Boström, D. G. Brown, R. J. Young, G. M. Keserü, *Nat. Rev. Drug Discov.* **2018**, *17*, 709–727.

78 a) W. P. Walters, J. Green, J. R. Weiss, M. A. Murcko, *J. Med. Chem.* **2011**, *54*, 6405–6416. b) S. Y. Chow, A. Nelson, *J. Med. Chem.* **2017**, *60*, 3591–3593.

79 D. P. Rotella, *ACS Chem. Neurosci.* **2016**, *7*, 1315–1316.

80 K. R. Campos, P. J. Coleman, J. C. Alvarez, S. D. Dreher, R. M. Garbaccio, N. K. Terrett, R. D. Tillyer, M. D. Truppo, E. R. Parmee, *Science* **2019**, *363*, eaat0805.

81 O. O. Grygorenko, D. M. Volochnyuk, S. V. Ryabukhin, D. B. Judd, *Chem. Eur. J.* **2019**, 1196–1237.

82 a) M. Yan, P. S. Baran, *Org. Process Res. Dev.* **2017**, *21*, 1091–1094. b) D. J. Foley, A. Nelson, S. P. Marsden, *Angew. Chem. Int. Ed.* **2016**, *55*, 13650–13657.

83 D. C. Blakemore, L. Castro, I. Churcher, D. C. Rees, A. W. Thomas, D. M. Wilson, A. Wood, *Nat. Chem.* **2018**, *10*, 383–394.

84 F. W. Goldberg, J. G. Kettle, T. Kogej, M. W. D. Perry, N. P. Tomkinson, *Drug Discov. Today* **2015**, *20*, 11–17.

85 T. I. Oprea, A. M. Davis, S. J. Teague, P. D. Leeson, *J. Chem. Inf. Model.* **2001**, *41*, 1308–1315.

86 a) M. M. Hann, T. I. Oprea, *Curr. Opin. Chem. Biol.* **2004**, *8*, 255–263. b) C. A. Lipinski, *Drug Discov. Today Technol.* **2004**, *1*, 337–341. c) G. M. Rishton, *Curr. Opin. Chem. Biol.* **2008**, *12*, 340–351.

87 A. Nadin, C. Hattotuwagama, I. Churcher, *Angew. Chem. Int. Ed.* **2012**, *51*, 1114–1122.

88 a) J. Baell, M. A. Walters, *Nature* **2014**, *513*, 481–483. b) J. L. Dahlin, M. A. Walters, *Future Med. Chem.* **2014**, *6*, 1265–1290. c) A. S. Kalgutkar, *J. Med. Chem.* **2020**, *63*, 6276–6302.

89 a) R. Doveston, S. Marsden, A. Nelson, *Drug Discov. Today* **2014**, *19*, 813–819. b) B. Raymer, S. K. Bhattacharya, *J. Med. Chem.* **2018**, *61*, 10375–10384.

90 R. J. Hall, P. N. Mortenson, C. W. Murray, *Prog. Biophys. Mol. Biol.* **2014**, *116*, 82–91.

91 a) N. Fuller, L. Spadola, S. Cowen, J. Patel, H. Schönherr, Q. Cao, A. McKenzie, F. Edfeldt, A. Rabow, R. Goodnow, *Drug Discov. Today* **2016**, *21*, 1272–1283. b) D. A. Erlanson, A. C. Braisted, D. R. Raphael, M. Randal, R. M. Stroud, E. M. Gordon, J. A. Wells, *Proc. Natl. Acad. Sci. U. S. A.* **2000**, *97*, 9367–9372. c) G. G. Ferenczy, G. M. Keserű, *J. Med. Chem.* **2013**, *56*, 2478–2486.

92 C. W. Murray, D. C. Rees, *Nat. Chem.* **2009**, *1*, 187–192.

93 M. Congreve, R. Carr, C. Murray, H. Jhoti, *Drug Discov. Today* **2003**, *8*, 876–877.

94 C. W. Murray, D. C. Rees, *Angew. Chem. Int. Ed.* **2016**, *55*, 488–492.

95 a) D. A. Erlanson, S. W. Fesik, R. E. Hubbard, W. Jahnke, H. Jhoti, *Nat. Rev. Drug Discov.* **2016**, *15*, 605–619. b) D. A. Erlanson, I. J. P. de Esch, W. Jahnke, C. N. Johnson, P. N. Mortenson, *J. Med. Chem.* **2020**, *63*, 4430–4444.

96 G. M. Keserű, D. A. Erlanson, G. G. Ferenczy, M. M. Hann, C. W. Murray, S. D. Pickett, *J. Med. Chem.* **2016**, *59*, 8189–8206.

97 A. D. Morley, A. Pugliese, K. Birchall, J. Bower, P. Brennan, N. Brown, T. Chapman, M. Drysdale, I. H. Gilbert, S. Hoelder, et al., *Drug Discov. Today* **2013**, *18*, 1221–1227.

98 a) C. N. Johnson, D. A. Erlanson, C. W. Murray, D. C. Rees, *J. Med. Chem.* **2017**, *60*, 89–99. b) C. N. Johnson, D. A. Erlanson, W. Jahnke, P. N. Mortenson, D. C. Rees, *J. Med. Chem.* **2018**, *61*, 1774–1784. c) P. N. Mortenson, D. A. Erlanson, I. J. P. de Esch, W. Jahnke, C. N. Johnson, *J. Med. Chem.* **2019**, *62*, 3857–3872. d) J. A. Johnson, C. A. Nicolaou, S. E. Kirberger, A. K. Pandey, H. Hu, W. C. K. Pomerantz, *ACS Med. Chem. Lett.* **2019**, *10*, 1648–1654.

99 a) B. Lamoree, R. E. Hubbard, *Essays Biochem.* **2017**, *61*, 453–464. b) C. Jacquemard, E. Kellenberger, *Expert Opin. Drug Discov.* **2019**, *14*, 413–416. c) D. E. Scott, A. G. Coyne, A. Venkitaraman, T. L. Blundell, C. Abell, M. Hyvönen, *ChemMedChem* **2015**, *10*, 296–303. d) Y. Cheng, T. C. Judd, M. D. Bartberger, J. Brown, K. Chen, R. T. Fremeau, D. Hickman, S. A. Hitchcock, B. Jordan, V. Li, et al., *J. Med. Chem.* **2011**, *54*, 5836–5857. e) F. Giordanetto, D. Pettersen, I. Starke, P. Nordberg, M. Dahlström, L. Knerr, N. Selmi, B. Rosengren, L.-O. Larsson, J. Sandmark, et al., *ACS Med. Chem. Lett.* **2016**, *7*, 884–889. f) X. Guillory, M. Wolter, S. Leysen, J. F. Neves, A. Kuusk, S. Genet, B. Somsen, J. K. Morrow, E. Rivers, L. van Beek, et al., *J. Med. Chem.* **2020**, *63*, 6694–6707.

100 A. Bancet, C. Raingeval, T. Lomberget, M. Le Borgne, J.-F. Guichou, I. Krimm, *J. Med. Chem.* **2020**, doi: 10.1021/acs.jmedchem.0c00242.

101 A. Trapero, A. Pacitto, V. Singh, M. Sabbah, A. G. Coyne, V. Mizrahi, T. L. Blundell, D. B. Ascher, C. Abell, *J. Med. Chem.* **2018**, *61*, 2806–2822.

102 D. M. George, E. C. Breinlinger, M. Friedman, Y. Zhang, J. Wang, M. Argiriadi, P. Bansal-Pakala, M. Barth, D. B. Duignan, P. Honore, et al., *J. Med. Chem.* **2015**, *58*, 222–236.

103 S. L. Schreiber, *Science* **2000**, *287*, 1964–1969.

104 a) M. D. Burke, *Science* **2003**, *302*, 613–618. b) K. M. G. O'Connell, W. R. J. D. Galloway, D. R. Spring in *Diversity-Oriented Synthesis: Basics and Applications in Organic Synthesis, Drug Discovery, and Chemical Biology*, (Eds.: A. Trabocchi), John Wiley & Sons, Inc., Hoboken, NJ, USA, **2013**, pp. 1–26.

105 a) M. D. Burke, S. L. Schreiber, *Angew. Chem. Int. Ed.* **2004**, *43*, 46–58. b) W. R. J. D. Galloway, D. R. Spring, *Divers. Oriented Synth.* **2013**, *1*, 21–28.

106 a) T. E. Nielsen, S. L. Schreiber, *Angew. Chem. Int. Ed.* **2008**, *47*, 48–56. b) W. R. J. D. Galloway, D. R. Spring, *Nat. Commun.* **2010**, *1*, 80.

107 S. Dandapani, L. A. Marcaurelle, *Curr. Opin. Chem. Biol.* **2010**, *14*, 362–370.

108 H. S. G. Beckmann, F. Nie, C. E. Hagerman, H. Johansson, Y. S. Tan, D. Wilcke, D. R. Spring, *Nat. Chem.* **2013**, *5*, 861–867.

109 D. Morton, S. Leach, C. Cordier, S. Warriner, A. Nelson, *Angew. Chem. Int. Ed.* **2009**, *48*, 104–109.

110 a) A. Deiters, S. F. Martin, *Chem. Rev*. **2004**, *104*, 2199–2238. b) C. O'Leary-Steele, P. J. Pedersen, T. James, T. Lanyon-Hogg, S. Leach, J. Hayes, A. Nelson, *Chem. Eur. J.* **2010**, *16*, 9563–9571.

111 W. R. J. D. Galloway, D. R. Spring, *Expert Opin. Drug Discov.* **2009**, *4*, 467–472.

112 a) A. Nören-Müller, I. Reis-Corrêa, H. Prinz, C. Rosenbaum, K. Saxena, H. J. Schwalbe, D. Vestweber, G. Cagna, S. Schunk, O. Schwarz, et al., *Proc. Natl. Acad. Sci. U. S. A*. **2006**, *103*, 10606–10611. b) H. Waldmann, *Nat. Chem. Biol.* **2009**, *5*, 76–77. c) I. Pavlinov, E. M. Gerlach, L. N. Aldrich, *Org. Biomol. Chem.* **2019**, *17*, 1608–1623.

113 a) S. Oh, S. B. Park, *Chem. Commun.* **2011**, *47*, 12754. b) W.-M. Dai, *Divers. Oriented Synth.* **2012**, *1*, 11–20. c) J. Kim, H. Kim, S. B. Park, *J. Am. Chem. Soc.* **2014**, *136*, 14629–14638.

114 a) E. Lenci, G. Menchi, A. Trabocchi, *Org. Biomol. Chem.* **2016**, *14*, 808–825. b) J. J. Ciardiello, W. R. J. D. Galloway, C. J. O'Connor, H. F. Sore, J. E. Stokes, Y. Wu, D. R. Spring, *Tetrahedron* **2016**, *72*, 3567–3578. c) J. Chauhan, T. Luthra, R. Gundla, A. Ferraro, U. Holzgrabe, S. Sen, *Org. Biomol. Chem.* **2017**, *15*, 9108–9120. d) Y. Gu, C. Tan, J. Gong, Z. Yang, *Synlett* **2018**, *29*, 1552–1571. e) S. Z. Tasker, A. E. Cowfer, P. J. Hergenrother, *Org. Lett.* **2018**, *20*, 5894–5898. f) G. Karageorgis, E. S. Reckzeh, J. Ceballos, M. Schwalfenberg, S. Sievers, C. Ostermann, A. Pahl, S. Ziegler, H. Waldmann, *Nat. Chem.* **2018**, *10*, 1103–1111. g) P. Verma, A. Chandra, G. Pandey, *J. Org. Chem.* **2018**, *83*, 9968–9977.

115 T. J. Pawar, H. Jiang, M. A. Vázquez, C. Villegas Gómez, D. Cruz Cruz, *Eur. J. Org. Chem.* **2018**, *2018*, 1835–1851.

116 For medicinal importance of macrocycles: F. Giordanetto, J. Kihlberg, *J. Med. Chem.* **2014**, *57*, 278–295.

117 For a review see: a) K. T. Mortensen, T. J. Osberger, T. A. King, H. F. Sore, D. R. Spring, *Chem. Rev.* **2019**, *119*, 10288–10317. b) L. A. Marcaurelle, E. Comer, S. Dandapani, J. R. Duvall, B. Gerard, S. Kesavan, M. D. Lee, H. Liu, J. T. Lowe, J.-C. Marie, et al., *J. Am. Chem. Soc.* **2010**, *132*, 16962–16976. c) R. W. Heidebrecht, C. Mulrooney, C. P. Austin, R. H. Barker, J. A. Beaudoin, K. C.-C. Cheng, E. Comer, S. Dandapani, J. Dick, J. R. Duvall, et al., *ACS Med. Chem. Lett.* **2012**, *3*, 112–117. d) A. Grossmann, S. Bartlett, M. Janecek, J. T. Hodgkinson, D. R. Spring, *Angew. Chem. Int. Ed.* **2014**, *53*, 13093–13097. e) A. Isidro-Llobet, K. Hadje Georgiou, W. R. J. D. Galloway, E. Giacomini, M. R. Hansen, G. Méndez-Abt, Y. S. Tan, L. Carro, H. F. Sore, D. R. Spring, *Org. Biomol. Chem.* **2015**, *13*, 4570–4580. f) S. Collins, S. Bartlett, F. Nie, H. Sore, D. Spring, *Synthesis* **2016**, *48*, 1457–1473. g) M. Dow, F. Marchetti, K. A. Abrahams, L. Vaz, G. S. Besra, S. Warriner, A. Nelson, *Chem. Eur. J.* **2017**, *23*, 7207–7211. h) A. Guarnieri-Ibáñez, F. Medina, C. Besnard, S. L. Kidd, D. R. Spring, J. Lacour, *Chem. Sci.* **2017**, *8*, 5713–5720. i) J. Zhang, M. Mulumba, H. Ong, W. D. Lubell, *Angew. Chem. Int. Ed.* **2017**, *56*, 6284–6288. j) J. J. Ciardiello, H. L. Stewart, H. F. Sore, W. R. J. D. Galloway, D. R. Spring, *Bioorg. Med. Chem.* **2017**, *25*, 2825–2843.

118 a) S. Bera, G. Panda, *ACS Comb. Sci.* **2012**, *14*, 1–4. b) R. Maltais, D. Poirier, *Eur. J. Org. Chem.* **2012**, *2012*, 5435–5439. c) Y.-C. Lee, S. Patil, C. Golz, C. Strohmann, S. Ziegler, K. Kumar, H. Waldmann, *Nat. Commun.* **2017**, *8*, 14043. d) D. J. Foley, P. G. E. Craven, P. M. Collins, R. G. Doveston, A. Aimon, R. Talon, I. Churcher, F. von Delft, S. P. Marsden, A. Nelson, *Chem. Eur. J.* **2017**, *23*, 15227–15232. e) J.-K. Yu, H.-W. Chien, Y.-J. Lin, P. Karanam, Y.-H. Chen, W. Lin, *Chem. Commun.* **2018**, *54*, 9921–9924. f) S. Mai, Y. Luo, X. Huang, Z. Shu, B. Li, Y. Lan, Q. Song, *Chem. Commun.* **2018**, *54*, 10240–10243. g) N. Mateu, S. L. Kidd, L. Kalash, H. F. Sore, A. Madin, A. Bender, D. R. Spring, *Chem. Eur. J.* **2018**, *24*, 13681–13687. h) H. P. A. Khan, T. K.

Chakraborty, *J. Org. Chem.* **2018**, *83*, 2027–2039. i) T. Liu, W. Jia, Q. Xi, Y. Chen, X. Wang, D. Yin, *J. Org. Chem.* **2018**, *83*, 1387–1393.

119 a) J. T. Lowe, M. D. Lee, L. B. Akella, E. Davoine, E. J. Donckele, L. Durak, J. R. Duvall, B. Gerard, E. B. Holson, A. Joliton, et al., *J. Org. Chem.* **2012**, *77*, 7187–7211. b) N. Kato, E. Comer, T. Sakata-Kato, A. Sharma, M. Sharma, M. Maetani, J. Bastien, N. M. Brancucci, J. A. Bittker, V. Corey, et al., *Nature* **2016**, *538*, 344–349.

120 a) H. Pajouhesh, G. R. Lenz, *NeuroRX* **2005**, *2*, 541–553. b) S. A. Hitchcock, L. D. Pennington, *J. Med. Chem.* **2006**, *49*, 7559–7583. c) Z. Rankovic, *J. Med. Chem.* **2015**, *58*, 2584–2608.

121 a) C. Agami, F. Couty, G. Evano, *Tetrahedron: Asymmetry* **2002**, *13*, 297–302. b) F. Couty, B. Drouillat, G. Evano, O. David, *Eur. J. Org. Chem.* **2013**, *2013*, 2045–2056. c) P. Quinodoz, B. Drouillat, K. Wright, J. Marrot, F. Couty, *J. Org. Chem.* **2016**, *81*, 2899–2910.

122 M. Maetani, N. Kato, V. A. P. Jabor, F. A. Calil, M. C. Nonato, C. A. Scherer, S. L. Schreiber, *ACS Med. Chem. Lett.* **2017**, *8*, 438–442.

123 a) G. M. Rishton, *Curr. Opin. Chem. Biol.* **2008**, *12*, 340–351. b) S. V. Ryabukhin, D. M. Panov, D. S. Granat, E. N. Ostapchuk, D. V. Kryvoruchko, O. O. Grygorenko, *ACS Comb. Sci.* **2014**, *16*, 146–153. c) E. Lenci, R. Innocenti, G. Menchi, A. Trabocchi, *Front. Chem.* **2018**, *6*, 522.

124 For a review see: a) R. Doveston, S. Marsden, A. Nelson, *Drug Discov. Today* **2014**, *19*, 813–819. b) D. J. Foley, PhD Thesis, University of Leeds (UK), **2015**. c) D. J. Foley, R. G. Doveston, I. Churcher, A. Nelson, S. P. Marsden, *Chem. Commun.* **2015**, *51*, 11174–11177. d) A. Karawajczyk, F. Giordanetto, J. Benningshof, D. Hamza, T. Kalliokoski, K. Pouwer, R. Morgentin, A. Nelson, G. Müller, A. Piechot, et al., *Drug Discov. Today* **2015**, *20*, 1310–1316. e) R. G. Doveston, P. Tosatti, M. Dow, D. J. Foley, H. Y. Li, A. J. Campbell, D. House, I. Churcher, S. P. Marsden, A. Nelson, *Org. Biomol. Chem.* **2015**, *13*, 859–865. f) J. D. Firth, P. G. E. Craven, M. Lilburn, A. Pahl, S. P. Marsden, A. Nelson, *Chem. Commun.* **2016**, *52*, 9837–9840. g) D. J. Foley, P. G. E. Craven, P. M. Collins, R. G. Doveston, A. Aimon, R. Talon, I. Churcher, F. von Delft, S. P. Marsden, A. Nelson, *Chem. Eur. J.* **2017**, *23*, 15227–15232. h) S. Rice, D. J. Cox, S. P. Marsden, A. Nelson, *Tetrahedron* **2019**, *75*, 130513.

125 M. Lüthy, M. C. Wheldon, C. Haji-Cheteh, M. Atobe, P. S. Bond, P. O'Brien, R. E. Hubbard, I. J. S. Fairlamb, *Bioorg. Med. Chem.* **2015**, *23*, 2680–2694.

126 J. L. Bilke, S. P. Moore, P. O'Brien, J. Gilday, *Org. Lett.* **2009**, *11*, 1935–1938.

127 J. Mayol-Llinàs, W. Farnaby, A. Nelson, *Chem. Commun.* **2017**, *53*, 12345–12348.

128 J. Mayol-Llinàs, A. Nelson, W. Farnaby, A. Ayscough, *Drug Discov. Today* **2017**, *22*, 965–969.

129 a) G. Karageorgis, S. Warriner, A. Nelson, *Nat. Chem.* **2014**, *6*, 872–876. b) G. Karageorgis, M. Dow, A. Aimon, S. Warriner, A. Nelson, *Angew. Chem. Int. Ed.* **2015**, *54*, 13538–13544. For a review see: c) G. Karageorgis, S. Liver, A. Nelson, *ChemMedChem* **2020**, doi: 10.1002/cmdc.202000524.

130 a) A. Green, F. Hobor, C. Tinworth, S. Warriner, A. Wilson, A. Nelson, *Chem. Eur. J.* **2020**, *26*,10682–10689. b) A. Leggott, J. E. Clarke, S. Chow, S. L. Warriner, A. J. O'Neill, A. Nelson, *Chem. Commun.* **2020**, *15*, 106–119.

131 S. L. Kidd, T. J. Osberger, N. Mateu, H. F. Sore, D. R. Spring, *Front. Chem.* **2018**, *6*, 460.

132 A. W. Hung, A. Ramek, Y. Wang, T. Kaya, J. A. Wilson, P. A. Clemons, D. W. Young, *Proc. Natl. Acad. Sci. U. S. A* **2011**, *108*, 6799–6804.

133 S. Haftchenary, S. D. Nelson, L. Furst, S. Dandapani, S. J. Ferrara, Ž. V. Bošković, S. Figueroa Lazú, A. M. Guerrero, J. C. Serrano, D. K. Crews, et al., *ACS Comb. Sci.* **2016**, *18*, 569–574.

134 a) H. Hassan, S. P. Marsden, A. Nelson, *Bioorg. Med. Chem.* **2018**, *26*, 3030–3033. b) R. Zhang, P. J. McIntyre, P. M. Collins, D. J. Foley, C. Arter, F. von Delft, R. Bayliss, S. Warriner, A. Nelson, *Chem. Eur. J.* **2019**, *25*,

6831–6839. c) A. R. Hanby, N. S. Troelsen, T. J. Osberger, S. L. Kidd, K. T. Mortensen, D. R. Spring, *Chem. Commun.* **2020**, *56*, 2280–2283. d) A. Trindade, E. Faulkner, A. Leach, A. Nelson, S. P. Marsden, *Chem. Commun.* **2020**, *56*, 8802–8805.

135 A. Sveiczer, A. J. P. North, N. Mateu, S. L. Kidd, H. F. Sore, D. R. Spring, *Org. Lett.* **2019**, *21*, 4600–4604.

136 T. A. King, H. L. Stewart, K. T. Mortensen, A. J. P. North, H. F. Sore, D. R. Spring, *Eur. J. Org. Chem.* **2019**, *2019*, 5219–5229.

137 N. Mateu, S. L. Kidd, L. Kalash, H. F. Sore, A. Madin, A. Bender, D. R. Spring, *Chem. Eur. J.* **2018**, *24*, 13681–13687.

138 D. G. Twigg, N. Kondo, S. L. Mitchell, W. R. J. D. Galloway, H. F. Sore, A. Madin, D. R. Spring, *Angew. Chem. Int. Ed.* **2016**, *55*, 12479–12483.

139 Y. Wang, J.-Y. Wach, P. Sheehan, C. Zhong, C. Zhan, R. Harris, S. C. Almo, J. Bishop, S. J. Haggarty, A. Ramek, et al., *ACS Med. Chem. Lett.* **2016**, *7*, 852–856.

140 S. L. Kidd, E. Fowler, T. Reinhardt, T. Compton, N. Mateu, H. Newman, D. Bellini, R. Talon, J. McLoughlin, T. Krojer, et al., *Chem. Sci.* **2020**, doi: 10.1039/D0SC01232G.

141 a) H.-J. Roth, *Curr. Opin. Chem. Biol.* **2005**, *9*, 293–295. b) Y. C. Martin, *Il Farmico* **2001**, *56*, 137–139.

142 A. Koutsoukas, S. Paricharak, W. R. J. D. Galloway, D. R. Spring, A. P. IJzerman, R. C. Glen, D. Marcus, A. Bender, *J. Chem. Inf. Model.* **2014**, *54*, 230–242.

143 G. Maggiora, M. Vogt, D. Stumpfe, J. Bajorath, *J. Med. Chem.* **2014**, *57*, 3186–3204.

144 P. Willett, J. M. Barnard, G. M. Downs, B. C. Information, U. Road, S. Sheffield, *J. Chem. Inf. Comput. Sci.* **1998**, *38*, 983–996.

145 Y. C. Martin, J. L. Kofron, L. M. Traphagen, *J. Med. Chem.* **2002**, *45*, 4350–4358.

146 a) A. Bender, *Expert Opin. Drug Discov.* **2010**, *5*, 1141–1151. b) J. Duan, S. L. Dixon, J. F. Lowrie, W. Sherman, *J. Mol. Graph. Model.* **2010**, *29*, 157–170.

147 D. C. Kombo, K. Tallapragada, R. Jain, J. Chewning, A. A. Mazurov, J. D. Speake, T. A. Hauser, S. Toler, *J. Chem. Inf. Model.* **2013**, *53*, 327–342.

148 W. H. B. Sauer, M. K. Schwarz, *J. Chem. Inf. Comput. Sci.* **2003**, *43*, 987–1003.

149 N. C. Firth, N. Brown, J. Blagg, *J. Chem. Inf. Model.* **2012**, *52*, 2516–2525.

150 L. B. Akella, D. DeCaprio, *Curr. Opin. Chem. Biol.* **2010**, *14*, 325–330.

151 Y. Shi, M. von Itzstein, *Molecules* **2019**, *24*, 2838–2848.

152 I. Colomer, C. J. Empson, P. Craven, Z. Owen, R. G. Doveston, I. Churcher, S. P. Marsden, A. Nelson, *Chem. Commun.* **2016**, *52*, 7209–7212.

153 For a further recent example see: T. D. Downes, S. P. Jones, H. F. Klein, M. C. Wheldon, M. Atobe, P. S. Bond, J. D. Firth, N. S. Chan, L. Waddelove, R. E. Hubbard, et al., *Chem. Eur. J.* **2020**, *26*, 8969–8975.

154 S. J. Chawner, M. J. Cases-Thomas, J. A. Bull, *Eur. J. Org. Chem.* **2017**, *2017*, 5015–5024.

155 G. Wuitschik, M. Rogers-Evans, K. Müller, H. Fischer, B. Wagner, F. Schuler, L. Polonchuk, E. M. Carreira, *Angew. Chem. Int. Ed.* **2006**, *45*, 7736–7739.

156 J. A. Bull, R. A. Croft, O. A. Davis, R. Doran, K. F. Morgan, *Chem. Rev.* **2016**, *116*, 12150–12233.

157 N. A. Meanwell in *Tactics in Contemporary Drug Design. Topics in Medicinal Chemistry*, Vol 9, (Eds.: N. A. Meanwell), Springer, Berlin, Heidelberg, **2013**, pp. 283–381.

158 J. A. Burkhard, G. Wuitschik, M. Rogers-Evans, K. Müller, E. M. Carreira, *Angew. Chem. Int. Ed.* **2010**, *49*, 9052–9067

159 C. White, M. A. McGowan, H. Zhou, N. Sciammetta, X. Fradera, J. Lim, E. M. Joshi, C. Andrews, E. B. Nickbarg, P. Cowley, et al., *ACS Med. Chem. Lett.* **2020**, *11*, 550–557.

160 a) H. Aoki, M. Okuhara, *Annu. Rev. Microbiol.* **1980**, *34*, 159–181. b) K.-F. Kong, L. Schneper, K. Mathee, *APMIS* **2010**, *118*, 1–36.

161 A. Brandi, S. Cicchi, F. M. Cordero, *Chem. Rev.* **2008**, *108*, 3988–4035.

162 a) D. S. Palacios, E. L. Meredith, T. Kawanami, C. M. Adams, X. Chen, V. Darsigny, M. Palermo, D. Baird, E. L. George, C. Guy, et al., *ACS Med. Chem. Lett.* **2019**, *10*, 1524–1529. b) V. S. Gehling, J. P. McGrath, M. Duplessis, A. Khanna, F. Brucelle, R. G. Vaswani, A. Côté, J. Stuckey, V. Watson, R. T. Cummings, et al., *ACS Med. Chem. Lett.* **2020**, *11*, 1213–1220.

163 K. F. Morgan, I. A. Hollingsworth, J. A. Bull, *Chem. Commun.* **2014**, *50*, 5203–5205.

164 T. Aftab, C. Carter, M. Christlieb, J. Hart, A. Nelson, *J. Chem. Soc. Perkin Trans. 1* **2000**, 711–722.

165 K. F. Morgan, I. A. Hollingsworth, J. A. Bull, *Org. Biomol. Chem.* **2015**, *13*, 5265–5272.

166 K. Morgan, R. Doran, R. Croft, I. A. Hollingsworth, J. A. Bull, *Synlett* **2015**, *27*, 106–110.

167 O. A. Davis, J. A. Bull, *Angew. Chem. Int. Ed.* **2014**, *53*, 14230–14234.

168 O. A. Davis, R. A. Croft, J. A. Bull, *Chem. Commun.* **2015**, *51*, 15446–15449.

169 O. A. Davis, R. A. Croft, J. A. Bull, *J. Org. Chem.* **2016**, *81*, 11477–11488.

170 D. Antermite, J. A. Bull, *Synthesis* **2019**, *51*, 3171–3204.

171 V. G. Zaitsev, D. Shabashov, O. Daugulis, *J. Am. Chem. Soc.* **2005**, *127*, 13154–13155.

172 a) W. R. Gutekunst, P. S. Baran, *J. Am. Chem. Soc.* **2011**, *133*, 19076–19079. b) W. R. Gutekunst, R. Gianatassio, P. S. Baran, *Angew. Chem. Int. Ed.* **2012**, *51*, 7507–7510.

173 D. P. Affron, O. A. Davis, J. A. Bull, *Org. Lett.* **2014**, *16*, 4956–4959.

174 D. P. Affron, J. A. Bull, *Eur. J. Org. Chem.* **2016**, *2016*, 139–149.

175 D. Antermite, D. P. Affron, J. A. Bull, *Org. Lett.* **2018**, *20*, 3948–3952.

176 See ref 170 and V. Hutskalova, P. K. Mykhailiuk, *Org. Biomol. Chem.* **2019**, *17*, 4342–4349.

177 M. Maetani, J. Zoller, B. Melillo, O. Verho, N. Kato, J. Pu, E. Comer, S. L. Schreiber, *J. Am. Chem. Soc.* **2017**, *139*, 11300–11306.

178 M. Shang, K. S. Feu, J. C. Vantourout, L. M. Barton, H. L. Osswald, N. Kato, K. Gagaring, C. W. McNamara, G. Chen, L. Hu, et al., *Proc. Natl. Acad. Sci. U. S. A.* **2019**, *116*, 8721–8727.

179 J. C. Beck, C. R. Lacker, L. M. Chapman, S. E. Reisman, *Chem. Sci.* **2019**, *10*, 2315–2319.

180 T. J. Osberger, S. L. Kidd, T. A. King, D. R. Spring, *Chem. Commun.* **2020**, *56*, 7423–7426.

181 Also see: N. Palmer, T. M. Peakman, D. Norton, D. C. Rees, *Org. Biomol. Chem.* **2016**, *14*, 1599–1610.

182 a) Q. Yang, M. Sheng, J. J. Henkelis, S. Tu, E. Wiensch, H. Zhang, Y. Zhang, C. Tucker, D. E. Ejeh, *Org. Process Res. Dev.* **2019**, *23*, 2210–2217. b) Q. Yang, M. Sheng, Y. Huang, *Org. Process Res. Dev.* **2020**, *24*, 1586–1601.

183 E. Vitaku, D. T. Smith, J. T. Njardarson, *J. Med. Chem.* **2014**, *57*, 10257–10274.

184 D. Antermite, L. Degennaro, R. Luisi, *Org. Biomol. Chem.* **2017**, *15*, 34–50.

185 G.-F. Zha, K. P. Rakesh, H. M. Manukumar, C. S. Shantharam, S. Long, *Eur. J. Med. Chem.* **2019**, *162*, 465–494.

186 3-Membered rings: a) M. Yar, E. M. McGarrigle, V. K. Aggarwal, *Angew. Chem. Int. Ed.* **2008**, *47*, 3784–3786. 4-membered rings b) S. P. Fritz, J. F. Moya, M. G. Unthank, E. M. McGarrigle, V. K. Aggarwal, *Synthesis* **2012**, *44*, 1584–1590. 5-membered rings: c) S. P. Fritz, T. H. West, E. M. McGarrigle, V. K. Aggarwal, *Org. Lett.* **2012**, *14*, 6370–6373. 5- and 6-membered rings: d) M. Yar, S. P. Fritz, P. J. Gates, E. M. McGarrigle, V. K. Aggarwal, *Eur. J. Org. Chem.* **2012**, *2012*, 160–166. 6-membered rings: e) M. Yar, E. M. McGarrigle, V. K. Aggarwal, *Angew. Chem. Int. Ed.* **2008**, *47*, 3784–3786. 6- and 7-membered rings: f) M. Yar, E. M. McGarrigle, V. K.

Aggarwal, *Org. Lett.* **2009**, *11*, 257–260. g) J. V. Matlock, T. D. Svejstrup, P. Songara, S. Overington, E. M. McGarrigle, V. K. Aggarwal, *Org. Lett.* **2015**, *17*, 5044–5047.

187 a) C.-V. T. Vo, G. Mikutis, J. W. Bode, *Angew. Chem. Int. Ed.* **2013**, *52*, 1705–1708. b) M. U. Luescher, J. W. Bode, *Org. Lett.* **2016**, *18*, 2652–2655. c) M. K. Jackl, I. Kreituss, J. W. Bode, *Org. Lett.* **2016**, *18*, 1713–1715.

188 C.-V. T. Vo, M. U. Luescher, J. W. Bode, *Nat. Chem.* **2014**, *6*, 310–314.

189 M. K. Jackl, I. Kreituss, J. W. Bode, *Org. Lett.* **2016**, *18*, 1713–1715.

190 a) S. Y. Hsieh, J. W. Bode, *Org. Lett.* **2016**, *18*, 2098–2101. b) S. Y. Hsieh, J. W. Bode, *ACS Cent. Sci.* **2017**, *3*, 66–72. c) M. K. Jackl, L. Legnani, B. Morandi, J. W. Bode, *Org. Lett.* **2017**, *19*, 4696–4699. d) C. Jindakun, S. Y. Hsieh, J. W. Bode, *Org. Lett.* **2018**, *20*, 2071–2075.

191 a) N. B. Bissonnette, J. M. Ellis, L. G. Hamann, F. Romanov-Michailidis, *Chem. Sci.* **2019**, *10*, 9591–9596. b) R. Gueret, L. Pelinski, T. Bousquet, M. Sauthier, V. Ferey, A. Bigot, *Org. Lett.* **2020**, *22*, 5157–5162.

192 L. R. E. Pantaine, J. A. Milligan, J. K. Matsui, C. B. Kelly, G. A. Molander, *Org. Lett.* **2019**, *21*, 2317–2321.

193 K. N. Betz, N. D. Chiappini, J. Du Bois, *Org. Lett.* **2020**, *22*, 1687–1691.

194 V. R. Bhonde, B. T. O'Neill, S. L. Buchwald, *Angew. Chem. Int. Ed.* **2016**, *55*, 1849–1853.

195 S. Greßies, F. J. R. Klauck, J. H. Kim, C. G. Daniliuc, F. Glorius, *Angew. Chem. Int. Ed.* **2018**, *57*, 9950–9954.

196 a) S. A. Ruider, S. Müller, E. M. Carreira, *Angew. Chem. Int. Ed.* **2013**, *52*, 11908–11911. b) T. Bera, B. Singh, T. A. Hamlin, S. C. Sahoo, J. Saha, *J. Org. Chem.* **2019**, *84*, 15255–15266.

197 a) C. K. Donawho, Y. Luo, Y. Luo, T. D. Penning, J. L. Bauch, J. J. Bouska, V. D. Bontcheva-Diaz, B. F. Cox, T. L. DeWeese, L. E. Dillehay, et al., *Clin. Cancer Res.* **2007**, *13*, 2728–2737. b) D. Xiao, C. Wang, A. Palani, H. C. Tsui, G. Reichard, S. Paliwal, N. Y. Shih, R. Aslanian, R. Duffy, J. Lachowicz, et al., *Bioorg. Med. Chem. Lett.* **2010**, *20*, 6313–6315. c) R. A. Duffy, C. Morgan, R. Naylor, G. A. Higgins, G. B. Varty, J. E. Lachowicz, E. M. Parker, *Pharmacol. Biochem. Behav.* **2012**, *102*, 95–100. d) M. Pizzonero, S. Dupont, M. Babel, S. Beaumont, N. Bienvenu, R. Blanqué, L. Cherel, T. Christophe, B. Crescenzi, E. De Lemos, et al., *J. Med. Chem.* **2014**, *57*, 10044–10057.

198 M. I. Calaza, C. Cativiela, *Eur. J. Org. Chem.* **2008**, *2008*, 3427–3448.

199 a) B. List, *Tetrahedron* **2002**, *58*, 5573–5590. b) W. Notz, F. Tanaka, C. F. Barbas, *Acc. Chem. Res.* **2004**, *37*, 580–591.

200 a) A. S. Anslow, L. M. Harwood, H. Phillips, D. Watkin, L. F. Wong, *Tetrahedron: Asymmetry* **1991**, *2*, 1343–1358. b) A. S. Anslow, L. M. Harwood, I. A. Lilley, *Tetrahedron: Asymmetry* **1995**, *6*, 2465–2468. c) L. M. Harwood, G. Hamblett, A. I. Jiménez-Díaz, D. J. Watkin, *Synlett* **1997**, *1997*, 935–938.

201 J. Maury, J. Clayden, *J. Org. Chem.* **2015**, *80*, 10757–10768.

202 F. Foschi, D. Landini, V. Lupi, V. Mihali, M. Penso, T. Pilati, A. Tagliabue, *Chem. Eur. J.* **2010**, *16*, 10667–10670.

203 a) N. S. Sheikh, D. Leonori, G. Barker, J. D. Firth, K. R. Campos, A. J. H. M. Meijer, P. O'Brien, I. Coldham, *J. Am. Chem. Soc.* **2012**, *134*, 5300–5308. Also see: b) T. K. Beng, J. S. Woo, R. E. Gawley, *J. Am. Chem. Soc.* **2012**, *134*, 14764–14771. c) A. Sadhukhan, M. C. Hobbs, A. J. H. M. Meijer, I. Coldham, *Chem. Sci.* **2017**, *8*, 1436– 1441.

204 K. R. Campos, A. Klapars, J. H. Waldman, P. G. Dormer, C. Y. Chen, *J. Am. Chem. Soc.* **2006**, *128*, 3538–3539.

205 T. Aeyad, J. D. Williams, A. J. H. M. Meijer, I. Coldham, *Synlett* **2017**, *28*, 2765–2768.

206 B. Anxionnat, B. Robert, P. George, G. Ricci, M. A. Perrin, D. Gomez Pardo, J. Cossy, *J. Org. Chem.* **2012**, *77*, 6087–6099.

207 A. Ford, H. Miel, A. Ring, C. N. Slattery, A. R. Maguire, M. A. McKervey, *Chem. Rev.* **2015**, *115*, 9981–10080.

208 a) L. D. Cama, B. G. Christensen, *Tetrahedron Lett.* **1978**, *19*, 4233–4236. b) R. W. Ratcliffe, T. N. Salzmann, B. G. Christensen, *Tetrahedron Lett.* **1980**, *21*, 31–34. c) T. N. Salzmann, R. W. Ratcliffe, B. G. Christensen, F. A. Bouffard, *J. Am. Chem. Soc.* **1980**, *102*, 6161–6163.

209 A. Caballero, P. J. Pérez, *Chem. Eur. J.* **2017**, *23*, 14389–14393.

210 D. Gillingham, N. Fei, *Chem. Soc. Rev.* **2013**, *42*, 4918.

211 M. C. Pirrung, H. Liu, A. T. Morehead, *J. Am. Chem. Soc.* **2002**, *124*, 1014–1023.

212 a) Y. Liang, H. Zhou, Z. X. Yu, *J. Am. Chem. Soc.* **2009**, *131*, 17783–17785. b) H. Huang, X. Guo, W. Hu, *Angew. Chem. Int. Ed.* **2007**, *46*, 1337–1339. c) Z. Li, B. T. Parr, H. M. L. Davies, *J. Am. Chem. Soc.* **2012**, *134*, 10942–10946.

213 R. Paulissen, H. Reimlinger, E. Hayez, A. J. Hubert, P. Teyssié, *Tetrahedron Lett.* **1973**, *14*, 2233–2236.

214 S. A. Johnson, H. R. Hunt, H. M. Neumann, *Inorg. Chem.* **1963**, *2*, 960–962.

215 G. G. Cox, J. J. Kulagowski, C. J. Moody, E.-R. H. B. Sie, *Synlett* **1992**, *1992*, 975–976.

216 C. G. Espino, K. W. Fiori, M. Kim, J. Du Bois, *J. Am. Chem. Soc.* **2004**, *126*, 15378–15379.

217 D. N. Zalatan, J. Du Bois, *J. Am. Chem. Soc.* **2009**, *131*, 7558–7559.

218 a) C. Jing, D. Xing, L. Gao, J. Li, W. Hu, *Chem. Eur. J.* **2015**, *21*, 19202–19207. b) S. M. Nicolle, W. Lewis, C. J. Hayes, C. J. Moody, *Angew. Chem. Int. Ed.* **2016**, *55*, 3749– 3753.

219 A. J. Boddy, D. P. Affron, C. J. Cordier, E. L. Rivers, A. C. Spivey, J. A. Bull, *Angew. Chem. Int. Ed.* **2019**, *58*, 1458–1462.

220 Q. Shi, N. S. Greenwood, M. C. Meehan, H. Park, M. Galella, B. Sandhu, P. Khandelwal, J. R. Coombs, W. P. Gallagher, C. A. Guerrero, et al., *Org. Lett.* **2019**, *21*, 9198–9202.

221 M. Regitz, *Justus Liebigs Ann. Chem.* **1964**, *676*, 101–109.

222 Davies, H. M. L.; Grazini, M. V. A.; Aouad, E. *Org. Lett.* **2001**, *3*, 1475–1477.

223 F. Ye, C. Wang, Y. Zhang, J. Wang, *Angew. Chem. Int. Ed.* **2014**, *53*, 11625–11628.

224 M. Lee, Z. Ren, D. G. Musaev, H. M. L. Davies, *ACS Catal.* **2020**, *10*, 6240–6247.

225 D. Pogocki, T. Ruman, M. Danilczuk, M. Danilczuk, M. Celuch, E. Wałajtys-Rode, *Eur. J. Pharmacol.* **2007**, *563*, 18–39.

226 C. Kadouri-Puchot, S. Comesse, *Amino Acids* **2005**, *29*, 101–130.

227 C. Galli, G. Illuminati, L. Mandolini, P. Tamborra, *J. Am. Chem. Soc.* **1977**, *99*, 2591–2597.

228 G. Illuminati, L. Mandolini, *Acc. Chem. Res.* **1981**, *14*, 95–102.

229 R. M. Beesley, C. K. Ingold, J. F. Thorpe, *J. Chem. Soc., Trans.* **1915**, *107*, 1080–1106.

230 a) C. J. Creighton, G. C. Leo, Y. Du, A. B. Reitz, *Bioorg. Med. Chem.* **2004**, *12*, 4375–4385. b) M. E. Maier, *Angew. Chem. Int. Ed.* **2000**, *39*, 2073–2077.

231 a) A. Klapars, S. Parris, K. W. Anderson, S. L. Buchwald, *J. Am. Chem. Soc.* **2004**, *126*, 3529–3533. b) C. Kitsiou, J. J. Hindes, P. I'Anson, P. Jackson, T. C. Wilson, E. K. Daly, H. R. Felstead, P. Hearnshaw, W. P. Unsworth, *Angew. Chem. Int. Ed.* **2015**, *54*, 15794–15798.

232 a) B. Hong, T. Luo, X. Lei, *ACS Cent. Sci.* **2020**, *6*, 622–635. b) M. Moir, J. J. Danon, T. A. Reekie, M. Kassiou, *Expert Opin. Drug Discov.* **2019**, *14*, 1137–1149.

233 a) T. Cernak, K. D. Dykstra, S. Tyagarajan, P. Vachal, S. W. Krska, *Chem. Soc. Rev.* **2016**, *45*, 546–576. b) J. Börgel, T. Ritter, *Chem* **2020**, *6*, 1877–1887.

234 Y. Sakakibara, E. Ito, T. Fukushima, K. Murakami, K. Itami, *Chem. Eur. J.* **2018**, *24*, 9254–9258.

235 L. S. Gerlis, J. M. Gumpel, *Rheumatology* **1981**, *20*, 50–53.

236 Y. Miyoshi, Y. Tanji, T. Taguchi, Y. Tamaki, S. Noguchi, *Clin. Cancer Res.* **2003**, *9*, 2229–2233.

237 A. Thompson, G. Kabalka, M. Akula, J. Huffman, *Synthesis* **2005**, *4*, 547–550.

238 Reaction of aryl triflate **161** in the reaction conditions of the cross-coupling reaction afforded no product.

239 N. Miyaura, K. Yamada, A. Suzuki, *Tetrahedron Lett.* **1979**, *20*, 3437–3440.

240 T. E. Barder, S. D. Walker, J. R. Martinelli, S. L. Buchwald, *J. Am. Chem. Soc.* **2005**, *127*, 4685–4696.

241 S. P. Green, K. M. Wheelhouse, A. D. Payne, J. P. Hallett, P. W. Miller, J. A. Bull, *Org. Process Res. Dev.* **2020**, *24*, 67–84.

242 M. Yang, T. R. Webb, P. Livant, *J. Org. Chem.* **2001**, *66*, 4945–4949.

243 E. Emer, J. Twilton, M. Tredwell, S. Calderwood, T. L. Collier, B. Liégault, M. Taillefer, V. Gouverneur, *Org. Lett.* **2014**, *16*, 6004–6007.

244 S. Hyde, J. Veliks, B. Liégault, D. Grassi, M. Taillefer, V. Gouverneur, *Angew. Chem. Int. Ed.* **2016**, *55*, 3785–3789.

245 W. H. Brooks, W. C. Guida, K. G. Daniel, *Curr Top Med Chem* **2011**, *11*, 760–770.

246 M. Melchert, A. List, *Int. J. Biochem. Cell Biol.* **2007**, *39*, 1489–1499.

247 L. A. Nguyen, H. He, C. Pham-Huy, *Int. J. Biomed. Sci.* **2006**, *2*, 85–100.

248 N. R. Srinivas, R. H. Barbhaiya, K. K. Midha, *J. Pharm. Sci.* **2001**, *90*, 1205–1215.

249 a) J. Gladysz, J. Michl, *Chem. Rev.* **1992**, *92*, 739–739. b) C. Bolm, J. A. Gladysz, *Chem. Rev.* **2003**, *103*, 2761–2762.

250 For a review see 207. For examples see: a) E. C. Lee, G. C. Fu, *J. Am. Chem. Soc.* **2007**, *129*, 12066–12067. b) B. Xu, S.-F. Zhu, X.-D. Zuo, Z.-C. Zhang, Q.-L. Zhou, *Angew. Chem. Int. Ed.* **2014**, *53*, 3913–3916. c) J.-X. Guo, T. Zhou, B. Xu, S.-F. Zhu, Q.-L. Zhou, *Chem. Sci.* **2016**, *7*, 1104–1108. d) M. L. Li, J. H. Yu, Y. H. Li, S. F. Zhu, Q. L. Zhou, *Science* **2019**, *366*, 990–994.

251 For reviews: a) K. Fuji, T. Kawabata, *Chem. Eur. J.* **1998**, *4*, 373–376. b) H. Zhao, D. C. Hsu, P. R. Carlier, *Synthesis* **2005**, *1*, 1–16. c) V. Alezra, T. Kawabata, *Synthesis* **2016**, *48*, 2997–3016. For examples: a) T. Kawabata, S. Kawakami, S. Majumdar, *J. Am. Chem. Soc.* **2003**, *125*, 13012–13013. b) J. H. Kim, Y. Chung, H. Jeon, S. Lee, S. Kim, *Org. Lett.* **2020**, *22*, 3989–3992.

252 G. Carbone, P. O'Brien, G. Hilmersson, *J. Am. Chem. Soc.* **2010**, *132*, 15445–15450.

253 S. Wu, S. Lee, P. Beak, *J. Am. Chem. Soc.* **1996**, *118*, 715–721.

254 K. Brak, E. N. Jacobsen, *Angew. Chem. Int. Ed.* **2013**, *52*, 534–561.

255 A. Nelson, *Angew. Chem. Int. Ed.* **1999**, *38*, 1583–1585.

256 J. Tan, N. Yasuda, *Org. Process Res. Dev.* **2015**, *19*, 1731–1746.

257 S. Jew, H. Park, *Chem. Commun.* **2009**, 7090–7103.

258 T. Respondek, E. Cueny, J. J. Kodanko, *Org. Lett.* **2012**, *14*, 150–153.

259 H. Ledon, G. Linstrumelle, S. Julia, *Tetrahedron* **1973**, *29*, 3609–3617.

260 G. Diaz-Muñoz, I. L. Miranda, S. K. Sartori, D. C. Rezende, M. Alves Nogueira Diaz, *Chirality* **2019**, *31*, 776–812.

261 E. Aller, G. G. Cox, D. J. Miller, C. J. Moody, *Tetrahedron Lett.* **1994**, *35*, 5949–5952.

262 a) J. F. Coope, B. G. Main, *Tetrahedron: Asymmetry* **1995**, *6*, 1393–1398. b) D. Özdemirhan, S. Sezer, Y. Sönmez, *Tetrahedron Asymmetry* **2008**, *19*, 2717–2720. c) R. Kourist, P. D. de Maria, U. T. Bornschuer, *ChemBioChem* **2008**, *9*, 491–498.

263 For examples see: a) I. D. Jurberg, H. M. L. Davies, *Chem. Sci.* **2018**, *9*, 5112–5118. b) T. Xiao, M. Mei, Y. He, L. Zhou, *Chem. Commun.* **2018**, *54*, 8865–8868. For a review see: c) Z. Yang, M. L. Stivanin, I. D. Jurberg, R. M. Koenigs, *Chem. Soc. Rev.* **2020**, doi: 10.1039/D0CS00224K.

264 a) C. Sambiagio, T. Noël, *Trends Chem.* **2020**, *2*, 92–106. b) C. Empel, R. M. Koenigs, *J. Flow Chem.* **2020**, *10*, 157–160.

265 A. J. Boddy, C. J. Cordier, K. Goldberg, A. Madin, A. C. Spivey, J. A. Bull, *Org. Lett.* **2019**, *21*, 1818–1822.

266 H. D. Banks, *J. Org. Chem.* **2006**, *71*, 8089–8097.

267 C. W. Bird, G. W. H. Cheeseman in *Compr. Heterocycl. Chem.*, Vol. 4 (Eds.: C. W. Bird, G. W. H. Cheeseman), Elsevier, **1984**, pp. 1–38.

268 N. De Rycke, O. David, F. Couty, *Org. Lett.* **2011**, *13*, 1836–1839.

269 M. Morgenthaler, E. Schweizer, A. Hoffmann-Röder, F. Benini, R. E. Martin, G. Jaeschke, B. Wagner, H. Fischer, S. Bendels, D. Zimmerli, et al., *ChemMedChem* **2007**, *2*, 1100–1115.

270 F. G. West, T. M. Bott, *Heterocycles* **2012**, *84*, 223–264.

271 P. Jaramillo, P. Pérez, P. Fuentealba, *J. Phys. Org. Chem.* **2007**, *20*, 1050–1057.

272 For reviews on ring opening/expansion of aziridines: (a) W. McCoull, F. A. Davis, *Synthesis* **2000**, *10*, 1347–1365. b) J. B. Sweeney, *Chem. Soc. Rev.* **2002**, *31*, 247–258. c) S. Stanković, M. D'hooghe, S. Catak, H. Eum, M. Waroquier, V. Van Speybroeck, N. De Kimpe, H.-J. Ha, *Chem. Soc. Rev.* **2012**, *41*, 643–665.

273 F. Couty, O. R. P. David in *Synthesis of 4- to 7-membered Heterocycles by Ring Expansion*, Vol. 41 (Eds.: M. D'hooghe, H. J. Ha), Springer, Cham., **2015**, pp. 1–47.

274 a) F. Couty, G. Evano, *Synlett* **2009**, *19*, 3053–3064. b) J. Dolfen, N. N. Yadav, N. De Kimpe, M. D'hooghe, H. J. Ha, *Adv. Synth. Catal.* **2016**, *358*, 3485–3511. c) G. Masson, D. G. Pardo, J. Cossy, **2020**, doi: 10.1002/ejoc.202000794.

275 W. Van Brabandt, R. Van Landeghem, N. De Kimpe, *Org. Lett.* **2006**, *8*, 1105–1108. Also see: a) K. Mollet, S. Catak, M. Waroquier, V. Van Speybroeck, M. D'hooghe, N. De Kimpe, *J. Org. Chem.* **2011**, *76*, 8364–8375. b) K. Mollet, M. D'hooghe, L. Broeckx, B. Danneels, T. Desmet, N. De Kimpe, *Tetrahedron* **2013**, *69*, 2603–2607.

276 a) J. A. Vanecko, F. G. West, *Org. Lett.* **2005**, *7*, 2949–2952. b) F. Couty, F. Durrat, G. Evano, J. Marrot, *Eur. J. Org. Chem.* **2006**, *2006*, 4214–4223. c) T. M. Bott, J. A. Vanecko, F. G. West, *J. Org. Chem.* **2009**, *74*, 2832–2836.

277 M. K. Ghorai, D. Shukla, K. Das, *J. Org. Chem.* **2009**, *74*, 7013–7022.

278 M. Ruggeri, A. W. Dombrowski, S. W. Djuric, I. R. Baxendale, *J. Org. Chem.* **2020**, *85*, 7276–7286.

279 M. D. Delost, D. T. Smith, B. J. Anderson, J. T. Njardarson, *J. Med. Chem.* **2018**, *61*, 10996–11020.

280 M. M. Heravi, V. Zadsirjan, B. Farajpour, *RSC Adv.* **2016**, *6*, 30498–30551.

281 a) Z. Chen, Z. Chen, Z. Yang, L. Guo, W. Du, Y. Chen, *Angew. Chem. Int. Ed.* **2019**, *58*, 15021–15025. b) Z. J. Zhang, L. Zhang, R. L. Geng, J. Song, X. H. Chen, L. Z. Gong, *Angew. Chem. Int. Ed.* **2019**, *58*, 12190–12194. c) G.-J. Mei, D. Li, G.-X. Zhou, Q. Shi, Z. Cao, F. Shi, *Chem. Commun.* **2017**, *53*, 10030–10033. d) N. Punna, K. Harada, J. Zhou, N. Shibata, *Org. Lett.* **2019**, *21*, 1515–1520.

282 J. R. Huff, P. S. Anderson, D. B. Olsen, S. S. Carroll, S. D. Young, S. F. Britcher, L. E. E. O. Tran, L. S. Payne, W. C. Lumma, T. A. Lyle, et al., *Antimicrob. Agents Chemother.* **1995**, *56*, 2602–2605.

283 a) Z. Xu, C. M. Tice, W. Zhao, S. Cacatian, Y.-J. Ye, S. B. Singh, P. Lindblom, B. M. McKeever, P. M. Krosky, B. A. Kruk, et al., *J. Med. Chem.* **2011**, *54*, 6050–6062. b) L. Zhuang, C. M. Tice, Z. Xu, W. Zhao, S. Cacatian, Y. Ye, S. B. Singh, P. Lindblom, B. M. Mckeever, P. M. Krosky, et al., *Bioorg. Med. Chem.* **2017**, *25*, 3649–3657.

284 a) T. Ullrich, K. Baumann, K. Welzenbach, S. Schmutz, G. Camenisch, J. G. Meingassner, G. Weitz-Schmidt, *Bioorg. Med. Chem. Lett.* **2004**, *14*, 2483–2487. b) S. Ina, Y. Kenjirou, N. Kyoji, 6-PHENYLTETRAHYDRO-1,3-OXAZIN-2-ONE DERIVATIVE AND PHARMACEUTICAL COMPOISITION CONTAINING THE SAME, PCT Int. Appl. US6251897B1, 2001.

285 J. M. Cassady, K. K. Chan, H. G. Floss, E. Leistner, *Chem. Pharm. Bull.* **2004**, *52*, 1–26.

286 a) S. C. Schmid, I. A. Guzei, J. M. Schomaker, *Angew. Chem. Int. Ed.* **2017**, *56*, 12229–12233. b) J. W. Hilborn, Z.-H. Lu, A. R. Jurgens, Q. K. Fang, P. Byers, S. A. Wald, C. H. Senanayake, *Tetrahedron Lett.* **2001**, *42*, 8919–8921. c) Y. F. Wang, T. Izawa, S. Kobayashi, M. Ohno, *J. Am. Chem. Soc.* **1982**, *104*, 6465–6466.

287 Ref 127 and a) L. Caggiano, D. J. Fox, S. Warren, *Chem. Commun.* **2002**, 2528–2529. b) H. Dao Thi, L. Decuyper, K. Mollet, S. Kenis, N. De Kimpe, T. Van Nguyen, M. D'hooghe, *Synlett* **2016**, *27*, 1100–1105. c) H. Dao Thi, G. Le Nhat Thuy, S. Catak, V. Van Speybroeck, T. Van Nguyen, M. D'hooghe, *Synthesis* **2018**, *50*, 1439–1456.

288 a) M. Hirama, T. Shigemoto, Y. Yamazaki, S. Ito, *J. Am. Chem. Soc.* **1985**, *107*, 1797–1798. b) M. Fujita, O. Kitagawa, T. Suzuki, T. Taguchi, *J. Org. Chem.* **1997**, *62*, 7330–7335. c) J.-R. Ella-Menye, V. Sharma, G. Wang, *J. Org. Chem.* **2005**, *70*, 463–469. d) R. Robles-Machín, J. Adrio, J. C. Carretero, *J. Org. Chem.* **2006**, *71*, 5023–5026. e) T. J. Donohoe, C. J. R. Bataille, W. Gattrell, J. Kloesges, E. Rossignol, *Org. Lett.* **2007**, *9*, 1725–1728. f) J. W. Rigoli, C. D. Weatherly, B. T. Vo, S. Neale, A. R. Meis, J. M. Schomaker, *Org. Lett.* **2013**, *15*, 290–293. g) U. Jakob, W. Bannwarth, *Tetrahedron Lett.* **2015**, *56*, 6340–6344.

289 T. Buyck, Q. Wang, J. Zhu, *J. Am. Chem. Soc.* **2014**, *136*, 11524–11528.

290 a) Y. Takeda, S. Okumura, S. Tone, I. Sasaki, S. Minakata, *Org. Lett.* **2012**, *14*, 4874–4877. b) S. Sun, C. Zhou, J.-T. Yu, J. Cheng, *Org. Lett.* **2019**, *21*, 6579–6583.

291 R. Yousefi, T. J. Struble, J. L. Payne, M. Vishe, N. D. Schley, J. N. Johnston, *J. Am. Chem. Soc.* **2019**, *141*, 618–625.

292 E. Miller, S. Kim, K. Gibson, J. S. Derrick, F. D. Toste, *J. Am. Chem. Soc.* **2020**, *142*, 8946–8952.

293 a) G. Cardillo, L. Gentilucci, A. Tolomelli, C. Tomasini, *Tetrahedron Lett.* **1997**, *38*, 6953–6956. b) C. Tomasini, A. Vecchione, *Org. Lett.* **1999**, *1*, 2153–2156.

294 a) T. B. Sim, S. H. Kang, K. S. Lee, W. K. Lee, H. Yun, Y. Dong, H.-J. Ha, *J. Org. Chem.* **2003**, *68*, 104–108. b) C. S. Park, M. S. Kim, T. B. Sim, D. K. Pyun, C. H. Lee, D. Choi, W. K. Lee, J.-W. Chang, H.-J. Ha, *J. Org. Chem.* **2003**, *68*, 43–49.

295 R. Morán-Ramallal, R. Liz, V. Gotor, *Org. Lett.* **2008**, *10*, 1935–1938.

296 All Log*P* and Mw values were calculated using ChemDraw® Version 18.0.0.231.

297 C. M. Alder, J. D. Hayler, R. K. Henderson, A. M. Redman, L. Shukla, L. E. Shuster, H. F. Sneddon, *Green Chem.* **2016**, *18*, 3879–3890.

298 G. Frenking, S. Fau, C. M. Marchand, H. Grützmacher, *J. Am. Chem. Soc.* **1997**, *119*, 6648–6655.

299 W. Mahy, M. Patel, D. Steadman, H. Woodward, B. N. Atkinson, F. Svensson, N. Willis, A. Flint, D. Papatheodorou, Y. Zhao, et al., *J. Med. Chem.* **2020**, *63*, 9464–9483.

300 T. Lassila, J. Hokkanen, S.-M. Aatsinki, S. Mattila, M. Turpeinen, A. Tolonen, *Chem. Res. Toxicol.* **2015**, *28*, 2292–2303.

301 Heating at 100 ºC with TfOH led to decomposition of the azetidine.

302 Y. Zheng, C. M. Tice, S. B. Singh, *Bioorg. Med. Chem. Lett.* **2014**, *24*, 3673–3682.

303 Y.-J. Zheng, C. M. Tice, *Expert Opin. Drug Discov.* **2016**, *11*, 831–834.

304 T. T. Talele, *J. Med. Chem.* **2020**, doi: 10.1021/acs.jmedchem.0c00829.

305 G. Müller, T. Berkenbosch, J. C. J. Benningshof, D. Stumpfe, J. Bajorath, *Chem. Eur. J.* **2017**, *23*, 703–710.

306 E. M. Carreira, T. C. Fessard, *Chem. Rev.* **2014**, *114*, 8257–8322.

307 J. Burkhard, E. M. Carreira, *Org. Lett.* **2008**, *10*, 3525–3526.

308 a) J. A. Burkhard, B. Wagner, H. Fischer, F. Schuler, K. Müller, E. M. Carreira, *Angew. Chem. Int. Ed.* **2010**, *49*, 3524–3527. Also see: b) G. Wuitschik, E. M. Carreira, B. Wagner, H. Fischer, I. Parrilla, F. Schuler, M. Rogers-Evans, K. Müller, *J. Med. Chem.* **2010**, *53*, 3227–3246.

309 For a related study see: S. L. Degorce, M. S. Bodnarchuk, J. S. Scott, *ACS Med. Chem. Lett.* **2019**, *10*, 1198–1204.

310 a) J. A. Burkhard, C. Guérot, H. Knust, E. M. Carreira, *Org. Lett.* **2012**, *14*, 66–69. b) A. A. Kirichok, I. Shton, M. Kliachyna, I. Pishel, P. K. Mykhailiuk, *Angew. Chem. Int. Ed.* **2017**, *56*, 8865–8869. c) B. A. Chalyk, A. A. Isakov, M. V. Butko, K. V. Hrebeniuk, O. V. Savych, O. V. Kucher, K. S. Gavrilenko, T. V. Druzhenko, V. S. Yarmolchuk, S. Zozulya, et al., *Eur. J. Org. Chem.* **2017**, *2017*, 4530–4542. d) A. A. Kirichok, I. O. Shton, I. M. Pishel, S. A. Zozulya, P. O. Borysko, V. Kubyshkin, O. A. Zaporozhets, A. A. Tolmachev, P. K. Mykhailiuk, *Chem. Eur. J.* **2018**, *24*, 5444–5449.

311 a) P. K. Gadekar, A. Roychowdhury, P. S. Kharkar, V. M. Khedkar, M. Arkile, H. Manek, D. Sarkar, R. Sharma, V. Vijayakumar, S. Sarveswari, *Eur. J. Med. Chem.* **2016**, *122*, 475–487. b) S. W. Reilly, S. Griffin, M. Taylor, K. Sahlholm, C. C. Weng, K. Xu, D. A. Jacome, R. R. Luedtke, R. H. Mach, *J. Med. Chem.* **2017**, *60*, 9905–9910. c) T. R. Hodges, J. R. Abbott, A. J. Little, D. Sarkar, J. M. Salovich, J. E. Howes, D. T. Akan, J. Sai, A. L. Arnold, C. Browning, et al., *J. Med. Chem.* **2018**, *61*, 8875–8894. d) K. Katayama, T. Tsunemi, K. Miyazaki, K. Uoto, R. Yoshioka, H. Terashima, M. Terakawa, K. Yamashiro, M. Haruyama, H. Maeda, et al., *Bioorg. Med. Chem. Lett.* **2020**, *30*, 127425. e) S. Noji, Y. Hara, T. Miura, H. Yamanaka, K. Maeda, A. Hori, H. Yamamoto, S. Obika, M. Inoue, Y. Hase, et al., *J. Med. Chem.* **2020**, *63*, 7163–7185.

312 a) G. S. Singh, Z. Y. Desta, *Chem. Rev.* **2012**, *112*, 6104–6155. b) M. M. M. Santos, *Tetrahedron* **2014**, *70*, 9735–9757. c) J. Bariwal, L. G. Voskressensky, E. V. Van Der Eycken, *Chem. Soc. Rev.* **2018**, *47*, 3831–3848.

313 a) T. L. Pavlovska, R. G. Redkin, V. V. Lipson, D. V. Atamanuk, *Mol. Divers.* **2016**, *20*, 299–344. b) B. Yu, D. Q. Yu, H. M. Liu, *Eur. J. Med. Chem.* **2015**, *97*, 673–698. c) B. Yu, Y.-C. Zheng, X.-J. Shi, P.-P. Qi, H.-M. Liu, *Anticancer. Agents Med. Chem.* **2016**, *16*, 1315–1324. d) N. Ye, H. Chen, E. A. Wold, P. Y. Shi, J. Zhou, *ACS Infect. Dis.* **2016**, *2*, 382–392.

314 a) K. Ding, Y. Lu, Z. Nikolovska-Coleska, S. Qiu, Y. Ding, W. Gao, J. Stuckey, K. Krajewski, P. P. Roller, Y. Tomita, et al., *J. Am. Chem. Soc.* **2005**, *127*, 10130–10131. b) Y. Zhao, S. Yu, W. Sun, L. Liu, J. Lu, D. McEachern, S. Shargary, D. Bernard, X. Li, T. Zhao, et al., *J. Med. Chem.* **2013**, *56*, 5553–5561. c) Y. Zhao, L. Liu, W. Sun, J. Lu, D. McEachern, X. Li, S. Yu, D. Bernard, P. Ochsenbein, V. Ferey, et al., *J. Am. Chem. Soc.* **2013**, *135*, 7223–7234. d) A. K. Gupta, M. Bharadwaj, A. Kumar, R. Mehrotra, *Top. Curr. Chem.* **2017**, *375*, 3.

315 a) A. Kumar, G. Gupta, A. K. Bishnoi, R. Saxena, K. S. Saini, R. Konwar, S. Kumar, A. Dwivedi, *Bioorganic Med. Chem.* **2015**, *23*, 839–848. b) A. Gollner, D. Rudolph, H. Arnhof, M. Bauer, S. M. Blake, G. Boehmelt, X. L. Cockroft, G. Dahmann, P. Ettmayer, T. Gerstberger, et al., *J. Med. Chem.* **2016**, *59*, 10147–10162. c) A. Aguilar, J. Lu, L. Liu, D. Du, D. Bernard, D. McEachern, S. Przybranowski, X. Li, R. Luo, B. Wen, et al., *J. Med. Chem.* **2017**, *60*, 2819–2839. d) A. Barakat, M. S. Islam, H. M. Ghawas, A. M. Al-Majid, F. F. El-Senduny, F. A. Badria, Y. A. M. M. Elshaier, H. A. Ghabbour, *Bioorg. Chem.* **2019**, *86*, 598–608.

316 a) Y. Li, J. Yang, A. Aguilar, D. McEachern, S. Przybranowski, L. Liu, C. Y. Yang, M. Wang, X. Han, S. Wang, *J. Med. Chem.* **2019**, *62*, 448–466. b) R. P. Wurz, V. J. Cee, *J. Med. Chem.* **2019**, *62*, 445–447.

317 J. Yang, Y. Li, A. Aguilar, Z. Liu, C. Y. Yang, S. Wang, *J. Med. Chem.* **2019**, *62*, 9471–9487.

318 a) M. Rottmann, C. McNamara, B. K. S. Yeung, M. C. S. Lee, B. Zou, B. Russell, P. Seitz, D. M. Plouffe, N. V. Dharia, J. Tan, et al., *Science* **2010**, *329*, 1175–1180. b) B. K. S. Yeung, B. Zou, M. Rottmann, S. B. Lakshminarayana, S. H. Ang, S. Y. Leong, J. Tan, J. Wong, S. Keller-Maerki, C. Fischli, et al., *J. Med. Chem.* **2010**, *53*, 5155–5164. c) N. J. White, S. Pukrittayakamee, A. P. Phyo, R. Rueangweerayut, F. Nosten, P. Jittamala, A. Jeeyapant, J. P. Jain, G. Lefèvre, R. Li, et al., *N. Engl. J. Med.* **2014**, *371*, 403–410. d) H. Turner, *Future Med. Chem.* **2016**, *8*, 227–238. e) T. D. Ashton, S. M. Devine, J. J. Möhrle, B. Laleu, J. N. Burrows, S. A. Charman, D. J. Creek, B. E. Sleebs, *J. Med. Chem.* **2019**, *62*, 10526–10562.

319 a) H. Takada, N. Kumagai, M. Shibasaki, *Org. Lett.* **2015**, *17*, 4762–4765. b) H. Zheng, X. Liu, C. Xu, Y. Xia, L. Lin, X. Feng, *Angew. Chem. Int. Ed.* **2015**, *54*, 10958–10962.

320 a) S. Chowdhury, M. Chafeev, S. Liu, J. Sun, V. Raina, R. Chui, W. Young, R. Kwan, J. Fu, J. A. Cadieux, *Bioorg. Med. Chem. Lett.* **2011**, *21*, 3676–3681. b) Y. P. Goldberg, N. Price, R. Namdari, C. J. Cohen, M. H. Lamers, C. Winters, J. Price, C. E. Young, H. Verschoof, R. Sherrington, et al., *Pain* **2012**, *153*, 80–85. c) S. K. Bagal, M. L. Chapman, B. E. Marron, R. Prime, R. I. Storer, N. A. Swain, *Bioorg. Med. Chem. Lett.* **2014**, *24*, 3690–3699.

321 J. A. Sclafani, J. Chen, D. V. Levy, H. Reese, M. Dimitri, P. Mudipalli, M. Christie, C. J. Neville, M. Olsen, R. P. Bakale, *Org. Process Res. Dev.* **2017**, *21*, 1616–1624.

322 W. Shi, Z. Jiang, H. He, F. Xiao, F. Lin, Y. Sun, L. Hou, L. Shen, L. Han, M. Zeng, et al., *ACS Med. Chem. Lett.* **2018**, *9*, 94–97.

323 For examples see: a) G. Rainoldi, M. Faltracco, L. Lo Presti, A. Silvani, G. Lesma, *Chem. Commun.* **2016**, *52*, 11575–11578. b) G. Rainoldi, M. Faltracco, C. Spatti, A. Silvani, G. Lesma, *Molecules* **2017**, *22*, 2016. c) S. Guo, P. Dong, Y. Chen, X. Feng, X. Liu, *Angew. Chem. Int. Ed.* **2018**, *57*, 16852–16856.

324 Analysis carried out on SciFinder on 06/04/2020 and 07/04/2020. A general substructure search was carried out with each ring size and heteroatom position iteratively with the following restrictions placed: 1) Exclude metal-containing results; 2) Exclude isotope-containing results; 3) Only include if hit has references; 4) Only include if hit is a single component; 5) Limit references to biological or preparative sources.

325 C. M. Starks, *J. Am. Chem. Soc.* **1971**, *93*, 195–199.

326 See ref 254 and a) G. Pupo, A. C. Vicini, D. M. H. Ascough, F. Ibba, K. E. Christensen, A. L. Thompson, J. M. Brown, R. S. Paton, V. Gouverneur, *J. Am. Chem. Soc.* **2019**, *141*, 2878–2883. b) G. Roagna, D. M. H. Ascough, F. Ibba, A. C. Vicini, A. Fontana, K. E. Christensen, A. Peschiulli, D. Oehlrich, A. Misale, A. A. Trabanco, et al., *J. Am. Chem. Soc.* **2020**, *142*, 14045–14051.

327 U. H. Dolling, P. Davis, E. J. J. Grabowski, *J. Am. Chem. Soc.* **1984**, *106*, 446–447.

328 a) M. J. O'Donnell, W. D. Bennett, S. Wu, *J. Am. Chem. Soc.* **1989**, *111*, 2353–2355. b) B. Lygo, P. G. Wainwright, *Tetrahedron Lett.* **1997**, *38*, 8595–8598. c) E. J. Corey, F. Xu, M. C. Noe, *J. Am. Chem. Soc.* **1997**, *119*, 12414–12415. d) T. Ooi, M. Kameda, K. Maruoka, *J. Am. Chem. Soc.* **1999**, *121*, 6519–6520. e) B. Lygo, B. Allbutt, S. R. James, *Tetrahedron Lett.* **2003**, *44*, 5629–5632. f) M. Kitamura, S. Shirakawa, K. Maruoka, *Angew. Chem. Int. Ed.* **2005**, *44*, 1549–1551. g) M.-H. Kim, S.-H. Choi, Y.-J. Lee, J. Lee, K. Nahm, B.-S. Jeong, H.-G. Park, S.-S. Jew, *Chem. Commun.* **2009**, 782–784. h) M. W. Ha, S. Hong, C. Park, Y. Park, J. Lee, M. Kim, J. Lee, H. Park, *Org. Biomol. Chem.* **2013**, *11*, 4030–4039.

329 a) S. Shirakawa, K. Liu, K. Maruoka, *J. Am. Chem. Soc.* **2012**, *134*, 916–919. b) S. Shirakawa, X. Wu, K. Maruoka, *Angew. Chem. Int. Ed.* **2013**, *52*, 14200–14203. c) T. Hashimoto, K. Sakata, F. Tamakuni, M. J. Dutton, K. Maruoka, *Nat. Chem.* **2013**, *5*, 240–244. d) L. Zong, X. Ban, C. W. Kee, C. H. Tan, *Angew. Chem. Int. Ed.* **2014**, *53*, 11849–11853. e) K. C. Nicolaou, G. Liu, K. Beabout, M. D. McCurry, Y. Shamoo, *J. Am. Chem. Soc.* **2017**, *139*, 3736–3746. f) M. Pawliczek, Y. Shimazaki, H. Kimura, K. M. Oberg, S. Zakpur, T. Hashimoto, K. Maruoka, *Chem. Commun.* **2018**, *54*, 7078–7080. f) T. Inukai, T. Kano, K. Maruoka, *Angew. Chem. Int. Ed.* **2020**, *59*, 2211–2214. g) M. Sicignano, R. Schettini, G. Pierri, M. L. Marino, I. Izzo, F. De Riccardis, L. Bernardi, G. Della Sala, *J. Org. Chem.* **2020**, *85*, 7476–7484. h) A. Eitzinger, M. Winter, J. Schörgenhumer, M. Waser, *Chem. Commun.* **2020**, *56*, 579–582.

330 M. J. O'Donnell, *Tetrahedron* **2019**, *75*, 3667–3696.

331 For examples of the use of PTC for controlling pericyclic reactions see: a) E. E. Maciver, S. Thompson, M. D. Smith, *Angew. Chem. Int. Ed.* **2009**, *48*, 9979–9982. b) C. P. Johnston, A. Kothari, T. Sergeieva, S. I. Okovytyy, K. E. Jackson, R. S. Paton, M. D. Smith, *Nat. Chem.* **2015**, *7*, 171–177.

332 M. Rabinovitz, Y. Cohen, M. Halpern, *Angew. Chem. Int. Ed. Engl.* **1986**, *25*, 960–970.

333 D. L. Hughes, U. H. Dolling, K. M. Ryan, E. F. Schoenewaldt, E. J. J. Grabowski, *J. Org. Chem.* **1987**, *52*, 4745–4752.

334 a) A. W. Herriott, D. Picker, *J. Am. Chem. Soc.* **1975**, *97*, 2345–2349. b) R. J. Fox, J. Qiu, *Org. Process Res. Dev.* **2020**, *24*, 235–241.

335 a) S. E. Denmark, R. C. Weintraub, *Heterocycles* **2010**, *82*, 1527–1540. b) S. E. Denmark, N. D. Gould, L. M. Wolf, *J. Org. Chem.* **2011**, *76*, 4260–4336.

336 P. H. Y. Cheong, C. Y. Legault, J. M. Um, N. Çelebi-Ölçüm, K. N. Houk, *Chem. Rev.* **2011**, *111*, 5042–5137.

337 a) E. de Freitas Martins, J. R. Pliego, *ACS Catal.* **2013**, *3*, 613–616. b) E. F. Martins, J. R. Pliego, *J. Mol. Catal. A Chem.* **2016**, *417*, 192–199.

338 B. Lygo, B. I. Andrews, *Acc. Chem. Res.* **2004**, *37*, 518–525.

339 a) M. T. Reetz, *Angew. Chem. Int. Ed. English* **1988**, *27*, 994–998. b) M. T. Reetz, S. Hütte, R. Goddard, *J. Am. Chem. Soc.* **1993**, *115*, 9339–9340. c) M. T. Reetz, S. Hütte, R. Goddard, C. Robyr, *Chem. Eur. J.* **1996**, *2*, 382–384.

340 a) Q. Jin, C. Zheng, G. Zhao, G. Zou, *J. Org. Chem.* **2017**, *82*, 4840–4850. b) X. Xia, Q. Zhu, J. Wang, J. Chen, W. Cao, B. Zhu, X. Wu, *J. Org. Chem.* **2018**, *83*, 14617–14625. c) R. He, C. Ding, K. Maruoka, *Angew. Chem. Int. Ed.* **2009**, *48*, 4559–4561. d) S. Hong, M. Jung, Y. Park, M. W. Ha, C. Park, M. Lee, H. G. Park, *Chem. Eur. J.* **2013**, *19*, 9599–9605. e) C. Cheng, X. Lu, L. Ge, J. Chen, W. Cao, X. Wu, G. Zhao, *Org. Chem. Front.* **2017**, *4*, 101–114. f) G.-Y. Ran, X.-X. Yang, J.-F. Yue, W. Du, Y.-C. Chen, *Angew. Chem. Int. Ed.* **2019**, *58*, 9210–9214.

341 a) J. Zhang, D. Cao, H. Wang, C. Zheng, G. Zhao, Y. Shang, *J. Org. Chem.* **2016**, *81*, 10558–10568. b) J. X. Zhang, H. Y. Wang, Q. W. Jin, C. W. Zheng, G. Zhao, Y. J. Shang, *Org. Lett.* **2016**, *18*, 4774–4777. c) X. Liu, D. Lu, J. Wu, J. Tan, C. Jiang, G. Gao, T. Wang, *Adv. Synth. Catal.* **2020**, *362*, 1490–1495. d) Y. Yang, Y. Jiang, W. Du, Y. Chen, *Chem. Eur. J.* **2020**, *26*, 1754–1758.

342 B. Xiang, K. M. Belyk, R. A. Reamer, N. Yasuda, *Angew. Chem. Int. Ed.* **2014**, *53*, 8375–8378.

343 C. Q. He, A. Simon, Y. H. Lam, A. P. J. Brunskill, N. Yasuda, J. Tan, A. M. Hyde, E. C. Sherer, K. N. Houk, *J. Org. Chem.* **2017**, *82*, 8645–8650.

344 K. Ohmatsu, Y. Ando, T. Nakashima, T. Ooi, *Chem* **2016**, *1*, 802–810.

345 a) K. Ohmatsu, M. Kiyokawa, T. Ooi, *J. Am. Chem. Soc.* **2011**, *133*, 1307–1309. b) K. Ohmatsu, Y. Hamajima, T. Ooi, *J. Am. Chem. Soc.* **2012**, *134*, 8794–8797.

346 a) M. T. H. Liu, K. Ramakrishnan, *Tetrahedron Lett.* **1977**, *18*, 3139–3142. b) C. J. Abelt, J. M. Pleier, *J. Am. Chem. Soc.* **1989**, *111*, 1795–1799.

347 A. C. S. Reddy, P. M. Reddy, P. Anbarasan, *Adv. Synth. Catal.* **2020**, *362*, 801–806.

348 For an example of a similar metal-catalysed diazo to ketone transformation see: M. J. James, P. O'Brien, R. J. K. Taylor, W. P. Unsworth, *Angew. Chem. Int. Ed.* **2016**, *55*, 9671–9675.

349 C. F. Macrae, I. Sovago, S. J. Cottrell, P. T. A. Galek, P. McCabe, E. Pidcock, M. Platings, G. P. Shields, J. S. Stevens, M. Towler, et al., *J. Appl. Crystallogr.* **2020**, *53*, 226–235.

350 K. M. Johnson, M. S. Rattley, F. Sladojevich, D. M. Barber, M. G. Nuñez, A. M. Goldys, D. J. Dixon, *Org. Lett.* **2012**, *14*, 2492–2495.

351 a) P. R. Savoie, J. T. Welch, *Chem. Rev.* **2015**, *115*, 1130–1190. b) C. R. Pitts, D. Bornemann, P. Liebing, N. Santschi, A. Togni, *Angew. Chem. Int. Ed.* **2019**, *58*, 1950–1954.

352 a) T. Umemoto, L. M. Garrick, N. Saito, *Beilstein J. Org. Chem.* **2012**, *8*, 461–471. b) A. Narayanan, K. Kohno, A. Nirmalchandar, R. Haiges, G. Iakobson, P. Beier, G. K. S. Prakash, *J. Org. Chem.* **2019**, *84*, 11724–11734.

353 a) L. Pitzer, F. Schäfers, F. Glorius, *Angew. Chem. Int. Ed.* **2019**, *58*, 8572–8576. b) S. Cembellín, T. Dalton, T. Pinkert, F. Schäfers, F. Glorius, *ACS Catal.* **2020**, *10*, 197–202.

354 An assessment of some parameters for the sensitivity of an enantioselective reaction has been reported recently: Y. Liu, G. Luo, X. Yang, S. Jiang, W. Xue, Y. R. Chi, Z. Jin, *Angew. Chem. Int. Ed* **2020**, *59*, 442–448.

355 R. S. Cahn, C. Ingold, V. Prelog, *Angew. Chem. Int. Ed. Engl.* **1966**, *5*, 385–415.

356 F. G. Bordwell, H. E. Fried, *J. Org. Chem.* **1991**, *56*, 4218–4223.

357 B. A. Jones, T. Balan, J. D. Jolliffe, C. D. Campbell, M. D. Smith, *Angew. Chem. Int. Ed.* **2019**, *58*, 4596–4600.

358 D. H. Ess, K. N. Houk, *J. Am. Chem. Soc.* **2007**, *129*, 10646–10647.

359 a) J. Li, S. G. Ballmer, E. P. Gillis, S. Fujii, M. J. Schmidt, A. M. E. Palazzolo, J. W. Lehmann, G. F. Morehouse, M. D. Burke, *Science* **2015**, *347*, 1221–1226. b) A. Adamo, R. L. Beingessner, M. Behnam, J. Chen, T. F. Jamison, K. F. Jensen, J. C. M. Monbaliu, A. S. Myerson, E. M. Revalor, D. R. Snead, et al., *Science* **2016**, *352*, 61–67. c) N. Collins, D. Stout, J.-P. Lim, J. P. Malerich, J. D. White, P. B. Madrid, M. Latendresse, D. Krieger, J. Szeto, V.-A. Vu, et al., *Org. Process Res. Dev.* **2020**, doi: 10.1021/acs.oprd.0c00143.

360 T. Jiang, S. Bordi, A. McMillan, K.-Y. Chen, F. Saito, P. Nichols, B. Wanner, J. Bode, *ChemRxiv* **2019**, *4*, doi: 10.26434/chemrxiv.7882799.

361 L. I. Manasevia, B. U. Maria, A. Prandi, L. Brasili, S. Franchini, *Synthesis* **2015**, *47*, 3767–3775.

362 M. J. Kohl, R. G. Lejeune, *Steroids* **2002**, *67*, 71–75

363 S. Wu, S. Lee, P. Beak, *J. Am. Chem. Soc.* **1996**, *118*, 715–721.

364 R. Taj, J. L. Sorensen, *Tetrahedron Lett*. **2015**, *56*, 7108–7111.

365 K. Gudmundsson, J. F. Miller, E. M. Turner, Chemical Compounds, PCT. Int. Appl. WO2006020415A1, 2006.

366 G. Povie, A.-T. Tran, D. Bonnaffé, J. Habegger, Z. Hu, C. Le Narvor, P. Renaud, *Angew. Chem. Int. Ed.* **2014**, *53*, 3894–3898.

367 P. H. Huy, Method of Converting Alcohol to Halide, WO2016202894A1, 2016.

368 A. Niida, H. Tanigaki, E. Inokuchi, Y. Sasaki, S. Oishi, H. Ohno, H. Tamamura, Z. Wang, S. C. Peiper, K. Kitaura, A. Otaka, N. Fujii, *J. Org. Chem.* **2006**, *71*, 3942–3951.

369 M. Muramatsu, Y. Hayakumo, S. Fujii, *The Journal of Biochemistry* **1967**, *62*, 408–418.

370 S. Fernández, E. Menéndez, V. Gotor, *Synthesis* **1991**, *1991*, 713–716.

371 D. Roberts, D. Elmore, *Biochem. J.* **1974**, *141*, 545-554.

372 X. Luo, G. Chen, L. He, X. Huang, *J. Org. Chem.* **2016**, *81*, 2943–2949.

373 T. Wang, H. An, T. A. Vickers, R. Bharadwaj, P. D. Cook, *Tetrahedron* **1998**, *54*, 7955–7976.

374 S. Rezazadeh, V. Devannah, D. A. Watson, *J. Am. Chem. Soc.* **2017**, *139*, 8110–8113.

375 E. Menéndez, V. Gotor, *Synthesis* **1993**, *1993*, 72–74.

376 J. K. Dutton, J. H. Knox, X. Radisson, H. J. Ritchie, R. Ramage, *J. Chem. Soc. Perkin Trans. 1* **1995**, 2581–2587.

377 S. C. Busman, G. D. Cuny, K. A. Zaklika, E. J. Ellis, Diazo Compounds for laser-induced mass transfer imaging materials, PCT Int. Appl. US19985756689A1, 1998.

378 D. G. Brown, E. J. Velthuisen, J. R. Commerford, R. G. Brisbois, *J. Org. Chem.* **1996**, *61*, 2540–2541.

379 D. Bélanger, X. Tong, S. Soumaré, Y. L. Dory and Y. Zhao, *Chem. Eur. J.* **2009**, 15, 4428.

380 H. M. L. Davies, M. V. A. Grazini, E. Aouad, *Org. Lett.* **2001**, *3*, 1475–1477.

381 A. Padwa, M. M. Sá and M. David Weingarten, *Tetrahedron*, **1997**, *53*, 2371–2386

382 E. Brenna, N. Caraccia, G. Fogliato, G. Fronza, C. Fuganti, *Tetrahedron* **1997**, *53*, 10555–10564.

383 M. A.Matulenko, E. S. Paight, R. R. Frey, Gomtsyan, S. DiDomenico, M. Jiang, C.-H. Lee, A. O. Stewart, H. Yu, K. L. Kohlhaas, K. M. Alexander, S. McGaraughty, J. Mikusa, K. C. Marsh, S. W. Muchmore, C. L. Jakob, E. A. Kowaluk, M. F. Jarvis, S. S. Bhagwat, *Bioorg. Med. Chem.* **2007**, *15*, 1586–1605.

384 N. Ríos-Lombardía, E. Busto, E. García-Urdiales, V. Gotor-Fernández, V. Gotor, *J. Org. Chem*. **2009**, *74*, 2571–2574.

385 W. F. Bailey, K. M. Lambert, Z. D. Stempel, K. B. Wiberg, B. Q. Mercado, *J. Org. Chem*. **2016**, *81*, 12116–12127.

386 C. E. Katz, J. Aubé, *J. Am. Chem. Soc*. **2003**, *125*, 13948–13949.

387 N. D. Hahn, M. Nieger, K. H. Dötz, *J. Organomet. Chem*. **2004**, *689*, 2662–2673.

388 E. Laurent, B. Marquet, R. Tardivel, *J. Fluor. Chem*. **1990**, *49*, 115–126.

389 J. R. Tagat, S. W. McCombie, D. V. Nazareno, C. D. Boyle, J. A. Kozlowski, S. Chackalamannil, H. Josien, Y. Wang, G. Zhou, *J. Org. Chem.* **2002**, *67*, 1171–1177.

390 J. Zheng, J.-H. Lin, L.-Y. Yu, Y. Wei, X. Zheng, J.-C. Xiao, *Org. Lett*. **2015**, *17*, 6150–6153.

391 M. Takemura, H. Takahashi, K. Kawakami, H. Takeshita, Y. Kimura, J. Watanabe, Y. Sugimoto, A. Kitamura, R. Nakajima, K. Kanai, T. Fujisawa, IMIDAZO(1,2-A)PYRIDINE DERIVATIVE, PCT Int. Appl. EP1479681A1, 2004.

392 F. Ye, S. Qu, L. Zhou, C. Peng, C. Wang, J. Cheng, M. L. Hossain, Y. Liu, Y. Zhang, Z.-X. Wang, J. Wang, *J. Am. Chem. Soc.* **2015**, *137*, 4435–4444.

393 R. C. Cambie, S. A. Coulson, L. G. Mackay, S. J. Janssen, P. S. Rutledge, P. D. Woodgate, *J. Organomet. Chem.* **1991**, *409*, 385–409.

394 M. Hu, C. Ni, J. Hu, *J. Am. Chem. Soc.* **2012**, *134*, 15257–15260.

395 C. Peng, J. Cheng, J. Wang, *J. Am. Chem. Soc.*, **2007**, *129*, 8708–8709.

396 G. Wu, Y. Deng, C. Wu, Y. Zhang, J. Wang, *Angew. Chem. Int. Ed*. **2014**, *53*, 10510–10514.

397 B. Song, F. Rudolphi, T. Himmler, L. J. Goossen, *Adv. Synth. Catal.*, **2011**, *353*, 1565–1574.

398 R. M. Kim, E. R. Parmee, Q. Tan,C. Yang, A. R. Lins, GLUCAGON RECEPTOR ANTAGONIST COMPOUNDS, COMPOSITIONS CONTAINING SUCH COMPOUNDS AND METHODS OF USE, PCT Int. Appl. WO2007136577A2, 2007.

399 D. Zhao, Y. Jiang, D. Ma, *Tetrahedron* **2014**, *70*, 3327–3332.

400 B. Wong, X. Linghu, J. J. Crawford, J. Drobnick, W. Lee, H. Zhang, *Tetrahedron* **2014**, *70*, 1508–1515.

401 L. Gao, G. S. Hwang, D. H. Ryu, *J. Am. Chem. Soc.* **2011**,*133*, 20708–20711.

402 T. Hashimoto, Y. Naganawa, T. Kano, K. Maruoka, *Chem. Commun.* **2007**, *48*, 5143–5145.

403 N. T. Kadunce, S. E. Reisman, *J. Am. Chem. Soc.* **2015**, *137*, 10480–10483.

404 G. Shapiro, PYRROLOPYRIMIDINE DERIVATIVES AS NR2B NMDA RECEPTOR ANTAGONISTS, PCT Int. Appl. WO2016044323A1, 2016.

405 J. C. Lee, J. Y. Yuk, *Synth. Commun.* **1995**, *25*, 1511–1515.

406 J. S. Baum, D. A. Shook, H. M. L. Davies, H. D. Smith, *Synth. Commun.* **1987**, *17*, 1709–1716.

407 L. Lomlim, J. Einsiedel, F. W. Heinemann, K. Meyer, P. Gmeiner, *J. Org. Chem*. **2008**, *73*, 3608–3611.

408 T. K. Beng, J. S. Woo, R. E. Gawley, *J. Am. Chem. Soc*. **2012**, *134*, 14764–14771.

409 J. Van Betsbrugge, D. Tourwé, B. Kaptein, H. Kierkels, R. Broxterman, *Tetrahedron* **1997**, *53*, 9233–9240.

410 E. J. Cochrane, D. Leonori, L. A. Hassall, I. Coldham, *Chem. Commun.* **2014**, *50*, 9910.

411 A. Nortcliffe, C. J. Moody, *Bioorg. Med. Chem.* **2015**, *23*, 2730–2735.

412 K. Ueno, S. Kubo, H. Tagawa, T. Yoshioka, W. Tsukada, *J. Med. Chem.* **1976**, *19*, 941–946.
413 O. G. L. Silva, L. M. B. Mateos, A. B.-L. Lorente, G. F. L. Gutierrez, Process for obtaining olopatadine and intermediates, EP2145882 (A1), 2010.
414 C. W. Y. Chung, P. H. Toy, *Tetrahedron* **2005**, *61*, 709–715.
415 S. Fujii, S. Y. Chang, M. D. Burke, *Angew. Chem. Int. Ed.* **2011**, *50*, 7862–7864.
416 R. Möckel, G. Hilt, *Org. Lett.* **2015**, *17*, 1644–1647.
417 D. O. Kiesewetter, J. A. Katzenellenbogen, M. R. Kilbourn, M. J. Welch, *J. Org. Chem.* **1984**, 4900–4905.
418 T. Furuya, A. E. Strom, T. Ritter, *J. Am. Chem. Soc.* **2009**, *131*, 1662–1663.
419 D. Vanderborn, C. Sewing, J. D. M. Herscheid, A. D. Windhorst, R. V. A. Orru, D. J. Vugts, *Angew. Chem. Int. Ed.* **2014**, *53*, 11046–11050.
420 I. Ugarriza, U. Uria, L. Carrillo, J. L. Vicario, E. Reyes, *Chem. Eur. J.* **2014**, *20*, 11650–11654.
421 T. Severin,, H. Poehlmann, *Chem. Ber.* **1978**, *111*, 1564–1577.
422 E. Emer, J. Twilton, M. Tredwell, S. Calderwood, T. L. Collier, B. Liégault, M. Taillefer, V. Gouverneur, *Org. Lett.* **2014**, *16*, 6004–6007.
423 J. R. Denton, D. Sukumaran, H. M. L. Davies, *Org. Lett.* **2007**, *9*, 2625–2628.
424 J. D. Beadle, A. Knuhtsen, A. Hoose, P. Raubo, A. G. Jamieson, M. Shipman, *Org. Lett.* **2017**, *19*, 3303–3306.
425 a) C. Marti, E. M. Carreira, *J. Am. Chem. Soc.* **2005**, *127*, 11505–11515. b) Z. Li, L. Rösler, K. Herr, M. Brodrecht, H. Breitzke, K. Hofmann, H. Limbach, T. Gutmann, G. Buntkowsky, *ChemPlusChem* **2020**, *85*, 1737–1746.
426 S. Muthusamy, C. Gunanathan, M. Nethaji, *J. Org. Chem.* **2004**, *69*, 5631–5637.
427 M. Borsche, *Chem. Ber.*, **1921**, *54*, 2854–2856.
428 C. Liang, J. Xia, D. Lui, X. Li, Q. Yao, J. Gao, *Eur. J. Med. Chem.*, **2014**, *74*, 742–750.
429 V. M. Muzalevskiy, E. S. Balenkova, A. V. Shastin, A. M. Magerramov, N. G. Shikhaliev, V. G. Nenajdenko, *Russ. Chem. Bull.* **2011**, *60*, 2343–2346.
430 L.-Y. Mei, X.-Y. Tang, M. Shi, *Chem. Eur. J.* **2014**, *20*, 13136–13142.
431 K. Dhara, T. Mandal, J. Das, J. Dash, *Angew. Chem. Int. Ed.* **2015**, *54*, 15831–15835.
432 R. P. Singh, U. Majumder, J. M. Shreeve, *J. Org. Chem.* **2001**, *66*, 6263–6267.
433 D. J. Vyas, R. Fröhlich, M. Oestreich, *J. Org. Chem.* **2010**, *75*, 6720–6723.
434 X. Yao, T. Wang, Z. Zhang, *Eur. J. Org. Chem.* **2018**, *2018*, 4475–4478.
435 B. M. Trost, J. Xie, J. D. Sieber, *J. Am. Chem. Soc.* **2011**, *133*, 20611–20622.
436 K. E. Eckert, A. J. Lepore, B. L. Ashfeld, *Helv. Chim. Acta* **2019**, *102*, e1900192.
437 P. Lan, D. Berta, J. A. Porco, M. S. South, J. J. Parlow, *J. Org. Chem.* **2003**, *68*, 9678–9686.
438 R. de Vivar, *Bol. Inst. Quim. Univ. Mexico,* **1956**, *8,* 10–15.
439 M. F. G. Stevens, J. A. Hickman, R. Stone, N. W. Gibson, G. U. Baig, E. Lunt, C. G. Newton, *J. Med. Chem.* **1984**, *27*, 196–201.
440 A. J. Brouwer, S. J. E. Mulders, R. M. J. Liskamp, *Eur. J. Org. Chem.* **2001**, *2001*, 1903–1915.
441 S. R. Chhabra, A. Mahajan, W. C. Chan, *J. Org. Chem.* **2002**, *67*, 4017–4029.
442 C. Hunter, R. F. W. Jackson, H. K. Rami, *J. Chem. Soc. Perkin Trans. 1* **2000**, 219–223.
443 H. King, J. Wright, *J. Chem. Soc.*, **1948**, 2314–2318.
444 A. Banerji, S. Maiti, *Tetrahedron* **1994**, *50*, 9079–9096.
445 C. Del Fiandra, M. Moccia, V. Cerulli, M. F. A. Adamo, *Chem. Commun.* **2016**, *52*, 1697–1700.
446 M. Lian, Z. Li, J. Du, Q. Meng, Z. Gao, *Eur. J. Org. Chem.* **2010**, *2010*, 6525–6530.
447 Y. Wang, H. Yin, X. Tang, Y. Wu, Q. Meng, Z. Gao, *J. Org. Chem.* **2016**, *81*, 7042–7050.

448 S. Benard, F. Guibbal, E. Jestin, O. Meilhac, Radiolabeled darapladib and analogs thereof and their use as imaging compounds, Int. Pat. App. WO2019063634A1, 2019.

449 M. D. Chappell, S. E. Conner, V. I. C. Gonzalez, J. E. Lamar, J. Li, J. S. Moyers, R. A. Owens, A. E. Allie, G. Zhu, GLUCAGON RECEPTOR ANTAGONISTS, PREPARATION AND THERAPEUTIC USES, PCT Int. Appl. WO2005118542 (A1), 2005.

450 a) A. M. J. Bouillot, N. Dodic, J. F. Gellibert, O. Mirguet, PYRIMIDINE DERIVATIVES AS ACTIVATORS OF SOLUBLE GUANYLATE CYCLASE, PCT Int. Appl. WO2010015653 (A1), 2010. b) J. Shen, Y. Wang, K. Wang, AZOLE HETEROCYCLIC COMPOUND, PREPARATION METHOD, PHARMACEUTICAL COMPOSITION AND USE, PCT Int. Appl. US2014171431 (A1), 2014.

451 T. Korenaga, T. Kosaki, R. Fukumura, T. Ema, T. Sakai, *Org. Lett.* **2005**, *7*, 4915–4917.

452 J. M. Birchall, R. Hazard, R. N. Haszeldine, A. W. Wakalski, *J. Chem. Soc. C* **1967**, 47–50.

453 S. Arai, T. Ishida, T. Shiori, *Tetrahedron Lett.* **1998**, *39*, 8299–8302.

454 R. Li, Z. Liu, L. Chen, J. Pan, W. Zhou, *Beilstein J. Org. Chem.* **2018**, *14*, 1421–1427.

455 C. Exner, A. Pfaltz, M. Studer, H.-U. Blaser, *Adv. Synth. Catal.* **2003**, *345*, 1253–1260.

456 G. Ma, W. Wan, J. Li, Q. Hu, H. Jiang, S. Zhu, J. Wang, J. Hao, *Chem. Commun.* **2014**, *50*, 9749–9752.

457 M. H. Franz, S. Röper, R. Wartchow, H. M. R. Hoffmann, *J. Org. Chem.* **2004**, *69*, 2983–2991.

458 M. Zielińska-Błajet, M. Kucharska, J. Skarżewski, *Synthesis* **2006**, *7*, 1176–1182.

459 P. Rabe, *Justus Liebig's Ann. der Chemie* **1932**, *492*, 242–266.

460 J. M. Tsangaris, T. A. Kabanos, *Monatshefte für Chemie Chem. Mon.* **1982**, *113*, 1393–1398.

461 A. P. Gorka, K. S. Sherlach, A. C. De Dios, P. D. Roepea, *Antimicrob. Agents Chemother.* **2013**, *57*, 365–374.

462 H. Brunner, J. Buegler, *Bulletin des Societes Chimiques Belges*, **1997**, *106*, 77–84.

463 O. Lifchits, M. Mahlau, C. M. Reisinger, A. Lee, C. Farès, I. Polyak, G. Gopakumar, W. Thiel, B. List, *J. Am. Chem. Soc.* **2013**, *135*, 6677–6693.

464 R. Craig, M. Litvajova, S. A. Cronin, S. J. Connon, *Chem. Commun.* **2018**, *54*, 10108–10111.

465 G. Kobayashi, *Yakugaku Zasshi*, **1950**, *70*, 381–383.

466 L. Hintermann, M. Schmitz, U. Englert, *Angew. Chem. Int. Ed.* **2007**, *46*, 5164–5167.

467 R. Li, Z. Liu, L. Chen, J. Pan, W. Zhou, *Beilstein J. Org. Chem.* **2018**, *14*, 1421–1427.

468 M. Lian, Z. Li, J. Du, Q. Meng, Z. Gao, *Eur. J. Org. Chem.* **2010**, *2010*, 6525–6530.

469 M. Gao, Y. Zhao, C. Zhong, S. Liu, P. Liu, Q. Yin, L. Hu, *Org. Lett.* **2019**, *21*, 5679–5684.

470 a) R. C. Neuman, R. Wolfe, *J. Org. Chem.* **1975**, *40*, 3147–3149. b) S. Lee, N. A. Beare, J. F. Hartwig, *J. Am. Chem. Soc.* **2001**, *123*, 8410–8411.

471 H. M. L. Davies, T. Hansen, M. R. Churchill, *J. Am. Chem. Soc.* **2000**, *122*, 3063–3070.

472 M. C. Hillier, C. Chen, *J. Org. Chem.* **2006**, *71*, 7885–7887.

473 C. R. Pitts, T. Lectka, *Chem. Rev.* **2014**, *114*, 7930–7953.

474 For a review see: a) F. Couty, B. Drouillat, G. Evano, O. David, *Eur. J. Org. Chem.* **2013**, *2013*, 2045–2056. b) C. Agami, F. Couty, G. Evano, *Tetrahedron: Asymmetry* **2002**, *13*, 297–302. c) F. Couty, D. Prim, *Tetrahedron: Asymmetry* **2002**, *13*, 2619–2624. d) F. Couty, G. Evano, N. Rabasso, *Tetrahedron: Asymmetry* **2003**, *14*, 2407–2412. e) F. Couty, G. Evano, M. Vargas-Sanchez, G. Bouzas, *J. Org. Chem.* **2005**, *70*, 9028–9031. f) M. Sivaprakasham, F. Couty, G. Evano, B. Srinivas, R. Sridhar, K. Rama Rao, *Arkivoc* **2007**, *2007*, 71–93.

475 P. Quinodoz, B. Drouillat, K. Wright, J. Marrot, F. Couty, *J. Org. Chem.* **2016**, *81*, 2899–2910.

476 a) A. Feula, L. Male, J. S. Fossey, *Org. Lett.* **2010**, *12*, 5044–5047. b) A. Feula, S. S. Dhillon, R. Byravan, M. Sangha, R. Ebanks, M. A. Hama Salih, N. Spencer, L. Male, I. Magyary, W.-P. Deng, et al., *Org. Biomol. Chem.* **2013**, *11*, 5083.

477 For a related bromocyclization see: S. Robin, G. Rousseau, *Eur J. Org. Chem.* **2000**, *2000*, 3007–3011.

478 N. E. Behnke, K. Lovato, M. Yousufuddin, L. Kürti, *Angew. Chem. Int. Ed.* **2019**, *58*, 14219–14223.

479 T. Bach, *Synlett* **2000**, *2000*, 1699–1707.

480 For a review see: C. S. Schindler, M. R. Becker, A. D. Richardson, *Chem. Sci.* **2020**, *68*, 42–61.

481 a) A. Padwa, *Chem. Rev.* **1977**, *77*, 37–68. b) A. C. Pratt, *Chem. Soc. Rev.* **1977**, *6*, 63–81. c) D. Sampedro, A. Soldevilla, P. J. Campos, R. Ruiz, M. A. Rodríguez, *J. Org. Chem.* **2008**, *73*, 8331–8336.

482 R. Sakamoto, T. Inada, S. Sakurai, K. Maruoka, *Org. Lett.* **2016**, *18*, 6252–6255.

483 E. Kumarasamy, S. K. Kandappa, R. Raghunathan, S. Jockusch, J. Sivaguru, *Angew. Chem. Int. Ed.* **2017**, *56*, 7056–7061.

484 M. R. Becker, A. D. Richardson, C. S. Schindler, *Nat. Commun.* **2019**, *10*, 5095.

485 G. L. Zhao, J. W. Huang, M. Shi, *Org. Lett.* **2003**, *5*, 4737–4739.

486 a) A. E. Taggi, A. M. Hafez, H. Wack, B. Young, D. Ferraris, T. Lectka, *J. Am. Chem. Soc.* **2002**, *124*, 6626–6635. b) S. France, M. H. Shah, A. Weatherwax, H. Wack, J. P. Roth, T. Lectka, *J. Am. Chem. Soc.* **2005**, *127*, 1206–1215. c) S. Takizawa, F. A. Arteaga, Y. Yoshida, M. Suzuki, H. Sasai, *Org. Lett.* **2013**, *15*, 4142–4145.

487 For related metal-mediated cycloadditions see: a) T. Akiyama, K. Daidouji, K. Fuchibe, *Org. Lett.* **2003**, *5*, 3691–3693. b) R. Shintani, G. C. Fu, *Angew. Chem. Int. Ed.* **2003**, *42*, 4082–4085. c) R. R. Liu, J. P. Hu, J. J. Hong, C. J. Lu, J. R. Gao, Y. X. Jia, *Chem. Sci.* **2017**, *8*, 2811–2815.

488 J.-B. Denis, G. Masson, P. Retailleau, J. Zhu, *Angew. Chem. Int. Ed.* **2011**, *50*, 5356–5360.

489 a) C. Denis, M. A. J. Dubois, A. S. Voisin-Chiret, R. Bureau, C. Choi, J. J. Mousseau, J. A. Bull, *Org. Lett.* **2019**, *21*, 300–304. b) M. A. J. Dubois, A. Lazaridou, C. Choi, J. J. Mousseau, J. A. Bull, *J. Org. Chem.* **2019**, *84*, 5943–5956.

490 a) C. Bosset, H. Beucher, G. Bretel, E. Pasquier, L. Queguiner, C. Henry, A. Vos, J. P. Edwards, L. Meerpoel, D. Berthelot, *Org. Lett.* **2018**, *20*, 6003–6006. b) S. Han, X. Ren, Q. Wu, A. Liang, J. Li, D. Zou, Y. Wu, Y. Wu, *Adv. Synth. Catal.* **2018**, *360*, 2308–2312. c) Z. Liu, N. Luan, L. Shen, J. Li, D. Zou, Y. Wu, Y. Wu, *J. Org. Chem.* **2019**, *84*, 12358–12365.

491 L. Degennaro, M. Zenzola, P. Trinchera, L. Carroccia, A. Giovine, G. Romanazzi, A. Falcicchio, R. Luisi, *Chem. Commun.* **2014**, *50*, 1698–1700.

492 M. Zenzola, L. Degennaro, P. Trinchera, L. Carroccia, A. Giovine, G. Romanazzi, P. Mastrorilli, R. Rizzi, L. Pisano, R. Luisi, *Chem. Eur. J.* **2014**, *20*, 12190–12200.

493 M. Andresini, S. De Angelis, A. Uricchio, A. Visaggio, G. Romanazzi, F. Ciriaco, N. Corriero, L. Degennaro, R. Luisi, *J. Org. Chem.* **2018**, *83*, 10221–10230.

494 a) E. Tayama, K. Watanabe, Y. Matano, *Eur. J. Org. Chem.* **2016**, *2016*, 3631–3641. b) E. Tayama, K. Watanabe, S. Sotome, *Org. Biomol. Chem.* **2017**, *15*, 6668–6678. For a related reaction see: c) B. Drouillat, F. Couty, J. Marrot, *Synlett* **2009**, *11*, 767–770.

495 A. Fawcett, A. Murtaza, C. H. U. Gregson, V. K. Aggarwal, *J. Am. Chem. Soc.* **2019**, *141*, 4573–4578.

496 For reviews see: a) S. Husinec, V. Savic, *Tetrahedron Asymmetry* **2005**, *16*, 2047–2061. b) G. Pandey, P. Banerjee, S. R. Gadre, *Chem. Rev.* **2006**, *106*, 4484–4517. c) L. M. Stanley, M. P. Sibi, *Chem. Rev.* **2008**, *108*, 2887–2902. d) T. Hashimoto, K. Maruoka, *Chem. Rev.* **2015**, *115*, 5366–5412. For selected examples see: e) J. L. Vicario, S. Reboredo, D. Badía, L. Carrillo, *Angew. Chem. Int. Ed.* **2007**, *46*, 5168–5170. f) B. M. Trost, S. M. Silverman, *J. Am. Chem. Soc.* **2012**, *134*, 4941–4954. g) S. Reboredo, E. Reyes, J. L. Vicario, D. Badía, L.

Carrillo, A. De Cózar, F. P. Cossío, *Chem. Eur. J.* **2012**, *18*, 7179–7188. h) T.-Y. Lin, C.-Z. Zhu, P. Zhang, Y. Wang, H.-H. Wu, J.-J. Feng, J. Zhang, *Angew. Chem. Int. Ed.* **2016**, *55*, 10844–10848. i) J. Otero-Fraga, S. Suárez-Pantiga, M. Montesinos-Magraner, D. Rhein, A. Mendoza, *Angew. Chem. Int. Ed.* **2017**, *56*, 12962–12966.

497 J. Hartung, S. N. Greszler, R. C. Klix, J. M. Kallemeyn, *Org. Process Res. Dev.* **2019**, *23*, 2532–2537.

498 a) L. E. Overman, M.-A. Kakimoto, *J. Am. Chem. Soc.* **1979**, *101*, 1310–1312. b) L. E. Overman, M. aki Kakimoto, M. E. Okazaki, G. P. Meier, *J. Am. Chem. Soc.* **1983**, *105*, 6622–6629. c) L. E. Overman, M. E. Okazaki, E. J. Jacobsen, *J. Org. Chem.* **1985**, *50*, 2403–2405.

499 T. E. Müller, K. C. Hultzsch, M. Yus, F. Foubelo, M. Tada, *Chem. Rev.* **2008**, *108*, 3795–3892.

500 a) C. F. Bender, R. A. Widenhoefer, *J. Am. Chem. Soc.* **2005**, *127*, 1070–1071. b) X. Han, R. A. Widenhoefer, *Angew. Chem. Int. Ed.* **2006**, *45*, 1747–1749. c) Z. Liu, J. F. Hartwig, *J. Am. Chem. Soc.* **2008**, *130*, 1570–1571.

501 For a review of different metals see: a) J. Hannedouche, E. Schulz, *Chem. Eur. J.* **2013**, *19*, 4972–4985. For Ir catalysis: b) K. D. Hesp, M. Stradiotto, *Org. Lett.* **2009**, *11*, 1449–1452. For Co catalysis: c) C. Lepori, P. Gómez-Orellana, A. Ouharzoune, R. Guillot, A. Lledós, G. Ujaque, J. Hannedouche, *ACS Catal.* **2018**, 4446–4451.

502 a) L. Ackermann, L. T. Kaspar, A. Althammer, *Org. Biomol. Chem.* **2007**, *5*, 1975–1978. b) L. Ackermann, A. Althammer, *Synlett* **2008**, *7*, 995–998.

503 a) N. D. Shapiro, V. Rauniyar, G. L. Hamilton, J. Wu, F. D. Toste, *Nature* **2011**, *470*, 245–249. b) X. Zhang, T. J. Emge, K. C. Hultzsch, *Angew. Chem. Int. Ed.* **2012**, *51*, 394–398. c) A. R. Brown, C. Uyeda, C. A. Brotherton, E. N. Jacobsen, *J. Am. Chem. Soc.* **2013**, *135*, 6747–6749. d) J.-S. Lin, X.-Y. Dong, T.-T. Li, N.-C. Jiang, B. Tan, X.-Y. Liu, *J. Am. Chem. Soc.* **2016**, *138*, 9357–9360. e) C. Chen, S. Jin, Z. Zhang, B. Wei, H. Wang, K. Zhang, H. Lv, X. Q. Dong, X. Zhang, *J. Am. Chem. Soc.* **2016**, *138*, 9017–9020. f) M.-A. Abadie, X. Trivelli, F. Medina, N. Duhal, M. Kouach, B. Linden, E. Génin, M. Vandewalle, F. Capet, P. Roussel, et al., *Chem. Eur. J.* **2017**, *23*, 10777–10788. g) J.-S. Lin, F.-L. Wang, X.-Y. Dong, W.-W. He, Y. Yuan, S. Chen, X.-Y. Liu, *Nat. Commun.* **2017**, *8*, 14841.

504 A. J. Musacchio, L. Q. Nguyen, G. H. Beard, R. R. Knowles, *J. Am. Chem. Soc.* **2014**, *136*, 12217–12220.

505 a) J. E. Redford, R. I. McDonald, M. L. Rigsby, J. D. Wiensch, S. S. Stahl, *Org. Lett.* **2012**, *14*, 1242–1245. b) R. Jana, T. P. Pathak, K. H. Jensen, M. S. Sigman, *Org. Lett.* **2012**, *14*, 4074–4077.

506 a) Y. Terada, M. Arisawa, A. Nishida, *Angew. Chem. Int. Ed.* **2004**, *43*, 4063–4067. b) C. Schmitz, W. Leitner, G. Franciò, *Chem. Eur. J.* **2015**, *21*, 10696–10702. c) S. Yu, C. Wu, S. Ge, *J. Am. Chem. Soc.* **2017**, *139*, 6526–6529.

507 K. Ye, Z. Song, G. S. Sauer, J. H. Harenberg, N. Fu, S. Lin, *Chem. Eur. J.* **2018**, *24*, 12274–12279.

508 Y. Zhang, Q. Yan, G. Zi, G. Hou, *Org. Lett.* **2017**, *19*, 4215–4218.

509 G. Flores-Constante, A. C. Sánchez-Chávez, L. A. Polindara-García, *Eur. J. Org. Chem.* **2018**, *2018*, 4586–4591.

510 a) S. G. Davies, R. L. Nicholson, P. D. Price, P. M. Roberts, A. J. Russell, E. D. Savory, A. D. Smith, J. E. Thomson, *Tetrahedron: Asymmetry* **2009**, *20*, 758–772. Also see ref 476.

511 J. L. Jeffrey, R. Sarpong, *Chem. Sci.* **2013**, *4*, 4092–4106.

512 a) C. Martínez, K. Muñiz, *Angew. Chem. Int. Ed.* **2015**, *54*, 8287–8291. b) P. Becker, T. Duhamel, C. J. Stein, M. Reiher, K. Muñiz, *Angew. Chem. Int. Ed.* **2017**, *56*, 8004–8008.

513 a) M. Yang, B. Su, Y. Wang, K. Chen, X. Jiang, Y.-F. Zhang, X.-S. Zhang, G. Chen, Y. Cheng, Z. Cao, et al., *Nat. Commun.* **2014**, *5*, 4707. b) D. Meng, Y. Tang, J. Wei, X.-Y. Shi, M. Yang, *Chem. Commun.* **2017**, *53*, 5744–5747.

514 a) D. A. Iovan, M. J. T. Wilding, Y. Baek, E. T. Hennessy, T. A. Betley, *Angew. Chem. Int. Ed.* **2017**, *56*, 15599–15602. b) K.-P. Shing, Y. Liu, B. Cao, X.-Y. Chang, T. You, C.-M. Che, *Angew. Chem. Int. Ed.* **2018**, *57*, 11947–11951.

515 Azides have also been employed in acid-mediated intramolecular Schmidt reactions: X. Wang, Y. Su, R. Li, P. Gu, *J. Org. Chem.* **2018**, *83*, 5816–5824.

516 a) D. Solé, A. Amenta, F. Mariani, M.-L. Bennasar, I. Fernández, *Adv. Synth. Catal.* **2017**, *359*, 3654–3664. b) Y. Wang, X. Wen, X. Cui, X. P. Zhang, *J. Am. Chem. Soc.* **2018**, *140*, 4792–4796. c) R. W. Kubiak, H. M. L. Davies, *Org. Lett.* **2018**, *20*, 3771–3775. d) K. Liu, C. Zhu, J. Min, S. Peng, G. Xu, J. Sun, *Angew. Chem. Int. Ed.* **2015**, *54*, 12962–12967.

517 S. Goudedranche, C. Besnard, L. Egger, J. Lacour, *Angew. Chem. Int. Ed.* **2016**, *55*, 13775–13779.

518 Racemic: a) X. Zhang, J. Ji, Y. Zhu, C. Jing, M. Li, W. Hu, *Org. Biomol. Chem.* **2012**, *10*, 2133–2138. Asymmetric: b) M. Li, R. Chu, J. Chen, X. Wu, Y. Zhao, S. Liu, W. Hu, *Org. Lett.* **2017**, *19*, 1290–1293.

519 C.-V. T. Vo, J. W. Bode, *J. Org. Chem.* **2014**, *79*, 2809–2815.

520 a) A. Noble, D. W. C. Macmillan, *J. Am. Chem. Soc.* **2014**, *136*, 11602–11605. b) C. K. Prier, D. W. C. MacMillan, *Chem. Sci.* **2014**, *5*, 4173–4178. c) D. W. C. MacMillan, J. D. Cuthbertson, J. A. Terrett, V. W. Shurtleff, M. H. Shaw, *Science* **2016**, *352*, 1304–1308.

521 a) D. T. Ahneman, A. G. Doyle, *Chem. Sci.* **2016**, *7*, 7002–7006. b) J. Xie, M. Rudolph, F. Rominger, A. S. K. Hashmi, *Angew. Chem. Int. Ed.* **2017**, *56*, 7266–7270.

522 a) J. E. Spangler, Y. Kobayashi, P. Verma, D. H. Wang, J. Q. Yu, *J. Am. Chem. Soc.* **2015**, *137*, 11876–11879. b) P. Jain, P. Verma, G. Xia, J. Q. Yu, *Nat. Chem.* **2017**, *9*, 140–144. c) H. J. Jiang, X. M. Zhong, J. Yu, Y. Zhang, X. Zhang, Y. D. Wu, L. Z. Gong, *Angew. Chem. Int. Ed.* **2019**, *58*, 1803–1807.

523 Y. Ma, X. Yao, L. Zhang, P. Ni, R. Cheng, J. Ye, *Angew. Chem. Int. Ed.* **2019**, *58*, 16548–16552.

524 a) C. J. Cordier, R. J. Lundgren, G. C. Fu, *J. Am. Chem. Soc.* **2013**, *135*, 10946–10949. b) X. Mu, Y. Shibata, Y. Makida, G. C. Fu, *Angew. Chem. Int. Ed.* **2017**, *56*, 5821–5824.

525 P. D. Bailey, P. A. Millwood, P. D. Smith, *Chem. Commun.* **1998**, 633–640.

526 V. Van Speybroeck, K. Moonen, K. Hemelsoet, C. V. Stevens, M. Waroquier, *J. Am. Chem. Soc.* **2006**, *128*, 8468–8478.

527 For hydrogenation of pyrroles see: R. Kuwano, M. Kashiwabara, M. Ohsumi, H. Kusano, *J. Am. Chem. Soc.* **2008**, *130*, 808–809.

528 a) F. Glorius, N. Spielkamp, S. Holle, R. Goddard, C. W. Lehmann, *Angew. Chem. Int. Ed.* **2004**, *43*, 2850–2852. b) C. Y. Legault, A. B. Charette, *J. Am. Chem. Soc.* **2005**, *127*, 8966–8967.

529 B. Qu, H. P. R. Mangunuru, S. Tcyrulnikov, D. Rivalti, O. V. Zatolochnaya, D. Kurouski, S. Radomkit, S. Biswas, S. Karyakarte, K. R. Fandrick, et al., *Org. Lett.* **2018**, *20*, 1333–1337.

530 Z. Nairoukh, M. Wollenburg, C. Schlepphorst, K. Bergander, F. Glorius, *Nat. Chem.* **2019**, *11*, 264–270.

531 H. Zhang, K. Muñiz, *ACS Catal.* **2017**, *7*, 4122–4125.

532 M. Lankelma, A. M. Olivares, B. de Bruin, *Chem. Eur. J.* **2019**, *25*, 5658–5663.

533 J. Min, G. Xu, J. Sun, *J. Org. Chem.* **2017**, *82*, 5492–5498.

534 X. Dong, Y. Han, F. Yan, Q. Liu, P. Wang, K. Chen, Y. Li, Z. Zhao, Y. Dong, H. Liu, *Org. Lett.* **2016**, *18*, 3774–3777.

535 For a review see: a) S. D. Griggs, D. T. Tape, P. A. Clarke, *Org. Biomol. Chem.* **2018**, *16*, 6620–6633. b) S. D. Griggs, N. Thompson, D. T. Tape, M. Fabre, P. A. Clarke, *Chem. Eur. J.* **2017**, *23*, 9262–9265.

536 Y. Ju, R. S. Varma, *J. Org. Chem.* **2006**, *71*, 135–141.

537 K. I. Fujita, T. Fujii, R. Yamaguchi, *Org. Lett.* **2004**, *6*, 3525–3528.

538 A. Takemiya, J. F. Hartwig, *J. Am. Chem. Soc.* **2006**, *128*, 6042–6043.

539 a) Z. Shao, J. Chen, Y. Tu, L. Li, H. Zhang, *Chem. Commun.* **2003**, 1918–1919. b) T. De Haro, C. Nevado, *Angew. Chem. Int. Ed.* **2011**, *50*, 906–910. c) Z. Lu, S. S. Stahl, *Org. Lett.* **2012**, *14*, 1234–1237. d) Q. Wang, W. Zhong, X. Wei, M. Ning, X. Meng, Z. Li, *Org. Biomol. Chem.* **2012**, *10*, 8566–8569. e) H. T. Huang, T. C. Lacy, B. Błachut, G. X. Ortiz, Q. Wang, *Org. Lett.* **2013**, *15*, 1818–1821. f) W. Kong, P. Feige, T. De Haro, C. Nevado, *Angew. Chem. Int. Ed.* **2013**, *52*, 2469–2473. g) X. Qi, C. Chen, C. Hou, L. Fu, P. Chen, G. Liu, *J. Am. Chem. Soc.* **2018**, *140*, 7415–7419.

540 a) S. Yu, W. Zhu, D. Ma, *J. Org. Chem.* **2005**, *70*, 7364–7370. b) Y. Hayashi, H. Gotoh, R. Masui, H. Ishikawa, *Angew. Chem. Int. Ed.* **2008**, *47*, 4012–4015. c) W. Xia, H. Yao, D. Liu, L. Zhao, Y. Zhou, H. Liu, *Adv. Synth. Catal.* **2016**, *358*, 1864–1869.

541 G. X. Ortiz, B. Kang, Q. Wang, *J. Org. Chem.* **2014**, *79*, 571–581.

542 I. Coldham, A. J. Collis, R. J. Mould, R. E. Rathmell, *Tetrahedron Lett.* **1995**, *36*, 3557–3560.

543 a) S. J. Hedley, W. J. Moran, D. A. Price, J. P. A. Harrity, *J. Org. Chem.* **2003**, *68*, 4286–4292. b) K. M. Goodenough, P. Raubo, J. P. A. Harrity, *Org. Lett.* **2005**, *7*, 2993–2996.

544 J. J. Topczewski, P. J. Cabrera, N. I. Saper, M. S. Sanford, *Nature* **2016**, *531*, 220–224.

545 P. S. Campbell, C. Jamieson, I. Simpson, A. J. B. Watson, *Chem. Commun.* **2017**, *54*, 46–49.

546 a) A. Dupas, P. Lhotellier, G. Guillamot, C. Meyer, J. Cossy, *Org. Lett.* **2019**, *21*, 3589–3593. b) D. Craig, S. R. J. Spreadbury, A. J. P. White, *Chem. Commun.* **2020**, *56*, 9803–9806..

547 a) B. Drouillat, I. V. Dorogan, M. Kletskii, O. N. Burov, F. Couty, *J. Org. Chem.* **2016**, *81*, 6677–6685. b) G. Masson, S. Rioton, D. Gomez Pardo, J. Cossy, *Org. Lett.* **2018**, *20*, 5019–5022. c) G. Masson, S. Rioton, D. Gomez Pardo, J. Cossy, *Eur. J. Org. Chem.* **2019**, *2019*, 5497–5507.

548 a) G. U. Georg, X. Guan, *Tetrahedron Lett.* **1992**, *33*, 17–20. b) G. L. Milligan, C. J. Mossman, J. Aubé, *J. Am. Chem. Soc.* **1995**, *117*, 10449–10459. c) D. Núñez-Villanueva, L. Infantes, M. T. García-López, R. González-Muñiz, M. Martín-Martínez, *J. Org. Chem.* **2012**, *77*, 9833–9839. d) Y. Huang, P. Li, X.-Q. Dong, X. Zhang, *Org. Biomol. Chem.* **2018**, *16*, 8819–8823.

549 J. M. Curto, M. C. Kozlowski, *J. Org. Chem.* **2014**, *79*, 5359–5364.

550 A. Barbero, A. Diez-Varga, F. J. Pulido, A. González-Ortega, *Org. Lett.* **2016**, *18*, 1972–1975.

551 E. Cini, G. Bifulco, G. Menchi, M. Rodriquez, M. Taddei, *Eur. J. Org. Chem.* **2012**, *2012*, 2133–2141.

552 C. A. Willoughby, S. L. Buchwald, *J. Am. Chem. Soc.* **1994**, *116*, 8952–8965.

553 W. Zawodny, S. L. Montgomery, J. R. Marshall, J. D. Finnigan, N. J. Turner, J. Clayden, *J. Am. Chem. Soc.* **2018**, *140*, 17872–17877.